FOURTH EDITION

Veterinary Ophthalmology

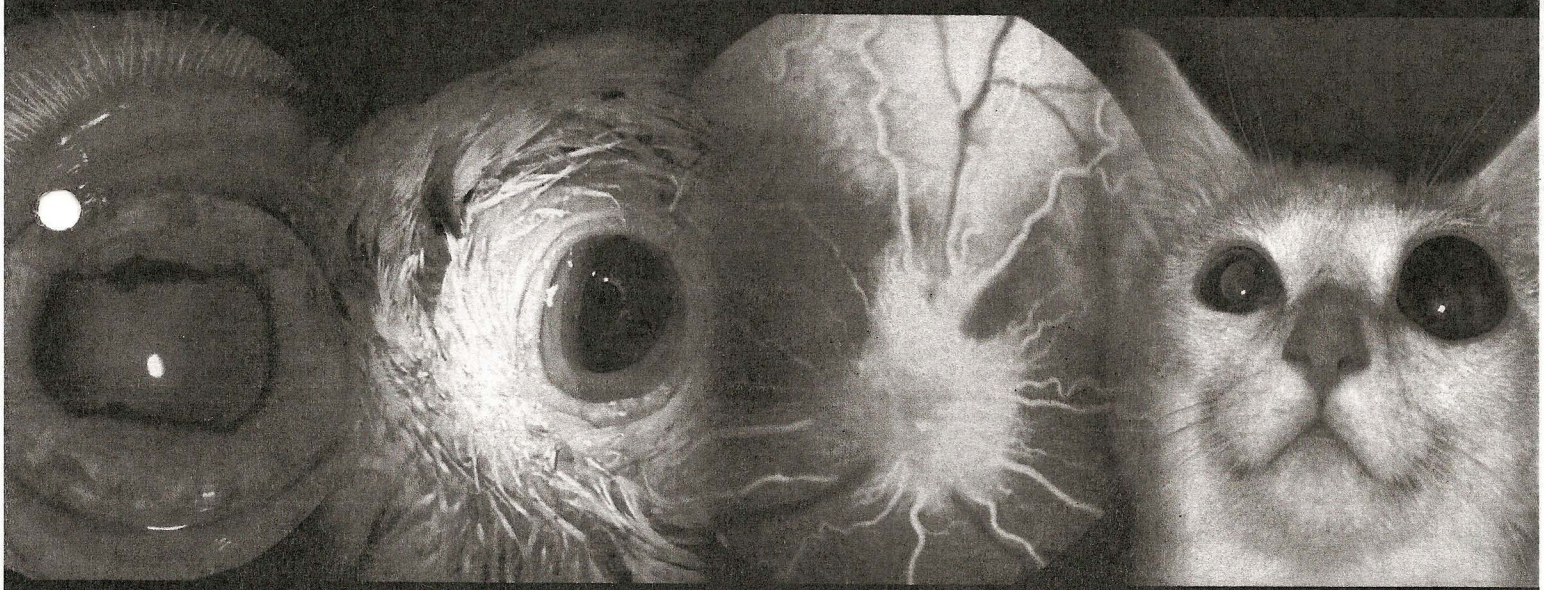

EDITED BY KIRK N. GELATT

VOLUME 1

Blackwell Publishing

Veterinary Ophthalmology

Fourth Edition

Volume I

Edited by

Kirk N. Gelatt, VMD

Diplomate, American College of Veterinary Ophthalmologists
Distinguished Professor of Comparative Ophthalmology
Department of Small Animal Clinical Sciences
College of Veterinary Medicine
University of Florida
Gainesville, Florida

Blackwell Publishing

Kirk N. Gelatt, VMD
Distinguished Professor of Comparative Ophthalmology
Department of Small Animal Clinical Sciences
College of Veterinary Medicine
University of Florida
Gainesville, Florida

©2007 Blackwell Publishing
All rights reserved

Blackwell Publishing Professional
2121 State Avenue, Ames, Iowa 50014, USA

Orders: 1-800-862-6657
Office: 1-515-292-0140
Fax: 1-515-292-3348
Web site: www.blackwellprofessional.com

Blackwell Publishing Ltd
9600 Garsington Road, Oxford OX4 2DQ, UK
Tel.: +44 (0)1865 776868

Blackwell Publishing Asia
550 Swanston Street, Carlton, Victoria 3053, Australia
Tel.: +61 (0)3 8359 1011

Authorization to photocopy items for internal or personal use, or the internal or personal use of specific clients, is granted by Blackwell Publishing, provided that the base fee is paid directly to the Copyright Clearance Center, 222 Rosewood Drive, Danvers, MA 01923. For those organizations that have been granted a photocopy license by CCC, a separate system of payments has been arranged. The fee code for users of the Transactional Reporting Service is ISBN-13: 978-0-7817-6657-9/2007.

First edition, © 1981, Lea & Febiger
Second edition, © 1991, Lea & Febiger
Third edition, © 1999 Lippencott Williams & Wilkins
Fourth Edition, 2007 Blackwell Publishing

Library of Congress Cataloging-in-Publication Data

Veterinary ophthalmology / [edited by] Kirk N. Gelatt. — 4th ed.
p. ; cm.
Includes bibliographical references and index.
ISBN-13: 978-0-7817-6657-9 (alk. paper)
ISBN-10: 0-7817-6657-5 (alk. paper)
1. Veterinary ophthalmology. I. Gelatt, Kirk N.
[DNLM: 1. Eye Diseases—veterinary. SF 891 V586 2007]
SF891.V48 2007
636.089'77—dc22

2006023434

The last digit is the print number: 9 8 7 6 5 4 3 2 1

ICBAS U BIBLIOTECA P PORTO
11389

CONTENTS

Volume I

Preface vii

Contributors ix

SECTION I: BASIC VISION SCIENCES 1

1 Ocular Embryology and Congenital Malformations 3
Cynthia S. Cook

2 Ophthalmic Anatomy 37
Don A. Samuelson

3 Physiology of the Eye 149
Glenwood G. Gum, Kirk N. Gelatt, and Douglas W. Esson

4 Optics and Physiology of Vision 183
Ron Ofri

SECTION II: FOUNDATIONS OF CLINICAL OPHTHALMOLOGY 221

5 Ocular Immunity 223
Daniel J. Biros

6 Clinical Microbiology 236
Laurence E. Galle and Cecil P. Moore

7 Clinical Pharmacology and Therapeutics
Part 1 Drug Delivery 271
Alain Regnier
Part 2 Antimicrobials, Antiinflammatory Agents, and Antiglaucoma Drugs 288
Alain Regnier
Part 3 Mydriatics/Cycloplegics, Anesthetics, Ophthalmic Dyes, Tear Substitutes and Stimulators, Intraocular Irrigating Fluids, Topical Disinfectants, Viscoelastics, Fibrinolytics and Antifibrinolytics, Antifibrotic Agents, Tissue Adhesives, and Anticollagenase Agents 332
Ian P. Herring

8 Fundamentals of Veterinary Ophthalmic Pathology 355
Bruce H. Grahn and Robert L. Peiffer

9 Ophthalmic Examination and Diagnostics
Part 1 The Eye Examination and Diagnostic Procedures 438
Franck J. Ollivier, Caryn E. Plummer, Kathleen P. Barrie
Part 2 Ocular Imaging 484
Maria E. Källberg
Part 3 Diagnostic Ultrasonography 507
Ursula M. Dietrich
Part 4 Electrodiagnostic Evaluation of Vision 520
Björn Ekesten

See Volume II for Chapters 10–30 and the Index

PREFACE

Veterinary Ophthalmology, now in its fourth edition, is testimony to the firm establishment of and progress in veterinary and comparative ophthalmology during the past nearly 50 years. When the first edition was released in 1981, the American College of Veterinary Ophthalmologists consisted of about 50 boarded ophthalmologists, and veterinary ophthalmology clinics were limited to a few private practices and academic institutions. Now, in 2006, veterinary ophthalmology is widely regarded as one of the premier clinical specialties in private practice. The American College has nearly 300 members, and the number of ACVO-boarded veterinary ophthalmologists continues to increase. Despite limited availability of training programs, we see steady growth in the number of private practices. Other countries worldwide have also established board certification organizations and are witnessing similar progress in the establishment of veterinary ophthalmology as a clinical specialty.

The first and second editions of this book were often referred to as the "blue bible" of veterinary ophthalmology because of the comprehensive information contained within their blue covers. When the third edition cover was changed to gold, the text was immediately became known as the "gold standard" for veterinary ophthalmology. It is our goal that this high standard as the leading text in veterinary ophthalmology continue with the fourth edition.

Veterinary Ophthalmology is a valuable reference for veterinary ophthalmologists; veterinary ophthalmology residents and graduate students; veterinary pathologists, pharmacologists, and toxicologists interested in the eye; vision scientists; and persons interested in comparative ophthalmology. It presents the current state of veterinary ophthalmology as documented by authors from America, Canada, England, France, Israel, Sweden, Switzerland, and the Netherlands. It includes practical information about the basic vision sciences; the foundations of clinical ophthalmology; ophthalmology of selected species, including canine, feline, equine, food animals, exotic, and laboratory animals; comparative neuroophthalmology; and ocular manifestations of systemic disease. Hundreds of color illustrations enhance the discussions and promote a deeper understanding of the information presented.

The fourth edition is organized similarly to previous editions, divided into two volumes with four major parts. Part I, "Basic Vision Sciences," consists of embryology and developmental abnormalities, anatomy, ocular physiology, and the physiology of vision and optics. The information in these chapters is unique and often very difficult to find in the comparative ophthalmic literature. Nevertheless, these disciplines form the critical basis for the remainder of the book.

In Part II, "Foundations of Clinical Ophthalmology," chapters are devoted to pharmacology, immunology, microbiology, pathology, and ocular examination and diagnostics. The information in these chapters is based on the experience and expertise of the authors and capsulized from numerous sources of materials that are often consuming and difficult to retrieve from the literature. Special attention is devoted to the continued progress in noninvasive imaging technology, which promises to advance clinical veterinary ophthalmology in the next several years (as it is doing in human ophthalmology at this time).

Part III, "Canine Ophthalmology," contains 14 chapters. Several chapters have been significantly expanded to present the status of diagnosis and therapy for specific diseases. In-depth discussion of surgical techniques and their outcomes provides invaluable guidance in best approaches to specific conditions, such as eyelid, corneosclera, and lens anomalies. Many gene and gene-mutation DNA tests for inherited retinal degenerations in purebred dogs are now available commercially; the most current and comprehensive summary of these tests and their application to diseases and diagnostics are explored in Chapter 21, "Diseases of the Canine Ocular Fundus."

In Part IV, "Special Ophthalmology," the expanded chapters on equine and feline ophthalmology reflect the greater numbers of these patients in our practices. The exotic and laboratory animal chapters again represent the importance of these species to veterinary ophthalmology. Comparative neuroophthalmology has a special place in veterinary ophthalmology, because such patients may present to either the ophthalmologist or neurologist. Finally, Chapter 30, "Ocular Manifestations of Systemic Diseases," is divided into canine, feline, equine, and food animal sections. This chapter focuses

on diagnosis, therapy, and prognosis of those diseases which often involve the eye and associated tissues.

A book of this magnitude requires a major commitment by a small group of authors who are experts in their chosen field and are willing to take time from their personal lives to present their experience and expertise to peers and colleagues worldwide. Such a book does not happen overnight, and with persistent hard work by all of the contributors, this effort has been completed in good time. A special thanks to our families from letting these veterinary ophthalmology "steal" again some family time for the good of our profession and our animal patients. I especially appreciate the assistance of the comparative ophthalmology faculty and staff at the University of Florida, particularly Edward O. MacKay and Tommy Rinkoski (PhD students) for their energy and computer expertise! A special thanks also goes to Antonia Seymour and Dede Anderson at Blackwell Publishing Professional for the opportunity to publish the fourth edition of *Veterinary Ophthalmology*.

Kirk N. Gelatt
Gainesville, Fl

CONTRIBUTORS

Kathleen P. Barrie, DVM, MS
Clinical Professor of Ophthalmology
Diplomate ACVO
Department of Small Animal Clinical Sciences
College of Veterinary Medicine
University of Florida
Gainesville, FL USA

Ellison Bentley, DVM
Clinical Assistant Professor of Comparative Ophthalmology
Diplomate ACVO
School of Veterinary Medicine
University of Wisconsin–Madison
Madison, WI USA

Daniel J. Biros, DVM
Postdoctoral Fellow
Diplomate ACVO
Schepens Eye Research Institute
Harvard Medical School
Boston, MA USA

Michael H. Boevé, DVM, PhD
Staff Ophthalmologist
Diplomate ECVO
Department of Clinical Sciences of Companion Animals
Faculty of Veterinary Medicine
Utrecht, The Netherlands

Dennis E. Brooks, DVM, PhD
Professor of Comparative Ophthalmology
Diplomate ACVO
Departments of Small Animal Clinical Sciences and Large Animal Clinical Sciences
College of Veterinary Medicine
University of Florida
Gainesville, FL USA

Carmen M. H. Colitz, DVM, PhD
Assistant Professor of Ophthalmology
Diplomate ACVO
Department of Veterinary Clinical Sciences
College of Veterinary Medicine
The Ohio State University
Columbus, OH USA

Cynthia S. Cook, DVM, PhD
Diplomate ACVO
Veterinary Vision,
San Mateo, CA USA

Cheryl L. Cullen, DVM
Clinical Associate Professor of Comparative Ophthalmology
Diplomate ACVO, Member, Hotchkiss Brain Institute
Department of Companion Animals
Faculty of Veterinary Medicine
Health Sciences Centre
University of Calgary
Calgary, Alberta Canada

Michael G. Davidson, DVM
Professor of Ophthalmology
Diplomate ACVO
Department of Companion Animal and Special Species Medicine
College of Veterinary Medicine
North Carolina State University
Raleigh, NC USA

Ursula M. Dietrich, Dr Med Vet
Assistant Professor of Ophthalmology
Diplomate ACVO; Diplomate ECVO
College of Veterinary Medicine
University of Georgia
Athens, GA USA

Björn Ekesten, DVM, PhD
Associate Professor of Ophthalmology
Diplomate ECVO
Department of Clinical Sciences
Faculty of Veterinary Medicine
Swedish University of Agricultural Science
Uppsala, Sweden

Douglas W. Esson, DVM
Resident in Ophthalmology
Eye Care for Animals
Tustin, CA USA

Laurence E. Galle, DVM
Assistant Professor of Ophthalmology
Diplomate ACVO
Department of Veterinary Medicine and Surgery
College of Veterinary Medicine
University of Missouri–Columbia
Columbia, MO USA

Kirk N. Gelatt, VMD
Distinguished Professor of Comparative Ophthalmology
Diplomate ACVO
Department of Small Animal Clinical Sciences
College of Veterinary Medicine

University of Florida
Gainesville, FL USA

Brian C. Gilger, DVM, MS
Professor of Ophthalmology
Diplomate ACVO
Department of Companion Animals and Special Species Medicine
College of Veterinary Medicine
North Carolina State University
Raleigh, NC USA

Elizabeth A. Giuliano, DVM, MS
Assistant Professor of Ophthalmology
Diplomate ACVO
Department of Veterinary Medicine and Surgery
College of Veterinary Medicine
University of Missouri–Columbia
Columbia, MO USA

Bruce H. Grahn, DVM
Professor of Ophthalmology
Diplomate ACVO
Department of Veterinary Internal Medicine
Western College of Veterinary Medicine
University of Saskatchewan
Saskatoon, SK Canada

Glenwood G. Gum, MS, PhD
Manager, Pharmacology/Pharmacokinetics
Biological Test Center
B. Braun Medical/McGaw, Inc
Irvine, CA USA

Diane V. H. Hendrix, DVM
Assistant Professor of Ophthalmology
Diplomate ACVO
Department of Small Animal Clinical Sciences
College of Veterinary Medicine
University of Tennessee
Knoxville, TN USA

Ian P. Herring, DVM, MS
Assistant Professor of Ophthalmology
Diplomate ACVO
Department of Small Animal Clinical Sciences
Virginia–Maryland Regional College of Veterinary Medicine
Virginia Tech
Blacksburg, VA USA

Maria E. Källberg, DVM, PhD
Assistant Professor of Ophthalmology
Department of Small Animal Clinical Sciences
College of Veterinary Medicine
University of Florida
Gainesville, FL USA

Thomas J. Kern, DVM
Associate Professor of Ophthalmology
Diplomate ACVO
Department of Clinical Sciences
College of Veterinary Medicine
Cornell University
Ithaca, NY USA

Andrew G. Matthews, BVM & S, PhD, FRCVS
Diplomate ECEIM
McKenzie, Bryson and Marshall
Kilmarnock, UK

Cecil P. Moore, DVM, MS
Professor of Ophthalmology
Diplomate ACVO
Department of Veterinary Medicine and Surgery
College of Veterinary Medicine
University of Missouri–Columbia
Columbia, MO USA

Kristina Narfström, DVM, PhD
Professor of Ophthalmology
Diplomate ECVO
Department of Veterinary Medicine and Surgery
College of Veterinary Medicine
University of Missouri–Columbia
Columbia, MO USA

Susan Nelms, DVM
Diplomate ACVO
Veterinary Eye Care
Bessemer, AL USA

Ron Ofri, DVM, PhD
Senior Lecturer, Veterinary Ophthalmology
Diplomate ECVO
Department of Clinical Sciences
Koret School of Veterinary Medicine
Hebrew University of Jerusalem
Rehovot Israel

Franck J. Olliver, DVM, PhD
Resident in Ophthalmology
Department of Small Animal Clinical Sciences
College of Veterinary Medicine
University of Florida
Gainesville, FL USA

Robert L. Peiffer Jr, DVM, PhD
Senior Investigator, Merck Research Laboratories
Diplomate ACVO
West Point, PA USA

Caryn E. Plummer, DVM
Resident in Ophthalmology
Department of Small Animal Clinical Sciences
College of Veterinary Medicine
University of Florida
Gainesville, FL USA

Alain Regnier, Dr Med Vet, PhD
Professor of Ophthalmology
Department of Clinical Sciences
School of Veterinary Medicine
Toulouse, France

Don A. Samuelson, PhD, MS
Professor of Comparative Ophthalmology
Department of Small Animal Clinical Sciences
College of Veterinary Medicine
University of Florida
Gainesville, FL USA

Lynne Sandmeyer, DVM, DVSc
Associate Professor of Ophthalmology
Diplomate ACVO
Department of Small Animal Clinical Sciences
Western College of Veterinary Medicine
University of Saskatchewan
Saskatoon, SK Canada

Merav Shamir, DVM
Senior Lecturer in Veterinary Neurology
Diplomate ECVN
Koret School of Veterinary Medicine

Hebrew University of Jerusalem
Rehovot, Israel

Simon Petersen-Jones, DVM, PhD, DVO, MRCVS
Associate Professor, Comparative Ophthalmology
Diplomate ECVO
Department of Small Animal Clinical Sciences
College of Veterinary Medicine
Michigan State University
East Lansing, MI USA

Patricia J. Smith, DVM, PhD, MS
Diplomate ACVO
Animal Eye Care
Fremont, CA USA

Bernard M. Spiess, DVM, Dr Med Vet
Professor of Ophthalmology
Diplomate ACVO; Diplomate ECVO
Department of Veterinary Surgery
University of Zurich
Zurich, Switzerland

Frans C. Stades, DVM, PhD
Associate Professor of Veterinary Ophthalmology
Diplomate ECVO
Department of Clinical Sciences of Companion Animals
Faculty of Veterinary Medicine
Utrecht University
Utrecht, The Netherlands

Jean Stiles, DVM, MS
Associate Professor of Ophthalmology
Diplomate ACVO
Department of Clinical Sciences
School of Veterinary Medicine
Purdue University, VCS Lynn Hall
West Lafayette, IN USA

Wendy M. Townsend, DVM, MS
Assistant Professor of Comparative Ophthalmology
Diplomate ACVO
Veterinary Medical Center
College of Veterinary Medicine
Michigan State University
East Lansing, MI USA

Samuel J. Vainisi, DVM
Diplomate ACVO
Animal Eye Clinic
Denmark, WI USA

Aubrey A. Webb, DVM, PhD
Faculty of Veterinary Medicine
Member, Hotchkiss Brain Institute
Health Sciences Centre
University of Calgary
Calgary, Alberta Canada

David A. Wilkie, DVM, MS
Professor of Comparative Ophthalmology
Diplomate ACVO
Department of Veterinary Clinical Sciences
College of Veterinary Medicine
Ohio State University
Columbus OH USA

David L. Williams, MA, VMB, PhD, CVO, MRCVS
Senior Lecturer, Veterinary Ophthalmology
Department of Clinical Veterinary Medicine
University of Cambridge
Cambridge, UK

Joseph C. Wolfer, DVM
Diplomate ACVO
Animal Eye Clinic
Toronto, Ontario, Canada

Section I

BASIC VISION SCIENCES

Chapter 1

Ocular Embryology and Congenital Malformations

Cynthia S. Cook

Investigations of normal and abnormal ocular development have often used rodents as animal models. Comparison with studies of humans and other animals demonstrates the sequence of developmental events is very similar across species.[1–5] Factors that must be considered when making interspecies comparisons include duration of gestation, differences in anatomic end point (e.g., presence of a tapetum, macula, or Schlemm's canal), and when eyelid fusion breaks (during the sixth month of gestation in the human versus 2 weeks postnatal in the dog) (Table 1.1).

This chapter describes normal events and abnormalities in this developmental sequence that can lead to malformations. Bearing in mind the species differences alluded to above, the mouse is a valuable model in the study of normal and abnormal ocular morphogenesis. In particular, studying the effects of acute exposure to teratogens during development has provided valuable information about the specific timing of events that lead to malformations.

GASTRULATION AND NEURULATION

Cellular mitosis following fertilization results in transformation of the single-cell zygote into a cluster of 12 to 16 cells. With continued cellular proliferation, this morula becomes a blastocyst, containing a fluid-filled cavity. The cells of the blastocyst will form both the embryo proper and the extraembryonic tissues (i.e., amnion and chorion). At this early stage, the embryo is a bilaminar disc consisting of hypoblast and epiblast. This embryonic tissue divides the blastocyst space into the amniotic cavity (adjacent to epiblast) and the yolk sac (adjacent to hypoblast) (Fig. 1.1).

Gastrulation (formation of the mesodermal germ layer) begins during day 10 of gestation in the dog (day 7 in the mouse; days 15–20 in the human). The primitive streak forms as a longitudinal groove within the epiblast (i.e., future ectoderm). Epiblast cells migrate toward the primitive streak, where they invaginate to form the mesoderm. This forms the three classic germ layers: ectoderm, mesoderm, and endoderm. Gastrulation proceeds in a cranial-to-caudal progression; simultaneously, the cranial surface ectoderm proliferates, forming bilateral elevations called the neural folds (i.e., future brain). The columnar surface ectoderm in this area now becomes known as the neural ectoderm (Fig. 1.2).

As the neural folds elevate and approach each other, a specialized population of mesenchymal cells, the neural crest, emigrates from the neural ectoderm at its junction with the surface ectoderm (Fig. 1.3). Migration and differentiation of the neural crest cells are influenced by the hyaluronic acid–rich extracellular matrix. This acellular matrix is secreted by the surface epithelium as well as by the crest cells, and it forms a space through which the crest cells migrate. Fibronectin secreted by the noncrest cells forms the limits of this mesenchymal migration.[6,7] Interactions between the migrating neural crest and the associated mesoderm appear to be essential for normal crest differentiation.[6,7] The neural crest cells migrate peripherally beneath the surface ectoderm to spread throughout the embryo, populating the region around the optic vesicle and ultimately giving rise to nearly all the connective tissue structures of the eye (Table 1.2).[8–10] The patterns of neural crest emergence and migration correlate with the segmental disposition of the developing brain.

It is important to note that mesenchyme is a general term for any embryonic connective tissue. Mesenchymal cells generally appear stellate and are actively migrating populations with extensive extracellular space. In contrast, *mesoderm* refers specifically to the middle embryonic germ layer. In other parts of the body (e.g., axial skeletal system), mesenchyme develops primarily from mesoderm, with a lesser contribution from the neural crest. In the craniofacial region, however, mesoderm plays a relatively small role in the development of connective tissue structures. In the eye, mesoderm probably gives rise only to the striated myocytes of the extraocular muscles and vascular endothelium. Most of the craniofacial mesenchymal tissue comes from neural crest cells.[9]

The neural tube closes initially in the craniocervical region and proceeds cranially and caudally. Once closure is complete, the exterior of the embryo is then completely covered by surface ectoderm, and the neural tube is lined by neural ectoderm. Neural segmentation then occurs to form the specific parts of the brain: forebrain (i.e., prosencephalon), midbrain (i.e., mesencephalon), and hindbrain (i.e., rhombencephalon) (Figs. 1.3

TABLE 1.1 Sequence Of Ocular Development

Human (Approximate Postfertilization Age)			Mouse (Day Postfertilization)	Dog (Day Postfertilization)	
Month	**Week**	**Day**		Postnatal	**Developmental Events**
1	3	22	8	13	Optic sulci present in forebrain
	4	24	9	15	Optic sulci convert into optic vesicles
			10	17	Optic vesicle contacts surface ectoderm
					Lens placode begins to thicken
		26			Optic vesicle surrounded by neural crest mesenchyme
2	5	28	10.5		Optic vesicle begins to invaginate, forming optic cup
					Lens pit forms as lens placode invaginates
					Retinal primordium thickens, marginal zone present
		32	11	19	Optic vesicle invaginated to form optic cup
					Optic fissure delineated
					Retinal primordium consists of external limiting membrane, proliferative zone, primitive zone, marginal zone, and internal limiting membrane
					Oculomotor nerve present
		33	11.5	25	Pigment in outer layer of optic cup
					Hyaloid artery enters through the optic cup
					Lens vesicle separated from surface ectoderm
					Retina: inner marginal and outer nuclear zones
			11.5	29	Basement membrane of surface ectoderm intact
					Primary lens fibers form
					Throchlear and abducens nerves appear
					Lid folds present
	6	37	12		Edges of optic fissure in contact
			12	30	Tunica vasculosa lentis present
					Lens vesicle cavity obliterated
					Ciliary ganglion present
		41	12	32	Posterior retina consists of nerve fiber layer, inner neuroblastic layer, transient fiber layer of Chievtiz, proliferative zone, outer neuroblastic layer, and external limiting membrane
			17	32	Eyelids fuse (dog)
	7				Anterior chamber beginning to form
			12.5	40	Secondary lens fibres present
		48	14	32	Corneal endothelium differentiated
	8	51			Optic nerve fibers reach the brain
					Optic stalk cavity is obliterated
					Lens sutures appear
					Acellular corneal stroma present
		54		30-35	Scleral condensation present
	9	57	17	40	First indication of ciliary processes and iris
					Extraocular muscles visible
				–	Eyelids fuse (occurs earlier in the dog)
	10			45	Pigment visible in iris stoma
					Ciliary processes touch lens equator
					Rudimentary rods and cones appear
				45-1P	Hyaloid artery begins to atrophy to the disc
3	12			–	Branches of the central retinal artery form

(continued)

TABLE 1.1 SEQUENCE OF OCULAR DEVELOPMENT *(continued)*

4	51	Pupillary sphincter differentiates
		Rental vessels present
	56	Ciliart muscle appears
	–	Eye axis forward (human)
–	56	Tapetum present (dog)
	2-14 P	Tunica vasculosa lentis atrophies
		Short eyelashes appear
5	40	Layers of the choroid are complete with pigmentation
6	–	Eyelids begin to open, light perception
	1 P	Pupillary dilator muscle present
7	1-14 P	Pupillary membrane atrophies
	1-16 P	Rod and cone inner and outer segments present in posterior retina
	10-13 P	Pars plana distinct
9	16-40t P	Retinal layers developed
	14 P	Regression of papillary membrane, TVL, and hyaloid artery nearly complete
		Lacrimal duct canalized

Data from references 2, 3, 46, and 159.

and 1.4). The optic vesicles develop from neural ectoderm within the forebrain, with the ocular connective tissue derivatives originating from the midbrain neural crest.

FORMATION OF THE OPTIC VESICLE AND OPTIC CUP

The optic sulci are visible as paired evaginations of the forebrain neural ectoderm on day 13 of gestation in the dog (Figs. 1.3, 1.4, 1.5, 1.6, and 1.7). The transformation from optic sulcus to optic vesicle is considered to occur concurrently with the closure of the neural tube (day 15 in the dog). Intracellular filaments and microtubules within the cytoskeleton alter cell shape and allow for cell movement. In addition to the mechanical influences of the cytoskeleton and the extracellular matrix, localized proliferation and cell growth contribute to expansion of the optic vesicle (Fig. 1.5).[10,11]

The optic vesicle enlarges and, covered by its own basal lamina, approaches the basal lamina underlying the surface

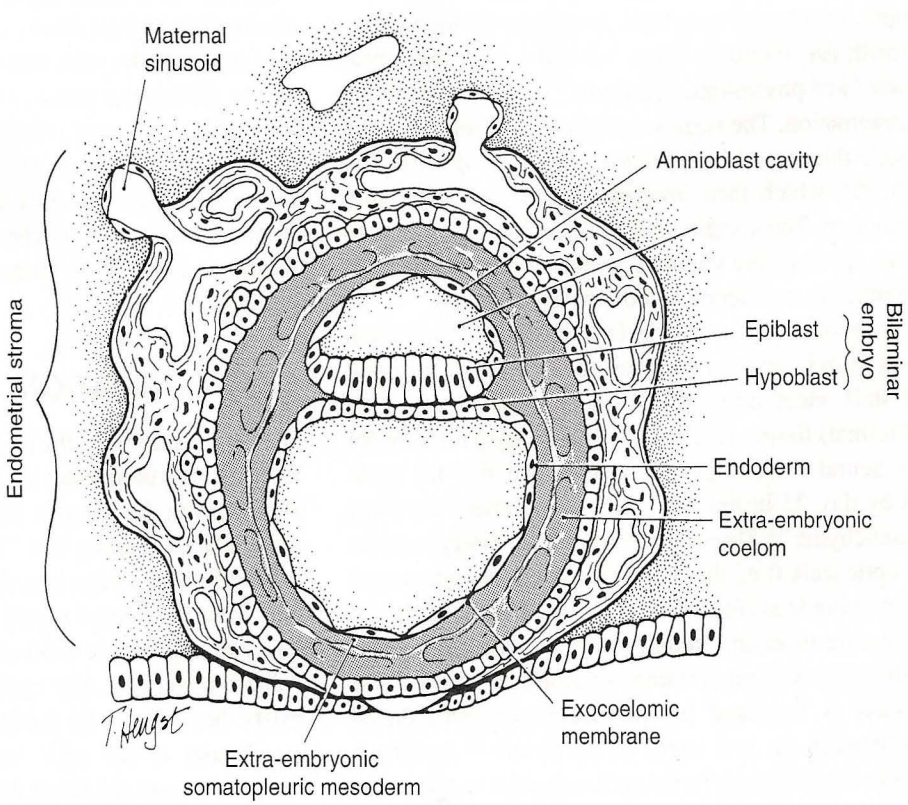

Figure 1.1. A blastocyst that has penetrated the maternal endometrium. An embryoblast has formed and consists of two cell layers: the epiblast above, and the hypoblast below. (Reprinted with permission from Cook C, Sulik K, Wright K. Embryology. In: Wright KW, ed. *Pediatric Ophthalmology and Strabismus.* St. Louis: Mosby–Year Book, 1995:3–59.)

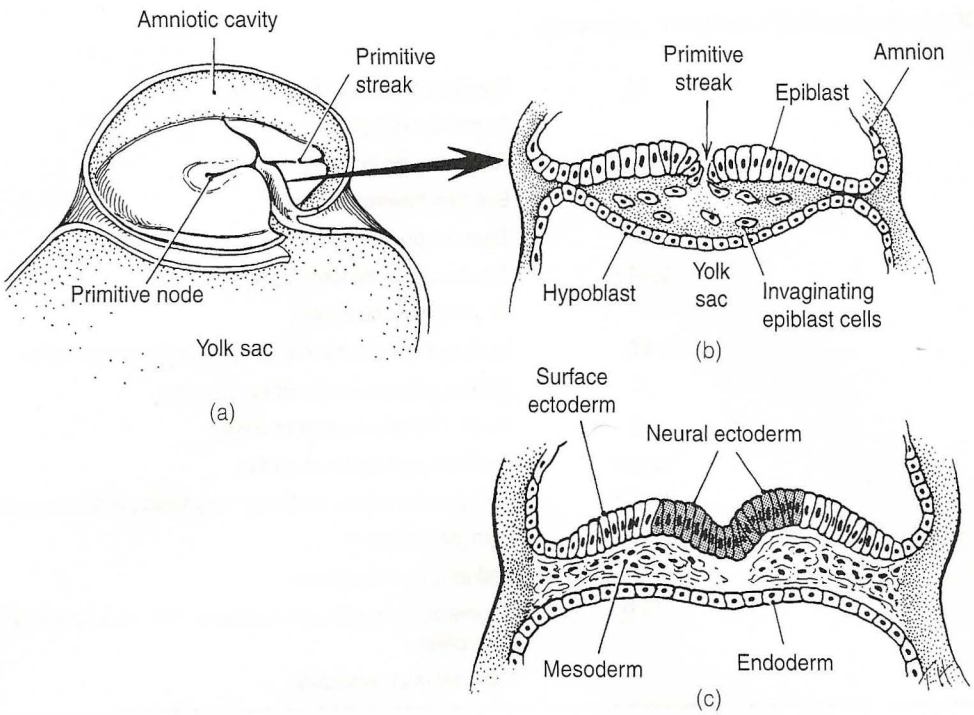

Figure 1.2. **A.** Dorsal view of an embryo in the gastrulation stage with the amnion removed. **B.** Cross-section through the primitive streak, representing invagination of epiblast cells between the epiblast and hypoblast layers. Note that the epiblast cells filling the middle area form the mesodermal layer. **C.** Cross-section through the neural plate. Note that the ectoderm in the area of the neural groove (shaded cells) has differentiated into neural ectoderm, whereas the ectoderm on each side of the neural groove is surface ectoderm (clear water cells). (Reprinted with permission from Cook C, Sulik K, Wright K. Embryology. In: Wright KW, ed. *Pediatric Ophthalmology and Strabismus.* St. Louis: Mosby–Year Book, 1995:3–59.)

ectoderm (Fig. 1.5). The optic vesicle appears to play a significant role in the induction and size determination of the palpebral fissure and of the orbital and periocular structures.[12] An external bulge indicating the presence of the enlarging optic vesicle can be seen at approximately day 17 in the dog.

The optic vesicle and optic stalk invaginate through differential growth and infolding (Figs. 1.6 and 1.7). Local apical contraction[13] and physiologic cell death[14] have been identified during invagination. The surface ectoderm in contact with the optic vesicle thickens to form the lens placode (Figs. 1.6, 1.7, and 1.8A, B), which then invaginates with the underlying neural ectoderm. The invaginating neural ectoderm folds onto itself as the space within the optic vesicle collapses, thus creating a double layer of neural ectoderm, the optic cup.

This process of optic vesicle/lens placode invagination progresses from inferior to superior, so the sides of the optic cup and stalk meet inferiorly in an area called the optic (choroid/retinal) fissure (Fig. 1.8F). Mesenchymal tissue (of primarily neural crest origin) surrounds and fills the optic cup, and by day 25 in the dog, the hyaloid artery develops from mesenchyme in the optic fissure. This artery courses from the optic stalk (i.e., the region of the future optic nerve) to the developing lens (Figs. 1.9 and 1.10). The two edges of the optic fissure meet and initially fuse anterior to the optic stalk, with fusion then progressing anteriorly and posteriorly. This process is mediated by glycosaminoglycan-induced adhesion between the two edges of the fissure.[15] Apoptosis has been identified in the inferior optic cup prior to formation of the optic fissure and, transiently, associated with its closure.[16] Failure of this fissure to close normally may result in inferiorly located defects (i.e., colobomas) in the iris, choroid, or optic nerve. Colobomas other than those in the "typical" six-o'clock location may occur through a different mechanism and are discussed later.

Closure of the optic cup through fusion of the optic fissure allows intraocular pressure (IOP) to be established. The protein in the embryonic vitreous humor (13% of plasma protein) is derived from plasma proteins entering the eye by diffusion out of permeable vessels in the anterior segment. After day 15, protein content in the vitreous decreases, possibly through dilution with aqueous humor produced by developing ciliary epithelium.[17]

LENS FORMATION

Before contact with the optic vesicle, the surface ectoderm first becomes competent to respond to lens inducers. Inductive signals from the anterior neural plate give this area of ectoderm a "lens-forming bias." Signals from the optic vesicle are required for complete lens differentiation, and inhibitory signals from the cranial neural crest may suppress any residual lens-forming bias in head ectoderm adjacent to the lens.[18,19] Adhesion between the optic vesicle and surface ectoderm exists, but there is no direct cell contact.[20–22] The basement membranes of the optic vesicle and the surface ectoderm remain separate and intact throughout the contact period.

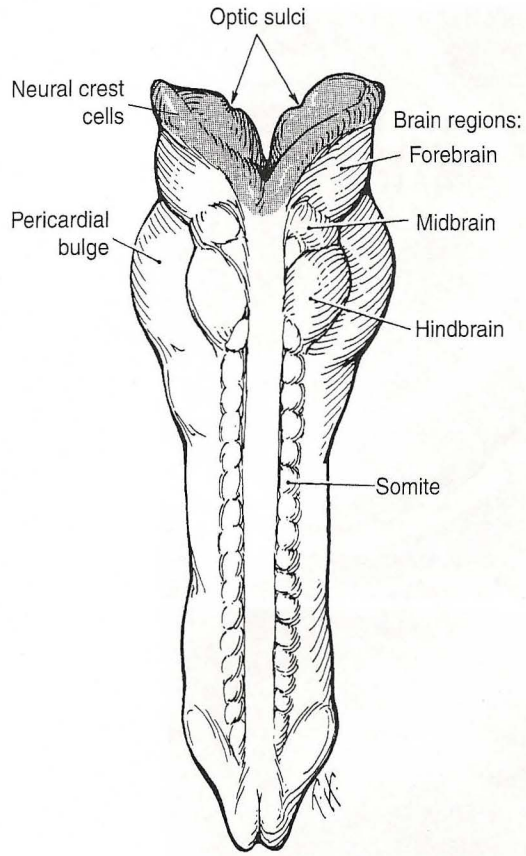

Figure 1.3. Dorsal view showing partial fusion of the neural folds to form the neural tube. Brain vesicles have divided into three regions: forebrain, midbrain, and hindbrain. The neural tube, groove, and facing surfaces of the large neural folds are lined with neural ectoderm (shaded cells), whereas surface ectoderm covers the rest of the embryo. Neural crest cells are found at the junction of the neural ectoderm and surface ectoderm. Neural crest cells migrate beneath the surface ectoderm, spreading throughout the embryo and specifically to the area of the optic sulci. Somites have formed along the lateral aspect of the closed cephalic neural tube. On the inside of both forebrain vesicles is the optic sulci. (Reprinted with permission from Cook C, Sulik K, Wright K. Embryology. In: Wright KW, ed. *Pediatric Ophthalmology and Strabismus.* St. Louis: Mosby–Year Book, 1995:3–59.)

Thickening of the lens placode can be seen on day 17 in the dog. A tight, extracellular matrix–mediated adhesion between the optic vesicle and the surface ectoderm has been described.[23–25] This anchoring effect on the mitotically active ectoderm results in cell crowding and elongation and in formation of a thickened placode. This adhesion between the optic vesicle and lens placode also assures alignment of the lens and retina in the visual axis.[26] Abnormal orientation of the optic vesicle as it approaches the surface ectoderm may result in induction of a smaller lens vesicle, which may assume an abnormal location within the optic cup.[25]

The lens placode invaginates, forming a hollow sphere, now referred to as a lens vesicle (Figs. 1.8C, D, 1.9, and 1.10). The size of the lens vesicle is determined by the contact area of the optic vesicle with the surface ectoderm and by the ability of the latter tissue to respond to induction. Aplasia may result from failure of lens induction or through later involutions of the lens vesicle, either before or after separation from the surface ectoderm.[23]

TABLE 1.2 EMBRYONIC ORIGINS OF SCULAR TISSUES

Neural Ectoderm	**Neural Crest**
Neural retina	Stoma of iris, ciliary body, choroids, and sclera
Retinal pigment epithelium	Ciliary muscles
Posterior iris epithelium Pupillary sphincter and dilator muscle (except in avain species)	Corneal stroma and endothelium Perivascular connective tissue and smooth muscle cells Striated muscles of iris (avain species only)
Bilayered ciliary epithelium	Menings of optic nerve
	Orbital cartilage and bone
	Connective tissue of the extrinsic ocular muscles
	Endothelium of trabecular mesh-work
Surface Ectoderm	**Mesoderm**
Lens	Extraocular myoblasts
Corneal and conjunctival epithelium	Vascular endothelium
Lacrimal gland	Schlemn's canal (human)
	Posterior sclera (?)

Data from references 8 and 47–49.

Lens vesicle detachment is the initial event leading to formation of the chambers of the ocular anterior segment. This process is accompanied by active migration of epithelial cells out of the keratolenticular stalk, cellular necrosis, apoptosis,

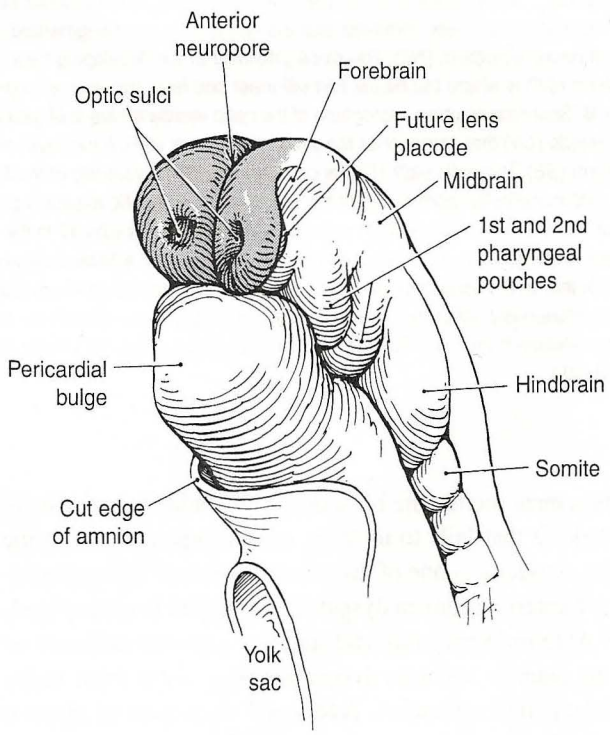

Figure 1.4. Development of the optic sulci, which are the first sign of eye development. Optic sulci on the inside of the forebrain vesicles consisting of neural ectoderm (shaded cells). The optic sulci evaginate toward the surface ectoderm as the forebrain vesicles simultaneously rotate inward to fuse.

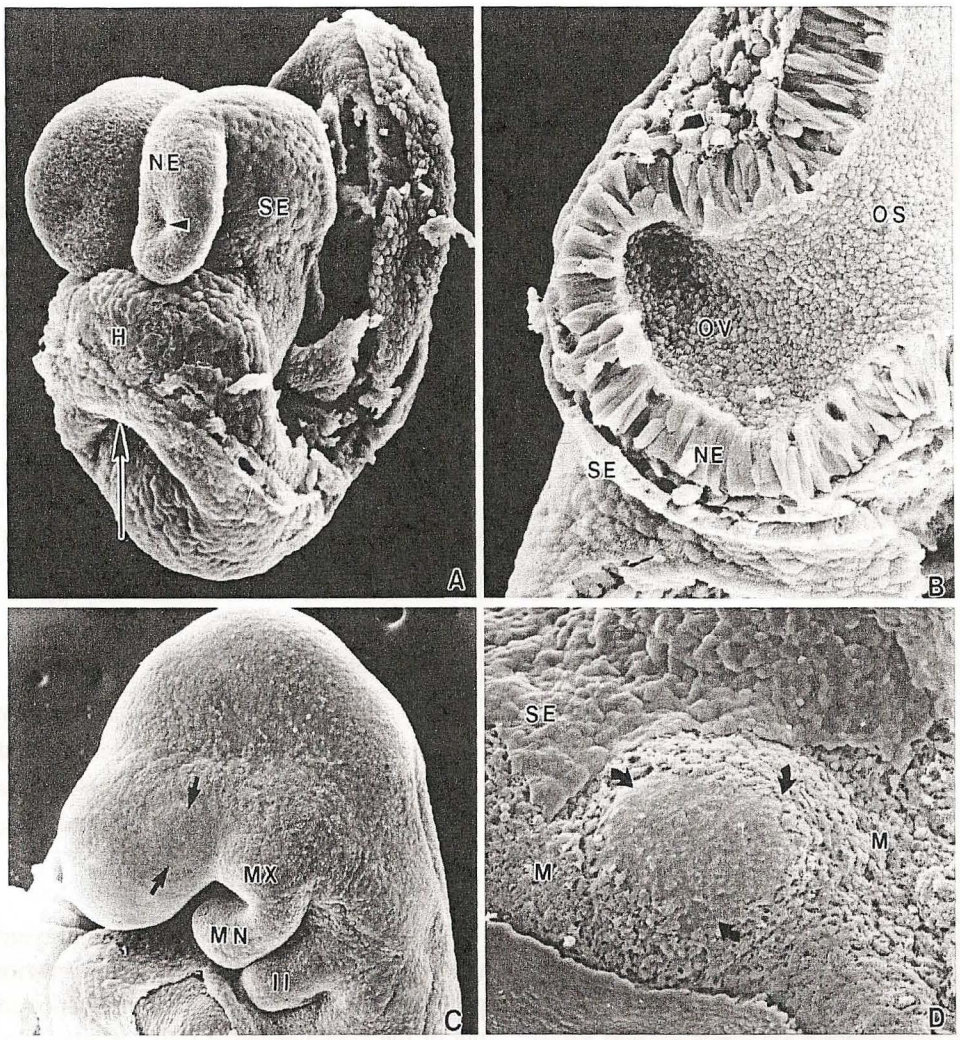

Figure 1.5. **A.** Scanning electron micrograph of a mouse embryo (six somite pairs) on day 8 of gestation, which is equivalent to day 13 of canine gestation. The amnion has been removed, and the neural folds have segmented into a forebrain region containing the optic sulci (*arrowhead*), which are evaginations of neural ectoderm (*NE*). The close proximity to the developing heart (*H*) can be seen. The area where the neural ectoderm (*NE*) meets the surface ectoderm (*SE*) is where the neural fold will meet and fuse; this area also gives rise to the neural crest cells. The entrance to the foregut is indicated by the arrow. **B.** Scanning electron micrograph of the optic vesicle on day 9 of gestation in the mouse (day 15 in the dog). Expansion of the optic sulcus results in an optic vesicle (*OV*) that approaches the surface ectoderm (*SE*). A thin layer of mesenchyme is still present between the neural ectoderm (*NE*) and the surface ectoderm (*SE*). The optic stalk (*OS*) is continuous with the ventricle of the forebrain. **C.** The bulge of the enlarging optic vesicle (*arrows*) can be seen externally. *MN,* mandibular prominence of the first visceral arch; *MX,* maxillary prominence of the first visceral arch; *II,* second visceral arch. **D.** Partial removal of the surface ectoderms (*E*) from an embryo of 25 somite pairs (day 17 in the dog; day 19 in the mouse) reveals the exposed basal lamina of the optic vesicle (*arrows*). Enlargement of the optic vesicle has displaced the adjacent mesenchyme (*M*) so that the basal lamina of the surface ectoderm (*E*) is in direct contact with that of the optic vesicle. (Part A reprinted with permission from Cook CS, Sulik KK. Sequential scanning electron microscopic analyses of normal and spontaneously occurring abnormal ocular development in C57B1/6J mice. *Scan Electron Microscopy* 1986;3:1215–1227. Parts B, C, and D reprinted with permission from Cook C, Sulik K, Wright K. Embryology. In: Wright KW, ed. *Pediatric Ophthalmology and Strabismus.* St. Louis: Mosby–Year Book, 1995:3–59.)

and basement membrane breakdown.[24,27] Induction of a small lens vesicle that fails to undergo normal separation from the surface ectoderm is one of the characteristics of the teratogen-induced anterior segment dysgenesis described in animal models.[25] Anterior lenticonus and anterior capsular cataracts as well as anterior segment dysgenesis may result from faulty keratolenticular separation. Additional discussion of anterior segment dysgenesis occurs later in this chapter.

Following detachment from the surface ectoderm (day 25 in the dog), the lens vesicle is lined by a monolayer of cuboidal cells surrounded by a basal lamina, the future lens capsule. The primitive retina promotes primary lens fiber formation in the adjacent lens epithelial cells. Surgical rotation of the chick lens vesicle by 180° results in elongation of the lens epithelial cells nearest the presumptive retina, regardless of the orientation of the transplanted lens.[28] Thus, while the retina develops independently of the lens, the lens appears to be dependent on the retinal primordium for its differentiation. The primitive lens filled with primary lens fibers is the embryonic lens nucleus. In the adult, the embryonic nucleus is the central sphere inside the Y sutures; there are no sutures within the embryonal nucleus (Figs. 1.11A and 1.12).

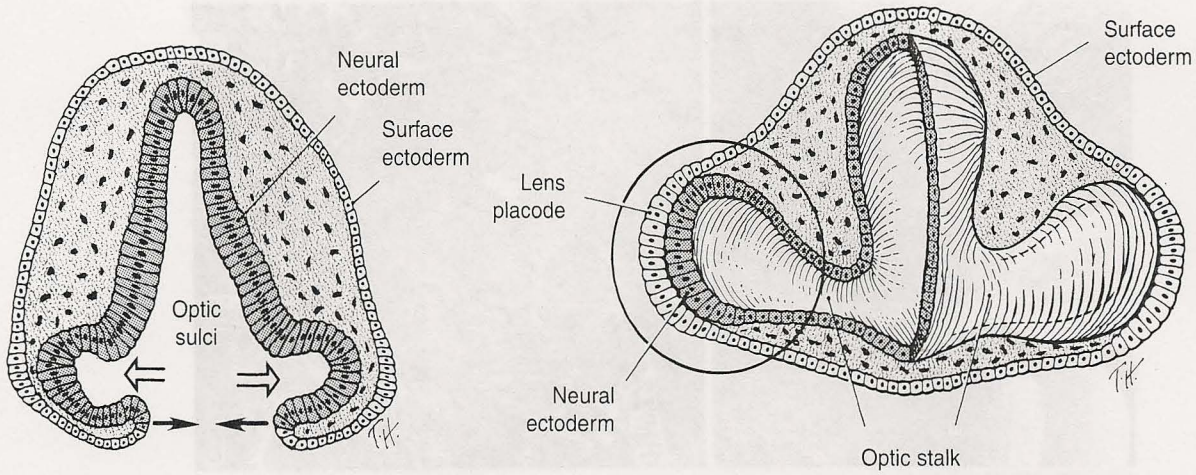

Figure 1.6. Cross-section at the level of the optic vesicle. Note that the neural tube is closed. The surface ectoderm now covers the surface of the forebrain, and the neural ectoderm is completely internalized. The surface ectoderm cells overlying the optic vesicles enlarge to form the early lens placode. (Reprinted with permission from Cook C, Sulik K, Wright K. Embryology. In: Wright KW, ed. Pediatric ophthalmology and strabismus. St. Louis: Mosby–Year Book, 1995:3–59.)

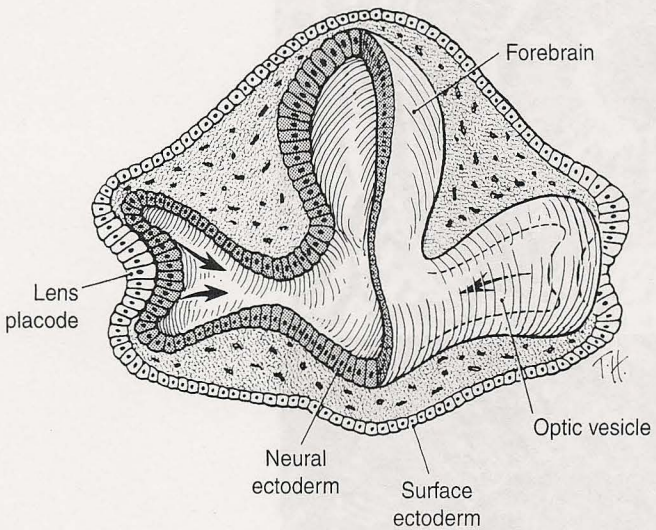

Figure 1.7. Transection showing invaginating lens placode and optic vesicle (*arrows*), thus creating the lens vesicle within the optic cup. Note the orientation of the eyes 180° from each other. (Reprinted with permission from Cook C, Sulik K, Wright K. Embryology. In: Wright KW, ed. *Pediatric Ophthalmology and Strabismus.* St. Louis: Mosby–Year Book, 1995:3–59.)

At birth, the lens consists almost entirely of lens nucleus, with minimal lens cortex. Lens cortex continues to develop from the anterior cuboidal epithelial cells, which remain mitotic throughout life. Differentiation of epithelial cells into secondary lens fibers occurs at the lens equator (i.e., lens bow) (Fig. 1.11B). Lens fiber elongation is accompanied by a corresponding increase in cell volume and a decrease in intercellular space within the lens.[29] The lens fibers exhibit a hexagonal cross-sectional shape and extensive surface interdigitations (Figs. 1.11C, D). The secondary lens fibers course anteriorly and posteriorly around the embryonal nucleus to meet at the Y sutures (Fig. 1.13).

The zonule fibers are termed the *tertiary vitreous,* but their origin remains uncertain. The zonules may form from the developing ciliary epithelium or the endothelium of the posterior tunica vasculosa lentis (TVL). Abnormalities could result in congenital ectopia lentis. Congenitally displaced lenses are often small and abnormally shaped (i.e., spherophakia), indicating a possible relationship between zonule traction and lens shape. Localized absence of zonules may result in a flattened lens equator, often described inaccurately as a lens coloboma.

VASCULAR DEVELOPMENT

The hyaloid artery is the termination of the primitive ophthalmic artery, a branch of the internal ophthalmic artery, and it remains within the optic cup following closure of the optic fissure. The hyaloid artery branches around the posterior lens capsule and continues anteriorly to anastomose with the network of vessels in the pupillary membrane (Figs. 1.14 and 1.15A, B).[30] The pupillary membrane consists of vessels and mesenchyme overlying the anterior lens capsule. This hyaloid vascular network that forms around the lens is called the anterior and posterior TVL. The hyaloid artery and associated TVL provide nutrition to the lens and anterior segment during its period of rapid differentiation. Venous drainage occurs via a network near the equatorial lens, in the area where the ciliary body will eventually develop. There is no discrete hyaloid vein.[30]

Once the ciliary body begins actively producing aqueous humor, which circulates and nourishes the lens, the hyaloid system is no longer needed. The hyaloid vasculature and TVL reach their maximal development by day 45 in the dog and then begin to regress.

As the peripheral hyaloid vasculature regresses, the retinal vessels develop. Vascular endothelial growth factor (VEGF)-A is a potent angiogenic peptide in the retina; antibody neutralization in vivo results in reduction in the hyaloid and retinal vasculature.[31] Spindle-shaped mesenchymal cells from the wall of the hyaloid artery at the optic disc form buds (*angiogenesis*) that invade the nerve fiber layer. In contrast, *vasculogenesis* is the

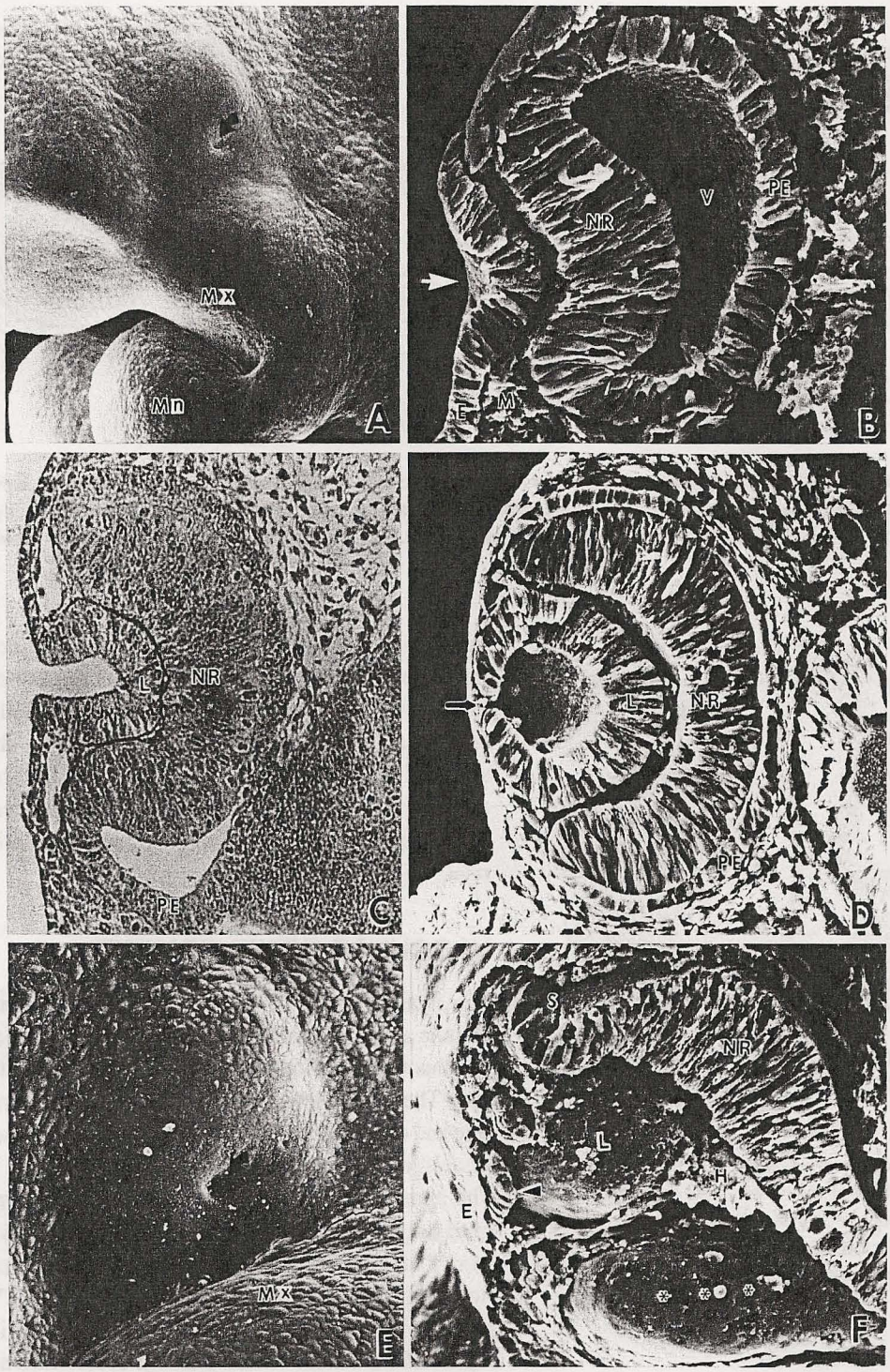

Figure 1.8. **A.** Mouse embryo on day 10 of gestation (29 somite pairs, equivalent to day 17 in the dog). On external examination, the invaginating lens placode can be seen (*arrow*). Note its position relative to the maxillary prominence (*Mx*) and mandibular (*Mn*) prominence of the first visceral arch. **B.** Frontal fracture through the lens placode (*arrow*) illustrates the associated thickening of the surface ectoderm (*E*). Mesenchyme (*M*) of neural crest origin is adjacent to the lens placode. As the precursor to the neural retina (*NR*), the distal portion of the optic vesicle concurrently thickens, whereas the proximal optic vesicle becomes a shorter, cuboidal layer that is the anlage of the retinal pigment epithelium (*PE*). The cavity of the optic vesicle (*V*) becomes progressively smaller. **C.** Light micrograph of the epithelium of the invagination lens placode (*L*). There is an abrupt transition between the thicker epithelium of the placode and the adjacent surface ectoderm, which is not unlike the transition between the future neural retina (*NR*) and pigment epithelium (*PE*). **D.** As the lens vesicle enlarges, the external opening of lens pore (*arrow*) becomes progressively smaller. The lens epithelial cells at the posterior pole of the lens elongate to form the primary lens fibers (*L*). *NR,* anlage of the neural retina; *PE,* anlage of the pigment epithelium (now a short cuboidal layer). **E.** External view of the lens pore (*arrow*) and its relationship to the maxillary prominence (*Mx*). **F.** Frontal fracture reveals the optic fissure (*) where the two sides of the invaginating optic cup meet. This forms an opening in the cup, allowing access to the hyaloid artery (*H*), which ramifies around the invaginating lens vesicle (*L*). The former cavity of the optic vesicle is obliterated except in the marginal sinus (*S*), at the transition between the neural retina (*NR*) and the pigment epithelium. *E,* surface ectoderm. (Reprinted with permission from Cook C. Embryogenesis of congenital eye malformations. *Vet Comp Ophthalmol* 1995;5:109–123.)

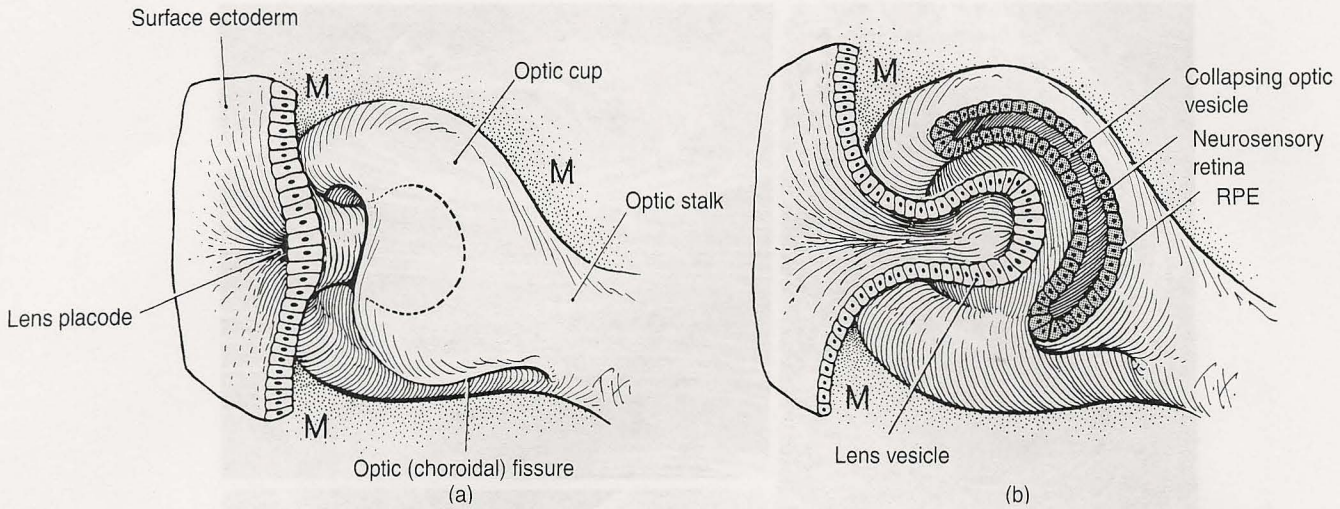

Figure 1.9. Formation of the lens vesicle and optic cup. Note that the optic fissure is present, because the optic cup is not yet fused inferiorly. **A.** Formation of lens vesicle and optic cup with inferior choroidal or optic fissure. Mesenchyme (*M*) surrounds the invaginating lens vesicle. **B.** Surface ectoderm forms the lens vesicle with a hollow interior. Note that the optic cup and optic stalk are of surface ectoderm origin. (Reprinted with permission from Cook C, Sulik K, Wright K. Embryology. In: Wright KW, ed. *Pediatric Ophthalmology and Strabismus.* St. Louis: Mosby–Year Book, 1995:3–59.)

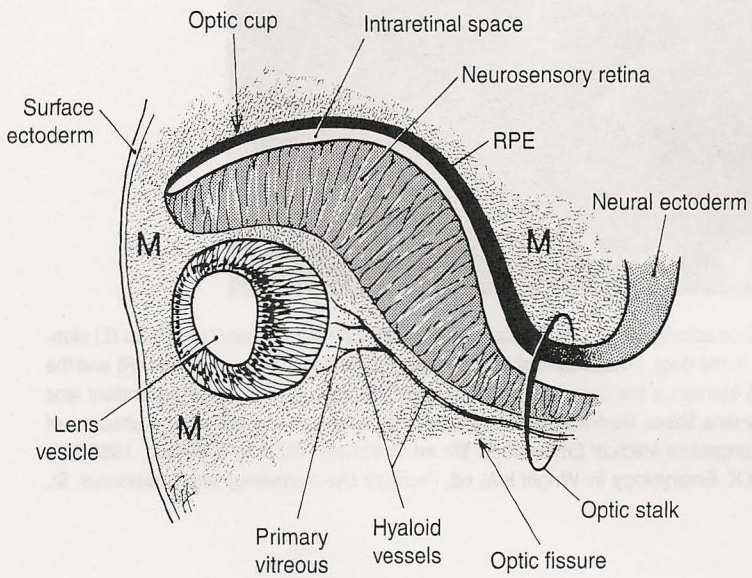

Figure 1.10. Cross-section through optic cup and optic fissure. The lens vesicle is separated from the surface ectoderm. Mesenchyme (*M*) surrounds the developing lens vesicle, and the hyaloid artery is seen within the optic fissure. (Reprinted with permission from Cook C, Sulik K, Wright K. Embryology. In: Wright KW, ed. *Pediatric Ophthalmology and Strabismus.* St. Louis: Mosby–Year Book, 1995:3–59.)

assembly of dispersed angioblasts into solid cords of mesenchymal cells that later canalize.[32,33] Controversy exists as to whether the process of retinal neovascularization occurs primarily through angiogenesis or vasculogenesis.[32–34] Recent studies indicate that spindle-shaped cells dispersed within the retina, previously thought to be angioblasts, may be immature retinal astrocytes, with retinal vascularization occurring primarily through angiogenesis.[32] The primitive capillaries have laminated walls consisting of mitotically active cells secreting basement membrane. Those cells in direct contact with the bloodstream differentiate into endothelial cells; the outer cells become pericytes. Zonulae occludens and gap junctions initially join adjacent cells, but later, the capillary endothelium is continuous.[35,36] The primitive capillary endothelial cells are multipotent and can redifferentiate into fibroblastic, endothelial, or muscle cells, possibly illustrating a common origin for these different tissue types.[36]

Branches of the hyaloid artery become sporadically occluded by macrophages prior to their gradual atrophy.[37] Placental growth factor (PlGF) and VEGF appear to be involved in hyaloid regression.[31,38] Proximal arteriolar vasoconstriction at birth precedes regression of the major hyaloid vasculature.[39] Atrophy of the pupillary membrane, TVL, and hyaloid artery occurs initially through apoptosis[40] and later through cellular necrosis[41] and is usually complete by the time of eyelid opening 14 days postnatally.

The clinical lens anomaly known as Mittendorf's dot is a small (1–2 mm) area of fibrosis on the posterior lens capsule, and it is a manifestation of incomplete regression of the hyaloid artery where it was attached to the posterior lens capsule. Bergmeister's papilla represents a remnant of the hyaloid vasculature consisting of a small, fibrous glial tuft of tissue emanating from the center of the optic nerve. Both are frequently observed as incidental clinical findings.

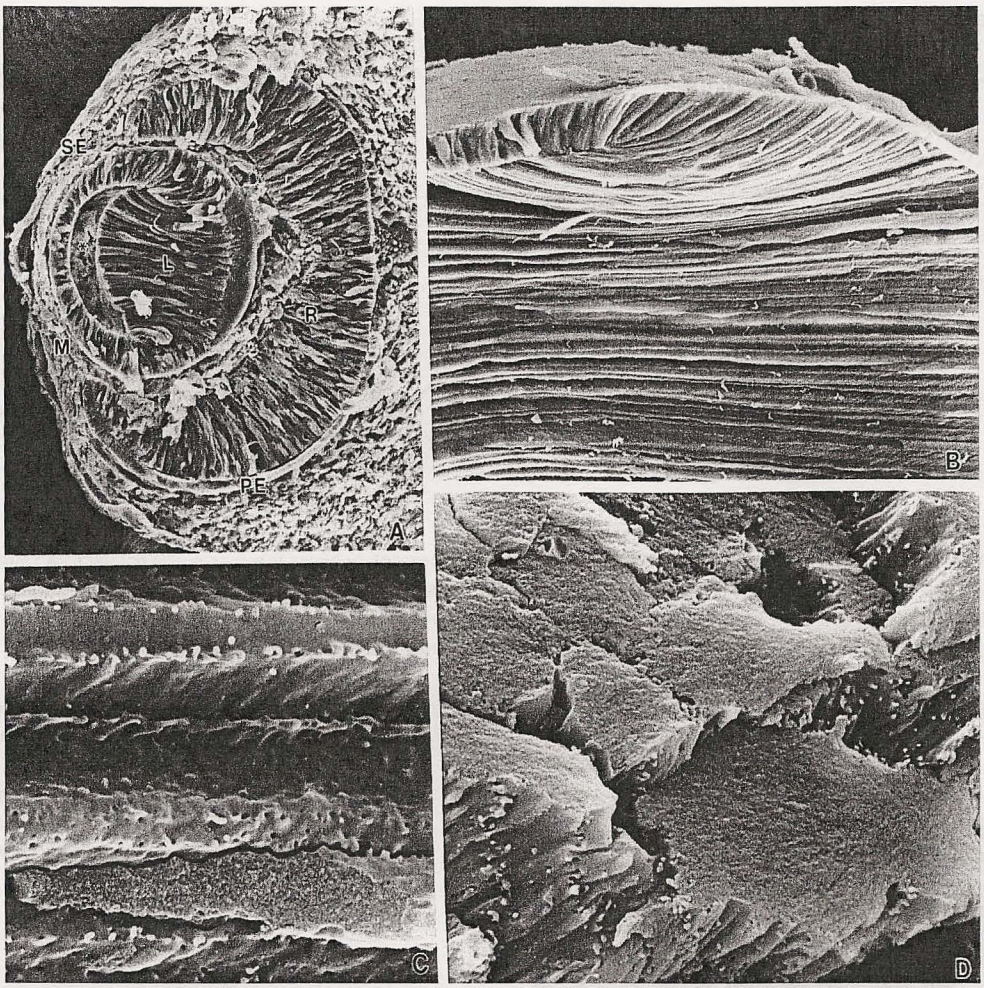

Figure 1.11. **A.** Following detachment of the lens vesicle from the surface ectoderm (*SE*), the posterior lens epithelial cells–primary lens fibers (*L*) elongate, obliterating the lens vesicle lumen (equivalent to day 29 of gestation in the dog). Invagination of the optic cup forms the inner neural retina (*R*) and the outer pigmented epithelium (*PE*). Mesenchyme of neural crest origin (*M*) surrounds the optic cup. **B.** Lens bow illustrating elongation of secondary lens fibers. **C** and **D.** Longitudinal view (**C**) and cross-section (**D**) of secondary lens fibers, illustrating the extensive interdigitations and the relative absence of extracellular space. (Part A reprinted with permission from Sadler TW. *Langman's Medical Embryology.* 5th ed. Baltimore: Williams & Wilkins, 1985:322. Parts B, C, and D reprinted with permission from Cook C, Sulik K, Wright K. Embryology. In: Wright KW, ed. *Pediatric Ophthalmology and Strabismus.* St. Louis: Mosby–Year Book, 1995:3–59.)

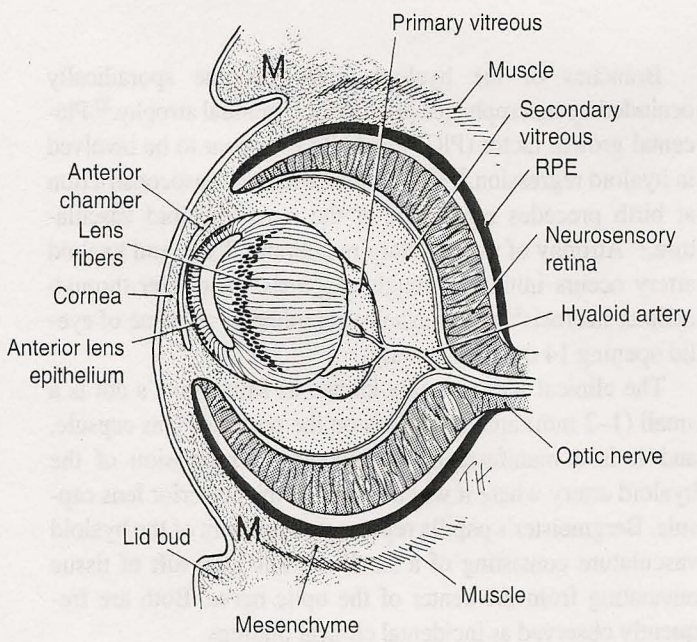

Figure 1.12. Overview of the developing eye surrounded by mesenchyme (*M*), which is mostly of neural crest origin. The hyaloid vasculature enters the optic cup through the optic fissure and surrounds the lens with capillaries that anastomose with the TVL. Axial migration of mesenchyme forms the corneal stroma and endothelium. (Reprinted with permission from Cook C, Sulik K, Wright K. Embryology. In: Wright KW, ed. *Pediatric Ophthalmology and Strabismus.* St. Louis: Mosby–Year Book, 1995:3–59.)

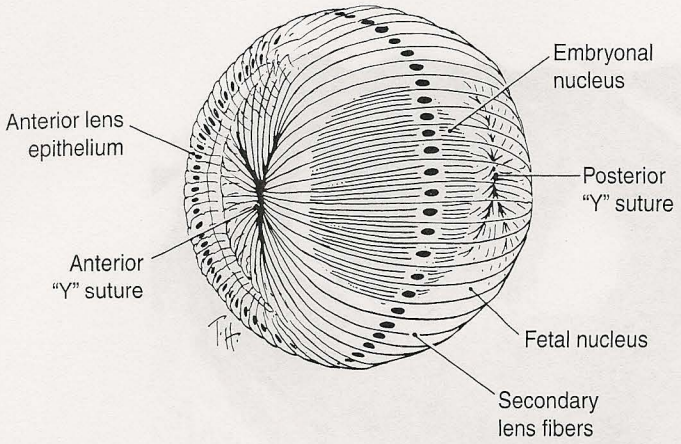

Figure 1.13. Secondary lens fibers and Y sutures. Secondary lens fibers elongate at the equator to span the entire lens, from the anterior to the posterior Y suture. The anterior Y suture is upright; the posterior Y suture is inverted. (Reprinted with permission from Cook C, Sulik K, Wright K. Embryology. In: Wright KW, ed. *Pediatric Ophthalmology and Strabismus.* St. Louis: Mosby–Year Book, 1995:3–59.)

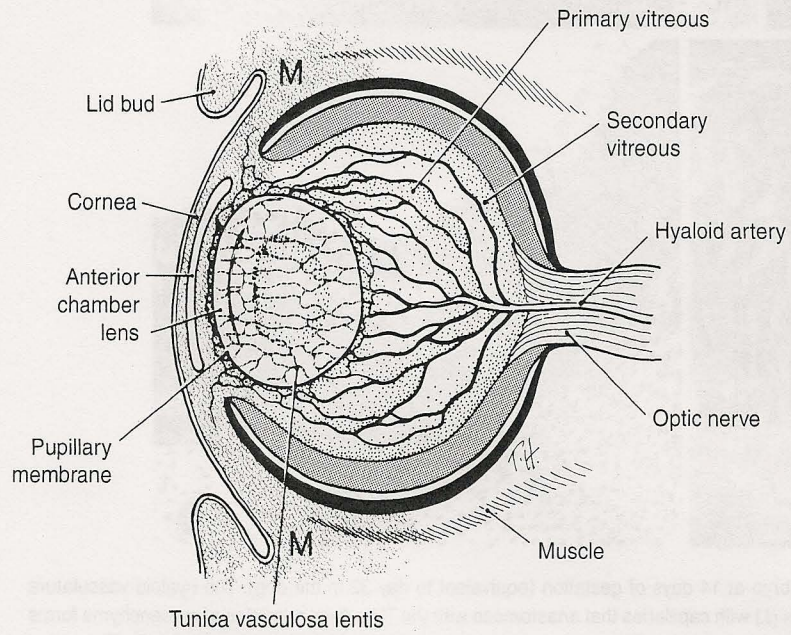

Figure 1.14. The hyaloid vascular system and TVL. (Reprinted with permission from Cook C, Sulik K, Wright K. Embryology. In: Wright KW, ed. *Pediatric Ophthalmology and Strabismus.* St. Louis: Mosby–Year Book, 1995:3–59.)

DEVELOPMENT OF THE CORNEA AND ANTERIOR CHAMBER

The anterior margins of the optic cup advance beneath the surface ectoderm and adjacent neural crest mesenchyme after lens vesicle detachment (day 25 in the dog). The surface ectoderm overlying the optic cup (i.e., the presumptive corneal epithelium) secretes a thick matrix, the primary stroma.[42,43] This acellular material consists of collagen fibrils and glycosaminoglycans. Mesenchymal neural crest cells migrate between the surface ectoderm and the optic cup, using the basal lamina of the lens vesicle as a substrate . Proteolysis of collagen IX triggers hydration of the hyaluronic acid, creating the space for cellular migration.[44] Initially, this loosely arranged mesenchyme fills the future anterior chamber, and it gives rise to the corneal endothelium and stroma, anterior iris stroma, ciliary muscle, and most structures of the iridocorneal angle (Fig. 1.16A). The presence of an adjacent lens vesicle is required for induction of corneal endothelium, identified by their production of the cell adhesion molecule n-cadherin.[45] Type I collagen fibrils and fibronectin secreted by the developing keratocytes form the secondary corneal stroma. Subsequent dehydration results in much of the fibronectin being lost and in a 50% reduction in stromal thickness.[6,46] The endothelium also is important to the dehydration of the stroma. Patches of endothelium become confluent and develop zonulae occludens during days 30 to 35 in the dog, and during this period, Descemet's membrane also forms. The cornea achieves relative transparency at the end of gestation in the dog. Following eyelid opening at approximately 14 days postnatal in the dog, there is an initial decrease in corneal thickness over 4 weeks, presumably as the corneal endothelium becomes functional. Then, a gradual increase in thickness occurs over the next 6 months.[47]

Neural crest migration anterior to the lens to form the corneal stroma and iris stroma also results in formation of a solid sheet of mesenchymal tissue, which ultimately remodels to form the anterior chamber. The portion of this sheet that bridges the future pupil is called the pupillary membrane (Figs. 1.16B, C, D). Vessels within the pupillary membrane form the TVL, which surrounds and nourishes the lens. These vessels are continuous with those of the primary vitreous (i.e., hyaloid). The vascular endothelium is the only intraocular tissue of mesodermal origin; even the vascular smooth muscle cells and pericytes that originate from mesoderm in the rest of the body are of neural crest origin.[9,48] In humans, the endothelial lining

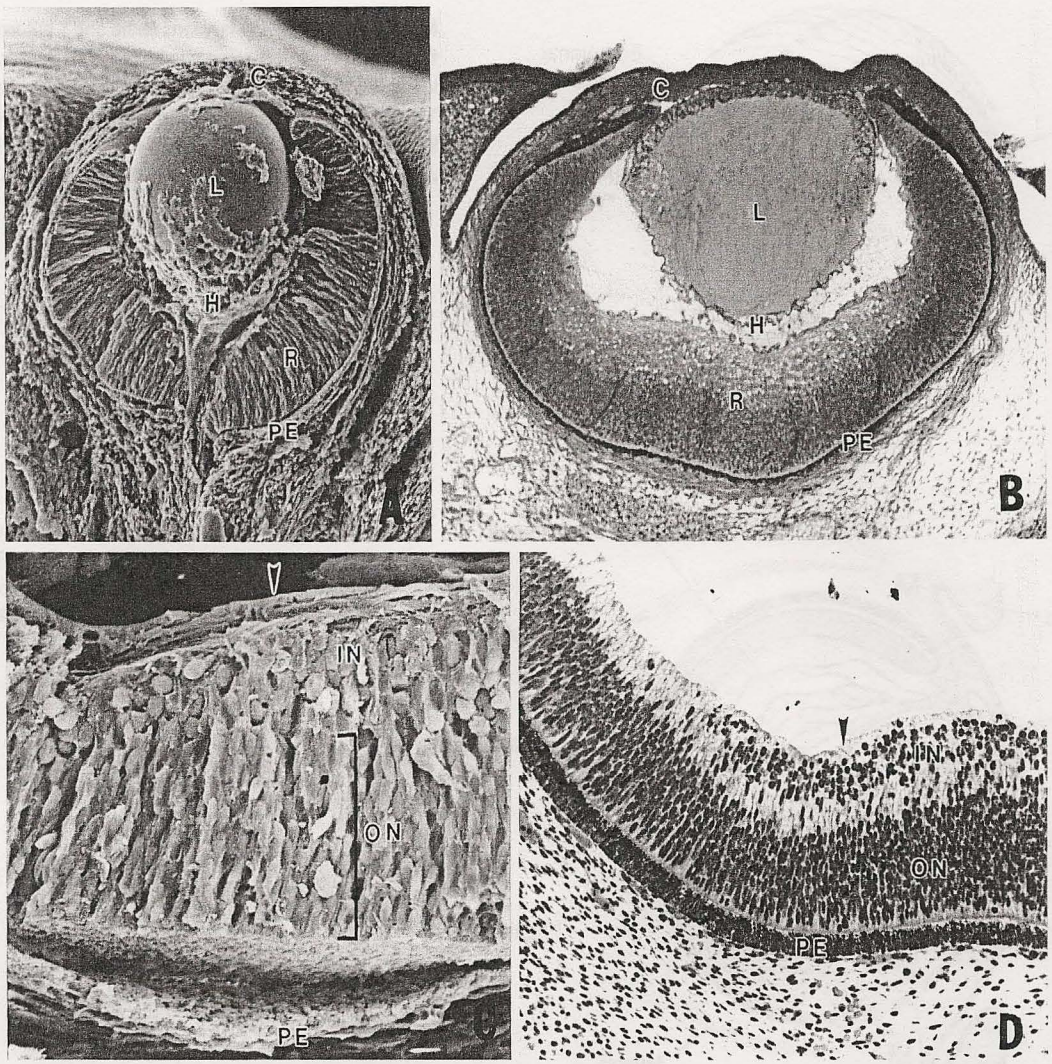

Figure 1.15. **A.** Scanning electron micrograph of a mouse embryo at 14 days of gestation (equivalent to day 32 in the dog). The hyaloid vasculature enters the optic cup through the optic stalk, and it surrounds the lens (*L*) with capillaries that anastomose with the TVL. Axial migration of mesenchyme forms the corneal stroma and endothelium (*C*). The retina (*R*) is becoming stratified, whereas the pigment epithelium (*PE*) remains cuboidal. **B.** The retina becomes stratified into an inner marginal zone and an outer nuclear zone. Note that the inner marginal zone is most prominent in the posterior pole. *C,* cornea; *H,* hyaloid artery; *L,* lens; *R,* retina; *PE,* pigment epithelium. **C.** Segregation of the retina into inner (IN) and outer (ON) neuroblastic layers. The ganglion cells are the first to differentiate, giving rise to the nerve fiber layer (*arrowhead*). The pigment epithelium (*PE*) has become artifactually separated in this specimen. **D.** Differentiation of the retina progresses from the central to the peripheral regions. Centrally, the inner (*IN*) and outer (*ON*) neuroblastic layers are apparent, with early formation of the nerve fiber layer (*arrowhead*). Peripherally, however, the retina consists of a single nuclear zone. Between the inner and outer neuroblastic layers is a clear zone, the transient fiber layer of Chievitz. This stage is equivalent to day 32 in the dog. *PE,* pigment epithelium. (Part A reprinted with permission from Sulik KK, Schoenwold GC. Highlights of craniofacial morphogenesis in mammalian embryos, as revealed by scanning electron microscopy. *Scan Electron Microscopy* 1985;4:1735–1752. Parts B, C, and D reprinted with permission from Cook C, Sulik K, Wright K. Embryology. In: Wright KW, ed. *Pediatric Ophthalmology and Strabismus.* St. Louis: Mosby–Year Book, 1995:3–59.)

of Schlemm's canal, like the vascular endothelium elsewhere, is of mesodermal origin. In the dog, atrophy of the pupillary membrane begins by day 45 of gestation and continues during the first 2 postnatal weeks.[49] Separation of the corneal mesenchyme (neural crest–cell origin) from the lens (surface ectoderm origin) results in formation of the anterior chamber.

In a microphthalmic or nanophthalmic globe, the cornea is correspondingly reduced in diameter. The term *microcornea* is used to describe a cornea that is proportionally smaller than normal for the size of the globe. As with lens induction, determination of the corneal diameter occurs at the time of contact by the optic vesicle with the surface ectoderm. This induction is also sensitive to timing; if the optic vesicle–ectoderm contact occurs earlier or later than normal, the ectoderm may not be fully capable of responding appropriately, resulting in microcornea.

DEVELOPMENT OF THE IRIS, CILIARY BODY, AND IRIDOCORNEAL ANGLE

The two layers of the optic cup (neuroectoderm origin) consist of an inner, nonpigmented layer and an outer, pigmented layer. Both the pigmented and nonpigmented epithelium of the iris and the ciliary body develop from the anterior aspect of the optic cup; the retina develops from the posterior optic cup. The optic vesicle is organized with all cell apices directed to

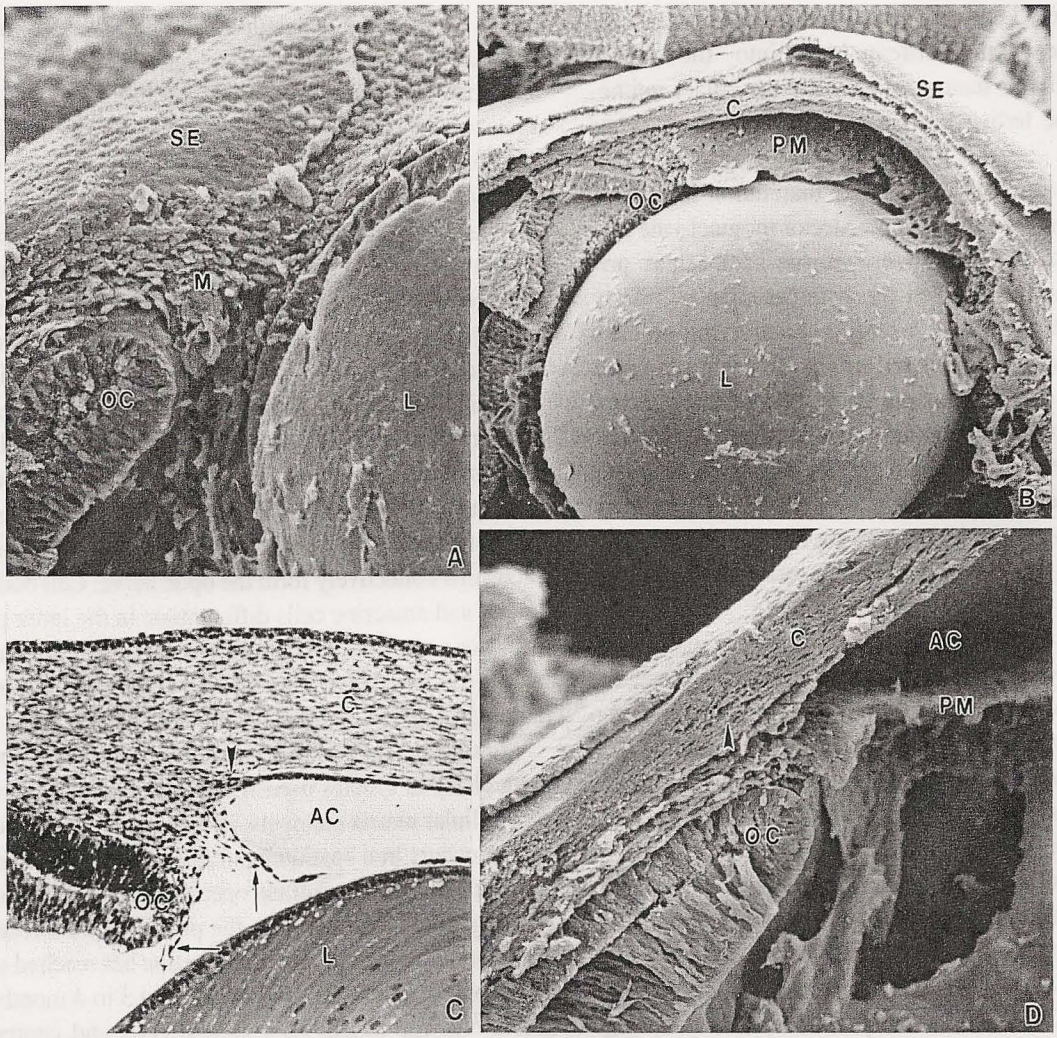

Figure 1.16. **A.** Scanning electron micrograph of a fetal human eye at approximately 42 days of gestation (equivalent to day 25 in the dog). The lens vesicle (*L*) has detached, and the neural crest–derived mesenchyme (*M*) is migrating axially between the optic cup (*OC*) and the surface ectoderm (*SE*). **B.** On day 54 in the human (day 32 in the dog), the pupillary membrane (*PM*) is seen within the anterior chamber. The corneal stroma (*C*) is apparent and is covered by the surface ectoderm (*SE*), which will become the corneal epithelium. *OC,* anterior margin of the optic cup, which will form the posterior epithelial layers of the iris, including the pupillary muscles. **C.** Light micrograph obtained at the same stage as in **B** illustrates the pupillary membrane and TVL (*arrows*) originating from the mesenchyme at the margin of the optic cup (*OP*). The limbal condensation that will become the scleral spur is indicated by the *arrowhead. AC,* anterior chamber; *C,* cornea; *L,* lens. **D.** Scanning electron micrograph of a fetal human eye at approximately 63 days of gestation. The anterior chamber (*AC*) is deeper and still bridged by the pupillary membrane (*PM*). Endothelialization of clefts within the neural crest–derived corneal stroma (*C*) by mesoderm will form Schlemm's canal (*arrowhead*) in the human eye. (Part A and D reprinted with permission from Cook C. Experimental models of anterior segment dysgenesis. *Ophthalmic Paediatr Genet* 1989;10:33–46. Parts A–D reprinted with permission from Cook C, Sulik K, Wright K. Embryology. In: Wright KW, ed. *Pediatric Ophthalmology and Strabismus.* St. Louis: Mosby–Year Book, 1995:3–59.)

the center of the vesicle. During optic cup invagination, the apices of the inner and outer epithelial layers become adjacent. Thus, the cells of the optic cup are oriented apex to apex.

A thin, periodic acid-Schiff–positive basal lamina lines the inner aspect (i.e., vitreous side) of the nonpigmented epithelium and retina (i.e., inner limiting membrane). By approximately day 40 of gestation in the dog, both the pigmented and nonpigmented epithelial cells show apical cilia that project into the intercellular space. There also is increased prominence of Golgi complexes and associated vesicles within the ciliary epithelial cells. These changes, as well as the presence of "ciliary channels" between the apical surfaces, probably represent the first production of aqueous humor.

The iris stroma develops from the anterior segment mesenchymal tissue (neural crest cell origin), and the iris pigmented and nonpigmented epithelium originate from the neural ectoderm of the optic cup. The smooth muscle of the pupillary sphincter and dilator muscles ultimately differentiate from these epithelial layers, and they represent the only mammalian muscles of neural ectodermal origin. In avian species, however, the skeletal muscle cells in the iris are of neural crest origin, with a possible small contribution of mesoderm to the ventral portion.[50–52]

Differential growth of the optic cup epithelial layers results in folding of the inner layer, representing early, anterior ciliary processes (Fig. 1.16B). The ciliary body epithelium develops

from the neuroectoderm of the anterior optic cup, and the underlying mesenchyme differentiates into the ciliary muscles. Extracellular matrix secreted by the ciliary epithelium becomes the tertiary vitreous and ultimately develops into lens zonules.

Three phases of iridocorneal angle maturation have been described.[53,54] First is separation of anterior mesenchyme into corneoscleral and iridociliary regions (i.e., trabecular primordium formation), followed by differentiation of ciliary muscle and folding of the neural ectoderm into ciliary processes. Second is enlargement of the corneal trabeculae and development of clefts in the area of the trabecular meshwork, which is accompanied by regression of the corneal endothelium covering the angle recess. Third is postnatal remodeling of the drainage angle, associated with cellular necrosis and phagocytosis by macrophages, resulting in opening of clefts in the trabecular meshwork and outflow pathways.

This change in the relationship of the trabecular meshwork to the ciliary body and iris root during the last trimester of human gestation occurs through differential growth with posterior movement of the iris and the ciliary body relative to the trabecular meshwork exposing the outflow pathways. This results in progressive deepening of the chamber angle and normal conformation of the ciliary muscle and ciliary processes.[55] This is in contrast to previous theories of cleavage of the iris root from the cornea or atrophy of angle tissue.[48,56,57] Posterior movement of the iris and ciliary body results in exposure of the trabecular meshwork.[55]

In species born with congenitally fused eyelids (i.e., dog and cat), development of the anterior chamber continues during this postnatal period before eyelid opening. At birth, the peripheral iris and cornea are in contact. Pectinate ligaments mature by 3 weeks, and rarefaction of the uveal and corneoscleral trabecular meshworks to their adult state occurs during the first 8 weeks after birth. There was no evidence of mesenchymal splitting, cell death, or phagocytic activity.[58,59]

RETINA AND OPTIC NERVE DEVELOPMENT

Infolding of the neuroectodermal optic vesicle results in a bilayered optic cup with the apices of these two cell layers in direct contact. Primitive optic vesicle cells are columnar, but by 20 days of gestation in the dog, they form a cuboidal layer containing the first melanin granules in the developing embryo. The neurosensory retina develops from the inner, nonpigmented layer of the optic cup and the retinal pigment epithelium (RPE) originates from the outer, pigmented layer. Bruch's membrane (the basal lamina of the RPE) is first seen during this time and becomes well developed over the next week, when the choriocapillaris is developing. By day 45, the RPE cells take on a hexagonal cross-sectional shape and develop microvilli that interdigitate with projections from photoreceptors of the nonpigmented (inner) layer of the optic cup.

At the time of lens placode induction, the retinal primordium consists of an outer, nuclear zone and an inner, marginal (anuclear) zone. Cell proliferation occurs in the nuclear zone, with migration of cells into the marginal zone. This process forms the inner and outer neuroblastic layers, separated by their cell processes that make up the transient fiber layer of Chievitz (Figs. 1.15C, D). Cellular differentiation progresses from inner to outer layers and, regionally, from central to peripheral locations. Peripheral retinal differentiation may lag behind that occurring in the central retina by 3 to 8 days in the dog.[49] Retinal histiogenesis beyond formation of the neuroblastic layers requires induction by a differentiated RPE. There are several rodent models of RPE dysplasia resulting in failure of later retinal differentiation and subsequent degeneration.[60,61] Retinal ganglion cells develop first within the inner neuroblastic layer, and axons of the ganglion cells collectively form the optic nerve. Cell bodies of the Müller and amacrine cells differentiate in the inner portion of the outer neuroblastic layer. Horizontal cells are found in the middle of this layer; the bipolar cells and photoreceptors mature last, in the outermost zone of the retina.[62–65]

Significant retinal differentiation continues postnatally, particularly in species born with fused eyelids. Expression of extracellular matrix elements, chondroitin sulfate, and heparin sulfate occurs in a spatiotemporally regulated manner, with a peak of chondroitin sulfate occurring at the time of eyelid opening. This corresponds to the period of photoreceptor differentiation.[66] At birth, the canine retina has reached a stage of development equivalent to the human at 3 to 4 months of gestation.[67] In the kitten, all ganglion cells and central retinal cells are present at birth with continued proliferation in the peripheral retina continuing during the first 2 to 3 postnatal weeks in dogs and cats.[67,68]

Possibilities for retinal regeneration have recently become reality with the discovery of neural stem cells in the mature eye of warm-blooded vertebrates.[69,70] These include cells at the retinal margin, pigmented cells in the ciliary body and iris, nonpigmented cells in the ciliary body, and Müller glia within the retina. Under the influence of growth factors, these neuroectodermal cells in the avian are capable of undergoing differentiation into retinal cells.[70]

SCLERA, CHOROID, AND TAPETUM

These neural crest–derived tissues are all induced by the outer layer of the optic cup (future RPE). Normal RPE differentiation is a prerequisite for normal development of the sclera and choroid. The choroid and sclera are relatively differentiated at birth, but the tapetum in dogs and cats continues to develop and mature during the first 4 months postnatally. The initially mottled, blue appearance of the immature tapetum is replaced by the bluish green to yellowish orange color of the adult. These color variations seen in immature dogs can prove a challenge to accurate funduscopic assessment.

Posterior segment uveoscleral colobomas most often result from a primary RPE abnormality. Subalbinotic animals have a

higher incidence of posterior segment colobomas with reduced RPE pigmentation being a marker for abnormal RPE development.[71] The most common example is the choroidal hypoplasia of collie eye anomaly.[72]

VITREOUS

The primary vitreous forms posteriorly between the primitive lens and the inner layer of the optic cup (Figs. 1.10 and 1.12). In addition to the vessels of the hyaloid system, the primary vitreous also contains mesenchymal cells, collagenous fibrillar material, and macrophages. The secondary vitreous forms as the fetal fissure closes, and it contains a matrix of cellular and fibrillar material, including primitive hyalocytes, monocytes, and hyaluronic acid.[73,74] Identification of microscopic vascular remnants throughout the vitreous in the vitreous of adult rabbits has led to speculation for interactive remodeling of the primary vitreous to form secondary vitreous.[75,76] Plasma proteins enter and leave the vitreous, and in the chick, there is a concentration of 13% of that found in plasma until a decline to 4% of plasma levels occurs during the last week prior to hatching.[17] Primitive hyalocytes produce collagen fibrils that expand the volume of the secondary vitreous.

The tertiary vitreous forms as a thick accumulation of collagen fibers between the lens equator and the optic cup. These fibers are called the marginal bundle of Drualt, or Drualt's bundle. Drualt's bundle has a strong attachment to the inner layer of the optic cup, and it is the precursor to the vitreous base and lens zonules. The early lens zonular fibers appear to be continuous with the inner, limiting membrane of the nonpigmented epithelial layer covering the ciliary muscle. Elastin and emulin (protein located at the elastin–microfibril interface) have been identified in developing zonules and Descemet's membrane.[77,78] Experimental exposure of chick embryos to homocysteine results in deficient zonule development and congenital lens luxation.[79]

Atrophy of the primary vitreous and hyaloid leaves a clear, narrow central zone, which is called Cloquet's canal. In the mouse, Doppler ultrasound biomicroscopy has been used to document in vivo the decrease in blood velocity associated with hyaloid regression between birth and postnatal day 13.[80] Most of the posterior vitreous gel at birth is secondary vitreous, with the vitreous base and zonules representing tertiary vitreous.

OPTIC NERVE

Axons from the developing ganglion cells pass through vacuolated cells from the inner wall of the optic stalk. A glial sheath forms around the hyaloid artery. As the hyaloid artery regresses, the space between the hyaloid artery and the glial sheath enlarges. Bergmeister's papilla represents a remnant of these glial cells around the hyaloid artery. Glial cells migrate into the optic nerve and form the primitive optic disc. The glial cells around the optic nerve and the glial part of the lamina cribrosa come from the inner layer of the optic stalk, which is of neural ectoderm origin. Later, a mesenchymal (neural crest origin) portion of the lamina cribrosa develops. Myelinization of the optic nerve begins at the chiasm, progresses toward the eye, and reaches the optic disc after birth.

EYELIDS

The eyelids develop from surface ectoderm, which gives rise to the epidermis, cilia, and conjunctival epithelium. Neural crest mesenchyme gives rise to deeper structures, including the dermis and tarsus. The eyelid muscles (i.e., orbicularis and levator) are derived from craniofacial condensations of mesoderm called somitomeres. In the craniofacial region, presumptive connective tissue–forming mesenchyme derived from the neural crest imparts spatial patterning information upon myogenic cells that invade it.[81] The upper eyelid develops from the frontonasal process; the lower eyelid develops from the maxillary process. The lid folds grow together and elongate to cover the developing eye (Fig. 1.17). The upper and lower lids fuse on day 32 of gestation in the dog. Separation occurs 2 weeks postnatally.

EXTRAOCULAR MUSCLES

The extraocular muscles arise from mesoderm in somitomeres (i.e., preoptic mesodermal condensations).[82–89] Spatial organization of developing eye muscles is initiated before they interact with the neural crest mesenchyme. Patterning of the segmental somitomeres follows that of the neural crest: somitomere I (forebrain), somitomere III (caudal midbrain), somitomeres IV and VI (hindbrain).[89] From studies of chick embryos, it has been shown that the oculomotor-innervated muscles originate from the first and second somitomeres, the superior oblique muscle from the third somitomere, and the lateral rectus muscle from the fourth somitomere.[90] The entire length of these muscles appears to develop spontaneously rather than from the orbital apex anteriorly, as had been previously postulated.[91,92] Congenital abnormalities are rarely identified and reported in the dog[93]; this may be a result of several factors, including that the extraocular muscles are normally less well developed in domestic mammals compared with man and our limited ability to assess minor abnormalities that would be manifest as impaired binocular vision.

DEVELOPMENTAL OCULAR ANOMALIES

Cyclopia and Synophthalmia

Formation of a single median globe (i.e., cyclopia) or two incompletely separated or fused globes (i.e., synophthalmia) may occur by two different mechanisms. The "fate maps," which have been produced for amphibian embryos, have revealed the original location of the neural ectodermal tissue that will form the globes as a single, bilobed area crossing the midline in the anterior third of the trilaminar embryonic disc. An early defect in separation of this single field could result in the formation of one or more median globes. After separation

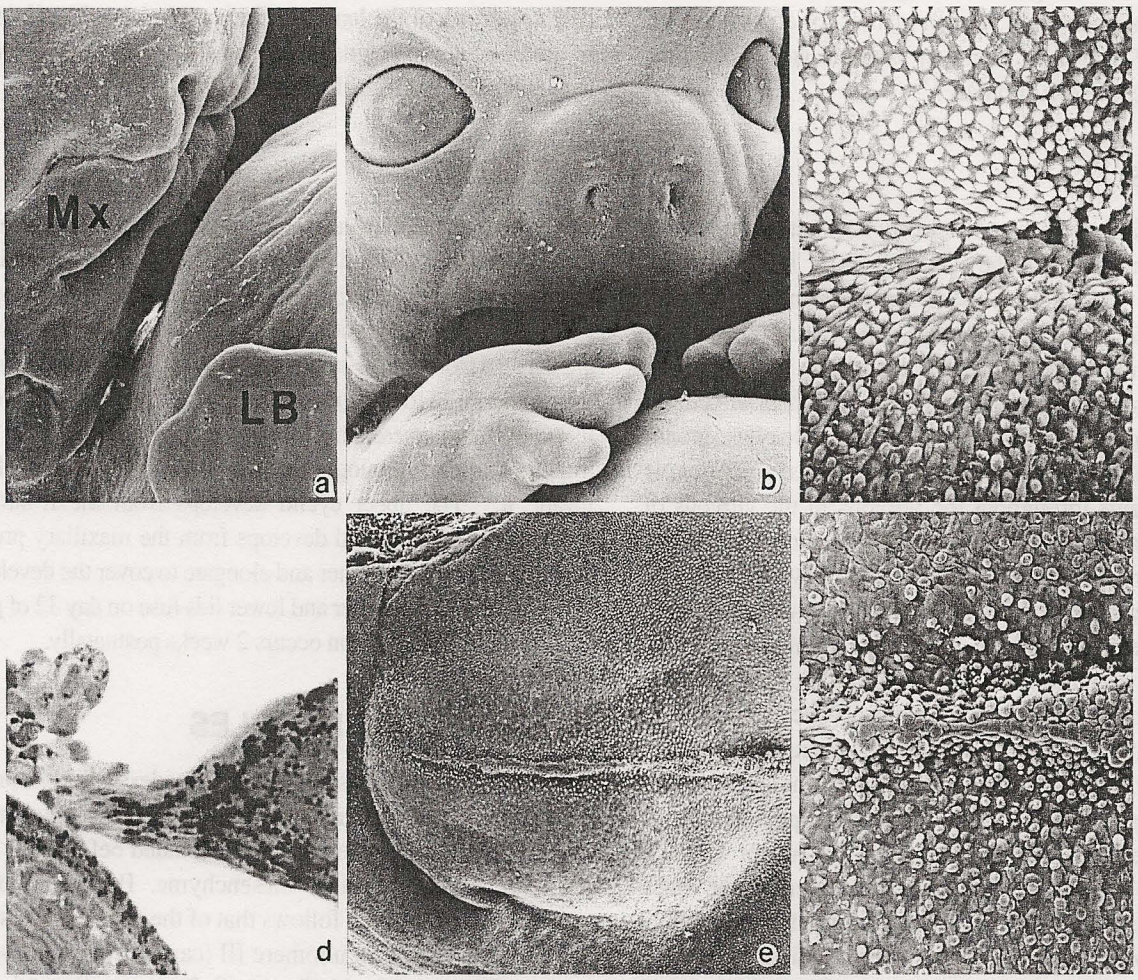

Figure 1.17. **A.** Lateral view of the head of a human embryo at 6 weeks of gestation. The individual hillocks that will form the external ear can be identified both cranial and caudal to the first visceral groove (*arrow*). The developing eye is adjacent to the maxillary prominence (*Mx*). *LB,* forelimb bud. **B.** Frontal view of the head of a human embryo at 8 weeks of gestation. Formation of the face is largely complete, and the eyelids are beginning to close. **C.** Eyelid closure begins at the medial and lateral canthi and progresses axially. **D.** Light micrograph of the eyelid marginal epithelium in a mouse at day 15 of gestation. The actively migrating epithelium forms a cluster of cells adjacent to the corneal epithelium. **E** and **F.** Surface view of the fused eyelids from a human embryo at 10 weeks of gestation. (Parts A, B, E, and F reprinted with permission from Sulik KK, Schoenwolf GC. Highlights of craniofacial morphogenesis in mammalian embryos, as revealed by scanning electron microscopy. *Scan Electron Microscopy* 1985;4:1735–1752. Part D reprinted with permission from Cook CS, Sulik KK. Sequential scanning electron microscopic analyses of normal and spontaneously occurring abnormal ocular development in C57B1/6J mice. *Scan Electron Microscopy* 1986;3:1215–1227.)

Figure 1.18. Synophthalmos in a Holstein calf, etiology unknown. Note the single median globe, palpebral fissure, cornea, and pupil. (Courtesy of Dr. B. Wilcock.)

into bilateral optic vesicles, later loss of the midline territory in the embryo could result in fusion of the ocular fields. This loss of midline territory is seen in holoprosencephaly, and the facial features characteristic of human fetal alcohol syndrome represent a mild end of the holoprosencephalic spectrum.[94,95] Cases of cyclopia or synophthalmos are invariably associated with severe craniofacial malformations (Fig. 1.18).

Cyclopia is rarely identified in dogs.[96] However, in sheep, ingestion of the alkaloids cyclopamine and jervine from the weed *Veratrum californicum* by pregnant ewes on day 14 of gestation (total duration of gestation, 150 days) is the best-documented example of teratogen-induced cyclopia and synophthalmia in domestic animals.[97–103] It has been shown that cyclopamine specifically blocks the Sonic hedgehog (Shh) signaling pathway.[100,101,104] The specific timing for *Veratrum*-induced cyclopia in sheep corresponds to the period of gastrulation and formation of the neural plate before separation of the optic fields. Exposure to the alkaloid earlier in gestation results in fetal death; later

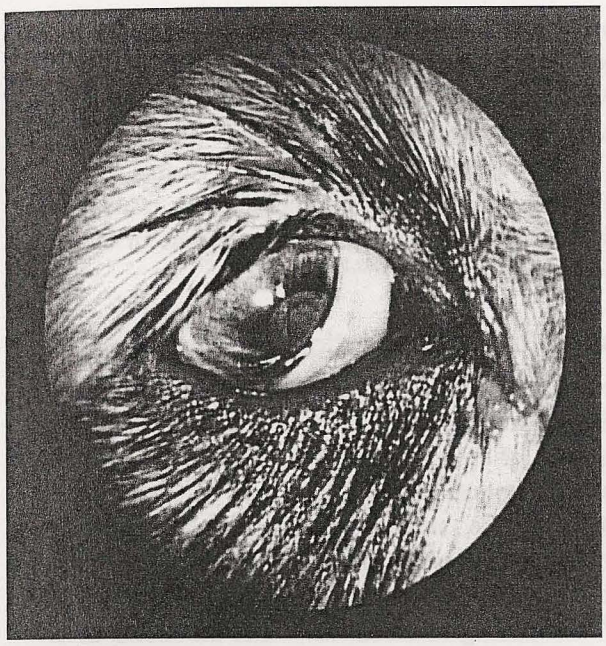

Figure 1.19. Microphthalmia and persistent pupillary membranes in a Chow Chow puppy. Note that the size of the palpebral fissure is proportional to the reduced size of the globe as a whole. This is consistent with microphthalmia induced at the optic vesicle stage.

exposure causes skeletal malformation or has no effect, thus demonstrating the importance of narrow, sensitive periods in development.

Microphthalmia and Anophthalmia

Microphthalmia may occur early in development through a deficiency in the optic vesicle or later through failure of normal growth and expansion of the optic cup (Fig. 1.19). A deficiency in the size of the globe as a whole is often associated with a correspondingly small, palpebral fissure. The fissure size is determined by the optic vesicle size during its contact with the surface ectoderm, so this supports a malformation sequence beginning at formation of the optic sulcus, optic vesicle, or earlier. Results from studies of teratogen-induced ocular malformations have been helpful in identifying sensitive developmental periods. Acute exposure to teratogens before optic sulcus formation results in an overall deficiency of the neural plate, with subsequent reduction in the optic vesicle size. When microphthalmia originates during development of the neural plate/optic sulcus, it is often associated with multiple ocular malformations, including anterior segment dysgenesis, cataract, retinal dysplasia, and persistence of the hyaloid.

Later initiation of microphthalmia can occur through failure to establish early intraocular pressure.[105,106] Placement of a capillary tube into the vitreous cavity of the embryonic chick eye reduces the IOP and markedly slows growth of the eye.[107] Histologic examination of the intubated eyes demonstrates a proportional reduction in the size of all ocular tissues except the neural retina and the lens, which are normal in size for the age of the eye. The retina in these eyes is highly convoluted, filling the small posterior segment. Thus, it has been concluded that growth of the neural retina occurs independent of the other ocular tissues. Experimental removal of the lens does not alter retinal growth.[108] Growth of the choroid and sclera appear to depend on IOP, as does folding of the ciliary epithelium.[109] Thus, failure of fusion of the optic fissure can result in microphthalmia and associated malformations (i.e., colobomatous microphthalmia). A delay in closure of this fissure during a critical growth period may result in inadequate globe expansion as well. If the fissure eventually closes, however, it may be difficult to distinguish between colobomatous and noncolobomatous microphthalmia. If the optic vesicle develops normally before abnormal (delayed) closure of the optic fissure, the palpebral fissure may not be reduced in size as much as the globe as a whole is reduced (Fig. 1.20). In most cases, microphthalmia occurs through a combination of cellular deficiency within the optic vesicle/cup compounded by failure of the optic fissure to close on schedule.[2,25,110]

Anophthalmos represents an extreme in the spectrum of microphthalmos. In most cases, careful examination of the orbital contents will reveal primitive ocular tissue (i.e., actual microphthalmos). True anophthalmos results from a severe developmental deficiency in the primitive forebrain, at a stage before optic sulcus formation. This usually results in a nonviable fetus.

Microphthalmos in domestic animals occurs sporadically and is associated with multiple malformations (Table 1.3), including anterior segment dysgenesis,[111–115] cataract,[116–120] persistent hyperplastic primary vitreous,[121–124] and retinal dysplasia.[113,116,121,123,125] In the Doberman pinscher, microphthalmia, anterior segment dysgenesis, and retinal dysplasia are thought to be inherited as autosomal recessive traits.[11] Inherited microphthalmia in Texas sheep has as its primary event abnormal development with involution of the lens vesicle

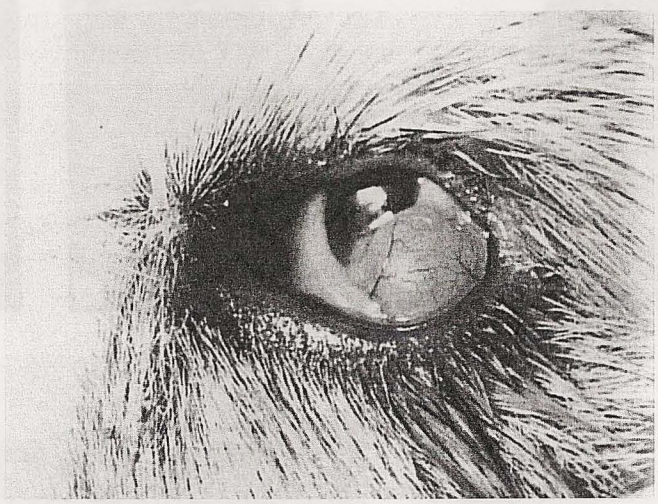

Figure 1.20. Microphthalmia and an inferior coloboma of the scleral and uveal tissue allowing vitreous prolapse into the subconjunctival space. Note the relatively larger, palpebral fissure than that seen in Fig. 1.19, which is consistent with colobomatous microphthalmia in which globe expansion is impaired by the inability to establish IOP because of the optic fissure failing to close. Both mechanisms of microphthalmos may occur in a single eye.

followed by proliferation of dysplastic mesenchyme, which develops into cartilage, smooth muscle, fat, and lacrimal gland.[126]

A similar spectrum of multiple ocular malformations has been described as a presumably inherited condition associated with central nervous system malformations in Angus,[127] Shorthorn,[128] and Hereford[129,130] cattle as well as in nondomestic species, including raptors,[131] camel,[132] and white-tailed deer.[133]

Table 1.3. Anomalies Associated with Microphthalmia in Dogs

Anomaly	Breed	Reference
Anterior segment dysgenesis	Saint Bernard	111
	Doberman	112–115, 220
Cataract	Old English Sheepdog	125
	Akita	116
	Miniature Schnauzer	117
	Chow Chow	221
	Cavalier King Charles Spaniel	119
	English Cocker Spaniel	120
	Irish Wolfhound	124
Retinal dysplasia	St. Bernard	111
	Doberman	112–115

Colobomatous microphthalmia is initiated later in gestation, as described in the next section.

In swine, congenital microphthalmia has been historically reported to be associated with maternal vitamin A deficiency.[134–136] Conversely, maternal excess of vitamin A and its analogue, retinoic acid, has been demonstrated to result in teratogenic ocular and craniofacial malformations in humans and laboratory animals.[25,110,137,138]

Colobomatous Malformations

A coloboma refers broadly to any congenital (present at birth) tissue defect. Ocular colobomas most frequently involve the vascular tunic of the eye, namely the iris and choroid. The spectrum encompasses minor defects (i.e., dyscoria) as well as major defects (i.e., aniridia). Aniridia occurs rarely in animals[139,140] but is seen as a malformation in humans associated with genetic syndromes, including Rieger syndrome (PITX2 gene)[141] and PAX6 gene mutations.[142] The iris stroma develops from neural crest mesenchyme induced by the bilayered epithelium of the anterior optic cup. Thus, a complete and full-thickness defect in the iris most likely results from incomplete axial expansion of the anterior optic cup. Iris hypoplasia represents the mild spectrum of this type of coloboma and is seen frequently in dogs (particularly those breeds characterized by subalbinism) and has been recognized as a genetic syndrome in horses.[143]

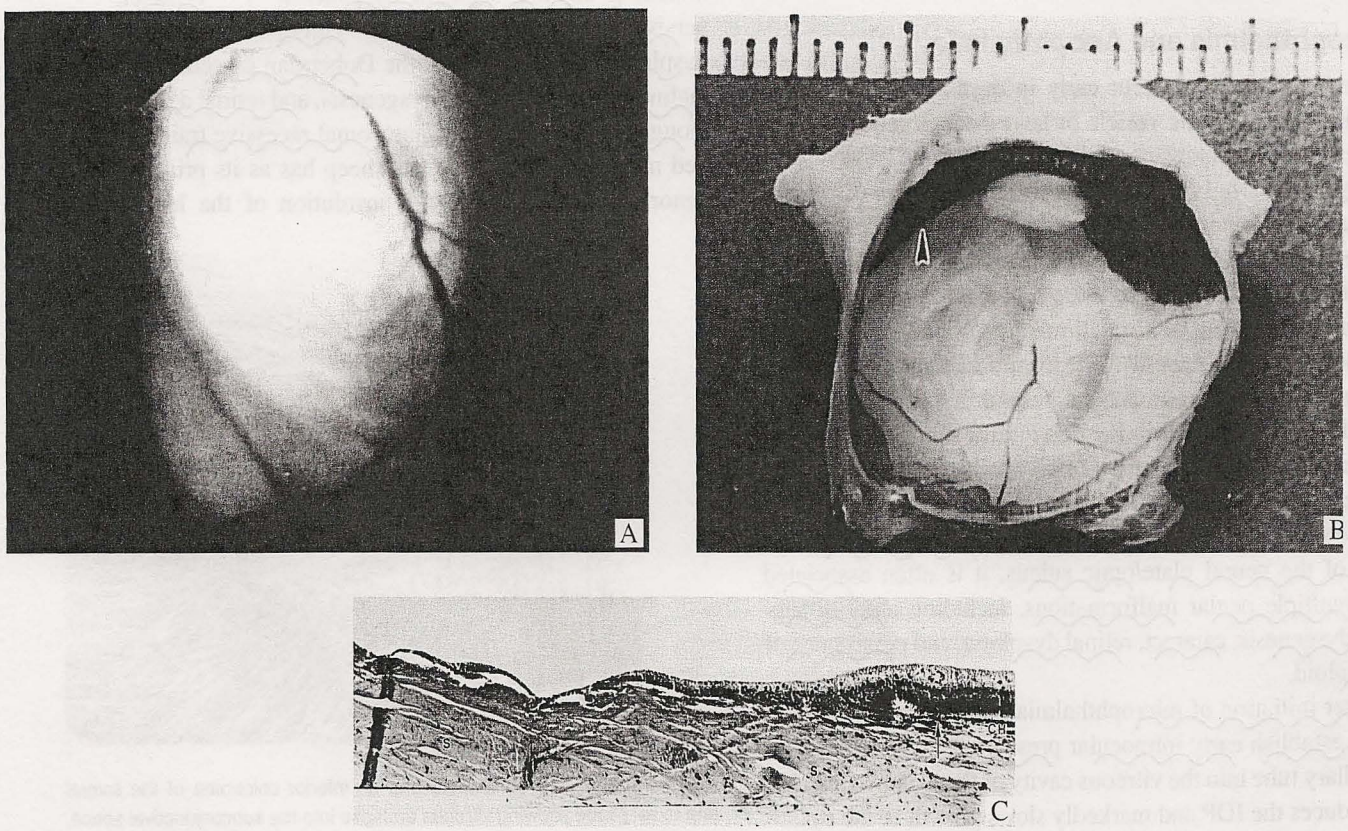

Figure 1.21. **A** and **B.** Clinical (**A**) and gross (**B**) photographs of the ocular fundus of an adult Australian Shepherd dog affected with MOD. Note the large excavation of the equatorial posterior segment. There is also a defect in the ciliary body (*arrowhead*), which was not apparent clinically. **C.** At the light microscopic level, defects such as this consist of a thin layer of sclera (*S*) lined by a glial membrane. Note the abrupt transition from normal retina, RPE, and choroid seen on the right to the sudden loss of RPE and choroid at the level indicated by the *arrow*. (Reprinted with permission from Cook C, Burling K, Nelson E. Embryogenesis of posterior segment colobomas in the Australian shepherd dog. *Prog Vet Comp Ophthalmol* 1991;1:163–170.)

The classic explanation for localized colobomatous malformations involves failure of the optic fissure to close. Such failure may result in secondary "colobomatous" microphthalmia (described previously), and in experimental models, there may be deviation of the fissure by 90° or more. When defects are located in any inferior location (particularly in a small globe), this is the most likely explanation.

Many colobomatous defects, however, occur in other locations.[144–146] Differentiation of the neural crest–derived stroma of the choroid and iris is determined by the adjacent structures of the outer layer of the optic cup: anteriorly, the iris and ciliary epithelium, and posteriorly, the RPE. In sequential analyses of animals exhibiting primary abnormalities in differentiation of the outer layer of the optic cup, anterior and posterior segment colobomas are associated with the uveal epithelium/RPE defects.[60,147,148]

Prenatal studies of colobomas in the Australian Shepherd dog have demonstrated a primary defect in the RPE, resulting in hypoplasia of the adjacent choroid and sclera (Figs. 1.21 and 1.22).[148] This condition is referred to as *merle ocular dysgenesis* (MOD) because of the correlation with the merle coat coloration.[71] A similar spectrum has been identified in cattle,[145] Great Dane dogs, and cats[146] exhibiting incomplete albinism. It is likely that the subalbinism is associated with abnormal RPE that fails to induce the overlying neural crest.

Choroidal hypoplasia in the Collie dog (i.e., *Collie eye anomaly,* or CEA)[149] may represent a malformation sequence similar to that of MOD (Figs. 1.23 and 1.24). Differences between CEA and MOD are illustrated in Table 1.4. CEA has been widely described in the Collie,[72] Border Collie,[150] Shetland Sheepdog,[149] and Australian Shepherd.[151] Variations of this congenital malformation, including scleral ectasia, sporadically

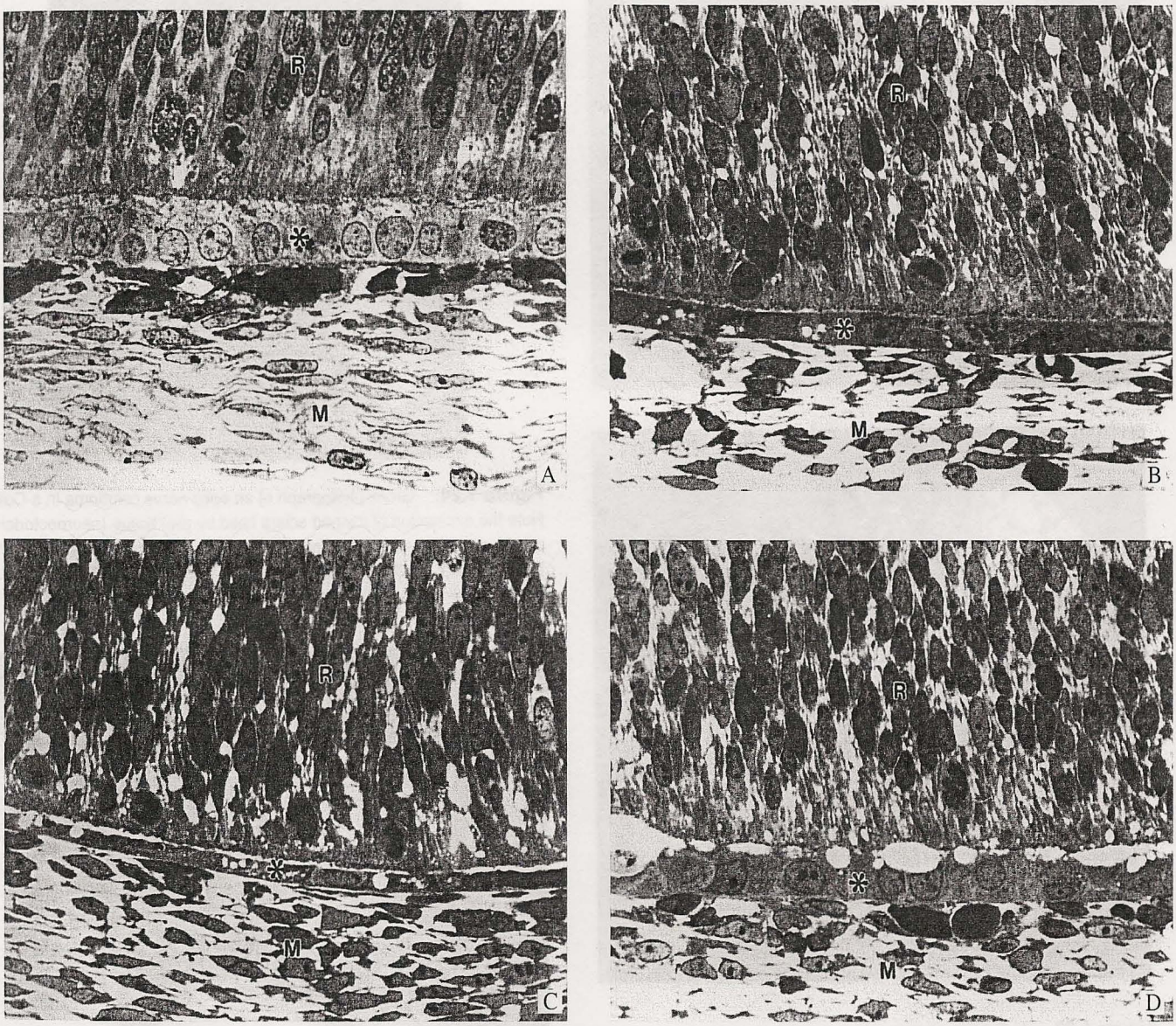

Figure 1.22. Sequential histology of merle ocular dysgenesis. **A.** Normal canine eye on day 30 of gestation. Note the cuboidal appearance of the nonpigmented RPE (*), which is closely apposed to the neural retina (*r*). The nuclei closest to the RPE are those of the outer neuroblastic layer. *M,* periocular mesenchyme—anlage of the choroid and sclera. **B.** MOD-affected eye on day 35 of gestation. The RPE (*) is shorted and contains a few intracytoplasmic vacuoles. **C** and **D.** MOD-affected eye on day 35 of gestation. The RPE (*) has become progressively thinner and exhibits a large number of vacuoles. Separation of the degenerating RPE from the neural retina also can be seen. (Reprinted with permission from Cook C, Burling K, Nelson E. Embryogenesis of posterior segment colobomas in the Australian shepherd dog. *Prog Vet Comp Ophthalmol* 1991;1:163–170.)

occur in other breeds as well.[152] It has been demonstrated that choroidal hypoplasia associated with CEA segregates as an autosomal recessive trait with nearly 100% penetrance.[153]

Dermoid

The presence of aberrant tissue (e.g., skin, cartilage, bone) within the orbit may originate early in development through abnormal differentiation of an isolated group of cells. Arrest or inclusions of epidermal and connective tissues (i.e., surface ectoderm and neural crest) may occur during closure of the fetal clefts. Abnormal invagination of ectodermal tissue later in gestation may result in a pocket of well-differentiated dermal tissue. Eyelid dermoids may occur though isolation of an island of ectoderm, later forming a nodule of tissue that is, strictly speaking, not abnormal in location but in configuration, a nonneoplastic overgrowth of tissue disordered in structure (Fig. 1.25). These

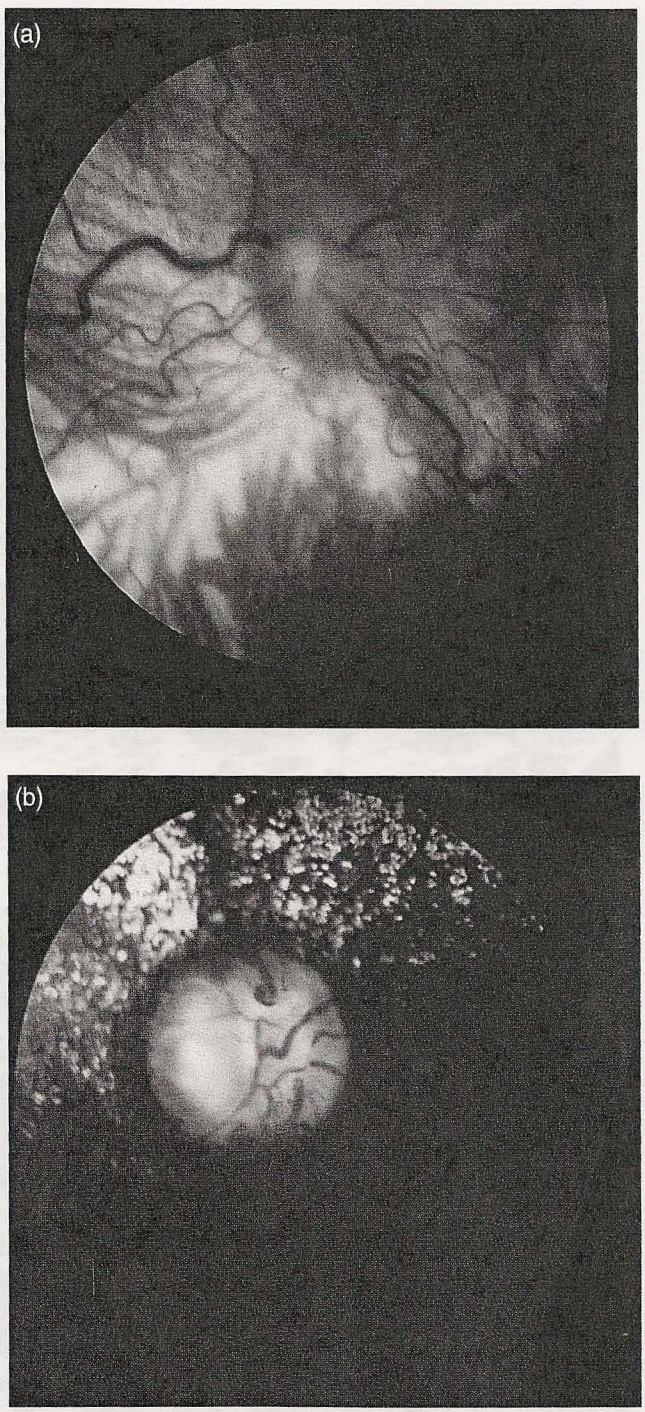

Figure 1.23. **A.** Fundus photograph of choroidal hypoplasia associated with Collie eye anomaly. Note the white sclera with superimposed choroidal and retinal vasculature. **B.** Optic nerve coloboma in a Collie affected with collie eye anomaly. The coloboma is located temporally adjacent to an area of mild choroidal hypoplasia (identified by absence of tapetum and visible choroidal vasculature).

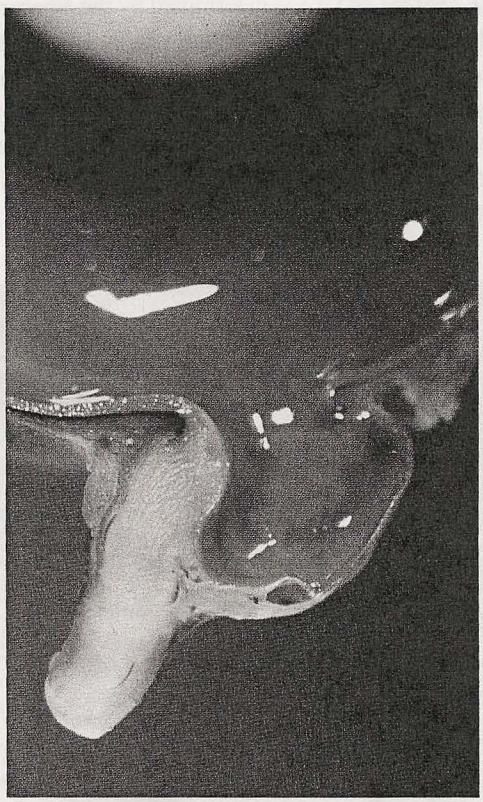

Figure 1.24. Gross photograph of an optic nerve coloboma in a Collie. Note the excavation of thinned sclera lined by glial tissue (neuroectoderm) continuous with retina. (Reprinted with permission from Wilcock, B. *Pathologic Basis of the Veterinary Disease,* 4th ed. McGavin MD, Zachary JF, eds. Elsevier, in press).

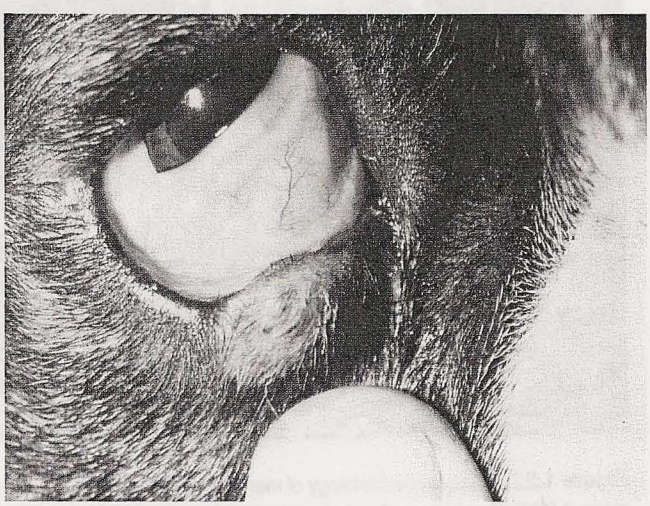

Figure 1.25. Eyelid dermoid in a Boxer dog. The tissue is histologically normal skin in a grossly normal location, but abnormal in configuration, representing a hamartoma. (Courtesy of Dr. R. Peiffer.)

tissue overgrowths are termed *hamartomas* (i.e., benign tissue mass resulting from faulty development). Limbal dermoids represent *choristomas* (i.e., mass formed by tissue not normally found at this site) (Fig. 1.26). Both eyelid epidermis and corneal epithelium originate from surface ectoderm, following induction by the optic vesicle, and there appears to be a narrow period during which the surface ectoderm can respond to inductive influences to produce a normal lens. The same may be true for induction of the cornea. Dermoids are seen in all species as an incidental finding, and they are seen as an inherited condition in cattle and some dog breeds.[154,155]

Anterior Segment Dysgenesis

The anterior segment dysgeneses identified in humans encompass a broad range of malformations, including Peters' anomaly, Axenfeld-Rieger syndrome, iridocorneal endothelium syndrome, posterior polymorphous dystrophy, and Sturge-Weber syndrome. Similar anomalies have been described in domestic animals, generally as sporadic occurrences.[140, 156–158] Anterior segment dysgenesis is often associated with microphthalmia.[111–115]

Table 1.4. Comparative Features of Merle Ocular Dysgenesis and Collie Eye Anomaly

	Merle Ocular Dysgenesis	Collie Eye Anomaly
Coat color	Homozygous Merle	No correlation
Microphthalmia	Frequent	Rare/mild
Choroidal hypoplasia	Extensive scleral/ retinal defects	Common, localized
Optic nerve coloboma	Rare	Frequent
Cataract	Frequent	Rare
Iris coloboma	Frequent	Rare

Reprinted with permission from Cook C, Burling K, Nelson E. Embryogenesis of posterior segment colobomas in the Australian shepherd dog. *Prog Vet Comp Ophthalmol* 1991;1:163–170.

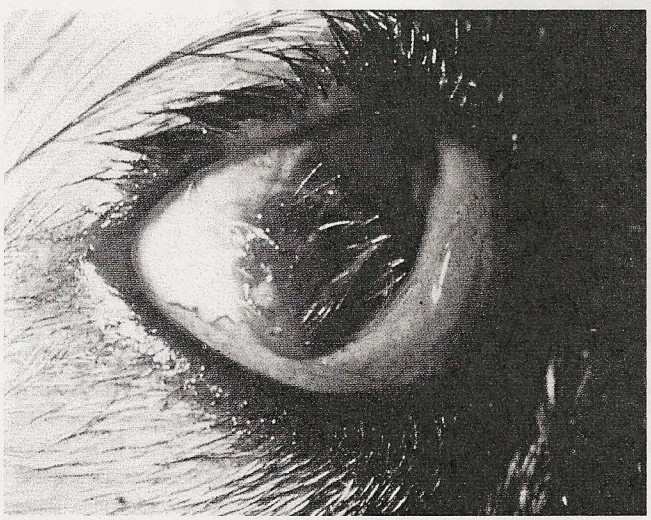

Figure 1.26. Limbal dermoid in a Pekingese dog. This is an example of a choristoma (histologically normal tissue in an abnormal location). (Courtesy of Dr. R. Peiffer.)

In domestic animals, *persistent pupillary membranes* represent the most common manifestation of anterior segment dysgenesis. In the embryo, the pupillary membrane forms a solid sheet of tissue that is continuous with the iris at the level of the collarette (Fig. 1.19). Regression occurs during the first 2 postnatal weeks, before eyelid opening in the dog. Persistence of some pupillary membrane strands was noted in 0.7% of 575 Beagles

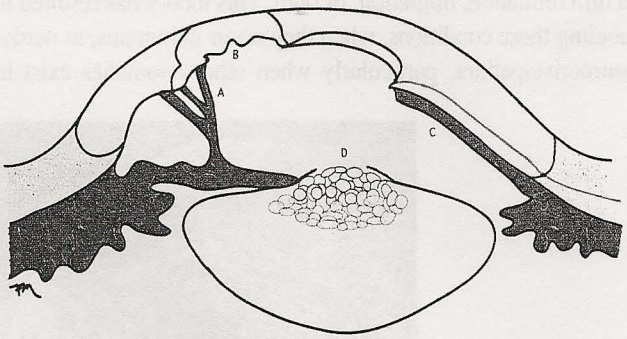

Figure 1.27. Clinical features of Peters' anomaly (anterior segment dysgenesis) resulting from abnormal separation of the lens vesicle from the surface ectoderm. **A.** Persistent pupillary membrane. **B.** Corneal opacity associated with defect in corneal endothelium, Descemet's membrane, and corneal stroma (neural crest). **C.** Iris hypoplasia. **D.** Anterior lenticonus and anterior polar cataract associated with partial defect in anterior lens capsule. (Drawing by Farid Mogannam.)

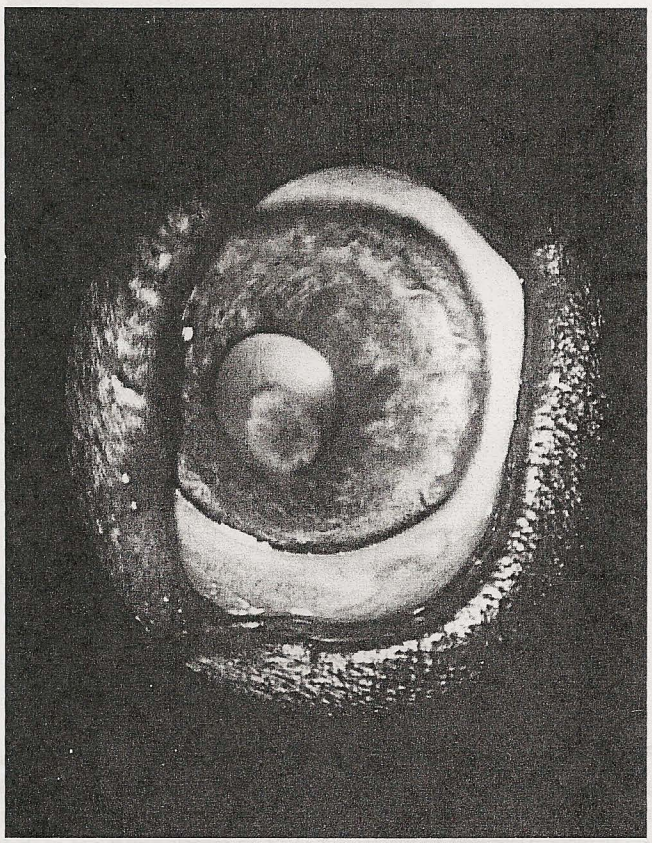

Figure 1.28. Clinical photograph of a puppy with Peters' anomaly exhibiting microphthalmia, a central corneal opacity, anterior axial cataract, and persistent pupillary membranes.

aged 16 to 24 weeks.[159] Inherited persistent pupillary membranes occur in the Basenji dog,[160,161] and they may be associated with corneal or lens opacities (or both) at the site of membrane attachments. Complete persistence of a sheet of tissue bridging the pupil is rare and results in visual impairment. Persistent pupillary membranes also occur sporadically in other breeds.[120]

Because most structures of the ocular anterior segment are of neural crest origin, it is tempting in cases of anterior segment anomalies to incriminate this cell population as being abnormal in differentiation, migration, or both. This theory has resulted in labeling these conditions, when they occur in humans, as ocular neurocristopathies, particularly when other anomalies exist in tissues that are largely derived from the neural crest (e.g., craniofacial connective tissue, teeth).[162–166] When considering this theory, it is important to realize two concepts. First, the neural crest is the predominant cell population of the developing craniofacial region, particularly the eye. In fact, the list of ocular tissues *not* derived from neural crest is relatively small (see Table 1.2). Thus, the fact that most malformations of this region involve crest tissues may reflect their ubiquitous distribution rather than their common origin. The normal development of the choroid and sclera (also of neural crest origin) in most of these "neural crest syndromes" argues against a primary neural crest anomaly. Second, the neural crest is an actively migrating

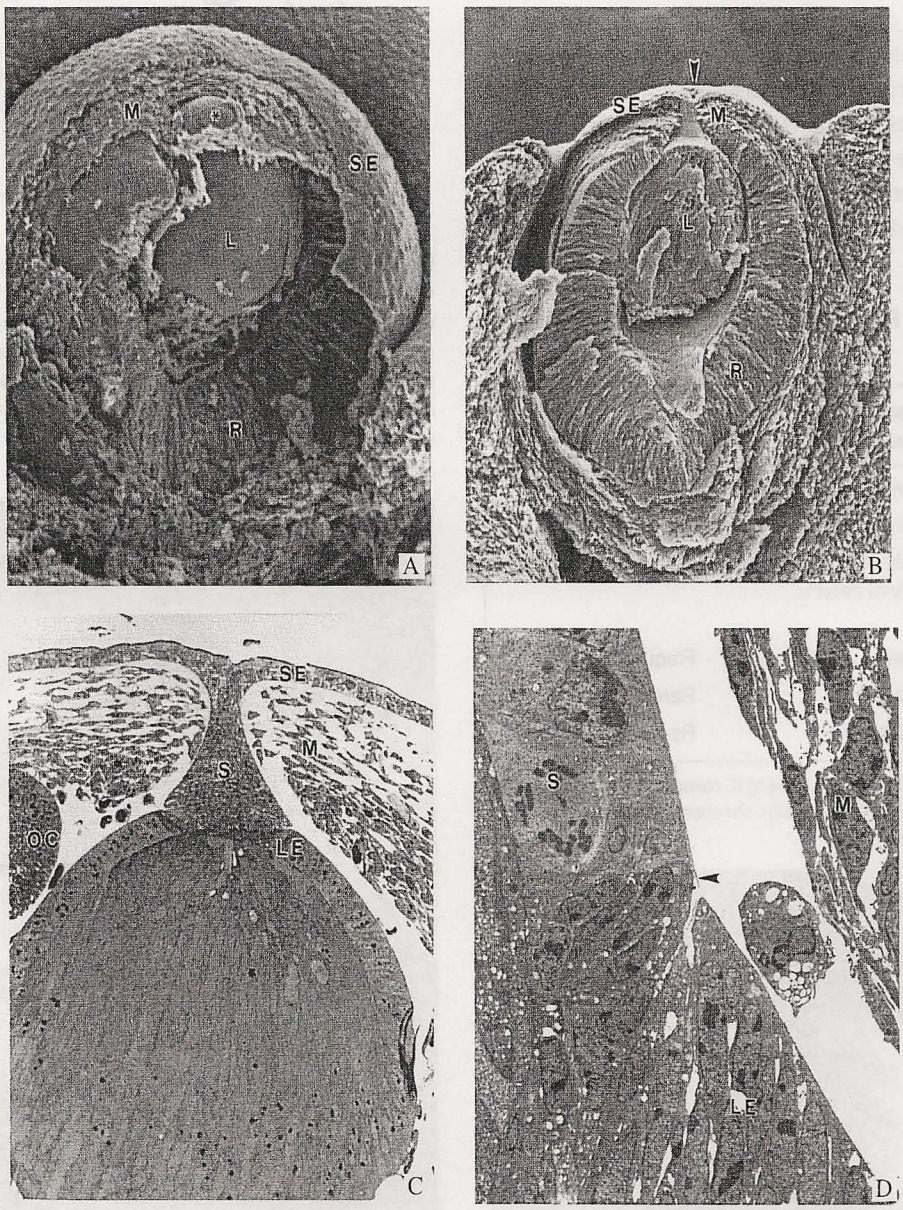

Figure 1.29. Keratolenticular dysgenesis induced by teratogen exposure in mice. **A.** Mouse embryo following acute exposure to ethanol during gastrulation. Delay in separation of the lens vesicle (*L*) from the surface ectoderm (*SE*) results in an anterior lenticonus (*) and failure of the mesenchyme (*M*) to complete its axial migration to form the corneal stroma, endothelium, and iris stroma. *R,* retinal primordium. (Original magnification, 166X.) **B, C,** and **D.** Mouse embryo following acute exposure to 13-cis-retinoic acid during gastrulation. A large keratolenticular stalk (*S*) persists and is continuous axially with the surface ectoderm (*SE*). The arrow in B indicates the incompletely closed lens pore; **D** is a transmission electron microscopic view of the stalk seen in **C.** There is discontinuity between the lens epithelium (*LE*) and the stalk epithelium (*S*). Adjacent neural crest mesenchyme (*M*) is visible, and two layers of basement membrane can be seen in **D:** bridging the lens–stalk junction as well as dividing the two zones. Mechanical interference with the axial migration of neural crest cells is responsible in this model for malformations, which mimics Peters' anomaly in the human. *OC,* optic cup. (Part A reprinted with permission from Cook CS, Nowotny AZ, Sulik KK. Eye malformations in a mouse model. *Arch Ophthalmol* 1987;105:1576–1581. Parts B, C, and D reprinted with permission from Cook CS, Sulik KK. Laminin and fibronectin in retinoid-induced keratolenticular dysgenesis. *Invest Ophthalmol Vis Sci* 1990;31:751–757.)

population of cells and can be easily influenced by adjacent cell populations. Thus, the perceived anomaly of neural crest tissue may, in many cases, be a secondary effect.

Much of the maturation of the iridocorneal angle occurs late during gestation and during early postnatal life in the dog, but earlier events may influence development of the anterior segment. Anterior segment dysgenesis syndromes characterized primarily by axial defects in corneal stroma and endothelium, accompanied by corresponding malformations in the anterior lens capsule and epithelium (i.e., Peters' anomaly), most likely represent a manifestation of abnormal keratolenticular separation (Figs. 1.27 and 1.28). This spectrum of malformations that mimic Peters' anomaly can be induced by teratogen exposure in mice before optic sulcus invagination (Figs. 1.29 and 1.30).[25,110,167] Similar syndromes of anterior segment dysgenesis have been identified in humans following ethanol exposure.[168–170]

The size of the lens vesicle is determined by the area of contact between the optic vesicle and the surface ectoderm. Thus, factors influencing the size of the optic vesicle or the angle at which the optic vesicle approaches the surface ectoderm may affect the ultimate size of the lens vesicle. Microphakia resulting from optic vesicle deficiencies may be initiated very early in gestation (i.e., during formation of the neural plate). Microphakia associated with lens luxation has been described in two unrelated Siamese kittens[171]; because the globes were apparently otherwise normal, a primary abnormality in the lens placode ectoderm can be postulated. Aphakia is much more rare and may occur through failure of contact between the optic vesicle and the surface ectoderm during the period when the surface ectoderm can respond to its inductive

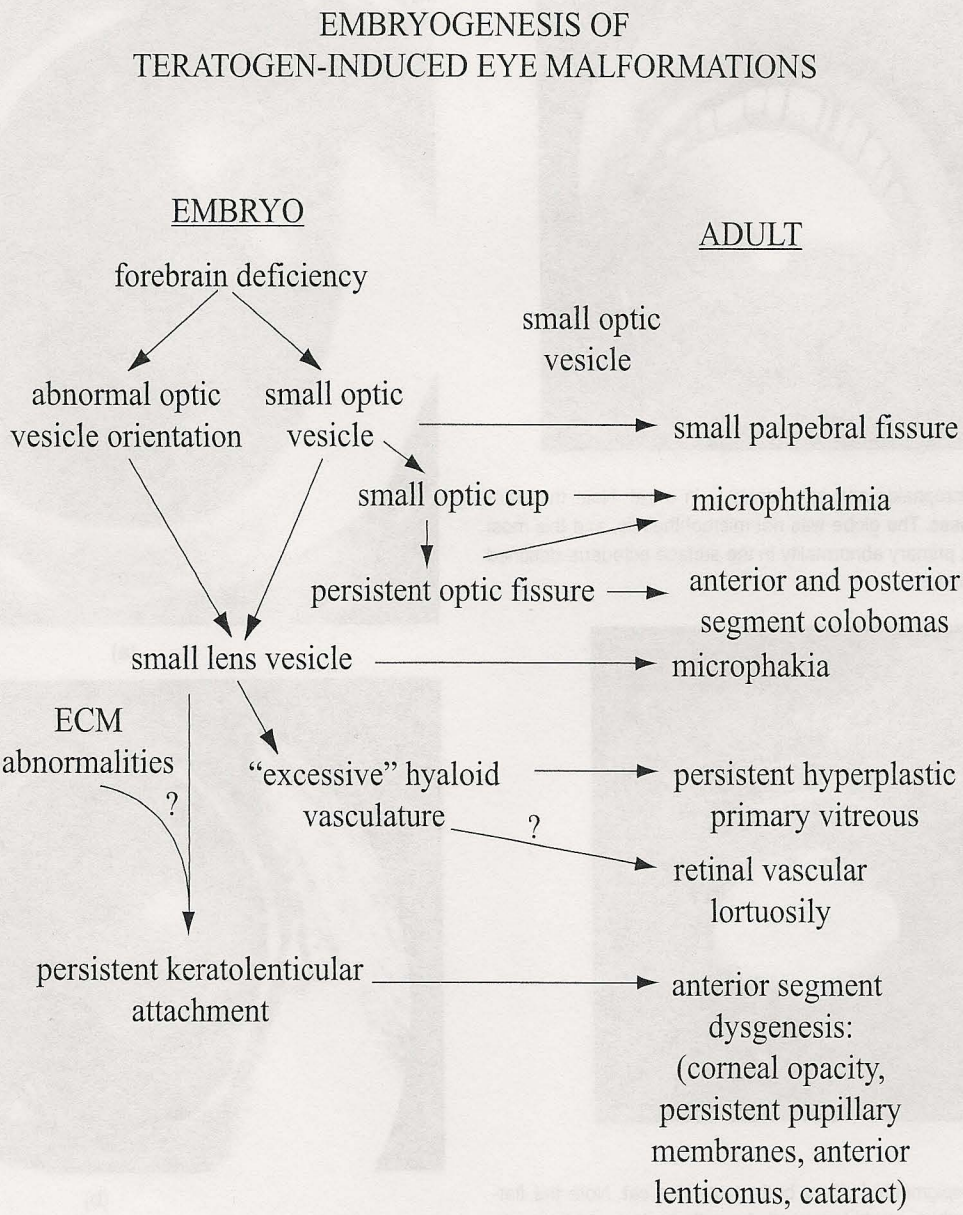

Figure 1.30. The relationship between microphthalmia and associated ocular malformations. An early embryonic insult (during gastrulation) leads to a deficiency in the forebrain and its derivatives, the optic sulci. The subsequently small optic vesicle often exhibits an abnormal relationship to the surface ectoderm, which is programmed (by the underlying neural crest) to form the lens. The result is a spectrum of malformations in the adult, including microphthalmia, microphakia, colobomas, persistent hyperplastic primary vitreous, and anterior segment dysgenesis. *ECM,* extracellular matrix. (Reprinted with permission from Cook C. Embryogenesis of congenital eye malformations. *Vet Comp Ophthalmol* 1995;5:109–123.)

influences. Because the anterior lens epithelium is required for induction of the corneal endothelium, this early initiation of aphakia would be associated with anterior segment dysgenesis. Alternatively, normal induction of a lens vesicle followed by later involution would be expected to result in an eye with more normal anterior segment morphology. The lens aplasia (lap) mouse demonstrates faulty lens basement membrane formation associated with apoptosis and involution of the rudimentary lens vesicle.[23,172,173] Sporadic cases of aphakia have been described in domestic animals, including a cat with associated retinal detachment but apparently normal iridocorneal structures (histopathology not available)[156] and a litter of Saint Bernard puppies with multiple ocular malformations.[111] In humans, in utero exposure to rubella or parvovirus B can result in aphakia; anterior segment structures are variably affected.[174] Abnormalities in lens shape (e.g., spherophakia, lens coloboma) may actually represent a primary abnormality in the ciliary processes, zonular fibers, or both, resulting in a lack of tension on the lens (Figs. 1.31 and 1.32). Thus, the term *coloboma* may be inaccurate when used in reference to a flattened equatorial portion of the lens that is not a true lens defect.

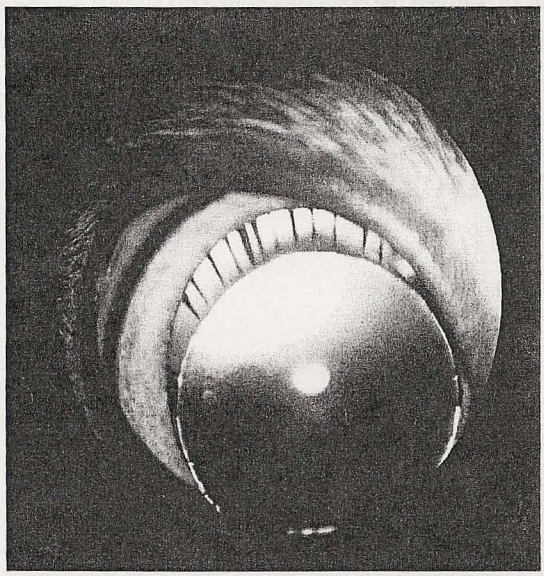

Figure 1.31. Microphakia and spherophakia in a cat. Note the elongated ciliary processes. The globe was not microphthalmic, and this most likely represented a primary abnormality in the surface ectoderm destined to become lens placode.

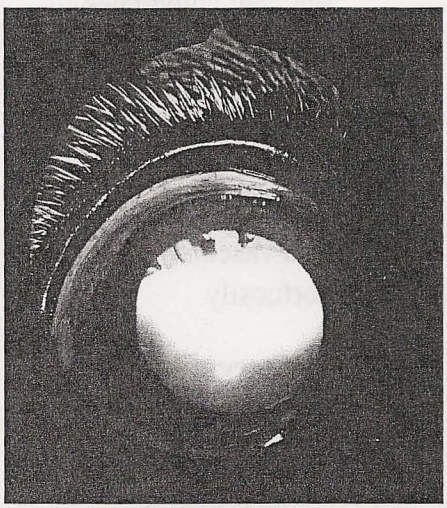

Figure 1.32. Nonpigmented ciliary body cysts in a cat. Note the flattened lens equator, which would incorrectly be called a lens coloboma. In this case, a medulloepithelioma of the ciliary body resulted both in the cysts and the localized absence of zonules. Failure of normal traction by the zonule on the lens equator resulted in this flattened appearance. (Case courtesy of K. Burling.)

Uveal Cysts

Uveal cysts occur through failure of adhesion of the inner and outer layers of the optic cup. They are most commonly identified as single or multiple spherical pigmented masses

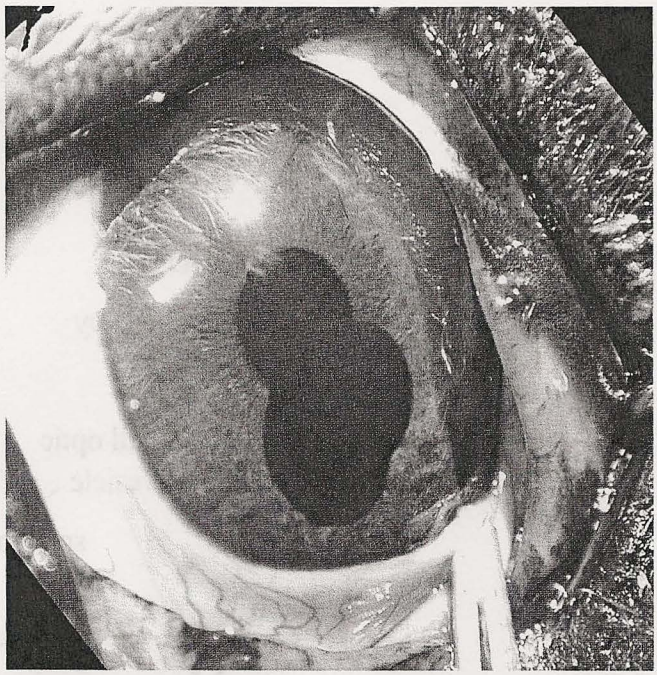

(a)

(b)

Figure 1.33. Iris cysts. **A.** Single iris cyst in a dog. **B.** Multiple iris cysts in a cat. In cats, these cysts are often thick-walled and remain attached to the posterior iris surface, causing anterior displacement of the iris and a shallow anterior chamber.

within the pupil or free-floating within the anterior chamber (Figs. 1.33 and 1.34). In the dog, they may be single or multiple and are often free-floating within the anterior chamber. They appear to have a genetic predilection. In the cat, they are more often thick-walled and remain attached to the posterior iris surface, causing anterior displacement of the iris and shallowing of the anterior chamber and may result in secondary glaucoma.[175] When they originate within the ciliary body they are nonpigmented (Fig. 1.32).

Congenital Ocular Anomalies in Rocky Mountain Horses

A syndrome of multiple ocular anomalies has been identified as a bilaterally symmetrical, inherited condition in the Rocky Mountain breed of horses[176,177] (Fig. 1.35). The condition is characterized by cysts of the posterior iris, ciliary body, and peripheral retina, indicating failure of adhesion of the inner and outer layers of the optic cup. These cysts are consistently

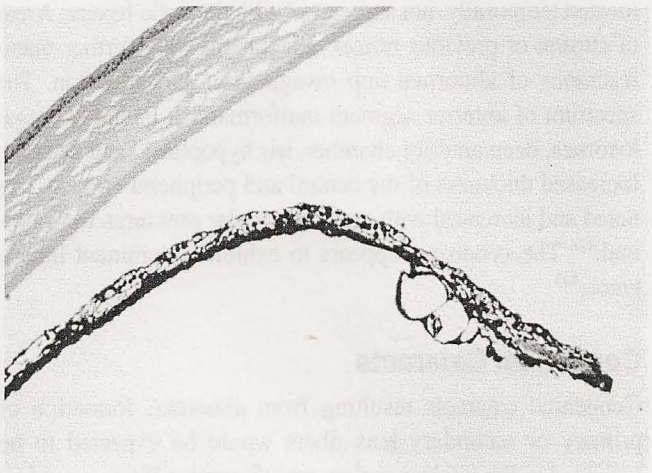

Figure 1.34. Histologic appearance of a uveal cyst on the posterior iris surface. These cysts form beneath the posterior pigmented epithelium and frequently separate to become free-floating spheres within the anterior chamber. (Courtesy of Dr. R. Peiffer.)

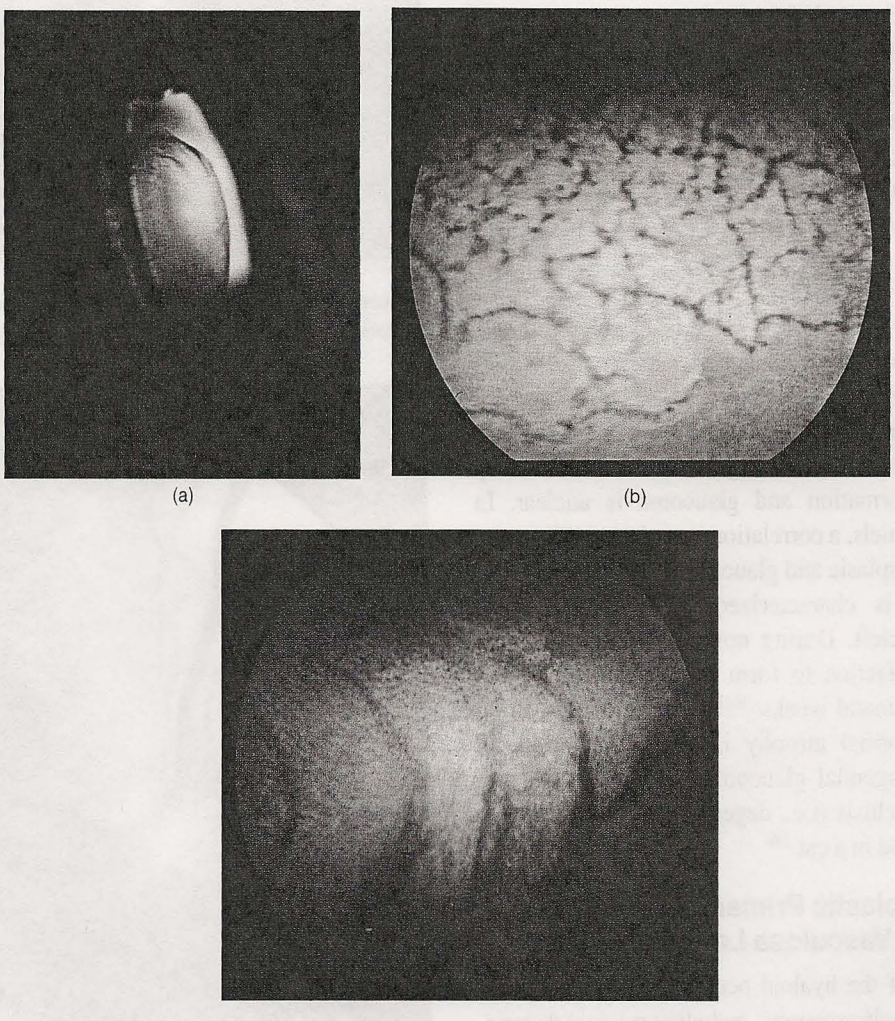

(a) (b) (c)

Figure 1.35. Spectrum of ocular lesions seen in Rocky Mountain horses. **A.** A large translucent cyst arising from the lateral part of the ciliary body extends into the vitreous cavity and occupies part of the temporal pupillary axis of the right eye. **B.** Retinal dysplasia is characterized by numerous pigmented folds located in the superior peripapillary neurosensory retina. (Reprinted with permission from Ramsey, DT, et al.: Congenital ocular abnormalities of Rocky Mountain horses. *Vet Ophthalmol* 2:47–59, 1999.). **C.** Multiple, well-delineated, darkly pigmented curvilinear streaks of retinal pigment epithelium are present in the peripheral right tapetal fundus. These streaks originate and terminate at the ora ciliaris retinae and extend toward the optic papilla. They represent demarcation lines from previous retinal detachments and are referred to clinically as "high-water markers." (Photos courtesy of Dr. D. Ramsey.)

located temporally, not associated with the optic fissure. Areas of current or previous retinal detachment were further manifestations of abnormal cup invagination and adhesion. The spectrum of anterior segment malformations included megalocornea, deep anterior chamber, iris hypoplasia, and cataract. Increased thickness of the central and peripheral corneas was noted and increased with age. Intraocular pressures were normal.[176] The syndrome appears to exhibit codominant inheritance.[143]

Congenital Cataracts

Congenital cataracts resulting from abnormal formation of primary or secondary lens fibers would be expected to be localized to the nuclear region, and they most likely would be nonprogressive. Abnormal lens vesicle invagination, separation, or defects in the lens epithelium or capsule would result in a cataract (with or without anterior or posterior lenticonus)[178] that would remain associated with the peripheral portion of the lens, with the secondary lens fibers forming underneath (e.g., Old English Sheepdog,[125] Cavalier King Charles Spaniel[119]). Congenital cataracts associated with mild microphthalmia in the Miniature Schnauzer[117,118,179] may result from early abnormalities in the lens placode/epithelium, and they may involve the lens nucleus, cortex, or both. In the Miniature Schnauzer, these lesions are recessively inherited, typically bilateral, and initially involve the posterior subcapsular region with rapid progression.[117,180]

Congenital Glaucoma

Malformations of the iridocorneal angle (i.e., goniodysgenesis) have been described in several breeds, including the Basset Hound[181,182] and the Bouvier des Flandres.[183] The iridocorneal angles of affected animals are malformed at birth, but the IOP often remains normal until middle age. Thus, the relationship between angle conformation and glaucoma is unclear. In English Springer Spaniels, a correlation was observed between pectinate ligament dysplasia and glaucoma.[184]

Goniodysgenesis is characterized by abnormal tissue bridging the ciliary cleft. During normal development, this sheet undergoes rarefaction to form the pectinate ligament during the first 3 postnatal weeks.[59,185] Failure of this membrane to undergo normal atrophy is thought to result in goniodysgenesis. Congenital glaucoma associated with presumed primary iridoschisis (i.e., degeneration of the anterior iris) has been described in a cat.[186]

Persistent Hyperplastic Primary Vitreous/ Persistent Tunica Vasculosa Lentis (PHPV/PTVL)

Variable persistence of the hyaloid occurs in association with many other types of malformations, including microphthalmia, microphakia, cataract, and retinal dysplasia (Fig. 1.36).[187] PHPV/PTVL may occur secondary to other malformations or as a primary, spontaneous failure of vascular regression. This condition has been described as an inherited trait in the Doberman[123,188] and the Bouvier des Flandres.[183] Normal vitreous may have antiangiogenic properties, and it may be essential for initiating regression of the hyaloid. Thus, the primary abnormality in PHPV/PTVL may rest with the product of the ciliary epithelium (i.e., secondary vitreous).

Retinal Dysplasia

Abnormal retinal differentiation results in rosettes and multifocal disorganization known as retinal dysplasia. Retinal folds without rosette formation may result from inequity in the relative growth rates of the inner (i.e., retinal) and outer (i.e., RPE) layers of the optic cup (Figs. 1.37 and 1.38). This is a particularly

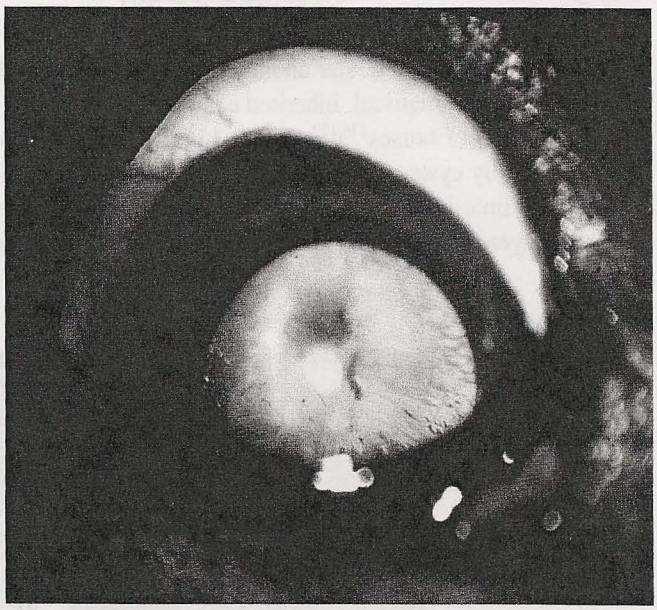

Figure 1.36. Persistent hyperplastic primary vitreous associated with a posterior subcapsular cataract in a puppy. This eye is also microphthalmic.

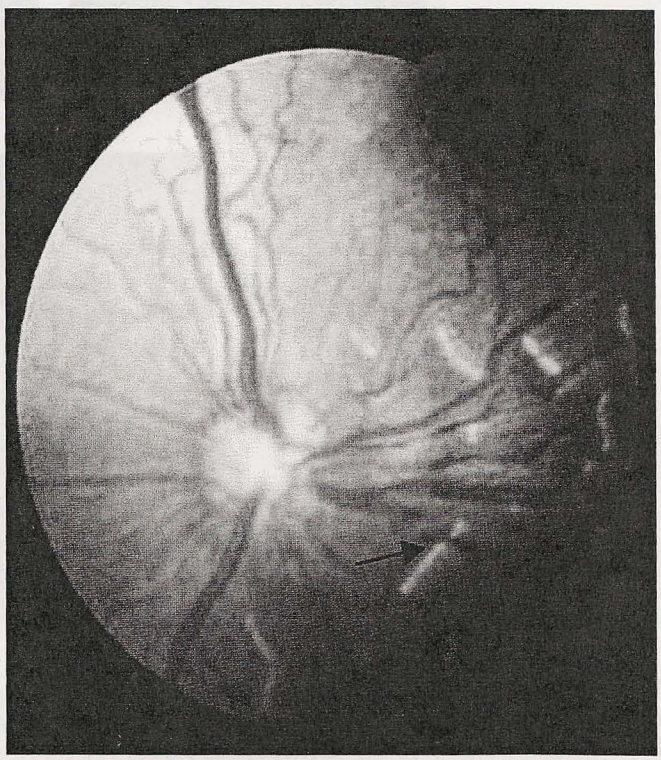

Figure 1.37. Fundus photograph of retinal folds in a young American Cocker Spaniel. These appear as single or multiple white curvilinear streaks. Elevation of a retinal vessel crossing a fold (*arrow*) can be seen.

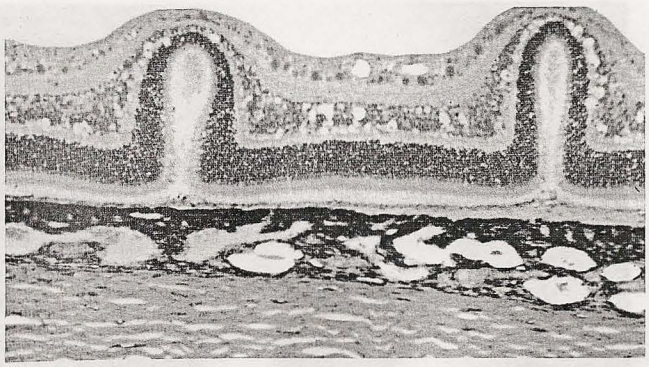

Figure 1.38. Histologic appearance of retinal folds. Note the normal stratification of the retinal layers and the mechanical distortion caused by disparate growth of the neural retina (inner optic cup) and the underlying RPE (outer optic cup). (Photo courtesy of Dr. R. Peiffer.)

likely pathogenesis in cases in which the folds resolve as the animal matures; it is seen most commonly among Collies. These folds do not represent abnormal differentiation and thus are not accurately referred to as dysplasia. Simple folding in the retina has been described in the American Cocker Spaniel[189] and the Beagle.[190,191] The genetic relationship between simple folds and true retinal dysplasia is undetermined.

True retinal dysplasia is characterized by disorganized development, the hallmark of which is the rosette. Abnormal or incomplete contact between the inner and outer layers of the optic cup during embryogenesis can result in dysplasia, the most severe form of which is associated with complete retinal nonattachment. This condition usually occurs in eyes that are microphthalmic with multiple ocular anomalies (e.g., Bedlington Terrier,[192,193] Sealyham Terrier[194]). In the Labrador Retriever, retinal dysplasia genetically associated with skeletal anomalies is inherited as an autosomal dominant trait.[195] A similar form of inherited skeletal–ocular dysplasia is seen in the Samoyed dog.[196,197]

Multifocal retinal rosettes in a retina that is partially attached to the underlying RPE represent the most common form of retinal dysplasia (Figs. 1.39 and 1.40). This condition has been described extensively in the English Springer Spaniel.[198–200] Retinal dysplasia occurs sporadically in other breeds[201] and species.[202] Multifocal, "geographic" retinal dysplasia most likely represents a later initiation of retinal disorganization. The dysplastic changes are first apparent at 45 to 50 days of gestation. Focal loss of cell junctions of the external limiting membrane is seen, with proliferation of neuroblasts in the retina forming rosettes.[203]

Retinal differentiation and maturation in the dog continues during the first 40 days postnatal. In addition, maturation of the tapetum during the first 6 months results in an inconsistent ability to detect mild forms of retinal dysplasia in puppies less than 10 weeks of age.[204]

An unusual form of RPE dysplasia with duplication of neural retina in the outer layer of the optic cup has been described in several mutant mouse strains.[60,61] Large colobomas of the choroid and sclera in the areas adjacent to the dysplastic RPE illustrate the importance of this layer in coordinating differentiation of the neural crest.

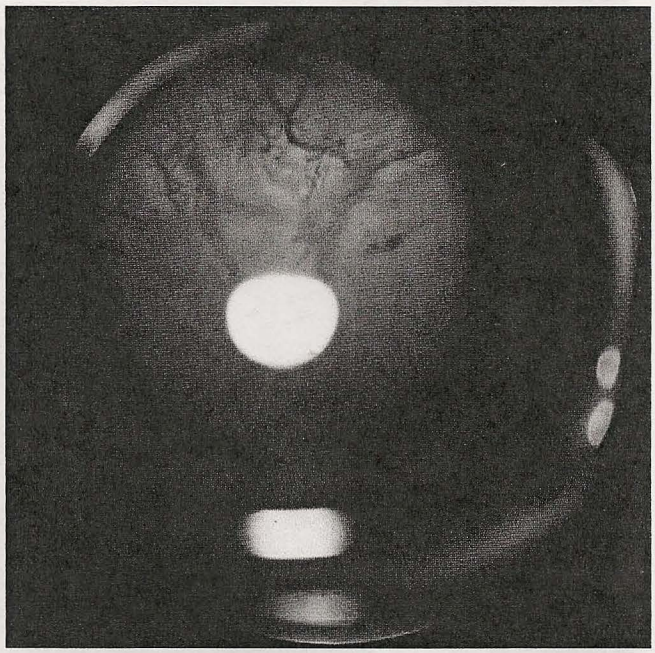

Figure 1.39. Geographic retinal dysplasia in an English Springer spaniel. The retina is detached and lies just posterior to the lens; there are many folds visible.

Figure 1.40. Histologic appearance of geographic retinal dysplasia. The retina exhibits disorganization and classic rosette formation. Note also the hypoplastic choroid. (Photo courtesy of Dr. R. Peiffer.)

Viral-induced "retinal dysplasia" has been associated with early postnatal exposure to canine herpesvirus[205,206] and prenatal exposure to bovine viral diarrhea virus,[207–209] bluetongue virus in lambs,[210] and feline panleukopenia virus.[211] Histopathologically, affected retinas are characterized by early inflammatory cell infiltrate and, later, by necrosis, gliosis, and diffuse disorganization of cell layers. Similar postnatal retinal disorganization can be induced in the dog by radiation exposure.[212,213] These conditions are more accurately classified as teratogen-induced necrosis and degeneration than as dysplasia.

Optic Nerve Hypoplasia

Though difficult to document experimentally, optic nerve hypoplasia most likely results from a primary abnormality in the number or ultimate differentiation of the ganglion cells (Fig. 1.41). Hypovitaminosis A in cattle can result in stenosis of the optic foramen with secondary optic nerve degeneration,

Figure 1.41. Optic nerve hypoplasia in an 8-week-old Alsatian puppy. This was a unilateral lesion, and the pup presented with anisocoria. (Photo courtesy of Dr. R. Peiffer.)

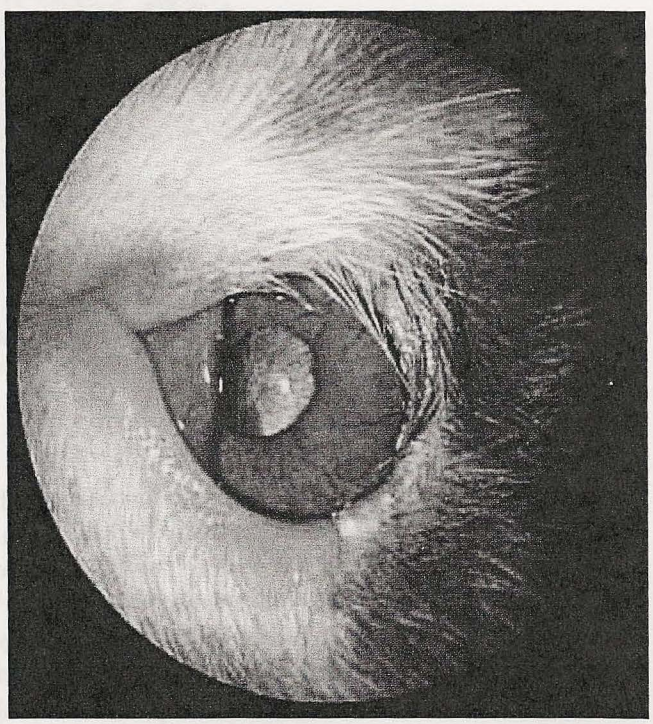

Figure 1.42. Eyelid coloboma in a kitten. The eyelid margin is absent from the temporal two thirds of the upper lid. There is keratitis due to exposure and trichiasis. The eye also exhibits microphthalmia, dyscoria, and persistent pupillary membranes.

incorrectly labeled hypoplasia. Colobomas of the optic nerve result from failure of the optic fissure to close, as described for "typical" colobomas. Myelination of the optic nerve progresses from the brain to the eye during the first 3 postnatal weeks.[214] Reduction in the amount of myelinization leads to a small optic disc that can mimic hypoplasia but is unassociated with vision deficits.

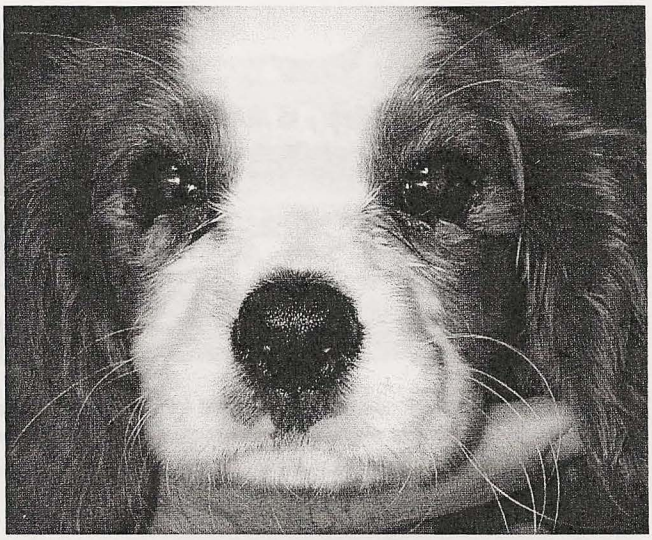

Figure 1.43 A Cavalier King Charles Spaniel with bilateral lower eyelid colobomas. Note the notch defects in the central portion of the lower lids and the abnormal hair growth adjacent to the defects.

Eyelid Coloboma

The eyelids and palpebral fissure are initially induced at the time of contact of the optic vesicle with the surface ectoderm. This is also the time of induction of the lens placode. Eyelid agenesis (coloboma) occurs in domestic cats, often with concurrent persistent pupillary membranes, keratolenticular dysgenesis, and subtle to severe microphthalmia (Fig. 1.42).[215–218] Eyelid colobomas occur less commonly in dogs (Fig. 1.43) and a case of upper eyelid agenesis has also been described in a peregrine falcon.[219]

The receptivity of the surface ectoderm to the inductive influences of the optic vesicle is highly spatiotemporally specific. The fairly consistent location of the defect in the temporal upper eyelid leads to suspicion of an abnormal orientation of the optic vesicle as it approaches the surface ectoderm, possibly eccentrically contacting the surface ectoderm in an area that is only partially receptive.

REFERENCES

1. Cook CS, Ozanics V, Jakobiec SA. Prenatal development of the eye and its adnexa. In: Tasman W, Jaeger E, eds. *Duane's Foundations of Clinical Ophthalmology.* Philadelphia: Lippincott; 1993: (Ch. 2), 1–93.
2. Cook CS. Embryogenesis of congenital eye malformations. *Vet & Comp Ophthalmol.* 1995; 5(2): 109–123.
3. Cook CS, Sulik KK. Sequential scanning electron microscopic analyses of normal and spontaneously abnormal ocular development in C57B1/6J mice. *Scan Elect Microsc.* 1986; 3: 1215–1227.
4. Hilfer SR. Development of the eye of the chick embryo. *Scan Elect Microsc.* 1983; III: 1353–1369.

5. O'Rahilly R. The timing and sequence of events in the development of the human eye and ear during the embryonic period proper. *Anat Embryo.* 1983; (168): 87–99.
6. LeDouarin NM, Teillet MA. Experimental analysis of the migration and differentiation of neuroblasts of the autonomic nervous system and of neurectodermal mesenchymal derivatives, using a biological cell marking technique. *Devel Biol.* 1974; 41: 162–184.
7. Noden DM. Periocular mesenchyme: Neural crest and mesodermal interactions. In: Tasman W, Jaeger E, eds. *Duane's Foundations of Clinical Ophthalmology.* Philadelphia: Lippincott; 1993: 1–23.
8. Noden DM. The embryologic origins of avian craniofacial muscles and associated connective tissues. *Am J Anat.* 1983; 168: 257–269.
9. Johnston MC, et al. Origins of avian ocular and periocular tissues. *Exp Eye Res.* 1979; 29(1): 27–43.
10. Hilfer SR, Randolph GJ. Immunolocalization of basal lamina components during development of chick otic and optic primordia. *Anatom Rec.* 1993; 235: 443–452.
11. Hilfer SR, Brady RC, Yang J-JW. Intracellular and extracellular changes during early ocular development in the chick embryo. In: Hilfer S, Sheffield J, eds. *Ocular Size and Shape: Regulation During Development.* New York: Springer-Verlag; 1981; 47–78.
12. Jones KL, Higgonbottom MC, Smith DW. Determining the role of the optic vesicle in orbital and periocular development and placement. *Pediatr Res.* 1980; 14: 703–708.
13. Wrenn JT, Wessells NK. An ultrastructural study of lens invagination in the mouse. *J Exp Zool.* 1969; (171): 359–368.
14. Schook P. A review of data on cell actions and cell interactions during the morphogenesis of the embryonic eye. *Acta Morphol Neerl Scand.* 1978; 16: 267–286.
15. Ikeda H, et al. Histological and histochemical studies of normal and faulty closure of the embryonic fissure in the eye of ICR mouse. *Jpn J Ophthalmol.* 1995; 39(1): 20–29.
16. Ozeki HF, et al. Apoptosis is associated with formation and persistence of the embryonic fissure. *Curr Eye Res.* 2000; 20(5): 367–372.
17. Beebe DC, et al. Transport and steady-state concentration of plasma proteins in the vitreous humor of the chicken embryo: Implications for the mechanism of eye growth during early development. *Dev Biol.* 1986; 114(2): 361–368.
18. Grainger RM, et al. Recent progress on the mechanisms of embryonic lens formation. *Eye.* 1992; 6(Pt 2): 117–122.
19. Grainger RM, Henry JJ, Henderson RA. Reinvestigation of the role of the optic vesicle in embryonic lens induction. *Develop.* 1988; 102: 517–526.
20. Cohen AI. Electron microscopic observations of the developing mouse eye. I. Basement membranes during early development and lens formation. *Dev Biol.* 1961; 3: 297–316.
21. Hunt HH. A study of the fine structure of the optic vesicle and lens placode of the chick embryo during incubation. *Dev Biol.* 1961; 3: 175–209.
22. Weiss P, Jackson SF. Fine structural changes associated with lens determination in the avian embryo. *Dev Biol.* 1961; (3): 532–554.
23. Aso S, Horiwaki S, Noda S. Lens aplasia: A new mutation producing lens abnormality in the mouse. *Lab An Sci.* 1995; 45(1): 41–46.
24. Garcia-Porrero JA, Collado JA, Ojeda JL. Cell death during detachment of the lens rudiment from ectoderm in the chick embryo. *Anat Rec.* 1979; 193: 791–804.
25. Cook CS, Sulik KK. Keratolenticular dysgenesis (Peters' anomaly) as a result of acute embryonic insult during gastrulation. *J Ped Ophthalmol & Strab.* 1988; 25(2): 60–66.
26. Beebe DC. Ocular growth and differentiation factors. In: Guroff G, ed., *Growth and Maturation Factors.* Vol. 3. New York: Wiley; 1985: 39–76.
27. Ozeki HF, et al. Suppression of lens stalk cell apoptosis by hyaluronic acid leads to faulty separation of the lens vesicle. *Exp Eye Res.* 2001; 72(1): 63–70.
28. Coulombre JL, Coulombre AJ. Lens development: IV. Size, shape and orientation. *Invest Ophthalmol Vis Sci.* 1969; 8: 251–257.
29. Beebe DC, et al. The mechanism of cell elongation during lens fiber cell differentiation. *Dev Biol.* 1982; 92(1): 54–59.
30. Schaepdrijver L, et al. The hyaloid vascular system of the pig. *Anat Embryol.* 1989: 549–554.
31. Feeney SA, et al. Role of vascular endothelial growth factor and placental growth factors during retinal vascular development and hyaloid regression. *Invest Ophthalmol Visual Sci.* 2003; 44(2): 839–847.
32. Hughes S, Yang H, Chan-Ling T. Vascularization of the human fetal retina: Roles of vasculogenesis and angiogenesis. *Invest Ophthalmol Visual Sci.* 2000; 41(5): 1217–1228.
33. Fruttiger M. Development of the mouse retinal vasculature: Angiogenesis versus vasculogenesis. *Invest Ophthalmol Visual Sci.* 2002; 43(2): 522–527.
34. Flower RW, et al. Postnatal retinal vascular development of the puppy. *Invest Ophthalmol Vis Sci.* 1985; 26(7): 957–968.
35. Mutlu F, Leopold IH. The structure of the fetal hyaloid system and tunica vasculosa lentis. *Arch Ophthalmo.* 1964; (71): 102–110.
36. Ashton N. Oxygen and the growth and development of retinal vessels. *Am J Ophthalmol.* 1966; 62: 412–435.
37. Jack RL. Regression of the hyaloid vascular system. An ultrastructureal analysis. *Am J Ophthalmol.* 1972; 74: 261–272.
38. Martin AC, et al. Pathogenesis of persistent hyperplastic primary vitreous in mice lacking the ARF tumor suppressor gene. *Invest Ophthalmol Vis Sci.* 2004; 45(10): 3387–3396.
39. Browning JA, et al. Proximal arterial vasoconstriction precedes regression of the hyaloid vasculature. *Curr Eye Res.* 2001; 22(6): 405–411.
40. Ito MF, Yoshioka MF. Regression of the hyaloid vessels and pupillary membrane of the mouse. *Anat Embryol.* 1999; 200(4): 403–411.
41. Zhu M, et al. The human hyaloid system: Cell death and vascular regression. *Exp Eye Res.* 2000; 70(6): 767–776.
42. Hay ED, Revel JP. Fine structure of the developing avian cornea. In: Wolsky A, Chen PS, eds. *Monographs in Developmental Biology.* Basel, Switzerland: Karger; 1969: 1.
43. Hay JP. Development of the vertebrate cornea. *Int Rev Cytol.* 1980; 63: 263–322.
44. Fitch J, et al. Collagen type IX and developmentally regulated swelling of the avian primary corneal stroma. *Dev Dyn.* 1998; 212(1): 27–37.
45. Beebe DC, Coats JM. The lens organizes the anterior segment: Specification of neural crest cell differentiation in the avian eye. *Dev Biol.* 2000; 220(2): 424–431.
46. Allen L, Burian HM, Braley AE. A new concept of the development of the anterior chamber angle. Its relationship to

developmental glaucoma and other structural anomalies. *Arch Ophthalmol.* 1955; 53: 783–798.
47. Montiani-Ferreira F, et al. Early postnatal development of central corneal thickness in dogs. *Vet Ophthalmol.* 2003; 6(1): 19–22.
48. Smelser GK, Ozanics V. The development of the trabecular meshwork in primate eyes. *Am J Ophthalmol.* 1971; 71: 366.
49. Aguirre GI, Rubin LF, Bistner SI. Development of the canine eye. *Am J Vet Res.* 1972; 33: 2399.
50. Yamashita TM, Sohal GSM. Development of smooth and skeletal muscle cells in the iris of the domestic duck, chick and quail. *Cell Tissue Res.* 1986; 244: 121–131.
51. Yamashita TM, Sohal GSM. Embryonic origin of skeletal muscle cells in the iris of the duck and quail. *Cell Tissue Res.* 1987; 249: 31–37.
52. Nakano KE, Nakamura H. Origin of the irideal striated muscle in birds. *J Embryol Exp Morph.* 1985; 88: 1–13.
53. Reme C, Urner U, Aeberhard B. The development of the chamber angle in the rat eye. *Graefe's Arch Clin Exp Ophthalmol.* 1983; 220: 139–153.
54. Reme C, Urner U, Aeberhard B. The occurrence of cell death during the remodeling of the chamber angle recess in the developing rat eye. *Graefe's Arch Clin Exp Ophthalmol.* 1983; 221: 113–121.
55. Anderson DR. The development of the trabecular meshwork and its abnormality in primary infantile glaucoma. *Trans Am Ophthalmol Soc.* 1981; 79: 458–485.
56. Barishak YR. The development of the angle of the anterior chamber in vertebrate eyes. *Doc Ophthalmol.* 1978; 45: 329–360.
57. Wulle KG. The development of the productive and draining system of the aqueous humor in the eye. *Adv Ophthalmol* 1972; (26): 296–355.
58. Samuelson DA, Gelatt KN. Aqueous outflow in the beagle. II. Postnatal morphologic development of the iridocorneal angle: Corneoscleral trabecular meshwork and angular aqueous plexus. *Curr Eye Res.* 1984; 3: 795–807.
59. Samuelson DA, Gelatt KN. Aqueous outflow in the beagle: Postnatal development of the pectinate ligament and trabecular meshwork. *Curr Eye Res.* 1984; 3: 783.
60. Cook CS, et al. RPE dysplasia with retinal duplication in a mutant mouse strain. *Exp Eye Res.* 1991; 52(4): 409–415.
61. Bumsted KM, Barnstable CJ. Dorsal retinal pigment epithelium differentiates as neural retina in the microphthalmia (mi/mi) mouse. *Invest Ophthalmol Visual Sci.* 2000; 41(3): 903–908.
62. Spira AW, Hollenberg MJ. Human retinal development: Ultrastructure of the inner retinal layers. *Dev Biol.* 1973; 31: 1–21.
63. Greiner JV, Weidman TA. Histogenesis of the cat retina. *Exp Eye Res.* 1980; 30(4): 439–453.
64. Greiner JV, Weidman TA. Histogenesis of the ferret retina. *Exp Eye Res.* 1981; 33(3): 315–332.
65. Greiner JV, Weidman TA. Embryogenesis of the rabbit retina. *Exp Eye Res.* 1982; 34(5): 749–765.
66. Erlich PB, et al. Major glycosaminoglycan species in the developing retina: Synthesis, tissue distribution and effects upon cell death. *Exp Eye Res.* 2003; 77(2): 157–165.
67. Shively JN, Epling GP, Jensen R. Fine structure of the postnatal development of the canine retina. *Am J Vet Res.* 1971; 32(3): 383–392.
68. Johns PR, Rusoff AC, Dubin MW. Postnatal neurogenesis in the kitten retina. *J Comp Neurol.* 1979; 187(3): 545–555.
69. Engelhardt M, et al. The neurogenic competence of progenitors from the postnatal rat retina in vitro. *Exp Eye Res.* 2004; 78(5): 1025–1036.
70. Fischer AJ. Neural regeneration in the chick retina. *Prog Retin Eye Res.* 2005; 24(2): 161–182. Epub 2004 Nov 11.
71. Bertram T, Coignoul F, Cheville N. Ocular dysgenesis in Australian Shepherd dogs. *J Am An Hosp Assoc.* 1984; 20: 177.
72. Barnett KC. Collie eye anomaly. *J Sm Anim Pract.* 1979; 20: 537–542.
73. Akiya S, et al. Electron microscopic study of the developing human vitreous collagen fibrils. *Ophthalmic Res.* 1986; 18(4): 199–202.
74. Bremer FM, Rasquin F. Histochemical localization of hyaluronic acid in vitreous during embryonic development. *Invest Ophthalmol Visual Sci.* 1998; 39(12): 2466–2469.
75. Los LI, et al. Vascular remnants in the rabbit vitreous body. II. Enzyme digestion and immunohistochemical studies. *Exp Eye Res.* 2000; 71(2): 153–165.
76. Los LI, Van Luyn MJA, Nieuwenhuis P. Vascular remnants in the rabbit vitreous body. I. Morphological characteristics and relationship to vitreous embryonic development. *Exp Eye Res.* 2000; 71(2): 143–151.
77. Bressan GM, et al. Emilin, a component of elastic fibers preferentially located at the elastin-microfibrils interface. *J Cell Biol.* 1993; 121(1): 201–212.
78. Horrigan SK, et al. Characterization of an associated microfibril protein through recombinant DNA techniques. *J Biol Chem.* 1992; 267(14): 10087–10095.
79. de las Casas CM, et al. High exogenous homocysteine modifies eye development in early chick embryos. *Birth Defects Res and Clin Mol Teratol.* 2003; 67(1): 35–40.
80. Brown AS, et al. Quantitation of hemodynamic function during developmental vascular regression in the mouse eye. *Invest Ophthalmol Vis Sci.* 2005; 46(7): 2231–2237.
81. Noden DM. Patterning of avian craniofacial muscles. *Dev Biol.* 1986; 116(2): 347–356.
82. Meier S, Tam PP. Metameric pattern development in the embryonic axis of the mouse. I. Differentiation of the cranial segments. *Differentiation.* 1982; 21(2): 95–108.
83. Meier S. The development of segmentation in the cranial region of vertebrate embryos. *Scan Electron Microsc.* 1982; (Pt 3): 1269–1282.
84. Tam PP, Meier S, Jacobson AG. Differentiation of the metameric pattern in the embryonic axis of the mouse. II. Somitomeric organization of the presomitic mesoderm. *Differentiation.* 1982; 21(2): 109–122.
85. Packard DS, Meier S. An experimental study of the somitomeric organization of the avian segmental plate. *Dev Biol.* 1983; 97(1): 191–202.
86. Tam PP. A study of the pattern of prospective somites in the presomitic mesoderm of mouse embryos. *J Embryol Exp Morphol.* 1986; 92: 269–285.
87. Jacobson AG. Somitomeres: Mesodermal segments of vertebrate embryos. *Development.* 1988; 104 Suppl: 209–220.

88. Tam PP, Trainor PAA. Specification and segmentation of the paraxial mesoderm. *Anat Embryol (Berl).* 1994; 189(4): 275–305.
89. Trainor PAA, Tam PP. Cranial paraxial mesoderm and neural crest cells of the mouse embryo: Co-distribution in the craniofacial mesenchyme but distinct segregation in branchial arches. *Development.* 1995; 121(8): 2569–2582.
90. Wahl CM, Noden DM, Baker R. Developmental relations between sixth nerve motor neurons and their targets in the chick embryo. *Dev Dyn.* 1994; 201(2): 191–202.
91. Sevel D. Reappraisal of the origin of human extraocular muscles. *Ophthalmology.* 1981; 88: 1330.
92. Sevel D. The origins and insertions of the extraocular muscles: Development, histologic features, and clinical significance. *Trans Am Ophthalmol Soc.* 1986; 84(1): 488–526.
93. Martin AC. Strabismus associated with extraocular muscle agenesis in a dog. *J Am Anim Hosp Assoc.* 1978; 14: 486–489.
94. Cohen MM, Sulik KK. Perspectives on holoprosencephaly: Part II. Central nervous system, craniofacial anatomy, syndrome commentary, diagnostic approach, and experimental studies. *J Craniofac Genet Dev Biol.* 1992; 12(4): 196–244.
95. Sulik KK, Johnston MC. Embryonic origin of holoprosencephaly: Interrelationship of the developing brain and face. *Scan Electron Microsc.* 1982; (Pt 1): 309–322.
96. Njoku CO, et al. Canine cyclopia. *Vet Rec.* 1978; 102(3): 60–61.
97. Saperstein G. Congenital defects in sheep. *J Am Vet Med Assoc.* 1975; 167: 314.
98. Binns W, et al. A congenital cyclopian-like malformation in lambs. *J Am Vet Med Assoc.* 1959; 134: 180–183.
99. Bryden MM, Evans HE, Keeler RF. Cyclopia in sheep caused by plant teratogens. *J Anat.* 1971; 110(3): 507.
100. Cooper MK, et al. Teratogen-mediated inhibition of target tissue response to Shh signaling. *Science.* 1998; 280(5369): 1603–1607.
101. Incardona JP, et al. The teratogenic veratrum alkaloid cyclopamine inhibits sonic hedgehog signal transduction. *Development.* 1998; 125(18): 3553–3562.
102. Keeler RF, Binns W. Teratogenic compounds of veratrum californicum (durand). II. Production of ovine fetal cyclopia by fractions and alkaloid preparations. *Can J Biochem.* 1966; 44(6): 829–838.
103. Keeler RF. Teratogenic compounds of veratrum californicum (durand) X. Cyclopia in rabbits produced by cyclopamine. *Teratology.* 1970; 3(2): 175–180.
104. Incardona JP, et al. Cyclopamine inhibition of sonic hedgehog signal transduction is not mediated through effects on cholesterol transport. *Dev Biol.* 2000; 224(2): 440–452.
105. Berman MB, Pierro LJ. Lens detachment and choroid fissure closure in the embryonic mouse eye. *Am Zool.* 1969; 9: 365.
106. Hero I, Farjah M, Scholtz CL. The prenatal development of the optic fissure in colobomatous microphthalmia. *Invest Ophthalmol Vis Sci.* 991; 32(9): 2622–2635.
107. Coulombre AJ. The role of intraocular pressure in the development of the chick eye. *J Exp Zool.* 1956; 133: 211–225.
108. Coulombre AJ, Coulombre L. Lens development. I. Role of the lens in eye growth. *J Exp Zool.* 1964; 156: 39–47.
109. Bard JB, Hay ED, Meller SM. Formation of the endothelium of the avian cornea: A study of cell movement in vivo. *Devel Biol.* 1975; 42: 334.
110. Cook CS. Experimental models of anterior segment dysgenesis. *Ophthalmic Ped Genet.* 1989; 10(1): 33–46.
111. Martin CL, Leipold HW. Aphakia and multiple ocular defects in Saint Bernard puppies. *Vet Med Small Anim Clin.* 1974; 69(4): 448–453.
112. Arnbjerg J, Jensen VJ. Spontaneous microphthalmia in two Doberman puppies with anterior chamber cleavage syndrome. *J Am Anim Hosp Assoc.* 1982; 18: 481–484.
113. Peiffer RL, Fischer CA. Microphthalmia, retinal dysplasia and anterior segment dysgenesis in a litter of Doberman Pinschers. *J Am Vet Med Assoc.* 1983; 183: 875.
114. Bergsjo T, et al. Congenital blindness with ocular developmental anomalies, including retinal dysplasia, in Doberman Pinscher dogs. *J Am Vet Med Assoc.* 1984; 184(11): 1383–1386.
115. Lewis DG, Kelly DF, Sansom J. Congenital microphthalmia and other developmental ocular anomalies in the Doberman. *J Sm Anim Pract.* 1986; 27: 559–566.
116. Laratta L, et al. Multiple congenital ocular defects in the Akita dog. *Cornell Vet.* 1985; 75(3): 381–392.
117. Gelatt KN, et al. Biometry and clinical characteristics of congenital cataracts and microphthalmia in the Miniature Schnauzer. *J Am Vet Med Assoc.* 1983; 183: 99–102.
118. Samuelson DA, et al. Prenatal morphogenesis of the congenital cataracts in the Miniature Schnauzer. *Lens Research.* 1987: 231–250.
119. Narfstrom K, Dubielzig R. Posterior lenticonus, cataracts and microphthalmia in the Cavalier King Charles Spaniel. *J Sm Anim Pract.* 1984; 25: 669–677.
120. Strande A, Nicolaissen B, Bjerkas I. Persistent pupillary membrane and congenital cataract in a litter of English Cocker Spaniels. *J Sm Anim Pract.* 1988; 29: 257–260.
121. Bayon A, et al. Ocular complications of persistent hyperplastic primary vitreous in three dogs. *Vet Ophthalmol.* 2001; 4(1): 35–40.
122. Boeve MH, et al. Persistent hyperplastic tunica vasculosa lentis and primary vitreous (PHTVL/PHPV) in the dog: A comparative review. *Prog Vet & Comp Ophthalmol.* 1992; 2(4): 163–172.
123. van der Linde-Sipman JS, Stades FC, de Wolff-Rouendaal D. Persistent hyperplastic tunica vasculosa lentis and persistent hyperplastic primary vitreous in the Doberman Pinscher: Pathological aspects. *J Am Anim Hosp Assoc.* 1983; 19: 791–802.
124. Kern TJ. Persistent hyperplastic primary vitreous and microphthalmia in a dog. *J Am Vet Med Assoc.* 1981; 178(11): 1169–1171.
125. Barrie KP, et al. Posterior lenticonus, microphthalmia, congenital cataracts and retinal folds in an old English Sheepdog. *J Am Anim Hosp Assoc.* 1979; 15: 715–717.
126. van der Linde-Sipman JS, van den Ingh TS, Vellema P. Morphology and morphogenesis of hereditary microphthalmia in Texel sheep. *J Comp Pathol.* 2003; 128(4): 269–275.
127. Rupp GP, Knight AP. Congenital ocular defects in a crossbred beef herd. *J Am Vet Med Assoc.* 1984; 184: 1149–1150.

128. Greene HJ, Leipold HW. Hereditary internal hydrocephalus and retinal dysplasia in shorthorn calves. *Cornell Vet.* 1974; 64: 367–375.
129. Kaswan RL, et al. Multiple hereditary ocular anomalies in a herd of cattle. *J Am Vet Med Assoc.* 1987; 191(1): 97–99.
130. Blackwell RL, Cobb EH. A hydrocephalus lethal in Hereford cattle. *J Hered.* 1959; (50)143.
131. Buyukmihci NC, Murphy CJ, Schulz T. Developmental ocular disease of raptors. *J Wildl Dis.* 1988; 24(2): 207–213.
132. Moore CP, et al. Congenital ocular anomalies and ventricular septal defect in a dromedary camel (*Camelus dromedarius*). *J Zoo Wildl Med.* 1999; 30(3): 423–430.
133. Wyand DS, et al. Intraocular lacrimal gland tissue with other ocular abnormalities occurring in a white-tailed deer. *J Comp Path.* 1972; 82: 219–221.
134. Manoly B. Blindness in newborn pigs. *Vet Rec.* 1951; 63: 398.
135. Hale F. The relation of vitamin A to anophthalmos in pigs. *Am J Ophthalmol.* 1935; 18: 1087–1093.
136. Roberts LD. Microphthalmia in swine. *J Hered.* 1948; 39: 146.
137. Mulder GB, et al. Effects of excess vitamin A on development of cranial neural crest–derived structures: A neonatal and embryologic study. *Teratology.* 2000; 62(4): 214–226.
138. Cook CS, Sulik KK. Laminin and fibronectin in retinoid-induced keratolenticular dysgenesis. *Invest Ophthalmol Vis Sci.* 1990; 31(4): 751–757.
139. Saunders LZ, Fincher MG. Hereditary multiple eye defects in grade Jersey calves. *Cornell Vet.* 1951; 41: 351–366.
140. Irby NL, Aguirre GD. Congenital aniridia in a pony. *J Am Vet Med Assoc.* 1985; 186: 281–283.
141. Perveen R, et al. Phenotypic variability and asymmetry of Rieger syndrome associated with PITX2 mutations. *Invest Ophthalmol Visual Sci.* 2000; 41(9): 2456–2460.
142. Sonoda S, et al. A novel PAX6 gene mutation (P118R) in a family with congenital nystagmus associated with a variant form of aniridia. *Graef's Arch Clin Exp Ophthal.* 2000; 238(7): 552–558.
143. Ewart SL, et al. The horse homolog of congenital aniridia conforms to codominant inheritance. *J Hered.* 2000; 91(2): 93–98.
144. Briziarelli G, Abrutyn D. Atypical coloboma in the optic disc of a Beagle. *J Comp Pathol.* 1975; 85(2): 237–240.
145. Gelatt KN, Huston K, Leipold HW. Ocular anomalies of incomplete albino cattle: Ophthalmoscopic examination. *Am J Vet Res.* 1969; 30: 1313–1316.
146. Gwin RM, et al. Multiple ocular defects associated with partial albinism and deafness. *J Am Anima Hospital Assoc.* 1981; 17: 401.
147. Zhao S, Overbeek PA. Regulation of choroid development by the retinal pigment epithelium. *Mol Vis.* 2001; 7: 277–282.
148. Cook CS, Burling K, Nelson EJ. Embryogenesis of posterior segment colobomas in the Australian Shepherd dog. *Prog Vet Comp Ophthalmol.* 1991; 1: 163–170.
149. Barnett KC, Stades FC. Collie eye anomaly in the Shetland Sheepdog in the Netherlands. *J Sm Anim Pract.* 1979; 20(6): 321–329.
150. Bedford PG. Collie eye anomaly in the Border Collie. *Vet Rec.* 1982; 111(2): 34–35.
151. Rubin LF, Nelson EJ, Sharp CA. Collie eye anomaly in Australian Shepherd dogs. *Prog Vet Comp Ophthal.* 1991; 1(2): 105–108.
152. Bedford PG. Collie eye anomaly in the Lancashire Heeler. *Vet Rec.* 1998; 143(13): 354–356.
153. Lowe JK, et al. Linkage mapping of the primary disease locus for Collie eye anomaly. *Genomics.* 2003; 82(1): 86–95.
154. Adams SB. Periocular dermoid cyst in a calf. *J Am Vet Med Assoc.* 1983; 182: 1255.
155. Barkyoumb SD, Leipold HW. Nature and cause of bilateral ocular dermoids in Hereford cattle. *Vet Path.* 1984; 21: 316–324.
156. Peiffer RL. Bilateral congenital aphakia and retinal detachment in a cat. *J Am Anim Hosp Assoc.* 1982; 18: 128–130.
157. Rebhum WC. Congenital anterior staphyloma with rudimentary lens in a calf. *J Am Vet Med Assoc.* 1977; 171: 440–442.
158. Swanson HL, et al. A case of Peters' anomaly in a Springer Spaniel. *J Comp Pathol.* 2001; 125(4): 326–330.
159. Bellhorn RW. A survey of ocular findings in eight- to ten-month-old Beagles. *J Am Vet Med Assoc.* 1974; 164(11): 1114–1116.
160. Roberts SR, Bistner SI. Persistent pupillary membrane in Basenji dogs. *J Am Vet Med Assoc.* 1968; 153(5): 533–542.
161. Bistner SI, Rubin LF, Roberts SR. A review of persistent pupillary membranes in the Basenji dog. *J Am Anim Hosp Assoc.* 1971; 7: 143–157.
162. Bahn CF, et al. Classification of corneal endothelial disorders based on neural crest origin. *Ophthalmology.* 1984; 91: 558–563.
163. Kupfer C, Kaiser-Kupfer MI. New hypothesis of developmental anomalies of the anterior chamber associated with glaucoma. *Trans Ophthal Soc UK.* 1978; (98): 213–215.
164. Kupfer C, Kuwabara T, Stark WJ. The histopathology of Peters' anomaly. *Am J Ophthalmol.* 1975; (80): 653–660.
165. Shields MB, et al. Axenfeld-Rieger syndrome. A spectrum of developmental disorders. *Surv Ophthalmol.* 1985; 29: 3 87–409.
166. Waring GO, Rodrigues MM, Laibson PR. Anterior chamber cleavage syndrome: A stepladder classification. *Surv Ophthalmol.* 1975; (20): 3–33.
167. Cook CS, Nowotny AZ, Sulik KK. Fetal alcohol syndrome: Eye malformations in a mouse model. *Arch Ophthalmol.* 1987; 105: 1576–1581.
168. Miller MT, et al. Anterior segment anomalies associated with the fetal alcohol syndrome. *J Pediatr Ophthalmol and Strabis.* 1984; (21): 8–18.
169. Miller MT, Israel J, Cuttone J. Fetal alcohol syndrome. *J Pediatr Ophthalmol and Strabis.* 1981; (18): 6–15.
170. Stromland K, Miller M, Cook C. Ocular teratology. *Surv Ophthalmol.* 1991; 35(6): 429–446.
171. Molleda JM, et al. Microphakia associated with lens luxation in the cat. *J Am Anim Hosp Assoc.* 1995; 31(3): 209–212.
172. Aso S, et al. Hypoplastic basement membrane of the lens anlage in the inheritable lens aplastic mouse (lap mouse). *Teratology.* 2000; 61(4): 262–272.

173. Aso S, et al. Apoptosis in the lens anlage of the heritable lens aplastic mouse (lap mouse). *Teratology.* 1998; 58(2): 44–53.
174. Hartwig NG, Vermeij-Keers C, Versteeg J. The anterior eye segment in virus induced primary congenital aphakia. *Acta Morphol Neerl Scand.* 1988; 26(4): 283–292.
175. Gemensky-Metzler AJ, Wilkie DA, Cook CS. The use of semiconductor diode laser for deflation and coagulation of anterior uveal cysts in dogs, cats and horses: A report of 20 cases. *Vet Ophthalmol.* 2004; 7(5): 360–368.
176. Ramsey DT, Hauptman JG, Petersen-Jones SM. Corneal thickness, intraocular pressure, and optical corneal diameter in Rocky Mountain horses with cornea globosa or clinically normal corneas. *Am J Vet Res.* 1999; 60(10): 1317–1321.
177. Ramsey DT, et al. Congenital ocular abnormalities of Rocky Mountain horses. *Vet Ophthalmol.* 1999; 2(1): 47–59.
178. Ori J, et al. Posterior lenticonus with congenital cataract in a Shih Tzu dog. *J Vet Med Sci.* 2000; 62(11): 1201–1203.
179. Monaco MA, Samuelson DA, Gelatt KN. Morphology and postnatal development of the normal lens in the dog and congenital cataract in the Miniature Schnauzer. *Lens Research.* 1985: 393–433.
180. Zhang R, et al. Analysis of eye lens–specific genes in congenital hereditary cataracts and microphthalmia of the Miniature Schnauzer dog. *Invest Ophthalmol Vis Sci.* 1991; 32(9): 2662–2665.
181. Martin CL, Wyman M. Glaucoma in the Basset Hound. *J Am Vet Med Assoc.* 1968; 153: 1320–1327.
182. Wyman CL, Ketring K. Congenital glaucoma in the Basset Hound: A biologic model. *Trans Sect Ophthalmol Am Acad Ophthalmol Otolaryngol.* 1976; 81(4, Pt 1): OP645–652.
183. Van Rensburg IBJ, et al. Multiple inherited eye anomalies including persistent hyperplastic tunica vasculosa lentis in Bouvier des Flandres. *Vet and Comp Ophthalmol.* 1992; 2(3): 133–139.
184. Bjerkas E, Ekesten B, Farstad W. Pectinate ligament dysplasia and narrowing of the iridocorneal angle associated with glaucoma in the English Springer Spaniel. *Vet Ophthalmol.* 2002; 5(1): 49–54.
185. Martin CL. Development of the pectinate ligament structure of the dog. *Am J Vet Res.* 1974; 35: 1433.
186. Brown A, Munger R, Peiffer RL. Congenital glaucoma and iridoschisis in a Siamese cat. *Vet & Comp Ophthalmol.* 1994; 4(3): 121–124.
187. Keller WF, Blanchard GL, Krehbiel JD. Congenital dysplasia in a canine eye: A case report. *J Am Anim Hosp Assoc.* 1972; 8: 29–34.
188. Stades FC. Persistent hyperplastic tunica vasculosa lentis and persistent hyperplastic primary vitreous in Doberman Pinschers: Genetic aspects. *J Am Anim Hosp Assoc.* 1983; 19: 957–964.
189. MacMillan AD, Lipton DE. Heritability of multifocal retinal dysplasia in American Cocker Spaniels. *J Am Vet Med Assoc.* 1978; 172: 568–572.
190. Heywood R, Wells GA. A retinal dysplasia in the Beagle dog. *Vet Rec.* 1970; 87: 178–180.
191. Schiavo DM, Field WE. Unilateral focal retinal dysplasia in Beagle dogs. *Vet Med Small Anim Clin.* 1974; 69(1): 33–34.
192. Rubin LF. Hereditary retinal detachment in Bedlington Terriers: A preliminary report. *Small Anim Clin.* 1963; 3: 387–389.
193. Rubin LF. Heredity of retinal dysplasia in Bedlington Terriers. *J Am Vet Med Assoc.* 1968; 152(3): 260–262.
194. Ashton N, Barnett KC, Sachs DD. Retinal dysplasia in Sealyham Terriers. *J Path Bact.* 1968; 96: 269–272.
195. Barnett KC, Bjorck GR, Kock E. Hereditary retinal dysplasia in the Labrador Retriever in England and Sweden. *J Sm Anim Pract.* 1970; 10: 755–759.
196. Meyers VN, et al. Short-limbed dwarfism and ocular defects in the Samoyed dog. *J Am Vet Med Assoc.* 1983; 183(9): 975–979.
197. Aroch I, Ofri R, Aizenberg I. Haematological, ocular and skeletal abnormalities in a Samoyed family. *J Sm Anim Pract.* 1996; 37(7): 333–339.
198. O'Toole D, et al. Retinal dysplasia of English Springer Spaniel dogs: Light microscopy of the postnatal lesions. *Vet Pathol.* 1983; 20(3): 298–311.
199. Lavach JD, Murphy JM, Severin GA. Retinal dysplasia in the English Springer Spaniel. *J Am Anim Hosp Assoc.* 1978; 14: 192–199.
200. Schmidt GM, et al. Inheritance of retinal dysplasia in the English Springer Spaniel. *J Am Vet Med Assoc.* 1979; 174: 1089–1090.
201. Bedford PG. Multifocal retinal dysplasia in the Rottweiler. *Vet Rec.* 1982; 111(13): 304–305.
202. Murphy CJ, et al. Retinal dysplasia in a hybrid falcon. *J Am Vet Med Assoc.* 1985; 187(11): 1208–1209.
203. Whiteley HE. Dysplastic canine retinal morphogenesis. *Invest Ophthalmol Vis Sci.* 1991; 32(5): 1492–1498.
204. Holle DM, et al. The geographic form of retinal dysplasia in dogs is not always a congenital abnormality. *Vet Ophthalmol.* 1999; 2(1): 61–66.
205. Albert DM, et al. Canine herpes-induced retinal dysplasia and associated ocular anomalies. *Invest Ophthalmol Vis Sci.* 1976; 15: 267–278.
206. Percy DH, et al. Lesions in puppies surviving infection with canine herpesvirus. *Vet Path.* 1971; 8: 37–53.
207. Bistner SI, Rubin LF, Saunders LZ. The ocular lesions of bovine viral diarrhea-mucosal disease. *Pathol Vet.* 1970; 7: 275.
208. Brown TT, et al. Pathogenetic studies of infection of the bovine fetus with bovine viral diarrhea virus. II. Ocular lesions. *Vet Path.* 1975; 12: 394–404.
209. Kahrs RF, Scott FW, de Lahunta A. Congenital cerebellar hypoplasia and ocular defects in calves following bovine virus diarrhea-mucosal disease infection in pregnant cattle. *J Am Vet Med Assoc.* 1970; 156: 1443.
210. Silverstein AM, et al. An experimental virus-induced retinal dysplasia in the fetal lamb. *Am J Ophthalmol.* 1971; 72: 22.
211. Percy DH, Scott FW, Albert DM. Retinal dysplasia due to feline panleukopenia virus infection. *J Am Vet Med Assoc.* 1975; 167: 935–937.
212. Shively JN, et al. Pathogenesis of radiation-induced retinal dysplasia. *Invest Ophthalmol Vis Sci.* 1970; 9: 888–900.
213. Shively JN, et al. Dose relationships of pathologic alterations in the developing retina of irradiated dogs. *Am J Vet Res.* 1972; 33: 2121–2134.
214. Fox MW. Postnatal ontogeny of the canine eye. *J Am Vet Med Assoc.* 1963; 143: 968–974.
215. Narfstrom K. Hereditary and congenital ocular disease in the cat. *J Feline Med Surg.* 1999; 1(3): 135–141.

216. Martin CL, Stiles J, Willis M. Feline colobomatous syndrome. *Vet & Comp Ophthalmol.* 1997; 7(1): 39–43.
217. Koch SA. Congenital ophthalmic abnormalities in the Burmese cat. *J Am Vet Med Assoc.* 1979; 174(1): 90–91.
218. Glaze MB. Congenital and hereditary ocular abnormalities in cats. *Clin Tech Small Anim Pract.* 2005; 20(2): 74–82.
219. Kern TJ, Murphy CJ. Partial upper eyelid agenesis in a peregrine falcon. *J Am Vet Med Assoc.* 1985; 187: 1207.
220. Stades FC. Persistent hyperplastic tunica vasculosa lentis and persistent hyperplastic primary vitreous (PHTVL/PHPV) in 90 closely related Doberman Pinschers: Clinical aspects. *J Am Anim Hosp Assoc.* 1980; 16: 739–751.
221. Collins B, et al. Familial cataracts and concurrent ocular anomalies in Chow Chows. *J Am Vet Med Assoc.* 1992; 200(10): 1485–1491.

Chapter 2

Ophthalmic Anatomy

Don A. Samuelson

The eye is undoubtedly the most uniquely crafted sensory organ of the vertebrate body. Its design incorporates all the major tissues in a remarkable, cameralike fashion, allowing individuals to be aware of their surroundings by emission and reflection of light. Along the path of vertebrate evolution, the eye has largely retained the same basic components and manner of development even though animal habits, as well as animal habitats, have become broadly diverse.

Nevertheless, each component or feature of the eye has undergone variable changes for one or more primary ecologic reasons. These changes, which have spawned additional secondary changes, have resulted in formation of the present ocular patterns.[1] Of the different factors that have influenced changes in eye morphology and physiology, the presence, absence, and variations in the intensity of light have been most significant. Adaptations to light intensity and duration have resulted in the division of vertebrates among the animal kingdom into three broad categories: diurnal, nocturnal, and arrhythmic.

Diurnal animals are essentially active during the day. They possess optimal visual acuity at that time and "poor" vision at night. Examples of diurnal animals are certain reptiles (e.g., turtles and colubrid snakes), many birds, nonhuman primates, marmots, squirrels, and pigs. Nocturnal animals are essentially active during the night, and they possess good vision under dimly lighted conditions. Included in this group are crepuscular animals that optimally use the twilight hours of morning and evening. Many animals can be described as being nocturnal or crepuscular, including bats, most reptiles, many rodents, ungulates, and carnivores. Larger representatives of the ungulates and carnivores comprise a third group of arrhythmic animals, which, for the most part, are equally active during the day and the night.[2] Each of these categories can be further subdivided according to feeding behavior (i.e., prey and predator).[3]

Certainly, time of visual activity and feeding behavior have played profound roles in evolution of the eye and modification of its components. These and other environmental pressures have resulted in formation of several highly evolved types of eyes from a common ancestral origin. Species of teleostean fishes, birds, and mammals have eyes with very good vision. Interestingly, the physiologic and morphologic mechanisms for attaining good quality of vision (i.e., presence of fovea and strong accommodative capabilities) are the same in each group of animals, even though evolution of these mechanisms occurred independently rather than sequentially. A similar adaptive pattern can be found among nocturnal species of vertebrates in the mechanisms regulating light by way of pupillary closure and photomechanical changes in the retina.[1,3] As the anatomy of various species are described in this chapter, we will see a natural tendency of many ocular components in distantly related species to converge evolutionarily under similar environmental conditions.

When studying comparative ophthalmology, a major hurdle is to comprehend all the different structures of the vertebrate eye, their individual functions, and how they combine to form the visual system. Comprehension of these essential schemes and concepts provides the basis for understanding clinical ophthalmology. Both normal and abnormal anatomy play important roles in ophthalmic diagnoses. Unlike those of many medical disciplines, however, most ophthalmic diagnoses are made on the basis of what one observes anatomically.

Commonly used diagnostic equipment such as the biomicroscope and the direct ophthalmoscope afford sufficient magnification to approach the histologic level; consequently, ophthalmologists are not content with only a knowledge of gross anatomy. In addition, no other routinely performed branch of surgery in veterinary medicine requires the same exactness of incision depth (to the level of micrometers) or of incision location and length (to the level of millimeters).

In conjunction with the anatomic patterns found in the vertebrate eye, there is a wide diversity of periocular structures collectively referred to as the *adnexa,* which provide protection and support for the globe as well as assist in its function. These structures are examined first.

ADNEXA—PROTECTIVE APPARATUS OF THE EYE

Orbit

The orbit is the bony fossa that separates the eye from the cranial cavity, surrounds and protects it, and provides several pathways through foramina for the various blood vessels and nerves involved in eye function. The size, shape, and position

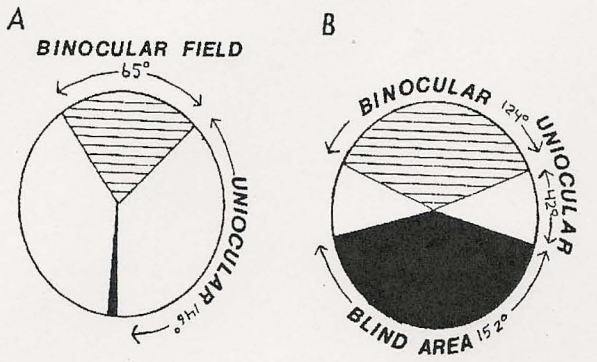

Figure 2.1. **A.** Equine visual field, showing a small binocular field, large panoramic uniocular areas, and a small blind area. **B.** Primate visual field, showing a large binocular field, small uniocular areas, and large blind area. (Redrawn from Duke-Elder S. *System of Ophthalmology. Vol. I. The Eye in Evolution.* London: Henry Kimpton, 1958.)

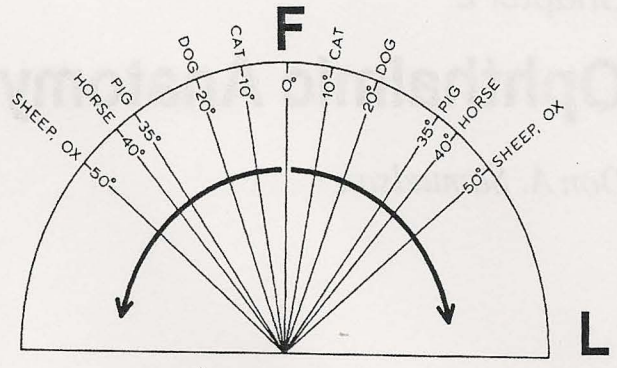

Figure 2.2. Comparison of angles formed by the optic axes of different domestic species. *F,* frontal; *L,* lateral. (Modified from Getty R. *Sisson and Grossman's the Anatomy of the Domestic Animal.* 5th ed. Philadelphia: WB Saunders, 1975.)

Table 2.1 Orbital Dimensions of Domestic Animals

Dimension	Feline (mm)	Canine (mm)	Bovine (mm)	Equine (mm)
Orbital Diameter				
Width	24	29	65	62
Height	26	28	64	59
Depth	—	49	120	98
Distance Between Orbits	23	36	151	173

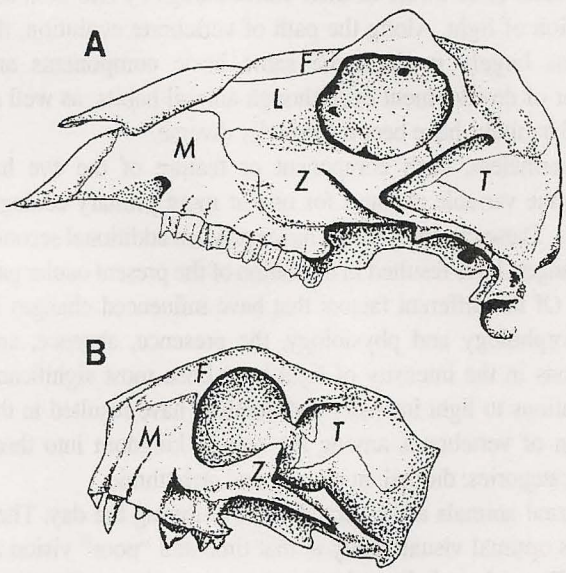

Figure 2.3. The enclosed orbit of the sheep (**A**) is typical of most grazing animals, whereas the open orbit of the domestic cat (**B**) exemplifies all carnivores. *F,* frontal; *L,* lacrimal; *M,* maxilla; *O,* orbit; *P,* parietal; *Z,* zygomatic. (Redrawn from Prince JH. *Comparative Anatomy of the Eye.* Springfield, IL: Charles C. Thomas, 1956.)

of the orbit are closely associated with the same two factors, time of visual activity and feeding behavior, that have markedly influenced global anatomy. The depth of the orbit contributes mostly to the protection and appearance of the eye, whereas the location of the orbit within the skull largely governs expanse of the visual field as well as the degree of depth of field for a given species or breed (Fig. 2.1; Table 2.1). In carnivores such as the cat and dog, the axes of their eyes are set rostrolaterally, approximately 10° and 20° from their midlines, respectively.[4] As a result, these animals have a great deal of binocular vision. In the horse and ruminants, which mainly have monocular vision, the orbits are quite far lateral in location, approximately 40° in horses and 50° from the midline in cattle (Fig. 2.2).

In addition to size, shape, and position, a separate feature divides all vertebrate orbits into two kinds: the enclosed, which is completely encompassed by bone; and the open or incomplete, which is partially surrounded by bone (Fig. 2.3). Among domestic animals, the horse, ox, sheep, cattle, and goat have enclosed orbits. By comparison, pigs and carnivores (i.e., dogs and cats) have open orbits. It is believed the enclosed orbit is essential for protection and skull reinforcement during dominance rituals, whereas the open orbit gives carnivores the ability to open their jaws widely at the sacrifice of orbital closure.[3]

The bony fossa consists of five to seven bones, depending on the species (Table 2.2). The orbit in the dog is composed of five, and sometimes six, bones, the supraorbital ligament that extends from the frontal to the zygomatic bones, and the periosteum (Fig. 2.4). The orbital rim is formed by the frontal, lacrimal, and zygomatic bones. Laterally, the orbit is formed by the supraorbital ligament, whereas the floor of the orbit, which is incomplete, is formed by the sphenoid and palatine bones. In animals with enclosed orbits, closure of the temporal side of the orbit is accomplished by union of the zygomatic process of the

Table 2.2 Orbital Bones by Species

Animal	Lacrimal	Zygomatic	Frontal	Sphenoid	Palatine	Maxillary	Ethmoid	Temporal
Dog	X	X	X	X	X	X		
Cat	X	X	X	X	X	X		
Horse	X	X	X	X	X			X
Ox	X	X	X	X	X	X		
Sheep	X	X	X	X	X	X		
Goat	X	X	X	X	X			
Pig	X	X	X	X	X		X	
Rabbit	X	X	X	X	X			X
Man	X	X	X	X	X	X	X	

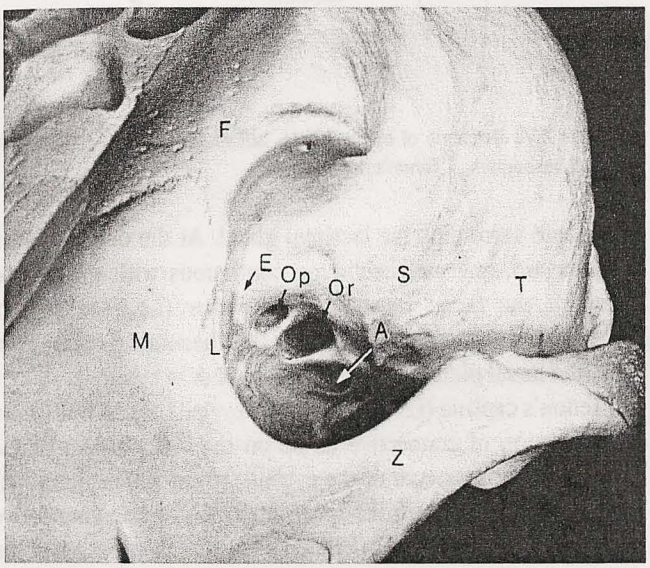

Figure 2.4. Canine orbit. Bones of the orbit shown: *F,* frontal; *L,* lacrimal; *M,* maxilla; *S,* sphenoid; *T,* temporal; *Z,* zygomatic. Orbital formina shown: *A,* rostral alar; *E,* ethmoidal; *Op,* optic; *Or,* orbital fissure.

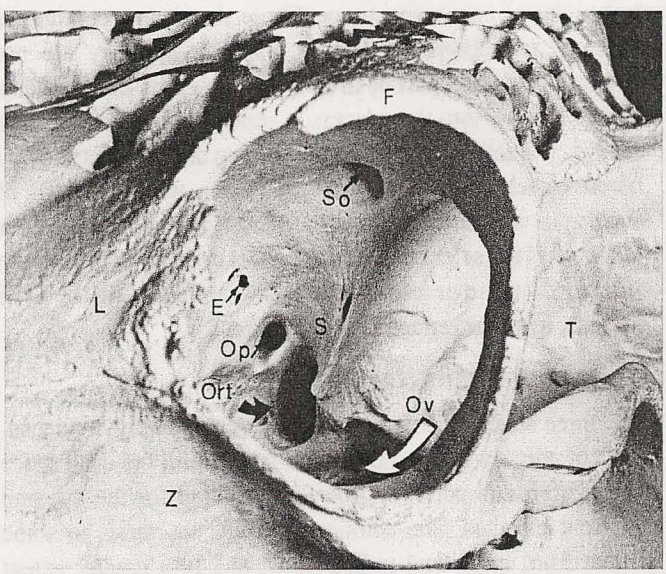

Figure 2.5. Bovine orbit. Bones of the orbit shown: *F,* frontal; *L,* lacrimal; *S,* sphenoid; *T,* temporal; *Z,* zygomatic. Orbital foramina shown: *E,* ethmoidal; *Op,* optic; *Ort,* orbitorotundum; *Ov,* ovale; *So,* supraorbital.

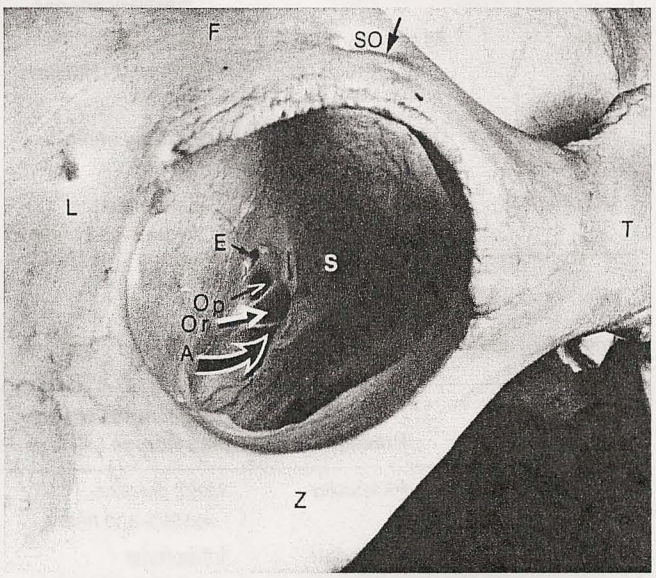

Figure 2.6. Equine orbit. Bones of the orbit shown: *F,* frontal; *L,* lacrimal; *S,* sphenoid; *T,* temporal; *Z,* zygomatic. Orbit foramina shown: *A,* rostral alar; *E,* ethmoidal; *Op,* optic; *Or,* orbital fissure; *So,* supraorbital.

frontal bone with the frontal process of the zygomatic bone (Fig. 2.5). In the horse, the zygomatic process of the temporal bone intervenes between these two and completes the orbital rim (Fig. 2.6).

Within the orbit, various foramina and fissures provide an osseous pathway by which blood vessels and nerves pass from the cranial cavity and alar canal into the orbital region. Those foramina, of rather constant position in domestic animals are the rostral alar, ethmoidal, lacrimal, orbital, ovale, optic, rotundum, and supraorbital. Other foramina closely related to the orbital structures are within the pterygopalatine region, and these are the maxillary, caudal palatine, and sphenopalatine (Tables 2.3 and 2.4). The orbital foramen is elongated in most domestic animals except the horse; therefore, it is referred to as the orbital fissure. In cattle, the orbital fissure and foramen rotundum are commonly fused to form the foramen orbitorotundum (Figs. 2.4, 2.5, and 2.6).

Table 2.3 Orbital Foramina and Associated Nerves and Vessels in Domestic Animals

Foramen or Fissure	Presence in Domestic Species	Associated Nerves and Vessels
Alar, rostral	Canine, equine, feline	Maxillary artery and nerve
Ethmoidal (1 or more)	All species	Ethmoidal vessels and nerve
Orbital	Canine, equine, feline	Abducens, oculomotor, ophthalmic, and trochlear nerves
Orbitorotundum	Bovine	III–IV cranial nerves, retinal, and internal maxillary arteries
Optic	All species	Optic nerve, internal ophthalmic artery
Rotundum	Canine, equine, feline	Maxillary nerve
Supraorbital	Bovine, canine, equine (feline variable)	Supraorbital vessels and nerve

Table 2.4 Foramina of the Pterygopalatine Region

Foramen	Presence	Associated Vessels and Nerves
Caudal palatine	All species	Major palatine vessels and nerve
Maxillary	All species	Infraorbital vessels and nerve
Sphenopalatine	All species	Sphenopalatine vessels and pterygopalatine nerve

Orbital Fascia

The orbital fascia consists of a thin, tough, connective tissue liner that envelops all the structures within the orbit, including the bony fossa itself. This fascia can be subdivided into three anatomic entities: the periorbita, fascia bulbi or Tenon's capsule, and fascial sheaths of the extraocular muscles (Fig. 2.7).

The periorbita is a conically shaped, fibrous membrane that lines the orbit and encloses the eyeball with its muscles, blood vessels, and nerves. Its apex is at the exit of the optic nerve from the orbit. At this point, it is continuous with the dural sheath of the optic nerve; in the orbit, it is thin, attaches firmly to the orbital bones, and forms their periosteum. In the dog, the periorbita does not always fuse with the periosteum of the frontal and the sphenoid bones.[5] Instead, the periosteum and periorbita often remain distinct and separate in these regions of the orbit. In animals with an incomplete lateral orbital wall, the periorbita is thicker laterally next to the orbital ligament. Anteriorly, in the dorsolateral part of the orbit, the periorbita

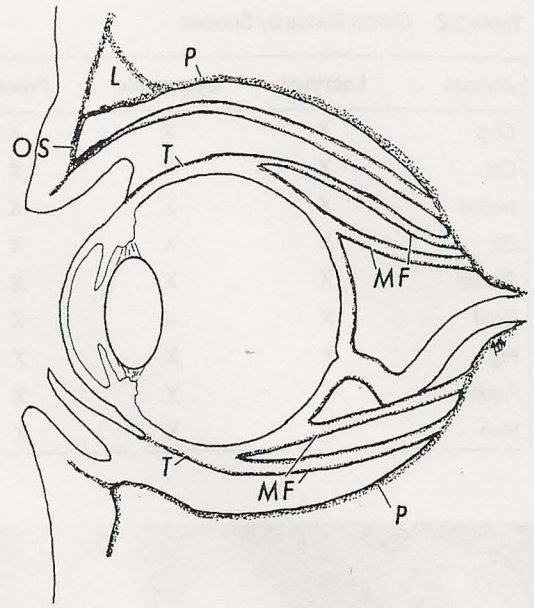

Figure 2.7. Divisions of orbital fascia. *MF,* muscle fascia; *P,* periorbita; *OS,* orbital septum; *T,* Tenon's capsule.

splits and surrounds the lacrimal gland. At the orbital rim, it splits again, one part becoming continuous with the periosteum of the facial bones and the other (i.e., the septum orbitale) merging with the eyelids and becoming continuous with the tarsal plates (i.e., the fibrous sheet in eyelids).

Tenon's capsule (i.e., sheath of the eyeball, fascia bulbi) is a condensation of connective tissue on the outer aspect of the sclera (i.e., fibrous coat of the eyeball), from which it is separated by a narrow, cleftlike space filled with loose connective tissue (i.e., Tenon's space). Tenon's capsule is attached to the sclera near the corneoscleral junction, and it blends or becomes continuous with the fascia surrounding the extraocular muscles.

The fascial sheaths of the extraocular muscles are dense, fibrous membranes loosely attached to the muscles with fine trabeculae of connective tissue. These sheaths are continuous with, or reflections of, Tenon's capsule, but they are not always considered part of it. In the dog, the muscular fasciae can be divided into three layers: a superficial, thick layer that extends caudally from the orbital septum and is penetrated by blood vessels and nerves; a middle layer, which consists of superficial and deep sheets that anteriorly attach to the outer junction of the sclera and cornea; and a deep layer next to the surface of the extraocular muscles that separates the recti muscles from the retractor oculi muscles.[5]

Extraocular Muscles and Fat

The three sheets of orbital fascia are separated by condensations of adipose tissue (i.e., orbital fat) that fill the dead space in the orbit and act as a protective cushion for the eye and adjacent muscles. The amount of orbital fat varies to some extent from individual to individual and to a greater extent from one animal species to another. Some animals, including birds and many reptiles (e.g., turtles and snakes) possess very little orbital fat, having relatively small orbits almost entirely filled by their globes.[2]

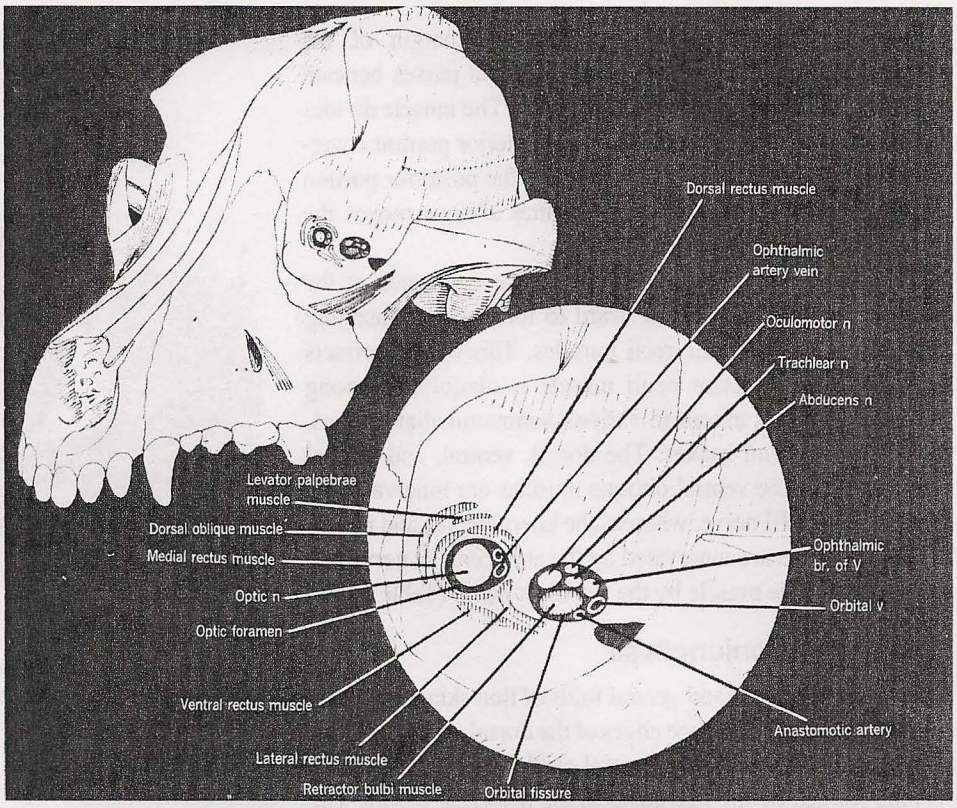

Figure 2.8. Orbital apex of the dog, illustrating structures passing through the optic foramen and orbital fissure as well as the extraocular muscle attachments. (Modified with permission from Evans H, Christensen G. *Miller's Anatomy of the Dog.* 2nd ed. Philadelphia: WB Saunders, 1979.)

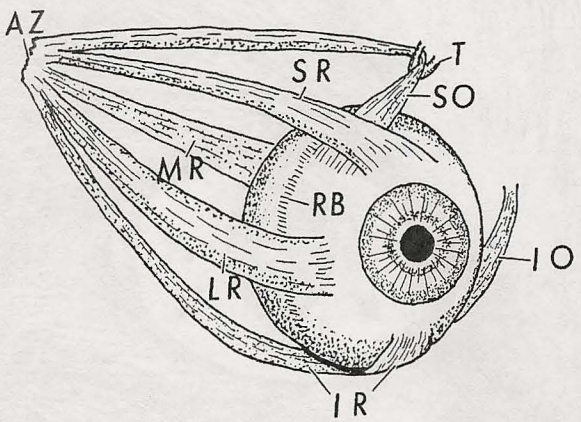

Figure 2.9. Arrangement of the orbital muscles of domestic animals. *AZ,* annulus of Zinn; *IO,* inferior oblique muscle; *IR,* inferior rectus muscle; *LR,* lateral rectus muscle; *RB,* retractor bulbi muscle attachments; *SO,* superior oblique muscle; *SR,* superior rectus muscle. (Redrawn from Prince JH, et al. *Anatomy and Histology of the Eye and Orbit in Domestic Animals.* Springfield, IL: Charles C. Thomas, 1960.)

The extraocular muscles suspend the globe in the orbit and provide ocular motility. There are four rectus muscles: the dorsal, ventral, medial, and lateral recti. They originate from the orbital apex (i.e., annulus of Zinn) and insert, in the dog, approximately 5 mm posterior to the limbus medially, 6 mm ventrally, 7 mm dorsally, and 9 mm laterally (Figs. 2.8 and 2.9). They move the eye in the direction of their names (Table 2.5). The dorsal (i.e., superior) oblique originates from the medial orbital apex, continuing forward dorsomedially to pass through a trochlea located near the medial canthus. It then turns acutely, passing dorsolaterally to the globe. It pulls the dorsal aspect of the globe medially and ventrally. The ventral

Table 2.5 Extrinsic Muscles of the Eye and Eyelids: Their Function and Nerve Supply

Muscle	Function	Nerve Supply
Eyeball		
Dorsal (superior) rectus	Rotate globe upward	Oculomotor
Ventral (inferior) rectus	Rotate globe downward	Oculomotor
Medial rectus	Rotate globe medially	Oculomotor
Lateral rectus	Rotate globe laterally	Abducens
Dorsal (superior) oblique	Rotate dorsal part of globe medially and ventrally	Trochlear
Ventral (inferior) oblique	Rotate ventral part of globe medially and dorsally	Oculomotor
Retractor oculi (bulbi)	Retract globe	Abducens
Eyelid		
Levator palpebrae superioris	Raise upper eyelid	Oculomotor
Orbicularis oculi	Close palpebral fissure	Facial
Retractor anguli oculi	Lengthen lateral palpebral fissure	Facial
Corrugator supercilii	Assist in elevating upper eyelid	Facial

oblique originates from the anterolateral margin of the palatine bone on the medial orbital wall and passes beneath the eye, crossing the ventral rectus tendon. The muscle divides as it reaches the lateral rectus, with the anterior portion covering the insertion of the lateral rectus and the posterior portion inserting beneath the rectus. The ventral oblique moves the globe medially and dorsally.[4]

The retractor oculi (i.e., bulbi) muscle originates at the orbital apex and continues forward to form a cone inserting posterior and deep to the recti muscles. This bundle retracts the globe. The retractor oculi muscle is ubiquitous among mammals, but it is absent in various nonmammalian groups, including birds and snakes. The dorsal, ventral, and medial recti as well as the ventral oblique muscles are innervated by the oculomotor III nerve, whereas the lateral rectus and retractor oculi muscles are innervated by the abducens VI nerve and the dorsal oblique muscle by the trochlear nerve (Table 2.5).

Eyelids and Conjunctivae

The eyelids are dorsal and ventral folds of thin skin continuous with the facial skin. The free edges of the dorsal and ventral lids meet to form the lateral and medial canthi (i.e., canthus). The opening formed by the free edges is the palpebral fissure. The fissure is prevented from assuming a circular shape by medial (i.e., nasal) and lateral (i.e., temporal) palpebral ligaments that attach the canthi to the orbital wall. The medial ligament inserts into the periosteum of the nasal bones, whereas laterally the retractor anguli oculi muscle inserts into the temporal fascia. The lateral ligament is absent in the dog, being replaced by the retractor anguli oculi muscle. Closure of the eyelids is achieved by contraction of the orbicularis oculi muscle located deep in the lids around the palpebral fissure. Opening or parting of the lids is by relaxation of the orbicularis oculi and contraction of the levator palpebrae superioris, which inserts into the upper tarsus (i.e., tarsal plate).

The free margin of the eyelid may contain a row of cilia or lashes. These lashes are directed away from the anterior surface of the cornea. The lower eyelids are devoid of lashes in most domestic species.

In the normal canine eye, the eyelids rest on the globe, with the upper and lower lids meeting laterally at the lateral canthus and medially at the medial canthus (Fig. 2.10). The upper eyelid has two to four rows of eyelashes (i.e., cilia) that usually begin near the medial quarter or third and either extend across to the lateral canthus or end shortly before the canthus. The lower eyelid has no cilia and has a hairless region approximately 2 mm wide adjacent to the lid margin extending the length of the lower lid and around the lateral canthus. The medial canthus, unlike the lateral canthus, has variable amounts of facial hair.

In the cat, the eyelids rest snugly on the cornea, and little, if any, sclera is exposed (Fig. 2.11). The lower eyelid has no cilia. The upper eyelid also exhibits none, but the leading row of hair from the medial third laterally appears to be distinct enough in most cats to be considered cilia. The lid margins are hairless and distinct.

In the horse, the eyelids fit snugly over the globe, except near the medial canthus, at which a protuberance of variable size

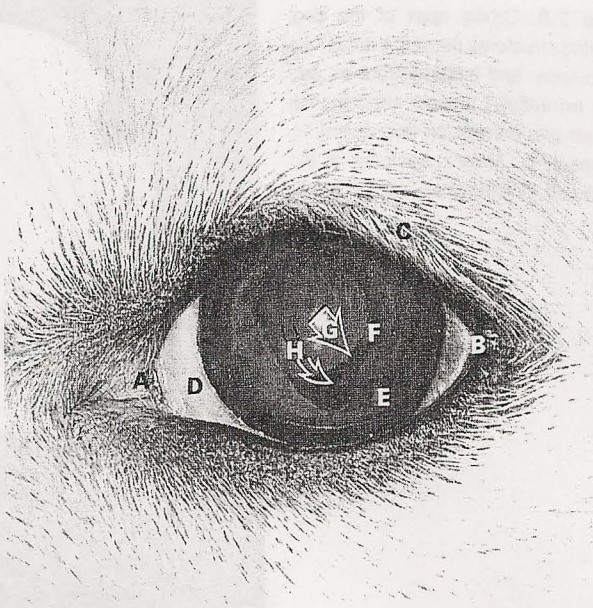

Figure 2.10. Surface anatomy of the dog's eye and adnexa at rest. *A,* medial canthus; *B,* lateral canthus; *C,* cilia; *D,* free margin of nonpigmented membrana nicitans; *E,* ciliary zone of iris; *F,* pupillary zone of iris; *G,* pupillary ruff; *H,* collarette.

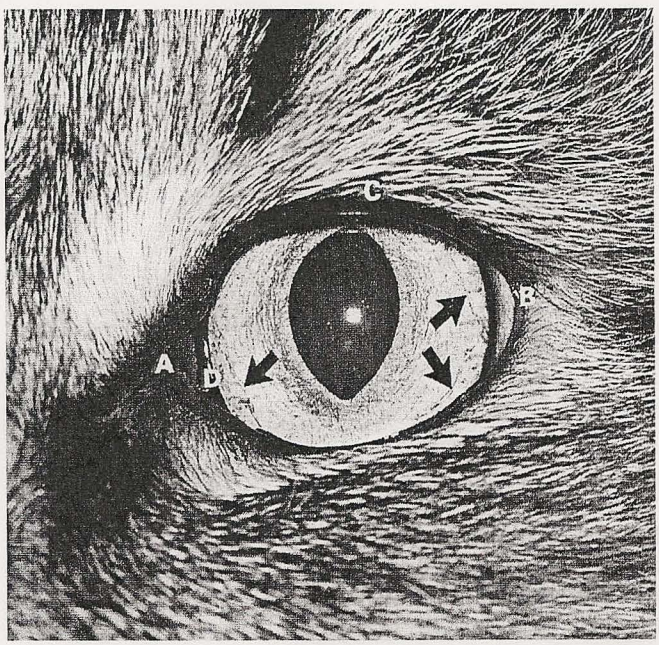

Figure 2.11. Surface anatomy of the cat's eye and adnexa at rest. *Arrows* show major arterial circle in ciliary zone of iris. *A,* medial canthus; *B,* lateral canthus; *C,* cilia; *D,* free margin of membrana nicitans.

(i.e., the lacrimal caruncle) is present (Fig. 2.12). The caruncle may or may not be pigmented. The lateral canthus is more rounded than that of the dog, and small amounts of sclera are visible both medially and laterally. The exposed lateral conjunctiva is often pigmented.

The cilia are well developed on the upper eyelid but absent on the lower lid. The cilia begin near the junction of the medial third and the middle third of the lid, and they extend almost to the lateral canthus. The facial hair is more sparse adjacent to the lower lid margins at both the medial and lateral canthi and often

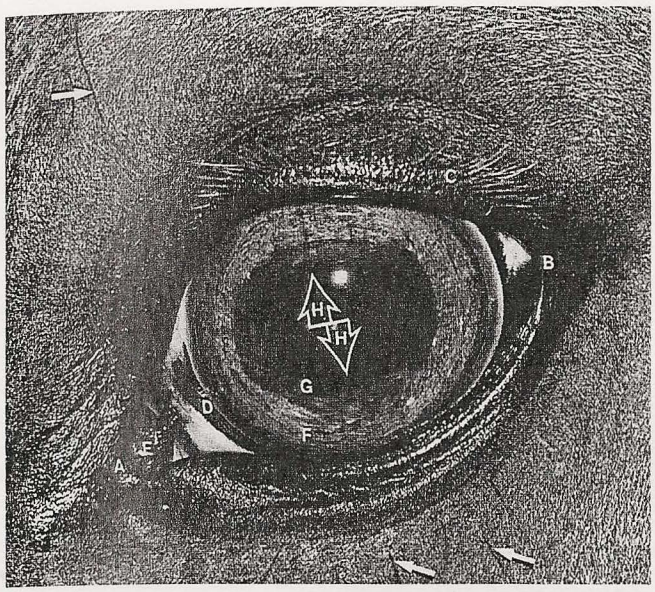

Figure 2.12. Surface anatomy of the equine eye and adnexa at rest. *Arrows* indicate vibrissae. *A,* medial canthus; *B,* lateral canthus; *C,* cilia; *D,* free margin of membrana nicitans; *E,* lacrimal caruncle; *F,* ciliary zone of iris; *G,* pupillary zone of iris; *H,* granulae iridica.

at the medial upper lid. Horizontal folds are present in both the upper and lower lids. Vibrissa are present on the base of the lower lid and on the medial aspect of the base of the upper lid.

The function of the eyelids is to protect and exclude light from the eyes, to sweep foreign bodies from the anterior surface of the eyeball, and to spread liquid tears across the cornea. The lids contain glands that lubricate the edges of the lids and help to prevent overflow of tear secretion. The ocular tear film is "pumped" by the lids to the nasolacrimal drainage channels. The lids also contain glands that contribute to the preocular tear film.

Histologically, the lid may be divided into four portions: the outermost layer of typical skin, the orbicularis oculi muscle layer, a tarsus and stromal layer, and the innermost layer of palpebral conjunctiva (Figs. 2.13 and 2.14). The outer layer of the eyelid, or the skin, is covered by a dense coat of fine hairs with small sebaceous and tubular glands. At the lid margins are a number of specialized hairs or cilia. The cilia of the upper lid are numerous in most domestic species. Cilia tend to be considerably shorter and finer on the lower lid and are commonly lacking in carnivores. Additional tactile hairs may be present on or in the vicinity of the lids. Bundles of smooth muscle fibers (i.e., the arrectores ciliorum) extend from the follicles of the eyelashes toward the tarsus. The muscle bundles are absent in carnivores and in humans, but they are rather common in ruminants.[3] The roots of the large cilia are in close association with prominent sebaceous glands (i.e., glands of Zeis) and modified sweat glands (i.e., glands of Moll, ciliary glands) (Fig. 2.15). These latter glands are spiral, but they are not highly coiled in appearance. The epithelium near the terminus of the gland consists of an outer myoepithelial layer and an inner layer of flattened glandular cells. The structure and location of the glands of Moll are similar in all domestic species, but their function is unknown.[6]

Within the stroma, bundles of striated muscle fibers are arranged in a row that extends nearly the full length of the eyelid.

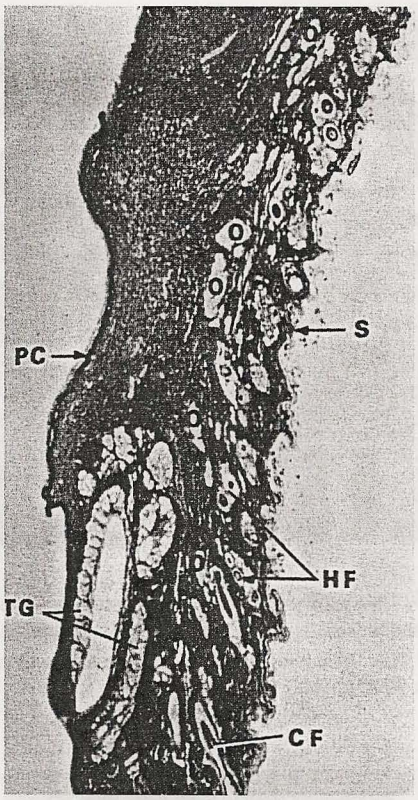

Figure 2.13. Upper eyelid of the dog. *HF,* hair follicle; *PC,* palpebral conjunctiva; *TG,* tarsal gland; *S,* skin; *CF,* cilia follicle; *O,* orbicularis oculi muscle fibers. (Original magnification, X10.)

Figure 2.14. Lower eyelid of the dog. The meibomian glands (*MG*) line the deep surface of the lid. Ciliary and sebaceous (*SG*) glands are closely associated with hair follicles (*HF*). (Original magnification, X100.)

In the upper eyelid, the levator palpebral superioris muscle, which originates from the orbital apex, fans out along the dorsal half of the midstroma. The muscles of the eyelids are separated from the posterior epithelial lining of the eyelids (i.e., palpebral conjunctiva) by a narrow layer of dense connective tissue

Figure 2.15. Ciliary gland of a horse from an area similar to that in Figure 2.14. The gland is lined by secretory cells (*SC*), superficial to which are myoepithelial cells (*MC*) surrounded by a basement membrane. (Original magnification, X770.)

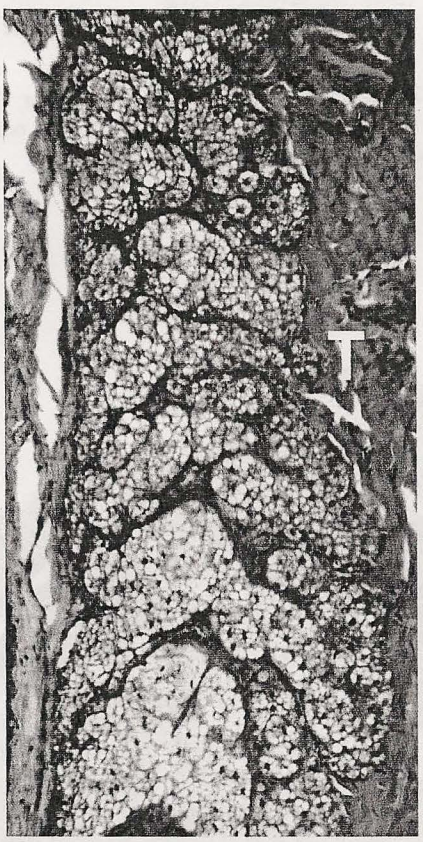

Figure 2.16. Canine meibomian gland consists of overlapping adenomeres, which collectively are enclosed by dense connective tissue of the tarsus (*T*). (Original magnification, X100.).

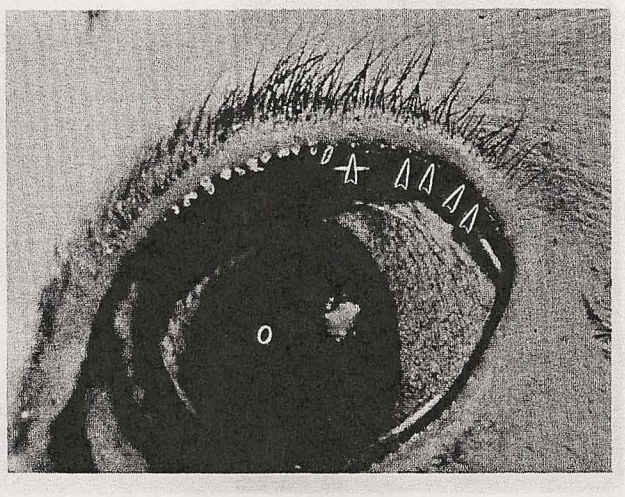

Figure 2.17. The meibomian glands and their ducts (*arrows*) are barely visible near the upper lid margin in this cat.

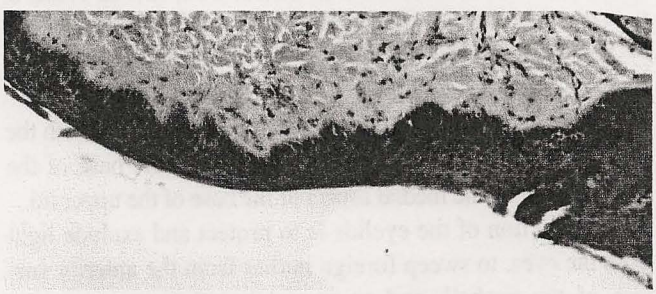

Figure 2.18. Light micrograph of the eyelid margin of the dog's lower lid. The meibomian gland orifice (*arrow*) opens in a trough on the lid margin. Note the keratinized stratified squamous epithelium associated with the orifice. (Original magnification, X100.)

referred to as the tarsus or tarsal plate. Near the margins of both eyelids, and visible through the conjunctiva on their posterior surfaces, are the meibomian (or tarsal) glands (Figs. 2.14, 2.16, 2.17, and 2.18). These glands form parallel rows of lobules, which have their duct openings close to the lid margins. The duct of the meibomian gland is extensively lined by a keratinized epithelium, which is visible at the gland's orifice (Figs. 2.18 and 2.19).[7] The glands, which are sebaceous in nature, are contained in the distal portion of the tarsus and contribute to the outer, oily component of the preocular tear film. The oily component consists of polar and unpolar lipids, with the former thought to contain the surfactant phospholipids needed to spread the lipid film over the aqueous (i.e., serous) layer.[8] Each gland is made of a number of holocrine acini, which are arranged in vertical columns and open into a central duct (Figs. 2.14 and 2.16). The meibomian glands are usually better developed in the upper eyelid, especially in the cat. Individual acini have associated plexi of nerve fibers, which are believed to stimulate their secretion.[9,10] The nerve fibers, which are smooth, varicose, and largely parasympathetic in origin, closely appose the basement membrane of each acinus. In the elephant, the eyelids lack meibomian glands, having unusually well-developed sebaceous glands (glands of Zeis) near the eyelid margins (personal observation).

The posterior region of the eyelids is lined with a mucous membrane known as the palpebral conjunctiva, which consists of a thin layer of loose connective tissue beneath a stratified columnar epithelium that becomes more stratified squamous toward the eyelid margin (Fig. 2.18). This conjunctiva, called the bulbar conjunctiva, is reflected onto the globe and is continuous

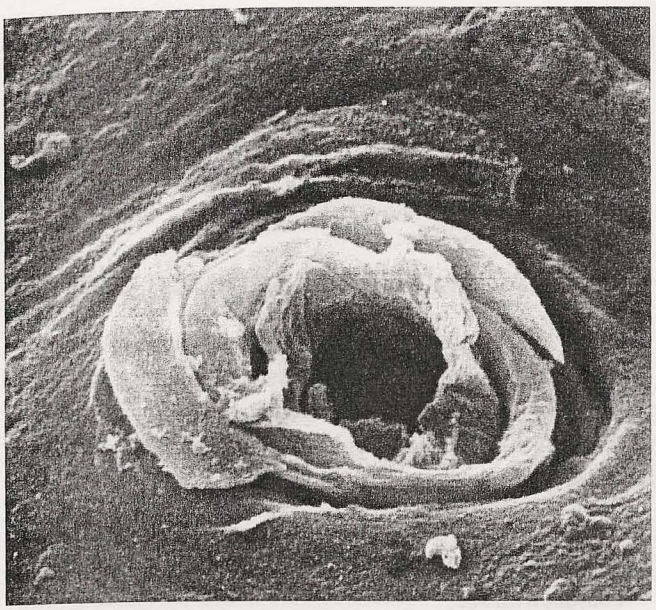

Figure 2.19. Scanning electron micrograph of the meibomian gland orifice (*arrow*) in a dog, revealing the keratinized stratified squamous epithelium. (Original magnification, X800.)

Figure 2.20. Palpebral conjunctiva of a canine eyelid is externally lined by a stratified columnar epithelium possessing numerous goblet cells (*GC*) near the fornix. (Original magnification, X250.)

with the corneal epithelium. The junction between the palpebral and bulbar conjunctiva is the fornix, and the epithelial lining in this region consists of the stratified cuboidal type.[11] The blind sac formed by the conjunctivae is termed the *cul-de-sac.*

Ventrally, an additional fold is formed by reflection of the conjunctiva over the nictitating membrane. These reflections form the conjunctival sac. All parts of the conjunctiva are continuous, but for descriptive purposes, it is divided into the palpebral, bulbar, and fornix conjunctiva.

Approximately a third of the way proximal to the duct of the meibomian gland, the epithelium of the palpebral conjunctiva changes from stratified squamous to stratified columnar (Fig. 2.14). From this level, goblet cells increasingly become more numerous. The distribution of goblet cells is heterogenous in the dog.[12] The highest densities occur along the lower nasal and middle fornix and the lower tarsal portion of the palpebral conjunctiva (Fig. 2.20). By comparison, the bulbar conjunctiva essentially lacks the goblet cells. At the fornix, the conjunctiva is arranged into small folds that contain protruding goblet cells and, dorsolaterally, openings of the lacrimal glands.[11] In the deeper regions of the conjunctiva, aggregates of lymphoid cells are common in the substantia propria.

The substantia propria of the conjunctiva is composed of two layers: a superficial adenoid layer, which in the dog and cat contains lymphatic follicles and glands; and a deep, fibrous layer. The nerves and vessels of the conjunctiva are in the fibrous layer. The arteries of the conjunctiva arise from the anterior ciliary arteries, which are branches of the external ophthalmic artery.

The lymphatics of the conjunctiva are arranged in two plexuses: a superficial and a deep system. Variations in the size and distribution of nodules occur between the upper and lower eyelids.[13] The lymphatic drainage is toward the commissures, at which they join the lymphatics of the eyelids. Drainage of the lateral commissure extends to the parotid lymph nodes, whereas the medial regions extend to the submaxillary lymph glands. In addition, the conjunctival lymphoid tissue of domestic species can have follicle-associated conjunctival epithelium where goblet cells are characteristically absent, being replaced by antigen-absorptive cells called M cells (microfold cells). The ultrastructural appearance of these cells, however, is not entirely identical to those described in mucosa-associated lymphoid tissues throughout the body.[14] It remains to be determined what role(s) the conjunctival lymphatic system plays in mucosal immunity.

The fornix conjunctiva is very thin and transparent, and it lies loosely on the underlying connective tissue. Approximately 3 mm from the limbus, the bulbar conjunctiva, Tenon's capsule, and sclera become closely united. The connective tissue is much more abundant here in the dog than in humans and some other species.

The conjunctiva is the most exposed of all the mucous membranes. Its primary functions are to prevent desiccation of the cornea, to increase mobility of the eyelids and the globe, and to provide a barrier against microorganisms and foreign bodies. This latter role is most important considering that conjunctival sacs house considerable microbial flora, including many potential pathogens.[15]

The third eyelid (i.e., nictitating membrane or membrana nictitans) is a large fold of conjunctiva that protrudes from the medial canthus over the anterior surface of the globe (Figs. 2.10, 2.11, and 2.12). It contains a cartilaginous, T-shaped plate, the horizontal part of which is parallel with the free or leading edge of the membrane (Fig. 2.21). It is rich in elastic tissue, and its free edge is usually pigmented in most animals among a given species. The stroma of the nictitans is fibrous connective tissue rich in glandular and lymphoid tissue (Fig. 2.22). The anterior (i.e., palpebral) surface is covered with nonkeratinized, stratified squamous epithelium. The bulbar surface is lined by a stratified squamous epithelium as well, having a distinct, three-dimensional, molded pattern of pads

and grooves in the dog.[11] The gland of the third eyelid, or the nictitans gland, surrounds the caudal end of the shaft of the cartilaginous plate. This gland is serous in the horse and cat, mixed (i.e., seromucoid) in cattle and the dog, and mostly mucoid in the pig.

The construction of the cartilage is largely elastic in the cat and the horse and hyaline in the dog. The three-dimensional form of the cartilage varies considerably among domestic species.[16] The appendix that is usually surrounded by glandular tissue and ends as a crossbar varies in thickness, being enlarged at the proximal end when comparing the cartilage of the cat to that of the dog. Moreover, the crossbar appears as a reverse S-form in the cat and as a crescent-shape in the dog. By comparison in the horse, the crossbar is distinctly hook-shaped.

In many terrestrial vertebrates, extraglandular tissue exists posterior to the third eyelid (i.e., Harder's gland). Morphologically, it looks like an extension of the nictitans gland, but it is deeply seated in the orbit. In some animals, it surpasses considerably in size the gland of the third eyelid. Typically, the secretory cells are columnar in shape and lined by myoepithelial cells. The adenomeres are arranged in tubules or a combination of tubules and alveoli (i.e., forming a compound tubular or tubuloalveolar gland). The glandular products are diverse in composition, consisting of mucus, serous, or lipid materials, with the latter being found in rodents and released uniquely in an exocytotic manner.[17] Harder's glands possess autonomically controlled nerves and are also under the control of gonadal, thyroid, and pituitary hormones. The functions of this gland remain speculative, but they may include immunologic defense, photoprotection, provision for thermoregulatory lipids, osmoregulation, and pheromone production. Harder's glands may also contribute to "saliva" and to the retinal–pineal axis, and may be a source of growth factors.[17]

In most domestic animals, there is no actual muscle that moves the nictitating membrane over the surface of the cornea; however, small bundles of smooth muscle do occur in the cat. Specifically, nine strands of smooth muscle fibers extend into the third eyelid of the cat and are believed to be involved with its protrusion and retraction.[18] In most instances, the movement may be indirect, resulting from contraction of the retractor oculi muscle, which retracts the globe into the orbital space and thus displaces orbital fat. In turn, this movement pushes the third eyelid across the cornea. In birds and other nonmammalian species without retractor oculi muscles, movement of the nictitating membrane is directly controlled by a pyramidalis muscle attached to the posterior surface of the sclera.[2]

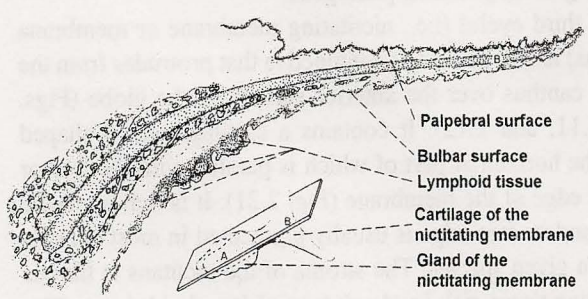

Figure 2.21. A histologic section of the mammalian nictitating membrane. (Modified from Evans H, Christensen G. *Miller's Anatomy of the Dog.* 2nd ed. Philadelphia: WB Saunders, 1979.)

LACRIMAL AND NASOLACRIMAL SYSTEM

An adequate supply of tears covering the partially exposed anterior segment of the globe and associated adnexa is necessary for optical integrity, maintenance of the cornea, and normal eye function. This fluid, called the preocular tear film, serves several functions, including:

1. Maintaining an optically uniform corneal surface,
2. Removing foreign material and debris from the cornea and conjunctival sac,
3. Permitting passage of oxygen and providing other nutritional requirements to the cornea, and
4. Providing an antimicrobial function.

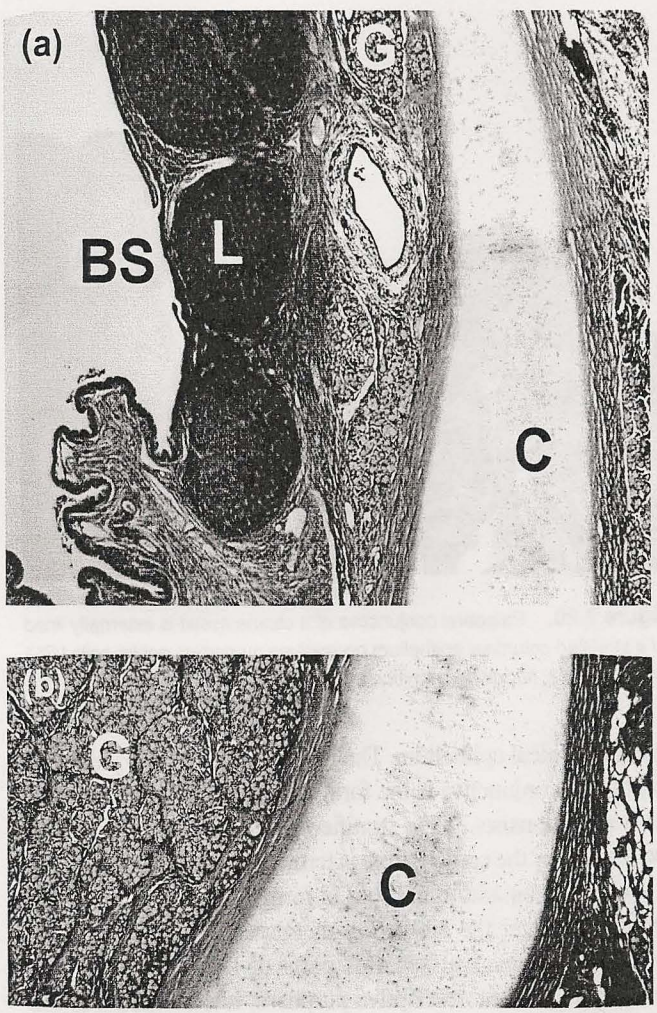

Figure 2.22. Nictitating membrane of the horse contains both glandular (*G*) and lymphoid (*L*) tissues, the latter superficially located within the stroma next to the bulbar surface (*BS*). *C*, cartilage. **A.** Middle third of the nictitating membrane. **B.** Base of the nictitating membrane. (Original magnification, X10.)

When tears are not present in adequate volume, keratoconjunctivitis sicca (i.e., dry eye) develops.

Tears are present over the surface of the eye as a triple-layered film. The outer, thin, superficial oily layer is provided by sebaceous glands of Zeis and the meibomian glands. This layer reduces evaporation of the underlying aqueous tears and forms a barrier along the lid margins that prevents tear overflow onto the face.

The second (i.e., middle) layer is the aqueous tear fluid layer, which is secreted by the lacrimal gland (61%), the accessory glands of Kraus and Wolfring (3%), and the gland of the third eyelid (35%).[19] Uptake of oxygen through this tear fluid is essential for normal corneal metabolism.

The third, innermost layer is the mucin layer, which is produced by the conjunctival goblet cells. This mucin layer is adsorbed to the corneal epithelial surface and distributed evenly during normal blinking. The mucin provides a hydrophilic surface over which the aqueous tear fluid spreads evenly.

As mentioned previously, the external eye is continuously exposed to an environment containing potentially pathogenic microorganisms. One of the mechanisms protecting the eye from potential infectious agents is the tear layer. Several antimicrobial substances exist in tears, but their roles in preventing infection are only partially understood.[20]

The composite secretion of tears is continuously spread over the surface of the eye in a uniform, thin layer by the constant action of the eyelids (and nictitans) during blinking. Excess fluid collects in the lower cul-de-sac by gravity and is mechanically "pumped" through the openings, the upper and lower puncta lacrimalae. These punctae are located just medial to the most medial meibomian gland and 1 to 2 mm inside the edge of the eyelid. They are surrounded by smooth muscle that works in coordination with the blinking of the eyelids to remove excess lacrimal fluid and prevent its backflow.

These structures mark the origin of the nasolacrimal drainage apparatus. They continue as the upper and lower canaliculi, which pass slightly vertically away from the eyelid margins and turn toward the medial canthus, pass through the periorbita, and join each other at a dilation, the lacrimal sac, located in the lacrimal fossa of the lacrimal bone (Fig. 2.23). This sac empties into the nasolacrimal duct, which passes through a short, bony canal and opens into the nasal cavity, where it continues as a duct until it reaches an opening at the floor of the nostril approximately 1 cm from the end of the nares. Some animals have an accessory opening in the canal as it passes by the root of the upper canine tooth.

The main component of this system is the lacrimal gland, which is a diamond-shaped structure in the dorsolateral aspect of the globe, lying within the periorbita. Fifteen to twenty small ducts open from it and into the superior conjunctival fornix. Histologically, the gland is a mixed tubuloalveolar type. Its function is production of the serous portion of tears. The innervation to the lacrimal gland is not fully understood, but the lacrimal branch of cranial nerve, sympathetic, and parasympathetic nerves are all involved in its function. Clinically, certain cholinergic drugs (e.g., pilocarpine) will stimulate tear secretion, whereas other drugs (i.e., anticholinergics) will decrease tear secretion.

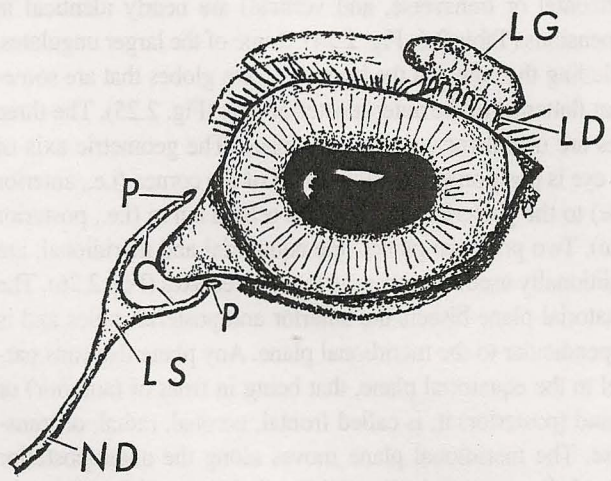

Figure 2.23. The nasolacrimal system. *C,* canaliculi; *LD,* Lacrimal ducts; *LG,* lacrimal gland; *LS,* lacrimal sac; *ND,* nasolacrimal duct.

GLOBE

Components

The globe is composed of three basic layers, or coats. The outer coat is fibrous tunic, and it is further divided into the cornea and sclera. The fibrous tunic gives the eye a constant shape and form, which are imperative for a functional visual system. In addition, the anterior portion of the fibrous tunic (i.e., the cornea) is transparent, thus enabling light to pass through, and is shaped in a manner that makes it a powerful lens that refracts light rays centrally, toward the visual axis of the eye. The second and middle layer is the uvea (meaning "grape"). The uvea, which is further divided into the choroid, the ciliary body, and the iris, is heavily pigmented and vascularized. It functions to modify both external and internal light, including reflection and scatter, as well as to provide nourishment and remove wastes for most of the eye's components. The third and most central layer is the nervous coat, which consists of the retina and associated optic nerve. Briefly, the retina contains light-sensitive cells (i.e., photoreceptors) that, after a series of intermediate modifying processes, transmit impulses to the brain via the optic nerve. The three tunics embrace the large, inner, transparent media of the eye: the aqueous humor, lens, and vitreous humor, which collectively function to transmit and refract light to the retina and provide an internal pressure that keeps the globe firmly distended.

Size, Shape, and Topography

The eyes in domestic animals are quite variable in size, but their shapes are comparatively uniform, being spherical in most instances, in which the three axes of the globe (anteroposterior,

horizontal or transverse, and vertical) are nearly identical in dimensions (Table 2.6; Fig. 2.24). Some of the larger ungulates, including the cow and the horse, possess globes that are somewhat flattened in the anteroposterior axis (Fig. 2.25). The three axes are useful for common reference. The geometric axis of the eye is positioned from the center of the cornea (i.e., anterior pole) to the posterior center of the scleral curve (i.e., posterior pole). Two principal planes, the equatorial and meridional, are traditionally used in references to the three axes (Fig. 2.26). The equatorial plane bisects the anterior and posterior poles and is perpendicular to the meridional plane. Any plane that runs parallel to the equatorial plane, that being in front of (anterior) or behind (posterior) it, is called frontal, coronal, radial, or transverse. The meridional plane moves along the anteroposterior axis of the eye, vertically dividing it into medial and lateral halves, even though meridional planes can be horizontal or oblique. Planes that run parallel to the meridional plane are described as being sagittal.

The long posterior ciliary arteries are visualized at the three-o'clock and nine-o'clock positions when viewed posteriorly, passing from the optic nerve to the equator in the superficial sclera (Fig. 2.27). Long ciliary nerves pass with the arteries. Numerous short posterior ciliary arteries penetrate the sclera around the circumference of the optic nerve. A variable number of vortex veins (usually four) emerge from the sclera posterior to the equator; typically, two vortex veins are present dorsally and two ventrally.

When working with individual enucleated eyes, several topographic features will help to establish their proper anatomic positions. For example, observation of the long posterior arteries and the longer horizontal dimension of the cornea determines the horizontal meridian. Placements of the ventral exit of the

Table 2.6 Dimensions of Globes of Domestic Species

Animal	Meridional A–P Axis of the Eye, A (mm)	Equatorial Axis, V (mm)	Horizontal, T (mm)	Ratio of A/V/T	Ratio of V/T
Horse	43.68	47.63	48.45	1:1.09:1.10	1:1.10
Mule	43.00	47.50	48.50	1:1.10:1.12	1:1.01
Cow	35.34	40.82	41.90	1:1.15:1.18	1:1.02
Calf	26.50	32.50	34.20	1:1.22:1.20	1:1.05
Sheep	26.85	30.02	30.86	1:1.11:1.15	1:1.02
Pig	24.60	26.53	26.23	1:1.08:1.06	1:0.99
Dog	21.73	21.34	21.17	1:0.98:0.97	1:0.99
Cat	21.30	20.60	20.55	1:0.97:0.96	1:0.99

Translated from Bayer J. *Angenheilkunde.* Vienna: Braumueller, 1914.

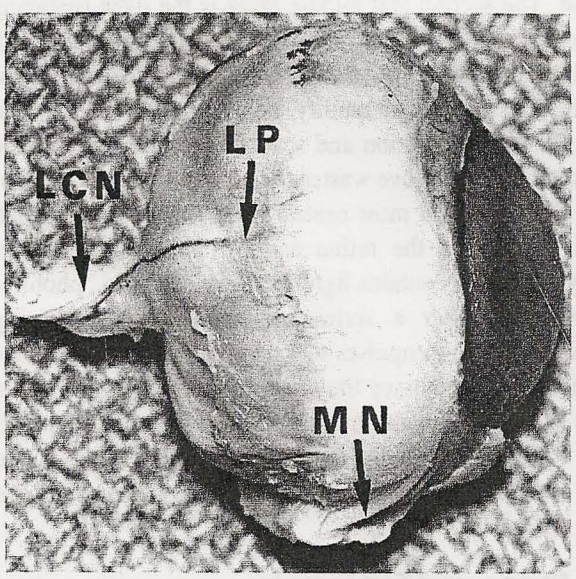

Figure 2.24. Lateral view of the feline globe. Note spherical shape and large cornea. *LCN,* long ciliary nerve; *LP,* long posterior ciliary artery; *MN,* membrane nictitans.

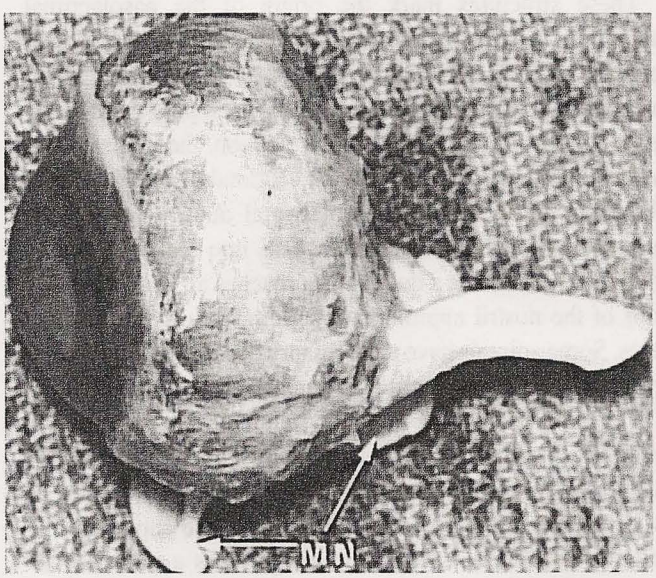

Figure 2.25. Lateral view of a bovine globe. Note the marked flattening in the anteroposterior axis and the marked ventral exit of the optic nerve from the posterior pole. *MN,* attached membrana nictitans.

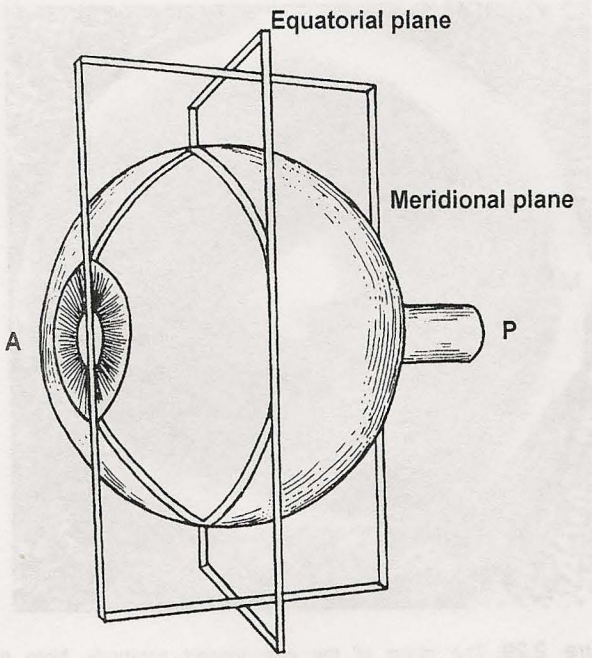

Figure 2.26. The equatorial and meridional planes of the eye. *A,* anterior pole; *P,* posterior pole. (Modified from Scheme HG, Albert DM. *Alder's Textbook of Ophthalmology.* Philadelphia: WB Saunders, 1969.)

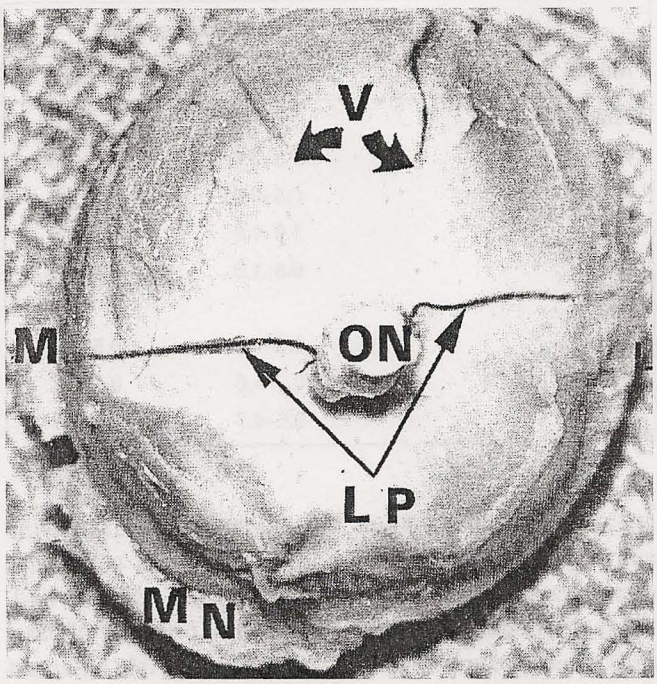

Figure 2.27. Posterior view of a feline globe. *LP,* long posterior ciliary artery; *L,* lateral; *M,* medial; *MN,* attached membrane nictitans; *V,* vortex veins; *ON,* optic nerve.

optic nerve and the dorsal oblique muscle tendon establish the dorsoventral aspect of the globe. And, finally, remnants of the membrana nictitans and the lateral placement of the optic nerve to the posterior pole exhibit the lateral and medial aspects.

The optic nerve in most domestic animals lies inferior and lateral to the posterior pole. Surrounding the optic nerve are many ciliary nerves and short posterior ciliary arteries. The posterior ciliary nerves pursue a long intrascleral course (up to 12 mm) before entering the suprachoroidal space to reach the iris, ciliary body, and limbus. In the dog, the long posterior ciliary arteries enter the sclera approximately 3 to 5 mm from the optic nerve in the horizontal meridian. In the cat, these arteries can enter the sclera immediately adjacent to the optic nerve (Figs. 2.25, 2.26, and 2.27). These vessels are visible on the nasal and temporal sides of the eye within the sclera at least as far as the equator before entering the choroidal space. At this point, each artery accompanies the long ciliary nerve to the iris and ciliary body. Recurrent vascular branches are given off to enter the choroid, but the main vessel trunk continues to be the major supply of the iris. The four large vortex veins lie posterior to the equator.

CORNEA

The cornea is the transparent, anterior fifth of the fibrous tunic of the globe. The functions of the cornea include support of intraocular contents, refraction of light (because of its curvature), and transmission of light (because of its transparency). Like the lens, the cornea is normally clear, avascular, and refracts light (40–42 diopters). The cornea relies on both aqueous humor and tears for nourishment and cleansing, and on the eyelids and membrana nictitans for protection from the external environment.

The cornea is elliptical in shape, with a horizontal diameter greater than the vertical. In the dog and the cat, the difference between these diameters is small, thus making their corneas appear to be almost circular (Fig. 2.28). In most ungulates, this difference is much more pronounced, allowing for a remarkable horizontal field of view (Fig. 2.29) that is further complemented by the lateral positioning of their orbits within their skulls. The combination of the exaggerated corneal dimensions and orbital positions in these grazing animals appears to be the adaptive result of their feeding behavior, affording them greater protection from predacious enemies.

Corneal thickness varies from species to species, from breed to breed, and from individual to individual. In most domestic animals, it is less than 1 mm. In the dog, it is 0.45- to 0.55-mm thick centrally and from 0.50- to 0.65-mm thick in the periphery. Table 2.7 lists thickness measurements of the central and peripheral cornea of various species. These data are based on postmortem measurements and should be corroborated by in vivo techniques such as specular microscopy and A-scan ultrasonography. Recently, profiles of corneal thickness have been made from dogs and cats by ultrasonic pachymetry and computer enhancement.[21–23] Only three locations were measured in the dog, but the cornea is not uniformly thick, being thickest at the temporal periphery and thinnest centrally (Table 2.8). The canine cornea thickens significantly with age, and with age taken into consideration, it is consistently thinner in females than in males.[21] Again, in the cat, the corneal thickness is not uniform, being thinnest along the nasal superior quadrant; overall, the mean axial thickness (0.546 mm–0.578 mm) is essentially identical to the mean perilimbal thickness (Table 2.8).[22,23] The mean thickness does increase significantly with age up to 100 months.

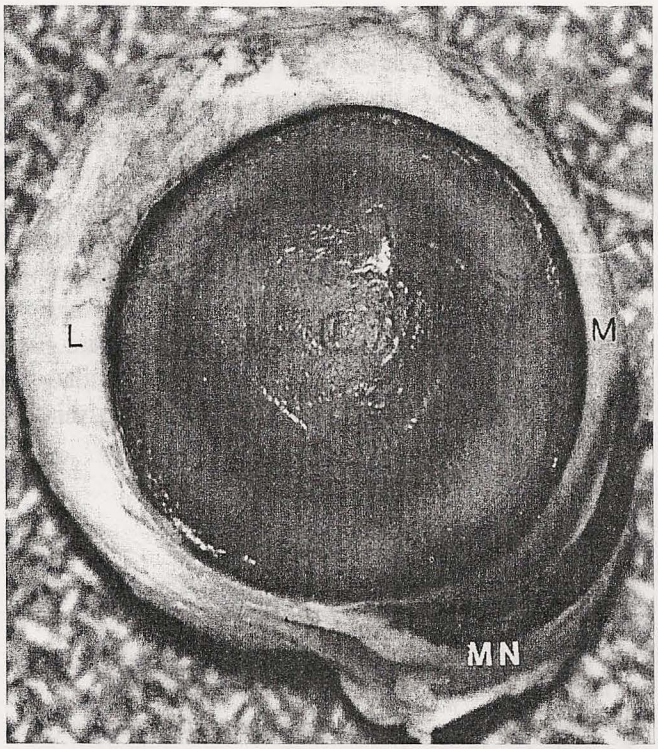

Figure 2.28. The globe of the dog viewed anteriorly. Note the slight horizontally elongated ellipse of the cornea. *L*, lateral; *M*, medial; *MN*, membrana nictitans.

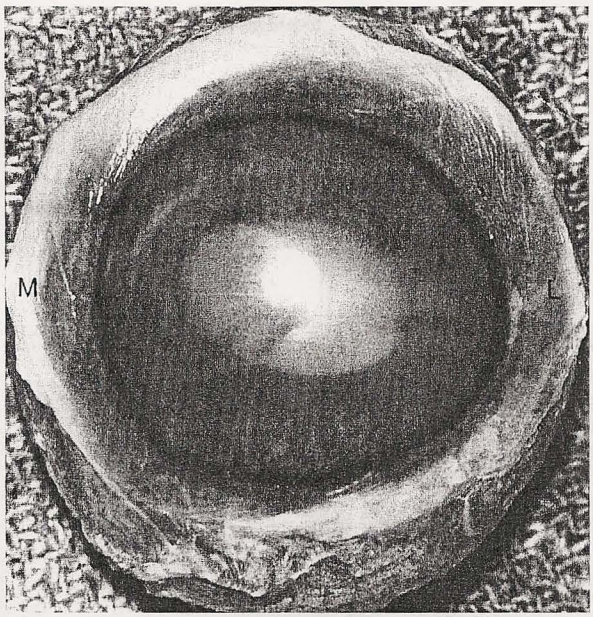

Figure 2.29. The globe of the cow viewed anteriorly. Note the horizontally elongated ellipse of the cornea. *L*, lateral; *M*, medial.

Table 2.7 Thickness of the Cornea in Domestic Animals

	Thickness (mm)	
Animal	**At Center**	**At Edge**
Horse	1.0–1.5	0.8
Cow	1.5–2.0	1.5–1.8
Sheep	0.8–2.0	0.3–0.5
Pig	1.0–1.2	0.5–0.8
Cat	0.8–1.0	0.4–0.6
Dog		
Large	0.8–1.0	0.5–0.6
Medium	0.8–1.0	0.5–0.7
Small	0.6–0.7	0.5–0.6

The cornea is richly supplied with sensory nerves, particularly pain receptors, and this sensitivity protects the cornea and helps to maintain its transparency (Fig. 2.30). The cornea is innervated by the long ciliary nerves, which are derived from the ophthalmic division of the trigeminal nerve.[24] The epithelial cell layers are richly innervated, and these nerve endings are unsheathed in the epithelium. The most superficial layers are primarily innervated with pain receptors, whereas more pressure receptors are found in the stroma. This explains why a superficial corneal injury is often more painful than a deeper wound. The extent to which the stroma is innervated in different animals is unknown. In the rabbit, nerve fiber endings occur within the corneal endothelium.[25]

As mentioned previously, the cornea, along with the lens, possesses the unique anatomic property of transparency. Anatomic factors that contribute to this transparency are:

1. Lack of blood vessels,
2. Nonkeratinized surface epithelium maintained by a preocular moisture film,
3. Lack of pigmentation, and
4. Size and organization of stromal collagen fibrils.

In addition, physiologic factors such as state of hydration are important.

On microscopic examination, animal corneas consist of four, and sometimes five, layers. From the outside and moving inward, the layers are the epithelium, Bowman's layer (rarely present), stroma, Descemet's membrane, and endothelium (i.e., mesothelium) (Fig. 2.31).

Anterior Epithelium

The corneal epithelium covers the anterior corneal surface, being nonkeratinized, stratified squamous. The epithelium is approximately 25- to 40-μm thick in the domestic carnivore and two to four times thicker in the larger and not always domesticated ungulate (Fig. 2.32). In the dog, cat, and bird, the anterior epithelium consists of a single cell layer of basal cells, which are columnar in shape and lie on a thin basement membrane; two or three layers of polyhedral (i.e., wing) cells; and two or three layers of nonkeratinized squamous cells. Among larger animals, the layers of polyhedral and squamous cells are more numerous. The cells are arranged to provide orderly replacement of the surface cells during desquamation.

Beneath the epithelium is a basement membrane, which is enhanced histologically when stained with periodic acid-Schiff (PAS) (Fig. 2.33A). The basal cells are firmly attached to the basal lamina of the basement membrane (i.e., anterior limiting lamina) by hemidesmosomes, anchoring collagen fibrils, and the glycoprotein laminin. Interestingly, of the different types of collagen believed to contribute to the basement membrane, evidence for type IV, which is ubiquitous throughout the basement membranes of the body, is weak (Table 2.9).[27,28] Hyaluronan and

Table 2.8 Thickness of the Cornea in the Cat and Dog as Determined by Ultrasonic Pachymetry

Corneal Location	Dog (mm)			Cat (mm)[d]
	Young[a]	Adult[b]	Aged[c]	
Superior peripheral	0.557±0.007	0.612±0.005 0. 780[e]	0.617±0.006	0.538±0.039 0.694[e]
Midsuperior-nasal peripheral				0.523±0.041
Nasal peripheral				0.530±0.042
Midnasal-inferior peripheral				0.538±0.042
Inferior peripheral		0.773[e]		0.539±0.037 0.760[e]
Midinferior-temporal peripheral				0.548±0.040
Temporal peripheral	0.540±0.006	0.581±0.006	0.643±0.006	0.559±0.043
Midtemporal-superior peripheral				0.558±0.037
Central	0.520±0.005	0.560±0.005 0.735[e]	0.597±0.006	0.546±0.048 0.767[e]

Data from Gilger BC, et al. Canine corneal thickness measured by ultrasonic pachymetry. *J Vet Res* 1991;52:1570–1572; and Schoster JV, Wickman L, Stuhr C. The use of ultrasonic pachymetry and computer enhancement to illustrate the collective corneal thickness profiles of 25 cats. *Vet Comp Ophthalmol* 1995; 5:68–73.

[a]20 dogs (both genders) 1 year old and younger were examined.

[b]29 dogs between 1 and 7 years old were examined.

[c]26 dogs over 7 years old were examined.

[d]25 cats (both genders) 2 years old and younger were examined.

[e]Corneal thickness based on formalin-fixed histologic preparations of 10 cat corneas and 12 dog corneas.

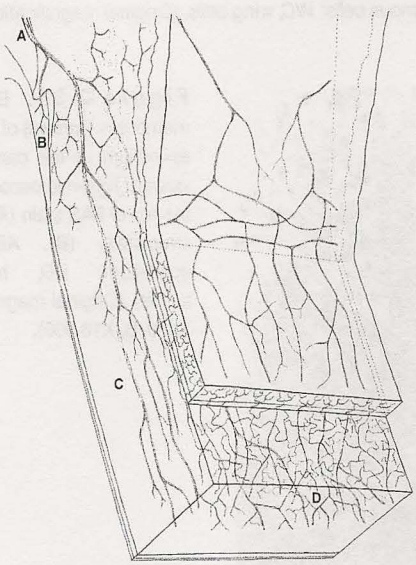

Figure 2.30. Innervation of the limbus and cornea. The long ciliary nerve (*A*) supplies the limbal region, then sends branches into the cornea. Nerves also supply the trabecular meshwork (*B*) and the region of the canal of Schlemm (i.e., angular aqueous plexus in nonprimates). Note the paucity of nerves in the deep cornea (*C*) and their absence in the region of Descemet's membrane as compared to the multitude of branched endings of nerves within the anterior stroma (*D*) and epithelium. (Modified from Hogan MJ, Alvarado JA, Weddell JE. *Histology of the Human Eye.* Philadelphia: WB Saunders, 1971.)

Figure 2.31. Histologic view of the canine cornea, revealing four layers: anterior epithelium (*AE*), stroma (*S*), Descemet's membrane (*DM*), and endothelium (*E*). (Original magnification, X100.)

fibronectin also have been associated with corneal epithelial attachment.[27] Ultrastructurally, the basement membrane consists of an osmiophilic layer, 30- to 55-nm thick, that is separated from the basal cell plasma membrane by a 25-nm wide, electron-lucent zone (Fig. 2.33B). Hemidesmosomes attach the basal cells to the basement membrane, which in turn anchors the epithelium to the stroma. The arrangement of hemidesmosomes varies among different animals, being linear among mammals and amphibians, in rosettes among birds and reptiles, and punctate without arrangement, or completely absent, among fish.[29] The epithelial cells have good regenerative powers (basal cell turnover time is approximately 7 days), but after removal of the basal lamina, weeks to months may be necessary for it to reestablish, and until the basement membrane is completely reformed, the epithelium can be easily removed from the stroma.[30,31]

The basal cells are tall, columnar cells with a flattened base and domed apex. They are crowded together, and as a result, the nuclei, which are located in the apical region, are often forced

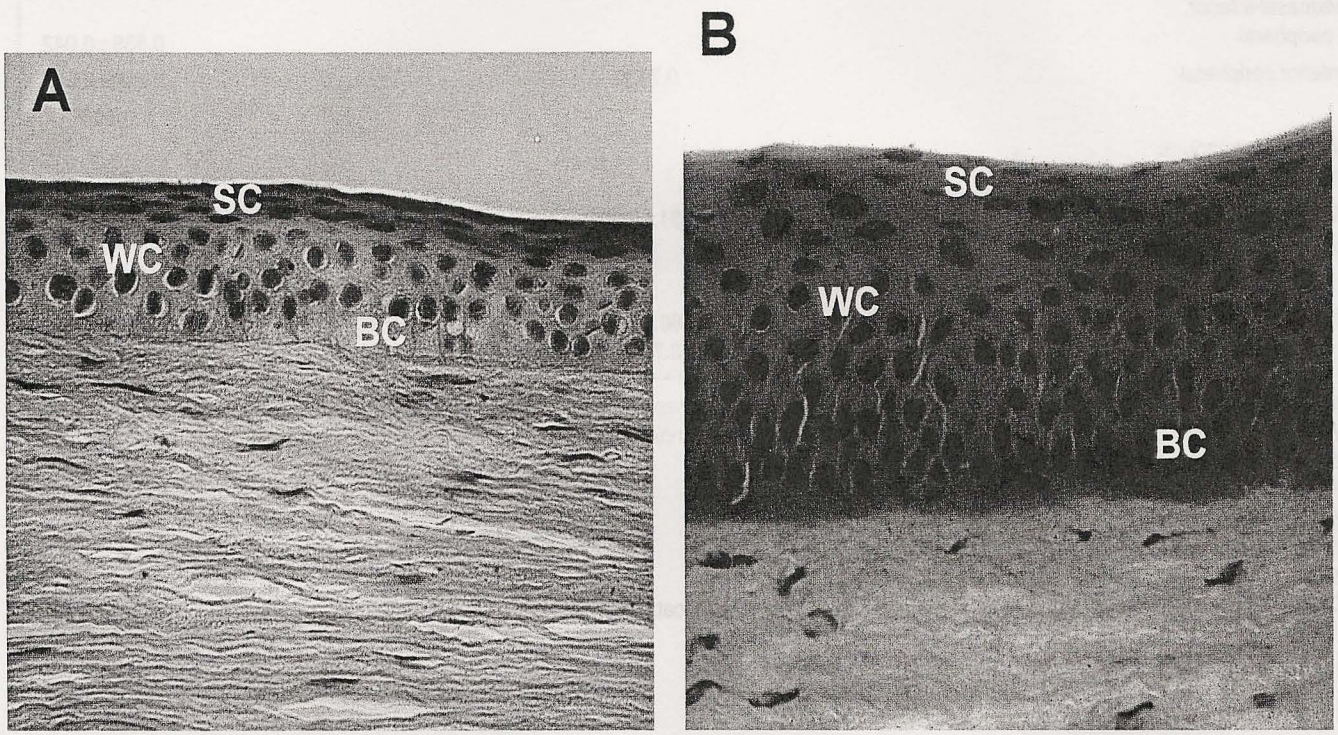

Figure 2.32. Anterior epithelia of canine (**A**) and ovine (**B**) corneas. *BC,* basal cells; *SC,* squamous cells; *WC,* wing cells. (Original magnification, X400.)

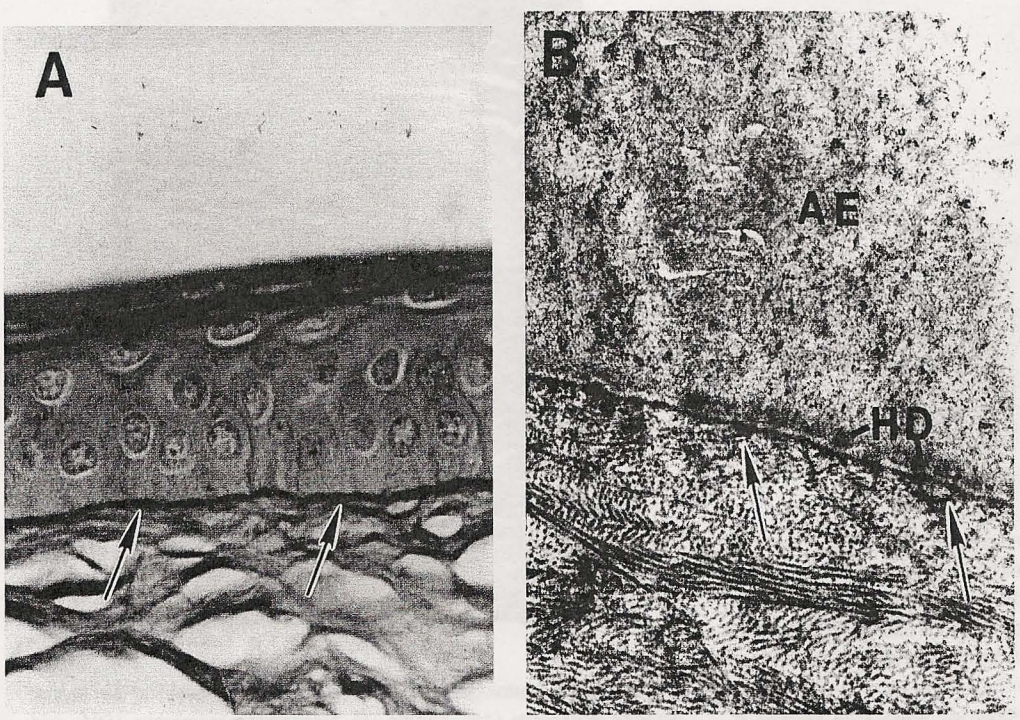

Figure 2.33. Basement membrane (*arrows*) of the anterior epithelium of the canine cornea viewed light-microscopically with the aid of PAS stain (**A**) and ultrastructurally (**B**). *AE,* anterior epithelium; *HD,* hemidesmosomes. (Original magnification: A, X400; B, X18,000).

Table 2.9 Location of Glycans and Collagen Types in the Cornea

Location	Types of Collagen	Glycans[a]	References
Anterior epithelium/ basement membrane	IV, VI, and VII	Laminin, fibronectin, hyaluronans	26, 27
Bowman's layer/anterior stroma	I, III, V, and VI	Heparin sulfate	48
Stroma	I, III, V, VI, and XII	Chondroitin 6- and 4-sulfates, dermatan sulfate	27, 39–41, 42, 45
Descemet's membrane	I, III, IV, V, VI, and VIII	Laminin, fibronectin tenascin, P component, heparin sulfate	52, 428, 429

[a]Includes glycoproteins and glycosaminoglycans.

into two or alternating layers. Mitosis is confined to the basal cells or those cells immediately superficial to the basal cells (i.e., stratum germinativum). Adjacent cell surfaces have small infoldings with numerous desmosomal attachments (Fig. 2.34).[32,33] Occasional lymphocytes are found in the basal epithelium and in the more superficial layers (Fig. 2.35). Desmosomes are absent between these extraneous cells and the adjacent epithelial cells.

Wing cells are a group of polygonal cells on top of the basal cells. Their depth varies from two or three layers to several layers deep, depending on the species and the location in the cornea (compare Fig. 2.32A with Fig. 2.32B). These layers form a transition zone between the columnar basal cells and the more superficial squamous cells.

The flattened superficial cells are several layers deep. During scanning electron microscopy (SEM), the cells appear to be flat and polygonal, with straight borders (Figs. 2.36 and 2.37). Both light and dark cell types can be identified. The light cells contain more microvillae and microplicae. These numerous projections scatter electrons and, as a resultant, produce a lighter appearance of the cell. The darker cells are the oldest and are occasionally seen to be in the process of desquamation (Fig. 2.36). Cells in the central cornea have more projections (i.e., microplicae and microvillae) than those in the periphery. The function of the microprojections is controversial, but they have been postulated to hold or stabilize the preocular tear film on the corneal surface.[34,35] The fine microplicae and microvillae that expand the surface area considerably allow mucin of the precorneal tear film to adhere firmly to the anterior epithelium. As mentioned earlier, the mucin component of the tear film is thicker than was previously believed.[36] Undoubtedly, the roughened texture of the squamous cells contributes to the substantial presence of mucin. The amount and composition of the mucin undoubtedly varies among species, being extremely well developed in aquatic mammals.[37]

Figure 2.34. Basal corneal epithelium and anterior stroma in a cow. Note the obliquely running lamellae in the anterior stroma (*arrows*). Bowman's layer is well developed, with randomly oriented thin collagen fibers (*BL*). Basal lamina (*B*) is separated from cytoplasmic membrane by a thin lucent line. Note also the columnar basal cells (*C*) with tortuous cytoplasmic membranes and perinuclear mitochondria (*M*). *HD,* hemidesmosomes; *K,* keratocyte. (Original magnification, X5800.)

Figure 2.35. Transmission electron microscopy (TEM) shows the basal corneal epithelium and associated basement membrane in a dog. A lymphocyte (*L*) is located tightly between adjacent basal cells. (Original magnification, X12,000.)

The cytoplasm of the superficial cells contains numerous tonofilaments and vesicles, but it generally lacks the mitochondria, rough endoplasmic reticulum, and ribosomes that occur in the basal and wing cells. Numerous desmosomal

Figure 2.36. SEM shows the surface of the anterior epithelium of a bovine cornea. The surface cells can be light or dark. Note the round bulges, where the nuclei lie within each cell. Note also that some cells appear to be desquamating. (Original magnification, X400.)

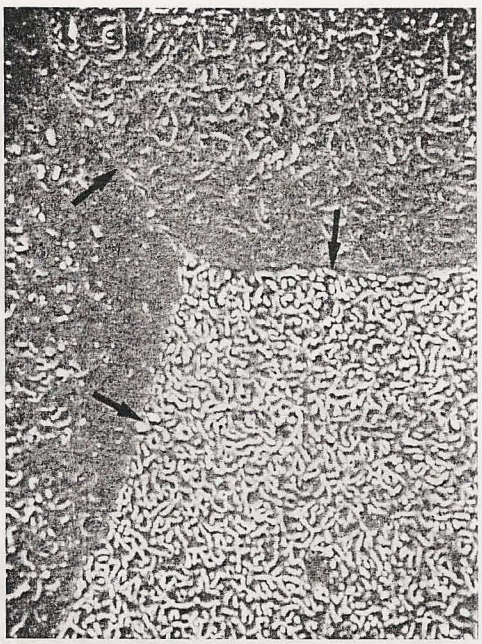

Figure 2.37. SEM shows the corneal epithelial surface of a horse. Junction of a light cell with two dark cells illustrates the increased numbers and better development of microplicae and microvillae in the light cell. Cell borders tend to be straight (*arrows*). (Original magnification, X3888.)

attachments are visible, and the surface cells have a zonula occludentes on their lateral membranes. Microprojections are visible on the surface cells (Fig. 2.38).[35,38] The origin of the microvillae appears to be from detached desmosomal junctions, but other authors have found no evidence for this.[32,38]

Corneal epithelium is thicker at the periphery of the cornea than in the center. With the junction of the bulbar conjunctiva, however, it abruptly thins, and pigmented cells are observed. The cornea is normally nonpigmented except at the periphery (i.e., limbus). At the limbus, pigment is scattered in all layers except the superficial squamous cells. Nerves that enter the epithelium lose their ensheathment and terminate in naked nerve endings among the wing cells (Fig. 2.39).[32]

Stroma

The corneal stroma (i.e., the substantia propria) comprises 90% of the thickness of the cornea. It consists of transparent, almost structureless lamellae of fibrous tissue, and these lamellae lie in sheets and split easily into planes (Fig. 2.40A). Between the lamella are fixed and infrequent wandering cells. The fixed cells are fibrocytes, which are called keratocytes, and the extensions of these cells contribute to formation and maintenance of the stromal lamellae. The keratocytes have thin nuclei, ill-defined borders, and delicate cell membranes (Fig. 2.40B). These cells can transform into fibroblasts when deep corneal injury occurs, and they may form scar tissue that is not transparent (Fig. 2.41). Wandering cells are usually leukocytes that have migrated from the limbus.

The lamellae are parallel bundles of collagen fibrils, with each lamella running the entire diameter of the cornea. All the collagen fibrils within a lamella are parallel, but between lamellae, they vary greatly in direction (Fig. 2.40). The lamellae of the posterior stroma are more regular in arrangement

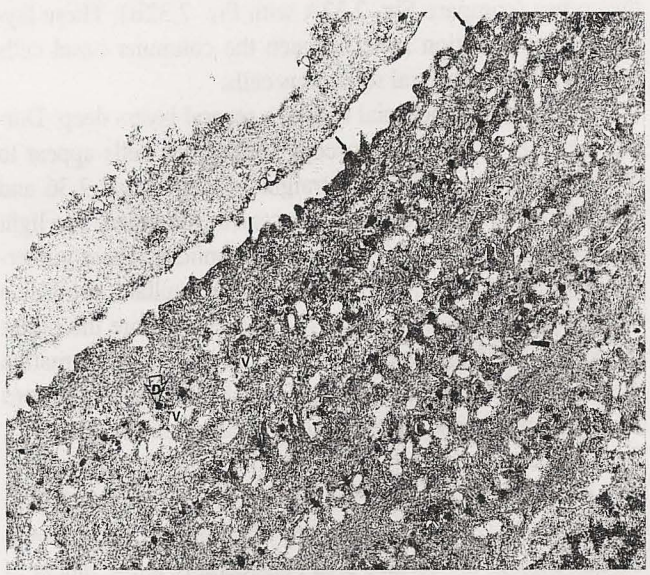

Figure 2.38. Superficial corneal epithelial cells of a dog. A degenerate cell on the surface is detaching. The microvillae on the underlying cell seems to be formed in the region of desmosomal attachments (*small arrows*), whereas others have flat tops, presumably from previous attachments. Note the multiple infolding of cytoplasmic membranes with numerous desmosomes (*D*). The cytoplasm is packed with tonofilaments, and numerous membrane-bound vacuoles (*V*) are present. (Original magnification, X18,000.)

than those of the anterior third of the stroma. The anterior lamellae are more oblique to the surface, and they have more branching and interweaving (Fig. 2.34).

Overall, the precise organization of the corneal stroma is the most important factor in maintaining corneal clarity. The bulk of the corneal stroma is composed of thin collagen fibrils that are uniformly positioned into lamellae and transverse the full diameter of the cornea. This special arrangement (with a periodicity of 620–640 Å) of stroma permits 99% of the light entering the cornea to pass without scatter.[32] Collagen of the stroma is made of at least five types (Table 2.9). Of these five, collagen type I is by far the most common, forming the small, evenly sized, striated fibrils. Type VI is associated only with the interfibrillar matrix, forming a network around the fibrils. Evidence from adult mice suggests that type VI is connected with type I through chondroitin/dermatan sulfate glycosaminoglycans (GAGs). In rabbits, this association is observed during development of the cornea as well.[39] Type VI, which is also close to the keratocyte, appears to play some kind of role in cell–matrix interactions, which would be especially important during development and repair.[40] In comparison, type V is combined or co-assembled with type I, and it is believed to be a factor responsible for the formation of the small, uniform diameter of the striated fibril, which is approximately 25 nm in most species.[41] Types III and XII are both believed to be developmental forms, with type III being the more common. How important they are during wound repair remains to be seen. The normal rabbit corneal endothelium, keratocytes, and corneal endothelia of chickens and mice have the potential to produce type XII.[42]

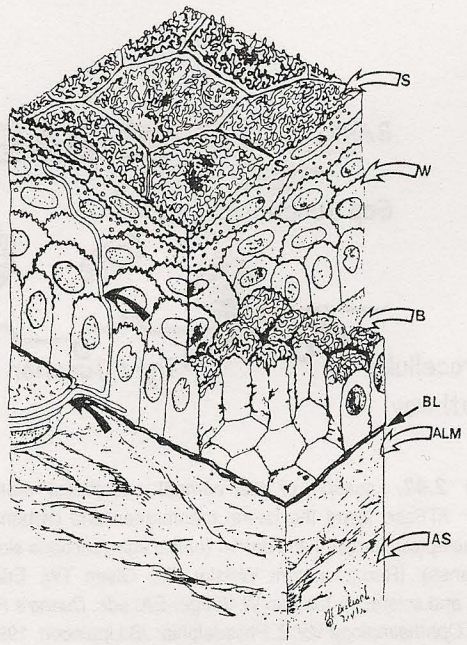

Figure 2.39. The corneal anterior epithelium and anterior stroma. Dark *arrows* indicate corneal nerve. *ALM,* cell-free zone or anterior limiting membrane; *AS,* anterior stroma; *B,* basal cells; *BL,* basal lamina; *S,* superficial squamous cells with microvillae; *W,* wing cell layer. (Modified from Hogan MJ, Alvarado JA, Weddell JE. *Histology of the Human Eye.* Philadelphia: WB Saunders, 1971.)

Collagen fibrils, along with the proteoglycans and their associated GAGs and glycoproteins, make up 15% to 25% of the corneal stroma, and they act as the principal support structure of the cornea. These collagen fibrils form the matrix for a specialized population of proteoglycans within the corneal stroma.[43] The cornea is from 75% to 85% water, and it is relatively dehydrated compared with other tissues. This state of dehydration is termed *deturgescence* and is, in part, a function of the endothelium and epithelium. These cells actively move water out of the stroma by energy-dependent Na^+/K^+ adenosine triphosphatase (ATPase) pumps, being most active in the

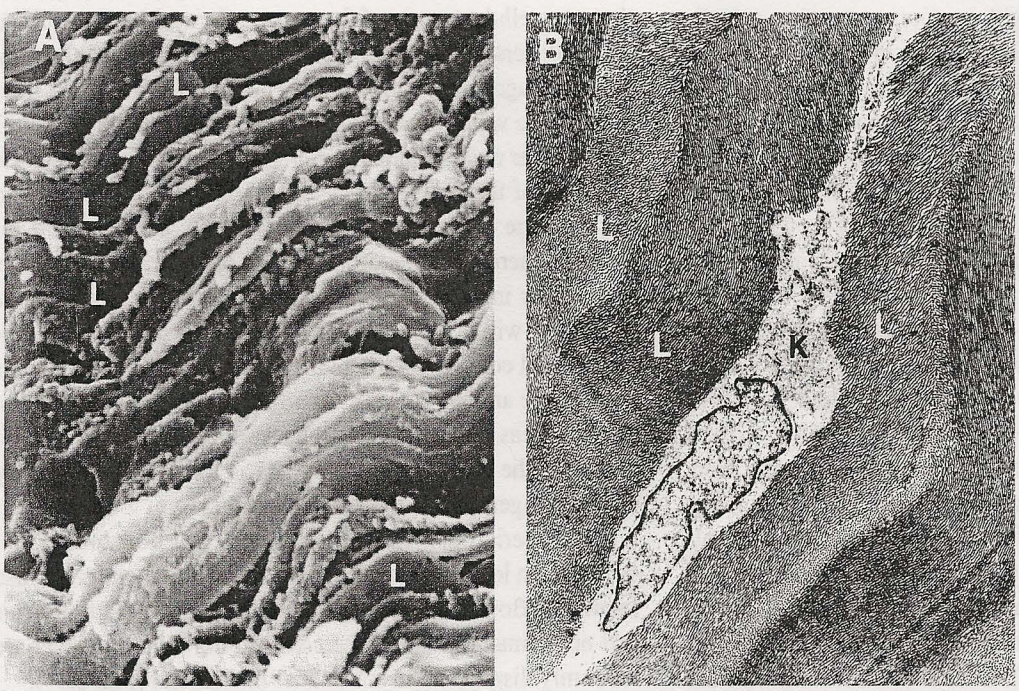

Figure 2.40. Corneal stroma, as shown by SEM in the dog (**A**) and TEM in the horse (**B**), consists of layers or lamellae (*L*) of collagen, which are sparsely interspersed with keratocytes (*K*). (Original magnification: A, X7400; B, X10,000.)

Figure 2.41. Wound healing in a canine cornea involves the proliferation of keratocytes (*K*), which maintain a plane of orientation running parallel to the longitudinal axis of the cornea. *M,* macrophage. (Original magnification, X2100.)

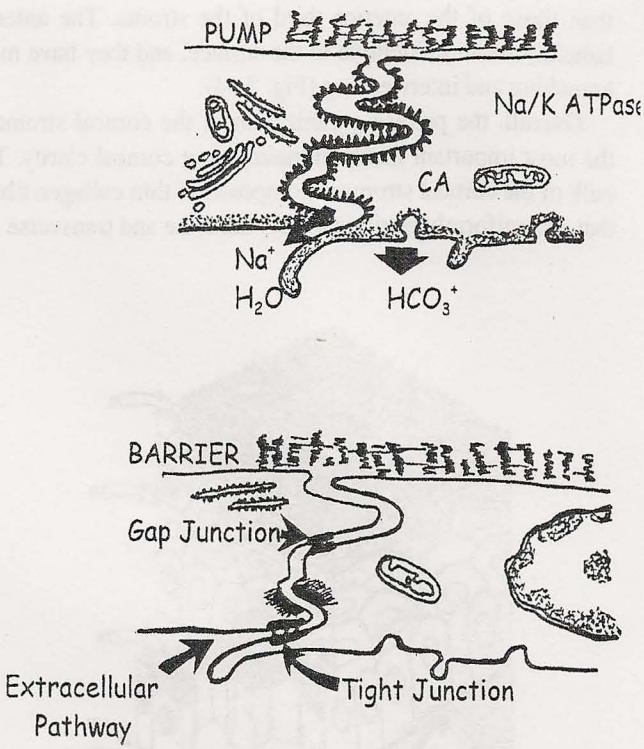

Figure 2.42. Location of the corneal endothelial metabolic pump (Na^+/K^+ ATPase along the lateral membranes and carbonic anhydrase along the apical margins) and barrier (apical tight junctions along the lateral membranes). (Redrawn from Watsky MA, Olsen TW, Edelhauser HF. Cornea and sclera. In: Tasman W, Jaeger EA, eds. *Duane's Foundation of Clinical Ophthalmology. Vol. 2.* Philadelphia: JB Lippincott, 1995.)

endothelium. Other "pumps" for deturgescence may also exist, including carbonic anhydrase. These cells pump Na^+ and Ca^{++} ions outward, into the aqueous humor and tears. Experimentally, removal of the epithelium produces an increase of 200% in corneal thickness after 24 hours because of the influx of water (i.e., edema). Removal of the endothelium produces an increase of 500% or more in thickness as the permeability increases sixfold, so the endothelium appears to be more important in maintenance of deturgescence in the cornea.[44] Figure 2.42 illustrates the primary roles the endothelium plays, both as a pump and as a barrier. The barrier component is provided by the tight junctions occurring apically along the lateral faces of adjoining cells next to the anterior chamber. These tight junctions are quite sensitive to calcium exposure, and they will break down when too much free Ca^{++} exists in the aqueous humor. The Na^+/K^+ ATPase pump is found further posteriorly, along the lateral membranes of neighboring cells (Fig. 2.42). A breakdown of the pump, the barrier, or both will result in rapid movement of water into the highly hydrophilic stroma.

The presence of selected GAGs allows the pumps to be effective. Thus, any change in the population of the GAGs, any significant damage to the epithelium or endothelium (i.e., the pumps), or any pressure exerted on the cornea will cause a physical rearrangement of the precise collagen organization, which in turn will result in opacity of the cornea. GAGs in the cornea consist of heparan sulfates, hyaluronic acid, undersulfated chondroitin sulfates, chondroitin 6-sulfate, chondroitin 4-sulfate, keratan sulfates, and dermatan sulfates. The most abundant of these is keratan sulfate, followed by dermatan sulfate.[45] Nearly all keratan sulfates are derived from stromal fibroblasts (i.e., keratocytes), whereas heparan sulfates are largely derived from the corneal epithelium, particularly as individuals mature. Hyaluronic acids, however, are formed to a fair degree by the corneal endothelium. Consequently, each corneal cell type contributes its own specific array of distinct GAG classes as well as, most likely, other glycoconjugates to the extracellular matrix of the cornea. Corneal keratan sulfate, which differs from that in cartilage by length, branching, and cross-linkage within the polymer, will absorb two to three times more water than chondroitin sulfates, but the latter will retain water eight to nine times better than keratan sulfate. On the basis of the different water-binding ability of GAGs, keratan sulfate is concentrated within the posterior bovine cornea, where it facilitates movement of water from the aqueous humor into the cornea.[46] Dermatan sulfate is more concentrated within the anterior stroma. In addition to the differential concentration of GAGs within the corneal stroma, the relative amount of keratan sulfate is lower toward the limbus, whereas the level of dermatan sulfate rises.[43] Concomitant with the loss of keratan sulfate is the loss of uniformly small collagen fibrils, as seen in the sclera.

The anteriormost stroma has a thin, cell-free zone corresponding in location with the anterior limiting membrane, also known as Bowman's layer (anterior lamina), in both humans and nonhuman primates. The collagen fibrils in this layer are randomly dispersed and are smaller in diameter (Fig. 2.34).

Bowman's layer is not seen in most animals as described in primates, though it is interpreted by some to occur throughout the mammalian eye.[47] In avian and human corneas, it is considered to be part of the corneal stroma and is 10- to 15-μm thick, relatively acellular, and composed of collagen fibrils of various types (Fig.2.43; Table 2.9). Although the different types of collagen are found in the stroma, the fibrils of Bowman's layer are smaller in diameter and less uniform than those of the stroma.[48] The anterior epithelium can produce most, if not all, of the collagen associated with this modified, acellular zone of the cornea. It is not elastic, but it is fairly tough and, when destroyed, may be replaced by scar tissue. From time to time, a Bowman's layer has been described in large, herbivorous mammals and most recently in the giraffe and various species of whales (Figs. 2.34 and 2.44).[49,50] Bowman's layer of the land-based species share similarities in size, morphology, and histochemistry, differing substantially from that of marine mammals, which may reflect a variation of roles that this structure plays. It has been assumed that Bowman's layer contributes additional stiffness and biomechanical strength to the cornea and to that end may be responsible for maintaining anterior corneal shape. Nevertheless, the construction of Bowman's layer in whales and to a lesser extent in giraffes varies from that of primates and birds. It is also interesting to note that among whales, Bowman's layer is not known to exist in deep-diving species, suggesting that its presence may be more closely associated with ocular function near or at the surface of the water. The bovine cornea possesses a similar structure beneath the anterior epithelium that rarely exceeds several micrometers in thickness but may represent a modified Bowman's layer.

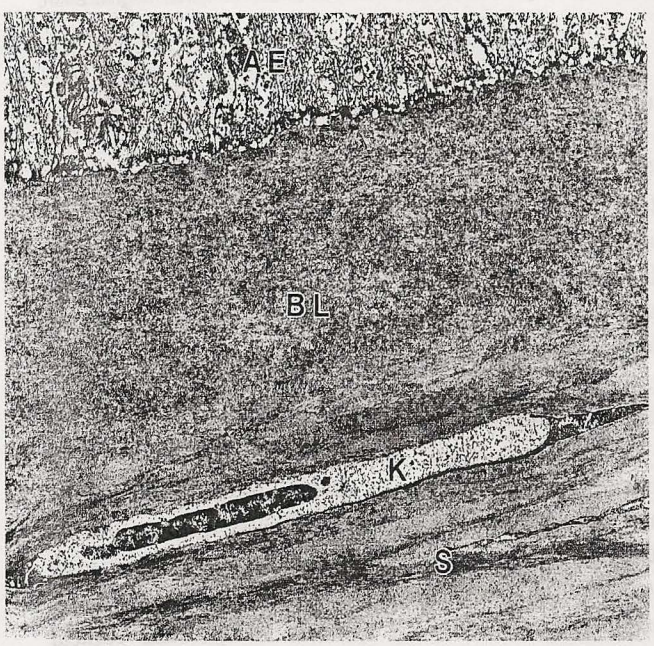

Figure 2.43. Bowman's layer or membrane (*BL*) in the chicken consists of an acellular zone or region of the anterior stroma immediately beneath the anterior epithelium (*AE*). Collagen fibrils in this area are the least organized of the entire stroma (*S*). (Original magnification, X3000.) (Courtesy of RD Whitley.)

Descemet's Membrane

Descemet's membrane is a homogenous, acellular membrane forming an inner protective boundary within the cornea. It is actually an exaggerated basement membrane of the posterior endothelium. It stains positively with PAS stain, as do other basement membranes, and it is produced by the posterior endothelium throughout life, thus forming a thicker membrane as the animal ages (Fig. 2.45).Clinically, the membrane shows elasticity, but it contains only fine collagen fibrils.[51] Descemet's membrane is normally under some tension and, if cut or ruptured, tends to curl like a scroll. Descemet's membrane ends at the apex of the trabecular meshwork in the limbal region. To some degree, its composition is similar to that of the trabeculae of the iridocorneal angle (ICA). This ever-thickening basement membrane contains a number of collagen types, including type VIII, which is found in the angle but not elsewhere in the cornea (Table 2.9).[52] Ultrastructurally, Descemet's membrane is distinctly layered in most animals, usually having a relatively thin anterior, unbanded zone next to the stroma, followed by a broad-banded zone and then by another broad, posterior unbanded zone located next to the endothelium (Fig. 2.45). Types III and IV make up the posterior unbanded zone, type IV and VIII the anterior banded zone, and types V and VI the anterior unbanded zone.[26]

Corneal Endothelium

The corneal endothelium is a single layer of flattened cells lining the inner cornea (Fig. 2.46). Some controversy exists regarding the regenerative ability of the endothelium, and indeed, it may vary with species and age. In general, however, active mitosis occurs primarily in the immature animal.[53–57] Specular microscopy and SEM of adult eyes reveal that the cells are usually hexagonally shaped (Figs. 2.47 and 2.48A). Closer inspection by SEM reveals that the surface is spotted with small microvillae and pores, and that the lateral edges of one cell interdigitate with another (Fig. 2.48B). In very young canines (i.e., 1–4 weeks of age), many of the cells do not have the typical hexagonal shape. Pronounced pleomorphism has also been observed in the kitten and the rabbit.[56] The reason for this pleomorphism is not known, but this cellular arrangement may result from increased mitotic activity with concomitant rapid corneal growth.[53]

Transmission electron microscopy (TEM) reveals the extensive, lateral, convoluted interdigitations between adjacent cells in the dog (Fig. 2.49). Along the lateral cell margins, the cell junctions, zonulae occludentes, maculae adherentes, and nexi occur. The abundance of mitochondria, smooth and rough endoplasmic reticulum, and a variety of vesicles, including pinocytotic vesicles, indicates these cells are metabolically active. There is gradual loss of the hexagonal shape in the oldest populations because of a concomitant, gradual decrease in the density of this epithelium. In young dogs, endothelial density is roughly less than 3000 cells/mm^2. As the animals age, endothelial density gradually lowers to 50% or less. With a smaller population, these cells spread out and

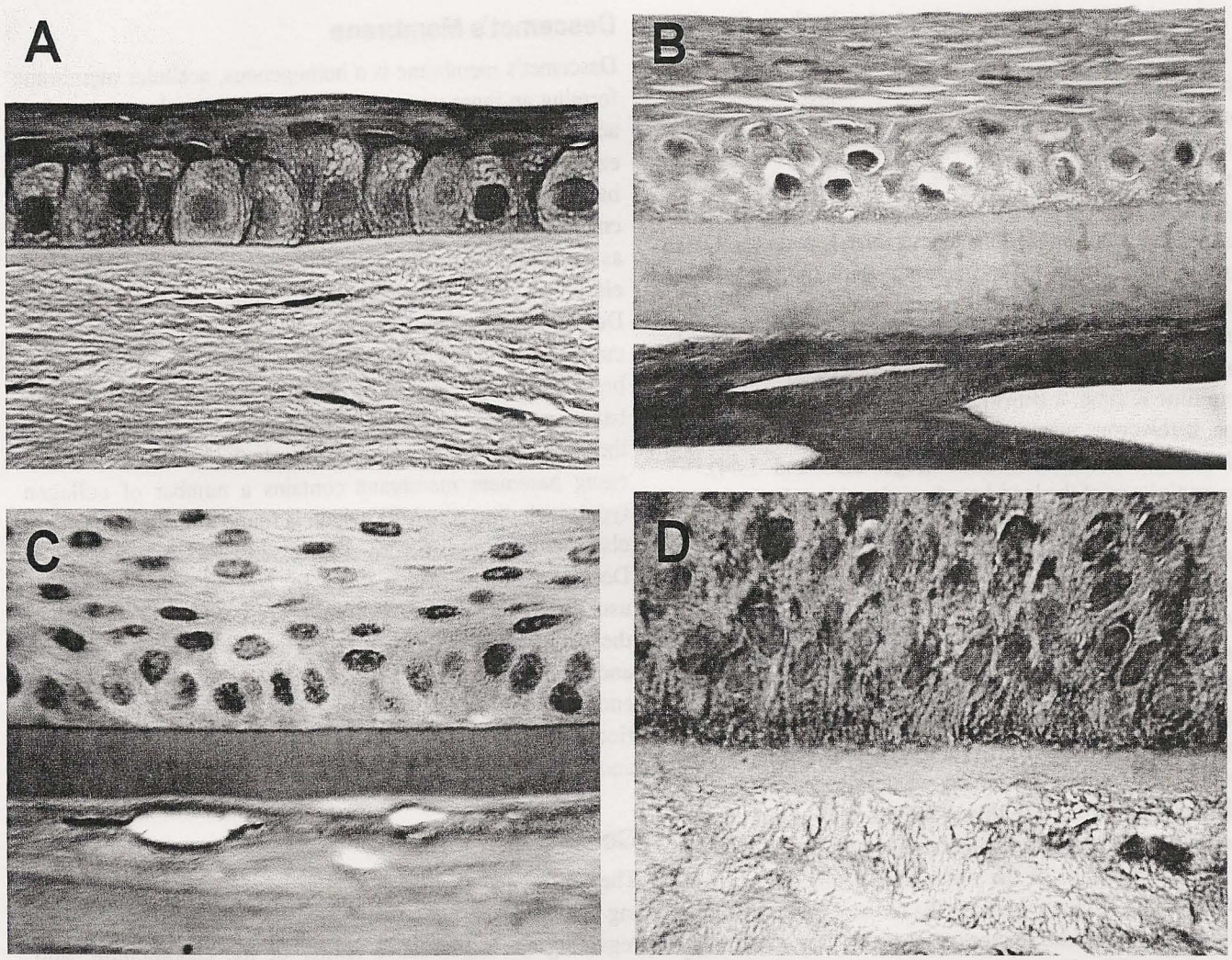

Figure 2.44. Bowman's layer among mammalian species. **A.** Rhesus monkey. (Original magnification, X400; Masson trichrome stain.) **B.** Bottle-nosed dolphin. (Original magnification, X400; Masson trichrome stain.) **C.** Pilot whale. (Original magnification, X400; PAS stain.) **D.** Giraffe. (Original magnification, X400; Masson trichrome stain.) (Courtesy of AZ Zivotoksky and D Zivotoksky.)

produce more pump sites to compensate for increasing leakage (Fig. 2.50). Thus, an age-related decrease in the density of corneal endothelial cells results in little change in thickness.[58] If the trend continues, however, the cells become too attenuated, which results in an insufficient pump unable to withstand the increasing leakage. This is the point known as corneal decompensation, and it usually occurs when the cell density falls to between 800 and 500 cells/mm^2.

Repair and Aging

Two processes are involved in healing of the epithelial surface of the cornea: cell migration to cover the injured area and mitosis to reconstitute the normal number of epithelial cells. The migratory activity occurs almost immediately following an abrasion of the cornea. Cell division soon follows to return the epithelium to normal thickness. Small epithelial defects may heal entirely, without any cell multiplication, simply by cell migration during the first 24 hours. When a considerable amount of anterior epithelium must be replaced, however, the anterior epithelium of the limbus becomes the primary source for production of new corneal anterior epithelial stem cells. Without the limbal epithelium, the proliferative capacity of the corneal epithelium is quite limited.[59]

Unfortunately, corneal endothelial cells do not respond to cell loss as quickly as do epithelial cells. Endothelial cells may be unable to retain a functional monolayer in inherited endothelial dystrophy, glaucoma, lens luxation, infectious diseases, aging, and after surgical (or other) trauma. In some species, including humans, nonhuman primates, the cat, and the dog, endothelial cells do not actively divide; instead, they enlarge and migrate to maintain a functional monolayer.[60,61] If this is not accomplished, a focal area of corneal edema is observed. This edema may be progressive, resulting in advanced corneal disease. In the species named, because no new endothelial cells are formed, any cells lost are replaced by the thinning and spreading of existing cells (Fig. 2.51),[61] and this results in a reduction of endothelial cell numbers and possible corneal decompensation. In the rabbit, corneal endothelial cells acquire a spindle-shape phase that provides a functional but incomplete barrier at the onset of injury.[62] After this phase, the cells become flattened and irregularly polyhedral in shape. The normal pump and barrier have both become reestablished, and then there is a

third phase in which the cells are further remodeled. This latter phase occurs 1 to 4 weeks after the injury. By comparison, wound healing in the cat's corneal endothelium is slower and not as complete as in the rabbit's. Stromal swelling in feline corneas will occur when cell density falls to less than 40% to 45% of normal measurements.[63]

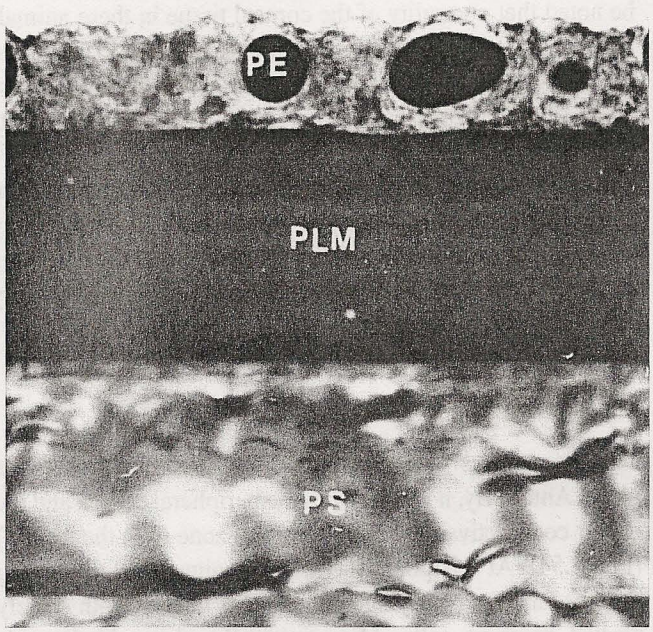

Figure 2.45. Posterior cornea of a horse. *PE,* posterior epithelium (corneal endothelium); *PLM,* posterior limiting membrane (Descemet's membrane); *PS,* posterior stroma. (Original magnification, X1200.)

Our understanding about the effects of aging on corneal morphology is limited. It has been known for some time that aging of the cornea and the lens can result in light scatter and reduced vision, but there has been little anatomic evidence to explain this change.[64,65] Most of the known age-related changes associated with the cornea involve the endothelium and Descemet's membrane. The aging Descemet's membrane becomes progressively thickened because of the continual addition of new basement membrane material by the endothelium.[66] This addition is quite remarkable from birth to adulthood; afterward, it is less pronounced but still distinct over a 5-year or longer span of time (Fig. 2.52).

As noted, the corneal endothelium demonstrates a steady decline in cell density with age. As the number of endothelial cell per area decreases, the average width of each cell increases.[67] Moreover, these cells become thinner, lose some of their general uniformity of size, and gradually become pleomorphic.

Little is known about age-related changes of the corneal stroma. By comparison, corneal wounding and repair has been studied extensively. A wounded cornea is often edematous and filled with inflammatory cells. To achieve successful wound healing of the stroma, the fibrous components must be reestablished in a way that follows, at least to some degree, normal development. Remember that the populations of proteoglycans (i.e., GAGs) are selective to keep the collagen fibrils organized and properly sized. If the relative concentrations of GAGs are substantially altered during wounding, the possibility of reforming the fibrous architecture for needed transparency is reduced and will remain so until the normal proteoglycan environment is rebuilt.[68–70]

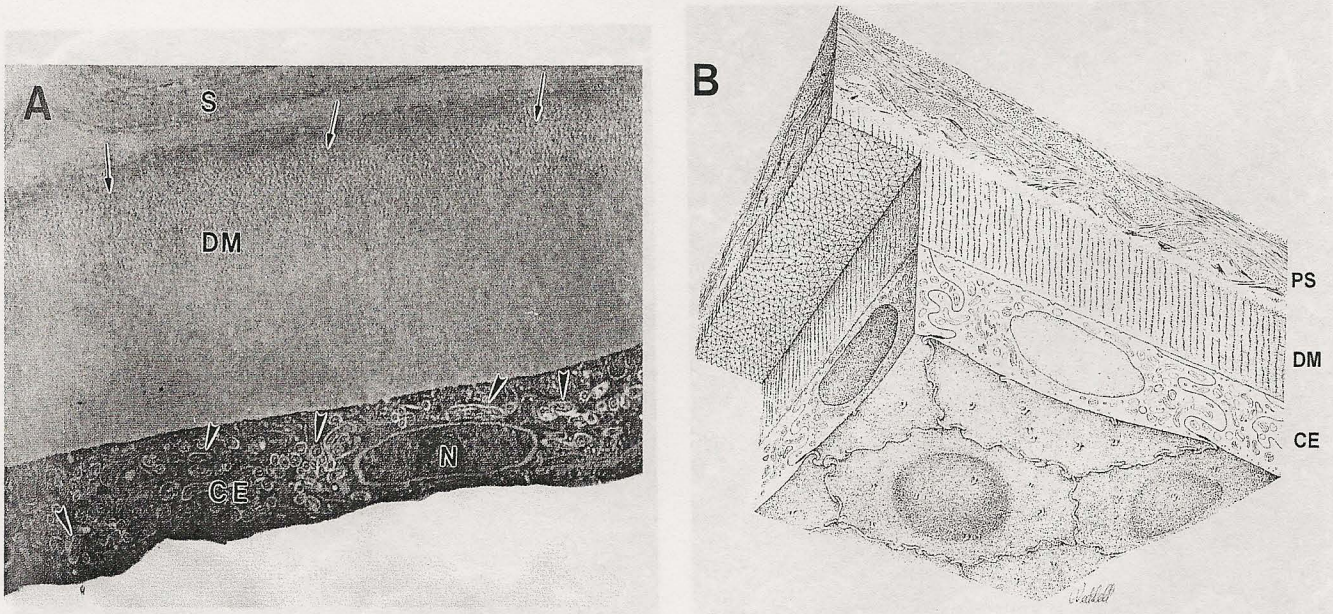

Figure 2.46. **A.** Descemet's membrane (*DM*) and corneal endothelium (*CE*) of an avian (i.e., chicken) cornea. Note the fine amorphous structure of the Descemet's membrane, though traces of banding are visible (*arrows*). The corneal endothelium does not possess hemidesmosomes as does the anterior epithelium to its basal lamina. *Arrowheads* point to the abundant mitochondria. *N,* nucleus; *S,* stroma. (Original magnification, X4000.) **B.** Three-dimensional drawing of the deep inner cornea showing the deepest corneal lamellae of the posterior stroma (*PS*), Descemet's membrane (*DM*), and the corneal endothelium (*CE*). (Revised from Hogan MJ, Alvarado JA, Weddell JE. *Histology of the Human Eye.* Philadelphia: WB Saunders, 1971.)

Hyaluronic acid is one of the first extracellular components to build up substantially after injury, filling lacunae in the stroma as well as between collagen lamellae.[71] Most often, it has been associated with dividing and migrating fibroblastlike cells within the stroma.[72] Gradually, hyaluronic acid decreases as the proteoglycans are reconstituted. If hyaluronic acid does not decrease in a timely manner, however, the normal flow of solutes will be altered, as will the normal spacing between collagen fibrils, which will reduce transparency and change the index of refraction.

Any angiogenic activity within the stroma should be reversed for successful repair. The presence of blood vessels in the cornea more centrally than at the limbus is indicative of corneal disease. The condition producing the vascularization may be local or generalized. There are some members of the animal kingdom, however, that have been described to be vascularized nonpathogenically, including the Rocky Mountain Bighorn sheep, armadillo, some Japanese salamanders (e.g., the giant, 5-foot long *Megalobatrachus maximus*), and certain laboratory mice (e.g., athymic, nude mice and euthymic hairless mice of the mutant strain *SKH1hr/hr*). Even so, it should be noted that normality of the corneal tissue in these animals has been little verified. By comparison, the Florida manatee (*Trichechus manatus latirostris*) does consistently possess blood vessels within the anterior epithelium and stroma of its cornea without any pathological association (Fig. 2.53).[73,74] The vessels occupy between 0.1% to 5% of the volume of the corneal tissue, mostly averaging less than 1% and most likely causing little interference with incoming light. Both fetuses and newborns have vascularized corneas, which are nearly identical to those of juvenile and adult animals.

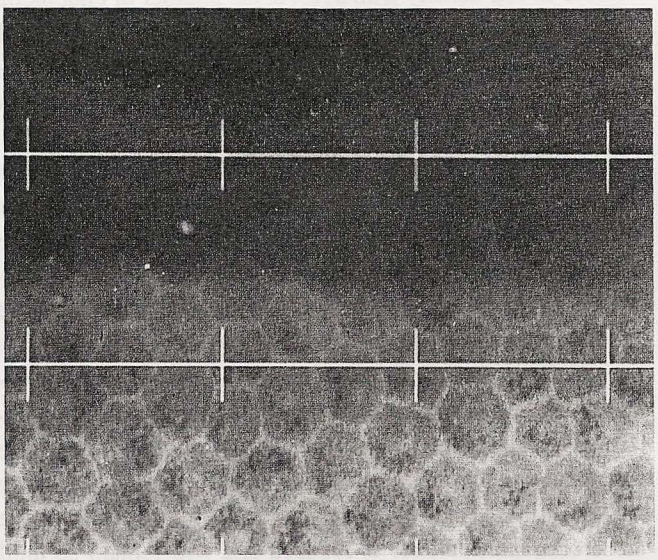

Figure 2.47. Specular micrograph of a young adult canine corneal endothelium shows the normal hexagonal arrangement of this tissue.

SCLERA

The sclera comprises the remainder of the fibrous tunic of the globe. Anteriorly, it merges with the peripheral cornea and the bulbar conjunctiva to form a transition zone (i.e., the limbus) (Fig. 2.54). At this point, the sclera is pigmented to varying degrees, and the overlying epithelium is thicker, with closely packed pigment cells. Microscopically, the epithelium is thicker than the adjacent corneal epithelium, with closely packed, small basal cells that have scanty cytoplasm. The stroma loses the regular arrangement characteristic of the cornea and takes on a less organized appearance of irregular,

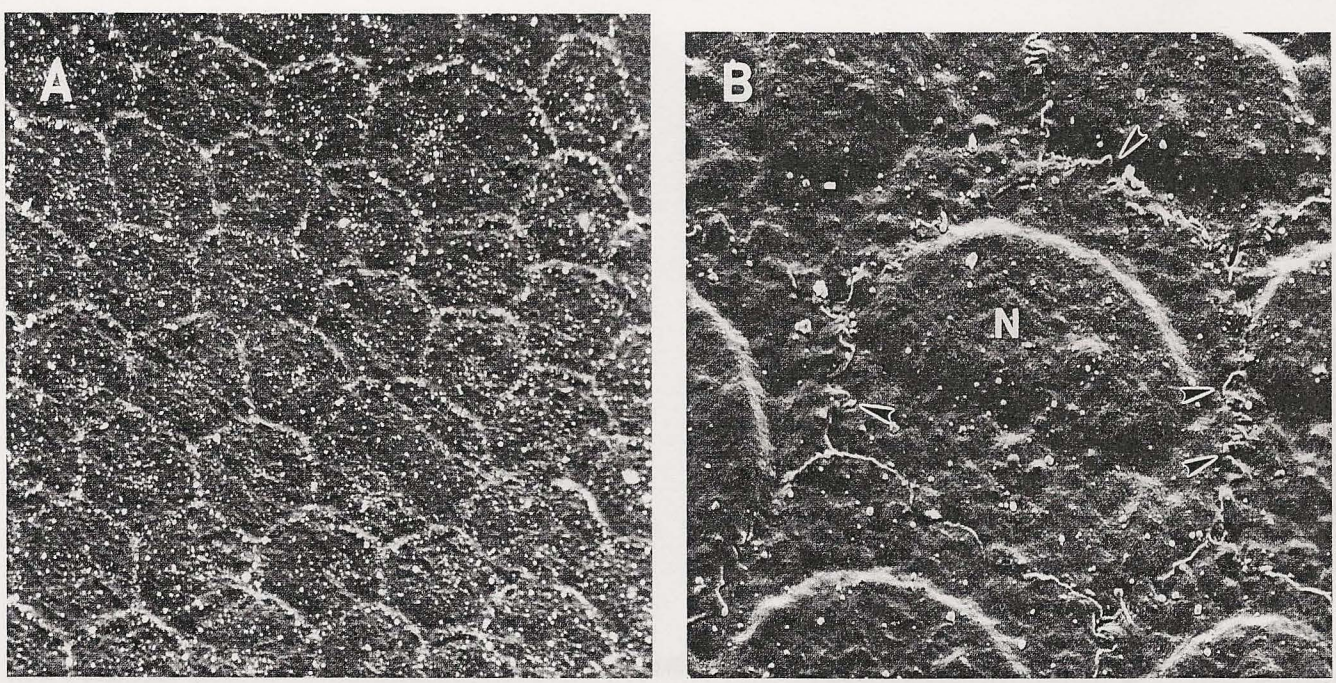

Figure 2.48. SEM of a 4-year-old canine corneal endothelium reveals occasional variability in cell size (*A*) and the lateral surface interdigitations between cells (*B, arrows*). The most prominent feature of the endothelial cell in the adult cornea is the nucleus (*N*), which bulges slightly into the anterior chamber. (Original magnification: A, X960; B, X3500.)

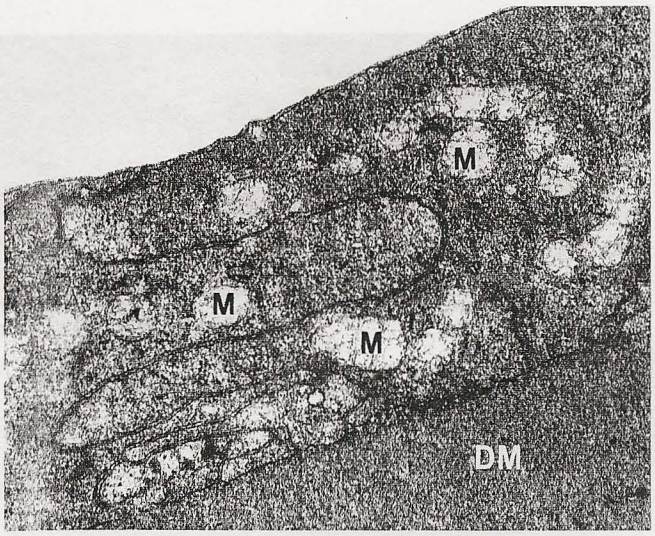

Figure 2.49. The lateral interdigitations observed between endothelial cells along the surface continue throughout the entire thickness of adjacent cells. Numerous mitochondria (*M*) are associated with these interdigitations. *DM,* Descemet's membrane. Canine cornea. (Original magnification, X16,000.)

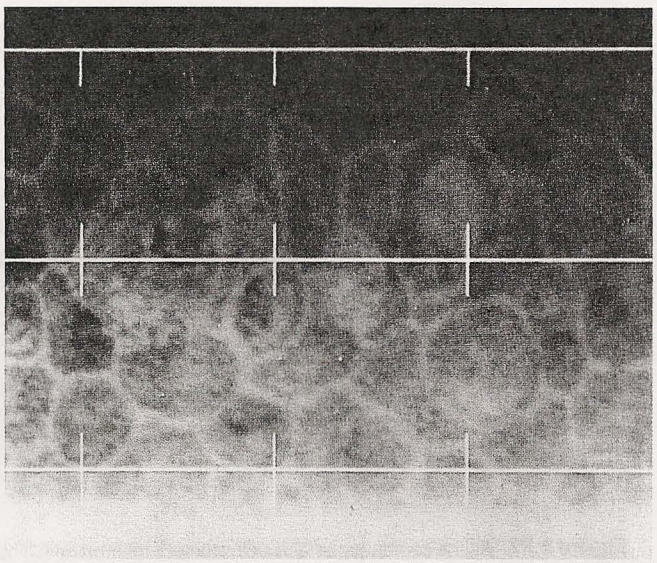

Figure 2.51. Specular micrograph of the corneal endothelium in a 7-year-old dog that had a cataract removed shows widening or spreading of adjacent cells to fill the areas in which endothelial cells had previously died. (Courtesy of R Gwin.)

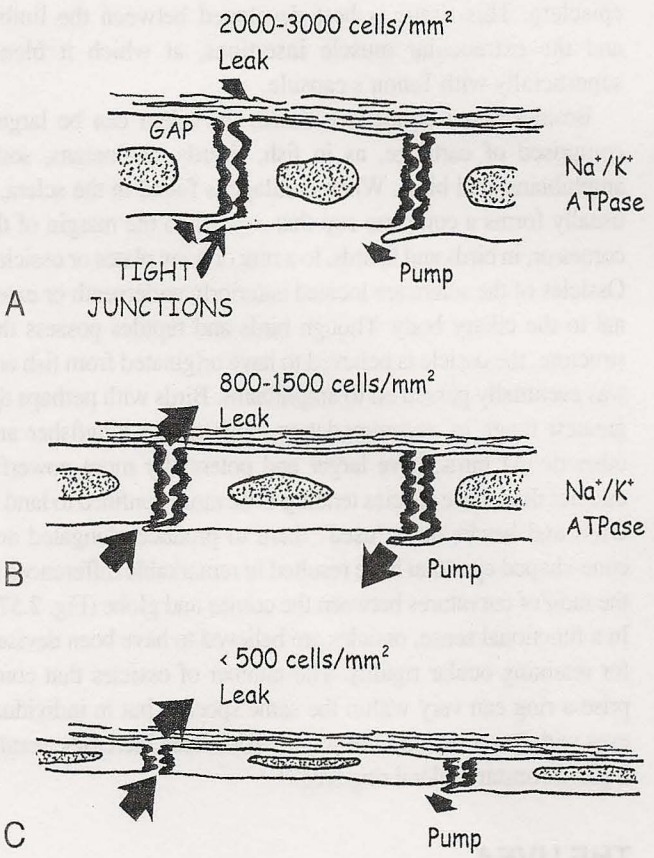

Figure 2.50. How corneal endothelial decompensation occurs as endothelial cells become so stretched that the remaining lateral membranes are insufficient to provide an adequate pump. **A.** Normal state with pump = leak. **B.** As cells diminish with age or disease, more pump sites are produced so that pump = leak. **C.** With minimal lateral membranes, corneal decompensation occurs and leak > pump. (Redrawn from Watsky MA, Olsen TW, Edelhauser HF. Cornea and sclera. In: Tasman W, Jaeger EA, eds. *Duane's Foundation of Clinical Ophthalmology. Vol. 2.* Philadelphia: JB Lippincott, 1995.)

dense connective tissue. Numerous blood vessels (i.e., the anastomosing branches of the anterior ciliary arteries) terminate in the loops of the marginal plexus, then drain back into the conjunctival venules. Bowman's layer exteriorly and Descemet's membrane interiorly also terminate in this area.

Along the outer portion of the stroma is an interconnecting network of veins known as the intrascleral plexus, which receives aqueous humor from the veins that drain the angular aqueous plexus (AAP) (Fig. 2.55). The intrascleral plexus is variably connected with the choroidal venous system (i.e., the vortex system) in domestic animals (Fig. 2.56).[75,76] The intrascleral plexus is variable in its relative size and depth in the sclera.[77–79] For example, in rabbits and primates, the plexus is formed on the outer side of circumferentially coursing canals, and it is composed of small vessels deep in the sclera. In carnivores, the intrascleral plexus is prominent and composed of from two to four large, anastomosing vessels in the midsclera. The intrascleral plexus receives afferent channels superficially via the episcleral network at the limbus as well. In the horse, the plexus, which is less prominent, collateralizes entirely with the anterior vortex system, because it is oriented radially to facilitate unidirectional flow outward from the angle region toward the vortex veins; in carnivores and primates, the reservoirs receiving aqueous humor are circumferentially oriented.

The color of the sclera depends on the thickness of its stroma (appearing blue when thin) and the fat content along its outer boundary (appearing yellow with increased content). The inner surface, which is referred to as the lamina fusca, is brown because of the adherent suprachoroidal pigment. The bulk of the sclera is called the sclera proper, which is very similar histologically to the limbus. The sclera contains elastic fibers that are interlaced among the collagen fibers, as are melanocytes (anteriorly) and fibrocytes. The collagen fibers, fibrocytes, and

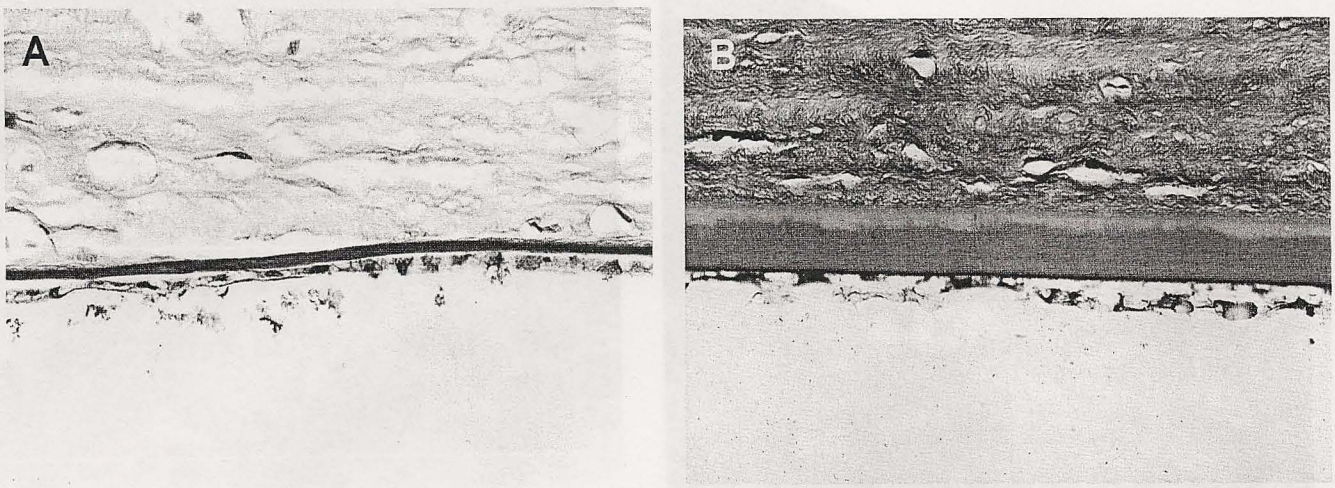

Figure 2.52. As the cornea grows older, Descemet's membrane (*D*) continues to expand in width, as seen when comparing a 1-year-old dog (**A**) with a 6-year-old individual (**B**). *CE,* corneal endothelium; *S,* stroma. (Original magnification, X400.)

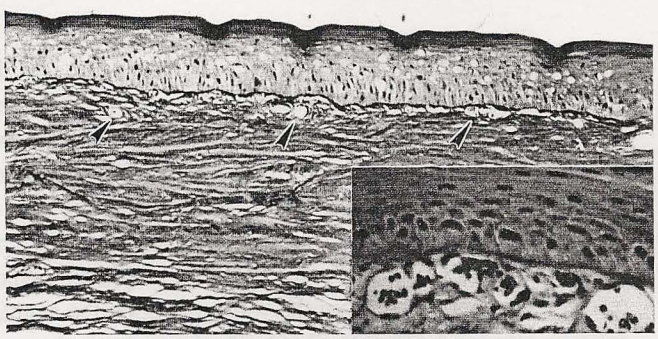

Figure 2.53. Anterior corneal stroma of adult manatee contains sparsely populated blood vessels (*arrows*). (Original magnification, X100.) **Insert.** Close-up of a cluster of these thin-walled vessels filled with erythrocytes. (Original magnification, X400.)

occasional melanocytes are arranged meridionally, obliquely, and radially in an irregular fashion. The sclera is more hydrated than the cornea and contains blood vessels. Its rigidity provides the resistance to intraocular fluid pressure, and several channels, or emissaria, are present for the passage of blood vessels and nerves. The most notable emissaria accommodate the optic nerve, long and short ciliary nerves, long posterior ciliary arteries, vortex veins, and anterior ciliary vessels.

Scleral thickness varies considerably among species and in different areas of the globe, but it is thinnest near the equator, especially at the insertions of the extraocular muscles, and in the dog is only 0.12-mm wide (Table 2.10). The region of the intrascleral venous plexus is the thickest area in animals with a well-developed plexus (e.g., the dog and cat), whereas in ungulates, the region of the optic nerve entrance or posterior pole is the thickest. At the point where the optic nerve passes through the sclera, it becomes sievelike in the area known as the lamina cribrosa. Abnormal tension in this region because of glaucoma disrupts the axoplasmic flow in individual nerve fibers of the optic nerve.

The external boundary of the scleral stroma consists of a thin collagenous and vascular membrane known as the episclera. This tissue is best developed between the limbus and the extraocular muscle insertions, at which it blends superficially with Tenon's capsule.

Besides dense connective tissue, the sclera can be largely comprised of cartilage, as in fish, lizards, chelonians, some amphibians, and birds. When cartilage is found in the sclera, it usually forms a complete cup that extends to the margin of the cornea or, in birds and lizards, to a ring of bony plates or ossicles. Ossicles of the sclera are located anteriorly underneath or external to the ciliary body. Though birds and reptiles possess this structure, the ossicle is believed to have originated from fish and was eventually passed on to amphibians. Birds with perhaps the greatest range of accommodation, such as the kingfisher and other diving birds, have larger and potentially more powerful ossicles than those species tending to be more confined to land.[80] Owls and hawks have "used" them to produce elongated and cone-shaped eyes that have resulted in remarkable differences in the radii of curvatures between the cornea and globe (Fig. 2.57). In a functional sense, ossicles are believed to have been devised for retaining ocular rigidity. The number of ossicles that comprise a ring can vary within the same species, but in individual eyes with fewer ossicles the single ossicle area increases, resulting in a constant scleral ring area.[81]

THE UVEA

The choroid, ciliary body, and iris form the uveal coat, or uvea. Unlike the fibrous coat, it is highly vascular and usually pigmented. The choroid and ciliary body are both attached to the internal surface of the sclera (Fig. 2.58). The iris originates from the anterior portion of the ciliary body, and it extends centrally to form a diaphragm in front of the lens. The iris and ciliary body are termed the *anterior uvea* and the choroid the *posterior uvea.*

Table 2.10 Thickness of the Sclera

Animal	Center of the Eyeground (mm)	Entry Point of the Optic Nerve (mm)	Equator of the Globe (mm)	Place of Crossing in the Cornea (mm)
Horse	1.5–2.2	1.35	0.5–0.3	1.1
	1.9		0.4	
Cow	1.9	2.20	1.0	1.2–1.5
Sheep	1.0–1.2	No increase in thickness	0.25–0.30	0.4–0.5
Pig	1.0–1.2	Thicker	0.5–0.8	—
Cat	0.09–0.20	0.13–0.60	0.09–0.20	1.1, in the form of a ring 5–7 mm wide
Dog	Similar to the cat, only thinner	0.3–0.4	0.12–0.20	0.6

Translated from Bayer *J. Angenheilkunde.* Vienna: Braumueller, 1914; and from Donovan RH, et al. Histology of the normal collie eye. *Ann Ophthalmol* 1974;6:257.

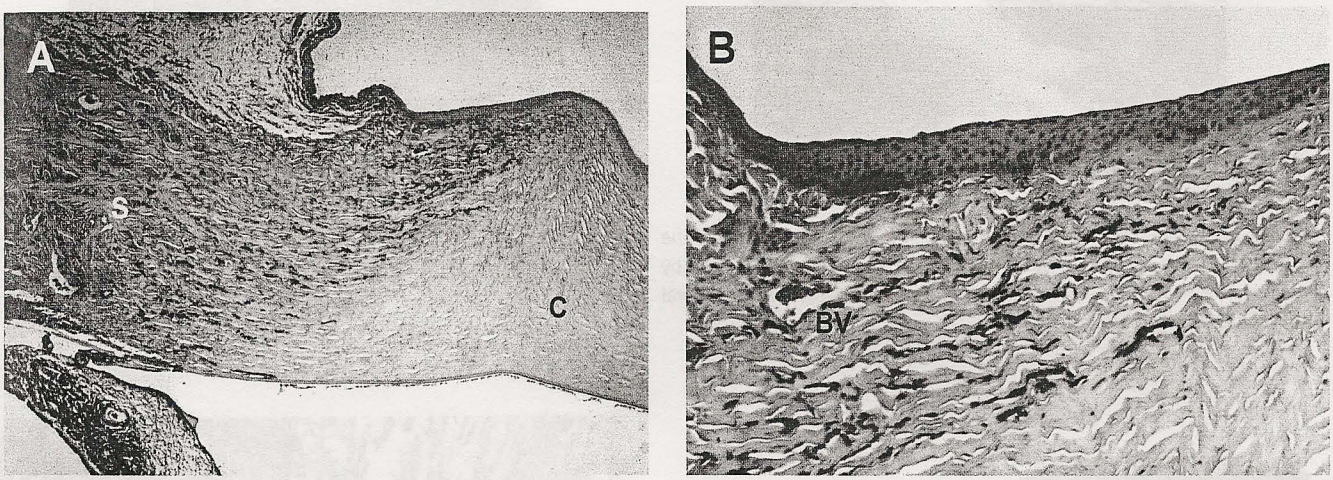

Figure 2.54. Canine limbus. **A.** Overall view shows merging of the irregular connective tissue of the sclera (*S*) with the highly organized connective tissue of the cornea (*C*). (Original magnification, X400.) **B.** Close-up of the outer limbus reveals an anterior epithelium that is markedly thickened, small blood vessels (*BV*), and melanocytes. (Original magnification, X250.)

Iris

The iris is a diaphragm that derives from the neural crest, mesoderm, and neuroectoderm. It extends centrally from the ciliary body to cover the anterior surface of the lens, except for a central opening, the pupil. It divides the anterior ocular compartment into anterior and posterior chambers, which communicate through the pupil. The shape of the moderately dilated pupil varies among species. Among mammals, it is round in primates, the dog, and the pig; is vertical when constricted in the cat; and it is oval in a horizontal plane in herbivores (i.e., horses, oxen, sheep, goats) (Figs. 2.10, 2.11, and 2.12). Along the upper edge of the pupil in herbivores, several round black masses are present (Fig. 2.59). They vary in size and are called granula iridica (i.e., corpora nigra). Similar smaller masses also exist on the lower edge of the pupil. These pigmented masses, which are extensions of the posterior pigmented epithelium, augment the effectiveness of pupillary constriction (i.e., miosis). Occasional myocytes of the sphincter muscle can be found in the basal portion of the granula iridica of goats and horses (Fig. 2.60). The presence of these cells indicates that these structures probably play more than a passive role during changes of pupillary size and shape. Eyes of animals with pupils that can be contracted to a slit are believed, in most instances, to be more sensitive to light than those with circular pupils.[3]

Grossly, the anterior iris is composed of a central pupillary zone and a peripheral ciliary zone. The demarcation between these two zones is the collarette, which is best demonstrated with moderate pupillary dilation. The portion of the ciliary zone adjacent to the pupil is sometimes more pigmented than the rest of the iris.

The peripheral half of the ciliary zone on frontal view contains a sinuous artery that passes circumferentially. The arteries enter at the nine- and the three-o'clock positions as terminations of the medial and lateral branches of the long posterior ciliary arteries (Fig. 2.11). Each artery branches dorsally and ventrally to pass circumferentially toward the opposite artery, and each forms an incomplete arterial circle, which is seen in the dog, pig, and horse at the twelve- and the two-o'clock positions.[82,83]

The function of the iris is to control the quantity of light entering the posterior segment through a central pupil. Contraction of the pupil reduces the amount of light entering the eye. Narrowing the pupil also eliminates the peripheral portion

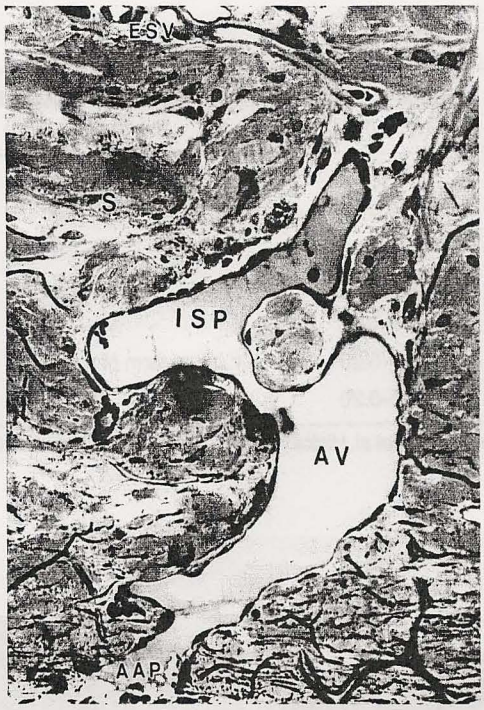

Figure 2.55. The intrascleral plexus (*ISP*) of a dog is located within the midsclera (*S*) and interconnected to the angular aqueous plexus (*AAP*) by aqueous veins (*AV*) that are sometimes prominent in size. *ESV,* episcleral veins. (Original magnification, X125.)

Figure 2.56. Corrosion cast of the canine ocular microvasculature demonstrates collateralization of the intrascleral plexus (*ISP*) with choroidal veins (*CV*) of the vortex system. (Original magnification, X410.)

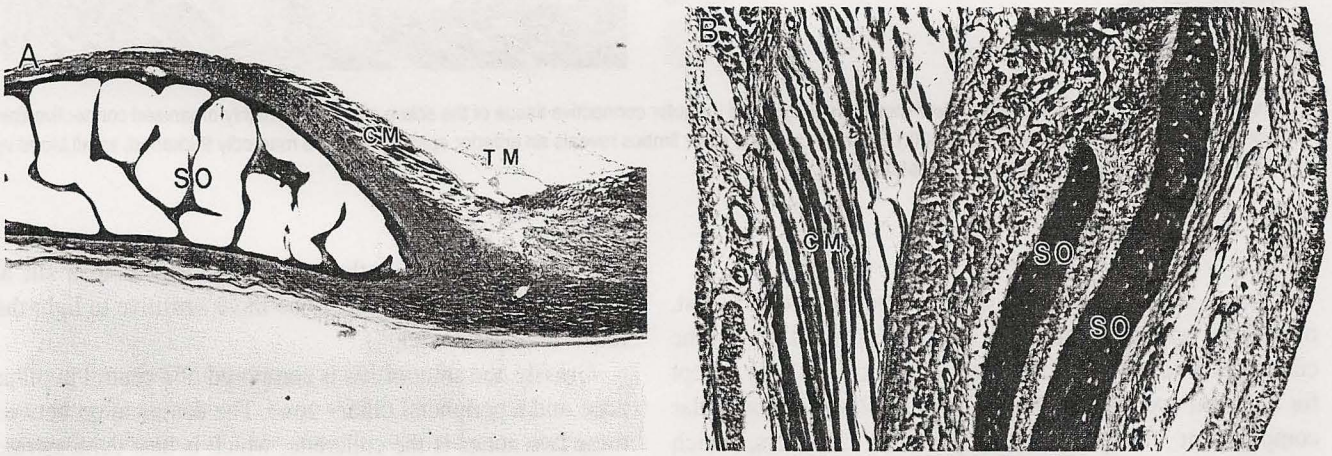

Figure 2.57. Scleral ossicles (*SO*) in birds vary somewhat in size and shape, being well developed with large interosseal spaces in owls (screech owl) (**A;** original magnification, X40) and comparatively thin in the chicken, with considerable overlap between adjacent ossicles (**B;** original magnification, X100). *CM,* ciliary body musculature (Crampton's muscle); *TM,* trabecular meshwork.

of the refractive system, and it diminishes lenticular spherical and chromatic aberrations. During periods of reduced light, the pupil dilates widely, allowing maximal stimulation of photoreceptor cells.

For the purpose of histologic discussion, the iris is divided into the anterior border layer, the stroma and sphincter muscle, and the posterior epithelial layers (Fig. 2.59). The anterior border layer consists of two cell types: fibroblasts, and melanocytes. The presence of a continuous epithelial sheet is frequently cited, but results of electron-microscopic studies have indicated them to be more fibroblastic in nature.[84–86] The anterior cells, which lack a basement membrane, form an almost-continuous layer with their cellular processes, but frequent small openings with large intercellular spaces and extension of underlying melanocyte processes break the continuity (Fig. 2.61). One or more layers of melanocytes are beneath the single layer of fibroblasts and compose the remainder of the anterior surface layer. For the most part, the melanocytes are oriented parallel to the iris surface, and their processes intermingle with other melanocytes

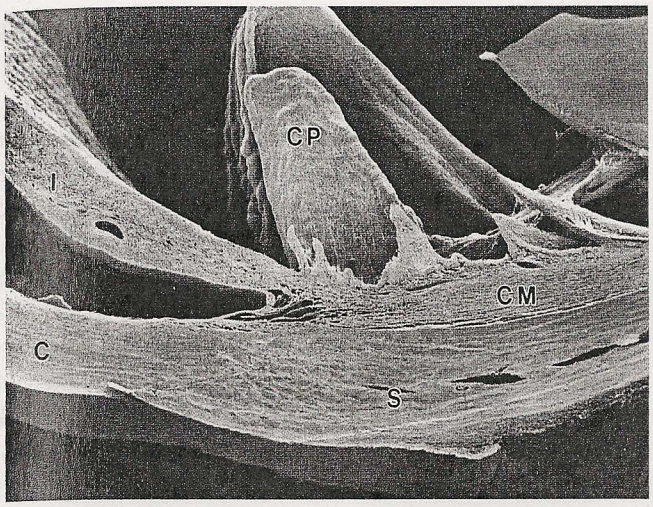

Figure 2.58. SEM of the canine anterior uvea. *C,* cornea; *CP,* ciliary processes; *CM,* ciliary body musculature; *I,* iris; *S,* sclera. (Original magnification, X25.)

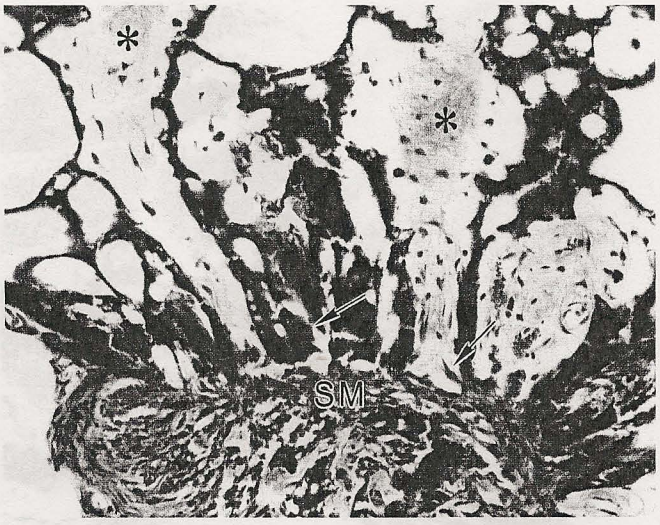

Figure 2.60. Myocytes of sphincter muscle (*SM*) line the pupillary margin of the goat iris and, occasionally, ingress (*arrows*) into the granula iridica, which also contains connective tissue elements (*). (Original magnification, X200.)

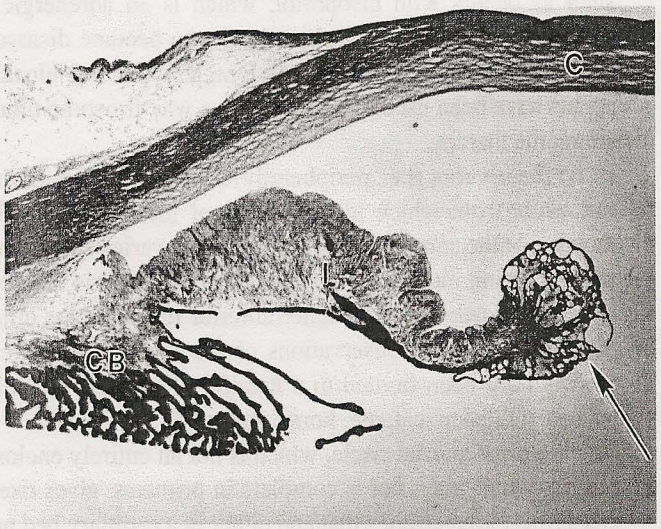

Figure 2.59. Iris (*I*) and anterior ciliary body (*CB*) of the goat. The *arrow* points to the granular iridica, which extends posteriorly along the posterior pigment epithelium. *C,* cornea.

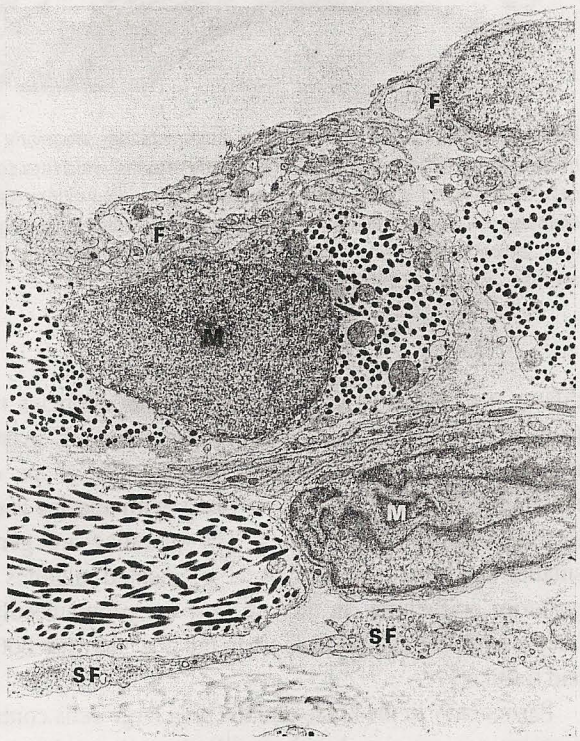

Figure 2.61. The anterior iris surface of the cat is composed of a fibroblastic surface layer (*F*) with ramifying processes and two layers of melanocytes (*M*) beneath fibroblasts. The lancelot shapes are pigment granules. *SF,* stromal fibroblast. (Original magnification, X9800.)

and anterior fibroblasts with no intercellular junctions. The pigment granules in the cat and dog are lanceolate to ovoid in shape, whereas they are round to ovoid in the horse.[76,87]

The iris stroma is composed of fine collagenous fibers, many chromatophores, and fibroblasts. The stroma is loosely arranged except around blood vessels and nerves, at which it can form dense sheaths. The collagen fibrils are organized to some extent in overlapping, wide arcades running from the pupil to the ciliary body.[88] Despite the dense histologic appearance, considerable extracellular space is evident ultrastructurally (Fig. 2.62). The ample space may be largely due to the unique orientation of the collagenous "skeleton" of the iris, consisting of a series of fibrous areas joining the iris root to its pupillary margin.[89]

Radial and meridional spaces, particularly those located anteriorly, receive materials including particles measuring up to 200 μm in diameter from the anterior chamber by diffusion into the stroma.[90,91] Fibroblasts and melanocytes are the predominant cell types that can be evenly distributed throughout the stroma of the iris or concentrated either anteriorly or posteriorly. In addition to the scattered melanocytes in the anterior stroma of many dog irides, a dense band of melanocytes can be present in the ciliary zone anterior to the

Figure 2.62. Canine iris stroma demonstrating irregularly placed melanocytes (*M*) except next to veins (*V*) and arteries, which are concentrically surrounded by the melanocytes. Note the marked differences in the diameter of collagen fibrils on the cross-section of different collagen bundles, indicating fusiform or spindle shape. Fibroblast processes (*arrows*) are also present. (Original magnification, X3500.)

dilator muscle, extending centrally to the sphincter muscle (Fig. 2.63A). The melanocytes are also especially prominent around the adventitia of blood vessels. The shape of the melanin granules in the stroma varies with species and with the maturity of the granules. The granules are generally smaller and more rodlike than the pigmented granules of the posterior epithelium. In the cat, they are pronouncedly rodlike, resembling tapetal rodlets; in the dog, they are both oval and rodlike.[87]

Particularly in the horse and the dog, large cells containing pigment are associated with capillaries and venules near the sphincter muscle.[86,92] These are believed to be macrophages of hematogenous origin. In humans, these cells are known as the clump cells of Koganei.[92] The cytoplasmic pigmented inclusions are so dense that they obscure the nucleus (Fig. 2.63B).

Iridal color varies considerably among individuals and among various breeds or species of animals. Color depends on the amount of pigmentation of the iridal stroma. The variation of color primarily results from the amount of pigmentation present, the type of pigmentation, and the degree of vascularization. In many instances, coloration of the irides of domestic animals tends to be dark, varying from dark brown to golden brown, gold, blue, and blue-green in color. Birds, on the other hand, have brightly colored irides. Traditionally, these bright colors were thought to result from the presence of carotenoids, an idea based on a single study of the yellow iris of chickens performed over 50 years ago. Carotenoid-bearing cells are referred to as xanthophores, and their presence certainly has been demonstrated to produce brightly colored irides. Recent studies, however, have found purines and pteridines to be the major iridal pigments in a variety of avian species, including doves and the great-horned owl.[93] Overall, pteridines and purines may be present more commonly than carotenoids as iris pigments in birds, and they are often found together as colored crystals. Combinations of purines/pteridines and carotenoids are probably common as well. Development of these pigments within an individual has been known to take a considerable amount of time, even as long as several years.[93]

As perhaps the most pigmented structure of the eye, the iris can bind many drugs, some of which can have toxicologic relevance. Even though melanin's ability to bind drugs, including chlorpromazine, benzodiazepines, and chloroquine, has been well documented, unexpectedly high accumulations of various drugs continue to be found in the iris and ciliary body.[94,95] In many instances, the drugs are reversibly bound, such as occurs with bisoprolol, which is an adrenergic β-antagonist that takes 1 week or longer to become disassociated from the uveal melanin of Beagles. Other β-blocking agents have been used in a time-release way for some time in glaucoma therapy.

At the iris root (i.e., peripherally) is an annular major arterial circle from which many vessels of the iris derive. The location of the annular major arterial circle varies among individuals, being most deep within the base of the iris but occasionally placed within the anteroinferior region of the ciliary body (Fig. 2.63A). Observations of the angioarchitecture of the iris have been limited to a handful of species, including primates, the dog, cat, pig, horse, and rat.[76,77,82]

The major arterial circle, which is not an entirely enclosed ring in nonprimates but is complete in primates, gives rise to numerous radial arteries that end either in a capillary bed near the pupillary margin (i.e., in the dog and cat) or in a minor arterial circle of the iris (i.e., in primates and the pig). There is some debate over the presence of secondary arterial circles in the equine iris.[76,82] The functional significance of the minor arterial circle is unclear.

The radial arteries to the pupil are generally tortuous in most animals (Fig. 2.64). The degree of tortuosity may reflect differences in pupil mobility between species. In the dog, transverse anastomosis of the radial arterioles is poorly developed, so a minor arterial circle does not exist.[82]

The radial arteries lose the internal elastic membrane that occurs in the major arterial circle artery, and they have only one layer of smooth muscle cells, compared with two to four in the latter artery (Fig. 2.65). A thick basement membrane is present externally, which also surrounds the smooth muscle cells, but this membrane is interrupted by frequent myoepithelial junctions.

A capillary network near the pupillary margin connects the terminal arterioles with the venules, which pass to the base of the iris behind the arterioles in the posterior stroma. The capillary

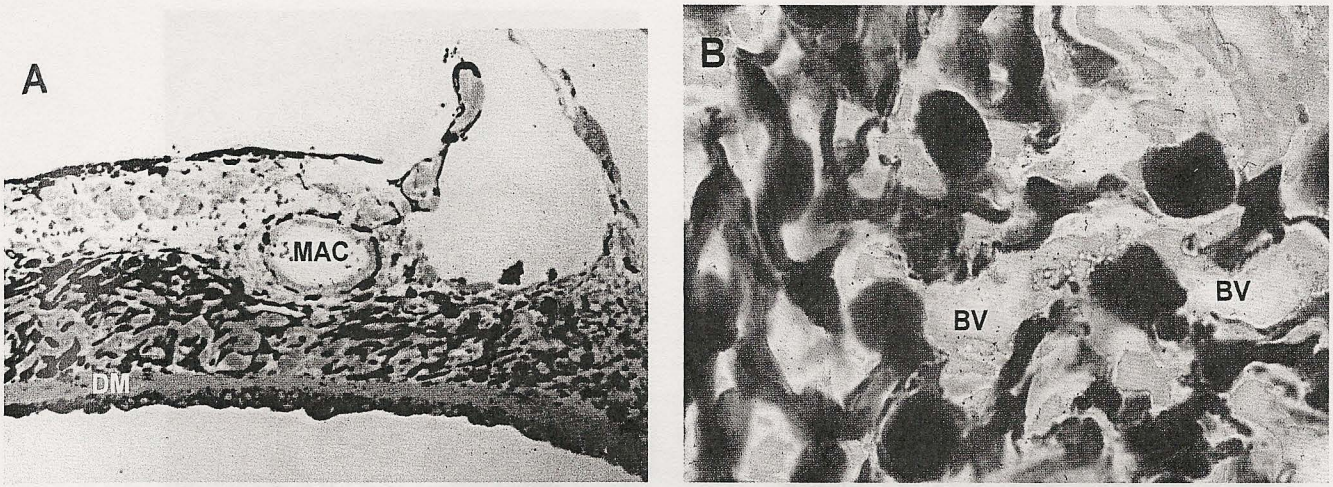

Figure 2.63. **A.** In many canine irides, melanocytes are concentrated in a wide band anterior to the dilator muscle (*DM*), as seen in the lower half of this iris. *MAC,* major arterial circle. (Original magnification, X100.) **B.** Large pigment-bearing cells are observed next to a small blood vessel (*BV*) near the sphincter muscle in this canine iris. (Original magnification, X400.)

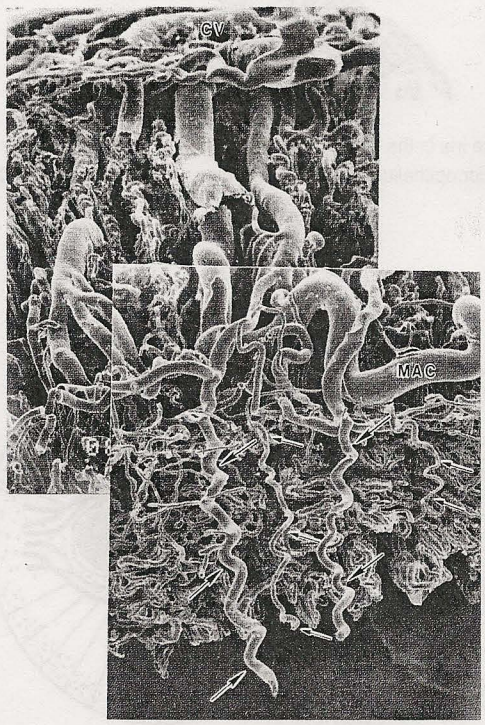

Figure 2.64. SEM corrosion cast of the anterior microvasculature of the equine eye. The iridal arteries (*small arrows*) and veins (*large arrows*) have a tortuous appearance as they progress toward the pupil. Note the iridal veins eventually empty posteriorly, into the anterior choroidal venous system (*CV*). *MAC,* major arterial circle. (Original magnification, X40.)

Figure 2.65. Radial artery in iris stroma of a horse. The endothelium has microvillae projecting into the lumen. A basal lamina (*arrows*) is found externally that also surrounds the smooth muscle processes (*S*). Melanocytes (*M*) and fibroblast processes (*F*) are found adjacent to the vessel. (Original magnification, X11,000.)

endothelium is not fenestrated, but the type of intercellular junctions varies with the species. The mouse, monkey, and human have a tight zonula occludens, but the rat, cat, and pig have 4-nm gap junctions between maculae occludentes.[96]

Venous drainage of the iris occurs through tortuous, radial vessels that empty directly into the anterior choroidal veins and out the vortex veins (Fig. 2.64), which typically number four in humans, the pig, and the cat but may vary in other species (e.g., the dog).[75,82,97] A unique variation of iridal venous drainage was recently discovered in the horse[76]: branches of the intrascleral venous plexus empty into the bases of the iridal veins, which in turn empty into the anterior choroidal venous circulation.

The iridal sphincter muscle, which is a flat band of thin, circular bundles of unstriated muscle fibers in mammals and striate muscle fibers in nonmammals, is located in the stroma near the pupil. In the dog and cat, it lies in the posterior

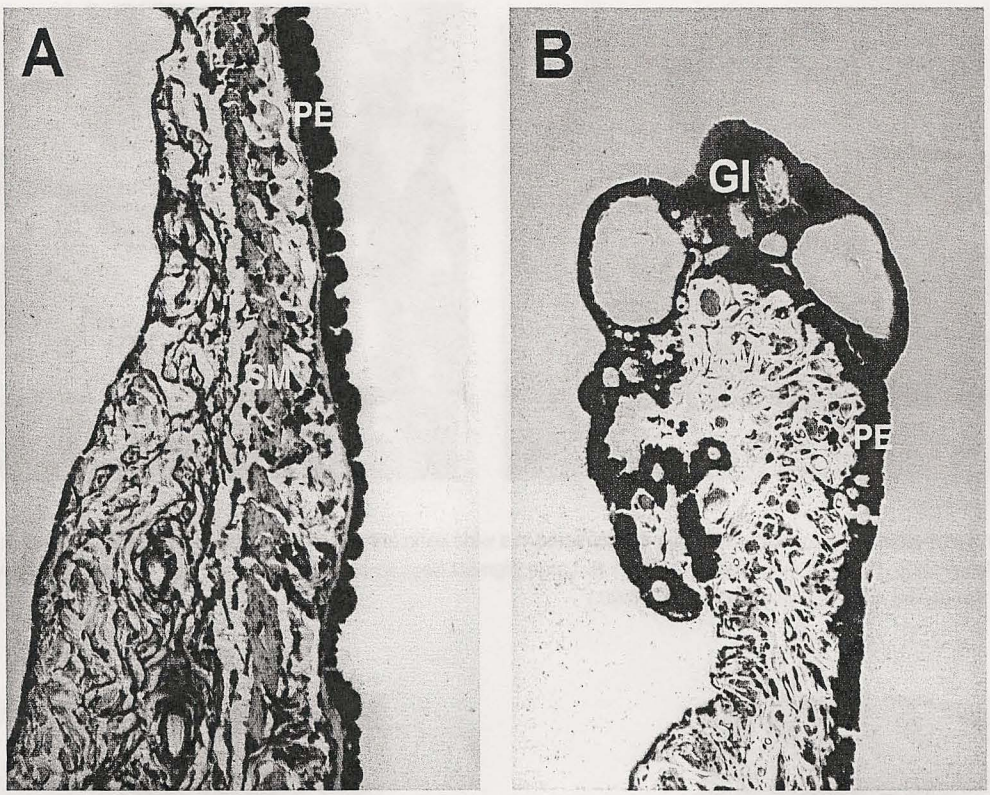

Figure 2.66. Sphincter muscle (*SM*) is located more posteriorly within the stroma of the iris in the dog (**A**) than in the horse (**B**). The sphincter muscle in the young horse is capped by the granula iridica (*GI*), which is a proliferation of the posterior epithelium (*PE*). (Original magnification: A, X200; B, X200.)

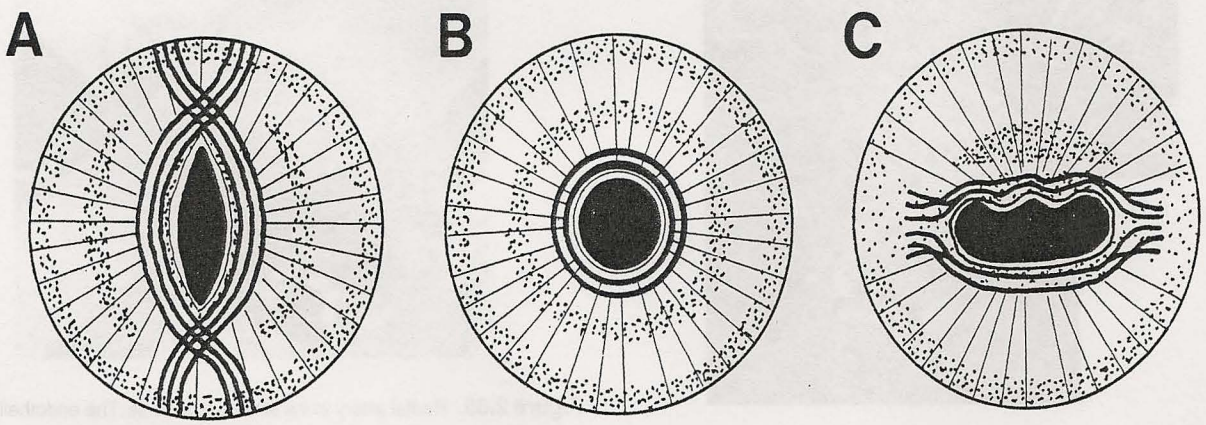

Figure 2.67. **A.** A typical vertically oriented slit pupil in which the sphincter muscles (*dark lines*) interlace, creating a scissorslike action during pupillary closure. **B.** The circular sphincter muscle and radiating dilators as found in primates, birds, the dog, and the pig, all having circular pupils. **C.** A horizontal pupil of an ungulate. (Redrawn from Prince JH. *Comparative Anatomy of the Eye.* Springfield, IL: Charles C. Thomas, 1956.)

stroma, separated from the pigmented epithelium and subjacent dilator muscle by a thin layer of connective tissue (Fig. 2.66A). In the horse, the sphincter occupies the main portion of the central stroma and is capped by the granular iridica when present (Fig. 2.66B). The shape of the sphincter varies among species according to the pupillary shape (Fig. 2.67).[3] The sphincter muscle is innervated primarily by parasympathetic nerve fibers.

The iridal dilator muscle is a single layer of unstriated muscle fibers in the posterior iridal stroma extending from the iris sphincter to the iris periphery. These muscle fibers apically (i.e., posteriorly) contain pigment around their nuclei and are innervated sympathetically (Fig. 2.68). The basal regions of each cell, which contains the myofilaments, overlap one another in a shinglelike fashion. This cell layer could be considered as a highly developed, pigmented myoepithelium. In

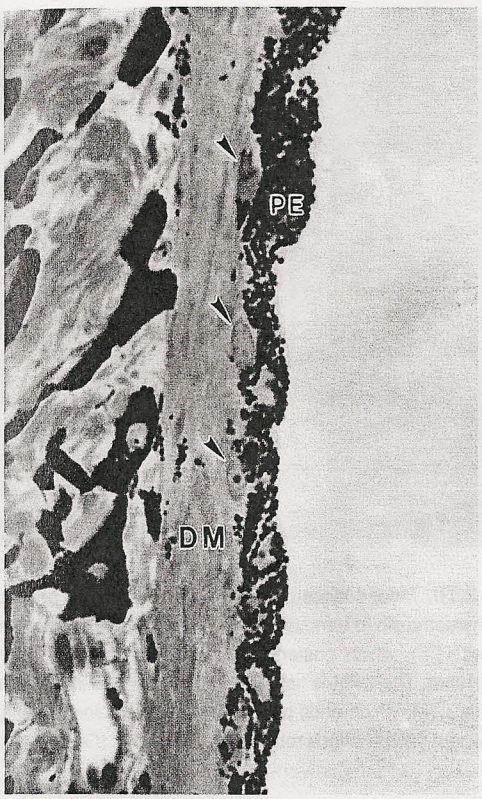

Figure 2.68. The canine iridal dilator muscle (*DM*) consists of a single layer of overlapping smooth muscle fibers. Apically, the nucleus (*arrows*) of each cell is partially surrounded by pigment granules. *PE*, posterior epithelium. (Plastic section; original magnification, X1000.)

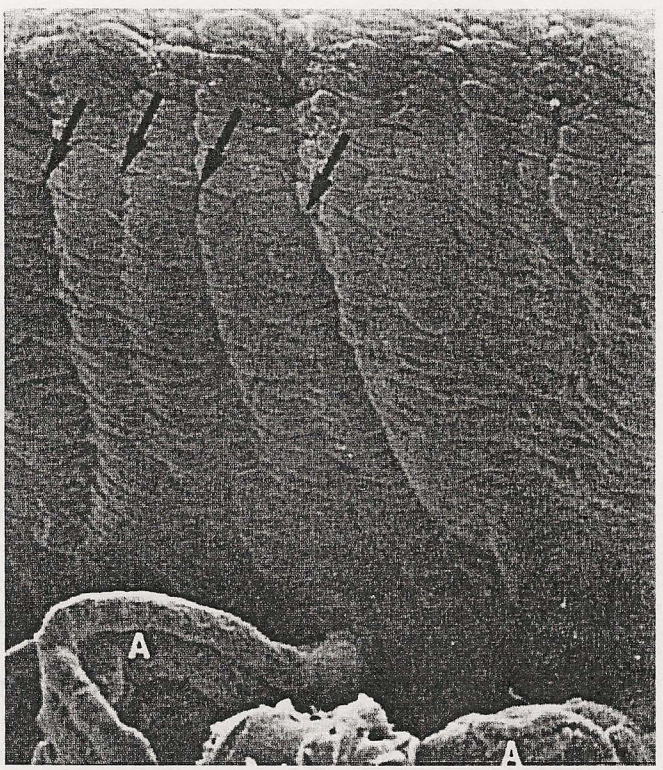

Figure 2.69. SEM of the posterior iris surface of a cat. *Arrows* point to radial folds (*A*). Tips of ciliary processes. Note circumferential orientation of clumps of posterior epithelium with small bumps from melanin granules. (Original magnification, X81.)

avian species, these intrinsic iris muscles are striated. The posterior iridal surface is then covered by two layers of pigmented epithelium that continue with the epithelium of the ciliary body. The anterior layer, which forms the dilator muscle, is directly continuous with the pigmented epithelium of the ciliary body, whereas the posterior layer, which is densely pigmented, is directly continuous with the nonpigmented epithelium of the ciliary body. In herbivores, both layers may extend anteriorly along the pupillary margin to form the granula iridica. In young animals, the granula iridica is smaller and more vacuolated (Fig. 2.66B).

The size of the dilator muscle varies with the species, being well developed in the dog and involving the full circumference of the iris. In the horse, it is less developed, and in species with elongated pupils, it is poorly developed adjacent to the long axis of the pupil.[4]

Ultrastructurally, the basal aspect of the posterior epithelium of the iris faces the posterior chamber and has numerous surface projections (Fig. 2.69). The posterior surface of the iris contains radial folds that extend to the base of the ciliary processes. These folds are radially oriented, but the pigmented epithelial cells are oriented with their long axis running circumferentially in the iris, thus giving rise to two patterns on the posterior surface.[84] A basement membrane separates the cells from the posterior chamber but does not follow all the invaginations of the cell surface. The lateral cell surfaces of the posterior epithelium have numerous slender cell processes with scattered desmosomes. In general, large spaces occur between the lateral cell membranes, which allow free access to the posterior chamber. The nucleus of the iridal posterior epithelium in the dog is oval and moderately indented, whereas the nuclei in the horse are often bizarre-shaped, being indented by adjacent pigment granules.

The epithelial (i.e., apical) portion of the dilator muscle (i.e., anterior epithelium) is located adjacent to the apical portion of the posterior epithelium and contains the cell nuclei. Melanin granules are mostly present in this portion of each cell. The myoepithelial (i.e., basal) portion has scattered melanin granules, and it forms irregular projections into the stroma, being covered by a basement membrane. In the horse, basement membrane material fills much of the intercellular space between projections of the myoepithelium.

In avian species and other lower vertebrates, these intrinsic iris muscles are striated, thus preventing the mydriatic agents and other drugs used in mammals from being used. Instead, paralytic agents such as cocaine (10% solution) must be administered. In addition to controlling the amount of light that enters the back of the eye, the iris of birds is believed to contribute to lenticular accommodation. Changes in the pupil diameters of chickens and pigeons result in changes in the positioning of their lenses (i.e., change in back vertex distance).[98] In some birds and other animals (e.g., the American alligator), the sphincter and dilator muscles are both striated and smooth. Specifically, in the great-horned owl, pupillary

constriction is performed mostly by skeletal muscle and pupillary dilation mostly by the radial myoepithelium, which contains smooth muscle myofilaments.[99] A similar arrangement occurs in the cormorant.[100] The additional smooth muscle along with the striated sphincter has been proposed as playing an important role in maintaining pupillary size.

The iris contains numerous myelinated and nonmyelinated nerves for sympathetic and parasympathetic innervations. The myelinated fibers do not follow the iris vessels per se, but they have a similar pattern as they follow the collagen fibers of the stroma. On entering the iris, each long ciliary nerve forms a dorsal and a ventral branch, to form a circular nerve in the ciliary body and also to meet their counterparts from the opposite side dorsally and ventrally in the iris. Radial nerve bundles from the circular nerve pass centrally to the pupil with a corkscrew shape, presumably to accommodate pupillary constriction. A circular plexus is formed near the collarette, from which branches continue toward the pupil and then divide and intersect to form a rhomboid-shaped mesh.[101]

Recently, it was proposed that the widely held belief that reflex constriction of the mammalian pupil in response to light depends exclusively on neural pathways between the eye and central nervous system needs to be revised.[102] In both golden hamsters and hooded rats, effective constriction of the pupil in response to light occurred after a variety of interventions, including bilateral intraorbital optic nerve section and unilateral intracranial optic nerve section with enucleation of the contralateral eye, combined in some cases with bilateral removal of the superior cervical ganglia, pinealectomy, or both. The constrictions that occurred after these different interventions were considerably slower than the usual, neuronally driven reflex.[102] Interestingly, the slow, nonneural pupillary reflex was not observed in albino animals, which suggests a melanin-mediated component to the slow pupillary light reflex.

Ciliary Body

The ciliary body is an anterior continuation of the choroid, and it joins with the iris. The largest component of the anterior uvea is triangular in sagittal section, with its apex continuing into the choroid, the inner side facing the lens and vitreous body, and the outer side facing the sclera (Fig. 2.58).

The ciliary body provides nourishment and removes wastes for the ocular structures that focus or refract light (i.e., the cornea and lens). Nutrients for the refractive structures are primarily supplied by the aqueous humor of the eye, which is an optically clear fluid originating from vascular sinuses within the folds and processes of the ciliary body and draining into the iridocorneal or anterior chamber angle, which forms the anterior boundary of the ciliary body. In the continuous process of aqueous humor formation and drainage, intraocular pressure (IOP) is created, which is responsible for providing the eye most of its rigidity.

Topographically, the ciliary body is divided into an anterior pars plicata (i.e., corona ciliaris) and a posterior pars plana. The pars plicata consists of a ring of 70 to 100 ciliary processes, depending on the species, with their intervening valleys (Fig. 2.70).[4] The processes, which increase greatly the production area of aqueous humor, are generally more prominent and numerous in animals with larger anterior chambers (i.e., the cow with 100 processes, the horse with 102 processes) than in animals with smaller anterior chambers (i.e., carnivores and primates with 74–76 processes) (Table 2.11).[4] Among lower vertebrates, they are often absent (in most fishes, lizards, and snakes).[2,3] In addition to aqueous production, ciliary processes play variable roles in lenticular accommodation, because these structures are intimately associated with the crystalline lens. In anurans, birds, and some reptiles, the ciliary processes are attached to the lens and participate directly in accommodation. By comparison, the processes in mammals primarily serve as a region for attachment of the lenticular zonules, which connect the lens with the ciliary body and its musculature, which in turn is responsible for accommodation.

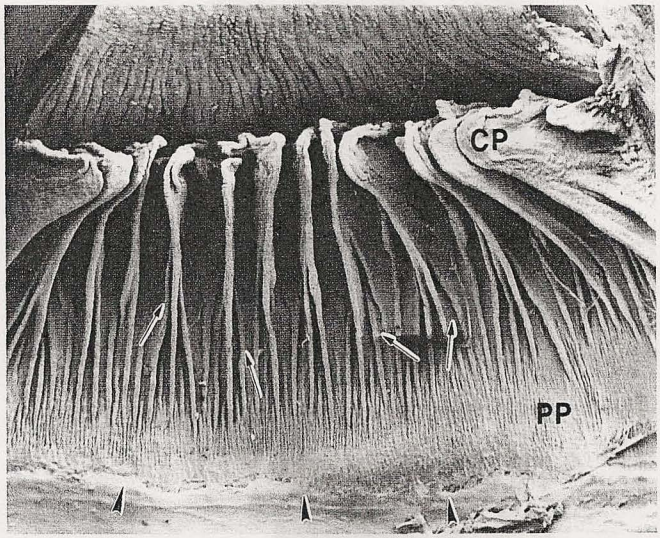

Figure 2.70. Inner surface of the ciliary body of a dog previously treated with α-chymotrypsin to remove the lenticular zonules possesses thin ciliary processes (*CP*), which posteriorly give rise to smaller secondary folds (*small arrows*). These folds flatten and disappear in the region called the pars plana (*PP*), which ends posteriorly at the adjoining retina, forming a line known as the ora ciliaris retinae (*large arrows*). (Original magnification, X18.)

The appearance of individual ciliary processes varies among species. In carnivores, the processes are thin and bladelike, with rounded tips that are invested with zonular fibers. Between the major ciliary processes, wide valleys with smaller, secondary folds are present. Many of the smaller secondary folds originating near the pars plana merge with the major processes at their base. The surface has numerous convolutions, but most of it is obscured by the investment of zonular fibers (Fig. 2.71).[103] The zonular fibers pass down into the valleys, and many fibers pass posteriorly to their origin on the pars plana.

In ungulates in general and the horse in particular, the ridge of the ciliary processes is capped by a broad, convoluted surface that overhangs the main body of the processes.[103] Numerous fibers run circumferentially, connecting the broad ridges together (Fig. 2.72). The combination of bridging fibers and

Table 2.11 Number and Shape of Processes in the Vertebrate Ciliary Body

Animal	Number	Size	Form
Anurans	3 (dorsal) Many (meridional) 1 (ventral)	Small	Variable
Lizards	Absent (ciliary roll)		Triangular
Snakes	Absent (ciliary roll)		Round
Crocodile	100		Tongue-shaped
Birds	Numerous	Small-Moderate	Thin, elongated
Shrew	Absent (ciliary roll)		
Carnivores	74–76	Moderate	Thin, finely convoluted
Herbivores (cow, horse)	100, 102	Large	Thick, broadly convoluted

Data from Duke-Elder S. *The Eye in Evolution.* Vol. I. London Henry Kimpton, 1958; Prince JH. *Comparative Anatomy of the Eye.* Springfield, IL Charles C. Thomas, 1956; and Prince JH, et al. *Anatomy and Histology of the Eye and Orbit in Domestic Animals.* Springfield, IL Charles C. Thomas, 1960.

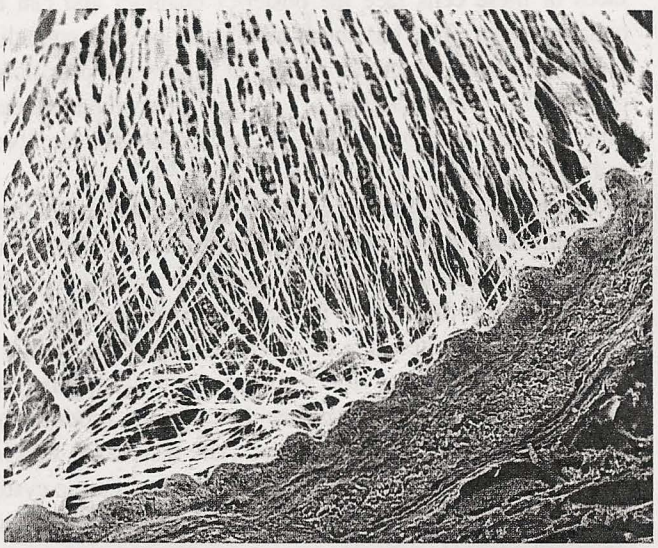

Figure 2.71. SEM (sagittal view) of the inner ciliary body of a dog reveals numerous zonular fibers attached along the epithelial surface. (Original magnification, X130.)

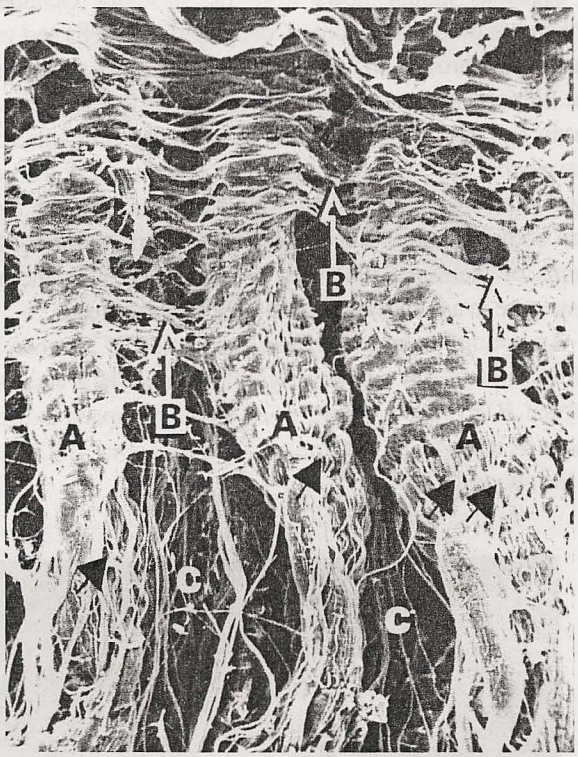

Figure 2.72. SEMS of the ciliary processes and zonular fibers in a horse. **A.** Ciliary process. **B.** *Arrows* point in the direction of the lens equator as well as to the horizontal fiber network joining adjacent process. **C.** Zonular fibers in valleys between processes. Note also the zonular fiber ensheathment of the ciliary processes (*small arrows*). (Original magnification, X41.)

the broad ridge on the processes makes the valleys less spacious than the convolutions. The cap of broad convolutions stops before the anterior tip of the ciliary processes, which are free of fibers and marked convolutions. The valleys between the processes have marked surface convolutions, and smaller folds are present.

The pars plana is the first flat, posterior portion extending from the posterior termination of the processes to the peripheral termination of the retina (i.e., ora ciliaris retinae) (Fig. 2.70). The width of the pars plana varies, because the retina extends more anteriorly in the inferior and medial quadrant in most species, enhancing peripheral vision. Therefore, the pars plana is wider superiorly and laterally. In the dog, the ora ciliaris retinae is 8 mm behind the limbus dorsally and laterally but only 4 mm ventrally and medially.[84] Both regions of the ciliary body are heavily pigmented. The main mass of the ciliary body, exclusive of the ciliary processes, consists of the smooth muscles in mammals and the skeletal muscle in nonmammals. Contraction of these muscles draws the ciliary processes and body both forward and inward, thus relaxing the lenticular zonules (suspensory ligament of the lens) and changing the shape and refraction of the lens (see Chapter 3). This muscle is often weakly developed in many nonprimate species and as a result offers poor accommodative ability.

The anteriormost component of the ciliary body is the ICA (i.e., filtration angle or anterior chamber angle). The ICA is

formed by the junction of the corneoscleral tunic, base of the iris, and an anterior recession of the ciliary body, which is known as the cilioscleral sinus or cleft (Fig. 2.58). Pectinate ligaments span the opening of the cilioscleral sinus from the pigmented corneoscleral junction to the root of the iris (Fig. 2.73). Behind the pectinate ligaments and within the cilioscleral sinus is a matrix of loose tissue strands, the trabecular meshwork. The trabecular meshwork consists of crisscrossing collagen cords that are covered by cells. In the cilioscleral sinus, the trabecular meshwork appears to be anterior tendinous extensions of ciliary body musculature. At the expense of the ciliary body musculature, a proportionally larger sinus is found in most domestic animals than is found in humans. Adjacent to the meshwork are aqueous collecting channels, which in turn empty into the intrascleral venous plexus and then the vortex veins.

Aqueous humor flows from the posterior chamber, in which it is produced by ciliary body epithelial cells and vasculature, and through the pupil, into the anterior chamber, and to the filtration angle. Aqueous flows between the pectinate ligaments and into the trabecular meshwork. Aqueous humor then leaves the eye either through the corneoscleral trabecular meshwork and associated outflow channels or through the ciliary body and anterior uvea (i.e., uveoscleral outflow). Most forms of increased IOP may be associated with increased resistance to aqueous outflow in both of these areas.

An optimal balance between production of aqueous fluid by the ciliary body and drainage through the ICA creates the normal IOP. This pressure is essential for maintaining the shape of the eye and retaining a close adherence of the retina to the choroid.

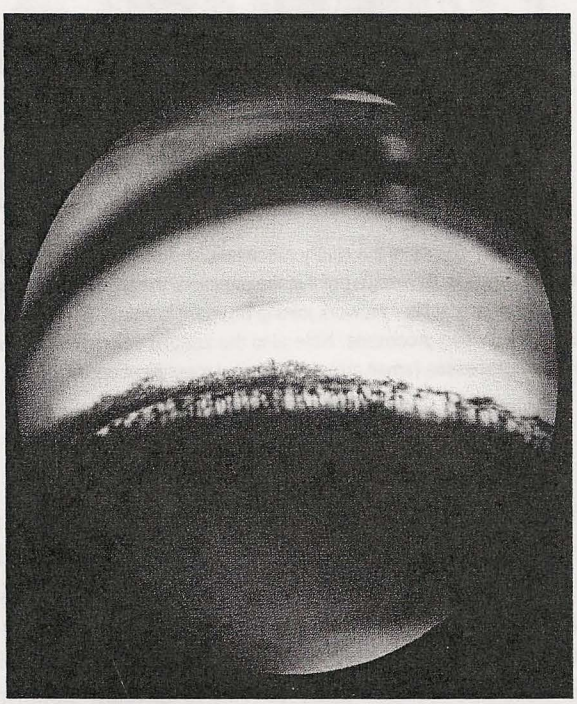

Figure 2.73. Gonioscopic view of the anterior ciliary body shows the fibrous strands, known as the pectinate ligament, that attach the anterior base of the iris to the limbus.

Histologically, the ciliary body is divided into the ciliary processes, ciliary body musculature, and ICA. Each is now discussed in more detail.

Ciliary Process

Each ciliary process consists of a central core of stroma and blood vessels covered by a double layer of epithelium; an inner, nonpigmented, cuboidal epithelium, which forms a complete, internal monocellular lining of the ciliary body; and an outer, pigmented, cuboidal epithelium, which also is only one cell layer thick (Fig. 2.74). In ungulates, the double-layered epithelium is more columnar than cuboidal.

The nonpigmented epithelium is confluent posteriorly with the sensory retina at the ora ciliaris retinae and anteriorly with the posterior pigmented epithelium of the iris. The basal surfaces of these cells face the posterior chamber and can be quite irregular. The basement membrane of this epithelial layer follows the general contour, but it does not pass down into the small irregularities or into the intercellular spaces. The basement membrane helps to anchor the zonular fibers and vitreous base.

The lateral cell surfaces of the nonpigmented epithelium have numerous villous processes along the bottom one half to two thirds. Cystic intercellular spaces in this region and in the pars plana are filled with intercellular material that have the staining characteristics of glycosaminoglycans (GAGs). The base of the cells also react positively for the same material (Fig. 2.75). The nonpigmented epithelium may produce the GAGs of the vitreous humor. These cells secrete the GAGs, which consist mostly of hyaluronans, laterally into the cystic intercellular spaces, which then communicate both with the vitreous base and basally.[104]

The lateral intercellular junctions of the nonpigmented epithelium consist of desmosomes, except at the apical end (Fig. 2.76). The apical ends possess gap junctions, zonula adherens, and zonula occludens, which probably represent the anatomic blood–aqueous humor barrier.[105–109]

The combination of this junctional complex and the redundant interdigitations of the lateral cell surfaces support the general belief that this portion of the ciliary processes is the site of aqueous humor production (Fig. 2.77). Furthermore, the enzyme carbonic anhydrase has been cytochemically localized at or in the nonpigmented epithelium.[109]

Cellular junctions between the nonpigmented and the pigmented epithelium of the ciliary process are very important, because these cell layers are tightly locked together in a physiologic way. The types of junctions found here reflect this importance, consisting of many gap junctions interspersed with desmosomes and unusual junctions termed *puncta adherentes,* which resemble desmosomes but lack the larger tonofilaments and associated intercellular central band (Fig. 2.76).[109] There are also dilated portions of the apical intercellular spaces with villous cytoplasmic processes protruding into them. These dilatations are termed *ciliary channels,* and they are usually near the apical termination of two adjacent cells (Fig. 2.78).

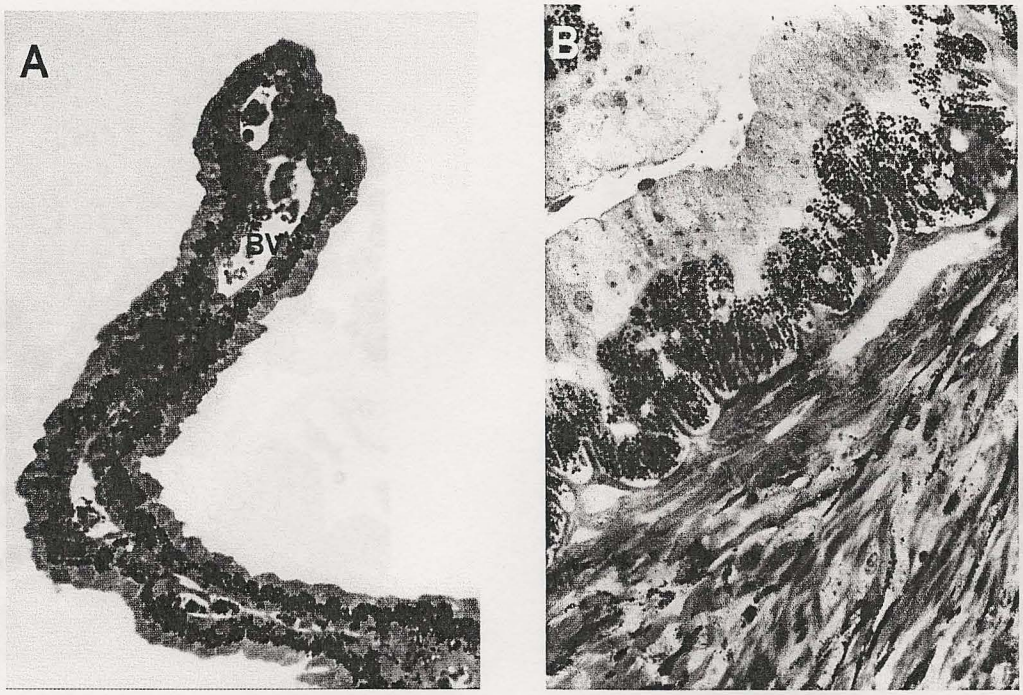

Figure 2.74. The ciliary epithelium that lines the processes and intervening valleys is bilayered. The outer layer is pigmented; the inner layer is nonpigmented. **A.** Cross-section of a canine ciliary process. The bilayered epithelium, which is cuboidal, lines blood vessels (*BV*), which together form a blood–aqueous barrier. (Plastic section; original magnification, X250.) **B.** Longitudinal section of an equine ciliary epithelium at the base of a process. Both layers are considerably more columnar than those in the dog. (Original magnification, X400.)

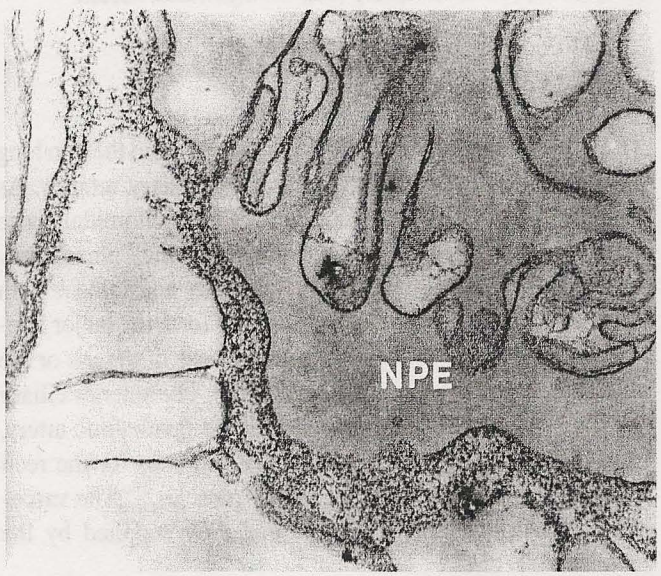

Figure 2.75. Colloidal iron stain demonstrates the presence of glycosaminoglycans (primarily hyaluronic acid) within the intercellular spaces between the nonpigmented epithelial cells (*NPE*) of the dog. (Original magnification, X25,000.)

The ciliary pigmented epithelium is the continuation of the retinal pigmented epithelium. Anteriorly, it continues as the anterior pigmented epithelial layer of the iris, which forms the dilator pupillae muscle. The pigmented epithelium is generally cuboidal and heavily laden with round-to-oval melanin granules.

The basal aspect of the epithelium faces the ciliary body stroma and is covered by a basement membrane (Fig. 2.78). In some instances, the basement membrane of adjacent capillaries in the ciliary processes comes into contact with the basement membrane of the pigmented epithelium to form a thickened, irregular, common basement membrane. The lateral cell surfaces of the pigmented epithelium are joined by desmosomes, and the basal cell surfaces have no specialized junctions. The nuclei of both pigmented and nonpigmented epithelia are located apically. Other than the melanin granules, the cytoplasm contains the same organelles, consisting of rough endoplasmic reticulum, smooth endoplasmic reticulum, free ribosomes (i.e., polysomes), and mitochondria.

A thin layer of loose connective tissue with blood vessels and nerves lies under the ciliary epithelium, separating the ciliary body epithelium from the underlying musculature. In the pars plana, this tissue contains a thin sheet or layer of elastic fibers continuous with the elastic layer of the basement membrane complex (i.e., Bruch's membrane) located between the retinal pigment epithelium (RPE) and choriocapillaris (i.e., capillary bed of choroid) (Fig. 2.79).

Anteriorly, this tissue is greatly thickened, consisting of numerous arterioles, venules, and capillaries that form plexi within each fold and process of the pars plicata (Figs. 2.74 and 2.78). The vascular plexus within the stroma of the ciliary process are "leaky," being lined with a fenestrated endothelium. Fibrocytes and melanocytes are sparsely populated within the stroma, being more concentrated toward the ciliary body musculature.

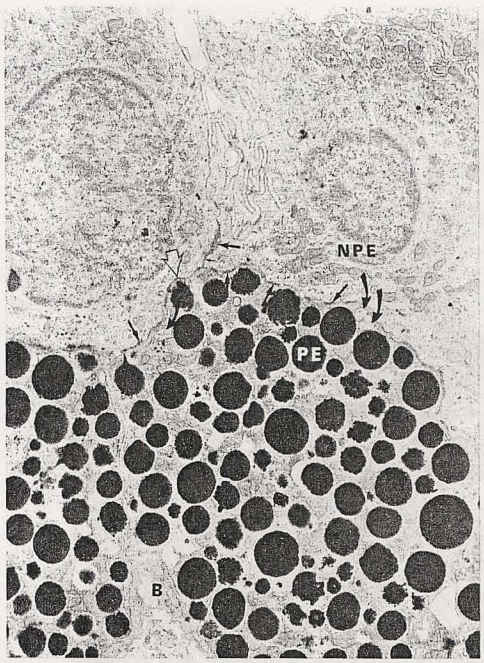

Figure 2.76. Apical junctions of nonpigmented epithelium and pigmented ciliary epithelium in a cat. The nonpigmented epithelial (*NPE*) nuclei are located apically; the wide intercellular spaces and villi can be seen in the basilar aspect of the intercellular spaces of the nonpigmented epithelium. The apical aspect of the nonpigmented intercellular space is the anatomic site of the blood–aqueous barrier and contains a fascia occludens (*small arrow*) and fascia adherentes (*large arrow*). The apical cell surfaces contain a fascia adherentes (*large arrow*), gap junctions (*open arrows*), and arch-shaped gap junctions (*curved arrows*). The basement membrane (*B*) of the pigmented epithelium (*PE*) is at the bottom. (Original magnification, X9800.)

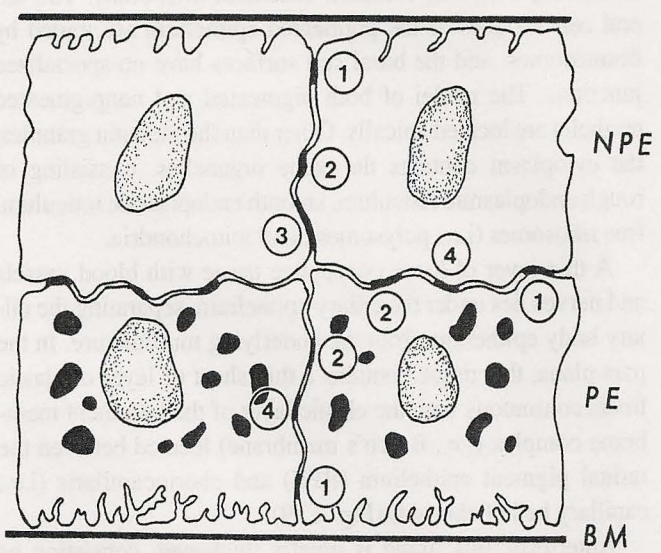

Figure 2.77. Relationship of the two layers of the ciliary epithelium and the basement membranes (*BM*) that cover their bases. The cells are joined by several types of cell junctions, including desmosomes (*1*), gap junctions (*2*), and puncta adherens (*3*). Only the apices of nonpigmented epithelial cells (*NPE*) are joined by a zonula occludens (*4*). *PE*, pigmented epithelium. (Redrawn from Streeten B. Ciliary body. In: Duane TD, Jaeger EA, eds. *Biomedical Foundations of Ophthalmology. Vol. 1.* Philadelphia: JB. Lippincott, 1988.)

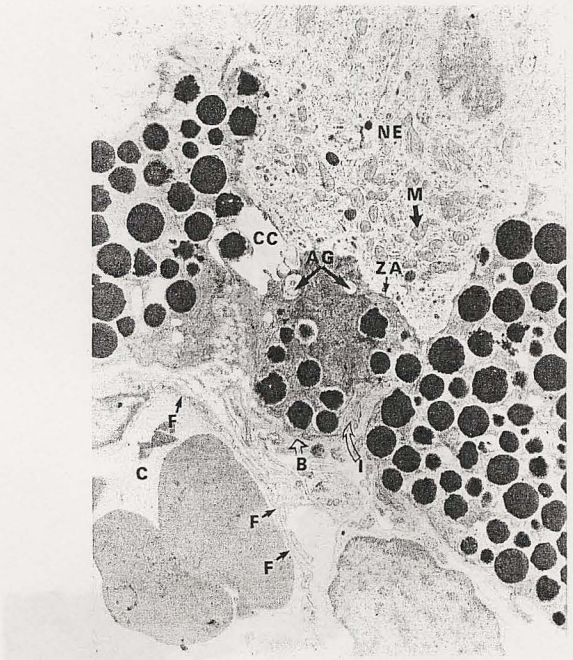

Figure 2.78. Ciliary epithelium with an underlying capillary in a ciliary process of a cat. The nonpigmented epithelium (*NE*) has numerous mitochondria (*M*). A large ciliary channel (*CC*) is present, as are multiple, arch-shaped gap junctions (*AG*) and zonules adherentes (*ZA*) in the apical intercellular space. The pigmented epithelium has numerous round melanin granules, and the basal surface has infoldings and a basement membrane (*B*). The capillary (*C*) abuts the epithelial basement membrane and exhibits fenestrations (*F*). A pericyte is adjacent to the capillary. (Original magnification, X9800.)

Ciliary Body Vasculature

The blood supply of the ciliary body derives from the two long posterior ciliary arteries and the anterior ciliary arteries. As the long posterior arteries pass into the suprachoroidal space equatorially along the lateromedial horizontal plane, they undergo several divisions, which anteriorly anastomose with branches of the anterior ciliary arteries to form the major arterial circle, which is located either in the base of the iris or the anterior ciliary body (Figs. 2.63 and 2.64). The anterior ciliary arteries, which arise from branches of the ophthalmic artery, typically enter the globe at the attachment sites for the recti muscles and help to supply the ciliary muscles.[109] The vasculature of the ciliary processes is primarily supplied by the major arterial circle.

Numerous anatomic variations of this vasculature have been found among mammals.[110–115] In primates and the rabbit, two types of arterioles supply the major and minor processes, whereas in other species, a single type of arteriole originates from the major arterial circle and supplies the process vasculature.[110–112,115] Discrete interspecies variations occur in the angioarchitecture of the ciliary processes (Table 2.12; Fig. 2.80). Rodents (i.e., the rat and guinea pig) have extensive interprocess connections and concentrically parallel capillaries that are irregularly dilated and travel posteriorly, emptying into the anteriormost choroidal veins. Carnivores (i.e., the dog and cat) have processes supplied by one arteriole that is directed posteriorly throughout its length, with capillary arcades that extend to

Figure 2.79. Pigmented epithelium and underlying stroma of the pars plana in a horse. Note the elastic tissue (*E*) in the stroma (*S*) that separates the capillary (*C*) and the pigmented epithelium. The basal aspect of the epithelium has numerous infoldings (*BI*). Desmosomes (*small arrows*) attach lateral cell membranes. (Original magnification, X5400.)

each process margin, from which they empty into venous sinuses at the base of each process. Ungulates (i.e., the pig, sheep, goat, and cow) possess processes with multiple arterioles occupying the process core, along with veins that drain into the choroidal circulation (Fig. 2.80).[111] The ciliary processes of carnivores, ungulates, primates, and the rabbit possess well-developed capillary beds responsible for extensive aqueous

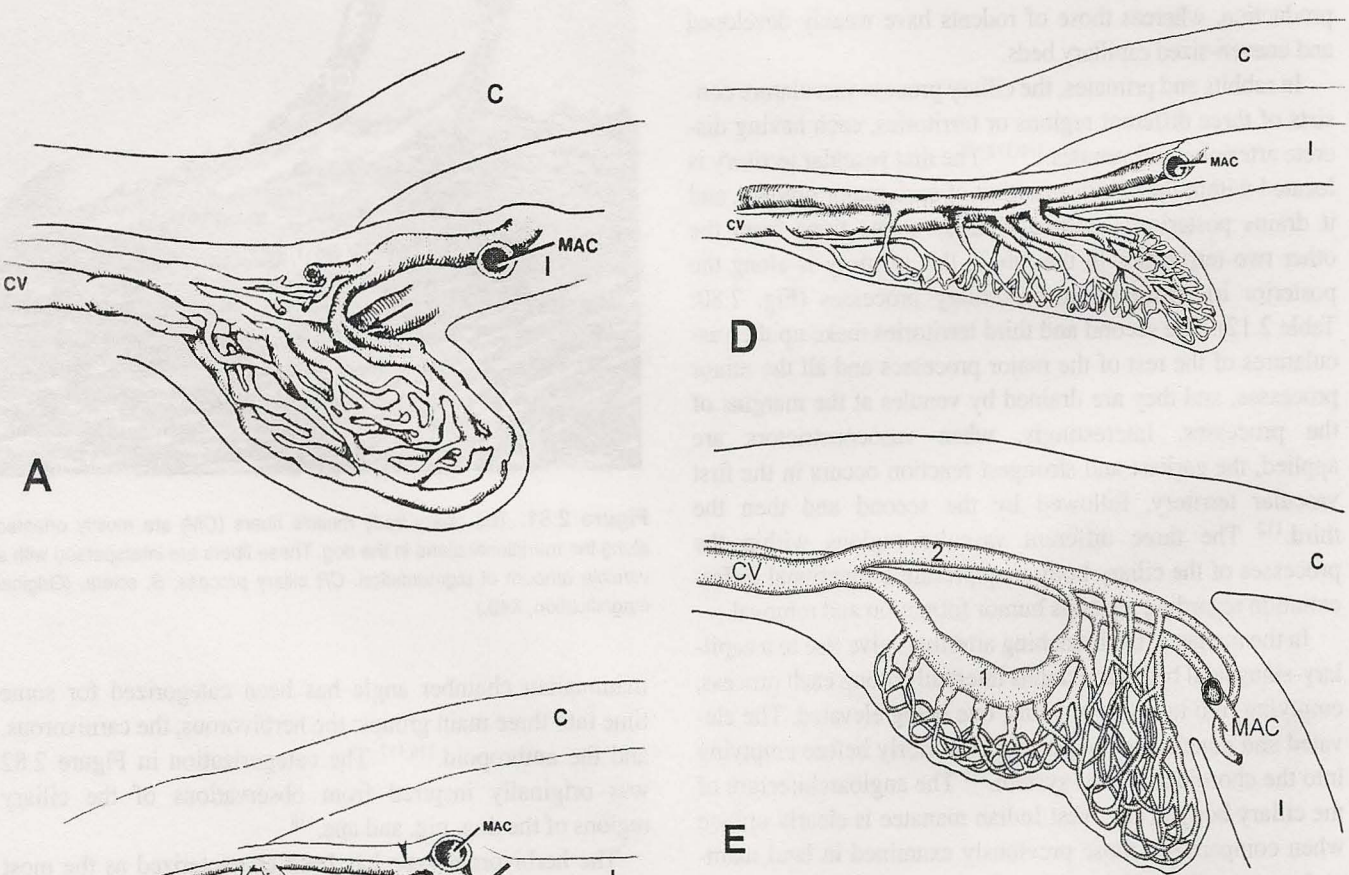

Figure 2.80. **A.** Dog. **B.** Cow. **C.** Mouse. **D.** Rabbit **E.** Manatee. (Modified from Morrison JC, DeFrank MP, Van Buskirk EM. Comparative microvascular anatomy of mammalian ciliary processes. *Invest Ophthalmol Vis Sci* 1987;28:1325–1340; Morrison JC, DeFrank MP, Van Buskirk EM. Regional microvascular anatomy of the rabbit ciliary body. *Invest Ophthalmol Vis Sci* 1987;28:1314–1324; and Natiello N, Samuelson D. Three-dimensional reconstruction of the angioarchitecture of the ciliary body of the West Indian manatee (*Trichechus manatus*). *Vet Ophthalmol* 2005;8:367–374).

Table 2.12 Microvasculature of the Ciliary Body Processes

Animal	Arteriolar Characteristics	Capillary Characteristics	Venous Characteristics
Rodents	Few anterior branches with midway focal, concentric constrictions	Irregular, convoluted, and mildly branched; interprocess capillary connections	Basally, posteriorly located; multiple venules
Rabbits	Anterior and posterior types; multibranched and basally located	Regularly shaped; moderately branched; anteriorly convoluted	Apically located, single posterior venule; multiple basally located anterior venules
Carnivores	Single, unbranched; located apically within each process with asymmetric constrictions at origin	Regularly shaped; highly branched and convoluted	Basally located, irregular sinuslike along entire length; multiple venules emptying into it
Ungulates	Multibranched and basally located with asymmetric constrictions at origin	Regularly shaped; highly to moderately branched	Basally located with multiple venules emptying into it along its length
Primates	Anterior and posterior types; multibranched and basally located	Regularly shaped; interprocess ciliary connections	Multiple, basally located venules emptying posteriorly

Data from Morrison JC, DeFrank MP, Van Buskirk EM. Regional microvascular anatomy of the rabbit ciliary body. *Invest Ophthalmol Vis Sci* 1987;28:1314–1324; Mastuo N. Scanning electron microscopic studies on the corrosion casts of the blood vessels of the ciliary body. *Acta Soc Ophthalmol Jap* 1973;77:928; and Funk R, Rohen JW. Scanning electron microscopic study on the vasculature of the human anterior eye segment. *Exp Eye Res* 1990;51:651–661.

production, whereas those of rodents have weakly developed and uneven-sized capillary beds.

In rabbits and primates, the ciliary process vasculature consists of three different regions or territories, each having discrete arterioles and venules.[110,112] The first vascular territory is located within the anterior portion of each major process, and it drains posteriorly, without venous connections from the other two territories. In the rabbit, this territory is along the posterior iris, forming iridial ciliary processes (Fig. 2.80; Table 2.12). The second and third territories make up the vasculatures of the rest of the major processes and all the minor processes, and they are drained by venules at the margins of the processes. Interestingly, when vasoconstrictors are applied, the earliest and strongest reaction occurs in the first vascular territory, followed by the second and then the third.[112] The three different vascular regions within the processes of the ciliary body may present a functional differentiation regarding aqueous humor formation and removal.

In the manatee, the branching arterioles give rise to a capillary-sinusoidal bed that extends internally along each process, emptying into two sets of veins, one being elevated. The elevated and nonelevated veins join posteriorly before emptying into the choroidal venous system.[115] The angioarchitecture of the ciliary body of the West Indian manatee is clearly unique when compared to those previously examined in land mammals.

Ciliary Body Musculature

Traditionally, the musculature of the ciliary body has been thought to be uniformly, poorly developed in most nonprimate mammals, being comprised of smooth muscle fibers running mainly along a meridional plane (Figs. 2.57 and 2.81). On the basis of ciliary body musculature development, the placental

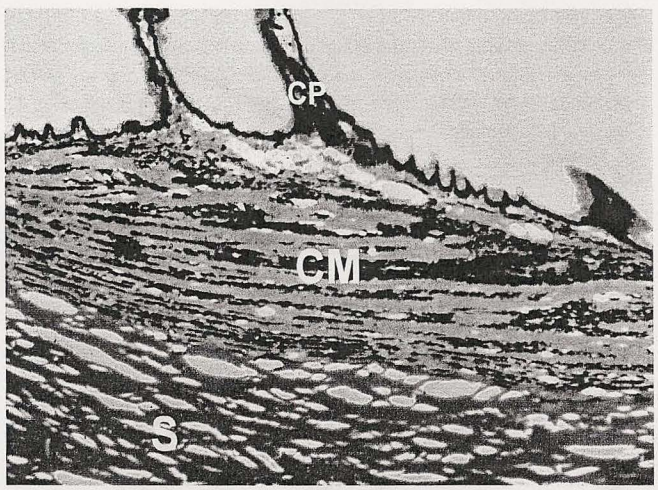

Figure 2.81. The ciliary body muscle fibers (*CM*) are mostly oriented along the meridional plane in the dog. These fibers are interspersed with a variable amount of pigmentation. *CP,* ciliary process; *S,* sclera. (Original magnification, X40.)

mammalian chamber angle has been categorized for some time into three main groups: the herbivorous, the carnivorous, and the anthropoid.[116,117] The categorization in Figure 2.82 was originally inspired from observations of the ciliary regions of the dog, pig, and ape.[118]

The herbivorous type has been characterized as the most common and primitive in orders of mammals up to and including ungulates. This type of angle consists of an inner layer of connective tissue that forms a baseplate of the ciliary body and extends from the root of the iris to the ora ciliaris retinae. It also consists of an outer layer of smooth muscle that presses against the sclera externally and runs meridionally from the corneoscleral junction toward the ora (Fig. 2.83A). The two layers have often been referred to as "leaves" that separate anteriorly and form the ciliary cleft. The ciliary cleft

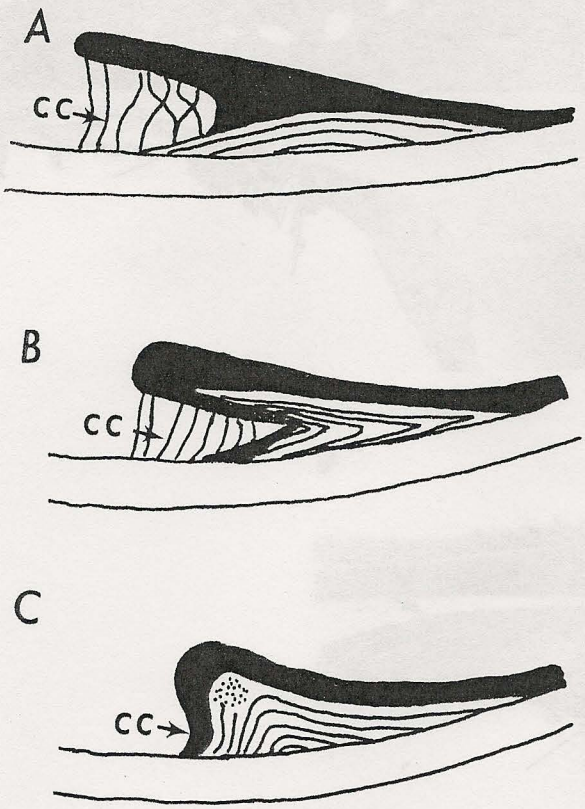

Figure 2.82. Degree of development of the ciliary body musculature among mammalian iridocorneal angle in the ungulate (**A**), carnivore (**B**), and ape (**C**). Development is most pronounced in primates (ape) and least pronounced in herbivorous species (ungulate). The carnivore lies in between. The size of the iridocorneal angle and its ciliioscleral cleft or sinus (*CC*) is inversely large or most pronounced in the ungulate. (Redrawn from Duke-Elder S. *System of Ophthalmology. Vol. I. The Eye in Evolution.* London: Henry Kimpton, 1958.)

is then a triangular area that varies both in depth (i.e., length) and height and that functionally may be considered to be a posterolateral extension of the anterior chamber into the ciliary body. This region was previously called the ciliioscleral sinus, but because it neither separates the ciliary body from the sclera nor is a part of the ciliary venous sinus, the term *ciliioscleral* has been changed to *ciliary cleft.*[117–119]

The ciliary cleft is not an empty space, as the name might imply. Rather, it is an area containing wide spaces filled with aqueous humor and interspersed with cell-lined cords of connective tissue. The spaces between the fibrous cords were initially described in the ox and the horse, and they have been often referred to as the Fontana's spaces.[120]

The carnivorous type possesses a bileaflet configuration as well, but the fibrous inner leaf or layer is usually replaced by meridionally oriented smooth muscle and some radially oriented muscle fibers (Figs. 2.82 and 2.83B).[118] As in the herbivorous type, the two leaves separate anteriorly and hold a wide, deep ciliary cleft. In both the herbivorous and carnivorous types, the ciliary cleft offers little support to properly anchor the iris. Compensation for wide and deep ciliary clefts is provided by a series of fibrous strands attaching the anterior iridal root and inner ciliary baseplate to the limbal cornea. Because of their comblike appearance from observations made from cow eyes, these strands are called the pectinate ligament.[121] Other names have included the suspensory ligaments of the iris, iris processes, and iris pillars (Table 2.13).[117]

Table 2.13 Anatomic Terminology of the Iridocorneal Angle

Pectinate ligament (120)
Pectinate fibers (103)
Suspensory ligaments of the iris (121)
Iris processes (32)
Iris pillars (118)
Ligamentum pectinatum[a]
Uveal trabecular meshwork (125)
Uveal meshwork (430)
Reticular meshwork (433)
Spongy tissue (103)
Fontana spaces (118)
Ciliary trabecular meshwork (433)
Reticulum trabeculare
Juxta-angular aqueous plexus (130)
Area cribriform (434)
Endothelial meshwork (435)
Cell-rich zone (430)
Inner wall of . . . (117)
Trabecular wall (117)
Pore tissue (436)
Ciliary cleft (117)
Ciliary sinus (118)
Ciliary canal (119)
Ciliosclera sinus (103)
Spatia anguli iridocornealis
Corneoscleral trabecular meshwork (125)
Corneoscleral meshwork (117)
Cribriform ligament (431)
Uveoscleral meshwork (145)
Trabeculum/trabecular meshwork (103, 117)
Scleral meshwork (430)
Angular meshwork (117)
Reticulum trabeculare
Angular aqueous plexus (117)
Aqueous plexus of Schlemm (437)
Angular aqueous sinus (117)
Schlemm's canal (438)
Trabecular vein (103)

Modified from Samuelson DA. A reevaluation of the comparative anatomy of the Eutherian iridocorneal angle and associated ciliary body musculature. *Vet Comp Ophthalmol* 1996;6:153–172.
[a]Italicized print indicates terms provided by the *Nomina Histologica* (2nd ed. Rev., 1992).

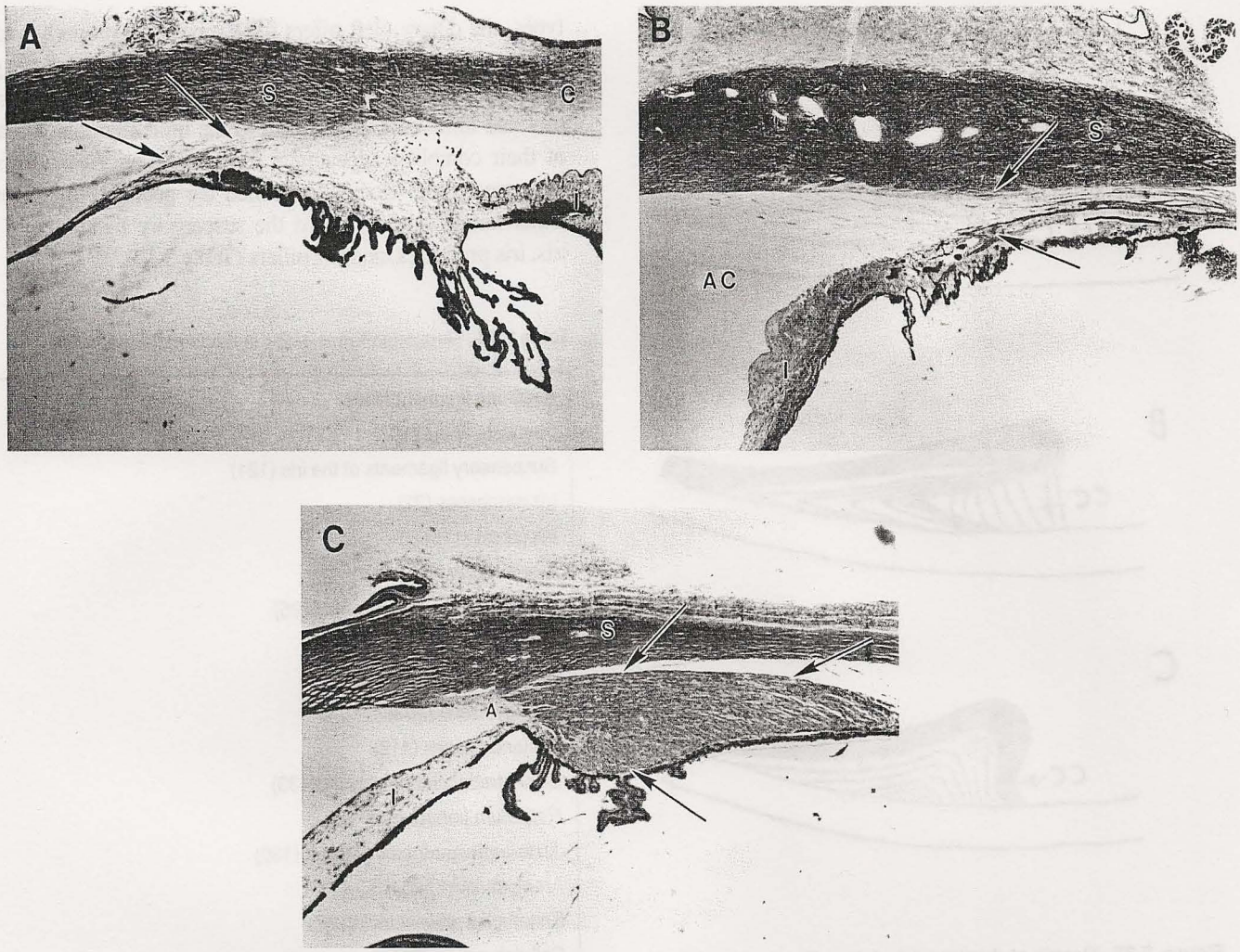

Figure 2.83. **A**. The deer has the traditional herbivorous type of iridocorneal angle and associated ciliary body musculature, which forms a single outer "leaf" (*arrows*) as it lines the outer, posterior portion of the iridocorneal angle. *C*, cornea; *I*, iris; *S*, sclera. (Original magnification, X20.) **B**. The cat possesses the traditional carnivorous type of iridocorneal angle, which forms a "bileaflet" anteriorly (*arrows*). *I*, iris; *S*, sclera. (Original magnification, X25.) **C**. The Rhesus monkey has the anthropoid type, which consists of a small iridocorneal angle and a well-developed ciliary body musculature (*arrows*). *I*, iris; *S*, sclera. (Original magnification, X20.)

The anthropoid type differs sharply in its configuration compared with the other types (Figs. 2.82 and 2.83C). The smooth musculature of primate ciliary bodies is generally believed to be the most highly developed among mammals. The muscle, which has three components (i.e., radial, meridional, and circular), forms a large, anterior pyramidal structure that provides a strong baseplate for iridal attachment. The anterior portion of the ciliary body musculature has, in fact, replaced both the ciliary cleft, which barely exists in the anthropoid angle, and the pectinate ligament, which vestigially consists of scattered iridal processes.

In addition to the three basic forms of ciliary body musculature and the associated ICA, three more designs have been described among nonprimate mammals (Fig. 2.84).[120] Among herbivores, two other types have been found: the small diurnal herbivore, as exemplified by the squirrel; and the large diurnal herbivore, as exemplified by the pig. In the small diurnal herbivore, a deep ciliary cleft is lined by inner and outer leaves of fibrous tissue and smooth muscle of the ciliary body. In the large diurnal herbivore, there is a well-developed ciliary cleft and outer leaf of ciliary muscle, which anteriorly includes circularly oriented muscle embedded within a scleral "spur." TEM of different ungulates has revealed that many of the muscle fibers, especially those located anteriorly, course more circumferentially than meridionally.[122] This difference in orientation of the musculature is most evident in the pig and water buffalo (Fig. 2.85). In these animals, circular muscle fibers are located near the innermost portion of the posterior end of the ciliary cleft (i.e., the ciliioscleral sinus). These fibers and the outer, meridional muscle fibers are separated from the posterior ICA by a small ridge of dense connective tissue, which is called a scleral spur because of its scleral-like appearance.

A third type occurs in "high" accommodative carnivores, such as the raccoon, mongoose, and ferret. In this configuration, the anterior ciliary body musculature is highly developed but not as an outer leaflet. Instead, the anterior musculature extends as a single leaflet either internally (i.e., the raccoon) or intermediately (Fig. 2.86).

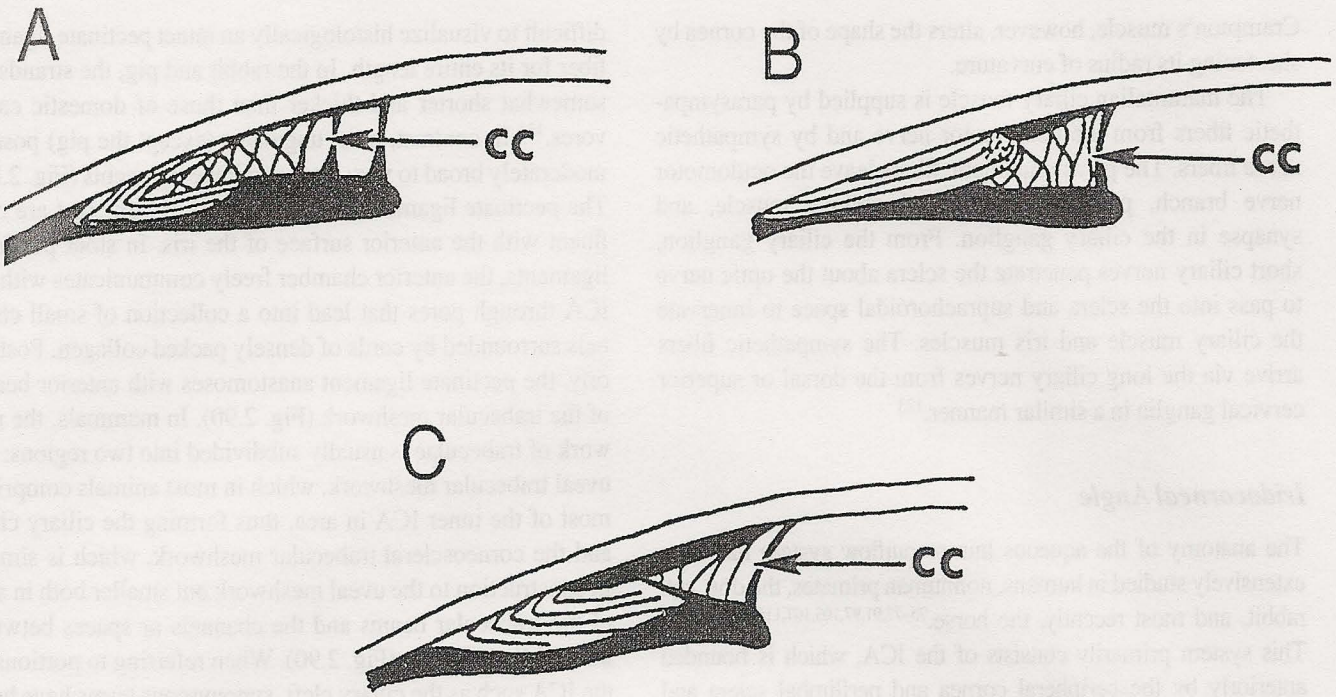

Figure 2.84. Three additional configurations of the eutherian nonprimate iridocorneal angle. Ciliary body musculature is indicated by linear shading. *CC,* ciliary cleft. **A.** Small diurnal herbivore. **B.** Large diurnal herbivore. **C.** "High" accommodative carnivore. (Reprinted with permission from Samuelson DA. A reevaluation of the comparative anatomy of the Eutherian iridocorneal angle and associated ciliary body musculature. *Vet Comp Ophthalmol* 1996;6:153–172.)

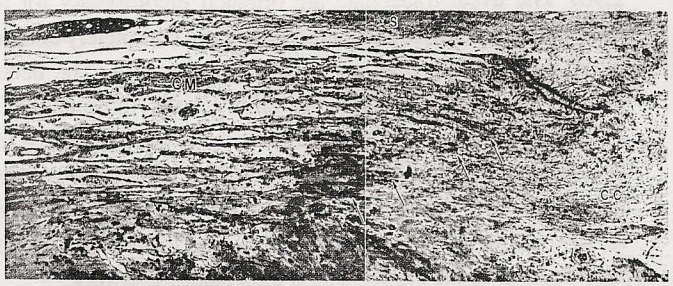

Figure 2.85. The anteriormost portion of the ciliary body muscle (*CM*) in the water buffalo has circularly oriented muscle fibers (*arrows*). *CC,* cilioscleral cleft; *S,* sclera. (Original magnification, X125.)

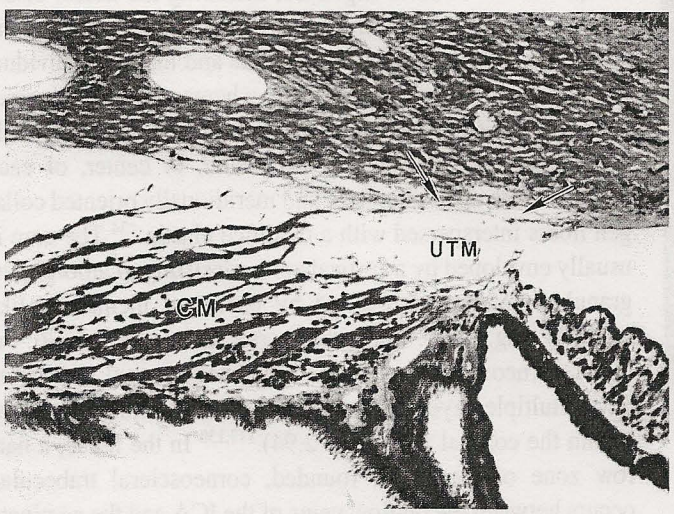

Figure 2.86. The mongoose has the "high" accommodative type of iridocorneal angle. *CM,* ciliary body musculature; *UTM,* trabecular meshwork. (Original magnification, X100.)

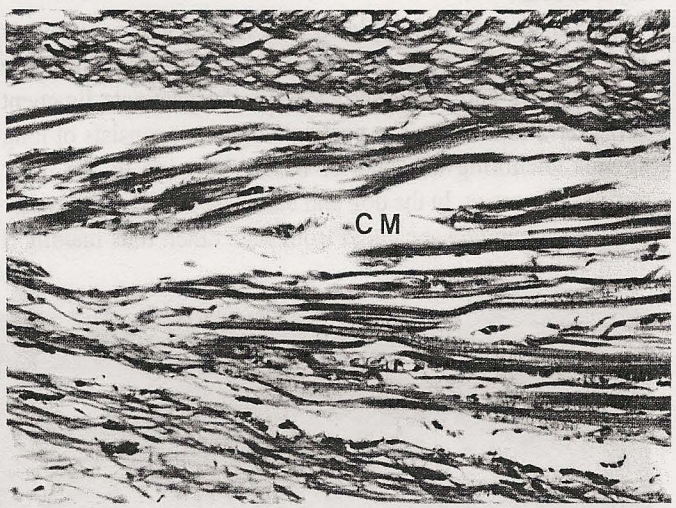

Figure 2.87. The muscle of Crampton (*CM*) in a bald eagle is one of several bundles of skeletal muscle within the ciliary body, each being oriented meridionally. (Original magnification, X125.)

In birds and other nonmammalian species, the ciliary body musculature consists of skeletal muscle cells that are primarily meridional (Fig. 2.87). At least two distinct bundles of muscle are positioned in this region of the avian eye: an anterior bundle, which is known as the muscle of Crampton, arises near the corneal margin; and a posterior bundle, which is known as Brücke's muscle. In birds such as the hawk, Brücke's muscle is well developed and sometimes is referred as two muscles: Müller's (anterior) and Brücke's.[2] Contraction of Brücke's muscle causes the ciliary body to push against or squeeze the lens, thus deforming it. Contraction of

Crampton's muscle, however, alters the shape of the cornea by shortening its radius of curvature.

The mammalian ciliary muscle is supplied by parasympathetic fibers from the oculomotor nerve and by sympathetic nerve fibers. The parasympathetic fibers leave the oculomotor nerve branch, penetrate the ventral oblique muscle, and synapse in the ciliary ganglion. From the ciliary ganglion, short ciliary nerves penetrate the sclera about the optic nerve to pass into the sclera and suprachoroidal space to innervate the ciliary muscle and iris muscles. The sympathetic fibers arrive via the long ciliary nerves from the dorsal or superior cervical ganglia in a similar manner.[123]

Iridocorneal Angle

The anatomy of the aqueous humor outflow system has been extensively studied in humans, nonhuman primates, the dog, cat, rabbit, and most recently, the horse.[75–77,91,97,103,107,116–122,124–132] This system primarily consists of the ICA, which is bounded anteriorly by the peripheral cornea and perilimbal sclera and posteriorly by the peripheral iris and anterior ciliary body musculature. From amphibians to higher mammals, the ICA consists of an irregular, reticular network of connective tissue beams called trabeculae that are lined partially or entirely by a single layer of cells.[117,120,131]

When viewing the angle from a frontal low-power view (e.g., gonioscopy, SEM), the most strikingly visible structure in carnivores and many herbivores is the pectinate ligament (Figs. 2.73 and 2.88). The pectinate ligament consists of long strands anchoring the anterior base of the iris to the inner peripheral cornea. In the dog and cat, these strands are usually slender and widely separated from each other, thus making it difficult to visualize histologically an intact pectinate ligament fiber for its entire length. In the rabbit and pig, the strands are somewhat shorter and thicker than those of domestic carnivores.[133] In contrast, most ungulates (except the pig) possess moderately broad to very stout pectinate ligaments (Fig. 2.89). The pectinate ligament is entirely lined by cells that are confluent with the anterior surface of the iris. In stout pectinate ligaments, the anterior chamber freely communicates with the ICA through pores that lead into a collection of small channels surrounded by cords of densely packed collagen. Posteriorly, the pectinate ligament anastomoses with anterior beams of the trabecular meshwork (Fig. 2.90). In mammals, the network of trabeculae is usually subdivided into two regions: the uveal trabecular meshwork, which in most animals comprises most of the inner ICA in area, thus forming the ciliary cleft; and the corneoscleral trabecular meshwork, which is similar in construction to the uveal meshwork but smaller both in size of the trabecular beams and the channels or spaces between the cell-lined beams (Fig. 2.90). When referring to portions of the ICA such as the ciliary cleft, synonymous terms have been frequently used. Table 2.13 lists many of these synonyms used to delineate regions within the mammalian ICA.

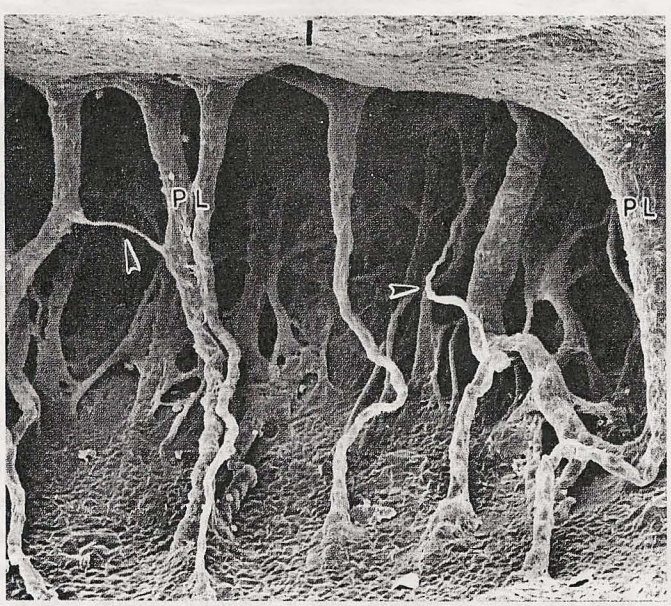

Figure 2.88. Frontal-view SEM of the canine iridocorneal angle. Fibrous pillars that attach the iris (*I*) to the limbus form the pectinate ligament (*PL*). *Arrows* indicate smaller fibrous connections between these pillars and uveal trabeculae located behind the pectinate ligament. (Original magnification, X160.)

The uveal meshwork interconnects the inner, anterior ciliary body musculature with the pectinate ligament (Figs. 2.85 and 2.90). The uveal trabeculae are oriented meridionally for the most part. In most animals, these beams are completely encased by an endothelium referred to as trabecular cells. The beams branch increasingly toward the ciliary body musculature in radial and circular directions. As a result, the posterior uveal trabeculae are smaller, with smaller intertrabecular spaces separating them (Fig. 2.91). Consequently, the posterior uveal meshwork often merges imperceptibly with the posterior, innermost regions of the corneoscleral trabecular meshwork.

The corneoscleral trabecular meshworks of domestic animals are characterized mainly by small trabeculae that in turn are separated by small intertrabecular spaces. In carnivores, these trabeculae are incompletely lined by trabecular cells. By comparison, in certain ungulates, including the horse, bison, and water buffalo, each trabecula is completely lined by trabecular cells (Fig. 2.92). In ruminants and the pig, individual trabeculae can be completely lined, whereas others are incompletely lined. Composition of the trabeculae varies very little among species.[120,124,125,130–132] The core, or center, of each beam is made up of circularly and meridionally oriented collagen fibers interspersed with a modified elastin.[134] The core is usually enveloped by a cortical zone consisting of amorphous, granular material surrounded by basement membrane–like material (Fig. 2.93). In the cat, horse, and water buffalo, the larger corneoscleral trabeculae and smaller uveal trabeculae have multiple layers of basement membrane–like material within the cortical zone (Fig. 2.94).[117,130] In the horse, a narrow zone of thickened, rounded, corneoscleral trabeculae occurs between the outflow veins of the ICA and the pectinate ligament (Fig. 2.95). These trabeculae possess no basement membrane–like material; instead, they have long-spacing collagen similar to that seen in Descemet's membrane.

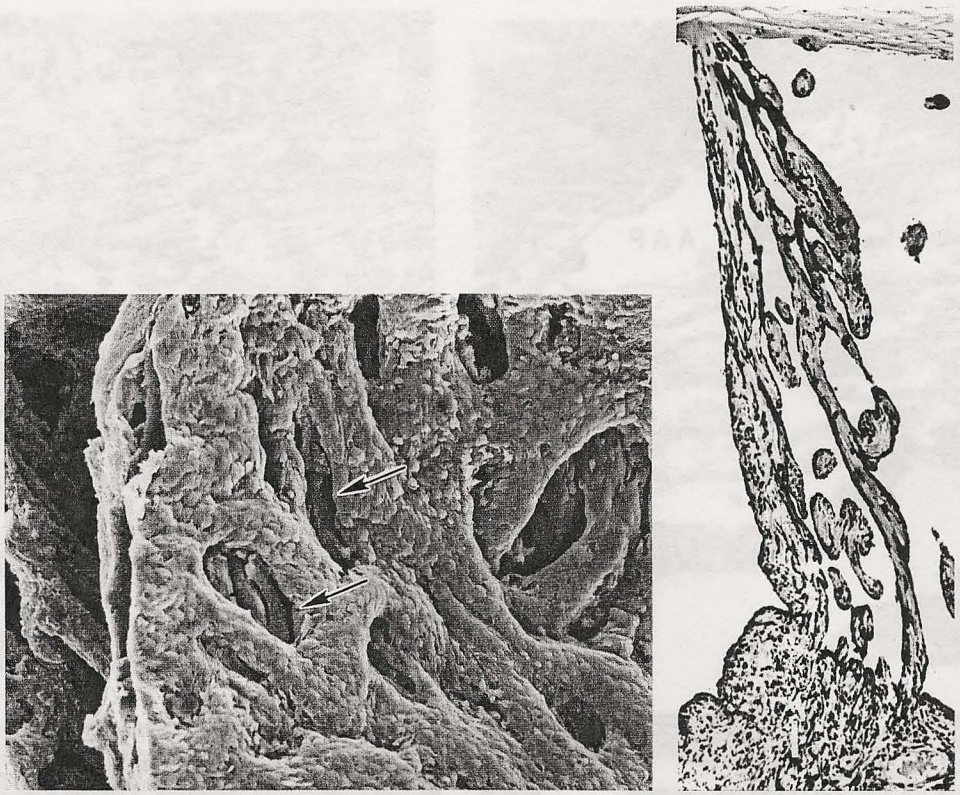

Figure 2.89. Frontal-view SEM (**A**) and sagittal-view light micrograph (**B**) of the equine pectinate ligament. Anteriorly, pores (*arrows*) form openings that permit the aqueous humor to move from the anterior chamber into the iridocorneal angle. (Original magnification: A, X200; B, X100.)

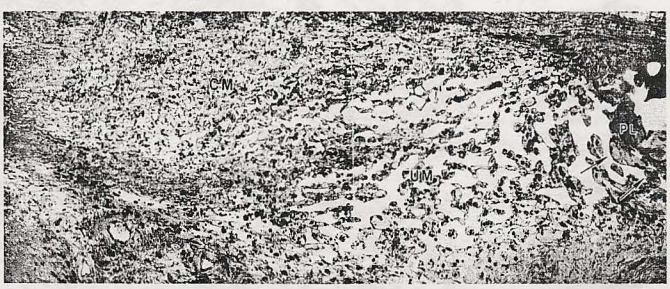

Figure 2.90. Iridocorneal angle of the bison. *Arrows* point to the attachment of the anterior uveal trabecular meshwork (*UM*) to the pectinate ligament (*PL*). The corneoscleral trabecular meshwork (*CM*), which has smaller trabecular beams and intertrabecular spaces, is located more posteriorly and externally. (Original magnification, X100.)

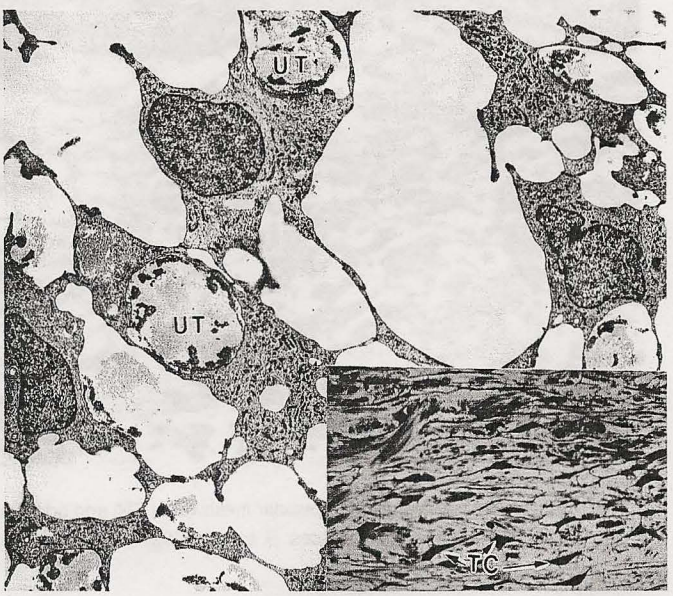

Figure 2.91. The inner, posterior uveal trabeculae (*UT*) are relatively small, resembling trabeculae of the corneoscleral trabecular meshwork as seen in the ovine iridocorneal angle. (Original magnification, X3400.) **Insert.** Most posteriorly, the fibrous beams of the uveal trabecular meshwork are loosely lined by trabecular cells (*TC*). (Original magnification, X200.)

Trabecular cells along the corneoscleral and uveal beams in the ICA are nearly identical in appearance in any given animal. Moreover, they largely resemble each other from one species to another, being fibroblastlike with slender cell processes that attach repeatedly to adjacent cells and their processes. These processes allow the corneoscleral trabecular meshwork to act as a sieve, thus reducing the size of the particles that can move into the corneoscleral meshwork.[91,135–137] The degree of meshwork porosity varies from animal to animal, such as being more porous in the dog than in the horse (Fig. 2.96). The trabecular cell also has the ability to ingest a wide variety of particles, which can range greatly in size.[138] The phagelike quality of the trabecular cell provides the ICA with an indigenous clearance mechanism for debris, thus reducing possibilities for an inflammatory response.[139,140]

Within the corneoscleral trabecular meshwork of the dog is a region known as the operculum that forms the anteriormost area of the ICA.[141] The operculum begins a region of the ICA having no direct contact with the AAP and comprises much of the nonfiltering portion of the trabecular meshwork.[142] It consists of both the peripheral extension of the corneal endothelium (and

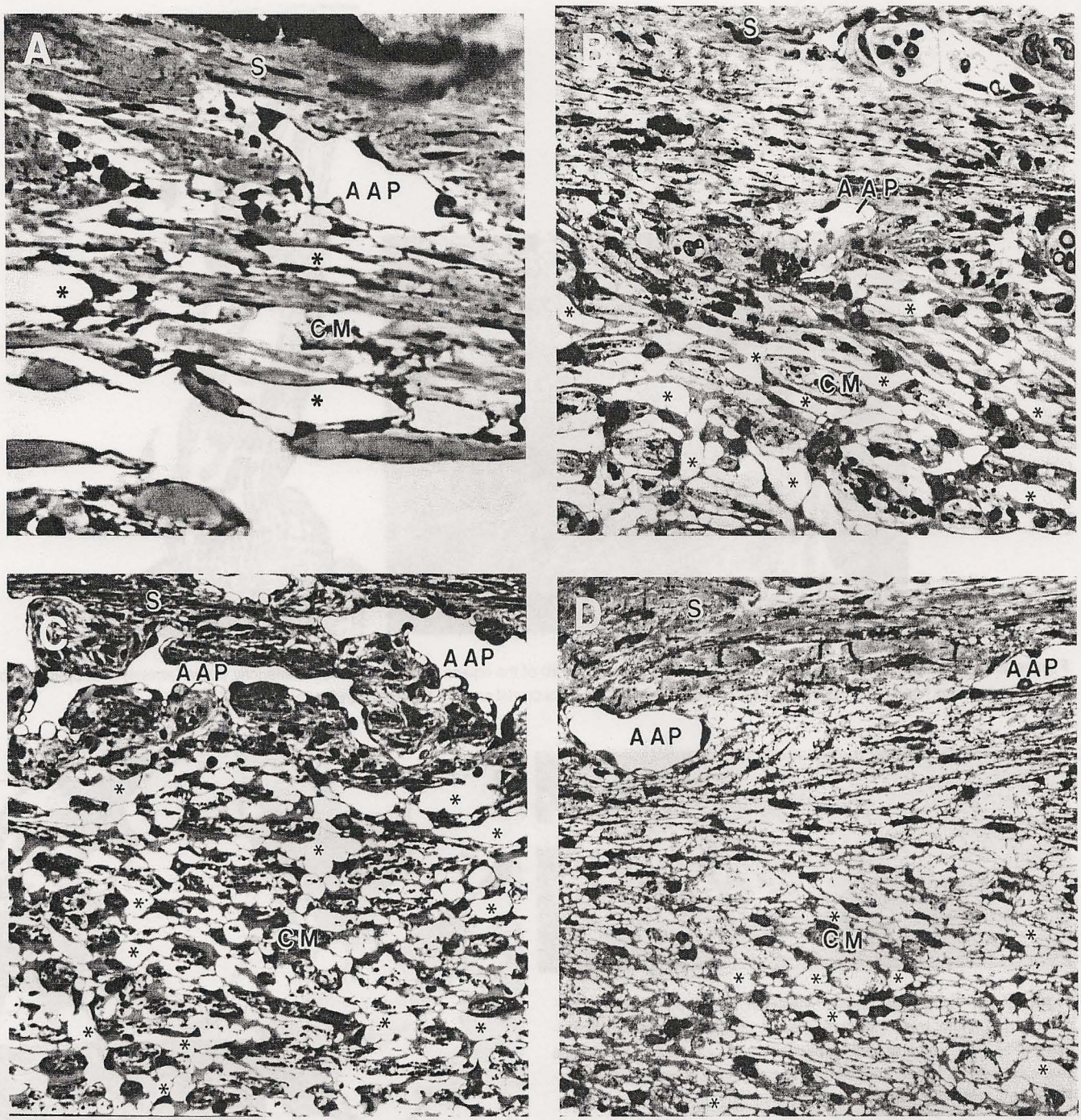

Figure 2.92. The corneoscleral trabecular meshwork (*CM*) and adjacent angular aqueous plexus (*AAP*) in the dog (**A**), bison (**B**), horse (**C**), and pig (**D**). *Asterisks* indicate intertrabecular spaces. *S,* sclera. (Original magnification: All, X400.)

the subjacent basement membrane) and the underlying, anteriormost portion of the corneoscleral trabecular meshwork. The operculum is especially well developed in the dog, rabbit, and nonhuman primates (Fig. 2.97).[120] The peripheral termination of the corneal endothelium and its basement membrane (i.e., Descemet's membrane) leads to what is sometimes called the cribriform ligament because it branches both posteroexternally, into the corneoscleral trabecular meshwork, and posterointernally, joining with the anterior uveal trabeculae. At present, the function of the operculum is not known; however, cells intimately associated with the operculum (i.e., Schwalbe's line cells) are secretory in nature, able to form and release certain enzymes, including enolase and hyaluronans synthase and phospholipids surfactant-like material (Fig. 2.98).[141,143–146] Before these studies, cells along the Schwalbe line were speculated to be developmental in nature and to represent an anterior, vestigial remnant of the pectinate ligament in the primate ICA.[146] While the role these cells play in the mature ICA has yet to be determined, Schwalbe's line cells represent a distinct subpopulation within most mammalian ICAs.

The external boundary of the corneoscleral trabecular meshwork is formed by the sclera and a plexus of aqueous humor collector vessels. In mammals and most lower vertebrates, the aqueous humor chiefly exits the eye through the

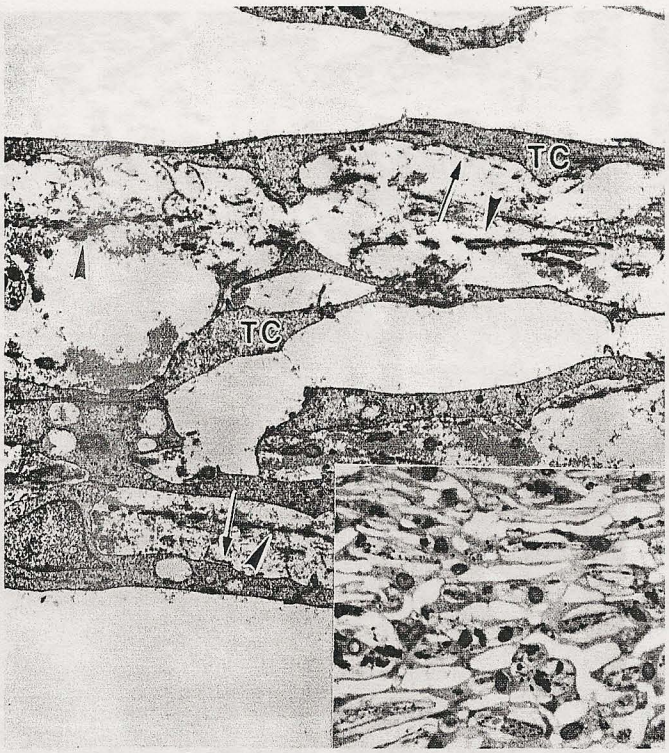

Figure 2.93. Corneoscleral trabecular beam in the bison. Each beam or trabecula has centrally placed elastic fibers (*arrowheads*) surrounded by collagen, which in turn is lined by a basement membrane–like material (*arrows*). *TC,* trabecular cells. (Original magnification, X3400.) **Insert.** Light micrograph of the corneoscleral trabeculae in the bison. (Original magnification, X400.)

Figure 2.94. The small uveal trabecula of a water buffalo possesses multiple layers of basement membrane–like material (*arrowheads*). These trabeculae often contain melanocytes (*ME*). *Asterisks* indicate intertrabecular spaces. (Original magnification, X15,000.)

Figure 2.95. Within the anterior corneoscleral trabecular meshwork in the horse is a narrow band of rounded trabeculae that consist of densely packed collagen, including long-spacing collagen (*arrows*). *Me,* elastic fiber. (Original magnification, X12,000.)

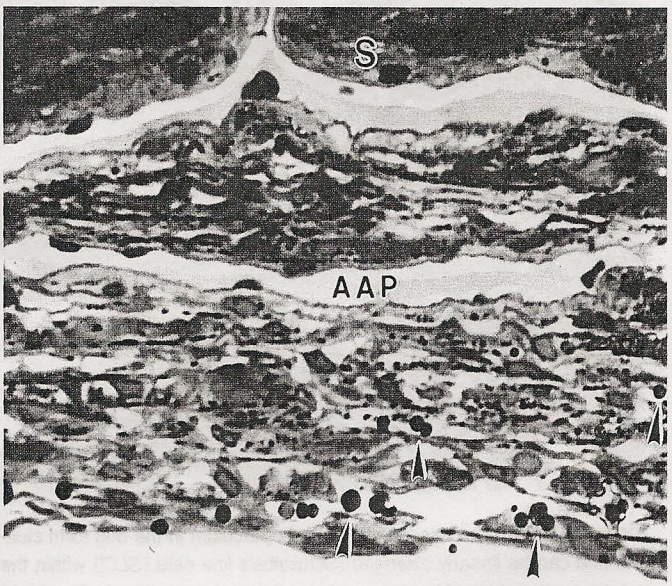

Figure 2.96. Microspheres up to 3 or 4 m in diameter (*arrowheads*) can move into the intertrabecular spaces of the corneoscleral trabecular meshwork in the dog. *AAP,* angular aqueous plexus; *S,* sclera. (Original magnification, X400.)

trabecular meshworks into these vessels (Fig. 2.92). In most mammals, these vessels consist of a small network of veins collectively termed the *angular aqueous plexus,* or *AAP.*[117,131] These vessels have radially oriented lumens, differing from the circumferentially coursing canal of Schlemm in primates.[147–149] The plexiform nature of the drainage vessels in most mammals allows removal of a substantial amount of aqueous humor. The single canal in primates most likely represents an evolutionary adaptation for removal of aqueous humor from a relatively small anterior chamber through a small, compact ICA bordered by a large and highly developed ciliary body musculature essential for accommodation.

The size of the individual collector vessels (i.e., trabecular veins) and the tissue immediately adjacent to the AAP varies considerably among mammals (Fig. 2.99). The trabecular veins in the cow, sheep, and water buffalo are large and

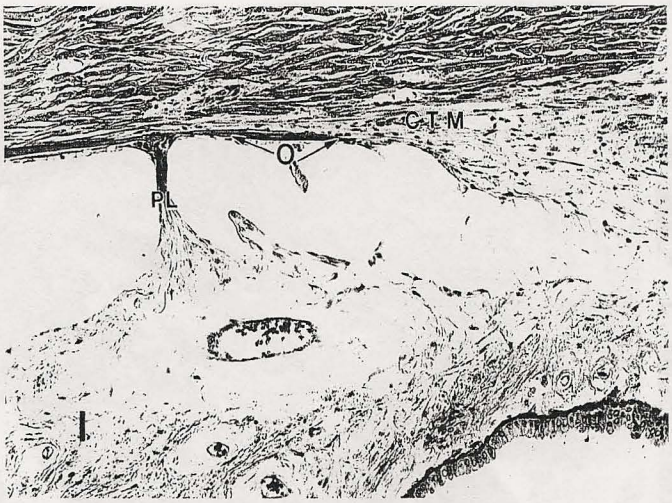

Figure 2.97. In the rabbit, as in most carnivores and monkeys, the peripheral corneal endothelium and its basement membrane extend posteriorly at variable lengths beyond the pectinate ligament (*PL*) and form the operculum (*O*). In turn, the operculum forms a lidlike cover over the anteriormost corneoscleral trabecular meshwork (*TM*). *I*, iris. (Original magnification, X100.)

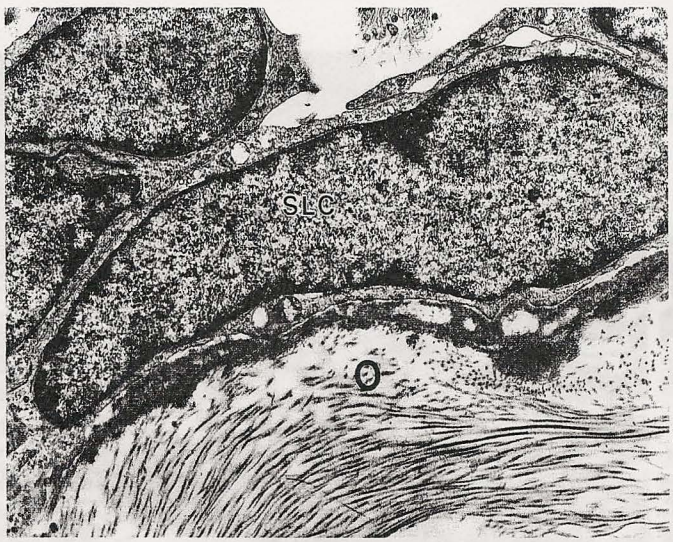

Figure 2.98. Cells associated with the operculum in the dog form clusters and can be linearly arranged (Schwalbe's line cells [*SLC*]) within the anteriormost regions of the corneoscleral trabecular meshwork. *O*, operculum. (Original magnification, X9800.)

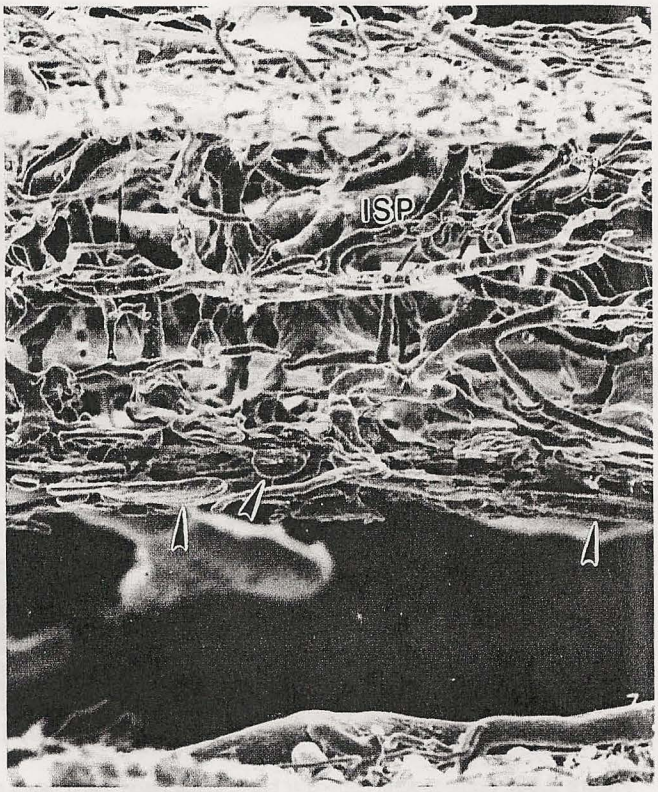

Figure 2.99. Frontal-view SEM corrosion cast of the limbal vasculature in the dog. *Arrows* indicate the variably dilated trabecular veins that collectively make up the angular aqueous plexus, which eventually empties into the intrascleral plexus (*ISP*). (Original magnification, X80.)

extensive. Those associated with the dog, cat, pig, and horse are less prominent but are still extensive. By comparison, the AAP of the bison is remarkably small, being only a fraction in size of that in the cow or sheep (Fig. 2.92).

The area adjacent to the trabecular veins typically consists of a zone of cellular elements intermixed with irregularly arranged elastin, collagen, and basement membrane–like material. These elements are much more compact in the horse than in other mammals, except for humans (Fig. 2.92). They constitute a separate zone, called the juxtacanalicular zone, that is readily distinguished from the rest of the outer corneoscleral trabecular meshwork. The function of this zone has yet to be determined, but it may contribute substantially to aqueous humor outflow resistance.

In some species, including the dog, rat, rabbit, and humans, smooth muscle–like cells (myofibroblastic cells) have been observed in the trabecular meshwork, especially adjacent to the aqueous humor outflow channels and along the distal or outer walls of the AAP and Schlemm's canal.[150,151] In the dog, the interior presence of myofibroblastic cells within the ICA suggests that these cells and the smooth muscle cells of the ciliary body along the same plane of orientation function to facilitate the removal of aqueous humor and are likely to be influenced by vascular mediators. Whether all myofibroblastic cells play a significant role in regulation of aqueous humor outflow is unknown.

GAGs form an integral component of trabeculae within the ICA and the area adjacent to the AAP (and canal of Schlemm). Treatment with hyaluronidase results in lowering of the IOP. GAGs appear to regulate IOP via their state of polymerization, which controls hydration capacity and swelling or shrinking.[152–156]

The manner by which aqueous humor flows into the trabecular veins of the AAP or canal of Schlemm continues to be debated.[120,147–149,157,158] Most of the aqueous humor is believed to move through large, vacuole-like structures of the inner endothelial cells (Figs. 2.92 and 2.100). These vacuoles become more prominent with increasing IOP.[158]

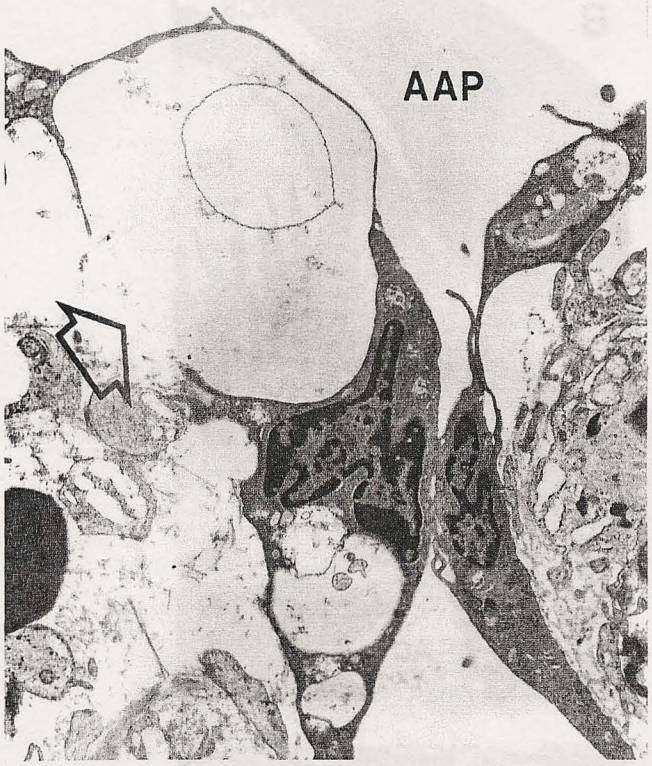

Figure 2.100. Close-up of the endothelial cells that line the angular aqueous plexus (*AAP*) of the horse. These cells frequently possess large vacuoles that often open at the base of each cell (*arrow*) and, less often, open next to the AAP. These vacuoles are believed to be avenues for aqueous humor to move through from the angle to the AAP. (Original magnification, X8000.)

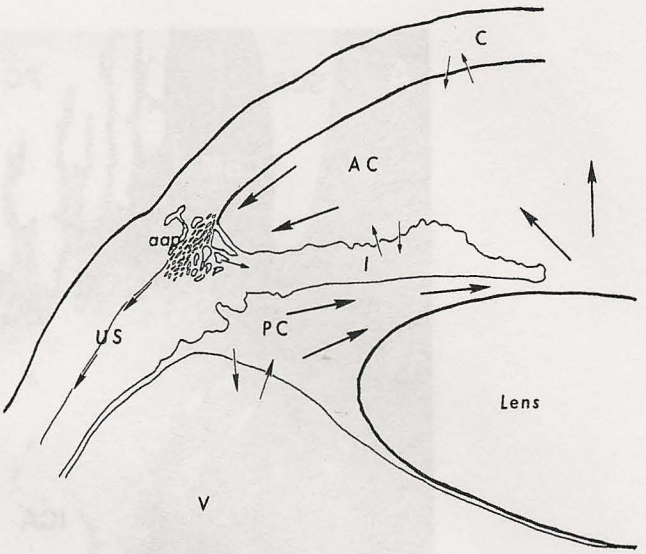

Figure 2.101. Aqueous humor, which is formed in the posterior chamber (*PC*), is partly exchanged across the vitreous face (*V*). Most of it flows into the anterior chamber (*AC*), where it is mainly removed by the trabecular meshwork and angular aqueous plexus (*aap*). Other drainage routes include the uveoscleral (*US*) pathway, exchange across iris vessels (*I*), and the corneal endothelium (*C*).

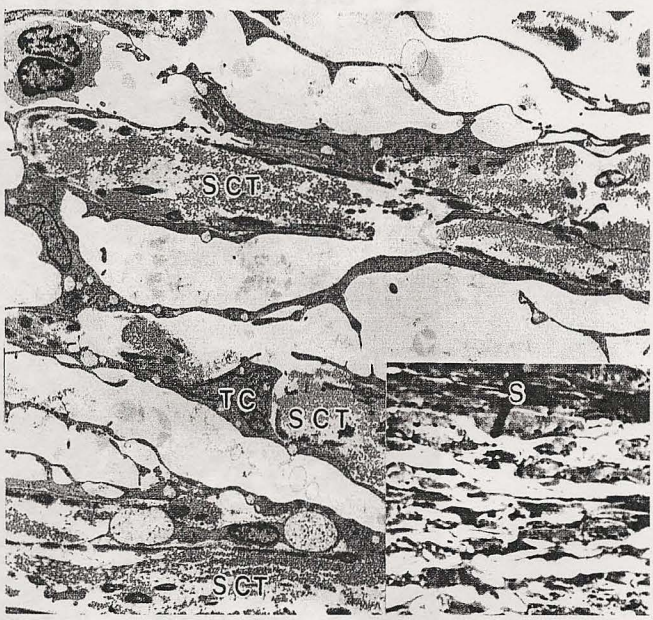

Figure 2.102. In the horse, there is a well-defined meshwork, called the supraciliary meshwork, between the ciliary body meshwork and the sclera. It is possibly responsible for removal of aqueous humor via uveoscleral outflow. *SCT,* supraciliary trabecula; *TC,* trabecular cell. (Original magnification, X3500.) **Insert.** Light micrograph of this meshwork. *S,* sclera. (Original magnification, X200.)

Uveoscleral Outflow

Aqueous humor is not entirely removed by the various angle collector vessels. Some drains either posteriorly into the vitreous humor, anteriorly within the iridal stroma and across the cornea, or exteroposteriorly along a supraciliary-suprachoroidal space into the adjacent sclera (Fig. 2.101).[91,126,159,160] The lattermost pathway is called the uveoscleral pathway, or unconventional outflow. Of the different ancillary routes, uveoscleral outflow is the most prominent, accounting for as much as 30% to 65% of the total aqueous humor being removed in nonhuman primates, 13% in the rabbit, 3% in the cat, 4% to 14% in humans, and 15% in the dog.[159,161] Results of particle-injection studies have demonstrated this pathway to be open to the level of the central choroid to those particles as large as 3 μm in diameter. One- to three-micron-diameter particles can move into the suprachoroidal space of the horse, chicken, and monkey eye, but only as far posteriorly as the ciliary body in the dog and cat, and they do not reach the supraciliary space in the rabbit.[91,135,136] The need for and use of uveoscleral outflow varies remarkably between species. In the horse, the uveoscleral pathway may be just as important as the conventional route for aqueous humor removal. Large spaces of the outer uveal meshwork become confluent posteriorly, with a uniquely wide and well-defined meshwork between the ciliary body musculature and the sclera (i.e., the supraciliary space). This region, which has been found only in the horse, is called the supraciliary meshwork and most likely represents a major pathway for aqueous humor removal (Fig. 2.102).[130]

Within the dog, cat, cow and horse, the outer anterior ciliary body musculature (CBM) forms longitudinal and circumferential attachments to trabeculae of the ICA.[162] Spaces between the endings of the CBM form avenues for the beginning of the uveoscleral pathway and varies in the amount of

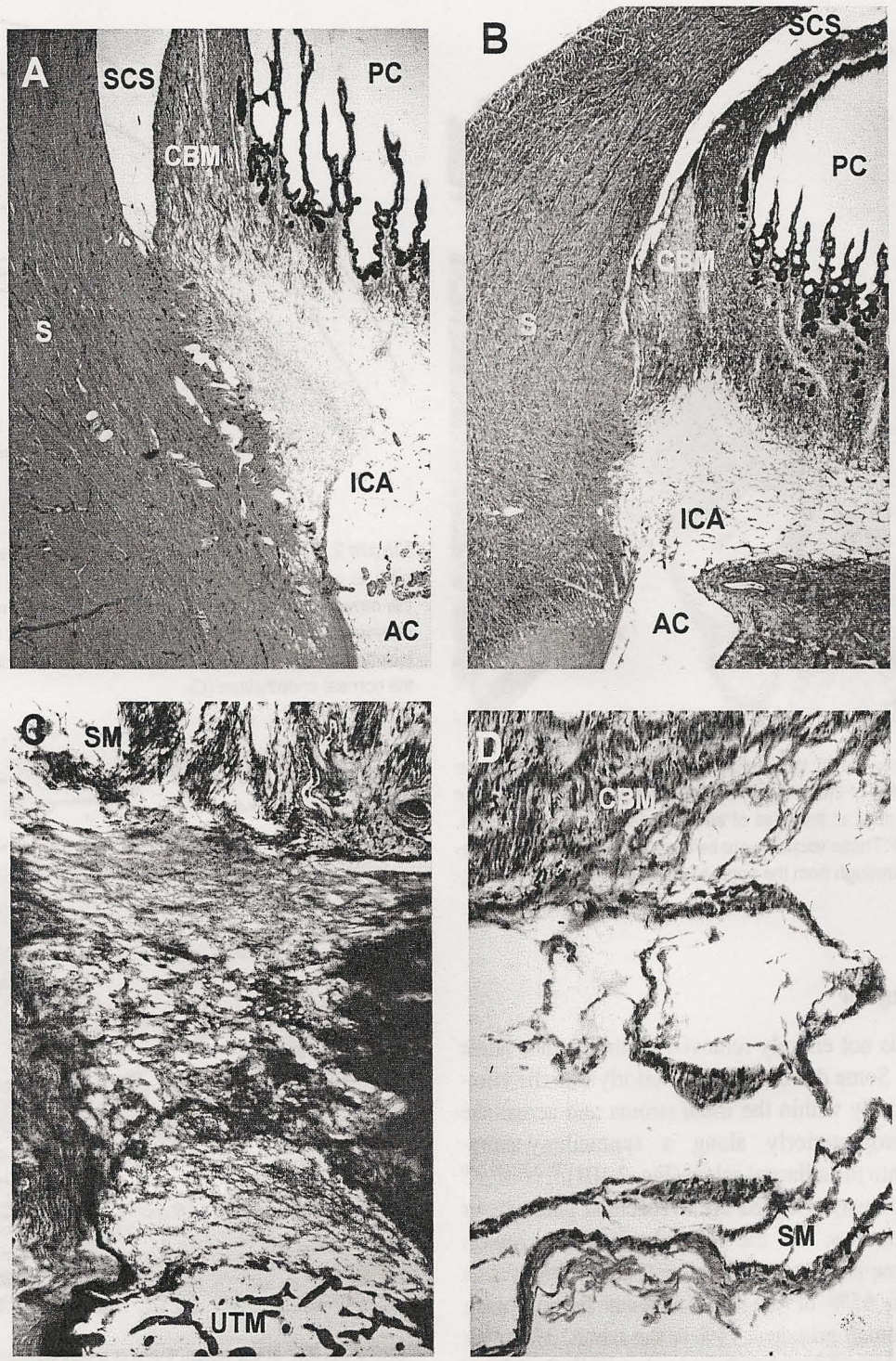

Figure 2.103. Anterior uveoscleral outflow pathway within domestic species viewed tangentially. **A.** Bovine anterior uvea. (Original magnification, X20.) **B.** Porcine anterior uvea. (Original magnification, X20.) **C.** Equine anterior uvea at region where the posterior iridocorneal angle (*ICA*) connects with the supraciliary meshwork (*SM*). (Original magnification, X20.) **D.** Feline supraciliary space with supraciliary meshwork (*SM*) with collagenous and smooth muscle trabeculae that connect the ciliary body musculature (*CBM*) with the sclera (*S*). (Original magnification, X100.) *AC,* anterior chamber; *PC,* posterior chamber; *UTM,* uveal trabecular meshwork. (All photographs are courtesy of Kara Kligman)

extracellular matrix (ECM) material, being most developed in the pig (Fig. 2.103).

In the pig, the corneoscleral trabecular meshwork is anchored by a scleral spur, which in turn anchors much of the outer CBM. As a result, the uveoscleral pathway is limited to small intertrabecular spaces of the posterior ICA that interface with the anterior CBM. Within the outer ciliary body, there are blood vessels in close proximity to the sclera. More posteriorly, the supraciliary space contains occasional collagenous trabeculae, some of which are attached to projections of the outer smooth muscle bundles.[162]

In the cow and domestic carnivores, outer anterior muscle bundles attach the CBM to the sclera concomitant with the presence of an anterior elastic sheath, which is especially well

developed in the dog. Initially, the uveoscleral pathway consists of small intercellular spaces lying between the attachments of the anterior smooth muscle bundles of the ciliary body and the posterior uveal trabecular meshwork. Within the supraciliary space, slender trabeculae are most numerous anteriorly extending from the ciliary body obliquely and radially.

In the horse, the outer anterior muscle bundles of the ciliary body are connected to branching connective tissue trabeculae within the uveoscleral pathway that are attached radially to the sclera.[130,162] Flow from the ICA to the supraciliary space appears direct with a modest amount of ECM. An elastic sheath lines this portion of the uveoscleral pathway. Trabeculae within the supraciliary space is extensive, consisting of either collagen or muscle. Those of muscle penetrate into the adjacent sclera. Both types of trabeculae are often branched and lined by melanocytes and become less numerous, narrower, and less branched posteriorly.

In the cat and dog, the outer anterior muscle bundles of the ciliary body, which are more abundant than in the other domestic species, form a fine meshwork of trabecular associations with the posterior ICA. The outer bundles are small throughout the entire ciliary body with branched attaching occasionally to the nearby sclera. Collagen trabeculae also attach the sclera to the ciliary body. Elastic fibers line these trabeculae as well as the inner portion of the sclera, especially anteriorly where the ciliary body begins and the ICA ends.

Aging

A number of age-related changes occur in the ciliary body. As the nonpigmented epithelium grows older, its basement membrane thickens greatly, resulting in a multilaminant, reticulated type.[109] This thickening eventually involves nearly all the epithelium in older individuals. The pigmented epithelial basement membrane similarly thickens with age, producing a nearly identical multilaminar appearance. The nonpigmented epithelium thins irregularly, especially at the base of the ciliary processes and along the pars plana (Fig. 2.104A). The stroma of the ciliary body, which separates the processes from the muscle, concomitantly thickens because of increased amounts of collagen and other extracellular materials. The degree of pigmentation in the ciliary body, however, lessens with age, particularly in the pigmented epithelium along the crests of the ciliary processes.[109] Age-related changes associated with the ICA are well documented in humans and the dog.[32,124,125,132,156]

The cortical zone within the trabecula broadens in older individuals. This thickening is contributed partly by additional basement membrane–like material and partly by additional amorphous material. The thickened cortical zone may contribute to increased thickening of the corneoscleral trabeculae within the canine ICA. In noncanine species, the cortical zone consists of fibronectin and both regular as well as "curly" or long-spaced collagen.[145,163] In the dog, curly collagen has rarely been encountered in the ICA, having been mostly associated with the peripheral extension of the corneal endothelium and its basement membrane (i.e., Descemet's membrane), which together can intrude as much as 0.5 mm into the ICA. Use of PAS stain, which reacts strongly with basement membrane material, on normal canine, laboratory-quality (i.e., Beagle) ICAs of different ages (3 months to 8 years) demonstrates positive reactions within the corneoscleral trabecular meshwork, especially along the posterior extension of Descemet's membrane. The apparent increase in PAS staining with age occurs mostly within the anteriormost portion of the corneoscleral trabecular meshwork, including the operculum. No age-related changes have been observed or reported within the uveal trabeculae of the canine ICA.[132]

The collagen cores also thicken because of both increased size of the collagen fibrils and an increment in the elastin associated with these cores. Perhaps the most discernable alterations of the canine ICA with regard to age are those associated with the extracellular fibers comprising the bulk of each trabecula. When comparing the average diameter of the collagen fibril as well as the distribution of diameter size within the inner and outer regions of the corneoscleral trabecular meshwork and subjacent sclera next to the aqueous plexus at different ages, several interesting changes have occurred (Fig. 2.104B,C).[164] Collagen fibrils within the outer corneoscleral trabecular meshwork increase their average diameter by approximately 25% during the second and third years of life compared with the latter half of the first year.[156] On the other hand, collagen fibrils within the inner corneoscleral trabecular meshwork and adjacent outer uveal trabecular meshwork become progressively thinner during the first 3 years of life. Early age-related changes in collagen fibrillar size are most remarkable within the sclera forming the outermost lining of the ICA, increasing nearly 100% in average diameter over a 2.5-year period. The increase of collagen fibrillar size within the inner scleral wall of the limbal region occurs unevenly, with some fibrils remaining small and others attaining considerable widths.

The elastic component within the ICA, which most likely provides the trabeculae with a necessary degree of resiliency, does not appear anatomically to be affected substantially by the beginning of the aging process. There may be changes, however, in the elastic fibers next to the AAP of old dogs that resemble those seen next to Schlemm's canal in old humans.[165,166]

The appearance of the trabecular (i.e., endothelial) cells in both the uveal and corneoscleral meshworks changes mostly during the first year of life. As the cells become more separated spatially, they elongate and possess less clustered cytoplasmic processes (Fig. 2.105). In older animals (>4 years of age), fewer cells are observed in both meshworks compared with those in younger animals (<1 year of age). Quantitative assessment of trabecular cells made from dogs that ranged in age from 3 months to 8 years reveals substantial age-related lowering of populations in both the uveal and corneoscleral trabecular meshworks (Fig. 2.106). By the end of the first year, the average cellular density of both meshworks has dropped by nearly 30%.[156] The lowering of cellular density during this period undoubtedly results from the overall increase in ICA size during the first year of life in the dog.[124,125] A

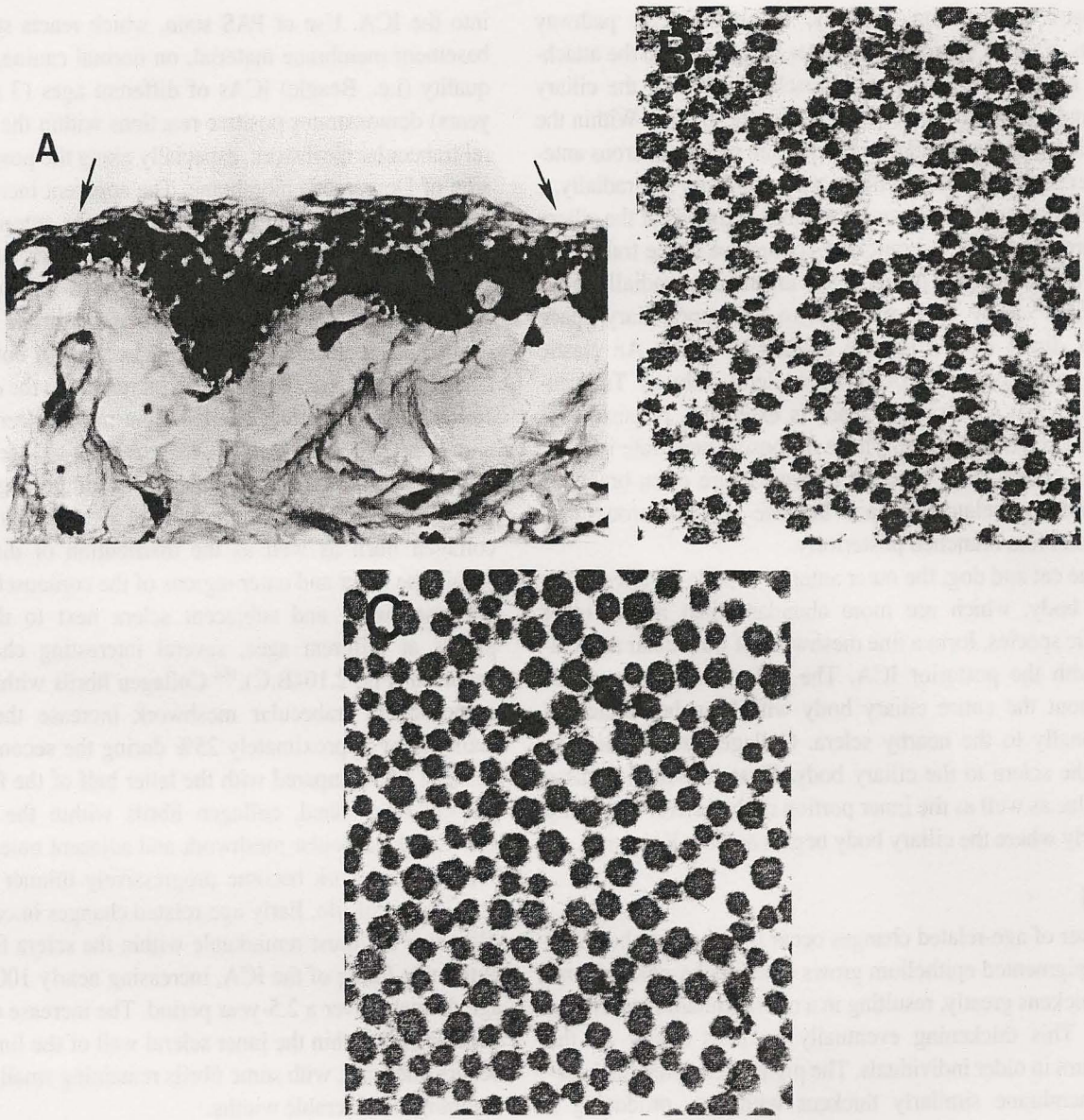

Figure 2.104. A. Pigmented and nonpigmented epithelia of the ciliary body in a 9-year-old dog. Note the irregularly attenuated portions (*arrows*) of the nonpigmented epithelium. (Original magnification, X400.) **B.** Core of a 1-year-old canine corneoscleral trabecula consists of small collagen fibrils when compared to that of a 6-year-old dog (**C**). (Original magnification: B, X10,000; C, X10,000.)

further substantial decrease in cellular density is not observed for another 5 years, until the seventh and eighth years of age. The size of the ICAs in the older dogs (7–8 years of age) is, in fact, slightly smaller than that in the younger mature dogs (1–6 years of age), which may be attributed to the age-related increase in lens size. These changes appear to reduce the area available for aqueous humor outflow and, quite possibly, make older individuals more susceptible to any kind of insult that could lead to glaucoma.

Innervation

As mentioned previously, the ciliary musculature is both sympathetically and parasympathetically innervated.[123,167] Cholinergic and adrenergic nerve endings have been observed in the various components of the ciliary body, including the trabecular meshwork, and within the ICA, most of these endings occur posteriorly. In the dog, cholinergic activity is most intense in the musculature, ciliary processes, and epithelium. Dense adrenergic innervation, however, is located in the subepithelial portions of the ciliary body.[168] Species differences in the distribution of these nerves to the eye among many lower mammals have been demonstrated,[169] but the function of the cholinergic and adrenergic nerves within the ciliary body remains speculative.[170,171]

Choroid

The choroid is the posterior portion of the uveal coat. It is composed primarily of blood vessels (mainly thin-walled veins) and pigmented support tissues. It is the main source of nutrition for the outer layers of the retina, which are immediately adjacent. In primates, the anterior margin of the choroid joins the ciliary body along an irregular junction known as the

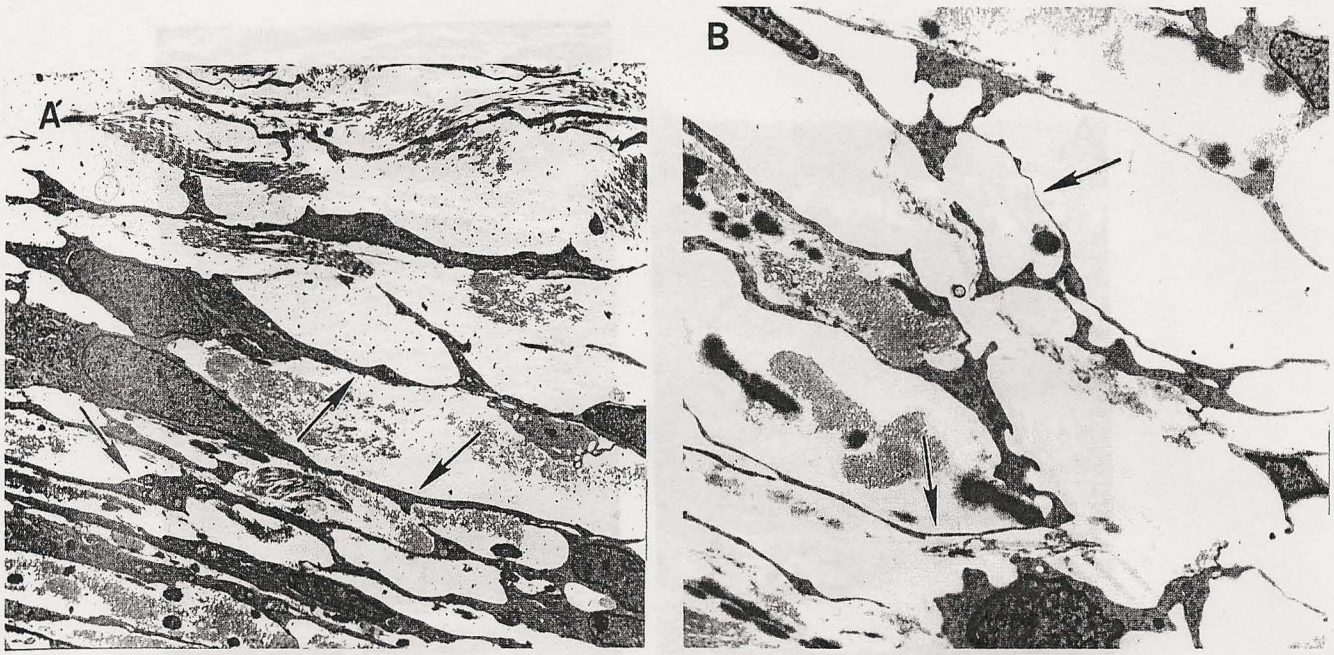

Figure 2.105. **A.** TEM shows that trabecular cells of the outer corneoscleral trabecular meshwork in the 3-month-old dog are clustered and interconnected by fairly prominent processes (*arrows*). (Original magnification, X4000.) **B.** TEM shows that trabecular cells in the 2-year-old dog are widely spaced and loosely interconnected by thin processes (*arrows*) in the outer corneoscleral trabecular meshwork. (Original magnification, X5000.)

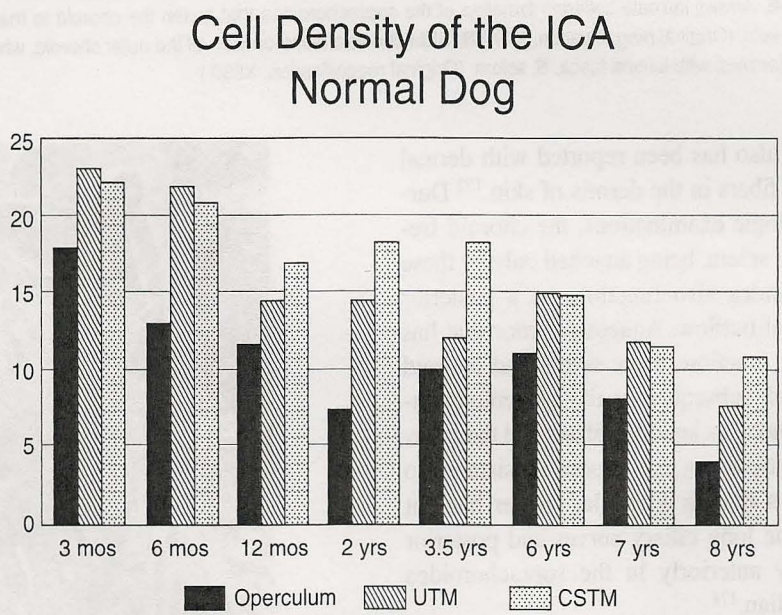

Figure 2.106. Graph of cell density (cells per 2500 sq. mm) within the different regions (operculum, uveal trabecular meshwork [*UTM*], and corneoscleral trabecular meshwork [*CSTM*]) of the iridocorneal angle of the dog at different ages.

ora serrata as the two structures interdigitate with each other along a serrated junction, as in humans. In most domestic animals, the junction is nonserrated and is called the ora ciliaris retinae. The choroid tends to thicken along the posterior pole, becoming thinner toward the equator. For morphologic discussions, the choroid can be divided externally to internally, as shown in Figure 2.107, into:

1. The suprachoroidea,
2. The stroma with large vessels,
3. The stroma with medium-sized vessels and tapetum, and
4. The choriocapillaris.

The tapetal layer varies among species, and it is absent in the pig, squirrel, and many nonhuman primates.

Suprachoroidea

The suprachoroidea consists of elastic, heavily pigmented connective tissue that forms a transition between the sclera and the choroid. Branching collagen lamellae traverse the potential suprachoroidal space to fasten the choroid to the lamina fusca of the inner sclera (Fig. 2.107). In pigmented rabbits, the choroidal melanocytes are situated predominantly in this region, being intimately associated with elastic fibers

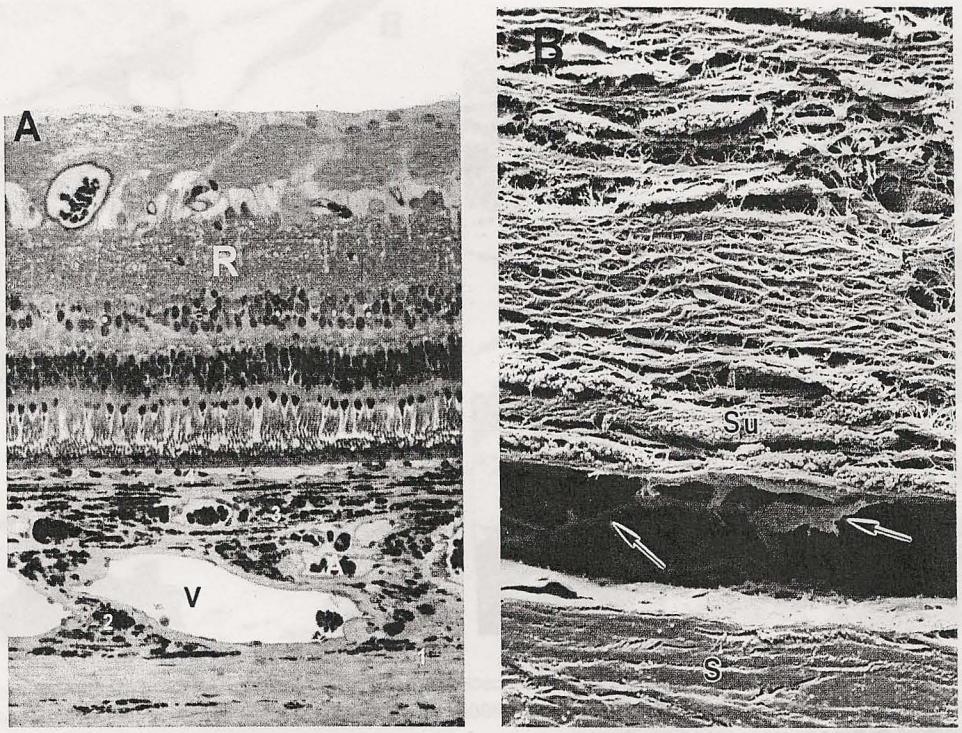

Figure 2.107. A. The canine choroid consists of the suprachoroidea (*1*), stroma with large blood vessels (*2*), stroma with medium-sized vessels and tapetum (*3*), and choriocapillaris (*4*). *Arrows* indicate collagen lamellae of the suprachoroidea that fasten the choroid to the lamina fusca of the sclera (*S*). *A,* artery; *R,* retina; *T,* tapetum; *V,* vein. (Original magnification, X40.) **B.** SEM shows a close-up view of the outer choroid, where the suprachoroidea (*Su*) forms fine collagenous attachments (*arrows*) with lamina fusca. *S,* sclera. (Original magnification, X850.)

and oxytaran fibers, and also has been reported with dermal pigment cells and elastic fibers in the dermis of skin.[172] During preparation for histologic examinations, the choroid frequently separates from the sclera, being attached only by these lamellae. The suprachoroidea also functions as a posterior component for uveoscleral outflow. Aqueous humor that has moved along this narrow junction of the sclera and choroid diffuses into the sclera and, subsequently, the systemic circulation. The layers of melanocytes and fibroblasts and the interspersing collagen and elastic fibers may produce resistance to uveoscleral drainage, even though a cellular barrier has not been found to exist.[173] The long ciliary nerves and posterior arteries course their way anteriorly in the suprachoroidea along the horizontal meridian.[174]

In birds, this region also contains a layer of nonvascular smooth muscle cells.[175] This muscle as well as that associated with the arteries are believed to be innervated by somatostatin-expressing neurons located within the avian choroid. The function of this band or layer of smooth muscle within the suprachoroidea is presently unknown, but its location suggests that it could play a significant role in uveoscleral aqueous humor outflow and IOP regulation.

Figure 2.108. SEM corrosion cast of the choroidal vasculature in the dog. *Large arrows* indicate collateralization of the intrascleral plexus (*ISP*) with the large choroidal veins (*V*). *Small arrows* indicate choroidal arteries. (Original magnification, X10.)

Large-Vessel Layer

Immediately internal to the suprachoroidea is a vascular plexus embedded in loose connective tissue containing melanocytes and fibrocytes. This plexus is composed mostly of large veins and scattered arteries (Fig. 2.108). These veins merge centripetally into four or more prominent vortex veins located obliquely near the equator between the horizontal and vertical meridians. In cross-section, the veins are cavernlike, occupying 50% or more of the total volume of the choroid (Figs. 2.107 and 2.109). They frequently collateralize with each other and communicate anteriorly with anterior ciliary

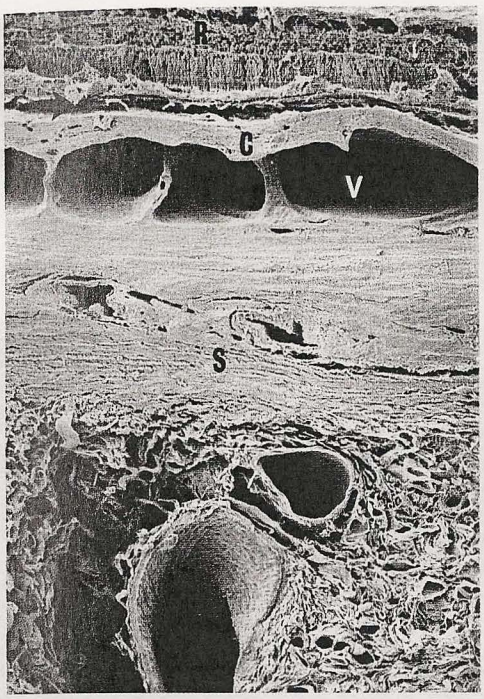

Figure 2.109. SEM of the posterior canine eye shows the choroid (*C*) is composed mostly of large, cavernous veins (*V*) that drain the choriocapillaris (*arrows*), which nourishes the outer retina (*R*). *S*, sclera. (Original magnification, X25.)

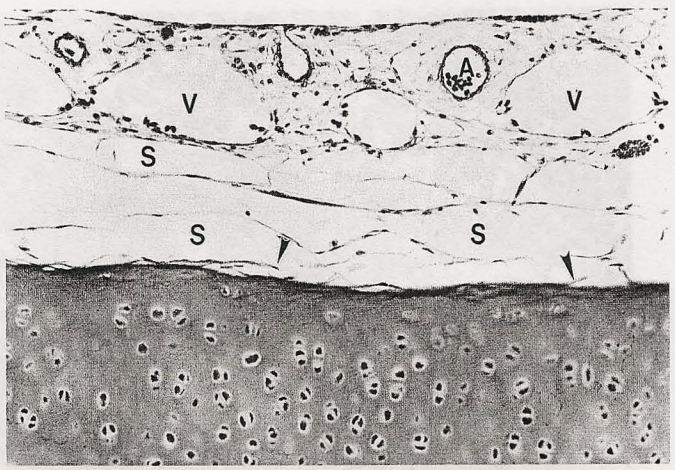

Figure 2.110. The outer choroid in the avian (i.e., chicken) eye consists of sinusoids (*S*) that extend to the suprachoroidea (*arrows*) and adjacent "cup" of hyaline cartilage. *A*, arteries; *V*, veins. (Original magnification, X200.)

veins, the intrascleral venous plexus, and the iridal veins.[87,176,177] The large arteries, which are much fewer in number, are mostly branches of the short posterior ciliary arteries, which enter the globe in the vicinity of the optic nerve and supply the retina, optic nerve, and the choroid. To a lesser extent, the choroid also receives blood from the long posterior ciliary arteries and the anterior ciliary arteries.[178]

In horses, the vessels, which also are mostly veins, tend to anastomose less than those in the canine eye and to run circumferentially along the anteroposterior axis.[76] Vasodilation of choroidal vessels can be achieved by stimulation of the facial nerve. Recently, the presence and spatial organization of nerves within the choroid of the rat, the rabbit, and humans have been documented.[179] In these three species, perivascular networks of diaphorase-positive nerve fibers with varicose terminals accompany the choroidal aeries and arterioles. An intrinsic, nitrergic nerve cell plexus, however, occurs only in the human eye, in the vicinity of the fovea. It remains to be seen if other animals, whether primates or not, possess a similar plexus.

In addition to providing the major source of oxygen and nutrients for the retina, the large vessels may act as a "cooling system," dissipating the heat produced from light absorption.[180,181] Because of the high amount of plasma proteins in the tissue fluid, the resulting osmotic pressure may also allow retinal fluids to pass into the choroid itself via the RPE and to assist in keeping the retina attached to the RPE.[182–184]

In the avian eye, the large veins are directly associated with another bed of vessels, which have been referred to as sinusoids, lacunae, or most recently, the lymphatic vessels.[1,175,185] These vessels, in fact, comprise a major portion of the choroidal volume, and they serve as a large reservoir that may assist in IOP regulation by removal of fluid from the blood vessels.[175,185] Morphologically, the vessels are similar to the lymphatic vessels, having an absence of innervation and a defined, basal lamina–associated smooth muscle, but having the presence of a fenestrated endothelium. These vessels are mostly located next to the suprachoroidea, and they may be thought of as a part of it. A portion of these vessels also extends into adjacent large veins as the latter exit the choroid (Fig. 2.110).

The combination of the accessory vessels in the outer choroid and a thin band of smooth muscle within the suprachoroidea distinguishes the avian from the mammalian choroid. As an experimental model for mammals, especially primates, the avian choroid should be used with considerable caution.

Medium-Sized Vessel and Tapetum Layer

A small layer of medium-sized vessels and pigmented reticular connective tissue lies internally to the large-vessel layer. These vessels are emissaries between a single sheet of capillaries and the layer of large blood vessels. The medium-sized vessels, especially the arteries, dichotomously branch, radiating slightly inward in a fanlike manner from the larger vessels. The cells surrounding these vessels consist of melanocytes and fibrocytes. In heavily pigmented individuals, the melanocyte is the predominant cell type. In most domestic animals, the melanocyte possesses characteristically oval-to-round melanin granules ranging from 0.1 to 4.0 μm in diameter (Fig. 2.111). The extracellular space consists of loosely arranged bundles of collagen mainly running parallel to the choroidal surface, and it is interspaced with numerous elastic fibers.

Nonmyelinated nerve fibers usually occur in association with the vascular system (Fig. 2.112). The nerves in the choroid are predominantly associated with the vascular system, and most of the nerves are associated with the arterial system. They arrive in the choroid as short ciliary nerves around the optic nerve and provide numerous collaterals in the posteroanterior route. They follow the short posterior ciliary artery branches, and they give off anastomotic branches. Most

Figure 2.111. TEM showed that choroidal melanocytes (*M*) in the pig are filled with oval-shaped melanosomes and interspersed between blood vessels (*BV*) as well as loosely arranged collagen fibers (*arrows*) and fibrocytes (*F*). (Original magnification, X4800.)

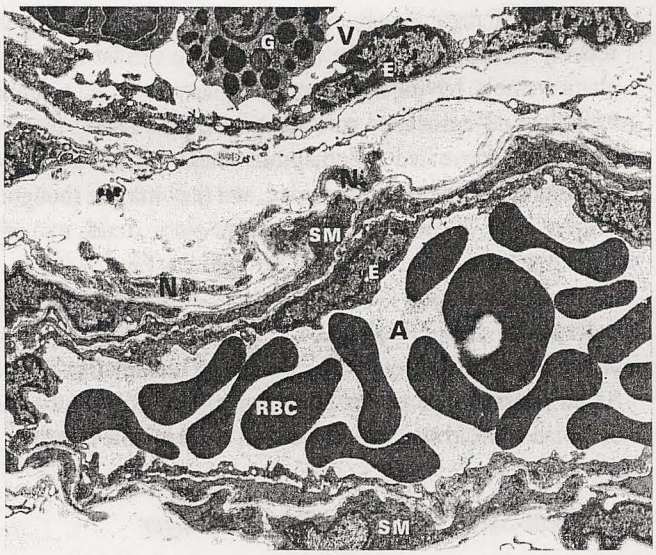

Figure 2.112. Choroidal artery and vein in the dog. The lower artery (*A*) is ensheathed with smooth muscle cells (*SM*), having a basal lamina, numerous dark densities, and pinocytotic vesicles on the cell surface. A nonmyelinated nerve fiber (*N*) is in close association with the smooth muscle. A vein (*V*) with a granulocyte (*G*) is separated from the artery by collagen fibrils and fibroblastic processes. The vein wall is thin, consisting of a nonfenestrated endothelium (*E*). (Original magnification, X4600.)

of the nerve endings are motor to the smooth muscles of the arteries.

In most domestic animals, the dorsal portion of the choroid at the medium-sized vessel layer contains a layer of reflective tissue called the tapetum lucidum. The tapetum is roughly triangular in shape when viewed funduscopically, and it varies in color (Fig. 2.113). It reflects light that has passed through the retina and thus restimulates the retinal photoreceptor cells. The tapetum lucidum is responsible both for the "eyeshine" seen at night when animals face a light and for the variable background color of the ocular fundus (background of the eye as viewed by light projected inside the eye) (Fig. 2.114). Animals without a

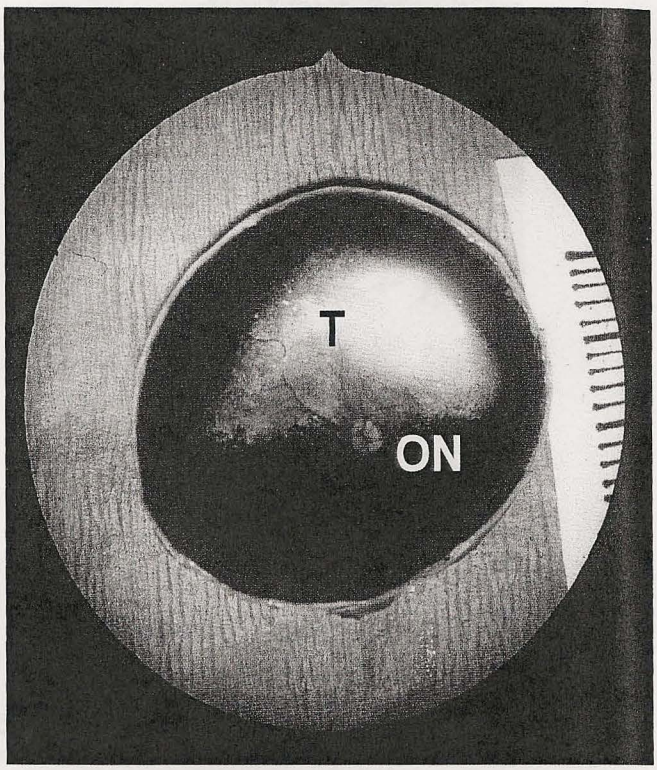

Figure 2.113. With the anterior half of the globe removed, the entire view of the tapetum lucidum (*T*) is seen in the dog. The tapetum lucidum, which is always located dorsally, usually ends along the horizontal plane next to or including the optic nerve head (*ON*).

Figure 2.114. "Eyeshine," or light being reflected back by the tapetum lucidum, in the bushbaby. The left eye reflects light poorly because of a cataract.

tapetum lucidum (i.e., humans, the squirrels, red kangaroo [*Macropus rufus*], and pig) have diurnal habits and red or orange to pale gray (depending on the amount of choroidal pigmentation) fundus reflections.[186] The red-to-orange backgrounds result from reflection of light from choroidal blood vessels in less-pigmented individuals.

The tapetal layer is composed of regularly arranged collagenous fibers in herbivores (i.e., the tapetal fibrosum in the horse, ox, sheep, and goat) and of specific polyhedral cells, or iridocytes, containing reflecting crystals in carnivores (i.e., the tapetal cellulosum in the dog and cat). Animals with a tapetum show great color variation depending on breed, species, age, and amount of pigmentation. When the eyes have been enucleated and placed in a standard formalin fixative, the color may fade or change, as in the dog.

Microscopically, the tapetum is interposed between the branching vessels in the choroid and the single layer of the choriocapillaris beneath the retina. The thickness of the tapetum varies, being multilayered at its center and thinning to a single cell (or lamella) at its periphery as well as adjacent to the optic nerve.

The tapetum lucidum develops late in animals born with immature eyes (e.g., the dog and cat). It is usually completely developed by 4 months of age. Animals born with mature eyes (e.g., ungulates and equines) have a well-developed tapetum at birth. The degree of pigmentation of the animal apparently has no affect on development of the tapetum. A comparison of pigmented and albino ferrets revealed no morphologic differences of their cellular tapeta at both the light microscopic and the transmission electron microscopic levels.[187]

Carnivores have cellular tapeta. Not all carnivores possess functionally developed tapeta, however, and not all animals with cellular tapeta of the choroid are carnivores.[188–190] The tapetum lucidum of the ranch mink (*Mustela* sp.) can consist of a few layers of tapetal cells with little reflective material and that are arranged haphazardly.[188] Little is known of the wild mink, but domestication of this animal may have influenced tapetal development, though ranch mink can have seven or more layers of tapetal cells.[191] The tapetum lucidum of the paca or spotted cavy (*Cuniculuc paca*), however, which is a member of the Rodentia, is cellular, consisting of several layers of ovoid-to-flattened cells within the superior choroid.[189,192] The electron-dense rodlets, which are typically uniform in diameter and highly organized in carnivores, vary in size, shape, and orientation in the paca, thus making this tapetum lucidum unlikely to provide constructive interference.

Histologically, the tapetum cellulosum is composed of rectangular-shaped cells that, in the central region, may be up to 35 cell layers deep in the cat, 15 layers deep in the dog, and 7 to 10 layers deep in the domestic ferret (Figs. 2.115 and 2.116; Table 2.14).[191,193–199] This number is gradually reduced toward the periphery until the tapetum cellulosum is replaced by regular choroidal stroma. From the underlying choroidal stroma, numerous small vessels penetrate the tapetal layer to form a single-layered capillary bed known as the choriocapillaris network on the surface of the tapetum. Iridocytes have a round nucleus with a prominent nucleolus; in tangential sections, the tapetal cells are polygonal.

The most striking ultrastructural feature of tapetal cells in the dog and cat is the presence of numerous slender, electron-dense rods in the cytoplasm. These rods in the cat are densely packed, uniform in size, circular in cross-section (approximately 0.23 μm × 4–5 μm), and circumferentially arranged into highly organized groups (Fig. 2.117). The sides of adjacent tapetal cells have a wider intercellular space, separated by collagen and elastic fibrils, than the ends of the cell, which are in closer apposition to each other. Within each cell, there may be several groups of rods, often oriented at right angles to each other but still maintaining their long axis parallel to the retinal surface. The rods are membrane-bound and pack the cytoplasm so that the remaining organelles are limited to the perinuclear region and the cell periphery. Melanin granules are present in small numbers in the tapetal cells adjacent to the choroid.[197,198] Moreover, in some choroidal melanocytes next to the tapetum lucidum of the cat and dog, the melanosomes can be regularly arranged.[199] This as well as the ability of the tapetal rods to bind calcium at a level similar to melanin suggest that in all likelihood, the iridocyte is a modified melanocyte.

The chemical composition of the tapetal layer varies among species. A high level of zinc (i.e., zinc cysteine) is present in the iridocytes in both the dog and ferret tapeta, whereas the iridocytes contain abundant riboflavin in the cat and are abundant in sulfur in the paca.[189] The tapetal rods are believed to contain the high concentrations of these substances.[200] In the cat, morphologic similarities between melanin granules (i.e., as in the anterior iris) and the tapetal rods, presence of both rods and melanin granules in the iridocytes, and localization of melanin

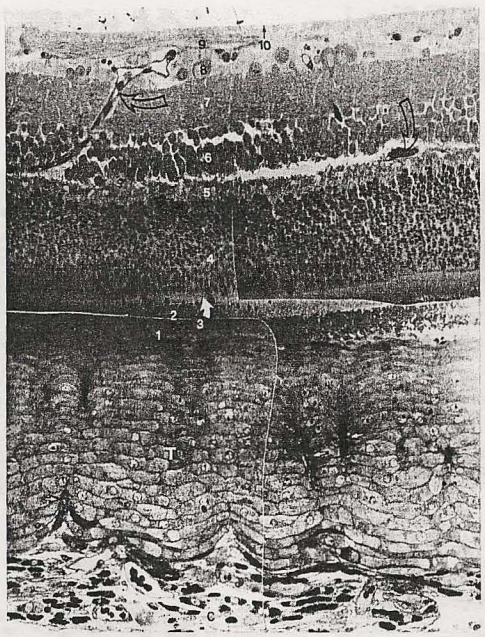

Figure 2.115. Montage of the kitten retina and inner choroid. *Dark arrows* point to capillaries penetrating tapetum. *Open arrows* indicate retinal blood vessels. *C,* choroid with numerous blood vessels and melanocytes; *T,* tapetal cells; *1,* retinal pigmented epithelium (not pigmented over tapetum); *2,* layer of rods and cones; *3,* internal limiting membrane; *4,* external nuclear layer; *5,* external plexiform layer; *6,* internal nuclear layer; *7,* internal plexiform layer; *8,* ganglion cell layer; *9,* nerve fiber layer; *10,* internal limiting membrane. (Plastic section; original magnification, X75.)

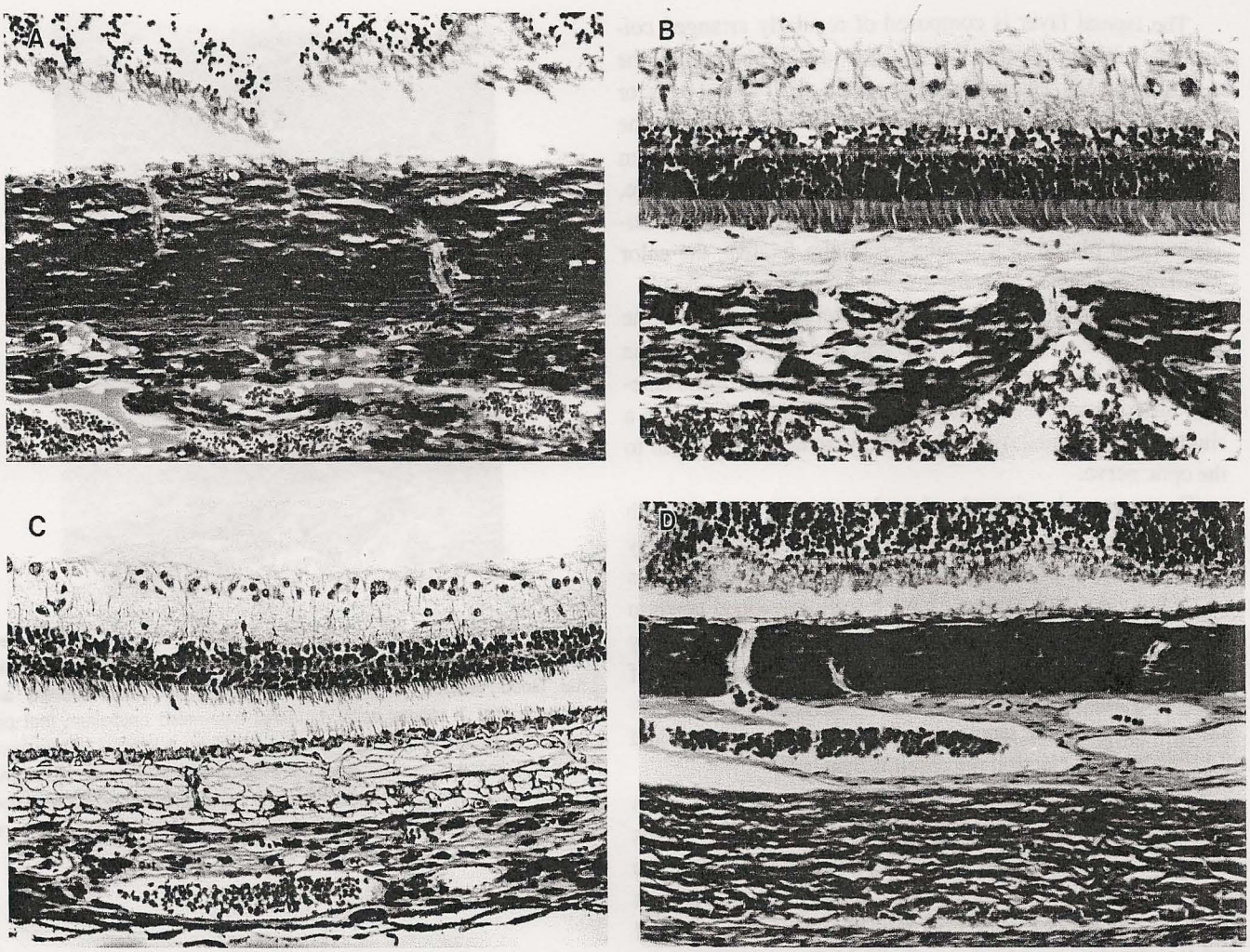

Figure 2.116. The carnivorous tapetum lucidum consists of layers of cells, called iridocytes, which vary in number, size, and composition. **A.** The cougar. **B.** The dog. **C.** The ferret. **D.** The cat. (Original magnification: All, X200.)

Table 2.14 Choroidal Tapeta Among the Vertebrates

Classification	Type of Tapetum	Reflective Material	Thickness; Number of Cell Layers or Crystals	Size of Fibrils or Rodlet Dimensions
Fishes				
Elasmobranchs, Squalus	Occlusible	Guanine crystals	60–80μm	12–13 superposed crystals
Elasmobranchs, Port Jackson Shark	Occlusible	Guanine	Length: 5–8μm Width: 0.1μm	15–20 superposed crystals
Placentals				
Carnivores				
Dog	Cellulosum	Zinc Cysteine	9–15 layers	Length: 4μm Diameter: 0.14μm Spacing: 0.20μm
		Zinc Cysteine	9–11 layers 15–20 layers	Length: 4μm Diameter: 0.18μm Spacing: 0.20μm
			43μm; 10–12 layers	
Cat	Cellulosum	Riboflavin	15–20 layers	Length: 4–6μm Diameter: 0.10–0.12μm Spacing: 0.15μm

		Riboflavin, Zinc	16–20 layers	
			30 layers	
			18–30 layers	Diameter: 8–10μm
				Length: 0.15μm
				Spacing: 0.08μm
			6–10 layers	Diameter: 5μm
				Length: 0.23μm
				Spacing: 0.40μm
			35 layers	
Ferret	Cellulosum	Zinc Cyteine	7–10 layers	
		Zinc Cyteine	5–7 layers	Diameter: 3–4μm
				Length: 0.13–0.15μm
			50μm; 10–15 layers	Diameter: 6μm
				Length: 0.20μm
				Spacing: 0.30μm
Ranch Mink	Cellulosum		30μm; 2–3 layers	Nonregular
Pinnipedes				
Seal (Grey seal)	Cellulosum	?	30–35 layers	Diameter: 5–6μm
				Length: 0.10μm
				Spacing: 0.15μm
Ungulates				
Cow	Fibrosum			Diameter: 0.15μm
				Spacing: 0.20μm
				Diameter: 0.20μm
Sheep	Fibrosum	Collagen	100–200μm	Diameter: 0.15μm
				Spacing: 0.20μm
			100–200μm	Diameter: 0.15μm
				Spacing: 0.08μm
			140 rows per layer: 9–16 layers	Diameter: 0.15μm
				Spacing: 0.18μm
Lemurs				
Lemur (Galago crassicaudatus)		Riboflavin		
Rodents				
Paca	Cellulosum	?	12–15	Diameter: 8–10μm
				Length: 0.2–0.25μm
				Spacing: 0.15μm
Primates				
Nonhuman (Aotus)	Fibrosum	Collagen		

From Ollivier FJ, et al. Comparative morphology of the tapetum lucidum (among selected species). *Vet Ophthalmol* 2004;1:11–23.

precursors are suggestive of a possible common origin for tapetal rods and melanin granules.[197,198,201]

In ungulates, closely and regularly arranged collagen fibers comprise the tapetum, which is often referred to as a fibrous tapetum. The fibrous tapetum is basically acellular, except for an occasional fibrocyte (Fig. 2.118). The collagen fibrils are organized into well-ordered lamellae that branch and interconnect with adjacent lamellae at the same level, being parallel with the retinal surface. Roughly several hundred of these lamellae or layers are estimated to comprise the fibrous tapetum of the sheep.[202] The collagen fibrils within each layer vary little in diameter, being approximately 80 nm, and have a regular spatial arrangement similar to that seen in the corneal stroma (Figs. 2.40 and 2.119).

Small blood vessels, typically capillaries, penetrate the tapetum at right angles to the long axes of the iridocytes in carnivores and to the collagen lamellae in herbivores, directly interconnecting the medium-sized blood vessels with the

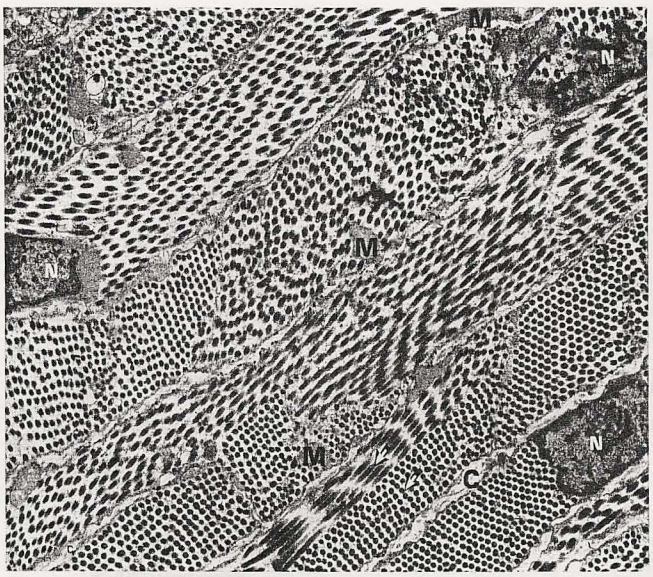

Figure 2.117. Tapetal cells of a cat. The main cytoplasmic components are the rods; mitochondria (*M*) are infrequent. The rods are uniform in a group concerning spatial orientation, but more than one group is often present within a cell (*arrows*). The sides of adjacent cells have wide intercellular spaces with scattered collagen fibrils (*C*), whereas the ends of the cells are in close apposition. *N,* nucleus of tapetal cell. (Original magnification, X7750.)

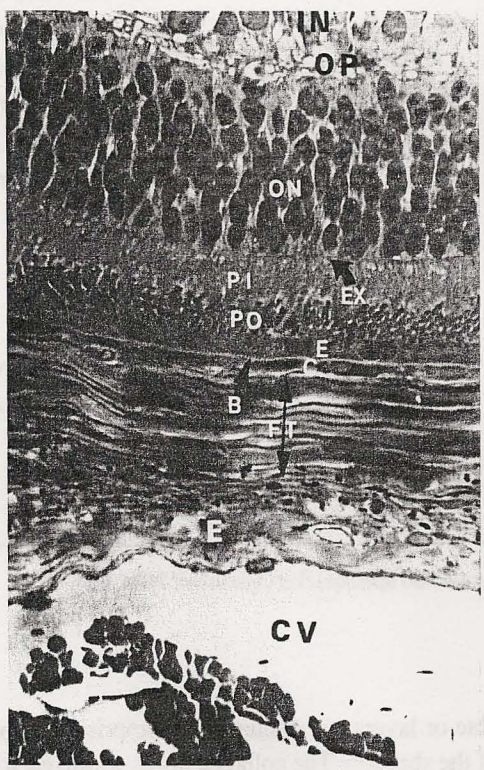

Figure 2.118. Inner choroid and outer retina of a young horse. Large choroidal veins (*CV*) lie under the fibrous tapetum (*FT*), which is separated from the outer retinal epithelium by the choriocapillaris (*C*) and Bruch's membrane (*B*). The epithelium (*E*) contains very few pigment granules over the tapetum. *EX,* external limiting membrane; *IN,* inner nuclear layer, *ON,* outer nuclear layer; *OP,* outer plexiform layer; *PI,* photoreceptor inner segments; *PO,* photoreceptor outer segments. (Original magnification, X375.)

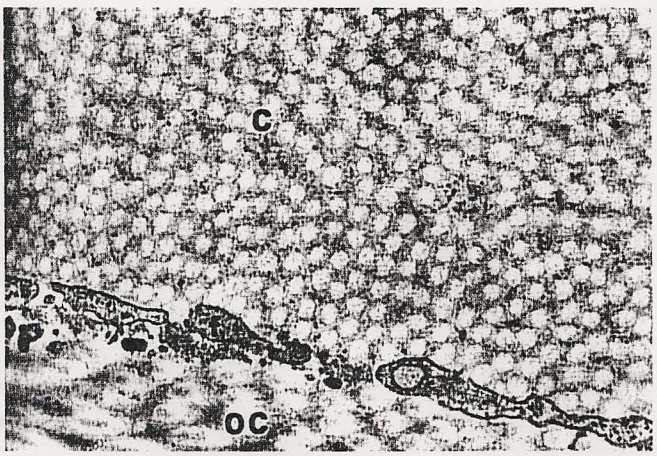

Figure 2.119. Fibrous tapetum in a horse. Collage fibrils (*C*) of quite uniform diameter and spatial orientation are seen in cross-section. Fibroblastic cell processes (*f*) are present between lamella. *OC,* obliquely sectioned collagen fibrils. (Original magnification, X17,500.)

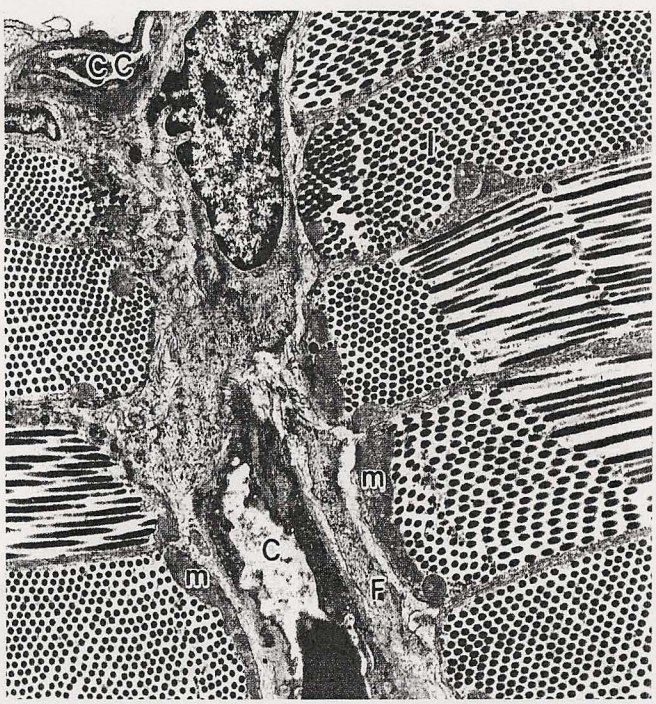

Figure 2.120. Capillaries (*C*) vertically interconnect medium-sized blood vessels with the choriocapillaris (*CC*) in the cat. The iridocytes (*I*), or tapetal cells, line up evenly next to these capillaries. The end of each iridocyte is bordered by mitochondria (*m*). *F,* fibrocyte. (Original magnification, X7200.)

choriocapillaris (Fig. 2.120). When observed end-on ophthalmoscopically, these vessels are sometimes called the "stars of Winslow." In the dog and cat, these vessels are separated from the iridocytes by a small amount of loose connective tissue and a lining of fibroblasts (Fig. 2.120).

In nonmammalian species, the tapeta lucida can be retinal instead of choroidal, especially among fish and to a lesser degree, reptiles. In most of these instances, either lipid- or guanine-laden material lies within the cytoplasm of the retinal pigment epithelium (retinal tapetal lucidum) (Table 2.15).[191,203] Among teolosts, movement of melanin granules within the retinal pigment epithelium can occur with the melanin granules

Table 2.15 Retinal Tapeta among the Vertebrates

Classification	Type of Tapetum	Reflective Material (Nature, Shape, Size)
Fishes		
Teleosts		
Seatrout	Occlusible	Spherules triglycerides; diameter 0.4μm
Gars	Occlusible	Spherules yellow pigment (phenolic compound); diameter 0.24μm
Toadfish	Argenteum stratum occlusible	Acid uric
Reptiles		
Crocodiles		
Alligator mississippiensis		Spherules guanine
Caiman crocodilus	Occlusible	Spherules guanine; length 0.7μm; diameter 0.12μm
Caiman sclerops	Nonocclusible	Guanine
Marsupials		
Opossum	Nonocclusible	Lipoidal spherules; cholesterol and esters
Placentals		
Bats		
Fruit Bat (Eidelon)		Spherules

From Ollivier FJ, et al. Comparative morphology of the tapetum lucidum (among selected species). *Vet Ophthalmol* 2004;1:11–23.

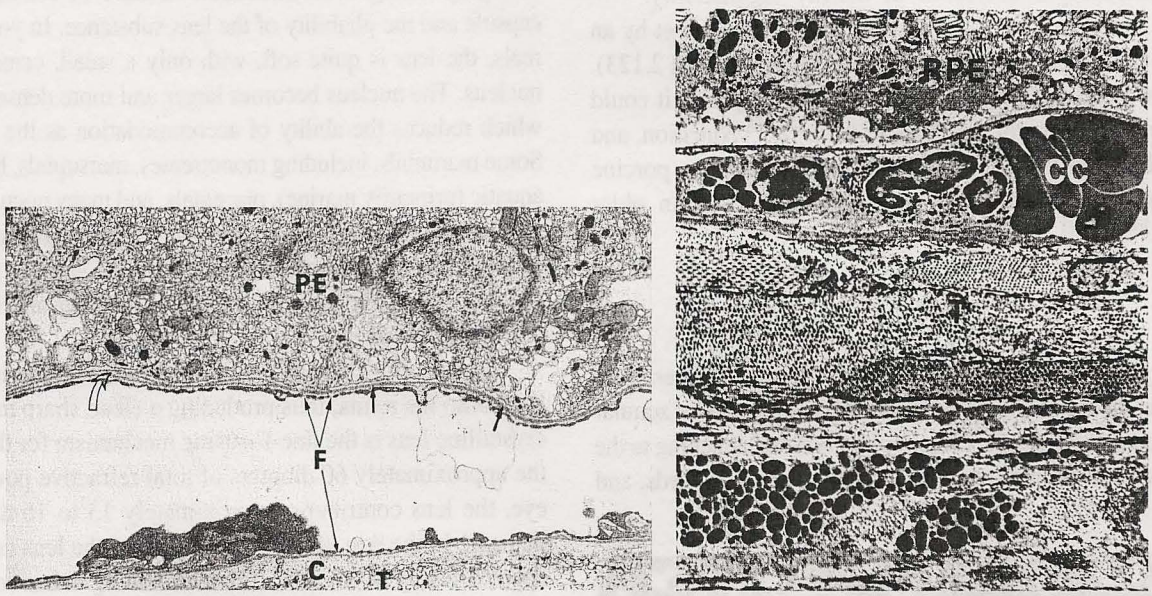

Figure 2.121. Choriocapillaris in the dog. **A.** The choriocapillaris (*CC*) forms the innermost layer of the choroid, being a wide capillary bed intimately associated with the RPE. *T,* tapetum cellulosum. (Original magnification, X3000.) **B.** Note the numerous fenestrations (*F*) in the endothelium with a diaphragm. Bruch's membrane in most places consists of only the fusion of the pigment epithelium and the endothelial basal lamina (*dark arrows*), but small amounts of the collagenous zone are visible when they separate (*light arrows*). Note how the tapetum (*T*) is buffered from the capillary by a layer of collagenous tissue (*C*). Note also the lack of pigment in the pigmented epithelium (*PE*) over the area of the tapetum. (Original magnification, X12,400.)

migrating toward the vitreous humor during ocular illumination, causing the reflective material to become masked or occluded. Consequently, these retinal tapeta are referred to as occlusible. In some fish (elasmobranchs), the retinal tapeta are occlusible, but not because of melanin movement. In these instances, the processes of the retinal pigment epithelium, which are filled with melanin granules, move inwardly along the perimeter of each photoreceptor's outer segment while concomitantly the visual cell moves toward the retinal pigment epithelium (e.g., retinomotor movement).

Choriocapillaris

The choriocapillaris is the innermost layer of choroidal vessels, forming a thin layer of capillaries separated from the RPE by a basement membrane complex known as Bruch's membrane (Fig. 2.121). The lumen of the choriocapillaris is fairly wide, allowing red blood cells to pass through two to three abreast. The endothelial lining of the choriocapillaris possesses numerous circular fenestrations, which are often arranged in rows. External to the endothelium is a basement

membrane forming the external layer of Bruch's membrane. Bruch's membrane is not as well developed a structure in the eyes of many domestic animals as it is in the eyes of primates. In most diurnal species that lack a tapetum lucidum, including pigs, primates, and so on, Bruch's membrane is pentalaminated, consisting of basal laminae of the RPE and choriocapillaris endothelia, two adjacent layers of collagen, and an intervening band of elastic fibers. In animals with tapeta, and especially with cellular tapeta, Bruch's membrane is reduced to a trilaminated structure consisting of the two basal laminae and a layer of collagen.

Aging

Besides providing oxygen and nutrients for the outer retina, the choroid serves largely as a "black box" of sorts because of the abundance of melanocytes that usually reside there. Changes in this black box with regard to age do occur, but they also appear to be minimal. In the pig, the amount of area occupied by melanocytes in the central choroid remains relatively unaltered throughout life; however, with time, the individual melanocyte decreases in density significantly.[204,205] Even so, the natural depletion of this cell type is offset by an increase in its size as the animal ages (Figs. 2.122 and 2.123). A similar trend appears to occur in the monkey, and it could well occur in most other animals as well.[206–208] Nutrition, and especially dietary zinc, has a profound effect on porcine choroidal pigmentation and other ocular melanin in older animals.[205,209–211]

LENS

The lens is a "fine-tuning," refractive structure that focuses sharp images on the retina for acute vision. It is suspended by zonular ligaments arising from the ciliary epithelium and attaching to the lens capsule at the lens equator. In many mammals, birds, and

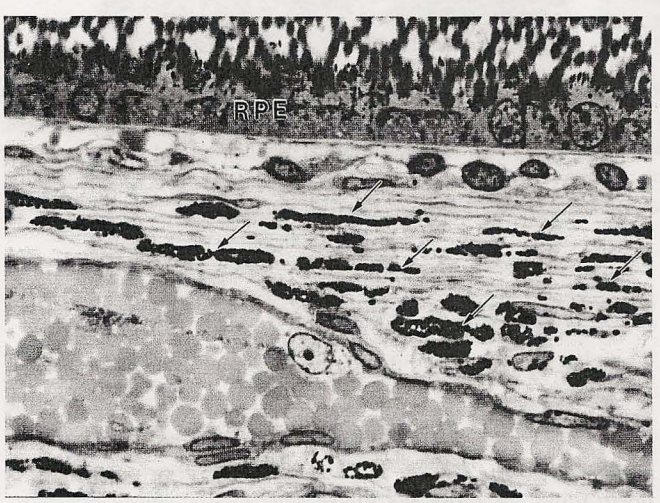

Figure 2.122. Central choroid of a 1-year-old Yorkshire boar contains numerous spindle-shaped melanocytes (*arrows*) throughout the entire medium- and large-vessel layers. (Plastic section; Toluidine blue O stain; original magnification, X1000.)

Figure 2.123. Central choroid of a 6-year-old Yorkshire boar has generally larger melanocytes than those in younger animals. Many of the melanocytes (*arrows*) are rounded, especially within the large-vessel layer. (Plastic section; Toluidine blue O stain; original magnification, X1000.)

reptiles, the lens is biconvex, with the degree of convexity changing during accommodation because of elasticity of the capsule and the pliability of the lens substance. In young mammals, the lens is quite soft, with only a small, central, denser nucleus. The nucleus becomes larger and more dense with age, which reduces the ability of accommodation as the lens ages. Some mammals, including monotremes, marsupials, herbivores, aquatic (primarily marine), placentals, and many nocturnal types such as the rat, have no accommodative mechanism.[3] Others, such as ungulates, accommodate weakly, having poor near vision; as a result, they rely more on smelling and hearing to detect nearer objects.

The basic function of the lens, as in a camera, is to focus light onto the retina, thus producing a clear, sharp image. The crystalline lens is the fine-focusing mechanism for the eye. Of the approximately 60 diopters of total refractive power of the eye, the lens contributes approximately 13 to 16 diopters in humans. In the dog, the dioptric power of the lens contributes approximately 40 diopters. The remaining refraction is provided by the cornea.

The refractive power of the lens is lessened because the change of refractive index is much greater at the air–cornea interface than at the aqueous–lens and lens–vitreous interfaces. To function, the lens must be transparent, in a stable position, and able to change its shape (i.e., accommodation). The lens is totally epithelial in nature, containing no pigment or blood vessels that would decrease transparency. It is held in place by numerous zonules, which extend from the ciliary body processes to the equatorial region of the lens. Contraction of ciliary body muscles reduces the tension on these lenticular zonules, which changes the lens shape because of the natural elasticity of the lens capsule, resulting in alteration of the dioptric power (increased) of the lens (accommodation). The lens is also held in place by the vitreous (i.e., the patella fossa) and the support of the iris. The lens is a transparent, avascular tissue deriving metabolic needs primarily from the aqueous humor. Any opacity of

the lens and its capsules is termed a *cataract.* Cataracts vary in degree of involvement, location, cause, and clinical significance. Nuclear sclerosis (discussed later) is neither a cataract nor a result of cataract formation, but a normal aging phenomenon.

The lens is proportionately larger in domestic animals than in humans. The dog lens has a volume of approximately 0.5 ml and averages 7 mm in thickness at the anteroposterior axis, with a 10-mm equatorial diameter. The proportion of lens volume to entire globe volume ranges from 1:8 to 1:10 in the dog. The equine lens, on the other hand, has a volume of approximately 3 ml and a lens–globe ratio of 1:20. Lens volumes of the sheep, cow, and pig lie between these figures and their respective lens–globe ratios (Table 2.16). The lens itself consists of an enveloping basement membrane structure called the lens capsule, an anterior epithelium, and a cellular stroma consisting of lens fibers (Fig. 2.124).

Table 2.16 Lens Data in Domestic Animals

Animal		Volume (ml)	Vol. = 1 to Eyeball Volume	Vol. In Percent of Eyeball Volume	Weight (g)	Lens Weight = 1 to Eyeball Wt.	Axis	Diameter	Position of Posterior Lens Surface	Radius of	
										Anterior Surface	Posterior Surface
Horse	Mathiessen	—	—	—	—	—	12.1	18.0	18.5	15.5	12.0
		—	—	—	—	—	13	19.0	19.0	21.0	13.0
		—	—	—	—	—	13.2	20.0	—	—	—
	Berlin	—	—	—	—	—	13.25	19.5	21.75	13.5	9.5
	Koschel	—	—	—	5.2	19.4	12.6	20.0	17.1	14.0	10.1
	Emmert	2.8	16.13	6.14	3.5	—	12.0	21.75	—	—	—
		3.5	—	—	3.6	—	14.0	22.0	—	—	—
	Linsenmeyera	3.04	—	—	—	—	13.27	21.25	—	—	—
	Klingsbert	—	—	—	—	—	—	—	20.4	18.85	11.19
	Nicolas and Fromaget	—	—	—	—	—	12.0	—	—	—	—
		—	—	—	—	—	15.0	21.0	—	17.7	11.3
	Arloing and Chauveau	—	—	—	—	—	14.0	17.0	—	—	—
	Frank and Leisering	—	—	—	—	—	12.0	21.0	—	15.0	10.0
	Dexler	—	—	—	—	—	12.1	20.98	19.5	19.3	11.85
	Rabl	—	—	—	—	—	12.28	21.14	—	—	—
	Bayer	—	—	—	—	—	12.75	21.0	21.11	15.5	10.0
Mule	Mathiessen	—	—	—	—	—	13.2	20.0	19.0	15.0	12.0
		—	—	—	—	—	12.2	18.0	—	—	—
Cow	Mathiessen	—	—	—	—	—	12.0	17.75	17.0	13.75	10.25
	Moenich	—	—	—	—	—	12.0	18.37	17.4	14.8	10.23
	Peschel	—	—	—	—	—	12.45	—	—	14.26	9.60
	Koschel	—	—	—	4.3	15.1	12.0	18.7	16.2	11.3	9.7
	Ox	2.2	—	—	2.25	—	—	—	—	—	—
	Emmert	2.3	14.5	6.9	2.4	—	12.0	17.25	—	—	—
		2.0	15.0	6.6	—	—	—	—	—	—	—
	Rabl	—	—	—	—	—	14.6	19.55	—	11.91	10.22
		—	—	—	—	—	14.88	18.65	—	11.77	10.33
		—	—	—	—	—	14.76	19.10	—	10.87	9.77
	Bayer	—	—	—	—	—	12.5	18.0	17.0	14.0	9.5
Calf	Wolfskehl	—	—	—	—	—	—	—	—	6.61	8.35
	Koschel	—	—	—	—	—	—	—	16.62	—	—

(Continued)

Table 2.16 Lens Data in Domestic Animals (Continued)

Animal		Volume (ml)	Vol. = 1 to Eyeball Volume	Vol. In Percent of Eyeball Volume	Weight (g)	Lens Weight = 1 to Eyeball Wt.	Axis	Diameter of Posterior Lens Surface	Position Surface	Radius of Anterior	Radius of Posterior
	Emmert	—	—	—	—	—	9.75	14.5	—	—	—
		1.0	18.0	5.5	—	—	10.25	15.5	—	—	—
	Bayer	—	—	—	—	—	10.5	14.0	14.0	10.15	9.25
Sheep	Koschel	—	—	—	2.3	10.0	10.4	14.5	—	8.9	7.9
	Emmert	0.9	—	—	—	—	10.0	14.5	—	—	—
		1.2	13.1	7.5	—	—	10.5	15.25	—	—	—
	Dexler	—	—	—	—	—	8.0	12.25	—	—	—
		—	—	—	—	—	12.44	15.73	—	—	—
	Rabl	—	—	—	—	—	12.04	15.53	—	8.79	8.09
Pig	Mathiessen	—	—	—	—	—	7.5	11.0	—	7.25	5.5
	Koschel	—	—	—	1.55	12.3	7.9	11.1	—	7.2	6.3
	Emmert	0.5	12.4	8.1	—	—	8.0	10.5	—	—	—
		0.8	—	—	—	—	8.0	10.5	—	—	—
	Linsenmeyerb	0.46	—	—	—	—	8.14	10.44	—	—	—
	Rabl	—	—	—	—	—	7.37	9.5	—	6.37	5.25
Dog	Koschel	—	—	—	1.07	9.3	—	—	—	6.2	5.5
		—	—	—	1.55	8.0	—	—	—	—	—
	Emmert	0.5	10.2	9.8	—	—	—	—	—	—	—
		—	—	—	—	—	7.13	10.6	—	—	—
	Rabl	—	—	—	—	—	7.69	10.92	—	—	—
Cat	Mathiessen	—	—	—	—	—	7.5	9.0	—	6.0	6.0
	Koschel	—	—	—	1.47	7.4	7.8	10.4	—	6.7	7.4
	Emmert	0.5	9.8	10.0	—	—	—	—	—	—	—

Translated from Bayer J. *Angenheilkunde.* Vienna; Braumueller, 1914.
[a]Average of 40 measurements.
[b]Average of 20 measurements.

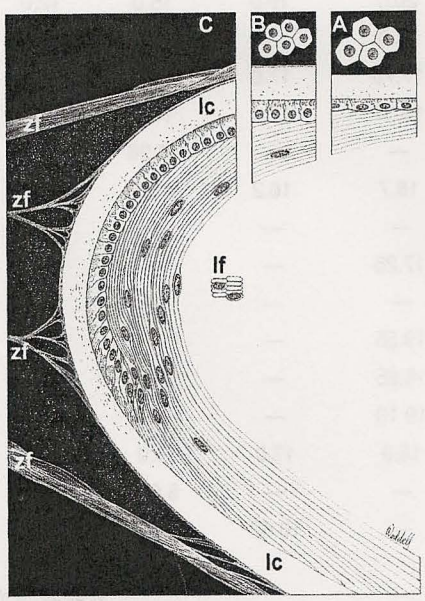

Figure 2.124. Composite drawing of the lens, capsule, and attachments. The anterior lens epithelium is seen face-on (*A*). The size and shape of these cells are compared with those in the intermediate zone (*B*) and in the equatorial zone (*C*). At the equator, the dividing cells elongate to form lens cortical cells (fibers). As they elongate anteriorly and posteriorly toward the sutures, their nuclei migrate somewhat anterior to the equator and form the lens bow. Zonular fibers (*zf*) attach to the anterior and posterior lens capsule (*lc*) and to the equatorial capsule, forming pericapsular or zonular lamellae of the lens. *Lf,* lens fibers seen in cross-section. (Modified from Hogan MJ, Alvarado JA, Weddell JE. *Histology of the Human Eye.* Philadelphia: WB Saunders, 1971.)

Lens Capsule

The lens is completely enclosed within a thick, PAS-positive elastic capsule, which is the exaggerated basement membrane of the lens epithelium. It has elastic properties but no elastic fibers.[32] The thickness of the capsule varies by region, with the thinnest being the posterior pole. The canine lens capsule is 8- to 12-μm thick at the equator, 50- to 70-μm anteriorly, and only 2- to 4-μm thick posteriorly. Most of the capsulate thickening occurs during the first year of life (Table 2.17).[212]

The lens capsule itself consists of fibrils and basement membrane material that are laminarly arranged (Fig. 2.125A). As the capsule continues to thicken, new fibrils are formed adjacent to the cell membrane of the epithelial cells, thus causing the outer fibrils to become more compressed. Only the epithelial cells can produce new capsule material. Ultrastructurally, the laminated appearance of the anterior capsule fades quickly with age. By 1 to 2 months after birth, the lens capsule assumes a homogenous appearance, which remains throughout life (Fig. 2.125B).

As in most basement membranes, the main component of the lens capsule is type IV collagen. Type IV collagen consists of a densely packed, three-dimensional branching network of fine microfibrils forming five-sided figures.[213]

Table 2.17 Lens Capsule Measurements in the Dog

Age	Anterior Pole (μm)	Equator (μm)	Posterior Pole (μm)
Neonatal	1.9	3.8	1.9
1 week	2.9	4.8	1.9
4 weeks	6.7	7.6	3.8
8 weeks	10.5	7.6	3.8
12 weeks	20.9	7.6	3.8
16 weeks	21.9	7.6	3.8
1 year	48.5	7.6	3.8

Courtesy of M Monaco.

Anterior Epithelium

Inside the anterior capsule is a single layer of lens epithelial cells. These epithelial cells continue to produce new capsule material, which, as stated previously, is the basement membrane for these cells. The cells are cuboidal to squamous centrally, become columnar near the equator, and elongate into slender hexagonal lens fibers. Nuclei are lost as they mature and move centrally. The lens epithelium lines only the anterior surface of the lens capsule and the equator postnatally. The posterior lens epithelium is used to form the embryonic primary lens fibers and, thus, normally is absent under the posterior lens capsule later in life. The epithelium is cuboidal early in life both near and at the anterior pole of the lens (Fig. 2.126A).[214] In older individuals, these cells become increasingly more squamous, undergoing the same kind of change in form that occurs in the corneal endothelium. Their cytoplasm, which becomes coarser in appearance, now has fewer organelles, and especially rough endoplasmic reticulum, than younger cells (Fig. 2.126B). The cell apices face the outer lens fibers, being attached to the underlying cortical fibers by tight junctions (i.e., zonula occludens) and macula adherens.[32,212,215,216]

Mature lens fibers become highly dependent on the anterior epithelium for maintaining a critical level of dehydration, which allows the soluble proteins to be functionally effective, and for providing a healthy level of reduced glutathione. The

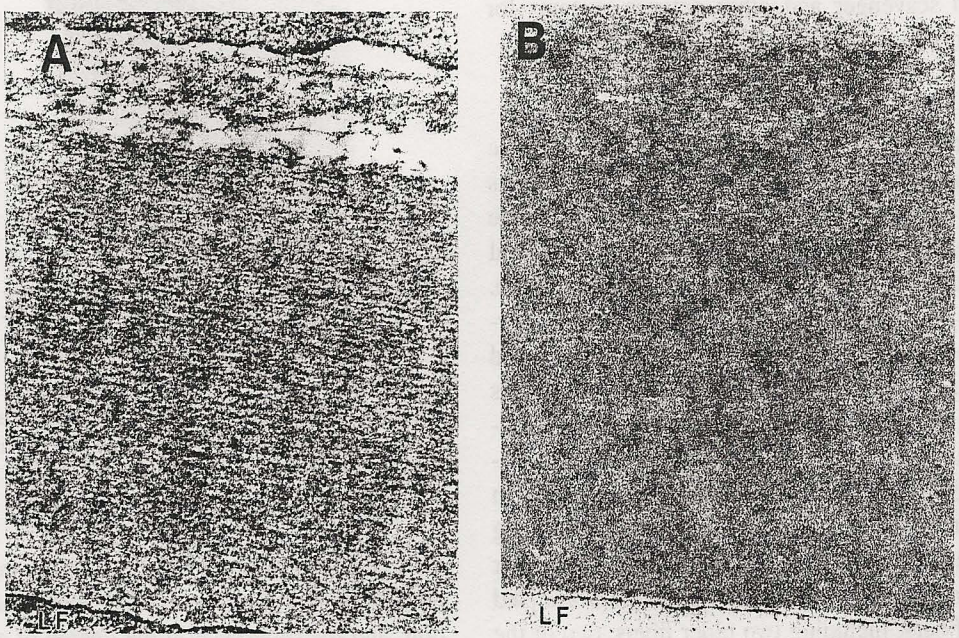

Figure 2.125. A. The canine lens capsule near the anterior pole shortly after birth consists of lamellae of fibrils and coarser basement membrane material. **B.** In the young adult, these lamellae are only partially visible by TEM along the outer region of the capsule; the rest of the capsule appears homogenous. *LF,* lens fiber. (Original magnification: A, X40,000; B, X25,000.)

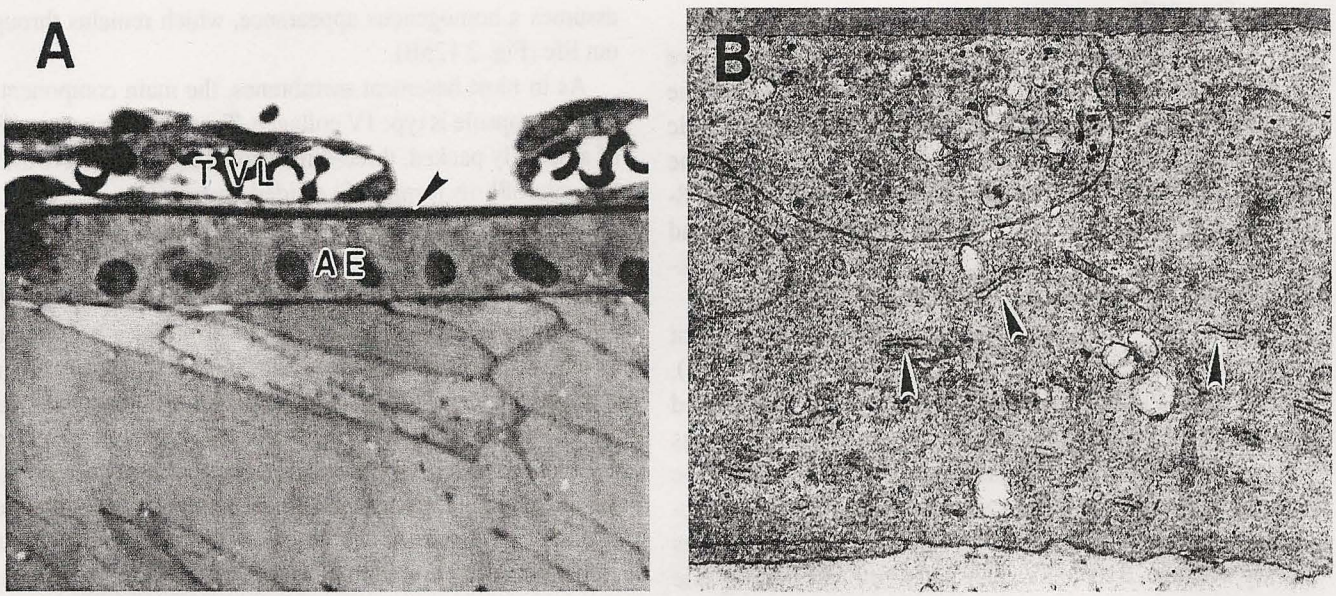

Figure 2.126. **A.** The anterior epithelium (*AE*) in a neonatal lens of a dog is cuboidal. Note the relatively thin capsule (*arrow*), which is bordered by the tunica vasculosa lentis (*TVL*). (Original magnification, X400.) **B.** Close-up of the anterior epithelium of an adult canine lens. The cytoplasm becomes less defined with age. *Arrows* indicate scattered mitochondria. (Original magnification, X3500.)

lens epithelium is highly susceptible to many potentially dangerous conditions, including changes of $[O^2]$, the presence of toxins, x-rays, and so on. It is also susceptible to ultraviolet (UV) light, both A and B, which is a major contributor to adverse aging of the lens and, quite possibly, to age-related cataracts. UVB radiation causes epithelial hyperplasia and anterior suture disintegration,[217,218] and excessive exposure to UV light may well lead to epithelial apoptosis, which has been closely associated with noncongenital cataracts, and to yellowing of the nucleus, both of which have been demonstrated experimentally in the murine lens.[218,219] Nocturnal (and arrhythmic) animals may be less able to cope with exposure to bright light, and scavenger and other defense systems for lenses may differ between animals within a given species.

Lens Fibers

Immediately anterior to the lens equator is a proliferative zone within the epithelium (Figs. 2.124 and 2.127). The cells within this zone begin to mitose at approximately the same time the primary lens fibers are formed during early fetal development. This zone of mitosis continues throughout life. The most recently formed cells elongate, with the apical portion of the cell extending forward beneath the epithelium and the basal portion posteriorly along the capsule (Fig. 2.128). As these cells are transformed into lens fibers, small ball-and-socket interdigitations begin to take shape (Fig. 2.129). Concomitantly, the lens fiber becomes roughly hexagonal in shape. The ball-and-socket junctions, which are present along the length of the fibers, are formed only at the six angular regions; in this way, any particular lens fiber is tightly coupled to six other lens fibers, including two older fibers, two of the same generation, and two younger fibers (Fig. 2.130). In addition to these cytoplasmic interdigitations are many gap junctions (i.e., nexi).[220] In the chicken, as much as 65% of the lens

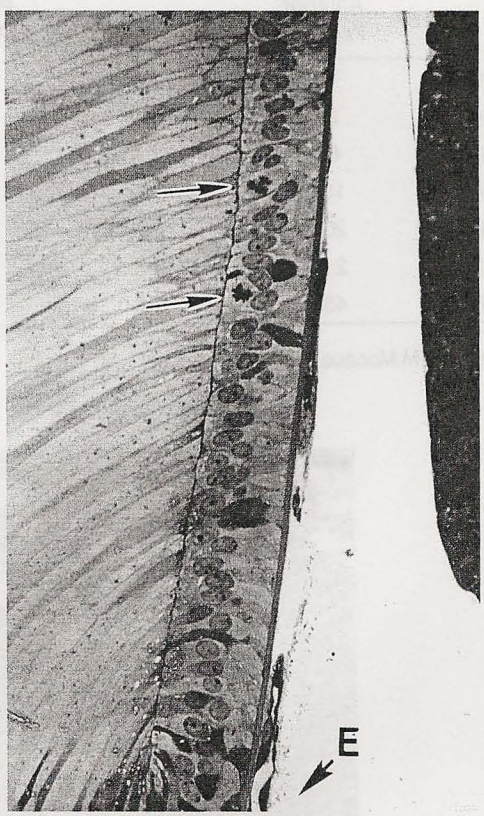

Figure 2.127. The anterior epithelium of a neonatal canine lens near the equator (*E*) has a proliferative zone at which cells mitose (*arrows*) and subsequently are pushed toward the equator. (Original magnification, X400.)

fiber cell membrane is associated with gap junctions.[221] The nucleus of each developing lens fiber retains its central location, and the difference in the degree of elongation between younger and older developing lens fibers creates the lens bow configuration of nuclei within the lens at the equator (Figs. 2.124, 2.128, and 2.131).

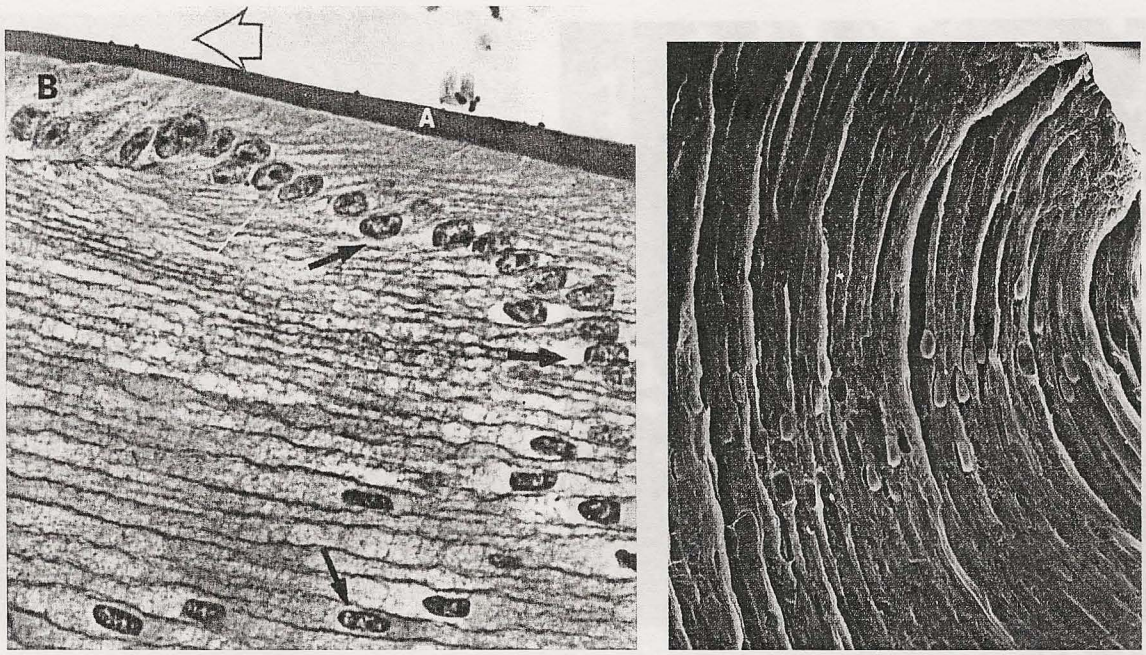

Figure 2.128. Young horse lens near the equator. **A.** Lens capsule. **B.** Columnar lens epithelium at equator. *Arrows* delineate the formation of the lens bow by the nuclei of the newly formed fibers. *Open arrow* points rostrally. (Original magnification, X500.)

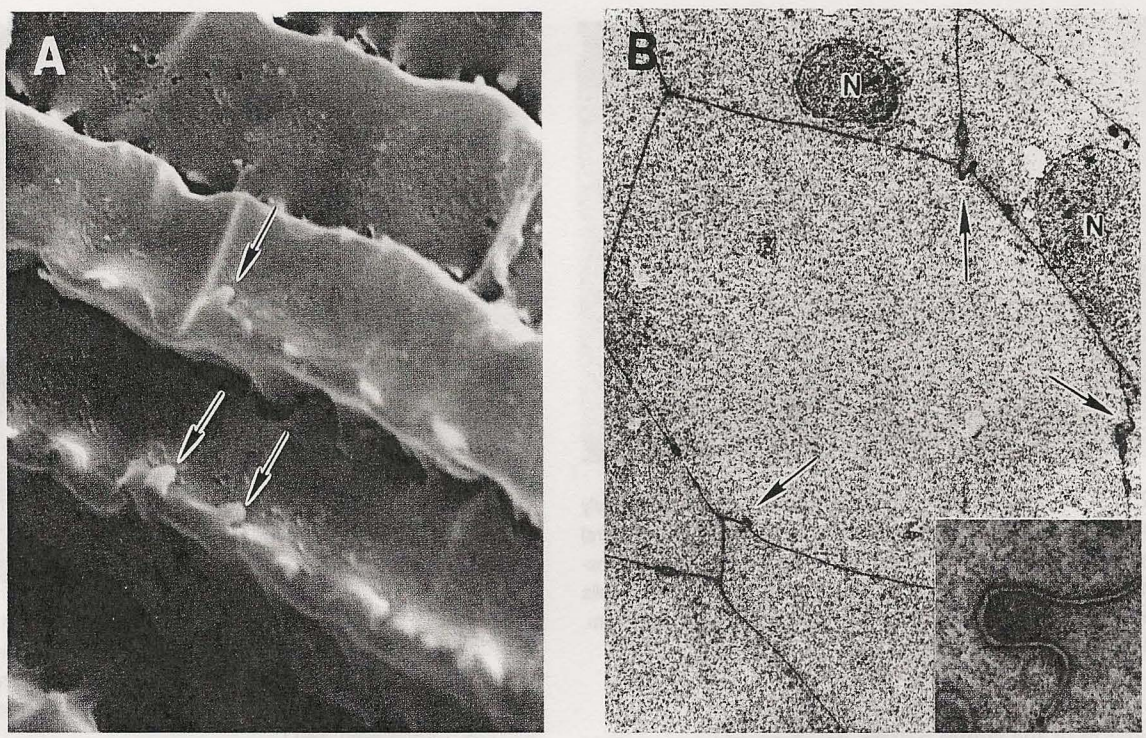

Figure 2.129. Newly formed canine secondary lens fibers are evenly hexagonal in cross-section. They form small ball-and-socket junctions (*arrows*) along their six angular edges. **A.** SEM. **B.** TEM. **Insert.** Close-up of one of the ball-and-socket junctions. *N,* nucleus. (Original magnification: A, X6600; B, X8000; Insert, X30,000.)

The lens fibers elongate toward the anterior and posterior poles, forming a U-shaped cell. The fibers do not reach the full distance from one pole to the next, much less the entire circumference of the lens; rather, they meet fibers from the opposite side to form the anterior and posterior lens sutures. The sutures are simply the junctions from opposite fibers at a given level in the lens. They vary in configuration both among species and at different levels within the lens.

The sutures usually form a Y-shaped pattern near the center of the lens, but in older eyes, they become more complex, with branching arms in the more superficial layers (Fig. 2.132). The suture patterns extend throughout the depth of the lens, but they are apparent in vivo only at optical interfaces. The sutures in the anterior half are typically in an upright Y-shaped pattern or one of its variations, whereas those on the posterior half are inverted Y-shaped patterns. Figure 2.133 illustrates

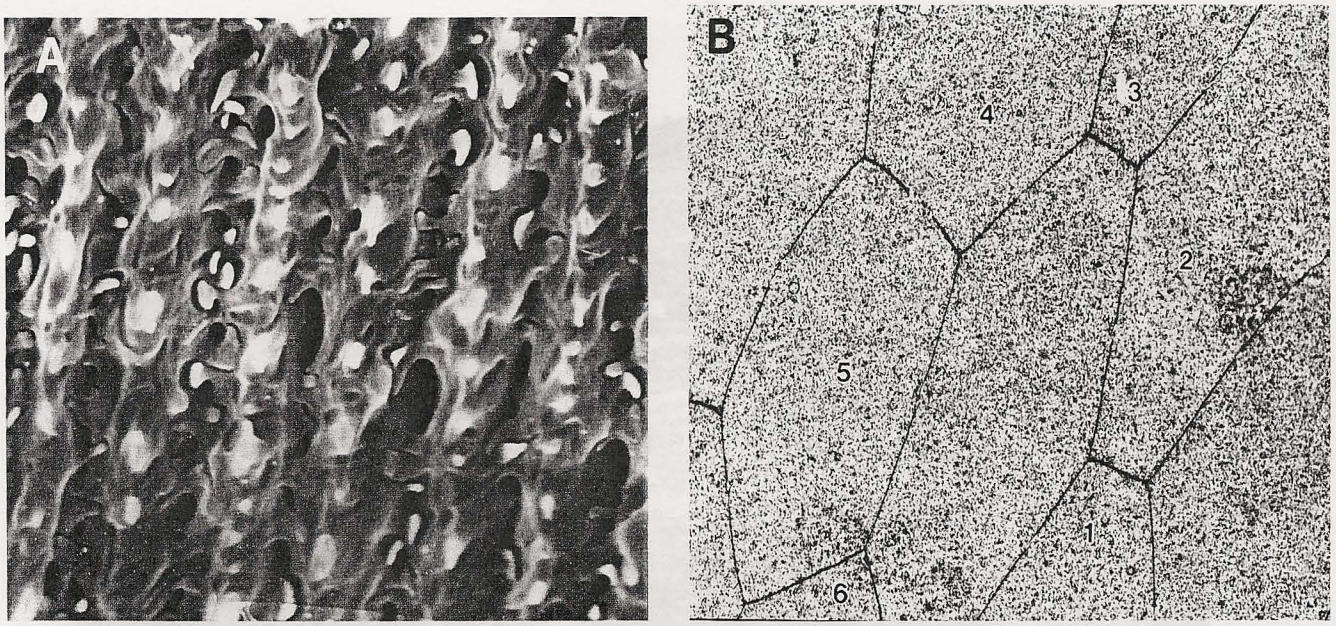

Figure 2.130. As the secondary lens fibers, as seen here in the dog, continue to develop, the ball-and-socket junctions become more pronounced (*A*) and the widths of the cells more flattened (*B*), though still retaining their hexagonal shape so that each cell remains closely engaged to two younger lens fibers (*1, 2*), two of the same generation (*3, 6*), and two older fibers (*4, 5*). (Original magnification: A, X4600; B, X3700.)

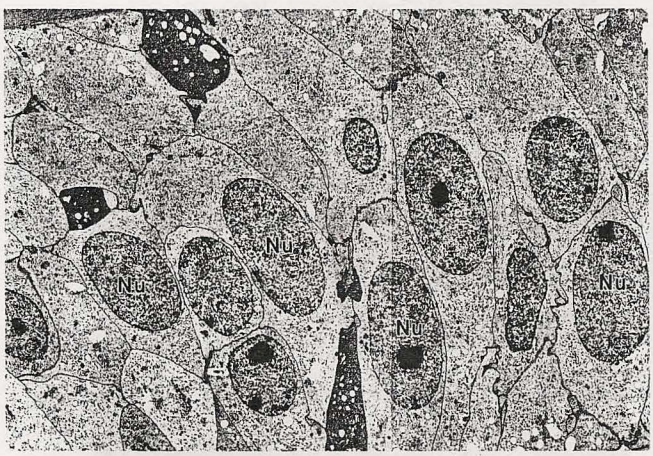

Figure 2.131. At the equator of a dog lens, the nuclei (*Nu*) of the newly forming secondary lens fibers are arranged linearly, taking up a central location within each cell. As these fibers mature, their nuclei are more rostrally or anteriorly placed, achieving a bowlike configuration. These cells possess a great deal of free ribosomes and rough endoplasmic reticulum. (Original magnification, X3000.)

Figure 2.132. Stereoscopic view of the posterior pole in an adult bovine lens demonstrates the distinct Y-shaped suture pattern where lens fibers attach to each other. Branching arms (*arrows*) of the Y-shaped sutures occur more superficially, representing the attachment of younger cells. (Original magnification, X40.)

how inversion of the suture pattern develops and how a fiber attaches to opposite sites on a suture arm in its anterior and posterior limits.[32] At the lens sutures, the fibers markedly interdigitate with each other (Fig. 2.134). The interdigitations can affect optical quality to some degree by varying the focal length of light in this region of the lens, especially during nuclear sclerosis, lens pathology, or both.[222] Overall, the combination of these well-developed regions for cell attachment, including the ball-and-socket junction, and the presence of the capsule and nexi make the lens a remarkably unified structure. Lens fibers that become attached to the suture have fully matured; these cells lie in the deep bow zone and, concomitantly, lose their nuclei and organelles.[223]

The mammalian adult lens consists of lens fibers formed chronologically throughout life. The oldest portion of the lens, which is formed during embryonic development, is in the center of the lens and known as the embryonic nucleus. It is a small, dark, lucent zone. Extending outwardly, the fetal nucleus, adult nucleus, and cortex are respectively encountered. These portions are frequently subdivided clinically into anterior and posterior divisions to further localize lesions.[224,225]

The surface of the lens fibers varies according to the location within the lens. In newly mature fibers (i.e., the outer cortex), the

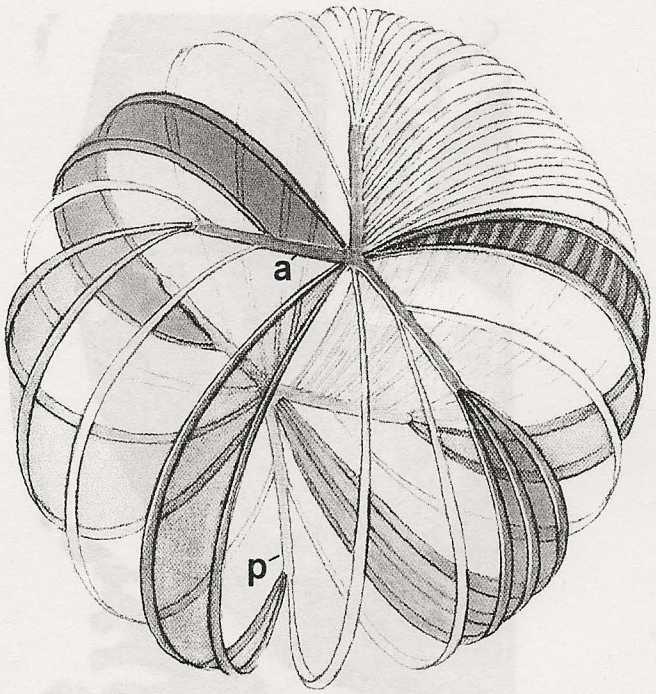

Figure 2.133. Drawing of the embryonal lens (i.e., nucleus) shows the anterior (*a*) Y suture, posterior (*p*) Y suture, and arrangement of the lens cells. The lens cells are depicted as wide, shaded bands. Those that attach to the tips of the Y sutures at one pole of the lens (*a*) attach to the fork of the Y at the opposite pole (*p*). (Revised from Hogan MJ, Alvarado JA, Weddell JE. *Histology of the Human Eye.* Philadelphia: WB Saunders, 1971.)

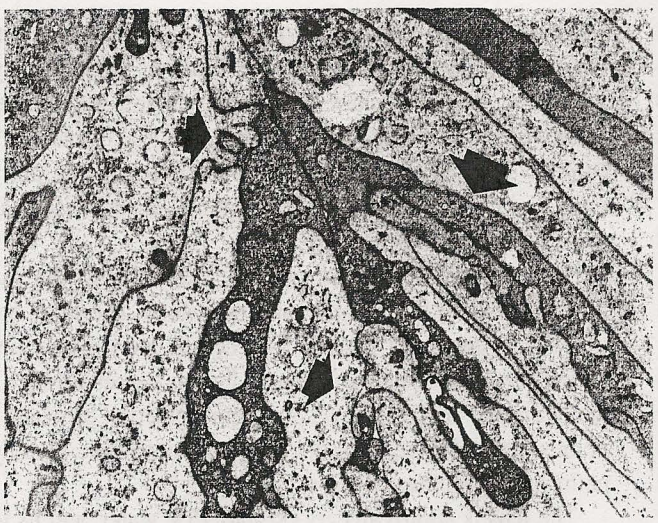

Figure 2.134. Close-up of a suture line in a dog lens reveals the great amount of cellular interdigitation (*arrows*) between adjacent lens fibers. (Original magnification, X5000.)

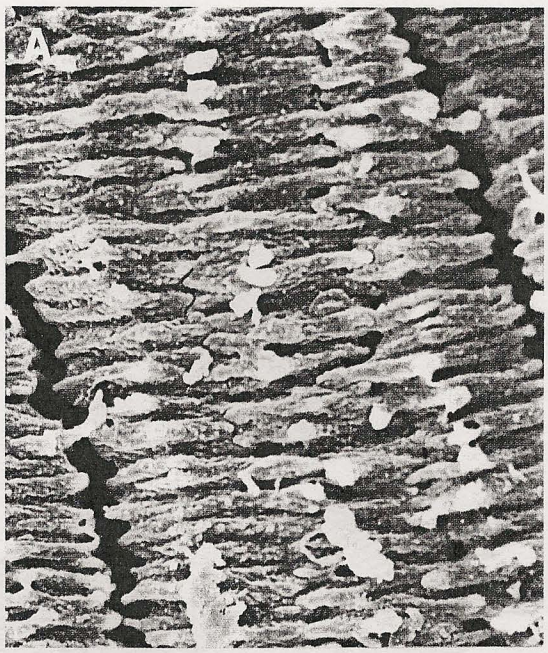

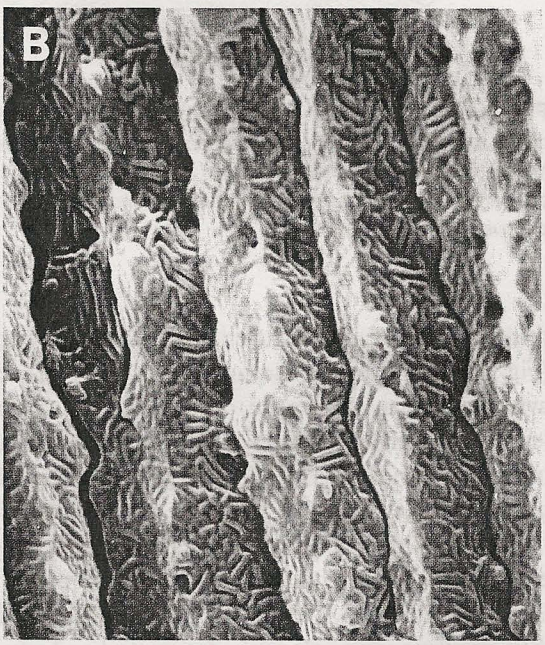

Figure 2.135. A. As lens fibers grow older, they are pushed toward the center of the lens (i.e., nucleus). Consequently, these fibers become more compressed and undulated. Note the secondary lens fibers within the inner cortex, as shown on this SEM. (Original magnification, X3400.) **B.** The lens fibers continue to become further compressed in the nucleus until their ball-and-socket junctions disappear, replaced by tongue-and-groove junctions that give these innermost cells a wrinkled appearance, as shown on this SEM. (Original magnification, X6000.)

ball-and-socket junctions are the dominant feature along each hexagonal edge (Fig. 2.130). This feature, however, is notably reduced in the lens fibers making up the inner cortex, lying next to the adult nucleus (Fig. 2.135A). The reduction in size of these interdigitations and the undulating appearance of the fiber undoubtedly result from the increasing compression that this region of the lens is undergoing. This change is even more remarkable in the region known as the lens nucleus, in which lens fibers have lost their ball-and-socket junctions entirely and instead possess tongue-and-groove junctions (Fig. 2.135B).

In birds, as in mammals, but to a greater extent, lenticular accommodation depends on the ability of the lens to change shape. The avian lens generally is softer and more flexible than the mammalian lens and consequently is allowed to be much more readily deformed during contraction of the musculature within the ciliary body and that of the peripheral iris.[226] As the musculatures contract, the ciliary body is thought to push against the midequatorial region of the lens, while the peripheral edge of

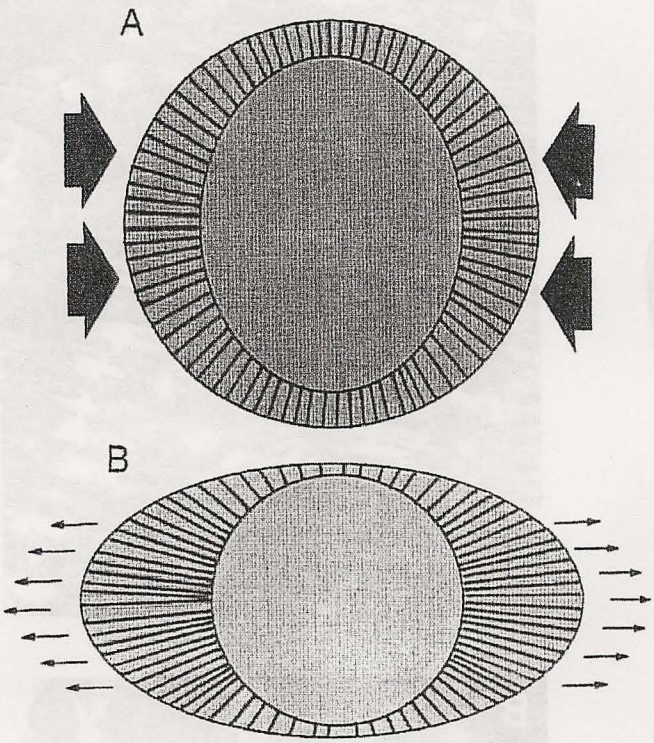

Figure 2.136. The avian lens is capable of marked changes in shape during accommodation because it can be physically pushed (*broad arrows*) into by the adjacent ciliary processes to form a more rounded form (**A**). By comparison, the lens "at rest" is stretched by zonules (small arrows) into a biconvex form (**B**).

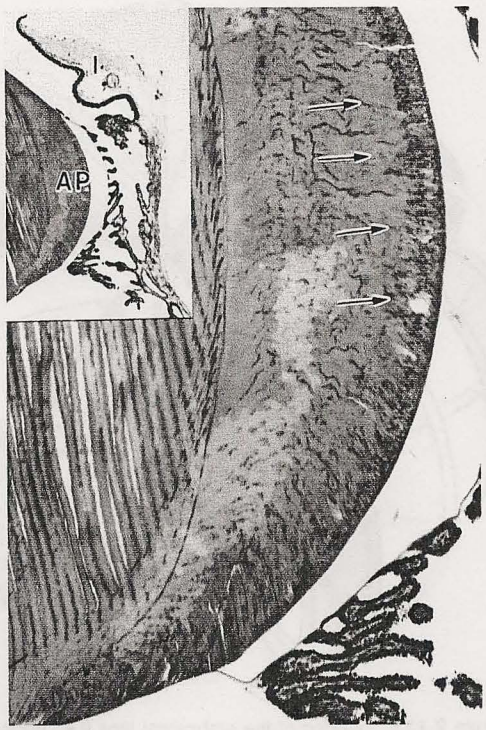

Figure 2.137. The "ringwulst," or annular pad (*AP*), of a screech owl's lens consists of radially arranged cells (*arrows*) that can withstand direct pressure placed on them. (Original magnification, X200.) **Insert.** Overview of the annular pad. *I*, iris. (Original magnification, X20.)

the iris presses against the anterior equatorial surface of the lens (Fig. 2.136). As an evolutionary adaptation to this activity, the avian lens has an annular pad, or "ringwulst," which consists of lens fibers that are relatively enlarged and arranged radially instead of concentrically (Fig. 2.137). The size of the pad appears to relate directly to the degree of accommodative ability.

Between the annular pad and the main lens body exists a cavum lenticuli that consist of globules tied off from the annular pad fibers and that separate the cells of the annular pad as they turn their course along the outermost lens body.[227] Annular pad fibers have a hexagonal circumference and are similar to young developing mammalian lens fibers. The annular pad fibers may be smooth-surfaced, lacking any anchoring cellular processes (as in the chicken, song thrush, and kestrel), or they may be studded with edge protrusions, including ball-and-socket junctions.[227] At the transition between the annular pad and the main lens body, the cells become considerably elongated, and their nuclei appear to be oval before their disappearance. The differentiation of germinative epithelial cells occurs in two phases: first into annular pad fibers that are elongated horizontally to the anteroposterior axis of the lens and then into main lens body fibers, which continue to elongate further and eventually lose their organelles.

Aging

Following regression of the hyaloid vascular system embryologically, the lens is deprived of blood supply postnatally. Subsequently, it depends on the aqueous humor and, to a lesser extent, the vitreous for nourishment. Transparency of the lens results from its relatively dehydrated state, lamellar arrangement of fibers, and solubility of lens proteins. The smooth and uniform thickness of the lens capsule and the epithelial cells in the pupillary region (i.e., the visual axis) also contribute to lens clarity.

The transparency of the cells and lens capsule are maintained as long as they are properly nourished. The small quantity of oxygen used by the lens comes from the aqueous humor. Glucose from the aqueous humor passes through the lens capsule, and metabolism of this glucose provides the main source of energy for the lens, with anaerobic glycolysis pathways being the most important.

The lens is approximately 60% to 75% water, and its total water content decreases with age. Relative dehydration and Na^+ and K^+ gradients are maintained by an active Na-K-ATPase pump, which is mostly located in the anterior epithelium. Lens proteins comprise 35% of the lens, which is a higher proportion than that in any other body tissue. Two forms have been described: soluble (i.e., crystallin) and insoluble (i.e., albuminoid). The proportion of soluble to insoluble proteins varies with species, age, and lens size.[225] Solubility of the proteins decreases with age as well, so the proportion of insoluble proteins is greater in an old than in a young lens and is greater in the older portion of the lens (i.e., the nucleus) than in the younger portion (i.e., the cortex). The albuminoid protein in the lens is largely associated with the cell membranes of the rigid, crenelated, and relatively dehydrated nuclear lens

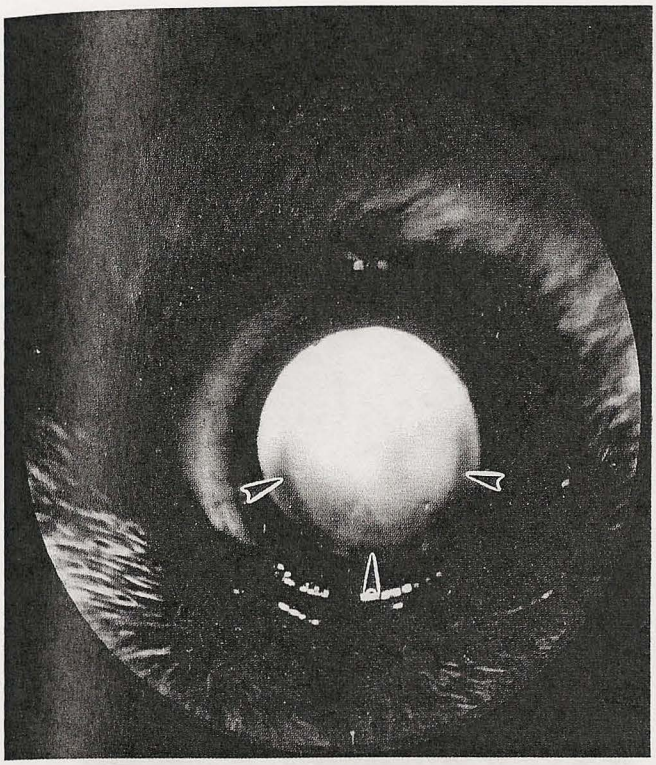

Figure 2.138. Nuclear sclerosis is a normal aging phenomenon of the mammalian lens. A substantial loss of lens elasticity occurs because of ever-increasing growth by the rigid center or nucleus of the lens, which can be discolored (*arrows*), as seen in this older dog.

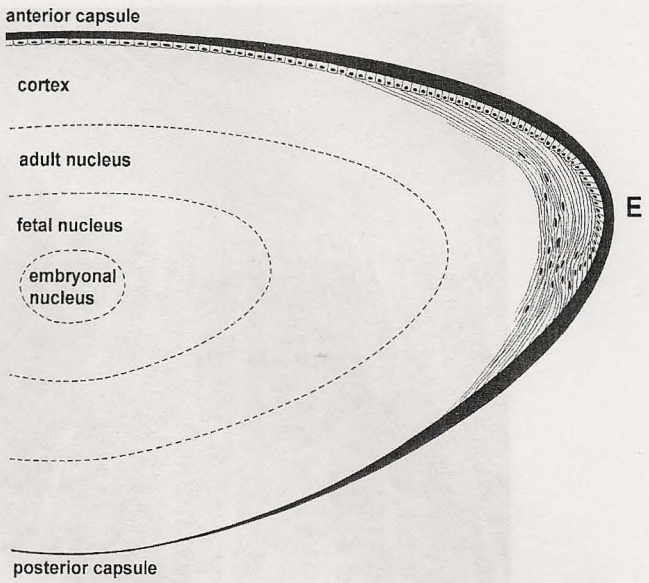

Figure 2.139. Schematic of the adult lens, showing nuclear zones. The thickness of the lens capsule in various zones is shown. (Revised from Hogan MJ, Alvarado JA, Weddell JE. *Histology of the Human Eye.* Philadelphia: WB Saunders, 1971.)

fibers. Thus, as the lens nucleus continues to expand with time, the volume needing to be dehydrated gradually lessens, which in turn reduces metabolically the demand on the aging anterior epithelium. Unfortunately, the lens nucleus has absolutely no flexibility. Consequently, as the lens becomes older, it also becomes less flexible or elastic.

Nuclear sclerosis, the gradual increase in density of the central zone that occurs in the lens with aging, is clinically evident (Fig. 2.138). In the dog, it becomes evident at approximately 6 years of age and older. This same loss of lens elasticity with aging accounts for the inability to accommodate (i.e., presbyopia) seen in humans after 40 years of age and necessitating use of bifocal eyeglasses.

In older mammalian lenses, the nucleus easily occupies the largest portion. Only recently, a detailed anatomic description of the mature nucleus has been made.[228] Lens fibers lose their flexibility as they become incorporated within the ever-growing nucleus, but their shape and organization varies considerably according to their location within the nucleus (i.e., adult nucleus, juvenile nucleus, fetal nucleus, and embryonic nucleus) (Fig. 2.139). Overall, the fibers are progressively larger in diameter and less orderly arranged toward the center of the lens. The differences seen in the nuclear fibers most likely reflect the increased forces of compaction that occur during lenticular aging.

Avian lenses are believed to remain soft and pliable throughout the lives of most birds. Though lens fibers are being added to the main lens body, the process appears to be slower than that in mammals, and it results in considerably less compaction. In a study on age-related changes to visual acuity in pigeons, little evidence of presbyopia was found.[229] Animals as old as 17 years increased only 9% in the mean viewing distance. Further analyses with an infrared photorefractor failed to support the occurrence of presbyopia in these birds.

Zonular Attachment

The lens is freely suspended from the ciliary body by a ring of transparent fibers called zonules. Zonular attachment is achieved by a complex arrangement of fibers that insert onto the lens capsule in a zone encompassing the equator and a short distance both anterior and posterior to the equator (Figs. 2.140A and B).[230] Each zonular fiber is made of numerous small fibrils, which are visible under SEM as they attach to the lens capsule (Fig. 2.140C). The zonular fiber spreads out greatly near the equator and terminates into smaller bundles. Each of these bundles, which are comprised of fibrils, also fan out and form a network that ramifies over the surface of the lens capsule, approximately 1.5 to 2.0 mm away from the lens equator. As each smaller bundle of fibrils blends into the outer capsule, it is interwoven with an adjacent bundle, thus providing added strength for its insertion.

In the dog, the fusion of the zonular fibrils and the superficial capsule as seen by TEM is a distinct layer (Fig. 2.140D). The fibrils that make up each bundle have a characteristic, 12-nm banded appearance. Adjacent bundles of these fibrils are compact and round. It was once believed that the zonular fibril consisted of collagen and was perhaps a condensation of vitreous; it was therefore referred to as the tertiary vitreous. Results of more recent studies, however, have revealed that the fibril is composed of a noncollagenous glycoprotein that more closely resembles elastin.[231,232] Zonular fibers are

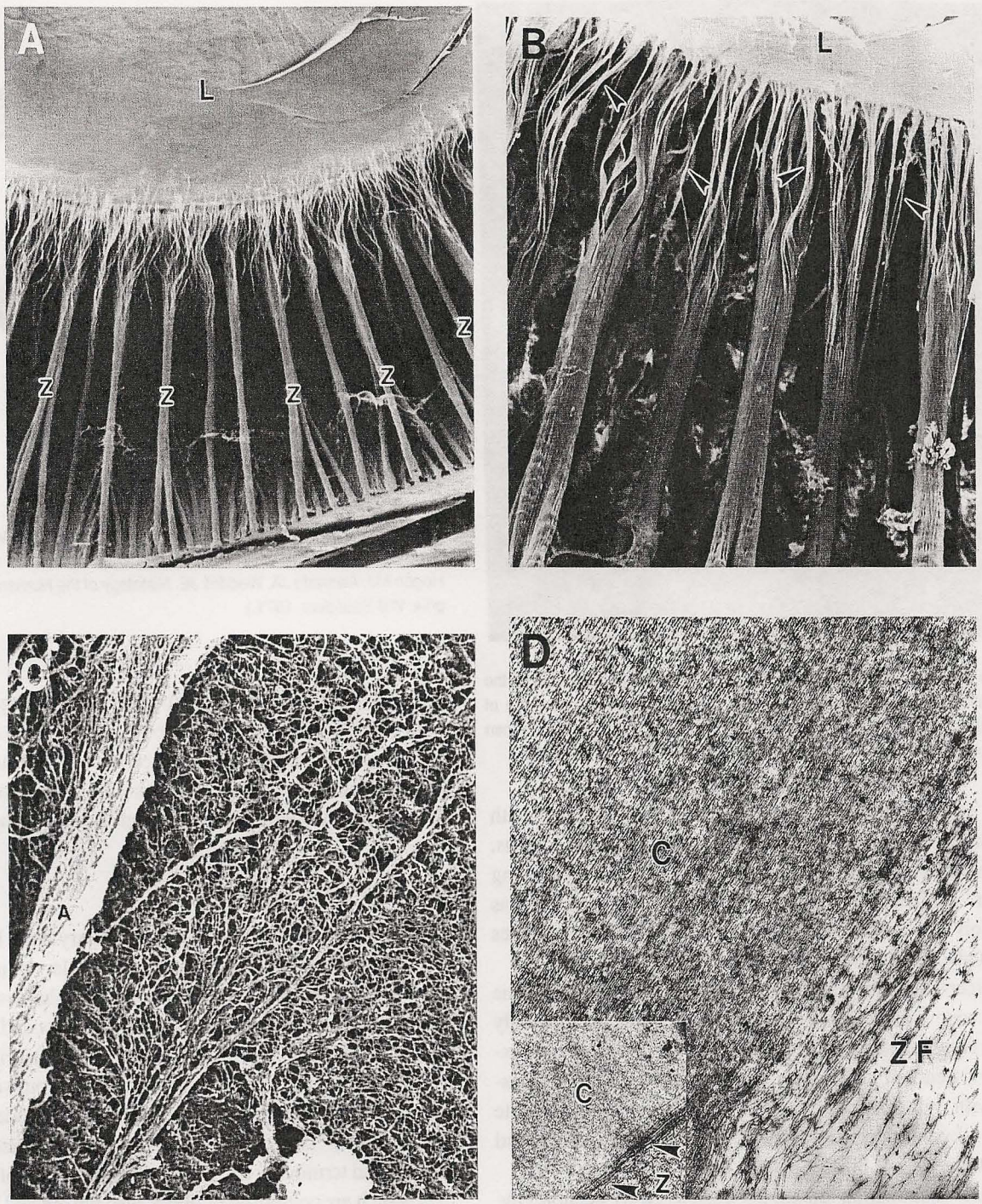

Figure 2.140. Zonular attachments to the lens in a dog. **A.** SEM shows zonules (*Z*) extend from the ciliary body onto the equator of the lens (*L*) in a ring-like manner, covering each ciliary process. (Original magnification, X30.) **B.** SEM shows that each zonule consists of bundles (*arrows*) of fibrils, which are most apparent next to the lens (*L*). (Original magnification, X78.) **C.** SEM shows termination of zonular fibrils, which unravel to form a dense meshwork over the capsule that greatly increases the surface area of attachment. *A,* zonular fiber. (Original magnification, X1600.) **D.** In the young, developing individual (i.e., neonate), the zonular fibrils (*ZF*) are imperceptibly intertwined with the outer layers of the lens capsule (*C*). (Original magnification, X24,000.) **Insert.** In the adult lens, zonular (*Z*) attachment (*arrows*) along the outer capsule (*C*) is more easily seen. (Original magnification, X15,000.)

believed to originate from the ciliary body, specifically the nonpigmented epithelium.[233] The fibrils do not penetrate the basement membrane entirely but intermix with the inner folds of the basement membrane (Fig. 2.141).

The arrangement of the zonular bundles in the dog varies a great deal even within the same eye. Five variations of the suspensory apparatus occur:

1. Bundles of zonules with broad lenticular attachments and regular, open arcades between bundles with isolated fibers crossing;
2. Irregular fiber distribution and interconnecting fibers between bundles, to the point of forming nets;
3. Bundles of different thickness and interconnecting fibers forming nets;

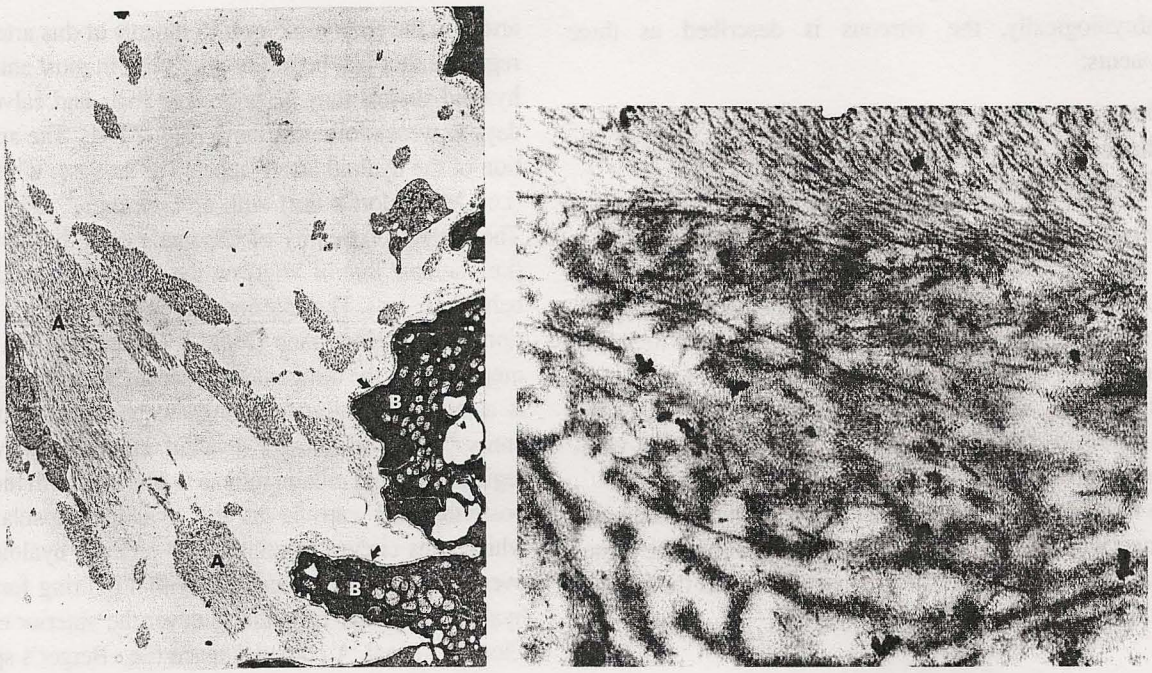

Figure 2.141. Zonular fibers in a horse at their origin from the nonpigmented ciliary epithelium. **A.** Bundle of zonular fibrils. **B.** Nonpigmented ciliary epithelium. *Arrows* indicate basal lamina of the epithelium. (Original magnification: X6750.) Right side image is an enlargement of the region where the zonule merges with the basal lamina. (Original magnification: X20,000.)

4. Long, fibrous bundles with interconnecting nets of fibers; and
5. Twisting of long, fibrous bundles with interconnecting fibers producing a membrane.[234]

The relationship of the zonules to ciliary processes varies to some extent among species. In primates, the zonular fibers originate largely from the pars plana, within 1 mm anterior to the ora serrata.[235–237] As the zonules course their way anteriorly, almost all have a close attachment to ciliary processes, adhering strongly to the valleys between the folds and along the sides of the processes.

In the cat, the zonular fibers largely appear to bypass the ciliary processes and insert in the valleys between (Fig. 2.142). In the dog, tips of the ciliary processes are free of zonular fibers, but the remaining process is ensheathed very intimately with the zonules (Figs. 2.71 and 2.143).[238] The fibers as a group can be followed to the base of the ciliary process. As the fibers insert into the lens capsule, they can fan out over a breadth of 300 μm and as a result overlap considerably with fibers arising from adjacent processes. The horse (Fig. 2.72) has numerous fibers both ensheathing the processes and in the valleys, and both types continue down to the pars plana. In addition, an extensive network of fibers runs horizontally, joining the ridges of the processes.

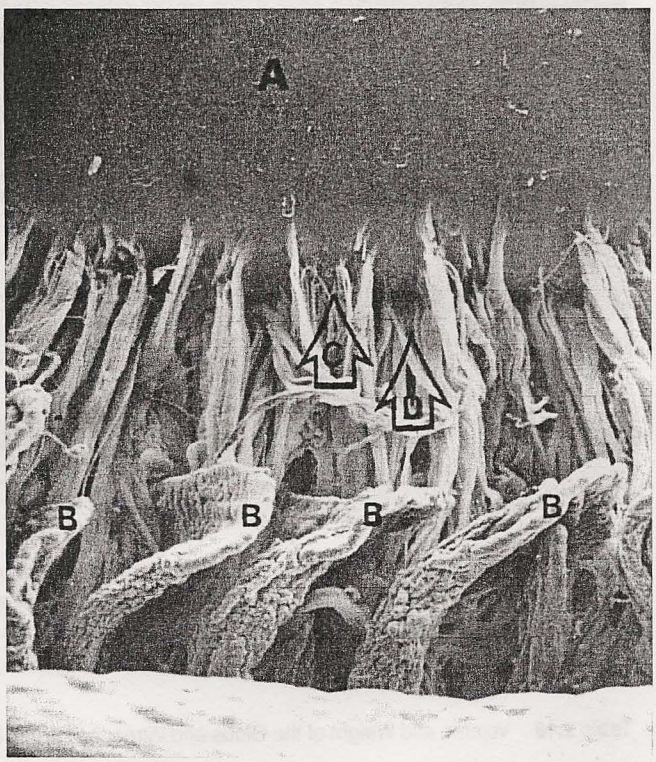

Figure 2.142. Caudal-view SEM of ciliary processes and zonular attachments to the lens in a cat. **A.** Posterior lens. **B.** Ciliary process. **C.** Posterior zonular fibers. **D.** Anterior zonular fibers. Note the zonular fibers extending from the valleys and producing a cluster of fibers at their lenticular insertion with gaps between bundles. (Original magnification, X40.)

VITREOUS

The vitreous humor is the largest single structure in the eye, occupying up to two thirds of the volume of the globe. It is a transparent, jellylike humor that fills the posterior cavity of the eye. The vitreous forms a gelatinous support for the retina and on its anterior surface is concave, forming the patellar fossa in which lies the lens. As a result, the vitreous functions to transmit light, to maintain the shape of the eye, and to help maintain the normal position of the retina. The weight and volume of the vitreous humor in selected domestic animals are listed in Table 2.18.

Embryologically, the vitreous is described as three components:

1. The primary vitreous,
2. The secondary vitreous, and
3. The tertiary vitreous.

The primary vitreous develops first and is composed mainly of the hyaloid artery system. The primary vitreous regresses with further development but is still easily demonstrable in normal young animals. The secondary vitreous, or the definitive vitreous, forms around the primary vitreous and is neuroectodermal in origin. The tertiary vitreous is actually the zonular fibers discussed previously. When speaking of the adult vitreous, one is usually referring to the secondary vitreous.

The vitreous encircles a central canal (i.e., the hyaloid canal or Cloquet's canal), extending from the optic disc to the posterior pole of the lens. This potential space contains the hyaloid artery in the embryonic eye. Remnants of this artery normally regress either just before or after birth in most animals; patent hyaloid vessels may be present in foals and calves for a few days to weeks following birth (Fig. 2.144). The anterior insertion of the hyaloid artery appears as a dense, white, small dot (i.e., Mittendorf's dot) with a "corkscrew" tail (Fig. 2.144). The anterior extremity of Cloquet's canal is seen as a circle (i.e., arcuate line of Vogt) on the anterior hyaloid membrane behind the lens. The anterior vitreous face is lined by the anterior hyaloid membrane (Figs. 2.144 and 2.145). It is not a membrane in the ultrastructural sense, but many authors feel it is a structure definitive enough to be considered a separate entity.[240,241] The anterior hyaloid curves forward from the region of the ora ciliaris retinae to blend in with the peripheral posterior lens capsule at the hyaloideocapsular ligament, which runs circumferentially. The anterior hyaloid continues over the posterior lens capsule within the ring formed by the hyaloideocapsular ligament to cover the anterior extremity of Cloquet's canal. A potential space (i.e., Berger's space) exists between the posterior lens capsule and the anterior hyaloid.

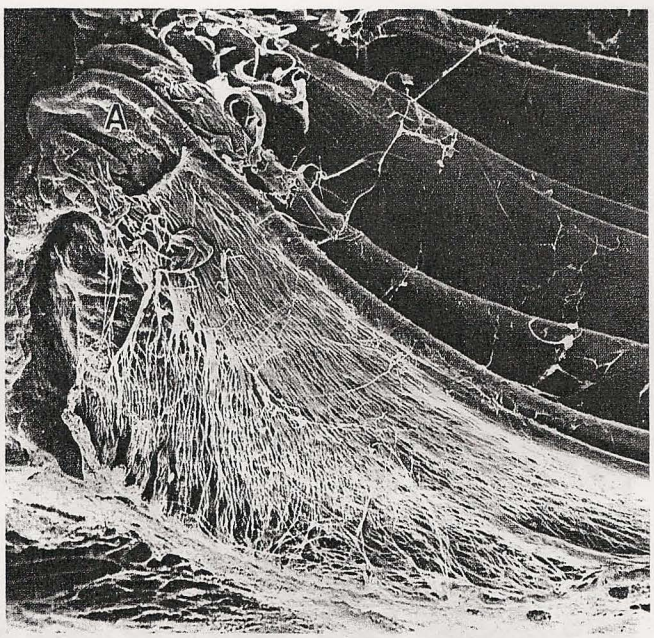

Figure 2.143. SEM shows that the apical portion (*A*) of each ciliary process in the dog is not intimately associated with zonular fibers (*arrows*). (Original magnification, X50.)

The vitreous attaches firmly to peripheral structures only at the edge of the optic nerve, near the ora ciliaris retinae and the posterior lens capsule. Attachment of the vitreous in the region of the ora ciliaris retinae is known as the vitreous base, and the broad attachment to the posterior lens capsule is the ligamentum hyaloideocapsulare (Fig. 2.145).

The vitreous is 99% water; collagen and hyaluronic acid comprise most of the remaining 1%. Collagen supplies the vitreous framework, and hyaluronic acid is found in the soluble portion. Nearly all visible light is transmitted through the normal vitreous. The collagen content is highest where the vitreous is a gel, and the collagen network is embedded in the internal limiting membrane of the retina, which produces part of the adult vitreous.[241] Specifically, collagen types II and IX comprise most of the extracellular fibers of the vitreous with a possibility of a third type consisting of a cross of types V and XI.[242] The collagen fibers interconnect with the hyaluronic acid by associated GAGs, consisting principally of chondroitin sulfate 4 and 6 and heparan sulfate.[243,244] In addition to collagen and hyaluronic acid, a cartilage matrix glycoprotein has been found in bovine, human, and rabbit vitreous.[245] This

Table 2.18 Volume and Weight of the Globe and Vitreous in Some Domestic Animals

	Globe		Vitreous		Ratio of Vitreous to Globe	
Animal	Volume (ml)	Weight (g)	Volume (ml)	Weight (g)	Volume	Weight
Human	7	6.77	4	3.9	0.6	0.6
Sheep	14	15.00	8	8.1	0.57	0.53
Pig	6	7.25	3.5	3.6	0.58	0.5
Calf	18	18.5	10	11.0	0.55	0.6
Ox	25	29.2	16	15.0	0.6	0.5
Rabbit	3	3.0	1	1.1	0.3	0.4

Modified from Jaffe N. *The Vitreous in Clinical Ophthalmology.* St Louis:, 1969.

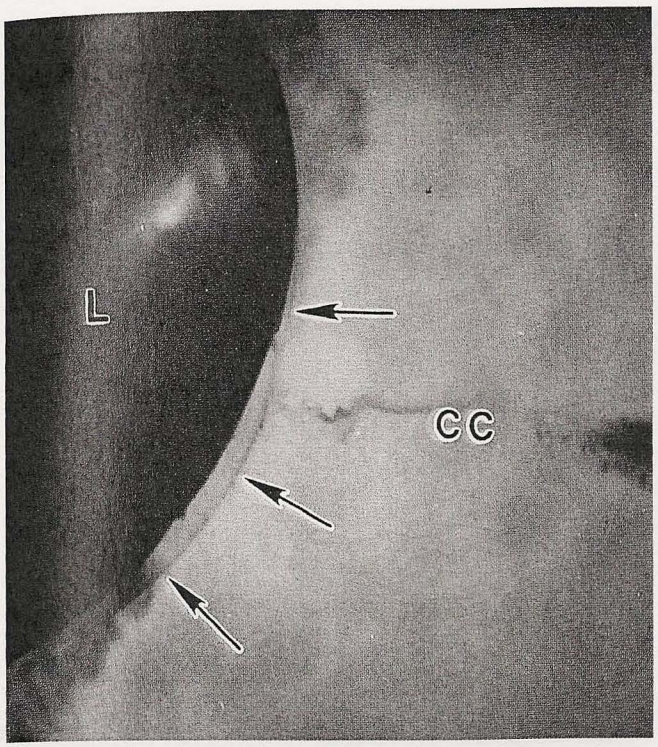

Figure 2.144. Anterior portion of Cloquet's canal (*CC*), which joins the anterior hyaloid membrane (*arrows*) behind the lens. (Original magnification, X15.)

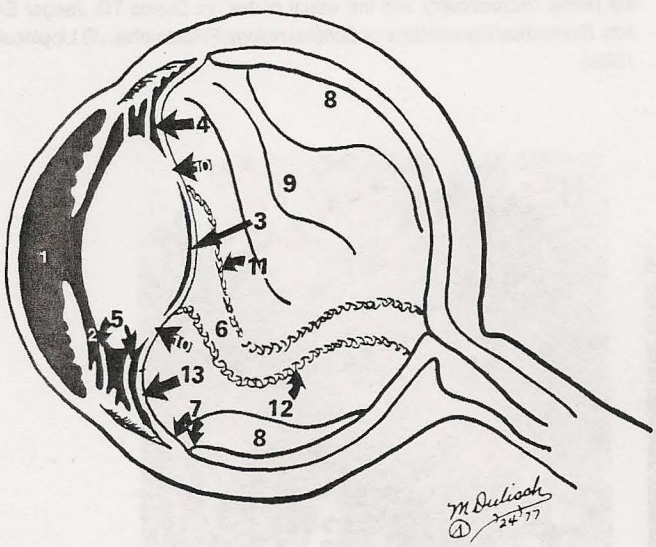

Figure 2.145. Schematic illustrating the spaces within the eye and the vitreous. *1,* anterior chamber; *2,* posterior chamber; *3,* Berger's space; *4,* Petit's canal; *5,* tertiary vitreous (zonules); *6,* Cloquet's canal; *7,* vitreous base; *8,* cortical vitreous; *9,* intermediate zone of vitreous with tracts; *10,* hyaloideocapsular ligament; *11,* dorsal plica; *12,* ventral plica; *13,* anterior hyaloid membrane. (Note that 3 and 4 are potential spaces only.)

material and a number of proteins, including vitrin, opticin, fibulin-1, and nidogen-1, are a part of the vitreal extracellular matrix and are produced primarily by the inner layer of the posterior half of the ciliary epithelium, and appear to be in a continuous state of turnover.[242,245]

The peripheral portion of the vitreous next to the retina is referred to as the cortex. The collagen fibrils of the cortical vitreous join the basement membrane of Müller and glial retinal cells at this location.

No actual membrane is present, but the posterior surface of the vitreous is often called the posterior hyaloid membrane. The vitreous proper has very few cells, and most of them are found in the cortex near the vitreous base. The main cell type is the hyalocyte, which is a histiocyte with a poorly developed lysosomal system. Hyalocytes can produce hyaluronic acid in vitro and have been thought to contribute to formation of the vitreous humor along with the nonpigmented epithelium of the ciliary body and the nonneuronal cells of the retina.[246] In the rabbit, however, involvement of this cell type in hyaluronic acid production has been brought into question.[247] Hyalocytes were found to disappear by the end of the third week after birth, even though hyaluronic acid increased substantially during that period of time. The possibility that these cells are related to remodeling events in the vitreous is most plausible. In addition to the hyalocyte, fibrocytes and glial cells comprise roughly one tenth of the total population of vitreal cells, lying mostly next to the ciliary body and the optic nerve head.[248]

The remainder of the vitreous humor is its central portion, which has been referred to as the retrolental and intermediate zones.[32] The central vitreous consists of layers of tracts, which in fact are layers of funnel-shaped sheets or plicae fitted one into another (Fig. 2.145). The most central tract is the hyaloid (i.e., retrolental) tract, which inserts near the hyaloideocapsular ligament. Between the cortex and central vitreous exists a border layer comprised of many compacted lamella, with each lamellae consisting of a meshwork of collagen fibrils.[249]

The entire vitreous is quite variable in its consistency because of the different proportions of gel to liquid vitreous that occur among species and at different ages. In the bovine, pig, and sheep, the entire vitreous is nearly homogenous in structure and of high density, much like human cortical vitreous. The cat and dog vitreous densities are reversed from that of primates: their cortex is fluid and the center is dense. Like ruminants, the pig and the horse do not show a separation into cortical and central zones, but the vitreous is of low optical density. The rabbit vitreous is of such low optical density that it could hardly be examined.[250–255] The consistency of the vitreous humor is also influenced by aging. In most species, holes and liquefaction (i.e., syneresis) occur in older individuals, particularly in the central region or the intermediate zone.

RETINA

The retina and optic nerve are derivatives of the forebrain; consequently, their morphology and physiology are similar to that of the brain. The sensory retina is connected to the brain by the optic nerve and the optic tracts. Photoreceptor cells of the retina comprise a complex layer of specialized cells, the rods and cones, which contain photopigments that change on exposure to light and produce chemical energy. This energy is then converted to electrical energy, which is ultimately transmitted to the visual cortex of the brain. The RPE furnishes important metabolites to photoreceptors; it also actively

phagocytizes the outermost photoreceptor segments as they are shed during normal outer-segment renewal. The retina receives almost all its nutrition from the retinal and choroidal capillaries, but a small amount probably derives from the vitreous. The retina has one of the highest rates of metabolism of any tissue in the body. If either source of nutrition is interrupted, ischemia will occur, which may lead to complete loss of retinal function. The eye requires a continuous supply of vitamin A (i.e., retinol), which is localized in the retina. The effects of vitamin A deficiency include retinal degeneration.[256]

The function of the retina as a direct extension of the brain is to receive light stimuli from the external environment and transmit this information accurately to the brain, where it is then interpreted to become vision. Once photoreceptors are stimulated by light, they transmit a nervous impulse that is received and modified in various ways by cells whose nuclei are in the inner nuclear layer (i.e., amacrine cells, bipolar cells, horizontal cells) (Fig. 2.146). The modified message is then transferred to ganglion cells, whose axons form the nerve fiber layer and extend through the optic nerve to the brain (i.e., lateral geniculate and cortex). Vision actually takes place in the visual cortex. Many ocular syndromes are associated with loss of function of one or more of these visual pathways, and it is important to understand the anatomic, physiologic, and embryologic relationships of the visual pathways before studying the disorders of this system.

Classically, 10 "layers" are described in retinal histology. The inner sensory retina contains nine, and the supportive pigmented epithelium is the tenth layer (Fig. 2.147). The optic

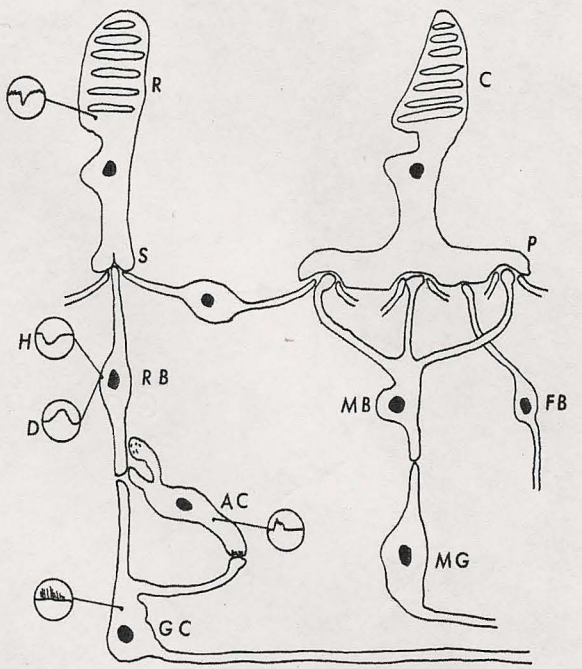

Figure 2.146. Microcircuitry of the retina with potential changes on spot illumination. The amacrine cell (*AC*) has a reciprocal inhibitory response onto the bipolar cell (*RB*) from which the information originated and acts to adjust the sensitivity of the ganglion cell (*GC*) synapse after receiving a signal. *C,* cone; *D,* depolarize; *H,* hyperpolarize; *P,* pedicle; *R,* rod; *S,* spherule. (Redrawn from Records RE, Zahn JR, Charles S, et al. Electrical signals of the retinal microcircuitry and the visual cortex. In: Duane TD, Jaeger EA, eds. *Biomedical Foundations of Ophthalmology.* Philadelphia: JB Lippincott, 1988.)

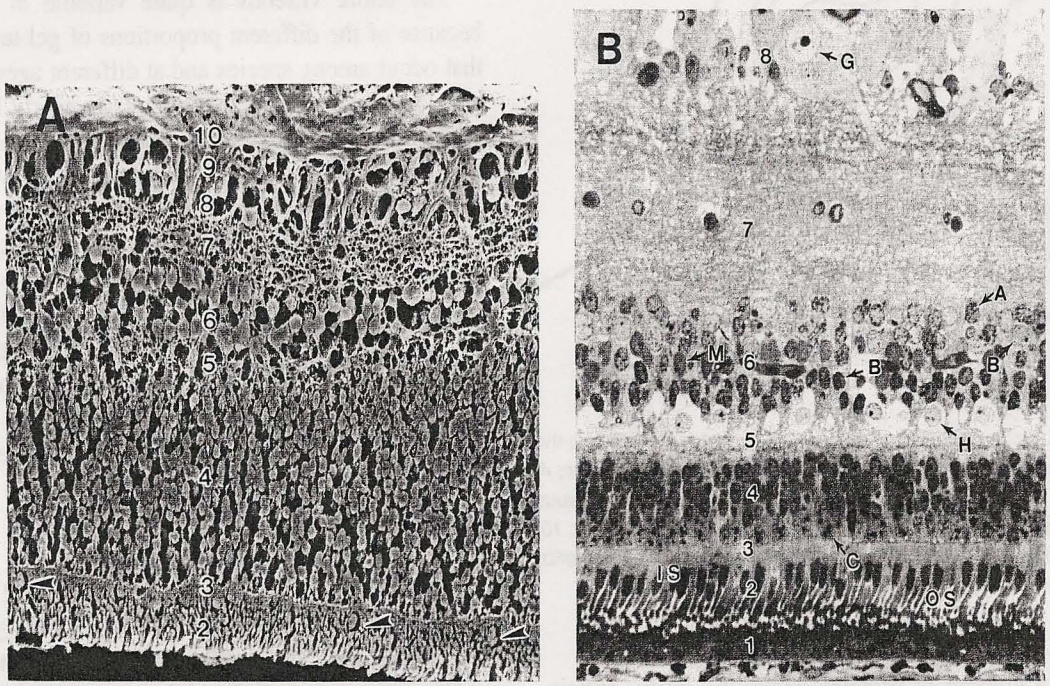

Figure 2.147. The sensory retina consists of nine discrete layers and a supportive pigmented epithelium that forms an outer, tenth layer, as demonstrated by SEM in the dog (**A**) and plastic section in the pig (**B**). The canine retina is rod dominant, being sparsely populated with cones (*arrows*). The porcine retina, by comparison, has a large population of cones and a much smaller rod-to-cone ratio than in the dog. Note the species differences in size or thickness of the outer and inner nuclear layers. *A,* amacrine cell nuclei; *B,* bipolar cell nuclei; *C,* cone nuclei; *G,* ganglion cell nuclei; *H,* horizontal cell nuclei; *M,* Müller cell nuclei; *1,* retinal pigment epithelium; *2,* layer of rods' and cones' outer (*OS*) and inner segments (*IS*); *3,* outer limiting membrane; *4,* outer nuclear layer; *5,* outer plexiform layer; *6,* inner nuclear layer; *7,* inner plexiform layer; *8,* ganglion cell layer; *9,* nerve fiber layer; *10,* inner limiting membrane. (Original magnification: Both, X250.)

retina extends from the optic disc to the ora ciliaris retinae, in which it is reduced to the two epithelial cell layers of the ciliary body.

The ten identifiable layers are usually considered from outside inward in the following order:

1. Retinal pigment epithelium (RPE),
2. Visual cell layer (rod and cone layer),
3. Outer limiting membrane,
4. Outer nuclear layer,
5. Outer plexiform layer,
6. Inner nuclear layer,
7. Inner plexiform layer,
8. Ganglion cell layer,
9. Nerve fiber layer, and
10. Inner limiting membrane.

Retinal Pigment Epithelium

The RPE is a layer of flat, polygonal cells that forms the outermost layer of the retina. It is the continuation of the outer pigmented epithelial layer of the ciliary body. The RPE is more adherent to the choroid than to the rest of the retinal tissue. This layer, which derives from the outer layer of the optic cup, is important in nutrient transport from the choriocapillaris to the outer layers of the retina. There are numerous infoldings of the cellular membrane at the base of each cell, and these are indicative of the extensive, ongoing transport between the RPE and the subjacent choriocapillaris. Each cell sends cytoplasmic processes inward to surround the visual receptors, to insulate them from bright light, and to increase their individual sensitivity. They also phagocytize the outer segments of photoreceptors as they are continuously shed.

The cells are usually densely pigmented, but they are devoid of pigment overlying the dorsal choroid that contains the tapetum lucidum. The absence of melanin permits light to pass through the RPE to the tapetum and then reflect back to the light-sensitive receptors.

On flat preparations, the RPE of most species forms a mosaic of hexagonal cells, which is most uniform in the posterior pole and in young animals (Fig. 2.148A). In most species, except the rat and rabbit, these cells are generally mononucleate. In general, the cells are larger and have more binucleate forms near the ora ciliaris retinae. Table 2.19 lists posterior-pole RPE size and binucleate frequency in various species with flat RPE preparations.[257]

The nucleus is centrally positioned and round to oval, with its long axis parallel to the retinal surface. The cytoplasm is predominantly filled with smooth endoplasmic reticulum (Fig. 2.148B). Mitochondria are numerous, being concentrated in the basal two thirds of the cell. In cells that do not overlie the tapetum lucidum, melanin granules are present, being either elongated or lanceolate and located in the apical to midportion of the cytoplasm. These granules are often seen in the long villous cytoplasmic processes, especially among avian species (Fig. 2.148C). In the tapetal region of the retina, the absence of melanin granules is quite conspicuous (Fig. 2.148D). On the other hand, other bodies, including residual bodies of lipofuscin and lamellated bodies, or phagosomes consisting of phagocytosed photoreceptor outer-segment discs are easily found.[193,258–262] Lysosomes also appear to increase in number in this region of the RPE.[261] The apparent increase of lysosomes may indicate enhanced shedding of the outer segment material over the tapetum; however, results of recent studies on melanogenesis suggest that the lysosomal system is closely associated with that of the melanosome and that the additional lysosomes may be a part of an underdeveloped or partially suppressed melanosomal system.[263–265]

The morphology and location of RPE melanosomes varies to some degree among different animals. The shape of melanosomes are typically oval, but they can be more elliptical

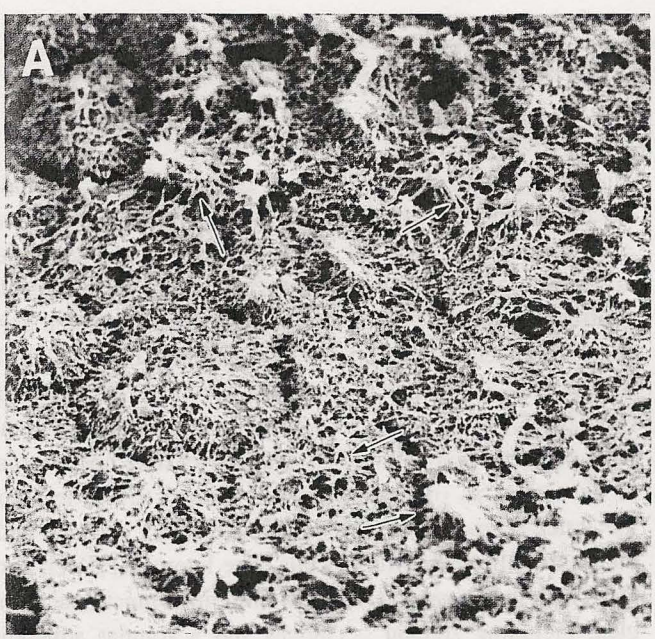

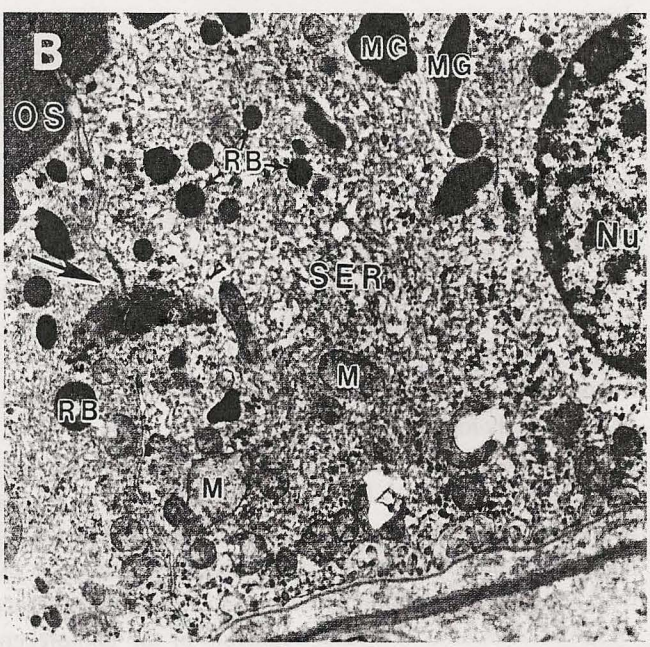

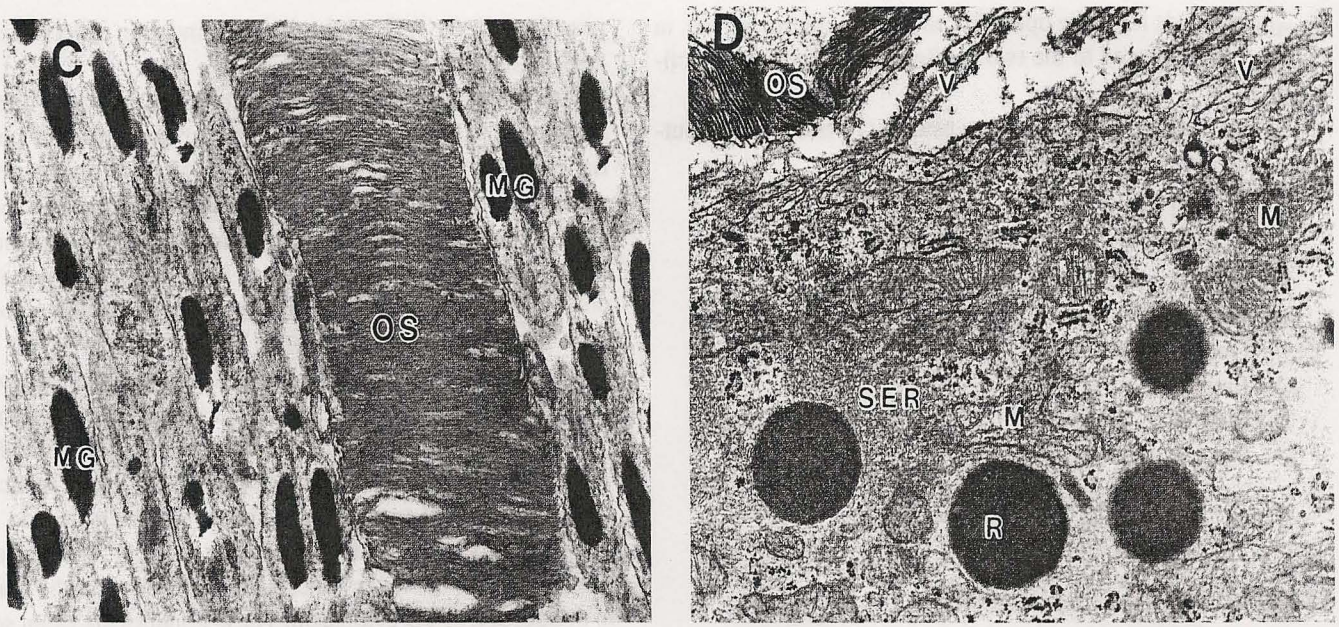

Figure 2.148. RPE. **A.** Surface-view SEM of the RPE in a dog with a partially detached retina reveals the hexagonal shape of these cells, which apically possess numerous cylindrical, villous cytoplasmic processes (*arrows*). (Original magnification, X3000.) (Courtesy of L Earle.) **B.** Pigment epithelium in a pig consists of an extensive smooth endoplasmic reticulum (*SER*), melanin granules (*MG*), and residual bodies (*RB*), which are apically located, and mitochondria (*M*), which are more basally positioned. *Arrow* indicates the junctional complex (see Fig. 2.149 for a close-up). *Nu,* nucleus; *OS,* outer segments. (Original magnification, X6000.) **C.** The avian villous cytoplasmic processes, as seen here in the chicken, contain long, narrow melanin granules (*MG*). These processes fasten the sensory retina, via the outer segments (*OS*), to the RPE, and they shield the outer segments from extraneous light. (Original magnification, X12,000.). **D.** In the nontapetal RPE of the cat, there is a complete absence of melanin granules. The residual bodies (*RB*) and mitochondria (*M*) are evenly distributed throughout the cytoplasm. *V,* villous process. (Original magnification, X10,000.)

Table 2.19 Retinal Pigment Epithelial Cell Size and Binucleate Frequency at the Posterior Pole

Species	Mean Cell Diameter (μm)	Mean Cell Height (μm)	Frequency of Binucleate Cells %
Human	14	10	3
Monkey	12	10	3
Rat	19	6	70
Rabbit	22	6	85
Dog	15	5	3
Sheep	17	8	1
Cow	13	5	1
Chicken	17	6	<1

Modified from Tso MOM, Friedman E. The retinal pigment epithelium. I. Comparative histology. *Arch Ophthalmol* 1967;78:641–649.

in diurnal species, especially birds and various reptiles, and to a lesser extent in primates (i.e., the monkey) and the squirrel.[266] The elliptical to nearly lanceolated melanosomes are frequently positioned within the microvilli, offering substantial shields against scattered light. Melanosomes within the RPE of arrhythmic and nocturnal species, such as the rat, hamster, mouse, bat, and so on, tend to be rounder, fewer in number, and less frequently located within the microvilli.

The inner apical surface of the RPE has numerous long villous processes that lie between and surround the outermost and oldest portion of the photoreceptor outer segments (Fig. 2.148). No cell membrane attachments exist between the RPE and the photoreceptors, but a viscous ground substance of GAGs surrounds the other segments of the photoreceptors.[64,104,267] On SEM examination, the apical villi are quite numerous, being clustered next to outer segments that have fractured and adhered to the RPE in preparation, such as that shown in Figure 2.149. The villous processes become unusually long near the site of retinal detachments and, as a result, contrast sharply with the apices of the RPE cells, which have lost their attachment with the outer segments. Detached RPE cells possess fewer apical processes, which are notably short (Fig. 2.148A). Microvilli are especially large and long in the RPE of many nonmammalian animals.[266] It is not unusual to have the tips of these processes extend to the level of the inner segments and even to make direct contact with the microvilli of the Müller cells. The lateral RPE cell surfaces near the apical end have a well-defined junctional complex, including zonular occludens and a zonular adherens (Fig. 2.150).

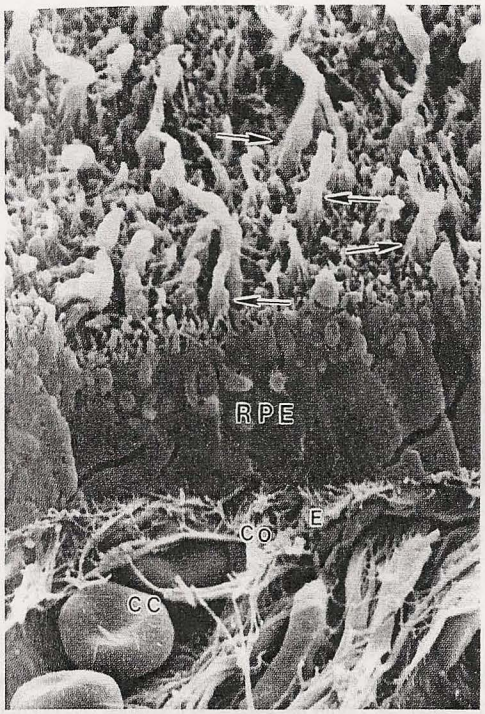

Figure 2.149. SEM shows cryofractured RPE and the underlying choriocapillaris (*CC*) of a sheep. *Arrows* indicate outer segments that remain fastened to apical villi. Note the strands of collagen (*Co*) and elastic fiber (*E*) that make up much of Bruch's membrane. (Original magnification, X6000.)

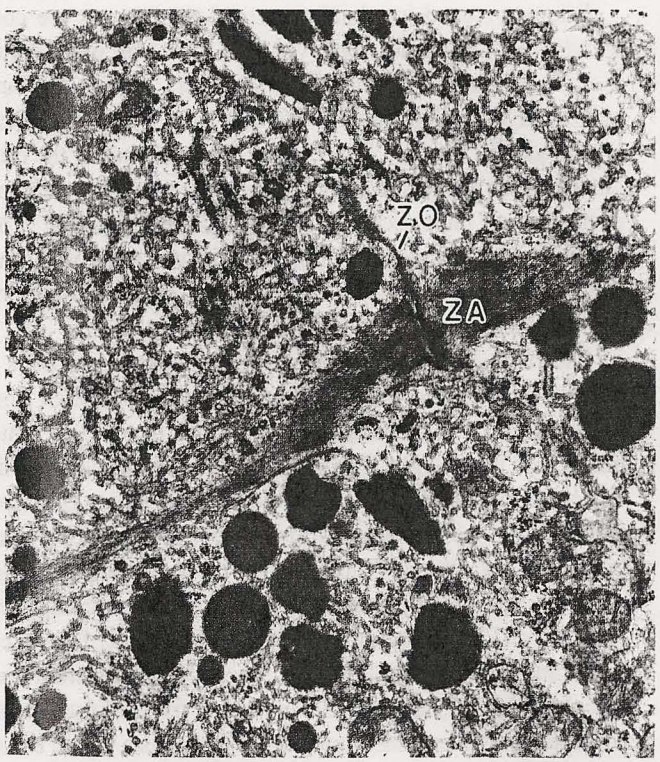

Figure 2.150. The junctional complex in the RPE of the pig consists of a zonular occludens (*ZO*) and a zonular adherens (*ZA*). (Original magnification, X10,000.)

The basal aspect of the RPE rests on a basement membrane over the choriocapillaris and its basement membrane and intercapillary regions. Marked basal infoldings of the cell membrane contrast sharply with the basement membrane, which is relatively smooth (Fig. 2.151). The size and organization of the

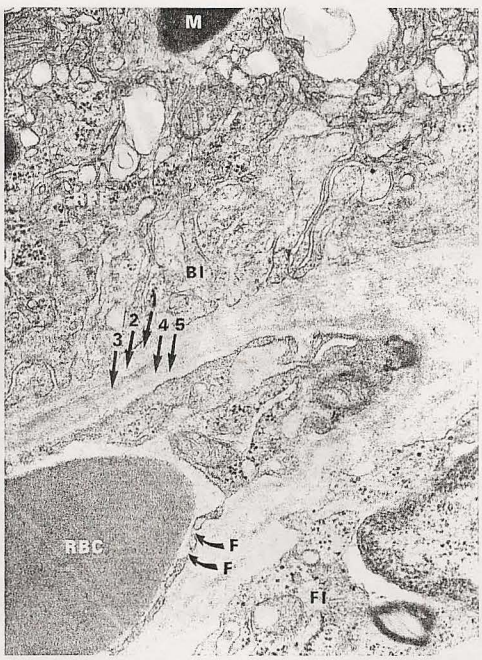

Figure 2.151. TEM shows the basal complex (i.e., Bruch's membrane) in capillary zone over the nontapetal region of a dog. Note the RPE with melanin (*M*) granules and basal infoldings (*BI*) of the RPE. The basal complex consists of *1*, basal lamina of RPE; *2*, inner collagenous zone; *3*, elastic layer; *4*, outer collagenous zone; *5*, basal lamina of choriocapillaris. *F*, fenestrations in choriocapillary endothelium; *FI*, fibroblast in anterior choroid; *RBC*, erythrocyte in choriocapillaris. (Original magnification, X43,600.)

basal infoldings vary to some degree among mammals.[261,262,268] In birds, the basal infoldings are especially developed and tightly packed as opposed to those in mammals, which tend to be smaller and irregularly positioned (Fig. 2.152).[268–270]

The basement membranes of the RPE and adjacent choriocapillaris collectively form a complex called Bruch's membrane. When fully developed, Bruch's membrane consists of five layers:

1. The basement membrane of the pigment epithelium of the retina,
2. An inner collagenous zone,
3. Elastic layer,
4. Outer collagenous zone, and
5. The basement membrane of the choriocapillaris.

In most species, the outer collagenous zone is thinner than the inner collagenous zone (Fig. 2.153). In animals with a cellular tapetum, the basement membrane of the pigment epithelium and the basement membrane of the choriocapillaris occasionally fuse, thus reducing the pentalaminated structure to a single layer. More often, however, the basement membrane of both epithelia remain, with a shared collagenous zone of variable thickness.

Neurosensory Retina (Neuroretina)

The sensory layer varies in thickness, being thickest near the optic disc and tapering to the ora ciliaris retinae. The width of each layer decreases, but the nerve fiber layer contributes the most to the variation in thickness. Most domestic animals have a central retina of approximately 200 to 240 μm and a peripheral

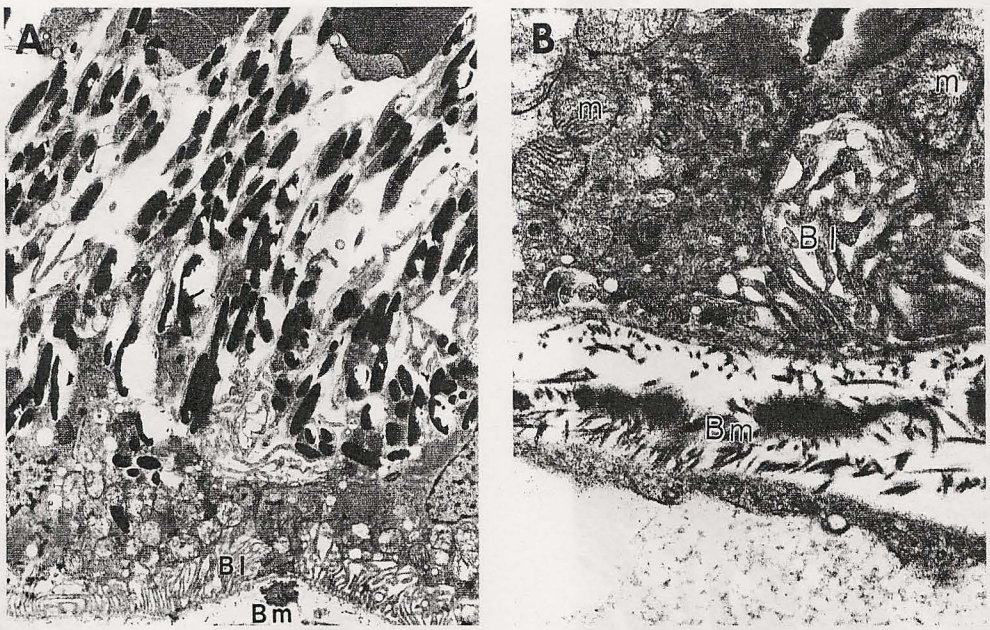

Figure 2.152. Avian (i.e., Great Egret) RPE. **A.** Apically, the long, slender cytoplasmic processes are filled with melanosomes, whereas basally, closely packed basal infoldings (*BI*) lie next to Bruch's membrane (*Bm*). (Original magnification, X5000.) **B.** Tightly packed basal infoldings (*BI*) occur in close proximity to many mitochondria (*m*). (Original magnification, X18,000) (Courtesy of S Loerzel.)

Figure 2.153. Close-up of Bruch's membrane in the pig shows the five components: basement membrane of the RPE (*BM 1*); the inner collagenous zone (*ICZ*); elastic layer (*EL*); outer collagenous zone (*OCZ*), which varies to some extent in thickness, usually being quite narrow; and the basement membrane of the choriocapillaris (*BM 2*). *Arrows* indicate fenestrations within the choriocapillary endothelium. (Original magnification, X65,000.)

retina of 100 to 190 μm.[4,271,272] In animals with poorly vascularized or avascular retinas, retinal thickness rarely exceeds 140 μm, which turns out to be the proposed oxygen diffusion maximum for retinal tissue (Table 2.19).[273–275] Thickness of the avascular retina of the marsupial bush-tailed possum (*Trichosurus vulpecula*), however, substantially exceeds the proposed maximal thickness by 20 μm or more, falling within the range for some vascular retinae.[275] By comparison, the thickness of the equine retina, which varies from 80 μm at the ora ciliaris retinae to 250 5m medial to the optic nerve, is for the most part less than 130 μm.[276]

When averaged intralaminar retinal thicknesses are compared between species with vascular and avascular retinae, those with vascular retinae have all layers, except the outer nuclear layer, being roughly 25% to 100% thicker than those with avascular retinae (Table 2.20). The thickness of the outer nuclear layer appears to be influenced more by the dominance of the type of photoreceptor than by vascularity (Table 2.20). The layer perhaps most influenced by the presence of absence of vascularity is the inner plexiform layer, being 50% thinner in avascular retinae (Table 2.20).[275]

The retinal photoreceptors are the primary visual cells of the eye (Fig. 2.146). The two types are the rods, which function in dim or reduced illumination, and the cones, which function in bright light. The cones provide sharp visual acuity and color sensitivity. The rods provide for detection of shapes and motion. The cone population is most dense in the central retina of most animals (Table 2.21). Primates and many avian and reptilian species possess cone-rich regions completely free of rods. These regions are called foveas (i.e., fovea centralis) and are responsible for the perception of different hues of color, high resolution, and binocular fixation (and depth perception). None of the domestic animals has a fovea, but an area of high cone density frequently occurs and is often called the area centralis. This area lies 3- to 4-mm dorsolateral to the optic disc in the dog and cat.[4,271,277] In mammals, the area centralis is, for the most part, more oval than round and extends along the horizontal plane.[278,279] The term *visual streak* is sometimes used synonymously for the area centralis. The visual streak is the region of the retina with greatest concentration of ganglion cells, the innermost layer of retinal neurons. Often, the two regions are nearly identical, or even

Table 2.20 Selected Examples of Retinal Thickness

Animal	Retinal Location (μm)		Reference
	Central	Peripheral	
Rat			
GCL/NFL	32 ± 9		275
IPL	60 ± 1		
ONL	35 ± 8		
TT	212	177	
Guinea Pig			
GCL/NFL	23 ± 1		275
IPL	27 ± 2		
ONL	21 ± 3		
TT	136	108	
Cat			
TT	228, 249	186, 195	275, 405, 432
Dog			
TT			433
Quail			
GCL/NFL	35 ± 4		275
IPL	49 ± 4		
ONL	48 ± 4		
TT	219	154	
Possum			
GCL/NFL	25 ± 3		275
IPL	30 ± 2		
ONL	41 ± 2		
TT	158	133	
Human			
TT	230	120	32

GLC, ganglion cell layer; IPL, inner plexiform layer; NFL nerve fiber layer; ONL, outer nuclear layer; TT, total thickness.

topographically identical. Instances do occur, however, in which peak ganglion-cell densities do not topographically match peak cone density.[280] Instead, a specific subpopulation of ganglion cells might be associated with the area centralis.[281,282]

Measurements of cone cell densities have been determined in a variety of species, including the dog and cat.[283,284] In the cat, the cones in the area centralis are approximately six to seven times more numerous than in the periphery (26,000–27,000 cells/mm^2 versus 4,000 cells/mm^2). By comparison, the rods of the cat are similar in density when comparing the peripheral retina (250,000 cells/mm^2) to the area centralis (275,000 cells/mm^2); however, the density of the rods nearly doubles (460,000 cells/mm^2) along a zone surrounding the area centralis.[258] In the pig, cone density of the central retina is slightly greater than in that of the cat, being nearly 39,000 cells/mm^2.[285,286] Likewise, the cone population in the peripheral retina of the pig is greater than in the cat, being 6,700 cells/mm^2. Overall, in the pig, the cones in the area centralis are approximately four times more numerous than those located peripherally, and the rod–cone ratios range from 3:1 centrally to 16:1 peripherally.

In the young rabbit, cone density within the visual streak is approximately 18,000 cells/mm^2, falling off dorsally to 7000 cells/mm^2 and ventrally to between 10,000 and 12,000 cells/mm^2.[287] Rod density is greatest just dorsally to the visual streak, being 300,000 cells/mm^2.

The distribution curves of rods and cones of many nonprimates are essentially the same as those in primates, with the main difference being quantitative.[284,288] In general, animals with foveas and well-developed areas centralis or visual streaks, including fish, reptiles, birds, squirrels, ungulates, carnivores, and primates, are essentially diurnal or arrhythmic.[2] True nocturnal species possess rod-dominant retinas

Table 2.21 Photoreceptor Densities and Ratios of Selected Vertebrates

Animal	Rod Peak Density (cells per mm^2)	Cone Peak Density (cells per mm^2)	Rod–Cone Ratios of Central Retina	References
Toad	21,000	25,000	1:1.2	441
Rabbit	300,000	18,000	>15:1	442
Snake[a]	None	20,000	N/A	301
Cat	460,000[b]	27,000	>10:1	284
Monkey	184,000[c]	141,000[d]	15–30:1[e]	443
Human	150,000[f]	199,000[d]	—	444
Tree Shrew	3,500[g]	36,000[h]	1:>10	445
Pig	162,000[b]	26,000	>5:1	286

[a]The garter snake possesses pure-cone retina.
[b]Region surroundingvea the area centralis.
[c]4- to 5-mm dorsal to the fovea.
[d]At the fovea.
[e]3- to 15-mm eccentricity.
[f]At the elliptical ring.
[g]At the inferior retina.
[h]At the inferior retina but not at the same location as the peak cone density.

lacking cone-rich centers. Predaceous birds can have two foveas, a principal central fovea and a shallower temporal fovea, except in eagles, in which the temporal is deepest. The central foveas provide enhanced lateral viewing for these animals, whereas the temporal foveas provide straight-ahead projection, enhancing their binocular field (Fig. 2.154).[289]

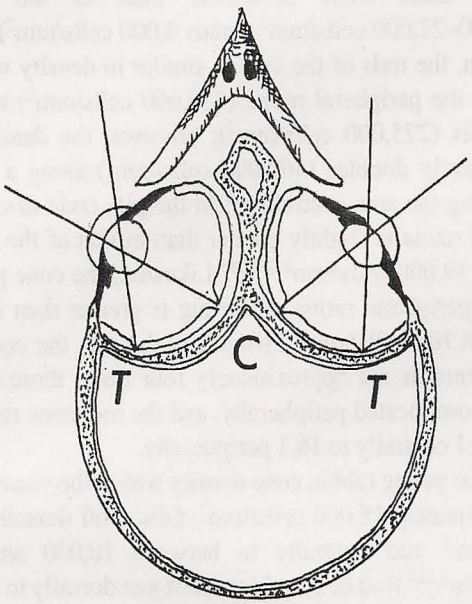

Figure 2.154. The foveal arrangement in the swallow, which possesses two fovea within each eye: one located temporally (*T*) for binocular vision and one located centrally (*C*) for panoramic vision. (Redrawn from Duke-Elder S. *System of Ophthalmology. Vol I. The Eye in Evolution.* London: Henry Kimpton, 1958.)

Visual Cell Layer (Rod and Cone Layer)

The visual cell layer actually contains only the outer parts of the photoreceptors known as the inner and outer segments, with their nuclei being in the outer nuclear layer. These segments, which are cylindrically to conically shaped, are closely packed together, side by side, and they are arranged radially, being parallel to incoming light through the pupil (Fig. 2.155). The segments react to the stimulation of light and initiate the mechanism of vision as well as the reflexes associated with it.

The rod outer segments are slender and are more sensitive than cones are to light. Rods function more effectively in low illumination (i.e., scotopic vision) and are inactivated by constant bright light; thus, they are well suited for night vision. On the other hand, they have less resolving power and produce a considerably lower visual acuity (i.e., sharpness). Cones are useful for vision during daylight (i.e., photopic vision) and can rapidly adapt to repeated stimuli, but they are less sensitive to light and therefore do not respond to low light levels.

The outer segments of the rods and cones are composed of stacks of membranous discs surrounded by the cell membrane. The rods form stacks of uniform width through their length and are longer than the cone outer segments (Figs. 2.155 and 2.156). The cone outer segments also consist of stacks of discs, but these segments are wider at their inner end, producing a cone shape (Fig. 2.157). In the area centralis, the cones are longer and more slender; nevertheless, they are easily distinguished from the rods (Fig. 2.155). The discs are actually flattened spheres. They consist of two membranes that are continuous at their ends and, in rods, are separate from the cell membrane as well as the adjacent discs.[32,290]

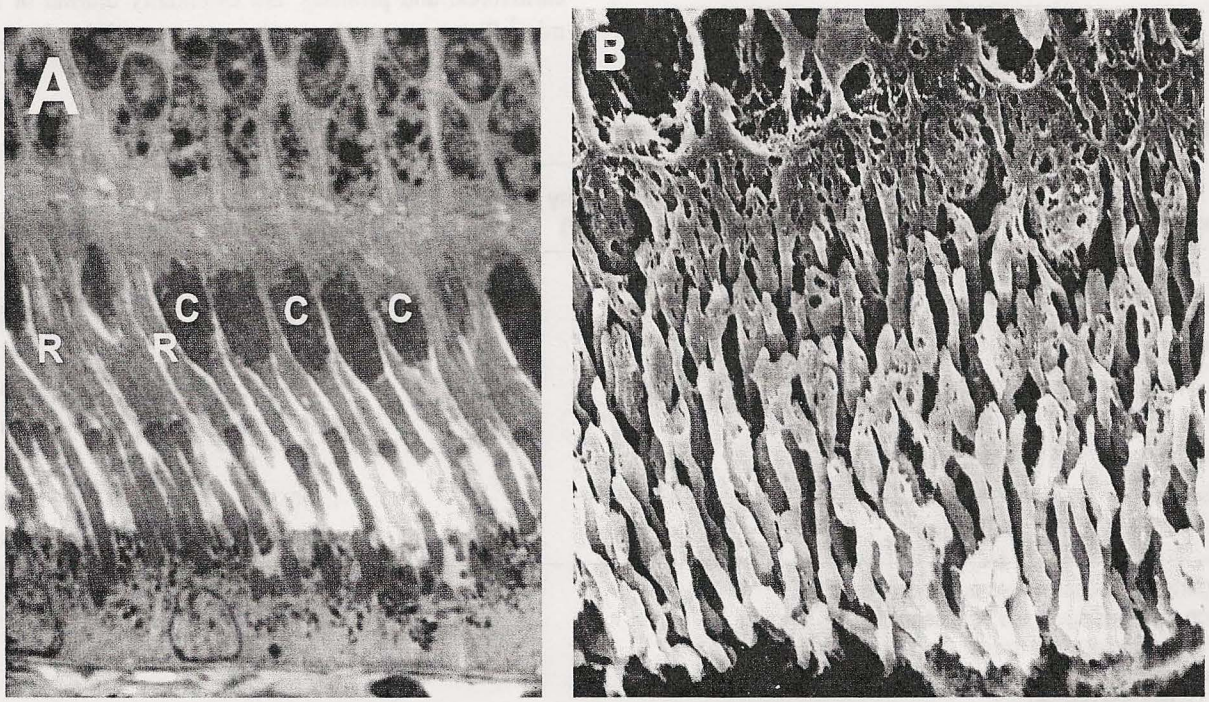

Figure 2.155. **A.** The visual cell layer of the pig contains many cones (*C*) among the rods (*R*) within the area centralis, making this animal well suited for day vision. (Original magnification, X400.) **B.** SEM shows the visual cell layer of the canine central retina contains mostly rods, with only scattered cones. Note that the rods are uniform in width throughout their length. (Original magnification, X2500.)

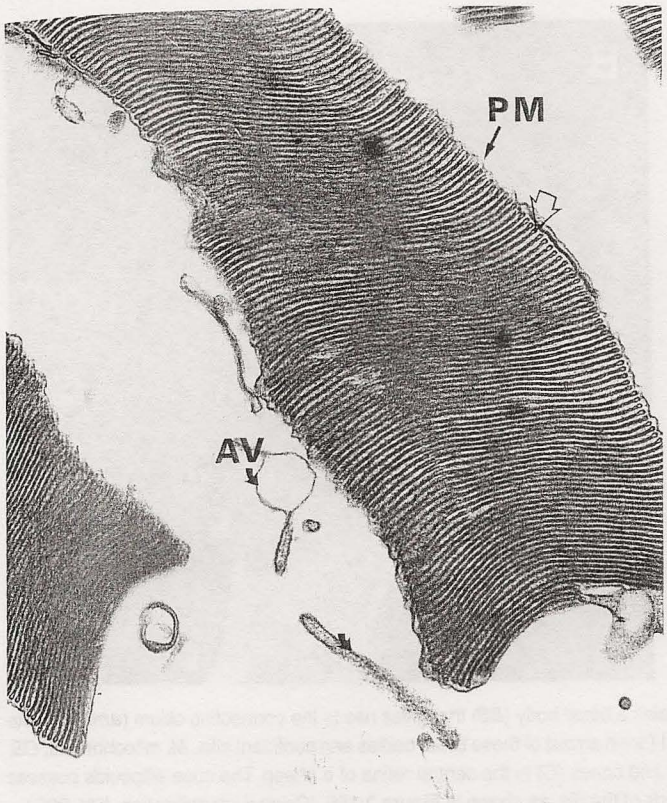

Figure 2.156. Tip of the outer segment discs in a rod of a young dog. Note that the discs or lamellae are separated from each other as well from as the plasma membrane (*PM*). The intralamellar space is slightly dilated at their periphery (*arrow*). Apical villi (*AV*) of pigmented epithelium are found between outer segments. (Original magnification, X54,000.)

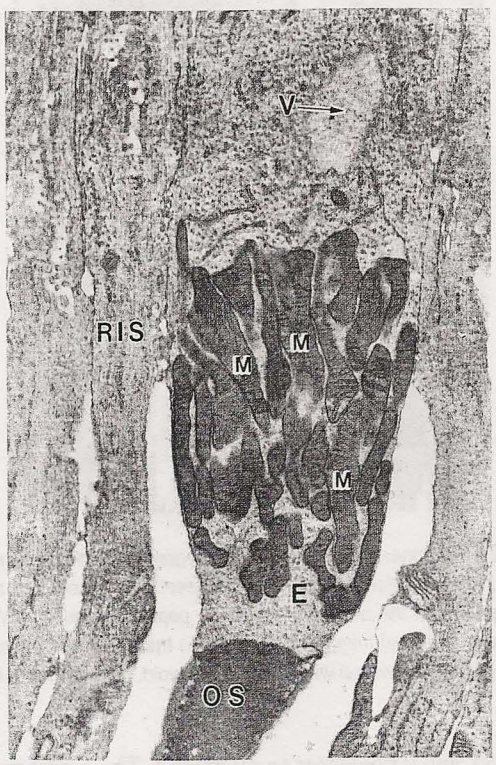

Figure 2.157. Inner portion of the outer segment (*OS*) and adjacent inner segment of a porcine cone. *E,* ellipsoid; *M,* mitochondria; *RIS,* rod inner segment; *V,* vitreal portion. (Original magnification, X10,000.)

In some mammalian cones, the proximal discs have continuity with the cell membrane, but it is uncertain how accurate this generality is among mammals.[290] Nevertheless, this invagination of the cell membrane, which forms the disc lamellae, constitutes the major morphologic difference between rods and cones.[291]

Within each mammalian cone outer segment, the discs contain one of three photopigments, which are sensitive to one of three different wavelength ranges. Birds, by comparison, possess four or even five classes of cone photopigments.[292] Four photopigments can detect essentially the same range of spectral bands that primate photopigments can sense (i.e., the colors red through violet). In addition, a fifth pigment has also been found, having its peak sensitivity in the near-UV portion (approximately 370 nm) of the light spectrum.[293]

The rod and cone outer segments are connected to the inner segments by a cilium, the basal body of which is in the distal inner segment (Fig. 2.158A). The cilium extends for a variable distance into the outer segment.

The outer portion of the inner segment is filled with long, tubular mitochondria and is termed the *ellipsoid* (Figs. 2.157 and 2.158B). Distally within the ellipsoid and to one side is the basal body, or one of a pair of centrioles, that gives rise to the connecting cilium. Rootlets with striations extend toward the vitreous body in the inner segment from the basal body. The cone ellipsoid is more broad and conical, and it contains more mitochondria than the rod ellipsoid. The outer rim forms a collar or calyx over the proximal portion of the outer segment.[32,104,290]

In the avian cone ellipsoid, a large oil droplet separates the numerous mitochondria from the connecting cilium (Fig. 2.159A). The appearance of this droplet may vary according to the species and type of cone.[294,295] The function of the oil droplet has undergone considerable speculation, and since the nineteenth century, it has been thought to serve as a light filter, allowing only specific wavelengths to be transmitted to the outer segment.[296,297] In diurnal birds, they are colored red, orange, yellow, yellowish-green, or green, whereas in crepuscular or nocturnal birds, they are pale yellow or colorless.[298,299] Because the entire visible spectrum cannot be absorbed by the different colored droplets, however, especially in the red spectrum, it has been proposed that the oil droplets enhance contrast and increase the number of object colors that can be discriminated, which in turn increases resolution and visual acuity.[1,300] The occurrence of oil droplets within the cone inner segments is widespread throughout vertebrates, including amphibians, reptiles, and nonplacental mammals.[4] In the snake (American garter), individual large oil droplets do not exist; instead, microdroplets are formed that lie next to mitochondrial cristae within the ellipsoid.[301] These microdroplets may be an adaptation for a small eye and act collectively as a single oil droplet.

The vitreal or inner portion of the inner segment is called the myoid in lower vertebrates because of the presence of myofilaments and contractile properties.[32,104,290] Although there is an absence of contractile structures in higher animals,

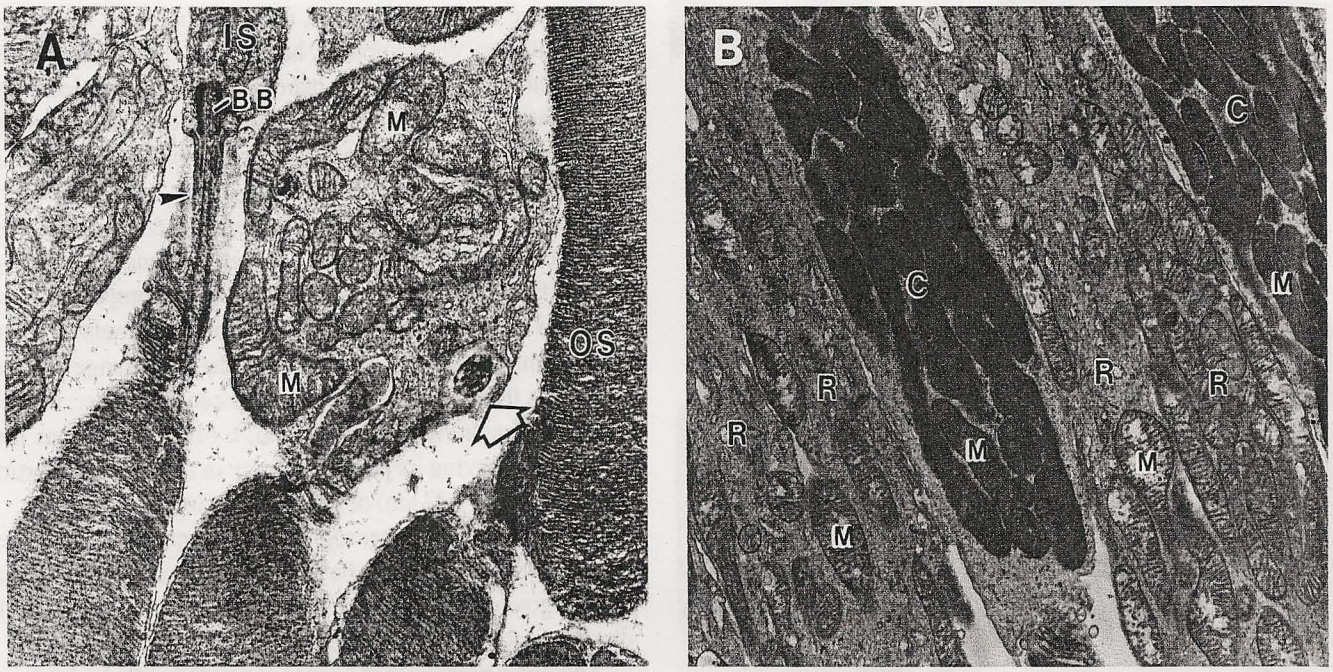

Figure 2.158. A. The outer portion of a rod inner segment (*IS*) of a dog contains a basal body (*BB*) that gives rise to the connecting cilium (*arrows*). Note the oblique plane of an adjacent inner segment reveals the peripheral placement (*open arrow*) of these basal bodies and confluent cilia. *M,* mitochondria; *OS,* outer segment. (Original magnification, X18,000.) **B.** The ellipsoids of rods (*R*) and cones (*C*) in the central retina of a sheep. The cone ellipsoids possess more mitochondria (*M*) than that of rods and are narrower than the cone ellipsoids of the pig, as shown in **Figure 2.156.** (Original magnification, X11,000.)

the term myoid is often used for this portion of the inner segment. The vitreal inner segment contains few mitochondria in rods and is relatively void of mitochondria in cones. The cytoplasm mostly consists of smooth and rough endoplasmic reticulum, free ribosomes, Golgi apparatus, small vesicles, and microtubules, and it is the principal site of protein synthesis. In the pig, the vitreal portion of cones also may contain a fairly prominent vesicle (Fig. 2.157). In the avian myoid, there is an area filled with glycogen, called the hyperboloid, that is best recognized light microscopically through use of histochemical localization (Fig. 2.159).

Rod and cone inner segments are separated from each other by long, villous extensions of Müller cells, which are called fiber baskets. These fiber baskets are virtually identical morphologically among the vertebrate species, but they are less numerous in retinas with intraretinal vasculatures (Fig. 2.160).[302] It has been hypothesized that these cell processes may serve to keep the extracellular portion of the visual cell layer dehydrated and thus help to maintain proper alignment of the outer segments.[303] These processes also most likely are involved in the exchange of metabolites with the RPE and help to provide a homeostatic environment for the outer segments.[304]

In addition to the rod and cone photoreceptors is a third class known as the double-cone photoreceptor, which is found in all vertebrate groups except placental mammals. The double cone consists of two closely associated, but separated, cone photoreceptors that differ in size, shape, and structure (Fig. 2.161). The significance of the double cone has yet to be determined, but it is the dominant photoreceptor in diurnal animals, occupying up to 82% of the retina at the inner segment level.[1,305] The chief cone of the double cone is the longer

Figure 2.159. Inner (*IS*) and outer (*OS*) segments of the photoreceptors in an owl. *Arrows* indicate oil droplets between the ellipsoid and adjacent outer segments in the somewhat sparsely populated cones. *ONL,* outer nuclear layer. (Original magnification, X3500.) **Insert.** Histochemical localization of glycogen (*arrows*) within the avian myoid. (Original magnification, X400.)

of the two, and it possesses an oil droplet. The accessory cone, on the other hand, lacks an oil droplet, having instead a conspicuous paraboloid (i.e., barrel-shaped body of glycogen). The presence of oil droplets in the accessory cone has been debated.[289,306]

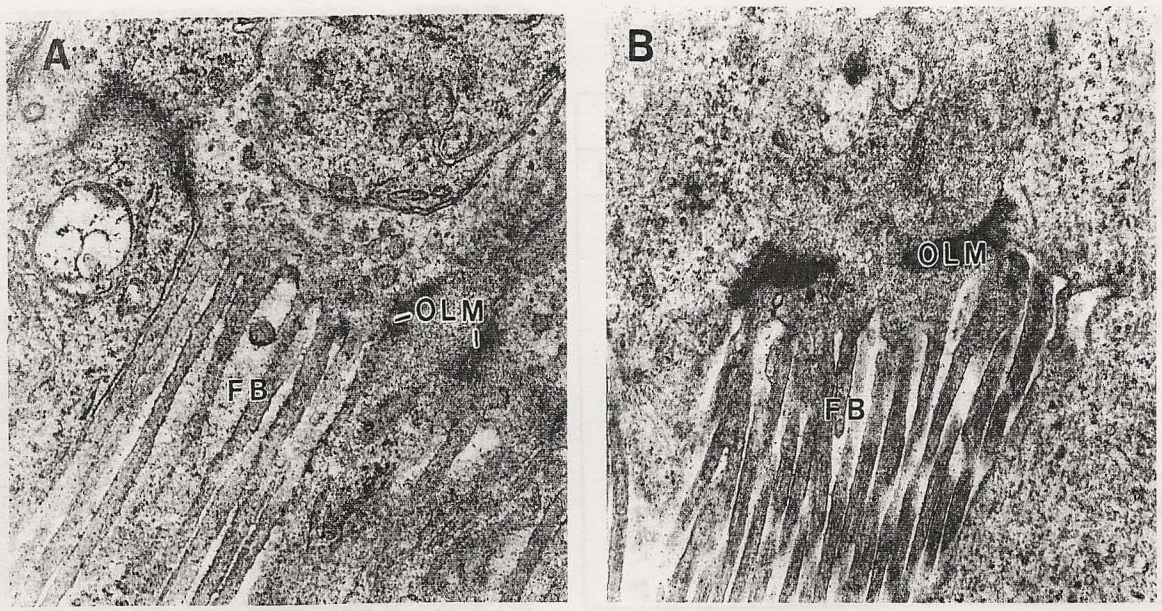

Figure 2.160. Long, villous extensions of Müller cells, known as fiber baskets (*FB*), occur ubiquitously in the vertebrate eye, as shown here in the dog (**A**) and the chicken (**B**). *OLM,* outer limiting membrane. (Original magnification: A, X35,000; B, X31,000.)

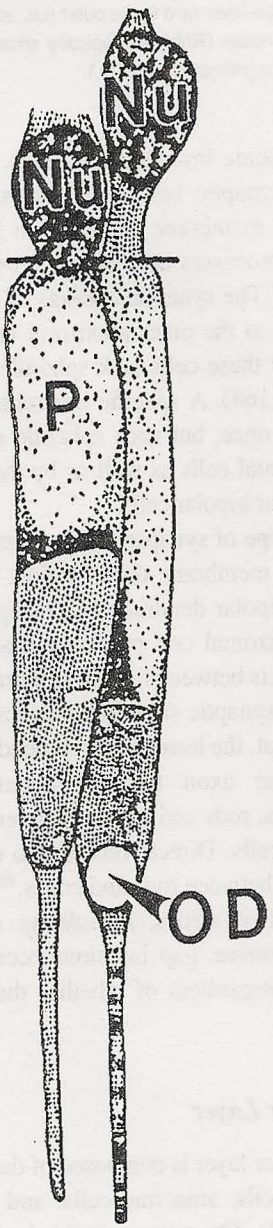

Figure 2.161. An avian double-cone photoreceptor. *Nu,* nucleus; *OD,* oil droplet; *P,* paraboloid. (Modified from Duke-Elder S. *System of Ophthalmology. Vol I. The Eye in Evolution.* London: Henry Kimpton, 1958.)

Outer Limiting Membrane

The inner segments of the visual cell layer are separated from nuclei of the photoreceptors by an extremely thin limiting membrane (Fig. 2.147). This membrane is actually composed of the densities of the cell junction, the zonular adherens, that firmly attach the inner segments of rods and cones to Müller cells and the Müller cells to each other (Fig. 2.160). The function of the external limiting membrane is to some degree speculative. In addition to holding the outer retina together, the external limiting membrane, because the rods and cones largely do not contact each other directly, most likely forms a barrier between the visual cell layer extracellular spaces and the rest of the sensory retina. Viewing the outer or external limiting membrane with light microscopy is enhanced by a partial constriction of each photoreceptor at the vitreal end of the myoid. These constrictions may help to maintain the location of the photoreceptor nuclei away from the highly metabolic inner segments, thus reducing the potential for oxidative injury.

Outer Nuclear Layer

This layer contains the soma or cell bodies of the photoreceptors. The number of rows of nuclei varies greatly according to species and location in the retina. In the central retina, the dog and cat possess the greatest depth of rows (12–15 and 19–20, respectively), whereas ungulates have fewer rows (5 in the horse and pig, 10 in the cow) (Table 2.22). The outer nuclear layer gradually thins in the peripheral retina as the density of rods and cones decreases. Cone nuclei are universally situated

Table 2.22 Rows of Nuclei in the Outer Nuclear Layer of Different Vertebrates

		Peripheral Retina	
Animal	**Central Retina**	**Dorsal**	**Ventral**
Mouse	12–16	10–12[a]	8–10[a]
Squirrel	2–3	2[a]	2–3[a]
Ferret	3–4	3[b]	3[b]
Ranch mink	8–10	6–8[b]	6–7[b]
Dog	10–15	8–9[b]	8–10[b]
Cat	12–18	8–10[b]	8–10[b]
Pig	5–6	3–4[b]	3–4[b]
Cow	8–10	3–4[c]	3–4[c]
Horse	4–6	3–4[c]	3[c]
Great-horned owl	3–4	2[b]	2[b]
Cormorant	3	2[b]	2[b]

[a]Measurements taken 0.5 mm from ora ciliaris retinae.
[b]Measurements taken 1.0 mm from ora ciliaris retinae.
[c]Measurements taken 2.0 mm from ora ciliaris retinae.

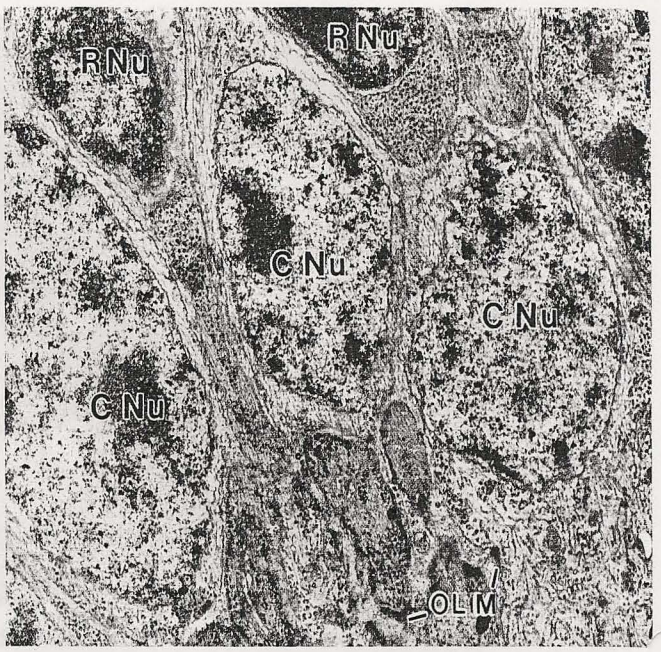

Figure 2.162. Within the outer nuclear layer of a sheep, cone nuclei (*CNu*) form a single layer next to the outer (i.e., external) limiting membrane (*OLM*). The rod nuclei (*RNu*) are typically smaller and more heterochromatic. (Original magnification, X6500.)

next to the external limiting membrane. In mammals, they are usually larger, oval, and more euchromatic (i.e., staining lighter) than the rod nuclei (Figs. 2.147 and 2.162). Rod nuclei are smaller, round to oval, darker, and more heterochromatic.

Additional structures in this layer are outer rod and cone connecting fibers, rod and cone axons, and Müller cell processes. The rod and cone connecting fibers are continuations of the inner segments to their origin from their respective nuclei. The axons of the rod and cone nuclei extend into the outer plexiform layer to synapse with horizontal and bipolar cells.

Outer Plexiform Layer

The outer plexiform layer consists of the terminal arborizations of rod and cone cell axons that synapse with the dendrites of horizontal and bipolar cells (Figs. 2.146 and 2.147). The rod axons typically end in pear-shaped spherule structures, whereas those of the cones end in larger, broader pedicles (Fig. 2.146). The rod spherule has one or more invaginations at which ribbon synapses occur, whereas the cone pedicle has numerous, more shallow invaginations of ribbon synapses (Fig. 2.163). The cone pedicles usually extend further vitreally into the outer plexiform layer.[32,258,290,307]

In the invagination of the synaptic expansion are two deeply inserted, horizontal cell processes (i.e., telodendrites) laterally and one or more bipolar cell processes centrally (Figs. 2.146 and 2.163). The synaptic contacts in the invagination are ribbon synapses. Within the presynaptic spherule at the site of synaptic contacts is a dense lamellar structure, the synaptic ribbon, which is oriented perpendicularly and close to the cytoplasmic invaginations (Figs. 2.163 and 2.164). A rim of clear synaptic vesicles envelops the synaptic ribbon, and increased membrane densities on both presynaptic and postsynaptic processes are usually present (Figs. 2.163 and 2.164).[32,308,309] The synaptic endings of rods that lie immediately adjacent to the outer plexiform layer occur within the soma, because these cells lack spherule-shaped axons (Figs. 2.163A and 2.164). A specific horizontal cell will contact a spherule only once, but each spherule may be contacted by several horizontal cells as well as by the dendritic processes from one to four bipolar cells.

A second type of synapse in this layer is flat and only distinguished by membrane densification. This process occurs between flat bipolar dendrites and receptor axons (i.e., cone pedicles). Horizontal cell processes may have conventional synaptic contacts between bipolar cell processes, and they can have both postsynaptic sites and presynaptic sites along their length. In the cat, the horizontal cell dendrites synapse only to cones, and the axon terminal connects exclusively to rods.[310,311] Thus, rods and cones are interconnected primarily by horizontal cells. Direct contact also exists between adjacent cones and between rods and cones.[309,312,313] For example, in two species of turtles, *Pseudemys scripta elegans* and *Chelydra serpentina,* gap junctions occur between adjacent cone pedicles regardless of whether they are red cones or green cones.[314]

Inner Nuclear Layer

The inner nuclear layer is composed of the soma of horizontal cells, bipolar cells, amacrine cells, and Müller cells (Figs. 2.146 and 2.147). The neurons in this layer maintain connec-

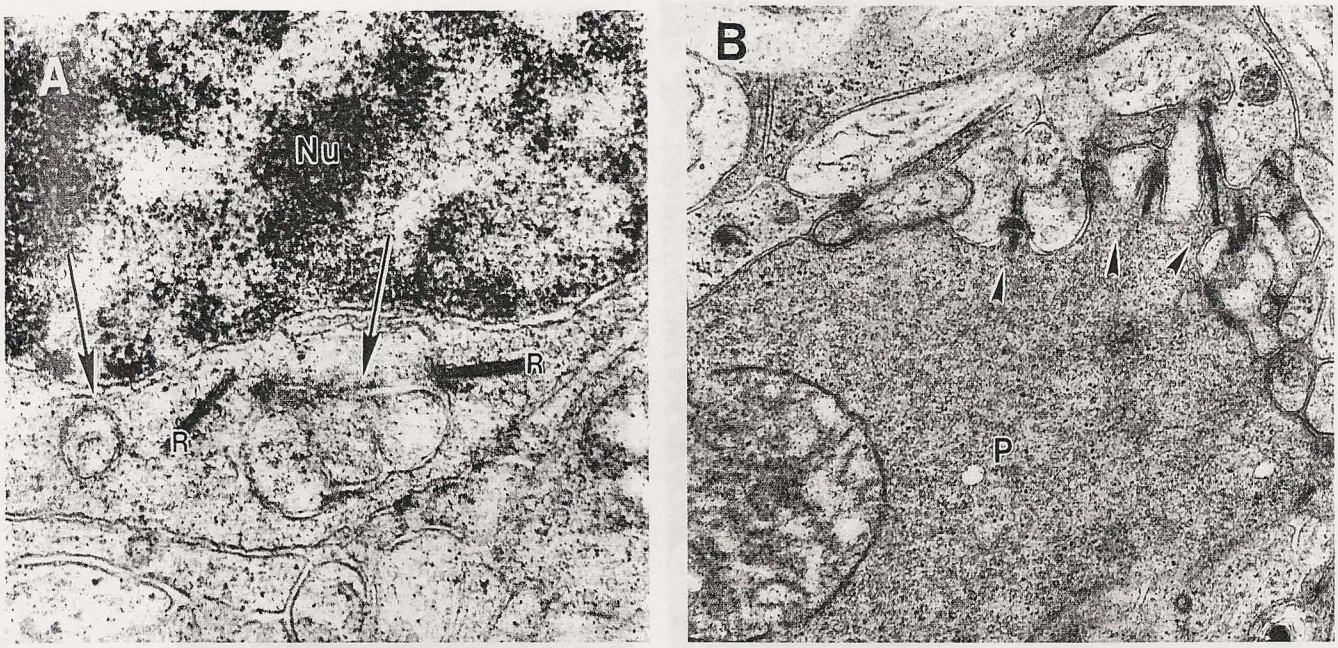

Figure 2.163. Synaptic ends of photoreceptors in the dog. **A.** Rod termination consists of a spherule, which has two invaginations (*arrows*) present adjacent to synaptic ribbons (*R*). *Nu,* nucleus. (Original magnification, X50,000.) **B.** Cone termination consists of a pedicle (*P*), which contains numerous invaginations (*arrows*) and associated ribbons. (Original magnification, X28,000.)

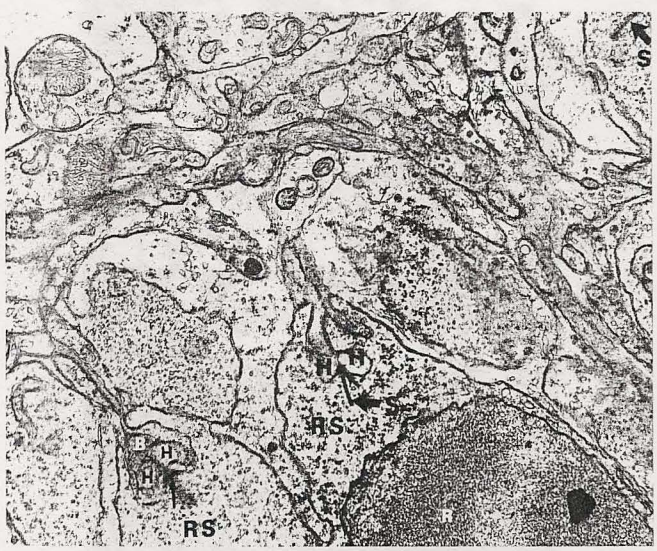

Figure 2.164. Outer plexiform layer of the cat. Synaptic vesicles fill spherules, and the *small arrows* point to an arciform density. *B,* bipolar cell process; *H,* horizontal cell process; *R,* rod nuclei; *RS,* rod spherules; *S,* ribbon synapse in rod spherule with synaptic ribbon. (Original magnification, X22,500.)

tions between the visual cell layer and the ganglion cell layer. These cells, which include the horizontal, bipolar, and amacrine cells, are involved in modification and integration of stimuli.

The horizontal cell nuclei are positioned along the outermost margin of the inner nuclear layer, whereas the amacrine cells are positioned along the innermost margin (Fig. 2.165). These two cell types have ramifying branches in their respective plexiform layers and act as integrating units. The bipolar nuclei and Müller cell nuclei compose the intermediate zone of the inner nuclear layer.[32,258,303]

Two types of horizontal cells have been identified in most vertebrates, small field and large field, but reports conflict regarding their connections and whether an axon is present. An axonless horizontal cell, known as type A, has been documented in several mammalian species synapsing with all kinds of cones.[315,316] In the second type, type B, it is generally believed that the dendritic endings of this horizontal cell synapse with the same cone pedicles as type A but that the cell has an axon as well, which synapses with rod spherules.[310] A third type, which also has an axon, is known to exist in the human retina.[317] The nuclei of horizontal cells are large, with a single, prominent nucleolus. The cells are also characterized by their wide, horizontally oriented cell processes.

In artiodactyl retinae, the externally positioned horizontal cells correspond to the A-type (axonless) cells in other mammalian species and have a delicate dendritic tree, while the more internally positioned horizontal cells correspond to the B-type cells and have single axons but with a more developed, robust dendritic tree.[318]

In the rabbit, the two horizontal cell types (i.e., types A and B) can be distinguished by use of different dyes.[319] Type B, which is slightly smaller (diameter, 100 μm) than type A (diameter, approximately 120 μm), outnumbers type A in the area of the visual streak by nearly 2.5 to 1 (1375 cells/mm^2 versus 555 cells/mm^2).[319] Peripherally, both types dwindle in density, with type B remaining more populated (400 cells/mm^2 versus 250 cells/mm^2). In the tree shrew, which has a retina that consists of 95% cones, the density of type B horizontal cells is up to three times as numerous as type A at any

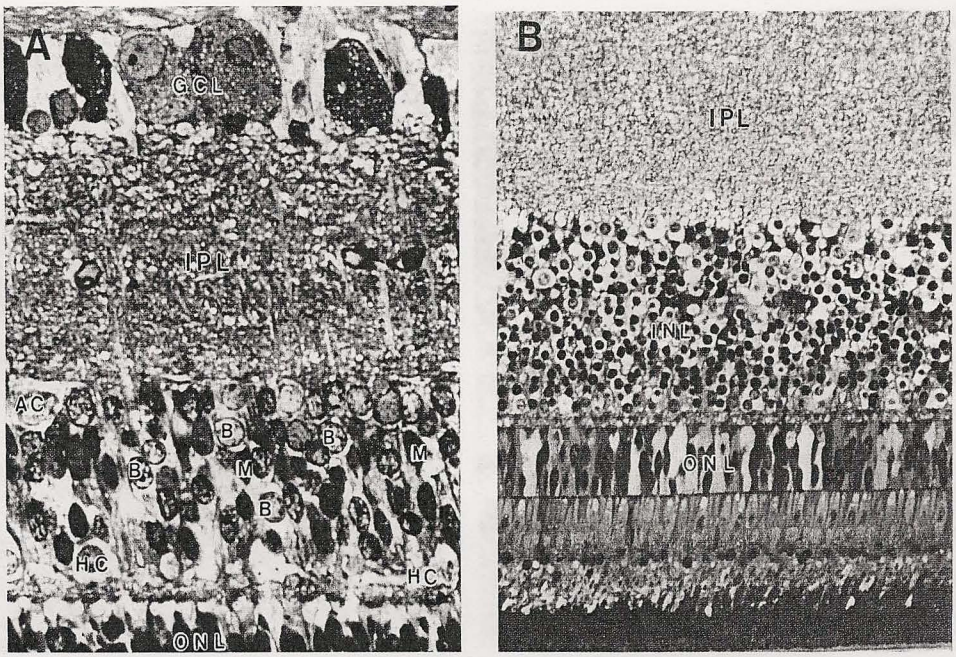

Figure 2.165. Inner nuclear layer and inner plexiform layer (*IPL*) of a pig (**A**) and a chicken (**B**). *AC,* amacrine cell; *B,* bipolar cell; *GCL,* ganglion cell layer; *HC,* horizontal cell; *M,* Müller cell; *ONL,* outer nuclear layer. (Original magnification: A, X100; B, X200.)

location within the retina.[320] In horses and related species (i.e., *Equus caballus, E. asinus, E. grevy*), type B horizontal cells outnumber type A by from 5:1 to 10:1.[321] Type A horizontal cells of equids are unusual among mammals in that they have very large dendritic fields. Their dendrites, which are fine and sparsely branched, appear to contact cones selectively, specifically blue cones, which comprise 10% to 25% of the cone population (Fig. 2.166). In the horse, type B cell densities range between 500 and 900 cell/mm^2 within the visual streak, being greater than 1000 cells/mm^2 in the area centralis, which is at the temporal end of the visual streak.[321] The density of type B cells drops sharply away from the visual streak to between 100 and 300 cells/mm^2. By comparison, type A cell density is between 50 and 100 cells/mm^2 within the visual streak and from 15 to 45 cells/mm^2 peripherally.

The bipolar cell is the second-most numerous neuron in the retina of most domestic animals, and it constitutes the radial connection between the photoreceptors and the ganglion cells. In cone-rich retinas, the numbers of bipolar cells increase remarkably, as do those of amacrine cells (Fig. 2.164B). Being radially oriented, their dendritic processes in the outer plexiform layer synapse with photoreceptors and horizontal cells, and their axonal processes terminate in the inner plexiform layer synapse with amacrine and ganglion cells (Fig. 2.146). Bipolar cells are subdivided according to their shape on the basis of Golgi impregnation staining and other selective labeling procedures, type of synaptic connections with photoreceptors, and axonal endings within the inner plexiform layer. Among mammalian retinas, the inner nuclear layer houses the somata of a single type of rod bipolar cell and a variety of cone bipolar types.

In the dark, a light signal is conventionally passed from a rod synapse onto a rod bipolar cell, which then contacts an amacrine (AII) cell that separates the signal into on and off pathways through synaptic activity with cone bipolar cells. These cells synapse with their respective ganglion cells, which move the on and off signals to the visual centers within the CNS. Consequently, rod bipolar cells (i.e., mop bipolar cells) apparently connect only with rod spherules and then

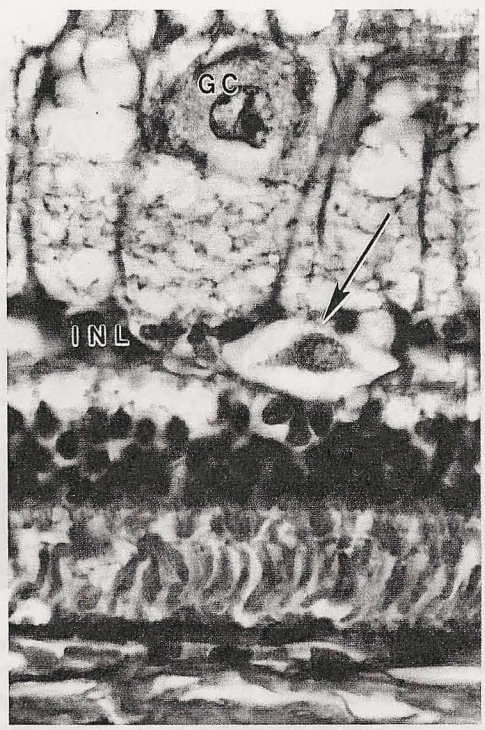

Figure 2.166. The equine retina has thin, inner nuclear layer (*INL*) with widely dispersed, large horizontal cells (*arrow*), some of which span the entire thickness of the INL. *GC,* ganglion cell. (Original magnification, X400.)

synapse with amacrine cells in the inner plexiform layer. These bipolar cells, which synapse with many rod spherules, do not synapse directly with ganglion cells. Among many species, the distribution of rod bipolar cells in the retina generally parallels the distribution of rod photoreceptors, which in the rabbit are greatest along the dorsal and ventral margins of the visual streak and area centralis, at densities of 5000 to 7000 cells/mm^2.[322] Overall, the density ratio of rods to rod bipolar cells varies little throughout the rabbit retina, ranging from 43:1 dorsally to 58:1 ventrally.

Cone bipolar cells, by comparison, can be divided into many types, consisting of 11 in the cat and 9 in both the rabbit and monkey.[319,323–326] Flat, diffuse bipolar cells synapse with several cones, whereas midget bipolar cells, which are of two types, invaginating and flat, synapse with cones singly. All cone bipolars can synapse with ganglion cells and amacrine cells in the internal plexiform layer. In some instances, cone bipolar cells can be presynaptic to rod amacrine (i.e., type AII) cells (i.e., narrow-field bistratified), as previously described[327]; as a result, certain bipolar cells are also part of the rod pathway because they receive input from rod-associated amacrine cells. The pattern of axonal arborization of the cone bipolar cells can vary considerably from one type to another. Axonal endings may occupy one or more specific strata within the inner plexiform layer.[327] The cytoplasm of bipolar cell axons can be identified ultrastructurally by their microtubules, and their nuclei are slightly smaller and more osmiophilic than those in horizontal cells (Fig. 2.167). For the most part, cone bipolar cells have narrow dendritic and axonal fields, which would be expected in radial transmission of information for high-spatial resolution. Nevertheless, a small population (<1% of the total population) of bipolar cells in the rabbit has dendritic arbors that spread across an area 50 to 200 5m in diameter.[328] Even so, the dendrites largely end at a common point in the outer plexiform layer, as do the axonal arbors within the inner plexiform layer. In this way, the entire population of this bipolar cell spatially links the outer and inner portions of the retina.

In rod-dominant retinas such as those of the rat, it has been assumed that cone bipolar cells form a relatively small portion of the inner nuclear layer. Results of immunocytochemical identification of cone bipolar cells in the rat retina, however, have shown that at least 50% of all bipolar cell are cone bipolar cells.[329] Since the photoreceptors of the rat retina are composed of approximately 99% rods, it would appear that cone bipolar cells function in a more substantial way than previously believed. In addition to the conventional route for scotopic vision previously described, a pathway involving direct contacts between rods and off cone bipolar cells can occur, but most likely varies in amount considerably from one species to another.[330]

In the nonmammalian retina of the Reeves' turtle (*Geoclemys reevesii*), nearly one quarter of the total bipolar cell population is dislocated within the outer nuclear layer, thus forming its most proximal layer.[331] As further examination of bipolar cells from other mammalian and nonmammalian retinas are made, new types and their respective roles will undoubtedly be discovered.

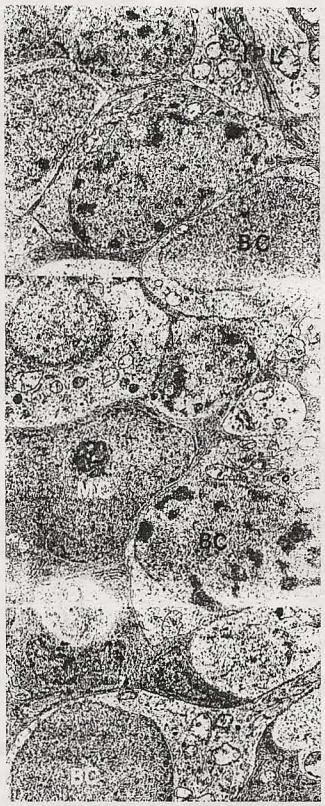

Figure 2.167. Collage of a canine inner nuclear layer. Bipolar cells (*BC*) form the largest population of neurons in this layer, being heterogenous in appearance and having euchromatic to somewhat heterochromatic nuclei. Müller cells (*MC*), which are fewer in number, are next to the bipolar cells. *IPL*, inner plexiform layer. (Original magnification, X10,100.)

Traditionally, the amacrine cell has been described as a neuron without an identifiable axon, whose processes terminate in the region of the inner plexiform layer.[290] Ultrastructural studies have, in fact, demonstrated that these neurons are of the pseudounipolar type, having axons with the characteristic synaptic vesicles but also having features in common with dendrites.[303] The amacrine cells are located vitreally in the inner nuclear layer, and they are recognized by occasional, indented euchromatic nuclei (Figs. 2.165 and 2.168). Their cytoplasm is more copious than that of bipolar cells, being filled with polysomes and rough endoplasm reticulum (i.e., Nissl bodies), mitochondria, neurofilaments, and tubules. Collectively, amacrine cells provide horizontal integration in the inner plexiform layer between bipolar cell terminals, ganglion cell dendrites, and other amacrine cells (Fig. 2.146).

Amacrine cells are categorized on the basis of the distribution of their axonal processes, which results in two major classes: diffuse and stratified. In addition, numerous basic types or subclasses of amacrine cells (up to 24 in the human retina and 27 in the squirrel) have been described on the basis of the degree of branching and stratification as determined by selective staining.[309,332] Diffuse amacrine cells have been subdivided on the basis of the size of their axonal fields into narrow- and wide-field types,[311,333] and their processes typically

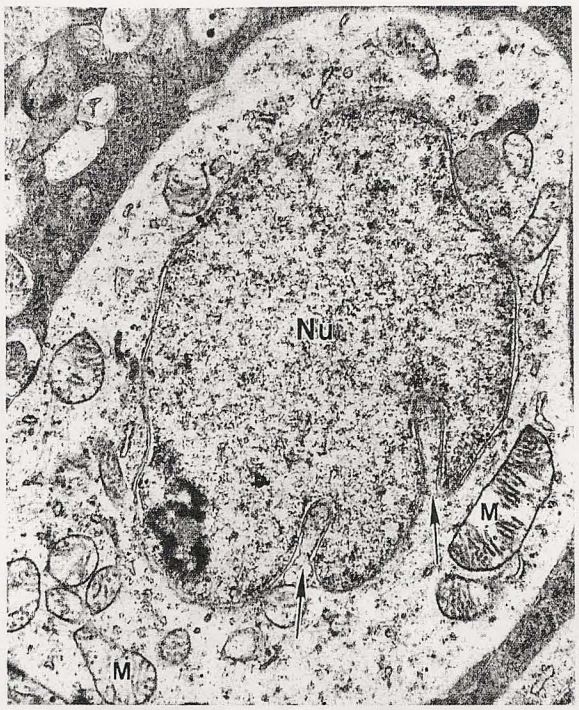

Figure 2.168. The amacrine cell of a dog possesses round, euchromatic nucleus (*Nu*) with occasional indentations (*arrows*) and a moderate amount of cytoplasm. *M,* mitochondria. (Original magnification, X14,000.)

extend throughout the entire thickness of the inner plexiform layer. Among the different types of diffuse amacrine cells known is a wide-field type (also referred to as narrow-field, or bistratified) that contacts both rod bipolar cells and ganglion cells (i.e., the rod [A17] amacrine cell).[334] Stratified amacrine cells, on the other hand, have been categorized primarily by the location of the layers in which their processes lie.[335,336] For example, certain types extend their processes to the outermost portion of the inner plexiform layer.[337] Among the different types of stratified amacrine cells is one that also contacts both rod bipolar cells and ganglion cells, and this is categorized as narrow-field, bistratified (i.e., rod [AII] amacrine cell). It is interesting to note that in certain photopic animals, such as the ground squirrel, the AII amacrine cell is not evident, suggesting the strong functional diversity of amacrine cell populations according to the dominance of rods versus cones among mammalian retinas.[338]

In addition to the different morphologic types, physiologic differences can also be correlated.[337,339] Over 30 different types of neurotransmitters exist within the synaptic processes of amacrine cells, including glycine, dopamine, taurine, acetylcholine, γ-aminobutyric acid, and a variety of neuropeptide substances, and those providing excitatory and inhibitory responses.[309]

More recently, a new type or population of amacrine cells was found in the ganglion cell layer of the retina and appropriately named the displaced amacrine cell.[339–341] Most amacrine cells of the peripheral cat retina consist of this type.[340] In the squirrel (*Spermophilus beecheyi*), three types of displaced amacrine cells occur, forming mirror-image pairs across the inner plexiform layer with similar amacrine cells within the proximal portion of the inner nuclear layer.[332]

In addition to the horizontal cell, bipolar cell, and amacrine cell, there is a fourth neuron of the inner nuclear layer, called the interplexiform cell, that is not found in all retinas.[309,332,342] This neuron, which is observed in the innermost zone of the inner nuclear layer, has both pre- and postsynaptic processes in the inner plexiform layer and presynaptic connections with horizontal and bipolar cells via a long horizontal process extending to the outer plexiform layer. As a result, it provides a feedback mechanism from the inner retina to the outer synaptic layer.

With the advent of immunohistochemical procedures, the intricate circuitry of the inner retina is now being explored in the rabbit, cat, and other species.[339,343,344] As specific associations between the different types of amacrine cells and those they contact (i.e., bipolar and ganglion cell populations) continue to be made, a clearer understanding of the visual-related events occurring among neurons of the inner nuclear layer, including the roles they play in the rod and cones pathways and ganglion cell directional selectivity, is possible.

Müller cells (radial glial cells) are the principal nonneuronal cell of the vertebrate retina and serve as supportive cells for most neurons in the retina. They tend to have more cytoplasm and to lie in the outer portion of the inner nuclear layer. Müller cells are elongated, branching cells that extend from the internal limiting membrane to beyond the external limiting membrane. They are important for internal structural support as well as for nutrition of the retina. Müller cell fibers fill almost all the extracellular space between neural cells. In both the outer nuclear and ganglion cell layers, Müller cells form close contacts to the neuronal somata, entirely encasing them, compared with the neuronal somata of the inner nuclear layer, which are only partially wrapped.[345,346] Their nuclei are angular and have denser chromatin than other nuclei in the inner nuclear layer (Fig. 2.167). In animals with an intraretinal vascular system, the outer processes are scanty in cellular cytoplasmic organelles and light-staining, whereas the inner fibers contain more numerous organelles. Numerous filaments are present, especially near the internal limiting membrane, and a very well-developed, smooth-surfaced endoplasmic reticulum is present.[302,347] The vitreal ends of the Müller cells possess end feet, which have the ability to phagocytize foreign substances and consequently may play an important role in normal retinal function.[348] The lateral sides of the end feet contain gap junctions, thus allowing these cells to transmit information throughout the retina.

In most animals, the Müller cell has a close spatial relationship with the blood vessels, indicating possible roles in the formation of the blood–retinal barrier, uptake of nutrients, and disposal of metabolites. In the rabbit retina, however, and quite possibly in retinas of other species, Müller cells do not contact blood vessels and may not participate in the blood–retinal barrier and transfer of metabolites.[345]

As a cell type within the vertebrate retina, the Müller cell is unique in that it consists of a single morphologic class or type.

These cells do vary in length according to the overall thickness of the retina, being shortest peripherally and longest centrally. Regarding their cell density, Müller cells have a neuronal-like distribution (Table 2.22). Peak density of the Müller cell occurs centrally in both the monkey (>30,000 cells/mm^2 parafoveally) and the rabbit (10,700–15,000 cells/mm^2 at the visual streak)[345,346]. In both the rabbit and monkey, Müller cell density drops considerably toward the periphery, to between 4400 and 6000 cells/mm^2 and 6000 cells/mm^2, respectively.

Inner Plexiform Layer

The inner plexiform layer is the synaptic region between the first- and second-order neurons, and it is notably thicker than the outer plexiform layer in all vertebrate retinas, especially those that possess fovea and well-defined area centralis (Figs. 2.146, 2.147, and 2.165). This layer comprises the cell processes of the inner nuclear and ganglion cell layers, at which synapses between bipolar, amacrine, and ganglion cells occur.

The bipolar cells synapse in ribbon synapses with two postsynaptic elements and hence are termed a *dyad.* The postsynaptic elements of the dyad consist of a ganglion cell dendrite and an amacrine process or two amacrine cell processes (Figs. 2.146 and 2.169). The predominant pairing is species variable, and in the cat, the rod bipolar terminals synapse only with the two types of amacrine cells previously mentioned. The cone bipolar cells synapse directly on a ganglion cell dendrite and an amacrine cell process, and the amacrine cells associated with rod bipolar cells act as internuncial neurons connecting with the ganglion cells.[308,349]

In addition to the ribbon synapses, abundant conventional synapses are present on the amacrine cells. These synapses involve bipolar terminals, ganglion cell dendrites, and other amacrine cells. Some act as reciprocal synapses back onto a bipolar terminal after participating in a dyad synapse (Fig. 2.169); thus, a single amacrine cell may connect presynaptically and postsynaptically to different areas of the same bipolar cell. In addition, serial synapses between two or more adjacent amacrine cell processes have been observed.[308] For example, in both the rabbit and cat, the rod narrow-field, bistratified amacrine cells are inserted in series along the rod pathway.[334]

The bipolar axons contain numerous synaptic vesicles and mitochondria, and they are the only structures to contain synaptic ribbons. The ganglion cell dendrites are the only processes in the plexiform layer without synaptic vesicles. They are pale, with smooth and rough endoplasmic reticulum, small mitochondria, and microtubules. The amacrine processes, which also are pale and possess large mitochondria and synaptic vesicles, are the most numerous because of the extensive arborization of their axons.

Aside from the neurochemical synapses, gap junctions occur between bipolar axons and ganglion somata as well as between rod AII amacrine cells and midget cone bipolar cells.[350] Functionally, the outer plexiform layer is organized to enhance static or spatial aspects to accentuate contrast in the retinal image. The inner plexiform layer appears to be concerned with temporal or dynamic activities, enhancing motion and direction responses.[308]

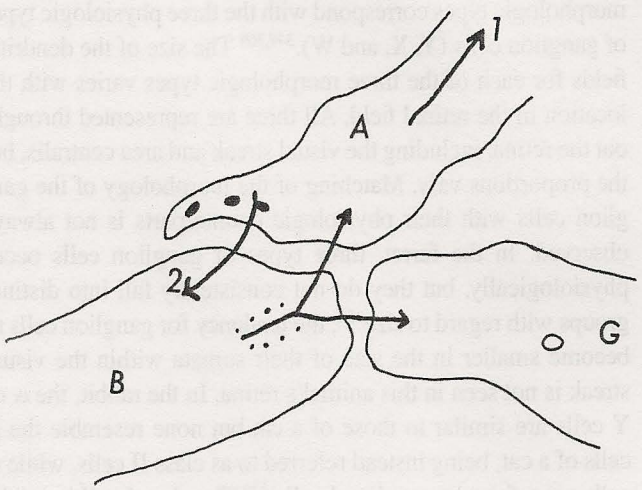

Figure 2.169. The bipolar–amacrine–ganglion cell interaction. The bipolar cell (*B*) projects onto both the ganglion (*G*) and the amacrine (*A*) cells. The amacrine cell controls or adjusts the bipolar cell in a negative feedback arrangement. *1,* further interactions; *2,* reciprocal inhibition. (Redrawn from Records RE, et al. Electrical signals of the retinal microcircuitry and the visual cortex. In: Duane TD, Jaeger EA, eds. *Biomedical Foundations of Ophthalmology. Vol. 2.* Philadelphia: JB Lippincott, 1988.)

Ganglion Cell Layer

The ganglion cell layer usually contains ganglion cells of three different types together with neuroglial cells and retinal blood vessels. It is the innermost cell layer of the retina and consists of a single layer of cells, except in the area centralis and visual streak, at which it can be two or three cell layers thick (except in primates and various nonmammalian animals, in which it can be six to nine cell layers thick) (Figs. 2.147, 2.165, and 2.170; Table 2.23).

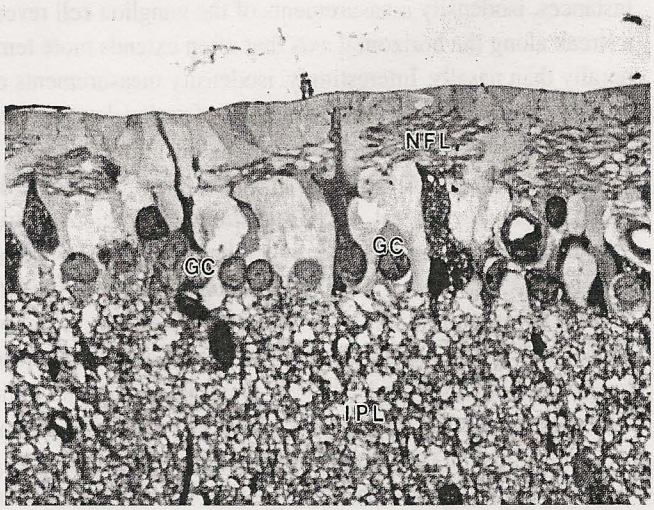

Figure 2.170. The ganglion cell layer of a pig is one or two cell layers thick at the paracentral retina. *GC,* ganglion cell; *IPL,* inner plexiform layer; *NFL,* nerve fiber layer. (Original magnification, X400.)

Table 2.23 Ganglion Cell Densities Within the Visual Streaks of Different Vertebrates

Animal	Ganglion Cell Density (per mm^2)	Description	Reference
Frog	3500	Weak, asymmetric streak located centrodorsally	364
Brush-tailed possum	5000	Horizontally positioned 0.6 mm above optic disc in tapetum, highest concentration near temporal end of streak	358
Honey possum	9000	At area centralis in midtemporal retina	358
Guinea pig	2300	Streak temporally located, 4–5 mm toward optic disc	363
Three-toed sloth	1500	Streak vertically oriented, with highest density in inferior temporal retina	362
Rabbit	5400	Prominent horizontal streak	360
	4700		345
Pigmented ferret	3300–4300	Prominent horizontal streak with highest density at area centralis	351
Dog	5300–13,000	Moderate to pronounced horizontal streak	353
	6400–14,400	extending temporally and nasally far from area centralis	356
Wolf	12,000–14,000	Pronounced horizontal streak	353
Horse	6500	Narrow horizontal streak slightly dorsal to optic disc with highest density temporally	357
Bottlenosed dolphin	670	At two spots: in nasal and temporal quadrants, 15–16 mm from optic disc	447

With measurement of isodensity lines of the ganglion cell within the retina, the occurrence of the visual streak and associated area centralis has been determined in many vertebrate species.[192,301,351,352] Animals with well-defined visual streaks include the cat, dog, wolf, ferret, horse, rabbit, chipmunk, squirrel, selected hysticomorph Amazonian rodents, brush-tail possum, lizard, snake, and birds.[301,352–360] Animals with less-defined visual streaks include nocturnal rodents (i.e., rat, mouse, and nocturnal paca), two-toed and three-toed sloths, elephant, koala, guinea pig, and anurans.[359,361–366] In most instances, isodensity measurements of the ganglion cell reveal a streak along the horizontal axis that often extends more temporally than nasally. Interestingly, isodensity measurements of different bat retinas reveal visual streaks of varied development similar to those found among other mammals (Table 2.23).[367]

Some variations of the shape and location of the streak do occur. In the dog and cat, the visual streak is more concentric than elongated.[356] In the horse, which has a narrow, elongated visual streak, the highest ganglion cell density occurs within its temporal portion, at which optimal resolution is believed to be restricted.[368] In the elephant, in addition to a concentration of ganglion cells along the horizontal plane inferior to the optic disc is another concentration of ganglion cells in the dorsal temporal retina, which may be an evolutionary adaptation enabling the animal to monitor its trunk.[361] Another unusual variation of the visual streak can be found in sloths.[362] In these animals, the visual streak is oriented vertically in the ventral temporal retina. The location of the visual streak may be an adaptation allowing the sloth to rotate uniquely its head 180 degrees while climbing upside down along horizontal branches.[362]

Three basic forms of ganglion cells have been described in the cat, and extensive research in the cat has related the morphology of these cells to their neurophysiology (see Chapter 4).[351] Boycott and Wassle[349] described α, β, and γ ganglion cells in the retina on the basis of dendritic fields, and these morphologic types correspond with the three physiologic types of ganglion cells (Y, X, and W).[349,369] The size of the dendritic fields for each of the three morphologic types varies with the location in the retinal field. All three are represented throughout the retina, including the visual streak and area centralis, but the proportions vary. Matching of the morphology of the ganglion cells with their physiologic counterparts is not always observed. In the ferret, three types of ganglion cells occur physiologically, but they do not consistently fall into distinct groups with regard to size[351]; the tendency for ganglion cells to become smaller in the size of their somata within the visual streak is not seen in this animal's retina. In the rabbit, the α or Y cells are similar to those of a cat but none resemble the β cells of a cat, being instead referred to as class II cells, while α cells are referred to as class I cells.[370] The class I cell is subdivided into four distinct types based on the level of dendritic branching, while the class II cells consist of three types, each having smaller fields than those of type class I.

Alpha or Y cells, which have rather sparsely branching dendrites and a large perikaryon, are relatively few in number, being found mostly within the peripheral retina. In the canine retina,

the density of the α cell can vary considerably. Depending on the retinal location, it can comprise between 3% to 14% of the total ganglion cell population in the dog and 1% to 18% in the wolf.[353] However, in the wolf, α ganglion cells can be completely absent in a substantial region of the temporal peripheral retina.[353]

Beta or X ganglion cells are smaller than α cells in similar areas and have more branches. They also are much more numerous than α cells, being more concentrated within the area centralis and visual streak than peripherally.

Gamma or W cells, which have a small perikaryon with a few thin, infrequently branching dendrites, are also numerous and mostly concentrated in the central retina.[371] The smaller ganglion cells are, for the most part, directly connected with midget bipolar cells, which in turn synapse solely with cones (Fig. 2.146). These ganglion cells are undoubtedly involved in high-resolution vision and project mostly to the superior colliculus.[371] In the cat, the γ cells comprise nearly one half the ganglion cells in most of the nasal retina but only one third of those in the temporal retina and area centralis[372]; however, γ cells of the temporal retina cross contralaterally to the brain twice as frequently as those that form uncrossed projections.

Ultrastructurally, the different types of ganglion cells have not been differentiated.[9] In general, they have abundant cytoplasm, which is characterized by aggregates of rough endoplasmic reticulum and ribosomes (i.e., Nissl substance) scattered through the cytoplasm, a smooth-surfaced endoplasmic reticulum, dense membrane-bound bodies, and mitochondria (Fig. 2.171).[32,258,373]

Figure 2.171. The inner plexiform and ganglion cell layers in a cat. Two rod bipolar synaptic terminals are identifiable with their synaptic ribbons (*small arrows*). Conventional synapses involving amacrine processes and bipolar cells, ganglion cells, or other amacrine cell processes are also visible (*open arrows*). In addition, Müller cells (*M*) with abundant smooth-surfaced endoplasmic reticulum are evident. The ganglion cells (*G*) contain electron-dense bodies, rough-surfaced endoplasmic reticulum (i.e., Nissl substance), and mitochondria. (Original magnification, X9700.)

Nerve Fiber Layer

Axons of ganglion cells gather in nerve fiber layer, then turn at right angles and course to the posterior pole, at which the optic nerve exits (Fig. 2.170). To maintain transparency of the retina, the nerve fibers lack myelin sheaths. Some neuroglial cells and the inner tips of Müller cells are also present among the nerve fibers. Large retinal vessels (from the short posterior ciliary arteries in the dog) occur in the nerve fiber layer as well as in the ganglion cell and inner plexiform layers.

The nerve fiber layer increases in thickness as it approaches the optic disc. The axons, which do not branch, pass radially to the optic nerve, except in the area centralis, where the concentration of axons arising from this region causes the more peripheral axons to arc around to reach the optic disc. In the cat, the mean axon diameter within the nerve fiber layer is 1.12 to 1.47 μm, being unimodal (0.6–0.8 μm) in distribution next to the optic disc and bimodal or even trimodal (0.0–0.8, 1.4–2.1, 3.3 μm) away from the optic nerve.[374] Axonal diameters within the optic nerve may be as much as 30% greater than those within the nerve fiber layer. Association ganglion cells that have branching axons have been reported in the calf, cat, and dog, but the termination and synapses that these fibers make are unknown.[290]

The neurons of the fiber layer are mainly centripetal (i.e., afferent) fibers carrying impulses from the retina to the brain, but in some species, centrifugal (i.e., efferent) fibers carrying impulses from the brain to the retina have been described. In birds, the presence of centrifugal fibers is well established, but in other animals, their presence and origin are controversial.[290,375] The axons are of various sizes, and the large axons originate from the large ganglion cells (i.e., Y or α cells).

In addition to Müller cells, glial cells are present in the inner retina, being found in the inner plexiform, ganglion cell, and nerve fiber layers. The astrocytes have long, branching processes and are found in a supportive role structurally and, perhaps, nutritionally around blood vessels and nerve axons (Fig. 2.172).[32,290]

Inner Limiting Membrane

The inner limiting membrane is a true basement membrane formed by the fused terminations of Müller cells. Along the innermost aspects of the sensory retina, the Müller cell processes, which are vertically oriented, flare out and abut the adjacent processes. On the inner or vitreal surface of these expansions, a basement membrane comprises the main part of the inner limiting membrane, with the remaining contribution from the vitreal fibrils inserting into the basement membrane itself.

Retinal Vasculature

Classically, variations of the retinal vasculature have been categorized into four basic patterns: holangiotic, merangiotic,

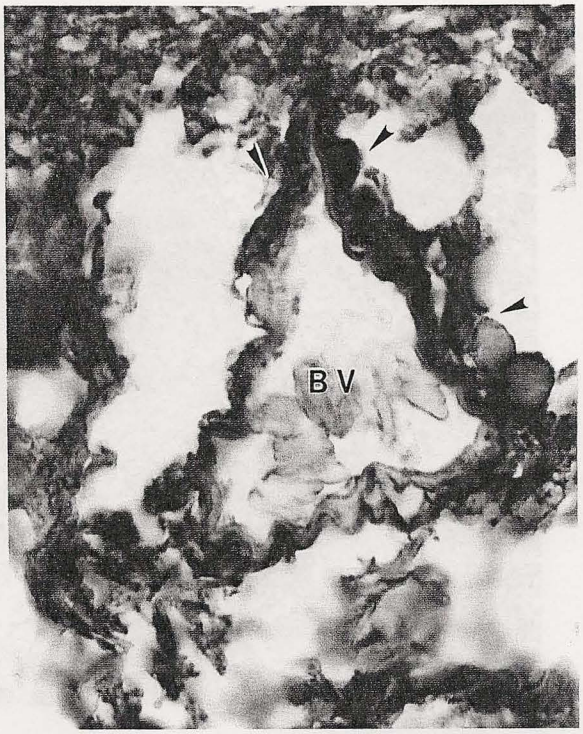

Figure 2.172. Within the canine inner retina, blood vessels (*BV*) are lined by numerous processes of astrocytes, which are revealed by immunohistochemical localization for glial fibrillar acid protein (*arrows*). (Original magnification, X1000) (Courtesy of A Komaromy.)

paurangiotic, and anangiotic. Most mammals possess the holangiotic pattern, in which most of the sensory retina receives a direct blood supply (see Chapter 27). The merangiotic pattern consists of blood vessels localized to a region of the retina. Lagomorphs (rabbits and pika) have this particular pattern. In the paurangiotic pattern, blood vessels within the retina occur only near the optic disc (peripapillarily). This pattern is seen in certain ungulates, such as the elephant, rhinoceros, horse, and marsupials. The anangiotic pattern is characterized by an absence of any vasculature within the sensory retina, and it occurs in many nonmammalian species, most notably birds, and in certain mammals, including monotremes, marsupials, and placentals (i.e., bats). In general, the retinal arterial supply in domestic animals is via the short posterior ciliary arteries, which are termed *cilioretinal arteries,* rather than via a central retinal artery origin, as in higher primates.[4,277,376,377]

In the holangiotic pattern of the cat, three major pairs of cilioretinal arteries and veins are present, originating around the optic disc periphery. They consist of a dorsomedial pair that curves laterally, a ventromedial pair, and a ventrolateral pair of arteries and veins. These vessels arc around the area centralis, leaving what appears clinically to be a vessel-free zone, but a capillary network is, in fact, present. The capillaries exist in the intercommunicating nets in a superficial (i.e., nerve fiber) and a deep (i.e., inner nuclear) layer. Adjacent to arterioles and arteries is a 100-μm to 200-μm capillary-free zone.[377]

In the dog, approximately 20 cilioretinal arterioles radiate from the optic disc and three to four major veins. Additional smaller veins join the larger veins on the optic disc and form a very short central retinal vein. The retinal vessels tend to be more tortuous in the dog than in other animals. The capillary network is extensive and similar to that of the cat in its depth, having a capillary-free zone around arterioles and a capillary network over the area centralis.

Histologically, the larger vessels of holangiotic retinas lie within the nerve fiber, ganglion cell, and inner plexiform layers. Capillaries, however, lie mostly within the inner nuclear layer and, to a lesser extent, within the ganglion cell and nerve fiber layers (Fig. 2.173A). Ultrastructurally, one to four endothelial cells line a capillary lumen. A basement membrane covers the endothelium as well as divides the surrounding mural cells (i.e., pericytes) and their processes (Fig. 2.173B).[258] Adjacent endothelial cells are attached by desmosomes and tight junctions.[303]

The paurangiotic retina of the horse contains approximately 30 fine arteries to arterioles and 30 veins to venules of approximately 25 and 35 μm in diameter, respectively, at the optic disc.[376] Ophthalmoscopically, they cannot be distinguished from each other, and they radiate 360 degrees outward from the disc for 6 mm horizontally and 3 to 4 mm vertically. The arteries do not form a capillary network at their terminations; rather, they pass directly into the venules, which have arteriolar annuli at the point of side-arm branching.[4,376]

The merangiotic retina, as seen in the rabbit, consists of a horizontal band of vessels that are confluent with medullated nerve fibers, emanating medially and laterally from each side of the optic disc. The vessels branch in a side-branch manner rather than dichotomously, which is usually the case in most mammals.[378] Four capillary areas are located within the horizontal band, including superficial net capillaries, deep capillaries of the nerve fiber layer, peripheral capillaries, and peripapillary capillaries.

In the anangiotic retina, vasculature within the inner eye is restricted to a structure called the pecten (pecten oculi), which lies vitreal to the optic nerve. The pecten is a highly pigmented, pleated structure reminiscent of ciliary processes, and it contains a rich plexus of small blood vessels (Fig. 2.174). The plexus is supplied by tributaries of the ophthalmotemporal artery and lacks any direct connections with the neighboring choroidal circulation.[379] The main function of the pecten is to provide nourishment for the inner retina and inner eye.[2,305] When viewed grossly, the pecten can be divided into three types: the pleated type seen in most birds; the conical type found in kiwi; and the vaned type reported in the ostrich.[305,380] Among the pleated pecten, the number of pleats and the size varies considerably within avian species. The variations appear to be associated with the general activity of bird behavior, including visual capability. The pecten, which are large and consist of numerous folds, such as those observed in the red-tailed hawk (*Buteo jamaicensis*), or small, especially relative to the size of the globe, with few folds, as seen in the emu (*Dromaius novaehollandiae*), are indicative of the variable involvement in the transport of substances to the avascular retina.[381–383]

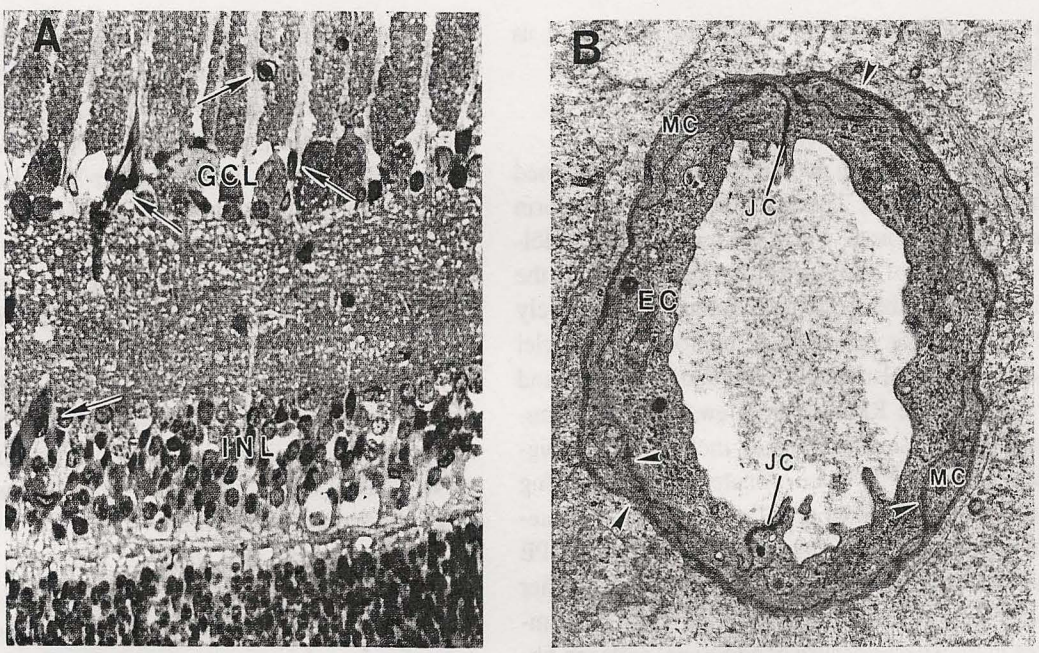

Figure 2.173. **A.** In holangiotic retina, as seen here in the pig, capillaries (*arrows*) are formed mostly within the ganglion cell layer (*GCL*) and inner nuclear layer (*INL*). *NFL,* nerve fiber layer; *ONL,* outer nuclear layer. (Original magnification, X125.) **B.** Close-up of a canine capillary in the ganglion cell layer reveals a basement membrane (*arrows*) that covers both endothelial cells (*EC*) and mural cells (*MC*). Adjacent endothelial cells are fused together by a junctional complex (*JC*) consisting of zonula adherens and zonula occludens. (Original magnification, X17,000.)

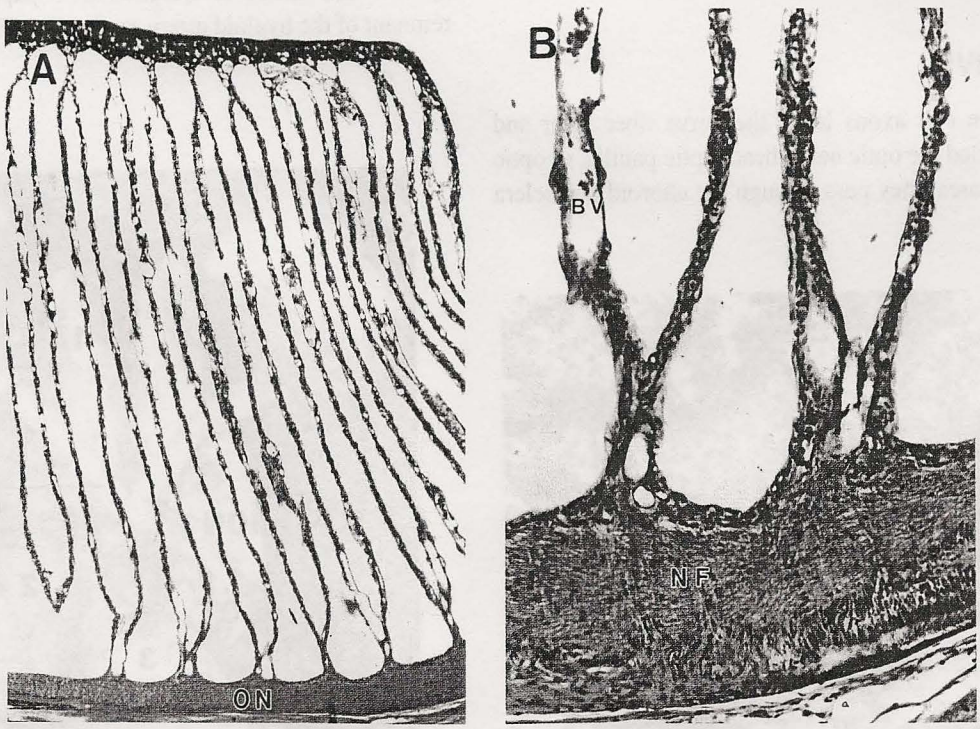

Figure 2.174. **A.** The avian pecten, as seen here in the chicken, consists of a pleated vascular plexus that lies vitreally atop the optic nerve head (*ON*). (Original magnification, X50.) **B.** Close-up of the base of the pecten as it internally lines the nerve fibers (*NF*) that form the optic nerve head. *BV,* blood vessels of the pecten. (Original magnification, X250.)

The amount of pigmentation varies among pecten of different birds, but melanin is especially developed along the apical portion, which may protect the blood vessels against exposure to incident UV light.[384] The amount of UV light the retina and pecten may receive has not been determined in birds; however, evidence indicates that at least some avian retinas use UV light for visual detection.[385] Thus, it seems reasonable to expect the vasculature of the pecten, which potentially serves the inner retina and vitreous, to be shielded from UV light and its potential for eliciting dangerous reactive oxygen radicals.[384] In addition to providing protection against the damaging influence of UV light, the extensive population of

melanocytes may offer structural support to the pecten as well.[382,386,387]

Aging

In aging eyes, the inner limiting membrane becomes thickened and increasingly vacuolated. The inner and outer plexiform layers can have cystoid spaces, which are formed within Müllerian cells. The layers of the sensory retina, especially the outer nuclear layer of the peripheral retina, progressively thin.[388] A displacement or migration of photoreceptor nuclei into the visual cell layer also occurs with age in humans and the rat.[389,390] Cells of the RPE become fewer but, concomitantly, become filled with residual bodies, including aging pigment (i.e., lipofuscin).[388,391–393] In primates, the underlining Bruch's membrane has a buildup of cellular debris–like material, including undigested material from deteriorating RPE cells. This type of buildup has not been found in any other species. In older pigs (5–6 years of age), the Bruch's membrane increases in thickness because of additional collagen fibrils (Fig. 2.175). In older equine retina, both cystoid degenerations and losses of regular layering occur within the peripheral retina next to the ora ciliaris retinae.[276] As older animals continue to be studied, our understanding of the aging retina will expand.

OPTIC NERVE

Retinal ganglion cell axons leave the nerve fiber layer and form what is called the optic nerve head, optic papilla, or optic disc. From this area, they pass through the choroid and sclera and into the orbit. The optic nerve is formed by ganglion cell axons, glial cells, and septae, which arise from the pia mater. The visual axons synapse in the lateral geniculate body and the rostral colliculus, whereas the pupillomotor fibers synapse in the pretectal area in the Edinger-Westphal nucleus or the nearby anteromedian nucleus. In addition, centrifugal (i.e., efferent) fibers occur in some species and may represent a method by which the brain can influence retinal function.[394]

The optic nerve extends from the globe to the optic chiasm, and it consists of four regions: intraocular, intraorbital, intracanalicular, and intracranial (Fig. 2.176).[394] Because of similar anatomic properties, the optic nerve is considered to be more of a nerve fiber tract of the brain than a peripheral nerve.[32] The intraocular optic nerve consists of retinal, choroidal, and scleral portions.

The terms *optic disc, papilla,* and *nerve head* are interchangeable and include the retinal and choroidal portions of the optic nerve. Optic papilla refers to an elevation of the nerve head, and its presence and development vary among species as well as individuals.[32] Within the optic papilla is a central depression called the physiologic cup (Fig. 2.177). The cup is lined by a plaque of glial cells known as the central supporting tissue meniscus of Kuhnt (Fig. 2.178). An exaggeration of this tissue is Bergmeister's papilla, which is the remnant of the hyaloid artery on the disc (Fig. 2.177).

Figure 2.175. Bruch's membrane in a 6-year-old pig is thicker than that in younger pigs because of a buildup of collagen fibrils, especially within the outer collagenous layer (*OCL*). *CC,* choriocapillaris. (Original magnification, X10,000.)

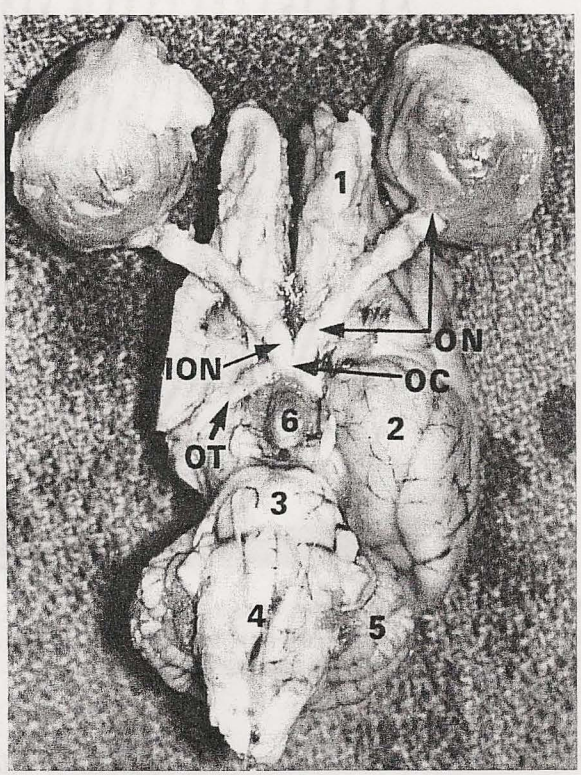

Figure 2.176. Ventral view of the dog brain–ocular relationship. The right cerebral hemisphere has been removed; note how physically close the eyes are to the brain. *ION,* intracranial optic nerve; *OC,* optic chiasm; *ON,* orbital optic nerve; *OT,* optic tracts; *1,* olfactory tract; *2,* piriform lobe; *3,* pons; *4,* medulla; *5,* cerebellum; *6,* pituitary.

Figure 2.177. SEM shows the internal view of the optic disc or nerve head of a dog. Centrally, the optic disc has a depression known as the physiologic cup (*PC*). The *arrow* indicates remnants of the hyaloid artery. (Original magnification, X40.)

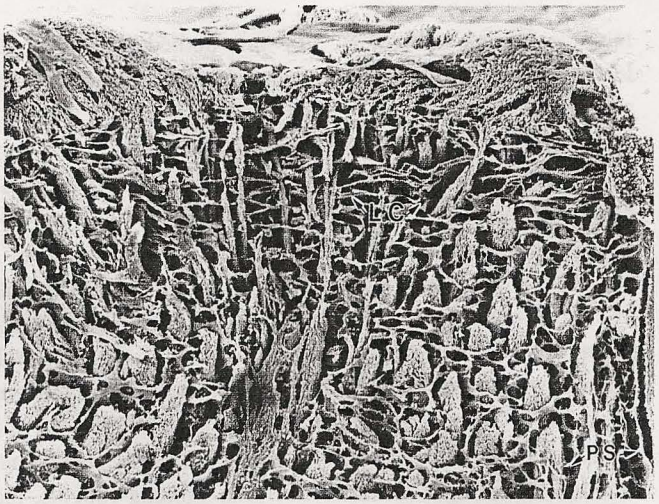

Figure 2.179. Trypsin digest of a canine optic nerve shows the network of collagen beams that make up the lamina cribosa (*LC*). These beams, which are largely a continuation of the fibrous tunic, are interconnected externally to pial septa (*PS*). (Original magnification, X25.) (Courtesy of DE Brooks.)

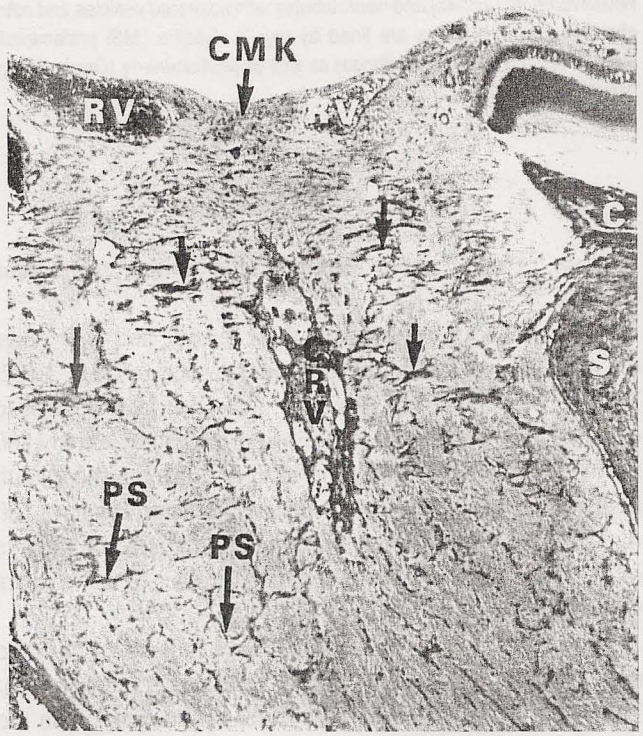

Figure 2.178. The optic nerve head and optic nerve of a dog. *Arrows* indicate lamina cribosa; note the number of astrocytes anterior to it. *C,* choroid; *CMK,* central miniscus of Kuhnt (accumulation of astrocytes in physiologic cup); *CRV,* central retinal vein; *RV,* retinal veins; *S,* sclera; *PS,* pial septa. (Original magnification, X720.)

Figure 2.180. Within the prelaminar region of the canine optic nerve, numerous thick-bodied astrocytes (*arrows*) are revealed by glial fibrillary acidic protein immunohistochemical localization. (Original magnification, X1000.) (Courtesy of A Komaromy.)

Converging nerve fibers of the retina cluster into fascicles or bundles as they become lined by glial (i.e., fibrous astrocytes) and collagenous (i.e., lamina cribrosa) elements. The astrocytes are oriented perpendicularly to the length of the bundle, thus separating the nerve fibers from all nonneuronal components (i.e., extracellular fibers of connective tissue, blood vessels, and microglia). Vitreally, the astrocytes and associated loose connective tissue form capillary-bearing trabeculae that support the nerve bundles as they turn 90 degrees into the scleral canal from the nerve fiber layer (Fig. 2.179).[395] This region is referred to as the choroidal or the anterior lamina cribrosa.

With the assistance of glial fibrillary acidic protein immunohistochemical localization, fibrous astrocytes can be observed throughout the optic nerve (Fig. 2.180). Two morphologic types of fibrous astrocytes can be distinguished: thin bodied and thick bodied.[396] Thick-bodied astrocytes are located throughout the optic nerve head and the prelaminar, laminar, and postlaminar regions. Within the posterior prelaminar region, these cells form glial tubes, which guide axons

into the lamina cribrosa.[396] The thin-bodied astrocytes are located more anteriorly, both accompanying and contacting axons.

Sclerally, the posterior region of the lamina cribrosa consists of meridional extensions of the sclera. In turn, these extensions consist of successive laminar sheets with radially aligned perforations (Fig. 2.179). Each lamina possesses a capillary in its center. As in the retina, the optic nerve capillaries are nonfenestrated, having tight junctions (i.e., zonula adherens).[397,398] The lamina cribrosa of the cat, dog, squirrel, and monkey is well-developed, having prominent collagenous laminae.[398,399] By comparison, the lamina cribrosa of the mouse, rat, and rabbit is poorly developed, lacking substantial amounts of collagen within the lamina. Among rodents, the lamina cribrosa in the rat optic nerve is least developed, consisting of only one or two beams of sparse connective tissue[400]; however, the lamina cribrosa of the guinea pig is considerably more developed, consisting of three or more beams of abundant connective tissue. Despite the disparity of development in these two animals, the extracellular composition of this portion of the optic nerve is nearly identical, consisting of type I, III, and VI collagen, elastin, and dermatan and chondroitin sulfate–containing proteoglycans.[401] Moreover, the extracellular matrix of these small eyes are comparable to that of the horse and the dog.[402]. Of the different types of collagen within the lamina cribrosa, type VI is predominant. The equine optic nerve possesses a well-constructed lamina cribrosa, which may afford additional protection to the optic nerve during episodes of elevated IOP.[402]

The axons within the optic nerve are easily distinguished by their tubular processes, which contain evenly dispersed neurofilaments and neurotubules and occasional vesicles and mitochondria (Fig. 2.181). The vesicles, mitochondria, and other cytoplasmic materials are being continuously moved within the axon toward the synaptic ending (orthogradely) and toward the cell body (retrogradely). Movement of these materials, which is known as axonal flow, is responsible for the constant supply of newly synthesized protein. Axonal flow within the optic nerve is normally unimpeded throughout the life of the ganglion cell; however, at the region where the nerve fibers exit the eye (i.e., lamina cribrosa), axonal flow is susceptible to blockage, which usually results from elevated IOP.[403,404] As the IOP rises in the eye, the laminar perforations lose their proper alignment, and axonal flow is interrupted.[404–407] Partial constriction of axoplasmic flow, however, has been found at the lamina cribrosa of normotensive eyes among a wide range of mammals, including the cat, human, rabbit, rat, guinea pig, sheep, ox, and pig.[408] This constriction may result from the pressure gradient across the lamina cribrosa, and it may contribute to, or be a factor in, low-tension glaucoma. In the dog, the axon is myelinated by oligodendrocytes throughout the entire optic nerve, including the optic disc. In the horse, cow, and humans, it begins posterior to the lamina cribrosa and is responsible for the marked

Figure 2.181. Axons within the optic nerve of a dog consist mostly of neurofilaments (*arrows*) and neurotubules with scattered vesicles and mitochondria (*M*). The axons are lined by myelin sheaths (*MS*) prelaminarly (i.e., anterior to the lamina cribosa) as well as postlaminarly. (Original magnification, X24,000.)

increase in optic nerve diameter after exiting the lamina cribrosa.[4]

The number of nerve fibers, their density, and their range of diameter vary considerably among species (Fig. 2.182; Table 2.24).[192,351,409–436] Animals with the least-developed eyes, such as the mole rat, contain approximately 900 to 1800 nerve fibers depending on the species, whereas those with highly developed eyes, such as various primates, can have 100 to 150 times that number. Interestingly, the size of the eye often does not correlate with the total number of nerve fibers within its optic nerve.

The orbital portion of the optic nerve is invested with the three meningeal sheaths of the central nervous system. The outermost is the thick dura mater, which fuses with the sclera anteriorly. Posteriorly, at the optic foramen, it divides into two layers. The outermost of these layers reflects onto orbital periosteum, and the innermost is continuous with the dura of the cranial vault (Fig. 2.183). The collagenous fibers of the dura run longitudinally on the external surface and circumferentially internally. The principal cell type is the fibroblast.[4,271]

The arachnoid sheath is internal to the dural sheath, and it is composed of collagen trabeculae covered by meningothelial cells of fibroblastic nature. The pia mater is closely applied to the nerve and sends septa radially into the nerve, thus dividing it into columns (Fig. 2.184). Small blood vessels accompany

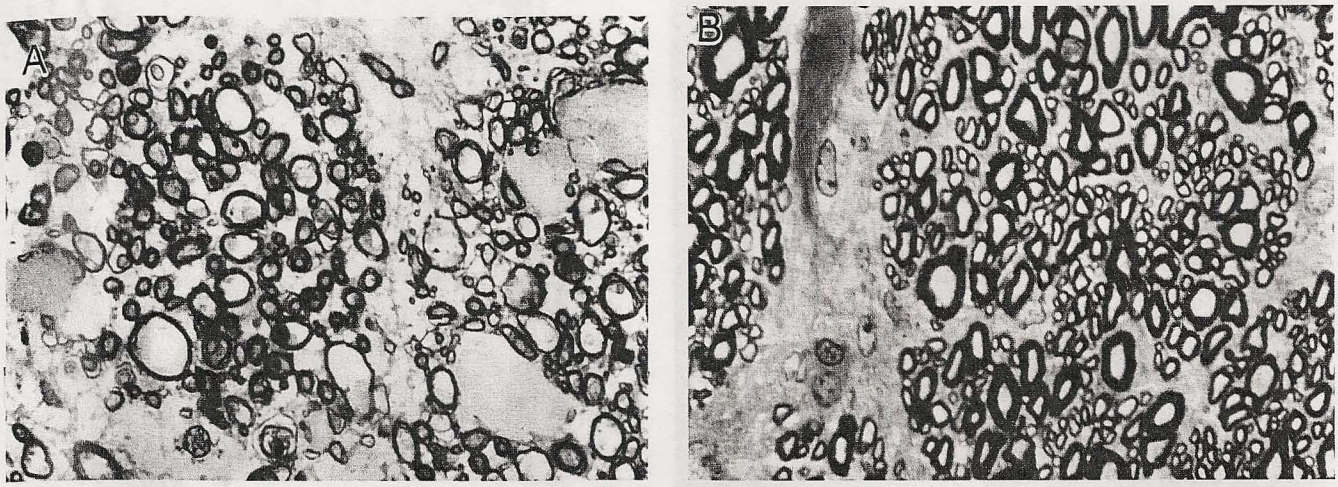

Figure 2.182. Cross-section of the optic nerve in a dog (**A**) and a horse (**B**) posterior to the laminar cribrosa. In both species, the widths of individual nerve fibers vary a great deal within a nerve fiber bundle. The myelin sheaths of the nerve fibers in the horse are generally thicker than those in the dog, reflecting the longer distances they extend in that species. (Original magnification: Both, X1000.)

Table 2.24 Axon Count and Density of Optic Nerves among Different Vertebrates

Animal	Total Axon Count	Axon Density (per mm^2)	Mean Fiber Diameter (μm)	Reference
Xenopus	68,000	N/A	N/A	364
Viper	53,700–69,600	N/A	0.735	446
Turtle	394,900	512,191	0.87 (0.42)[a]	410
Rat	102,085	568,000	0.6–0.83	409
Guinea pig	159,000[b]	N/A	N/A	411
Eastern chipmunk	565,000	490,451	0.83	412
Three hystricomorph rodents	480,000–550,000[c]	N/A	N/A	359
Capybara	370,000[c]	N/A	N/A	359
Nocturna paca	230,000[c]	N/A	N/A	359
Rabbit	394,000	354,395	1.0	413
Pigmented ferret	82,000–88,000[c]	N/A	N/A	351
Dog	145,000–165,000	~50,000	1.5	414–417
Cat	193,000	78,000	1.6	418
Horse	1.08 million	62,800	1.9	419
Human and monkey	1.1–1.2 million	150,000	1.0 and 0.8	420–422
Anubis baboon	1.41–1.81 million[c]	—	—	423
Opossum	100,000	264,061	1.6 (0.59)[a]	424
Marsupial "quokka"	180,000–224,000[c]	N/A	N/A	425
Bat	17,500	N/A	0.7	426

[a]Based on unmyelinated axons.
[b]Based on ganglion cell counts, accounting for displaced amacrine cells.
[c]Based on ganglion cell counts, without accounting for displaced amacrine cells, which can compromise 10–50% of cells within the ganglion cell layer.

the pial septa into the optic nerve. In the rabbit, cerebrospinal fluid from the subarachnoid space permeates across the pia and penetrates the nerve fibers and surrounding extracellular materials. Cerebrospinal fluid of the optic nerve meninges also penetrates the perineural sclera and spreads into the choroid, eventually entering the choriocapillaris, venules, and veins.[437]

VASCULATURE OF THE EYE AND ORBIT

Among domestic animals, the main supply of blood to the eye and orbit is via the internal maxillary artery (as a branch of the external carotid artery), which after passing through the alar canal branches to give rise to the external ophthalmic artery.

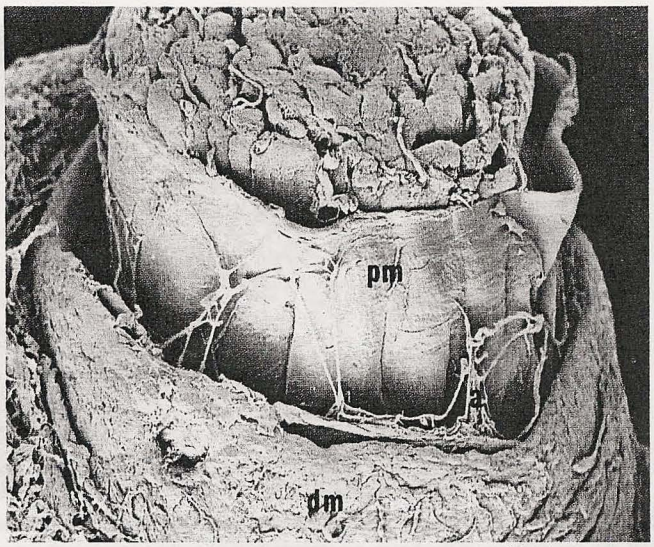

Figure 2.183. SEM shows how the orbital optic nerve is protected by the three meningeal layers, or sheaths, of the central nervous system; the thick dura mater (*dm*), which is internally lined by the arachnoid and its trabeculae; and the pia mater (*pm*). (Original magnification, X33.)

Figure 2.184. Pial septae within the pig bulbar optic nerve can contain melanocytes (*Me*) and separate the nerve fiber bundles into long columns. (Original magnification, X200.)

By comparison, in primates, the entire global microcirculation and most of the orbital circulation is supplied via the internal carotid artery, which gives rise to the internal ophthalmic artery.[4]

Domestic species possess both internal and external ophthalmic arteries, but the external ophthalmic artery provides most of the circulation to the eye. Both the long and short posterior ciliary arteries as well as the lacrimal, muscular, and supraorbital arteries derive from the external ophthalmic artery. The internal ophthalmic artery, which is relatively small, provides the blood supply for the optic nerve and anastomoses with the external ophthalmic artery or one of its branches (Fig. 2.185); this anastomosis is especially prominent in the dog.

The blood vessels of the retina and choroid arise from both the long and short posterior ciliary arteries. Domestic animals generally have a number of small arteries entering the retinal layers from around the optic disc. In adult domestic animals, a single central retinal artery does not exist.

In the horse, the choroidal vasculature is fed by short posterior ciliary arteries, which originate from the four posterior ciliary arteries, including the lateral and medial posterior arteries that continue anteriorly. Additionally, choroidoretinal arteries form a network around the optic nerve, giving rise to small retinal arterioles that characterize the pauangiotic fundus of this species as well as giving rise to peridiscal choroidal branches.[448]

In small mammals, the arterial supply to the eye is comparable but can be understandably reduced. In the hamster, the primary blood supply for the eye is derived from the long posterior ciliary artery, which initially enters the optic nerve head region and separates into three branches, consisting of the medial and lateral long posterior ciliary arteries and the central retinal artery.[449] The central retinal artery, in turn, branches into six radiating arterioles, which characterize the holangiotic fundus of this animal.

Venous drainage of the eye varies considerably among domestic species (Fig. 2.186).[4] In the dog, the two main venous channels within the orbit are the supraorbital and the inferior orbital veins. The lacrimal, superior vortex, ethmoidal, and several muscular veins empty into a large dilatation of the supraorbital vein. The inferior vortex and malaris veins empty into the inferior orbital veins, which anastomose anteriorly and join the supraorbital dilatation at the apex of the orbit posteriorly. Two prominent veins drain the dilatation: the orbital vein, which enters the intracranial system; and an internal maxillary vein, which connects to the external jugular vein.[4]

The cat has an external rete or vascular network that is more venous than arterial.[4] The anterior ciliary veins, four vortex veins, and a pair of fine long posterior veins empty into the rete.[87] The inferior vortex vein and anterior ciliary veins initially join the inferior orbital veins, and the superior vortex vein drains initially into the superior orbital veins. The rete is drained by a large ophthalmic vein, which passes into the external jugular. The supraorbital vein also empties anteriorly into the facial vein via the angular and inferior orbital veins, which eventually empty into the internal jugular vein.[4]

In the horse, the principal venous channels of the eye consist of the ophthalmic, orbital, supraorbital, and reflex veins. The dorsal ophthalmic vein receives blood from the superior vortex, palpebral, and lacrimal veins (Fig. 2.187). The dorsal ophthalmic vein is joined posteriorly by the anterior ciliary, supraorbital, muscularis, infratrochlear veins, and ultimately,

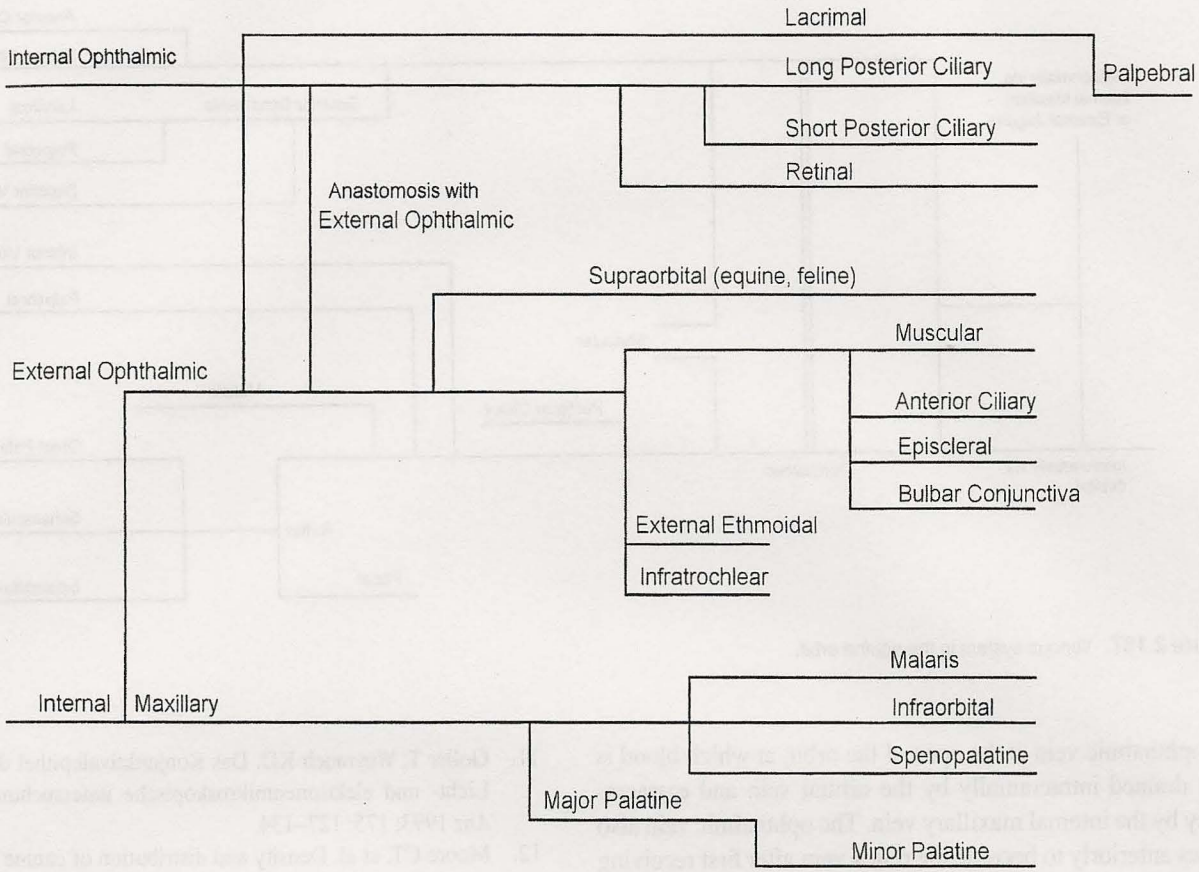

Figure 2.185. Arterial system of the mammalian orbit. Note that variations exist in different animals.

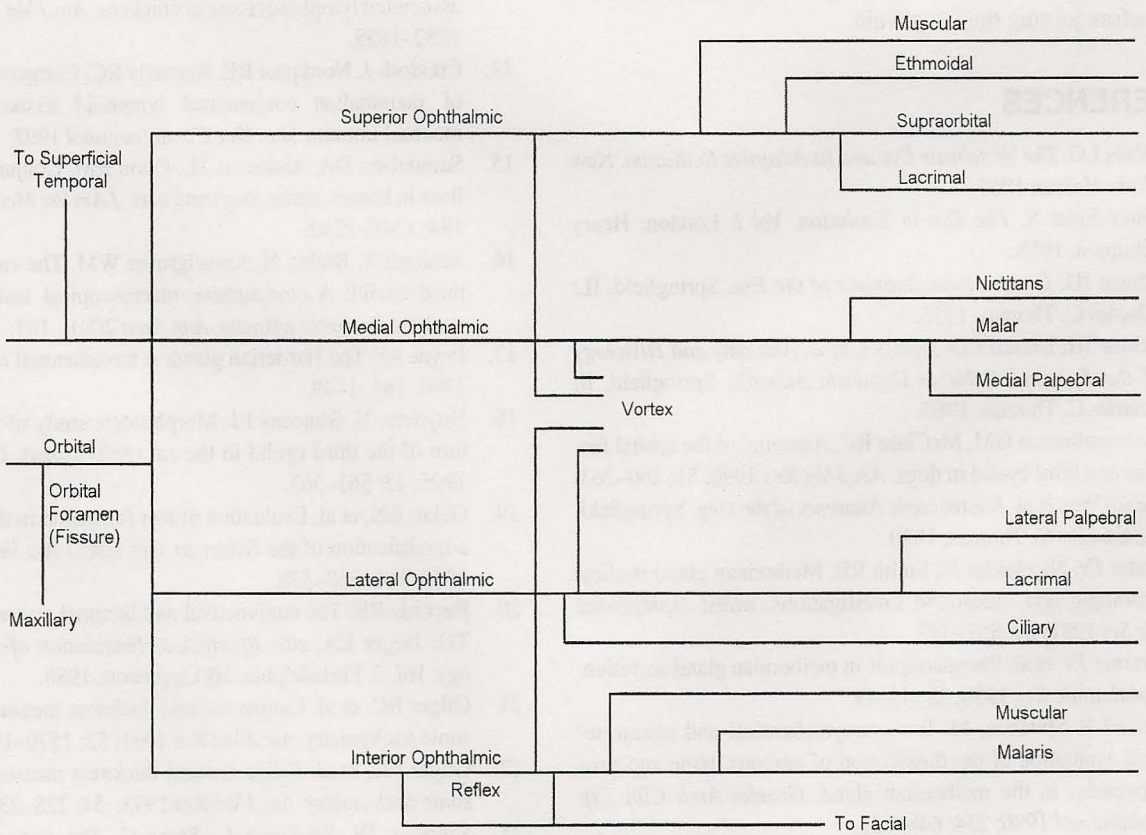

Figure 2.186. Venous system of the mammalian orbit. (Modified from Prince JH, Diesen CD, Eglitis I, et al. *Anatomy and Histology of the Eye and Orbit in Domestic Animals.* Springfield, IL: Charles C. Thomas, 1960.)

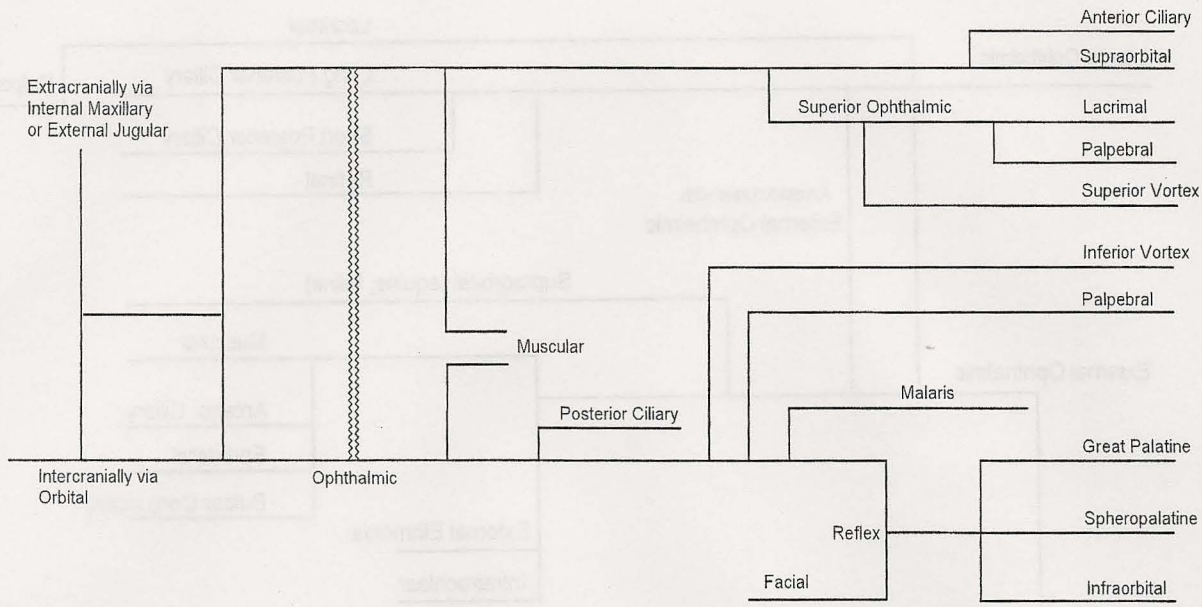

Figure 2.187. Venous system in the equine orbit.

the ophthalmic vein at the apex of the orbit, at which blood is then drained intracranially by the orbital vein and extracranially by the internal maxillary vein. The ophthalmic vein also passes anteriorly to become the reflex vein after first receiving the inferior vortex veins via muscular veins, posterior ciliary vein, inferior vortex vein, and palpebral veins.[4] The reflex vein receives the great palatine, sphenopalatine, and infraorbital veins before joining the facial vein.

REFERENCES

1. Walls LG. *The Vertebrate Eye and Its Adaptive Radiation.* New York: Hafner, 1967.
2. Duke-Elder S. *The Eye in Evolution. Vol I.* London: Henry Kimpton, 1958.
3. Prince JH. *Comparative Anatomy of the Eye.* Springfield, IL: Charles C. Thomas, 1956.
4. Prince JH, Diesen CD, Eglitis I, et al. *Anatomy and Histology of the Eye and Orbit in Domestic Animals.* Springfield, Il: Charles C. Thomas, 1960.
5. Constantinescu GM, McClure RC. Anatomy of the orbital fasciae and third eyelid in dogs. *Am J Vet Res* 1990; 51: 260–263.
6. Adam WS, et al. *Microscopic Anatomy of the Dog.* Springfield, IL: Charles C. Thomas, 1970.
7. Jester JV, Nicolaides N, Smith RE. Meibomian gland studies: histologic and ultrasound investigations. *Invest Ophthalmol Vis Sci* 1981; 20: 537–547.
8. Greiner JV, et al. Phospholipids in meibomian gland secretion. *Ophthalmic Res* 1996; 28: 44–49.
9. Seifert P, Spitznas, M. Immunocytochemical and ultrastructural evaluation of the distribution of nervous tissue and neuropeptides in the meibomian gland. *Graefes Arch Clin Exp Ophthalmol* 1996; 234: 648–656.
10. Chung CW, Tigges M, Stone RA. Peptidergic innervation of the primate meibomian gland. *Invest Ophthalmol Vis Sci* 1996; 37: 238–245.
11. Goller T, Weyrauch KD. Das Konjunktivalepithel des hundes. Licht- und elektronenmikroskopische untersuchungen. *Anat Anz* 1993; 175: 127–134.
12. Moore CT, et al. Density and distribution of canine conjunctival goblet cells. *Invest Ophthalmol Vis Sci* 1987; 28: 1925–1932.
13. Fix AS, Arp LH. Morphologic characterization of conjunctiva-associated lymphoid tissue in chickens. *Am J Vet Res* 1991; 52: 1852–1859.
14. Chodosh J, Nordquist RE, Kennedy RC. Comparative anatomy of mammalian conjunctival lymphoid tissue: A putative mucosal immune site. *Dev Comp Immunol* 1998; 22: 621–630.
15. Samuelson DA, Andresen TL, Gwin RM. Conjunctival fungal flora in horses, cattle, dogs and cats. *J Am Vet Med Assoc* 1984; 184: 1240–1242.
16. Schlegel T, Brehm H, Amselgruber WM. The cartilage of the third eyelid: A comparative macroscopical and histological study in domestic animals. *Ann Anat* 2001; 183: 165–169.
17. Payne AP. The Harderian gland: A tercentennial review. *J Anat* 1994; 185: 1–49.
18. Nuyttens JJ, Simoens PJ. Morphologic study of the musculature of the third eyelid in the cat (*Felix catus*). *Lab Anim Sci* 1995; 45: 561–563.
19. Gelatt KN, et al. Evaluation of tear formation in the dog, using a modification of the Schirmer tear test. *J Am Vet Med Assoc* 1975; 166: 368–370.
20. Records RE. The conjunctival and lacrimal system. In: Duane TD, Jaeger EA, eds. *Biomedical Foundation of Ophthalmology. Vol. 2.* Philadelphia: JB Lippincott, 1988.
21. Gilger BC, et al. Canine corneal thickness measured by ultrasonic pachymetry. *Am J Vet Res* 1991; 52: 1570–1572.
22. Gilger BC, et al. Feline corneal thickness measured by ultrasonic pachymetry. *Am J Vet Res* 1993; 54: 228–230.
23. Schoster JV, Wickman L, Stuhr C. The use of ultrasonic pachymetry and computer enhancement to illustrate the collective corneal thickness profiles of 25 cats. *Vet Comp Ophthalmol* 1995; 5: 68–73.

24. Mawas J. The innervation of the human cornea. *Bull Soc Ophthalmol Fr* 1951; 2: 162–168.
25. Wolter J. Innervation of the corneal endothelium of the eye of the rabbit. *Arch Ophthalmol* 1957; 58: 246–256.
26. Smolek MK, Klyce. Cornea. In: Wasman W, Jaeger EA, eds. *Biomedical Foundations of Ophthalmology. Vol. 1.* Philadelphia: JB Lippincott, 1993: 1–20.
27. Nakamura M, Mishima H, Nishida T, Otori T. Binding of hyaluron to plasma fibronectin increases the attachment of corneal epithelial cells to a fibronectin matrix. *J Cell Physiol* 1994; 159: 415–422.
28. Nakamura M, et al. Glycosaminoglycan and collagen fibrillar interactions in the mouse corneal stroma. *Matrix Biol* 1994; 14: 283–286.
29. Buck RC. Ultrastructural characteristics associated with the anchoring of corneal epithelium in several classes of vertebrates. *J Anat* 1983; 137: 743–756.
30. Khodadoust AA, et al. Adhesion of regeneration corneal epithelium: The role of basement membrane. *Am J Ophthalmol* 1968; 65: 339–348.
31. Gelatt KN, Samuelson DA. Recurrent corneal erosions and epithelial dystrophy in the Boxer dog. *J Am Anim Hosp Assoc* 1982; 18: 453–460.
32. Hogan MJ, Alvarado JA, Weddell JE. *Histology of the Human Eye.* Philadelphia: WB Saunders, 1971.
33. Shively JN, Epling G. Fine structure of the canine eye: cornea. *Am J Vet Res* 1970; 13: 713–717.
34. Blumcke S, Morgenroth K. The stereo ultrastructure of the external and internal surface of the cornea. *J Ultrastruct Res* 1976; 18: 502–518.
35. Harding C, et al. A comparative study of corneal epithelial cell surfaces utilizing the scanning electron microscope. *Invest Ophthalmol* 1974; 13: 906–912.
36. Prydal JI, Campbell FW. Study of precorneal tear film thickness and structure by interferometry and confocal microscopy. *Invest Ophthalmol Vis Sci* 1992; 33: 1996–2005.
37. Brightman AH, Gerd S, Campbell TW, Fedde MR. A study of viscosity of marine mammal tears. *Vet Ophthalmol* 2003; 6: 359 (abstract).
38. Hoffman F, Schweichel JU. The microvilli structure of the corneal epithelium of the rabbit in relation to cell function: A transmission and scanning electron microscopic study. *Ophthalmic Res* 1972/1973; 4: 175.
39. Takahashi T, Cho HI, Kublin CL, Cintron C. Keratan sulfate and dermatan sulfate proteoglycans associated with type IV collagen in fetal rabbit cornea. *J Histochem Cytochem* 1993; 41: 1447–1457.
40. Doane KJ, Yang G, Birk DE. Corneal cell-matrix interactions: Type VI collagen promotes adhesion and spreading of corneal fibroblasts. *Exp Eye Res* 1992; 200: 490–499.
41. Linsenmayer TF, et al. Type V collagen: Molecular structure and fibrillar organization of the chicken alpha 1 (V) NH2-terminal domain, a putative regulator of corneal fibrillogenesis. *J Cell Biol* 1993; 121: 1181–1189.
42. Zhan Q, Burrows R, Cintron C. Localization of type XII collagen in normal and healing rabbit cornea by in situ hybridization. *Exp Eye Res* 1995; 60: 551–561.
43. Borcherding LJ, et al. Proteoglycans and collagen fibre organization in human corneoscleral tissue. *Exp Eye Res* 1978; 21: 59–70.
44. Watsky MA, Olsen TW, Edelhauser HF. Cornea and sclera. In: Tasman W, Jaeger EA, eds. *Duane's Foundation of Clinical Ophthalmology. Vol. 2.* Philadelphia: JB Lippincott, 1995: 1–29.
45. Cintron C, Covington HI. Proteoglycan distribution in developing rabbit cornea. *J Histochem Cytochem* 1990; 38: 675–680.
46. Castoro JA, Bettelheim AA, Bettelheim FA. Water concentration gradients across bovine cornea. *Invest Ophthalmol Vis Sci* 1988; 29: 963–968.
47. Hayashi S, Osawa T, Tohyama K. Comparative observations on corneas with special reference to Bowman's layer and Descemet's membrane in mammals and amphibians. *J Morphol,* 2002; 254: 247–258.
48. Gordon MK, et al. Type V collagen and Bowman's membrane. Quantitation of mRNA in corneal epithelium and stroma. *J Biol Chem* 1994; 269: 2459–2466.
49. Murphy CJ, Kern TJ, Howland HC. Refractive state, corneal curvature, accommodative range and ocular anatomy of the Asian elephant (*Elephas maximus*). *Vision Res* 1991; 32: 2013–2121.
50. Samuelson DA, Ganesh KC, Miles SM, Zivotofsky AZ, Zivotofsky D, and Lewis PA. Morphology and histochemistry of Bowman's layer in selected vertebrates. *Invest Ophthalmol Vis Sci* 2005; 45(ARVO suppl): S2181.
51. Jakus MA. Studies on the cornea. II: The fine structure of Descemet's membrane. *J Biophys Biochem Cytol* 1956; 2: 243–250.
52. Tamura Y, et al. Tissue distribution of type VIII collagen in human adult and fetal eyes. *Invest Ophthalmol Vis Sci* 1991; 32: 2636–2644.
53. Laing RA, et al. Changes in the corneal endothelium as a function of age. *Exp Eye Res* 1976; 22: 587–594.
54. Oh JO. Changes with age in the corneal endothelium of normal rabbits. *Acta Ophthalmol* 1963; 41: 568–573.
55. Chi HH, Teng CC, Katzin HM. Healing process in the mechanical denudation of the corneal endothelium. *Am J Ophthalmol* 1960; 49: 693–703.
56. MacCallum DK, et al. Evidence for corneal endothelial cell hypertrophy during postnatal growth of the cat cornea. *Invest Ophthalmol Vis Sci* 1983; 24: 247–250.
57. von Sallman L, Caravaggio LL, Grimes P. Studies on the corneal endothelium of the rabbit. I. Cell division and growth. *Am J Ophthalmol* 1961; 51: 955–969.
58. Andrew S, et al. Density of corneal endothelial cells and corneal thickness in eyes of euthanized horses. *Am J Vet Res* 2001; 62: 479–482.
59. Huang AJ, Tseng SC. Corneal epithelial wound healing in the absence of limbal epithelium. *Invest Ophthalmol Vis Sci* 1991; 32: 96–105.
60. Van Horn DL, et al. Regenerative capacity of the corneal endothelium in rabbit and cat. *Invest Ophthalmol Vis Sci* 1977; 16: 597–613.
61. Gwin RM, Warren JK, Samuelson DA. Effects of phacoemulsification and extracapsular lens removal on corneal thickness and endothelial cell density in the dog. *Invest Ophthalmol Vis Sci* 1983; 24: 227–236.
62. Yee RW, et al. Correlation of corneal endothelial pump site density, barrier function, and morphology in wound repair. *Invest Ophthalmol Vis Sci* 1985; 26: 1191–1201.
63. Landsham N. Relationship between morphology and functional ability of regenerated corneal endothelium. *Invest Ophthalmol Vis Sci* 1988; 29: 1100–1109.

64. Weale RA. *The Aging Eye.* London: Lewis, 1963.
65. Birren JE, Williams MV. A perspective on aging and visual function. In: Sekuler R, Kline D, Dismukes K, eds. *Aging and Human Visual Function.* New York: Alan R. Liss, 1982: 7–22.
66. Cogan DG, Kuwabara T. Growth and regenerative potential of Descemet's membrane. *Trans Ophthalmol Soc UK* 1971; 91: 875–894.
67. Gwin RM, et al. Decrease in canine corneal endothelial cell density and increase in corneal thickness as a function of age. *Invest Ophthalmol Vis Sci* 1982; 22: 267–271.
68. Dische Z, Cremer-Bartels G, Kaye GI, Buddecke E. Metabolic heterogeniety of KS in bovine cornea and its role in the maintenance of corneal collagen structure. *Doc Ophthalmol Proc Ser* 1979; 18: 253–264.
69. Dische Z, Cremer-Bartels G, Kaye GI. Differences between two fractions of glycosaminoglycans of the corneal stroma in their structural relation to collagen. *Proc Natl Acad Sci USA* 1985; 82: 760–764.
70. Kangas TA, Edelhauser HF, Twining SS, O'Brien WJ. Loss of stroma glycosaminoglycans in transient stromal edema. *Invest Ophthalmol Vis Sci* 1990; 31: 1994–2002.
71. Fagerholm P, Fitzsimmons T, Harfstrand A, Schenholm M. Reactive formation of hyaluronic acid in the rabbit corneal alkali burn. *Acta Ophthalmol Suppl* 1992: 67–72.
72. Fitzsimmons TD, et al. Endogenous hyaluronan in corneal disease. *Invest Ophthalmol Vis Sci* 1994; 35: 2774–2782.
73. Samuelson DA, Travers A, Lewis PA, Harper JY. Corneal angiogenesis in the Florida manatee. *Invest Ophthalmol Vis Sci* 2004; 44(ARVO suppl): S4805.
74. Harper JY, Samuelson DA, Reep RL. Corneal vascularization in the Florida manatee (*Trichechus manatus*) and three-dimensional reconstruction of vessels. *Vet Ophthalmol* 2005; 8.
75. Van Buskirk EM. The canine eye: The vessels of aqueous drainage. *Invest Ophthalmol Vis Sci* 1979; 18: 223–230.
76. Smith P, Samuelson D, Brooks D. Aqueous drainage paths in the equine eye: Scanning electron microscopy of corrosion cast. *J Morphol* 1988; 198: 33–42.
77. Sharpnack DD, et al. Vascular pathways of the anterior segment of the canine eye. *Am J Vet Res* 1984; 45: 1287–1294.
78. Troncoso MV. The intrascleral vascular plexus and its relations to the aqueous outflow. *Am J Ophthalmol* 1942; 65: 1153–1162.
79. Ujiie K, Bill A. The drainage routes for aqueous humor in monkeys as revealed by scanning electron microscopy of corrosion casts. *Scan Electron Microsc* 1984; 2: 84A.
80. Curtis EL, Miller RC. The sclerotic ring of North American birds. *Auk* 1938; 55: 225–243.
81. Canavese B, Fazzini U, Colitti M. Morphometric analysis of the scleral bony ring with different numbers of ossicles in the eye of *Coturnix japonica. Anat Histol Embryol* 1994; 23: 128–136.
82. Anderson BG, Anderson WD. Vasculature of the equine and canine iris. *Am J Vet Res* 1977; 38: 1791–1799.
83. Saari M. Vasculature of the pig iris. *Ann Med Exp Biol* 1972; 50: 1–11.
84. Donovan RH, et al. Histology of the normal collie eye. II. *Uvea Ann Ophthalmol* 1974; 6: 1175–1189.
85. Rohen J. Comparative and experimental studies on the iris of primates. *Am J Ophthalmol* 1961; 52: 384–396.
86. Tousimis A, Fine B. Ultrastructure of the iris: An electron microscopic study. *Am J Ophthalmol* 1959; 48: 397–417.
87. Tousmis A. Pigment cells of the mammalian iris. *NY Acad Sci Ann* 1963; 100: 447–466.
88. Shively JN, Epling GP. Fine structure of the canine eye: iris. *Am J Vet Res* 1969; 30: 13–25.
89. Wyatt HJ. A "minimum-wear-and-tear" meshwork for the iris. *Vision Res,* 2000; 40: 2167–2176.
90. Rodriques MM, Hackett J, Donohoo P. Iris. In: Duane TD, Jaeger EA, eds. *Biomedical Foundations of Ophthalmology. Vol. 1.* Philadelphia: JB Lippincott, 1988: 1–18.
91. Smith PJ, et al. Unconventional aqueous humor outflow of microspheres perfused into the equine eye. *Am J Vet Res* 1986; 47: 2445–2453.
92. Woberman P, Fine B. The clump cells of Koganei. The light and electron microscopic study. *Am J Ophthalmol* 1972; 73: 90–101.
93. Oliphant LW. Cytology and pigments of non-melanophore chromatophores in the avian iris. In: *Advances in Pigment Cell Research.* New York: Alan R. Liss, 1988: 65–82.
94. Salazar-Bookaman MM, Wainer I, Patil PN. Relevance of drug-melanin interactions to ocular pharmacology and toxicology. *J Ocul Pharmacol* 1994; 10: 217–239.
95. Steiner K, Buhring KU, Merck E. The melanin binding of bisoprolol and its toxicological relevance. *Lens Eye Toxic Res* 1990; 7: 319–333.
96. Szalay J, Nunziata B, Henkind P. Permeability of iridal blood vessels. *Exp Eye Res* 1975; 21: 531–543.
97. Risco JM, Nopanitaya W. Ocular microcirculation: Scanning electron microscopy. *Invest Ophthalmol Vis Sci* 1980; 19: 5–12.
98. Glasser A, Howland HC. In vitro changes in back vertex distance of chick and pigeon lenses: Differences and the effects of aging. *Vision Res* 1995; 35: 1813–1824.
99. Oliphant L. The musculature and pupillary response of great horned owl iris. *Exp Eye Res* 1983; 37: 583–595.
100. Loerzel SM, et al. Vecuronium bromide, phenylephrine and atropine combinations as mydriatics in juvenile double–stressed cormorants (*Phalacrocora auratus*). *Vet Ophthalmol* 2002; 5: 149–154.
101. Saari M. Myelinated nerves of the pig iris. *Acta Ophthalmol* 1971; 49: 921–937.
102. Lau KC, So KF, Campbell G, Lieberman AR. Pupillary constriction in response to light in rodents, which does not depend on central neural pathways. *J Neurol Sci* 1992; 113: 70–79.
103. Troncoso MU. Microanatomy of the eye with the slit lamp microscope. II. Comparative anatomy of the ciliary body, zonula and related structures in mammalia. *Am J Ophthalmol* 1942; 25: 1–30.
104. Fine BS, Yanoff M. *Ocular histology.* 2nd ed. New York: Harper & Row, 1979.
105. Shabo AL, Maxwell DS, Kreiger AD. Structural alterations in the ciliary process and the blood-aqueous barrier of the monkey after systemic urea injections. *Am J Ophthalmol* 1976; 81: 162–172.
106. Smith RS. Ultrastructural studies of the blood-aqueous barrier. I. Transport of an electron-dense tracer in the iris and ciliary body of the mouse. *Am J Ophthalmol* 1971; 71: 1066–1077.
107. Smith RS, Rudt LA. Ultrastructural studies of the blood-aqueous barrier. II. The barrier to horseradish peroxidase in primates. *Am J Ophthalmol* 1973; 76: 937–947.
108. Smith RL, Raviola G. The structural basis of the blood-aqueous barrier in the chicken eye. *Invest Ophthalmol Vis Sci* 1983; 24: 326–338.

109. Streeten B. Ciliary body. In: Duane TD, Jaeger EA, eds. *Biomedical Foundations of Ophthalmology. Vol. 1.* Philadelphia: JB. Lippincott, 1988: 1–38.
110. Morrison JC, Van Buskirk EM. Anterior collateral circulation in the primate eye. *Ophthalmology* 1983; 90: 707–715.
111. Morrison JC, DeFrank MP, Van Buskirk EM. Comparative microvascular anatomy of mammalian ciliary processes. *Invest Ophthalmol Vis Sci* 1987; 28: 1325–1340.
112. Morrison JC, DeFrank MP, Van Buskirk EM. Regional microvascular anatomy of the rabbit ciliary body. *Invest Ophthalmol Vis Sci* 1987; 28: 1314–1324.
113. Matsuo N. Scanning electron microscopic studies on the corrosion casts of the blood vessels of the ciliary body. *Acta Soc Ophthalmol Jap* 1973; 77: 928.
114. Funk R, Rohen JW. Scanning electron microscopic study on the vasculature of the human anterior eye segment. *Exp Eye Res* 1990; 51: 651–661.
115. Natiello N, Samuelson D. Three-dimensional reconstruction of the angioarchitecture of the ciliary body of the West Indian manatee (*Trichechus manatus*). *Vet Ophthalmol* 2005; 8(6): 367–373.
116. Henderson T. The anatomy and physiology of accommodation in Mammalia. *Trans Ophthalmol Soc UK* 1926; 280–308.
117. Tripathi RC. Comparative physiology and anatomy of aqueous humor outflow pathway. In: Davson H, ed. *The Eye. Vol. 5.* New York: Academic Press, 1974: 163–272.
118. Duke-Elder S. *System of Ophthalmology. Vol. I.* London: Henry Kimpton, 1958: 460–467.
119. Troncoso MU. Comparative anatomy, physiology and evolution of the angle of the anterior chamber in Mammalia. *XV Int Cong Ophthalmol Cairo* 1938; 4: 98–119.
120. Samuelson DA. A reevaluation of the comparative anatomy of the Eutherian iridocorneal angle and associated ciliary body musculature. *Vet Comp Ophthalmol* 1996; 6: 153–172.
121. Hueck A. *Die Bewegung der Krystall-Linse.* Dorpat, 1839.
122. Samuelson DA, Lewis PA. Comparative morphology of the iridocorneal angle of selected artiodactyls (ungulates). *Vet Comp Ophthalmol* 1995; 5: 89–103.
123. Gum GG. Ophthalmic physiology. In: Gelatt KN, ed. *Veterinary Ophthalmology.* Philadelphia: Lea & Febiger, 1991: 130–134.
124. Samuelson DA, Gelatt KN. Aqueous outflow in the Beagle. I. Postnatal morphologic development of the iridocorneal angle: Pectinate ligament and ureal trabecular meshwork. *Curr Eye Res* 1984; 6: 783–794.
125. Samuelson DA, Gelatt KN. Aqueous outflow in the Beagle. II. Postnatal morphologic development of the iridocorneal angle: Corneoscleral trabecular meshwork and angular aqueous plexus. *Curr Eye Res* 1984; 6: 795–807.
126. McMaster PRB, Macri FJ. Secondary aqueous humor outflow pathways in the rabbit, cat, and monkey. *Arch Ophthalmol* 1968; 79: 297–303.
127. Martin CL. The normal canine iridocorneal angle as viewed with the scanning electron microscope. *J Am Anim Hosp Assoc* 1975; 11: 180–192.
128. Bill A. The drainage of aqueous humor. *Invest Ophthalmol* 1975; 14: 1–6.
129. Inomata H, Bill A, Smelzer G. Aqueous humor pathways through the trabecular meshwork and into Schlemm's canal in the cynomolgous monkey (*Macaca irus*). *Am J Ophthalmol* 1972; 73: 760–798.
130. Samuelson D, Smith P, Brooks D. Morphologic features of the aqueous humor drainage pathways in horses. *Am J Vet Res* 1989; 50: 720–727.
131. Tripathi RC. Ultrastructure of the exit pathway of the aqueous in lower mammals. *Exp Eye Res* 1971; 12: 311–314.
132. Bedford PCG, Grierson I. Aqueous drainage in the dog. *Res Vet Sci* 1986; 41: 172–186.
133. Simones P, DeGeest JP, Lauwers H. Comparative morphology of the pectinate ligaments of domestic mammals, as observed under the dissecting microscope and the scanning electron microscope. *J Vet Med Sci,* 1996; 58: 977–982.
134. Gong H, Trinkaus-Randall V, Freddo TF. Ultrastructural localization of elastin in normal infant and adult trabecular meshwork using atropoelastin antibody. *Invest Ophthalmol Vis Sci* 1989; 30(suppl): 204.
135. Samuelson DA, Gum GG, Gelatt KN, Barrie KP. Aqueous outflow in the Beagle: Unconventional outflow, using different-sized microspheres. *Am J Vet Res* 1985; 40: 242–248.
136. Garcia GA, et al. Microsphere evaluation of aqueous outflow in the chicken eye. *Invest Ophthalmol Vis Sci* 1986; 27(suppl): 200.
137. Johnson M, et al. The filtration characteristics of the aqueous outflow system. *Exp Eye Res* 1990; 50: 407–418.
138. Samuelson DA, Gelatt KN, Gum GG. Kinetics of phagocytosis in the normal canine iridocorneal angle. *Am J Vet Res* 1984; 45: 2359–2366.
139. Grierson I, Lee WR. Erythrocyte phagocytosis in the human trabecular meshwork. *Br J Ophthalmol* 1973; 57: 400–415.
140. Sherwood M, Richardson TM. Kinetics of the phagocytic process in the trabecular meshwork of cats and monkeys. *Invest Ophthalmol Vis Sci* 1981; 20(suppl): 65.
141. Samuelson, DA, Plummer C, Gelatt K. Schwalbe line's cell in the normal and glaucomatous dog. *Vet Ophthalmol* 2001; 4: 47–53.
142. Rohen JW, Lutjen-Drecoll E. Morphology of aqueous outflow pathways in normal and glaucomatous eyes. In: Ritch R, Shields MB, Krupin T, eds. *The Glaucomas.* St. Louis: CV Mosby, 1989: 41–74.
143. Raviola G. Schwalbe's line cells: A new cell type in the trabecular meshwork of Macaca mulatta. *Invest Ophthalmol Vis Sci* 1982; 22: 45–56.
144. Stone RA, Kuwayama Y, Laties AM, Marangos PJ. Neuron-specific enolase-containing cells in the Rhesus monkey trabecular meshwork. *Invest Ophthalmol Vis Sci* 1984; 25: 1332–1334.
145. Lutjen-Decoll E, Rohen JW. Functional morphology of the trabecular meshwork. In: Tasman W, Jaeger EA, eds. *Biomedical Foundations of Ophthalmology. Vol. 1.* Philadelphia: JB Lippincott, 1992: 1–33.
146. Allen L, Burian HM, Braley AE. The anterior border ring of Schwalbe and the trabecular zone. *Arch Ophthalmol* 1955; 53: 799–806.
147. Tripathi RC. Mechanism of the aqueous outflow across the trabecular wall of Schlemm's canal. *Exp Eye Res* 1971; 11: 116–121.
148. Kayes J. Pore structure of the inner wall of Schlemm's canal. *Invest Ophthalmol* 1967; 6: 381–394.
149. Grierson I, Lee WR, Abraham S. Pathways for drainage of aqueous humor into Schlemm's canal. *Trans Ophthalmol Soc UK* 1977; 97: 719–725.
150. de Kater AW, Spurr-Michand SJ, Gibson IK. Localization of smooth muscle myosin-containing cells in the aqueous outflow pathway. *Invest Ophthalmol Vis Sci* 1990; 31: 347–353.

151. Ryland TR, et al. Localization of smooth muscle actin in the iridocorneal angle of normal and spontaneous glaucomatous Beagle dogs. *Vet Ophthalmol* 2003; 6: 205–209.
152. Grierson I, Lee WR. Acid mucopolysaccharides in the outflow apparatus. *Exp Eye Res* 1975; 21: 417–431.
153. Samuelson DA, Gum GG, Gelatt KN. Action of hyaluronidase on aqueous outflow resistance in normal and glaucomatous dogs. *Invest Ophthalmol Vis Sci* 1987; 28(suppl): 131.
154. Gum GG, Samuelson DA, Gelatt KN. Effect of hyaluronidase on aqueous outflow resistance in normal and glaucomatous dogs. *Am J Vet Res* 1992; 53: 767–770.
155. Knepper PA, Goosens W, Hvizd M, Palmberg PF. Glycosaminoglycans of the human trabecular meshwork in primary open angle glaucoma. *Invest Ophthalmol Vis Sci* 1996; 37: 1360–1367.
156. Samuelson DA, Gelatt KN. The aging iridocorneal angle and glaucoma. In: Mohr U, ed. *Pathobiology of the Aging Dog.* ILSI Press, 1998.
157. Allingham RR, et al. Relationship between outflow facility and inner wall pores and vacuoles in Schlemm's canal. *Invest Ophthalmol Vis Sci* 1989; 30(suppl): 222.
158. Lee WR, Grierson I. Pressure effects on the endothelium of the trabecular wall of Schlemm's canal: A study by scanning electron microscopy. *Albr von Graefes Arch Klin Ophthalmol* 1975; 196: 255–265.
159. Bill A, Phillips CI. Uveoscleral drainage of aqueous humor in human eyes. *Exp Eye Res* 1971; 12: 275–281.
160. Bill A. Some aspects of the ocular circulation. *Invest Ophthalmol Vis Sci* 1985; 26: 410–424.
161. Barrie KP, et al. Quantitation of uveoscleral outflow in normotensive and glaucomatous Beagles by H-labeled dextran. *Am J Vet Res* 1985; 46: 84–88.
162. Kligman KC, Lewis PA, Samuelson DA. Morphology of the uveoscleral pathway in domestic species. I*nvest Ophthalmol Vis Sci* 2004; 44(ARVO suppl): S43.
163. Floyd BB, Cleveland PH, Worthen DM. Fibronectin in human trabecular drainage channels. *Invest Ophthalmol Vis Sci* 1985; 26: 797–804.
164. Gelatt KN, Samuelson DA. Collagen fiber organization in the iridocorneal angle of Beagles with inherited glaucoma. *Invest Ophthalmol Vis Sci* 1986; 27(suppl): 310.
165. Lutjen-Drecoll E, Shimizu T, Rohrbach M, Rohen JW. Quantitative analysis of "plaque material" in the inner and outer wall of Schlemm's canal in normal and glaucomatous eyes. *Exp Eye Res* 1986; 443–456.
166. Lutjen-Drecoll E, Rohen JW. Morphology of aqueous outflow pathways in normal and glaucomatous eyes. In: Ritch R, Shields MB, Krupin T, eds. *The Glaucomas.* St. Louis: Mosby-Year Book, 1996: 89–123.
167. Miller ME, Christensen GE, Evans H. *Anatomy of the Dog.* Philadelphia: WB Saunders, 1964.
168. Gwin RM, Gelatt KN, Chiou CY. Adrenergic and cholinergic innervation of the anterior segment of the normal and glaucomatous dog. *Invest Ophthalmol Vis Sci* 1979; 18: 674–682.
169. Ehinger B. Adrenergic nerves to the eye and to related structures in man and the cynomolgus monkey *(Macaca irus). Invest Ophthalmol* 1966; 5: 42–52.
170. Ehinger B. Distribution of adrenergic nerves in the eye and some related structures in the cat. *Acta Physiol Scand* 1966; 66: 123–128.
171. Nomura T, Smelser G. The identification of adrenergic and cholinergic nerve endings in the trabecular meshwork. *Invest Ophthalmol* 1974; 13: 525–532.
172. Funata M, Mimatsu T, Tokoro T. Electron microscopic study of the choroidal melanocytes and elastic fibers. *Nip Ganka Gak Zas* 1990; 94: 352–358.
173. Koseki T. Ultrastructural studies of the lamina suprachoroidea in the human eye. *Nip Ganka Gak Zas* 1992; 96: 757–766.
174. Castro-Correia J. Studies on the innervation of the uveal tract. *Ophthalmologica* 1967; 154: 497–520.
175. DeStefano ME, Mugnaini E. Fine structure of the choroidal coat of the avian eye. *Invest Ophthalmol Vis Sci* 1997; 38: 1241–1260.
176. Wong VG, Macri FJ. Vasculature of the cat eye. *Arch Ophthalmol* 1964; 72: 351–358.
177. Natiello M, Lewis P, Samuelson, D. Comparative anatomy of the ciliary body of the West Indian manatee (*Trichechus manatus*) and selected species. *Vet Ophthalmol* 2005; 8: 375–386.
178. Torczynski E. Choroid and suprachoroid. In: Duane TD, Jaeger EA, eds. *Biomedical Foundations of Ophthalmology. Vol. 1.* Philadelphia: JB Lippincott, 1988; Chapter 22: 1–33.
179. Flugel C, Tamm ER, Mayer B, Lutjen-Drecoll E. Species differences in choroidal vasodilative innervation: Evidence for specific intrinsic nitrergic and VIP-positive neurons in the human eye. *Invest Ophthalmol Vis Sci* 1994; 35: 592–599.
180. Auker CR, Parver LM, Doyle T, Carpenter DO. Choroidal blood flow. I. Ocular tissue temperature as a measure of flow. *Arch Ophthalmol* 1982; 100: 1323–1326.
181. Parver LM, Auker CR, Carpenter DO, Doyle T. Choroidal blood flow. II. Reflexive control in the monkey. *Arch Ophthalmol* 1982; 100: 1327–1330.
182. Bill A. Blood circulation and fluid dynamics in the eye. *Physiol Rev* 1975; 55: 383–417.
183. Bill A, Sperber G, Ujiie K. Physiology of the choroidal vascular bed. *Int Ophthalmol* 1983; 6: 101–107.
184. Bill A. A method to determine osmotically effective albumin and gamma globulin concentrations in tissue fluids, its application to the uvea and a note on the effects of capillary "leaks" on tissue fluid dynamics. *Acta Physiol Scand* 1968; 73: 511–522.
185. Meriney SD, Pilar G. Cholinergic innervation of the smooth muscle cells in the choroid coat of the chick eye and its development. *J Neurosci* 1987; 7: 3827–3839.
186. Young DL, Braekevelt CR. Fine structure of the retinal epithelial regions of the red kangaroo (*Macropus rufus*). *Anat Anz* 1993; 175: 299–303.
187. Tjalve H, Frank A. Tapetum lucidum in the pigmented and albino ferret. *Exp Eye Res* 1984; 38: 314–351.
188. Braekevelt CR. Fine structure of the retinal epithelium and tapetal lucidum of the ranch mink, *Mustela vison. Acta Anat Basel* 1989; 135: 296–302.
189. Braekevelt CR. Fine structure of the tapetum lucidium of the paca, *Cuniculus paca. Acta Anat Basel* 1993; 146: 244–250.
190. Lascano C, et al. Structural specializations of the eye in the vizcacha (*Lagostomus maximus maximus*). *Anat Rec* 1999; 255: 34–43.
191. Ollivier FJ, et al. Comparative morphology of the tapetum lucidum (among selected species). *Vet Ophthalmol* 2004; 7: 11–22.
192. Silveira LC, Picano-Diniz CW, Oswaldo-Cruz E. Distribution and size of ganglion cells in the retinae of large Amazon rodents. *Vis Neurosci* 1989; 2: 221–235.

193. Hebel R. Entwicklung und struktur der retina und des tapetum lucid um des hundes. *Ergeb Anat Entwickl-Gesch* 1971; 45: 3–92.
194. Wyman M, Donovan EF. The ocular fundus of the normal dog. *J Am Vet Med Assoc* 1965; 145: 17.
195. Braekevelt CR. Fine structure of the tapetum lucidum of the domestic ferret. *Anat Embryol* 1981; 163: 201–214.
196. Braekevelt CR. The fine structure of the feline tapetum lucidum. *Anat Histol Embryol* 1990; 19: 97–105.
197. Pedler C. The fine structure of the tapetum cellulosum. *Exp Eye Res* 1963; 2: 189–195.
198. Bernstein MH, Pease DC. Electron microscopy of the tapetum lucidum of the cat. *J Biophys Biochem Cytol* 1959; 5: 35–40.
199. Chijiiwa T, Ishibashi T, Inomata H. Histological study of choroidal melanocytes in animals with tapetum lucidum cellulosum. *Graefes Arch Clin Exp Ophthalmol* 1990; 228: 161–168.
200. Pirie A. The chemistry and structure of the tapetum lucidum in animals. In: Graham-Jones O, ed. *Aspects of Comparative Ophthalmology.* New York: Pergamon Press, 1965: 57–68.
201. Bussow H, Baumgarten HG, Hansson C. The tapetal cell: A unique melanocyte in the tapetum lucidum cellulosum of the cat (*Felis domestica L.*). *Anat Embryol* 1980; 158: 289–302.
202. Bellairs R, Harkness LR, Harkness RD. The structure of the tapetum of the eye of the sheep. *Cell Tissue Res* 1975; 157: 73–91.
203. Schwab IR, et al. Evolution of the tapetum. *Trans Am Ophthalmol Soc* 2002; 100: 187–199.
204. Cavitt K, Samuelson D, Brooks D, Hendricks D, Whitley D, Leone N. Morphometric evaluation of choroidal pigmentary changes associated with low zinc nutrition in pigs. *Invest Ophthalmol Vis Sci* 1991; 32(suppl): 1175.
205. Samuelson DA., et al. The influence of low zinc nutrition on choroid in the pig. I. The melanocyte. *Vet Ophthalmol,* 1999; 2: 27–34.
206. Hu F, Montagna W. The development of pigment cells in the eyes of rhesus monkeys. *Am J Anat* 1971; 132: 119–132.
207. Hu F, Endo H, Alexander NJ. Morphological variations of pigment granules in eyes of the rhesus monkey. *Am J Anat* 1973; 136: 167–182.
208. Hu F, Mah K. Changes in melanosomes with age in iridal stromal melanocytes of rhesus macaques. *Mech Aging Dev* 1979; 32: 95–102.
209. Samuelson DA, et al. The association of macromelanosomes and low zinc nutrition in the pig. *Invest Ophthalmol Vis Sci* 1992; 33(Suppl): 1193.
210. Samuelson DA, et al. X-ray microanalysis of ocular melanin in pigs maintained on normal and low zinc diets. *Exp Eye Res* 1993; 56: 63–70.
211. Samuelson DA, et al. The influence of low zinc nutrition on choroid in the pig eye. II. The melanosome. *Vet Ophthalmol* 1999; 2: 35–45.
212. Monaco MA, Samuelson DA, Gelatt KN. Morphology and postnatal development of the normal lens in the dog and congenital cataract in the Miniature Schnauzer. *Lens Res* 1985; 2: 393–433.
213. Barnard K, Burgess SA, Cater DA, Wooley DM. Three-dimensional structure of type IV collagen in the mammalian lens capsule. *J Struct Biol* 1992; 108: 6–13.
214. Samuelson DA, et al. Prenatal morphogenesis of the congenital cataracts in the Miniature Schnauzer. *Lens Res* 1987; 4: 231–250.
215. Benedetti EL, et al. A portrait of plasma membrane specializations in eye lens epithelium and fibers. *Biochem Biophys Acta* 1976; 157: 353.
216. Rafferty NS, Esson EA. An electron-microscope study of adult mouse lens: Some ultrastructural specializations. *J Ultrastruct Res* 1974; 46: 239–253.
217. Wegener AR. In vivo studies on the effect of UV-radiation on the eye lens in animals. *Doc Ophthalmol* 1994; 88: 221–232.
218. Vrensen GF. Aging of the human eye lens—A morphological point of view. *Comp Bioch Physiol A Physiol* 1995; 111: 519–532.
219. Li WC, et al. Lens epithelial cell apoptosis appears to be a common cellular basis for non-congenital cataract development in humans and animals. *J Cell Biol* 1995; 130: 169–181.
220. Philipson BT, Hanninen L, Balazs EA. Cell contacts in human and bovine lenses. *Exp Eye Res* 1975; 21: 505–519.
221. Kuszak J, Maisel H, Harding CV. Gap junctions of chick lens fiber cells. *Exp Eye Res* 1978; 27: 495–498.
222. Kuszak JR, Sivak JG, Weerheim JA. Lens optical quality is a direct function of lens sutural architecture. *Invest Ophthalmol Vis Sci* 1991; 32: 2119–2129.
223. Kuwabara T, Imaizumi M. Denucleation process of the lens. *Invest Ophthalmol* 1974; 13: 973–981.
224. Martin C. Slit lamp examination of the normal canine anterior ocular segment. Part II: Description. *J Small Anim Pract* 1969; 10: 151–162.
225. Daniel WJ, Noonan NE, Gelatt KN. Isolation and characterization of the crystallins of the normal and cataractous canine. *Curr Eye Res* 1984; 3: 911–922.
226. Glasser A, et al. The mechanism of lenticular accommodation in chickens. *Vision Res* 1995; 35: 1525–1540.
227. Willekens B, Vrensen G. Lens fiber organization in four avian species: a scanning electron microscopic study. *Tissue Cell* 1985; 17: 359–377.
228. Taylor VL, et al. Morphology of normal human lens. *Invest Ophthalmol Vis Sci* 1996; 37: 1396–1414.
229. Hodos W, Miller RF, Fite KV. Age-dependent changes in visual acuity and retinal morphology in pigeons. *Vision Res* 1991; 31: 669–677.
230. Farnsworth PN, et al. Surface ultrastructure of the human lens capsule and zonular attachments. *Invest Ophthalmol Vis Sci* 1976; 15: 36–40.
231. Dische Z, Murty VLN. An insoluble structural glycoprotein: A major constituent of the zonula zinni. *Invest Ophthalmol Vis Sci* 1974; 13: 991.
232. Streeten BW, Licari P. Immunohistochemical comparison of zonular fibrils and elastic tissue microfibrils. *Invest Ophthalmol Vis Sci* 1981; 21: 130–135.
233. Gloor BP. Zur entwicklung des glaskorpers undder zonule: VI. Autoradiographische untersuchurgen zur entwicklung der zonule der maus mit ^{3}H-markeirten aminoauren und ^{3}H- glucose. *Albr von Graefes Arch Klin Exp Ophthalmol* 1974; 189: 99–104.
234. Tucker R. Comparative and functional studies on the suspensory apparatus of the lens (Mammalia). *Z Morphol Tiere* 1973; 74: 171.
235. Raviola G. The fine structure of the ciliary zonule and ciliary epithelium with special regard to the organization and insertion of the zonular fibrils. *Invest Ophthalmol Vis Sci* 1971; 10: 851–869.
236. Streeten BW. Zonular apparatus. In: Duane TD, Jaeger EA, eds. *Biomedical Foundations of Ophthalmology. Vol. 1.* Philadelphia: JB Lippincott, 1992.

237. Rohen JW. Scanning electron microscopic studies of the zonular apparatus in human and monkey eyes. *Invest Ophthalmol Vis Sci* 1979; 18: 133–144.
238. Gelatt KN, Samuelson DA. The role of lens luxation in inherited glaucoma in the Beagle. *Anim Eye Res* 1998; 17: 1–8.
239. Jaffe NS. *The Vitreous in Clinical Ophthalmology.* 1st ed. St. Louis: CV Mosby, 1969.
240. Rosen E. Anterior hyaloid membrane. *Am J Ophthalmol* 1965; 59: 1069–1079.
241. Balazs EA. Functional anatomy of the vitreous. In: Duane TD, Jaeger EA, eds. *Biomedical Foundations of Ophthalmology. Vol. 1.* Philadelphia: JB Lippincott, 1994; Chapter 17: 1–17.
242. Bishop PN, et al. The role of the posterior ciliary body in the biosynthesis of vitreous humor. *Eye* 2002; 16: 454–460.
243. Goes RM, et al. Chondroitin sulfate proteoglycans are structural renewable constituents of the rabbit vitreous body. *Curr Eye Res* 2005; 30: 405–413.
244. Noulas AV, et al. Pig vitreous gel: macromolecular composition with particular reference to hyaluronan-binding proteoglycans. *Biochimie* 2002; 84: 295–302.
245. Haddad A, et al. The origin of the intrinsic glycoproteins of the rabbit vitreous body: An immunohistochemical and autoradiographic study. *Exp Eye Res* 1990; 50: 555–561.
246. Jacobson B. Biosynthesis of hyaluronic acid in the vitreous: V. Studies on a particular hyalocyte glycosyl transferase. *Exp Eye Res* 1976; 27: 247–249.
247. Andre JC, Haddad A, Fife RJ, Pelletier G. Morphologic and molecular changes during the postnatal development of the rabbit vitreous. *Exp Eye Res* 1992; 55: 67–71.
248. Balazs EA, et al. Studies on the structure of the vitreous body: XII. Cytological and histochemical studies on the cortical tissue layer. *Exp Eye Res* 1964; 3: 57–71.
249. Faulborn J, Bowald S. Combined macroscopic light microscopic, scanning, and transmission electron microscopic investigation of the vitreous body. II. The anterior vitreous cortex. *Ophthalmic Res* 1982; 14: 117–123.
250. Eisner G, Bachmann E. Vergleichend morphologische spaltlampenuntersuchung des glaskorpers beim rind. *Albr von Graefes Arch Klin Exp Ophthalmol* 1974; 191: 329–342.
251. Eisner G. Zue anatomie des glaskorpers. *Albr von Graefes Arch Klin Exp Ophthalmol* 1975; 193: 33–56.
252. Eisner G, Bachmann E. Vergleichend morphologische spaltlempenuntersuchung des glaskorpers bei der katze. *Albr von Graefes Arch Klin Exp Ophthalmol* 1974; 191: 343–350.
253. Eisner G, Bachmann E. Vergleichend morphologische spaltlampuntersuchung des glaskorpers beim pferd. *Albr von Graefes Arch Klin Exp Ophthalmol* 1974; 192: 1–8.
254. Eisner G, Bachmann E. Vergleichend morphologische spaltlampenuntersuchung des glaskorpers von schaf, schwein, hund, affen und kaninchen. *Albr von Graefes Arch Klin Exp Ophthalmol* 1974; 192: 9–17.
255. Eisner G. Clinical anatomy of the vitreous. In: Duane TD, Jaeger EA, eds. *Biomedical Foundations of Ophthalmology. Vol. 1.* Philadelphia: JB. Lippincott, 1988; Chapter 16: 1–34.
256. Herron WL, et al. Vitamin A deficiency induced "rod thinning" to permanently decrease the production of rod outer segment material. *Invest Ophthalmol Vis Sci* 1974; 13: 54–59.
257. Tso MO, Friedman E. The retinal pigment epithelium. I. Comparative histology. *Arch Ophthalmol* 1967; 78: 641–649.
258. Shively JN, Epling GP, Jensen R. Fine structure of the canine eye: Retina. *Am J Vet Res* 1970; 31: 1339–1359.
259. Leure-xdu Pree A. Ultrastructure of the pigment epithelium in the domestic sheep. *Am J Ophthalmol* 1968; 65: 383–398.
260. Nilsson SE, et al. The morphology of the sheep retina. I. The receptor cells and the pigment epithelium. *Acta Ophthalmol* 1973; 51: 599–611.
261. Braekevelt CR. The retinal epithelial fine structure in the domestic cat. *Anat Histol Embryol* 1990; 19: 58–66.
262. Braekevelt CR. The retinal epithelial fine structure in the grey seal. *Acta Anat Basel* 1986; 127: 255–261.
263. Jimbow K. Current update and trends in melanin pigmentation and melanin biology. *Keio J Med* 1995; 44: 9–18.
264. Orlow SJ. Melanosomes are specialized members of the lysosomal lineage of organelles. *J Invest Dermatol* 1995; 105: 3–7.
265. Schraermeyer U. Does melanin turnover in the eyes of adult vertebrates? *Pig Cell Res* 1993; 6: 193–204.
266. Kuwabara T. Species differences in the retinal pigment epithelium. In: Zinn GM, Marmor MF, eds. *The Retinal Pigment Epithelium.* Cambridge, MA: Harvard Press, 1979: 58–82.
267. Spitznas M, Hogan MJ. Outer segments of photoreceptors and the retinal pigment epithelium: Interrelationship in the human eye. *Arch Ophthalmol* 1970; 84: 810–819.
268. Braekevelt CR. Retinal pigment epithelial fine structure in the red-tailed hawk (*Buto jamaicensis*). *Anat Histol Embryol* 1990; 21: 48–56.
269. Braekevelt CR, Thorlakson IJ. Fine structure of the retinal pigment epithelium of the great horned owl (*Bubo virginianus*). *Histol Histopathol* 1993; 8: 17–23.
270. Braekevelt CR. Fine structure of the retinal pigment epithelium (RPE) of the emu (*Dromaius novaehollandiae*). *Tissue Cell* 1998; 30: 149–156.
271. Donovan RH, et al. Histology of the normal collie eye. III. Lens, retina and optic nerve. *Ann Ophthalmol* 1974; 6: 1299–1307.
272. Brown KT. The electroretinogram: Its components and their origins. *Vision Res* 1968; 18: 633–677.
273. Dollery CT, Bulpitt CJ, Kohner EM. Oxygen supply to the retina and choroidal circulation at normal and increased arterial oxygen tensions. *Invest Ophthalmol* 1969; 8: 588–594.
274. Chase J. The evolution of retinal vascularization in mammals: A comparison of vascular and avascular retinae. *Ophthalmology* 1982; 89: 1518–1525.
275. Buttery RG, Hinrichsen CFL, Weller WL, Haight JR. How thick should a retina be? A comparative study of mammalian species with and without intraretinal vasculature. *Vision Res* 1991; 31: 169–187.
276. Ehrenhofer MC, et al. Normal structure and age-related changes of the equine retina. *Vet Ophthalmol* 2002; 5: 39–47.
277. Henkind P. The retinal vascular system of the domestic cat. *Exp Eye Res* 1966; 5: 10–20.
278. Smith PJ. Effect of dietary zinc levels on photic retinopathy in the pig. PhD dissertation, University of Florida, Gainesville, 1995.
279. DeSchaepdrijver L. Vergelijkende Morfologische Studie van de Retinale Circultie bij de Hond, de Kat en het Varken. PhD thesis, Universiteit Gent Faculteit van de Diergenesskunde, 1993.
280. Rapaport DH, Stone J. The area centralis of the retina in the cat and other mammals: Focal point for function and development of the visual system. *Neurosci* 1984; 11: 289–301.

281. Enroth-Cugell C, Robson JG. The contrast sensitivity of retinal ganglion cells of the cat. *J Physiol Lond* 1966; 187: 517–522.
282. Provis JM. The distribution and size of ganglion cells in the retina of the pigmented rabbit: A quantitative analysis. *J Comp Neurol* 1979; 185: 121–137.
283. Koch SA, Rubin LF. Distribution of cones in retina of the normal dog. *Am J Vet Res* 1972; 33: 361–363.
284. Steinberg RH, Reid M, Lacy PL. The distribution of rods and cones in the retina of the cat. *J Comp Neurol* 1973; 148: 229–235.
285. Schrieber P, et al. Photoreceptor density inversely proportional to axial length. *Invest Ophthalmol Vis Sci* 1994; 35(suppl): 1801.
286. Chandler MJ, Smith PJ, Samuelson DA. Photoreceptor density and the area centralis of the domestic pig retina. *Vet Ophthalmol* 1999; 2: 179–184.
287. Famiglietti EV, Sharpe SJ. Regional topography of rod and immunocytochemically characterized "blue" and "green" cone photoreceptors in rabbit retina. *Vis Neurosci* 1995; 12: 1151–1175.
288. Krebs W, Krebs I. *Primate Retina and Choroid: Atlas of Fine Structure in Man and Monkey.* New York: Springer-Verlag, 1991.
289. Meyer DB. The avian eye and its adaptations. In: Crestelli F, ed. *Handbook of Sensory Physiology. Vol. VII/5.* Berlin: Springer-Verlag, 1977: 564–566.
290. Rodieck RW. *The Vertebrate Retina: Principles of Structure and Function.* San Francisco: WH Freeman, 1973.
291. Cohen AI. Rods and cones and the problem of visual excitation. In: Straatsma BR, Hall MO, Allen, RA, eds. *The Retina—Morphology, Function and Clinical Characteristics.* Los Angeles: University of California Press, 1969: 31–62.
292. Waldvogel JA. The bird's eye view. *Am Scientist* 1990; 78: 342–353.
293. Chen D, Collins JS, Goldsmith TH. The ultraviolet receptor of bird retinas. *Science* 1984; 225: 337–340.
294. Braekevelt CR. Retinal photoreceptor fine structure in the red-tailed hawk (*Buteo jamaicensis*). *Anat Histol Embryol* 1993; 22: 222–232.
295. Braekevelt CR. Fine structure of the retinal photoreceptors of the great horned owl (*Bubo virginianus*). *Histol Histopathol* 1993; 8: 25–34.
296. Schultze M. Zur anatomie und physiologie der retina. *Arch Mikrosk Anat* 1866; 3: 215–244.
297. King-Smith PE. Absorption spectra and function of coloured oil drops in the pigeon retina. *Vision Res* 1969; 9: 1391–1399.
298. Iskandar LA, Abdel-Sayad SZ, Abdel-Khalek LR. Absorption spectrum of visual pigments and sensitivity curve of Egyptian pigeon (*Colombia livia*). *Proc Zool Soc A R Egypt* 1986; 11: 117–124.
299. Iskandar LA, Ghorab HM, Bucci TJ, Abdel-Khalek LR. Photoreceptors and oil droplets colour: A comparative histology of the retina of owl and pigeon. *Proc Zool Soc A R Egypt* 1986; 11: 125–136.
300. Vorobyev M. Coloured oil droplets enhance colour discrimination. *Proc Biol Sci* 2003; 270: 1255–1261.
301. Wong RO. Morphology and distribution of neurons in the retina of the American garter snake, *Thamnophis sitalis. J Comp Neurol* 1989; 283: 587–601.
302. Uga S, Smelser GK. Comparative study of the fine structure of retinal Müller cells in various vertebrates. *Invest Ophthalmol* 1973; 12: 434–448.
303. Sigelman J, Ozanics V. Retina. In: Duane TD, Jaeger EA, eds. *Biomedical Foundations of Ophthalmology. Vol. 1.* Philadelphia: JB Lippincott, 1988: Chapter 19: 1–63.
304. Magalhaes MM. Functional cytoarchitecture of the retina Müller cell. In: Yamada E, Mishima S, eds. *The Structure of the Eye. Jpn J Ophthalmol*, 1976.
305. Meyer DBC. The avian eye and its adaptations. In: Crescitelli F, ed. *Handbook of Sensory Physiology.* Berlin: Springer-Verlag, 1977: 559–561.
306. Young SR, Martin GR. Optics of retinal oil droplets: A model of light collection and polarization detection in the avian retina. *Vision Res* 1984; 24: 129–137.
307. Kaas, et al. Receptor pedicle density in the cat's retina. *Brain Res* 1972; 42: 496–497.
308. Dowling JE, Werblin FS. Synaptic organization of the vertebrate retina. *Vision Res Suppl* 1971; 3: 1–15.
309. Park SS, Sigelman J, Gragoudas ES. The anatomy and cell biology of the retina. In: Tasman W, Jaeger EA, eds. *Duane's Foundations of Clinical Ophthalmology. Vol 1.* Philadelphia: Lippincott-Raven, 1994: Chapter 19: 1–63.
310. Kolb H. The connections between horizontal cells and photoreceptors in the retina of the cat: Electron microscopy of Golgi preparations. *J Comp Neurol* 1974; 155.
311. Kolb H, Famiglietti EV. Rods and cone pathways in the inner plexiform layer of cat retina. *Science* 1974; 186: 47–49.
312. Witkovsky P. Functional anatomy of the retina. In: Tasman W, Jaeger EA, eds. *Foundations of Clinical Ophthalmology. Vol 1.* Philadelphia: Lippincott-Raven, 1992: Chapter 20: 1–29.
313. Copenhagen DR, Owen WG. Functional characteristics of lateral interactions between rods in the retina of the snapping turtle. *J Physiol* 1976; 259: 251.
314. Kolb H, Jones J. Electron microscopy of Golgi-impregnated photoreceptors reveals connections between red and green cones in the turtle retina. *J Neurophysiol* 1985; 54: 304–317.
315. Gallego A. Studies on horizontal cells and a note on microglial cells. *Prog Ret Res* 1986; 5: 165–206.
316. Boycott BB, Hopkins JM, Sperling HG. Cone connections of the horizontal cells of the rhesus monkey's retina. *Proc R Soc Lond* 1987; 229: 345–379.
317. Kolb H, Linberg KA, Fisher SK. Neurons of the human retina—A Golgi study. *J Comp Neurol* 1992; 318: 147–187.
318. Sandmann D, Boycott BB, Peichl L. The horizontal cells of artiodactyls retinae: Comparison with Cajal's descriptions. *Vis Neurosci* 1996; 13: 735–746.
319. Mills SL, Massey SC. Morphology of bipolar cells labeled by DAPI in the rabbit retina. *J Comp Neurol* 1992; 321: 133–149.
320. Muller B, Peichl L. Horizontal cells in the cone-dominated tree shrew retina: Morphology, photoreceptor contacts, and topographical distribution. *J Neurosci* 1993; 13: 3628–3646.
321. Sandmann D, Boycott BB, Peichl L. Blue-cone horizontal cells in the retinae of horses and other equidae. *J Neurosci* 1996; 16: 3381–3396.
322. Young HM, Vaney DI. Rod-signal interneurons in the rabbit retina: I. Rod bipolar cells. *J Comp Neurol* 1991; 310: 139–153.
323. Boycott BB, Wassle H. Morphological classification of bipolar cells of the primate retina. *Eur J Neurosci* 1991; 3: 1069–1088.
324. Kolb H, Nelson R. Hyperpolarizing, small-field, amacrine cells in cone pathways of cat retina. *J Comp Neurol* 1996; 371: 415–436.

325. Cohen E, Sterling P. Convergence and divergence of cones onto bipolar cells in the central area of cat retina. *Phil Trans R Soc Lond B* 1990; 330: 323–328.
326. Strettoi E, Masland RH. The organization of the inner nuclear layer of the rabbit retina. *J Neurosci* 1995; 15: 875–888.
327. Merighi A, Raviola E, Dacheux RF. Connections of two types of flat cone bipolars in the rabbit retina. *J Comp Neurol* 1996; 371: 164–178.
328. Jeon C-J, Masland RH. A population of wide-field bipolar cells in the rabbit's retina. *J Comp Neurol* 1995; 360: 403–412.
329. Euler T, Wassle H. Immunocytochemical identification of cone bipolar cells in the rat retina. *J Comp Neurol* 1995; 361: 461–478.
330. Protti DA, et al. Light signaling in scotopic conditions in the rabbit, mouse and rat retina: A physiological and anatomical study. *J Neurophysiol* 2005; 93: 3479–3488.
331. Tauchi M. Single cell shape and population densities of indoleamine-accumulating and displaced bipolar cells in Reeves' turtle retina. *Proc R Soc Lond B Biol Sci* 1990; 238: 351–367.
332. Linberg KA, Suemune S, Fisher SK. Retinal neurons of the California ground squirrel, *Spermophilus beecheyi:* A Golgi study. *J Comp Neurol* 1996; 365: 173–216.
333. Kolb H, Famiglietti EV. Rod and cone pathways in the retina of the cat. *Invest Ophthalmol Vis Sci* 1976; 15: 935–946.
334. Strettoi E, Dacheux RF, Raviola E. Synaptic connections of rod bipolar cells in the inner plexiform layer of the rabbit retina. *J Comp Neurol* 1990; 295: 449–466.
335. Isayama T, Elderd WD. Y-immunoreactive amacrine cells in the retina of the turtle, *Pseudemys scripta elegans. J Comp Neurol* 1988; 271: 56–66.
336. Williamson DE, Eldred WD. Synaptic organization of two types of amacrine cells with CRF-like immunoreactivity in the turtle retina. *Vis Neurosci* 1991; 6: 257–269.
337. Ammermuller J, Weiler R. Physiological and morphological characterization of OFF-center amacrine cells in the turtle retina. *J Comp Neurol* 1988; 273: 137–148.
338. Cuenca N, et al. The neurons of the ground squirrel retina as revealed by immunostains for calcium binding proteins and neurotransmitters. *J Neurocytol* 2002; 31: 649–666.
339. Vaney DI, Young HM, Gynther IC. The rod circuit in the rabbit retina. *Vis Neurosci* 1991; 7: 141–154.
340. Wong ROL, Hughes A. The morphology, number, and distribution of a large population of confirmed displaced amacrine cells in the adult cat retina. *J Comp Neurol* 1987; 255: 159–177.
341. Chang SK, Straznicky C. The generation and changing retinal distribution of displaced amacrine cells in Bufo marinus from metamorphosis to adult. *Anat Embryol Berl* 1992; 186: 175–181.
342. Iuvone PM. Neurotransmitters and neuromodulators in the retina-regulation, interaction, and cellular effects. In: Adler R, Farber D, eds. *The Retina: A Model for Cell Biology Studies. Part II.* Orlando, FL: Academic Press, 1986.
343. Casini G, Rickman DW, Brecha NC. A-II amacrine cell population in the rabbit retina: Identification by parvalbumin immunoreactivity. *J Comp Neurol* 1995; 356: 132–142.
344. Casini G, Brecha NC. Vasoactive intestinal polypeptide-containing cells in the rabbit retina: Immunohistochemical localization and quantitative analysis. *J Comp Neurol* 1991; 305: 313–327.
345. Robinson SR, Dreher B, McCall MJ. Non-uniform retinal expansion during the formation of the rabbit's visual streak: Implications for the ontogeny of mammalian retinal topography. *Vis Neurosci* 1989; 2: 201–219.
346. Distler C, Dreher Z. Glial cells of the monkey retina. II. Müller cells. *Vision Res* 1996; 36: 2381–2394.
347. Nilsson SE, et al. The morphology of the sheep retina. II. The inner nuclear layer, the ganglion cells and the plexiform layers. *Acta Ophthalmol* 1973; 51: 612–627.
348. Nishizono H, et al. Evidence that Müller cells can phagocytize egg-lecithin-coated silicone particles. *Tissue Cell* 1993; 25: 305–310.
349. Boycott BB, Wassle H. The morphological types of ganglion cells of the domestic cat's retina. *Am J Physiol* 1974; 226: 397–400.
350. Kolb H. The inner plexiform layer in the retina of the cat: Electron microscopic observations. *J Neurocytol* 1979; 8: 295–329.
351. Henderson Z. Distribution of ganglion cells in the retina of adult pigmented ferret. *Brain Res* 1985; 358: 221–228.
352. Wakakuwa K, Washida A, Fukuda Y. Distribution and soma size of ganglion cells in the retina of the eastern chipmunk (*Tamias subiricus asiaticus*). *Vision Res* 1985; 25: 877–885.
353. Peichl L. Topography of ganglion cells in the dog and wolf retina. *J Comp Neurol* 1992; 324: 603–620.
354. Wilhelm M, Straznicky C. The topographic organization of the retinal ganglion cell layer of the lizard, *Ctenophorus nuchalis. Arch Histol Cytol* 1992; 55: 251–259.
355. Toth P, Staznicky C. The morphological characterization and distribution of displaced ganglion cells in the anuran retina. *Vis Neurosci* 1989; 3: 551–561.
356. Gonzalez-Soriano J, et al. A quantitative study of ganglion cells in the German Shepherd dog retina. *Anat Histol Embryol* 1995; 24: 61–65.
357. Hebel R. Distribution of retinal ganglion cells in five mammalian species (pig, sheep, ox, horse, dog). *Anat Embryol* 1976; 150: 45–51.
358. Freeman B, Tancred E. The number and distribution of ganglion cells in the retina of the brush-tailed possum, *Trichosurus vulpecula. J Comp Neurol* 1978; 177: 557–567.
359. Silveira LC, Picano-Diniz CW, Oswaldo-Cruz E. Distribution and size of ganglion cells in retinae of large Amazon rodents. *Vis Neurosci* 1989; 2: 221–235.
360. Vaney DI. A quantitative comparison between the ganglion cell populations and axonal outflows of the visual streak and periphery of the rabbit retina. *J Comp Neurol* 1980; 189: 215–233.
361. Stone J, Halasz P. Topography of the retina in the elephant, *Loxodonta africana. Brain Behav Evol* 1989; 34: 84–95.
362. Costa BL, Pessoa VF, Bousfield JD, Clarke RJ. Unusual distribution of ganglion cells in the retina on the three-toed sloth (*Bradypus variegatus*). *Braz J Med Biol Res* 1987; 20: 741–748.
363. Do Nascimento JL, Do Nascimento RS, Damasceno BA, Silveira LC. The neurons of the retinal ganglion cell layer of the guinea pig: Quantitative analysis of their distribution and size. *Braz J Med Biol Res* 1991; 24: 199–214.
364. Graydon ML, Giorgi PP. Topography of the retinal ganglion cell layer of Xenopus. *J Anat* 1984; 139: 145–157.
365. Schmid KL, Schmid LM, Wildsoet CF, Pettigrew JD. Retinal topography in the koala (*Phascolarctos cinereus*). *Brain Behav Evol* 1992; 39: 8–16.

366. Andrade da Costa BL, Pessoa VF, Bousfield JD, Clarke RJ. Ganglion cell size and distribution in the retina of the two-toed sloth (*Choloephus didactylus L.*). *Braz J Med Biol Res* 1989; 22: 233–236.
367. Pettigrew JB, et al. Peak density and distribution of ganglion cells in the retinae of microchiropteran bats: Implications for visual resolution. *Brain Behav Evol* 1988; 32: 39–56.
368. Timney B, Keil K. Visual acuity in the horse. *Vision Res* 1992; 32: 2289–2293.
369. Levick WR. Form and function of cat retinal ganglion cells. *Nature* 1975; 254: 659–662.
370. Famiglietti EV. Class I and class II ganglion cells of rabbit retina: A structural basis for X and Y (brisk) cells. *J Comp Neurol* 2004; 478: 323–346.
371. Stone J, Keens J. Distribution of small and medium-sized ganglion cells in the cat's retina. *J Comp Neurol* 1980; 192: 235–246.
372. Stein JJ, Berson DM. On the distribution of gamma cells in the cat retina. *Vis Neurosci* 1995; 12: 687–700.
373. Beauchemin ML. The fine structure of the pig's retina. *Albr von Graefes Arch Klin Exp Ophthalmol* 1974; 190: 27–45.
374. Fitzgibbon T, Funke K. Retinal ganglion cell axon diameter spectrum of the cat: Mean axon diameter varies according to retinal position. *Vis Neurosci* 1994; 11: 425–439.
375. Matsuyama M. Peculiar patterns of nerve fibers in the retina. I. Normal animal eye. *J Pediatr Ophthalmol* 1973; 10: 77.
376. Michaelson IC. *Retinal Circulation in Man and Animals.* Springfield, IL: Charles C. Thomas, 1954.
377. Matlu F, Leopold IH. Structure of the retinal vascular system of the dog, monkey, rat, mouse, and cow. *Am J Ophthalmol* 1964; 58: 261–270.
378. Hyvarinen L. Vascular structures of the rabbit retina. *Acta Ophthalmol* 1967; 45: 852–861.
379. Iskandar LA, Samuelson DA, Whitley RD. The pecten and the posterior circulation in the avian eye. *Invest Ophthalmol Vis Sci* 1988; 29(suppl): 381.
380. Sillman AJ. Avian vision. In: Farmer DA, King JK, Parkes KC, eds. *Avian Biology.* New York: Academic Press, 1973: 349–387.
381. Braekevelt CR. Fine structure of the pecten oculi in the American crow (*Corvus brachyrhynchos*). *Anat Histol Embryol* 1994; 23: 357–366.
382. Braekevelt CR. Fine structure of the pecten oculi of the red-tailed hawk (*Buteo jamaicensis*). *Anat Histol Embryol* 1991; 20: 354–362.
383. Braekevelt CR. Fine structure of the pecten oculi of the emu (*Dromaius novaehollandiae*). *Tissue Cell* 1998; 30: 157–165.
384. Kiama SG, Bhattacharjee J, Maina JN, Weyrauch, KD. A scanning electron microscope study of the pecten oculi of the black kite (*Milvus migrans*): Possible involvement of melanosomes in protecting the pecten against damage by ultraviolet light. *J Anat* 1994; 185: 637–642.
385. Bennett AT, Cuthill IC. Ultraviolet vision in birds: What is its function? *Vision Res* 1994; 34: 1471–1478.
386. Braekevelt CR. Fine structure of the pecten oculi in the great horned owl (*Bubo virginianus*). *Histol Histopathol* 1993; 8: 9–15.
387. Smith BJ, Smith SA, Braekevelt CR. Fine structure of the pecten oculi in the barred owl (*Strix varia*). *Histol Histopathol* 1996; 11: 89–96.
388. Gao H, Hollyfield JG. Aging of the human retina. Differential loss of neurons and retinal pigment epithelial cells. *Invest Ophthalmol Vis Sci* 1992; 33: 1–17.
389. Gartner S, Henkind P. Aging and degeneration of the human macula. I. Outer nuclear layer and photoreceptors. *Br J Ophthalmol* 1981; 65: 23–28.
390. Lai YL. Outward movement of photoreceptor cells in normal rat retina. *Invest Ophthalmol Vis Sci* 1980; 19: 849–856.
391. Fite KV, Bengston L. Aging and sex-related changes in the outer retina of Japanese quail. *Curr Eye Res* 1989; 8: 1039–1048.
392. Feeney-Burns L, Hilderbrand ES, Eldridge S. Aging human RPE: Morphometric analysis of macular, equatorial and peripheral cells. *Invest Ophthalmol Vis Sci* 1984; 25: 195–200.
393. Aouididi S, Dorey K, Delori FC, Samuelson D. Lipofuscin accumulation in zinc deficient pigs. *Invest Ophthalmol Vis Sci* 1994; 35(suppl): 1502.
394. Brooks DE, Komaromy AM, Kallberg ME. Comparative retinal ganglion cell and optic nerve morphology. *Vet Ophthalmol* 1999; 2: 3–11.
395. Hayreh SH. Anatomy and physiology of the optic nerve head. *Trans Am Ophthalmol Otolaryngol* 1974; 78: 240.
396. Trivino A, et al. Immunohistochemical study of human optic nerve head astroglia. *Vision Res* 1996; 36: 2015–2028.
397. Anderson DR, Baverman S. Reevaluation of the optic disk vasculature. *Am J Ophthalmol* 1976; 82: 165–174.
398. Brooks DE, Samuelson DA, Gelatt KN. Ultrastructural changes in laminar optic nerve capillaries of Beagles with primary open-angle glaucoma. *Am J Vet Res* 1989; 50: 929–935.
399. Tansley K. Comparison of the lamina cribrosa in mammalian species with good and indifferent vision. *Br J Ophthalmol* 1956; 40: 178–182.
400. Johanssen JO. The lamina cribrosa in the eyes of rats, hamsters, gerbils and guinea pigs. *Acta Anat Basel* 1987; 128: 55–62.
401. Morrison J, et al. Structure and composition of the rodent lamina cribrosa. *Exp Eye Res* 1995; 60: 127–135.
402. Brooks et al. Immunohistochemistry of the extracellular matrix of the normal equine lamina cribrosa. *Vet Ophthalmol* 2000; 3: 127–132.
403. Williams LW, et al. Orthograde rapid axoplasmic transport and ultrastructural changes of the optic nerve. Part I. Normotensive and acute hypertensive Beagles. *Glaucoma* 1983; 5: 177–188.
404. Samuelson DA, et al. Orthograde rapid axoplasmic transport and ultrastructural changes of the optic nerve. Part II. Beagles with primary open-angle glaucoma. *Glaucoma* 1983; 5: 189–196.
405. Brooks DE, Samuelson DA, Gelatt KN. Morphologic changes in the lamina cribrosa of Beagle dogs with primary open angle glaucoma. *Am J Vet Res* 1989; 50: 908–914.
406. Brooks DE, et al. Histomorphometry of the equine scleral lamina cribrosa. *Vet Comp Ophthalmol* 1994; 4: 184–192.
407. Quigley HA, Addicks EM. Regional differences in the structure of the lamina cribrosa and their relation to glaucomatous optic nerve damage. *Arch Ophthalmol* 1981; 99: 137–143.
408. Hollander H, Marakov F, Stefani FH, Stone J. Evidence of constriction of optic nerve axons at the lamina cribrosa in the normotensive eye in humans and other mammals. *Ophthalmic Res* 1995; 27: 296–309.
409. Fukuda Y, Sugimoto T, Shirokawa T. Strain differences in quantitative analysis of the rat optic nerve. *Exp Neurol* 1982; 75: 525–532.

410. Geri GA, Kimsey RA, Dvorak CA. Quantitative electron microscopic analysis of the optic nerve of the turtle, Pseudemys. *J Comp Neurol* 1982; 207: 99–103.
411. Do Nascimento JL, Do Nascimento RS, Damasceno BA, Silveira LC. The neurons of the retinal ganglion cell layer of the guinea pig: Quantitative analysis of their distribution and size. *Braz J Med Biol Res* 1991; 24: 199–214.
412. Wakakuwa K, et al. An electron microscopic analysis of the optic nerve of the eastern chipmunk (*Tasmias sibiricusasiaticus*): Total fiber count and retinoptic organization. *Vision Res* 1987; 27: 1891–1901.
413. Vaney DI, Hughes A. The rabbit optic nerve: Fiber diameter spectrum, fiber count, and comparison with retinal ganglion cell count. *J Comp Neurol* 1976; 170: 241–252.
414. Bruesch S, Arey L. The number of myelinated and unmyelinated fibers in the optic nerve of vertebrates. *J Comp Neurol* 1942; 77: 631–665.
415. Krinkle A, Frohlich E, Krinkle G. An analysis of the distribution of the myelinated nerve fibers in the optic fascicles of a Beagle dog. *Experentia* 1985; 41: 464–465.
416. Novokhatshii A, Reshetniak V. Quantitative characteristics of degeneration of the fibers of the optic nerve after section. *Ark Anat Gistol Embriol* 1987; 93: 55–58.
417. Brooks DE, et al. Histomorphometry of the optic nerves of normal dogs and dogs with hereditary glaucoma. *Exp Eye Res* 1995; 60: 71–89.
418. Williams RW, Bastiani MJ, Chalupa LM. Loss of axons in the cat optic nerve following fetal unilateral enucleation: An electron microscopic analysis. *J Neurosci* 1983; 3: 133–144.
419. Brooks DE, et al. Histomorphometry of the optic nerves of normal horses and horses with glaucoma. *Vet Comp Ophthalmol* 1995; 5: 193–210.
420. Jonas J, Muller-Bergh J, Schlotzer-Schrehardt U, Naumann G. Histomorphometry of the human optic nerve. *Invest Ophthalmol Vis Sci* 1990; 31: 736–744.
421. Jonas J, et al. Human optic nerve fiber count and optic disc size. *Invest Ophthalmol Vis Sci* 1992; 33: 2012–2018.
422. Sanchez R, Dunkelberger G, Quigley H. The number and diameter distribution of axons in the monkey optic nerve. *Invest Ophthalmol Vis Sci* 1986; 27: 1342–1350.
423. Fischer QS, Kirby MA. Number and distribution of retinal ganglion cells in anubis baboons (*Papio anubis*). *Brain Behav Evol* 1991; 37: 189–203.
424. Kirby MA, Clift-Fornsberg L, Wilson PD, Rapisardi SC. Quantitative analysis of the optic nerve of the North American opossum (*Didelphis virginiana*): An electron microscopic study. *J Comp Neurol* 1982; 211: 318–327.
425. Beazley LD, Dunlop SA. The evolution of an area centralis and visual streak in the marsupial, *Setonix brachyurus*. *J Comp Neurol* 1983; 216: 211–231.
426. Qijiu W, Junfeng L, Yumei X. The numbers and diameter spectra of bats (*Pipistrellus abramus*). *Acta Zool Sin* 1981; 27: 337–342.
427. Shen JY, Kelly DE, Hyman S, McComb JG. Intraorbital cerebrospinal fluid outflow and posterior uveal component of the hamster eye. *Cell Tissue Res* 1985; 240: 77–87.
428. Levy SG, et al. The composition of wide-spaced collagen in normal and diseased Descemet's membrane. *Curr Eye Res* 1996; 15: 45–52.
429. Fitch JM, Birk DE, Linsenmayer C, Linsemayer TF. Stromal assemblies containing collagen types IV and VI and fibronectin in the developing embryonic avian cornea. *Dev Biol* 1991; 144: 379–391.
430. Virchow H. Die kammerbucht und das gerustwerk der selben. In: Graefe-Saemisch, ed. *Handbuch der Geramten Augenheilk.* 2nd ed. Vol. 1. Leipzig, 1910.
431. Martin CL. Gonioscopy and anatomical correlations of the drainage angle of the dog. *J Small Anim Pract* 1969: 10: 171–184.
432. Fritz W. Uber die membrana descemets und das ligamentum pectinatum iridis bei den saugtieren und menschen. *Sbr Akad Wissensch Math Naturw Kl Wein* 1906; 115: 485–568.
433. Flugel C, Tamm E, Lutjen-Drecoll E. Different cell populations in bovine trabecular meshwork: An ultrastructural and immunocytochemical study. *Exp Eye Res* 1991; 52: 681–690.
434. Rohen J. Morphology and pathology of the trabecular meshwork. In: Smelser GK, ed. *The Structure of the Eye.* New York: Academic Press, 1961.
435. Ashton N. The exit of the aqueous. *Trans Ophthalmol Soc UK* 1960; 80: 379–421.
436. Flocks M. The anatomy of the trabecular meshwork as seen in tangential sections. *Arch Ophthalmol* 1956; 56: 708–718.
437. Uberreiter O. Die kammerwasservenen beim hunde. *Tierarztl Mschr* 1959; 46: 721–722.
438. Rouget C. Note sur la structure de l'oeil et en particulier sur appareil irio-choroidien. *C Seanc Mem Soc Biol* 1856; 3: 114–132.
439. Linsenmeier RA. Effects of light and darkness on oxygen distribution and consumption in the cat retina. *J Gen Physiol* 1986; 88: 521–542.
440. Brown KT. The electroretinogram: Its components and their origins. *Vision Res* 1968; 8: 633–766.
441. Zhang YD, Straznicky C. The morphology and distribution of photoreceptors in the retina of *Bufo marinus*. *Anat Embryol Berl* 1991; 183: 97–104.
442. Famiglietti EV, Sharpe SJ. Regional topography of rod and immunocytochemically characterized "blue" and "green" cone photoreceptors in rabbit retina. *Vis Neurosci* 1995; 12: 1151–1175.
443. Wikler KC, Williams RW, Rakic P. Photoreceptor mosaic: Number and distribution of rods and cones in the rhesus monkey retina. *J Comp Neurol* 1990; 297: 499–508.
444. Jonas JB, Schneider U, Naumann GO. Count and density of human retinal photoreceptors. *Graefes Arch Clin Exp Ophthalmol* 1992; 230: 505–510.
445. Muller B, Peichl L. Topography of cones and rods in the tree shrew retina. *J Comp Neurol* 1989; 282: 581–594.
446. Ward R, et al. The optic nerve of the viper, *Vipera aspis*. *J Hirnforsch* 1989; 30: 565–576.
447. Mass AM, Supin A. Ganglion cell topography of the retina in the bottlenosed dolphin, *Tursiops truncatus*. *Brain Behav Evol* 1995; 45: 257–265.
448. Simoens P, Muylle S, Lauwers H. Anatomy of the ocular arteries in the horse. *Equine Vet J* 1996; 28: 360–367.
449. Ninomiya H, Inomata T. Microvasculature of the hamster eye: Scanning electron microscopy of vascular corrosion casts. *Vet Ophthalmol* 2005; 8: 7–12.

Chapter 3

Physiology of the Eye

Glenwood G. Gum, Kirk N. Gelatt, and Doug W. Esson

Adequate knowledge regarding physiology of the eye and visual system of the animal species commonly confronting the veterinary ophthalmologist provides an important foundation for clinical comparative and veterinary ophthalmology. Most diagnostic procedures, interactions of ocular tissues and drugs, ophthalmic diseases, and surgical procedures require thorough understanding of the normal physiology as well as the pathophysiology of the eye and its associated structures. This chapter presents the ophthalmic physiology of the eye, especially regarding the outer eye, anterior segment, and lens; the optics and physiology of vision are presented in Chapter 4.

PROTECTIVE MECHANISMS OF THE EYE

Eyelids

The eyelids of domestic animals are designed to protect the anterior segment of the eye, especially the cornea. The eyelids contain the meibomian glands, large sebaceous glands that secrete the outer, oily layer of the preocular tear film. Some accessory lacrimal glands may also be present in the conjunctiva of some species, and in others, the gland of the nictitating membrane contributes to the aqueous layer of the preocular film. The normal blinking of the eyelids maintains the physiologic thickness of the preocular tear film, aids movement of the tears both to and within the nasolacrimal system, and helps eliminate small particles from the corneal and conjunctival surfaces. Reflex closure of the eyelids protects the anterior segment from external trauma.

Along with the associated medial and lateral canthal ligamentous and muscle attachments, the eyelids determine the shape and width of the palpebral fissure. For example, a wide, round palpebral fissure is normal among brachycephalic breeds, and a narrow, almond-shaped palpebral fissure is normal among dolichocephalic breeds. The shape of the palpebral fissure also depends on the relationship of the globe to the orbit. A small globe in a deep orbit allows a narrow palpebral fissure; the opposite occurs with a large globe in a shallow orbit. In other domestic animals, the shape of the palpebral fissure is more constant among the breeds. The nictitating membrane, or third eyelid, aids in protection of the conjunctiva and cornea by moving, either passively or actively, over the cornea when the globe is retracted. The nictitating membrane contains one or more important accessory, superficial tear-producing glands that contribute to the aqueous portion of the preocular tear film. The nictitating membrane also helps to support the position of the lower eyelid through its mass in the ventromedial cul-de-sac, and it forms part of the lacrimal pool in the medial canthus. In birds, the nictitating membrane is nearly transparent, and its movement is under direct muscular control.

In the dog, the upper eyelid, which contains the cilia or eyelashes, is more movable than the lower. When the eyelids are closed, most of the ambient light is prevented from entering the eyes. The frequency of blinking in a dog eye is approximately 3 to 5 times per minute, and a blink in one eye is accompanied by a blink in the other approximately 85% of the time. It is not unusual for a restrained dog to blink 10 to 20 times per minute. Another study indicated mean canine blink rates of 12.4 per minute are normal, with approximately 66% of these blinks being incomplete.[1] Eyelid closure is mediated by the efferent fibers of the facial nerve (CN VII). The oculomotor (CN III) innervates the levator palpebral superioris, and the facial nerves innervate the corrugator supercilii, which are responsible for opening the eyelids. The three eyelid reflexes are divided into the corneal, palpebral, and menace (Table 3.1). In general, carnivores are born with their eyelids fused, the eyelids opening between 10 and 14 days of age. The eyelids of herbivores, however, are usually open at birth.

In the cat, both eyelids lack cilia. Complete blinks are infrequent, occurring at a rate of approximately 1 to 5 every 5 minutes. The lids of both eyes blink together approximately 70% of the time. The eyelids of pigmented cats allow no more than 5% of light at longer wavelengths to be transmitted. Kittens normally open their eyelids between 10 and 15 days of age; however, both eyes do not always open on the same day.[2] The nictitating membrane of the feline species is large and more active and may passively cover part of the cornea or be drawn, as during excitement, into the medial canthus. The nictitans can extend at least two thirds of the way across the cornea. The smooth muscle that draws the membrane into

Table 3.1 Eyelid Reflexes

	Cornea	Palpebral	Menace[a]
Stimulus	Tactile	Tactile	Menacing gesture
Receptors	Somesthetic	Somesthetic	Cones, Rods
Afferent pathway	Ophthalmic and maxillary branch of trigeminal nerve	Trigeminal nerve	Optic nerve
Efferent pathway	Facial nerve	Facial nerve	Facial nerve
Effectors	Eyelid muscles	Eyelid muscles	Eyelid muscles
Response	Blink	Blink	Blink

[a]If sufficient cortex of one cerebral hemisphere is damaged, the menace reaction cannot be elicited in the contralateral eye of the dog. Pathology of the cerebellar cortex can also affect the menace reaction.

the medial canthus is innervated exclusively by postganglionic adrenergic sympathetic nerve fibers with cell bodies located in the anterior cervical ganglion. Their axons follow the oculomotor nerve. Normally, the nictitans show no spontaneous activity, because the smooth muscle lacks tight junctions like that of the visceral smooth muscle. Each muscle cell is innervated by one or more axons, thus substantiating that activation of the smooth muscle in the nictitating membrane is neurogenic and that the myogenic conduction normally found in visceral smooth muscles does not occur.[3] The muscle appears to be insensitive to stretch. The endings are adrenergic, but the muscle responds to the administration of acetylcholine and histamine. The cat is the only common domestic animal with an appreciable number of muscle fibers in the nictitating membrane, which in this species permits approximately 10% of applied light to pass.[4] In all animals, if the globe is retracted by the retractor bulbi muscles or decreases in size, the membrane passively begins to cover the eye. In the case of globe retraction, this may be partially caused by the globe displacing the orbital fat forward.

In the horse, the cilia are long and numerous on the upper eyelid, except near the medial canthus. The frequency of blinking varies from 5 to 25 times per minute, and approximately 30% of blinks are accompanied by a blink in the contralateral eye. Long tactile hairs, or vibrissae, occur on both the dorsal brow and lower eyelid. The vibrissae are long, stout, single shafts of hair that are usually thicker than adjacent skin hair; they may provide additional sensation for the eyelids.

In cattle, sheep, and pigs, the upper eyelid is the most mobile, and the majority of cilia are present on the upper eyelid. Pigs and some ruminants have a deeper structure, the Harder's gland, in addition to the superficial gland of the nictitating membrane. Its function, however, is unknown. In the pig, the meibomian glands are poorly developed, and the main eyelid glands are sweat glands. The frequency of blinking is approximately 5 times per minute in cattle, and approximately 60% of the time, both eyes blink together. The pig blinks approximately 10 times per minute; 90% of blinks are bilateral.[5]

In birds, the lower eyelid is larger and more movable than the upper eyelid. There are no feathers corresponding to eyelashes on the lids, but there are feathers corresponding to eyebrows. Chicks are hatched with their eyes open. The avian nictitating membrane, which is much more translucent than that in other domestic animals, replaces the eyelids for blinking. Two muscles extraneous to the lid pull the nictitating membrane over the entire anterior segment as many as 15 to 20 times per minute, even with the other eyelids closed. The nictitans also contain a superficial tear gland, and some species have a deeper Harder's gland.

Tear Production and Drainage

Both the optical and normal function of the cornea with its hydrophobic epithelium depend on the integrity of the lacrimal system. The preocular tear film maintains an optically uniform corneal surface by smoothing out minor irregularities, removing foreign matter from the cornea and conjunctiva, lubricating the conjunctiva and cornea, providing nutrients to the avascular cornea, and in some species, "controlling" the local bacterial flora. The preocular film also undergoes constant evaporation and formation of transient "dry spots." Hence, the rate of tear evaporation appears to be directly related to the rate of blinking, because ideally, the rate of blinking is much faster than the development of these dry spots.

In all species studied, the preocular tear film can be divided into three layers. The outer layer (~0.1 μm) is a very thin, oily layer, consisting of waxy and cholesterol esters as well as polar and neutral lipids.[6] The lipids in humans include unsaturated and branched-chain fatty acids and alcohols, 8 to 32 carbon chains in length. This outer layer prevents evaporation of the underlying layers and overflow of tear film onto the eyelids and is produced by sebaceous glands (i.e., tarsal and meibomian gland) of the eyelids. These glands undergo holocrine secretion (release of the entire cell and its contents). Androgens as well as neurotransmitters may be involved in the regulation of meibomian gland secretion. Androgen receptor mRNA and protein have been isolated from rat, rabbit, and human meibomian acinar epithelial cells. Additionally, the neuropeptides calcitonin gene-related peptide, substance P, neuropeptide Y, and vasoactive intestinal peptide have been identified in association with meibomian glands in humans and guinea pigs.[7] The middle aqueous layer (~7 μm) is the thickest (>60%) and performs the primary functions of the tear film. This layer consists of approximately 98% water and approximately 2% solids, made up predominantly of proteins. The aqueous layer contains inorganic salts, glucose, urea, proteins, glycoproteins, and biopolymers.[8] The lacrimal gland, superficial gland of the nictitating membrane, Harderian gland, and accessory lacrimal glands in the conjunctiva all contribute to its formation. Destruction or excision of the

lacrimal gland or third eyelid gland will result in a variable amount of reduction in aqueous tear production.[9–11] The aqueous tear layer is evaluated clinically through use of the Schirmer tear test.[9,12] Topical anesthetics anticholinergics (e.g., atropine sulfate), preanesthetics (e.g., acetylpromazine maleate-ketamine HCl), and general anesthesia can induce short-term reduction in the aqueous tear estimates as derived through the Schirmer tear test.[9,13–15]

The deep, or mucin, layer (~0.02–0.05 μm) is composed of tear mucins produced by the apocrine conjunctival goblet cells as well as an underlying glycocalyx that is associated with the corneal and conjunctival microvilli. The distribution of human and canine goblet cells has been shown to be similar, with densities being highest in the lower nasal and middle fornices but essentially absent from bulbar areas adjacent to the cornea.[16] The deep gland, or Harderian gland, of the nictitans may also contribute to this layer. Mucin may be produced by goblet cells in response to mechanical, immune, histamine, antigenic, or (direct or indirect) neural stimulation.[17] The mucin layer contains glycoproteins, which are carbohydrate–protein complexes characterized by the presence of hexosamines, hexoses, and sialic acid. These glycoproteins play a critical role in lubricating the corneal surface, thus making its hydrophobic surface more hydrophilic (to permit spreading), and in stabilizing the preocular film.[18] At least two secreted mucins and two membrane-bound mucins have been identified in the normal canine ocular mucus layer.[19] The mucin layer as well as the integrity of the outermost layer of corneal epithelium are necessary for retention of the tear film on the cornea.[20] The deep layer ensures stability of the tear film by lowering its surface tension and permitting the spread of tear film after blinking. Clinical estimation of the rate of evaporation (and, indirectly, of the mucus component of the preocular film) is performed through determining the time (in seconds) for the "tear film breakup."[21,22]

Tears are a clear and slightly alkaline solution, with an average pH of 7.5.[23] In humans, bovines, and the rabbit, the tear electrolyte concentration is similar to that in plasma, except for potassium, which is three to six times more abundant in tears, thus indicating an active transport mechanism.[23–25] The glucose concentration is lower in human tears than in plasma, but its level corresponds with that in plasma, thereby allowing a crude means of evaluating blood glucose levels by placing a calorimetric paper test strip (Glucostix, Bayer, Elkhart, IN) in the conjunctival cul-de-sac. This procedure provides a semiquantitative method for determining hyperglycemia.[26] In human patients with diabetes, the elevated glucose levels in tears appear to result from the tissue fluids, not from the lacrimal gland secretions.[27]

The precorneal tear film contains both nonspecific and specific antimicrobial substances. Nonspecific substances include lysozyme, lactoferrin, α-lysine, and complement. Specific antimicrobial substances include secretory immunoglobulins A, G, and M. Protein levels in canine tears average 0.35 g/dL, with 93% globulin, 4% albumin, and 3% lysozyme, which is a ubiquitous antibacterial enzyme that hydrolyzes bacterial cell walls.[28] Lysozyme is produced by the conjunctival goblet cells and has antibacterial and antifungal properties. Its levels are increased in conjunctivitis.[28] Relative to humans and nonhuman primates, domestic animals have very low levels of lysozyme (e.g., the horse has one half to one fourth that of human tears), and the cat has none.[12,29–31] Lysozyme activity has not been detected in cattle, but it has been detected in sheep and goats.[26]. Lactoferrin has been identified in the tear film of humans, cattle, and other mammals, and it reversibly binds the iron, which is available for bacterial metabolism and growth. Immunoglobulin A contributes to ocular defense by coating bacterial and viral microorganisms, leading to agglutination, neutralization, and lysis. Immunoglobulin A is present in greater concentrations in the tear film than are immunoglobulins G and M.[7]

The lacrimal nerve, which is a branch of the trigeminal nerve, is mainly sensory, but it also provides the lacrimal gland with its parasympathetic and sympathetic fibers.[32,33] Both adrenergic and cholinergic distribution patterns around the acini and blood vessels of the canine lacrimal gland are similar; however, the cholinergic fibers appear to be greater in number than the adrenergic fibers.[33] The acinar cells are primarily responsible for secretion of proteins in lacrimal gland fluid. These proteins are synthesized in the endoplasmic reticulum, modified in the Golgi apparatus, and stored in secretory granules. Stimulation of the cholinergic and adrenergic fibers in the lacrimal gland causes release of these proteins into the lacrimal fluid. This process requires a series of separate cellular pathways that use secondary messengers and is controlled by a process called signal transduction.[34]

Four types of tears are reported in humans:

1. Psychogenic tears, or tears of emotion;
2. Continuous (or "basal") tears, which are needed for normally functioning preocular and tear film;
3. Reflex tears, which are produced by exposure of the eye to light, cold, wind, or other irritants; and
4. Tears induced by drugs directly stimulating the glands.

Animals probably have all these types except psychogenic tears. Lacrimation is stimulated by painful irritants, eye diseases, mechanical or olfactory stimuli of the nasal mucous membranes, and sinus diseases. Human patients with keratoconjunctivitis sicca are deficient in both basal and reflex tears, with lower concentrations of lysozyme and lactoferrin compared with persons with healthy eyes.[35,36] Clinical estimation of the total and basal aqueous portions of tear formation in the dog and cat is made using the Schirmer I tear test with the test strip positioned in the middle of the inferior conjunctival fornix for 1 minute.[37,38] Attempts to determine basal levels of tear formation use the Schirmer II tear test, with the external ocular surfaces anesthetized and the lower conjunctival fornix dried by Dacron swabs. Basal tear levels in the dog and cat are approximately 50% of the total tear formation in those species.[37,38]

The nasolacrimal drainage system eliminates used tear film and any excessive tears. Preocular tear film accumulates along the palpebral margin of each eyelid and is forced by blinking

to move medially into the lacrimal puncta. When the tears are in the lacrimal pool and the facial muscles relax, the tears flow into the canaliculi by capillary action. Normal breathing movements also facilitate this flow into the canaliculi. Reflex blinking of the eyelids closes the lacrimal sac, which acts as a pump. Pseudoperistaltic motion of the nasolacrimal duct allows movement of the tears into the nasal cavity.[39] Similar studies have not been reported in domestic animals, but autoregulation of the lacrimal system with receptors in the excretory portion has been suggested in studies of human tear flow.[39] Evaluation of canalicular function in humans suggests that destruction of either canaliculus alone does not affect excretion of tears; in domestic animals, the lower canaliculus seems to be the most important for tear drainage.[40]

Cornea

The sensitivity of the cornea is a major factor in protecting the eye. Rapid blink and retraction of the globe with prolapse of the nictitating membrane are fundamental reflexes when the cornea is touched or irritated. During extreme pain, the reflex is exaggerated, and blepharospasm sometimes occurs to the extent that the lids cannot be opened voluntarily. Corneal sensitivity may vary by species, area of the cornea, and in the dog, by skull types. Corneal sensitivity in dogs, as measured by the Cochet-Bonnet esthesiometer and histology of the corneal nerves, indicated corneal sensitivity was highest in the dolichocephalic skull types and lowest in the brachycephalic types.[41] Corneal sensitivity in the mesaticephalic skull types was intermediate. Corneal sensitivity was greatest peripherally and was lower centrally. Sensory innervation to the cornea is provided via the ophthalmic branch of the trigeminal nerve. The nerves are myelinated at the corneal periphery, and they lose their myelin as they traverse into the central portion. The nerves overlap extensively in the cornea so that stimulation at one point excites many afferent fibers. Corneal innervation arises from the corneal limbal plexus, which comprises a 0.8-mm to 1-mm wide, ringlike band surrounding the peripheral cornea. Morphologically, this plexus may be further subdivided into a predominantly perivascular, outer, periscleral zone and a denser and more highly branched inner, pericorneal zone. Stromal innervation originates as 14 to 18 prominent, radially directed stromal bundles, distributed at regular intervals around the limbus. Each bundle contains approximately 30 to 40 axons, which undergo repetitive dichotomous branching to form the axonal trees that innervate the entire cornea. Nerve fibers entering the basal epithelial layer form unique, preterminal arborizations known as "epithelial leashes," which exhibit a highly ordered distribution and give rise to a profusion of smaller, ascending branches.[42] Hence, superficial corneal ulcers are often more painful than deep corneal ulcerations.

The somatosensory sensations of pressure, cold, and warmth are not documented fully in the cornea, but touch and pain receptors exist. The sensory fibers of the cornea exhibit an "axon reflex" that, when stimulated, results in miosis, hyperemia, ocular hypertension, and increased protein levels in the aqueous humor. The humoral mediators appear to be prostaglandins, histamine, and acetylcholine.[43] Substance P, a peptide neurotransmitter, is located in approximately 20% of the nerve cell bodies, which is a minor proportion of the sensory nerve supply to the cornea. This neurotransmitter does not appear to be involved with nociception in the cornea, but it may act as a neurogenic mediator of inflammatory responses.[43,44] This reflex is responsible for the clinical signs of anterior uveitis associated with painful conditions of the cornea, conjunctiva, and eyelids. β-Adrenergic receptors have been isolated on the corneal epithelial cells that appear to be activators of cyclic nucleotides, thus turning on the enzyme system within the epithelial cells.[45] Levels of nerve growth factor (NGF) have been demonstrated to be elevated in the cornea and precorneal tear film following corneal epithelial wounding in dogs; however, topical application of NGF failed to modulate corneal wound healing in the normal dog eye.[46]

With the sclera, the cornea maintains the shape of the globe and the intraocular pressure (IOP). The health of the cornea is influenced by the preocular film, aqueous humor, IOP, and eyelids. Problems in any one of these can cause corneal disease that results in loss of transparency and therefore loss of vision.

Because the cornea is the most powerful refractive surface of the eye, it must remain transparent. The approximately six-cell-thick corneal epithelial layer absorbs some short-wavelength light, but it permits the transmission of most light in the visible spectrum. Its transparency depends on its relative acellularity, absence of blood vessels, state of relative dehydration, arrangement of stromal collagen fibrils, and extracellular matrix. Quiescent fibroblasts in normal corneal tissue contribute to optical clarity by producing nearly transparent lens crystallinelike proteins. Synthesis of these proteins drops dramatically following injury, coinciding with increased reflectance, and does not increase again until several weeks following injury when the scar is remodeling and the haze is improving.[47]

The aqueous humor, limbal capillaries, and tears furnish the metabolic needs of the avascular cornea. To maintain a state of relative dehydration, the cornea requires energy in the form of adenosine triphosphate (ATP), which is generated by the breakdown of glucose (furnished mainly by the aqueous humor). The corneal epithelium obtains oxygen for aerobic glycolysis from the preocular tear film (at the rate of 3.5–4.0 μL/cm per hour in humans). The endothelium and keratocytes in the deep stroma receive their oxygen from the aqueous humor. Glucose is supplied by the limbal capillaries and the tears. The corneal epithelium obtains most of its glucose from the stroma and converts it to glucose-6-phosphate, after which 85% is metabolized into pyruvate via the glycolytic pathway. Most of this pyruvate is then metabolized into lactic acid, but some is diverted into the citric acid cycle to produce ATP. Glucose is stored in the corneal epithelium as glycogen, which can be used for energy under stressful conditions (e.g., trauma and surgical wounds). If glycogen stores are depleted, normal healing of the epithelium and cellular locomotion over the surface is inhibited.[48] In the absence of oxygen, as when the

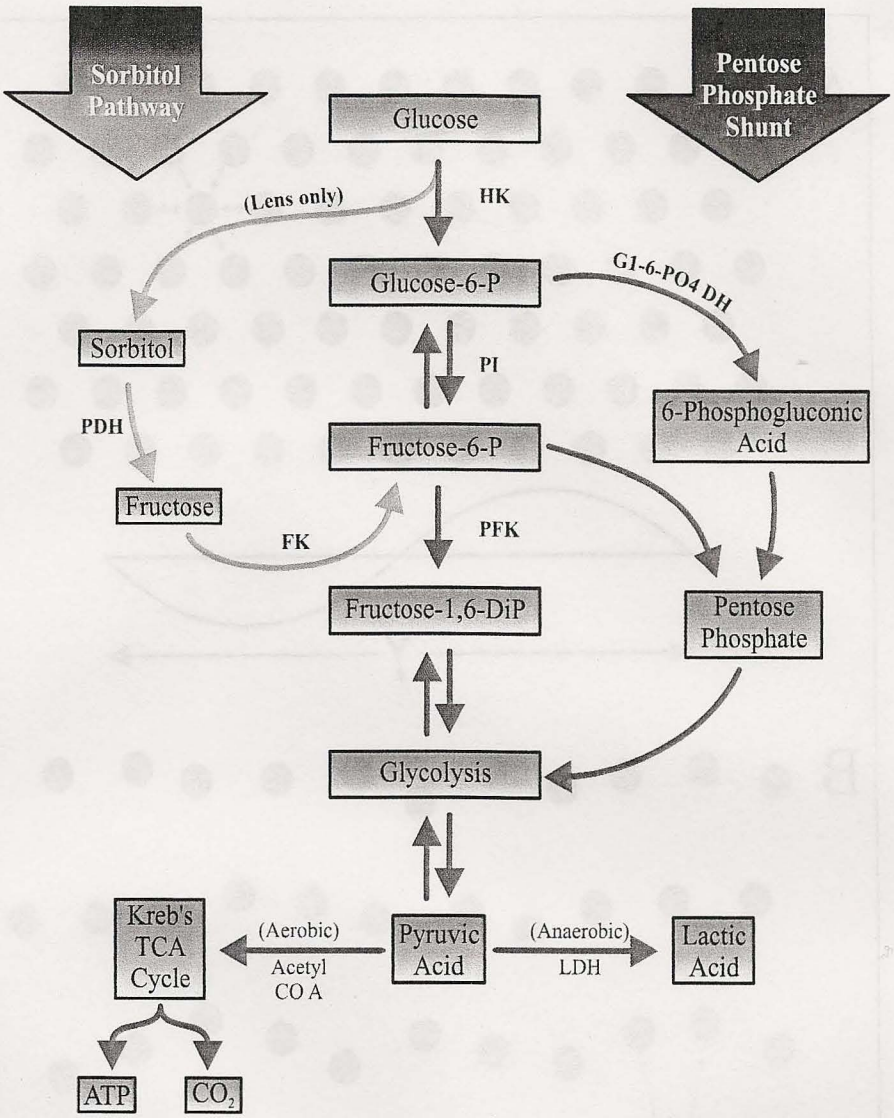

Figure 3.1. Metabolism of glucose in the cornea and lens. Tricarboxylic acid (TCA) cycle: coupled to electron transport and oxidative phosphorylation for the production of ATP. Pentose phosphate shunt: hexoses are converted to pentose for use in nucleic acid synthesis and generation of nicotinamide-adenine dinucleotide phosphate (NADPH). *FK,* fructokinase; *Gl-6-PO_4DH,* glucose-6-phosphate dehydrogenase; *HK,* hexokinase; *LDH,* lactic dehydrogenase; *PDH,* polyol dehydrogenase; *PFK,* phosphofructokinase; *PI,* phosphohexoisomerase.

eyelids are closed, energy is provided through anaerobic glycolysis. If excessive lactic acid is produced by this process, corneal hydration occurs.[49–52] The remainder of the glucose use within the corneal epithelium is also metabolized via the pentose phosphate shunt, which produces nicotinamide-adenine dinucleotide phosphate (NADPH), an important resource for free radical control (Fig. 3.1). Other metabolites from this pathway are ribose-5-phosphate (ribose-P) and reduced triphosphate-pyridine nucleotide. Ribose-P is used in nucleic acid synthesis of DNA or RNA, whereas triphosphate-pyridine nucleotide is used by the corneal epithelium for synthesis of lipids.[50] The metabolic needs of the keratocytes are limited, and they relate to maintenance of the collagen fibrils and glycosaminoglycans (GAGs) within the stroma. The corneal endothelium has large glucose needs (approximately five times that of the epithelium) to sustain its pump mechanism. Its metabolic pathway is mainly anaerobic glycolysis, with the citric acid and pentose phosphate pathways also being significant.

The state of relative corneal dehydration or deturgescence depends on many factors. Anatomic integrity of the epithelium and endothelium provide two-way, physical barriers against the influx of tears and aqueous humor. Loss of the corneal epithelium results in a 200% increase of corneal thickness because of hydration; loss of the endothelium results in a 500% increase of corneal thickness.[49] Following eyelid opening in the canine, there is an initial decrease in corneal thickness until approximately 6 weeks of age, which presumably mirrors maturation of corneal endothelial function. After 6 weeks, the corneal thickness increases with age until approximately 30 weeks.[53] Osmotic forces between the tears, aqueous humor, and corneal stroma probably affect corneal hydration, but the exact mechanism is unknown. The role of electrolyte concentration is also unknown. Cation concentration of the cornea is regulated by Na^+,K^+-ATPase located in the epithelium and endothelium. If this enzyme is inhibited by either drugs (e.g., Quabain) or the lack of energy, the cornea

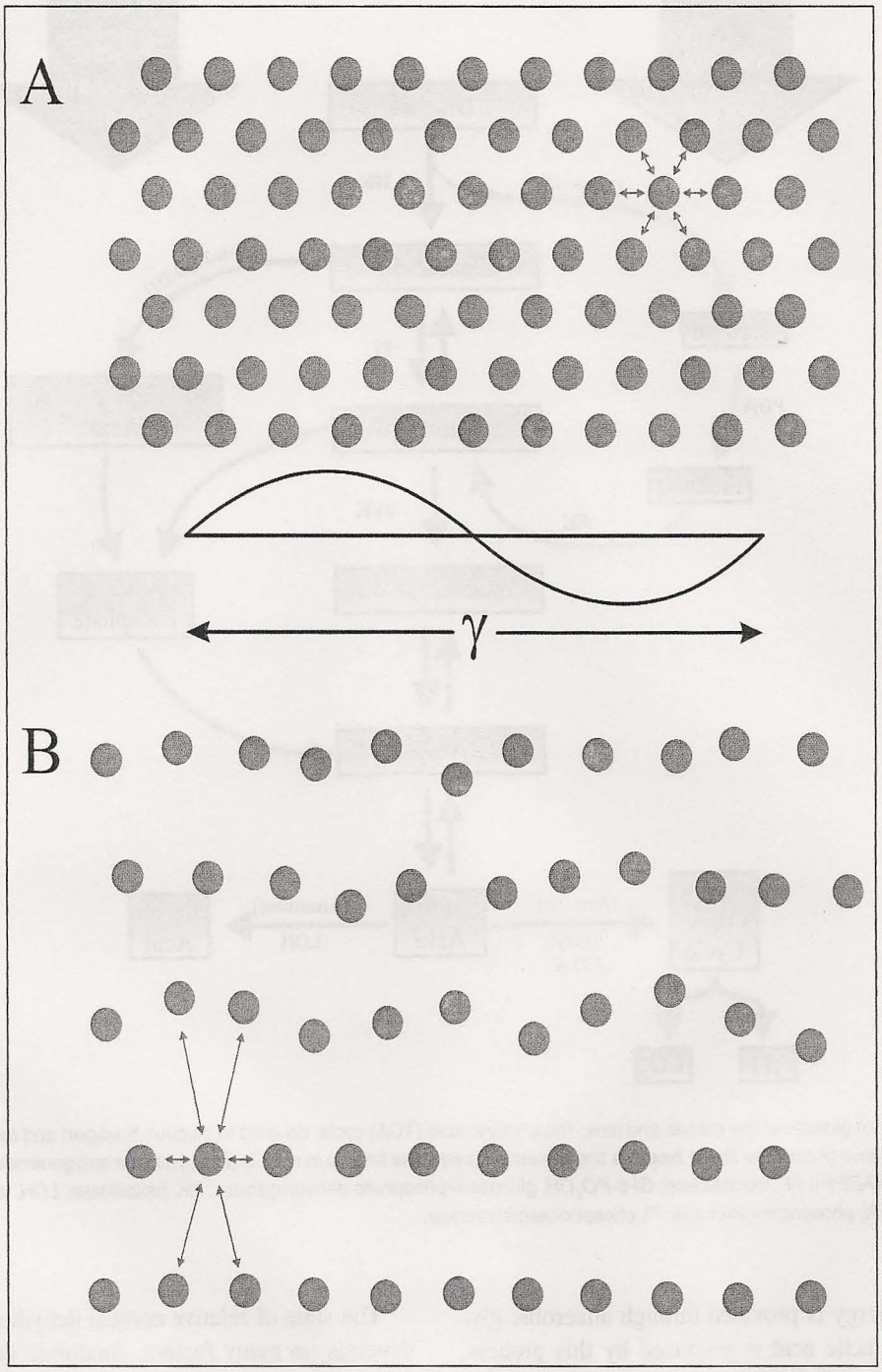

Figure 3.2. **A.** Cross-section of the corneal fibrils arranged in a lattice formation. Forces of repulsion between the fibrils are shown schematically, and a representative wavelength is shown below for comparison. **B.** Swelling of the cornea and disorder in the rows of fibrils consequent to weakening of the forces of alignment from the neighboring rows. This causes the bluish color of corneal edema. (Modified with permission from Maurice DM. The physics of corneal transparency. In: Duke-Elder S, ed. *Transparency of the Cornea.* Oxford: Blackwell Scientific Publications, 1960.)

becomes overhydrated. Evaporation of the preocular tear film results in hypertonicity of the tear film, causing water to flow out of the cornea and into the tear film. There is a net flux of water and ions toward the epithelium and tears. Increased IOP causes corneal edema, which is reversible if the pressure is returned to normal. This phenomenon may be caused by influx of aqueous humor, loss of endothelial function, disruption of the collagen arrangement by stretching, or some combination of these.

Collagen fibrils with 64-mm to 66-mm periodicity, along with glycoproteins and GAGs, make up 20% to 25% of the corneal stroma and act as a supporting structure. The remaining corneal stroma contains between 75% and 80% water. The uniform-thickness collagen fibrils are arranged in parallel lamellae running at oblique angles to each other, and they are separated by less than a wavelength of light (Fig. 3.2).[51] This parallel arrangement of the corneal collagen fibers extends from the center of the cornea to its periphery, where the fibrils develop a concentric configuration to form a "weave" at the limbus, which in turn provides strength and helps to maintain its curvature. Corneal collagen is similar to collagen from other sources, which has a high concentration of glycine,

proline, and hydroxyproline. In the human cornea, several types of collagen have been reported, including types I and VI (Bowman's layer); I (50–55%), III (1–2%), V (10%), and VI (stroma); and V, VIII, IX, and XII (Descemet's membrane).[52] The predominant corneal GAGs consist of keratin sulfate. In the central cornea of humans is also a nonsulfated chondroitin sulfate; in the peripheral cornea are chondroitin-4-sulfate and dermatan sulfate. The central cornea of humans contains no hyaluronic acid (HA), except at the limbus. These GAGs fill the interfibrillar or interstitial spaces of the stroma and attach to the collagen fibrils or proteins of the cornea. The regular arrangement of collagen and the GAG concentration differ in the cornea and sclera, thus allowing one to be transparent and the other to be opaque. The GAGs act as anions binding cations and water. These substances appear to be responsible for maintaining the regular arrangement of the collagen fibrils by controlling distribution of water in the stroma.[54,55] Corneal keratin sulfate, which differs from keratin sulfate found in cartilages by the length of the polymer, degree of branching, and an *O*-glycosidic linkage with either serine or threonine, absorbs two to three times as much water as chondroitin sulfate, but once water is absorbed by the chondroitin sulfate, it is retained eight to nine times better than by keratin sulfate. Keratin sulfate is concentrated near the posterior cornea near the endothelium, where it facilitates movement of water from the aqueous humor into the cornea.[52] Spontaneous chronic corneal epithelial defects (SCCED) in the canine have been shown to be associated with altered basement membrane structure and physiology. Affected corneas display epithelial dysmaturation, inflammatory stromal infiltrates, and the presence of a PAS-positive acellular zone composed of collagen.[56]

Drug Transport through the Cornea, Limbus, and Bulbar Conjunctiva

Movement of substances through the cornea, limbus, and bulbar conjunctiva is important clinically because of the frequent use of topical ophthalmic medications. After passage through the preocular (precorneal film), the corneal epithelium presents a reasonable barrier to the passage of most compounds because of the extensive close contacts and junctional complexes between the corneal basal cells. True zonula occludens–type (i.e., tight) junctions have not been reported in the corneal epithelial cells.

The most important characteristic of the topically applied drug is its solubility. To pass through an intact cornea that consists of an outer lipid layer (i.e., the epithelium), a middle aqueous layer (i.e., the stroma), and an inner lipid layer (i.e., the endothelium), the drug must possess both lipophilic and hydrophilic properties. Drugs having both polar (i.e., water-soluble) and nonpolar (i.e., lipid-soluble) forms, such as chloramphenicol and alkaloids, penetrate the cornea well. Because the cornea is the path of least resistance for the passage of a drug, some evidence indicates a drug may enter the globe through the sclera with a loss of integrity or when a continuous high concentration of a drug is applied to the bulbar conjunctiva.[57] Polar compounds (e.g., fluorescein) penetrate the cornea well only if the epithelium is absent, as in corneal ulceration. The size of the molecule, concentration of the drug, pH of the drug, and the drug's or formulation's ability to reduce surface tension also affect corneal penetration.[58] Recent studies have also concluded that the conjunctival/scleral route can be an effective route for drugs to enter the iris and ciliary body.[56] Excellent reviews of the permeability of the cornea to topically applied drugs have been published elsewhere.[59–61]

IRIS AND PUPIL

The iris muscles consist of an antagonist constrictor (sphincter) that encircles the pupil and radial dilator muscles. The sphincter muscle consists of an annular band of smooth muscles near the pupillary margin of the iris that derive from mesodermal tissue. The dilator muscle consists of a series of myoepithelial cells that stretch from near the pupillary margin to the base of the iris and are contiguous posteriorly with the outer pigmented ciliary body epithelium. Pupil size varies on the basis of the balance between these two muscle groups. The constrictor muscle, which is the stronger of the two, is innervated by the oculomotor nerve (CN III) and provides primarily parasympathetic control; the dilator muscles are innervated by primarily sympathetic nerves. The constrictor muscles cause miosis, and the dilator muscles are responsible for mydriasis. Bright light decreases pupil size.

The sympathetic activity in the iridal dilator muscle and ciliary body musculature (discussed later) may be mediated by a combination of β-receptors (β_1 and β_2) and α-receptors (α_1 and α_2). The α_1-receptors are responsible for cardiostimulation, and the α_2-receptors elicit bronchodilation, vasodilation in the skeletal muscles, and uterine contractions. The β_1-receptors generally mediate excitatory responses, except in the intestines. The β_2-receptors are thought to be located, at least in part, in the presynthetic nerve terminals. Species differences of the α- and β-receptors have been demonstrated among humans, the rabbit, nonhuman primates, the cat, and the dog, and they are summarized in Table 3.2.[62–80] The ocular effects of these β- and α-receptors on the human eye are summarized in Table 3.3.[62–64]

Table 3.2 Adrenergic Receptors in the Iris and Ciliary Body

Species	Iris Sphincter	Iris Dilator	Ciliary Muscles
Human	α and β equally	Mainly α, very few or no β	Mainly β, very few α
Rabbit	Mainly β, few α	Mainly α, few β	Mainly α, few β
Monkey	Mainly α, perhaps β	Mainly α, few β	Only β, no α
Cat	Mainly β, some α	Mainly α, some β	Mainly β, some α
Dog	α and β	α and β	?

Table 3.3 Effector Sites and Receptor Types in Humans

Eye Tissue	*Receptor Type(s)*	*Response*
Iris dilator	α_1	Contraction (mydriasis)
Ciliary body muscles	β	Relaxation
Aqueous humor	β_2	Increased outflow; increase formation
	α	Slight decrease
Conjunctival blood vessels	α	Vasoconstriction
	β_2	Vasodilation
Müller's muscle	α	Contraction (lid retraction)

Table 3.4 Components of the Pupillary Light Reflex

Stimulus	Illumination of the Retina
Receptors	Photoreceptors (rods and cones)
Afferent pathway	Optic nerve–optic tract to pretectal area (ipsi- and contralateral via posterior commissure)
Efferent pathway	Pretectal area to anteromedian nuclei (dog) (ipsi- and contralateral), which is rostal to the Edinger-Westphal nuclei, and then parasympathetic fibers to ciliary ganglion (via CN III)
	Postganglionic fibers to the iris
Effector	Sphincter muscle of the iris
Response	Miosis (constriction of the pupil, both direct and consensual reflex)

Components of the pupillary light reflex are listed in Table 3.4. Most synapses in the ciliary ganglion are involved in relaying impulses that result in accommodation; the remainder are concerned with constriction of the pupil. Morphine acts on subcortical cells (i.e., oculomotor nuclear complex) to cause constriction of the canine pupil[71] and dilation of the feline pupil because of the release of catecholamines from the adrenal glands.[72] Endogenous prostaglandin $F_{2\alpha}$ appears to be involved in maintaining muscle tone in the sphincter muscle of the iris. Prostaglandins most likely act directly on these muscles, and they appear to act to a lesser extent on the dilator muscles of the canine iris.[73] Several biologically active peptides have been isolated in the nerve supply of the intraocular muscles. Neuropeptide Y, a 36-amino-acid peptide, is found in the terminal vesicles of sympathetic neurons and co-stored with norepinephrine. It appears that neuropeptide Y has a modulatory role on the iris dilator muscles of the eye that enhances adrenergic-induced contractions of these vessels. By itself, however, neuropeptide Y does not have any potent contractile qualities.[74]

Horner's syndrome results from sympathetic denervation of the iris dilator muscle and denervation of the tarsal and orbital muscles. The clinical signs are miosis, ptosis, and enophthalmos, with passive protrusion of the nictitating membrane.[75] The iris dilator muscle becomes hypersensitive to catecholamines after the muscle has been denervated, via the phenomenon of *denervation hypersensitivity*. Thus, an injection or instillation in the eye of a relatively small amount of epinephrine causes mydriasis in animals with Horner's syndrome. Hypersensitivity is greater in postganglionic denervation than in preganglionic denervation.

Absence of a light stimulus to the retina most likely does not initiate an active reflex response leading to pupillary dilation. Some of the stimuli for pupil dilation (i.e., mydriasis) are sudden body pain, asphyxia, and anxiety. Pupillary dilation can be produced by stimulation of sympathetic fibers (e.g., startle reflex) or by inhibition of the parasympathetic outflow from the ventral tegmental area and anteromedian nucleus, the rostral extension of the Edinger-Westphal nucleus.[76] Four pupillodilator pathways have been identified in the brain stem of the cat:

1. A descending excitatory pathway from the hypothalamus, which projects to the intermediolateral cell column (C8–T2);
2. A descending inhibitory pathway from the hypothalamus, which projects to the Edinger-Westphal nucleus;
3. An ascending inhibitory pathway from the reticular formation, which projects to the Edinger-Westphal nucleus; and
4. An ascending inhibitory pathway from the dorsal horn, which projects to the Edinger-Westphal nucleus (Fig. 3.3).[77]

Pupillary functions include regulating light entering the posterior segment of the eye, increasing the depth of focus for near vision, and minimizing optical aberrations by the lens. Local irritation (e.g., contusion or corneal abrasion) results in conjunctival and iridal hyperemia, increased levels of proteins in the aqueous humor, increased and later decreased IOP, and miosis. The neural pathways and humoral mediators are unknown, but axonal reflexes have been suggested (discussed previously).

Iridal color and pupil size vary widely among species, and the irides of the young are often a different color than those of the adult. Iris color, or the amount of melanin, may influence the effects of many drugs.[78] In domesticated cats, the constricted pupil is a vertical slit, whereas in the larger, wild felidae, it is circular. On dilation, the vertical sides of the domestic feline pupil expand to produce a circular pupil. The constrictor muscle fibers are vertically oriented, and the dilator fibers are absent at the dorsal and ventral parts of the pupil. Because the central iris rests against the axial lens, the lens pushes the iris forward during accommodation.

In young horses, the pupil is more circular than in adults. Under illumination, the ends of the oval pupil of mature horses do not constrict as the dorsal and ventral borders do. In bright daylight, the superior granula iridica occludes the central pupillary opening, resulting in two apertures and assisting

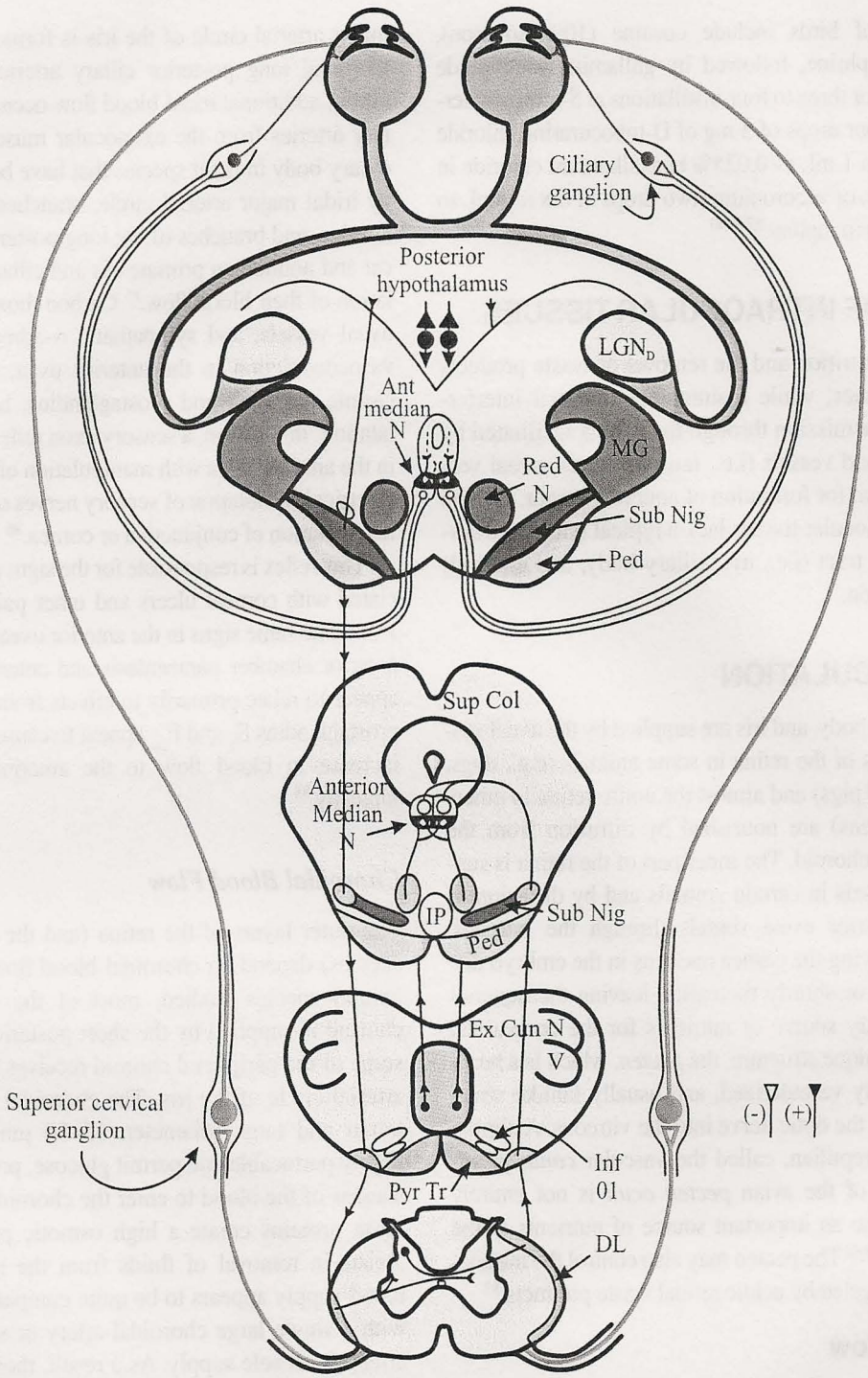

Figure 3.3. Pupillomotor pathways. **1.** A descending, excitatory multisynaptic pathway leaving the hypothalamus and projecting through the sympathetic nervous system. **2.** A descending, inhibitory multisynaptic pathway leaving the hypothalamus and projecting to the Edinger-Westphal nucleus. (or anteromedian nuclei) **3.** An ascending, inhibitory system leaving the reticular formation and projecting to the Edinger-Westphal nucleus. (or anteromedian nuclei) **4.** An ascending, inhibitory system leaving the dorsal horn and projecting to the Edinger-Westphal nucleus. (or anteromedian nuclei) (Modified with permission from Loewy AD, Araujo JC, Kerr FW. Pupillodilator pathways in the brain stem of the cat: Anatomical and electrophysiological identification of a central autonomic pathway. *Brain Res* 1973;60:65.)

with focusing through the creation of a Scheiner's disc phenomenon.[79] With very low illumination or administration of a mydriatic, the dorsal and ventral borders of the pupil dilate, thereby forming a circular pupil. The pupil of a horse responds relatively sluggishly to a penlight stimulus and seldom closes fully.

The avian pupil is circular and highly motile. The consensual pupillary reflex is usually absent (because of total decussation of nerve fibers at the optic chiasm), but occasionally, a strong beam of light may traverse the posterior ocular layers and the thin medial orbital bones to stimulate the opposite retina. The highly colored avian irides can be affected by diet. Because the constrictor and dilator muscles are mainly striated with varying amounts of nonstriated fibers, the pupil is not affected by traditional mydriatic agents, but it can be dilated by neuromuscular blocking drugs. Those reported to be effective in

selected species of birds include cocaine (10% solution), followed by epinephrine, followed by gallamine triethiodide applied to the eye for three to four instillations at 5-minute intervals or by two to four drops of 3 mg of D-tubocurarine chloride powder dissolved in 1 mL of 0.025% benzalkonium chloride in pigeons and raptors, or vecuronium (two drops of 0.8 mg/mL to 4 mg/mL solutions) in raptors.[57,80,81]

NUTRITION OF INTRAOCULAR TISSUES

The provision of nutrition and the removal of waste products for intraocular tissues, while maintaining minimal interference with light transmission through the eye, is facilitated by two systems of blood vessels (i.e., retinal vessels, uveal vessels), the mechanism for formation of aqueous humor, and the vitreous body. Intraocular tissues lack a typical lymphatic system, and the uveal tract (i.e., iris, ciliary body, and choroid) assumes this function.

OCULAR CIRCULATION

The choroid, ciliary body, and iris are supplied by the uveal vessels. The outer parts of the retina in some animals (e.g., dogs, cats, ruminants, and pigs) and almost the entire retina in others (e.g., horses, chickens) are nourished by diffusion from the uveal vessels in the choroid. The inner part of the retina is supplied by retinal vessels in certain animals and by diffusion of nutrients from anterior uveal vessels through the vitreous. Blood vessels supplying the cornea and lens in the embryo disappear before birth or shortly thereafter, leaving the aqueous humor as the primary source of nutrients for the cornea and lens. Birds have a unique structure, the *pecten,* which is a heavily pigmented, highly vascularized, and usually fanlike structure projecting from the optic nerve into the vitreous. A similar structure occurs in reptilian, called the vascular *conus papillaris.* The function of the avian *pecten oculi* is not entirely known, but it may be an important source of nutrients to the inner retinal layers.[80,82] The pecten may also control the intraocular pH, which is affected by acidic retinal waste products.[83]

Ocular Blood Flow

The vascular pressure promoting flow, the resistance of blood vessels, and the viscosity of the blood all influence the flow of blood through all tissues, including the eye. The pressure head for blood flow (i.e., perfusion pressure) is the difference in pressure between the arteries and the veins. In the eye, the IOP approximates the venous pressure, so the perfusion pressure is the difference in pressure between the small arteries entering the eye and the IOP.[84] Of clinical importance is that the perfusion pressure to the eye is reduced by lowering the blood pressure or raising the IOP, as occurs in the glaucomas.

Anterior Uveal Blood Flow

Of the total blood flow to the eye in humans, approximately 5% flows to the iris and 7% to the ciliary body. In most species, the major arterial circle of the iris is formed by the nasal and the temporal long posterior ciliary arteries. In humans and the rabbit, additional iridal blood flow occurs from the anterior ciliary arteries from the extraocular muscles. Blood flow to the ciliary body in most species that have been studied is provided by iridal major arterial circle, branches of the anterior ciliary arteries, and branches of the long posterior ciliary arteries. The cat and nonhuman primate iris and ciliary body have autoregulation of their blood flow.[85] Carbon dioxide dilates the anterior uveal vessels, and sympathetic α-adrenergic receptors cause vasoconstriction in the anterior uvea. Parasympathetic muscarinic receptors and prostaglandins, however, cause vasodilatation. In addition, a sensory axon reflex causes vasodilatation in the anterior uvea with manipulation of the iris, mechanical or electrical stimulation of sensory nerves of the eye, and mechanical irritation of conjunctiva or cornea.[86]

This reflex is responsible for the signs of anterior uveitis associated with corneal ulcers and other painful extraocular problems. The same signs in the anterior uveal vessels in response to anterior chamber paracentesis and anterior segment infections appear to relate primarily to effects from prostaglandins.[87] The prostaglandins E_1 and $F_{2\alpha}$ appear to cause a twofold to threefold increase in blood flow to the anterior uvea when applied topically.[88]

Choroidal Blood Flow

The outer layers of the retina (and the entire retina in some species) depend on choroidal blood flow for nutrients. In the animal species studied, most of the blood supply to the choroid is supplied by the short posterior ciliary arteries, but some of the peripheral choroid receives blood from the major arterial circle of the iris. The choroidal capillaries are fenestrated and large (diameter, 15–50 μm). These vessels are highly permeable and permit glucose, proteins, and other substances of the blood to enter the choroid. Within the choroid, these proteins create a high osmotic pressure gradient that assists in removal of fluids from the retina. The choroidal blood supply appears to be quite compartmentalized, perhaps with a single large choroidal artery or short posterior ciliary artery as its sole supply. As a result, these "watershed zones" may be nonperfused, with marked elevations of IOP appearing in the dog as pyramidal-shaped areas of choroidal and retinal degenerations extending from the optic nerve head.

The rate of uveal blood flow is rapid (1.2 mL/min in the cat),[89] with a mean combined retinal and choroidal circulation time of 3 to 4 seconds.[90] In humans, 98% of the blood flow passes through the uveal tract, of which 85% is through the choroid. With this high rate of blood flow, oxygen extraction from each millimeter of blood is low (~5–10%). The oxygen content of choroidal venous blood is 95% of that in arterial blood. Reduced flow rates result in higher oxygen extraction, so that total extraction is reached. This protects the oxygen supply to the retina, and it also protects the eye from light-generated thermal damage. Choroidal vessels have little to no autoregulatory mechanism, but carbon dioxide is a potent

vasodilator of choroidal vessels.[91–94] Choroidal vessels are under the strong influence of sympathetic stimulation, which can result in a 60% reduction of choroidal blood flow. Parasympathetic fibers have been found in the choroid of monkeys, but no studies concerning the relationship of these fibers to blood flow have been conducted. α-Adrenergic drugs cause vasoconstriction of choroidal vessels, but β-adrenergic drugs have no effect.[91] In the rabbit, α- and β-adrenergic blockade cause choroidal vasodilation and vasoconstriction, respectively.[94] Nitric oxide appears to be a putative neurotransmitter of parasympathetic origin in the choroidal perivascular autonomic nerve fibers, and it may be an endothelium-derived vasoactive relaxing factor.[93]

Retinal Blood Flow

In humans, approximately 5% of the total blood flow is through the retina. In the cat, 20% of the oxygen consumed by the retina is delivered through the retinal circulation and the remainder through the choroidal circulation.[85] Similar data are not available for other domestic animals. Blood flow in the innermost part of the retina is practically unaffected by moderate changes in perfusion pressure. The theoretic oxygen diffusion maximum of 143 μm presents a physical problem for those animal species with avascular retinas; as a result, avascular retinas are usually very thin, with short photoreceptors, no tapetums, high glycogen levels in the Müller cells, and no retinal taper.

Autoregulation of retinal blood flow, which is almost perfect in the cat, monkey, and pig, protects the retinal circulation from large variations in perfusion pressure.[85,95] Both metabolic and myogenous autoregulation are present in the eye. Metabolic control of retinal blood flow is similar to that of blood flow to the brain. In the brain, increased PO_2 and decreased PCO_2 cause vasoconstriction, and decreased PO_2 and increased PCO_2 cause vasodilatation. In the cat, maximum retinal vasodilatation occurs with an increased PCO_2 of 75 to 80 mm Hg, so as to increase flow from 15 to 50 mL/min.[85] In immature eyes with developing blood vessels, high oxygen consumption may cause a syndrome known as retrolental fibroplasia. The increased oxygen causes vasoconstriction and inhibition of vascular development, with obliteration of vessels. After withdrawal of the increased oxygen, vasoproliferation, retinal edema, and hemorrhages cause traction bands that result in retinal detachment. Neural control of retinal blood flow is limited to those vessels indirectly affecting retinal flow. Retinal vessels have α-adrenergic–binding sites that, when stimulated, cause vasoconstriction, thus increasing retinal vascular resistance.[96,97] Retinal arteries most likely autoregulate through a myogenic mechanism, which is activated on the basis of stretch. During sympathetic stimulation, myogenic autoregulatory responses appear to increase.[97] Opening and closing of capillary beds in many tissues occurs with varying metabolic needs. Spontaneous contractions and dilatations of small retinal arterioles have been observed in kittens but are rare in adult cats.[91] In general, it is believed that both choroidal and retinal blood flow are constant through all capillary beds; however, regional blood flow in the retina decreases from the optic disc to the periphery.[98] In humans, blood flow to the nasal side of the retina is approximately three times less than that to the temporal side, but no significant difference has been noted between superior and inferior retina blood flow.[99] Autoregulation of the retinal and optic nerve in normal and glaucomatous eyes demonstrates some differences.[100]

Local regulation of the retinal and choroidal circulations apparently is controlled by several interrelated factors. The vascular endothelial cells may produce nitric oxide, endothelins, prostaglandins, and renin-angiotension products in response to chemical stimuli (e.g., acetylcholine, brachykinin), changes in blood pressure and blood vessel wall stress, changes in local oxygen levels, and other stimuli.[101] As the mechanisms of local autoregulation become better understood, pharmacologic modulation of these processes may become possible.

Blood Flow of the Optic Nerve Head

Blood flow of the optic nerve head in humans, the cat, and the rabbit possesses autoregulation over a wide range of IOPs (~30–75 mm Hg), but in humans, this autoregulation is most efficient when IOP is 6 to 30 mm Hg.[102,103] Blood supply to the optic nerve head is usually provided primarily by branches from the short posterior ciliary arteries. Studies of blood flow in the optic nerve head have been limited, however, by the small tissue mass involved.

The optic nerve head is subjected to several different pressures as well as to the tissue stress at the level of the scleral lamina cribrosa. Axons from the retinal ganglion cells exit the eye under the effect of IOP, passing through the lamina scleral cribrosa at progressively decreasing tissue pressures to become the optic nerve. The retrolaminar pressure for these axons in the dog is approximately 7 mm Hg and relates directly to the cerebrospinal pressure.[104] Both short- and long-term elevations in IOP may also produce tissue changes within the lamina scleral cribrosa that may influence blood flow and axon vitality. With local ischemia, retinal excitatory endogenous neurotransmitters (e.g., glutamate, aspartate) may be released, thereby inducing toxic effects, especially on the retinal ganglion cells, and initiating a cascade of cellular apoptosis.

OCULAR BARRIERS

The blood–ocular barriers contain endothelial and epithelial tight junctions with varying degrees of "leakiness." These barriers prevent almost all protein movement and are effective against low-molecular-weight solutes such as fluorescein and sucrose. The complexities of these structures differ between the various vascular beds, which allows movement of some substances from one compartment to the other.

The two barriers within the eye are the blood–retinal barrier and the blood–aqueous barrier. Other lesser barriers of the eye exist as well. The corneal epithelium, though a significant barrier to most substances, lacks true zonula occludens–type (i.e., tight) junctions. The iris blood vessels have tight junctions but

lack fenestrations; nevertheless, they are relatively impermeable to large molecules, as demonstrated by anterior segment fluorescein angiography. Permeability of the iridal vessels may be influenced by age and species differences.[105]

Blood–Retinal Barrier

The endothelial portion of the blood–retinal barrier is the endothelium of the retinal capillaries, is nonfenestrated, and has tight junctions preventing both inward and outward movement of materials. The epithelial portion of the blood–retinal barrier is the retinal pigment epithelium. This barrier separates the choroidal tissue fluid, which is similar to plasma, from the retinal tissue fluid. The most permeable point of the blood–retinal barrier is the optic nerve head, at which substances from the choroid can pass into the nerve.[106] The choroidal capillaries are highly permeable to and permit passage of all low-molecular-weight compounds and proteins. Thus, nutrients from the choroidal blood supply pass readily into the retinal pigment epithelium, where mechanisms exist to pass them on into the retina. This high-protein permeability of the choroidal vessels also elevates osmotic pressure, which helps fluid to pass out of the retina. The retinal pigment epithelium probably has an active transport mechanism that contributes to the flow of fluid from the retina.

No significant barrier exists between the aqueous humor and the vitreous body, or between the vitreous body and the retina. In the normal eye, passage of compounds into the anterior vitreous apparently occurs around the periphery of the lens, through the anterior vitreous face and hyaloideocapsular (Wieger's) ligament that forms the caudal border of the posterior chamber. Lens removal, however, can increase the passage of selected drugs from the anterior chamber into the vitreous and retina. Hence, the blood–aqueous barrier is responsible for controlling the passage of substances from the anterior uveal vessels to the retina.

Blood–Aqueous Barrier

The blood–aqueous barrier depends primarily on the tight junctions between the nonpigmented ciliary body epithelium. The ciliary vessels are similar to choroidal vessels regarding high-protein permeability. The ciliary body blood vessels are highly fenestrated, and they leak most of their plasma components into the stroma. Fortunately, however, the epithelial portion of the blood–aqueous barrier is the inner, nonpigmented ciliary epithelium, which controls the flow of fluid into the posterior chamber. This barrier is not as effective as the retinal epithelial barrier, because protein passes into the aqueous humor by pinocytosis and through openings in the rest of the anterior uvea. No barrier is present between the aqueous humor and the vitreous humor, which allows the diffusion of solutes from the posterior aqueous into the vitreous humor, or between the anterior uvea and the sclera.[107] The endothelial portion consists of tight junctions and contributes to the blood–aqueous barrier iris vessels.[108] Because the anterior region of the iris does not have a continuous cellular layer, the extracellular space of this region is in contact with the aqueous humor. Diffusion of solutes across the iridal vascular endothelium is possible, but no data exist that indicate an active transport system.[109] The blood–aqueous barrier permits free passage of some substances from the aqueous humor into surrounding tissues and into the bloodstream.[106] Breakdown of the blood–aqueous barrier is seen clinically as an aqueous flare in anterior uveitis and secondary or plasmoid aqueous following loss of the aqueous humor, as in anterior chamber paracentesis.

In 1957, prostaglandins were first identified in the aqueous humor and were termed *irin*. Prostaglandins are synthesized in large amounts from arachidonic acid released by esterified sites in membrane phospholipids after trauma, iridocyclitis, and intraocular surgery. Prostaglandins are thought to be primarily responsible for the blood–aqueous barrier breakdown following anterior chamber paracentesis.[110,111] Their role in anterior uveitis is the subject of current research, but prostaglandins are not the only mediators in this process.[112] Aqueous humor protein concentrations and prostaglandin E^2 metabolites following anterior chamber paracentesis in the dog are reduced by pretreatment with aspirin (i.e., a prostaglandin inhibitor) and flunixin meglumine (i.e., a nonsteroidal antiinflammatory agent).[87,88,111]

AQUEOUS HUMOR AND INTRAOCULAR PRESSURE

The ciliary body has several functions, including:

1. Formation of aqueous humor by active secretion, ultrafiltration, and simple diffusion;
2. Generation of IOP through the aqueous dynamic process;
3. Influence through its musculature on the conventional (i.e., corneoscleral trabecular meshwork or pressure-sensitive) aqueous humor outflow;
4. Provision of both the blood supply and nerve supply for the anterior segment;
5. Control with its musculature over the accommodation process;
6. Constitution of the blood–aqueous barrier; and
7. Formation of the entry for the nonconventional (i.e., uveoscleral or pressure-insensitive) aqueous humor outflow.

The ciliary body is also rich in antioxidant systems, with significant concentrations of catalase, superoxide dismutase, and glutathione peroxidase types I and II. In addition, the ciliary body is the major drug detoxification center in the eye, with its microsomes containing the cytochrome P_{450} proteins, which catalyze many drugs. In avian species, the ciliary body musculature is composed of distinct anterior and posterior components that alter the corneal curvature for corneal accommodation and move the ciliary body anteriorly for lenticular accommodation.[113,114]

Aqueous Humor Formation

Aqueous humor is the transparent fluid that fills the anterior chamber, pupil, and posterior chamber. With a refractive index

of 1.335, its density is slightly greater than that of water. As aqueous humor is formed by the ciliary body processes, it enters the posterior chamber and flows through the pupil into the anterior chamber, where it leaves the eye through the corneoscleral trabecular and uveoscleral outflow pathways. This continuous flow of aqueous humor supplies the avascular cornea and lens with nutrients and also removes their waste products. The rate of aqueous humor formation equals the outflow, so the IOP is maintained at a relatively constant level and the refracting surfaces of the eyes are kept in the normal position. Aqueous humor resembles an ultrafiltrate of plasma (Tables 3.5 and 3.6).[53,115–121] Breakdown of the blood–aqueous

Table 3.5 Concentrations of Organic Compounds in Aqueous Humor, Plasma, and Vitreous

Compounds	Aqueous	Plasma	Vitreous	Species
Amino acids	2.86	1.87	1.23	Dog
(μmol/mL)	—	—	30	Cat
	—	—	14–30	Cow
	—	—	30.0	Horse
	2.10	—	—	Monkey
Ascorbate	0.55	—	—	Dog
(μmol/mL)	0.1	—	—	Cat
	1.21	—	—	Cow
	—	—	0.43–0.98	Horse
	1.18	0.02	0.02	Monkey
	0.96	0.04	0.46	Rabbit
Glucose	5.11	7.00	—	Dog
(μmol/mL)	4.55	5.96	3.17	Cat
	2.00	3.11	3.0–3.4	Cow
	5.44	5.05	5.55	Horse
	3.0	4.1	—	Monkey
	6.9	7.2	3.0	Rabbit
Hyaluronate	—	—	35	Dog
(μg/mL)	—	—	31–53	Cat
	4.4	—	251–1190	Cow
	—	0.29	—	Horse
	<2.0	—	423	Monkey
	<3.0	10.3	31	Rabbit
Lactate	—	—	—	Dog
(μmol/mL)	—	—	—	Cat
	—	—	1.64	Cow
	—	—	1.94	Horse
	4.3	3.0	—	Monkey
	12.1	8.2	12.0	Rabbit
Protein	0.38	6.5	—	Dog
(mg/100 mL)	0.15–0.55	7.8	—	Cat
	0.17	7.5	379–960	Cow
	0.2	7.3	—	Horse
	33.3	—	—	Monkey
	25.9	—	—	Rabbit
Urea	7.45	—	—	Dog
(μmol/mL)	5.16	7.88	8.5	Cat
	—	5.59	14.2	Cow
	—	4.5	4.83	Horse
	6.1	7.3	—	Monkey
	7.0	9.1	7.63	Rabbit

Table 3.6 Concentrations of Inorganic Compounds in Aqueous Humor, Plasma, and Vitreous

Compounds	Aqueous	Plasma	Vitreous	Species
Bicarbonate (μmol/mL)	Ratio aqueous:plasma = 1.13	—	—	Dog
	30.4	25.3	—	Cat
	36.0	—	—	Cow
	Ratio aqueous:plasma = 0.82	—	19.6–32.4	Horse
	22.5	18.8	—	Monkey
	33.6	27.4	19.6–32.4	Rabbit
Calcium (mEq/L)	2.9	5.2	—	Dog
	2.7	4.8	—	Cat
	—	—	3.5–4.0	Cow
	3.0	5.5	4.9–7.3	Horse
	2.5	4.9	—	Monkey
	3.5	6.2	1.5	Rabbit
Chloride (mEq/L)	124.8	115.9	—	Dog
	—	—	—	Cat
	—	—	116–124	Cow
	12.1	10.1	112–120	Horse
	125.0	110.0	—	Monkey
	105.1	111.8	104.7	Rabbit
Oxygen (mm Hg)	45	—	—	Dog
	—	—	53	Cat
	—	—	—	Cow
	—	—	—	Horse
	—	—	—	Monkey
	30	77	17.0	Rabbit
Phosphate (μmol/mL)	0.53	1.26	—	Dog
	0.48	1.87	—	Cat
	—	—	0.42–0.92	Cow
	0.33	0.31	1.00	Horse
	0.14	0.68	—	Monkey
	0.89	1.49	0.40	Rabbit
Potassium (mEq/L)	5.0	4.4	5.3	Dog
	4.4	4.0	—	Cat
	7.1	4.7	4.9–5.6	Cow
	5.1	5.5	4.9–7.3	Horse
	3.9	4.0	—	Monkey
	5.2	5.5	9.5	Rabbit
Sodium (mEq/L)	149.4	154	—	Dog
	158.5	163.6	—	Cat
	149.5	143	131–148	Cow
	117.4	143.5	118–163	Horse
	152	148	—	Monkey
	143	146	134	Rabbit

barrier modifies the composition of the aqueous humor, primarily by the addition of proteins and prostaglandins, which is exhibited clinically as aqueous flare. With the addition of proteins, the aqueous composition closely approximates that of plasma and is termed *plasmoid aqueous.* Plasmoid aqueous in domestic animals clots easily because of high levels of fibrinogen. Unless treated pharmacologically, this clotting may cause many of the complications encountered during intraocular surgery of animals.

The metabolic needs of the cornea and lens alter the aqueous humor composition, as seen by the differences in concentration of some substances between the anterior and the posterior

chambers. The level of substances in the blood also affects the level of those same substances in the aqueous humor; one example is the hyperglycemia of diabetes mellitus, which results in elevated aqueous sugar concentration. Other factors affecting composition of aqueous humor are alterations in the rate of blood flow through the ciliary processes and modifications of the secretory activity of the ciliary body nonpigmented epithelium.

The chemical components of the aqueous humor are proteins, immunoglobulins, enzymes, and lipids, all of which are present in much lower concentrations than in the plasma. This is due to the blood–aqueous barrier as well as because of electrolytes and other inorganic compounds. Carbohydrates, urea, and amino acids are also found in the aqueous humor at various concentrations. The carbohydrate level in aqueous humor is approximately 80% that of the plasma. Because the carbohydrates enter the aqueous humor by diffusion, however, this difference most likely results from their use by the lens and cornea.[122] Urea concentration in the aqueous humor is also approximately 80% that of plasma. Results of previous studies in the dog have indicated that urea penetrates the blood–aqueous barrier very slowly; therefore, a steady level as compared to that in plasma is never reached, which results in a lower concentration of urea in the aqueous.[123] In most mammalian species, the concentration of amino acids in the aqueous humor is higher than that in the plasma, and this suggests an active transport of amino acids across the ciliary epithelium is most likely involved in this secretory process.[124,125] In the dog, however, amino acid concentrations in the aqueous humor are lower than those in the plasma.[115] In this species, the vitreous may act as a "sink" for some of the amino acids, thus causing the deficiency.[124,125] In addition, the vitreous may function as a reservoir for certain drugs and other compounds.

The major cations in the aqueous humor are sodium, potassium, calcium, and magnesium, with sodium making up 95% of the total cation concentration. Sodium enters the aqueous through an active transport mechanism, with a net flow of water into the posterior chamber. This "pump" probably accounts for most of the aqueous humor formed by secretion. The major anions in aqueous humor are chloride, bicarbonate, phosphate, ascorbate, and lactate. The chloride and bicarbonate ions enter with sodium, but their concentrations vary among species. For example, in the horse, the aqueous chloride concentration exceeds that of plasma, whereas the level of aqueous bicarbonate is less than that of plasma bicarbonate. In the guinea pig, the bicarbonate concentration is higher and the chloride concentration is lower.[126] Because the total anion concentration equals the total cation concentration, the combined chloride and bicarbonate concentrations equal the sodium concentration. Lactate in the aqueous humor is found in much higher concentrations than in the plasma. Results of previous studies indicate that glucose metabolism by the cornea, ciliary body, lens, and retina contributes to the lactate concentration of the aqueous humor. Lactate concentrations do not appear to accumulate in the posterior chamber above the plasma concentration.[127]

Ascorbate concentration in the aqueous humor exceeds that in plasma because of an active transport mechanism.[128] The level of aqueous ascorbate is lower in young animals than in adults, but the reason for this is unclear.[122] It has been suggested that ascorbate plays a role in storage of catecholamines in the iris, is a cofactor in electron transfer reactions, is a reducing agent in hydroxylation reactions (e.g., lysine to proline in collagen connective tissue), partially absorbs ultraviolet radiation, serves as an antioxidant, and helps to regulate production of GAGs in the trabecular meshwork.[128,129] Aqueous humor ascorbate levels appear to be higher in diurnal animals than in nocturnal animals, thus suggesting a possible protective effect against light-induced damage.

Aqueous humor is formed by three basic mechanisms: diffusion, ultrafiltration, and active secretion by the nonpigmented ciliary epithelium. Diffusion of solutes occurs down the concentration gradient, or from the area of higher concentration to the area of lower concentration. Lipid-soluble compounds are examples of diffusible substances. Ultrafiltration occurs when movement of a compound across a cell membrane is increased by a hydrostatic force, and it results from differences between the pressure of the ciliary body capillaries and the IOP. Active transport requires energy (usually ATP) to secrete material against a concentration gradient. Active transport of certain solutes (by the ciliary epithelium) is the most important factor in aqueous humor formation.[130,131] The Na^+ ion is the major constituent actively transported from blood to the aqueous humor. An enzyme complex, Na^+,K^+-ATPase, is an active transport system present in the nonpigmented ciliary epithelium; this enzyme complex is membrane-bound and is found in the highest concentrations along the lateral interdigitation of these cells. Alterations in this complex will cause a marked decrease in aqueous formation.[130,132,133] Differences in osmolarity between plasma and aqueous humor are small, thereby making the rate of aqueous production dependent on the rate of solute transfer.[134] Carbonic anhydrase (CA) catalyzes the reaction:

$$CO_2 + H_2O \longrightarrow HCO_3^- + H^+$$

Entry of bicarbonate into the aqueous is associated with entry of water into the posterior chamber. Administration of topical and systemic carbonic anhydrase inhibitors slows the reaction, thus decreasing the rate of aqueous formation (Fig. 3.4). These drugs are useful therapeutic agents in treatment of glaucomas.[135]

Aqueous humor circulates within the anterior chamber because of the temperature difference between the air-cooled cornea and the iris. This process is known as thermal circulation. The convection current causes an upward flow of aqueous near the dorsal cornea. This circulation is responsible for the deposition of cellular material and keratic precipitates on the corneal endothelium in a vertical streak or spindle.

The rate of aqueous humor formation equals the rate of aqueous outflow, thereby determining the IOP. The flow of aqueous humor through the ciliary body epithelium and into the posterior chamber is caused by hydrostatic pressure against an osmotic

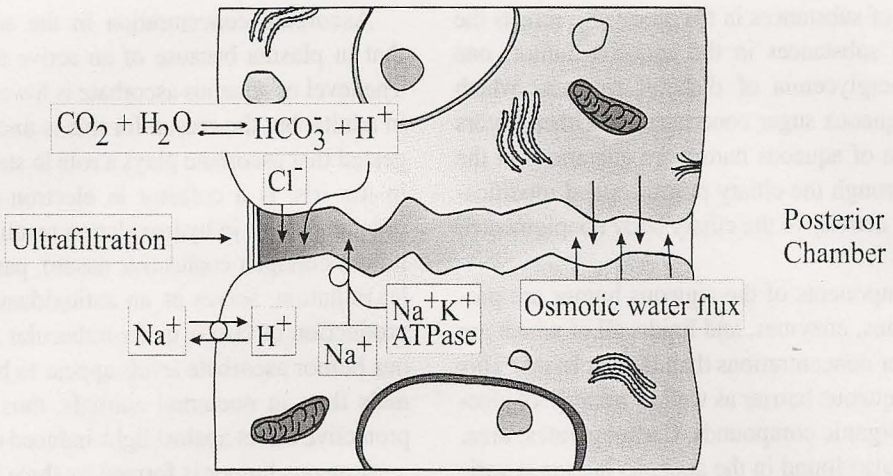

Figure 3.4. Theoretic diagram of aqueous production based on the gradient osmotic flow model. The highest concentrations of Na^+,K^+-ATPase are along lateral cell walls. The role of Cl-transport is not clear. (Modified with permission from Caprioli J. The ciliary epithelia and aqueous humor. In: Moses RA, Hart WM, eds. *Adler's Physiology of the Eye.* St. Louis: CV Mosby, 1987.)

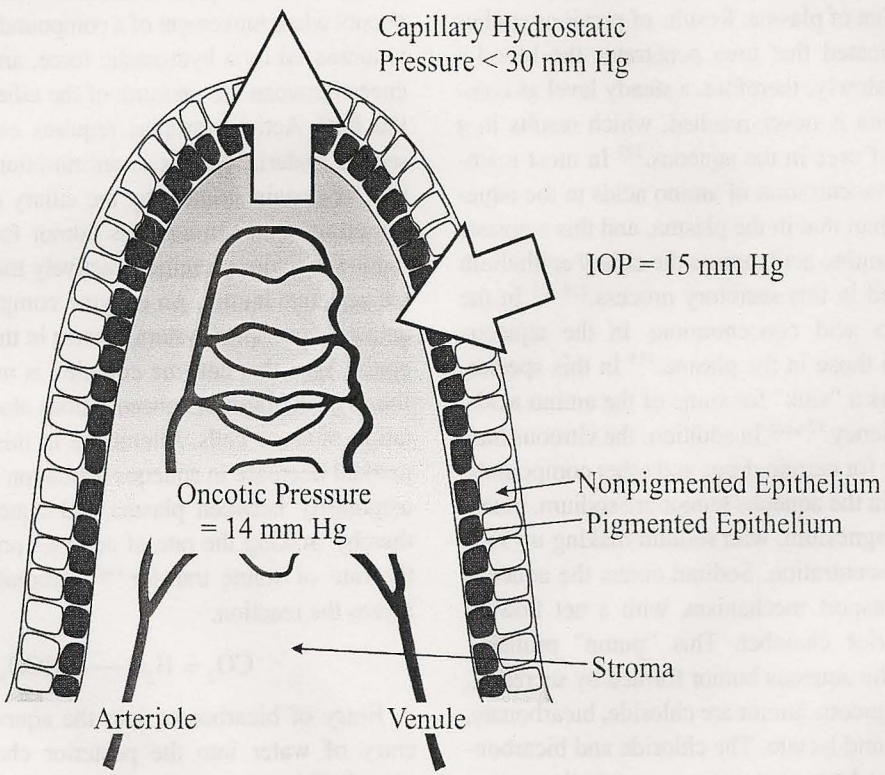

Figure 3.5. Schematic of the ciliary body process showing the hydrostatic forces involved in formation of aqueous humor.

pressure gradient (i.e., ultrafiltration) and by a metabolic pump (discussed earlier). The rate of aqueous formation from within the ciliary stromal tissue is influenced by humoral as well as by sympathetic and parasympathetic innervation to maintain a steady-state IOP. An increase in IOP causes a reduction in aqueous inflow, which is related to an alteration in the hydrostatic pressure gradient. This indicates that IOP only partially depends on systemic blood pressure (Fig. 3.5).[136,137]

Within the ciliary epithelium, an adenylate cyclase enzyme–receptor complex exists that is responsible for forming a second messenger complex, cyclic adenosine monophosphate (cAMP). Adenylate cyclase is activated by catecholamines, gonadotropins (i.e., glycoprotein hormones), organic fluorides, and other compounds such as cholera toxin and forskolin (a diterpene), which in turn cause a decrease in aqueous inflow and IOP.[137,138] This enzyme system may be a common pathway through which IOP is regulated within the eye.

Aqueous Humor Outflow

The rate of aqueous humor formation varies among species. Aqueous humor dynamics involve the balance between

production (i.e., active secretion) and both conventional and nonconventional outflow. Conventional outflow involves the flow of aqueous humor through the corneoscleral trabecular meshwork; the nonconventional route involves uveoscleral outflow.[139,140] In conventional outflow, the primary resistance to aqueous outflow appears to be localized to the inner wall of the interscleral plexus and the outer trabecular meshwork.

Though it is often not considered, the "backpressure" created by the venous portion of the conventional or corneoscleral (i.e., pressure-sensitive) aqueous humor pathways on Schlemm's canal or the intrascleral plexus constitutes approximately 50% to 75% of the resistance that determines IOP. Minor anatomic variations in the venous system have been demonstrated in several species (i.e., nonhuman primates, dogs, cats, rabbits) that appear to determine the exit of aqueous humor from the anterior chamber. To date, however, results of pressure studies in humans, nonhuman primates, rabbits, and dogs reveal venous pressure in all species studied to be approximately 8 to 12 mm Hg.[141–144] Measurements of the venous pressure of these vessels include direct cannulation (using very fine glass pipettes) and indirect partial-to-complete compression schemes (using a string-gauge system or a fluid-filled chamber).[144]

Arteriovenous anastomoses within the episcleral vasculature have been recently demonstrated in the rabbit, dog, owl monkey, and cynomolgus monkey. These vascular shunts may function in the rabbit and dog where the episcleral vasculature appears to lack a capillary system and in the monkey species as an emergency system to elevate IOP after anterior chamber paracentesis or to flush retrogradely the outflow channels.[145,146] Many formulae have been developed for the formation and exit of aqueous humor in both humans and animals. These formulae have evolved over several decades of studies and now appear to be accurate for humans, the rabbit, selected nonhuman primates, the dog, and the cat (Table 3.7). In large animals, uveoscleral outflow, which appears to be independent of IOP, may be a substantial route that cannot be measured by tonography.

Table 3.7 Aqueous Humor Dynamics Formulae

I. Flow = $(P_1 - P_e)R$
F = Aqueous production
P_1 = IOP
P_e = ESV pressure (episcleral venous pressure)
R = Resistance
II. Inflow = Outflow
III. Secretion – C_{pseudo} $(P_1 - P_e) = C(P_1 - P_e)/1 + Q(P_1 - P_e) + U$
C_{pseudo} = Pseudofacility
P_1 = IOP
P_e = EVP (episcleral venous pressure)
C = Total facility
Q = Outflow obstruction coefficient
U = Uveoscleral outflow

The term *pseudofacility* refers to pressure-dependent ultrafiltration formation of aqueous humor. It was assumed that any measurement procedure for aqueous humor dynamics that temporarily elevated IOP (e.g., perfusion of the anterior chamber, tonography, perilimbal suction cup) would temporarily decrease the rate of humor formation. This slight decrease in the rate of formation would alter the pressure-sensitive outflow measurements obtained by tonography and were termed *false facility,* or pseudofacility. Results of studies that involved compressing the venous pressure of the aqueous humor outflow systems in humans and nonhuman primates suggest the pseudofacility to be as high as a 20% error. Fluorophotometric measurements of rates of humor formation, however, indicate these sudden (but limited) increases in IOP do not suppress the rate of humor formation. Fluorophotometry in both normal and glaucomatous human eyes indicate that rates of aqueous humor formation are essentially the same.[147] Another possible explanation is immediate dilatation of the intraocular blood vessels and slow accumulation of aqueous humor. In current reports, pseudofacility may still be used as a "correction" factor in the humor formulae.

Other influences on the rate of aqueous humor formation and regulation of IOP have been proposed. In the cat, a center in the diencephalon has been found that, when stimulated, causes alterations in the IOP.[148] Central nervous system regulation of IOP is not understood, however, and hormonal control of aqueous humor production may be involved. Because of the similarities between the ciliary and renal epithelium, antidiuretic hormone, cortisol, and prolactin have been suggested as factors in regulating aqueous humor dynamics.[141] The effect of drugs on aqueous humor dynamics is discussed in Chapters 7 (Part 2) and 21.

The outflow of aqueous humor is primarily through the trabecular meshwork, but a small percentage (depending on the species) leaves by diffusion through the iris, ciliary body, and vitreous. This unconventional, or uveoscleral, outflow is independent of the IOP, but it is affected by the state of the ciliary body and by the hydrostatic pressure difference between the anterior chamber and the suprachoroidal space.[150–153] Contraction of the ciliary body musculature decreases unconventional outflow, possibly by reducing the extracellular spaces; in turn, relaxation increases outflow via this route.

The available information on aqueous humor dynamics in animals is summarized in Table 3.8.[154] Results of earlier studies indicated that volume of the anterior chamber directly relates to the rate of aqueous outflow, so that animals with large eyes have faster outflow rates per minute.[155] The resistance to aqueous outflow is inversely proportional to the facility of outflow (C_{out}). Results of recent studies indicate that the main site of resistance to outflow is the endothelial lining of the angular aqueous plexus and the extracellular matrix (Fig. 3.6).[156,157] The site of filtration may be different from the site of flow resistance as well.[158]

Aqueous humor can pass directly into the angular aqueous plexus (or Schlemm's canal in nonhuman primates and domestic chickens) through transcellular pores, large vacuoles, or

Table 3.8 Estimates of aqueous humor dynamics in selected species

	Dog	Cat	Rabbit	Cow	Horse	Nonhuman Primate
"C" outflow (μL/mmHg/min by tonography)	0.24–0.30	0.27–0.32	0.22–0.28	—	0.90	0.24–0.28
Uveoscleral outflow (μL/min)	15%	3%	13–25%	—	—	5–40%
IOP (mmHg)	15–18	17–19	15–20	20–30	17–28	13–15
Episcleral venous pressure (mmHg)	10–12	8	9	—	—	—
Aqueous formation	—	0.8 (tracers)	—	—	—	—

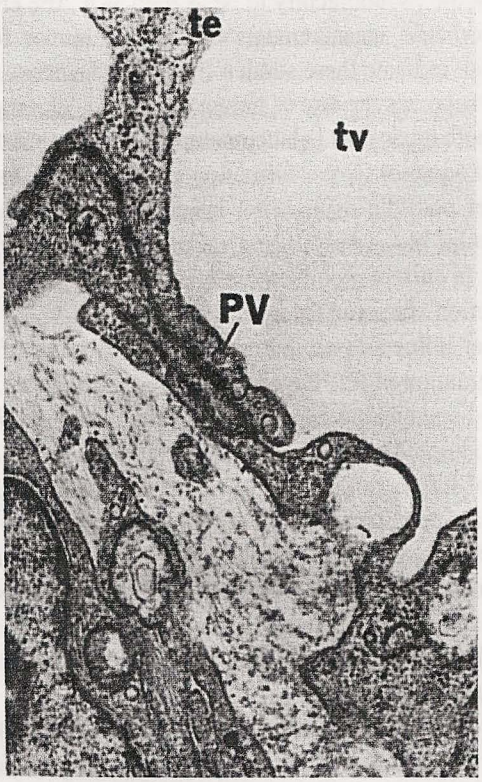

Figure 3.6. Transmission-electron micrograph showing the angular aqueous plexus in a canine eye. *Arrows* indicate cell junctions between the endothelial cells. Numerous pinocytotic vesicles are present. *PV,* pinocytotic vesicle: *te,* endothelium of trabecular vein; *tv,* trabecular vein (angular aqueous plexus). (Original magnification, X37,800.) (Courtesy of DA Samuelson.)

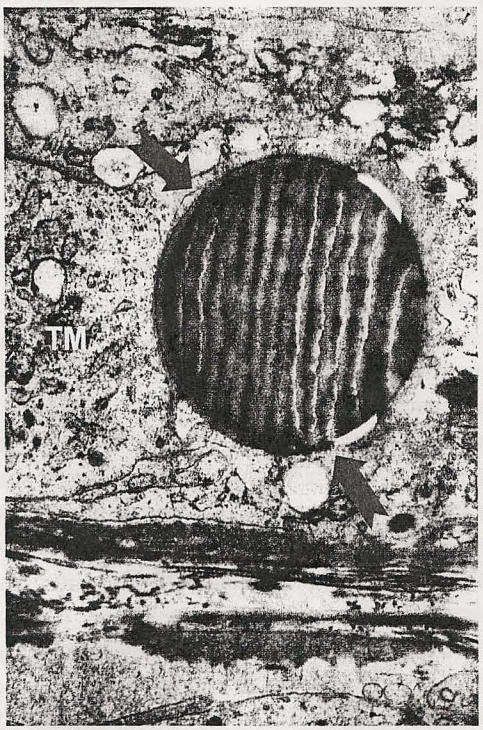

Figure 3.7. Phagocytic activity of the trabecular meshwork cell. *Arrows* indicate a 3-μm latex sphere being ingested into a trabecular meshwork cell. (Original magnification, X7,700.) (Photo provided by DA Samuelson.)

pinocytotic vesicles. Another mechanism exists that involves phagocytic activity by macrophages and native trabecular meshwork cells (Fig. 3.7). This self-cleaning filter mechanism is activated by the presence of large particulate material. A malfunction of endothelial phagocytosis and reduced numbers of trabecular endothelial cells may contribute to the abnormal state of primary open-angle glaucoma.[159]

The nonfiltering portion of the canine iridocorneal angle has been shown to contain Schwalbe's line (SL) cells, which have both secretory and epithelial characteristics. Changes in morphology and number of SL cells correlated with the progression of disease in glaucomatous dogs.[160]

Resistance developed by the pressure-sensitive aqueous humor outflow pathways appears to relate to the trabecular meshwork cells and their extracellular matrix. The extracellular matrix is quite complex, and it consists of the different glycoproteins and the proteoglycans. The important proteins and glycoproteins in humans include laminin (i.e., the basement membrane "glue") and fibronectin, which both bind and organize the extracellular matrix and attach to the cell surfaces. Proteins important in the meshwork include the interstitial collagens, type IV basement membrane collagen, type V and VI collagens, and elastin.[161] The trabecular meshwork, which is immediately adjacent to Schlemm's canal in humans and certain other animal species, or the intrascleral venous plexus in most domestic animals, is called the juxtacanalicular zone and probably accounts for the major site of aqueous outflow resistance.

The GAGs in the aqueous outflow pathway appear to play important physiologic roles, including maintenance of structural integrity, cell matrix interactions, binding and sequestration of growth factors, and modulation of interstitial fluid exchange.[162] They form highly viscous and elastic gel solutions that function as a biologic gel filtration system and account for a significant amount of the resistance to

aqueous humor outflow. Flow in a gel filtration system can be approximated by Darcy's Law:

$$U = K(\Delta P/L)$$

where U equals a linear flow rate (expressed in cm/hour), ΔP equals pressure drop over the gel bed (expressed in cm of H_2O), L equals bed height (expressed in cm), and K equals a constant of proportionality, which depends on the properties of the gel material and the eluant. GAGs may act to maintain low-flow movement of fluid, unidirection, and the pressure gradient between the trabecular lamellae and the aqueous venous plexus of the eye.[163] These endothelial cells also allow entrance of the aqueous humor into the exit channels by vacuolation.[143,156,163,164] The aqueous humor then flows into the episcleral and subconjunctival plexus of the veins and, finally, into the general circulation.

In humans, the major types of proteoglycans within the trabecular meshwork include chondroitin, dermatan sulfate, and heparitin sulfate. HA and a small amount of keratan sulfate have also been found, and the relative amount and ratios of all these proteoglycans may change with age. In normal young rabbits, the trabecular meshwork GAGs consist of HA, keratan sulfate, heparitin sulfate, and conjugates of dermatan sulfate–chondroitin sulfate 4 and 6.[165] Aging in rabbits results in changes to the trabecular meshwork GAGs, with less keratan sulfate. In normal young dogs, the trabecular meshwork contains HA, chondroitin sulfate, dermatan sulfate, and heparitin sulfate.[166] Results of recent studies indicate that an enzyme-resistant GAG is present in the trabecular meshwork in glaucomatous human eyes and in glaucomatous Beagle eyes.[167–169] It appears this enzyme-resistant GAG causes an increase in outflow resistance, which in turn contributes to the abnormal state of aqueous dynamics in the glaucomatous eye. Other glycoproteins as well as the basement membrane material of the trabecular meshwork may also be important extracellular matrix contributing to outflow resistance. A subset of juvenile onset and primary open angle glaucomas have been shown to be associated with mutations in the trabecular meshwork inducible glucocorticoid response (TIGR) or myocilin gene.[170,171] Mutated myocilin is not normally secreted and accumulates in cells which may critically impair the function of the trabecular meshwork.[172,173] Myocilin induction may also underlay the mechanism of human steroid-induced glaucoma.[174]

Methods to Measure Aqueous Dynamics

Aqueous humor dynamics have been investigated in animals using a number of both invasive and noninvasive methodologies (Table 3.9). Most of these procedures have been performed in the rabbit, cat, and nonhuman primates, and limited information is available for the dog, cat, horse, and cow. Perfusion of the anterior chamber of in vivo and in vitro eyes has been performed in many species to determine total or gross aqueous humor outflow. The constant-pressure perfusion technique is the most frequently used. It involves maintaining a constant level of IOP with periodic, intermittent, or continuous volumes of perfusate.

Table 3.9 Methods to Investigate Aqueous Humor Dynamics

I. Techniques to investigate the formation of aqueous humor:
Cannulation of anterior chamber: constant-rate/constant-pressure perfusion.
Direct view/measurement of newly formed aqueous humor.
Use of markers in aqueous humor (radioactive, flourescein, paraminophippuric acid). Measure the decay rate of intracamerally injected isotopes.
II. Procedures to investigate the exit of aqueous humor:
Ocular perfusion to lower IOP.
Perilimbic suction cup.
Tonography (conventional outflow/pressure sensitive).
Use of markers (flourescein, nitrotetrazolin, latex spheres, radioactive tracers). Both conventional and uveoscleral outflow routes are measured.
III. Methods to measure the episcleral venous pressure:
Partial to complete collapse of the episcleral veins to cause alteration in the blood flow.
Torsion balance
Pressure chamber (filled with air or saline)
Air jet
Ocular compression
Direct cannulation and measurement by transducer.

The constant-rate procedure (involving injection of a constant volume of perfusate) is infrequently reported. In the perfusion decay test, either a preselected volume of perfusate is injected or a preselected level of IOP is achieved. Once the perfusate has been injected, the time for the IOP to regain the baseline or preexisting level is measured. In many ways, the perfusion techniques are similar to the noninvasive tonography methods. The two-step or two levels of constant perfusion of the anterior chamber, as reported by Bárány and Scotchbrook,[175] has become the most frequently reported procedure. Briefly, the technique includes constant perfusion of the anterior chamber at two different levels of IOP (~2–3 and 8–10 mm Hg above baseline) for several minutes. The total (i.e., perfusion) facility is determined by dividing the difference in perfusion rates between the two levels of IOP by the pressure difference between those two levels. Pseudofacility may account for approximately 0.02 μL/min per mm Hg with this procedure in humans.

A large amount of literature has been published on anterior chamber perfusion in several species. The type of perfusate, duration of perfusion (i.e., the "washout effect"), in vivo and in vitro eye preparations, level of IOP during perfusion, addition of certain enzymes, and drugs (including anesthesia and other substances) may directly influence the perfusion rate. If perfusion of the anterior chamber is planned, the literature should be consulted and carefully evaluated. Also of interest, the rates of perfusion obtained in the animals investigated have correlated closely with the values obtained by the noninvasive tonographic and fluorophotometric methods.

Several methods have been used to demonstrate anatomic routes and quantity of uveoscleral outflow as well as of conventional (i.e., corneoscleral) outflow. The combination of conventional and uveoscleral outflow pathways equals the total volume of aqueous humor that exits the eye (as well as that formed by the ciliary body). The percentages accounted for by uveoscleral outflow range from 4% to 14% in humans, 30% to 65% in nonhuman primates, 3% in the cat, 15% in the dog, and 13% in the rabbit. The horse appears to have a more extensive uveoscleral outflow system, but the volume and percentage of the total outflow system have not been reported. The horse has an extensive angular aqueous plexus as well. Also of interest, topical pilocarpine appears to decrease uveoscleral outflow, perhaps by reducing the potential spaces within the anterior ciliary body, in nonhuman primates, the cat, and the dog. Atropine slightly increases the uveoscleral outflow.

Uveoscleral outflow can be demonstrated using observable tracers measuring 10.0 nm to 1.0 μm in diameter. These tracers include microspheres, fluorescein-labeled dextran, Evans blue, nitro blue tetrazolium, India ink, trypan blue, thorotrast, blue dextran, colored proteins, C-inulin, ferritin, saccharated iron, and yeast cells. As one would anticipate, the smaller diameter (i.e., pore) tracers penetrate the different tissues to greater extents. After perfusion at different levels of IOP and for different time intervals, the eyes (especially the root of the iris, the entire ciliary body, the suprachoroidal space, and choroid, even as far posterior as the optic nerve) are examined by light microscopy, scanning-electron microscopy, and transmission-electron microscopy for these markers. These same methods have also demonstrated the ability of the trabecular endothelium and wandering macrophages to phagocytize particulate material within the outflow pathways. To estimate the amount of uveoscleral outflow (either as μl or %), isotopes are injected into the anterior chamber; the time, amount of the isotope, or both, are standardized. Tracers have included I-albumin,[125] I-diodone (i.e., iodopyracet),[131] I-gamma globulin,[125] H-labeled dextran,[3] and C-inulin.[14] At the conclusion of perfusion, either the ocular tissues are dissected into the different sections and analyzed for radioactivity, or the entire globe is sectioned and the radioactivity of each area is measured by scintillation counter.

Measurements of tracers in the fluids within the intrascleral veins, episcleral veins, and vortex veins are alternate methods of determining the different routes of aqueous humor outflow. These methods require the anatomy of these venous systems to be determined. There may be mixing between the systems, and the tracer concentrations in the anterior chamber and blood must be established at the same time. Atraumatic entry to the intrascleral or episcleral venous system (or both) must be available.

Both invasive and noninvasive techniques may be used to estimate the rate of aqueous humor formation. As one would anticipate, early methods were invasive and essentially measured the dilution of intracamerally injected substances over short periods of time. With the volume of aqueous humor within the anterior and posterior chambers determined and the amount of dilution of the tracer estimated, the total amount of aqueous humor produced per unit of time could be determined. Early studies used ascorbic acid, cysteine, inulin, and other small, measurable substances. Probably the weakest part of these studies was determination of the volumes of both the anterior and posterior chambers. When studying glaucomatous animals (in which these chambers may be altered considerably), these volumes may be difficult to determine. On the basis of these invasive experiments, fluorophotometry was developed as both an experimental and a clinical procedure to noninvasively determine the rate of aqueous humor formation in many species, including humans.

In recent years, fluorophotometry has been employed as a noninvasive method for studying aqueous humor flow dynamics, for evaluating ocular pharmaceutical agents used in treatment of glaucoma, and for determining iris permeability in both healthy and diseased states. Fluorophotometry of the anterior chamber and vitreous can assess the permeability of the blood–retinal barriers in the healthy and diseased eye. Fluorophotometry has been used extensively in humans, nonhuman primates, and the rabbit, but it will become more popular in veterinary medicine as a tool for assessing aqueous flow dynamics and permeability coefficients involved in both normal and abnormal ocular states.[176–179] Critical in the determination of aqueous humor production rates is the anterior and posterior chamber volumes (Table 3.10).[180,181]

Ocular Rigidity

Another concept involved in IOP is ocular rigidity, which is the resistance offered by the fibrous tunics of the eye (i.e., sclera and cornea) to a change in intraocular volume. Ocular rigidity may also be defined as the change in IOP per incremental change in the intraocular volume; this resistance manifests as a change in IOP. Ocular rigidity (k) is determined by Schiotz tonometry, and it estimates the change in volume (open-manometer system) when the instrument is placed on

Table 3.10 Comparative Physical Dimensions of the Eye

	Human (mL)	Cat (mL)	Dog (mL)	Rabbit (mL)	Cow (mL)	Horse (mL)
Anterior chamber	0.3	0.6	0.4	0.3	1.7	2.4
Posterior chamber	0.06	0.3	0.2	0.06	1.5	1.6
Lens volume	0.2	0.3	0.5	0.2	2.2	3.1
Vitreous volume	3.9	2.8	3.2	1.5	20.9	28.8

the cornea as well as after injections of exact volumes or preselected elevations in IOP. This logarithmic relationship between IOP and volume of the globe is:

$$Log\ P_2/P_1 = k(V_2 - V_1)$$

Ocular rigidity is a constant characteristic of each eye, but it also depends on IOP. Hence, the distensibility of each globe varies among individuals as well as with the level of IOP. The dog and cat have greater scleral elasticity than adult humans, so less resistance is offered with indentation tonometry, and buphthalmia occurs more readily with prolonged, increased IOP.[182,183] Manometric studies to develop Schiotz tonometer calibration tables for the dog, rabbit, and cat have not been successful clinically and may be associated with different individual rigidities for the cornea and sclera.[184]

Intraocular Pressure

Clinical tonometric methods of determining IOP are discussed in Chapter 9, and the tonometric values of IOP in normal domestic animals are listed in Table 3.11.[185–204] For the most part, the range of normal IOPs in the different domestic animal species has not been ascertained. One reasonable method that can be applied clinically is to determine the mean IOP and then establish two (95% of the population) or three (99% of the population) standard deviations. In humans, IOP can demonstrate brief or short-term elevations as well as long-term increases. In animals, many of these observations also occur, but others have not been reported (Table 3.12). Diurnal IOP variations generally occur in most animals and humans; in humans, the highest pressure occurs in the morning and the lowest in the afternoon.[205] The circadian IOP cycles in the rabbit, cat, and nonhuman primates are opposite to those in the dog and in humans, with the highest levels of IOP occurring during the day and the lowest pressures at night.[186,187] Results of studies involving both normotensive and glaucomatous Beagles indicate similar intraocular variations to those in humans, with the morning IOP usually being the highest. In the normal dog, the range in IOP varies by 18 to 22 mm Hg daily, whereas in the glaucomatous Beagle, perhaps associated with abnormal IOP control mechanisms, the valleys and peaks in IOP may be 10 to 15 mm Hg different. Seasonal

Table 3.11 Intraocular Pressures in Animals

Species	Tonometer	IOP Results Mean ± SD	Investigator
Dog	Mackay-Marg	15.7 ± 4.2	Miller et al.
	TonoPen	16.7 ± 4.0	
	Mackay-Marg	17.8 ± 0.9 (pm) 21.5 ± 0.8 (am)	Gelatt et al.
Cat	Mackay-Marg		Miller et al.
	TonoPen		
Rabbit	Pneumatonograph		Vareilles et al.
			Smith et al.
Horse	Mackay-Marg		Cohen and Reinke
	Mackay-Marg		McClure et al.
	TonoPen		Kotani et al.
	Mackay-Marg		Trim et al.
	Mackay-Marg		Miller et al.
	TonoPen		
	Mackay-Marg		Smith et al.
	Mackay-Marg		Van der Woerdt et al.
Cow	Mackay-Marg		Gum
			Kotani et al.
Monkey (ketamine)	Pneumatonograph		Bito et al.
	TonoPen		Komaromy et al.
Alligator	TonoPen		Whittaker et al.
Ferrets	TonoPen		Sapienza et al.
Raptors			
Hawks	TonoPen		Stiles et al.
Eagle			
Owl			
Rat	TonoPen		Mermoud et al.

Table 3.12 Short- and Long-Term Fluctuations in Intraocular Pressure

Short-Term	Long-Term
Diurnal changes	Aging
Forced eyelid closure	Race/breed
Contraction of retractor bulbi muscles	Hormones Glucocorticoids
Coughing/Valsalva maneuver	Growth hormone
Abrupt changes in blood pressure	Estrogen
Pulse	Progesterone
Struggling/electroshock	Obesity
Changes in body/head position	Myopia
Succinylcholine	Gender
Acidosis	Season

variations have been reported in humans and the rabbit; IOPs are lower in the summer and higher during the winter months in the rabbit.[187] This has not been substantiated in the dog at this time, but Magrane[206] has suggested that attacks of acute congestive glaucoma in the American Cocker Spaniel occur more often in the period from October through March.

LENS

The second-most powerful refracting surface in the eye is the lens. Like the cornea, it is a transparent tissue without a direct blood supply. Differences between the lens and cornea are their sources of nutrients, solubility of structural proteins, amount of glycoproteins, and physical characteristics responsible for transparency. The lens depends primarily on the surrounding aqueous humor for its metabolic needs. Most of the lenticular proteins are soluble with a small amount of glycoproteins, whereas the cornea consists mostly of insoluble collagen and relatively large numbers of glycoproteins. Transparency of the cornea depends on the precise, regular arrangement of the collagen fibers; transparency of the lens depends primarily on the highly ordered lens cell arrangement as well as on the solubility and physical arrangements of its proteins.

The lens behaves as a very large, single cell or syncytium both biochemically and electrically. The lens consists of approximately 65% water, 35% protein, and small amounts of lipids, inorganic ions, carbohydrates, ascorbic acid, glutathione, and amino acids. Both the anterior and posterior lens capsules are the lens's extracellular matrix and, like the typical epithelial basement membrane, consist of type IV collagen and heparitin sulfate proteoglycan. The thickness of the anterior lens capsule in dogs increases with age.[207] The protein content of the lens is higher than that of any other organ. Protein synthesis ceases with formation of the lens fiber cells, and all the protein changes that occur after this stage are posttranslational modifications. Lens proteins may be divided into soluble proteins, or crystallins, and into insoluble, or albuminoid, proteins. Soluble proteins comprise approximately 85% of the total lens proteins, but this amount decreases with age as the soluble proteins become insoluble. This percentage also varies among species and with the pathophysiologic state of the lens. When the lens becomes cataractous, the level of insoluble proteins increases. Most of the insoluble proteins occur in the lens nucleus, whereas the soluble proteins are concentrated in the lens cortex.[208] The insoluble proteins are associated primarily with membranes of the lens fibers; the soluble proteins consist of the bulk of the refractive fibers of the lens and are considered to be the structural proteins of the lens.

The soluble proteins are divided into four groups on the basis of their molecular size: α-, β-heavy (β_H), β-light (β_L), and γ-crystallins.[209] δ-Crystallin accumulates only in the lenses of birds and reptiles, and it is the first and major crystallin (70%) in the lens of the developing chicken.[210] The combination of α- and γ-crystallin accounts for approximately 50% of the total mammalian lens proteins; the remainder are β-crystallin. There is a high degree of similarity within the β-crystallin lens proteins among the different animal species.[211,212] During aging of the canine lens as well as the lenses of other species, the relative proportions of α- and β_L-crystallin increase and β_H- and γ-crystallin decrease.[208,213–215] These changes appear to be accelerated in age-matched cataractous lenses.[213,214] Proteinase activity in the aging lens has been shown to increase as well. The relationship of proteinase and cataract formation has not been established,[216] but these same enzymes may be important in spontaneous cataract resorption.

The long prismatic lens fiber cells are organized in tightly packed units with interdigitations that appear as a three-dimensional jigsaw puzzle. The interdigitations are specialized gap junctions that join all the lens cells, thus permitting them to act as a syncytium. The cytoskeletal proteins occur in the urea-extractable fraction of the lens proteins. These microfilaments include the usual actin, vimentin, spectrin, and intermediate filaments as well as the lens-specific intermediate filaments such as beaded filaments. Vimentin is the most intermediate filament in the human lens cell, occurring in the epithelial and cortical fiber cells but not the nuclear fiber cells. The functions of the beaded filaments, which consist of two classes (i.e., 90- and 48-kD filaments), probably relate to crystallin packing and density distribution as well as attachment sites for the crystallin molecules.

Lens proteins are immunologically organ-specific, but they are not species-specific. The lens capsule prevents lens proteins from contacting the reticuloendothelial and circulatory systems prenatally, so if lens proteins are released postnatally into the aqueous humor, the body's defense system recognizes them as foreign. The result is production of antibodies against the body's own lens, and a lens-induced uveitis may occur. Lymphocytes and neutrophils may play an important role in lens-induced uveitis following surgery or injury.[217,218] The lens capsule in humans is permeable only to small-molecular-weight proteins (<50,000 kD), which include the low-molecular-weight crystallins.

The lens epithelium is the major site of energy production in the lens. Energy is used for active transport of inorganic ions and amino acids and for protein synthesis. The active transport

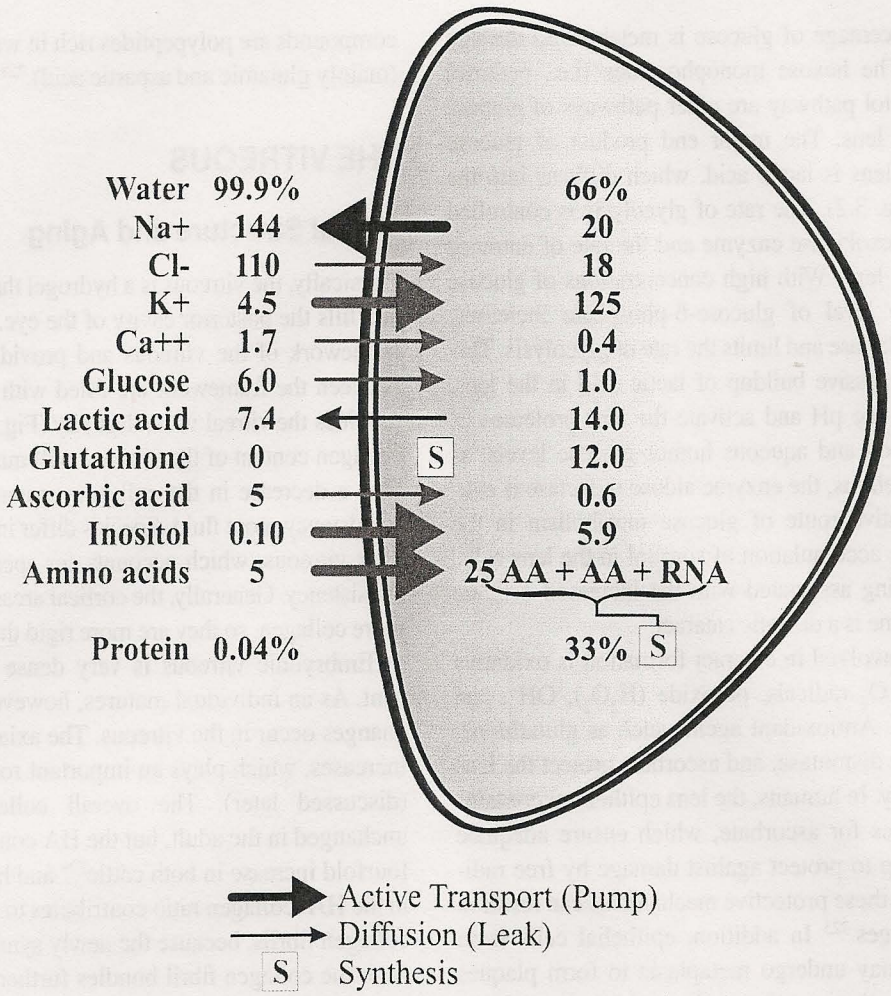

Figure 3.8. Chemical composition of the aqueous humor and lens. Water and protein are expressed as percentages of lens weight. Na^+, Cl^-, K^+, and Ca^{++} ions are expressed in µEq per ml of lens water. Other compounds are expressed in µmol per g of lens weight or µmol per mL of aqueous humor. *AA*, amino acids; *RNa*, ribonucleic acid. (Modified with permission from Cotlier E. The lens. In: Moses RA, Hart WM, eds. *Adler's Physiology of the Eye.* 8th ed. St. Louis: CV Mosby, 1987, pp 268–290.)

of cations and amino acids involves the action of Na^+-K^+–activated ATPase to maintain high K^+ ion and amino acid concentrations and low Na^+ ion, Cl^- ion, and water concentrations within the lens. The movement of water is passive and occurs with the active cation transport. As the Na^+ ion is transported from the lens, K^+ is transported into the lens (Fig. 3.8) in a manner similar to that of the transport mechanism in red blood cells. A deficiency of lens Na^+,K^+-ATPase results in cataracts in mice because of breakdown of the pump mechanism.[219] The lens epithelium of birds and reptiles has a thickened annular pad, which may modify the transport mechanisms in these species.

Glutathione and ascorbic acid are present at high levels in the lens. Exceptions are the dog, rabbit, and guinea pig, which have lower levels of ascorbic acid in the lens than in the aqueous humor.[180] The function of lenticular ascorbic acid most likely relates to the oxidation–reduction reactions or is coupled to glutathione metabolism.[220] Glutathione is a tripeptide of L-glutamate, L-cysteine, and glycine synthesized in the lens. Its function is to furnish sulfhydryl groups for the lens proteins, thereby preserving their solubility, and for the Na^+,K^+-ATPase reaction, thereby maintaining the transport "pumps." Other biologic functions include participation in amino acid transport with γ-glutamyl transpeptidase and as a substrate for glutathione peroxidase, which destroys cytotoxic lipid hydroperoxides. In a normal lens, glutathione is predominantly in the reduced form (GSH); the level of the oxidized form of glutathione is only 2.1% to 2.6% that of the reduced GSH. Levels of both the reduced and the oxidized forms of glutathione are decreased in cataract formation, except in advanced cataract patients, in whom the level of the oxidized form is 9% that of the reduced form.[221]

The lens capsule functions as a semipermeable membrane that prevents only large molecules from passing through. It has only a mechanical function in maintaining the shape of the lens in association with accommodation and in providing for the attachment of the zonules. A contractile system appears to exist in the lens epithelial and cortical cells, and though its physiologic function is not completely understood, it appears to stabilize the shape of the lens.[222]

The source of energy for the lens is glucose, which diffuses from the aqueous humor. Energy is derived from anaerobic glycolysis and is used for active cation transport and protein synthesis. Oxygen is not necessary for normal lens metabolism,

though a small percentage of glucose is metabolized through the Krebs cycle. The hexose monophosphate (i.e., pentose) shunt and the sorbitol pathway are other pathways of glucose metabolism in the lens. The major end product of glucose metabolism in the lens is lactic acid, which diffuses into the aqueous humor (Fig. 3.2). The rate of glycolysis is controlled by the amount of hexokinase enzyme and the rate of entrance by glucose into the lens. With high concentrations of glucose (>175 mg/dL), the level of glucose-6-phosphate increases, which inhibits hexokinase and limits the rate of glycolysis. This process prevents excessive buildup of lactic acid in the lens, which would lower the pH and activate the lens proteases.[223] With very high blood and aqueous humor glucose levels, as occur in diabetes mellitus, the enzyme aldose reductase is activated as an alternative route of glucose metabolism in the lens.[224] The result is accumulation of sorbitol in the lens cells, which causes swelling associated with the increased osmotic pressure. The outcome is a diabetic cataract.

A major factor involved in cataract formation is oxidative damage caused by O_2 radicals, peroxide (H_2O_2), OH^-, and ultraviolet radiation. Antioxidant agents such as glutathione, catalase, superoxide dismutase, and ascorbate protect the lens from oxidative injury. In humans, the lens epithelium contains transporter molecules for ascorbate, which ensure adequate metabolism and help to protect against damage by free radicals. A deficiency in these protective mechanisms can result in cataractogenic changes.[225] In addition, epithelial cells from cataractous lenses may undergo metaplasia to form plaques composed of fibrous tissue and ectopic membrane produced by epithelial cells.[226]

Removal of the cataractous lens leaves the aphakic eye hypermetropic. The image in an aphakic eye is out of focus, right-side up, reversed (i.e., like a mirror image), and enlarged. With one lens removed, binocular or stereoscopic vision is impaired. The loss of a lens or lenses, however, does not appear clinically to be a significant problem for domestic animals. This sudden adaptation to an aphakic condition may be explained, at least in part, by an observation made in the cat. If a cat's eye is surgically rotated approximately 90 degrees, the cat can discriminate horizontal from vertical visual cues without needing time for orientation. The exact anatomic site of this immediate adjustment is not known.[227] Basic differences between human and animal lenticular physiology are growth rate, hydration, accommodative capacity, color, and concentration of fluorescent compounds (Table 3.13). The fluorescent compounds are polypeptides rich in water-soluble amino acids (mainly glutamic and aspartic acid).[228]

THE VITREOUS

Vitreal Structure and Aging

Physically, the vitreous is a hydrogel that consists of 98% water and fills the posterior cavity of the eye. Collagen makes up the framework of the vitreous and provides its plasticity. Spaces between the framework are filled with hyaluronic acid, which provides the vitreal viscoelasticity (Fig. 3.9). An increase in the collagen content of the vitreous will make it more solid, or gel-like; a decrease in the collagen content will make the vitreal consistency more fluid. Species differ in the collagen content of their vitreous, which accounts for species variation in vitreal consistency. Generally, the cortical areas of the vitreous contain more collagen, so they are more rigid than other portions.

Embryonic vitreous is very dense and therefore translucent. As an individual matures, however, important structural changes occur in the vitreous. The axial length of the vitreous increases, which plays an important role in growth of the eye (discussed later). The overall collagen content remains unchanged in the adult, but the HA concentration undergoes a fourfold increase in both cattle[229] and humans.[230] This change in the HA–collagen ratio contributes to greater dispersal of the collagen fibrils, because the newly synthesized HA molecules push the collagen fibril bundles further apart, thus increasing the optical clarity of the vitreous. These changes in HA–collagen interactions as well as in the GAG contents of the vitreous do not cease on reaching adulthood but continue throughout life, and they are believed to be responsible for the vitreal liquefaction observed as part of the aging process in some species.[231] In humans, rheologic (i.e., the gel-liquid state of the vitreous) changes begin in the central vitreous at 5 years of age and continue throughout life, so that in the geriatric patient, more than 50% of the vitreous is eventually liquefied.[232] As liquefaction progresses, the collagen bundles are packed into the remaining gel fraction, whereas HA molecules are redistributed to the liquid fraction. A common complication of this progressive liquefaction is separation of the posterior vitreous cortex from the retinal inner limiting membrane. This detachment, which predisposes to retinal tears, has been implicated as a risk factor in rhegmatogenous retinal detachment in the dog.[232]

Table 3.13 Comparative Physiology of the Lens in Primates and Lower Animals

Species	Growth Rate	Hydration State	Accommodation	Color	Fluorescent Polypeptides
Humans, nonhuman primates	Slowly decreases throughout life	Maintained at 65% water throughout life	Present	Pale Yellow	Present
Lower mammals (cow, rabbit, rat)	Fast in early stages of life; little to no growth during the late stages of life	Dehydrated with aging (35–50% water)	Little to none	Colorless	Absent

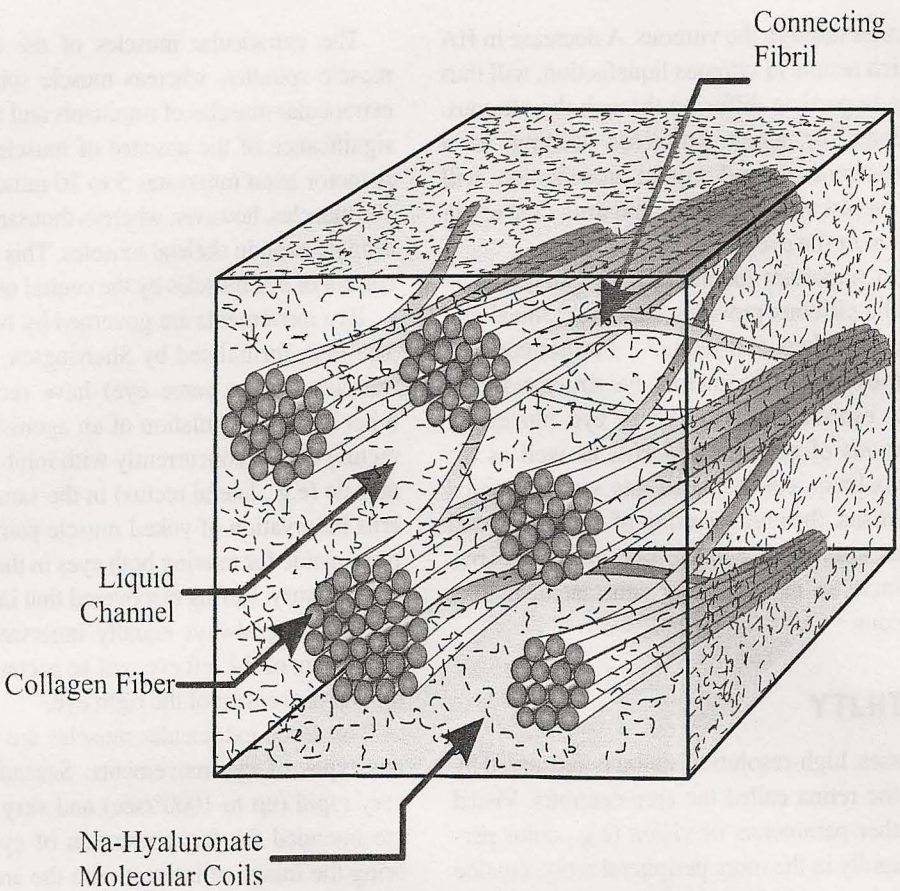

Figure 3.9. Schematic of the vitreal ultrastructure. Parallel collagen fibrils are packed into bundles that aggregate and ultimately form visible fibers. Hyaluronic acid and water molecules fill the interfibrillar spaces. (Modified with permission from Sebag J, Balazs EA. Morphology and ultrastructure of human vitreous fibers. *Invest Ophthalmol Vis Sci* 1989;30:1867–1873).

Vitreous Functions

The vitreous is the largest structure in the eye, occupying approximately 80% of the globe.[231] Though it is frequently ignored by both researchers and clinicians, the vitreous contributes to the development, optics, structure, physiology, and metabolism of the eye.

The vitreous plays an important role in growth of the eye by contributing to the increase in globe size. Inserting a drainage tube into the vitreous cavity of chicken embryos lowers intravitreal pressure and stops growth of the eye,[234] and vitrectomy of rabbit eyes has a similar inhibitory effect.[235] On the other hand, vitreal elongation will cause an increase in the axial length of the globe. This lengthens the path of the incoming light, thus providing for greater light refraction. In some aquatic species, such as goldfish, this increased vitreal refractivity is a physiologic mechanism that compensates for the loss of refractive power when the cornea is submerged in water.[236] In terrestrial species, the increased refraction by the vitreous may lead to myopia. Vitreal elongation resulting in axial myopia has been induced through visual deprivation in a number of species, including nonhuman primates,[237] chickens,[238] and the cat.[239] This elongation of the vitreous is affected by the synthesis of collagen. Synthesis, molecular reconfiguration, and hydration of HA molecules likewise change the volume of the vitreous and hence of the eye.[231] It has been suggested that in addition to its refractive role, the vitreous has functions in the process of vision. In humans, there is evidence the vitreous functions in accommodation by moving anteriorly against the lens, thus changing the lens diameter and the axial length.[240]

Several anatomic factors contribute to the optical clarity of the vitreous. These include the small diameter of the vitreal collagen fibers, their wide dispersion in the vitreal cavity, and the largely acellular makeup of the vitreous.[231] Another important factor in optical clarity is the blood–vitreous barrier; it is believed HA acts as a barrier that prevents diffusion of macromolecules and cells into the vitreous[241] except in cases of trauma or cortex disruption. Inflammatory responses,[241] neovascularization,[242] and collagenase activity[243] are likewise suppressed in the vitreous. As a result of these anatomic and physiologic properties, the vitreous transmits 90% of light at wavelengths between 300 and 1400 nm.[244]

The vitreous also plays an important role in ocular metabolism. It serves as a storage site for retinal metabolites, including glycogen,[245] amino acids,[246] and potassium.[247] Retinal and lenticular waste products, including lactic acid[231] and free radicals,[248] are also taken up by the vitreous, which thus serves to protect the lens and retina from toxic compounds. In the cow, these molecules (and water) can diffuse across the vitreous through pores that are 400 nm in diameter.[249] HA serves as a barrier to this diffusion process[250]; therefore, molecule size and HA concentration are two of the primary factors affecting

diffusion of molecules through the vitreous. A decrease in HA concentration, which results in vitreous liquefaction, will thus lead to an increase in particle diffusion through the vitreous. Therefore, pathologic or aging processes leading to a decreased HA concentration and vitreal liquefaction will affect the nutrient supply, waste removal, and drug delivery in the posterior segment of the eye.

Perhaps the most important function of the vitreous is its mechanical role. The vitreous provides both mechanical and structural support to the lens and retina.[251] Furthermore, its viscoelastic properties protect the internal eye structures from trauma and stress, especially during rapid eye movement (REM). Concentrations of collagen and HA, as well as the nature of their cross-links, contribute to this viscoelasticity. For example, in humans, the concentration of vitreal HA and collagen is twice as high as that in the pig, and this corresponds to a 60% increase in the Spring constant of human versus porcine vitreous.[252]

OCULAR MOTILITY

As Chapter 4 discusses, high-resolution vision is subserved by a small section of the retina called the area centralis. Visual acuity as well as other parameters of vision (e.g., color perception) decrease rapidly in the more peripheral retina outside the area centralis. To keep an object of interest in the center of the visual field so that its image will stimulate the area centralis (or fovea), vertebrates rely on the actions of seven extraocular muscles.

Domestic species have four rectus extraocular muscles—dorsal (or superior), ventral (inferior), nasal (medial), and temporal (lateral)—all of which move the eye in those respective directions. All four are innervated by the oculomotor nerve (CN III), except for the lateral rectus muscle, which is innervated by the abducens nerve (CN VI). Two oblique muscles are additionally present. The ventral oblique, which is innervated by the oculomotor nerve, pulls the ventral part of the eyeball both nasally and dorsally; the dorsal oblique, which is innervated by the trochlear nerve (CN IV), pulls the dorsal part of the eyeball both nasally and ventrally. The retractor bulbi, which is not present in all species, is innervated by the abducens nerve.

The oculomotor nerve is usually thought to be strictly a motor nerve. In sheep, afferent nerves enter the brainstem through the oculomotor nerve.[253] These afferent nerves carry impulses (especially from the conjunctiva) to the brainstem, where the input influences the anterior body and neck muscles. The cell bodies of these afferents are located in the trigeminal semilunar ganglion.

The extraocular muscles of the eyes of birds are similar to those of mammals, but there are no retractor bulbi muscles. Birds make obvious use of their upper body and neck muscles to obtain a spatial perspective of objects. The shapes of eyeballs also vary considerably among different species of birds. The eyeballs are relatively large, and the two eyes weigh almost as much as the brain.[254]

The extraocular muscles of the dog, cat, and bird lack muscle spindles, whereas muscle spindles are present in the extraocular muscles of ruminants and the pig.[255] The functional significance of the absence of muscle spindles is not known. A motor axon innervates 5 to 10 muscle fibers in the extrinsic eye muscles, however, whereas thousands may be innervated by a single axon in skeletal muscles. This situation allows for finer control of eye muscles by the central nervous system.

Eye movements are governed by two fundamental laws.[256] The first, formulated by Sherrington, states that antagonistic muscles (in the same eye) have reciprocal innervation. In other words, stimulation of an agonistic muscle (e.g., medial rectus) occurs concurrently with inhibition of the antagonistic muscle (e.g., lateral rectus) in the same eye. The second governs innervation of yoked muscle pairs (i.e., the two muscles responsible for moving both eyes in the same direction). In the 19th century, Hering discovered that in mammals, yoked muscle pairs are always equally innervated; therefore, a lateral movement of the left eye will be accompanied by an identical, medial movement of the right eye.

The seven extraocular muscles are responsible for numerous types of eye movements. Saccadic eye movements are very rapid (up to 1000°/sec) and very brief (<0.1 sec). They are intended for fast correction of eye position and rapidly bring the image of interest onto the area centralis. Thus, saccadic movements are used mostly when tracking a fast-moving object or to begin pursuit of a formerly stationary object. Once the image of the object has been "captured" by the area centralis, smooth pursuit eye movements are used to match the speed of the object and to maintain its image in the area centralis. Required minor corrections and adjustments are, again, executed by saccadic movements. This combination of alternating rapid and slow eye movements is called the optokinetic nystagmus (discussed later), which can be used to track objects moving at speeds under 100°/sec.[257] Saccades and smooth pursuit constitute the two types of conjugate (or version) eye movements in which the two eyes move together without changing the angle between them.

Vergence eye movements, in contrast, change the angle of intersection between the two eyes. These can be either convergent (i.e., increasing the angle between the visual axes to focus on a near target) or divergent (i.e., decreasing the angle between the visual axes to focus on a far target). Vergence movements are usually slow (<21°/sec), and they have two roles. The first is to aid in visualizing nearby objects, which is a process that combines convergent eye movement, accommodation, and miosis. The second is to resolve any small misalignments between the two visual axes that otherwise may result in a disparity between the retinal images of the two eyes.

The afferent stimulus for all these eye movements is the visualized object. If the head is moving, however, eye movement is controlled by a different afferent limb, which allows for a faster tracking response. In this case, the stimulus is the acceleration of the head. Linear acceleration stimulates the otoliths of the vestibular apparatus, and angular acceleration stimulates the hair cells of the semicircular canals. These

organs provide the afferent input for the vestibulo-ocular reflex (VOR), the neuronal pathways of which are discussed in detail in Chapter 29. The reflex produces immediate, but slow, eye movements, which compensate for movement of the head and help to keep the image stabilized on the area centralis. Thus, if the head moves up, the VOR moves the eyes down, and if the head moves to the left, the VOR moves the eyes to the right. It appears that the cat makes greater use than the dog of the VOR arc to follow moving objects. Comparison of the dog and cat when visually following a bouncing ball is most dramatic.

Nystagmus is usually characterized by a rapid eyeball movement in one direction and a slow movement in the opposite direction. Nystagmus can be either horizontal or vertical. The types of nystagmus are categorized on the basis of their causes, and they include optokinetic, rotatory, postrotatory, ocular, caloric, galvanic, anesthetic, brainstem, cerebellar, and vestibular.

In optokinetic nystagmus, the eyelids must be open, and the fast phase is opposite in direction to the movement of the visual stimuli. However, the visual stimuli can be moving with the head stationary, or the head and body can be moving with the visual stimuli stationary. In the latter case, the fast phase is in the same direction as the movement of the head. This can be used as an objective means of detecting vision in animals. Optokinetic nystagmus usually occurs in the horizontal plane and is less well substantiated in the vertical plane. In rotatory nystagmus, the fast phase is in the same direction as the rotation of the head. In postrotatory nystagmus, which is seen after rotation stops, the fast phase is opposite the direction of the rotation of the head. Postrotatory nystagmus lasts approximately 10 seconds after rotation stops. In rotatory and postrotatory nystagmus, the stimuli are acceleration and deceleration, respectively. At a constant rate of rotation, nystagmus does not occur if the lids are closed. Optokinetic nystagmus occurs if the eyelids are open. Ocular nystagmus is associated with congenital blindness and has a wandering or searching movement of the eyes rather than the distinct fast and slow phases. Caloric nystagmus is elicited by placing warm (48°C) water or cold (18°C) water in one ear canal. Caloric nystagmus is elicited by expansion or contraction of the endolymph in the semicircular canals adjacent to the ear canal.[241] Cold water in one ear usually causes nystagmus to the opposite side; warm water causes nystagmus to the same side. Galvanic nystagmus results from galvanic (i.e., direct current) stimulation of the vestibular nerve. Nystagmus during induction of general anesthesia is the result of decreased inhibition of the brain centers that initiate nystagmus; brainstem, cerebellar, and vestibular nystagmus are caused by pathologic changes in the respective areas. Components of optokinetic, rotatory, and postrotatory nystagmus reflexes are shown in Table 3.14. By convention, the direction of nystagmus is indicated by the fast phase.

There are several other types of eye movements. During certain stages of sleep, REM occurs, usually in bursts lasting from 5 to 60 minutes. Numerous REM bursts, which are traditionally associated with dreaming, may occur during a single sleep. Sleep patterns vary with age, however. Discrete eye movement bursts during certain stages of sleep are infrequent in newborn kittens, but after 3 weeks of age, adult patterns of sleep develop.[259] Another important class of movements are those that maintain eye position while gazing at a stationary target.[256] These movements are required to maintain fixation on the object even when both the observer and the target are immobile. Though slow drifts are also used for this purpose, position maintenance movements are usually characterized by their low magnitude (several minutes/arc) and high frequency (1–50 per second). Hence, they have also been called microsaccades or micronystagmus.

Kittens are born with a divergent strabismus that is evident following eyelid opening at approximately 12 to 14 days postnatally. Normal interocular alignment, which depends on visual stimuli, develops during the second postnatal month.[260] Crossed eyes (i.e., convergent strabismus), which is commonly seen in adult Siamese cats and certain albino mammals, results from a genetic neuroanatomic defect in the primary visual pathway that involves the retinogeniculate and the geniculocortical projections.[261,262]

The oculocardiac reflex may be stimulated by pressure on the globe, tension on the extraocular muscles or iris, or increased

Table 3.14 Components of Optokinetic, Rotatory, and Postrotatory Nystagmus

	Optokinetic	Rotatory and Postrotatory
Stimulus	Visual	Movement of endolymph in the semicircular canals
Receptors	Photoreceptors (rods and cones)	Hair cells of the cupula
Afferent pathway	Optic nerve to occipital visual cortex and frontal visual cortex	Vestibular nerve (CN VIII) to vestibular nuclei and cerebellum
Efferent pathway	Corticotectal and corticotegmental tract to oculomotor; abducens, and trochlear nerve via MLF[a]	Vestibular nuclei to oculomotor, abducens, and trochlear nerve via MLF
Effectors	Extraocular muscles (except retractor oculi)	Extraocular muscles (except retractor oculi)
Response	Saccadic eye movements (slow phase followed by a fast phase)	Saccadic eye movements (slow phase followed by a fast phase)

MLF, medial longitudinal fasciculus.
[a]The corticotectal tract mediates eye movements in nonorbital directions; the corticotegmental tract mediates horizontal eye movements via parameridian pontine reticular formation.

intraorbital pressure caused by injection, hemorrhage, or a foreign body. The oculocardiac reflex has been reported in humans, the dog, cat, horse, rabbit, mice, and a cockatiel.[263–268] Sensory stimulation of the eye and orbital areas results in stimulation of the vagal nucleus in the brainstem, thus causing a reflexive slowing of the heart. The afferent arc of the reflex involves the sensory branches of the ophthalmic division of the trigeminal nerve (CN V) to its sensory nucleus. The efferent arc is via the vagus nerve (CN X) to the heart. The most common effect of the reflex is bradycardia, but other clinically significant effects are cardiac arrest and ventricular fibrillation. Endotracheal intubation may cause vagal stimulation as well, resulting in similar reflexive cardiac alterations.[269] This reflex may be evoked in conscious or lightly anesthetized animals. In the latter, hypoxia probably facilitates the reflex, which will induce fatigue after repeated stimulation. In the dog, as the IOP increases, the heart rate may also increase, thus indicating the possibility of an intraocular-sympathetic-cardiac reflex as well as a trigeminovagal reflex.[270]

REFERENCES

1. Carrington SD, Bedford PGC, Guillon JP, Woodwards EG. Polarized light biomicroscopic observations on the precorneal film. 1. The normal tear film of the dog. *J Small Anim Pract* 1987; 28: 605–622.
2. Blakemore C, Cummings RM. Eye-opening in kittens. *Vis Res* 1975; 15:1417–1418.
3. Marshall JM. Vertebrate smooth muscle. In: Mountcastle VB, ed. *Medical Physiology.* Vol. 1. St. Louis: CV Mosby, 1974.
4. Crawford ML, Marc RE. Light transmission of cat and monkey eyelids. *Vis Res* 1976;16: 323–324.
5. Gum GG. Physiology of the eye. In: Gelatt KN, ed. *Veterinary Ophthalmology.* 2nd ed. Philadelphia: Lea & Febiger, 1991.
6. Holly FJ, Lemp MA. Tear physiology and dry eyes. *Surv Ophthalmol* 1977; 22: 69–87.
7. Davidson H, Kuonen V. The tear film and ocular mucins. *Vet Ophthalmol* 2004 Mar–Apr; 7(2): 71–77.
8. Hicks SJ, Corfield AP, Kaswan RL, Hirsh S, Stern M, Bara J, Carrington SD. Biochemical analysis of ocular surface mucin abnormalities in dry eye: The canine model. *Exp Eye Res* 1998; 67: 709–718.
9. McLaughlin SA, Brightman AH 2d, Helper LC, Primm ND, Brown MG, Greeley S. Effect of removal of lacrimal and third eyelid glands on Schirmer tear test results in cats. *J Am Vet Med Assoc* 1988; 193: 820–822.
10. Johnson BW, Whiteley HE, McLaughlin SA. Effects of inflammation and aqueous tear film deficiency on conjunctival morphology and ocular mucus composition in cats. *Am J Vet Res* 1990; 51: 820–824.
11. Saito A, Izumisawa Y, et al. The effect of third eyelid gland removal on the ocular surface of dogs. *Vet Ophthalmol* 2001 Mar; 4(1): 13–18.
12. Marts BS, Bryan GM, Prieuo DJ. Schirmer tear test measurements and lysozyme concentration of equine tears. *J Equine Med Surg* 1977; 1: 427–432.
13. Vestre WA, et al. Decreased tear production associated with general anesthesia in the dog. *J Am Vet Med Assoc* 1979; 174: 1006–1007.
14. Ludders JW, Heavner JE. Effect of atropine on tear formation in anesthetized dogs. *J Am Vet Med Assoc* 1979; 175: 585–586.
15. Arnett BD, et al. Effect of atropine sulfate on tear production in the cat when used with ketamine hydrochloride and acetylpromazine maleate. *J Am Vet Med Assoc* 1984; 185: 214–215.
16. Moore CP, Wilsman NJ, et al. Density and distribution of canine conjunctival goblet cells. *Invest Ophthalmol Vis Sci* 1987 Dec; 28(12): 1925–1932.
17. Davidson H, Kuonen V. The tear film and ocular mucins. *Vet Ophthalmol* 2004 Mar–Apr; 7(2): 71–77.
18. Van Haeringen NJ. Clinical biochemistry of tears. *Surv Ophthalmol* 1981; 26: 84–96.
19. Hicks SJ, Carrington SD. Demonstration of discrete and membrane-bound ocular mucins in the dog. *Exp Eye Res* 1997 Apr; 64(4): 597–607.
20. Mishima S. Some physiological aspects of the pre-corneal tear film. *Arch Ophthalmol* 1965; 73: 233–241.
21. Carrington SD, Bedford PGC, Guillon JP, Woodward EG. Polarized light biomicroscopic observations on the pre-corneal tear film. 2. Keratoconjunctivitis sicca in the dog. *J Small Anim Pract* 1987; 28: 671–679.
22. Carrington SD, Bedford PGC, Guillon JP, Woodward EG. Polarized light biomicroscopic observations on the pre-corneal tear film. 3. The normal tear film of the cat. *J Small Anim Pract* 1987; 28: 821–826.
23. Magrane WG, Dorr G. unpublished data, 1973.
24. Maidment DC, et al. Electrolyte and protein levels in bovine tears. *Br Vet J* 1985; 141: 169–173.
25. Mircheff AK. Lacrimal fluid and electrolyte secretion: A review. *Curr Eye Res* 1989; 8: 607–617.
26. Daubs JG. A comparison of enzyme reagent strip tests for lacrimal glucose. *Am J Optom Physiol Opt* 1976; 53: 232–235.
27. Milder B, Weil BA. *The Lacrimal System.* Norwalk, CT: Appleton-Century-Crofts, 1983.
28. Roberts SR, Erickson OF. Dog tear secretion and tear proteins. *J Small Anim Pract* 1962; 3: 1.
29. Erickson OF, Feeney L, McEwen WK. Filter-paper electrophoresis of tears. II. Animal tears and the presence of a "slow-moving lysozyme." *Arch Ophthalmol* 1956; 55: 800–806.
30. Luchter FJ, Gurisatti C. Queratoconjunctivitis de los bovinos. *Rev Med Vet* 1974; 55: 139.
31. Bonavida B, Sapse AT, Sercarz EE. Rabbit tear proteins. I. Detection and quantitation of lysozyme in nonstimulated tears. *Invest Ophthalmol* 1968; 7: 435–440.
32. Elsby JM, Wilson H. Lacrimal secretion in the cat. *Br J Pharm Chemother* 1967; 29: 29.
33. Powell CC, Martin CL. Distribution of cholinergic and adrenergic nerve fibers in the lacrimal glands of dogs. *Am J Vet Res* 1989; 50: 2084–2088.
34. Dartt DA. Signal transduction and control of lacrimal gland protein secretion: A review. *Curr Eye Res* 1989; 8: 619–636.
35. Farris RL, Stuchell RN, Mandel ID. Basal and reflex human tear analysis. I. Physical measurements: Osmolarity, basal volumes, and reflex flow rate. *Ophthalmol* 1981; 88: 852–857.
36. Stuchell RN, Farris RL, Mandel ID. Basal and reflex human tear analysis. II. Chemical analysis: Lactoferrin and lysozyme. *Ophthalmol* 1981; 88: 858–861.
37. Gelatt KN, Peiffer RL Jr, Erickson JL, Gum GG. Evaluation of tear formation in the dog, using a modification of the Schirmer tear test. *J Am Vet Med Assoc* 1975; 166: 368–370.

38. Berger SL, King VL. The fluctuation of tear production in the dog. *J Am Anim Hosp Assoc* 1998; 34: 79–83.
39. Francois J, Neetens A. Tear flow in man. *Am J Ophthalmol* 1973; 76: 351–358.
40. Jones LT, Marquis MM, Vincent NJ. Lacrimal function. *Am J Ophthalmol* 1972; 73: 658–659.
41. Barrett PM, Scagliotti RH, Merideth RE, Jackson PA, Alarcon, FL. Absolute corneal sensitivity and corneal trigeminal nerve anatomy in normal dogs. *Prog Vet Comp Ophthalmol* 1991; 1: 245–254.
42. Marfurt C, Murphy C, Florczak J. Morphology and neurochemistry of canine corneal innervation. *Invest Ophthalmol Vis Sci* 2001 Sep; 42(10): 2242–2251.
43. Bynke G, Hakason R, Sundler F. Is substance P necessary for corneal nociception? *Eur J Pharmacol* 1984; 101: 253–258.
44. Keen P, Tullo AB, Blyth WA, Hill TJ. Substance P in the mouse cornea; Effects of chemical and surgical denervation. *Neurosci Lett* 1982; 29: 231–235.
45. Waltman SR, Hart WM. The cornea. In: Moses RA, Hart WM, eds. *Adler's Physiology of the Eye.* 8th ed. St. Louis; CV Mosby, 1987.
46. Woo HM, Bentley E, Campbell SF, Marfurt CF, Murphy CJ. Nerve growth factor and corneal wound healing in dogs. *Exp Eye Res* 2005 May; 80(5): 633–642.
47. Jester JV, Moller-Pedersen T, Huang J, Sax CM, Kays WT, Cavangh HD, Petroll WM, Piatigorsky J. The cellular basis of corneal transparency; Evidence for "corneal crystallins." *J Cell Sci* 1999 Mar; 112: 613–622.
48. Tripathi RC, Raja SC, Tripathi BJ. Prospects for epidermal growth factor in the management of corneal disorders. *Surg Ophthalmol* 1990; 34: 457–462.
49. Cotlier E. The cornea. In: Moses RA, ed. *Adler's Physiology of the Eye.* Vol. 6. St. Louis: CV Mosby, 1975.
50. Zubay G. *Biochemistry.* New York: Macmillan, 1988.
51. Maurice DM. The physics of corneal transparency. In: Duke-Elder S, ed. *Transparency of the Cornea.* Oxford: Blackwell Scientific Publications, 1960.
52. Forrester JV, Dick AD, McMenamin P, Lee WR. *The Eye: Basic Sciences in Practice.* Philadelphia: WB Saunders, 1996.
53. Montiani-Ferreira F, Petersen-Jones S, Cassotis N, Ramsey DT, Gearhart P, Cardoso F. Early postnatal development of central corneal thickness in dogs. *Vet Ophthalmol* 2003; 6: 19–22.
54. Funderburgh JL, Funderburgh ML, Rodrigues MM, Krachmer JH, Conrad GW. Altered antigenicity of keratan sulfate proteoglycan in selected corneal diseases. *Invest Ophthalmol Vis Sci* 1990; 31: 419–428.
55. Kennedy JK, White CA. *Bioactive Carbohydrates in Chemistry, Biochemistry and Biology.* New York: Ellis Horwood, 1983.
56. Bentley E. Spontaneous chronic corneal epithelial defects in dogs: A review. *J Am Anim Hosp Assoc* 2005; 41: 158–165.
57. Schoenwald RD, Deshpande GS, Rethwisch DG, Barfknecht CF. Penetration into the anterior chamber via the conjunctival/scleral pathway. *J Ocul Pharm Ther* 1997; 13: 41–59.
58. Gelatt KN, Mackay EO, Gelatt JK, Stengard-Ollies K, Aza J. Effects on intraocular pressure and pupil size in glaucomatous Beagles after topical pilocarpine instilled with standard (pH 5) and buffer-tip (pH 7) droptainer. *J Ocul Pharm Ther* 1997; 13: 95–104.
59. Burstein NL, Anderson JA. Review: Corneal penetration and ocular bioavailability of drugs. *J Ocul Pharmacol* 1985; 1: 309–326.
60. Shell JW. Pharmacokinetics topically applied ophthalmic drugs. *Surg Ophthalmol* 1982; 26: 207–218.
61. Benson H. Permeability of the cornea to topically applied drugs. *Arch Ophthalmol* 1974; 91: 313–327.
62. Shields MB. *Textbook of Glaucoma.* 3rd ed. Baltimore: Williams & Wilkins, 1992: 431–488.
63. Zimmerman TJ. Topical ophthalmic beta blockers: A comparative review. *J Ocul Pharmacol* 1993; 9: 373–384.
64. Bartlett JD, Jaanus SD. *Clinical Ocular Pharmacology.* 2nd ed. London: Butterworth-Heinemann, 1989: 69–148.
65. Colasabti BK, Trotter RR. Effects of selective beta-1 and beta-2 adrenocepter agonists and antagonists on intraocular pressure in the cat. *Invest Ophthalmol Vis Sci* 1981; 20: 69–76.
66. Macri FJ, Cevario SJ. A pharmacodynamic study of the inhibitory effects of L-norepinephrine, L-epinephrine, and D,L-isoproterenol on aqueous humor formation in the enucleated arterially perfused cat eye. *Invest Ophthalmol* 1974; 13: 392–395.
67. Neufield AH, Sears MI. Cyclic AMP in ocular tissues of the rabbit, monkey, and human. *Invest Ophthalmol* 1974; 13: 475–477.
68. Vareilles P, Silverstone D, Plazonnet B, Le Douarec J, Sears ML, Stone CA. Comparison of the effects of timolol and other adrenergic agents on intraocular pressure in the rabbit. *Invest Ophthalmol Vis Sci* 1977; 16: 987–996.
69. Potter DE, Rowland JM. Adrenergic drugs and intraocular pressure: Effects of selective ß-adrenergic agonists. *Exp Eye Res* 1978; 27: 615–625.
70. Yoshitomi T, Yushi I. Double reciprocal innervations in dog iris sphincter and dilator muscles. *Invest Ophthalmol Vis Sci* 1986; 27: 83–91.
71. Lee HK, Wang SC. Mechanism of morphine-induced miosis in the dog. *J Pharmacol Exp Ther* 1975; 193: 415–431.
72. Wallenstein MC, Wang SC. Mechanism of morphine-induced mydriasis in the cat. *Am J Physiol* 1979; 236: R292–296.
73. Yoshitomi T, Yushi I. Effects of indomethacin and prostaglandins on the dog iris sphincter and dilator muscles. *Invest Ophthalmol Vis Sci* 1988; 29: 127–132.
74. Piccone M, Littzi J, Krupin T, Stone RA, Davis M, Wax MB. Effects of neuropeptide Y on the isolated rabbit iris dilator muscles. *Invest Ophthalmol Vis Sci* 1988; 29: 330–332.
75. Jones BR, Studdert VP. Horner's syndrome in the dog and cat as an aid to diagnosis. *Aust Vet J* 1975; 51: 329–332.
76. Toyoshima K, Kawana E, Sakai H. On the neuronal origin of the afferents to the ciliary ganglion in cat. *Brain Res.* 1980 3; 185: 67–76.
77. Loewy AD, Araujo JC, Kerr FW. Pupillodilator pathways in the brain stem of the cat: Anatomical and electrophysiological identification of a central autonomic pathway. *Brain Res* 1973; 60: 65–91.
78. Ogidigben MJ, Potter DE. Comparative effects of alpha-2 and DA-2 agonists on intraocular pressure in pigmented and non-pigmented rabbits. *J Ocul Pharmacol* 1993; 9: 187–199.
79. Murphy CJ, Howland HC. On the gekko pupil and Scheiner's disc. *Vision Res* 1986; 26(5): 815–817.
80. Bellhorn RW, Bellhorn MS. The avian pecten. I. Fluorescein permeability. *Ophthalmol Res* 1975; 7: 1.
81. Mikaelian I, Paillet I, Williams D. Comparative use of various mydriatic drugs in kestrels (*Falco tinnunculus*). *Am J Vet Res* 1994; 55: 270–272.
82. Wingstrand KG, Munk O. The pectin oculi of the pigeon with regard to its function. *Biol Skr* 1965; 14: 5.

83. Brach V. The effect of intraocular ablation of the pecten oculi of the chicken. *Invest Ophthalmol* 1975; 14: 166–168.
84. Bill A. The uveal venous pressure. *Arch Ophthalmol* 1963; 69: 780–782.
85. Alm A, Bill A. The oxygen supply to the retina. II. Effects of high intraocular pressure and of increased arterial carbon dioxide tension on uveal and retinal blood flow in cats. *Acta Physiol Scand* 1972; 84: 306–319.
86. Jalnpol LM, Axelrod A, Tessler H. Pathways of the eye's responses to topical nitrogen mustard. *Invest Ophthalmol* 1976; 15: 486–489.
87. Regnier AM, Dossin O, Cutzach EE, Gelatt KN. Comparative effects of two formulations of indomethacin eyedrops on the paracentesis-induced inflammatory response of the canine eye. *Vet Comp Ophthalmol* 1996; 5: 242–246.
88. Green K, Peterson CA, Diddiqui A. Ocular blood flow after experimental alkali burns and prostaglandin administration. *Arch Ophthalmol* 1985; 103: 569–571.
89. Bili A. A method for quantitative determination of blood flow through the cat uvea. *Arch Ophthalmol* 1962; 67: 156–162.
90. Freidman E, Smith TR. Estimation of retinal blood flow in animals. *Invest Ophthalmol* 1965; 4: 1122–1128.
91. Bill A. Blood circulation and fluid dynamics in the eye. *Physiol Rev* 1975; 55: 383–417.
92. Yu DY, Alder VA, Cringle SJ, Brown MJ. Choroidal blood flow measured in the dog eye in vivo and in vitro by local hydrogen clearance polarography: Evalidation of a technique and response to raised intraocular pressure. *Exp Eye Res* 1988; 46: 289–303.
93. Mann RM, Riva CE, Stone RA, Barnes GE, Cranstoun SD. Nitric oxide and choroidal blood flow regulation. *Invest Ophthalmol Vis Sci* 1995; 36: 925–930.
94. Kiel JW, Shepherd AP. Autoregulation of choroidal blood flow in the rabbit. *Invest Ophthalmol Vis Sci* 1992; 33: 2399–2410.
95. Attariwala A, Giebs C, Glucksberg MR. The influence of elevated intraocular pressure on vascular pressures in the cat retina. *Invest Ophthalmol Vis Sci* 1994; 35: 1019–1025.
96. Forster BA, et al. Adrenergic alpha, and alpha$_2$ binding sites are present in bovine retinal blood vessels. *Invest Ophthalmol Vis Sci* 1987; 28: 1741–1746.
97. Hoste AM, et al. Effect of alpha-1 and beta agonists on contraction of bovine retinal resistance arteries in vitro. *Invest Ophthalmol Vis Sci* 1989; 30: 44–50.
98. Laatikairen LT. Regional blood flow in the cat retina. *Exp Eye Res* 1976; 23: 47–56.
99. Feke GT, Tagawa H, Deupree DM, Goger DG, Sebag J, Weiter JJ. Blood flow in the normal human retina. *Invest Ophthalmol Vis Sci* 1989; 30: 58–65.
100. Pillunat LE, Stodtmeister R, Wilmanns I, Christ T. Autoregulation of ocular blood flow during changes in intraocular pressure. *Graefe's Arch Clin Exp Ophthalmol* 1985; 223: 219–223.
101. Brown SA, Jampol LM. New concepts of regulation of retinal vessel tone. *Arch Ophthalmol* 1996; 114: 199–204.
102. Shonat RD, Wilson DF, Riva CE, Cranstoun SD. Effect of acute increases in intraocular pressure on intravascular optic nerve head oxygen tension in cats. *Invest Ophthalmol Vis Sci* 1992; 33: 3174–3180.
103. Weinstein JM, Duckrow RB, Beard D, Brennant RW. Regional optic nerve blood flow and its autoregulation. *Invest Ophthalmol Vis Sci* 1983; 24: 1559–1565.
104. Morgan WH, Yu DY, Cooper RL, Alder VA, Cringle SJ, Constable IJ. The influence of cerebrospinal fluid pressure on the lamina cribrosa tissue pressure gradient. *Invest Ophthalmol Vis Sci* 1995; 36: 1163–1172.
105. Bellhorn RW. Permeability of blood-ocular barriers of neonatal and adult cats to fluorescein-labeled dextrans of selected molecular sizes. *Invest Ophthalmol Vis Sci* 1981; 21: 282–290.
106. Rodriquez-Peralta L. The blood aqueous barrier in five species. *Am J Ophthalmol* 1975; 80: 713–725.
107. Elgin SS. Arteriovenous oxygen difference across the uveal tract of the dog eye. *Invest Ophthalmol* 1964; 3: 417–426.
108. Freddo TF, Sacks-Wilner R. Interendothelial junctions of the rabbit iris vasculature in anterior uveitis. *Invest Ophthalmol Vis Sci* 1989; 30: 1104–1111.
109. Bito LZ. The physiology and pathophysiology of intraocular fluids. *Exp Eye Res* 1977; 25(suppl): 273–289.
110. Neufeld AH, Sears ML. Prostaglandin and eye. *Prostaglandins* 1973; 4: 157–175.
111. Regnier A, Whitley RD, Benard P, Bonnefoi M. Effect of flunixin meglumine on the breakdown of the blood–aqueous barrier following paracentesis in the canine eye. *J Ocul Pharmacol* 1986; 2: 165–170.
112. Bhattacherjee P. The role of arachidonate metabolites in ocular inflammation. In: Bito LZ, Stjernschantz J, eds. *The Ocular Effects of Prostaglandins and Other Eicosamids.* New York: Alan R. Liss, 1989.
113. Murphy CJ, Glasser A, Howland HC. The anatomy of the ciliary region of the chicken eye. *Invest Ophthalmol Vis Sci* 1995; 36: 889–896.
114. Glasser A, Howland HC. A history of studies of visual accommodation in birds. *Q Rev Biol* 1996; 71: 475–509.
115. Bito LZ, Davson H, Levin E, Murray M, Snider N. The relationship between the concentration of amino acids in the ocular fluids and blood plasma of dogs. *Exp Eye Res* 1965; 4: 374–380.
116. Cole DF. Comparative aspects of the intra-ocular fluids. In: Davson H, Graham LT, eds. *The Eye,* Vol 5, New York, Academic Press, 1974.
117. Tulamo R, et al. Determination of concentration of hyaluronate in equine serum. *Am J Vet Res* 1990; 51: 740–742.
118. Caprioli J. The ciliary epithelia and aqueous humor. In: Moses RA, Hart WM, eds. *Adler's Physiology of the Eye.* St. Louis: CV Mosby, 1987.
119. McLaughlin BG, McLaughlin PS. Equine vitreous humor chemical concentrations: Correlation with serum concentrations and postmortem changes with time and temperature. *Can J Vet Res* 1988; 52: 476–480.
120. Blogg JR, Coles EH. Aqueous humor proteins—A review. *Vet Bull* 1970; 40: 347.
121. Graymore CN. *Biochemistry of the Eye.* New York: Academic Press, 1970.
122. Duke-Elder S. The aqueous humor. In: *System of Ophthalmology. Vol. IV. Physiology of the Eye.* St. Louis: CV Mosby, 1968.
123. Davson H, Weld CB. Studies on the aqueous humor. *Am J Physiol* 1941; 134: 1.
124. Dickinson JC, Durham DG, Hamilton PB. Ion exchange chromatography of free amino acids in aqueous fluids and lens of the human eye. *Invest Ophthalmol Vis Sci* 1968; 7: 551–563.
125. Reddy VN, Chakrapani B, Lim CP. Amino acid transport across blood–aqueous barrier of mammalian species. *Exp Eye Res* 1977; 25: 555–562.

126. Davson H. The intraocular fluids. In: Davson H, ed. *The Eye,* Vol. 1, 2nd ed. New York: Academic Press, 1969.
127. Riley MV. Intraocular dynamics of lactic acid in the rabbit. *Invest Ophthalmol Vis Sci* 1972; 11: 600–607.
128. Chu TC, Candia OA. Active transport of ascorbate across the isolated rabbit ciliary epithelium. *Invest Ophthalmol Vis Sci* 1988; 29: 594–599.
129. DiMattio J. A comparative study of ascorbic acid entry into aqueous and vitreous humors of the rat and guinea pig. *Invest Ophthalmol Vis Sci* 1989; 30: 2320–2331.
130. Cole DF. Secretion of the aqueous humor. *Exp Eye Res* 1977; 25(suppl): 161–176.
131. Pederson JE, Green K. Aqueous humor dynamics: Experimental studies. *Exp Eye Res* 1973; 15: 277–297.
132. Bonting SL, Becker B. Studies on Na^+-K^+ activated adenosine triphosphatase. *Invest Ophthalmol* 1964; 3: 523–533.
133. Garg LC, Oppelt WW. The effect of ovabain and acetazolamide on transport of sodium and chloride from plasma to aqueous humor. *J Pharm Exp Ther* 1970; 175: 237–247.
134. Maren TH. The development of topical carbonic anhydrase inhibitors. *J Glaucoma* 1995; 4: 49–62.
135. Higginbotham EJ. Topical carbonic anhydrase inhibitors. *Ophthalmol Clin North Am* 1989.
136. Macri FJ, Cevareo SJ. Ciliary ganglion stimulation. II. Neurogenic intraocular pathway for excitatory effects on aqueous humor production and outflow. *Invest Ophthalmol* 1975; 14: 471–476.
137. Green K. Physiology and pharmacology of aqueous humor inflow. *Surg Ophthalmol* 1984; 29: 208–214.
138. Caprioli J, Sears M, Bausher L, Gregory D, Mead A. Forskolin lowers intraocular pressure by reducing aqueous inflow. *Invest Ophthalmol Vis Sci* 1984; 25: 268–277.
139. Samuelson DA, Gum GG, Gelatt KN, Barrie KP. Aqueous outflow in the beagle: Unconventional outflow, using different-sized micropheres. *Am J Vet Res* 1985; 46: 242–248.
140. Cruise LJ, McClure R. Posterior pathway for aqueous humor drainage in the dog. *Am J Vet Res* 1981; 42: 992–995.
141. Talusan ED, Schwartz B. Episcleral venous pressure: Differences between normal, ocular hypertensive, and primary open angle glaucoma. *Arch Ophthalmol* 1981; 99: 824–828.
142. Maepea O, Bill A. The pressure in the episcleral veins, Schlemm's canal and the trabecular meshwork in monkeys: Effects of changes in intraocular pressure. *Exp Eye Res* 1989; 49: 645–663.
143. Tripathi RC, Tripathi BJ. The mechanism of aqueous outflow in primates, lower mammals and birds. A comparative study. *Exp Eye Res* 1973; 17: 393–394.
144. Gelatt KN, Gum GG, Merideth RE, Bromberg N. Episcleral venous pressure in normotensive and glaucomatous Beagles. *Invest Ophthalmol Vis Sci* 1982; 23: 131–135.
145. Rohen JW, Funk RHW. Functional morphology of the episcleral vasculature in rabbits and dogs: Presence of arteriovenous anastomoses. *J Glaucoma* 1994; 3: 51–57.
146. Funk RHW, Rohen JW. Scanning electron microscopic study of episcleral arteriovenous anastomoses in the owl and cynomolgus monkey. *Curr Eye Res* 1995; 15: 321–327.
147. Beneyto-Martin P, Fernandez-Vila PC, Perez TM. Determination of the pseudofacility by fluorophotometry in the human eye. *Int Ophthalmol* 1995–1996; 19: 219–223.
148. Glaster J. Response of the intraocular pressure to diencephalic stimulation. *Br J Ophthalmol* 1960; 44: 649–664.
149. Niederer W, Richardson BP, Donatsch P. Hormonal control of aqueous humor production. *Exp Eye Res* 1975; 20: 329–340.
150. Bill A. Formation and drainage of aqueous humor in cats. *Exp Eye Res* 1966; 5: 185–190.
151. Barrie KP, Gum GG, Samuelson DA, Gelatt KN. Quantitation of uveoscleral outflow in normotensive and glaucomatous beagles by ^{3}H-labeled dextran. *Am J Vet Res* 1985; 46: 84–88.
152. Gelatt KN, Gum GG, Williams LW, Barrie KP. Uveoscleral flow of aqueous humor in the normal dog. *Am J Vet Res* 1979; 40: 845–848.
153. Emi K, Pederson JE, Toris CB. Hydrostatic pressure of the suprachoroidal space. *Invest Ophthalmol Vis Sci* 1989; 30: 233–238.
154. Gelatt KN, Brooks DE, Samuelson DA. Comparative glaucomatology. Part I. Spontaneous models. *J Glaucoma* 1997: 1998; 7: 187–201.
155. Tripathi RC. Comparative physiology and anatomy of the aqueous outflow pathway. In: Davson H, Graham L, eds. *Biochemistry of the Eye.* Vol. 5. New York: Academic Press, 1974.
156. Tripathi RC, Tripathi BJ. The mechanism of aqueous outflow in lower mammals. *Exp Eye Res* 1972; 14;:73–79.
157. Samuelson DA, Gelatt KN. Aqueous outflow in the beagle. I. Postnatal development of the indocorneal angle: Pectinate ligament and uveal trabecular meshwork. *Curr Eye Res* 1984; 3: 783–794.
158. Johnson M, Johnson DH, Kamm RD, DeKater AW, Epstein DL. The filtration characteristics of the aqueous outflow system. *Exp Eye Res* 1990; 50: 407–418.
159. Samuelson DA, Gelatt KN, Gum GG. Kinetics of phagocytosis in the normal canine iridocorneal angle. *Am J Vet Res* 1984; 45: 2359–2366.
160. Samuelson D, Plummer C, Lewis P, Gelatt K. Schwalbe line's cell in the normal and glaucomatous dog. *Vet Ophthalmol* 2001; 4: 47–53.
161. Samples JR. Glycoproteins and glaucoma. *J Glaucoma* 1993; 2: 1–2.
162. Knepper PA, Goossens W, Palmberg PF. Glycosaminoglycan stratification of the juxtacanalicular tissue in normal and primary open angle glaucoma. *Invest Ophthalmol Vis Sci* 1996; 37: 2414–2425.
163. Knepper PA, McLone DG. Glycosaminoglycan and outflow pathways of the eye and brain. *Pediatr Neurosci* 1985–1986; 12: 240–251.
164. Samuelson DA, Gelatt KN. Aqueous outflow in the Beagle. II. Postnatal morphologic development of the iridocorneal angle: Corneoscleral trabecular meshwork and angular aqueous plexus. *Curr Eye Res* 1984; 3: 795–807.
165. Knepper PA, Breen M, Weinstein HG, Blacik LJ. Intraocular pressure and glycosaminoglycan distribution in the rabbit eye: Effect of age and dexamethasone. *Exp Eye Res* 1978; 27: 567–575.
166. Gum GG. Glycosaminoglycans in the iridocorneal angle of the normal and glaucomatous beagle. PhD thesis. University of Florida, 1986.
167. Gum GG, Gelatt KN, Knepper PA. The isolation for a GAG?ase-resistant material in the trabecular meshwork of glaucomatous Beagles (abstract). *Proc 8th Int Cong Eye Res* 1988: 34.
168. Gum GG, Wanigatunga S, Wagener KB. ^{13}NMR spectroscopy of a GAG?ase resistant material isolated from the trabecular meshwork of the glaucomatous Beagle (abstract). *Invest Ophthalmol Vis Sci* 1989; 30(suppl): 355.

169. Gum GG, Gelatt KN, Knepper PA. Histochemical localization of glycosaminoglycans in the aqueous outflow pathways in normal Beagles and Beagles with inherited glaucomas. *Prog Vet Comp Ophthalmol* 1993; 3: 52–57.
170. Huang W, Jaroszewski J, Ortego J, Escribano J, Coca-Prados M. Expression of the TIGR gene in the iris, ciliary body, and trabecular meshwork of the human eye. *Ophthalmic Genet* 2000; 21: 155–169.
171. Fingert JH, Stone EM, Sheffield VC, Alward WL. Myocilin glaucoma. *Surv Ophthalmol* 2002; 47: 547–561.
172. Ohlmann A, Tamm ER. The role of myocilin in the pathogenesis of primary open-angle glaucoma. *Ophthalmology* 2002; 99: 672–677.
173. Sapir-Pichhadze R, Blumenthal EZ. Steroid induced glaucoma. *Harefuah* 2003; 142: 137–140.
174. Shepard AR, Jacobson N, Sui R, Steely HT, Lotery AJ, Stone EM, Clark AF. Characterization of rabbit myocilin: Implications for human myocilin glycosylation and signal peptide usage. *BMC Genet* 2003; 4: 5.
175. Bárány EH, Scotchbrook S. Influence of testicular hyaluronidase on the resistance to flow through the angle of the anterior chamber. *Acta Physiol Scand* 1954; 30: 240–248.
176. McLaren JW, Brubaker RF. A scanning ocular spectrofluorophotometer. *Invest Ophthalmol Vis Sci* 1988; 29: 1285–1293.
177. Bartels SP. Aqueous humor flow measured with fluorophotometery in timolol-treated primates. *Invest Ophthalmol Vis Sci* 1988; 29: 1498–1504.
178. Kurnik RT, Burde RM, Becker B. Breakdown of the blood–aqueous barrier in the rabbit eye by infrared radiation. *Invest Ophthalmol Vis Sci* 1989; 30: 717–722.
179. Brubaker RF. Flow of aqueous humor in humans. *Invest Ophthalmol Vis Sci* 1991; 32: 3145–3166.
180. McLaren JW, Trocme SD, Reif S, Brubaker RF. Rate of flow of aqueous humor determined from measurements of aqueous fluid. *Invest Ophthalmol Vis Sci* 1990; 31: 339–346.
181. Toris CB, Yablonski ME, Wang YL, Hayaski M. Prostaglandin A_2 increases uveoscleral outflow and trabecular outflow facility in the cat. *Exp Eye Res* 1995; 61: 649–657.
182. Wyman M. Applied anatomy and physiology of the anterior chamber angle. *Vet Clin North Am* 1973; 3: 439–451.
183. Peiffer RL, Gum GG, Gelatt KN. Pressure-volume relationships of the normal canine eye. *Am J Vet Res* 1978; 39: 1927–1931.
184. Gelatt KN, Gum GG. Comparisons of anterior chamber manometric recordings (mm Hg) and Schiotz tonometer scale-units in normal and glaucomatous dogs. *Anim Eye Res* 1995; 14: 49–58.
185. Gum GG. Unpublished data, 1990.
186. Miller PE, Pickett JP, Majors LJ, Kurzman ID. Clinical comparison of the Mackay-Marg and TonoPen applanation tonometers in the dog. *Prog Vet Comp Ophthalmol* 1991; 1: 171–176.
187. Gelatt KN, Gum GG, Barrie KP, Williams LW. Diurnal variation in intraocular pressure in normotensive and glaucomatous Beagles. *Glaucoma* 1981; 3: 121–125.
188. Miller PE, Pickett JP, Majors LJ, Kurzman ID. Evaluation of two applanation tonometers in cats. *Am J Vet Res* 1991; 52: 1917–1921.
189. Vareilles P, Conquet P, Ledonarec JC. A method for the routine extraocular pressure (IOP) measurement in the rabbit: Range of IOP variation in this species. *Exp Eye Res* 1977; 24: 369–375.
190. Komaromy AM, Brooks DE, Kubilis PS, Dawson WW, Sapp HL, Nelson G, Collins BR, Sherwood MB. Diurnal intraocular pressure curves in healthy Rheses macaques (*Macaca mulatta*) and rheses macaques with normotensive and hypertensive primary open-angle glaucoma. *J Glaucoma* 1998; 7: 128–131.
191. Smith SD, Geogory DS. A circadian rhythm of aqueous flow underlies the circadian rhythm of IOP in NZW rabbits. *Invest Ophthalmol Vis Sci* 1989; 30: 775–778.
192. Cohen CM, Reinke DA. Equine tonometry. *J Am Vet Med Assoc* 1970; 156: 1884–1887.
193. McClure JR, Gelatt KN, Gum GG, Manning JP. The effect of parenteral acepromazine and xylazine on intraocular pressure in the horse. *Vet Med Small Anim Clin* 1976; 71: 1727–1730.
194. Kotani T, Tuzuki K, Izumisawa Y, Yamashita K, Oukuma N, Yamura S. Which are the optimal tonometers for different animal species? Horses. *Anim Eye Res* 1993; 12: 55–61.
195. Trim CM, Colbern GT, Martin CL. Effect of xylazine and ketamine on intraocular pressure in horses. *Vet Rec* 1985; 117: 442–443.
196. Miller PE, Pickett JP, Majors LJ. Evaluation of two applanation tonometers in horses. *Am J Vet Res* 1990; 51: 935–937.
197. Smith PJ, Gum GG, Whitley RD, Samuelson DA, Brooks DE, Garcia-Sanchez GA. Tonometric and tonographic studies in the normal pony eye. *Equine Vet J Ophthalmol Suppl* 1990; 10: 36–38.
198. Van Der Woerdt A, Gilger BC, Wilkie DA, Strauch SM. Effect of auriculopalpebral nerve block and intravenous administration of xylazine on intraocular pressure and corneal thickness in horses. *Am J Vet Res* 1995; 56: 155–158.
199. Kotani T, Tuzuki K, Oukuma N, Tamura S, Izumishawa Y, Yamashita K. Which are the optimal tonometers for different animal species? Cattle. *Anim Eye Res* 1993; 12: 47–53.
200. Bito LZ, Merritt SQ, DeRousseau CJ. Intraocular pressure of Rhesus monkeys (*Macaca mulatta*). *Invest Ophthalmol Vis Sci* 1979; 18: 785–793.
201. Whittaker CJ, Heaton-Jones TG, Kubilis PS, et al. Intraocular pressure variation associated with body length in young American alligators (*Alligator mississippiensis*). *Am J Vet Res* 1995; 56: 1380–1383.
202. Sapienza JS, Porcher D, Collins BR, Gum GG, Brooks DE. Tonometry in clinically normal ferrets (*Mustela putorius furo*). *Prog Vet Comp Ophthalmol* 1991; 1: 291–294.
203. Stiles J, Buyukmihci NC, Farver TB. Tonometry of normal eyes in raptors. *Am J Vet Res* 1994; 55: 477–479.
204. Mermoud A, Baerveldt G, Minckler DS, Lee MB, Rao NA. Intraocular pressure in Lewis rat. *Invest Ophthalmol Vis Sci* 1994; 35: 2455–2460.
205. Shiose Y. Intraocular pressure: New perspectives. *Surv Ophthalmol* 1990; 34: 413–435.
206. Magrane WG. Canine glaucoma. MS thesis. Graduate School of Medicine, University of Pennsylvania, 1956.
207. Bernays ME, Peiffer RL. Morphologic alterations in the anterior lens capsule of canine eyes with cataracts. *Am J Vet Res* 2000; 61: 1517–1519.
208. Harding JJ, Dilley KJ. Structural proteins of the mammalian lens: A review with emphasis on changes in development, aging and cataract. *Exp Eye Res* 1976; 22: 1–73.
209. Bloemendal H, Herbrink P. Growing insight into the structure of ß-crystallin. *Ophthalmol Res* 1974; 6: 81.
210. Das GC, Piatigorsky J. Promoter activity of the two chicken δ-crystalline genes in the Hela cell extract. *Curr Eye Res* 1988; 7: 331.

211. Ramaekers FCS, van Kan PL, Bloemendal H. A comparative study of ß-crystallins from ungulates, whale and dog. *Ophthalmic Res* 1979; 11: 143.
212. Piatigorsky J. Lens differentiation in vertebrates. A review of cellular and molecular features. *Differentiation* 1981; 19: 134–153.
213. Daniel WJ, Noonan NE, Gelatt KN. Isolation and characterization of the crystallins of the normal and cataractous canine lens. *Curr Eye Res* 1984; 3: 911–922.
214. Piatigorsky J, Kador PF, Kinoshita JH. Differential synthesis and degradation of protein in the hereditary Philly mouse cataract. *Exp Eye Res* 1980; 30: 69–78.
215. Zigler JS Jr, Carper DA, Kinoshita JH. Changes in lens crystallins during cataract development in the Philly mouse. *Ophthalmic Res* 1981; 13: 237.
216. Srivastava OP, Srivastava K. Human lens membrane proteinase: Purification and age-related distributional changes in the water-soluble and insoluble protein fractions. *Exp Eye Res* 1989; 48: 161–175.
217. McMahon MS, Weiss JS, Riedel KG, Albert DM. Clinically unsuspected phacoanaphylaxis after extracapsular cataract extraction with intraocular lens implantation. *Br J Ophthalmol* 1985; 69: 836–840.
218. Simpson W, Wild G, Figg K, Milford-Ward A. Human T-cell mediated response to homologous lens antigen. *Exp Eye Res* 1989; 48: 49–54.
219. Kinoshita JH. Mechanisms initiating cataract formation. *Invest Ophthalmol* 1974; 13: 713–724.
220. Berger J, Shepard D, Morrow F, Sadowski J, Haire T, Taylor A. Reduced and total ascorbate in guinea pig eye tissues in response to dietary intake. *Curr Eye Res* 1988; 7: 681–686.
221. Gelatt KN, Bruss M, DeCostanza SM, Noonan NE, Das ND, Wolf ED. Reduced oxidized, and protein-bound glutathione concentrations in normal and cataractous lenses in the dog. *Am J Vet Res* 1982; 43: 1215–1217.
222. Rafferty NS, Scholz DL, Goldberg M, Lewyckyj M. Immunocytochemical evidence for an actinomyosin system in lens epithelial cells. *Exp Eye Res* 1990; 51: 591–600.
223. Kuck JF Jr. Metabolism of the lens. In: Graymore CN, ed. *Biochemistry of the Eye.* New York: Academic Press, 1970.
224. Sato S, Kador PF. Rat lens aldehyde reductase. *Invest Ophthalmol Vis Sci* 1989; 30: 1618–1622.
225. Andley UP, Clark BA. Generation of oxidants in the near-UV photooxidation of human lens α-crystalline. *Invest Ophthalmol Vis Sci* 1989; 30: 706–713.
226. Bernays ME, Peiffer RL. Morphologic alterations in the anterior lens capsule of canine eyes with cataracts. *Am J Vet Res* 2000; 61: 1517–1519.
227. Mitchell DE, Giffin F, Muir D. Behavioral compensation of cats after early rotation of one eye. *Exp Brain Res* 1976; 25: 109–113.
228. Garcia-Castineiras S, Dillon J, Spector A. Non-tryptophan fluorescence associated with human lens protein: Apparent complexity and isolation of bitryosine and anthranilic acid. *Exp Eye Res* 1978; 26: 461–476.
229. Balazs EA, Laurent TC, Larent UBG. Studies on the structure of the vitreous body. VI. Biochemical changes during development. *J Biol Chem* 1959; 234: 422–430.
230. Balazs EA, Denlinger JL. Aging changes in the vitreous. In: *Aging and Human Visual Function.* New York: Alan R. Liss, 1982.
231. Sebag J. *The Vitreous: Structure, Function and Pathology.* New York: Springer-Verlag, 1989.
232. Balazs EA. Function anatomy of vitreous. In: Jakobies FA, ed. *Ocular Anatomy, Embryology and Tetralogy.* Philadelphia: Harper and Row, 1982.
233. Hendrix DV, Nasisse MP, Cowen P, Davidson MG. Clinical signs, concurrent diseases, and risk factors associated with retinal detachment in dogs. *Prog Vet Comp Ophthalmol* 1993; 3: 87–91.
234. Coulombre AJ. The role of intraocular pressure in the development of the chicken eye. *J Exp Zool* 1956; 133: 211.
235. Arciniegas A, Amaya LE, Ruiz LA. Myopia—A bioengineering approach. *Ann Ophthalmol* 1980; 12: 805.
236. Seltner RL, Weerheim JA, Sivak JG. Role of the lens and vitreous humor in the refractive properties of the eyes of three strains of goldfish. *Vis Res* 1989; 29: 681–685.
237. Raviola E, Wiesel TN. An animal model of myopia. *N Engl J Med* 1985; 312: 1609–1615.
238. Hodos W, Fitzke FW, Hayes BP, Holden AL. Experimental myopia in chicks: Ocular refraction by electroretinography. *Invest Ophthalmol Vis Sci* 1985; 26: 1423–1430.
239. Belkin M, Yinon U, Rose L, Reisert I. The effect of visual environment on refractive error of cats. *Doc Ophthalmol* 19677; 42: 433–437.
240. Coleman DJ. Unified model for accommodative mechanism. *Am J Ophthalmol* 1970; 69: 1063–1079.
241. Hultsch E. Peripheral uveitis in the owl monkey-experimental model. *Mod Probl Ophthalmol* 1977; 18: 247–251.
242. Jacobson B, Dorfman T, Basu PK, Hasany SM. Inhibition of vascular endothelial cell growth and trypsin activity by vitreous. *Exp Eye Res* 1985; 41: 581–595.
243. Lutty GA, Thompson DC, Gallup JY. Vitreous—An inhibitor of retinal extract-induced neovascularization. *Invest Ophthalmol Vis Sci* 1983; 24: 52–56.
244. Boettner EA, Wolter JR. Transmission of the ocular media. *Invest Ophthalmol* 1962; 1: 776–783.
245. Weiss H. The carbohydrate reserve in the vitreous body and retina of the rabbit eye during and after pressure ischaemia and insulin hypoglycemia. *Ophthalmol Res* 1972; 3: 360–371.
246. Reddy VN. Dynamics of transport systems in the eye. *Invest Ophthalmol Vis Sci* 1979; 18: 1000–1008.
247. Newman EA. Regional specialization of retinal glial cell membrane. *Nature* 1984; 309: 155–157.
248. Ueno N, Sebag J, Hirokawa H, Chakrabarti B. Effects of visible light irradiation on vitreous structure in the presence of a photosensitizer. *Exp Eye Res* 1987; 44: 863–870.
249. Fatt I. Hydraulic flow conductivity of the vitreous gel. *Invest Ophthalmol Vis Sci* 1977; 16: 565–568.
250. Foulds WS, Allan D, Moseley H, Kyle PM. Effect of intravitreal hyaluronidase on the clearance of tritiated water from the vitreous to the choroid. *Br J Ophthalmol* 1985; 69: 52–532.
251. Schmidt GM, Coulter DB. Physiology of the eye. In: Gelatt KN, ed. *Veterinary Ophthalmology.* 1st ed. Philadelphia: Lea & Febiger, 1981: 129–159.
252. Weber H, Landwehr G, Kilp H, Neubauer H. Mechanical properties of the vitreous in pig and human donor eyes. *Ophthalmol Res* 1982; 14: 335–343.
253. Manni E, Bortolami R, Pettorossi VE, Callegari E. Trigeminal efferent fibers in the trunk of the oculomotor nerve of lambs. *Exp Neurol* 1976; 50: 465–476.
254. Martin GR. An owl's eye: Schematic optics and visual performance in *Strix alucol. J Comp Physiol* 1982; 145: 341.

255. Harker DW. The structure and innervation of sheep superior rectus and levater palpebrae extraocular muscles. *Invest Ophthalmol* 1972; 11: 970–979.
256. Alpern M. Eye movements and strabismus. In: Barlow HB, Mollon JD, ed. *The Senses.* Cambridge: Cambridge University Press, 1982: 201–211.
257. Feldon SE, Burde RM. The oculomotor system. In: Hart WM Jr, ed. *Adler's Physiology of the Eye.* St. Louis: Mosby–Year Book, 1992: 134–183.
258. Rose WR. Otitis externa: The caloric test. *Vet Med Small Anim Clin* 1977; 72: 63–67.
259. Hoppenbrouwers T, Sterman MB. Development of sleep state patterns in the kitten. *Exp Neurol* 1975; 49: 822–838.
260. Sherman SM. Development of interocular alignment in cats. *Brain Res* 1972; 37: 187–203.
261. Shatz CJ, Levay S. Siamese cat: Altered connections of visual cortex. *Sci* 1979; 204: 328–330.
262. Robertson TW, Hickey TL, Guillery RW. Development of the dorsal lateral geniculate nucleus in normal and visually deprived Siamese cats. *J Comp Neurol* 1980; 191: 573–579.
263. Rhode J, et al. A study of the electrocardiographic alterations. *Am J Ophthalmol* 1958; 46: 367–382.
264. Walsh FB, Hoyt WF. Sensory innervation of the eye and orbit. In: *Clinical Neuro-ophthalmology.* 3rd ed. Baltimore: Williams & Wilkins, 1969.
265. Clutton RE, et al. Significance of the oculocardiac reflex during ophthalmic surgery in the dog. *J Small Anim Pract* 1988; 29: 573.
266. Panneton WM, Burton H. Projections from the paratrigeminal nucleus and the medullary spinal dorsal horns to the peribrachial area in the cat. *Neuroscience* 1985; 15: 779–797.
267. Short CE, Rebhun WC. Complications caused by the oculocardiac reflex during anesthesia in a foal. *J Am Vet Med Assoc* 1980: 176: 630–631.
268. Pipo RA, Broadstone RV, Murphy CJ. Lethal oculocardiac reflex in a cockatiel. *Vet Comp Ophthalmol* 1996; 6: 27–29.
269. Brunson DB. Anesthesia in ophthalmic surgery. Symposium on Ophthalmology. *Vet Clin North Am Small Anim Pract* 1980; 10: 481–495.
270. Howard DR, Sawyer DC. Electroretinography of acute hypoxic and increased intraocular pressure status in the dog. *Am J Vet Res* 1975; 36: 81–84.

Chapter 4

Optics and Physiology of Vision

Ron Ofri

INTRODUCTION

The aim of this chapter is to describe the physical, anatomical, and physiological aspects of the process of vision. With this aim in mind, the chapter has been divided into three parts. The first part is devoted to visual optics. It covers the physical changes that light undergoes during its passage through the various structures of the eye until it reaches the retina. Some readers may wonder at the amount of space that has been devoted to optical aberrations in the eye and to species we do not normally see in our clinic, such as fish and the penguin. However, understanding how various species cope with these aberrations, or with their unique habitat, is fundamental to the understanding of visual optics.

The second part of this chapter describes what happens once light reaches the retina. This section is devoted to the neuronal processes of vision and describes the generation, processing, and propagation of the visual signal in the retina, visual pathways, and cortex. The final part of this chapter is devoted to visual perception. It describes how the optical and neuronal processes covered in the first two sections combine into a visual sensation, enabling the detection of movement, details, and color that make vision such a rich experience.

VISUAL OPTICS

Physical Optics

Light

The nature of light has long been a subject of controversy. Light has alternately been described as a wave (first proposed by Huygens in 1678) or as photon particles (first proposed by Newton in 1672). These descriptions are not mutually exclusive. Quantum optics, first proposed by Planck, use both models to explain the dual nature of light and its interaction with matter. Both models also are applicable in the eye: the wave theory explains the physical changes light undergoes during its passage through the eye, and the particle theory explains the energy transformation that occurs when light strikes the photoreceptors.

Light behaves as a wave as it passes through transparent media such as air, vacuum, or the visual axis of the eye. Much like a wave of water, a wave of light has two principal characteristics (Fig. 4.1). Its amplitude, A, is the maximum value of the field generated by the propagating wave; it determines the wave's intensity. The wavelength, λ, is the distance between adjacent wave crests; it determines the wave's location in the electromagnetic spectrum. As Figure 4.2 shows, light, which is the visible portion of the electromagnetic spectrum, occupies a small fraction of that spectrum, which ranges from cosmic and gamma rays ($\lambda < 10^{-10}$ meters) to power transmission ($\lambda > 10^{5}$ meters). In humans, visible light normally ranges in wavelength from 390 (i.e., deep blue) to 760 (i.e., deep red) nm.[1] However, additional wavelengths, outside the 390 to 760 nm spectrum, can be seen by other species. For example, many avian species possess ultraviolet vision that allows them to detect light with $\lambda < 300$ nm, thus enabling them to see hues that we cannot perceive.[2] This capability is used both in foraging and selection of mates.[3] At the other end of the spectrum, fish living in black-water rivers, in which the maximally transmitted light is longer than 600 nm, have evolved infrared vision, enabling them to detect light with $\lambda > 760$ nm that is prevalent in their environment.[4] This is not to be confused with the infrared "vision" of snakes, however, which relies on the heat-detection properties of the pit organs.[5]

On the other hand, light also possesses the properties of particles, which manifest as it is generated (at the light source) and absorbed (e.g., by the retinal photoreceptors). These nonmaterial particles, termed *photons,* represent quanta of energy that can be emitted or absorbed. The amount of energy in a given photon is inversely proportional to its wavelength; therefore, blue light, which has a shorter wavelength than red light (Fig. 4.2), possesses more energy than the latter. The light energy of the photon is absorbed by the visual chromophore molecule in the outer segment of the photoreceptor (provided that the chromophore is sensitive to that photon's wavelength). This energy is then used to isomerize the chromophore (from 11-*cis*-retinal into all-*trans*-retinal in the case of rhodopsin), thereby initiating conversion of a light stimulus into an electric signal. This process is called the *phototransduction process* and

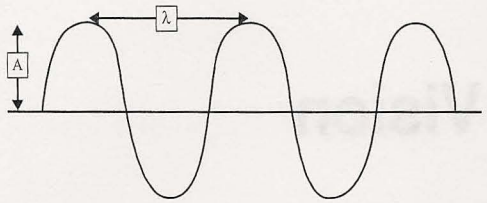

Figure 4.1. Representation of light as a wave, which is characterized by two parameters. Its amplitude (*A*) is the maximum value the wave obtains as it propagates. Its wavelength (λ) is the distance between two consecutive peaks.

is discussed in detail later in this chapter. The particle nature of light also manifests in other clinically important processes. Fluorescein molecules, for example, absorb photons of blue light and re-emit (i.e., fluoresce) photons with a lower energy content (in the yellow-green portion of the spectrum).[1]

Photometry

Photometry is the quantitative measurement of visible light. Photometry measures a number of interrelated properties of light, using a basic unit called a *candela.* Two important characteristics of light are its luminous intensity, which describes the intensity of a light source (as measured in candela), and its luminance, which describes its brightness reflected from a surface (as measured in foot-Lamberts or candela/m^2). These two properties are related, but they are not necessarily proportional. A handheld penlight is a bright source of light, but it possesses low intensity and therefore cannot be used to illuminate a stadium. A streetlight provides high-intensity light, which illuminates a large area, but it is not bright and does not provide enough illumination to conduct cataract surgery. Table 4.1 provides the luminances of several common sources of light. Other important characteristics of light are its luminous flux, which describes (as measured in lumens) the flow of light from a given point, and its illumination, which describes (as measured in foot-candles or lumens/m^2) the luminous flux falling on the surface of a given area.

Luminance is measured using photometers, which are divided into two major classes. Visual photometers provide a subjective reading, because the observer compares the illumination of the measured light with that of a standard light. Photoelectric photometers convert the measured light into an electric current, which is displayed by the instrument. Photometry measurements are extremely important in visual electrophysiologic recordings (e.g., electroretinography) because they are used to describe such variables as threshold, ambient light, and stimulus parameters.

Transmission and Reflection

As noted, humans see light with a wavelength of 390 to 760 nm. This limitation is a result of two factors. The first is the absorption spectrum of the visual chromophore, discussed previously. The second limiting factor is the transmission, reflection, and attenuation of the various wavelengths by the ocular media. Transmission of light through the various ocular surfaces depends on several factors, and the two most significant are the wavelength of the light and the angle of incidence. In humans, radiation wavelengths of 300 to 2500 nm are transmitted through the cornea.[6] Not all wavelengths, however, are transmitted through the cornea equally. For example, the human cornea transmits from 95% to 98% of light in the 600- to 1000-nm range but only 80% to 94% of light in the 450- to 600-nm range.[7]Transmittance through the human cornea is also affected by age.[8] In the rabbit, the cornea transmits 89% to 93% of the light at 370 to 500 nm, falling to 50% transmittance at 310 nm and 2% at wavelengths below 290 nm.[9]

Additional attenuation of transmission occurs inside the eye (Fig. 4.3). Even though light with wavelengths of up to

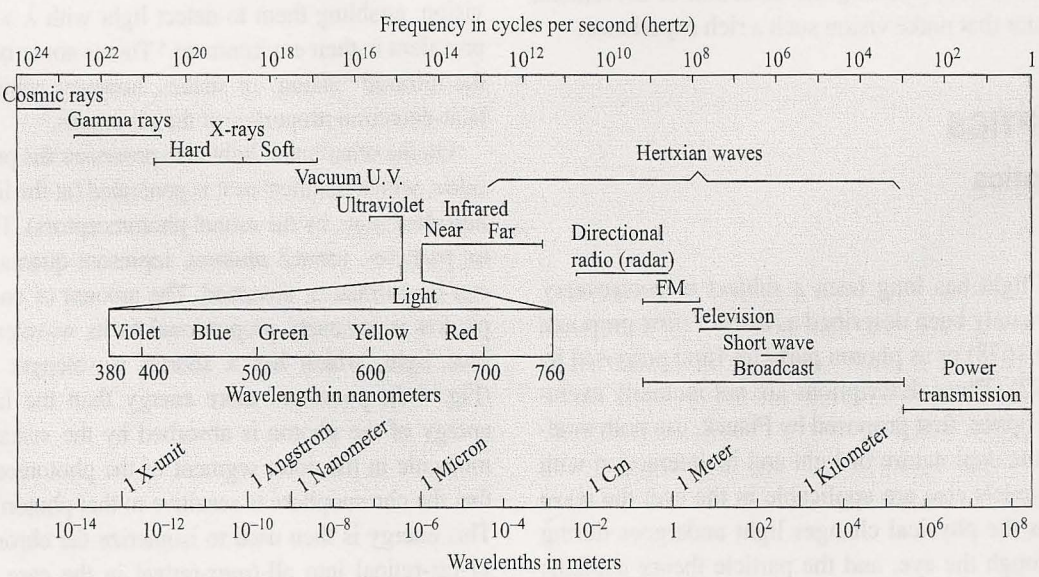

Figure 4.2. Spectrum of electromagnetic radiation. Most humans can see radiation with a wavelength of between 390 and 760 nm. (Reprinted with permission from Kaufman JE, Christensen JF, eds. *IES Lighting Handbook,* 5th ed. New York: Illuminating Engineering Society of North America, 1972.)

Table 4.1 Luminances of Natural and Artificial Light Sources[a]

Source	Luminance (cd/m2)
Sun	10^9
Car light	10^7
Incandescent tungsten lamp	10^6–10^7
Fluorescent lamp	10^4–10^5
Clear sky at noon	10^4
Full moon	10^3
Street lamp	0.1–1.0
Moonless night sky	10^{-3}–10^{-6}

Adapted from Millodot M. *Dictionary of Optometry and Visual Science*, 4th ed. Oxford; Butterworth Heinemann, 1997.

[a]In general, only the photopic system is active at a luminance <10 cd/m^2; at a luminance >10^{-3} cd/m^2, the scotopic system functions alone. Both systems are active at intermediate luminance values, which are defined as mesopic vision.

2500 nm passes the cornea, there is barely any transmission of wavelengths greater than 1950 nm through the aqueous humor; and in humans, the lens only transmits wavelengths between 390 and 1400 nm.[6] In other words, the aqueous and lens act as color filters, preventing light with very short and very long wavelengths (which has passed the cornea) from reaching the retina. In this context, it is noteworthy that humans can detect ultraviolet radiation ($\lambda < 390$ nm) following lens extraction, because the lens serves as a filter, blocking out light of shorter wavelengths.[1,6] Even structures normally forgotten by clinicians, such as tear film[10] and eyelids,[11] act as color filters. Thus, when cumulative transmittances are calculated for the successive components of the eye, a maximal transmittance rate in humans of 84% is obtained for light in the 650- to 850-nm range.[6] Obviously, transmission will be further reduced by ocular opacities. Grade II nuclear cataracts in rats cause a 50% reduction in transmission of light compared with grade I cataracts.[12] Furthermore, transmittance of light by the eye does not automatically result in vision, because transmitted radiation must be absorbed by a photopigment sensitive to that wavelength before the light can be seen.

Ocular surfaces can also reflect back incoming light. Light that strikes a surface at an oblique angle is reflected back; it is not transmitted into the new medium. The critical angle for reflection is determined by the difference in the indices of refraction (discussed later) between the two mediums. Most of the reflection that takes place in the eye occurs at the cornea because of the large difference in refraction index between the cornea and air. Reflection that occurs at the cornea–air interface affects not only incoming light but also outgoing light. Thus, internal reflection of outgoing light back into the eye prevents the ophthalmologist from examining the iridocorneal angle. Goniolenses filled with fluid are used to decrease the difference in refraction indices between the cornea and air, thus increasing the critical angle and permitting rays emanating from the iridocorneal angle to pass through the cornea.[1]

Radiation that is not transmitted or reflected can be either scattered in the eye or absorbed by pigments. Foremost among these pigments are the photopigments of the photoreceptor outer segments, which absorb photons and thus initiate the visual process. Additional absorption processes in the eye may have clinical implications. Use of Nd:YAG lasers for cyclophotocoagulation[13] or photocoagulation of intraocular tumors[14] is based on the preferential absorbance of 1064-nm radiation by melanin-containing tissue. In addition, absorption

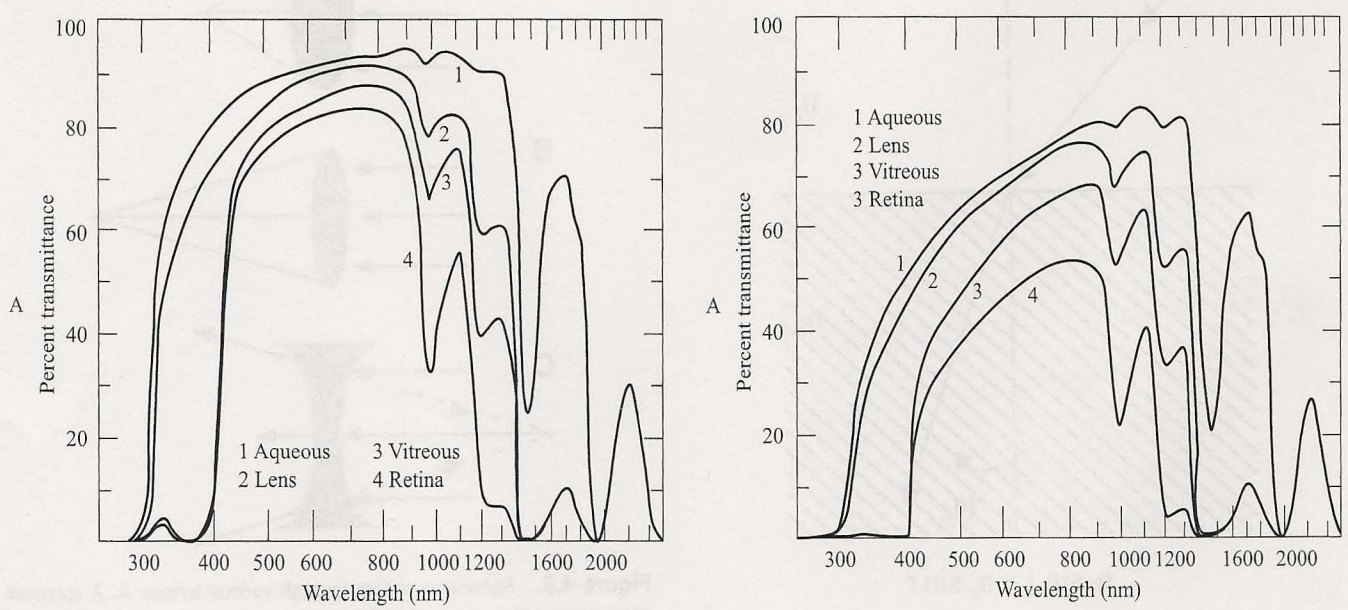

Figure 4.3. Transmittance rates of light through various structures of the human eye. **A.** Total light transmitted, including direct transmittance and scattered light, at each wavelength. **B.** Directly transmitted light, not including losses from reflection or scatter, at each wavelength. (Reprinted with permission from Boettner EA, Wolter JR. Transmission of the ocular media. *Invest Ophthalmol* 1962;1:776–783.)

of ultraviolet solar radiation has been implicated in diseases such as pannus in the dog,[15] squamous cell carcinoma in cattle,[16] and cataract and drusen formation in humans.[17]

Geometric Optics

Refraction

In vacuum, light travels at a constant speed (c) of approximately 3×10^8 m/sec. As it strikes denser media, light undergoes three changes:

1. Its velocity is reduced,
2. Its wavelength shortens, and
3. It is bent (unless it struck the surface of the medium at a 90° angle).

These changes are expressed in the equation:

$$n = c/v = \lambda/\lambda_m$$

where n is the index of refraction (or bending); c and λ are the speed and wavelength, respectively, in vacuum; and v and λm are the velocity and wavelength, respectively, in the new medium. The amount of refraction that occurs as light passes from one medium to another is described by Snell's law (Fig. 4.4) and is determined by the angle of incidence and by the refractive indices of both media. Because various structures of the eye differ in their refraction indices, light is successively refracted (bent) as it passes from air through the precorneal tear film, cornea, aqueous humor, lens, and vitreous on its way to the retina.

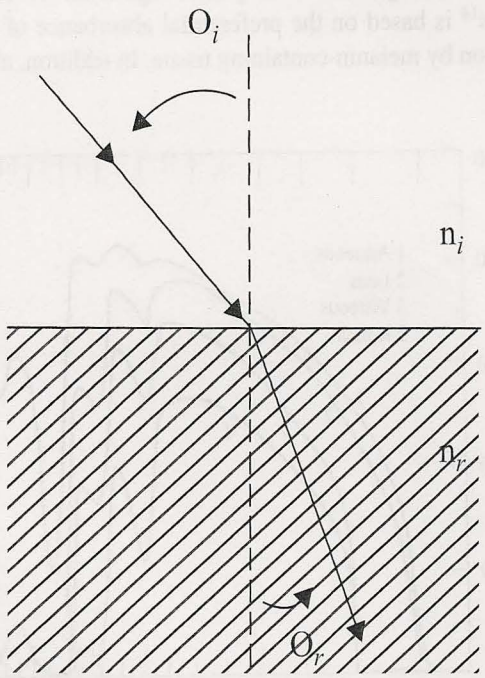

Figure 4.4. Refraction of light as it passes from one medium to another is governed by Snell's law. The angle of refraction (O_r) is a function of the angle of incidence (O_i) and the refractive indices of the two mediums. In this representation, $n_i < n_r$; therefore, $O_i > O_r$.

Vergence

An object that bends (or refracts) light is called a lens. When a single ray of light strikes a lens, the ray undergoes simple refraction. Most objects or images, however, generate a pencil of light rays rather than a single ray. When a pencil of rays strikes a lens, they spread apart (i.e., diverge) or come together (i.e., converge) (Fig. 4.5). Divergence, or negative vergence, occurs when light strikes a concave lens; convergence, or positive vergence, occurs when light strikes a convex lens. The vergence power (i.e., amount of bending) of a lens is measured in units called *diopters*. One diopter (D) is the verging power of a lens with a focal length (f) of one meter. In broader terms:

$$D = 1/f$$

The focal length of a lens is the distance between the center of the lens and the point at which parallel rays of light are brought into focus by that lens. The focal length of a lens is directly proportional to its curvature radius. Therefore, the verging power (or the diopter power) of the lens increases as its curvature increases. As Figure 4.5 shows, a convex lens with a focal length of 0.1 m will have a power of +10 D (D = $1/f$ = 1/0.1 m = 10D). A flatter, convex lens with a focal length of 0.2 m will be "weaker," with a power of +5 D (D = $1/f$ = 1/0.2 m = 5D). A concave lens with a focal length of 0.2 m will have a power of −5 D. The vergence powers of lenses in an optical system are additive. Thus, if the lenses in Figures 4.5A and 4.5B were placed next to each other, the resulting optical system would have a theoretical power of +15 D. If all

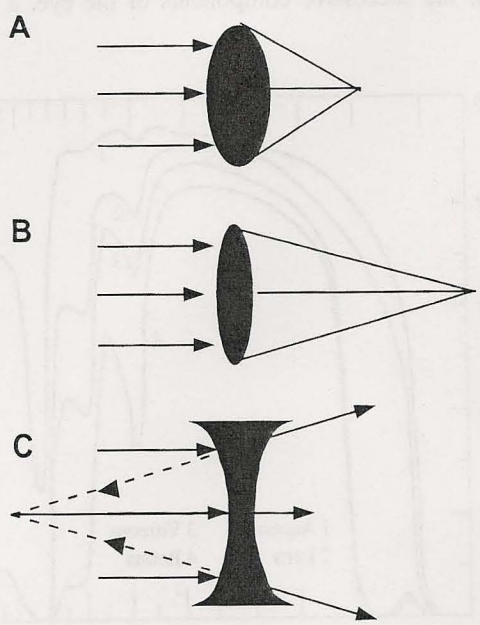

Figure 4.5. Refraction of light through various lenses. **A.** A spherical convex lens with a power of 10 D focuses parallel light rays at a distance of 0.1 m. **B.** A flatter, spherical convex lens with a power of 5 D focuses parallel rays at a distance of 0.2 m. **C.** Parallel rays passing through a concave spherical lens diverge. A virtual image is formed by tracing back (*dashed lines*) the diverging rays.

three lenses in Figure 4.5 were united into one system, it would have a power of +10 D. This principle holds in the eye, because the refractive contributions of the successive ocular surfaces are added to form a focused image on the outer segments of the photoreceptors.

The positive power of the convex lens indicates that it forms a *real image,* which means that incoming rays from the object are converged and focused on the other side of the lens. The negative power of the concave lens indicates that it forms a *virtual* or *aerial image,* which means that the diverging rays are traced, using imaginary extensions, backward to a "focused" virtual image "located" on the same side of the lens as the object. These principles are manifested in ophthalmoscopy. The direct ophthalmoscope provides a real image of the patient's fundus, whereas indirect ophthalmoscopy entails use of a handheld convex lens and therefore provides a virtual image of the fundus.

Visual Optics

Refractive Structures of the Eye

As mentioned, light is successively refracted by the various ocular structures as it passes through the eye on its way to the retina. Table 4.2 lists the refractive indices and powers of various ocular surfaces in humans. The most anterior optical surface of the eye is the precorneal tear film. By strict definition, it could be argued that the tear film is the most refractive layer of the eye. This is because of the large difference in refractive indices as light passes from air, which has a refractive index of almost 1, into the tear film, which has a refractive index of 1.336.[18] Factoring the refractive indices of air and the tear film into Snell's law reveals that the precorneal tear film has a refractive power of 43 D.[18] Alterations in the composition[19] or breakup time[18] of the tear film may change the refractive power of the eye by as much as 1.3 D and may contribute to the blurry vision complaints commonly encountered in (human) dry eye patients.[20] The effect of tear deficiencies on the quality of vision in our animal patients has yet to be studied.

Table 4.2 Refraction Constants in the Human Eye

Structure	Refractive Index	Refractive Power (D)	Reference
Tears	1.336	43.0[a]	18
Cornea	1.376	42.3[a]	22, 32
Anterior surface	1.401	48.2	32
Posterior surface	1.373	–5.9	32
Lens	1.41	19.11	22
Anterior surface		8.4	250
Posterior surface		14.0	250
Vitreous/aqueous	1.336		22
Retina	1.363		250

[a]The refractive power of the cornea and tears is not additive. Rather, that of the former arises from the latter and its interface with air. The net power of the tears and the anterior and posterior cornea is 43 D.

The cornea is the next organ through which incoming light passes. The corneal stroma has a refractive index of 1.376. Because this value is slightly higher than the refractive index of the tear film, passage of light from the tear film into the anterior layers of the cornea results in an additional 5 D of refractive power.[21] However, these 5 D are "lost" when light passes from the posterior cornea into the aqueous humor, which has a refractive index nearly identical to that of the tears. When combined, the precorneal tear film and the cornea contribute a net refractive power of 43 D, which conventionally (though somewhat erroneously) is attributed to the cornea (Table 4.2). Therefore, in humans, for example, the cornea contributes approximately 70% of the total 60 D power of the eye, thus making it our largest refractive organ.[21]

Another factor affecting the refractive power of the cornea, besides the refractive index, is its curvature. Because the cornea converges light, it acts as a convex lens. As stated earlier, the refractive power of such a lens depends to a large extent on its curvature radius. Therefore, in large eyes, which are characterized by flat corneas, the refractive power of the cornea is reduced. Conversely, in small eyes with spherical corneas, its power is increased. Table 4.3 shows the relationship between size of the eye and refractive power of the cornea in several species. Furthermore, the central and peripheral corneas have different curvatures and consequently differ in their refractive powers (see "Spherical and Chromatic Aberrations" later in this chapter).

As noted, the refraction that occurs as light passes from the cornea into the aqueous humor and during its passage through the aqueous has little overall significance. Therefore, the next significant refractive structure through which light passes after the cornea is the pupil. The pupillary aperture is not considered to be a classic refractive structure, but it does make an important contribution to the resolving power of the eye. As the pupil dilates in dim light, the number of photons entering the eye increases, thereby also increasing retinal illumination. Mydriasis, however, also decreases the depth of focus of the eye. This is especially critical in animals with limited accommodative capability (discussed later). The implication for

Table 4.3 Eye Size and Corneal Power

Species	Axial Length (mm)	Corneal Power (D)	References
Goldfish	4.2	129 (in air)	24
Rat	6.3	112.7	24
Rabbit	18.0	44.6	24
Cat	21.3	43.0	251
Dog	19.5–21.9	37.8–43.2[a]	83, 91, 93
Elephant	38.8	21.3	95
Horse	43.7	15.7–19.5	74, 252

[a]The range of values in the dog probably reflects a breed difference, because larger breeds have flatter corneas.[83]

such species is that as the pupil dilates, the range of distances at which objects remain in focus decreases. For example, with an eye that is focused at a distance of 1 m, objects at a distance of between 0.56 and 5.00 m will be in focus when pupil diameter is 1 mm; the range decreases to between 0.78 and 1.40 m when the pupil dilates to 4 mm.[22] Furthermore, as the pupil dilates, the relative significance of optical aberrations inherent in the eye increases (discussed later), thereby reducing its resolving power. Therefore, the pupillary light reflex is, in effect, a constant balancing of two conflicting requirements for vision: maximal retinal illumination and visual resolution. As a rule of thumb, constricting the pupil by half increases visual resolution by a factor of two.[23]

The lens is another structure that makes a significant contribution to the overall refractive power of the eye (Tables 4.2 and 4.4). As in the case of the cornea, the refractive power of the lens is determined both by its refractive index and its curvature. In humans and in many nonaquatic species, the refractive index of the lens is ~1.41. Since this refractive index is relatively similar to that of the aqueous humor (range, in most species, 1.334–1.338),[24] the lens in these species has a rather low refractive power. In humans, the calculated refractive power of the lens is approximately 19 D.[25] The refractive index of the lens increases in aquatic species, where it can be as high as 1.65, resulting in significantly higher refractive power.[26]

The second factor determining lenticular refractivity, the lens curvature, also differs between aquatic and nonaquatic species. Generally, it can be said that the lens is spherical in fish and aquatic mammals, while it is more discoid in terrestrial species.[27] Therefore, it will have a higher refractive power in the former compared to the latter (Table 4.4). The reasons for the effect of habitat on the refractive index and curvature of the lens are discussed later in this chapter. Of course, the curvature (and, hence, the refractive power) of the lens can also be changed actively through a process termed *accommodation* (see next section).

Though usually forgotten by ophthalmologists, the vitreous also plays an important role in refractive development of the eye. Vitreous elongation increases the axial length of the eye, thereby increasing the refractive path of light and inducing myopia. In certain species of fish, this mechanism serves to increase ocular refraction and compensate for loss of corneal refractive power. In different goldfish strains, for example, the vitreous body can contribute anywhere from 37% to 70% of the total axial length of the eye.[28] In visual-deprivation studies conducted during critical developmental periods in species as diverse as chickens,[29] fish,[30] and tree shrews,[31] the deprivation-induced myopia also was a result of elongation of the vitreous body.

It should be noted that light is also refracted *during* its passage through ocular structures such as the cornea and lens, not just at their interface with other structures. This refraction results from changes in refractive indices in various layers of these structures. Some of these refractive gradients are probably too small to affect the overall optical performance of the eye, however. For example, refractive indices in the various corneal layers ranges from 1.401 to 1.373 D in humans,[32] whereas the rat retina has a refractive range of 1.369 to 1.385 D.[33] In other cases, however, regional differences are significant and must be taken into account; for example, in the goldfish eye, the refractive indices of the lens cortex and nucleus are 1.35 and 1.57 D, respectively.[34]

Table 4.4 Lens Power and Refractive Indices

Species	Lens Power (D)	Refractive Index	References
Rat	243.9	1.683	24
Rabbit	75.0	1.6	24
Cat	52.9	1.554	24
Dog	41.5[a]		84
Horse	14.9–15.4	1.42	252

[a]Value in the dog is based on dioptric strength of intraocular lens needed to regain emmetropia in aphakic dogs.

Accommodation

Accommodation is a rapid change in the refractive power of the eye, which is intended to bring the images of objects at different distances into focus on the retina. The stimulus for the accommodative response is a blurred, or defocused, retinal image.[35] Eyes of vertebrates accommodate by one or more of the following mechanisms: changing the corneal curvature, changing the distance between the cornea and retina, changing the curvature or position of the lens, or having two or more separate optical pathways of different refractive powers.[36]

Humans and other primates accommodate by changing the curvature of the lens. To view distant objects, sympathetic innervation induces relaxation of the ciliary body muscle, which in turn leads to stretching of the lens zonules. The increased tension of the zonules results in a greater pull on the lens capsule, thus causing the lens to become more discoid and decreasing its overall axial thickness and refractive power in a process of *disaccommodation.*[36] To accommodate for near objects, the reverse process takes place. Parasympathetic input induces contraction of the ciliary body muscles, leading to relaxation of the zonular fibers and reduced tension on the lens capsule. In turn, this liberates the inherent elasticity of the lens, resulting in a more spheroid lens possessing greater axial thickness and refractive power.[24,36] These changes in lenticular curvature allow primates such as the young (<5 years) rhesus monkey to accommodate by as much as 34 D.[37] As the animal ages, however, it gradually loses its accommodative capability in a process termed *presbyopia,* and monkeys older than 25 years can accommodate only to an average of 5 D.[37] A similar and dramatic reduction has been reported in the chicken, as lenticular accommodation decreases from more than 20 D at hatching to less than 5 D at one year of age.[38] Mechanisms proposed for presbyopia

include reduction in ciliary muscle contractility, changes in the refractive index of the lens, age-related changes in the relative position of the lens and ciliary body, and loss of the lens capsule and lens fiber elasticity.[36,39–41]

As with most other aspects of vision research, the mammalian species in which accommodative capabilities have been studied most extensively is the cat. The elasticity of the feline lens capsule is 5% of the elasticity in humans; thus, the cat obviously does not accommodate by changing its lens curvature.[42,43] Instead, *translation* (i.e., the anteroposterior movement of the entire lens) is responsible for accommodative changes in the feline eye.[24] This movement is made possible by the relative abundance of meridional (i.e., longitudinal) fibers in the feline ciliary body muscle and by the relative scarcity of circular fibers, which predominate in primates.[44] Parasympathetic stimulation of the meridional muscle fibers in the cat results in forward displacement of the lens by up to 0.6 mm,[45] thus inducing anywhere between 2 and 8 D of accommodation.[24] The dog's accommodative power is reportedly lower, only 1 to 3 D in range.[24,46] However, in other carnivores, the same mechanism is used to achieve a significantly greater magnitude of accommodation (usually associated with primates). Forward lens movement in the raccoon induces accommodation of up to 19 D, which is the greatest accommodative capability of any nonprimate, terrestrial mammal studied.[47] A similar wide range of accommodative capability also exists in other closely related species. For example, the grey squirrel does not accommodate,[48] whereas the California ground squirrel can accommodate up to 6 D.[49] It should be noted that lens displacement in mammals results from ciliary muscle contraction, but in fish, such displacement is affected by a specialized smooth muscle, the retractor lentis.[50,51]

Rodents and ungulates are generally described as lacking accommodative capability.[24,52] In the former, this lack of accommodation is explained by the absence of a well-defined ciliary muscle,[53] though the small pupil size in species such as the rat does provide these animals with a great depth of focus.[54] Lack of accommodation in ungulates,[24,52] some of which possess a more developed ciliary muscle,[53,55] is more difficult to explain and may account for the low visual acuity in such species as the cow.[56] The horse has a much higher visual acuity than the cow, but its accommodative power is also limited to plus or minus 1 D in either direction.[57]

Another species in which accommodation has been studied extensively is the chicken, which employs several accommodative mechanisms. Lenticular accommodation in the chicken is achieved when the ciliary[58] or peripheral iris[59] muscles contract. This contraction is transmitted through the ciliary processes and results in changes similar to those that occur in primates. These changes include thickening of the lens by 0.2 mm,[56] steepening of its curvature, and a bulging of the lens into both the anterior and vitreous chambers (thereby reducing their depths).[60] However, unlike mammals, chickens also possess a mechanism for changing the corneal curvature. Just like lenticular accommodation, corneal accommodation in the chicken also results from ciliary muscle contraction, which flattens the peripheral cornea and increases the curvature of the central cornea.[61–63] Corneal accommodation is reported to play an important role in chicken accommodation, contributing 8 to 9 D compared to 15 to 19 D of lenticular accommodation,[60–62] though other researchers claim the contribution is insignificant.[64] Changes in intraocular pressure do not contribute to lenticular accommodation in the chicken,[59] but they may contribute to changes in refractive power brought about by choroidal stretching.[65] It should be noted that the chicken, as well as other avian and reptile species, may accommodate independently in both eyes, resulting in *anisometropia* (i.e., unequal degree of refraction in the two eyes) of up to 6 D.[66,67]

Abnormal Refractive States and Optical Errors

The "purpose" of refraction and the accommodative processes described in the previous sections is to focus an image on the outer segments of the photoreceptors.

Emmetropia and Ametropia

An *emmetropic* eye is one in which parallel light rays (from a distant object) are focused on the outer segments when the eye is at rest. A nonemmetropic, or *ametropic,* eye is one in which the focused image (from a distant object) falls anterior to the retina (i.e., nearsighted or myopic eye) or posterior to it (i.e., farsighted or hypermetropic eye) (Fig. 4.6).

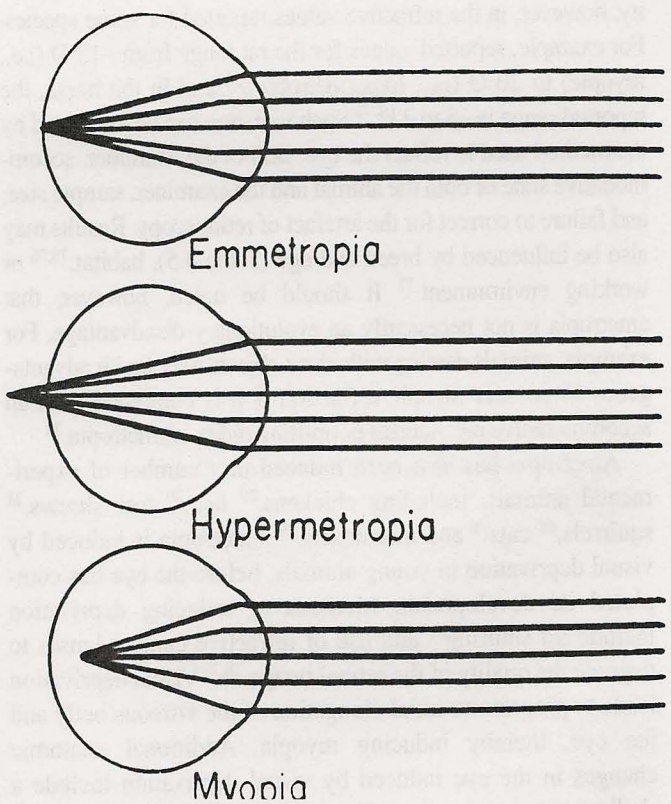

Figure 4.6. In emmetropia, parallel light rays are focused on the retina. In hypermetropia, light rays are focused behind the retina. In myopia, the light is focused in front of the retina. (Reprinted with permission from Guyton AC. *Textbook of Medical Physiology.* 7th ed. Philadelphia: WB Saunders, 1986.)

Retinoscopy is the most commonly used method to determine the refractive state of the eye. It is based on two assumptions: first, that light emerging from the eye (i.e., emergent rays) follows the same optical path as light entering the eye; and second, that the fundus reflex originates at the level of the outer segments. If those two assumptions hold, then emergent rays exit an emmetropic eye as parallel rays, a hypermetropic eye as diverging rays, and a myopic eye as converging rays.[68] Therefore, the location of the focal point formed by the emergent rays can be used to determine the refractive state of the eye.[68]

However, it should be noted that the second assumption is not completely accurate. The fundus reflex does not originate at the outer segments but closer to the observer, at the level of the inner limiting membrane.[69] Thus, there is a gap (equal to the thickness of the retina) between the point at which we actually measure the reflected light and the point at which we should measure it. This gap, termed the *artefact of retinoscopy,* results in shifting refraction values in the direction of hypermetropia and needs to be corrected using an established formula.[69] This error is relatively minor (+0.25 D) in young humans,[70] but it becomes significant in small eyes, reaching values as high as +10 and +11 D in the rat and the gerbil, respectively.[71]

Table 4.5 lists refractive values in various species. Few species are truly emmetropic, though once the values are corrected for eye size, many terrestrial species are within 1 D of emmetropia. In general, most mammals are within plus or minus 1 D of emmetropia.[24,72] Most selachians, amphibians, and snakes tend to be somewhat hypermetropic, while most cyclostomes and teleosts are myopic.[73] There is a large variability, however, in the refractive values reported for some species. For example, reported values for the rat range from −13 D (i.e., myopic) to 20 D (i.e., hypermetropic),[24] and in the horse, the reported range is −3 to 3 D.[74] Such variation can be explained by the method used to refract the eye, skill of the examiner, accommodative state of both the animal and the examiner, sample size, and failure to correct for the artefact of retinoscopy. Results may also be influenced by breed and age (Table 4.5), habitat,[75,76] or working environment.[77] It should be noted, however, that ametropia is not necessarily an evolutionary disadvantage. For example, animals dealing with close objects may find it advantageous to possess myopic refraction if it is combined with an accommodative mechanism permitting reflex emmetropia.[24]

Ametropia has also been induced in a number of experimental animals, including chickens,[29] fish,[30] tree shrews,[31] squirrels,[48] cats[78] and marmosets.[79] Ametropia is induced by visual deprivation in young animals, before the eye has completed its development. Methods of inducing deprivation include lid suturing[31] and use of refractive contact lenses to degrade the quality of the retinal image.[78,79] Visual deprivation leads to progressive axial elongation of the vitreous body and the eye, thereby inducing myopia. Additional anatomic changes in the eye induced by visual deprivation include a shallow anterior chamber, thinner lens, and changes in corneal curvature.[31] The aim of these experiments is to develop animal models for the study of the pathogenesis of myopia in humans, particularly for deprivation myopia in children born with various ocular opacities.[80]

Table 4.5 Refractive Values in Selected Animal Species

Species	Refractive Value (D)	References
Cat		
Street cat	−0.8	75
Laboratory cats	+1.4	75
Dog		
Mean value	−0.27–(−0.39)	76, 77
Indoor dogs	−0.64	76
Outdoor dogs	+0.17	76
Brachycephalic	+0.23	76
Mesaticephalic	−0.62	76
Dolichocephalic	−0.20	76
Small breeds	−0.58	76
Medium breeds	−0.66	76
Large breeds	+0.13	76
Horse	+0.33	106
Asian elephant	+0.23	95
Thomson Gazelle		
Newborn	+3.44	96
Age 50 days	+0.13	96
Rhinoceros	+1.08	272
Rabbit	+0.5	253
Ostrich		
At hatching	−4.5	72
Age 7 days	+0.4	72
Chicken		
At hatching	+6.5	254
14 days	+2.0–(−0.5)	254
Adult	−0.20	79
Penguin		
In water	+8.0–(+13.0)	113
In air	+0.25–(−1.75)	113
Hooded seal		
In water	+2.0–(+3.0)	273
In air	−2.0–(−4.0)	273

Aphakic Eyes and Intraocular Lenses

Because of the significant refractive role of the lens, cataract surgery (or any surgical lens extraction) resulting in aphakia leaves the eye severely hypermetropic. The aphakic eye lacks the refractive contribution of the lens; therefore, light is not sufficiently refracted, resulting in an image formation "behind" the retina. Since the early 1980s, veterinary ophthalmologists have sought to alleviate this problem by implanting intraocular lenses (IOLs) in the eyes of dogs following cataract extraction. The purpose is to compensate for loss of refraction by the lens, thereby returning the eye to an emmetropic state. Early attempts using 14.5- to 29.0-D IOLs left the eyes hypermetropic.[81,82] Today, following the results of studies involving large numbers of dogs of various breeds, the consensus is the ideal IOL for dogs should have a power of

40.0 to 41.5 D.[76,83,84] The 1.5-D range of recommended values probably results from breed differences (Table 4.5).[76,84] However, it is important to note that though 41-D IOLs are used to bring aphakic dogs to emmetropia, this does *not* mean that aphakic dogs suffer from hypermetropia of 41 D. Indeed, the hypermetropia in aphakic dogs has been shown to range from 14.4 to 15.2 D.[83,84] The reason that a 41-D IOL is needed to correct 15 D of hypermetropia is that an IOL is placed in the capsular bag, surrounded by aqueous humor. This environment results in a reduction of its overall refractive power (due to the small difference in refractive indices between the aqueous humor and the IOL), and therefore this power has to be higher than the aphakia it is intended to resolve. If dogs were to be fitted with spectacles to correct aphakia, then indeed these spectacles would require 15-D lenses!

Future directions for IOL implants likely will include development of implants for additional species and implants with accommodative capability. Preliminary results in the cat indicate that IOLs for this species should have a strength of 52 to 53 D.[85] A pilot study in the horse concluded that an IOL of 22.5 D overcorrects the aphakic equine eye.[86] Additional developments being studied include IOLs with accommodative capabilities. In species that accommodate through changes in lens curvature, accommodative capability can be restored by implanting an endocapsular inflatable balloon; the balloon is then inflated with silicone liquid or gel. This technique, which has been successful in the rabbit,[87] pig,[88] and macaque,[89] enables the animal to accommodate up to 6 D. Bifocal implants are also being designed.[90] Ideally, in the near future, every cataractous animal patient will be refracted and fitted with an appropriate IOL that will bring the eye to an emmetropic state.

Though veterinary ophthalmologists have made significant progress in improving refraction of aphakic animals, little attention has been paid to improved refraction in phakic animals. Various surgical techniques, mostly involving use of lasers, are used to correct ametropia and astigmatism in humans, and preliminary work shows that some of these techniques are applicable in the dog,[91] thus opening the door to future research in this area.

Astigmatism

Astigmatism is a state of unequal refraction of light along the different meridians of the eye. Normally, a given refractive structure of the eye (e.g., the cornea) has a constant curvature radius in all its meridians (though the cornea may flatten toward the limbus). Astigmatism occurs when one of the ocular refractive structures (or the retina) has different curvature radii along its different meridians. Because of these differing curvatures, light entering the eye through the vertical meridian may be refracted more (i.e., direct, or with-the-rule, astigmatism) or less (i.e., inverse, or against-the-rule, astigmatism) than light entering through the horizontal meridian. Therefore, light entering along one meridian will be focused on the retina and result in high-resolution vision, whereas light along another meridian will be unfocused, leading to low-resolution vision (Fig. 4.7). Such an aberration is corrected with a cylindrical lens rather than with a spherical lens that is used to correct ametropia. In humans, most cases of astigmatism result from abnormalities in the anterior surface of the cornea; of these, 90% are direct astigmatism. Only a minority of cases result from lenticular or posterior corneal surface abnormalities.[92]

Some pathologic processes may induce astigmatism. Corneal disease resulting in edema or scarring will inevitably lead to an uneven corneal surface, resulting in astigmatism. Focal cataracts will cause refractive astigmatism because of variations in refractivity among different lenticular zones.[92] In addition, cataract surgery,[93] penetrating keratoplasty,[94] and other procedures that involve incising and suturing of the cornea may result in astigmatism because of imperfect alignment of wound edges; however, such surgically induced astigmatism frequently resolves over time.[93,94] Noteworthy astigmatism has been described in some wildlife species, including the Asian elephant[95] and the newborn gazelle,[96] though its significance is unknown.

However, in most cases, astigmatism in the animal kingdom is physiologic rather than pathologic. Several avian species, including the pigeon,[97,98] chicken,[99] crane, and quail,[98] as well as several amphibian species, including the frog and toad,[99] possess lower-field myopia. In these species, the astigmatism helps the animal match the average viewing distances of different areas of the visual field.[99] The eyes of these animals are emmetropic along the horizontal and in the upper visual field, but they become progressively myopic below the horizontal. This allows the animal to keep the ground in focus while foraging for food and, at the same time, monitor the sky for predators.[98,100] This may be why predators such as raptors do not possess this adaptation.[100] The same principle is also found in

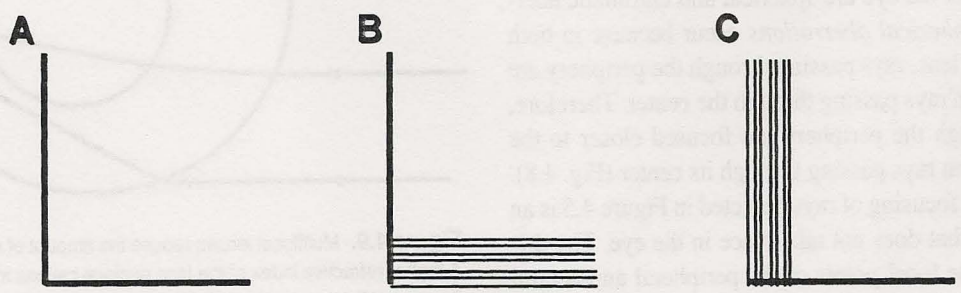

Figure 4.7. A. A normal eye can see focused horizontal and vertical lines. **B** and **C.** An astigmatic eye will see a focused line in one orientation and a blurred line along the perpendicular axis. (Modified from Duke-Elder S. *System of Ophthalmology. Vol V. Ophthalmic Optics and Refraction.* London: Henry Kimpton, 1970.)

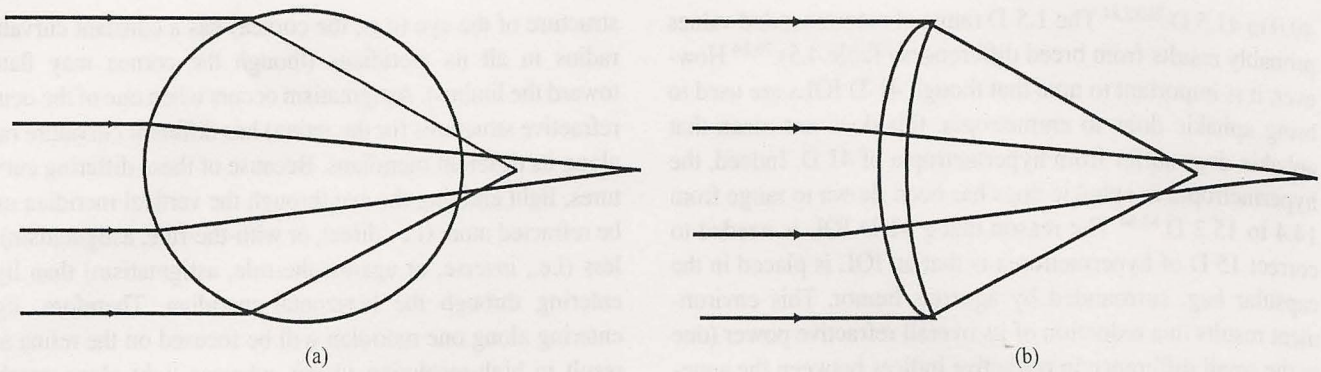

Figure 4.8. Spherical aberrations occur when light passes through the lens (*A*) and cornea (*B*). In both cases, peripheral rays are refracted (bent) more than central rays. Therefore, the focal point of the peripheral rays is closer to the lens/cornea than the focal point of the peripheral rays, resulting in a blurred image. The distance between the two focal points is called spherical aberration and is measured in diopters (D).

eyes of partially aquatic mammals, such as the dolphin,[101] harbor seal,[102] and harbor porpoise.[103] Regional changes in the refractive powers of different parts of the cornea allow these animals to maintain high-resolution vision in both water and air. Therefore, physiologic astigmatism may be an evolutionary mechanism helping animals to improve their spatial-resolution capabilities in different environments.[104]

The horse was also believed to possess a similar, passive "accommodating" mechanism, resulting from a nonsymmetrical eye shape. According to the ramp retina theory, the superior retina was believed to be farther from the lens than the inferior retina. Therefore, the horse would raise its head to view distant objects and lower it to view nearby objects.[105,106] Anatomical measurements have now discredited this theory,[57,106] and the horse is believed to possess an active (though limited) accommodation mechanism of 1 to 2 D.[57,106] The head movement previously associated with this behavioral "focusing" is now believed to occur when the horse is interchanging monocular and binocular visual fields.[106]

Spherical and Chromatic Aberrations

The eye is not a perfect optical system. Indeed, Duke-Elder quotes Hermann von Helmholtz, the 19th-century German physicist who invented the ophthalmoscope, as saying that "if an optician should try to sell me an instrument possessing such faults, I would feel justified in using the most severe language with regard to the carelessness of his work and return the instrument under protest."[92] Two of the most significant optical problems that affect the eye are spherical and chromatic aberrations. Positive *spherical aberrations* occur because in both the cornea and the lens, rays passing through the periphery are refracted more than rays passing through the center. Therefore, rays passing through the periphery are focused closer to the cornea (or lens) than rays passing through its center (Fig. 4.8). In other words, the focusing of rays depicted in Figure 4.5 is an "ideal" refraction that does not take place in the eye. The difference between the focal points of the peripheral and central rays, the spherical aberration, is measured in diopters.

Both the cornea and the lens possess anatomical adaptations that are intended to minimize the extent of their inherent spherical aberrations. In the lens, the higher refractive index of the lenticular nucleus increases the refractive power of the central lens. This results in moving its focal point closer to the lens, closer to the focal point of the peripheral lens. A gradient variation in the refractive index of the lens would result in the formation of a multifocal lens, with further attenuation of the spherical aberration (Fig. 4.9). Corneal spherical aberrations are minimized because the peripheral cornea is flatter than the central (apical) cornea. This decreases the refractive power of the peripheral cornea and moves its focal point away from the cornea and closer to that of the central cornea. Therefore, refractive surgeons attach great importance to centering the apical cornea so that the aberration-free zone is aligned with the pupil, thereby contributing to a high-quality retinal image.[21] The possible effects of corneoscleral transpositions on visual optics in our animal patients have yet to be investigated.

Another structure that plays a critical role in reducing spherical aberrations is the pupil. Contraction of the pupil blocks rays of light that entered the eye through the most peripheral (and refractive) cornea. It also prevents light from passing through the peripheral lens. Thus, miosis allows only

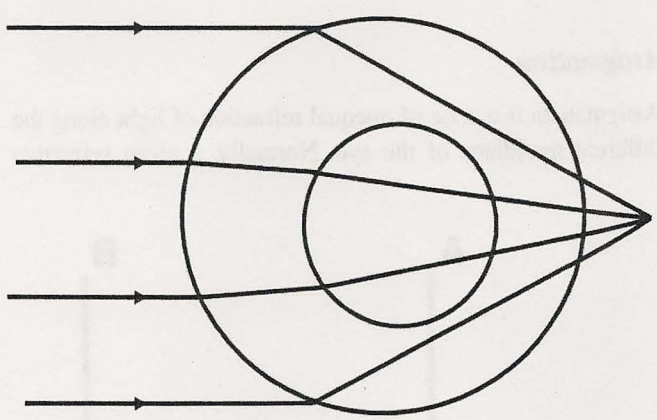

Figure 4.9. Multifocal lenses reduce the amount of spherical aberrations. A higher refractive index of the lens nucleus causes increased refraction of the central light rays (compared to the refraction of the central rays in Figure 4.8A). Consequently, the focal point of the central rays is shifted closer to the lens and closer to the focal point of the peripheral rays, thus eliminating the spherical aberrations seen in Figure 4.8A.

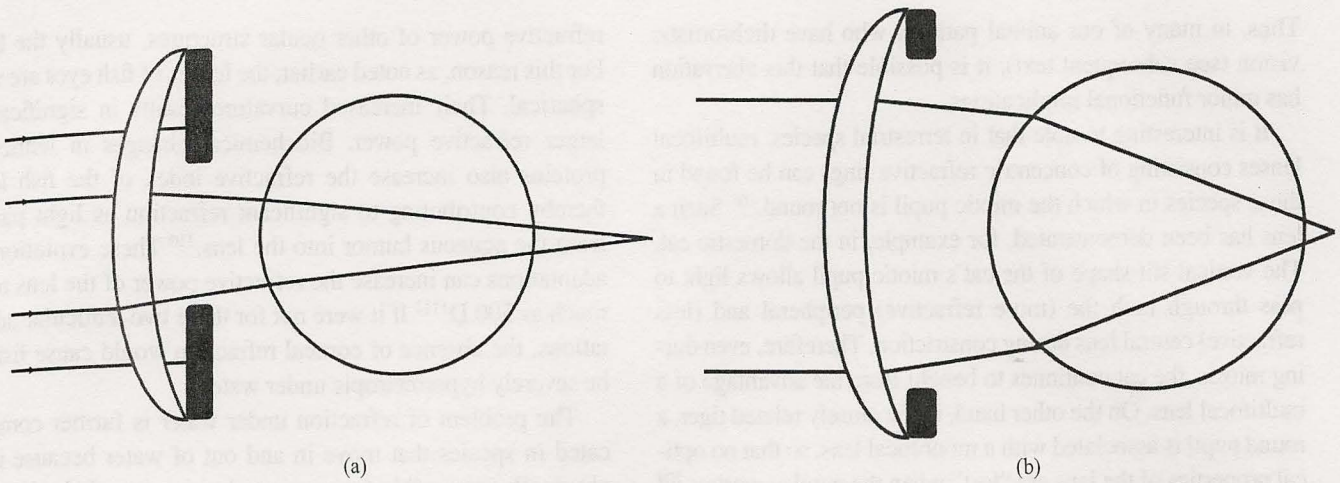

Figure 4.10. Pupillary diameter affects the magnitude of spherical aberrations. A miotic pupil (*A*) blocks the peripheral rays, thereby eliminating the spherical aberrations. Only central rays reach the retina, resulting in a focused image. A mydriatic pupil (*B*) admits peripheral rays into the eye, thereby increasing the amount of spherical aberrations. Fig 4.10B is the basis for the blurred vision experienced following pharmacological dilation of the pupil.

rays that pass through the central cornea and lens to reach the retina, and thereby it contributes to the formation of a well-focused image (Fig. 4.10A). A mydriatic pupil, on the other hand, allows more peripheral rays to enter the eye, and their passage through the peripheral cornea and lens increases the amount of spherical aberrations (Fig 4.10B). In humans, an 8 mm pupil induces 1 D of spherical aberrations,[107] which is the reason for the significant blurring of vision that we experience after our pupils have been pharmacologically dilated.

Chromatic aberrations result from the fact that the refractive index *n* (see equation on page 184), is not constant, but rather is wavelength dependent. Once again, therefore, the diagram in Figure 4.5 is somewhat misleading because it portrays an ideal situation pertaining to monochromatic light. However, when white light enters a prism (or a lens), each wavelength contained in that light is refracted by a different amount. The n_m of a given wavelength is inversely proportional to λ. Therefore, waves with a short wavelength (e.g., blue light) have a higher n_m than waves with a long wavelength (e.g., red light). Consequently, blue light will be more refracted than red light, and its focal point will be closer to the lens (Fig 4.11A). The distance between the focal points of the short and long wavelengths is the chromatic aberration, and once again, this distance is measured in diopters.

As in the case of spherical aberrations, anatomical adaptations may contribute to decreasing the effect of the chromatic aberrations. For example, fish have been shown to possess multifocal lenses consisting of concentric rings of differing refractive properties.[108] Thus, blue light passing through one ring will be less refracted than red light passing through another ring, thereby compensating for the blue light's higher n_m. Consequently, the image formed on the retina will be *chromatically focused* (Fig. 4.11B). Obviously, chromatic aberrations are less significant in species that have limited color vision because some of the defocused wavelengths may not be absorbed by the photoreceptors and hence are not perceived.

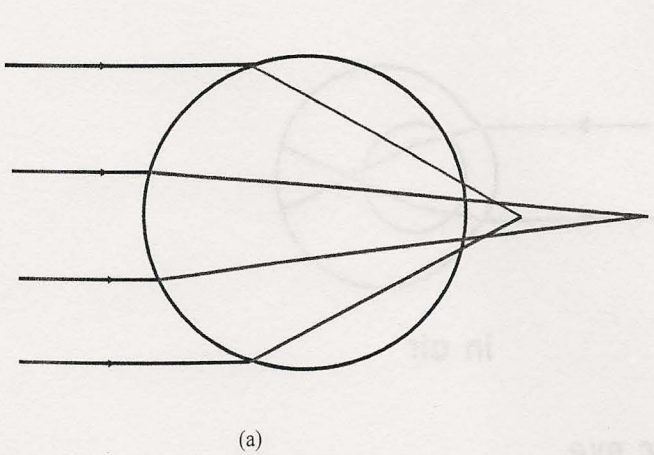

Figure 4.11A. Chromatic aberrations in the lens. White light is composed of numerous wavelengths, each of which is characterized by a different refractive index (n_m). Light with a short wavelength (e.g., blue light) has a higher n_m than light with a long wavelength (e.g., red light). Consequently, blue light will be more refracted than red light, and its focal point will be closer to the lens. The distance between the focal points of the short and long wavelengths is the chromatic aberration; this distance is measured in diopters.

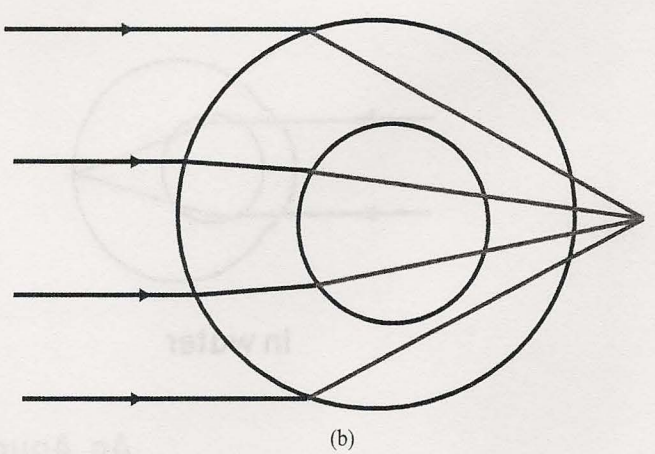

Figure 4.11B. Multifocal lenses reduce the magnitude of chromatic aberrations. A higher refractive index of the lens nucleus causes increased refraction of the red light (compared to its reduced refraction in Figure 4.11A). Consequently, the focal point of the red light is shifted closer to the lens and closer to the focal point of the blue light, thus eliminating the chromatic aberrations seen in Figure 4.11A.

Thus, in many of our animal patients who have dichromatic vision (see subsequent text), it is possible that this aberration has minor functional implications.

It is interesting to note that in terrestrial species, multifocal lenses consisting of concentric refractive rings can be found in those species in which the miotic pupil is not round.[108] Such a lens has been demonstrated, for example, in the domestic cat. The vertical slit shape of the cat's miotic pupil allows light to pass through both the (more refractive) peripheral and (less refractive) central lens during constriction. Therefore, even during miosis, the cat continues to benefit from the advantage of a multifocal lens. On the other hand, in the closely related tiger, a round pupil is associated with a monofocal lens, so that no optical properties of the lens are "lost" when the pupil constricts.[109]

Emmetropia Under Water

In aquatic species, the cornea is in contact with water rather than air. Because of the very small (~0.003) difference between the refractive indices of the cornea and water, the cornea of these species has virtually no refractive power. Fish are forced to compensate for this absence by increasing the refractive power of other ocular structures, usually the lens. For this reason, as noted earlier, the lenses of fish eyes are very spherical. Their increased curvature results in significantly larger refractive power. Biochemical changes in lenticular proteins also increase the refractive index of the fish lens, thereby contributing to significant refraction as light passes from the aqueous humor into the lens.[110] These evolutionary adaptations can increase the refractive power of the lens to as much as 500 D![111] If it were not for these two lenticular adaptations, the absence of corneal refraction would cause fish to be severely hypermetropic under water.

The problem of refraction under water is further complicated in species that move in and out of water because it is physically impossible for an eye to be emmetropic both in air and under water (Fig. 4.12). Eyes that are emmetropic in the air will be hypermetropic under water because the refractive power of the cornea is lost due to its submersion in water. Conversely, eyes that are emmetropic under water become extremely myopic in the air because the cornea (due to Snell's law) contributes refraction that the eye did not possess under water (compare values for penguins and seals in Table 4.5). Therefore, species that live and function in both habitats must

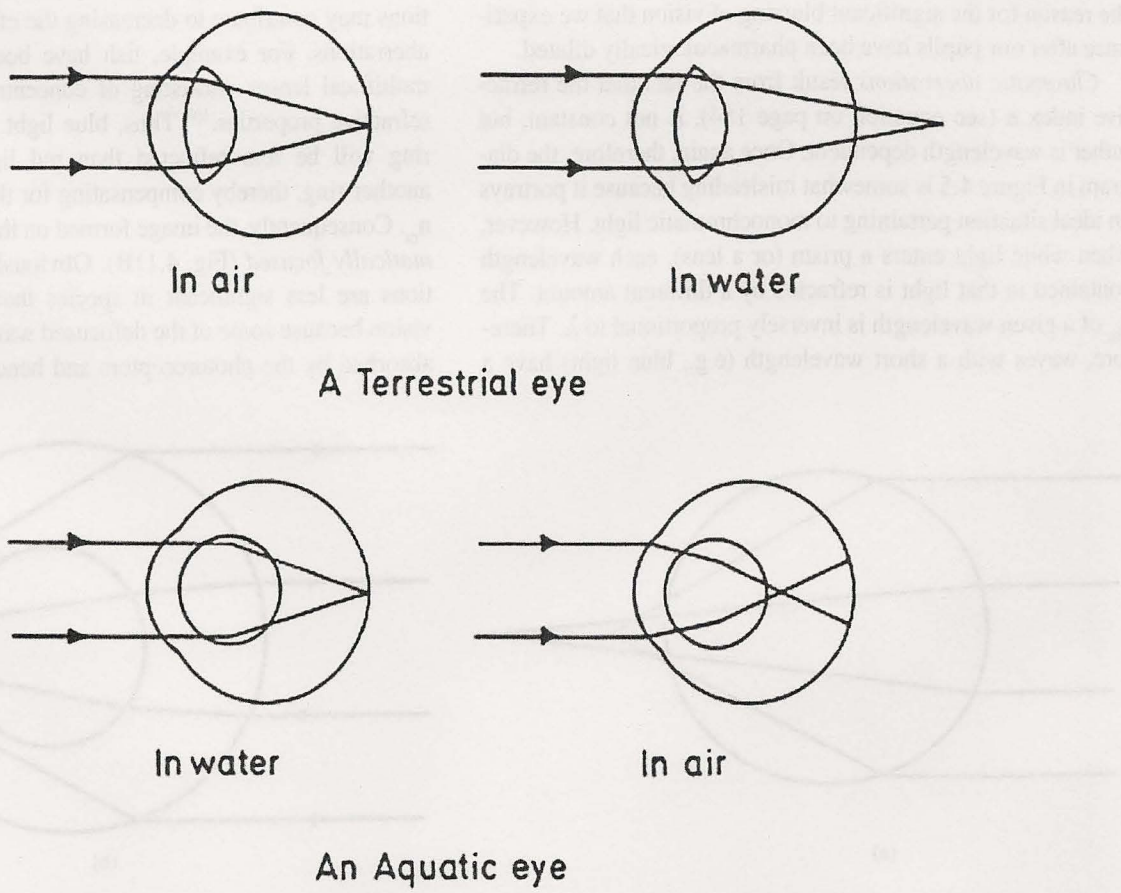

Figure 4.12. No eye can be emmetropic both in air and under water. An eye of terrestrial animals, which is emmetropic in an aerial environment, loses the refractive contribution of the cornea under water and becomes farsighted (top panel). An eye of a fish that is emmetropic under water becomes severely nearsighted (myopic) in the air because it "gained" corneal refraction that it did not possess under water (bottom panel). Note the difference in shapes of the lenses between the two species. The lens of the fish is more spherical in order to increase its refractive power (to compensate for the absence of corneal refraction under water). (Reprinted with permission from Sivak JG, Millodot M. Optical performance of the penguin eye in air and water. *J Comp Physiol* 1977;119:241–247.)

"choose" whether they will be emmetropic in the air or under water. It is very interesting to observe that both of these evolutionary strategies exist in the animal kingdom. Birds that hunt under water, such as cormorants[112] and penguins,[113,114] are emmetropic in the air (Table 4.5). These species overcome the resulting underwater hyperopia by increasing the accommodative power of the lens. During accommodation in the cormorant, for example, the lens bulges through the pupil, forming a lenticonus that increases the lenticular optical pathway and refractive power.[112] This gives the lens in some diving birds an accommodative power of 60 D and an incredible accommodation rate of more than 600 D/sec, 10 times as fast as nondiving birds.[112]

On the other hand, many aquatic mammals developed an opposing evolutionary strategy. Sea lions, harbor seals, and other Pinnipeds are emmetropic under water. Consequently, these animals become severely myopic when they come out of the water to breath. Various mechanisms have evolved to make up for the increased refractive power of the eye in an aerial environment. In some dolphin species, a specialized, flattened region with very low refractive power has evolved in the nasal cornea, providing for focused aerial vision, whereas the rest of the cornea is convex, providing for underwater vision. The animal shifts its head as it exits the water to allow light to enter through the flat "window."[101] A similar solution, with different curvatures in different regions of the cornea, has evolved in both harbor seals[102] and harbor porpoises.[103] As the animal moves from water to air, the resulting miosis allows the iris to block light from highly refractive quadrants of the cornea from entering the eye; under water, mydriasis allows light from these quadrants to enter the eye. In penguins, the entire cornea is flat, thus minimizing the alteration in refractive state when moving from air to water. In these animals, the cornea is the major refractory organ on land, and lens accommodation provides for underwater refraction.[113,114] More primitive amphibians (e.g., crocodiles) that lack this compensatory accommodative capability simply cannot focus when submerged and rely on other senses when hunting under water.[115]

VISUAL PROCESSING: FROM PHOTORECEPTORS TO CORTEX

The Retina

Visual Pigments

The process of vision begins with absorption of a photon by a photopigment in the outer segment of the photoreceptor. A visual photopigment consists of two parts. The first is a vitamin A_1–derived chromophore molecule, 11-*cis*-retinaldehyde (i.e., retinal). This molecule can be found in both rod and cone photopigment. The second component of the photopigment is opsin, which is an apo-protein that determines the wavelength of the photon the pigment will absorb. This part of the photopigment differs between cones and rods, and between different types of cones (see "Color Vision" later in this chapter).

Most of our understanding about the processes occurring in the outer segments comes from studying rhodopsin, which is the photopigment of rods. Rhodopsin is an integral part of the membrane of the outer segment discs, and it is estimated that each rod has approximately 10^9 rhodopsin molecules.[116] Rhodopsin is a long polypeptide chain (molecular weight, 27,000–40,000 d) that traverses the disc membrane as a helix.[117,118] As a photon is absorbed by the pigment, 60% of its energy is transferred to the molecule.[119] This energy is then used to initiate a chain bleaching reaction, which results in the breaking off of opsin and the photoisomerization of the chromophore (through several intermediate compounds) into all-*trans*-retinaldehyde, or R* (Fig. 4.13). This bleaching process (so called because it results in loss of color by the molecule) can be recorded as the early receptor potential.

In most mammals studied to date, maximal absorption by rhodopsin occurs at between 495 and 500 nm, thus showing a high degree of evolutionary conservation in the molecule.[117] The absorption peaks of the cone pigments in various species are presented in Table 4.6. Most mammals possess at least two classes of cone pigments: those sensitive to one short wavelength and those sensitive to one or more long wavelengths. Though they are more difficult to study because of the smaller

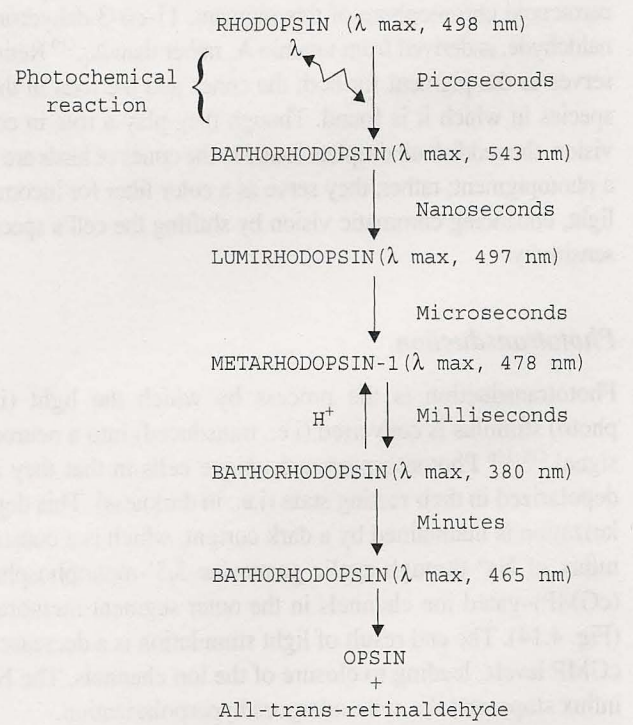

Figure 4.13. Stages in the bleaching of rhodopsin. Photoreaction is indicated by a curved line. Wavelengths (λ) are absorption maxima of rhodopsin intermediates, and the times shown are approximate decay times of the intermediates at physiologic temperature. Hypsorhodopsin (not shown) was discovered by illuminating rhodopsin at 4° K (λ max, 430 nm for hypsorhodopsin). The loss of color (bleaching) occurs when all-*trans*-retinaldehyde is reduced to all-*trans*-retinol (not shown). (Modified from Saari JC. Metabolism and photochemistry in the retina. In: Moses RA, Hart WM, eds. *Alder's Physiology of the Eye.* 8th ed. St. Louis: CV Mosby, 1987:356–372.)

Table 4.6 Spectral Sensitivity in Selected Species

Species	Cone Peak Sensitivity (nm)	Method of Determination[a]	References
Rat	510	1, 2	255
Cat[b]	454, 561	1	256
	450, 550	2	257
Dog[c]	429–435, 555	1, 2	46, 258, 259
Horse	428, 539	1,2	260, 261
Pig	439, 556	2	262
Cow	451, 555	2	263
Sheep	445, 552	2	263
Goat	443, 552	2	263
Guinea pig	429, 529	1, 2	264

[a]Method of determination: 1, behavioral; 2, electrophysiology; 3, microspectrophotometry.
[b]There are suggestions that the cat is trichromatic, with an additional class of cones peaking at 500 nm or 520 mm.[265,257]
[c]Three species of foxes also have similar values.[259]

number of cones and problems in extraction, cone pigments such as iodopsin[117] appear to be similar to rhodopsin in both structure and function.[119]

Another photopigment, which is found in the retinas of freshwater vertebrates such as fish and amphibians, is retinal$_2$.[116] The carotenoid chromophore of this pigment, 11-*cis*-3-dehydroretinaldehyde, is derived from vitamin A_2 rather than A_1.[119] Retinal$_2$ serves as the pigment for both the cones and the rods in those species in which it is found. Though they play a role in color vision, the reddish oil droplets found in the cones of birds are not a photopigment; rather, they serve as a color filter for incoming light, enhancing chromatic vision by shifting the cell's spectral sensitivity.

Phototransduction

Phototransduction is the process by which the light (i.e., photo) stimulus is converted (i.e., transduced) into a neuronal signal.[116–126] Photoreceptors are unique cells in that they are depolarized in their resting state (i.e., in darkness). This depolarization is maintained by a dark current, which is a constant influx of Na^+ through cyclic guanosine-3,5'-monophosphate (cGMP)–gated ion channels in the outer segment membrane (Fig. 4.14). The end result of light stimulation is a decrease in cGMP levels, leading to closure of the ion channels. The Na^+ influx stops, and the cell undergoes hyperpolarization.

The numerous steps in the cascade that ends in decreased cGMP levels are illustrated in Figure 4.15. One of the key molecules participating in this cascade is transducin (T), which is a G protein composed of three subunits (Tα, Tβ, and Tγ). In darkness, transducin is bound to guanosine diphosphate (T-GDP). Another important molecule is phosphodiesterase (PDE), which, when activated, hydrolyzes cGMP into GMP. In both transducin and PDE, γ is the inhibitory subunit.

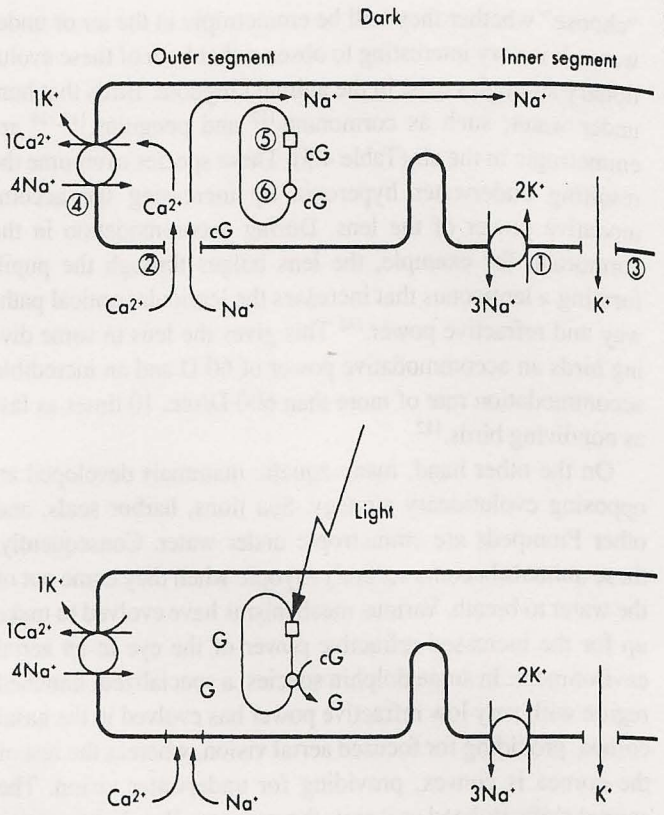

Figure 4.14. Ion flow through the rod outer and inner segments in light and dark. In dark (*top*), Na^+ extruded from the inner segment by a Na^+/K^+ pump (*1*) flows into the outer segment through a sodium channel (*2*) in the outer segment that is open when cGMP (*cG*) is bound. Na^+ returns to the inner segment where the main outward current is carried by K^+ (*3*). Ca^{2+} also enters the outer segment via the sodium channel (*2*); its cytoplasmic concentration is kept low by a $Na^+/Ca^{2+}:K^+$ exchanger (*4*). Following absorption of a photon by rhodopsin (*5*), a phosphodiesterase (*PDE*) (*6*) is activated that reduces the concentration of cGMP, allowing the Na^+ channel to close (*bottom*). Ca^{2+} extrusion by the exchanger (*4*) continues even though its entry is blocked by the closed Na^+ channels, producing a transient decrease in cytoplasmic Ca^{2+} concentration following stimulation. (Reprinted with permission from Saari JC. The biochemistry of sensory transduction in vertebrate photoreceptors. In: Hart WM Jr, ed. *Adler's Physiology of the Eye.* 9th ed. St. Louis: Mosby–Year Book, 1992:460–484.)

Following isomerization of the photopigment by light into R*, the bleached molecule changes its conformation and binds to transducin, forming a T-GDP-R* complex. This binding changes the affinity of the complex to GDP, which drops off and is replaced by guanosine triphosphate (GTP), leading to the formation of a T-GTP-R* complex. Additional affinity changes now occur, and the complex breaks up. R* falls off and is free to activate additional T-GDP molecules. Tβ-Tγ also falls off, thereby removing the inhibitory effect on the Tα-GTP complex. The activated complex migrates to the disc membrane, where it activates PDE by removing its γ inhibitory subunits. Because PDE contains two γ subunits, two Tα-GTP complexes are required for complete PDE activation. The activated PDE hydrolyzes cGMP into GMP, resulting in decreased cGMP levels (from 60 μM to < 10 μM) and leading to closure of the Na^+ channels and cell hyperpolarization. It has been calculated that the absorption of a single photon may lead to closure of 4% of the outer segment channels.

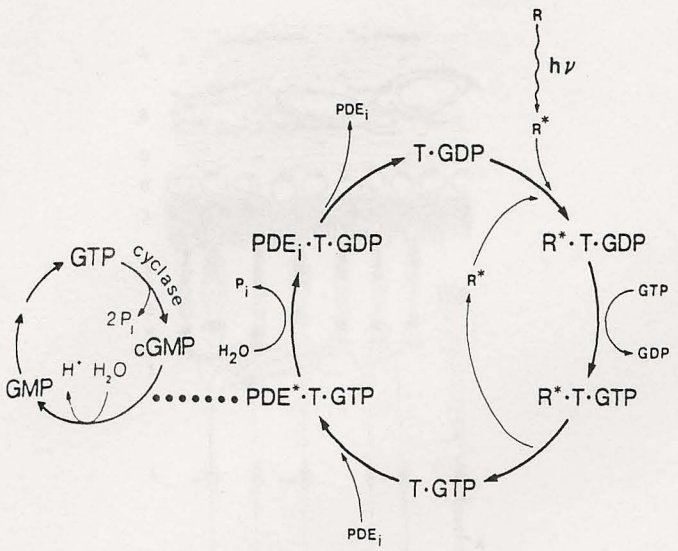

Figure 4.15. The cGMP cascade of phototransduction. Light causes activation of rhodopsin (*R*). Activated rhodopsin (*R**) binds to the transducin GDP (T-GDP) complex, leading to reduction in affinity to GDP. GDP is replaced by GTP, forming an R*-T-GTP complex, leading to dissociation of R*. The remaining T-GTP complex activates phosphodiesterase (PDE*), an enzyme that hydrolyzes cGMP into GMP. The reduction in cGMP levels leads to closure of the Na^+ channels and hyperpolarization. (Reprinted with permission from Falk G. Retinal physiology. In: Heckenlively JR, Arden GB, eds. *Principles and Practice of Clinical Electrophysiology of Vision.* St. Louis: Mosby–Year Book 1991:69–84.)

There are two potential amplification steps in the phototransduction reaction. Each R* molecule may activate 500 T-GDP complexes, and each activated PDE molecule may hydrolyze 800 cGMP molecules. Taking into account the two Tα-GTP complexes required for complete PDE activation, the net result is amplification of the signal by a factor of 10^5. This signal gain makes it possible to record electrical currents generated in rods following the absorption of a single photon. Cones, on the other hand, need to absorb 40 times as many photons to generate the same current, thus accounting for their decreased light sensitivity.

The cascade is eventually turned off by an equally complex chain reaction. Tα-GTP is hydrolyzed into Tα-GDP, thus freeing up the PDE inhibitory γ subunit. The γ subunit rebinds to PDE, thus stopping the hydrolysis of cGMP, and Tα-GDP rebinds to Tβ-Tγ, thus deactivating the transducin molecule. At the same time, the enzyme rhodopsin kinase phosphorylyates R*. This phosphorylation increases the affinity of rhodopsin to arrestin, and their binding prevents further transducin activation by R*. Meanwhile, guanylate cyclase activity in the outer segment increases, which leads to synthesis of cGMP. As its concentration rises, it eventually causes reopening of the channel and photoreceptor depolarization.

Understanding of the phototransduction process has enabled us to gain insight into the pathogenesis of several types of photoreceptor dysplasias and degenerations. Rod-cone dysplasia type 1 in Irish Setters has been shown to be caused by a mutation in one DNA base in the gene coding for the β subunit of PDE. The resulting defect prevents PDE from hydrolyzing cGMP, resulting in cGMP buildup and leading to cell death.[127] Mutations in rhodopsin have been shown to cause progressive retinal degeneration in the English Mastiff, making it a naturally occurring animal model for some forms of human retinitis pigmentosa.[128] Photoreceptor dysplasia in Miniature Schnauzers[129] and early retinal degeneration in the Norwegian Elkhound[130] may likewise be the result of a specific defect in one of the phototransduction molecules. The genetics of canine retinal diseases are discussed extensively in Chapter 21.

Synthesis and Regeneration of the Visual Pigments

As indicated earlier, light stimulation causes bleaching of the photopigment; conversely, the pigment undergoes regeneration during darkness. Prolonged and intense light stimulation will eventually bleach all of the retinal photopigment. Prolonged and total darkness will enable all of the photopigment to regenerate. At intermediate levels of illumination, between these two extremes, a dynamic and continuous process of bleaching and regeneration occurs, leading to equilibrium and contributing to adaptation to existing light levels.[118,119,134–138]

The first step in the photopigment regeneration process, as outlined in Figure 4.16, is reduction of all-*trans*-retinal to

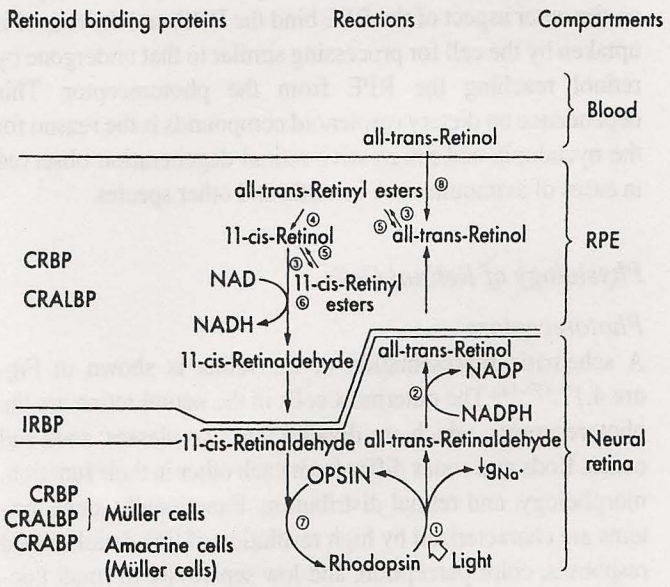

Figure 4.16. Regeneration of photopigment. Reactions 3 to 6 occur in the RPE; reactions 1, 2, and 7 occur in the photoreceptor. **1.** Light is absorbed by rhodopsin, causing bleaching of the pigment and formation of all-*trans*-retinaldehyde. **2.** All-*trans*-retinaldehyde is reduced into all-*trans*-retinol, which is transported to the RPE using an interstitial retinoid-binding protein (IRBP). **3.** In the RPE, retinol is esterified into all-*trans*-retinyl. **4.** The ester undergoes hydroisomerization into 11-*cis*-retinol. **5.** Retinyl esters are hydrolyzed. **6.** 11-*cis*-retinol is oxidized into 11-*cis*-retinaldehyde, which is transported by IRBP back to the photoreceptor. **7.** The chromophore and pigment form rhodopsin. **8.** All-*trans*-retinol may also reach the RPE from the liver via systemic circulation. Additional retinoid-binding proteins located in amacrine and Müller cells include cellular retinol–binding protein (CRBP), cellular retinoic acid–binding protein (CRABP), and cellular retinaldehyde–binding protein (CRALBP). (Reprinted with permission from Saari JC. The biochemistry of sensory transduction in vertebrate photoreceptors. In: Hart WM Jr, ed. *Adler's Physiology of the Eye.* 9th ed. St. Louis: Mosby-Year Book, 1992:460–484.)

all-*trans*-retinol. This is the only step of the regeneration process that occurs in the outer segment of the photoreceptor; the rest occurs in the retinal pigment epithelium (RPE). Because of compartmentalization of the enzymes, virtually no pigment regeneration occurs in mammalian neural retinas that have been detached from the RPE.

Retinol diffuses out of the outer segment into the subretinal space and makes its way to the RPE. An interstitial retinoid-binding protein (IRBP) plays a role in the intercellular movement of retinol, though the exact mechanism of diffusion or transport has yet to be elucidated. Once inside the RPE, the retinol is esterified into retinyl, which is eventually isomerized into 11-*cis*-retinaldehyde. This retinoid is translocated from the RPE back to the outer segment (again using IRBP), where it binds with opsin (synthesized in the inner segment) to reform rhodopsin.

Obviously, bleached pigment is not the only substrate for 11-*cis*-retinaldehyde synthesis in the RPE. Dietary uptake still remains the main source of substrates. Carotenoid compounds in food are oxidized into vitamin A (retinol) in the walls of the small intestine. The vitamin is then esterified and transported to the liver, where it is bound to retinol-binding protein (RBP). Retinol-bound RBP is transported through the bloodstream and eventually reaches the choriocapillaris. Specific receptors on the outer aspect of the RPE bind the RBP, and the retinol is uptaken by the cell for processing similar to that undergone by retinol reaching the RPE from the photoreceptor. This dependence on dietary carotenoid compounds is the reason for the nyctalopia and progressive retinal degeneration observed in cases of avitaminosis A in cattle and other species.

Physiology of Retinal Cells

Photoreceptors

A schematic representation of the retina is shown in Figure 4.17.[139–142] The outermost cells in the neural retina are the photoreceptors, which are divided into two classes: rods and cones. Rods and cones differ from each other in their function, morphology, and retinal distribution. Functionally, cone systems are characterized by high resolution of fine details, rapid responses, color perception, and low sensitivity to small fluctuations in light intensity. Rod systems are characterized by poor visual resolution and no color perception, but they are extremely sensitive to changes in light levels and detection of motion. Therefore, cones are particularly suitable for daylight (i.e., photopic) vision, whereas rods contribute mostly to dim-light (i.e., scotopic) vision.

The functional differences between rods and cones as well as the animal's lifestyle dictate the retinal distribution (Table 4.7). In most mammalian species (including humans), rods outnumber cones, but nocturnal animals have a greater proportion of rods and diurnal animals a greater proportion of cones. Likewise, predators that depend on precisely locating their prey and species that display bright colors for sexual purposes have relatively more cones; prey species that depend on detecting peripheral motion (by predators) when grazing have

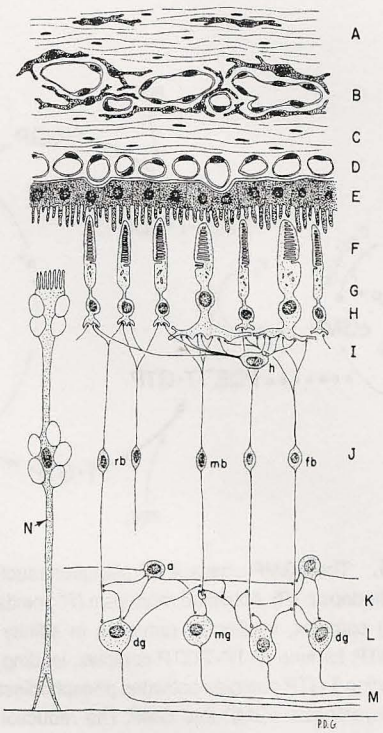

Figure 4.17. Organization of the retina and choroid. The rod spherules have synaptic contact with rod bipolar (*rb*) cells, which in turn have axosomatic and axodendritic synaptic contact with diffuse ganglion cells (*dg*). The cone pedicles have synaptic contacts with a single midget bipolar cell (*mb*), which connects a single cone to a single midget ganglion cell (*mg*) and with flat bipolar cells (*fb*), which connect several cones via axosomatic and axodendritic synapses with diffuse ganglion cells (*dg*). Horizontal cells (*h*) contact rod spherules and cone pedicles. Amacrine cells (*a*) contact the dendrites of all bipolar cells and both types of ganglion cells. *A,* suprachoroid layer; *B,* vessel layer; *C,* connective tissue in lieu of tapetum lucidum (the pigment epithelial cells lack pigment at the level of the tapetum); *D,* choriocapillary layer; *E,* pigment epithelium; *F,* layer of rods and cones; *G,* outer limiting membrane; *H,* outer nuclear layer; *I,* outer plexiform (synaptic) layer; *J,* inner nuclear layer; *K,* inner plexiform (synaptic) layer; *L,* ganglion cell layer; *M,* optic nerve fiber layer adjacent to the inner limiting membrane; *N,* supporting glial cells (Müller cells). (Reprinted with permission from Dellmann HD, Brown EM. Textbook of veterinary histology. Philadelphia: Lea & Febiger, 1976.)

more rods. There are also regional differences in photoreceptor concentration. In most mammalian and avian species, the retina contains a specialized region that is characterized by a high density of cones. This area subserves the highest-resolution vision of the animal, though as Table 4.7 demonstrates, the concentration of the cones in this region can vary greatly between species. In diurnal species possessing high acuity, such as humans and many avian species, this region is called the *fovea.* The fovea is actually a retinal depression (or pit) that contains no rods, thus permitting more dense packing of cones. In most other species, this region is called the *area centralis.* Though this area has the highest concentration cones, in nocturnal species, such as the cat, rods outnumber the cones even in the *area centralis* (Table 4.7). Thus, the animal acquires higher scotopic sensitivity, albeit sacrificing visual acuity. The fovea and area centralis are surrounded, respectively, by a *macula* and *visual streak,* which are regions

Table 4.7 Photoreceptor Concentration in Cats and Humans

	Human	Cat
Number of rods ($\times 10^6$)	110–125	
Number of cones ($\times 10^6$)	6.5	
Maximal cone concentration (per mm^2)	199,000	27,000
Maximal rod concentration (per mm^2)	160,000	460,000
Cone concentration at ora serrata (per mm^2)	5,000	<3,000
Rod concentration at ora serrata (per mm^2)	40,000	250,000
Rod to cone ratio (area centralis)	No rods	11:1
Rod to cone ratio (ora serrata)	50:1	100:1

Source of data for humans: Osterberg G. Topography of the layer of rods and cones in the human retina. *Acta Ophthal.* 1935;6 (suppl):1–103. Source of data for cats: Steinberg RH, Reid M, Lacy PL. The distribution of rods and cones in the retina of the cat (*Felis domesticus*). *J Comp Neurol* 1973;148:229–248.

of decreasing cone density. The concentration of cones continues decreasing with retinal eccentricity, and in most species, the more peripheral retina contains virtually no cones; rods, which are used for motion detection and scotopic vision, populate this region.

Morphologically, photoreceptors are divided into four parts:

1. The outer segment,
2. The inner segment,
3. The nucleus, and
4. The synaptic terminal.

The outer segment is the part of the cell where phototransduction, as well as disc formation and shedding, occurs. The outer segments are connected by a cilium to the inner segment, which is an area rich in mitochondria (ellipsoid), Golgi apparatus, and endoplasmic reticulum (myoid). Opsin is synthesized in the endoplasmic reticulum of the inner segment and is transported through the cilium to the base of the outer segment, where it is incorporated into the outer segment's plasma membrane, which undergoes invagination to form a new disc. In rods, the disc detaches from the membrane and the outer segment is filled with a stack of free-floating discs. In cones, the disc remains part of the membrane, thus exposing it to a greater supply of chromophore (relative to the disconnected rod disc). As new discs are formed at the base of the outer segment, older discs are displaced toward the distal end, from which they will eventually be shed and then phagocytized by the RPE in a diurnal cycle (following light onset). Experiments in which radiolabeled prescursors have been injected into the inner segments show that labeled proteins appear at the outer segment base within 2 hours; another 8 to 10 weeks pass before the discs containing these proteins are shed and phagocytized.

Morphologic differences between rods and cones are discussed in great detail in Chapter 2. Some of these differences are a direct consequence (or cause) of the functional differences between the two types of photoreceptors. The rod outer segment is long and thin, which permits a high density of rods in the periphery, thus increasing the probability of absorbing scarce photons at night. Cones are two to three times thicker than rods, except in the central retina, where they are also thin to permit a high receptor density. Rod axons are thin, which is consistent with the cell's slow response to light, whereas cone axons are thick, enabling faster conduction.

The nuclei of the photoreceptors constitute the outer nuclear layer (ONL) of the retina, which is separated from the inner segments by an outer limiting membrane. The axonal terminals of the rods and cones are called spherules and pedicles, respectively. Their synaptic invaginations synapse with dendritic processes of bipolar and horizontal cells at the outer plexiform layer (OPL).

Horizontal and Bipolar Cells

The soma of both the horizontal and bipolar cells are located in the inner nuclear layer (INL).[143–145] Horizontal cells occupy the outermost layer of the INL and synapse almost exclusively in the OPL. Physiologically, horizontal cells are divided into two types. Luminous (L) type horizontal cells hyperpolarize in response to light stimulation; these cells synapse with rods or a single class of cones. Color (C) type horizontal cells, which synapse with more than one cone class, respond by hyperpolarizing or depolarizing in a wavelength-dependent manner. The role of horizontal cells in the visual process is poorly understood, but it is hypothesized they integrate responses from photoreceptors and increase sensitivity to changes in illumination (i.e., contrast) and color, which is a phenomenon termed *lateral inhibition.*

Bipolar cell somata are also located in the INL. Their dendrites synapse with photoreceptors and horizontal cells in the OPL, and their axons terminate in the inner plexiform layer (IPL), where they synapse with amacrine and ganglion cells. Therefore, the function of bipolar cells is to serve as *second-order* neurons of the retina, connecting, directly or indirectly, the *first-order* (photoreceptors) and *third-order* (ganglion cells) neurons. A bipolar cell receptive field is the sum of the receptive fields of the photoreceptors to which it synapses. A rod bipolar cell can receive input from scores of rods, constituting a converging pathway with a large receptive field (Fig. 4.18). Such a pathway enhances scotopic vision, because the absorption of just one photon anywhere in the receptive field is sufficient to stimulate the rod bipolar pathway. Cone bipolar cells are divided into different types, based on their function and retinal location. Cone bipolars in the peripheral retina are called diffuse bipolars, functioning much like rod bipolars, converging input from several cones. Foveal cones, on the other hand, are characterized by a diverging pathway, in which one cone outputs to two or more *midget bipolar* cells.

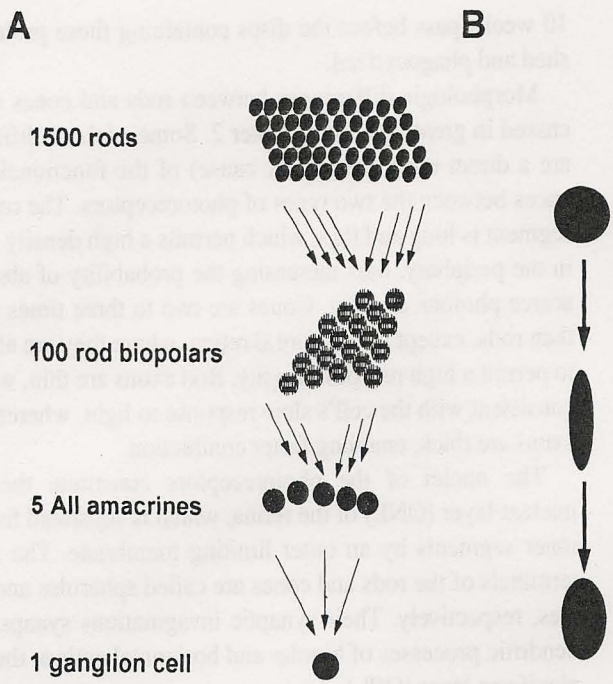

Figure 4.18. Schematic representation of the rod and cone pathways. **A.** The output of numerous rods converges through several bipolar cells and a smaller number of amacrine cells and onto one ganglion cell. This allows the rod system to enhance the response to a weak stimulus (scotopic vision). **B.** The cone pathway is characterized by a minimal cone–bipolar–ganglion cell ratio, which allows for maximum discrimination (high acuity), fast transmission, and other characteristics of the cone system.

Because each midget bipolar cell inputs from just one cone, it will have a much smaller receptive field. This feature, combined with the antagonistic center-surround properties of the receptive fields (see subsequent discussion), contributes to the higher visual resolution that characterizes the cone systems.

Bipolar cells may also be classified on the basis of the response generated by light stimulation of their central receptive field. "ON-center" cells depolarize when their center is stimulated by light, whereas "OFF-center" cells hyperpolarize in response to central stimulation (Fig. 4.19). The peripheral (i.e., toroidal) receptive field of these cells is antagonistic to the center. For example, an ON-center bipolar cell will also depolarize when its periphery is "stimulated" by darkness; therefore, a high degree of contrast between central and toroidal stimulants will cause an enhanced response of the bipolar cells. This is one possible mechanism for increased contrast sensitivity, which is essential for high-resolution vision. Conversely, light stimulation of both the center and periphery of an ON-center bipolar cell will result in a decreased response by the cell, because the response of the periphery will inhibit the response of the center.

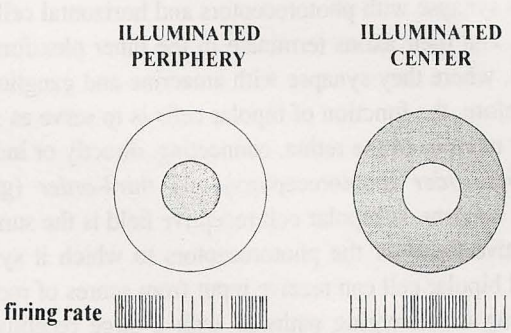

Figure 4.19. Antagonism of central and peripheral receptive fields of a bipolar or ganglion cell. The concentric receptive field has a central region in which stimulation by light has one effect on a cell's firing and a surrounding region in which that stimulation has an opposite effect. In the case of an ON-center cell (*on the right*), stimulation of the center causes increased activity, whereas stimulation of the surround causes decreased activity. In an off-center cell (*on the left*), stimulation of the center will cause decreased activity, whereas stimulation of the surround will increase the cell's activity. (Modified from Masland RH. The functional architecture of the retina. *Sci Am* 1986;255:102–111.)

Other INL cells

The INL is populated by three more types of cells (in addition to displaced ganglion cells).[146–148] Little is known about the interplexiform neuron, which is a cell that inputs from the IPL and outputs to the OPL. Interplexiform neurons have been found in several species, including the cat and primates. They synapse directly with amacrine and bipolar cells and indirectly with photoreceptors; therefore, they may modulate photoreceptor output as a function of IPL activity.

The second class of cells found in the INL is Müller cells, which are ependymoglial cells (i.e., they have both a structural support and a metabolic role). Long processes of the Müller cells extend from the INL toward the inner and outer retina, where they join to form both the inner and outer limiting membranes. Thus, the Müller cells can be regarded as retinal radial cells, extending through its entire thickness and lending it architectural support. Müller cells also fill in all gaps in the neuroretina not occupied by other elements, and their outer processes surround the individual photoreceptors, isolating them from each other and keeping them properly aligned.

Metabolically, Müller cells store glycogen, which helps to protect the retina from fluctuations in systemic glucose levels. These cells also help to maintain the anionic balance in the retina by uptaking the K^+ secreted by the photoreceptors. Müller cells remove the excess K^+ from the retina, thus acting

as a "K^+ sink" and contributing to generation of the b-wave of the electroretinogram. Müller cells are also active in uptake and metabolism of neurotransmitters (including GABA, dopamine and glutamate) and in retinal phagocytosis following injury.

Amacrine cells, which are the third type of INL cells, occupy the innermost tier of this layer (though displaced amacrine cells are also found in the ganglion cell layer). More than 20 types of amacrine cells have been identified in the mammalian retina. All are characterized by the fact they do not possess any recognizable axons, and they are classified by their location in the INL strata, by the size and shape of their dendritic tree (e.g., linear, beads, starburst), and by the neurotransmitter they release (e.g., acetylcholine, serotonin, dopamine).

Amacrine cells form a very complex and confusing network of connections with bipolar axon terminals, with ganglion cell dendrites, and with other types of amacrine cells. Their responses increase the sensitivity of ganglion cells to changes in illumination, thus contributing to motion, direction, and contrast detection. Therefore, it can be said that amacrine and horizontal cells play a similar role (i.e., lateral processing of the signal) in the IPL and OPL, respectively. Figure 4.20 shows, as an example, how amacrine cells affect the antagonism of the peripheral receptive field of ganglion cells. Signals from the central receptive field are relayed from the photoreceptors through bipolar cells and directly to the ganglion cells. Signals from the peripheral field are relayed through bipolar cells to amacrine cells, which through lateral inhibition affect an "off-surround" response. In birds and other nonmammalian species, amacrine cells are the target cells of centrifugal fibers from higher cortical centers, which further modulate the retinal responsiveness.

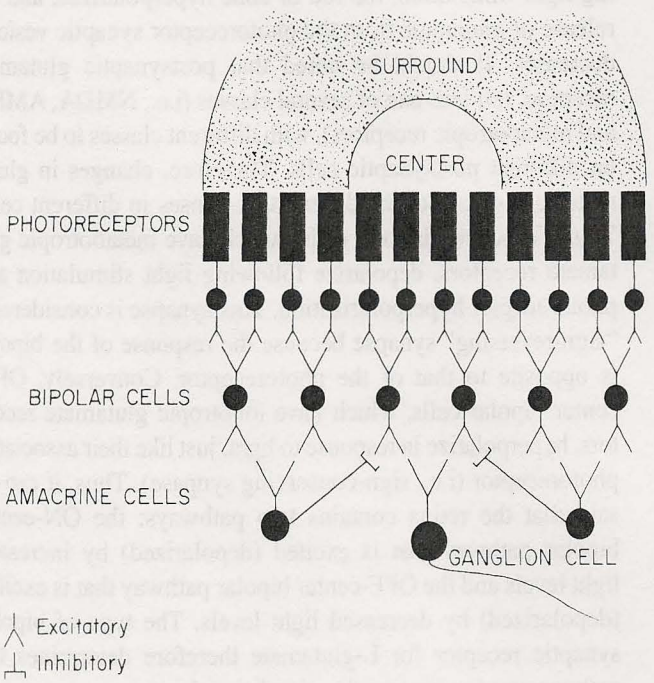

Figure 4.20. Center-surround organization of the receptive field. Photoreceptors activated by stimuli in the center stimulate bipolar cells, which in turn excite ganglion cells. Photoreceptors activated by stimuli in the surround stimulate bipolar cells, which in turn excite amacrine cells. Amacrine cells will inhibit ganglion cells. Horizontal cells are involved with the center-surround receptive field concept as well. (Modified from Dowling JE, Boycott BB. Organization of the primate retina: electron microscopy. *Proc R Soc Lond B Biol Sci* 1966;166:80–111.)

Ganglion Cells

All information processed by the retina eventually converges on the ganglion cells, the innermost cell layer in the retina, and its final output neuron.[149–154] Though much signal processing has occurred in the bipolar, horizontal, and amacrine cells, the ganglion cells are the most complex information processing cells in the retina. There are several ways to categorize ganglion cells:

1. *Size and retinal location.* Midget (β) ganglion cells are located in the central retina, and the small size of these cells permits denser packing, thus allowing each to input from fewer cones and bipolars. In species with high-resolution vision, the functional ratio of bipolar cells to β ganglion cells approaches 1:1 in the foveal region. Larger (α) ganglion cells are found in the more peripheral retina, and their large size permits convergence of input from many amacrine cells. Axonal diameter is proportional to the somata size; therefore, central β cells possess smaller-diameter axons than peripheral α cells.
2. *Input cell.* In mammals, most ganglion cells input directly from bipolar cells. Therefore, the receptive fields of these cells function in a manner similar to those of their associated bipolar cells (i.e., ON-center-OFF-surround, or vice versa). These cells are called X cells. Other ganglion cells (i.e., Y type) input mainly from amacrine cells. Conversely, ganglion cells can also be classified on the basis of the cell to which they output. M ganglion cells synapse in the magnocellular layers of the dorsal lateral geniculate nucleus (DLGN), whereas P ganglion cells terminate in the parvocellular layers.
3. *Information processing.* The luminance (magno) pathway both processes and relays information regarding changes in light levels and motion. The resolution (parvo) pathway processes information pertaining to fine details and the color of the stimulus.

Obviously, these classifications are not exclusive; rather, they constitute different descriptions of the same cells. Beta, X, or parvo cells are numerous, small, and centrally located; these cells input from cone systems and bipolar cells. The small diameter and therefore slower conducting axons of these cells transmit information on stimulus color (i.e., wavelength) and fine detail. Alpha, Y, or magno cells are fewer in number, larger in size, and peripherally located; these cells input from rod systems and amacrine cells. Their larger diameter and faster conducting axons relay information on subtle changes in illumination levels (i.e., contrast) and stimulus motion (i.e., temporal resolution). These cells are characterized by transient (i.e., phasic) response, as compared to the more sustained (i.e., tonic) response of the β cells. In the cat, 55% of the ganglion cells are β cells; α cells constitute only

3% to 5% of the ganglion cell population. Most of the axons of both types of cells terminate in the DLGN, with only a few collateral fibers synapsing in the superior colliculus.

There are numerous other types of ganglion cells in the mammalian retina as well. The W, or γ, cells have small somata and axons, but their response to light can be either sustained or transient. They serve in cone systems and contribute to high-resolution photopic vision. Half of these cells project to the superior colliculus rather than to the DLGN, but little is known about their circuitry (or that of the other ganglion cell classes).

Ganglion cells usually have an intrinsic, basal firing rate in darkness. Changes in the number of spikes in response to light or darkness are similar to those of the corresponding ON or OFF bipolar cells with which they synapse in the IPL. The resulting action potentials allow the signal generated by the ganglion cells to be propagated through their axons, which constitute the optic nerve fibers, all the way to the (relatively) distant lateral geniculate nucleus.

RETINAL SYNAPSES AND NEUROTRANSMITTERS

Obviously, with so many different types and classes of retinal cells, there are numerous potential pathways for transferring a signal from the photoreceptors to the ganglion cell axons.[144,155–159] Furthermore, new cell types, projections, and synapses are constantly being discovered.

The synaptic terminal of a mammalian cone, which is large and flat, is called a pedicle. The rod terminal, which is rounder and smaller, is called a spherule. Both pedicles and spherules contain mitochondria, synaptic vesicles, and synaptic ribbons. Both also contain invaginations, in which one bipolar and two horizontal cells (that together constitute the synaptic triad) synapse. Photoreceptors usually have more than one synaptic invagination. A typical rod synapses with two triads, and a cone may have multiple contacts with three or more bipolar cells. In addition, photoreceptors send out processes to neighboring spherules and pedicles, thus providing for direct electrical junctions between photoreceptors. Because of these couplings, current can spread from one rod, for example, to adjacent rods. Therefore, the stimulation of a single rod can activate other photoreceptors, resulting (once again) in the large receptive field that converges on the bipolar cell. The junctions also allow rod signals to be transmitted through cone pathways.

The two basic pathways of the retina are the cone pathway and the rod pathway (Fig. 4.18). The cone pathway typically is short, involving only two types of synapses: cone to bipolar cell and bipolar to ganglion cell. As mentioned, in the central retina this is a diverging pathway, with one cone synapsing to two bipolar cells, thereby transmitting the signal to an ON-center and an OFF-center ganglion cell. The anatomic and physiologic features of this pathway as well as their implications for cone-mediated vision have already been discussed. To recap briefly, the various types of opsins in cone outer segments contribute to color vision; the dense packing of cones in the central retina, the minimal cone–bipolar–ganglion cell ratio, and the small size of the receptive fields all contribute to a small-size receptive field essential to high-resolution vision. The axonal anatomy of the cones, combined with the lack of lateral processing by amacrine cells, contribute to fast conduction and quick response to light flickers.

The rod pathway features a greater number of permutations (Fig. 4.17). As noted, rod spherules synapse to cone pedicles, and using this electrical synapse, rod signals can be relayed by the cone pathway, resulting in a greater range of illumination for the cone pathway. Rods also synapse with rod bipolar cells and, through them, with AII amacrine cells. In turn, these either synapse with the various ganglion cells or feedback to bipolar cells and contribute to lateral processing of the signal. The converging nature of the rod to bipolar to amacrine cell to ganglion cell pathway (Fig. 4.18) is the basis for many of its physiologic characteristics. It has been estimated that up to 1,500 rods may converge on 100 rod bipolar cells, which synapse with 5 amacrine cells, eventually converging on a single ON, β ganglion cell. This large, summated receptive field represented by each ganglion cell sensitizes it to motion, direction, contrast, and low levels of illumination.

Because photoreceptors are depolarized in the dark, they are constantly releasing an excitatory neurotransmitter. This neurotransmitter is L-glutamate, which serves as the "vertical neurotransmitter" of the retina, relaying information from the photoreceptors, via the bipolars, to the ganglion cells. Following light stimulation, the rod or cone hyperpolarizes, and the release of glutamate from the photoreceptor synaptic vesicles decreases. It should be noted that postsynaptic glutamate receptors fall into one of several classes (i.e., NMDA, AMPA, and metabotropic receptors), with different classes to be found on different postsynaptic cells. Therefore, changes in glutamate release can evoke different responses in different cells. Thus, ON-center bipolar cells, which have metabotropic glutamate receptors, depolarize following light stimulation and photoreceptor hyperpolarization. This synapse is considered a "sign-reversing" synapse because the response of the bipolar is opposite to that of the photoreceptor. Conversely, OFF-center bipolar cells, which have ionotropic glutamate receptors, hyperpolarize in response to light, just like their associated photoreceptor (i.e., sign-conserving synpase). Thus, it can be said that the retina contains two pathways: the ON-center bipolar pathway that is excited (depolarized) by increased light levels and the OFF-center bipolar pathway that is excited (depolarized) by decreased light levels. The type of bipolar synaptic receptor for L-glutamate therefore determines the pathway used to process the visual signal.

Acetylcholine is another excitatory transmitter found in the retina. It is released by starburst (i.e., cholinergic) amacrine cells. By definition, an excitatory transmitter causes depolarization in the cell with which it synapses, which in this case is a ganglion cell. Because amacrine cells do not possess an axon, release of acetylcholine occurs at an isolated and localized dendritic site, beyond which the transmitter does not

spread. As the stimulus moves across the receptive field, acetylcholine is released by additional dendrites. Progression of the depolarizing wave across the ganglion cell makes that cell sensitive to the direction of the stimulus.

The main inhibitory transmitter in the retina is γ-aminobutyric acid (GABA). As such, it is used mainly for lateral processing of the signal by both horizontal and amacrine cells, which have an inhibitory function in the OPL and IPL, respectively. Together with glycine, GABA acts to inhibit ganglion cells by opening their Cl^- channels. Dopamine and serotonin (indoleamine) are two more transmitters found in amacrine cells, and they probably play an important role in signal modulation. Dopaminergic amacrine cells, for example, synapse only with other amacrine cells and not with ganglion or bipolar cells. As in the case of glutamate, it should be noted some of these transmitters can activate several classes of receptors. Acetylcholine can bind to muscarinic and nicotinic receptors, and dopamine can bind to D_1 and D_2 receptors, thus making further signal refinements possible. That numerous other transmitters (mostly neuroactive peptides such as enkephalin and glucagon) have been found in the retina as well as the discovery that interplexiform neurons also secrete inhibitory transmitters make us realize there is still much to learn about the pathways and circuits in the retina.

From Retina to Visual Cortex

As noted, the axons of the retinal ganglion cells constitute the optic nerve fibers.[160–168] These axons converge at the optic disc, where they are joined in bundles to form the nerve. Ganglion cells are the only retinal neurons that generate an action potential, and myelination, which in some species (e.g., the dog) starts at this level, provides for rapid saltatory conduction of the electrical signal. All of the neuronal processing of the visual signal that has so far taken place in the retina, including information about stimulus size, contrast, color, movement, and location, is coded "merely" as alterations in the firing rate of the ganglion cells!

Ganglion cells transmit visual information as a cohort of individual signals generated by multiple cells representing different points in the visual field. Therefore, a single object will generate numerous signals that are transmitted in parallel pathways by many ganglion cells. Consequently, arrangement of the ganglion cell axons within the optic nerve is not random. Instead, the fibers are arranged in a retinotopic manner, meaning that the precise spatial arrangement of the retina is maintained within the nerve. Fibers from the superior retina form the superior half of the optic disc, and fibers from the inferior retina form the inferior half. This precise arrangement is a condition for the subsequent accurate projection of the visual field in both the DLGN and the visual cortex.

As the nerve approaches the chiasm, the location of fibers within the nerve gradually shifts in preparation for decussation at the optic chiasm (Fig. 4.21). Generally, fibers from the temporal retina remain on the ipsilateral side of the brain, and fibers from the nasal retina cross over to the contralateral side. The amount of decussation, however, varies between species,

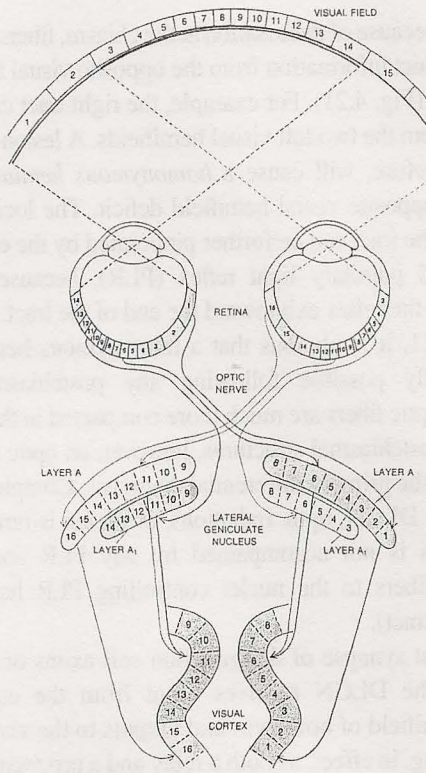

Figure 4.21. Projection of the visual field onto retina, lateral geniculate nucleus (LGN), and visual cortex. The visual field is divided into 16 segments. An inverted image of the field is projected onto the retina by the reversing lens. The left eye does not see the extreme right side of the total field (segments 15 and 16), and the right eye does not see the extreme left side of the total field (segments 1 and 2). Segments 3 to 14 are seen by both eyes (binocular vision). Because of decussation at the chiasm, the right LGN receives the temporal hemifield of the right eye (segments 3–8) and the nasal hemifield of the left eye (segments 1–8). The left LGN receives the nasal hemifield of the right eye (segments 9–16) and the temporal hemifield of the left eye (segments 9–14). The representation in the various layers of the LGN (only two layers, A and A1, are shown) are in register so that a vertical penetration will represent the same point in the visual field of both eyes. The two sets of representation are fused in the cortex. (Reprinted with permission from Guillery RW. Visual pathways in albinos. *Sci Am* 1974;240:44–54.)

perhaps representing a broad evolutionary scale. In birds, all the fibers cross over to the contralateral side. Likewise, many amphibian and reptilian species have complete crossover; in others, as little as 5% of the fibers stay on the ipsilateral side. In the horse, 15% of the fibers stay on the ipsilateral side, as do 25% in the dog and 33% in the cat. In humans, only half of the fibers cross over. Partial crossover of fibers allows both hemispheres to continue receiving visual input even when one retina or optic nerve has been completely destroyed, thus enabling the animal to maintain better physiologic function and correlation with other sensory input. Because the topography of decussating fibers is characterized by spatial precision, lesions in different areas of the chiasm (or the optic nerve) will cause specific visual deficits; these are discussed in more detail in Chapter 29.

The optic tract runs from the optic chiasm to the DLGN. Several other tracts (discussed later) exit the optic tract before it reaches the DLGN and relay visual information to extracortical

centers. Because of decussation at the chiasm, fibers of the optic tract conduct information from the opposite visual hemifield of both eyes (Fig. 4.21). For example, the right tract carries information from the two left visual hemifields. A lesion in the optic tract, therefore, will cause a *homonymous hemianopia,* or a bilateral opposite visual hemifield deficit. The location of the lesion in the tract can be further pinpointed by the extent of the consensual pupillary light reflex (PLR), because the fibers mediating the reflex exit toward the end of the tract. Looking at Figure 4.21, it is obvious that a homonymous hemianopia is theoretically possible following any postchiasmal lesion. Because optic fibers are much more compacted in the tract than in other postchiasmal structures, however, an optic tract lesion should be the primary differential diagnosis. Complete destruction of the DLGN, optic radiations, or cortex is rare, and such destruction is not accompanied by any PLR abnormalities (because fibers to the nuclei controlling PLR have already exited the tract).

The first synapse of the ganglion cell axons occurs in the DLGN. The DLGN receives input from the contralateral visual hemifield of both eyes and outputs to the visual cortex, thus serving, in effect, as both a relay and a processing station. In most species with both a ventral lateral geniculate nucleus (VLGN) and a DLGN, the optic tract terminates in the DLGN. Primates do not have a VLGN; therefore, the optic tract synapses in the lateral geniculate nucleus (LGN). The DLGN of the cat and the LGN of the macaque monkey have been studied extensively, and though anatomic differences do exist between the two (e.g., the cat DLGN comprises four layers and the macaque LGN comprises six), the functional principles of both are very similar and are discussed here as one.

The basis for the functional architecture of the LGN is its retinotopic organization. Each layer of the LGN constitutes a precise map of the contralateral visual hemifield. Thus, in the cat, uncrossed fibers from the temporal hemifield of the right eye terminate in layers A_1 and C_1 of the right DLGN; fibers crossing over from the nasal hemifield of the left eye terminate in layers A and C of the right DLGN. Furthermore, the four resulting maps are in register, which means that if an electrode vertically penetrated the four layers, the cells it would pass through all represent the same point in the visual field of both retinas (Fig. 4.21). Thus, the path of the electrode would represent a vertical line of projection of that point onto the DLGN.

The maps of the DLGN preserve more than just topography of the visual field. They also reflect the physiologic processing of the signal that has occurred in the retina. Thus, layers A and A_1 of the cat DLGN input from X-type ganglion cells, whereas layers C and C_1 input from Y-type cells. Therefore, the four cells through which the above-mentioned line of projection passes receive both X- and Y-type data about an identical receptive field in both eyes. This provides the basis for the merging of visual information that occurs in the cortex.

The actual synapses between the ganglion cell axons and the dendrites of the thalamic cells take place in a structure termed the *synaptic glomerulus.* The thalamic cells may be of two types: interneurons, which provide for some signal processing, or projecting cells. Axons of these projecting cells exit the DLGN and form the optic radiations, and these axons relay the visual signal from the DLGN to the primary visual cortex, where they synapse. In some species, these radiations also contain axons that descend from the visual cortex to the DLGN and superior colliculus.

Several other pathways also relay visual information from the retina to extracortical centers. Fibers exiting the optic tract relay information to the pretectal nucleus, and through it to the Edinger-Westphal nucleus; these nuclei control the PLR. Other optic tract fibers synapse in the superior colliculus, which controls saccadic eye movement and also inputs information from other sensory organs (i.e., ears and spinal cord) and is therefore involved in correlation of sensory information. In addition, information from the retina reaches additional nuclei involved in controlling optokinetic reflexes, circadian rhythms, and endocrinic activity of the hypothalamus.

Visual Cortex

Location of the Primary Visual Cortex

Mapping of the visual cortex in humans was first performed during World War I by Holmes,[169] who studied deficits in wounded British soldiers suffering from brain injuries. The first animal in which the visual cortex was mapped was the cat, studied by Talbot in 1940.[170] Since then, the visual cortex has been mapped in more than a dozen species of laboratory animals,[171–184] the sheep,[185] and the dog.[186–184]

Early work on the visual cortex in humans and the cat revealed that the primary visual area (so called because it is the main recipient of DLGN output) occupies the region known as Brodmann's area 17.[169,170] This area is a histologically defined region in the occipital lobe, possessing unique cytoarchitectural and myeloarchitectural characteristics, the boundaries of which were determined for humans in the early 20th century.[188] In all mammalian species mapped to date, this area lies in posterior pole of the occipital lobe. In the cat, it occupies the posteromedial portion of the cortex, extending from the crown of the lateral gyrus on the dorsal surface to the superior bank of the splenial sulcus on the medial surface.[189] In the dog, it is located at the junction of the marginal and endomarginal gyri.[186,187] In humans, the primary visual cortex is located between the lunate sulcus (rostrally) and the inferior occipital sulcus (posterolaterally). This area has also been called the striate cortex, or V I (i.e., Visual I), a physiologic term coined by Woolsey and Fairman in 1946.[190]

The stereotaxic coordinates for the representation of the area centralis in the feline cortex are P3-L5 (i.e., 3-mm posterior to the interaural plane and 5-mm lateral to the midline) (Figs. 4.22 and 4.23).[191] Anatomically, it is located on the crown of the lateral gyrus, near the junction of the lateral and posterior lateral gyri.[189] In the dog, interbreed variation has been observed,[186,187] but on average, projection of the canine area centralis is 13.4-mm anterior to the interaural plane and 8.4-mm lateral to the midline (Fig. 4.24).[186,187] Knowing the

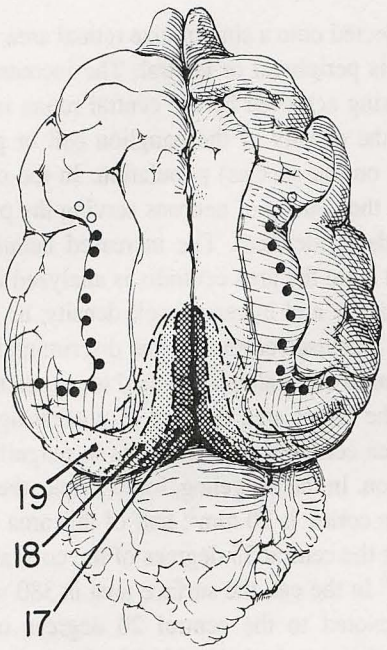

Figure 4.22. Visual areas 17, 18, and 19 of the cat brain. The shaded area shows the suprasylvian region of the cat brain. (Modified from Spear PD, Baumann TP. *J Neurophysiol* 1975;38:1414.)

precise coordinates is important when recording cortical visual–evoked potentials, because the electrodes must be precisely positioned to record a maximal signal. In humans, a displacement of just 2.5 cm in the location of the active electrode decreases the amplitude of the recorded signal by 75%.[192]

Neuronal Organization

Cells of the primary visual cortex, V I, are arranged in six layers, which are defined on the basis of the cytoarchitecture and myelination patterns of the cells.[193] Layer 4 is heavily myelinated and gives this region its characteristic histological appearance that was recognized as early as the 19th century. It is in this layer that incoming LGN axons synapse with cortical neurons. More precisely, magnocellular projections synapse in layer 4Ca, while parvocellular projections synapse in layer 4Cb, thus maintaining the segregation and dual processing of visual information that has characterized the visual system to this point. Layers 2 and 3 contain excitatory neurons that project to other cortical visual areas (see "Number of Maps" later in this chapter), while layers 1 and 2 receive feedback input from these same extrastriate visual areas. Similar descending feedback loops project from layers 5 and 6 back to the DLGN.[194]

One mm^3 of V1 tissue contains approximately 4,700 neurons, 2,900 microglia, 3,400 oligodendrocytes, and 49,000 astrocytes.[195] Most of the neurons are GABAnergic, inhibitory interneurons that do not project outside of V I.[196] Rather, they are devoted to processing of the signal in the striate cortex. Only a minority of the cells are excitatory, spiny (stellate or pyramidal) neurons that project outside area 17.

Representation of the Visual Field

The area V I receives its input from the DLGN, and this input consists of the entire contralateral visual hemifield as

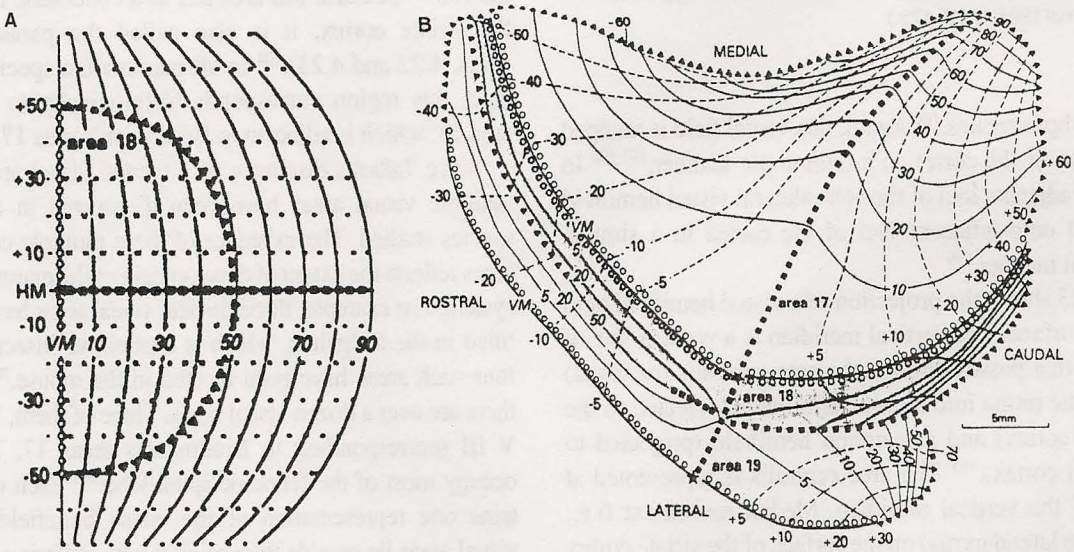

Figure 4.23. The visual hemifield on the cat cortex. **A.** Perimeter chart showing extent of the visual hemifield. Azimuths are illustrated by solid lines and elevations by dashed lines.

▼ - The most peripheral part of the visual hemifield.

★, representation of the area centralis;

○, representation of the vertical meridian;

■, representation of the horizontal meridian.

B. Visual hemifield in areas 17 (V I), 18 (V II), and 19 of the unfolded cat cortex. Areas 17 and 18 border each other along the vertical meridian. The area centralis is represented at the intersection of the border and the horizontal meridian representation. (Reprinted with permission from Tusa RJ, Rosenquist AC, Palmer LA. Retinotopic organization of areas 18 and 19 in the cat. *J Comp Neurol* 1979;185:657–678.)

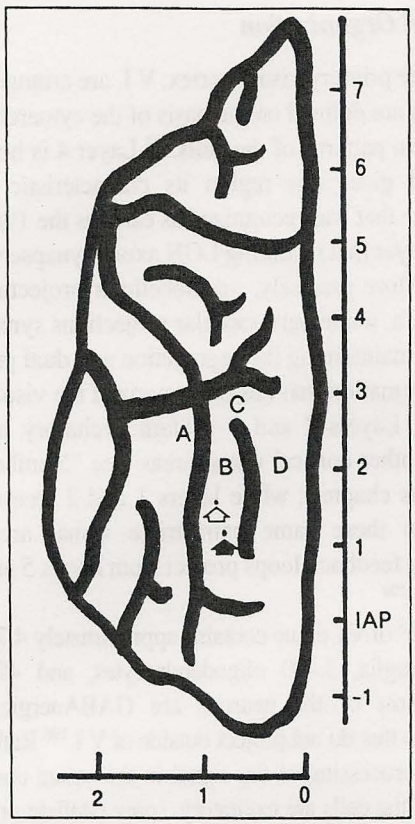

Figure 4.24. Dorsal view of the left hemisphere of the canine brain. The *solid arrow* points to the location of the cortical area of central vision in Beagles. The *hollow arrow* points to the location of the cortical area of central vision in Greyhounds. The vertical axis represents distance (cm) anterior (positive values) and posterior (negative values) to the interaural plane (IAP); the horizontal axis represents distance (cm) lateral to the midline. *A,* marginal sulcus; *B,* marginal gyrus; *C,* endomarginal sulcus; *D,* endomarginal gyrus. (Reprinted with permission from Ofri R, Dawson WW, Samuelson DA. Mapping of the cortical area of central vision in two dog breeds. *Vet Comp Ophthalmol* 1994;4:172–178.)

projected on both retinas.[189] Again, this visual field is mapped on the surface of the cortex in a retinotopic manner.[197,198] In other words, adjacent loci of the contralateral visual hemifield are projected onto adjacent loci of the cortex in a simple, point-to-point manner.[199]

Figure 4.23 shows the projection of a visual hemifield onto the cortical surface. The vertical meridian is a vertical line of demarcation that passes through the area centralis (or fovea) and divides the retina into a nasal hemifield (projected to the contralateral cortex) and a temporal hemifield (projected to the ipsilateral cortex).[168] The area centralis is represented at the center of the vertical meridian. Medial movement (i.e., away from the lateral gyrus) on the surface of the striate cortex represents peripheral movement (i.e., away from the area centralis) in the visual field.[189,200]

Because of the importance of visual input from the area centralis, large cortical areas are devoted to processing the signals originating from this region. *Magnification factor* is a term coined in 1961 to quantify the disproportionate amount of cortical area devoted to processing visual information from the area centralis.[201] In the retina, each degree of the visual field is projected onto a similar-size retinal area, regardless of whether it is peripheral or central. The increased resolution and processing achieved by the central retina is obtained by increasing the density of the ganglion cell or photoreceptor (depending on the species) population. In the cortex, on the other hand, the density of neurons serving the peripheral and central fields is identical. The increased detail with which visual input from the area centralis is analyzed is not a result of thicker layers and increased cell density, as in the retina. Rather, this increased cortical visual discrimination is a result of the increased cortical area devoted to representing the area centralis. The larger area devoted to processing information from the area centralis in turn results in magnification of its representation. In the hedgehog, for example, the surface area of the striate cortex is 20 mm^2; half of this area is devoted to representing the central 35 degrees of the contralateral visual hemifield.[180] In the cat, the surface area is 380 mm^2, 50% of which is devoted to the central 20 degrees of the visual field.[189] In other words, half of V I is devoted to the central 20 degrees of the feline retina, and half of V I is devoted to the rest of the visual field. Both the surface area of V I and the area centralis magnification are much larger in the cat than in the primitive hedgehog, reflecting the higher evolutionary development of the feline visual system.

Number of Maps

The extent of visual resolution and evolution in a given species is reflected not only in the surface area of the striate cortex and the magnification factor but also in the number of visually responsive areas.[200,202] A second visual area, known as V II, was discovered by Talbot in 1942 while working on the cat.[203] Because this area lies as a concentric ring lateral to the striate cortex, it is also called the parastriate cortex (Figs. 4.22 and 4.23).[204] In all mammalian species studied to date, this region corresponds histologically to Brodmann's area 18, which is adjacent to Brodmann's area 17.[200]

Since Talbot's discovery of a second visual area in the cat, multiple visual areas have been discovered in almost every species studied. The existence of these multiple cortical visual areas reflects the extent of development of the mammalian visual system. For example, three cortical visual areas have been identified in the hedgehog, which is a primitive insectivore,[180] and four such areas have been located in the mouse.[205] In the cat, there are over a dozen visual areas. Three of them, V I, V II, and V III (corresponding to Brodmann's areas 17, 18, and 19), occupy most of the feline occipital lobe.[200] Each of these contains one representation of the visual hemifield. Additional visual areas lie outside the occipital lobe, differing in their size, neural organization, region of the visual field they map, and type of information processed.[206–208] On the basis of many behavioral studies in nonhuman primates, where more than 30 such areas have been described, it is assumed these extraoccipital areas deal with "higher" visual processing, such as shape and location discrimination as well as facial recognition.[209–211] It should be noted that the mammalian sensory and auditory organs also have multiple cortical representations of their stimuli.[212]

Functional Architecture of the Striate Cortex

The functional architecture of the striate cortex has been extensively studied by Hubel and Wiesel, who received a Nobel Prize for their work on cat and monkey cortical organization.[213,214] As noted previously, incoming fibers from the DLGN synapse in layer 4 of V I, which is populated by *simple cells.*[215] These cells maintain the functional orientation of their respective ganglion cells and DLGN layers (regarding stimulus orientation, movement, direction, and antagonistic center-surround), but they are monocular in nature. Simple cells output to more *complex cells* in other cortical layers.[216] Complex cortical cells receive binocular input (from several simple cells), but input from one eye is dominant over that of the other eye. In addition, other cortical cells, termed *color opponent cells,* display antagonistic center-surround properties (similar to those of bipolar and ganglion cells) regarding color.

The basic cortical unit that processes an incoming signal is termed a *column,* which descends through all six layers of the cortex.[217,218] As in the DLGN, vertical penetration through the six cortical layers of the column will result in passage through cells with (approximately) identical receptive fields. Therefore, adjacent retinal receptive fields project onto adjacent columns in V I. As stated, there is no difference in size between columns serving the central and the peripheral retina; rather, more columns are used to process visual input from the central retina.

There are several functional types of columns in V I devoted to stimulus size, color, orientation, and ocular dominance. An example of the last two types is shown in Figure 4.25. In an orientation column, all the cells respond best only to one stimulus orientation; in other words, cells in a given column may fire in response to a horizontal bar but not to a vertical or diagonal bar. Movement of 50 μm along one axis of the cortical surface will bring a shift of 10 degrees in the orientation preference of the cells. Movement of 0.1 mm along the same axis will shift the orientation preference by 20 degrees. Therefore, a column 0.9-mm wide will contain cells responding to 180-degree changes in orientation, thus containing all the possible permutations.

Movement along another axis of the cortical surface will result in movement across dominance columns. A dominance column is an area approximately 0.4-mm wide in which input from one eye is dominant over that of the other eye. The dominance is strongest at the center of the column and falls off gradually, so that input is almost equally binocular at the column periphery. As movement continues into the adjacent column, there is a gradual buildup of dominance by the other eye, which, again, will be most dominant at the adjacent column's center.

A *hypercolumn* is a complete set of both column types. It contains, along one axis 0.9 mm in length, all possible permutations of orientation preferences. Along a different axis 0.8 mm in length, it contains all possible ocular dominance combinations. Therefore, every given cell in a hypercolumn will respond best just to one stimulus orientation from one eye, thus representing the first level of cortical signal processing.

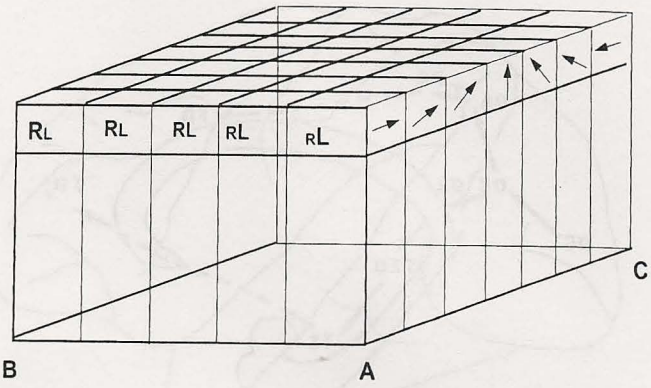

Figure 4.25. Cortical hypercolumn in V I. A hypercolumn is made of an aggregate of orientation columns (AC axis) and dominance columns (AB axis). In an orientation column, all cells respond preferentially to a given orientation of the stimulus (*arrows* along the AC axis). Moving a cortical surface electrode 50 μm along the AC axis would bring it into the adjacent orientation column, in which cells respond preferentially to a stimulus that is shifted by 10 degrees (*shifted arrow*). Movement of 0.1 mm will result in movement through two columns and shift the orientation preference by 20 degrees. Movement of 0.9 mm will encompass orientation preferences of 180 degrees. Dominance columns (along the AB axis) are 0.4-mm wide and made of cells that receive preferential input from one eye. In the center of the hypercolumn, cells receive equal input from the left and right eyes (*R* and *L* are of equal size). Movement in one direction along the AB axis will result in progressively stronger input from the left eye and weaker input from the right eye (note progressively larger *L* and smaller *R*). Movement in the other direction will result in progressively stronger input from the right eye (larger *R*) and weaker input from the left eye (small *L*).

Additional processing of the visual signal occurs both at the striate cortex and in other visual areas. In addition to hypercolumns for orientation and dominance selectivity, the striate cortex also contains a parallel and separate system to process spectral information. Cells belonging to this system are arranged in "blobs" (on the basis of their staining for cytochrome oxidase) and respond selectively to different combinations of stimulus wavelength.[219] Similar processing occurs at V II, but afterward, the visual pathways diverge while still maintaining the functional segregation of the magnocellular (stereopsis, movement, directionality, and contrast sensitivity) and of the parvocellular (spatial resolution and color sensitivity) systems (Fig. 4.26).[220–222] Areas of the middle temporal lobe appear to be associated with analysis of movement, including speed, orientation, and direction, and with stereoscopic depth.[223] The parietal lobe appears to function in spatial recognition and localization of objects in space,[222] and V 4 is rich in color-processing cells.[220,221] The temporal lobe deals with object (i.e., facial) recognition and discrimination.[224] At the same time, there is also extensive feedback activity, with signals conducted along efferent pathways from extrastriate areas to V I and from there back to the LGN.

In less than half a second, the isomerization of rhodopsin by a photon has set off a chain reaction through the various retinal layers, along the optic nerve and tract, and in the DLGN, that has resulted in a processed cortical signal. A sight to behold!

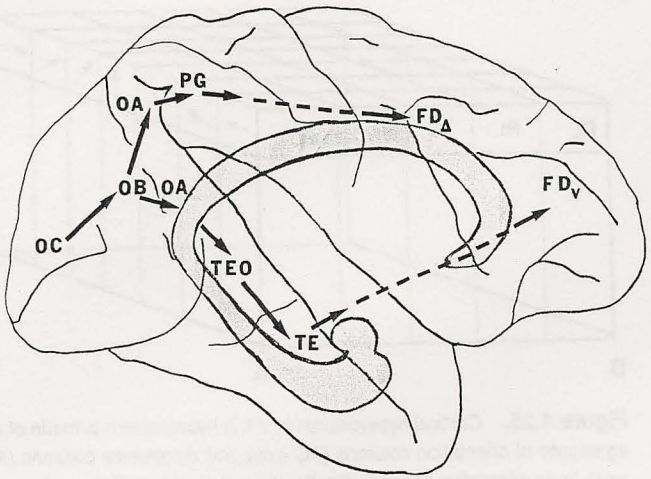

Figure 4.26. Occipitotemporal and occipitoparietal pathways. The occipitotemporal pathway, which is involved with objective identification, interconnects with the prestriate and inferior temporal areas (*OB, OA, TEO, TE*) and links with the limbic system (shaded area [hippocampus]) and the ventral frontal lobe (*Fdv*). The occipitoparietal pathway is involved with perception of an object in space and interconnects with the prestriate and inferior parietal areas (*OB, OA, PG*). It links with the dorsal limbic system and dorsal frontal lobe (*FDΔ*). *OC,* primary visual cortex. (Modified from Mishkin K, Ungerleider LG, Macko KA. Object vision and spatial vision: Two cortical pathways. *Trends Neurosci* 1986;6:414–417.)

VISUAL PERCEPTION

Light and Dark Adaptation

The eye can respond to changes in levels of background luminance by changing its sensitivity.[134,225–227] A decrease in luminance will activate the rod system, resulting in increased sensitivity (i.e., lower threshold) and scotopic vision. An increase in background luminance will lead to *mesopic vision* in which both the rod and cone systems are active. Further increases in background illumination will result in light adaptation. At luminance levels greater than 0.03 cd/m^2, only the photopic cone system is active, resulting in lower sensitivity (i.e., higher threshold). As noted previously, however, what is lost in sensitivity is gained in improved color vision and visual acuity, which characterize cone function and output.

Several mechanisms are responsible for changes of visual sensitivity in response to changes of luminance. Foremost among these are changes in the concentrations of available photopigment in the outer segments.[134–138] As noted earlier, light causes dissociation of retinal and opsin, leading to bleaching of the photopigment. This, in turn, results in depletion of the available photopigment and leads to a proportional increase in the visual threshold (i.e., lower sensitivity). With the onset of darkness, opsin binds again to the chromophore, which will lead to an increase in photopigment concentration. The resulting increase in sensitivity is directly proportional to the concentration of available photopigment.

These photochemical processes contribute significantly to visual adaptation, but they are relatively slow. Visual adaptation, however, also has a fast component, which is mediated by synaptic and lateral activity in retinal neurons.[140,142–143] This part of the adaptation process results from the center-surround antagonism in receptive fields of bipolar and ganglion cells. Steady background illumination, which will fall on the surround receptive field, causes a decrease in the response of the central visual field. Conversely, sudden onset of a focal stimulus in a dark room elicits a higher response (shifting of a response-intensity curve to the left).

A third mechanism contributing to light and dark adaptation is the size of the pupil, which helps regulate the amount of light that may reach the retina. However, its contribution to the overall process is relatively minor. It has been estimated that in humans, photochemical reactions resulting in pigment regeneration provide adaptation over 8 log units of illumination. Neural processing in the retina provides adaptation over an illumination range of 3 log units, while pupillary dilation and constriction provide adaptation over illumination changes of just one log unit.

Contrary to popular belief, cones also dark adapt. However, this is a relatively fast process, complete in 5 to 10 minutes, that increases our sensitivity to light by just 2 log units. Dark adaptation in rods is a much longer process, which makes a more significant contribution to the overall sensitivity of the eye. The duration of the rod dark adaptation and its contribution to the range of visible illumination varies between species based on the degree of development of their scotopic system. In humans, the process of dark adaptation lasts 20 to 30 minutes, while in nocturnal animals increased sensitivity to low light levels can be recorded up to 1 hour after onset of darkness.

A converse process is that of light adaptation, where the eye adapts itself to detecting stimuli against a background of light. As the luminance of the background light increases, eventually the eye reaches a point of saturation at which the stimulus cannot be detected against the bright background.

Flicker Detection

Temporal responsiveness of the eye has two aspects: motion detection and flicker detection. The eye responds to flashes of light, but as the frequency of these flashes increases, a point is reached at which the eye can no longer distinguish the individual flashes. At this point, which is termed the *critical flicker frequency* (CFF), the eye perceives a steady light even though this light is made up of numerous flickers.[228–230] There are separate CFFs for the rod and cone systems (just as there are separate adaptation mechanisms for the rod and cone systems). Therefore, CFF is a function of stimulus intensity, wavelength, illumination, and the retinal area stimulated. Figure 4.27 shows the effect of the last two variables on CFF. It can be appreciated that flickers of low-intensity light projected on the peripheral retina, and consequently stimulating the rod pathway, "fuse" at a frequency of approximately 10 Hz. Flickers characterized by high illumination projected onto the central retina will activate the cone pathway and therefore fuse at much higher frequencies. As implied in Figure 4.27, if the picture in your television or computer monitor is flickering, one way to overcome the problem is to reduce the screen's intensity!

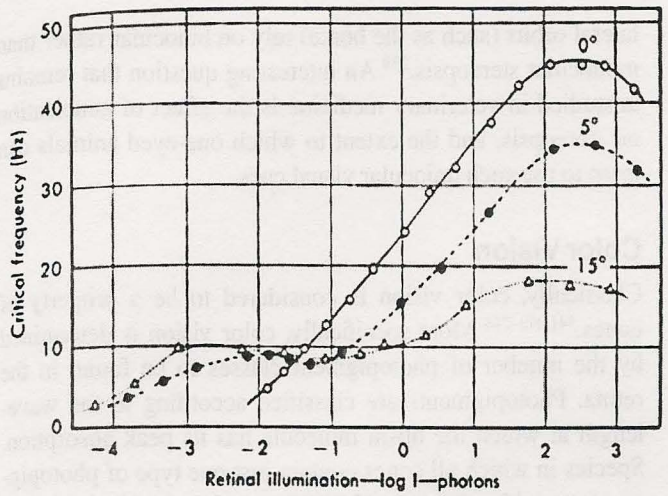

Figure 4.27. Critical flicker frequency as a function of retinal illumination (X axis) for light projected on three different retinal locations. As can be seen, the highest CFF values are attained for light flashing on the foveal region (0° - ^). The lowest values are for light flashing in the retinal periphery (15° - Δ). CFF values also increase with illumination. Both of these characteristics illustrate that cones' CFF is higher than rods' CFF. (Reprinted with permission from Hart WM, Jr. The temporal responsiveness of vision. In: Hart WM Jr, ed. *Adler's Physiology of the Eye.* 9th ed. St. Louis: Mosby–Year Book, 1992:548–579.)

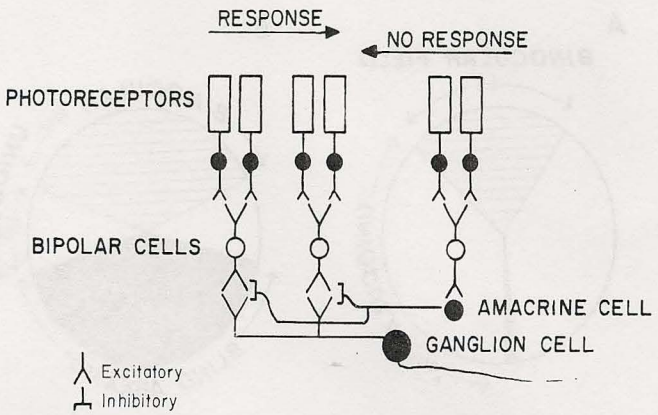

Figure 4.28. A possible mechanism to explain directionally selective retinal ganglion cells. A stimulus moving in a no-response direction activates photoreceptors, which in turn excite amacrine cells that inhibit ganglion cell dendrites when the succeeding photoreceptors are activated. A stimulus moving in the response direction activates photoreceptors, which in turn activate bipolar and ganglion cells. In this case, amacrine cells inhibit ganglion cells after the stimulus has passed. (Reprinted with permission from Barlow HB, Levick WR. The mechanism of directionally selective units in the rabbit's retina. *J Physiol* 1965;178:496.)

As noted, CFF is affected by numerous factors, and therefore it is difficult to make interspecies comparisons. However, in general, the CFF for the canine rod system is similar to that of humans (10–20 Hz). The CFF for the canine cone system is higher than that of humans, and values of 60 to 90 Hz have been reported.

Motion Perception

The functional basis for movement detection in the retina and brain has already been discussed. Lateral processing by amacrine cells contributes to movement and direction sensitivity in the retina (Fig. 4.28).[147,148] Movement detection is also one of the characteristics of the magnocellular pathway.[151,152] The large dendritic tree and transient responses of the α- or Y-type cells make them particularly adapted for motion detection. Because of this pathway segregation, sensitivity to motion is regarded as a characteristic of the peripheral retina; however, this concept is a generalization. The peripheral retina perceives motion and may be sensitive to certain speeds, directions, or objects that function as "attention-grabbing" stimuli. Subtle movement, however, is best detected by the more central retina, which has a lower threshold for motion detection. Therefore, contrary to popular belief, motion sensitivity is directly correlated with visual acuity. Thus, a human can detect objects 10 times slower than a cat can.[231] Similarly, the peripheral retina has a higher motion detection threshold than the area centralis.

Psychophysically, there are three ways of discerning motion.[232–234] Movement can be perceived if an object is moving across our visual field while our eyes and head are stationary. Stimulation of different retinal regions results in the perception of movement. Motion can also be perceived when either the head or the eyes are moved to pursue a moving object. These head or eye movements help the eye to maintain a steady image of a moving object on the retina, thereby allowing more time for visual processing of its properties. (Ocular motility is discussed in greater detail in Chapter 3.) It is interesting to note that even though each of these perceptual mechanisms involves the use of different pathways, all three result in similar sensations and experiences. A somewhat different problem results from the rapid saccadic eye movements. Theoretically, these movements should result in a blurry image because of the speed with which the object would move across the visual field. It is suspected that neuronal suppression is responsible for the "smooth" image that is eventually perceived following saccadic movements.

Binocular Vision and Depth Perception

A binocular visual field is one in which both eyes see simultaneously. The magnitude and extent of binocular vision depends, to a large extent, on placement of the orbits within the skull (Fig. 4.29). In species with frontal eyes (e.g., carnivores), most of the visual field is covered by binocular vision; there are two small, peripheral uniocular fields and a large blind spot behind the skull (Fig. 4.29). In species with more lateral eyes (e.g., herbivores), there is a small, central, binocular field; two large, peripheral uniocular fields; and a small blind spot (Fig. 4.29). Placement of the orbit is discussed in greater detail in Chapter 2.

Depth perception, or stereopsis, is most commonly associated with binocular vision, and the extent to which the visual fields of the two eyes overlap.[235–238] For every object located in the binocular visual field, two images are formed (one by each eye). Because of differences in viewing angles between the two eyes, however, these two images are nearly always disparate. Therefore, a neural mechanism must exist that

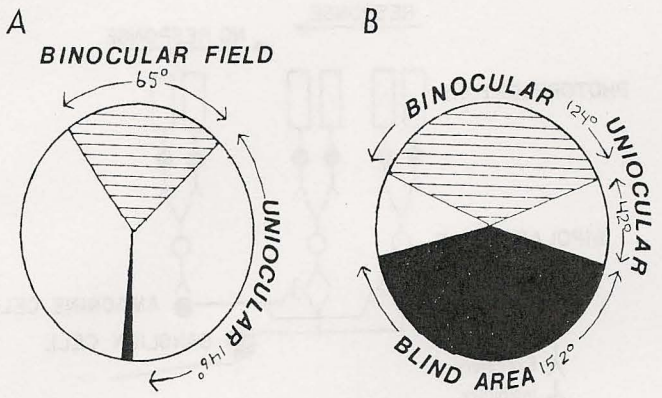

Figure 4.29. **A.** Equine visual field showing a small binocular field, large panoramic uniocular areas, and a small blind area. **B.** Primate visual field showing a large binocular field, small uniocular areas, and a large blind area. (Modified from Duke-Elder S. *System of Ophthalmology. Vol. I. The Eye in Evolution.* London: H. Kimpton, 1970).

correlates disparate images and either fuses them into one response or suppresses one of them. Failure of such a mechanism will result in *diplopia* (i.e., double vision) or *visual rivalry* (i.e., visual confusion).

As discussed previously, the first synapse following decussation occurs at the DLGN; however, no binocular interaction occurs at this site. The segregation between the output of the two eyes is also maintained at the first cortical synapse (i.e., the simple cells populating layer 4 of V I). These cells output to adjacent layers of V I and to other extrastriate visual areas, where many of the neurons receive binocular input. These neurons act as "disparity detectors." Their response can either be amplified due to fusion of two slightly disparate images from both eyes or slightly inhibited due to suppression of an image from the less dominant eye. Both binocular and disparity-selective neurons have been described in the cortices of a number of species with laterally placed eyes, including the sheep, goat, and rabbit.[239,240] Their existence would account for the superior binocular stereopsis that has been demonstrated behaviorally in the horse, despite its relatively small binocular field.[241] It should be noted that the previously discussed segregation into magnocellular and parvocellular pathways is also maintained in regard to stereopsis. The parvocellular pathway is associated with static stereopsis and fine disparities, and the magnocellular path is associated with motion stereopsis and coarse disparities.

Another prerequisite for binocular vision is optic nerve decussation. Obviously, species with no decussation at the optic chiasm (e.g., birds) lack input required to generate the binocular cortical maps discussed previously. Such species rely on cerebral commissures connecting the two hemispheres to make stereopsis possible. It should also be noted that depth perception (i.e., stereopsis) is possible in uniocular visual fields thanks to visual cues such as aerial and geometric perspectives, shadows, movement, texture gradients, and interposition.[238] Such cues have long been thought to play a central role in providing stereopsis for animals with laterally placed eyes. However, it has been shown that even species with lateral orbits (such as the horse) rely on binocular rather than monocular stereopsis.[239] An interesting question that remains unstudied in veterinary medicine is the effect of enucleation on stereopsis, and the extent to which one-eyed animals can learn to use such uniocular visual cues.

Color Vision

Classically, color vision is considered to be a property of cones.[141,242–244] More specifically, color vision is determined by the number of photopigment classes to be found in the retina. Photopigments are classified according to the wavelength at which the opsin molecule has its peak absorption. Species in which all cones contain just one type of photopigment are said to be monochromatic, and their color vision is limited to different shades of that one color. In dichromatic species, there are two classes of cones, each containing a photopigment characterized by a different absorption curve, while trichromatic and tetrachomatic species have three or four classes of cones, respectively, as characterized by their photopigments (Fig. 4.30; Table 4.6).

As Figure 4.30 shows, the absorbance curve of a given photopigment is bell-shaped. Peak absorbance (or maximum sensitivity) occurs at a primary wavelength, but the photoreceptor can also be hyperpolarized (to a lesser extent) by a relatively broad range of wavelengths. Furthermore, in species with overlap of two or more absorbance curves, a given light stimulus will stimulate (to differing degrees) cones of different classes. The extent of stimulation of the various cone classes will determine the color perceived. For example, the dashed line seen in Figure 4.30 would describe a "green-red" color, because this light stimulated a given number of green cones and a smaller number of red cones. A different light, with a slightly higher red component, would stimulate a slightly higher number of red cones (and fewer green cones), and its line would be shifted to the right. An observer would describe this color as "more reddish-green." Under optimal conditions, humans can detect color differences as subtle as 1 to 2 nm.[245] Therefore, the "richness" of color vision, or the

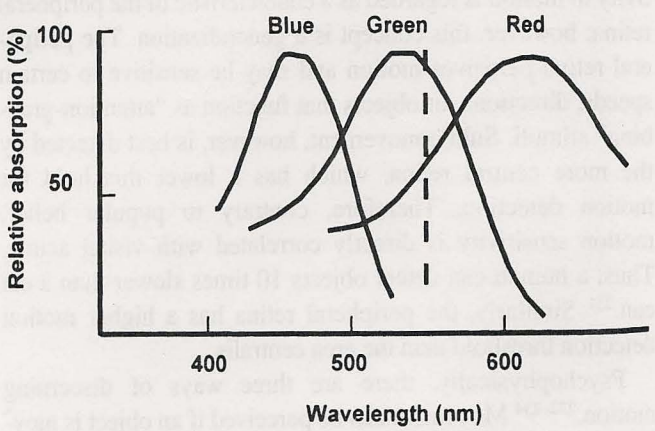

Figure 4.30. Cone absorption in a trichromatic species. The absorption peaks are for blue (455 nm), green (530 nm), and red (625 nm) light. The *dashed line* denotes a random "green-red" color.

number of hues that can be perceived, is a function of the number of cone classes and the degree of their overlap.

Humans possess three populations of opsins, with maximal absorbance of short (~420 nm, or blue), medium (~530 nm, or green), and long (~560 nm, or red) wavelengths. The associated cone populations are therefore commonly known as S, M, and L cones, respectively. The green photopigment is the most abundant in the human retina, while the blue is the scarcest. It is important to understand (for purposes of discussing color vision with pet owners) that most so-called color blind people are not truly color blind. True color blindness, whereby a person has no cones and relies only on rod vision, is called *achromotopsia,* and it is an extremely rare condition affecting 0.00003% of the population. Most "color blind" people are in fact dichromats, who are usually missing the green (1%) or red (1%) photopigment.

The peak absorbances of cones in animal species commonly seen by veterinarians are provided in Table 4.6. As can be seen, and contrary to popular misconception, most of our patients, including the dog, horse, and ruminant species, are dichromats rather than color blind. Most of these species have a short wavelength cone population, with maximal absorbance of 435 to 455 nm, and a middle/long wavelength cone population with peak absorbance of 530 to 555 nm. Thus, their color vision is comparable to that of *deuternopes,* or humans missing the green cone population (Fig. 4.31). Cats are exceptional: microspectrophotometry studies in cats indicate a trichromatic cone system, but feline behavioral studies reveal only a dichromatic capability.[246] Some animal species are monochromatic and therefore perceive only various shades of one color. These are mostly nocturnal species (e.g., the rat) that function in environments where color vision is of little consequence. At the other end of the spectrum, many avian and fish species have tetrachromatic vision due to the presence of an additional opsin molecule with peak absorbance in the ultraviolet range (320–400 nm).[247] We can only imagine the richness of color vision in such species!

Figure 4.31. A dog's view of the world. Note the lack of green shades and the low visual resolution (especially for distant objects). (Reproduced from http://www.veterinaryvision.com with permission by Dr C. Cook.)

Perception of color also depends on the luminosity of the light source. Colors are best perceived in bright light, when the photopic system is active. As the source luminosity decreases, so does the perception of color. At low illumination, when only the rod system is functional, the observer can see only varying shades of gray. This is probably why the absorption peak of rhodopsin is almost constant (495–500 nm) in most species. There is no evolutionary force driving development of color-vision capabilities in photoreceptors that are active in the dark. For similar reasons, some nocturnal species, including nocturnal primates (e.g., the owl monkey), have not developed color vision and have remained monochromatic (Table 4.6).

Color vision, however, is not determined only by the stimulus and the photopigment. As noted in the beginning of this chapter, attenuation and filtering of different wavelengths by the various ocular layers may prevent certain colors from reaching the retina, thus affecting our ability to perceive them.[6–9] Another extraretinal factor that determines color perception is the architecture of the DLGN and visual cortex.[145,220,221] Both areas are populated by color-sensitive cells, termed *opponent color cells.* These cells are activated in response to a given color but are inhibited by another, in a manner similar to the on-off responses characterizing the retinal bipolar and ganglion cells. For example, yellow-blue cells respond to yellow light, but they are inhibited by blue light. Other cells may be triggered by red light and inhibited by green. *Double opponent cells* will respond in an antagonistic manner to both spatial and spectral stimuli. Thus, some cells may be "red-on-center, green-off-surround," or "blue-on-center, yellow-off-surround." Obviously, the number of possible double opponent cell types is potentially very large, depending on the number of cone classes.

Oil droplets found in the cones of birds also play a role in color vision by filtering out different wavelengths of incoming light and shifting the wavelength sensitivity of the photoreceptor. The yellowing of the lens in some species, such as the horse, may have a similar function, as it filters out the blue wavelengths of incoming light.

Visual Acuity

Visual acuity is the maximal resolving power of the eye, or the minimal angle that can be visually resolved. There are a number of ways to express visual acuity, but the best known method is based on the Snellen chart. Determination of Snellen acuity requires verbal cooperation by the test subject, however, and therefore is not applicable in veterinary medicine. In animals, visual acuity can be determined using behavioral tests, electrophysiologic recordings (to determine the smallest pattern that elicits a retinal or cortical response), or pursuit (i.e., optokinetic) eye responses (to determine the smallest stimulus that elicits a tracking eye movement). There are two ways to express the results of these tests (Fig. 4.32). Cycles per degree (cpd) is the number of cycles (a dark and a

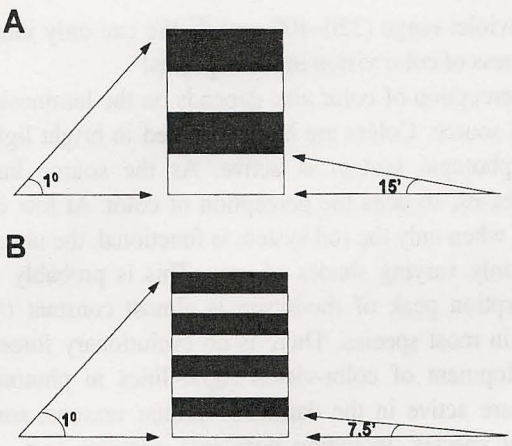

Figure 4.32. Visual acuity expressed in cpd and MAR. The acuity of the observer on the left is denoted in cpd, which expresses the number of cycles (each cycle consisting of a dark and a light bar) seen within a 1-degree visual field. The observer on the right has an identical visual acuity, but it is denoted in MAR, which expresses the angle (in minutes) subtended by a single bar. **A.** The acuity of the observer on the left is 2 cpd (two pairs of light and dark bars). Because there are four bars in a degree, each is 15-ft wide; therefore, the acuity of the observer on the right is 15 MAR. **B.** The observer on the left can discriminate four pairs of dark and light bars in a 1-degree field and therefore has an acuity of 4 cpd. The width of each bar is now 7.5-ft, however, and the acuity of the observer on the right is therefore 7.5 MAR.

white bar) that can be seen within a field subtended by a 1-degree visual angle. Minutes of arc (MAR) describes the angle (in minutes) subtended by the narrowest bar that can be discriminated. These values are inversely related. If a subject can resolve very narrow bars (resulting in a low MAR value), it will be able to see many bars (a high cpd value) within a 1-degree visual field. (A chart converting between Snellen, cpd, and MAR values is provided elsewhere.[46]) A human adult typically has a Snellen acuity of 20/15, which is equivalent to 45 seconds of arc or 36 cpd. Values for various animal species are provided in Table 4.8. Figure 4.31 shows the optical quality of the images formed by a dog's eye.

Many factors influence visual acuity. These include both stimulus and ocular parameters. The two most important stimulus parameters are the luminance and contrast of the stimulus. At low luminance levels, when only the scotopic system is active, the signal generated by the photoreceptors is transmitted by the converging rod pathway, resulting in low acuity (Fig. 4.18). Visual acuity improves significantly at high luminance (i.e., photopic) levels because of the 1:1 ratio between the activated cones and their ganglion cells; at these levels, acuity is largely a function of the physical size and distance between cones. Likewise, a high degree of contrast is required for high acuity. If there is little contrast between two adjacent bars, it will be very difficult to distinguish between them. Therefore, acuity and contrast sensitivity should, theoretically, be proportional to each other. Because of optical limitations and physiologic signal processing, however, there is a loss of contrast sensitivity at both high and low spatial frequencies. Other stimulus parameters influencing visual acuity include stimulus duration (acuity declines for brief stimuli because of insufficient exposure) and stimulus movement (movement faster than the tracking response will, again, result in insufficient retinal exposure).

Table 4.8 Visual Resolution in Animals

Species	Resolution (cycles/degree)	Method of Determinations[a]	References
Dog	4.3–11.6	2	249, 266
Cat	3.5–8.6	1, 2	267, 268
Cow	1.8	1	56
Horse	18–23	1	269
	16.5	3	106
	10.3	2	270
Human	30		
Eagle	132–143	1, 3	271

[a]Method of determination: 1, behavioral; 2, electrophysiology, 3, calculated based on retinal anatomy.

The refractive error of the eye is among the most important ocular factors influencing visual acuity. Maximal acuity can be obtained only in an emmetropic eye, when the image is focused on the retina. Ammetropia leads to loss of acuity and has been associated with resulting behavioral problems such as increased nervousness.[74] Refractive errors may be corrected by accommodation; however, this mechanism is limited in most nonavians and nonprimates. Another handicap in many animal species is the presence of a tapetum lucidum in the choroid. Light striking the tapetum is reflected back onto the retina at various angles, resulting in light scatter and diminished acuity.

The size of the pupil is another important consideration in visual acuity. Pupil size changes with illumination levels, thus resulting in improved acuity. At scotopic levels, mydriasis permits a greater number of photons to enter the eye, thus increasing the resolution of the rod system. At photopic levels, miosis decreases the optical aberrations inherent in the eye. Furthermore, a miotic pupil increases the depth of focus, thereby increasing the distance over which objects remain in focus without active accommodation. With extreme mydriasis or miosis, however, optical and chromatic aberrations again result in a decline of visual acuity.

Visual acuity is also determined, to a large extent, by retinal anatomy; the correlation between visual acuity and the rod and cone pathways has already been discussed. Visual acuity decreases as a function of increased retinal eccentricity because of the decreased number of cones and ganglion cells in the peripheral retina (Table 4.7) and because signals from the peripheral retina are processed by the converging rod pathway. This decline in the peripheral ganglion cell population has been noted in the cat[248] and horse.[74] Additionally, the peripheral retina is populated mostly by α- or Y-type ganglion cells, which are characterized by large dendritic trees, further contributing to the low acuity of this region. Thus, it is not surprising that low visual acuity has been demonstrated in the peripheral retina of the dog.[249]

Conversely, the architecture of the central retina has evolved to provide maximal visual acuity. It is characterized

by a maximal number of cones and ganglion cells, by a low photoreceptor–ganglion cell ratio, and by a large population of β- or X-type ganglion cells. The presence of these factors defines the existence of a specialized retinal region, the area centralis (or visual streak). In primates and birds, this region has further evolved into a fovea (and its surrounding macula), which is an anatomic pit in the retina in which there are no rods. These regions are also characterized by the absence of structures that might interfere with absorption of incoming light, such as blood vessels, ganglion cell axons, and (in foveas) the INL.

Obviously, differences in cone–rod ratios and variations in ganglion cell types are not limited to regional retinal variations. Such differences are also found between species, depending on their environment (diurnal vs. nocturnal), life style (herbivorous vs. carnivorous), and other evolutionary factors (Table 4.7). The low cone concentration and small number of optic nerve fibers, combined with the presence of a light-scattering tapetum, are the limiting reason for the low acuity values in the cat. Because of these retinal anatomy constraints, the low acuity values of our patients can never be improved by visual aids such as glasses or LASIK surgery, contrary to suggestions by the general public. However, what cats lack in cone function they may gain in rod function. The maximal rod concentration in cats and humans is 460,000/mm^2 and 160,000/mm^2, respectively. Therefore, though their view of the world may not be as colored or detailed as ours, cats continue to see while we are left groping in the dark!

REFERENCES

1. Miller D, et al. Optics, refraction and contact lenses. In: Wilson FM, ed. *Basic and Clinical Science Course III.* San Francisco: American Academy of Ophthalmology, 1991: 1–123.
2. Bleiweiss R. Ultraviolet plumage reflectance distinguishes sibling bird species. *Proc Natl Acad Sci USA* 2004; 101: 16561–16564.
3. Smith EL, Greenwood VJ, Bennett AT. Ultraviolet colour perception in European starlings and Japanese quail. *J Exp Biol* 2002; 205: 3299–3306.
4. Levine JS, MacNichol EF Jr. Color vision in fishes. *Sci Am* 1982; 246: 140–149.
5. Safer AB, Grace MS. Infrared imaging in vipers: Differential responses of crotaline and viperine snakes to paired thermal targets. *Behav Brain Res* 2004; 154: 55–61.
6. Boettner EA, Wolter JR. Transmission of the ocular media. *Invest Ophthalmol* 1962; 1: 776–783.
7. Beems EM, van Best JA. Light transmission of the cornea in whole human eyes. *Exp Eye Res* 1990; 50: 393–396.
8. van der Berg TJTP, Tan KEWP. Light transmittance of the human cornea from 320 to 700 nm for different ages. *Vision Res* 1994; 34: 1453–1456.
9. McLaren JW, Brubaker RF. Measurement of transmission of ultraviolet and visible light in the living rabbit cornea. *Curr Eye Res* 1996; 15: 411–421.
10. Michalos P, et al. Do human tears absorb ultraviolet light? *CLAO J* 1994; 20: 192–193.
11. Ando K, Kripke DF. Light attenuation by the human eyelid. *Biol Psych* 1996; 39: 22–25.
12. Nishimoto K, Sasaju K. In vivo light scattering in the lens versus in vitro spectral transmissions in the nuclear region. *Ophthalmic Res* 1995; 27: 1–11.
13. Weigt AK, Herring IP, Marfurt CF, Pickett JP, Duncan RB Jr, Ward DL. Effects of cyclophotocoagulation with a neodymium: yttrium-aluminum-garnet laser on corneal sensitivity, intraocular pressure, aqueous tear production, and corneal nerve morphology in eyes of dogs. *Am J Vet Res* 2002; 63: 906–915.
14. Rol P, Fankhauser F, Giger H, Durr U, Kwasniewska S. Transpupillar laser phototherapy for retinal and choroidal tumors: A rational approach. *Graefes Arch Clin Exp Ophthalmol* 2000; 238: 249–272.
15. Mayer SJ. Stratospheric ozone depletion and animal health. *Vet Rec* 1992; 131: 120–122.
16. Anderson DE, Badzioch M. Association between solar radiation and ocular squamous cell carcinoma in cattle. *Am J Vet Res* 1991; 52: 784–788.
17. Bressler NM, Bressler SB. Preventative ophthalmology. Age-related macular degeneration. *Ophthalmology* 1995; 102: 1206–1211.
18. Montes-Mico R, Alio JL, Munoz G, Perez-Santonja JJ, Charman WN. Postblink changes in total and corneal ocular aberrations. *Ophthalmology* 2004; 111: 758–767.
19. Fish SK, Pflugfelder SC, de Paiva CS. The effect of tear film composition on refraction. *Invest Ophthalmol Vis Sci* 2004; 45: ARVO abstract 3887.
20. Tutt R, Bradley A, Begley C, Thibos LN. Optical and visual impact of tear break-up in human eyes. *Invest Ophthalmol Vis Sci* 2000; 41: 4117–4123.
21. Courville CB, Smolek MK, Klyce SD. Contribution of the ocular surface to visual optics. *Exp Eye Res* 2004; 78: 417–425.
22. Duke-Elder S. The dioptric imagery of the eye. In: *System of Ophthalmology. Vol. V. Ophthalmic Optics and Refraction.* London: Henry Kimpton, 1970: 93–152.
23. Schaeffel F, de Queiroz A. Alternative mechanisms of enhanced underwater vision in the garter snakes *Thamnophis melanogaster* and *Thamnophis couchii. Copeia* 1990; 1: 50–58.
24. Hughes A. The topography of vision in mammals of contrasting life style: Comparative optics and retinal organization. In: Crescitelli F, ed. *The Visual System in Vertebrates—Handbook of Sensory Physiology VII.* Berlin: Springer-Verlag, 1977.
25. Smith G. The optical properties of the crystalline lens and their significance. *Clin Exp Optom* 2003; 86: 3–18
26. Sivak JG. Optical characteristics of the eye of the spiny dogfish (*Squalus acanthias*). *Rev Can Biol* 1978; 37: 209–217.
27. Schmidt-Morand D. Vision in the animal kingdom. *Vet Int* 1992; 1: 3–32.
28. Seltner RL, Weerheim JA, Sivak JG. Role of the lens and vitreous humor in the refractive properties of the eyes of three strains of goldfish. *Vision Res* 1989; 29: 681–685.
29. Liu J, Pendrak K, Capehart C, Sugimoto R, Schmid GF, Stone RA. Emmetropisation under continuous but non-constant light in chicks. *Exp Eye Res* 2004; 79: 719–728.
30. Shen W, Vijayan M, Sivak JG. Inducing form-deprivation myopia in fish. *Invest Ophthalmol Vis Sci* 2005; 46: 1797–1803.

31. McBrien NA, Norton TT. The development of experimental myopia and ocular component dimensions in monocularly lid-sutured tree shrews (*Tupaia belangeri*). *Vision Res* 1992; 32: 843–852.
32. Patel S, Marshall J, Fitzke FW III. Refractive index of the human corneal epithelium and stroma. *J Refract Surg* 1995; 11: 100–105.
33. Chen E. Refractive indices of the rat retinal layers. *Ophthalmic Res* 1993; 25: 65–68.
34. Axelrod D, Lerner D, Sands PJ. Refractive index within the lens of a goldfish eye determined from the paths of thin laser beams. *Vision Res* 1988; 28: 57–65.
35. Wang B, Ciuffreda KJ. Depth-of-focus of the human eye in the near retinal periphery. *Vision Res* 2004; 44: 1115–1125.
36. Kaufman PL. Accommodation and presbyopia: Neuromuscular and biophysical aspects. In: Hart WM Jr, ed. *Adler's Physiology of the Eye,* 9th ed. St. Louis: Mosby–Year Book, 1992: 391–411.
37. Bito LZ, et al. Age-dependent loss of accommodative amplitude in rhesus monkeys: An animal model for presbyopia. *Invest Ophthalmol Vis Sci* 1982; 23: 23–31.
38. Choh V, Sivak JG, Meriney SD. A physiological model to measure effects of age on lenticular accommodation and spherical aberration in chickens. *Invest Ophthalmol Vis Sci* 2002; 43: 92–98.
39. Haefliger E, Parel JM. Accommodation of an endocapsular silicone lens (Phaco-Ersatz) in the aging rhesus monkey. *J Refract Corneal Surg* 1994; 10: 550–555.
40. Jungschaffer DA, et al. Refractive changes induced by electrocautery of the rabbit anterior lens capsule. *J Cataract Refract Surg* 1994; 20: 132–137.
41. Beers AP, van der Heijde GL. Age related changes in the accommodation mechanism. *Opto Vision Sci* 1996; 73: 235–242.
42. Fisher RF. The elastic constants of the human lens capsule. *J Physiol (Lond)* 1969; 201: 1–19.
43. Fisher RF. The elastic constants of the human lens. *J Physiol (Lond)* 1971; 212: 147–180.
44. Prince JH, et al. *Anatomy and histology of the eye and orbit in domestic animals*. Springfield: Charles C. Thomas, 1960.
45. O'Neill WD, Brodkey JS. Linear regression of lens movement with refractive state. *Arch Ophthalmol* 1969; 82: 795–799.
46. Miller PE, Murphy CJ. Vision in dogs. *J Am Vet Med Assoc* 1995; 207: 1623–1634.
47. Rohen JW, et al. Functional morphology of accommodation in the raccoon. *Exp Eye Res* 1989; 48: 523–527.
48. McBrien NA, et al. Experimental myopia in a diurnal mammal (*Sciurus carolinensis*) with no accommodative ability. *J Physiol* 1993; 469: 427–441.
49. McCourt ME, Jacobs GH. Refractive state, depth of focus and accommodation of the eye of the California ground squirrel (*Spermophilus beecheyi*). *Vision Res* 1984; 24: 1261–1266.
50. Shand J, Doving KB, Collin SP. Optics of the developing fish eye: Comparisons of Matthiessen's ratio and the focal length of the lens in the black bream Acanthopagrus butcheri (*Sparidae, Teleostei*). *Vision Res.* 1999; 39: 1071–1078.
51. Andison ME, Sivak JG. The functional morphology of the retractor lentis muscle of a teleost fish, *Astronotus ocellatus*. *Can J Zool* 1994; 72: 1880–1886.
52. Piggins D, Phillips CJC. The eye of the domesticated sheep with implications for vision. *Anim Sci* 1996; 62: 301–308.
53. Samuelson DA. A reevaluation of the comparative anatomy of the eutherian iridocorneal angle and associated ciliary body musculature. *Vet Comp Ophthalmol* 1996; 6: 153–172.
54. Block MT. A note on the refraction and image formation of the rat's eye. *Vision Res* 1969; 9: 705–711.
55. Samuelson DA, Lewis PA. Comparative morphology of the iridocorneal angle among selected atriodactyls (Ungulates). *Vet Comp Ophthalmol* 1995; 5: 89–103.
56. Rehkamper G, Perrey A, Werner CW, Opfermann-Rungeler C, Gorlach A. Visual perception and stimulus orientation in cattle. *Vision Res* 2000; 40: 2489–2497.
57. Sivak JG, Allen DB. An evaluation of the 'ramp' retina in the horse eye. *Vision Res* 1975; 15: 1353–1356.
58. West JA, Sivak JG, Doughty MJ. Functional morphology of lenticular accommodation in the young chicken (*Gallus domesticus*). *Can J Zool* 1991; 69: 2183–2193.
59. Glasser A, Murphy CJ, Troilo D, Howland HC. The mechanism of lenticular accommodation in chicks. *Vision Res* 1995; 35: 1525–1540.
60. Choh V, Sivak JG, Irving EL, Wong W. Ultrasound biomicroscopy of the anterior segment of the enucleated chicken eye during accommodation. *Ophthal Physiol Opt* 2002; 22: 401–408.
61. Schaeffel F, Howland HC. Corneal accommodation in chick and pigeon. *J Comp Physiol* 1987; 160: 375–384.
62. Glasser A, Troilo D, Howland HC. The mechanism of corneal accommodation in chicks. *Vision Res* 1994; 34: 1549–1566.
63. Murphy CJ, Glasser A, Howland HC. The anatomy of the ciliary region of the chicken eye. *Invest Ophthalmol Vis Sci* 1995; 36: 889–896.
64. Sivak JG, et al. Ocular accommodation in chickens: Corneal vs lenticular accommodation and effect of age. *Vision Res* 1986; 26: 1865–1872.
65. Suburo AM, Marcantoni M. The structural basis of ocular accommodation in the chick. *Rev Can Biol Exp* 1983; 42: 131–137.
66. Schaeffel F, Wagner H. Barn owls have symmetrical accommodation in both eyes, but independent pupillary responses to light. *Vision Res* 1992; 32: 1149–1155.
67. Schmid KL, Howland HC, Howland M. Focusing and accommodation in tuatara (*Sphenodon punctatus*). *J Comp Physiol A* 1992; 170: 263–266.
68. Davidson MG. Clinical retinoscopy for the veterinary ophthalmologist. *Vet Comp Ophthalmol* 1997; 7: 128–137.
69. Glickstein M, Millodot M. Retinoscopy and eye size. *Science* 1970; 168: 605–606.
70. Millodot M, O'Leary D. The discrepancy between retinoscopic and subjective measurements: Effect of age. *Am J Optom Physiol Optics* 1978; 55: 309–316.
71. Millodot M, Sivak J. Hypermetropia of small animals and chromatic aberration. *Vision Res* 1978; 18: 125–126.
72. Ofri R, Millodot S, Shimoni R, Horowitz IH, Ashash E, Millodot M. Development of the refractive state in eyes of ostrich chicks (*Struthio camelus*). *Am J Vet Res* 2001; 62: 812–815.
73. Gillum W. Mechanisms of accommodation in vertebrates. *Ophthalmic Semin* 1976; 1: 253–286.
74. Miller PE, Murphy CJ. Equine vision: Normal and abnormal. In: Gilger BC, ed. *Equine Ophthalmology.* Philadelphia: Elsevier Saunders, 2005: 371–408.
75. Belkin M, et al. Effects of visual environment on refractive error of cats. *Doc Ophthalmol* 1977; 42: 433–437.
76. Gaiddon J, Bouhana N, Lallement PE. Refraction by retinoscopy of normal, aphakic and pseudophakic canine eyes:

Advantage of a 41-diopter intraocular lens? *Vet Comp Ophthalmol* 1996; 6: 121–124.
77. Murphy CJ, Zadnik K, Mannis MJ. Myopia and refractive errors in dogs. *Invest Ophthalmol Vis Sci* 1992; 33: 2459–2463.
78. Mower GD. The relationship between relative eye usage and ocular dominance shifts in cat visual cortex. *Brain Res Dev Brain Res* 2005; 154: 147–151.
79. Troilo D, Nickla DL. The response to visual form deprivation differs with age in marmosets. *Invest Ophthalmol Vis Sci* 2005; 46: 1873–1881.
80. Jampolsky A. Consequences of retinal image clarity versus occlusion (absent) versus diffusion. *Trans Am Ophthalmol Soc* 1994; 92: 349–376.
81. Pollet L. Refraction of normal and aphakic canine eyes. *J Am Anim Hosp Assoc* 1982; 18: 323–326.
82. Peiffer RL Jr, Gaiddon J. Posterior chamber intraocular lens implantation in the dog: Results of 65 implants in 61 patients. *J Am Anim Hosp Assoc* 1991; 27: 453–462.
83. Gaiddon J, et al. Use of biometry and keratometry for determining optimal power for intraocular lens implants in dogs. *Am J Vet Res* 1991; 52: 781–783.
84. Davidson MG, et al. Refractive state of aphakic and pseudophakic eyes of dogs. *Am J Vet Res* 1993; 54: 174–177.
85. Gilger BC, Davidson MG, Colitz CM. Experimental implantation of posterior chamber prototype intraocular lenses for the feline eye. *Am J Vet Res* 1998; 59: 1339–1343.
86. Millichamp NJ, Dziezyc J, Martinez E. Cataract surgery in horses—A progress report. *Proc Am Coll Vet Ophthalmol* 1996; 27: 54.
87. Hara T, et al. Complications associated with endocapsular balloon implantation in rabbit eyes. *J Cataract Refract Surg* 1994; 20: 507–512.
88. Nishi O, et al. Refilling the lens with an inflatable endocapsular balloon: Surgical procedure in animal eyes. *Graeffe's Arch Clin Exp Ophthalmol* 1992; 230: 47–55.
89. Sakka Y, et al. Accommodation in primate eyes after implantation of refilled endocapsular balloon. *Am J Ophthalmol* 1996; 121: 210–212.
90. Percival P. Indications for the multizone bifocal implant. *J Cataract Refract Surg* 1990; 16: 193–197.
91. Rosolen SG, et al. Refractive corneal surgery on dogs: Preliminary results of keratomileusis using a 193 nanometer excimer laser. *Vet Comp Ophthalmol* 1995; 5: 18–24.
92. Duke-Elder S. Simple refractive errors. In: *System of Ophthalmology. Vol. V. Ophthalmic Optics and Refraction.* London: Henry Kimpton, 1970: 255–295.
93. Nelms SR, et al. Comparison of corneal and scleral surgical approaches for cataract extraction by phacoemulsification and intraocular lens implantation in normal dogs. *Vet Comp Ophthalmol* 1994; 4: 53–60.
94. Hammoudi DS, Segev F, Abdolell M, Rootman DS. Outcome of penetrating keratoplasty performed by cornea fellows compared with that of an experienced staff surgeon. *Cornea* 2005; 24: 410–416.
95. Murphy CJ, Kern TJ, Howland HC. Refractive state, corneal curvature, accommodative range and ocular anatomy of the Asian elephant (*Elephas maximus*). *Vision Res* 1992; 32: 2013–2021.
96. Ofri R, Millodot S, Tadmor Y, Matalon E, Kass PH, Horowitz IH, Millodot M. The development of the refractive state in the newborn Thomson gazelle. *J Comp Physiol A* 2004; 190: 831–835.
97. Fitzke FW, et al. Refractive sectors in the visual field of the pigeon eye. *J Physiol Lond* 1985; 369: 33–44.
98. Hodos W, Erichsen JT. Lower-filed myopia in birds: An adaptation that keeps the ground in focus. *Vision Res* 1990; 30: 653–657.
99. Schaeffel F, et al. Lower-field myopia and astigmatism in amphibians and chickens. *J Opt Soc Am A* 1994; 11: 487–495.
100. Murphy CJ, Howland M, Howland HC. Raptors lack lower-field myopia. *Vision Res* 1995; 35: 1153–1155.
101. Dawson WW, Schroeder JP, Sharpe SN. Corneal surface properties of two marine mammal species. *Marine Mammal Sci* 1987; 3: 186–197.
102. Renouf D. Sensory function in the harbor seal. *Sci Am* 253: 90–95.
103. Kroger RH, Kirschfeld K. Optics of the harbor porpoise eye in water. *J Opt Soc Am* 1993; 10: 1481–1489.
104. Shilo S. Astigmatism of the mammalian cornea: Evolutionary and perceptive significance. *Doc Ophthalmol* 1977; 44: 403–419.
105. Farrall H, Handscombe M. Equine vision. *Equine Vet J* 1999; 31: 354–355.
106. Harmann AM, Moore S, Hoskins R, Keller P. Horse vision and an explanation for the visual behaviour originally explained by the "ramp retina." *Equine Vet J* 1999; 31: 384–390.
107. Millodot M. *Dictionary of Optometry and Visual Science,* 4th ed. Oxford: Butterworth Heinemann, 1997.
108. Kroger RHH, Campbell MCW, Fernald RD, Wagner HJ. Multifocal lenses compensate for chromatic defocus in vertebrate eyes. *J Comp Physiol A* 1999; 184: 361–369.
109. Malmstrom T, Kroger RHH. Relationship between lens optics and pupil shape in terrestrial vertebrates. *Invest Ophthalmol Vis Sci* 2004; 45: ARVO abstract 1742.
110. Pierscionek BK, Augusteyn RC. The refractive index and protein distribution in the blue eye trevally lens. *J Am Optom Assoc* 1995; 66: 739–743.
111. Pettigrew JD, Collin SP. Terrestrial optics in an aquatic eye: The sandlance, *Limnichthytes fasciatus* (*Creediidae, Teleostei*). *J Comp Physiol* 1995; 177: 397–408.
112. Katzir G, Howland HC. Corneal power and underwater accommodation in great cormorants (*Phalacrocorax carbo sinensis*). *J Exp Biol* 2003; 206: 833–841.
113. Sivak JG, Millodot M. Optical performance of the penguin eye in air and water. *J Comp Physiol* 1977; 119: 241–247.
114. Howland HC, Sivak JG. Penguin vision in air and water. *Vision Res* 1984; 24: 1905–1909.
115. Fleishman LJ, et al. Crocodiles don't focus underwater. *J Comp Physiol* 1988; 163: 441–443.
116. Dowling J. Visual adaptation and photoreceptor mechanisms. In: Dowling J, ed. *The Retina.* Cambridge: Belknap Press of Harvard University, 1987: 187–223.
117. Hargrave PA, McDowell JH, Feldmann RJ, Atkinson PH, Rao JKM. Argos P. Rhodopsin's protein and carbohydrate structure: Selected aspects. *Vision Res* 1984; 24: 1487–1499.
118. Ruprecht JJ, Mielke T, Vogel R, Villa C, Schertler GF. Electron crystallography reveals the structure of metarhodopsin I. *EMBO J* 2004; 23: 3609–3620.
119. Saari JC. The biochemistry of sensory transduction in vertebrate photoreceptors. In: Hart WM Jr, ed. Adler's physiology of the eye. 9th ed. St. Louis: Mosby–Year Book, 1992: 460–484.
120. Ridge KD, Abdulaev NG, Sousa M, Palczewski K. Phototransduction: Crystal clear. *Trends Biochem Sci* 2003; 28: 479–487.

121. Maeda T, Imanishi Y, Palczewski K. Rhodopsin phosphorylation: 30 years later. *Prog Retin Eye Res* 2003; 22: 417–434.
122. Baylor DA. Photoreceptor signals and vision. *Invest Ophthalmol Vis Sci* 1987; 28: 34–49.
123. Liebman PA, Parker KR, Dratz EA. The molecular mechanism of visual excitation and its relation to the structure and composition of the rod outer segment. *Annu Rev Physiol* 1987; 49: 765–791.
124. Warren R, Molday RS. Regulation of the rod photoreceptor cyclic nucleotide-gated channel. *Adv Exp Med Biol* 2002; 514: 205–223.
125. Chabre M, Deterre P. Molecular mechanism of visual transduction. *Eur J Biochem* 1989; 179: 255–266.
126. Yau KW. Phototransduction mechanism in retinal rods and cones. *Invest Ophthalmol Vis Sci* 1994; 35: 9–32.
127. Aguirre GD, et al. Rod-cone dysplasia in Irish setters: A defect in cyclic GMP metabolism in visual cells. *Science* 1978; 201: 1133–1134.
128. Zhu L, Jang GF, Jastrzebska B, Filipek S, Pearce-Kelling SE, Aguirre GD, Stenkamp RE, Acland GM, Palczewski K. A naturally occurring mutation of the opsin gene (T4R) in dogs affects glycosylation and stability of the G protein-coupled receptor. *J Biol Chem* 2004; 279: 53828–53839.
129. Parshall CJ, et al. Photoreceptor dysplasia: An inherited progressive retinal atrophy of Miniature Schnauzer dogs. *Prog Vet Comp Ophthalmol* 1991; 1: 187–203.
130. Acland GM, Aguirre GD. Retinal degeneration in the dog: IV. Early retinal degeneration (ERD) in Norwegian Elkhounds. *Exp Eye Res* 1987; 44: 491–521.
131. Chader GJ. Animal mutants of hereditary retinal degeneration: General consideration and studies on defects in cyclic nucleotide metabolism. *Prog Vet Comp Ophthalmol* 1991; 1: 109–126.
132. Clements PJM, et al. Recent advances in understanding the spectrum of canine generalised progressive retinal atrophy. *J Small Anim Pract* 1996; 37: 155–162.
133. Zhang Q, Baldwin VJ, Acland GM, Parshall CJ, Haskel J, Aguirre GD, Ray K. Photoreceptor dysplasia (PD) in Miniature Schnauzer dogs: Evaluation of candidate genes by molecular genetic analysis. *J Hered* 1999; 90: 57–61.
134. Lamb TD, Pugh EN Jr. Dark adaptation and the retinoid cycle of vision. *Prog Retin Eye Res* 2004; 23: 307–380.
135. Thompson DA, Gal A. Vitamin A metabolism in the retinal pigment epithelium: Genes, mutations, and diseases. *Prog Retin Eye Res* 2003; 22: 683–703.
136. Gonzalez-Fernandez F. Evolution of the visual cycle: The role of retinoid-binding proteins. *J Endocrinol* 2002; 175: 75–88.
137. Burns ME, Baylor DA. Activation, deactivation, and adaptation in vertebrate photoreceptor cells. *Annu Rev Neurosci* 2001; 24: 779–805.
138. Saari JC. Biochemistry of visual pigment regeneration. *Invest Ophthalmol Vis Sci* 2000; 41: 337–348.
139. Wikler KC, Rakic P. Distribution of photoreceptor subtypes in the retina of diurnal and nocturnal primates. *J Neurosci* 1990; 10: 3390–3401.
140. Taylor WR, Smith RG. Transmission of scotopic signals from the rod to rod-bipolar cell in the mammalian retina. *Vision Res* 2004; 44: 3269–3276.
141. Dacey DM, Packer OS. Colour coding in the primate retina: Diverse cell types and cone-specific circuitry. *Curr Opin Neurobiol* 2003; 13: 421–427.
142. Bloomfield SA, Dacheux RF. Rod vision: Pathways and processing in the mammalian retina. *Prog Retin Eye Res* 2001; 20: 351–384.
143. Dacheux RF, Raviola E. The rod pathway in the rabbit retina: A depolarizing bipolar and amacrine cell. *J Neurosci* 1986; 6: 331–345.
144. Kaneko A. Physiological and morphological identification of horizontal, bipolar and amacrine cells in goldfish retina. *J Physiol* 1970; 207: 623–633.
145. Twig G, Levy H, Perlman I. Color opponency in horizontal cells of the vertebrate retina. *Prog Retin Eye Res* 2003; 22: 31–68.
146. Dowling J, Ehinger B. Synaptic organization of the amine-containing interplexiform cells of the goldfish and cebus monkey retinas. *Science* 1975; 188: 270–273.
147. Bloomfield SA. Plasticity of AII amacrine cell circuitry in the mammalian retina. *Prog Brain Res* 2001; 131: 185–200.
148. Vaney DI, Taylor WR. Direction selectivity in the retina. *Curr Opin Neurobiol* 2002; 12: 405–410.
149. De Monsasterio FM, Gouras P. Functional properties of ganglion cells of the rhesus monkey retina. *J Physiol Lond* 1975; 251: 167–195.
150. Wilder HD, Grunert U, Lee BB, Martin PR. Topography of ganglion cells and photoreceptors in the retina of a New World monkey: The marmoset *Callithrix jacchus*. *Vis Neurosci* 1996; 13: 335–352.
151. Dacey DM. Physiology, morphology and spatial densities of identified ganglion cell types in primate retina. *CIBA Found Symp* 1994; 184: 12–34.
152. Silveira LC, Saito CA, Lee BB, Kremers J, da Silva Filho M, Kilavik BE, Yamada ES, Perry VH. Morphology and physiology of primate M- and P-cells. *Prog Brain Res* 2004; 144: 21–46.
153. Chalupa LM, Gunhan E. Development of ON and OFF retinal pathways and retinogeniculate projections. *Prog Retin Eye Res* 2004; 23: 31–51.
154. Troy JB, Shou T. The receptive fields of cat retinal ganglion cells in physiological and pathological states: Where we are after half a century of research. *Prog Retin Eye Res* 2002; 21: 263–302.
155. Wu SM. Synaptic transmission in the outer retina. *Annu Rev Physiol* 1994; 56: 141–168.
156. He S, Dong W, Deng Q, Weng S, Sun W. Seeing more clearly: Recent advances in understanding retinal circuitry. *Science* 2003; 302: 408–411.
157. Boycott BB, Hopkins JM, Sperling HG. Cone connections of the horizontal cells of the rhesus monkey's retina. *Proc R Soc Lond B* 1987; 229: 345–379.
158. Wassle H. Parallel processing in the mammalian retina. *Nat Rev Neurosci.* 2004; 5: 747–757.
159. Lukasiewicz PD. Synaptic mechanisms that shape visual signaling at the inner retina. *Prog Brain Res* 2005; 147: 205–218.
160. Warwick R. The visual pathway. In: Wolff E, ed. *Anatomy of the Eye and Orbit.* 7th ed. Philadelphia: WB Saunders, 1976: 325–395.
161. Horton JC, Greenwood MM, Hubel DH. Non-retinotopic arrangement of fibres in cat optic nerve. *Nature* 1979; 282: 720–722.
162. Fitzpatrick D, Itoh K, Diamond IT. The laminar organization of the lateral geniculate body and the striate cortex in the squirrel monkey (*Saimiri sciureus*). *J Neurosci* 1983; 3: 673–702.
163. Shapley R, Perry VH. Cat and monkey retinal ganglion cells and their visual functional roles. *Trends Neurosci* 1986; 9: 229–235.
164. Conley M, Fitzpatrick D. Morphology of retinogeniculate axons in the macaque. *Vis Neurosci* 1989; 2: 287–296.

165. Anderson DR, Quigley HA. The optic nerve. In: Hart WM Jr, ed. *Adler's Physiology of the Eye,* 9th ed. St. Louis: Mosby–Year Book, 1992: 616–640.
166. Oster SF, Deiner M, Birgbauer E, Sretavan DW. Ganglion cell axon pathfinding in the retina and optic nerve. *Semin Cell Dev Biol* 2004; 15: 125–136.
167. Yucel YH, Zhang Q, Weinreb RN, Kaufman PL, Gupta N. Effects of retinal ganglion cell loss on magno-, parvo-, koniocellular pathways in the lateral geniculate nucleus and visual cortex in glaucoma. *Prog Retin Eye Res* 2003; 22: 465–481.
168. Oster SF, Sretavan DW. Connecting the eye to the brain: The molecular basis of ganglion cell axon guidance. *Br J Ophthalmol* 2003; 87: 639–645.
169. Holmes G. Disturbances of vision by cerebral lesions. *Br J Ophthalmol* 1918; 2: 353–384.
170. Talbot SA. Arrangement of visual area of cat's cortex. *Am J Physiol* 1940; 129: 477–478P.
171. Allman J. The representation of the visual field in the cerebral cortex of the owl monkey (*Aotus trivirgatus*). PhD dissertation, University of Chicago, 1970.
172. Cowey A. Projection of the retina on to striate and prestriate in the squirrel monkey (*Saimiri sciureus*). *J Neurophysiol* 1964; 27: 366–393.
173. van Essen DC, Maunsell JHR. The middle temporal visual area in the macaque: Myeloarchitecture, connections, functional properties and topographic organization. *J Comp Neurol* 1981; 199: 293–326.
174. Allman JM, Kaas JH, Lane RH. The middle temporal visual area (MT) in the bushbaby, Galago sengalensis. *Brain Res* 1973; 57: 197–202.
175. Kaas JH, et al. Cortical visual areas in the tree shrew (*Tupaia glis*): A correlation between cortical evoked potential maps and architectonic subdivision. *Brain Res* 1972; 42: 491–496.
176. Thompson JM, Woolsey CN, Talbot SA. Visual areas I & II of cerebral cortex of rabbit. *J Neurophysiol* 1950; 13: 277–288.
177. Choudhury BP. Retinotopic organization of the guinea pig's visual cortex. *Brain Res* 1978; 144: 19–29.
178. Adams AD, Forrester JM. The projection of the rat's visual field on the cerebral cortex. *Q J Exp Physiol* 1968; 53: 327–336.
179. Woolsey TA. Somatosensory, auditory and visual cortical areas of the mouse. *Johns Hopkins Med J* 1967; 121: 91–112.
180. Kaas JH, Hall WC, Diamond IT. Cortical visual areas I & II in the hedgehog: Relation between evoked potential mapping and architectonic subdivisions. *J Neurophysiol* 1970; 33: 595–615.
181. Woolsey CN, et al. Visual cortex of the marmoset. *Fed Proc* 1955; 14: 166.
182. Olavarria J, Mendez B. The representations of the visual field on the posterior cortex of *Octodon degus. Brain Res* 1979; 161: 539–543.
183. Tiao YC, Blakemore C. Functional organization in the visual cortex of the golden hamster. *J Comp Neurol* 1976; 168: 459–482.
184. Hall WC, et al. Cortical visual areas in the grey squirrel (*Sciurus carolinesis*): A correlation between cortical evoked potential maps and architectonic subdivisions. *J Neurophysiol* 1971; 34: 437–452.
185. Clarke PGH, Whitteridge D. The cortical visual areas of the sheep. *J Physiol Lond* 1976; 256: 497–508.
186. Ofri R. Electrophysiological and histological mapping of the cortical area of central vision in the dog. PhD dissertation, University of Florida, 1993.
187. Ofri R, Dawson WW, Samuelson DA. Mapping of the cortical area of central vision in two dog breeds. *Vet Comp Ophthalmol* 1994; 4: 172–178.
188. Brodmann K. Beitrage zur histologischen Localisation der Grosshirnrinde. Dritte Mitteilung. Die Rindenfelder der niederen Affen. *J Psychol Neurol* 1905; 4: 177–226.
189. Tusa RJ, Palmer LA, Rosenquist AC. The retinotopic organization of area 17 (striate cortex) in the cat. *J Comp Neurol* 1978; 177: 213–236.
190. Woolsey CN, Fairman D. Contralateral, ipsilateral and bilateral representation of cutaneous receptors in somatic area I & II of the cerebral cortex of pig, sheep and other mammals. *Surgery* 1946; 19: 684–702.
191. Bilge M, et al. A map of the visual cortex in the cat. *J Physiol Lond* 1967; 191: 116P–118P.
192. Halliday AM, Michael WF. Changes in pattern-evoked responses in man associated with the vertical and horizontal meridians of the visual field. *J Physiol Lond* 1970; 208: 499–513.
193. Bartels A, Zeki S. The chronoarchitecture of the cerebral cortex. *Philos Trans R Soc Lond B Biol Sci* 2005; 360: 733–750.
194. Manger PR, Rosa MG. Visual thalamocortical projections in the flying fox: Parallel pathways to striate and extrastriate areas. *Neuroscience* 2005; 130: 497–511.
195. Fitzpatrick D, Lund JS, Schmechel DE, Towles AC. Distribution of GABAergic neurons and axon terminals in the macaque striate cortex. *J Comp Neurol* 1987; 264: 73–91.
196. O'Kusky J, Colonnier M. A laminar analysis of the number of neurons, glia, and synapses in the visual cortex (area 17) of adult macaque monkeys. *J Comp Neurol* 1982; 210: 278–290.
197. Ejima Y, Takahashi S. Positioning of retinotopic areas and patterning of cerebral cortex layout. *Neuroreport* 2005; 16: 9–12.
198. Heider B, Jando G, Siegel RM. Functional architecture of retinotopy in visual association cortex of behaving monkey. *Cereb Cortex* 2005; 15: 460–78.
199. Allman JM, Kaas JH. A representation of the visual field in the caudal third of the middle temporal gyrus of the owl monkey (*Aotus trivirgatus*). *Brain Res* 1971; 31: 85–105.
200. van Essen DC. Visual areas of the mammalian cerebral cortex. *Annu Rev Neuro Sci* 1979; 2: 227–263.
201. Daniel PM, Whitteridge D. The representation of the visual field on the cerebral cortex in monkeys. *J Physiol Lond* 1961; 159: 203–221.
202. Allman JM. Maps in context: Some analogies between visual cortical and genetic maps. In: Vaina LM, ed. *Matters of Intelligence.* Boston: D. Reidl, 1987: 369–393.
203. Talbot SA. A lateral localization in cat's visual cortex. *Fed Proc* 1942; 1: 84.
204. Sanides F, Hoffman J. Cyto- and myeloarchitecture of the visual cortex of the cat and of the surrounding integration cortices. *J Hirnforsch* 1969; 11: 79–104.
205. Wagor E, Mangini NJ, Pearlman AL. Retinotopic organization of striate and extrastriate visual cortex in the mouse. *J Comp Neurol* 1980; 193: 187–202.
206. Hubel DH, Wiesel TN. Visual area of the lateral suprasylvian gyrus (Clare-Bishop area) of the cat. *J Physiol Lond* 1969; 202: 251–260.
207. Palmer LA, Rosenquist AC, Tusa RJ. The retinotopic organization of lateral suprasylvian visual areas in the cat. *J Comp Neurol* 1978; 177: 237–256.
208. Tusa RJ, Palmer LA. Retinotopic organization of areas 20 and 21 in the cat. *J Comp Neurol* 1980; 193: 147–164.

209. Rosa MG, Palmer SM, Gamberini M, Tweedale R, Pinon MC, Bourne JA. Resolving the organization of the New World monkey third visual complex: The dorsal extrastriate cortex of the marmoset (Callithrix jacchus). *J Comp Neurol* 2005; 483: 164–191.
210. Rosa MG, Tweedale R. Brain maps, great and small: Lessons from comparative studies of primate visual cortical organization. *Philos Trans R Soc Lond B Biol Sci* 2005; 360: 665–691.
211. Fort A, Besle J, Giard MH, Pernier J. Task-dependent activation latency in human visual extrastriate cortex. *Neurosci Lett* 2005; 379: 144–148.
212. Stent GS. *Function and Formation of Neural Systems.* Berlin: Dahlem Konferenz, 1977.
213. Hubel DH, Wiesel TN. Functional architecture of macaque monkey visual cortex. *Proc R Soc Lond* B 1977; 198: 1–59.
214. Hubel DH, Wiesel TN. Brain mechanisms of vision. *Sci Am* 1979; 269: 150–162.
215. Binzegger T, Douglas RJ, Martin KA. A quantitative map of the circuit of cat primary visual cortex. *J Neurosci* 2004; 24: 8441–8453.
216. Lehky SR, Sejnowski TJ, Desimone R. Selectivity and sparseness in the responses of striate complex cells. *Vision Res* 2005; 45: 57–73.
217. Tagawa Y, Kanold PO, Majdan M, Shatz CJ. Multiple periods of functional ocular dominance plasticity in mouse visual cortex. *Nat Neurosci* 2005; 8: 380–388.
218. Martinez LM, Wang Q, Reid RC, Pillai C, Alonso JM, Sommer FT, Hirsch JA. Receptive field structure varies with layer in the primary visual cortex. *Nat Neurosci* 2005; 8: 372–379.
219. Livingstone MS, Hubel DH. Anatomy and physiology of a color system in the primate visual cortex. *J Neurosci* 1984; 4: 309–356.
220. Livingstone MS, Hubel DH. Psychophysical evidence for separate channels for the perception of form, color, movement and depth. *J Neurosci* 1987; 7: 3416–3468.
221. Livingstone MS, Hubel DH. Segregation of form, color, movement and depth: Anatomy, physiology and perception. *Science* 1988; 240: 740–749.
222. Mishkin M, Ungerleider LG, Macko KA. Object vision and spatial vision: Two cortical pathways. *Trends Neurosci* 1968; 6: 414–417.
223. Newsome WT, Mikami A, Wurtz RH. Motion selectivity in macaque visual cortex. III. Psychophysics and physiology of apparent motion. *J Neurophysiol* 1986; 55: 1340–1351.
224. Perrett DI, Rolls ET, Caan W. Visual neurons responsive to faces in the monkey temporal cortex. *Exp Brain Res* 1982; 47: 329–342.
225. Arshavsky VY. Rhodopsin phosphorylation: From terminating single photon responses to photoreceptor dark adaptation. *Trends Neurosci* 2002; 25: 124–6.
226. Hurley JB, Chen J. Evaluation of the contributions of recoverin and GCAPs to rod photoreceptor light adaptation and recovery to the dark state. *Prog Brain Res* 2001; 131: 395–405.
227. Fain GL. Dark adaptation. *Prog Brain Res* 2001; 131: 383–394.
228. Raninen A, Franssila R, Rovamo J. Critical flicker frequency to red targets as a function of luminance and flux across the human visual field. *Vision Res.* 1991; 31: 1875–1881.
229. Berman SM, Greenhouse DS, Bailey IL, Clear RD, Raasch TW. Human electroretinogram responses to video displays, fluorescent lighting, and other high frequency sources. *Optom Vis Sci* 1991; 68: 645–662.
230. Armitage JA, Bui BV, Gibson R, Vingrys AJ. Postnatal development of flicker sensitivity in guinea pigs. *Clin Exp Optom* 2001; 84: 270–275
231. Pasternak T, Merigan WH. Movement detection by cats: Invariance with direction and target configuration. *J Comp Physiol Psych* 1980; 94: 943–952.
232. Angelaki DE. Eyes on target: What neurons must do for the vestibuloocular reflex during linear motion. *J Neurophysiol* 2004; 92: 20–35.
233. Clifford CW, Ibbotson MR. Fundamental mechanisms of visual motion detection: Models, cells and functions. *Prog Neurobiol* 2002; 68: 409–437.
234. Vaney DI, Taylor WR. Direction selectivity in the retina. *Curr Opin Neurobiol* 2002; 12: 405–410.
235. Parker AJ, Cumming BG. Cortical mechanisms of binocular stereoscopic vision. *Prog Brain Res.* 2001; 134: 205–216.
236. Casagrande VA, Boyd JD. The neural architecture of binocular vision. *Eye* 1996; 10: 153–160.
237. Read J. Early computational processing in binocular vision and depth perception. *Prog Biophys Mol Biol* 2005; 87: 77–108.
238. Tychsen L. Binocular vision. In: Hart WM Jr, ed. *Adler's Physiology of the Eye,* 9th ed. St. Louis: Mosby–Year Book, 1992: 773–853.
239. van Sluyters TC, Steward DL. Binocular neurons of the rabbit visual cortex. *Exp Brain Res* 1974; 19: 166–195.
240. Clarke PGH, Donaldson IML, Whitteridge D. Binocular visual mechanisms in cortical areas I and II of the sheep. *J Physiol* (London) 1976; 256: 509–526.
241. Timney B, Keil K. Local and global stereopsis in the horse. *Vision Res* 1999; 39: 1861–1867.
242. Yokoyama S. Molecular evolution of color vision in vertebrates. *Gene* 2002; 300: 69–78
243. Pichaud F, Briscoe A, Desplan C. Evolution of color vision. *Curr Opin Neurobiol* 1999; 9: 622–627.
244. Gegenfurtner KR, Kiper DC. Color vision. *Annu Rev Neurosci* 2003; 26: 181–206.
245. Weale RA. *Focus on Vision.* London: Hodder and Stoughton, 1982.
246. Ringo J, Wolbarsht ML, Wagner HG, Crocker R, Amthor F. Trichromatic vision in the cat. *Science* 1977; 198: 753–755.
247. Smith EL, Greenwood VJ, Bennett ATD. Ultraviolet colour perception in European starlings and Japanese quail. *J Exp Biol* 2002; 205: 3299–3306.
248. Stone J. A quantitative analysis of the distribution of ganglion cells in the cat's retina. *J Comp Neurol* 1965; 124: 337–352.
249. Ofri R, Dawson WW, Gelatt KN. Visual resolution in normal and glaucomatous dogs determined by pattern electroretinogram. *Prog Vet Comp Ophthalmol* 1993; 3: 111–116.
250. Millodot M. Image formation in the eye. In: Barlow HB, Mollon JD, eds. *The Senses.* Cambridge: Cambridge University Press, 1982: 46–61.
251. Habib MS, et al. Myopic intrastromal photorefractive keratectomy with the neodymium-yttrium lithium fluoride picosecond laser in the cat cornea. *Arch Ophthalmol* 1995; 113: 499–505.
252. Farrall H, Handscombe MC. Follow-up report of a case of surgical aphakia with an analysis of equine visual function. *Eq Vet J Suppl* 1990; 10: 91–93.
253. Pak MA. Ocular refraction and visual contrast sensitivity of the rabbit, determined by the VECP. *Vision Res* 1984; 24: 341–345.

254. Irving EL, et al. Chick eye optics: Zero to fourteen days. *J Comp Physiol* 1996; 179: 185–194.
255. Neitz J, Jacobs GH. Reexamination of spectral mechanisms in the rat (*Rattus norvegicus*). *J Comp Psychol* 1986; 100: 21–29.
256. Loops MS, Millican CL, Thomas SR. Photopic spectral sensitivity of the cat. *J Physiol Lond* 1987; 382: 537–553.
257. Guenther E, Zrenner E. The spectral sensitivity of dark and light-adapted cat retinal ganglion cells. *J Neurosci* 1993; 13: 1543–1550.
258. Neitz J, Geist T, Jacobs GH. Color vision in the dog. *Vis Neurosci* 1989; 3: 119–125.
259. Jacobs GH, et al. Photopigments of dogs and foxes and their implication for canid vision. *Vis Neurosci* 1993; 10: 173–180.
260. Carrol J, Murphy CJ, Neitz M, ver Hoeve JN, Neitz J. Photopigment basis for dichromatic color vision in the horse. *J Vision* 2001; 1: 80–87.
261. Timney B, Macuda T. Vision and hearing in horses. *J Am Vet Med Assoc* 2001; 218: 1567–1574.
262. Neitz J, Jacobs GH. Spectral sensitivity of cones in an ungulate. *Vis Neurosci* 1989; 2: 97–100.
263. Jacobs GH, Deegan II JF, Neitz J. Photopigment basis for dichromatic color vision in cows, goats and sheep. *Visual Neurosci* 1998; 15: 581–584.
264. Jacobs GH, Deegan JF II. Spectral sensitivity, photopigments and color vision in the guinea pig (*Cavia porcellus*). *Behav Neurosci* 1994; 108: 993–1004.
265. Ringo J, et al. Trichromatic vision in the cat. *Science* 1977; 198: 753–755.
266. Odom JV, Bromberg NM, Dawson WW. Canine visual acuity: Retinal and cortical field potentials evoked by pattern stimulation. *Am J Physiol* 1983; 245: R636–R641.
267. Belleville S, Wilkinson F. The development of vernier acuity in the cat. *Invest Ophthalmol Vis Sci* 1990; 31: 1175–1180.
268. Pasternak T, Horn K. Spatial vision of the cat: Variation with eccentricity. *Vis Neurosci* 1991; 6: 151–158.
269. Timney B, Keil K. Visual acuity in the horse. *Vision Res* 1992; 32: 2289–2293.
270. ver Hoeve JN, Neitz J, Murphy CJ. Horse sense: Electrophysiologic measures of equine vision. *Invest Ophthalmol Vis Sci* 1999; 40: ARVO abstract S22.
271. Reymond L. Spatial visual acuity of the eagle *Aquila audax:* A behavioural, optical and anatomical investigation. *Vision Res* 1985; 25: 1477–1491.
272. Howland HC, Howland M, Murphy CJ. Refractive state of the rhinoceros. *Vision Res* 1993; 33: 2649–2651.
273. SivakJG, et al. The eye of the hooded seal, *Cystophora cristata,* in air and water. *J Comp Physiol* 1989; 165: 771–777.

Section II

FOUNDATIONS OF CLINICAL OPHTHALMOLOGY

Chapter 5

Ocular Immunity

Daniel J. Biros

INTRODUCTION

Comparative ophthalmologists have come a long way in understanding how the immune response affects ocular disease in domestic animals. From cancer to infection, trauma to autoimmunity, almost all ocular pathology can be linked to one or more components of the immune response. Further, recognition of most ocular diseases and delivery of the most effective treatments for common eye problems are becoming more dependent on an accurate and up-to-date understanding of ocular immunity both in health and disease. The goal of this chapter is twofold: to distinguish ocular immunity as an extreme type of a regional immune response and to explain how most of the time the delicate tissue of the eye is well protected from the powerful and often destructive forces of the immune system but at other times becomes highly vulnerable when the forces of ocular immunity break down.

WHAT IS OCULAR IMMUNITY?

Ocular immunity is a highly specialized form of a regional immune response whereby the body alters immune system functionality in order to preserve the delicate tissues of the eye. Regional immunity is important because to protect itself against a great range of invading pathogens, the body must possess diverse strategies. As a result, a range of immune effector mechanisms has evolved. Many subsets of not only T cells but also immunoglobulin classes exist to provide the best possible protection against pathogen invasion and disease. Individual body tissues are able to select among this wide range of defense mechanisms to preserve physiologic function while overcoming the virulence of the invading pathogen.

The eye has developed specific and unique mechanisms to maintain homeostasis and minimize the potential for damage inflicted by immunogenic inflammation (Table 5.1). Otherwise known as ocular immune privilege, ocular immunity is defined by (a) the unique passive and active immunomodulatory properties of its microenvironment, (b) its ability to alter the functionality of immune cells, and (c) its expression of immune tolerance in an allograft tissue transplantation setting. The phenomenon now known as immune privilege was first reported by van Dooremal in a paper published in 1873[1] and later rediscovered by Medawar in the late 1940s.[2] Medawar later won the Nobel prize for his work. It was Medawar who first defined an immune privileged site as one of immunologic ignorance, stating that the unique properties of immune privilege sites were passive in nature. Less than a decade later, in 1953, Billingham first reported the corneal epithelium as immune privileged tissue.[3] Only later would we understand that the unique immune properties held within the corneal epithelium would significantly contribute to the high success rate of corneal transplantation in humans. Nonetheless, it wasn't until around 1975 that Billingham, Kaplan, Streilein, and their colleagues discovered that ocular immunity actually possesses active and systemic mechanisms in addition to the passive localized features pointed out by Medawar.[4–6] This discovery led to the current definitions of immune privilege described primarily as a unique set of

Table 5.1 Concepts in Regional Immunity Applied to the Eye

Concept	Ophthalmic Manifestation
Semiconfined microenvironment	Aqueous humor produced by the ciliary body; vitreous
Tissue-specific antigen presenting cells	Macrophages and dendritic cells in the iris stroma, trabecular meshwork, ciliary body, choriocapillaris stroma; microglia of retina
Innate immune cells	Iridal, choroidal, and ciliary body stromal macrophages
Blood–ocular barrier	Tight junctions in ciliary body and retinal pigment epithelium; vascular endothelium of iris and retinal vessels
Afferent lymphatics	No lymphatic vessels except in choroid; uveoscleral pathway
Nerves	Autonomic nerves in iris, ciliary body, choroid; corneal C-type fibers

characteristics of a tissue (or a site) in the body based specifically on its response to tissue transplantation: *immune privileged tissue* is tissue that survives for a prolonged period of time in a nonimmune privileged site,[7–10] and *immune privileged site* is a part of the body that can contain a transplanted non–immune privileged tissue for a prolonged period of time.[4] Active and passive mechanisms of ocular immune privilege (to be discussed in more detail later) are listed in Table 5.2. Known immune privileged tissues and sites are listed in Tables 5.3 and 5.4.

PRINCIPLES OF INNATE AND ADAPTIVE IMMUNITY

Before examining the details of what drives the ocular immune response, we should first understand the components of the two primary levels of immune regulation: innate and adaptive immunity. In general, the innate immune system is based on the phagocyte response as a first line of defense in an infection. Receptors found on circulating neutrophils and macrophages locate and bind, for example, many common bacterial surface markers. This leads to phagocytosis of the pathogen and release of cytokines into the environment. These cytokines in turn mediate the behavior of other immune cells. The innate response occurs within minutes to hours of injury or infection and is seen clinically as acute inflammation: redness, pain, swelling, heat, and impairment or loss of tissue function. Vasodilation and vasopermeability also characterize innate immunity and are integral to mounting a successful immune response to the pathogen by permitting the travel of innate immune cells to the site of infection.

The adaptive immune response depends on successful presentation of a pathogenic antigen to a circulating antigen-presenting cell (APC). These antigen-loaded APCs then migrate from the affected tissue to a regional lymph node to activate and trigger the production of a clonal population of lymphocytes. The stimulated lymphocytes travel out of the lymph node and circulate to the site of infection to release a targeted killing of the pathogen. This is accomplished either by direct killing of the pathogen by the lymphocyte or by directing other lymphocytes to release cytokines that direct other immune cells to clear the pathogen. Adaptive immunity takes up to 7 days to elicit a specific population of lymphocytes to direct a highly specific and directed targeting of the pathogen. The mechanisms of adaptive immunity are designed to eliminate the four classes of pathogens: extracellular bacteria, parasites, and fungi; intracellular bacteria and parasites; viruses; and parasitic worms. Several immune effectors and their functional properties are listed in Table 5.5. The T cell response is a primary focus of study in ocular immunity. The anterior chamber–associated immune deviation (ACAID) response (discussed later) is an example of regional immune deviation from a conventional T cell

Table 5.2 Tissue Characteristics in Ocular Immunity

1. Blood–tissue barrier
2. No lymphatic vessels
3. Low MHC molecule expression
4. Presence of functional immunomodulatory factors
5. Extended allograft survival compared with other tissues
6. Capable of APC-mediated immune deviation
7. Abundant Fas ligand expression
8. Ability to generate regulatory T cells

Table 5.3 Immune Privilege Sites

1. Brain
2. Eye: central cornea, anterior chamber, vitreous cavity, subretinal space
3. Pregnant uterus
4. Testis
5. Hair follicles
6. Adrenal cortex
7. Certain tumors
8. Hamster cheek pouch

Table 5.4 Immune Privilege Tissues

1. Brain and spinal cord
2. Eye: cornea, lens, pigment epithelium, retina
3. Placenta
4. Ovary
5. Testis
6. Liver
7. Certain tumors
8. Hamster cheek pouch

Table 5.5 Functions of Immune Effectors

Immune Effectors	Functional Properties
Neutrophils	Secrete toxic cytokines and promote angiogenesis
Macrophages	Secrete mediators, causing bystander tissue damage
Complement-fixing antibodies	Activate complement
Activated complement	Triggers generalized inflammation
NK cells	Lyse MHC class I
Th1 and Th2 cells	Secrete proinflammatory cytokines, bystander damage
Cytotoxic T cells	Destroys MHC class I–expressing target cells
Noncomplement-fixing antibodies	Neutralizes pathogens
iC3b	Promotes ACAID

response leading to adaptive immunity. In order to fully understand the principles of ocular immunity and ACAID, it is worthwhile to review the mechanisms of the T cell in adaptive immunity.[11]

T Cell Activation

There are two distinct signals in T cell activation. The first is accomplished through antigen recognition and the second through accessory activation receptors such as B7 and ICAM-1 on the surface of the APC and CD28 and LFA-1 on the surface of the T cell. Two classes of major histocompatibility complex (MHC) molecules on the surface of APC present processed antigen to the T cell receptor (TCR). Class I MHC presents intracellular processed antigens, and class II MHC presents exogenous antigens such as those from bacteria or fungus. Based on genetic recombination, individuals possess a wide variety of types of TCR; T cells therefore are able to recognize a wide variety of antigens. Nonetheless, T cells can bind processed antigen only in the context of the MHC of the same individual. CD8 and CD4 receptors on T cells also bind to MHC class I and MHC class II, respectively. CD4 and CD8 markers are found only on mature T cells but do contribute to T cell activation as part of Signal 1 (antigen recognition).

Without the second, or accessory, activation receptor signal, T cell activation will not happen. Activation is mediated through B7 on the APC-binding CD28 on the T cell or ICAM-1 on the APC-binding LFA-1 on the T cell. This signal is most important when activating naïve T cells and serves to amplify the intracellular signals triggered during the TCR–MHC interaction. After the accessory T cell–APC ligands are formed, there is an upregulation of interleukin (IL)-2 and IL-2 receptor on the T cell. The autocrine function of IL-2 results in T cell proliferation and clonal expansion of the antigen-specific T cells.

T Cell Differentiation

Three factors in general determine the nature of the T cell produced in an adaptive response: the manner of antigen presentation, the type of APC, and the microenvironment in which the T cells are activated.[12] The nature of the innate immune response also influences the outcome of adaptive immunity.[13] There are roughly three types of Th cells in adaptive immunity: Th1, Th2, and Th3. They are defined by the cytokines produced and the type of effector response elicited. Th1 cells are characterized by interferon-gamma (IFN-γ), tumor necrosis factor (TNF), and IL-2 production. They result in functions including delayed type hypersensitivity (DTH), tumor rejection, and allograft rejection, and they can mediate B cell switching to complement-fixing IgG. Th2 cells produce IL-4, IL-5, and IL-13 and are associated with allergic responses. Th3 cells make TGF-β, IL-4, and IL-10 and can suppress Th1 and Th2 activity. The Th3 cells have only recently been characterized and are shown to be the result of oral tolerance and also the immunomodulatory effect of aqueous humor on activated T cells. Th3 cells have a potential to suppress autoimmunity mediated by Th1 cells.

Intracellular signals triggered by surface receptor activation drive the T cell response by regulating proliferation, driving lymphokine production, and promoting expression of surface receptors. The level of intracellular signaling during T cell activation is dictated in part by the affinity of the TCR to the bound MHC. High-affinity binding leads to a Th1 response, and low-affinity binding leads to a Th2 (and possibly a Th3) response. Factors that may affect affinity include amino acid substitution of the processed antigen and unfavorable MHC binding leading to differentiated TCR signaling.

Macrophages and dendritic cells may also present antigen to T cells through their roles as innate immune response mediators, leading primarily to a Th1 response. These macrophages and dendritic cells upregulate MHC class II expression via pathogen-associated molecular patterns (PAMP) found on the surface of pathogens. PAMP-induced production of IFN-γ, TNF, and IL-12 also contributes to the development of the Th1 response.

Unlike macrophages and dendritic cells, activated B cells have the ability to present antigen to T cells, leading to a Th2 response. B cells bind antigen to their surface immunoglobulin and process it to be presented on MHC class II, which in turn finds appropriate TCR for T cell activation in a Th2 manner. Overexpression of B cell–activating protein B7.2 and secretion of IL-1 are thought to contribute to a Th2 response. Absence of IFN-γ or IL-12 during Th differentiation also leads to a preferential development of a Th2 response.

Natural killer T (NKT) cell activation is another way to induce a Th2 cell response. NKT cells bind the processed antigen in the cleft of CD-1, an MHC class I analogue found on cells such as intestinal epithelium, and secrete IL-4, a Th2-associated cytokine. On the other hand, natural killer (NK) cells in certain circumstances promote Th1 response when activated by cells devoid of MCH class I. Once activated, NK cells secrete IFN-γ.

Cytokines found in the T cell microenvironment can also influence T cell differentiation. IL-4 and IFN-γ suppress the production of each other, promoting either a Th2 or Th1 response, respectively. Th3 cells, by their production of TGF-β, can suppress both Th1 and Th2 cells. Other environments rich in constitutive TGF-β production, including the aqueous humor, can also promote suppression of a Th1 or Th2 response by favoring production of Th3 cells. This process of Th3 promotion is a characteristic of immune privileged tissue and works to promote a vastly different immune environment than what is found in conventional tissues such as the skin.

T Cell Termination

When pathogens are cleared or when the need for a T cell response is no longer necessary, it is imperative that the T cell response stops in order to prevent ongoing inflammation and unnecessary tissue damage. The desire to halt hypersensitivity responses, autoimmunity, and allograft rejection stem from the body's recognition of ending adaptive immunity and reestablishing homeostasis, immune privilege, and an environment

that promotes self-tolerance. The general term used in the events surrounding Th1 termination is *immunosuppression.* Four types of immunosuppression are categorized: anergy, passive death, active death, and cytokine-mediated suppression.[14]

Anergy

In general, anergy occurs when Signal 1, the processed antigen binding the TCR, is not followed by Signal 2, the activation of CD28. The corollary also holds because anergy also appears when Signal 2 occurs without Signal 1. When one signal is not accompanied by another, there is no production of IL-2 and the T cells fail to proliferate. Examples of anergy may be found when the pathogen was adequately cleared by the innate immune response or when there is a significant reduction of PAMPs such that APCs reduce the expression of accessory molecules. CTLA-4 upregulation on the surface of activated T cells leads to reduced binding of CD28 as both CD28 and CTLA-4 compete for B7 on the APC. CTLA-4 mediates suppressive signals in the activated Th cell and is thought to be a self-regulating mechanism since it is only found on activated T cells.

Lack of PAMPs may also induce anergy due to antigen presentation in the absence of inflammation. Reduced levels of MHC and accessory molecules are the result of this type of anergy. Presentation of many autoantigens also may trigger this type of anergy, leading to peripheral tolerance. Immune privilege tissues also are thought to exhibit Th cell anergy due to inherent low expression of MHC molecules.

Passive Cell Death

Also known as death by neglect, antigen specific T cells that never encounter their antigen will not survive. Both naïve and memory Th cells are susceptible to passive cell death. Memory Th cells need ongoing low-level stimulation in order to retain immunologic memory. It is thought that small amounts of antigen in the host acquired through immunization or previous infection contribute to the maintenance of memory T cells. Passive T cell death is by apoptosis and is Fas-independent (see active T cell death below). Activated T cells can counter this death by neglect by upregulating intracellular expression of Bcl-2 and Bcl-x. IL-2 production also can prevent passive death of Th cells.

Active T Cell Death

Activated Th cells express Fas (CD95) on their surface. Fas binds with Fas-ligand (Fas-L or CD95L) found on other cells, including other Th cells, to induce apoptotic death. Apoptosis is achieved through membrane degradation, enzymatic destruction of DNA, and cellular bleb formations that are taken up by other cells. The upregulated Bcl-2 and Bcl-x expression that protects the Th cell from passive cell death does not protect the Th cell from Fas-mediated apoptosis. This type of immunosuppression is also considered to be self-regulatory in that both repeated Th cell stimulation and IL-2 production promote active T cell death. The fact that T cells also express Fas-L also demonstrates a mechanism of Th cell regulation against overproliferation. Immune privileged tissues express large amounts of Fas-L, contributing to allograft survival and suppression of Th1 responses. However, Fas-Fas-L–mediated apoptosis is suppressed by healthy aqueous humor, suggesting that TGF-β, a potent anti-apoptotic factor constitutively produced in the anterior chamber, may counter the effects of active Th cell death in the eye. Further, Fas-Fas-L–mediated Th cell apoptosis is enhanced by neutrophil degranulation, another event that is suppressed by the immunomodulatory factors found in the eye. Therefore the precise role of active Th cell death in the eye is not fully understood.

Immunosuppression by Cytokines

Finally, T cells can be regulated by the cytokines found in their environment. These can be endogenous cytokines produced by resident cells or cytokines found as a product of the immune cells in the environment. As mentioned earlier, Th cell populations are defined and sustained by the types of factors they produce. They are also influenced by the cytokines that either promote or suppress their development. IL-12 and IFN-γ promote development of Th1 cells, whereas IL-4, IL-10, and TGF-β suppress Th1 development. Th1 cells are associated with DTH and the induction of cytolytic $CD8^+$ T cells, and they promote B cell class switching to complement-fixing antibody production. Th2 cells are sustained by IL-1 and IL-4 production but are suppressed by IL-12, IFN-γ, and TGF-β. Th2 cells mediate allergic responses and promote B cell growth and immunoglobulin class switching to non-complement-fixing antibodies. They also suppress inflammation induced by macrophages. Th3 cells are promoted by TGF-β in conjunction with IL-4 and IL-10, and by α-MSH. Th3 cell activity is inhibited by IFN-γ and possibly by TNF. Th3 cells, as mentioned earlier, suppress Th1 and Th2 cell activity, and because of their production of TGF-β, they also may mediate B cell immunoglobulin switching to IgA.

The presence of particular populations of activated immune cells will influence the differentiation of Th cells. If active NK cells are present in an inflammatory environment, they promote a Th1 response because they make IFN-γ. By contrast, if activated NKT cells are present, a Th2 type response is invoked because of their production of IL-4. If APCs that are *not* producing IL-12 and IFN-γ are present, a Th2 response is likely, and so on. It is conceivable that specific immune responses may be selected on the basis of the cytokines found in a given microenvironment. As discussed later, the ocular microenvironment is a clear example of such selectivity.

OVERVIEW OF AN IMMUNE RESPONSE

The general immune response is reviewed in this section in the context of something we can relate to in ophthalmology: corneal allograft rejection. More specific details of immune response are discussed later in the section "Immunology of

Corneal Transplantation." The donor graft contains alloantigens against which the recipient will have an adaptive immune response. In order to establish a full-blown immune response, a series of events must occur in the immune system. In the first, or inductive, phase, APCs present the donor-derived alloantigens to alloreactive T cells. This is the afferent limb of the immune reflex. APCs develop in the bone marrow and are either dendritic cells or macrophages. APCs leave the bone marrow and normally reside throughout the body's parenchyma. APCs possess on their surface abundant amounts of MCH class I and II. Alloreactive T cells may recognize allogeneic MHC class I and II in one of two ways: by a direct binding of the T cell receptor to the MHC molecule as a ligand or by the detection of an MHC-derived peptide in the groove of another MHC molecule. It is in the latter type of presentation that minor histocompatibility antigens are processed and presented to T cells. Stimulated APCs also secrete proinflammatory cytokines (IL-12) and upregulate other APC surface markers (B7, ICAM, CD40) integral to T cell activation. The APCs are constantly circulating throughout the body, and once they encounter antigen, they migrate through the lymphatics to the parafollicular cortex of the draining regional lymph node where T cells continuously migrate. Once a naïve T cell encounters an APC bearing surface antigen peptides, the T cells undergo clonal expansion, which begins the second, or efferent, limb of the immune reflex. It is generally accepted that as in nongraft-related immune responses, T cells can be activated only by APCs bearing processed alloantigen on their surfaces. Further, this encounter must occur in the secondary lymphoid organs such as the spleen or lymph nodes, not in the site of the graft.

The clonally expanded T cells leave the lymph node where they expanded and travel to the site of the graft, where they initiate effector responses that can destroy the allograft. At the graft site, effector T cells are easily reactivated by virtually any cell that presents alloantigen, namely, keratocytes, epithelium, and endothelium. The corneal graft is different from a healthy cornea in that its cells now express costimulatory molecules similar to professional APCs—the same molecules that can serve as targets for T cell effector function. The graft also reacts to proinflammatory cytokines secreted by reactivated effector T cells by upregulating expression of MHC even more, making it possible to intensify the effector immune response. In summary, mechanisms of the termination of the T cell response arise when antigen presentation drops off, when MHC expression falls, or when immunosuppressive factors neutralize the inflammatory environment.

OCULAR SURFACE IMMUNITY

The ocular surface is an extension of the skin and exhibits many of the immune properties of mucosal surfaces. Most of the healthy ocular surface is *not* an immune privileged site, and other than the central cornea, does not contain any immune privileged tissue. The conjunctival tissue is replete with $CD1^+$ dendritic cells and macrophages, which serve as sentinels protecting the eye from pathogens.[15,16] The extensive vascular network allows for rapid and robust immune affector and effector immune responses, utilizing the draining lymph node as a link between afferent and efferent immunity. There is also a resident population of $CD8^+$ T cells located between epithelium and in the substatia propria.[17–20] Function of these $CD8^+$ cells is unclear other than that they partake in immune response regulation. $CD4^+$ and B cells are normally found at the mucosal surfaces in far fewer numbers. Other specialized epithelial cells also assist in afferent immunity, similar to M cells found in the gastrointestinal tract. And while $CD8^+$ cells are the predominant cell type in the ocular surface efferent immune response, both $CD4^+$ and B cells increase in number during conjunctival inflammation. Distribution of the immune cells on the ocular surface varies: the healthy perilimbal conjunctiva contains the highest concentration of immune cells. Mast cells also constitute a significant population of ocular surface immune cells.[21,22]

The lacrimal tissue specializes in tear production and provides via the tear secretions delivery of ocular surface immunoglobulins, mostly IgA and to a much lesser extent IgG, and others.[23–25] B cells, T cells, and macrophages are all found in healthy lacrimal tissue.[26–28] The role of these cells is poorly understood, but they may play a part in both afferent and efferent arms of the adaptive immune response. Ocular surface inflammatory diseases are widespread among species. They include pathogen-induced inflammation (bacterial and viral origin, especially feline herpesvirus), autoimmunity (keratoconjunctivitis sicca, allergy, nodular granulomatous episcleritis), and cancer (squamous cell carcinoma). Chemical toxicities also elicit a marked and sometimes vision-threatening innate immune response, resulting in massive chemosis, conjunctival inflammation, and in many cases acute corneal necrosis with corneal perforation. It is important to remember the cornea, especially the central cornea, is very limited in a rapid immune response; it is immune privileged tissue and an immune privileged site. For this reason, perhaps, it is essentially vulnerable to acute inflammation extending from the surrounding conjunctival ocular surface. On the other hand, the healthy central cornea is capable of accepting allografts at a rate far higher than that of other body tissues, in part because of its specialized immunity, which is discussed in the section "Immunology of Corneal Transplantation."

ANTERIOR CHAMBER–ASSOCIATED IMMUNE DEVIATION

The anterior chamber, vitreous chamber, and subretinal space are all endowed with a unique type of immunity that protects the delicate and irreplaceable tissue of the eye from inflammation.[5,6,29–35] APCs in the eye capture antigen within the eye, then migrate out of the eye via the trabecular meshwork (in the case of antigen presentation in the anterior chamber) into the bloodstream to the spleen, where they form clusters with $CD4^+$, $CD8^+$, and NKT cells in the splenic marginal zone.

Within these clusters, the APCs secrete chemokines (CXCL2 or MIP-2), which recruit more NKT cells to the site.[36,37] These NKT cells bind the APC and produce a specialized microenvironment that contains TGF-β2, IL-10, and thrombospondin.[38,39] More APCs and marginal zone B cells arrive at these cluster formations. Finally, T cells specific to the eye-derived antigen start to aggregate at the cluster. These T cells are activated by both the eye-derived APCs that first encountered the antigen and the splenic B cells.[40,41]

Once activated, the T cells, known as regulatory T cells (Treg), become the afferent $CD4^+$ and efferent $CD8^+$ cells characterized in ACAID.[42,43] The $CD4^+$ cells suppress the activation and differentiation of naïve T cells into the proinflammatory Th1 effector cells. The $CD8^+$ efferent cells suppress expression of Th1-mediated immunity (including DTH). Afferent Tregs act in the secondary lymphoid organs, and efferent Tregs act in the peripheral tissues, including the eye.[44–46]

ACAID is an immune response that can be adoptively transferred to other mice, either through the blood of an ACAID-induced mouse 24 to 48 hours post antigen injection or through systemic injection of iris or ciliary body APCs from a mouse that received antigen into the anterior chamber 24 hours previously.[47,48] The spleen is necessary for ACAID to occur because APCs treated *in vitro* with TGF-β preferentially travel to the spleen after intravenous injection into naïve mice.[49]

As noted, ACAID is a systemic response, not simply a local response. Before ACAID was discovered, the eye was thought to escape active immune responses by immunologic ignorance by sequestering antigens away from immune recognition. Ocular immunity, including ACAID, is much more than immunologic ignorance. It is now understood that the ACAID response could not happen without the unique combination of immunomodulatory factors found within the ocular microenvironment.

THE OCULAR MICROENVIRONMENT

The ocular microenvironment is capable of both the innate and adaptive immune responses despite the specialized barriers that contain the ocular media and preserve the highly metabolic retinal tissue. In other words, the blood–ocular barrier is not absolute. If activated immune cells reach the eye, they have the potential to cause irreversible damage to the highly regulated ocular tissue. To respond to the ongoing threat of activated immune cells reaching the eye, the ocular environment contains numerous soluble and membrane-bound factors to counter or neutralize the active immune response and minimize inflammation in the eye. These intraocular factors are not the "silver bullet" for saving the eye from immune-mediated damage: their immunomodulatory properties may also lead to unwanted events such as unimpeded tumor growth in the eye or permissive intraocular growth of a pathogen. A controlled amount of inflammation may be welcomed in these aforementioned circumstances to save the eye from being consumed by cancer or bacteria. Finding the right balance of immunosuppressive and proinflammatory events is the key to maintaining ocular function and vision. A good place to begin investigating the ocular microenvironment is the aqueous humor.

Immunomodulatory Properties of Aqueous Humor

When macrophages come in contact with aqueous humor or with TGF-β2, a factor found in the anterior chamber, they alter their functionality by producing TGF-β, failing to produce IL-12, and deviating from their usual manner of antigen presentation.[50] They stimulate a population of $CD8^+$ suppressor cells (the effector suppressor cells found in ACAID), inhibiting Th1 type immunity. These functionally altered macrophages also mediate Th2 responses that induce non-complement-fixing antibody production by B cells. Aqueous humor, however, cannot prevent lysis by fully functional cytotoxic T cells. There are many other factors in addition to TGF-β2 in the aqueous humor (Table 5.6). Most of these factors contribute to suppressed IFN-γ production by Th1 cells. Vasoactive intestinal peptide (VIP) and somatostatin suppress antigen- and mitogen-mediated T cell proliferation.[51,52] α-MSH suppresses IFN-γ production by T cells but does not suppress T cell proliferation.[53] TGF-β2 with α-MSH can also directly suppress activation and proliferation of Th1 cells. α-MSH with or without TGF-β2 can also induce a population of Treg cells with Th3-like properties.[54]. Further, effector $CD4^+$ (but not $CD8^+$) cells that enter the healthy eye do not carry out their effector functions but rather are converted by the local soluble factors into regulatory cells that can suppress other

Table 5.6 Soluble Immunomodulatory Factors in the Eye

Factor	Immunomodulatory Property
TGF-β2	Suppresses T cell, NK cell, and macrophage activation; confers tolerance-promoting properties on APCs; with α-MSH induces regulatory T cells
α-MSH	Suppresses IFN-γ production; inhibits PMN activation; promotes IL-10 production by APC
VIP	Inhibits T cell activation and differentiation
CGRP	Inhibits APC function; inhibits LPS- and IFN-γ-activated macrophages
Somatostatin	Inhibits T cell activation
Thrombospondin	Confers tolerance-promoting properties on APCs
MIF	Inhibits NK cell mediated lysis
Cortisol	Suppresses inflammation; causes APC to produce IL-10 instead of IL-12
IL-1 receptor antagonist	Inhibits proinflammatory effects of IL-1α/β
CD46, CD55, CD59	Inhibits complement activation
CD95L (Fas-L)	Inhibits neutrophil inflammation

activated Th1 cells. The induction of these Th3 cells may also be important in maintaining tolerance to autoantigens.

Aqueous humor factors can also inhibit innate immune cell function.[55] Calcitonin gene–related peptide inhibits nitric oxide formation from stimulated APCs.[56] Migration inhibitory factor (MIF) inhibits NK cell–mediated lysing of target cells.[57] Both Fas-L and α-MSH inhibit neutrophil function.[58] Complement activation is also prevented by at least two soluble aqueous humor factors. One factor, iC3b, prevents C3 conversion to C3b (see Table 5.5), and another separate factor prevents antibody binding to C1q.[59] Also, aqueous humor does not impair noncomplement-fixing (antiviral) antibodies.

Cell Surface Molecules That Promote Ocular Immunity

Three mechanisms of sustaining ocular immunity have been identified on the cells within the eye: apoptosis of activated T cells, inhibition of complement, and inhibition of T cell activation (Table 5.7). Fas-L is found on cells within the eye and is in part responsible for promoting apoptosis of Fas^+ T cells that enter the eye.[34,60–63] Complement inhibitors, including complement receptor–related protein, or Crry, are found on ocular cells, and in the case of Crry, when it was experimentally neutralized in the eyes or rats, the result was spontaneous ocular inflammation.[64,65] It has also been suggested that activated T cell suppression may occur through direct cell-to-cell contact with CD86 (B7.2), which is found on the iris pigment epithelia cells in mice.[66] When activated T cells enter the eye through the iris pigment epithelium, CD86 bind to the CTLA-4 receptor on the T cells and not only suppress IFN-γ production by the T cells but also convert them to Treg cells that have the potential to suppress other Th1-type cells.

IMMUNOLOGY OF CORNEAL TRANSPLANTATION

This section focuses on the highly unique immunologic properties of corneal tissue transplantation. The first documented successful corneal transplantation in humans occurred over 100 years ago. To date, orthotopic corneal allografting is the most common allograft transplantation, with approximately 50,000 procedures performed annually in the United States alone.[67,68] Animal model systems have provided much of the information characterizing the cellular and molecular immunology, which is likely driven by immune privilege of the cornea and anterior chamber. There is much less information on the immunology of corneal allografting in domestic animals. Most clinical corneal surgeries in domestic animals have utilized conjunctival autografting to successfully repair corneal damage from infection, trauma, and other immune-mediated processes. Corneal allografts in low-risk settings (no vascularization in the host corneal bed, no previous history of corneal grafting) enjoy almost 100% success, whereas graft failure in high-risk settings was almost always due to significant immune-mediated rejection.[68–71] The most recent understanding of corneal transplantation can be narrowed down to two basic areas: the condition of the host cornea and the unique immunomodulatory properties of the healthy corneal graft.

First, the quality of the host corneal bed plays a significant role in determining graft outcome. High-risk corneas no longer hold the properties of ocular immunity. As a result, graft rejection is strongly correlated with high-risk eyes. High-risk eyes also demonstrate growth of lymphatics, which alter the immune properties of the cornea by connecting the cornea to the immune system directly and allowing antigenic information to escape the graft site.[72,73] Blood-borne immune effectors can also gain access to the grafted site in high-risk eyes.

Second, the corneal graft itself expresses features of healthy ocular immunity. Unlike most solid tissues, normal corneas have a lack of bone marrow–derived APCs necessary to initiate an immune response.[74] Most adventitial (i.e., bone marrow–derived) cells on the cornea lie near the limbus. In settings where there is a reconstitution of Langerhans cells into corneal tissue, grafts become highly vulnerable to rejection. Corneal cells also express Fas-L (CD95L), which triggers apoptosis in $CD95^+$ effector T cells.[61,62] DAF, CD59, and CD46 are other molecules found on corneal endothelium that inhibit complement effector functions induced during an alloimmune response.[64] These surface molecules protect the corneal endothelium from injury. Further, expression of MHC class I and class II molecules is diminished and functionally impaired on corneal parenchymal cells, especially the corneal endothelium.[75–77] Corneal epithelium strongly express class I, whereas keratocytes express less class I than do the other fibroblasts in the body. Similar to other cells in the body, IFN-γ can upregulate class I antigen expression in corneal epithelial and endothelial cells. However, IFN-γ-induced class II antigens are upregulated only in the corneal epithelium, not in the endothelium. Therefore, induction and expression of alloimmunity is subdued as a result of the decreased antigenic load of corneal tissue in contrast to other tissue with normal MHC expression.

Experimentally, in low-risk eyes, uncomplicated allogeneic corneal grafts are accepted with virtually no acute rejection (in 7–14 days) when contrasted with other orthotopic solid organ grafts. Further, sustaining these grafts without rejection is often accomplished without the aid of local immunosuppressive therapy. Also, grafts with only MHC alloantigens against the host survive better than those with only minor histocompatibility antigen disparity. High-risk eyes, however, are another story. Most high-risk allografts develop acute, irreversible graft rejection, and very few grafts survive indefinitely. In both high- and low-risk recipients, grafts expressing only minor histocompatibility antigens are rejected at a higher rate than grafts with only MHC alloantigen disparity.[78–80]

Finally, all layers of the cornea secrete the immunosuppressive cytokine TGF-β, and keratocytes constitutively produce excessive IL-1 receptor antagonist (relative to local endogenous production of IL-1α).[81–86] During an alloimmune

response, these molecules modulate the activity of APC, T cells, B cells, NK cells, and macrophages to enhance tolerance of the graft in the host. Because the corneal graft forms part of the anterior border of the anterior chamber, antigens from the graft escape into the aqueous humor and are presented to the systemic immune system via the ACAID pathways. This enables a muted or absent DTH response to the graft as well as decreased production of complement-fixing antibodies that could elicit graft destruction.[33,87] Experimental data have shown that allogenic corneal grafts induce donor-specific ACAID in the host, impairing DTH.[88,89]

T cells play a significant role in corneal graft rejection. While the exact effectors responsible for corneal graft rejection remain unknown, T lymphocytes are thought to play a dominant role in the rejection process. Severe combined immune-deficient (SCID) mice will accept indefinitely corneal grafts from allogenic donors despite immunogenetic disparity, suggesting that adaptive immunity plays a central role in graft rejection.[90] $CD4^+$ Th1 cells (cells that secrete IFN-γ and mediate DTH) appear to have an integral role in graft rejection, whereas B cells and $CD8^+$ cells do not.

There are two populations of alloreactive T cells that can be responsible for graft rejection: *indirect alloreactive T cells* and *direct alloreactive T cells.*[91–93] The indirect population binds peptides that come from alloantigenic proteins found on graft parenchymal cells. Host APC process the proteins into peptides and load them onto class I and class II molecules for the T cells to bind. Therefore, the T cells that bind these APCs recognize donor-derived peptides in the context of self-MHC molecules. The direct alloreactive T cells, on the other hand, recognize allogenic MCH class I and II molecules directly. These cells are responsible for acute graft rejection in most solid tissue grafts, and they are sensitized primarily by passenger leukocytes (dendritic cells and macrophages) expressing high levels of class I and class II. Sensitization occurs when passenger leukocytes leave the graft and migrate via the lymphatics to the draining lymph node, where they encounter naïve direct alloreactive T cells. These T cells return to the graft and destroy it. Since corneal tissue has fewer dendritic cells and macrophages than most other solid tissue, and since corneal cells express less MHC on their surface, less acute rejection is seen in corneal allografting. In general, acute rejection of corneal grafts is seen in high-risk eyes, and subacute rejection (between 14 and 56 days) is seen in low-risk corneal grafting. Unsensitized, direct alloreactive T cells are estimated in healthy humans in high precursor frequencies (1%–5% of peripheral T cells), whereas indirect alloreactive T cells are estimated in much lower precursor frequencies (<1:10,000). This is why HLA matching plays such a minor part in increasing corneal allograft survival in humans.

To date it is suggested that there are two waves of rejection in allosensitization. The first wave is initiated by donor-derived APCs that migrate quickly into the draining lymph node. These APCs quickly activate direct alloreactive T cells, contributing to acute rejection.[94] The second wave, which overlaps the first wave, consists of recipient-derived APCs that infiltrate the graft, then travel to the draining lymph node. These APCs express peptides derived from donor alloantigens in the MHC molecules, triggering the expansion of indirect alloreactive T cells and subacute rejection.

A third but less understood pathway called peripheral sensitization is also thought to exist and was first described by Medawar.[95] In this pathway, naïve alloreactive T cells are activated in the graft itself. Direct alloreactive T cells are thought to be responsible for this phenomenon. They migrate to the graft and bind donor MHC class I and II antigens directly on the graft cells. It is not clear whether the activated T cells expand locally in the graft or migrate to the draining lymph node for expansion and differentiation.

It is important to note that most of these studies were performed on rodent or human tissue; therefore, comparisons to transplantation immunology in domestic animals must be made with this in mind. In conclusion, the normal eye is an immune privileged site for orthotopic allogenic corneal transplants, tolerance of grafts is seen only in eyes that have immune privilege, and minor histocompatibility antigens are more detrimental than major histocompatibility antigens to graft survival.

WHEN OCULAR IMMUNITY FAILS

When proteins in the blood leak into the immune privileged eye, they neutralize TGF-β2 and accelerate degradation of the immunomodulatory factors found in the anterior chamber. Growth factors found in the blood can trigger the intraocular production of proinflammatory immunity. Upregulation of antigen processing, including autoantigen presentation, can promote loss of ocular immunity and destroy ocular tissue. Experimentally, immunosuppressive microenvironments have the potential to reemerge following intraocular inflammation, with active TGF-β2 (induced by local production of IL-6 during inflammation) being a leading promoter of this reestablished environment.[96–99]

Experimental Uveitis

The success of overriding the protective mechanisms in ocular immunity has been demonstrated in experimental models that depend on immunizing the animal with an autoantigen in adjuvant. Experimental autoimmune disease utilizes, in part, delivery of PAMPs to the immune system via an adjuvant such as mycobacteria in order to overcome the normal defenses that suppress induction of autoreactive inflammation. Adjuvant also enables induction of innate and adaptive immune responses in a tissue that may normally suppress such responses (i.e., immune privileged tissues). The PAMPs in the adjuvant activate nuclear factor kappa B (NF-κB)–regulated proinflammatory cytokines. Further, some bacterial antigens cross-react with autoantigens, amplifying the immune response. This method, when used with an ocular autoantigen such as interphotoreceptor retinoid–binding protein, is termed *experimental autoimmune uveitis* (EAU).[100–102]

Nonlethal amounts of PAMPs (endotoxin) may also be given systemically to induce uveitis by breaking down the

blood–ocular barrier. Macrophages within the eye subsequently produce nitric oxide, oxygen reactive intermediates, and proinflammatory cytokines. Ocular immunity is abolished, and the ocular environment is susceptible not only to the transient inflammation caused by the endotoxin but also to subsequent autoimmunity, indicating that the eye may have undergone a permanent change to its microenvironment, making it susceptible to future autoimmune attacks. This form of experimental uveitis is termed *endotoxin-induced uveitis* (EIU).[96–99,103]

High-Risk Corneas

Ocular immunity fails in high-risk corneas for several reasons. A high-risk, or inflamed, cornea has compromised immune privilege where host sensitization occurs rapidly. As previously mentioned, direct and indirect alloreactive T cells play an integral role in host sensitization and graft rejection. Lymph vessels are found in the bed of high-risk corneal grafts and can readily transport alloantigens to the draining lymph node. Further, recipient APCs can conveniently enter the graft from the vascularized graft bed. Donor-derived APCs are initially MHC class II negative but can quickly undergo maturation as they pass through the inflamed graft bed. These donor-derived APCs can go on to activate direct alloreactive T cells in the draining lymph node. All of these mechanisms serve to enhance graft rejection by exposing donor alloantigens, compromising immune privilege, and depriving the eye of its immunological ignorance.

OCULAR IMMUNITY AND CANCER

As mentioned earlier in the chapter and listed in Tables 5.2 and 5.3, certain tumors show characteristics of immune privileged tissue. In fact, from the perspective of an immunologist, many tumors have evolved elaborate ways to evade immune detection and grow permissively in the body. It is reported that spontaneous tumors express antigens that have the potential to elicit an immune response. One question to be raised is, do cancer cells within the eye behave differently than they do in other parts of the body due to the principles of ocular immunity? The question has been answered in the early studies on ACAID.[104–106] P815 tumor cell lines injected into the healthy anterior chamber exhibited indefinite growth and eventual destruction of ocular tissue. When ocular immunity is abolished or uveitis is allowed to coincide with the injection of the P815 cells into the anterior chamber, tumor growth is inhibited. The uninhibited tumor growth in the healthy eyes is supported by the active immune suppression imparted by the ACAID response with the help of the immunosuppressive ocular microenvironment.[107] When the immunosuppressive factors are neutralized or degraded and ACAID is no longer evident, then the ocular environment loses its unique immune properties and tumor rejection ensues.

Another question is, can we use what we know about ocular immunity to treat certain tumors in the body? If certain tumors escape the immune system by the same mechanisms as the eye uses to suppress inflammation, then there may be opportunities to treat certain cancers by inviting the termination of immune privilege to the cancer tissue. Tumor escape mechanisms include an immunosuppressive microenvironment,[108–117] reduced or nonexistent class I expression,[118–123] inhibition of the antigen processing pathways,[124,125] inhibition of tumor-infiltrating APCs, induction of deviant immune effector cells,[126,127] and loss of tumor antigen gene transcription.[128]

THERAPEUTIC POTENTIAL

Several types of immunity and transplantation settings can be investigated as opportunities for using what we now know as ocular immunity in the treatment of not only ophthalmic disease but also systemic immune disorders. Induction of Th3 cells either by oral tolerance or cytokine therapy can reduce the detrimental effects of autoreactive Th1 cells. Corneal allograft survival in a high-risk setting is another obvious area to look for ways to improve surgical and visual outcome. Experimentally, corneal allografts can be given healthy epithelium or can be treated with ocular immunomodulatory factors promoting a deviation from conventional immune recognition pathways that would lead to graft rejection. Moving away from conjunctival autografts toward corneal allografting as a treatment for high- and low-risk corneal inflammatory diseases remains an ongoing challenge to the veterinary ophthalmologist but offers a significant advance to the visual outcome in our veterinary patients. Breakthroughs in gene therapy, cytokine therapy, and clinical application of other novel immunomodulatory factors will offer brand new ways to approach restoring ocular immunity in the face of ocular inflammation and consequential vision loss.

REFERENCES

1. van Dooremaal J. The development of living tissues transplanted into foreign ground. *Albrecht Von Graefe's Arch Ophthalmol* 1873; 19: 359–373.
2. Medawar P. Immunity to homologous grafted skin. III. The fate of skin homografts transplanted to the brain, to subcutaneous tissue, and to the anterior chamber of the eye. *Br J Exp Pathol* 1948; 129: 58–69.
3. Billingham RE, Boswell T. Studies on the problem of corneal homografts. *Proc R Soc Lond B Biol Sci* 1953; 141: 392–406.
4. Barker CF, Billingham RE. Immunologically privileged sites. *Adv Immunol* 1977; 25: 1–54.
5. Kaplan HJ, Streilein JW. Immune response to immunization via the anterior chamber of the eye. I. F. lymphocyte-induced immune deviation. *J Immunol* 1977; 118: 809–814.
6. Kaplan HJ, Streilein JW. Immune response to immunization via the anterior chamber of the eye. II. An analysis of F1 lymphocyte-induced immune deviation. *J Immunol* 1978; 120: 689–693.
7. Hori J, Joyce N, Streilein JW. Epithelium-deficient corneal allografts display immune privilege beneath the kidney capsule. *Invest Ophthalmol Vis Sci* 2000; 41: 443–452.
8. Hori J, Joyce NC, Streilein JW. Immune privilege and immunogenicity reside among different layers of the mouse cornea. *Invest Ophthalmol Vis Sci* 2000; 41: 3032–3042.

9. Ng TF, Osawa H, Hori J, et al. Allogenic neonatal neuronal retina grafts display partial immune privilege in the subcapsular space of the kidney. *J Immunol* 2002; 169: 5601–5606.
10. Wenkel H, Streilein JW. Evidence that retinal pigment epithelium functions as an immune-privileged tissue. *Invest Ophthalmol Vis Sci* 2000; 41: 3467–3473.
11. Weiss A. *T-lymphocyte Activation,* 4th ed. Philadelphia: Lippincott-Raven, 1999: 411.
12. Alberola-Ila J, Takaki S, Kerner JD, et al. Differential signaling by lymphocyte antigen receptors. *Annu Rev Immunol* 1997; 15: 125–154.
13. Fearon DT, Locksley RM. The instructive role of innate immunity in the acquired immune response. *Science* 1996; 272: 50–53.
14. Van Parijs L, Abbas AK. Homeostasis and self-tolerance in the immune system: Turning lymphocytes off. *Science* 1998; 280: 243–248.
15. Gillette TE, Chandler JW, Greiner JV. Langerhans cells of the ocular surface. *Ophthalmology* 1982; 89: 700–711.
16. Marceau F, Boisjoly HM, Wagner E, et al. Long-term culture and characterization of human limbal microvascular endothelial cells. *Exp Eye Res* 1990; 51: 645–650.
17. Chandler JW, Gillette TE. Immunologic defense mechanisms of the ocular surface. *Ophthalmology* 1983; 90: 585–591.
18. Dua HS, Gomes JA, Jindal VK, et al. Mucosa specific lymphocytes in the human conjunctiva, corneoscleral limbus and lacrimal gland. *Curr Eye Res* 1994; 13: 87–93.
19. Franklin RM and Remus LE. Conjunctival-associated lymphoid tissue: Evidence for a role in the secretory immune system. *Invest Ophthalmol Vis Sci* 1984; 25: 181–187.
20. Sacks EH, Wieczorek R, Jakobiec FA, et al. Lymphocytic subpopulations in the normal human conjunctiva. A monoclonal antibody study. *Ophthalmology* 1986; 93: 1276–1283.
21. McMenamin PG, Crewe J, Morrison S, et al. Immunomorphologic studies of macrophages and MHC class II-positive dendritic cells in the iris and ciliary body of the rat, mouse, and human eye. *Invest Ophthalmol Vis Sci* 1994; 35: 3234–3250.
22. Morgan SJ, Williams JH, Walls AF, et al. Mast cell numbers and staining characteristics in the normal and allergic human conjunctiva. *J Allergy Clin Immunol* 1991; 87: 111–116.
23. McGill JI, Liakos GM, Goulding N, et al. Normal tear protein profiles and age-related changes. *Br J Ophthalmol* 1984; 68: 316–320.
24. Peppard JV and Montgomery PC. Studies on the origin and composition of IgA in rat tears. *Immunology* 1987; 62: 193–198.
25. Sullivan DA, Allansmith MR. Source of IgA in tears of rats. *Immunology* 1984; 53: 791–799.
26. Franklin RM. The ocular secretory immune system: A review. *Curr Eye Res* 1989; 8: 599–606.
27. Franklin RM, McGee DW, Shepard KF. Lacrimal gland-directed B cell responses. *J Immunol* 1985; 135: 95–99.
28. Martin CL, Munnell J, Kaswan R. Normal ultrastructure and histochemical characteristics of canine lacrimal glands. *Am J Vet Res* 1988; 49: 1566–1572.
29. Jiang LQ, Streilein JW. Immune privilege extended to allogenic tumor cells in the vitreous cavity. *Invest Ophthalmol Vis Sci* 1991; 32: 224–228.
30. Ksander BR, Streilein JW. Analysis of cytotoxic T cell responses to intracameral allogenic tumors. *Invest Ophthalmol Vis Sci* 1989; 30: 323–329.
31. Niederkorn JY. Immune privilege in the anterior chamber of the eye. *Crit Rev Immunol* 2002; 22: 13–46.
32. Streilein JW. Regional immunity and ocular immune privilege. In: Streilein JW, ed. *Immune Response and the Eye. Chemical Immunology Vol. 73.* Basel, Switzerland: Karger AG, 1999; 11–38.
33. Streilein JW, Niederkorn JY and Shadduck JA. Systemic immune unresponsiveness induced in adult mice by anterior chamber presentation of minor histocompatibility antigens. *J Exp Med* 1980; 152: 1121–1125.
34. Wenkel H, Streilein JW. Analysis of immune deviation elicited by antigens injected into the subretinal space. *Invest Ophthalmol Vis Sci* 1998; 39: 1823–1834.
35. Wilbanks GA, Streilein JW. Distinctive humoral immune responses following anterior chamber and intravenous administration of soluble antigen. Evidence for active suppression of IgG2-secreting B lymphocytes. *Immunology* 1990; 71: 566–572.
36. Faunce DE, Sonoda KH, Stein-Streilein J. MIP-2 recruits NKT cells to the spleen during tolerance induction. *J Immunol* 2001; 166: 313–321.
37. Sonoda KH, Exley M, Snapper S, et al. CD1-reactive natural killer T cells are required for development of systemic tolerance through an immune-privileged site. *J Exp Med* 1999; 190: 1215–1226.
38. Sonoda KH, Faunce DE, Taniguchi M, et al. NK T cell-derived IL-10 is essential for the differentiation of antigen-specific T regulatory cells in systemic tolerance. *J Immunol* 2001; 166: 42–50.
39. Takeuchi M, Alard P, Streilein JW. TGF-beta promotes immune deviation by altering accessory signals of antigen-presenting cells. *J Immunol* 1998; 160: 1589–1597.
40. Faunce DE, Stein-Streilein J. NKT cell-derived RANTES recruits APCs and $CD8^+$ T cells to the spleen during the generation of regulatory T cells in tolerance. *J Immunol* 2002; 169: 31–38.
41. D'Orazio TJ, Mayhew E, Niederkorn JY. Ocular immune privilege promoted by the presentation of peptide on tolerogenic B cells in the spleen. II. Evidence for presentation by Qa-1. *J Immunol* 2001; 166: 26–32.
42. Niederkorn JY, Streilein JW. Alloantigens placed into the anterior chamber of the eye induce specific suppression of delayed-type hypersensitivity but normal cytotoxic T lymphocyte and helper T lymphocyte responses. *J Immunol* 1983; 131: 2670–2674.
43. Wilbanks GA, Streilein JW. Characterization of suppressor cells in anterior chamber-associated immune deviation (ACAID) induced by soluble antigen. Evidence of two functionally and phenotypically distinct T-suppressor cell populations. *Immunology* 1990; 71: 383–389.
44. Niederkorn JY. Anterior chamber-associated immune deviation. In: Streilein JW, ed. *Immune Response and the Eye. Chemical Immunology* Vol. 73. Basel, Switzerland: Karger AG, 1999; 59–71.
45. Stein-Streilein J, Streilein JW. Anterior chamber associated immune deviation (ACAID): Regulation, biological relevance, and implications for therapy. *Int Rev Immunol* 2002; 21: 123–152.
46. Streilein JW, Masli S, Takeuchi M, et al. The eye's view of antigen presentation. *Hum Immunol* 2002; 63: 435–443.
47. Wilbanks GA, Mammolenti M, Streilein JW. Studies on the induction of anterior chamber-associated immune deviation

(ACAID). II. Eye-derived cells participate in generating blood-borne signals that induce ACAID. *J Immunol* 1991; 146: 3018–3024.

48. Wilbanks GA, Streilein JW. Studies on the induction of anterior chamber-associated immune deviation (ACAID). 1. Evidence that an antigen-specific, ACAID-inducing, cell-associated signal exists in the peripheral blood. *J Immunol* 1991; 146: 2610–2617.
49. Wilbanks GA, Streilein JW. Macrophages capable of inducing anterior chamber associated immune deviation demonstrate spleen-seeking migratory properties. *Reg Immunol* 1992; 4: 130–137.
50. Kaiser CJ, Ksander BR, Streilein JW. Inhibition of lymphocyte proliferation by aqueous humor. *Reg Immunol* 1989; 2: 42–49.
51. Taylor AW, Streilein JW, Cousins SW. Immunoreactive vasoactive intestinal peptide contributes to the immunosuppressive activity of normal aqueous humor. *J Immunol* 1994; 153: 1080–1086.
52. Taylor AW, Yee DG. Somatostatin is an immunosuppressive factor in aqueous humor. *Invest Ophthalmol Vis Sci* 2003; 44: 2644–2649.
53. Taylor AW, Streilein JW, Cousins SW. Identification of alpha-melanocyte stimulating hormone as a potential immunosuppressive factor in aqueous humor. *Curr Eye Res* 1992; 11: 1199–1206.
54. Namba K, Kitaichi N, Nishida T, et al. Induction of regulatory T cells by the immunomodulating cytokines alpha-melanocyte-stimulating hormone and transforming growth factor-beta2. *J Leukoc Biol* 2002; 72: 946–952.
55. Streilein JW, Stein-Streilein J. Does innate immune privilege exist? *J Leukoc Biol* 2000; 67: 479–487.
56. Taylor AW, Yee DG, Streilein JW. Suppression of nitric oxide generated by inflammatory macrophages by calcitonin gene-related peptide in aqueous humor. *Invest Ophthalmol Vis Sci* 1998; 39: 1372–1378.
57. Apte RS, Sinha D, Mayhew E, et al. Cutting edge: Role of macrophage migration inhibitory factor in inhibiting NK cell activity and preserving immune privilege. *J Immunol* 1998; 160: 5693–5696.
58. Gregory MS, Repp AC, Holhbaum AM, et al. Membrane Fas ligand activates innate immunity and terminates ocular immune privilege. *J Immunol* 2002; 169: 2727–2735.
59. Goslings WR, Prodeus AP, Streilein JW, et al. A small molecular weight factor in aqueous humor acts on C1q to prevent antibody-dependent complement activation. *Invest Ophthalmol Vis Sci* 1998; 39: 989–995.
60. Ferguson TA, Stuart PM, Herndon JM, et al. Apoptosis, tolerance, and regulatory T cells—old wine, new wineskins. *Immunol Rev* 2003; 193: 111–123.
61. Griffith TS, Brunner T, Fletcher SM, et al. Fas ligand-induced apoptosis as a mechanism of immune privilege. *Science* 1995; 270: 1189–1192.
62. Stuart PM, Griffith TS, Usui N, et al. CD95 ligand (FasL)-induced apoptosis is necessary for corneal allograft survival. *J Clin Invest* 1997; 99: 396–402.
63. Yamagami S, Kawashima H, Tsuru T, et al. Role of Fas-Fas ligand interactions in the immunorejection of allogenic mouse corneal transplants. *Transplantation* 1997; 64: 1107–1111.
64. Bora NS, Gobleman CL, Atkinson JP, et al. Differential expression of the complement regulatory proteins in the human eye. *Invest Ophthalmol Vis Sci* 1993; 34: 3579–3584.
65. Sohn JH, Kaplan HJ, Suk HJ, et al. Chronic low-level complement activation within the eye is controlled by intraocular complement regulatory proteins. *Invest Ophthalmol Vis Sci* 2000; 41: 3492–3502.
66. Sugita S, Streilein JW. Iris pigment epithelium expressing CD86 (B7-2) directly suppresses T cell activation in vitro via binding to cytotoxic T lymphocyte-associated antigen 4. *J Exp Med* 2003; 198: 161–171.
67. Price FW, Jr., Whitson WE, Marks RG. Progression of visual acuity after penetrating keratoplasty. *Ophthalmology* 1991; 98: 1177–1185.
68. Smith RE, McDonald HR, Nesburn AB, et al. Penetrating keratoplasty: Changing indications, 1947 to 1978. *Arch Ophthalmol* 1980; 98: 1226–1229.
69. Mader TH, Stulting RD. The high-risk penetrating keratoplasty. *Ophthalmol Clin North Am* 1991; 4: 411–426.
70. Volker-Dieben HJ, Kok-van Alphen CC, Lansbergen Q, et al. Different influences on corneal graft survival in 539 transplants. *Acta Ophthalmol (Copenh)* 1982; 60: 190–202.
71. Wilson SE, Kaufman HE. Graft failure after penetrating keratoplasty. *Surv Ophthalmol* 1990; 34: 325–356.
72. Cursiefen C, Chen L, Dana MR, et al. Corneal lymphangiogenesis: Evidence, mechanisms, and implications for corneal transplant immunology. *Cornea* 2003; 22: 273–281.
73. Cursiefen C, Ikeda S, Nishina PM, et al. Spontaneous corneal hem- and lymphangiogenesis in mice with destrin-mutation depend on VEGFR3 signaling. *Am J Pathol* 2005; 166: 1367–1377.
74. Streilein JW, Toews GB, Bergstresser PR. Corneal allografts fail to express Ia antigens. *Nature* 1979; 282: 326–327.
75. Treseler PA, Foulks GN, Sanfilippo F. The expression of HLA antigens by cells in the human cornea. *Am J Ophthalmol* 1984; 98: 763–772.
76. Wang HM, Kaplan HJ, Chan WC, et al. The distribution and ontogeny of MHC antigens in murine ocular tissue. *Invest Ophthalmol Vis Sci* 1987; 28: 1383–1389.
77. Whitsett CF, Stulting RD. The distribution of HLA antigens on human corneal tissue. *Invest Ophthalmol Vis Sci* 1984; 25: 519–524.
78. Joo CK, Pepose JS, Stuart PM. T-cell mediated responses in a murine model of orthotopic corneal transplantation. *Invest Ophthalmol Vis Sci* 1995; 36: 1530–1540.
79. Nicholls SM, Bradley BB, Easty DL. Effect of mismatches for major histocompatibility complex and minor antigens on corneal graft rejection. *Invest Ophthalmol Vis Sci* 1991; 32: 2729–2734.
80. Sonoda Y, Streilein JW. Orthotopic corneal transplantation in mice—evidence that the immunogenetic rules of rejection do not apply. *Transplantation* 1992; 54: 694–704.
81. Jager MJ, Bradley D, Streilein JW. Immunosuppressive properties of cultured human cornea and ciliary body in normal and pathological conditions. *Transpl Immunol* 1995; 3: 135–142.
82. Kennedy MC, Rosenbaum JT, Brown J, et al. Novel production of interleukin-1 receptor antagonist peptides in normal human cornea. *J Clin Invest* 1995; 95: 82–88.
83. Streilein JW, Bradley D, Sano Y, et al. Immunosuppressive properties of tissues obtained from eyes with experimentally manipulated corneas. *Invest Ophthalmol Vis Sci* 1996; 37: 413–424.
84. Donnelly JJ, Xi MS, Rockey JH. A soluble product of human corneal fibroblasts inhibits lymphocyte activation. Enhancement by interferon-gamma. *Exp Eye Res* 1993; 56: 157–165.

85. Kawashima H, Prasad SA, Gregerson DS. Corneal endothelial cells inhibit T cell proliferation by blocking IL-2 production. *J Immunol* 1994; 153: 1982–1989.
86. Khaw PT, Schultz GS, MacKay SL, et al. Detection of transforming growth factor-alpha messenger RNA and protein in human corneal epithelial cells. *Invest Ophthalmol Vis Sci* 1992; 33: 3302–3306.
87. Streilein JW. Immune regulation and the eye: A dangerous compromise. *Faseb J* 1987; 1: 199–208.
88. Sonoda Y, Streilein JW. Impaired cell-mediated immunity in mice bearing healthy orthotopic corneal allografts. *J Immunol* 1993; 150: 1727–1734.
89. Yamada J, Streilein JW. Induction of anterior chamber-associated immune deviation by corneal allografts placed in the anterior chamber. *Invest Ophthalmol Vis Sci* 1997; 38: 2833–2843.
90. Niederkorn JY. The immunology of corneal transplantation. *Dev Ophthalmol* 1999; 30: 129–140.
91. Shoskes DA, Wood KJ. Indirect presentation of MHC antigens in transplantation. *Immunol Today* 1994; 15: 32–38.
92. Liu Z, Sun YK, Xi YP, et al. Contribution of direct and indirect recognition pathways to T cell alloreactivity. *J Exp Med* 1993; 177: 1643–1650.
93. Lee RS, Grusby MJ, Glimcher LH, et al. Indirect recognition by helper cells can induce donor-specific cytotoxic T lymphocytes in vivo. *J Exp Med* 1994; 179: 865–872.
94. Liu Y, Hamrah P, Zhang Q, et al. Draining lymph nodes of corneal transplant hosts exhibit evidence for donor major histocompatibility complex (MHC) class II-positive dendritic cells derived from MHC class II-negative grafts. *J Exp Med* 2002; 195: 259–268.
95. Medawar P. Transplantation of tissues and organs: Introduction. *Br Med Bull* 1965; 21: 97–101.
96. Mo JS, Streilein JW. Immune privilege persists in eyes with extreme inflammation induced by intravitreal LPS. *Eur J Immunol* 2001; 31: 3806–3815.
97. Ohta K, Wiggert B, Yamagami S, et al. Analysis of immunomodulatory activities of aqueous humor from eyes of mice with experimental autoimmune uveitis. *J Immunol* 2000; 164: 1185–1192.
98. Ohta K, Yamagami S, Taylor AW, et al. IL-6 antagonizes TGF-beta and abolishes immune privilege in eyes with endotoxin-induced uveitis. *Invest Ophthalmol Vis Sci* 2000; 41: 2591–2599.
99. Streilein JW, Ohta K, Mo JS, et al. Ocular immune privilege and the impact of intraocular inflammation. *DNA Cell Biol* 2002; 21: 453–459.
100. Taylor A, Namba K. In vitro induction of CD25+ CD4+ regulatory T cells by the neuropeptide alpha-melanocyte stimulating hormone (alpha-MSH). *Immunol Cell Biol* 2001; 79: 358–367.
101. Caspi RR. Immunogenetic aspects of clinical and experimental uveitis. *Reg Immunol* 1992; 4: 321–330.
102. Caspi RR, Roberge FG, Chan CC, et al. A new model of autoimmune disease. Experimental autoimmune uveoretinitis induced in mice with two different retinal antigens. *J Immunol* 1988; 140: 1490–1495.
103. Ohta K, Wiggert B, Taylor AW, et al. Effects of experimental ocular inflammation on ocular immune privilege. *Invest Ophthalmol Vis Sci* 1999; 40: 2010–2018.
104. Jiang LQ, Jorquera M, Streilein JW. Subretinal space and vitreous cavity as immunologically privileged sites for retinal allografts. *Invest Ophthalmol Vis Sci* 1993; 34: 3347–3354.
105. Niederkorn J, Streilein JW and Shadduck JA. Deviant immune responses to allogenic tumors injected intracamerally and subcutaneously in mice. *Invest Ophthalmol Vis Sci* 1981; 20: 355–363.
106. Wenkel H, Chen PW, Ksander BR, et al. Immune privilege is extended, then withdrawn, from allogenic tumor cell grafts placed in the subretinal space. *Invest Ophthalmol Vis Sci* 1999; 40: 3202–3208.
107. Apte RS, Mayhew E, Niederkorn JY. Local inhibition of natural killer cell activity promotes the progressive growth of intraocular tumors. *Invest Ophthalmol Vis Sci* 1997; 38: 1277–1282.
108. Beissert S, Ullrich SE, Hosoi J, et al. Supernatants from UVB radiation-exposed keratinocytes inhibit Langerhans cell presentation of tumor-associated antigens via IL-10 content. *J Leukoc Biol* 1995; 58: 234–240.
109. Gabrilovich D, Ishida T, Oyama T, et al. Vascular endothelial growth factor inhibits the development of dendritic cells and dramatically affects the differentiation of multiple hematopoietic lineages in vivo. *Blood* 1998; 92: 4150–4166.
110. Gabrilovich DI, Chen HL, Girgis KR, et al. Production of vascular endothelial growth factor by human tumors inhibits the functional maturation of dendritic cells. *Nat Med* 1996; 2: 1096–1103.
111. Huang M, Wang J, Lee P, et al. Human non-small cell lung cancer cells express a type 2 cytokine pattern. *Cancer Res* 1995; 55: 3847–3853.
112. Kuppner MC, Hamou MF, Bodmer S, et al. The glioblastoma-derived T-cell suppressor factor/transforming growth factor beta 2 inhibits the generation of lymphokine-activated killer (LAK) cells. *Int J Cancer* 1988; 42: 562–567.
113. Oyama T, Ran S, Ishida T, et al. Vascular endothelial growth factor affects dendritic cell maturation through the inhibition of nuclear factor-kappa B activation in hemopoietic progenitor cells. *J Immunol* 1998; 160: 1224–1232.
114. Ranges GE, Figari IS, Espevik T, et al. Inhibition of cytotoxic T-cell development by transforming growth factor beta and reversal by recombinant tumor necrosis factor alpha. *J Exp Med* 1987; 166: 991–998.
115. Sato T, McCue P, Masuoka K, et al. Interleukin 10 production by human melanoma. *Clin Cancer Res* 1996; 2: 1383–1390.
116. Takeuchi M, Kosiewicz MM, Alard P, et al. On the mechanisms by which transforming growth factor-beta 2 alters antigen-presenting abilities of macrophages on T cell activation. *Eur J Immunol* 1997; 27: 1648–1656.
117. Young MR, Wright MA, Lozano Y, et al. Mechanisms of immune suppression in patients with head and neck cancer: Influence on the immune infiltrate of the cancer. *Int J Cancer* 1996; 67: 333–338.
118. Chen HL, Gabrilovich D, Virmani A, et al. Structural and functional analysis of beta2 microglobulin abnormalities in human lung and breast cancer. *Int J Cancer* 1996; 67: 756–763.
119. Gattoni-Celli S, Kirsch K, Timpane R, et al. Beta 2-microglobulin gene is mutated in a human colon cancer cell line (HCT) deficient in the expression of HLA class I antigens on the cell surface. *Cancer Res* 1992; 52: 1201–1204.
120. Lassam N, Jay G. Suppression of MHC class I RNA in highly oncogenic cells occurs at the level of transcription initiation. *J Immunol* 1989; 143: 3792–3797.
121. Maeurer MJ, Gollin SM, Storkus WJ, et al. Tumor escape from immune recognition: Loss of HLA-A2 melanoma cell surface expression is associated with a complex rearrangement of the

short arm of chromosome 6. *Clin Cancer Res* 1996; 2: 641–652.

122. Marincola FM, Shamamian P, Alexander RB, et al. Loss of HLA haplotype and B locus down-regulation in melanoma cell lines. *J Immunol* 1994; 153: 1225–1237.
123. Versteeg R, Kruse-Wolters KM, Plomp AC, et al. Suppression of class I human histocompatibility leukocyte antigen by c-myc is locus specific. *J Exp Med* 1989; 170: 621–635.
124. Restifo NP, Esquivel F, Kawakami Y, et al. Identification of human cancers deficient in antigen processing. *J Exp Med* 1993; 177: 265–272.
125. Weis JH, Seidman JG. The expression of major histocompatibility antigens under metallothionein gene promoter control. *J Immunol* 1985; 134: 1999–2003.
126. Bakker AB, Phillips JH, Figdor CG, et al. Killer cell inhibitory receptors for MHC class I molecules regulate lysis of melanoma cells mediated by NK cells, gamma delta T cells, and antigen-specific CTL. *J Immunol* 1998; 160: 5239–5245.
127. Ikeda H, Lethe B, Lehmann F, et al. Characterization of an antigen that is recognized on a melanoma showing partial HLA loss by CTL expressing an NK inhibitory receptor. *Immunity* 1997; 6: 199–208.
128. Maeurer MJ, Gollin SM, Martin D, et al. Tumor escape from immune recognition: Lethal recurrent melanoma in a patient associated with downregulation of the peptide transporter protein TAP-1 and loss of expression of the immunodominant MART-1/Melan-A antigen. *J Clin Invest* 1996; 98: 1633–1641.

Chapter 6

Clinical Microbiology

Laurence E. Galle and Cecil P. Moore

Eye infections have long been recognized as a major cause of ocular disease and represent a substantial portion of the ocular cases requiring medical or surgical attention, or both. Infectious agents may cause or complicate a variety of animal ocular diseases, including orbital cellulitis, blepharitis, conjunctivitis, keratitis, uveitis, and endophthalmitis. The significance of infectious ocular disease is not limited by species, however, because virtually all vertebrates are susceptible to one (or more) of a variety of infectious agents that affect the eye. This chapter presents the major groups of organisms involved in, with an emphasis on specific agents recognized as causes of, significant ocular disease in animals. Because an understanding of which organisms are considered to be normal flora versus which are considered to be pathogenic is necessary for effective management of infectious ocular disease, commensal organisms of the ocular surface are discussed as well. Life cycles, epidemiology, pathogenic mechanisms, host responses, and diagnostic approaches are presented for the pertinent viruses, bacteria, fungi, protozoa, and algae. For specific clinical aspects of infectious diseases, however, the reader is directed to the appropriate clinical chapters.

OCULAR VIROLOGY

Virus Replication and Mechanisms of Virus-Induced Injury

Understanding mechanisms of viral pathogenesis requires a general understanding of the stages of viral replication. Because viruses have no inherent replicative ability, they must enter host cells and utilize host cell processes for their own replication. The method by which viruses induce injury to ocular tissues is quite variable. Many directly destroy ocular cells in the process of replication, as is typical for alphaherpesviruses. Alternatively, other viruses may indirectly damage ocular cells by inciting an immune or inflammatory response that is deleterious to tissues, induces tumor formation, or causes tissue injury via immunosuppression. The "ideal" virus will infect the host, become persistent or latent in its host, and be steadily or intermittently released so that it may infect other hosts.

The classic stages of viral infection are *adsorption, penetration, uncoating, transcription, translation, replication, assembly,* and *release.*[1] Viruses are usually very specific in their mechanisms for infecting a target cell. As a virion comes in contact with a target cell, it interacts with and attaches to specific receptors or components of cell membrane, usually via specific glycoproteins, in a process known as adsorption. After adsorption, the virus must be internalized by the target cell. This process of penetration may occur through pinocytosis or translocation in the case of nonenveloped viruses, or fusion of the cell membrane with the viral envelope in the case of enveloped viruses. Uncoating is the process of releasing viral proteins of the tegument and the viral genome from the capsid. The proteins of the tegument contain viral enzymes necessary to begin the transcription, translation, and nucleic acid replication processes (Fig. 6.1).

Transcription and translation of viral nucleic acids and replication of viral nucleic acids occur in a specific order dependent on the type of nucleic acid present in the virion. DNA viruses are often transcribed to mRNA and translated to viral proteins shortly after uncoating and prior to beginning DNA replication. The replication and transcription of RNA viruses is more complicated. Nonretroviral RNA viral nucleic acids may be classified as positive or negative RNA strands. RNA of positive strand RNA viruses is similar to mRNA and is transcribed and translated prior to replication. A complementary or negative strand of RNA is then created as a template for replication of the positive strand RNA genome. RNA of negative strand RNA viruses, however, must be converted to a positive strand mRNA by RNA-dependent RNA polymerase (RDRP) before transcription and translation into proteins may begin. Then RDRP uses the positive strand RNA as a template to create the negative RNA strands to be included in the new virions.[2]

Retroviruses get their name from their unique method of genome replication. Upon uncoating of the virus, the viral protein reverse transcriptase creates a DNA template from the viral RNA genome. This proviral DNA is incorporated in the host genome where it is replicated to RNA via transcription, and RNA is used for translation and new viral genomic

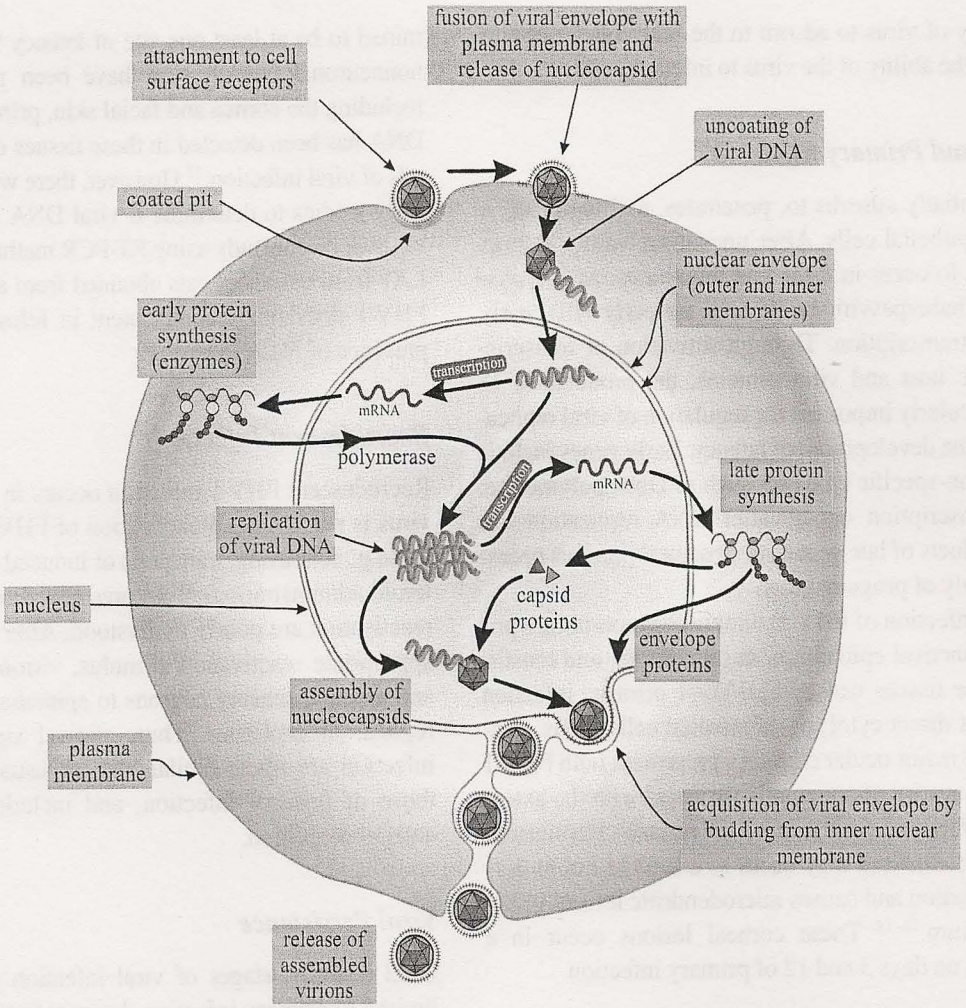

Figure 6.1. Stages of replication of a herpesvirus. (Reprinted with permission from Quinn PJ, Markey BK, Carter ME, Donnelly WJC, Leonard FC. Replication of viruses. In: *Veterinary Microbiology and Microbial Disease.* Oxford: Blackwell Science; 2002:283–289)

material. This unique mechanism of inserting proviral DNA into the host genome is often exploited for gene therapy using specific retroviral vectors.

After replication of the viral genome and formation of viral structural proteins, progeny virions are assembled within the host cell and readied for release. Release of progeny virus may occur by budding through the host cell membrane or through rupture of the host cell. Enveloped viruses acquire their envelope from the host cell membrane.

Feline Herpesvirus-1 (Feline Rhinotracheitis Virus)

Features and Epidemiology

Feline herpesvirus type 1 (FHV-1) is a member of the *Herpesviridae* family, subfamily *Alphaherpesvirinae.* The three subfamilies of herpesviruses are classified and defined by certain characteristics of growth, replication, and latency. Being a member of the alphaherpesvirus subfamily, FHV-1 has a short replication cycle, spreads rapidly in cell culture, causes lysis of infected cells, and achieves latency in sensory ganglia of its host. The natural host range of FHV-1 is restricted to domestic and wild feline populations. However, the virus is generally widespread within the feline population, with an estimated 50% to 97% of cats being seropositive.[3–5]

FHV-1 is an enveloped double-stranded DNA virus with a genome of approximately 134 kilobase (kb) pairs arranged as one long component (104 kb) and one short component (30 kb).[6,7] The nucleocapsid is 1400 Å in diameter and consists of the DNA genome surrounded by a protein coat called tegument. The envelope surrounds the nucleocapsid and is composed of glycoproteins, resulting in a virion that is approximately 140 nm in diameter with icosohedryl geometry.

There appears to be little genomic variation among FHV-1 strains. Restriction endonuclease digestion demonstrates the FHV-1 genome to be highly conserved with existence of three major genotype groups: C7301, F2, and C7805. The C7301 genotype is reported to be most prevalent of the three groups.[8,9] In spite of the FHV-1's minimal genetic diversity, recent studies of experimental infection have shown variable pathogenecity among FHV-1 field isolates of the same restriction endonuclease pattern.[1] Other reports have identified mutations and genetic rearrangements of genes responsible for encoding specific glycoproteins among different FHV-1 isolates. Natural rearrangement of FHV-1 glycoprotein C (gC) was shown to

alter the ability of virus to adsorb to the host cell membrane, thus affecting the ability of the virus to infect the cell.[11]

Replication and Primary Infection

FHV-1preferentially adsorbs to, penetrates, and replicates in conjunctival epithelial cells. After uncoating, viral transcription is thought to occur in three specific phases, as is typical with other alphaherpesviruses: immediate early (IE), early, and late gene transcription. Through activation of transcription of specific host and viral proteins, the products of IE genes are particularly important for regulation of viral replication cycle and the development of latency. Early genes include many replication-specific enzymes such as DNA polymerase. Late gene transcription occurs after DNA replication has begun; the products of late genes are structural proteins necessary for assembly of progeny virus.

In primary infection of FHV-1, viral replication occurs primarily in conjunctival epithelium, nasal mucosa, and tonsils. Lesions in these tissues caused by FHV-1 primary infection are the result of direct cytolysis of infected cells. Thus, conjunctivitis is the major ocular clinical sign present with FHV-1 infection. The severity of conjunctivitis varies with the extent and severity of virus replication and release. Replication within corneal epithelium may occur to a limited extent during primary infection and causes microdendritic lesions of the corneal epithelium.[12–14] These corneal lesions occur in a biphasic pattern on days 3 and 12 of primary infection.

Latency

Latency has been classically described as the period during which actively replicating virus cannot be detected and clinical signs are not present. During primary infection progeny virus infect sensory nerve endings at the primary site of infection and ascend sensory neurons in retrograde manner to associated sensory ganglia where they become latent. Because FHV-1 primary infection typically occurs in the conjunctiva and nasal mucosa, tissues receiving sensory innervation from the trigeminal nerve, FHV-1 typically becomes latent in trigeminal ganglia.

While latency appears to be a biologically quiescent period of viral infection, there is minimal transcription of a small portion of the viral genome called latency-associated transcript (LAT) during latent herpesvirus infections. Though LATs are also transcribed during actively replicating infections, they are the only detectable transcribed virus gene during latency.[15] Prior to detection and identification of LAT, latent infections and sites of latency could be identified only through cocultivation of latently infected tissues in cell culture. With the identification of LAT and the refinement of reverse transcriptase–polymerase chain reaction (RT-PCR) techniques, identification of LAT has become the standard for identifying latently infected virus.

Utilizing cocultivation techniques, sites of latency for alphaherpesviruses have been determined to be sensory ganglia. The trigeminal ganglia have been unequivocally determined to be at least one site of latency for FHV-1.[15–19] Other nonneuronal latency sites have been proposed for FHV-1, including the cornea and facial skin, primarily because FHV-1 DNA has been detected in these tissues during quiescent periods of viral infection.[17] However, there was no attempt in these early studies to determine if viral DNA was truly from latent virus. A recent study using RT-PCR methods to identify FHV-1 LAT from tissues of cats obtained from a shelter suggests that FHV-1 does not become latent in feline cornea despite the presence of FHV-1 DNA.[16]

Recrudescent Infections

Recrudescent FHV-1 infection occurs in animals when latent virus is reactivated. Reactivation of FHV-1 occurs after natural (e.g., rehousing, transport) or induced stress (e.g., corticosteroid administration),[20] but precise molecular mechanisms of reactivation are poorly understood. After latent virus receives appropriate reactivation stimulus, virions begin to replicate and descend sensory neurons to epithelial tissues where viral replication continues. Thus, clinical signs of recrudescent infection are often similar, though usually less severe than those of primary infection, and include conjunctivitis and corneal ulceration.

Viral Persistence

Until recently, stages of viral infection were thought to be limited to primary infection, latent infection, or recrudescent infection. However, with the advancement of molecular diagnostics and the high sensitivity of polymerase chain reaction (PCR), viral DNA can often be detected in tissues from cases that do not clearly fit into one of the three previously mentioned stages.[21] Persistent HSV-1 DNA has been demonstrated for chronic inflammatory lesions in the eyelids, conjunctiva, and cornea as presence of viral DNA without detectable viral protein synthesis in a murine model.[22] Persistent viral infection is suspected to be accompanied by low-level viral protein production capable of driving chronic or persistent immune responses. Alternatively, recent evidence supports that viral DNA CpG sequences are, in fact, immunogenic and may be capable of driving chronic inflammatory responses in persistently infected tissues.[23] Though similar studies have not been reported for feline herpesvirus-1, FHV-1 DNA has been detected in tissues from clinical patients without evidence of primary infection or latent infection and in normal feline corneas without detectable production of LAT.[16] Given the many similarities between HSV-1 and FHV-1, both alphaherpesviruses, it is possible that a persistent viral state also exists for FHV-1 and may be involved in pathogenesis of FHV-1 associated ocular syndromes.

Immune Responses

Initial response to primary FHV-1 infection is believed to be dependent on macrophages, interferon, and complement.[24,25]

Development of serum-neutralizing (SN) titers occurs at low magnitude after primary infection (<1:64) but increases after re-exposure to the virus or recrudescent infections. Humoral immunity diminishes the severity of infection but does not prevent infection or the development of latency. Viral glycoproteins (60, 68, and 105 KD) have been shown to be the major viral antigen responsible for induction of the humoral response.[26]

FH-1–Associated Syndromes

Pathogenic mechanisms of conjunctivitis and corneal ulceration occurring with primary or recrudescent FHV-1 infection are well described and were discussed in the previous sections. There are, however, several clinical syndromes known or believed to be associated with FHV-1 infection for which pathogenesis is unknown or unclear (Table 6.1).

Keratoconjunctivitis Sicca (KCS)

Keratoconjunctivitis sicca resulting from infection with FHV-1 has been described and occurs in natural and experimental infection.[12] Though the exact pathogenesis is unclear, it is likely that reduction of tear production is the result of virus-mediated destruction and obstruction of lacrimal secretory ductules.

Stromal Keratitis

Stromal keratitis in cats with FHV-1 infections is analogous to HSV-1–induced stromal keratitis (HSK) in humans. Data produced to date suggest that stromal damage is immunopathologic in origin.[27–30] Histologic observations from cats with chronic, naturally occurring stromal keratitis have revealed fibrosis, collagen degeneration, and numerous lymphocytes, plasma cells, and macrophages. Experimentally, stromal keratitis does not occur during primary infection unless the normal immune response is suppressed by corticosteroids.[12] In this scenario, development of stromal keratitis is preceded by chronic epithelial ulceration and delayed virus clearance (and prolonged virus shedding) as well as acquisition of viral antigen by the corneal stroma. The sequential stromal accumulation of polymorphonuclear cells as well as T and B lymphocytes correlates temporally with the return of normal immune function, eventually leading to stromal inflammation and fibrosis. The events surrounding experimental FHV-1 stromal keratitis are most compatible with a delayed hypersensitivity, or Th1 cell–mediated response.[31] The precise mechanisms for development of stromal keratitis remain unclear. Antigens responsible for the immune response have not been identified, and stromal keratitis occurs during times when the virus is apparently quiescent and viral protein production cannot be detected. Sequestered viral antigens is one theory to explain the pathogenesis of HSK, but viral antigens cannot be detected. These factors have led some to suggest that HSK is an autoimmune disease against virus-altered host proteins or that it is the result of molecular mimicry. More recently evidence for the immunogenicity of viral DNA with high levels of CpG sequences has been demonstrated.[23] Studies are in progress to determine if persistent viral DNA may play a role in the development of HSK.

Eosinophilic Keratitis

Studies on scrapings and swabs of affected corneas show a clear link between eosinophilic keratitis (EK) and FHV-1 infection. PCR has demonstrated the presence of FHV-1 DNA in 45 of 59 cases of confirmed eosinophilic keratitis.[32] However, the role of FHV-1 in EK has not been determined. While there is some degree of overlap between the clinical appearance of eosinophilic keratitis and eosinophilic conjunctivitis, a study using PCR on tears collected from confirmed cases of feline eosinophilic conjunctivitis failed to amplify FHV-1 DNA.[33]

Corneal Sequestration

Corneal sequestration has been reported to be associated with FHV-1 infection.[32] One study clearly demonstrated a relationship between FHV-1 and corneal sequestra when cats were infected and subsequently given immunosuppressive doses of corticosteroids.[12] Subsequent investigation of naturally occurring feline corneal disease by PCR found 86 of 156 corneal sequestra samples to contain FHV-1 DNA, whereas only 1 of 17 normal corneas contained FHV-1 DNA.[32] Further analysis demonstrated that Persian and Himalayan breeds were significantly less likely to have FHV-1 DNA in sequestra samples than were other breeds. These findings suggest that sequestra in Persian and Himalayan breeds are likely due to some nonviral etiology. While there is a significant relationship between corneal sequestra and FHV-1 in non-Persian, non-Himalayan breeds, the role of the virus in pathogenesis has not been determined.

Symblepharon

Symblepharon as a manifestation of FHV-1 is seen primarily in young animals that have experienced severe conjunctivitis and viral-induced cytolysis of conjunctival epithelium. Exposure of underlying substantia propria allows for adhesion to occur between adjacent ulcerated tissues.

Uveitis

Numerous herpesviruses are known to cause uveitis in humans. Likewise, FHV-1 has been demonstrated to be associated with feline uveitis. A recent study of cats with uveitis demonstrated FHV-1 DNA via PCR in the aqueous humor in cats with uveitis; the same study found 22 of 44 cats with idiopathic uveitis had intraocular FHV-1–specific antibody production with Goldman-Witmer coefficient (C value) greater than eight.[34] These data support a role for FHV-1 in idiopathic uveitis, but the pathogenesis remains to be determined.

Feline Calicivirus Infection

Features

Feline calicivirus is a single-stranded RNA virus of the family *Caliciviridae* and genus *Vesivirus.*

Epidemiology and Pathogenic Mechanisms

Feline calicivirus is considered to cause as much as 50% of all respiratory diseases in the cat, and it has often been referred to as a potential cause of conjunctivitis in this species as well.

Table 6.1 Ocular Syndromes Reported to be Associated with Selected Animal Viruses

Feline herpesvirus-1	Primary Infection
	• Most frequently conjunctivitis; symblepharon; dendritic corneal ulcers are less common
	Recrudescent Infection or Viral Persistence
	• Conjunctivitis
	• Corneal ulceration
	• Eosinophilic keratitis
	• Corneal sequestration
	• Keratoconjunctivitis sicca
	• Stromal keratitis
	• Uveitis
	Retinopathy or retinitis
Feline immunodeficiency virus	Anterior uveitis
	Anterior hyalites (vitritis)
	Conjunctivitis
Feline leukemia virus	Anisocoria
	Lymphoma
	Retinal dysplasia with intrauterine infections
	Anemic retinopathy
	Uveal lymphoma
	Spastic pupil syndrome
	Experimental uveitis
Feline sarcoma virus	Uveal melanoma
	Periocular fibrosarcoma
Feline panleukopenia virus	Retinal dysplasia with intrauterine infections
Feline infectious peritonitis virus	Granulomatous uveitis
Canine herpesvirus-1	Retinal dysplasia with intrauterine infections
	Dendritic ulcers reported in 2 dogs
Equine herpes virus-2	Ulcerative and nonulcerative keratitis
Canine adenovirus-1	Uveitis; corneal endothelialitis with corneal edema
	Conjunctivitis
Bovine herpesvirus-1	Keratitis
Bovine viral diarrhea	Retinal dysplasia with intrauterine infection between days 76 and 150 of gestation
Malignant catarrhal fever	Anterior uveitis with lyphocytic vasculitis
	Keratitis

Results of numerous experimental studies, however, clearly indicate that calicivirus infection produces clinical signs that are nearly always restricted to the oral cavity and the respiratory system.[35–39] In addition, studies addressing the effects of infection with different calicivirus strains clearly reveal that glossal ulceration is the most prominent sign and that conjunctivitis is rarely observed.[37–39] Furthermore, a comparative study regarding the effects of infection by 10 different calicivirus strains in 66 cats revealed histologic changes in the conjunctiva of only one cat.[35] Taken together, these data strongly suggest that caliciviruses are rarely pathogenic to the feline conjunctiva.

Feline Infectious Peritonitis

Features

Feline infectious peritonitis virus (FIP) is single-stranded, enveloped RNA virus and is a member of the *Coronaviridae* family. FIP is genetically very similar to *feline*

enteric coronavirus and may, in fact, be a mutant or variant of FECV.[40] One study found distinct genetic similarities between FIP and FECV isolated from the same geographic environment that are not present when compared to either feline coronavirus isolated from other environments.[41]

Pathogenic Mechanisms

Clinical signs of FIP infection are classically categorized into effusive (wet) and noneffusive (dry) forms of the disease. Vasculitis develops from immune complex deposition, and resultant increased vessel permeability allows exudation in the effusive form of FIP. Noneffusive FIP occurs when a cell-mediated immune response develops to the coronavirus, resulting in pyogranulomatous inflammation in affected tissues.[42]

Ocular involvement is more typical in the noneffusive forms of FIP, with uveitis being a common finding of many affected cats.[43] Characteristic clinical signs are aqueous flare, keratic precipitates, iris swelling and color changes, hyphema, and retinal hemorrhages.

Similarities between FIP and FECV and the relatively frequent exposure to FECV have long caused frustration in interpretation of laboratory diagnostics for suspected cases of FIP.[44] Cross-reactivity of serology between the viruses makes the interpretation of such tests difficult. Traditional RT-PCR techniques are highly sensitive to the presence of feline coronavirus RNA but are incapable of distinguishing FIP from FECV. Recently, however, RT-PCR for subgenomic mRNA of the feline coronavirus M gene was adapted to identify FIP-infected peripheral blood monocytes.[45] That study was able to detect 75 of 81 postmortem confirmed cases of FIP, while none of 17 cats with other non-FIP pathologies were positive with this assay.

Feline Immunodeficiency Virus

Features

Feline immunodeficiency virus (FIV) is a member of the *Retroviridae* family, subfamily *Lentivirnae.* It is a single-stranded, enveloped RNA virus best known for causing an immunodeficiency syndrome in cats similar to that caused by human immunodeficiency virus (HIV). The biologic similarities between these viruses create much interest in FIV as a research model for human disease.

Pathogenic Mechanisms

Many of the clinical signs of FIV are related to the immunodeficiency syndrome it creates with resultant secondary infections. While this is particularly true of systemic clinical signs, ophthalmic clinical signs are more vague and not necessarily related to secondary infections. Two infectious organisms that have received considerable attention with respect to their interaction with FIV are *Toxoplasma gondii* and *Chlamydophila felis* (formerly known as *Chlamydia psittaci*). Each of these organisms is more thoroughly discussed in its appropriate section in this chapter.

Conjunctivitis

Mild, chronic, or self-limiting conjunctivitis may be seen in FIV-infected cats.[17,46] One study of cats with chronic conjunctivitis reported 8.5% of the cats tested were positive for FIV[47] compared to 2.6% FIV infection of normal cats. Another study of FIV-infected cats demonstrated 11% to have chronic conjunctivitis.[46]

Anterior Uveitis

Feline immunodeficiency virus has been reported to cause anterior uveitis in the absence of secondary or opportunistic infections. Lymphocytic-plasmacytic inflammation of the anterior uvea is present histologically, but the pathogenesis of this lesion is undetermined.

Associated Anterior Hyalitis (Vitreitis)/Pars Planitis

Dense, white blood cell infiltration of the anterior peripheral vitreous adjacent to the lens zonules, producing the appearance of a "snowbank," characterizes the pars planitis seen with FIV infection.[48] The pathogenesis of this lesion is unknown, but the cellular infiltrate is primarily plasma cells.

Anisocoria

Mild-to-moderate mydriasis has been described with FIV infection. The pathogenesis of the lesion is not determined, but central nervous system disease was suggested as a possible cause. Anisocoria from FIV infection is usually permanent and slowly progressive.

Intraocular Neoplasia

Cats infected with FIV are reported to be more likely to develop B-cell lymphoma, and one retrospective study reported 7 cats with intraocular lymphoma to be infected with FIV.[49] However, attempts thus far to demonstrate virus within intraocular melanoma have failed.[50] While a direct correlation between FIV and intraocular neoplasia is not clear, it is possible that FIV-related immunosuppression and reduced immune surveillance allows certain neoplastic processes to progress.

Retinopathy

Large, geographic, irregular areas of hyperreflectivity and areas of retinal thinning of the sensory retina have been described with FIV.[48] While there are also reports of retinal perivasculitis in some cases of FIV, the histologic appearance of FIV retinopathy is that of panretinal degeneration without inflammation.[51] Support for this retinopathy being a primary condition, and not the result of secondary infection, comes from the fact that such lesions have been described in both naturally and experimentally infected cats. These lesions have developed during the acute phase of infection (i.e., the first 6 months) in experimentally infected cats and during the AIDS-like stages in naturally infected cats. The pathogenesis

of this lesion is probably the same as that of the microvascular retinopathy that occurs during infection with HIV and of the neurologic degeneration that occurs in FIV-infected cats and HIV-infected humans. Two hypotheses have been proposed:

1. Neurotoxin: Both FIV and HIV are capable of enhancing excitatory amino acid toxicity in cultured fetal neurons. This toxicity can be blocked using N-methyl-D-aspartate receptor antagonists. However, glial cells must be present for the toxicity to occur, which suggests the effect of the virus is indirect and is mediated by glial cells. These viruses do not appear to infect neurons, but they can infect microglia and, possibly, astrocytes.

2. Altered Hemodynamics: FIV or HIV results in increased vascular permeability and altered hemodynamics. The finding of cotton-wool spots and hemorrhages indicates that vascular compromise occurs. The pathogenesis of these lesions and their importance, however, remain unclear.

Feline Leukemia Virus

Features

Feline leukemia virus (FeLV) is an enveloped, single-stranded RNA virus in the *Retroviridae* family, subfamily *Oncovirinae.*

Pathogenic Mechanisms

Systemic

Transmission of FeLV can occur horizontally or vertically. Horizontal transmission occurs via saliva with prolonged intimate contact and is more likely to occur in environments where biting or grooming is prevalent.[52] After successful transmission of the virus, viremia develops, and the virus is disseminated to lymphoid tissue and bone marrow. From effects on cells at these sites, the virus causes hematologic changes, immunosuppression, and tumor formation.

Ocular

Uveal Lymphosarcoma: One of the most frequent ocular manifestations of FeLV is uveal lymphosarcoma. Uveal lymphosarcoma is typically infiltrative, and appearance may range from mild diffuse iris thickening or focal anterior uveal masses to extensive uveal infiltration. Affected eyes will most often exhibit some degree of anterior uveitis, including aqueous flare, anterior chamber fibrin, keratic precipitates, and synechia. In fact, FeLV should be considered a rule-out for idiopathic feline uveitis because one histopathologic study found it to be a frequent cause of uveitis. Lymphosarcoma and uveitis may also result in secondary glaucoma. Uveal lymphosarcoma is often present as one component of multicentric disease but may also present without evidence of other organ involvement. Nonuveal lymphosarcoma may also cause ocular clinical signs by infiltrating the orbit, eyelids, conjunctiva, or nictitans.

Retinal Dysplasia: Infection of fetal kittens with FeLV may result in retinal dysplasia. Affected kittens develop inflammation, followed by necrosis and disorganization of the retina, resulting in rosettes, and retinal folds with infolding of the retinal pigment epithelium, and gliosis.[53] Retinal neoplasia has also been suggested to occur in one kitten experimentally infected with FeLV.[53]

Anemic Retinopathy: Anemic retinopathy results from decrease of hemoglobin concentration to below 5mg/dl. It is believed that resultant hypoxia from decrease in oxygen-carrying capacity triggers a compensatory venule dilation to maintain retinal perfusion. Capillaries subsequently become fragile, resulting in hemorrhage at all depths of the retina.[54]

Spastic Pupil Syndrome: It is likely that spastic pupil syndrome represents FeLV infection of the parasympathetic portion of the cranial nerve III. Supporting data for this proposed mechanism, however, is limited.

Other: A recent study reports the identification of FeLV proviral DNA via PCR in 11 normal feline corneas of 17 FeLV seropositive cats and in none of the corneas of seronegative cats.[55] Immunohistochemistry localized FeLV to the corneal epithelium. While the role corneal FeLV might play in FeLV-related ocular disease has not been determined, the immediate implications for these data are in the selection of donor corneas for corneal grafting procedures.

Feline Sarcoma Virus

Features

Feline sarcoma virus (FeSV) belongs to the family *Retroviridae* and subfamily *Oncovirinae.* It is a variant of FeLV that has incorporated host oncogenes.

Pathogenic Mechanisms

Experimental FeSV Uveitis

In an experimental study in which FeSV was injected subcutaneously, anterior uveitis, including iritis, posterior synechia, and cataract formation, was present 37 days postinoculation. Histologically, the inflammation was primarily infiltration of lymphocytes and plasma cells into the anterior uvea, and inflammatory changes were attributable to virus–antibody interactions or cell-mediated immune response. Virus was identified in aqueous humor of infected cats.[56]

Experimental FeSV-Induced Uveal Melanoma

Development of uveal melanomas has been demonstrated following the anterior chamber inoculation of FeSV in experimental studies. More recently, FeLV/FeSV proviral DNA was identified in 3 of 36 globes enucleated for uveal melanoma.[50] Status of systemic infection with FeLV or FeSV was not known. The role naturally occurring FeLV or FeSV may play in the development of uveal melanoma remains unknown.

Fibrosarcomas

Fibrosarcomas of the eyelids have been reported to be associated with FeSV in young cats. A recent study of 6 cats affected with ocular sarcoma, however, failed to demonstrate FeLV or FeSV.[57]

Feline Panleukopenia Virus

Features

Feline panleukopenia virus is a nonenveloped, single-stranded DNA virus and a member of the family *Parvoviridae* and genus *Parvovirus.*

Pathogenic Mechanisms

The major ocular pathology of feline panleukopenia is retinal dysplasia associated with intrauterine infection. In one case report of a 6-week-old kitten, lesions were characterized by retinal thinning, loss of the normal architecture, and rosette formation.[58] Virus was recovered from the cerebrum, and cerebellar hypoplasia was present as well. Hydrancephaly has also been reported in association with perinatal panleukopenia infection; the optic nerves were small with increased perineural connective tissue.[59]

Canine Herpesvirus

Features

Canine herpesvirus type 1 (CHV-1), like FHV-1, is an enveloped, double-stranded DNA virus. It is a member of the *Herpesviridae* family and the *Alphaherpesvirinae* subfamily. Its host range is restricted to the dog, and replication and biologic behavior are similar to FHV-1.

Pathogenic Mechanisms

Systemic

Transmission can take place in utero, following contact with contaminated vaginal secretions, or postparturition. In puppies, death is caused by disseminated virus replication in parenchymal organs and the CNS. Transient vaginitis may be the only clinical manifestation in adults. The lesions result from direct viral cytolysis.

Ocular

Experimental infection of newborn puppies with CHV-1 results in keratitis, uveitis, retinal necrosis, and optic neuritis.[60] Panuveitis with intranuclear inclusions can be seen 4 days after experimental infection, with subsequent retinal necrosis, retinal maturation retardation, and retinal folding and hypertrophy. One recent report identified CHV-1 as the etiology of dendritic corneal ulceration in 2 dogs.[61] CHV-1 was identified using cell culture, PCR, indirect immunofluorescent antibody (IFA), and electron microscopy in the affected dogs, whereas the virus could not be isolated in normal dogs or dogs with nondendritic corneal ulcers. It was suggested that immunosuppression likely played a key role in the development of viral keratitis in both dogs.

Canine Distemper Virus

Features

Canine distemper virus is an enveloped, negative strand RNA virus. It is a member of the family *Paramyxoviridae,* genus *Morbillivirus.*

Pathogenic Mechanisms

General

Canine distemper virus has an affinity for tissues of neural and epithelial origin. It causes pathology via direct cytolysis of infected cells.

Systemic

The primary route of infection is the respiratory tract. The virus spreads from the oropharynx to the regional lymph nodes and tonsils, and viremia disseminates the virus to lymph tissues throughout the body. Virus persists in the epithelial tissues of dogs unable to mount a protective immune response.

Ocular

Affected tissues include conjunctival epithelium, lacrimal gland, retina, optic nerve, and optic tracts. Mucoid to catarrhal ocular exudates are often present in acute distemper. Keratoconjunctivitis sicca may occur as a direct result of acute distemper and may be a short-lived or chronic change. In the earliest report, posterior segment abnormalities resultant from distemper included retinitis, optic neuritis, and destruction of the optic tracts.[62] Acute retinitis is characterized by congestion, edema of the nerve fiber layer and the inner plexiform layer, and perivascular cuffing.[62–64] Intranuclear inclusions may be seen in retinal glia. Sequelae are optic nerve degeneration, focal-to-diffuse areas of retinal degeneration characterized ophthalmoscopically in the tapetal fundus by hyperreflectivity, and RPE pigment loss in the nontapetal fundus. Retinochoroiditis has been demonstrated to occur in 9 of 22 dogs infected with distemper. Distemper inclusions have also been found in the ciliary body of one dog.[65]

Canine Adenovirus-1

Features

Members of the DNA virus family *Adenoviridae* are divided into two genera: *Mastadenovirus* and *Aviadenovirus.* The former includes *Canine adenovirus-1* (CAV-1). These viruses are nonenveloped, regular icosahedrons 65 to 80 nm in diameter.

Pathogenic Mechanisms

Systemic

Canine adenovirus is acquired via oropharyngeal route and is a recognized cause of pharyngitis and tonsilitis. Virus replicates and spreads to regional lymph nodes, kidney, liver,

and vascular endothelium. CAV-1 is the causative organism of infectious canine hepatitis and may thus cause severe or fatal illness.

Ocular

Ophthalmic signs of CAV-1 occur from natural infection and from vaccination with modified live vaccines. Initial clinical findings are mild anterior uveitis with mild corneal edema and anterior uveitis. These early clinical signs are resultant from viral replication in the anterior uvea and corneal endothelium[66] and are histologically characterized by mononuclear inflammatory cell response in the iris and trabecular meshwork.[65] A second phase of ocular inflammation is characterized by severe corneal edema. This latter phase of primarily corneal disease is the result of a type III hypersensitivity reaction (i.e., immune complex disease or Arthus reaction) affecting the corneal endothelium; replicating virus is not detectable from the eye in this latter phase, whereas viral antigen and antibody are easily demonstrated.

Type III hypersensitivity has been readily demonstrated in an experimental setting.[67,68] Twenty-four dogs were inoculated with infectious canine hepatitis (ICH). Nine dogs received virulent virus subcutaneously, and 15 dogs received attenuated virus intravenously. After 4 to 8 days, the aqueous humor was removed and the anterior chambers injected with 0.2 mL of anti-ICH serum. Fourteen of the 24 dogs developed eye disease, and in two dogs, corneal edema was severe. Purified viral antigen and anti-ICH serum were then injected into the anterior chamber of 8 dogs. Intense iritis with severe edema occurred, and the reaction was found to be more severe if complement was added to the immune complexes.

Prevalence

Ocular disease is estimated to occur in 20% of naturally occurring cases and in 0.4% of dogs given modified live vaccine. Afghan Hounds have been suggested to be predisposed to more severe ocular lesions after inoculation with attenuated CAV-1 vaccine.[69]

Equine Herpesvirus

Features

Five equine herpesviruses (EHV) have been identified: EHV-1 (i.e., rhinopneumonitis virus), EHV-3 (i.e., coital exanthema), and EHV-4 are members of the *Alphaherpesvirus* subfamily, and EHV-2 and EHV-5 are members of the *Gammaherpesvirus* subfamily. Continued improvements in molecular virology are advancing our understanding and classification of viruses. At one time, EHV-2 was classified as a betaherpesvirus but is now more appropriately classified as a gammaherpesvirus. Similarly, EHV-2 and EHV-5 are very closely related[70,71]; many early reports of EHV-2 may have, in fact, been EHV-5.

Viral Pathogenesis

Only three equine herpesviruses have been associated with ocular disease. Alphaherpesviruses EHV-1 and EHV-4 are known to cause conjunctivitis as a component of upper respiratory disease. Keratitis attributable to EHV-2 has been described repeatedly in the literature as punctate, lacelike, ulcerative, or nonulcerative lesions of the cornea in individual cases and in herd outbreaks of corneal disease.[72–74] Early reports isolated replicating EHV-2 from affected eyes, whereas later reports demonstrated presence of the virus via PCR. Though EHV-2 is widely reported to be associated with corneal disease, it is not clear whether the virus is actually responsible for corneal disease or is merely an incidental finding in the face of corneal disease. Gammaherpesviruses are ubiquitous in equine populations but may have regional variability in prevalence. They are also reported to infect and become latent in mononuclear white blood cells. A preliminary study of 10 horses with normal eyes, using PCR specific for equine gammaherpesviruses EHV-2 and EHV-5, found 8 horses to have a gammaherpesvirus DNA present in nasopharyngeal swabs and 5 to have gammaherpesvirus present in conjunctival swabs.[75] Given the relatively high prevalence of gammaherpesvirus DNA detected from horses with normal eyes in this limited population, it seems possible that gammaherpesviruses detected from horses with corneal disease may be an incidental finding. Further studies are needed to determine if EHV-2 or EHV-2 play a role in equine corneal disease.

Bovine Herpesvirus-1 (Infectious Bovine Rhinotracheitis)

Features

The infectious bovine rhinotracheitis virus belongs to the family *Herpesviridae* and subfamily *Alphaherpesvirinae*. Its structure and behavior is typical of other alphaherpesviruses.

Pathogenic Mechanisms

Systemic

Upper respiratory disease is caused by direct viral cytolysis.

Ocular

Ocular disease may occur with or without respiratory signs. Conjunctivitis is the predominant feature with variable severity ranging from chemosis and hyperemia to severe ulcerative conjunctivitis, with formation of white conjunctival plaques composed of mononuclear cells (i.e., plasma cells and lymphocytes).[76,77] Keratitis is also possible.

Bovine Virus Diarrhea

Features

Bovine virus diarrhea (BVD) is a member of the *Togaviridae* family and genus *Pestivirus* (i.e., mucosal disease viruses). The virus exists in a lipid-containing envelope with surface

projections that surround a spherical nucleocapsid. Virions are 40 to 70 nm in diameter. Replication occurs in the cytoplasm, and assembly is assumed to occur during budding through the plasma membrane.

Pathogenic Mechanisms

BVD is subdivided into cytopathic and noncytopathic forms dependent on behavior in cell culture and presence of certain protein sequences. Cytopathic BVD is characterized by the production of NS3 structural protein, whereas noncytopathic BVD produces the noncleaved structural protein NS23.[78] Calves that are infected with noncytopathic BVD prior to 150 days of gestation are immunotolerant of the virus and become persistently infected, whereas infection with cytopathic virus at this stage is often fatal. Persistently infected animals are lifelong carriers and may shed virus in large quantities throughout their lives.[79] Calves surviving infection between 76 and 150 days of gestation often have congenital ocular defects, including retinal dysplasia, cataracts, and microphthalmos.[80–82]

Malignant Catarrhal Fever

Features

Malignant catarrhal fever virus belongs to the family *Herpesvirinae* and subfamily *Alcelaphinae.*

Pathogenic Mechanisms

General

Malignant catarrhal fever is a pansystemic, vasculopathic disease of cloven-hooved animals worldwide (e.g., deer).[83] In the peracute form, death from hemorrhagic gastroenteritis occurs 1 to 3 days after the onset of clinical signs. In the alimentary form, clinical signs are fever, diarrhea, diffuse exanthema, lacrimation, and lymphadenopathy. In the head and eye form, typically seen in Africa, mucopurulent nasal discharge, corneal opacity, edema of the head and neck, and neurologic manifestations are common. Nasal and lacrimal discharge, dermatitis, and lymphadenopathy may be the only external signs in the ocular form of the disease.

Ocular

Lymphocytic vasculitis of retinal, scleral, and uveal vessels is the predominant insult. Anterior uveitis is associated with corneal edema and keratitis. The predominantly lymphocytic vascular infiltrates contrasts this disease from BVD, thromboembolic meningoencephalitis (TEME), infectious bovine rhinotracheitis, and infectious keratitis.[84,85] An immunologic mechanism is suspected (e.g., type IV [DTH response]).

Bluetongue Virus

Features

Bluetongue virus is nonenveloped RNA virus, a member of the family *Reoviridae,* and a member of the genus *Orbivirus.*

Pathogenic Mechanisms

The bluetongue virus replicates in hematopoietic cells and endothelial cells of blood vessels. The ocular lesions are similar to those caused by BVD in both calves and lambs.[86] Vaccination of ewes during the first trimester of gestation with attenuated live vaccine produces necrotizing retinitis and CNS damage. Target tissues are the brain, spinal cord, and retina. The severity of disease depends on when in gestation the ewes are vaccinated. In lambs infected at 50 to 58 days, early lesions predominantly affect the retinal vasculature (i.e., endothelial nuclei rounded and vesicular).

Marek's Disease

Features

Marek's disease virus is a member of the family *Herpesviridae* and subfamily *Gammaherpesvirinae*

Viral Pathogenesis

Marek's disease is slowly cytopathic, like other gammaherpesviruses, and is tumorgenic with an ability to transform T lymphocytes. Systemic manifestations of Marek's disease are neurolymphomatosis (range paralysis) and acute Marek's disease. Ocular manifestations of Marek's disease include severe panuveitis and ocular lymphomatosis.[87]

Diagnostic Methods

Cytology

Cytology may be a useful diagnostic tool for a few viruses. Presence of multinucleate epithelial cells is suggestive of HSV-1 infection in humans, but these cells are not present in FHV-1 infections. Intranuclear inclusions in epithelial cells may be seen in conjunctival scrapings during primary FHV-1 infection, but they are not identifiable with routinely used Wright-Giemsa–type cytologic stains. The inflammatory cell infiltrate seen in acute FHV-1 infection consists predominantly of neutrophils and therefore has little diagnostic significance. At least early in the course of disease, examination of Schorr's-stained conjunctival scrapings for intranuclear inclusion bodies can be useful in making the diagnosis of canine distemper.

Immunofluorescence

Immunofluorescent antibody (FA) testing has long been used to diagnose viral infections in animals. Immunoflourescence can be performed in a direct or indirect manner. The fundamental principle behind each method of FA is that the sample to be tested for viral antigens is fixed on a slide, and a fluorescent molecule is attached to the viral antigen through one or more viral-specific antibodies. The direct method uses a single antibody (or a single application of polyclonal antibodies) with conjugated fluorescent molecule to react with the sample. The indirect FA (IFA) method first uses a nonfluorescent antibody

to react with the sample (the primary antibody) and follows up with a secondary fluorescent antibody with an affinity for the first antibody used. Both methods require the use of a fluorescent microscope for evaluation. The IFA is more commonly utilized than direct FA for most diagnostic testing.

Limitations of FA in virological diagnosis are in the effective sensitivity of these assays. For example, FHV-1 can be detected with IFA on day 1 through 6, but not on day 9 of experimental infection.[13] Twelve days postinfection, FHV-1 detection rate using virus isolation was 99%, whereas IFA detection rate was 20%.[88] Similarly, positive IFA results were reported in only 8.8% of cases in which FHV-1 was suspected as being causative.[47] Another study demonstrated 28% of clinically normal cats to be positive via FA; 50% of cats with acute FHV-1 infection and 36% of cats with chronic FHV-1 infection were positive in the same study.[5] Another limitation to FA is the stage of infection and concentration of viral epitopes. Many viral infections, such as FHV-1, decrease replication and release of virus and associated antigens with chronicity. Thus, long-standing infections are less likely to have detectable antigen. In addition to the biologic sensitivity of FA testing, sensitivity and specificity is dependent on technician interpretation. Technicians must tediously examine numerous cells and subjectively determine if the magnitude of cell fluorescence is above that which would be considered "background" fluorescence.

Sample collection involves collecting scrapings or swabs of affected tissue and spreading on microscopic slides or collecting tissue biopsies. Smears or scrapings should be acetone-fixed to preserve epitopes for reaction.

Virus Isolation

Virus isolation (VI) has long been considered the "gold standard" for diagnosing viral infections. However, VI suffers from significant limitations. Many viruses (e.g., FHV-1) are labile and may be destroyed using standard collection and transport mechanisms. Special transport media and rapid delivery to a laboratory are not always available in field situations. Isolating a virus requires cell culture techniques. It is relatively laborious and expensive for laboratories to maintain large libraries of cells in culture for VI compared to maintenance of reagents for newer diagnostic methods such as PCR. With the decreased sensitivity compared to newer molecular methods, VI use is declining. Samples should be obtained with Dacron swabs and placed in culture as soon as possible.[89] If not collecting samples directly onto cell culture, swabs should be placed in appropriate transport media and shipped on ice to the laboratory as fast as possible. Freezing of the sample should be avoided because many viruses are inactivated by repeated freeze–thaw cycles.

Serology

Serology has long been used for diagnosis of several viral infections. A fourfold rise in neutralizing titer between acute and convalescent sampling is considered to be diagnostic of infection for many viruses. Unfortunately, routinely performed serologic titers have not proved to be useful in diagnosing many of the most important ocular pathogens, such as FHV-1 infection in the cat. Two reasons for this are the relatively low titer response after primary infection and the inability to distinguish response in primary infection from that with repeated vaccination. Though neutralizing titers predictably rise after experimental reactivation of latent virus, titers of great magnitude are rarely seen in cats with recrudescent infections. In one study,[5] comparison of FHV-1 enzyme-linked immunosorbent assay (ELISA) titers with clinical signs suggestive of FHV-1 infection, or IFA and VI, demonstrated no correlation between titer magnitude and the likelihood of a positive test result. A prior study demonstrated serum titer to be inversely proportional to the probability of getting positive FA or VI result. It is likely that the negative FA results are due to antigen inhibition by secretory antibody.[47]

As previously noted, similarities between FIP and FECV prevent the effective use of serologic methods in the diagnosis of FIP.

Polymerase Chain Reaction

PCR has significantly improved the ability to diagnose many viral pathogens. The major advantage of PCR is its inherent exponential amplification of small amounts of DNA to a detectable signal.[90] The key to this exponential molecular amplification is that the target DNA sequence is doubled during each of approximately 30 cycles of the amplification reaction. Thus, one viral copy, under ideal conditions, would be amplified to 5.37×10^8 copies in 30 cycles of amplification. The general concept behind PCR is that a simple double-stranded template DNA is reacted with oligonucleotide primers, free nucleotide bases to be used in constructing new DNA molecules, and DNA polymerase. These components are mixed in a sample tube with appropriate salt concentrations and buffers. The sample is heated to approximate 90°C to melt or separate the double-stranded DNA, cooled to allow annealing of the oligonucleotide primers to the template DNA, and heated slightly to allow DNA polymerase to build new DNA strands from the oligonucleotide primers, template DNA, and nucleotides. This series of reaction temperatures constitutes one cycle of the PCR reaction. The entire PCR reaction is comprised of numerous cycles (approximately 25 to 40) to exponentially amplify the target DNA sequence.

Three common variations of PCR methodology are nested PCR, RT-PCR, and real-time PCR. Nested PCR utilizes a second set of oligonucleotide primers, directed at a sequence internal to the first amplified sequence, and repeats the cycling program a second time. The major advantage of nested PCR is increased sensitivity. Increased sensitivity, however, may have adverse effects in some situations, as discussed later. RT-PCR is a method of amplifying RNA for detection. DNA polymerases used in PCR will not amplify

RNA sequences. Therefore, RNA sequences must first be reverse transcribed to DNA so that standard PCR can be performed. This technique is frequently utilized to detect mRNA sequences transcribed from DNA, but it may also be used to detect RNA of certain RNA viruses. Real-time PCR is a modification of the standard PCR reaction that measures the rate and amount of amplification of target DNA sequence; thus real-time PCR allows quantification of the target DNA. Such measurement is made possible through the use of molecules that fluoresce when bound to double-stranded DNA or specialized primer sets that fluoresce as they are utilized in the PCR reaction (Taqman technology). Using either technology, the amount of fluorescence is measured once during each cycle of the PCR reaction. Comparison of the fluorescent measurements to standard curves of amplification reactions of known quantities of DNA allows for estimation of the amount of target DNA present in the initial sample.

PCR for FHV-1

PCR has been utilized extensively for diagnosis of clinical FHV-1 infections and in research studies. The most frequently reported target gene utilized for FHV-1 PCR is the thymidine kinase gene. Both standard and nested PCR assays have been described. Sensitivity of these assays has been reported as being capable of detecting as little as 0.08 fg (less than one viral copy) to 390 fg (approximately 3 × 103 virus copies) of viral DNA.[91,92]

The high sensitivity of PCR, combined with the ubiquitous nature of FHV-1, has the potential of creating a diagnostic dilemma for the clinician. With as many as 80% of exposed cats being latently infected, it is not uncommon to detect FHV-1 DNA sequences in samples taken from normal eyes. Additionally, the ability of latent FHV-1 infections to be reactivated and to shed virus with stress can further confound interpretation of positive PCR results. For example, cats with non-FHV-1–induced corneal disease may be stressed enough by corneal disease that they reactivate a latent infection and begin to shed virus. Such a scenario would yield a legitimate positive PCR result but may lead a clinician to an incorrect diagnosis. The clinician must be cautious in selection of PCR and interpretation of positive PCR results.

Real-time PCR and RT-PCR have recently been utilized to further characterize FHV-1 infections, though their use for clinical diagnostics is not widespread. Attempts were made to correlate the amount of virus with stage of infection using real-time PCR.[93] Results correlate with virus isolation methods, but this diagnostic method may have limited ability in discriminating latently or persistently affected "normal" patients from those with low levels of virus shedding during clinical disease. RT-PCR has been used experimentally to identify latent infections in trigeminal ganglia.[16]

PCR for FIP Virus

As previously discussed, FIP is believed to be a mutation of FECV. Because these viruses are so closely related, it has not been possible until recently to distinguish them via molecular methods. RT-PCR for subgenomic mRNA of the feline coronavirus M gene adapted to identify FIP-infected peripheral blood monocytes was able to detect 75 of 81 postmortem confirmed cases of FIP.[45] None of 17 cats with other non-FIP pathologies were positive with this assay.

Sample Collection

Collection of samples for PCR must be done with consideration of pathogen and host biology and interaction of the pathogen and host. FHV-1 is an obligate intracellular organism that only leaves the cell with replication and release. To maximize the opportunity of detecting a herpesvirus infection via PCR, the clinician must collect as many host cells as possible for analysis. Thus, a scraping is preferred over a swab, and a biopsy is preferred over a scraping. Site of infection or affected tissue should also be considered. For collection of conjunctival swabs, a topical anesthetic is instilled in the eye and a sample is collected on a Dacron swab by rolling it through the ventral cul-de-sac. Swabs are placed in 1 mL of phosphate-buffered saline (PBS). Alternatively, for epithelial keratitis, scrapings may be collected; keratectomy or other tissue specimens are similarly placed in PBS. Once collected, samples should be frozen (–20°C) until the PCR assay can be performed, and it must not be allowed to warm appreciably before analysis. Prior to analysis, swab specimens are processed via lysing the cells by heating at 98°C for 10 minutes. Tissue samples must first be digested with enzymes (proteinase K) and the DNA extracted before cycling.

OCULAR BACTERIOLOGY

Morphology and Life Cycle

Bacteria are prokaryotic organisms consisting of a cell membrane (i.e., cell wall or envelope), cytoplasm, one strand of DNA, and in some instances, specialized surface structures such as capsules or fimbriae (pili). Bacteria lack a nucleus or mitotic apparatus, but the bacterial DNA is organized into a single, circular strand of chromosome. In addition to this single, closed-loop chromosome, bacterial cytoplasm contains smaller molecules of DNA, termed *plasmids,* and ribosomal RNA. Plasmids carry information for drug resistance, that is, R factors, or code for toxins that can affect host cellular functions. Bacteria reproduce by asexual binary fission, involving ingrowth of the cell wall and cleavage of the intracellular compartment with division of cell contents.

Bacterial cell walls are comprised of phospholipids and proteins that play key roles in many cell functions. Cell membranes of bacteria contain the electron transport system, serve as an osmotic barrier, and regulate transport of solutes. The cell wall is also the site of many antigenic determinants for various bacteria, whereby variability of surface polysaccharides allow serologic differentiation of isolates. Endotoxin, when present, is located within the cell wall, where a lipid component (i.e., lipid A) is primarily responsible for toxicity.

Mycoplasmas lack a rigid cell wall, and some agents, such as *Borrelia* and *Leptospira* sp., have flexible, thin walls.

Specialized bacterial surface structures include the outer capsules and fimbria. The external layer of the bacterial capsule can prevent phagocytosis and aid in adherence of the bacteria to tissues. Capsules may be well organized and distinct or more mucuslike and diffuse, forming a slime layer that contributes to formation of a biofilm.[94] Some bacteria have a capsule with a chemical structure that mimics host tissue, thereby camouflaging the organism from the host's immune system.[95] Fimbriae (or pili) are short, hairlike extensions of the cell membrane that mediate adhesion to specific surfaces. Fimbriae aid in the initial colonization of the host, but they may also increase susceptibility of bacteria to phagocytosis.

The bacterial growth cycle typically consists of four phases: the lag phase, the logarithmic growth phase, the stationary growth phase, and a decline phase. Bacteria vary in their temperature requirements for growth and can be divided into psychrophiles (0–20°C), mesophiles (20–40°C), and thermophiles (40–90°C). Most bacteria are mesophiles, with some important mesophiles, such as *Staphylococcus* sp., capable of growth at temperatures below their normal growth range. Others, such as *Streptococcus* and *Proteus* sp., possess the ability for psychrophilic growth.

Iron is an essential nutrient for bacteria. Iron availability affects bacterial growth and can influence the nature of a bacterial infection. The fact that the eye is iron-deficient may aid in its resistance to bacteria. Bacteria may undergo phenotypic changes, however, and develop ways to acquire iron from infected tissue. Under conditions of iron-restricted growth, pathogenic bacteria may produce exotoxins and thereby acquire iron from damaged host cells.[96]

Classification

Gram-staining properties and cell morphology remain the most practical means of classifying bacteria. Other important distinguishing features are fermentation products, ability to metabolize various substrates, sensitivity to different antibiotics, and colony morphology. Commercially available kits are now widely used, especially in nonreference laboratories. Though common, concerns have been expressed about the accuracy and expense of some of these rapid identification methods. DNA typing has been exploited to develop rapid diagnostic systems and to illuminate bacterial heterogeneity, thus allowing refinement of taxonomic designations; specific taxonomic categorization requires approval of an official international body. DNA sequencing has also made apparent the variations within groups of organisms.[97]

Dynamics of Ocular Surface Flora

Commensal Flora

Microbial populations of the ocular surface vary greatly between species (Table 6.2). Several factors appear to influence the prevalence of individual microorganisms; these include geography and climate, season, species, sampling and culturing techniques, and the immediate environment. Normal, noninvasive mucosal bacterial populations are primarily comprised of commensal flora present in large numbers and transient flora that may be recovered infrequently and in smaller numbers. These noninvasive normal microbial inhabitants of the ocular surface play a major role in prevention of infectious ocular disease. By limiting available nutrients, occupying surface space, and secreting inhibiting substances, these commensal flora are presumed to inhibit pathologic microbial species from colonizing the ocular surface and to provide an important means of checks and balances in ocular surface microbiology. Disruption of this homeostatic mechanism with long-term use of topical antimicrobials may result in overgrowth of pathogenic microbes with subsequent ocular disease (Table 6.2).

Opportunistic Bacteria

Bacteria that are either nonpathogenic or generally considered to be weakly pathogenic may cause disease in an immunocompromised host or present as a coinfection. Opportunistic organisms may colonize tissue after gaining entry into an unusual anatomic site via trauma or other insult. Mixed infections may occur whereby a combination of organisms that individually are incapable of causing significant infection may complement each other, thus producing pathogenic factors sufficient to cause disease. Research opportunities exist for investigating determinants of mixed infections in both humans and animals. Some examples of opportunistic bacteria commonly isolated in cases of animal disease include *Staphylococcus epidermidis, Bacillus* sp., *Corynebacterium* sp., *Escherichia coli, Klebsiella* sp., *Enterobacter* sp., *Serratia* sp., and *Pseudomonas* sp. (other than *Pseudomonas aeruginosa*).[101,104,105,112–114]

Aerobic Pathogens

Gram-Positive Bacteria

Staphylococcus Sp.

Staphylococci are ubiquitous and indigenous microflora of the skin and mucous membranes, and they are common causes of suppurative ocular and periocular infections.[103,112,115–118] *Staphylococci* are Gram-positive organisms that appear cytologically as individual cocci, pairs of cocci, small groups of four to six organisms, or grapelike clusters. They are facultative anaerobes, fermentative, catalase-positive, oxidase-negative, and nonmotile. When Gram-positive cocci are seen in corneal or conjunctival scrapings, *Staphylococcus* sp. must be differentiated from *Streptococcus* sp., *Micrococcus* sp., and yeasts such as *Candida* sp. and *Pityrosporum* sp.

Coagulase (named because it clots plasma) and hemolysins are the most widely recognized enzymes produced by staphylococci. Other enzymes produced by staphylococci include staphylokinase, catalase, lipase, collagenase, hyaluronidase, nuclease, fibrinolysin, gelatinase, protease, phosphatase, and lysozyme. Staphylococci may also produce enterotoxins with

Table 6.2 Summary of Findings of Studies of Normal Ocular Flora

Canine	Wide variation in prevalence of individual organisms Gram-positive organisms most commonly isolated (98, 99) Bacteria recovered from 68–78% of normal dog eyes (100–102) • Staphylococci most common isolates • Coagulase-positive *S. aureus* isolated in up to 45% of eyes • Small numbers of multiple other bacterial species
Feline	65% of eye cultures were negative (103) *S. aureus* and *S. epidermidis* predominated in eyes with positive growth
Equine	Similar bacterial genera from normal eyes of horses in different geographic regions of the world • Gram-positive aerobic bacterial most common • *Bacillus cereus, Corynebacterium* sp., and *Staphylococcus epidermidis* common Gram-positive isolates • Considerable variation noted in prevalence of individual organisms Comparison of normal microflora from 2 horse populations (104,105) • Gram-positive isolates predominated in both stabled and hospitalized horses • *Corynebacterium, Bacillus, Staphylococcus,* and *Streptomyces* prevalent Gram-positive genera • Gram-negative organisms less common overall, with *Neisseria, Moraxella,* and *Acinetobacter* prevalent Gram-negative genera isolates Mycoplasmas not identified
Bovine	Ocular microflora of eyes of calves brought into commercial units (106) • Nonhemolytic *Moraxella bovis* in 50–60% of calves 1–2 months after grouping • Overall rate of isolation of *M. bovis* was 13% with an upsurge in isolates in late summer • *Brahamella catarrhalis* and *Mycoplasma bovoculi* present in a few calves initially but increased after grouping to 26% and 45%, respectively • Other isolates included *Staphylococcus epidermidis* (65%), *Streptococcus faecalis* (48%), *Bacillus* sp. (45%), *Ureaplasma* sp. (13%), *Acholeplasma laidlawii* (9%), *Mycoplasma bovirhinis* (8%), *Mycoplasma bovis* (2%), *Escherichia coli* (2%)
Ovine	Conjunctival sacs of 100 healthy ewes and 20 lambs cultured (106) • *Branhamella ovis* was the only organism regularly isolated • *Mycoplasma conjunctivae* was isolated from 9 normal ewes
Camelids	Bacterial and mycoplasma cultures of healthy conjunctivae of 3 species of captive camelids (108) • Eleven genera of bacterial isolates • *Staphylococcus epidermidis* and *Pseudomonas* sp. most frequent isolates • Nine varieties of pseudomonads found, representing at least 3 *Pseudomonas* sp. • Many isolates (particularly the pseudomonads) potentially pathogenic • Mycoplasmas not isolated
Birds	Bacteriologic flora from conjunctiva and cornea of healthy psittacine birds (109) • Bacteria isolated from 59% of bird eyes cultured Conjunctival flora of eyes of normal captive exotic birds (110) • 83% yielded bacterial isolates • 70% of isolates Gram-positive • *Mycoplasma* sp. were absent • Stained conjunctival scrapings did not reveal chlamydial inclusions Bacterial genera isolated most frequently (both studies): *Staphylococcus* and *Corynebacterium*

(continued)

Table 6.2 Summary of Findings of Studies of Normal Ocular Flora *(continued)*

	Conjunctival flora of 100 clinically ducklings • 57% of Gram-negative isolates indicated intestinal flora from fecal contamination of water source
Rabbits	Conjunctiva of 54 New Zealand white rabbits with no signs of ocular or upper respiratory infection (111) • 99% yielded isolates • *Bacillus* sp. and *Staphylococcus* sp. predominated • *Pasteurella multocida* and *Bordetella bronchiseptica* infrequently isolated

a wide range of biologic activities. In the human eye, alpha toxin (dermonecrotoxin) has been associated with chronic staphylococcal conjunctivitis.[119]

Staphylococcal isolates commonly recovered from ocular sources are coagulase-positive species, *S. aureus* and *S. intermedius,* and a coagulase-negative species, *S. epidermidis.* Coagulase-negative staphylococci vary in pathogenic potential, but because they may produce some of the same biologically active products (e.g., hemolysins, dermonecrotoxin), they are recognized as being increasingly important opportunistic pathogens. Slime production, which allows adherence to biomaterials (discussed later), and multiple antibiotic resistance have been reported with *S. intermedius.*

Streptococcus Sp. and Related Cocci

Streptococci are ubiquitous, suppurative bacteria that may be found among normal mucosal flora. Enterococci are opportunists and can be found in the intestinal tract of most mammals. Exotoxins produced by cocci include hemolysins, nuclease, protease, and streptokinase. The polysaccharide capsules of some strains are antiphagocytic or function as adhesions. Streptococcal keratitis is relatively common in domestic animals, especially the horse, in which streptococcal endophthalmitis may also occur.[113,120–123] Most pathogenic streptococci produce hemolysins, with the type of hemolysis produced varying with the species. Generally, alphahemolytic streptococci are the most pathogenic for animals. Streptococci may also be grouped serologically by typing of a C-substance, which is a group-specific surface carbohydrate. Streptococci with C-substance are typed and referred to as Lancefield groups. Groups C and D (now *Enterococcus* sp.) are frequently encountered ocular isolates. *S. equi* and *S. zooepidemicus* are in the Lancefield C group.

Corynebacterium Sp. and Rhodococcus Sp.

Corynebacteria sp. and *Rhodococcus* sp. may be found as flora of normal skin and mucosal surfaces. These bacterial organisms grow in the intestine and, following fecal dissemination, propagate in soil. With tissue invasion, these organisms are pyogenic and may cause a variety of suppurative conditions. Virulence factors include production of hemolysin, phospholipase, and cholesterol oxidase. *Corynebacteria* sp. have been recovered from corneal ulcers in domestic animals, usually as mixed infections. In such cases, the specific etiologic role of corynebacterial organisms is not clear. Following periocular trauma, corynebacteria may cause blepharitis, orbital cellulitis, or orbital abscesses, particularly in large animal species.

Bacillus Sp.

Bacillus sp. are a heterogeneous group of large, spore-forming, Gram-positive, rod-shaped organisms that are mostly saprophytic, inhabiting soil, water, and vegetation. They are either aerobic or facultatively anaerobic. *B. anthracis* is the major animal pathogen in the genus, causing anthrax in both animals and humans. *B. piliformis* causes Tyzzer's disease in mice and foals. *B. cereus* may produce both enzymes and toxins and has been associated with severe endophthalmitis following penetrating trauma in humans.[124] *B. subtilis* produces a weak hemolysin and protease, but its pathogenic role in eye disease is not clear. *Bacillus* sp. are isolated from corneal ulcers in animals, but they are not believed to play a major pathogenic role because other, more pathogenic organisms are usually present as a coinfection.

Actinomycetes

Actinomycetes comprise a heterologous group of procaryotes that can form Gram-positive, branching filaments less than 1 μm in diameter. *Actinomycetes* of greatest interest are *Actinomyces* sp., *Nocardia* sp., and *Streptomyces* sp. *Actinomyces* sp., which are commonly present on the mucous membranes of normal animals, and may cause pyogranulomatous disease of the head and periocular structures of cattle. *Nocardia* sp. and *Streptomyces* sp. are soil microorganisms. *Nocardia* sp., though essentially saprophytic, may cause suppurative and pyogranulomatous lesions, particularly in immunosuppressed hosts. The cell walls of *Nocardia* organisms prevent effective phagocytosis. *Streptomyces* are prolific producers of antimicrobial substances and have been commonly isolated from normal equine conjunctiva.[105]

Gram-Negative Bacteria

Pseudomonas Sp.

Pseudomonas sp. are Gram-negative rods widely distributed in nature, including in soil and water, as saprophytic bacteria. These organisms are also found on the skin and mucous membranes of animals and are occasionally isolated as inhabitants

of the normal intestinal tract. *P. aeruginosa* is frequently isolated in cases of severe keratitis and is well known for its ability to cause rapid and progressive destruction of corneal tissues in a variety of vertebrate species.[113,118,125–127] Regardless of the species, abraded corneas are particularly susceptible to the devastating effects of *P. aeruginosa* infection. In companion animals, pseudomonas keratitis is a serious and relatively common disease; it can also be particularly devastating to the large, slow-healing equine cornea.

Pathogenic factors associated with *Pseudomonas* sp. that contribute to invasiveness and tissue destruction include proteases, exotoxins, and hemolysins.[128–130] Pyocyanin, which is a pigment produced by *P. aeruginosa,* may contribute to tissue damage by inhibiting cellular oxygen uptake. On microscopic examination of smears collected from corneal lesions, *Pseudomonas* sp. are morphologically indistinguishable from other Gram-negative bacilli, though the bacteria tend to be slightly larger. Antibiotic susceptibility testing is especially important with *P. aeruginosa* isolates, because multiple-drug resistance associated with R factors is not uncommon.[120] Additional virulence factors of *P. aeruginosa* are discussed later.

Moraxella Sp.

Moraxella sp. were originally discovered as a human ocular pathogen. *M. bovis* is the primary cause of infectious bovine keratoconjunctivitis (IBK, or bovine "pink eye") and is of great economic importance to cattle producers. *Moraxella* sp. have also been reported to cause ocular infections of small ruminants and the horse.[131–133]

The Moraxella organism is a relatively large, plump, Gram-negative coccobacillus. Multiple factors affect the pathogenicity of *M. bovis,* including exposure to ultraviolet light, environmental irritants, concurrent infections, and the genetic, nutritional, and immune status of the host. Nonpiliated, nonpathogenic forms can exist in a carrier state in the host; carrier animals are asymptomatic but shed the organism. *M. bovis* may harbor in nasal, ocular, or vaginal secretions, and it may be transmitted by direct contact, aerosol, and fomites. The face fly, *Musca autumnalis,* is the primary mechanical vector for IBK. Certain stimuli (e.g., ultraviolet light) can cause direct conversion of nonhemolytic, nonpiliated organisms to pathogenic forms in carrier animals; a rapid, logarithmic growth phase of the organism accompanies this transformation. Additional discussion of virulence factors of *M. bovis* is presented later.

Other Glucose-Nonfermenting, Gram-Negative Bacteria

Other Gram-negative organisms commonly isolated from animals include those of the genera *Neisseria, Branhamella,* and *Acinetobacter.*[113,134,135] Mucous membranes of mammals are a natural habitat for *Neisseria* sp. Pathogenic *Neisseria* sp., however, may colonize mucosal surfaces, including the conjunctiva, and in human patients, colonization may extend onto the cornea. *Neisseria* sp. are Gram-negative cocci from 0.6 to 1.0 μm in diameter. They typically grow in pairs with adjacent ends flattened, thus forming a kidney-bean shape. Clusters of organisms are occasionally seen. On scraped specimens, *Neisseria* sp. are often seen on the surface of the epithelial cells or within leukocytes. Surface components of the Neisseria bacterium are thought to play a critical role in its pathogenicity. The presence of pili or capsules gives *Neisseria* sp. enhanced ability to adhere to host cells and renders the organism relatively resistant to phagocytosis. Neisseria organisms produce oxidase and autolytic enzymes. On autolysis, endotoxin is liberated and, in turn, is responsible for hemorrhages on mucous membranes. An immunoglobulin A protease is also found in pathogenic strains. Prevalence of penicillinase-producing organisms is increasing, and these resistant organisms may be virulent for the eye.

Branhamella ovis is a Gram-negative diplococcus similar to *Moraxella* sp. This agent has been cultured from normal eyes of small ruminants and from eyes of sheep and goats with keratoconjunctivitis. *B. ovis* may occur as a coinfection with chlamydial or mycoplasmal conjunctivitis, and it may complicate the ocular disease, thereby causing more serious lesions, such as corneal ulceration.[136] Other causes of bacterial eye infections in domestic ruminants include *Acinetobacter* sp. and *B. catarrhalis. Acinetobacter* sp. have been isolated from cases of equine infectious keratitis, in which it was considered to be a significant pathogen.[113,120].

Enteric Bacteria

Enteric bacteria are a diverse group of Gram-negative bacteria found in the normal intestinal tract as well as in soil, sewage, and as plant pathogens. These organisms are commonly referred to as coliform bacteria, and they include the genera *Escherichia, Citrobacter, Salmonella, Shigella, Klebsiella, Enterobacteria, Serratia, Proteus,* and *Yersinia.* Most of these organisms are opportunistic invaders of the eye and exhibit greatest pathogenicity when host defenses are reduced or there is tissue damage. Organisms from these genera have also been recovered from humans with keratitis, blepharitis, conjunctivitis, dacryocystitis, orbital infections, and endophthalmitis, and from animals with a variety of ocular diseases.[113,117,118,137]

In their outer cell membranes, enteric bacteria produce lipopolysaccharides, which are potent endotoxins and important factors in their pathogenicity. Endotoxins released when the bacteria die and lyse have been associated with production of immune ring infiltrates in Gram-negative corneal infections in humans. *Escherichia coli* and *Serratia* sp. endotoxins and proteases have been shown experimentally to induce inflammatory infiltrates and corneal necrosis.[137]

Haemophilus Sp.

Haemophilus sp. require factors from blood for growth, hence the derivation of its name. *Haemophilus* sp. can be normal flora of the oral cavity and nasopharynx but have also been a primary etiologic agent for acute mucopurulent conjunctivitis

in humans. The organisms have little affinity for the avascular cornea, and corneal involvement as a complication of conjunctivitis is rare. *Haemophilus* sp. favor an intracellular environment and readily parasitize epithelial cells and white blood cells. Virulent strains are usually encapsulated; unencapsulated strains are often more elongated. Natural pathogenicity appears to relate directly to capsule formation, which confers resistance to complement-mediated immunity. Other surface components, such as lipooligosaccharides, are important in bacteremia and hematogenous spread. The organisms produce endotoxin but not exotoxin.

Ocular lesions of TEME, which is caused by *Haemophilus somnus,* are typically found in the posterior uvea.[138] Acute septic TEME most commonly occurs in feedlot cattle and may cause thromboembolic chorioretinitis, resulting in funduscopically visible exudates and hemorrhages. When an infected animal survives the acute septicemia, the foci of chorioretinal exudates may subsequently be noted as areas of necrosis and chorioretinal scarring. Retinal detachments may result from retinal edema and subretinal exudates, and blindness may occur either from ocular lesions or septic thrombosis of brain tissues.

Miscellaneous Ocular Bacterial Pathogens

Several different genera of aerobic bacteria have been isolated from animals with infectious conjunctivitis or keratoconjunctivitis. *Pasteurella multocida* is an important cause of conjunctivitis in the rabbit,[139] in which this eye disease is associated with acute or chronic respiratory disease. Infections with *Pasteurella* sp. in calves may cause conjunctivitis in addition to rhinitis, pharyngitis, and pneumonia.[140] Other bacterial genera associated with eye infections of animals are *Leptospira* sp., *Borrelia* sp., *Brucella* sp., and *Mycobacterium* sp.,[141–144] primarily causing infectious uveitis. *Listeria monocytogenes* causes encephalitis in cattle and may also cause ocular signs, including facial paralysis and ptosis, that are most often unilateral (on the side of the central lesion).[140] *L. monocytogenes* has also caused ophthalmitis in sheep[145] and has been reported to cause keratitis in one horse.[146]

Nonspore-forming obligate anaerobes constitute a large group of Gram-positive and Gram-negative bacteria that exist not only in the environment but also as commensals on the mucous membranes of animals and humans, particularly in the intestinal tract as part of the normal flora. They are nutritionally demanding and require strict anaerobic conditions for isolation. They are most commonly implicated in necrotic and suppurative deep-tissue infections, often as mixed infections with facultative anaerobic bacteria. In veterinary ophthalmology, *Peptostreptococcus* sp., *Bacteroides* sp., and *Fusobacterium* sp. have been isolated from cases of orbital cellulitis or orbital abscess in animals.[147] *Clostridium* sp. can cause or contribute significantly to deep soft-tissue infections. Occasionally, clostridial organisms have been isolated from infected animal corneas, usually as a component of mixed infections. The role of clostridial organisms in ocular surface disease is presently unclear.

Mycoplasma Sp. and Chlamydophila Sp.

Mycoplasma Sp.

As the smallest prokaryotic cells capable of self-replication, the mycoplasmas (mollicutes) are ubiquitous, free-living saprophytes and animal pathogens. The collective term *pleuropneumonialike organisms* has been used as another designation for mycoplasmas. Both pathogens and nonpathogens are found on the mucous membranes. Outside the host, pathogenic species may survive for a few days in microenvironments protected from sunlight. Mycoplasmas lack a true cell wall; instead, they are enclosed in a plasma membrane composed of protein, glycoprotein, glycolipid, and phospholipid. This accounts for their plasticity and pleomorphism, including cocci, spiral, filament, and ringlike structures. Mycoplasmas have Gram-negative plasma membranes, but they stain poorly with Gram-stain. Giemsa and other Romanowsky stains produce better results. Fragility, pleomorphism, and weak staining make direct examination of stained smears of limited value in making the diagnosis.

Pathogenic mycoplasmas adhere to host mucous membranes, where they remain extracellular, producing hemolysins, proteases, nucleases, and other toxic factors. Latency can occur, and various stresses may predispose an animal to mycoplasmal infections, which may be low-grade and chronic. Mycoplasmas tend to be relatively host-specific. Domestic species affected with mycoplasmal eye disease include the cat and ruminants. Mycoplasmal eye infections are characterized by serous discharge and conjunctival hyperemia. Numerous *Mycoplasma* sp., including *M. felis, M. gatea, M. arginini,* and *Acholeplasma laidlawii* have been recovered from the eyes of cats.[148] It remains controversial, however, to what extent mycoplasmas are pathogenic to cats. Results of numerous studies confirm that mycoplasmal organisms can be recovered from the conjunctival sac of clinically normal cats.[148–150] Furthermore, attempts to induce disease by inoculating cats with different mycoplasmal strains have failed to produce disease. Conversely, inoculating 6- to 10-week-old kittens with the *M. felis* strain has been reported to cause clinical signs.[151] That *M. felis* is a conjunctival pathogen is supported by observations that this organism is recovered at a higher frequency from ill versus clinically normal cats.[137] A review of feline studies leads to the conclusion that *M. gatea* is part of the normal flora of domestic cats but that *M. felis* can, under certain conditions, induce conjunctival inflammation. On the basis of available data, it is difficult to attribute a major role to any *Mycoplasma* sp. in the pathogenesis of naturally occurring feline conjunctivitis.

In sheep, *M. conjunctivae* and *M. agalactiae* are important causes of conjunctivitis.[107,152–154] In goats, *M. agalactiae* causes systemic disease affecting the eyes, joints, mammary glands, or gravid uteri. Also in goats, *M. mycoides* subsp.

mycoides causes septicemia, mastitis, arthritis, uveitis, and keratoconjunctivitis, including perilimbal corneal opacities.[155] Eye lesions may occur in goats without systemic signs. *M. bovoculi* and *Ureaplasma* sp. have been isolated from the eyes of cattle affected with contagious conjunctivitis.[155] *M. bovis, M. laidlawii,* and *M. bovirhinis* have also been associated with bovine conjunctivitis, but they have been less commonly reported. Keratitis is uncommonly associated with pure mycoplasmal infections; however, *M. bovoculi* will enhance the pathogenicity of *M. bovis* to the point that the combined infection results in extensive corneal lesions.[156] Bovine mycoplasmal conjunctivitis tends to occur seasonally (in the summer months) and is usually mild and self-limiting.

Chlamydophila Sp.

Members of the genus *Chlamydophila* are obligate intracellular organisms that possess a cell wall similar to those of other Gram-negative bacteria. They have a unique developmental cycle, with two morphologically distinct forms: infectious (i.e., elementary bodies) and reproductive (i.e., reticulate bodies). Elementary bodies are small (200–300 nm), extracellular forms of the organism that enter the cell by endocytosis. After cell entry, they differentiate into larger, noninfectious but metabolically active, reticulate bodies. The reticulate bodies multiply through binary fission and, at approximately 20 hours following infection, begin to mature within the membrane-bound inclusion to form new elementary bodies. Release of infectious elementary bodies generally begins at approximately 40 hours after infection and results in cell lysis.

Chlamydophila sp. were previously identified as *Chlamydia* sp.[157] Currently identified members of the *Chlamydophila* genus include the following: *Chlamydophila psittaci, Chlamydophila felis, Chlamydophila abortus, Chlamydophila caviae, Chlamydophila pecorum, Chlamydophila pneumoniae,* and *Chlamydophila trachomatous. C. pscittaci, C. felis, C. abortus,* and *C. caviae* were all previously grouped as *Chlamydia psittaci,* an organism that gained widespread recognition as a pathogen causing a variety of zoonotic diseases in vertebrates and invertebrates. *C. felis* is a highly contagious disease of cats and spreads rapidly by direct contact. It is most commonly found in multiple cat households, catteries, or shelters.[158,159] Major systemic clinical signs are typically limited to the respiratory tract and the eyes. The primary ocular manifestation is conjunctivitis. Organisms are shed in tears and nasal secretions and may persist in the ocular tissues for several months following remission of ocular signs. Initial chemosis followed by suppurative conjunctivitis is typical of feline chlamydial ocular infections. Petechial hemorrhages may occur, and conjunctival lymphoid follicles may develop with chronicity.

Experimental infection with *C. pscittaci* (*C. felis*) was characterized by the onset of unilateral conjunctivitis within 5 to 10 days of exposure. Blepharospasm, chemosis, and vascular congestion were the initial clinical signs. Serous ocular discharge became mucoid or mucopurulent within 3 to 5 days. All cats subsequently became bilaterally affected, and the clinical signs persisted for 22 to 25 days. Histologically, chlamydial conjunctivitis is initially characterized by a neutrophilic infiltrate (day 7), with macrophages, lymphocytes, and plasma cells becoming progressively more numerous between days 10 and 21.[159,160]

The exact prevalence of chlamydophila infection in the cat is not known. In one report,[161] cats on 45% of sheep farms in Great Britain had serologic evidence of exposure, and in several studies,[161,162] the organism was recovered from the eyes of approximately 30% of cats with conjunctivitis. In other studies,[163,164] the seroprevalence of *Chlamydophila* sp. in the cat has been reported to be from 5.0% to 12.7%. Recovery from chlamydophila infection can result in persistent infections. Experimental ocular exposure has resulted in conjunctival shedding for up to 8 months[165]; chronic shedding of organisms from the urogenital and gastrointestinal tracts has also been documented. The site of persistence has not been unequivocally determined, but chlamydial organisms have been identified in the gastric mucosa of the cat.[166]

In sheep, *C. psittaci* was previously associated with conjunctivitis, keratitis, polyarthritis, pneumonia, orchitis, epididymitis, and abortion.[167] Certainly, the diseases in many of the reports may have been caused by what is now known as *C. abortus.*[168,169] Persistent, inapparent infection with intermittent shedding is common among ovine chlamydial diseases. The elementary bodies are relatively resistant and may remain viable for several days. Conjunctivitis and keratoconjunctivitis associated with *Chlamydophila* sp. in swine have also been reported.[170]

In general, *Chlamydia* sp. are considered to have a restricted host range; however, there are several documented cases involving transmission of *C. felis* from cats to humans.[171–173] In addition, apparent transmission of *Chlamydia* sp. from a macaw to a cat has been reported.[174] Psittacosis transmitted from birds to humans is a well-recognized zoonosis.[175]

Pathogenic Mechanisms of Bacterial Disease

Adhesion Phenomena and Virulence Factors

The "infectivity" of a microorganism is greatly influenced by its ability to initiate the infectious process. Bacterial adhesion to epithelial cells is recognized as a critical initial stage in the colonization of mucosal surfaces and in the pathogenesis of ocular infections.[176] Adhesins (i.e., protein determinants of adherence) have been identified for most bacterial pathogens and been shown to function in vivo.[177,178] Some adhesins are expressed in bacterial pili.[179]

Host cell receptors that form linkages with bacterial adhesins have been identified as carbohydrates or carbohydrate moieties of cell membrane glycoproteins.[180] Sialic acid is reported to be a receptor molecule for bacterial adhesin.[181] Basal and migrating corneal epithelial cells have different cell membrane sugars than superficial cells,[182] thus accounting for the differences in susceptibility of adherence by organisms to these cells. Cell adhesion phenomena have been studied

extensively for two bacterial genera, *Pseudomonas*[130,179,183] and *Moraxella,* each of which has considerable significance in veterinary ophthalmology.

The capacity of an organism to cause tissue inflammation and destruction depends on production of one or more virulence factors. Virulence factors include proteases, elastases, hemolysins, and cytotoxins. Among the bacteria of interest in veterinary ophthalmology, *P. aeruginosa* and *M. bovis* are, again, the organisms most extensively studied for virulence traits. Adhesive phenomena and virulence factors of these two bacterial species are reviewed here.

Pathogenic Mechanisms of Pseudomonas aeruginosa

Pseudomonas aeruginosa is generally recognized as the most virulent corneal pathogen. It adheres more readily to corneal epithelial cells than do most other bacterial species.[184] Corneal destruction by *Pseudomonas* sp. is attributed to a variety of enzymes, endotoxins, and exotoxins; however, adherence of the organism to the epithelial surface is the necessary first step in pathogenesis of pseudomonas keratitis. Pseudomonas organisms adhere poorly to intact epithelium or bare stroma, but they adhere readily to injured epithelium at the edge of an epithelial defect. Therefore, trauma is a necessary prerequisite for bacterial adherence and subsequent corneal infection.

As mentioned, *Pseudomonas* sp. adhere poorly to bare corneal stroma. Pseudomonas organisms reach the corneal stroma by a process of adherence to epithelium, penetration of the epithelial cell, and transcellular migration. The interaction between *P. aeruginosa* and corneal epithelium was studied in a rabbit model during the first hour after inoculation with both scanning- and transmission-electron microscopy.[129] The initiating events in Pseudomonas corneal ulceration in the rabbit model involved adherence of organisms to damaged or exposed basal epithelial cells by an interaction between bacterial and cellular membranes, which required 15 to 30 minutes to occur. After 30 minutes, the organisms were engulfed by the epithelial cell and reached the corneal stroma through transcellular migration.

Several human corneal epithelial glycosylated proteins studied in vitro provide receptor sites for *P. aeruginosa* pili binding; the binding of pili to these proteins is specific, competitive, and saturable.[179] Several single proteins have been confirmed, and all are characterized as glycoproteins, with the sugar mannose being identified as an important component of the human corneal receptors for *P. aeruginosa.* It is possible that adherent bacteria might secrete proteases to create openings in cells, thus exposing intracellular proteins (i.e., cytokeratins) that enhance pathogenesis by further bacterial adherence and colonization of the host tissue.[179]

P. aeruginosa produces several proteases and toxins that damage tissue and interfere with host defense systems.[130] Proteases are required for virulence because of their contribution to establishing infection and affecting the course of corneal healing, primarily through degradation of the basement membranes and extracellular matrix. Exotoxin A, which is lethal to corneal cells, is also required along with a protease to establish infection. Exoenzyme S, which is another secreted toxin, appears to contribute to tissue damage and dissemination of the organism. Exoproducts contribute directly to keratitis through toxic effects on corneal cells and degradation of corneal proteins and indirectly through activation of corneal proteases.[130]

P. aeruginosa produces at least two major matrix metalloproteinases, which are designated elastase and alkaline protease.[185,186] Both have been reported to attack the helical structure of native type I collagen very slowly, whereas elastase has also been reported to degrade native type III and type IV collagen more rapidly, generating specific fragments.[187] Both have been reported to degrade rabbit corneal proteoglycans both in vitro and in vivo.[188–190] These enzymes play a role in the ulcerative process of Pseudomonas keratitis in rabbit models as well.[188,191]

Pathogenic Mechanisms of Moraxella bovis

The importance of pili adhesions has been recognized in the pathogenesis of *Moraxella bovis.*[192–194] Experimental inoculation of piliate *M. bovis* organisms into the eyes of calves caused persistent infection and clinical disease, whereas inoculation of nonpiliate *M. bovis* did not.[192] In studies of the interaction between *M. bovis* and bovine corneal epithelium, piliated bacteria attaching to undamaged superficial cells tended to adhere to dark cells.[193] Dark cells have been characterized as older, hypermature epithelial cells with smaller, more densely packed microvilli.[195] The pili elaborated by *M. bovis* are filamentous homopolymers of pili protein subunits.[194] Two distinct types of pili, designated I and Q, have been identified and purified from *M. bovis,* and the Q-pili have been cloned.[194,196] In vivo pilin gene rearrangement and pilin-type switching have been evaluated by DNA hybridization and immunoblot assay. Q-pili are specific for colonization of bovine corneal epithelium, whereas I-pili enable maintenance of an established infection.[197]

The presence of pili alone is insufficient to cause disease following infection with *M. bovis.*[198] The betahemolysin of *M. bovis* is also required. Evidence suggests the hemolysin is an enzyme that correlates with cytotoxicity for bovine leukocytes and corneal epithelial cells in vitro.[199] The hemolysin of *M. bovis* is a transmembrane, pore-forming, calcium-dependent, heat-labile protein that is produced in culture during logarithmic phase growth.[200] A stable cytolysin, which is released as an exotoxin from *M. bovis* during early logarithmic phase growth, has been recently demonstrated as well.[201]

A positive in vivo correlation between levels of hemolytic and cytotoxic activity with the progressive stages of calf-corneal epithelial cell damage has been demonstrated, but the investigators were unable to purify the hemolysin as a single protein.[202] Previous evidence suggests the hemolytic activity is associated with outer membrane–bound vesicles released by *M. bovis* during the logarithmic growth phase.[199] A cytolysin of *M. bovis* has been partially characterized.[201] The results reported by Beard and Moore[202] support the possibility

that hemolytic and cytolytic activities are attributable to the same effector molecule; their findings substantiate the importance of hemolysin in the pathogenesis of *M. bovis*–induced disease, possibly causing clinical signs either directly as a result of damage to ocular cells or indirectly through lysis of leukocytes attracted to the affected site. This latter effect would result in delayed corneal healing and might contribute to corneal damage through release of endogenous enzymes, which could then act on corneal substrates.[203] A cell detachment factor produced by *M. bovis* has also been identified and characterized.[204]

Diagnostic Bacteriology

The laboratory bacteriologic workup includes preparing and examining microscopic Gram-, Giemsa-, or Wright-stained slides and inoculating culture media for isolation and subsequent organism identification. Results of cultures are more sensitive than cytology results, but examination of stained slides may give immediate information about the causative organism, thus allowing prompt, focused therapy. Because polymicrobial eye infections are common among animals, culture, speciation, and susceptibility testing may be essential to the successful management of ocular infections.

Specimen Collection

Techniques of collecting specimens for cytology and culture rely on scrapings, swabs, or aspirates of affected tissue. Scrapings using a Kimura spatula, Beaver blade, or Bard-Parker blade are best for cytology, and these scrapings may also be used for direct cultures. Calcium alginate swabs moistened with trypticase soy broth will yield higher retrieval rates than scrapings from infected corneas. Dacron/rayon swabs soaked in thioglycolate broth are equally effective. Cotton is less desirable, however, because of the absorption of sample material by the cotton fibers. Scrapings are generally effective in retrieving filamentous organisms.

Procedures followed in processing diagnostic bacteriologic specimens depend largely on the disease and the organisms suspected. Therefore, an appropriate patient history, with suggestion by the clinician as to the most likely diseases, is quite important. Steps generally followed in the examination of specimens for bacterial analysis, including direct microscopic examination of the specimen, are outlined in Figure 6.2.

Direct Examination

In ophthalmic cases, materials submitted for examination include swabs, scrapings, or aspirates.[205–209] Examination of

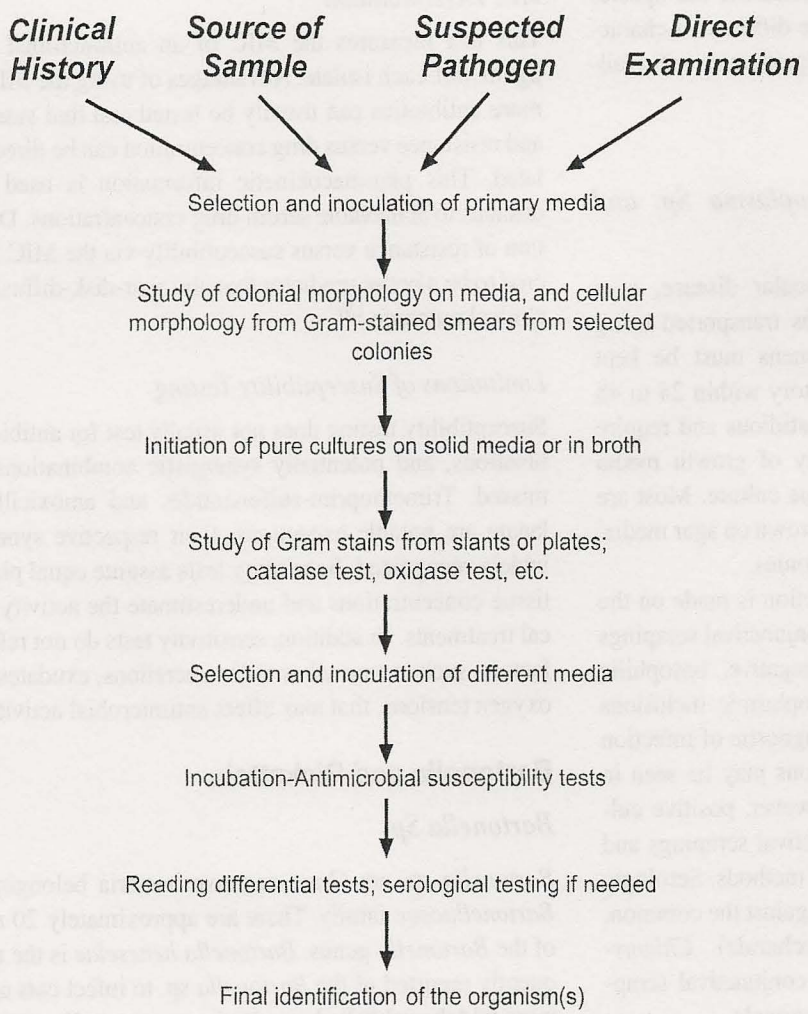

Figure 6.2. Examination of specimens for bacterial analysis. (Modified with permission from Carter GR, Wise DJ. Outline of procedures for the bacteriologic and mycologic examination of clinical specimens. In: Carter GR, Chengappa MM, Roberts AW, eds. *Essentials of Veterinary Microbiology.* 6th ed. Ames: Iowa State Press, 2004:95.)

submitted materials following staining of smears or wet-mount preparations should be routinely performed as an initial screen for pathogenic agents. Specific examination procedures (e.g., differential stains) will vary with the disease and the suspected causative agents. Findings from direct examination may aid in the selection of appropriate culture media. Fluorescent antibody procedures, when available, may also be performed on smears of fluids, tissues, or exudates.

Isolation and Identification Procedures

Figure 6.2 reflects a routine approach in processing specimens for bacterial identification. Information from responses to those items listed at the top of the flow chart essentially determine which primary media will be selected. In some cases, a strong presumptive diagnosis can be made on the basis of a direct examination. For example, if Gram-negative bacteria are found, the results of triple sugar-iron-agar slants (i.e., step 3) may be particularly useful. A fluorescent antibody procedure may also be used to identify some organisms from clinical materials.

Patient history, species, tissue involved, Gram-stain reaction, and microscopic morphology may suggest the most probable genus or family of the organism in question. With this knowledge, certain differential tests can be performed to confirm the genera and eventually to establish the species identification. Flow charts addressing the differential characteristics of organisms with veterinary significance are available (see Fig. 6.2).[210]

Diagnosis of Infections with Mycoplasma Sp. and Chlamydophila Sp.

In suspected cases of mycoplasmal ocular disease, eyes should be cultured and moistened swabs transported using sterile modified Hayflick broth. Specimens must be kept refrigerated and be delivered to a laboratory within 24 to 48 hours of collection. Mycoplasmas are fastidious and require specific growth factors, with the quality of growth media needing to be equal to that used for tissue culture. Most are anaerobic or microaerophiles and, when grown on agar media, typically form fried egg–shaped microcolonies.

The diagnosis of *Chlamydophila* infection is made on the basis of cytologic evaluation of stained conjunctival scrapings from acutely infected animals. Gram-negative, basophilic (i.e., Wright or Giemsa stains), intracytoplasmic inclusions within conjunctival epithelial cells are diagnostic of infection with *Chlamydophila* sp. Because inclusions may be seen in fewer than 50% of affected animals, however, positive cultures or immunologic staining of conjunctival scrapings and serologic testing are additional diagnostic methods. Serologic tests primarily detect antibodies directed against the common, genus-specific antigen (i.e., lipopolysaccharide). *Chlamydophila* organisms can be cultured from conjunctival scrapings as well as from the blood of affected animals.

Molecular Biologic Techniques to Diagnose Chlamydophila Disease

Because many of the genes in *Chlamydiphila* sp. are highly conserved,[211] it is possible to detect many species with one set of primers. The detection of *Chlamydophila* sp., formerly known as *Chlamydia psittaci,* by targeting sequences of the ompA (i.e., outer membrane protein) gene has been described.[212,213]

Susceptibility Testing

Agar-Disk-Diffusion Test (Kirby-Bauer Test)

On the basis of human pathogens and human standards, the agar-disk-diffusion test measures the inhibition of bacterial growth against a concentration of antimicrobial agent that diffuses from an impregnated paper disk placed on agar.[214] Zone size can be directly correlated with minimal inhibitory concentration (MIC); in other words, the larger the zone size, the lower the MIC. Limitations of this test include inoculation variables and interpretation of zone sizes. Inoculation variables include depth of agar, incubation time, and preparation (i.e., contents) of the agar. Because antibiotics diffuse at different rates throughout the agar, published standards must be used to interpret the sensitivities.

MIC Determination

This test measures the MIC of an antimicrobial agent (in μg/mL)for each isolate. Advantages of using the MIC are that more antibiotics can usually be tested and that susceptibility and resistance versus drug concentration can be directly correlated. This pharmacokinetic information is used to relate dosages to achievable serum drug concentrations. Determination of resistance versus susceptibility via the MIC is considered to be a better predictor than the agar-disk-diffusion test of clinical outcome.[120]

Limitations of Susceptibility Testing

Susceptibility testing does not usually test for antibiotic combinations, and potentially synergistic combinations may be missed. Trimethoprim-sulfonamides and amoxicillin-clavulanate are notable exceptions; their respective synergies are widely recognized. Sensitivity tests assume equal plasma and tissue concentrations and underestimate the activity for topical treatments. In addition, sensitivity tests do not reflect local factors, such as normal or reflex secretions, exudates, or local oxygen tensions, that may affect antimicrobial activity.

Bartonella and Rickettsia

Bartonella Sp.

Bartonella sp. are Gram-negative bacteria belonging to the *Bartonellaceae* family. There are approximately 20 members of the *Bartonella* genus. *Bartonella heneselae* is the most frequently reported of the *Bartonella* sp. to infect cats and is the most widely published species in veterinary literature. Other

Bartonella sp. reported to infect cats with less frequency include *B. clarridgeiae, B. koehlerae,* and *B. quintana.*[215–218]

Pathogenic Mechanisms

Bartonella sp. are transmitted by arthropods, and the primary vector for *Bartonella henselae* in cats is the cat flea (*Ctenocephalides felis*).[219,220] Though cats can be experimentally inoculated with *Bartonella henselae,* transmission among cats does not occur in an environment free of fleas.[221,222] *Bartonella* sp. are intracellular bacteria. Infection is suspected to be primarily of red blood cells, but infection of vascular endothelium is also reported.[223]

Naturally occurring *B. henselae* infection is mild and transient, and clinical findings may include pyrexia, lymphadenopathy, lethargy, and anorexia. Mild neurologic signs including nystagmus and tremors, and focal motor seizures are less frequent.[222,224–228] Though clinical signs are usually mild and often self-limiting, cats experimentally infected have been shown to develop nephritis, myocarditis, and hepatitis.[222,225] Additionally, a case of fatal myocarditis associated with natural *B. henselae* infection has been reported.[229]

Ocular

The primary ocular clinical sign reported to be associated with *Bartonella hensela* infection is uveitis.[230] Intraocular specific IgG production with C value greater than 1 was documented in 7 of 49 cats with naturally occurring uveitis and in 4 of 9 cats experimentally infected with *B. henselae,* whereas 0 of 49 apparently healthy cats had local specific IgG production.[231] It should be noted, however, that C values higher than 8 would be considered a more rigid criteria for the determination of local antibody production. The same study documented the presence of *Bartonella* DNA in aqueous humor in 3 of 24 cats with uveitis, 4 of 9 experimentally infected cats, and 1 of 49 apparently healthy cats. Recently, a dog with anterior uveitis and lesions of the tapetal fundus concurrent with fever was (1:512) to *Bartonella vinsonii.* Attempts to identify the bacterium from aqueous humor using PCR were unsuccessful. The patient did, however, improve with azithromycin.[232]

Diagnostic tests available for bartonellosis include serology, blood culture, and PCR. Antibody titers of greater than 1:256 may correlate well with blood cultures, but reports of low predictive value of these tests make them less desirable. Blood culture is considered to be the most accurate means of assessing and identifying infected patients and is most widely used. Samples should be collected into EDTA and frozen for immediate transport to the laboratory. PCR has been described for *Bartonella henselae* and offers more rapid turnaround time than blood culture.[233]

Rickettsia Sp.

Rickettsia sp. consist of minute, obligate intracellular bacteria that are transmitted by ticks. They are rod-shaped or coccobacilli, and they vary from 0.3 to 0.6 μm in length. *Rickettsiae* contain both RNA and DNA, and they replicate through binary fission, primarily within the vascular endothelium or perivascular cells. They are nonmotile and aerobic. Of the many species of *Rickettsia* identified in animals, ocular disease has most commonly been associated with infections by *R. rickettsii* and *Ehrlichia canis.*[234,235,235] *Anaplasma platys* (formerly *Ehrlichia platys*) has been reported as a cause of canine uveitis as well.[236]

R. rickettsii causes an acute, febrile illness in dogs and humans, which is referred to as Rocky Mountain spotted fever (RMSF). Tick vectors, *Dermacentor variabilis* and *D. andersoni,* may become infected horizontally during feeding on infected mammals or following transstadial replication within the tick midgut and transovarial transmission between generations of ticks. After several hours of attachment to the host, the tick vector may infect the new host into which the organisms invade and replicate within the vascular endothelia of the small blood vessels.

Infection with *R. rickettsii* produces a multifocal vasculitis, thereby setting into motion a complex cascade of pathophysiologic events, including platelet activation, complement- and coagulation-system activation, chemotaxis, and vascular necrosis with extravasation of serum and blood. Perivasculitis subsequently develops, with infiltration of granulocytic and mononuclear inflammatory cells. RMSF may cause fever, skin and mucosal hemorrhages, and in some cases, neurologic signs. Multiple organ failure may result in acute death among severe cases. The pathogenesis of the ocular disease in RMSF relates directly to the vascular lesions. Altered vascular permeability in the conjunctiva, uvea, and retina result in conjunctival hemorrhages, signs of uveitis (i.e., corneal edema, iris stromal hemorrhage, miosis, aqueous flare, hyphema), and retinal hemorrhages. Unilateral or bilateral optic neuritis also occurs.

E. canis causes canine monocytic ehrlichiosis, which results in a spectrum of acute, subclinical, and chronic disease. Currently, three strains of the organism are recognized. The tick vector is *Rhipicephalus sanguineus,* which can transmit the disease more than 5 months after detaching from the canine host. This allows ticks to overwinter and infect hosts the following spring. The organism replicates in mononuclear inflammatory cells, which allow its spread throughout the body. Circulating leukocytes are also targeted. As perivascular tissues become infected with the *E. canis* organism, severe vasculitis may occur, resulting in bleeding and platelet consumption. Clusters of intracytoplasmic organisms (i.e., morulae) may be seen microscopically in blood monocytes.

Following an incubation period of between 8 and 20 days, *E. canis* may cause acute, subclinical, or chronic disease. During the acute phase, the parasite enters the bloodstream and lymphatics, and it localizes in the mononuclear phagocytic cells of the spleen, liver, and lymph nodes, where replication occurs. Then, infected mononuclear cells disseminate the *Rickettsia* organisms throughout other organ systems, where they induce vascular changes. Ocular disease is associated with acute vasculitis, perivasculitis, and thrombocytopenia, and it includes conjunctival hyperemia, corneal edema and

deep vascularization, aqueous flare, iridal congestion, miosis, and fibrinous debris on the anterior lens capsule. Hyphema, chorioretinitis, vitreal and retinal hemorrhages, and in some cases, optic neuritis have also been noted. As the disease becomes chronic, retinal vascular engorgement and compromise of the blood–retinal barrier may result from hyperproteinemia and hyperviscosity syndrome.

The diagnosis of canine ehrlichiosis is made on the basis of both clinical and hematologic findings: the presence of morulae in stained blood smears, bone marrow cytology (i.e., hypoplastic bone marrow with plasmacytosis and mastocytosis), and serology using an IFA test. An ELISA procedure has been developed that is both sensitive and specific for detecting antibodies. Immunoblot and PCR techniques are recently developed diagnostic procedures as well. *E. canis* can also be cultured on a monocyte–macrophage (DH82) continuous cell line.

Anaplasma platys is a small rickettsial parasite that causes infectious cyclic thrombocytopenia in dogs. The organism infects platelets rather than leukocytes and is a serologically distinct ehrlichiae. *E. platys* enter platelets by endocytosis following adherence and forming intracellular morulae. *A. platys* incubates for 8 to 15 days, with the highest percentage of infected platelets occurring during the initial parasitemic episode. During this phase, a precipitous decrease in platelet count occurs, and the organism is no longer seen. Repetitive cycles of parasitemia and subsequent thrombocytopenia may recur initially at 1- to 2-week intervals and then diminish in severity and frequency over time. *A. platys* may be diagnosed on the basis of the characteristic blue inclusions in platelets on blood smears stained with Giemsa or new methylene blue; unfortunately, the value of this method may be limited by the presence of very low numbers of parasites. An IFA test to detect serum antibodies to *A. platys* has been developed as well.

Confirmation of RMSF involves serologic testing, direct immunofluorescence staining of skin biopsies, or isolation of the organism. Serologic tests that can measure both immunoglobulin M and immunoglobulin G are the micro-IFA test and the ELISA. Both acute and convalescent titers are needed for a definitive diagnosis to be made, with a fourfold increase in titer considered to be diagnostic. Serologic diagnosis may be confounded by subclinical infection and a high seroprevalence rate in certain endemic areas, as well as by cross-reactions from nonpathogenic rickettsial strains. False-negative serologic tests may also occur.

OCULAR MYCOLOGY

Life Cycle and Taxonomic Classification

Fungi are eukaryotic organisms that grow as either single-cell yeasts or multicellular, filamentous molds. Yeasts are unicellular, elliptical to spherical, generally 3 to 5 μm in diameter, and reproduce by budding. Molds are characterized by branching tubular filaments (or hyphae) and are generally 2 to 10 μm in diameter. The terms *yeast* and *mold* are useful designations for fungi; however, these terms are not mutually exclusive. Depending on the environment, some species of fungi may grow as either yeast or mold forms, and these species are described as dimorphic. Interestingly, some fungi exhibit multiple forms simultaneously, including budding, pseudohyphae, and hyphae; therefore, these species are described as polymorphic. Environmental temperature, nutrient factors, and genetic factors determine the type of growth observed.

The reproductive cycle of fungi may be sexual, asexual, or both. The sexual form of a fungal organism is referred to as a telemorph; the asexual form is referred to as an anamorph. The entire fungal replication process, consisting of all known reproductive forms, is referred to as a holomorph. In sexual reproduction, propagules arise through a process of plasmogamy, which is followed by karyogamy of compatible nuclei and subsequent meiosis. The point at which meiosis occurs varies among species. In contrast to meiotic reproduction, asexual reproduction is characterized by propagules formed directly from existing nuclei through mitosis. Via asexual reproduction, molds produce aerial fruiting hyphae that bear spores, the dispersion of which is chiefly through air currents, water, and animals.

The optimum temperature for growth of fungi is 20° to 30°C, but pathogenic fungi causing systemic mycoses can tolerate 37°C. Fungal growth is by simple mitosis of somatic nuclei and budding or apical extension of the cell wall. Elongation of buds with persistent attachment of cells in some yeasts produces filamentous forms known as pseudohyphae. In filamentous fungi, as hyphae grow by apical extension, they may intertwine to form a mycelial network or colony. Hyphae are often divided at regular intervals by cross-partitions called septa, which have one or more small pores that allow for cytoplasmic communication. Chitin is a primary component of the cellular structure of many fungi. Chitin is composed of N-acetylglucosamine residues linked by glycosidic bonds similar to those found in cellulose. Fungal cell wall structures, which contain ergosterol, other lipids, and glycoproteins, serve as unique targets for antifungal drugs.

Fungi were previously classified as plants, but they lack chlorophyll. Therefore, fungi have been placed in their own kingdom. Fungi are nonmotile and most are strictly aerobic. Because fungi are nonphotosynthetic, they must obtain nutrition by secreting enzymes and absorbing the digested substrate. Medically important fungi have been separated into four traditional classes: *Basidiomycetes* sp., *Ascomycetes* sp., *Zygomycetes* sp., and *Deuteromycetes* sp. (or *Fungi Imperfecti*). The first three categories have characteristic sexual reproductive structures, whereas the imperfect fungi are so named because a sexual stage has not been found, and thus these fungi must be more artificially classified by features of their asexual reproductive structures.

Host Response and Pathogenic Mechanisms

Fungi are commonly recovered from the eyelids and conjunctiva of normal animals, and they are believed to reflect random

environmental exposure. Fungi appear not to be permanent floral residents of the ocular surface but only transient colonizers of the external eye. Filamentous fungi are the predominate fungal isolates reported from the eyes of normal animals. In equine studies, fungi most frequently isolated from normal eyes include the genera *Aspergillus, Alternaria, Penicillium, Fusarium, Cladosporium,* and *Absidia.*[104,105,237] Some minor differences have been noted between results of ocular culture studies done on horses in different geographic locations, but fungal isolates from normal eyes in the different regions have been strikingly similar.

Local defenses to fungi are generally quite effective, because ocular infection is not common unless anatomic barriers are compromised. An intact corneal epithelium provides excellent resistance to fungal penetration and infection. Normal ocular surface flora, normal lacrimal flow, and mechanical movements of the eyelids (and third eyelids) create an environment unfavorable to the growth of many opportunistic fungi. In addition, because many fungi will not grow at elevated temperatures, normal body temperature is high enough to prevent some from becoming pathogenic. The lower temperature of the cornea relative to the rest of the body and the eye, however, may partially explain the predilection for keratomycosis as the most common ocular infection with fungi. The role of local antibodies and complement in protection against ocular fungal infection is unclear.

A breach of the intact corneal epithelial barrier is usually a prerequisite for keratomycosis, and penetrating injuries may result in direct inoculation of fungi into the cornea. After trauma, colonization of an ocular wound by fungi may occur, particularly when corticosteroids have been administered, whether alone or in combination with antibacterial agents. The clinical observation that topical corticosteroids enhance the risk of fungal ocular infections suggests that local immune factors may be important in protecting the eye from fungal invasion. Local immunosuppression by corticosteroids possibly results primarily from effects on cellular immune mechanisms, because immunity to fungal infections is considered to be more cell-mediated than antibody-mediated. Systemic or topical antibacterial agents alter normal flora and can decrease natural microbial barriers as well as encourage colonization and growth of fungi.

The clinical appearance of keratomycosis ranges from ulceration to corneal abscessation. The host responds to keratomycosis by recruitment of a cellular immune response in the cornea. Corneal abscesses are usually populated by mixed inflammatory cells, with a large percentage of neutrophils. Healing of the affected avascular cornea is usually assisted by the ingrowth of blood vessels from the limbus. This vascularization response often appears to be slowed or delayed as it reaches the infected area. One in vitro study using fungal isolates from keratomycosis demonstrated that filtered supernatant of the culture media was capable of minimizing differentiation of human umbilical vein endothelium in cell culture.[238] These findings support the possibility that certain fungal isolates can prevent or slow vascular ingrowth into the cornea as means of self-protection.

Many fungal species have been identified in animal ocular disease. Among domestic animals, fungal keratitis occurs most frequently in the horse. Keratomycosis has also been reported in the dog and cat.[239–242] Fungal infections of the equine cornea are usually attributed to environmentally common organisms (i.e., *Aspergillus* sp., *Penicillium* sp., *Fusarium* sp.), which correlates with results of epidemiologic studies showing these fungi are also frequently isolated from normal eyes.[105,113,116,120,123,243–246] Recently, four cases of equine fungal keratitis were reported in which the organism was identified as *Cylindrocarpon destructans;* this organism has been previously unreported in either diseased or normal equine eyes.[247] Topical antibiotic-corticosteroid therapy generally may increase fungal colonization of the eyelids and conjunctiva and therefore may be a significant predisposing factor for oculomycosis.

Growth characteristics of fungi may result in only superficial infection or, when altered by the local tissue environment, in the invasion of deep tissues. Descemet's membrane provides a significant barrier to fungal penetration in corneal infection, but intraocular extension of keratomycosis is possible. Several pathogenic genera, including *Candida* and *Aspergillus,* are capable of causing both superficial and deep ocular disease.

The second avenue for fungal invasion of the eye is endogenous (i.e., via the bloodstream). In humans, intraocular infections (i.e., oculomycoses) generally occur during systemic immune depression. In animals, by contrast, systemic mycoses often occur in otherwise healthy patients living in endemic areas. In animals, intraocular fungal disease most often results from systemic mycoses contracted through respiratory tract exposure. Primary causes of oculomycoses are the dimorphic fungi *Histoplasma, Blastomyces,* and *Coccidioides,* as well as the yeast *Cryptococcus,* which may cause uveitis, chorioretinitis, endophthalmitis, or optic neuritis in animals.

Host inflammatory response to oculomycosis is generally suppurative in acute cases and pyogranulomatous in chronic cases. Host tissues may be damaged directly by inflammatory processes (i.e., by elaborating inflammatory mediators and oxidative products) or by degradative enzymes produced directly by the fungal organisms. One recent report found *Histoplasma* sp. in cytology samples from a white ulcerated lesion in a horse; the horse responded favorably to topical antifungals, suggesting that *Histoplasma* sp. was not incidental.

Diagnostic Methods

Direct Examination

Fungal infections of the eyelids, conjunctiva, and cornea can be identified by scraping surface lesions. Organisms may be seen after direct staining of smears from scraped specimens and subsequent identification by culture. Deep nonulcerative keratitis or intraocular infection requires culture of a biopsy specimen (i.e., cornea) or aspirates (i.e., anterior chamber/vitreous). Histopathology of a deep corneal biopsy or enucleated specimen allows demonstration of fungal organisms through special staining procedures.

Direct smears can be examined by various techniques. Calcofluor white powder is a fluorescent material that binds to chitin in fungal cell walls. When excited by light at a wavelength of 500 nm, the bound calcofluor fluoresces blue-green. A solution of 0.1% calcofluor can be mixed with 10% potassium hydroxide to result in a rapid, extremely sensitive technique, and Gram stain, simple methylene blue, or India ink wet preparations are useful as rapid diagnostic procedures to identify many yeasts. Histologic sections stained with Giemsa stain, periodic acid-Schiff (PAS), or methenamine silver are sensitive and result in permanent preparations. Use of special stains allows confirmation of fungal infection and differentiation between yeast and hyphal forms, but specific identification of species may require fungal cultures. Diagnosis of fungal keratitis using peroxidase-labeled lectins in an experimental rabbit model has been described.[248]

Fungal Cultures

Sabouraud dextrose agar is the medium most commonly used for culturing ocular fungi. Enriched media such as brain-heart infusion agar with 5% blood is used for dimorphic fungi. When incubated at 37°C, mycelial fungal growth may convert to the yeast phase of the dimorphic organism. Gentamicin or chloramphenicol are useful additions to culture media to suppress bacterial overgrowth, but media should not include cycloheximide, which inhibits fungal growth.

Specimens from external infections of the ocular surface should be collected with a spatula and inoculated by streaking directly onto culture media. Inoculation streaks provide a means of differentiating possible pathogens, which grow in the streak areas, from airborne contaminants, which grow in the nonstreak areas. Scrapings or biopsy specimens from corneal ulcers (i.e., keratomycosis) or aspirates from the anterior chamber or the vitreous cavity (i.e., oculomycosis) should be directly inoculated onto Sabouraud agar, brain-heart infusion broth medium, and blood agar plates. Incubation should be at 24° to 30°C for at least 30 days. Species such as *Candida* and *Fusarium* will normally grow within 4 days, but as many as 25% of fungal isolates may require up to 2 weeks of incubation. When *Histoplasma* sp. or *Blastomyces* sp. are suspected, cultures must be incubated for at least 4 weeks.

Definitive identification is often made on the basis of the morphologic structure of the organism, including the direct microscopic appearance of the fungus in the clinical specimen, the morphology of the colony and type of pigmentation, the microscopic appearance of the fruiting heads and spores from mold colonies, and the morphology of the yeast and type of budding. Biochemical tests can be used for yeasts and, to a more limited extent, to identify some molds. Other tests specific to the particular fungus, such as the germ-tube test for *Candida albicans,* may be useful.

Serologic Tests

A number of serologic tests are available for the diagnosis of systemic mycoses.[249]

Complement-Fixation Test

The complement-fixation (CF) test is used for the diagnosis of histoplasmosis, blastomycosis, and coccidioidomycosis. Cross-reactivity between *Histoplasma* sp. and *Blastomyces* sp. may occur. CF titers for mycotic agents may be low (e.g., 1:8, 1:16), and nonspecific anticomplementary activity may be problematic. Appropriate controls must be used and acceptable limits of complement activity established. Titers of 1:8 or greater are considered to be presumptive evidence of histoplasmosis, blastomycosis, and coccidioidomycosis. Lower titers (e.g., 1:2, 1:4) may also be important, but a supplementary gel diffusion precipitation test should be performed. CF titers may serve as a prognostic aid. When titers decrease over a period of several weeks, the prognosis is usually good; if titers continue to increase over 8 weeks or longer, the prognosis is more guarded.

Gel Diffusion Precipitin Test

The gel diffusion precipitin (GDP) test is an immunodiffusion test with less cross-reactivity than the CF test. The test is based on the reaction in agar gel of specific antibody to fungal cell extracts or culture filtrates. In addition to its specificity, it is relatively simple to perform. The GDP has been developed for blastomycosis, histoplasmosis, coccidioidomycosis, aspergillosis, candidiasis, and sporotrichosis. In cases of mixed infections, false-negative results may be problematic. In addition, the GDP test is not useful in the diagnosis of advanced histoplasmosis in the cat.

Latex Agglutination Test

The slide latex agglutination (LA) test is rapid, sensitive, and specific for the presence of fungal antigen. This test has been developed for the diagnosis of cryptococcosis, coccidioidomycosis, sporotrichosis, candidiasis, and histoplasmosis, and it has been used extensively to detect antigen in body fluids (e.g., cryptococcal antigen in cerebrospinal fluid). The course of disease may also be monitored during therapy by quantitating the antigen in fluids.

Fluorescent Antibody Test

Fluorescein-labeled antibodies may be used to rapidly identify fungi in tissues and culture, and this test may also be used on fixed specimens. It is particularly useful in the absence of culture and when serum is not available. Fluorescein-labeled lectins with defined specificity for different sugars also have been used to identify fungi in paraffin sections for surgical and postmortem specimens. The indirect fluorescent antibody test may also be used to detect antibody to fungal agents when other procedures are unavailable.

Tube Agglutination Test

The tube agglutination test is a sensitive procedure for the diagnosis of sporotrichosis and cryptococcosis using yeast cells as antigen. It is used in conjunction with the LA antigen test to quantitate anticryptococcal antibody for prognostic purposes.

Fluorescent Immunoassay

The fluorescent immunoassay is an immunochemical procedure used to detect antibodies to *Candida* sp., *Histoplasma* sp., *Blastomyces* sp., and *Coccidioides* sp. This procedure eliminates the need for titration and subjective determination of end points. Cross-reaction between *Histoplasma* sp. and *Blastomyces* sp. has not been observed, because sensitivity permits serum dilutions of 1:75 to dilute cross-reacting antibodies. This test compares favorably to conventional methods in correlating clinical response and predicting relapse of disease.

Susceptibility Testing

In vitro susceptibility testing of fungi to antifungal drugs has been performed by measuring a suitable concentration end point (i.e., the MIC) for various antifungal drugs.[250,251] The MIC is the amount of drug (μg/mL) that inhibits essentially all visible growth in treated test wells compared with duplicate, untreated test wells. Standardized in vitro susceptibility test criteria are not available, though attempts have been made to estimate MIC susceptibility versus resistance on the basis of correlating clinical responses to antifungal therapy.[123] Clear correlations have not yet evolved, however, between antifungal drug MIC and clinical outcome.

Polymerase Chain Reaction

The ease with which PCR diagnostics can be performed, the relatively minimal expense of such testing, and the rapidity with which results can be delivered make PCR testing for fungal keratitis desirable. Recent studies demonstrate the ability of PCR to accurately detect mycotic keratitis in humans.[252,253] These results are encouraging, and it is very tempting to use PCR in veterinary patients suspected of having keratomycosis. However, the high sensitivity of PCR may, in fact, be a limiting factor in the applicability of PCR to diagnosis of keratomycosis in veterinary species. Fungal organisms are often part of the commensal flora depending on geography, season, and environment; standard PCR cannot distinguish transient fungal flora from those that are involved in pathogenesis of disease. A recent report using real-time PCR demonstrated correlation of quantified PCR results with fungal culture. More research is necessary to determine if real-time PCR results also correlate with clinical disease.[254]

TOXOPLASMA SP.

Taxonomy, Morphology, and Life Cycle

Toxoplasmosis is an infection caused by the obligate intracellular protozoal parasite *Toxoplasma gondii.* The cat is the only known definitive host for the parasite, but intermediate hosts include many warm-blooded species. The parasite's life cycle is divided into intestinal (i.e., sexual) and tissue (i.e., asexual) phases. The intestinal or coccidian phase is limited entirely to the cat, whereas the tissue phase occurs in both the cat and the intermediate hosts. The asexual phase includes formation of tachyzoites and bradyzoites. Tachyzoites are crescent-shaped (3×7 μm) and represent the pathogenic, propagative form of the parasite, which is present during active infectious disease. Bradyzoites are comma-shaped (2×7 μm) and found in chronic disease. Bradyzoites replicate slowly and accumulate within cysts, which are generally 50 to 200 μm in diameter.

Cats become infected by ingesting bradyzoite cysts from the tissues of an infected intermediate host, usually rodents or birds. After ingestion, bradyzoites rapidly transform into tachyzoites, penetrate the cat's intestinal mucosa, and undergo an enteroepithelial cycle of sexual proliferation that results in development and shedding of oocysts. Oocysts detach from the intestinal epithelium and are shed in the feces. After primary infection, cats can shed millions of fecal oocysts, each of which is 11 to 14 μm by 9 to 11 μm in size and contains four sporozoites in two sporocysts. In the external environment, the oocyst undergoes sporulation within 1 to 3 days, when it then becomes infectious.

Transmission and Pathogenic Mechanisms

Cats and intermediate hosts can become infected by ingesting bradyzoite cysts or tachyzoites (in meat, unpasteurized milk, contaminated water), by ingesting or inhaling oocysts shed in feline feces, or by congenital transmission of tachyzoites. After ingestion, bradyzoites rapidly transform into tachyzoites, penetrate the intestinal wall, enter the circulatory system, and disperse systemically. Proliferation of tachyzoites initiates destruction of host cells before development of an immune response (usually 1–2 weeks for humoral and 2–4 weeks for cellular immunity). In toxoplasmosis, tissue damage results from both intracellular growth of the organism and the host's immunologic responses. The type and severity of disease depends on the number of organisms, strain of *T. gondii,* organs infected, and the immune status and response of the host. Congenital transmission of toxoplasmosis occurs when an infection is acquired during pregnancy; this means of transmission occurs in humans and herbivores but is relatively uncommon in carnivores. The fetus or neonate of a dam with previous antibodies to *Toxoplasma* sp. will usually not develop congenital toxoplasmosis. When the nonimmune dam is infected during pregnancy, however, the disease is usually more severe in the fetus than in the dam. Transplacental transmission of *Toxoplasma* sp. increases when the infection is acquired in the second or third trimesters of pregnancy, but more severe fetal disease generally occurs when the infection is acquired during the first trimester. After congenital infection, recurrent disease in an otherwise healthy animal may result from reactivation of encysted organisms. In humans, infections have also been acquired from blood transfusions and contaminated donor tissue.

Host Responses

When host immune defenses are initiated, the proliferative stage of the infection is curtailed, though organisms may

encyst and remain viable in infected tissues for the life of the animal. Macrophages activated by interferon-gamma are the principal cells involved in control of *T. gondii* infection. Inflammatory reactions are usually minimal around the bradyzoite cysts, however, possibly because of the incorporation of host elements into the cyst walls, which masks the expression of parasitic antigens. Infection progresses when the cysts rupture, thereby releasing parasites that proliferate and invade neighboring cells. Bradyzoite cysts can be located in many tissues and are typically abundant in the brain, skeletal muscle, myocardium, and viscera. An intact cell-mediated immune system is extremely important for resisting *T. gondii* infection. Chronic immunosuppression can reactivate latent infection via bradyzoite cyst rupture, initiate rapid transformation into tachyzoites, and allow progressive development of infection. Immunocompromise, as occurs with immunosuppressive retroviral infections, may result in reactivation of a previous, latent infection.

The role of T. *gondii* in anterior uveitis is controversial. Ocular toxoplasmosis in humans is characterized by a necrotizing retinochoroiditis, with anterior uveitis being rarely documented. Most cases of human ocular toxoplasmosis are thought to result from a reactivated, congenital infection. In domestic species, ocular toxoplasmosis is most common in the cat.[255–257] In contrast to *T. gondii* infection in humans, the most common clinical finding with naturally occurring *T. gondii* infection in cats is nongranulomatous anterior uveitis. Additionally, *T. gondii* cannot typically be demonstrated from eyes with anterior uveitis. Experimental infections in the cat have resulted primarily in chorioretinal lesions, but retrospective studies of spontaneous feline ocular toxoplasmosis indicate that multifocal granulomatous panuveitis (particularly iridocyclitis) is the prevalent ocular manifestation.[258,259]

In cases of ocular inflammation associated with *Toxoplasma* sp. cellular immune memory to uveal antigens may perpetuate the inflammatory disease, as damaged uveal or retinal cells stimulate lymphocytes and plasma cells, which may then initiate production of autoantibodies and further contribute to the uveitis. Interestingly, in cats with uveitis, organisms are found relatively infrequently on histologic examination of the uveal tissues. High levels of toxoplasma-specific antibody within the uvea of cats with subacute or chronic anterior uveitis may reflect nonspecific recruitment of toxoplasma-sensitized lymphocytes.[255] Furthermore, in chronically inflamed eyes, other lymphocytes may be recruited as well, thus resulting in the presence of a wide variety of antibodies not specifically associated with the primary cause of the uveitis but further exacerbating the disease.[260]

Diagnostic Methods

Laboratory diagnosis of *Toxoplasma gondii* infection includes recovery and isolation of the parasite, histologic identification, and serologic evaluation of the patient. Isolation of the parasite from blood, spinal and ocular fluids, sputum, or placenta by direct inoculation into cell culture of mice is diagnostic of an acute infection. Recovery of the parasite from tissues (except placenta) can represent either an acute or a chronic infection. Serologic tests for the diagnosis of toxoplasmosis include the Sabin-Feldman test (i.e., methylene blue dye test), CF test, hemagglutination test, LA test, IFA, and ELISA. Measurement of IgM antibodies may facilitate making the diagnosis during the acute phase of toxoplasmosis. Serologic diagnosis of toxoplasmosis may be confounded by the high seroprevalence of *T. gondii*–specific antibodies in normal cats.[261,262] Measurement of aqueous humor–specific antibodies compared with serum levels, the C-value, has been found to be useful in documenting local antibody production.[263–265] Even so, the possibility of nonlocal production of *T. gondii* antibodies present in the anterior chamber must be recognized.

The *Toxoplasma* parasite can be identified histologically by routine microscopic examination of hematoxylin and eosin–stained and Giemsa-stained tissue sections. Identification of tachyzoites indicates an active infection, whereas detection of cysts indicates chronic disease (except for cysts in placental or fetal tissues, which by the nature of these tissues connotes acute or subacute disease). Fluorescent antibody and peroxidase-antiperoxidase techniques are reliable methods for detection. The PCR is both sensitive and specific, and it may be used for detecting *Toxoplasma* DNA in cases in which cysts cannot be visualized. In vitro diagnostic tests and the presence or absence of clinical disease are not always readily correlated, because the prevalence of asymptomatic infected cats is not known and infected immunocompromised cats may not have predictable serologic responses.

PROTOTHECA SP.

Taxonomy and Life Cycle

Prototheca sp. are achlorophyllous algae that are morphologically similar to the algal genus *Chlorella.* Cells are spherical to oval in shape and range from 1 to 13 μm in diameter, with some cells exhibiting slightly longer lengths. The hyaline cell wall is approximately 0.5-μm thick, the cytoplasm is granular and basophilic, and the nucleus is small and centrally located. Reproduction is through endosporulation, with cleavage of the parent cell resulting in the release of from 2 to 20 or more endospores. The nucleus may not be visible in the immature forms, and empty hyaline shells may be visible among intact algal cells within lesions. The three recognized species are *P. stagnora, P. zopfii,* and *P. wickerhamii,* with the latter two being pathogenic.

Pathogenic Mechanisms

Prototheca sp. are an environmental contaminant that, when ingested by the host, may rarely cause disease. The organism is minimally pathogenic and does not spread between hosts. Immunosuppression, especially of cell-mediated immunity, favors establishment of infection. Systemic protothecosis occurs in the dog, in which it typically manifests as colitis with intermittent, bloody diarrhea.[266–268] The colon is the

probable site of primary infection and entry for disseminated disease.

Virulence may vary between species of *Prototheca. P. wickerhamii* appears to be less pathogenic, causing only localized skin disease in the dog and cat; *P. zopfii* is nearly always isolated from disseminated cases in the dog.[269,270] In the dog, predispositions for the Collie breed and females have been noted.[270,271]

Host Response

Because protothecosis becomes widely disseminated in the dog, a number of organ systems, including the lymphatics, kidneys, and lungs, are commonly involved. Intermittent or protracted bloody diarrhea, weight loss, and debility are the usual clinical findings. CNS and ocular involvement are also relatively common and are associated with severe depression, deafness, ataxia, circling, paresis, and blindness. Renal failure has been reported as well. In some cases, chronic ulcerative skin lesions with draining tracts or crusty exudates on the trunk or extremities are seen. Whereas protothecosis in the cat is limited to cutaneous disease, canine dermatologic lesions usually reflect disseminated disease with concurrent involvement of the lymphatics, viscera, brain, or eyes.[272]

Host reactions vary considerably. Typically, there is a mild, mixed inflammatory cell response, and minimal necrosis is noted at the periphery of lesions. Cellular infiltrates consist of macrophages, lymphocytes, neutrophils, and substantial numbers of plasma cells. In some instances, a granulomatous or pyogranulomatous response is apparent, in which organisms may be seen within macrophages and multinucleate giant cells. Multifocal aggregates of the *Prototheca* organism are found in the affected tissues. Ocular responses include focal or diffuse granulomatous chorioretinitis as well as retinal separation and degeneration, with masses of organisms present between the retina and choroid.[271,273]

Diagnostic Methods

Identifying organisms on Wright-stained fluid specimens obtained by vitreous centesis or cerebrospinal fluid collection is a reliable method of diagnosis. Gram's iodine also works well to stain smears for organisms. Gomori's methenamine-silver or PAS stains of histologic specimens enhance identification of organisms. *Prototheca* sp. grow readily in a variety of laboratory media, including Sabouraud's cycloheximide-free dextrose agar at 25° to 37°C. Fungistatic discs may be used to differentiate *Candida* sp. from *Prototheca* sp. Similarly, a clotrimazole disc will allow differentiation between *P. wickerhamii* (i.e., susceptible) and *P. zopfii* (i.e., resistant).

REFERENCES

1. Quinn PJ, Markey BK, Carter ME, et al. Replication of viruses. In: *Veterinary Microbiology and Microbial Disease,* Oxford: Blackwell Science; 2002: 283–289.
2. Ball LA. Replication Strategies of RNA Viruses. In: Knipe, DM, Howley PM, eds. *Field's Virology,* 4 ed. Philadelphia: Lippincott, Williams & Wilkins; 2001: 105–118.
3. Studdert MJ, Martin MC. 1970. Virus diseases of the respiratory tract of cats. 1. Isolation of feline rhinotracheitis virus. *Aust Vet J;* 46: 99–104.
4. Ellis TM. 1981. Feline respiratory virus carriers in clinically healthy cats. *Aust Vet J* 57: 115–118.
5. Maggs DJ, Lappin MR, Reif JS, et al. 1999. Evaluation of serologic and viral detection methods for diagnosing feline herpesvirus-1 infection in cats with acute respiratory tract or chronic ocular disease. *J Am Anim Hosp Assoc* 214; 4: 502–507.
6. Grail A, Harbour DA, Chia W. 1991. Restriction endonuclease mapping of the genome of feline herpesvirus type 1. *Arch Virol* 116; 1–4: 209–220.
7. Rota PA, Maes RK, Ruyechan WT. 1986. Physical characterization of the genome of feline herpesvirus-1. *Virology* 154; 1: 168–179.
8. Maeda K, Kawaguchi Y, Ono M, Tajima T, Mikami T. Restriction endonuclease analysis of field isolates of feline herpesvirus type 1 and identification of heterogeneous regions. *J Clin Microbiol* 1995; 33: 217–221.
9. Maeda K, Kawaguchi Y, Ono M, Tajima T, Mikami T. Comparisons among feline herpesvirus type 1 isolates by immunoblot analysis. *J Vet Med Sci 1995;* 57: 147–150.
10. Hamano M, Maeda K, Mizukoshi F, Une Y, et al. Experimental infection of recent field isolates of feline herpesvirus type 1. *J Vet Med Sci* 2003; 65: 939–943.
11. Hamano M, Maeda K, Mizukoshi F, Mochizuki M, et al. Genetic rearrangements in the gC gene of the feline herpesvirus type 1. *Virus Genes* 2004; 28: 55–60.
12. Nasisse MP, Guy JS, Davidson MG, Sussman WA, Fairley NM. Experimental ocular herpesvirus infection in the cat. Sites of virus replication, clinical features and effects of corticosteroid administration. *Invest Ophthalmol Vis Sci* 1989; 30: 1758–1768.
13. Nasisse MP. Feline herpesvirus ocular disease. *Vet Clin N Am: Sm Anim Pract* 1990; 20: 667–680.
14. Roberts SR, Dawson CR, Coleman V, Togni B. Dendritic keratitis in a cat. *J Am Anim Hosp Assoc* 1972; 161: 285–289.
15. Ohmura Y, Ono E, Matsuura T, Kida H, Shimizu Y. Detection of feline herpesvirus 1 transcripts in trigeminal ganglia of latently infected cats. *Arch Virol* 1993; 129(1–4): 341–347.
16. Townsend WM, Stiles J, Guptill-Yoran L, Krohne SG. Development of a reverse transcriptase-polymerase chain reaction assay to detect feline herpesvirus-1 latency-associated transcripts in the trigeminal ganglia and corneas of cats that did not have clinical signs of ocular disease. *Am J Vet Res* 2004; 65: 314–319.
17. Reubel GH, Ramos RA, Hickman MA, Rimstad E, Hoffmann DE, Pedersen NC. Detection of active and latent feline herpesvirus 1 infections using the polymerase chain reaction. *Arch Virol* 1993; 132: 409–420.
18. Gaskell RM, Dennis PE, Goddard LE, Cocker FM, Wills JM. Isolation of felid herpesvirus I from the trigeminal ganglia of latently infected cats. *Journal of General Virology* 1985; 66(Pt 2): 391–394.
19. Nasisse MP, Davis BJ, Guy JS, Davidson MG, Sussman W. Isolation of feline herpesvirus 1 from the trigeminal ganglia of acutely and chronically infected cats. *J Vet Intern Med* 1992; 6: 102–103.
20. Gaskell RM, Povey RC. Experimental induction of feline viral rhinotracheitis virus re-excretion in FVR-recovered cats. *Vet Rec* 1977; 100: 128–133.

21. Mitchell WJ, Gressens P, Martin JR, DeSanto R. Herpes simplex virus type 1 DNA persistence, progressive disease and transgenic immediate early gene promoter activity in chronic corneal infections in mice. *J Gen Virol* 1994; 75(Pt 6): 1201–1210.
22. Maggs DJ, Chang E, Nasisse MP, Mitchell WJ. Persistence of herpes simplex virus type 1 DNA in chronic conjunctival and eyelid lesions of mice. *J Virol* 1998; 72: 9166–9172.
23. Lundberg P, Welander P, Han X, Cantin E. Herpes simplex virus type 1 DNA is immunostimulatory in vitro and in vivo. *J Virol* 2003; 77: 11158–11169.
24. Tham KM, Studdert MJ. Antibody and cell-mediated immune responses to feline herpesvirus 1 following inactivated vaccine and challenge. *Zentralblatt Fuer Veterinaermedizin Reihe B* 1987; 34: 585–597.
25. Tham KM, Studdert MJ. Clinical and immunological responses of cats to feline herpesvirus type 1 infection. *Vet Rec* 1987; 120: 321–326.
26. Burgener DC, Maes RK. Glycoprotein-specific immune responses in cats after exposure to feline herpesvirus-1. *Am J Vet Res* 1988; 49: 1673–1676.
27. Doymaz MZ, Rouse BT. Herpetic stromal keratitis: An immunopathologic disease mediated by CD4+ T lymphocytes. *Invest Ophthalmol Vis Sci* 1992; 33: 2165–2173.
28. Hendricks RL, Janowicz M, Tumpey TM. Critical role of corneal Langerhans cells in the CD4- but not CD8-mediated immunopathology in herpes simplex virus-1-infected mouse corneas. *J Immunol* 1992; 148: 2522–2529.
29. Niemialtowski MG, Rouse BT. Predominance of Th1 cells in ocular tissues during herpetic stromal keratitis. *J Immunol* 1992; 149: 3035–3039.
30. Russell RG, Nasisse MP, Larsen HS, Rouse BT. Role of T-lymphocytes in the pathogenesis of herpetic stromal keratitis. *Invest Ophthalmol Vis Sci* 1984; 25: 938–944.
31. Nasisse MP, English RV, Tompkins MB, Guy JS, Sussman W. Immunologic, histologic, and virologic features of herpesvirus-induced stromal keratitis in cats. *Am J Vet Res* 1995; 56: 51–55.
32. Nasisse MP, Glover TL, Moore CP, Weigler BJ. Detection of feline herpesvirus 1 DNA in corneas of cats with eosinophilic keratitis or corneal sequestration. *Am J Vet Res* 1998; 59: 856–858.
33. Allgoewer I, Schaffer EH, Stockhaus C, Vogtlin A. Feline eosinophilic conjunctivitis. *Vet Ophthalmol* 2001; 4: 69–74.
34. Maggs DJ, Lappin MR, Nasisse MP, Maggs DJ, Lappin MR, Nasisse MP. Detection of feline herpesvirus-specific antibodies and DNA in aqueous humor from cats with or without uveitis. *Am J Vet Res* 1999; 60: 932–936.
35. Hoover EA, Kahn DE. Experimentally induced feline calicivirus infection: Clinical signs and lesions. *J Am Anim Hosp Assoc* 1975; 16: 463–468.
36. Love DN. Pathogenicity of a strain of feline calicivirus for domestic kittens. *Aust Vet J 1975;* 51: 541–546.
37. Ormerod E, McCandlish IA, Jarrett O. Diseases produced by feline caliciviruses when administered to cats by aerosol or intranasal instillation. *Vet Rec* 1979; 104: 65–69.
38. Wardley RC, Povey RC. The clinical disease and patterns of excretion associated with three different strains of feline calicivirus. *Res Vet Sci* 1976; 23: 14.
39. Wardley RC, Povey RC. The pathology and sites of persistence associated with three different strains of feline calicivirus. *Res Vet Sci* 1977; 23: 15–19.
40. Poland AM, Vennema H, Foley JE, Pedersen NC. Two related strains of feline infectious peritonitis virus isolated from immunocompromised cats infected with a feline enteric coronavirus. *J Clin Microbiol* 1996; 34: 3180–3184.
41. Vennema H, Poland A, Foley J, Pedersen NC. Feline infectious peritonitis viruses arise by mutation from endemic feline enteric coronaviruses. *Virology* 1998; 243: 150–157.
42. Evermann JF, Henry CJ, Marks SL. Feline infectious peritonitis. *J Am Anim Hosp Assoc* 1995; 206: 1130–1134.
43. Martin CL, Stiles J. Ocular infections. In: Greene CE, ed. *Infectious Diseases of the Dog and Cat,* 2nd ed. Philadelphia: WB Saunders; 1998: 658–717.
44. Sparkes AH, Gruffydd-Jones TJ, Harbour DA. An appraisal of the value of laboratory tests in the diagnosis of feline infectious peritonitis. *J Am Anim Hosp Assoc* 1994; 30: 345–350.
45. Simons FA, Vennema H, Rofina JE, et al. A mRNA PCR for the diagnosis of feline infectious peritonitis. *J Virolog Meth* 2005; 124: 111–116.
46. Yamamoto JK, Hansen H, Ho EW, et al. Epidemiologic and clinical aspects of feline immunodeficiency virus infection in cats from the continental United States and Canada and possible mode of transmission. *J Am Anim Hosp Assoc* 1989; 194: 213–220.
47. Nasisse MP, Guy JS, Stevens JB, English RV, Davidson MG. Clinical and laboratory findings in chronic conjunctivitis in cats: 91 cases (1983–1991). *J Am Anim Hosp Assoc* 1993; 203: 834–837.
48. English RV, Davidson MG, Nasisse MP, Jamieson VE, Lappin MR. Intraocular disease associated with feline immunodeficiency virus infection in cats. *J Am Anim Hosp Assoc* 1990; 196: 1116–1119.
49. Fischer BL, Vail DM, Dubielzig RR. A study of factors influencing survival after enucleation in feline ocular lymphosarcoma (abstract). Proceed 30th Meet Am Coll Vet Ophthalmol, 1999: 81.
50. Stiles J, Bienzle D, Render JA, Buyukmihci NC, Johnson EC. Use of nested polymerase chain reaction (PCR) for detection of retroviruses from formalin-fixed, paraffin-embedded uveal melanomas in cats. *Vet Ophthalmol* 1999; 2: 113–116.
51. English RV, Nelson P, Johnson CM, Nasisse M, Tompkins WA, Tompkins MB. Development of clinical disease in cats experimentally infected with feline immunodeficiency virus. *J Infect Dis* 1994; 170: 543–552.
52. Hardy WD. Hematopoetic tumors of cats. *J Am Anim Hosp Assoc* 1981; 17: 921–940.
53. Albert DM, Lahav M, Colby ED, Shadduck JA, Sang DN. Retinal neoplasia and dysplasia. I. Induction by feline leukemia virus. *Invest Ophthalmol Vis Sci* 1977; 16: 325–337.
54. Fischer CA. Retinopathy in anemic cats. *J Am Anim Hosp Assoc* 1970; 156: 1415–1427.
55. Herring IP, Troy GC, Toth TE, et al. Feline leukemia virus detection in corneal tissues of cats by polymerase chain reaction and immunohistochemistry. *Vet Ophthalmol* 2001; 4: 119–126.
56. Lubin JR, Albert DM, Essex M, de NF, Riis R. Experimental anterior uveitis after subcutaneous injection of feline sarcoma virus. *Invest Ophthalmol Vis Sci* 1983; 24: 1055–1062.
57. Cullen CL, Haines DM, Jackson ML, Peiffer RL, Grahn BH. The use of immunohistochemistry and the polymerase chain reaction for detection of feline leukemia virus and feline sarcoma virus in six cases of feline ocular sarcoma. *Vet Ophthalmol* 1998; 1: 189–193.

58. Percy DH, Scott FW, Albert DM. Retinal dysplasia due to feline panleukopenia virus infection. *J Am Anim Hosp Assoc* 1975; 167: 935–937.
59. Greene CE, Gorgasz EJ, Martin CL. Hydranencephaly associated with feline panleukopenia. *J Am Anim Hosp Assoc* 1982; 18: 767–768.
60. Albert DM, Lahav M, Carmichael LE, Percy DH. Canine herpes-induced retinal dysplasia and associated ocular anomalies. *Invest Ophthalmol Vis Sci* 1976; 15: 267–278.
61. Ledbetter EC, Riis R, Kern TJ, Haley NJ, Schatzberg SJ. Corneal ulceration associated with naturally occurring canine herpesvirus-1 infection in two adult dogs (abstract). Proceed 36th Ann Meet Am Coll Vet Ophthalmol 2005: 13.
62. Coats G. Retinal degeneration following distemper in a dog. Proceed Royal Soc Med (Section Ophthalmology) 1913: 14–18.
63. Parry HB. Degeneration of the dog retina. IV. Retinopathies associated with dog distemper-complex virus infections. *Brit J Ophthalmol* 1954; 38: 295–309.
64. Jubb KV, Saunders LZ, Coates HV. The intraocular lesions of canine distemper. *J Comp Pathol* 1957; 67: 21–29.
65. Render JA, Carlton WW, Vestre WA. Canine distemper inclusions in the ciliary body of dog. *J Am Anim Hosp Assoc* 1982; 181: 164–165.
66. Aguirre G, Carmichael L, Bistner S. Corneal endothelium in viral induced anterior uveitis. Ultrastructural changes following canine adenovirus type 1 infection. *Arch Ophthalmol* 1975; 93: 219–224.
67. Carmichael LE. The pathogenesis of ocular lesions of infectious canine hepatitis. II. Experimental ocular hypersensitivity produced by the virus. *Pathol Vet* 1965; 2: 344–359.
68. Carmichael LE. The pathogenesis of ocular lesions of infectious canine hepatitis. I. Pathology and virologic observations. *Pathol Vet* 1964; 1: 73–95.
69. Curtis R, Barnett KC. Canine adenovirus-induced ocular lesions in the Afghan hound. *Cornell Vet* 1981; 71: 85–95.
70. Kleiboeker SB, Turnquist SE, Johnson PJ, Kreeger JM. Detection and nucleotide sequencing of a DNA-packaging protein gene of equine gammaherpesviruses. *J Vet Diag Invest* 2004; 16: 67–74.
71. Agius CT, Nagesha HS, Studdert MJ. Equine herpesvirus 5: Comparisons with EHV2 (equine cytomegalovirus), cloning, and mapping of a new equine herpesvirus with a novel genome structure. *Virology* 1992; 191: 176–186.
72. Miller TR, Gaskin JM, Whitley RD, Wittcoff ML. Herpetic keratitis in a horse. *Eq Vet J* 1990; 10(suppl): 15–17.
73. Thein P. The association of EHV-2 infection with keratitis and research on the occurrence of equine exanthema (EHV-3) in horses in Germany. In: Bryan JT, Gerber H, ed. *Equine Infectious Diseases IV.* Princeton, NJ: Veterinary Publishing; 1978: 33–41.
74. Kershaw O, von Oppen T, Glitz F, Deegen E, Ludwig H, Borchers K. Detection of equine herpesvirus type 2 (EHV-2) in horses with keratoconjunctivitis. *Virus Res* 2001; 80: 93–99.
75. Galle LE, Kleiboeker SB, Johnson PJ, Giuliano EA, Scotty NS. Prevalence of equine herpesvirus DNA from conjunctival swabs in Missouri. Proceed 34th Ann Meet Am Coll Vet Ophthalmol 2003: 8.
76. Timoney PJ, O'Connor PJ. An outbreak of the conjunctival form of infectious bovine rhinotracheitis virus infection. *Vet Rec* 1971; 89: 170.
77. Rebhun WC, Smith JS, Post JE, Holden HR. An outbreak of the conjunctival form of infectious bovine rhinotracheitis. *Cornell Vet* 1978; 68: 297–301.
78. Meyers G, Thiel HJ. Molecular characterization of pestiviruses. *Adv Virus Res* 1996; 47: 53–118.
79. Castrucci G, Osburn BI, Ferrari M, Traldi V. An experimental contribution to the study of the pathogenesis of bovine viral diarrhea virus infection. *Comp Immunol Microbiol Infect Dis* 1992; 15: 163–169.
80. Osburn BI, Castrucci G. Diaplacental infections with ruminant pestiviruses. *Arch Virol* 1991; 3(suppl): 71–78.
81. Bistner SI, Rubin LF, Saunders LZ. The ocular lesions of bovine viral diarrhea-mucosal disease. *Pathol Vet* 1970; 7: 275–286.
82. Kahrs RF, Scott FW, de Lahunta A. Congenital cerebella hypoplasia and ocular defects in calves following bovine viral diarrhea-mucosal disease infection in pregnant cattle. *J Am Vet Med Assoc* 1970; 156: 1443–1450.
83. Wyand DS, Helmboldt CF, Nielsen SW. Malignant catarrhal fever in white-tailed deer. *J Am Anim Hosp Assoc* 1971; 159: 605–610.
84. Whiteley HE, Young S, Liggitt HD, DeMartini JC. Ocular lesions of bovine malignant catarrhal fever. *Vet Pathol* 1985; 22: 219–225.
85. Jubb KV, Saunders LZ, Stenius PI. Die histologischen Augenveranderungen beim bosartigen Katarrhalfieber des Rindes. *Schweizer Archiv fur Tierheilkunde* 1960; 102: 392.
86. Silverstein AM, Parshall CJ, Osburn BI, Prendergast RA. 1971. An experimental, virus-induced retinal dysplasia in the fetal lamb. *Am J Ophthalmol* 1971; 72: 22.
87. Ficken MD, Nasisse MP, Boggan GL. Marek's disease virus isolates with unusual tropism and virulence for ocular tissues. Clinical findings, challenge studies, and pathologic features. *Avian Path* 1991; 20: 461–467.
88. Moore CP, Nasisse MP. Clinical microbiology. In: Gelatt KN, ed. *Veterinary Ophthalmology,* 3rd ed. Philadelphia: Lippincott Williams & Wilkins; 1999: 259–290.
89. Crane LR, Gutterman PA, Chapel T, Lerner AM. Incubation of swab materials with herpes simplex virus. *J Infect Dis* 1980; 141: 531.
90. Van Gelder RN. Cme review: Polymerase chain reaction diagnostics for posterior segment disease. *Retina* 2003; 23: 445–452.
91. Stiles J, McDermott M, Bigsby D, et al. Use of nested polymerase chain reaction to identify feline herpesvirus in ocular tissue from clinically normal cats and cats with corneal sequestra or conjunctivitis. *Am J Vet Res* 1997; 58: 338–342.
92. Weigler BJ, Babineau CA, Sherry B, Nasisse MP. High sensitivity polymerase chain reaction assay for active and latent feline herpesvirus-1 infections in domestic cats. *Vet Rec* 1997; 140: 335–338.
93. Vogtlin A, Fraefel C, Albini S, et al. Quantification of feline herpesvirus 1 DNA in ocular fluid samples of clinically diseased cats by real-time TaqMan PCR. *J Clin Microbiol* 2002; 40: 519–523.
94. Elder MJ, Stapleton F, Evans E, Dart JK. Biofilm-related infections in ophthalmology. *Eye* 1995; 9(Pt 1): 102–109.
95. Davis BD. Bacterial architecture. In: Davis BD, Dulbecco R, Eisen HN, Ginsberg HS, eds. *Microbiology,* 4th ed. Philadelphia: Lippincott Williams & Wilkins; 1990: 38–39.
96. Griffiths E. The iron-uptake systems of pathogenic bacteria. In: Bullen JJ, Griffiths E, eds. *Iron and Infection: Molecular,*

Physiological, Clinical Aspects. Chichester, England: John Wiley & Sons, 1987: 69–137.
97. Bukanov N, Ravi VN, Miller D, Srivastava K, Berg DE. Pseudomonas aeruginosa corneal ulcer isolates distinguished using the arbitrarily primed PCR DNA fingerprinting method. *Curr Eye Res* 1994; 13: 783–790.
98. Gaskin JM. Microbiology of the canine and feline eye. *Vet Clin N Am: Sm Anim Pract* 1980; 10: 303–316.
99. Gerding PA, Jr., Kakoma I. Microbiology of the canine and feline eye. *Vet Clin N Am: Sm Anim Pract* 1990; 20: 615–625.
100. Bistner SI, Roberts SR. Conjunctival bacterial: Clinical appearance can be deceiving. *Mod Vet Pract* 1969; 50: 45–47.
101. Urban M, Wyman M, Rheins M, Marraro RV. Conjunctival flora of clinically normal dogs. *J Am Anim Hosp Assoc* 1972; 161: 201–206.
102. McDonald PJ, Watson DJ. Microbial flora of normal canine conjunctivae. *J Sm Anim Pract* 1976; 17: 809–812.
103. Campbell LH, Fox JG, Snyder SB. Ocular bacteria and mycoplasma of the clinically normal cat. *Feline Pract* 1973; 3: 12.
104. Whitley RD, Moore CP. Microbiology of the equine eye in health and disease. *Vet Clin N Am: Large Anim Pract* 1984; 6: 451–466.
105. Moore CP, Heller N, Majors LJ, Whitley RD, Burgess EC, Weber J. Prevalence of ocular microorganisms in hospitalized and stabled horses. *Am J Vet Res* 1988; 49: 773–777.
106. Barber DM, Jones GE, Wood A. Microbial flora of the eyes of cattle. *Vet Rec* 1986; 118: 204–206.
107. Dagnall GJ. An investigation of colonization of the conjunctival sac of sheep by bacteria and mycoplasmas. *Epidemiol Infect* 1994; 112: 561–567.
108. Gionfriddo JR, Rosenbusch R, Kinyon JM, Betts DM, Smith TM. Bacterial and mycoplasmal flora of the healthy camelid conjunctival sac. *Am J Vet Res* 1991; 52: 1061–1064.
109. Zenoble RD, Griffith RW, Clubb SL. Survey of bacteriologic flora of conjunctiva and cornea in healthy psittacine birds. *Am J Vet Res* 1983; 44: 1966–1967.
110. Wolf ED, Amass K, Olsen J. Survey of conjunctival flora in the eye of clinically normal, captive exotic birds. *J Am Anim Hosp Assoc* 1983; 183: 1232–1233.
111. Chalmers WS, Kewley DR. Bacterial flora of clinically normal conjunctivae in the domestic duckling. *Avian Pathol* 1984; 14: 69–74.
112. Murphy JM, Lavach JD, Severin GA. Survey of conjunctival flora in dogs with clinical signs of external eye disease. *J Am Anim Hosp Assoc* 1978; 172: 66–68.
113. Moore CP, Fales WH, Whittington P, Bauer L. Bacterial and fungal isolates from Equidae with ulcerative keratitis. *J Am Anim Hosp Assoc* 1983; 182: 600–603.
114. Petersen-Jones SM. Quantification of conjunctival sac bacteria in normal dogs and those that suffer from keratoconjunctivitis sicca. *Vet Comp Ophthalmol* 1997; 7: 29–35.
115. Brooks DE, Andrew SE, Biros DJ, et al. Ulcerative keratitis caused by beta-hemolytic Streptococcus equi in 11 horses. *Vet Ophthalmology* 2000; 3(2–3): 121–125.
116. McLaughlin SA, Brightman AH, Helper LC, Manning JP, Tomes JE. Pathogenic bacteria and fungi associated with extraocular disease in the horse. *J Am Anim Hosp Assoc* 1983; 182: 241–242.
117. Gerding PA, Jr., McLaughlin SA, Troop MW. Pathogenic bacteria and fungi associated with external ocular diseases in dogs: 131 cases (1981–1986). *J Am Anim Hosp Assoc* 1988; 193: 242–244.
118. Burd EM. Bacterial keratitis and conjunctivitis. In: Smolin G, Throft RA, eds. *The Cornea,* 3rd ed., Boston: Lippincott Williams, & Wilkins; 1994: 115–167.
119. Packer AJ, Koontz FP. Ocular staphylococcal infections. *Am J Ophthalmol* 1984; 140: 645.
120. Moore CP, Collins BK, Fales WH. Antibacterial susceptibility patterns for microbial isolates associated with infectious keratitis in horses: 63 cases (1986–1994). *J Am Anim Hosp Assoc* 1995; 207: 928–933.
121. Rebhun WC. Bacterial ulcers of the equine cornea. *Eq Pract* 1981; 3: 40–49.
122. Barratt-Jones SM, Young SM, Canton DD, Mohr FC. *Streptococcus equi* infection as a cause of panophthalmitis in a horse. *J Eq Vet Sci* 1991; 11: 229–231.
123. Brooks DE, Andrew SE, Dillavou CL, Ellis G, Kubilis PS. Antimicrobial susceptibility patterns of fungi isolated from horses with ulcerative keratomycosis. *Am J Vet Res* 1998; 59: 138–142.
124. Ho PC, O'Day DM, Head WS. Fulminating panophthalmitis due to exogenous infection with *Bacillus cereus:* Report of 4 cases. *Br J Ophthalmol* 1982; 66: 205–208.
125. Wyman M, Swanson C, Kowalski JJ, Powers JD, Boraski EA. Experimental *Pseudomonas aeruginosa* ulcerative keratitis model in the dog. *Am J Vet Res* 1983; 44: 1135–1140.
126. Hazlett LD, Zelt R, Cramer C, Berk RS. *Pseudomonas aeruginosa* induced ocular infection. A histological comparison of two bacterial strains of different virulence. *Ophthalmic Res* 1985; 17: 289–296.
127. Miller PE. *Pseudomonas aeruginosa*-associated corneal ulcers in captive cranes. *J Zoo Wildlife Med* 1994; 25: 449–454.
128. Kernacki KA, Berk RS. Characterization of the inflammatory response induced by corneal infection with *Pseudomonas aeruginosa. J Ocular Pharm* 1994; 10: 281–288.
129. Stern GA, Lubniewski A, Allen C. The interaction between *Pseudomonas aeruginosa* and the corneal epithelium. An electron microscopic study. *Arch Ophthalmol* 1985; 103: 1221–1225.
130. Twining SS, Kirschner SE, Mahnke LA, Frank DW. Effect of *Pseudomonas aeruginosa* elastase, alkaline protease, and exotoxin A on corneal proteinases and proteins. *Invest Ophthalmol Vis Sci* 1993; 34: 2699–2712.
131. Hughes DE, Pugh GW Jr. Isolation and description of a Moraxella from horses with conjunctivitis. *Am J Vet Res* 1970; 31: 457–462.
132. Huntington PJ, Coloe PJ, Bryden JD, Macdonald F. Isolation of a Moraxella sp from horses with conjunctivitis. *Aust Vet J* 1987; 64: 118–119.
133. Spradbrow PB. The bacterial flora of the ovine conjunctival sac. *Aust Vet J* 1968; 44: 117–118.
134. Bankemper KW, Lindley DM, Nusbaum KE, Mysinger RH. Keratoconjunctivitis associated with *Neisseria ovis* infection in a herd of goats. *J Vet Diag Invest* 1990; 2: 76–78.
135. Dagnall GJ. Some cultural characteristics of *Branhamella ovis* isolated from the conjunctival sac of sheep. *Vet Microbiol* 1993; 37: 45–52.
136. Dagnall GJ. The role of *Branhamella ovis*, Mycoplasma conjunctivae and *Chlamydia psittaci* in conjunctivitis of sheep. *Br Vet J* 1994; 150: 65–71.

137. Okumoto M. Enterobacteriaceae. In: Tasman W, Jaeger EA, eds. *Duane's Foundations of Clinical Ophthalmology.* Philadelphia: JB Lippincott; 1990: 52–53.
138. Dukes TW. The ocular lesions in thromboembolic meningoencephalitis (ITEME) of cattle. *Can Vet J* 1971; 12: 180–182.
139. Harkness JE. *Biology and Medicine of Rabbits and Rodents,* 3rd ed. Philadelphia: Lea & Febiger, 1989.
140. Rebhun WC. Ocular manifestations of systemic diseases in cattle. *Vet Clin N Am: Large Anim Pract* 1984; 6: 623–639.
141. Gwin RM, Kowalski JJ, Wyman M, Winston S. Ocular lesions associated with *Brucella canis* infection in a dog. *J Am Anim Hosp Assoc* 1980; 16: 607–609.
142. Burgess EC, Gillette D, Pickett JP. Arthritis and panuveitis as manifestations of *Borrelia burgdorferi* infection in a Wisconsin pony. *J Am Anim Hosp Assoc* 1986; 189: 1340–1342.
143. Riecke JA, Rhoades HE. *Brucella canis* isolated from the eye of a dog. *J Am Anim Hosp Assoc* 1975; 166: 583–584.
144. Roberts SJ. Comments on equine leptospirosis. *J Am Anim Hosp Assoc* 1969; 155: 442–445.
145. Walker JK, Morgan JH. Ovine ophthalmitis associated with *Listeria monocytogenes*. *Vet Rec* 1993; 132: 636.
146. Sanchez S, Studer M, Currin P, Barlett P, Bounous D. Listeria keratitis in a horse. *Vet Ophthalmol* 2001; 4: 217–219.
147. Collins BK, Moore CP, Dubielzig RR, Gengler WR. Anaerobic orbital cellulitis and septicemia of a dog. *Can Vet J* 1991; 32: 683–685.
148. Tan RJ, Lim EW, Ishak B. Ecology of mycoplasmas in clinically healthy cats. *Aust Vet J* 1977; 53: 515–518.
149. Blackmore DK, Hill A. The experimental transmission of various mycoplasmas of feline origin to domestic cats (*Felis catus*). *J Sm Anim Pract* 1973; 14: 7–13.
150. Heyward JT, Sabry MZ, Dowdle WR. Characterization of mycoplasma species of feline origin. *Am J Vet Res* 1969; 30: 615–622.
151. Tan RJ, Miles JA. Incidence and significance of mycoplasmas in sick cats. *Res Vet Sci* 1974; 16: 27–34.
152. Dagnall GJ. Experimental infection of the conjunctival sac of lambs with *Mycoplasma conjunctivae*. *Br Vet J* 1993; 149: 429–435.
153. Egwu GO. In vitro antibiotic sensitivity of *Mycoplasma conjunctivae* and some bacterial species causing ovine infectious keratoconjunctivitis. *Sm Rumin Res* 1992; 7: 85–92.
154. Rodriguez JL, Poveda JB, Rodriguez F, Espinosa DL, Monteros A. Ovine infectious keratoconjunctivitis caused by *Mycoplasma agalactiae*. *Sm Rumin Res* 1996; 22: 93–96.
155. Gourley RN. Myeloplasmosis in cattle, sheep, and goats. *Is J Vet Sci* 1981; 17: 531–536.
156. Rosenbusch RF. Influence of mycoplasma preinfection on the expression of *Moraxella bovis* pathogenicity. *Am J Vet Res* 1983; 44: 1621–1624.
157. Everett KD, Bush RM, Andersen AA. Amended description of the order Chlamydiales, proposal of Parachlamydiaceae fam. nov. and Simkaniaceae fam. nov., each containing one monotypic genus, revised taxonomy of the family Chlamydiaceae, including a new genus and five new species, and standards for the identification of organisms. *Intern J System Bacteriol* 1999; 49(Pt 2): 415–440.
158. Bannasch MJ, Foley JE. Epidemiologic evaluation of multiple respiratory pathogens in cats in animal shelters. *J Feline Med Surg* 2005; 7: 109–119.
159. Cai Y, Fukushi H, Koyasu S, et al. An etiological investigation of domestic cats with conjunctivitis and upper respiratory tract disease in Japan. *J Vet Med Sci* 2002; 64: 215–219.
160. Hoover EA, Kahn DE, Langloss JM. Experimentally induced feline chlamydial infection (feline pneumonitis). *Am J Vet Res* 1978; 39: 541–547.
161. Wills JM, Howard PE, Gruffydd-Jones TJ, Wathes CM. Prevalence of *Chlamydia psittaci* in different cat populations in Britain. *J Sm Anim Pract* 1988; 29: 327–329.
162. Shewan PE, Povey RC, Wilson MR. A survey of the conjunctival flora of clinically normal cats and cats with conjunctivitis. *Can Vet J* 1980; 21: 231–233.
163. Lazarowics M. A serological survey in cats for antibodies to respiratory virus and chlamydia. *Z Versuchstierked* 1977; 19: 325.
164. Studdert MJ, Studdert VP, Wirth HJ. Isolation of *Chlamydia psittaci* from cats with conjunctivitis. *Aust Vet J* 1982; 57: 515–517.
165. Wills JM, Gruffydd-Jones TJ, Richmond SJ, Gaskell RM, Bourne FJ. Effect of vaccination on feline *Chlamydia psittaci* infection. *Infect Immun* 1987; 55: 2653–2657.
166. Hargis AM, Prieur DJ, Gaillard ET. Chlamydial infection of the gastric mucosa in twelve cats. *Vet Pathol* 1983; 20: 170–178.
167. Hopkins JB, Stephenson EH, Storz J, Pierson RE. Conjunctivitis associated with chlamydial polyarthritis in lambs. *J Am Anim Hosp Assoc* 1973; 163: 1157–1160.
168. Navarro JA, Garcia de la Fuente JN, Sanchez J, et al. Kinetics of infection and effects on the placenta of *Chlamydophila abortus* in experimentally infected pregnant ewes. *Vet Pathol* 2004; 41: 498–505.
169. Nietfeld JC. Chlamydial infections in small ruminants. *Vet Clin N Am: Food Anim Pract* 2000; 17: 301–314.
170. Rogers DG, Andersen AA, Hogg A, Nielsen DL, Huebert MA. Conjunctivitis and keratoconjunctivitis associated with chlamydiae in swine. *J Am Anim Hosp Assoc* 1993; 203: 1321–1323.
171. Ostler HB, Schachter J, Dawson CR. Acute follicular conjunctivitis of epizootic origin. Feline pneumonitis. *Arch Ophthalmol* 1969; 82: 587–591.
172. Schachter J, Arnstein P, Dawson CR, Hanna L, Thygeson P, Meyer KF. 1968. Human follicular conjunctivitis caused by infection with a psittacosis agent. Proceed Soc Exp Biol Med 1968; 127: 292–295.
173. Hartley JC, Stevenson S, Robinson AJ, et al. Conjunctivitis due to *Chlamydophila felis* (Chlamydia psittaci feline pneumonitis agent) acquired from a cat: Case report with molecular characterization of isolates from the patient and cat. *J Infect* 2001; 43: 7–11.
174. Lipman NS, Yan LL, Murphy JC. Probable transmission of *Chlamydia psittaci* from a macaw to a cat. *J Am Anim Hosp Assoc* 1994; 204: 1479–1480.
175. Williams LP Jr. Review of the epidemiology of chlamydiosis in the United States. *J Am Anim Hosp Assoc* 1989; 195: 1518–1521.
176. Smith H. The revival of interest in mechanisms of bacterial pathogenicity. *Biol Rev Camb Philos Soc* 1995; 70: 277–316.
177. Razin S, Jacobs E. Mycoplasma adhesion. *J Gen Microbiol* 1992; 138: 407–422.
178. Rhem MN, McDevitt DL, Penland RL, Hook M, Wilhelmus KR. The role of adhesion molecules in the pathogenesis of

Staphylococcus aureus keratitis. *Invest Ophthalmol Vis Sci* 1996; 37: 417.
179. Wu X, Gupta SK, Hazlett LD. Characterization of *P. aeruginosa* pili binding human corneal epithelial proteins. *Curr Eye Res* 1995; 14: 969–977.
180. Beachey EH. Bacterial adherence: Adhesin-receptor interactions mediating the attachment of bacteria to mucosal surface. *J Infect Dis* 1981; 143: 325–345.
181. Ramphal R, Pyle M. Evidence for mucins and sialic acid as receptors for *Pseudomonas aeruginosa* in the lower respiratory tract. *Infect Immun* 1983; 41: 339–344.
182. Gipson IK, Riddle CV, Kiorpes TC, Spurr SJ. Lectin binding to cell surfaces: Comparisons between normal and migrating corneal epithelium. *Develop Biol* 1983; 96: 337–345.
183. Gupta SK, Masinick SA, Hobden JA, Berk RS, Hazlett LD. Bacterial proteases and adherence of *Pseudomonas aeruginosa* to mouse cornea. *Exp Eye Res 1996;* 62: 641–650.
184. Reichert R, Stern G. Quantitative adherence of bacteria to human corneal epithelial cells. *Arch Ophthalmol* 1984; 102: 1394–1395.
185. Morihara K. Production of elastase and proteinase by *Pseudomonas aeruginosa*. *J Bacteriol* 1964; 88: 745–757.
186. Kawaharajo K, Abe C, Homma JY, Kawano M, Goto E. Corneal ulcers caused by protease and elastase from *Pseudomonas aeruginosa*. *Jpn J Exper Med* 1974; 44: 435–442.
187. Heck LW, Morihara K, McRae WB, Miller EJ. Specific cleavage of human type III and IV collagens by *Pseudomonas aeruginosa* elastase. *Infect Immun* 1986; 51: 115–118.
188. Brown SI, Bloomfield SE, Tam W. The cornea-destroying enzyme of *Pseudomonas aeruginosa*. *Invest Ophthalmol Vis Sci* 1974; 13: 174–180.
189. Kessler E, Kennah HE, Brown SI. Pseudomonas protease. Purification, partial characterization, and its effect on collagen, proteoglycan, and rabbit corneas. *Invest Ophthalmol Vis Sci* 1977; 16: 488–497.
190. Kreger AS, Gray LD. Purification of *Pseudomonas aeruginosa* proteases and microscopic characterization of pseudomonal protease-induced rabbit corneal damage. *Infect Immun* 1978; 19: 630–648.
191. Twining SS, Davis SD, Hyndiuk RA. Relationship between proteases and descemetocele formation in experimental Pseudomonas keratitis. *Curr Eye Res* 1986; 5: 503–510.
192. Pedersen KB, Froholm LO, Bovre K. Fimbriation and colony type of *Moraxella bovis* in relation to conjunctival colonization and development of keratoconjunctivitis in cattle. *Acta Pathol Microbiol Scand* 1972; 80: 911–918.
193. Chandler RL, Bird RG, Smith MD, Anger HS, Turfrey BA. Scanning electron microscope studies on preparations of bovine cornea exposed to *Moraxella bovis*. *J Comp Pathol* 1983; 93: 1–8.
194. Ruehl WW, Marrs CF, Fernandez R, Falkow S, Schoolnik GK. Purification, characterization, and pathogenicity of *Moraxella bovis* pili. *J Exp Med* 1988; 168: 983–1002.
195. Pfister RR. The normal surface of corneal epithelium: A scanning electron microscopic study. *Invest Ophthalmol Vis Sci* 1973; 12: 654–668.
196. Marrs CF, Schoolnik G, Koomey JM, Hardy J, Rothbard J, Falkow S. Cloning and sequencing of a *Moraxella bovis* pilin gene. *J Bacteriol* 1985; 163: 132–139.
197. Ruehl WW, Marrs CF, George L, Banks SJ, Schoolnik GK. Infection rates, disease frequency, pilin gene rearrangement, and pilin expression in calves inoculated with *Moraxella bovis* pilin-specific isogenic variants. *Am J Vet Res* 1993; 54: 248–253.
198. Pugh GW Jr., Hughes DE, McDonald TJ. Keratoconjunctivitis produced by *Moraxella bovis* in laboratory animals. *Am J Vet Res* 1968; 29: 2057–2061.
199. Ostle AG, Rosenbusch RF. *Moraxella bovis* hemolysin. *Am J Vet Res* 1984; 45: 1848–1851.
200. Clinkenbeard KD, Thiessen AE. Mechanism of action of *Moraxella bovis* hemolysin. *Infect Immun* 1991; 59: 1148–1152.
201. Gray JT, Fedorka-Cray PJ, Rogers DG. Partial characterization of a *Moraxella bovis* cytolysin. *Vet Microbiol* 1995; 43(2–3): 183–196.
202. Beard MK, Moore LJ. Reproduction of bovine keratoconjunctivitis with a purified haemolytic and cytotoxic fraction of *Moraxella bovis*. *Vet Microbiol* 1994; 42: 15–33.
203. Kagonyera GM, George LW, Munn R. Light and electron microscopic changes in corneas of healthy and immunomodulated calves infected with *Moraxella bovis*. *Am J Vet Res* 1988; 49: 386–395.
204. Halenda RM, Riley LK. Identification and characterization of a cell detachment factor produced by *Moraxella bovis* (abstract). *Invest Ophthalmol Vis Sci* 1996; 37: S417.
205. Varga JH, Wolf TC, Jensen HG. Swab culture of corneal ulcers. *Ophthalmology* 1992; 99: 1346.
206. Benson WH, Lanier JD. Comparison of techniques for culturing corneal ulcers. *Ophthalmology* 1992; 99: 800–804.
207. Jacob P, Gopinathan U, Sharma S, Rao GN. Calcium alginate swab versus Bard Parker blade in the diagnosis of microbial keratitis. *Cornea* 1995; 14: 360–364.
208. Stonecipher KG, Jensen H. Diagnosis, laboratory analysis, and treatment of bacterial corneal ulcers. *Opto Clin* 1995; 4: 53–64.
209. McLeod SD, Kolahdouz-Isfahani A, Rostamian K, Flowers CW, Lee PP, McDonnell PJ. The role of smears, cultures, and antibiotic sensitivity testing in the management of suspected infectious keratitis. *Ophthalmology* 1996; 103: 23–28.
210. Quinn PJ, Carter ME, Markey BK, Carter GE. *Clinical Veterinary Microbiology*. London: Wolfe, 1994.
211. Kaltenboeck B, Kousoulas KG, Storz J. Structures of and allelic diversity and relationships among the major outer membrane protein (ompA) genes of the four chlamydial species. *J Bacteriol* 1993; 175: 487–502.
212. Sykes JE, Studdert VP, Anderson G, Browning GF. Comparison of *Chlamydia psittaci* from cats with upper respiratory tract disease by polymerase chain reaction analysis of the ompA gene. *Vet Rec* 1997; 140: 310–313.
213. Di Francesco A, Baldelli R. Feline chlamydiosis in Italy: PCR amplification and analysis of the ompA and groEL-homolog genes. *New Microbiol* 2002; 25: 341–344.
214. Prescott JF, Baggot JD. Antimicrobial susceptibility testing and antimicrobial drug dosage. *J Am Anim Hosp Assoc* 1985; 187: 363–368.
215. La VD, Tran-Hung L, Aboudharam G, Raoult D, Drancourt M. *Bartonella quintana* in domestic cat. *Emerg Infect Dis* 2005; 11: 1287–1289.
216. Droz S, Chi B, Horn E, Steigerwalt AG, Whitney AM, Brenner DJ. *Bartonella koehlerae* sp. nov., isolated from cats. *J Clin Microbiol* 1999; 37: 1117–1122.
217. Gurfield AN, Boulouis HJ, Chomel BB, et al. Coinfection with *Bartonella clarridgeiae* and *Bartonella henselae* and with

different *Bartonella henselae* strains in domestic cats. *J Clin Microbiol* 1997; 35: 2120–2123.
218. Chomel BB, Carlos ET, Kasten RW, et al. Bartonella henselae and *Bartonella clarridgeiae* infection in domestic cats from the Philippines. *Am J Trop Med Hygien* 1999; 60: 593–597.
219. Shaw SE, Kenny MJ, Tasker S, Birtles RJ. Pathogen carriage by the cat flea *Ctenocephalides felis* (Bouche) in the United Kingdom. *Vet Microbiol* 2004; 102(3–4): 183–188.
220. Chomel BB, Kasten RW, Floyd-Hawkins K, et al. Experimental transmission of *Bartonella henselae* by the cat flea. *J Clin Microbiol* 1996; 34: 1952–1956.
221. Abbott RC, Chomel BB, Kasten RW, et al. Experimental and natural infection with *Bartonella henselae* in domestic cats. *Comp Immunol, Microbiol Infect Dis* 1997; 20: 41–51.
222. Guptill L, Slater L, Wu CC, et al. Experimental infection of young specific pathogen-free cats with *Bartonella henselae*. *J Infect Dis* 1997; 176: 206–216.
223. Dehio C. Bartonella interactions with endothelial cells and erythrocytes. *Trend Microbiol* 2001; 9: 279–285.
224. Kordick DL, Hilyard EJ, Hadfield TL, et al. *Bartonella clarridgeiae,* a newly recognized zoonotic pathogen causing inoculation papules, fever, and lymphadenopathy (cat scratch disease). *J Clin Microbiol* 1997; 35: 1813–1818.
225. Kordick DL, Brown TT, Shin K, Breitschwerdt EB. Clinical and pathologic evaluation of chronic *Bartonella henselae* or *Bartonella clarridgeiae* infection in cats. *J Clin Microbiol* 1999; 37: 1536–1547.
226. Kordick DL, Breitschwerdt EB. Relapsing bacteremia after blood transmission of *Bartonella henselae* to cats. *Am J Vet Res* 1997; 58: 492–497.
227. O'Reilly KL, Bauer RW, Freeland RL, et al. Acute clinical disease in cats following infection with a pathogenic strain of *Bartonella henselae* (LSU16). *Infect Immun* 1999; 67: 3066–3072.
228. Mikolajczyk MG, O'Reilly KL. Clinical disease in kittens inoculated with a pathogenic strain of *Bartonella henselae*. *Am J Vet Res* 2000; 61: 375–379.
229. Chomel BB, Wey AC, Kasten RW, Stacy BA, Labelle P. Fatal case of endocarditis associated with *Bartonella henselae* type I infection in a domestic cat. *J Clin Microbiol* 2003; 41: 5337–5339.
230. Lappin MR, Black JC. 1999. *Bartonella* spp. infection as a possible cause of uveitis in a cat. *J Am Anim Hosp Assoc* 1999; 21: 1205–1207.
231. Lappin MR, Kordick DL, Breitschwerdt EB. *Bartonella* spp antibodies and DNA in aqueous humor of cats. *J Feline Med Surg* 2000; 2: 61–68.
232. Michau TM, Breitschwerdt EB, Gilger BC, Davidson MG. *Bartonella vinsonii* subspecies *berkhoffi* as a possible cause of anterior uveitis and choroiditis in a dog. *Vet Ophthalmol* 2003; 6: 299–304.
233. Roy AF, Corstvet RE, Tapp RA, O'Reilly KL, Cox HU. Evaluation and use of a nested polymerase chain reaction assay in cats experimentally infected with *Bartonella henselae* genotype I and *Bartonella henselae* genotype II. *J Vet Diag Invest* 2001; 13: 312–322.
234. Davidson MG, Breitschwerdt EB, Nasisse MP, Roberts SM. Ocular manifestations of Rocky Mountain spotted fever in dogs. *J Am Anim Hosp Assoc* 1989; 194: 777–781.
235. Leiva M, Naranjo C, Pena MT. Ocular signs of canine monocytic ehrlichiosis: A retrospective study in dogs from Barcelona, Spain. *Vet Ophthalmol* 2005; 8: 387–393.
236. Glaze MB, Gaunt SD. Uveitis associated with *Ehrlichia platys* infection in a dog. *J Am Anim Hosp Assoc* 1986; 189: 916–917.
237. Samuelson DA, Andresen TL, Gwin RM. Conjunctival fungal flora in horses, cattle, dogs, and cats. *J Am Anim Hosp Assoc* 1984; 184: 1240–1242.
238. Welch PM, Gabal M, Betts DM, Whelan NC, Studer ME. In vitro analysis of antiangiogenic activity of fungi isolated from clinical cases of equine keratomycosis. *Vet Ophthalmol* 2000; 3(2–3): 145–151.
239. Miller DM, Blue JL, Winston SM. Keratomycosis caused by Cladosporium sp in a cat. *J Am Anim Hosp Assoc* 1983; 183: 1121–1122.
240. Mendoza L, Donato A, Padhye A. Canine mycotic keratoconjunctivitis caused by *Acremonium kiliense*. *Sabouraudia* 1985; 23: 447–450.
241. Qualls CW Jr., Chandler FW, Kaplan W, Breitschwerdt EB, Cho DY. Mycotic keratitis in a dog: Concurrent Aspergillus sp and Curvularia sp infections. *J Am Anim Hosp Assoc* 1985; 186: 975–976.
242. Peiffer RL, Jackson WF. Mycotic keratopathy of the dog and cat in the southeastern United States. A preliminary report. *J Am Anim Hosp Assoc* 1979; 15: 93–97.
243. Kern TJ, Brooks DE, White MM. Equine keratomycosis: Current concepts of diagnosis and therapy. *Eq Vet J* 1983; 2(Supplement): 33–38.
244. Beech J, Sweeny CR, Irby N. Keratomycosis in 11 horses. *Eq Vet J* 1983; 2(suppl): 39–44.
245. Barton MH. Equine keratomycosis. *Compend Contin Ed Pract Vet* 1992; 14: 936–944.
246. Grahn B, Wolfer J, Keller C, Wilcock BP. Equine keratomycosis: Clinical and laboratory findings in 23 cases. *Prog Vet Comp Ophthalmol* 1992; 3: 2–7.
247. Hendrix DV, Chmiemlewski NT, Smith PJ, Brooks DE, Gelatt KN, Whittaker C. Keratomycosis in four horses caused by *Clindrocarpen destructans*. *Vet Comp Ophthalmol* 1996; 6: 252–257.
248. Garcia ML, Herreras JM, Dios E, Argueso P, Almaraz A. Evaluation of lectin staining in the diagnosis of fungal keratitis in an experimental rabbit model. *Mol Vision* 2002; 8: 10–16.
249. Jackson JA. Immunodiagnosis of systemic mycoses in animals: A review. *J Am Anim Hosp Assoc* 1986; 18: 702–705.
250. Stevens DA. Antifungal drug susceptibility testing. A critical review. *Mycopathologia* 1984; 87: 135–140.
251. Drutz DJ. In vitro antifungal susceptibility testing and measurement of levels of antifungal agents in body fluids. *Review Infect Dis* 1987; 9: 392–397.
252. Kumar M, Shukla PK. Use of PCR targeting of internal transcribed spacer regions and single-stranded conformation polymorphism analysis of sequence variation in different regions of rRNA genes in fungi for rapid diagnosis of mycotic keratitis. *J Clin Microbiol* 2005; 43: 662–668.
253. Kumar M, Mishra NK, Shukla PK. Sensitive and rapid polymerase chain reaction based diagnosis of mycotic keratitis through single stranded conformation polymorphism. *Am J Ophthalmol* 2005; 140: 851–857.
254. Belknap EB, Bardem CA, Yin C, Colitz CMH, Belknap JK. Real-time PCR as a diagnostic tool for equine fungal keratitis: A preliminary study (abstract). Proceed 36th Ann Meeting Am Coll Vet Ophthalmol 2005: 7.
255. Chavkin MJ, Lappin MR, Powell CC, Cooper CM, Munana KR, Howard LH. *Toxoplasma gondii*-specific antibodies in the

aqueous humor of cats with toxoplasmosis. *Am J Vet Res* 1994; 55: 1244–1249.
256. Davidson MG, Nasisse MP, English RV, Wilcock BP, Jamieson VE. Feline anterior uveitis: A study of 53 cases. *J Am Anim Hosp Assoc* 1991; 27: 77–83.
257. Dubey JP, Carpenter JL. Histologically confirmed clinical toxoplasmosis in cats: 100 cases (1952–1990). *J Am Anim Hosp Assoc* 1993; 203: 1556–1566.
258. Davidson MG, Lappin MR, English RV, Tompkins MB. A feline model of ocular toxoplasmosis. *Invest Ophthalmol Vis Sci* 1993; 34: 3653–3660.
259. Peiffer RL Jr., Wilcock BP. Histopathologic study of uveitis in cats: 139 cases (1978–1988). *J Am Anim Hosp Assoc* 1991; 19: 135–138.
260. Chavkin MJ, Lappin MR, Powell CC, Roberts SJ, Parshall CJ, Reif JS. Seroepidemiologic and clinical observations of 93 case of uveitis in cats. *Prog Vet Comp Ophthalmol* 1992; 2: 29–36.
261. Lappin MR, Cayatte S, Powell CC, Gigliotti A, Cooper C, Roberts SM. Detection of *Toxoplasma gondii* antigen-containing immune complexes in the serum of cats. *Am J Vet Res* 1993; 54: 415–419.
262. Burney DP, Lappin MR, Cooper C, Spilker MM. Detection of *toxoplasma gondii*-specific IgA in the serum of cats. *Am J Vet Res* 1995; 56: 769–773.
263. Lappin MR, Roberts SM, Davidson MG, Powell CC, Reif JS. Enzyme-linked immunosorbent assays for the detection of *toxoplasma gondii*-specific antibodies and antigens in the aqueous humor of cats. *J Am Anim Hosp Assoc* 1992; 201: 1010–1016.
264. Hill SL, Lappin MR, Carman J, et al. Comparison of methods for estimation of *toxoplasma gondii*-specific antibody production in the aqueous humor of cats. *Am J Vet Res* 1995; 56:1181–1187.
265. Lappin MR, Burney DP, Hill SA, Chavkin MJ. Detection of *toxoplasma gondii*-specific IgA in the aqueous humor of cats. *Am J Vet Res* 1995; 56: 774–778.
266. Cook JR, Jr., Tyler DE, Coulter DB, Chandler FW. Disseminated protothecosis causing acute blindness and deafness in a dog. *J Am Anim Hosp Assoc* 1984; 18: 1266–1272.
267. Merideth RE, Gwin RM, Samuelson DA, Gelatt KN, Buffolano W. Systemic protothecosis with ocular manifestation in a dog. *J Am Anim Hosp Assoc* 1984; 20: 153–156.
268. Schultze AE, Ring RD, Morgan RV, Patton CS. Clinical, cytologic and histopathologic manifestations of protothecosis in two dogs. *Vet Ophthalmol* 1998; 1: 239–243.
269. Buyukmihci N, Rubin LF, DePaoli A. Protothecosis with ocular involvement in a dog. *J Am Anim Hosp Assoc* 1975; 167: 158–161.
270. Migaki G, Font RL, Sauer RM, Kaplan W, Miller RL. Canine protothecosis: Review of the literature and report of an additional case. *J Am Anim Hosp Assoc* 1982; 181: 794–797.
271. Carlton WW, Austin L. Ocular protothecosis in a dog. *Vet Pathol* 1973; 10: 274–280.
272. Hosaka S, Hosaka M. A case report of canine protothecosis. *J Vet Med Sci* 2004; 66(5): 593–597.
273. Font RL, Hook SR. Metastatic protothecal retinitis in a dog. Electron microscopic observations. *Vet Pathol* 1984; 21: 61–66.

Chapter 7

Clinical Pharmacology and Therapeutics

Part 1: Drug Delivery

Alain Regnier

DRUG DELIVERY

Introduction

Ocular responses to drugs are correlated with the concentration of active ingredient at the intended site of action, referred to as the biophase. In ocular therapy, drug choice is based not only on pharmacodynamic potency but also on pharmacokinetic properties to select the most suitable route of administration and dosage regimen; these, in turn, must ensure the presence of an effective drug concentration in the target biophase for an appropriate period while limiting diffusion of the drug to other ocular structures or parts of the body. The dosage regimen and route of administration should also be adapted to clinical management of the patient in order to maximize owner compliance.[1–3]

Although the external eye is readily accessible for drug administration, efficient drug delivery to the eye is difficult because the eye is a unique organ in that it has several functional and structural protective mechanisms. Mechanisms such as blinking, permanent lacrimation, and lacrimal drainage, which are necessary to preserve visual acuity, also favor rapid removal of drugs that are applied to the ocular surface. The globe itself is protected physically by tough layers of sclera and cornea that can exclude not only noxious chemicals but also drugs from the inner eye. Additionally, the internal ocular structures are isolated anatomically from the systemic circulation by blood–ocular barriers, which are critical for maintaining the delicate homeostasis of the ocular transparent media but which act as major obstacles for the access of topical or systemic medications to intraocular target tissues. Depending on site of the ocular tissue target to be reached, drugs used in ophthalmology are administered locally or systemically, and the main factors to be considered when drug delivery to the eye is attempted therefore include (a) how to cross the external layers of the globe (cornea, conjunctiva and sclera) or blood–ocular barriers to reach an intraocular site; (b) how to localize drug actions at the ocular tissues while minimizing systemic effects; and (c) how to prolong the duration of drug actions such that the frequency of drug administration can be minimized.[4]

Topical Administration

Topical administration is the most common route of administration for ophthalmic drugs because of its advantages, including simplicity of application and convenience to reach both extra- and intraocular tissue targets. The pharmacokinetic profile of topically applied ophthalmic drugs is influenced by precorneal factors (i.e., lacrimation, drainage) and the specific characteristics of the formulation itself that will determine the amount of drug penetrating the eye.

Ophthalmic Solutions and Suspensions

Eye drops represent the pharmaceutical formulations most widely used in ophthalmology and consist of solutions and suspensions. Ophthalmic solutions are formulations in which the drug is totally dissolved in a given solvent. Typically, they are low-viscosity, aqueous solutions mixable with the aqueous tear film. Thus, the drug must be, at least to some degree, water soluble. Some exceptions exist, like compounded preparations of cyclosporine in corn or olive oil.[5] To minimize irritation of the eye, ophthalmic solutions must ideally have an osmolality (tonicity) of about 300 mOsm/kg, which is the tonicity of normal tears. However, various studies have shown that the eye can tolerate solutions with an osmolality in the range of 200 to 600 mOsm/kg, or 0.2% to 2.0% in NaCl equivalents.[3,6] Sodium chloride, boric acid, and dextrose are used to modify tonicity. Ophthalmic solutions must fall within a pH between 4.5 to 9 to be comfortable to patients and not induce tearing and blinking reflexes.[3,6] To improve stability and sterility, ophthalmic solutions are formulated with appropriate vehicles that may contain buffers, organic or inorganic carriers, emulsifiers, and wetting agents. The advantages of solutions include relative ease in dispensing and use. In addition, most agents are well tolerated, cause little discomfort, and do not affect vision.[5] When frequent applications of ophthalmic solutions are required in horses (i.e., in the treatment of severe corneal infections), a continuous irrigation system, such as a subpalpebral lavage system or a nasolacrimal cannula, is necessary to provide frequent instillations with minimum handling.[7]

Pharmaceutical derivatives of low aqueous solubility, such as acetates and alcohols used as topical corticoids, require formulations as ophthalmic suspensions.[5] A suspension consists of particles of active ingredient in a saturated aqueous vehicle that includes dispersing and suspending agents designed to be instilled into the eye. The drug particles contained in suspension must be less than 10 μm, uniform in size, and micronized to prevent irritation of the ocular surface.[3,8] Similarly to the ophthalmic solutions, the suspensions should be formulated at a tonicity and a pH that are safe for the ocular surface.[3] Compared to solutions, ophthalmic suspensions have some disadvantages associated with the formulation and use. For manufacturers, suspensions present problems with regard to both method of sterilization and drug concentration, which can be manipulated only by increasing the number of particles. These problems may be overcome by the reformulation of ophthalmic suspensions as solutions, either by formulating water-soluble derivatives of the parent drugs (i.e., sodium phosphate salts for glucocorticoids) or complexing poorly water-soluble compounds with drug carriers such as cyclodextrins to increase their water solubility.[9] From a practical point of view, potential disadvantages of ophthalmic suspensions include the possibility of irritation due to suspended crystals or particles[10] and the need to be adequately shaken before use to disperse drug particles evenly throughout the vehicle and avoid incorrect dosing.[5,11]

All multidose eye preparations must include a bacteriostatic preservative (i.e., benzalkonium chloride, benzethonium chloride, methylparaben, propylparaben, mercurial compounds, thimerosal) to prevent or inhibit microbial growth during clinical use.[6,10] At appropriate concentrations, these preservatives must be safe, must be compatible with the other ingredients of the preparation, and must remain effective throughout the period of use of the eye drops. It is assumed that preserved eye drops in multidose containers do not become heavily contaminated for up to 1 month after opening, enabling these eye drops to be used for a maximum of 4 weeks.[12] Most preservatives, however, may have local deleterious effects, either by toxicity or hypersensitivity, and patients who become intolerant to preservatives then require eye drops prepared without added preservatives. Preserved ophthalmic preparations cannot be instilled on the injured eye or used during surgical intervention in the anterior chamber because of possible toxicity to the corneal endothelium, anterior uvea, or both.[10]

Unpreserved eye drops are supplied in unit dose containers or multidose bottles, but the range is still limited so they cannot be used in all cases.[12] Unpreserved eye drops supplied in multidose bottles should be stored at 2° to 8°C after opening to reduce the rate of replication of any microbial contaminants, and they should not be kept in use for more than 7 days.[12]

Drug Disposition after Instillation of Eye Drops

As indicated in Figure 7.1.1, an ophthalmic drug topically applied to the eye is distributed in three ways. It is drained by the nasolacrimal apparatus, may penetrate into the eye through the corneal and/or noncorneal routes, and is absorbed into the systemic circulation via the conjunctiva and nasopharynx.

Precorneal Area

Nasolacrimal Drainage and Tear Turnover When eye drops are administered to the ocular surface, they first mix with the tear film compartment, the volume of which is about 7 to 10 μl (with 1 μl covering the cornea and about 3 to 4 μl residing in each conjunctival sac), as estimated in man and rabbit.[13,14] The drop volume delivered by many ophthalmic dropper bottles is about 40 μL in average,[15] but actually it varies within a range of 25 to 70 μL depending on the design of the dropper tip, the physicochemical properties of the medication to be dispensed, and the manipulation of the dropper bottle.[16] Since the palpebral fissure is capable of holding only 25–30 μL of fluid,[17] the volume of most ophthalmic drops largely exceeds the volume of the cul-de-sac, so complete retention of this drop volume is unlikely to occur. As a consequence, the sudden increase of volume created by instillation of an eye drop will be diminished rapidly by escape of a large proportion of the instilled fluid into the nasolacrimal system and spillage over the lower eyelid.[18] Scintigraphic studies of ophthalmic solutions has shown that as a result of rapid drainage, most of the instilled solution is lost within the first 15 to 30 seconds.[14,19] The extra solution volume that enters the nasolacrimal apparatus will flow then to the nasopharynx, where swallowing of the drained fraction may contribute to some systemic side effects (i.e., salivation with atropine). Following removal of a substantial proportion of the drug subsequently to administration of such an excess volume, a second mechanism of clearance, represented by continual turnover of the tear film, will prevail until restoration of the normal tear volume occurs.[20] In normal, nonirritated human eyes, the secretion and drainage of tears occur at a rate of approximately 1 μL/min corresponding to a 15% turnover of the tear film per minute.[20] This washout results in almost complete disappearance of the applied fluid remaining on the ocular surface via lacrimal drainage within approximately 10 minutes.[20]

Factors Influencing the Drainage Rate The rate at which the instilled drug is eliminated from the ocular surface due to drainage by the nasolacrimal system is influenced by three main factors: the size of the drop delivered to the eye, the

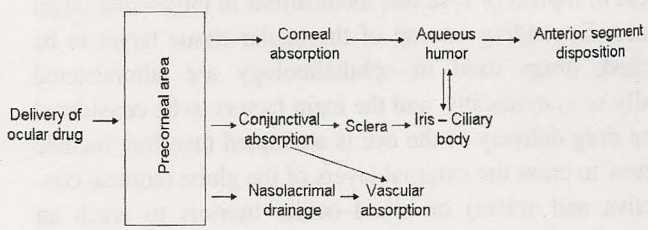

Figure 7.1.1

blinking frequency, and the tear flow dynamics. Within the cul-de-sac, the drainage rate of an instilled volume has been shown to be proportional to the volume of the drop that is above the normal lacrimal fluid volume. The larger the volume instilled, the more rapidly it is drained through the nasolacrimal system.[4] This is illustrated by data from pharmacokinetic models indicating that tear drainage within the first minute following topical application is 13 μL/min and 30 μL/min for a 25-μL and a 50-μL eye drop respectively.[21] As a result, 90% of a topically instilled dose in a rabbit eye is cleared within 2 minutes for an instilled volume of 50 μL, 4 minutes for an instilled volume of 25 μL, and 7.5 min for an instilled volume of 5 μL.[22] Thus, a strategy for minimizing the rate of drug loss through drainage would be to reduce the volume instilled to 5–15 μL.[23,24] Efficiency of this method, has been demonstrated experimentally and clinically.[25,26] For example, a single administration of a 10-μL drop of phenylephrine 10% to human volunteers resulted in the same mydriasis as a 30-μL drop of the same concentration.[26] A similar observation was made with 15-μL and 70-μL drops of clonidine 0.25 or 0.50% that produced an identical hypotensive ocular effect when applied to human eyes.[27]

For the same reasons, instillation of one drop immediately after another will reduce the availability of the first drug instilled because it will suffer a loss due to nasolacrimal drainage that is proportional to the time interval between instillations.[1] As an instilled drop is removed in about 10 minutes, dosage guidelines therefore recommend that at least 10 minutes elapse between the instillation of drops of different medications.[14]

Tear flow dynamics may also alter the drug residence time in the precorneal compartment if the instilled medication is an irritant by virtue of its pH and/or tonicity. As previously discussed, the pH of an ophthalmic preparation should be kept as close to the physiological pH as possible to avoid local irritation or foreign body sensation with enhanced lacrimation and blinking that will promote drug clearance through the lacrimal system.[14,28]

Penetration across the Cornea

After topical ocular application, drugs may be absorbed into the inner eye through the corneal or conjunctival-scleral route. The rate and extent of absorption through one route or the other is dependent both on transport characteristics of the cornea, conjunctiva, and sclera and on the physicochemical properties of the drug itself. Generally, the cornea has been regarded as the main route of absorption for clinically used ocular drugs because most of them have been developed with adequate properties for corneal absorption.[29,30]

Corneal Barriers The cornea consists of three primary layers, the epithelium, stroma, and endothelium, representing distinct barriers to absorption organized as an aqueous phase (stroma) sandwiched by two lipid layers (epithelium and endothelium). Kinetic studies using in vitro and in vivo techniques have shown that drugs penetrate the corneal epithelium either by partitioning through the cells (transcellular route) or diffusing between the cells (paracellular route).[31–33] This penetration is attributable to the presence of annular tight junctions (zonula occludens), which completely surround and seal the superficial cells to all but the smallest hydrophilic molecules.[34] It is thus anticipated that the transcellular drug penetration will be related to oil/water (o/w) partition coefficient because of the lipophilic nature of the epithelium, whereas paracellular movement will more likely be related to characteristics such as molecular size and aqueous diffusity.[35,36] As a consequence, the transcellular route across the lipid cell membrane will contribute to the epithelial transfer of lipophilic molecules, while small hydrophilic (polar) compounds will diffuse through the intercellular space, which represents the aqueous pore pathways of the corneal epithelium.[33,37] Ultrastructural studies determined that the intercellular space at its most confined point has a size ranging from 0.6 to less than 3 nm.[32]

If the epithelial layer is a rate-limiting barrier for highly polar drugs, at the opposite, the stroma with its 78% water content allows the free passage of compounds possessing high aqueous solubility and acts as a barrier to lipophilic molecules.[18] Although the endothelium is cellular, its permeability displays a strong dependence on both o/w partition coefficient and molecular size. This indicates that the endothelium does not provide significant resistance to lipophilic and hydrophilic ophthalmic drugs.[38] The significant permeability of the endothelium likely relates to the fact that it is only one cell thick and that these cells are connected by junctional gaps that do not provide any barrier for drug penetration.[4,18]

Thus, in order for an ophthalmic drug to penetrate the cornea, it must exhibit intermediate solubility characteristics, being soluble to some degree in both oil and water to penetrate the epithelium and stroma.[4] It is postulated that a good predictor of corneal penetration rate of drugs is the o/w partition coefficient and that maximal corneal penetration is obtained with drugs whose o/w partition coefficient range from 10:1 to 1000:1.[36] For moderately lipophilic drugs such as timolol and dexamethasone, the corneal epithelium contributes 50% to the total resistance to transport while the stroma and endothelium each contribute 25%.[28] For hydrophilic drugs such as epinephrine and pilocarpine, the corneal epithelium contributes more to the total resistance.[28]

Most ophthalmic drugs, being weak acids or bases, are present in solutions as both the unionized and ionized forms of the molecule. The ionized form can be a cation or an anion and is in equilibrium with the unionized form, also called the free-base form of the drug.[1,4,18] Penetration of ionizable drugs through the cornea follows the pH partition theory because they are hydrophilic in the ionized form and lipophilic when unionized.[1,4] When such a drug is applied on the eye, its unionized form predominantly penetrates the epithelium (Fig. 7.1.2). The paracellular pathway allows for only a small degree of permeation by the ionized form. Once the free base reaches the stroma, its abundance drives the reaction to convert the unionized form to the ionized form, which is the favored stromal diffusion. Upon reaching the endothelium,

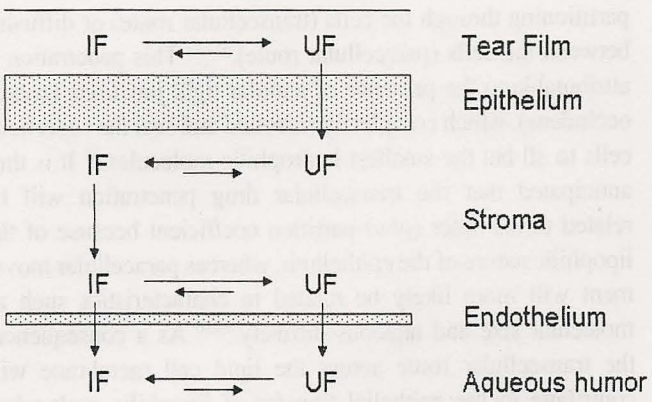

Figure 7.1.2.

another equilibrium is found, and penetration is achieved by both the ionized and unionized forms, because the endothelium is relatively permeable to drugs.[4,21]

Factors Influencing Corneal Absorption In the case of ionizable drugs, the pH of the ophthalmic preparation and of the tear fluid affect ocular drug penetration by influencing the ratio of the ionized (dissociated) and unionized (nondissociated) forms of the molecule in equilibrium. The degree of ionization of a drug in solution, and hence its capacity to diffuse across cellular barriers, is determined by its dissociation constant (pKa) and the solvent's pH. The dissociation constant is governed by the following relationship: pH = pKa + log[base]/[salt]. Thus, small changes in the pH can significantly affect the degree of drug dissociation in the formulation.[14] By using buffer solutions, the pH can be adjusted to increase the proportion of the unionized fraction, the more-lipophilic species, of the drug molecule, thereby facilitating penetration across the lipid barrier of the corneal epithelium. If we consider the activity of tropicamide and atropine on the isolated iris sphincter, tropicamide has 1/70 the affinity of atropine for muscarinic receptors. Both drugs topically applied as a 1% solution, however, are equally effective as mydriatics because a larger proportion of tropicamide (pKa = 5.4) compared to atropine (pKa = 9.7) will exist as unionized at tear pH and will be rapidly transferred through the cornea to intraocular target tissues.[40] Penetration of pilocarpine, a weak base, increases more than 10-fold when its pH is changed from 7 to 9.5. However, the pH of pilocarpine formulations must be kept within 4.5 to 5.5 to ensure drug stability.[40]

Protein binding of topical drugs is known to occur in the precorneal tear film, rendering the bound fraction no longer available for absorption. As local inflammation increases tear protein content, drug loss by this route may gain significance during topical treatment.[18] Experimentally, a 75- to 100-fold reduction in pupillary response to pilocarpine was found in rabbits by addition of 3% albumin to tear fluid.[14] In an effort to minimize this effect, agents such as cetylpyridinium that compete with the drug's binding site to lacrimal proteins were shown to increase ocular availability of topically applied drugs such as pilocarpine.[14]

Penetration through the cornea is controlled by the gradient of drug concentration. However, the possible increase of drug concentration in the formulation is limited by the extent of induced lacrimation, since after instillation of a hyperosmotic solution, fluids are osmotically removed from the surrounding ocular tissues so that complete dilution to isotonicity occurs rapidly.[14]

Hydrophilic drugs that penetrate poorly through the intact epithelium reach very high levels in the cornea when the epithelium is damaged or inflamed. In the case of a corneal ulcer, drug is further retained by the craterlike effect of irregular tissue margins.[2] Experimentally, it has been shown that penetration into the cornea and anterior chamber of a topically applied hydrophilic antifungal agent is increased up to ninefold when 25% to 50% of the surface area of the corneal epithelium is removed.[41] The possible clinical implication of these findings is that corneal epithelial debridement may be performed in some situations (i.e., keratomycosis or corneal abscess beneath an intact epithelium) to allow better penetration of therapeutic drugs into the deep corneal stroma and anterior chamber.[41] At the opposite, the effect of epithelial damage should be low or negligible for lipophilic drugs, which normally penetrate the epithelium very readily.[35] As discussed in a later section, the permeability of corneal epithelium may also be altered by chemical action of compounds such as surfactant or chelating agents.

Noncorneal Absorption Route

In the two last decades, studies have shown that the conjunctival-scleral absorption of ocularly applied drugs contributes to the ocular absorption known as noncorneal absorption. The noncorneal absorption route through conjunctiva and sclera is important mostly for very hydrophilic and large molecules that are not able to penetrate through the corneal barrier.[42] The conjunctiva is more permeable than the cornea through a significant paracellular route, which makes its permeability to molecules of varying physicochemical characteristics, such as β-blockers, hydrophilic macromolecules, and [^{3}H]mannitol, 2 to 30 times higher than that of the cornea.[37,43–46] In addition, data indicate that there is not a large difference between the permeability coefficients of ionized and unionized forms, which can also be explained by the richness of paracellular routes of the conjunctival membrane.[47]

Once the drug penetrates the conjunctiva, there are two distinct possibilities for it to reach the intraocular target tissues. It can diffuse through the sclera to enter certain intraocular tissues bypassing the anterior chamber. Data of in vitro experiments on scleral permeability indicate that the scleral permeability is approximately 10 times more than in the cornea.[46,48] The primary route for solute transport through the sclera is by passive diffusion through the interfibrillar aqueous media of the gel-like proteoglycans.[49] Transscleral diffusion is unaffected by the intraocular pressure, at pressures ranging from 0 to 60 mmHg, and allows the transfer of compounds with a molecular weight as high as 150 kDa.[50,51] Other in vitro data also indicate that if a topically applied drug is preferentially absorbed by the scleral route, its transfer will be more

rapid through the sclera than it would be through the cornea.[52] Access to the posterior segment is also possible through the sclera for hydrophilic drugs and could be four times more effective than through the cornea.[47] Recent investigations demonstrated that scleral permeability is enhanced with exposure to prostaglandins (PGs) or PG analogues, such as latanoprost,[53,54] suggesting that the prospect of increasing transscleral permeability by PG cotreatment might allow sufficient transscleral transport to provide delivery of macromolecules, such as trophic factors, to the retina.[53,54] The other possibility for drug penetration through the conjunctival-scleral pathway is that once the drug is absorbed into the conjunctival-scleral tissue, a significant portion enters scleral vessels that supply the uvea, particularly the anterior ciliary arteries, and deposits within the ciliary body.[55] Although the proportion of drug entering the eye by the two routes of the conjunctival-scleral pathway is not known, vessel uptake and deposition at the iris-ciliary body was found to be significant for drugs such as the topical carbonic anhydrase inhibitors.[55]

No ophthalmic drug delivery systems have been designed to specifically promote noncorneal drug penetration, but it is possible that this end result can be obtained from the inserts and microparticulate systems (e.g., nanoparticles) because they are placed in the fornices. When timolol was applied to rabbit eyes, the drug concentration in the conjunctiva and the amount of drug penetrating the iris-ciliary body and aqueous humor were significantly higher using ocular inserts rather than eye drops. In light of these findings, it was concluded that after application of the insert into the fornix, the iris-ciliary body would absorb the drug that has penetrated through the conjunctiva and sclera.[56] The mucoadhesive polymer polycarbophil was also shown to enhance the ocular uptake of gentamicin, presumably by facilitating the drug transfer through the conjunctival-scleral pathway, which was facilitated by the prolonged contact time between the mucoadhesive polymer and the underlying bulbar conjunctiva.[57]

Systemic Absorption

Mechanisms and Consequences As mentioned earlier, a large part from each drop applied to any eye is drained through the nasolacrimal system, where the vascularized lining of the nasolacrimal duct and nasopharyngeal mucosa is available for absorption.[4,14] It has been shown in the rabbit that the epithelium of the nasolacrimal passage is able to absorb lipophilic substances, and it is most likely that lipophilic components of tear fluid or drugs from tear drop are also readily absorbed by the nasolacrimal ducts in other species.[58]

Systemic drug absorption also results from uptake by fenestrated blood vessels located in the conjunctiva/episclera and must also be considered.[4,14,18] This seems the case for the ophthalmic β-blockers, which show an extremely low drug concentration in plasma after corneal application compared to conjunctival and scleral applications.[47] Both transconjunctival absorption and transnasal absorption after drainage via the nasolacrimal duct are generally undesirable not only because the dose fraction that is removed by the systemic circulation fails to contribute to the production of an ocular effect but also because it may participate in systemic side effects. The significance of circulatory system access by topical agents is that these medications entering the systemic circulation through the nasolacrimal mucosa bypass the primary metabolism in the liver in this way. The administration of eye drops has therefore been compared with a slow intravenous injection, which can account for the systemic toxicity of some topically applied ophthalmic preparations such as β-blockers. The systemic toxicity that may be observed in the dog after topical application of some ophthalmic preparations such as phenylephrine, glucocorticoids, and timolol has been reviewed recently.[59,60] Reduction of vascular absorption may be promoted by either decreasing nasolacrimal drainage of the instilled drug or increasing its ocular penetration. In humans, nasolacrimal occlusion (NLO) and eyelid closure are simple techniques that not only increase the ocular bioavailability of topically applied ocular drugs but also reduce the severity of adverse systemic effects. In one experiment, systemic absorption of topical timolol was reduced more than 60% and ocular absorption increased by 70% in patients practicing NLO or eyelid closure for 5 minutes after eye drop application.[61,62] These maneuvers eliminate the pump action of the eyelids, increase corneal contact time, and minimize the amount of drug delivered to the lacrimal and nasopharyngeal mucosa, hence improving the efficacy and safety margin for eye drops.[61,63] However, the effect of NLO on the systemic absorption is probably best for drugs that are mostly absorbed from the nasopharyngeal mucosa, because it has no effect on systemic absorption via conjunctiva.[64] It has also been proposed to reduce drug uptake by conjunctiva by inducing vasoconstriction in conjunctiva and nasal mucosa with topical phenylephrine.[65] In rabbits, it was found that the systemic bioavailability of timolol from eye drops was decreased from 73% to 38% by co-administering timolol with phenylephrine.[65]

Systemic Delivery of Peptides through Ocular Route Since most of the instilled drugs are absorbed systemically, the technique to deliver peptide drugs into systemic circulation via ocular route has been extensively studied in experimental animals.[28,66] Currently, most peptide drugs are administered by parenteral injection because extensive hydrolysis within the gastrointestinal tract results in poor oral bioavailability. Because repeated injections are poorly accepted by patients, nonoral routes have been investigated as alternatives for systemic drug delivery. Among those is the ocular route, since the mucous membrane in the conjunctiva and nasal cavity are permeable to macromolecular compounds.[66] Small peptides such as thyrotropin-releasing hormone (MW 360) and luteinizing hormone-releasing hormone (MW 1200) are easily absorbed by the ocular route compared to larger polypeptides such as insulin (MW 6000), which need to be combined with permeation enhancers or emulsants, like saponin, the nonionic surfactants BL-9 and Brij-78, and certain alkylglycosides to penetrate ocular membranes after topical application.[28,67] The delivery of systemic insulin through the ocular route was investigated in the late 1990s in healthy cats and dogs[68,69] and in the diabetic dog.[70]

Such data demonstrated that systemic absorption of insulin may occur subsequently to topical ocular administration. To the author's knowledge, the ocular route of insulin administration is not currently used in small animals, but systemic delivery of antidiuretic hormone (ADH) through ocular route is exploited in the treatment of canine diabetes insipidus.

Inside the Eye

Distribution

Following intraocular penetration of topically applied drugs, their subsequent distribution and retention at the target site is critical to their therapeutic success. Those drugs that diffuse through the cornea enter the aqueous humor first and then are distributed to the iris-ciliary body, lens, and vitreous. Drug levels reached in the iris-ciliary body are similar to those achieved in the aqueous humor, but levels in the lens and vitreous body are consistently lower.[14] Topically applied drugs that penetrate the eye via the noncorneal route of entry reach higher concentrations in the iris-ciliary body than in the aqueous humor because scleral penetration permits the drug to reach the target tissue first without entering the aqueous humor.[1,14] Aqueous outflow is presumed to be the primary route of drug elimination from the eye, although loss of drug may occur by additional pathways (i.e., retinal blood flow) or processes such as metabolism and drug binding to distinctive tissues.[1,14]

Melanin Binding

The iris and ciliary body have a heavily pigmented layer of epithelial cells, which can influence the pharmacological effect of instilled ophthalmic drugs, because accumulation of drug in this pigmented tissue by melanin binding decreases the free drug concentration available for target tissues.[2] Melanin acts as a site of loss for the drug so that the concentration at the target decreases, leading initially to smaller ocular effects. This explains that the higher the amount of melanin in the eye, the smaller is the initial mydriatic effect of atropine.[71] Subsequently, the pigmented iris accumulates relatively greater amounts of substance than the albino iris, and the pigmented anterior uvea forms a drug reservoir. During the elimination phase of the drug action, the pigment granules slowly release the drug as a sustained-release preparation, resulting in prolonged duration of action. It was found in the rabbit that pilocarpine can accumulate up to 10 times more in the pigmented than in the albino anterior uvea and that its miotic effects are significantly prolonged in the pigmented rabbit eyes compared to albino eyes.[72,73] Similarly, when applied topically to albino and pigmented eye, the duration of the mydriatic effect of atropine is 3 to 4 times longer in the pigmented than in the albino eye.[71] Affinity to melanin of the iris-ciliary body was reported for antibiotics, such as amikacin,[74] minocycline,[75] and sparfloxacin,[76] that concentrate in the pigmented layers of the eye. The reduced hypotensive ocular effect of timolol observed in people with darker irides was attributed to melanin binding.[77]

By affecting the bioavailability of topically applied drugs, ocular pigmentation may also decrease their local toxic effects. In the rabbit, for example, it was found that ocular pigmentation protects the retina from the toxic action of gentamicin. This protective effect probably reflects binding of the drug by the melanin, which thereby reduces the concentration of the free gentamicin.[78]

Drug Metabolism

Ocular drug metabolism was a neglected area of research until the discovery during the last 10 years that topically applied drugs may be metabolized during transport across the corneal epithelium and/or after reaching their sites of action in the anterior segment of the eye and that metabolism can be exploited to develop new ophthalmic drugs with superior pharmacological properties to the parent compound, such as prodrugs and soft drug analogues.[2,36] Enzyme systems identified to play a role in ocular drug metabolism include esterases, N-acetyltransferase, catechol-O-methyltransferase, monoamine oxidase, lysosomal enzymes, peptidases, and sulphate transferase.[1] Esterase activity is the highest in the iris-ciliary body, followed by the cornea, and then the aqueous humor.[2] Depending on the nature of the drug, these enzymes contribute to either an activating or inactivating effect. The latter metabolic process results in loss of activity of the drug. The esterases, for example, are responsible for activating dipivalyl epinephrine, the prodrug of epinephrine, and for inactivating pilocarpine.[28] After pilocarpine instillation in the rabbit, about 40% of the original compound in the cornea and 75% of that in the anterior chamber are breakdown products of pilocarpine, mainly pilocarpic acid.[35] Topical idoxuridine, an antiviral drug, is also subject to metabolic breakdown in the corneal epithelium, where it is converted to 2'-deoxyuridine and iodouracil, which can be recovered from the anterior chamber.[35] The metabolism of ocularly applied drugs during or after corneal penetration has been exploited to design ocular drugs according to the prodrug or the soft drug approach. Whereas the prodrug approach allows for control of the absorption process (i.e., an inactive drug converted in vivo to an active drug), soft drugs are designed to take advantage of a predicable and controllable elimination process. Thus, soft drugs are therapeutic molecules that are metabolized at a controlled rate to an inactive drug.[1]

Drug Delivery Kinetics and Ocular Bioavailability

Because most of the instilled medicinal drop is rapidly lost from the preocular area, ophthalmic solutions exhibit a fast drug pulse delivery with an initially high concentration that rapidly declines to a concentration below the therapeutic range, as shown in Figure 7.1.3. From a pharmacokinetic standpoint, the disappearance of a drug from ophthalmic solution follows a first-kinetic order in which the instilled drug available for target tissues declines exponentially as the medication is lost through the nasolacrimal system and is washed away by the tear turnover.[18] With ophthalmic suspensions, the

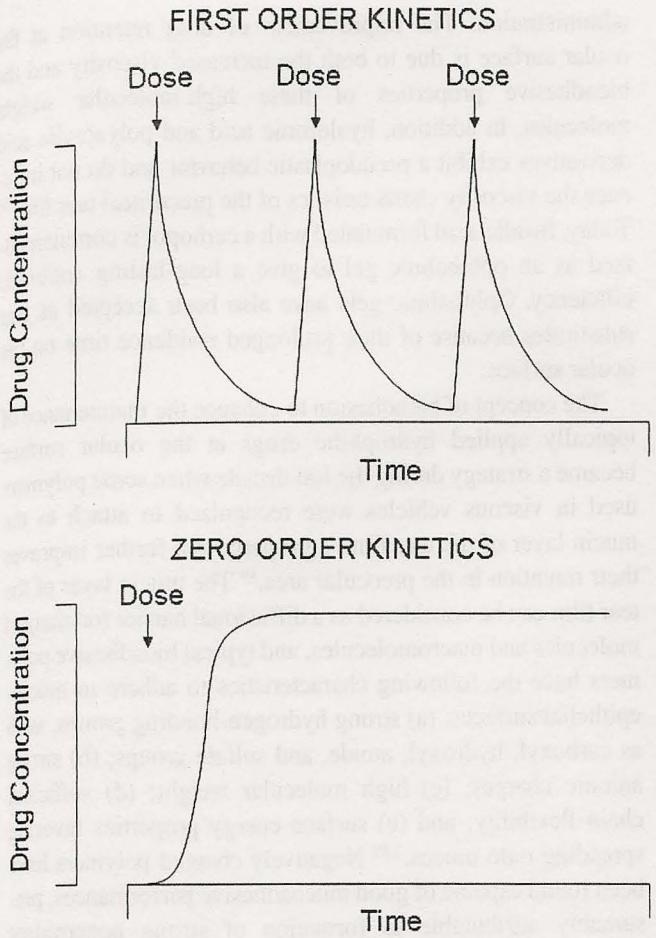

Figure 7.1.3.

drug administration is also pulsed, but suspensions are said to be advantageous compared to solutions because the retention of particles and their dissolution prolong contact time between the drug and the ocular surface and allow the drug concentration to persist in the tear fluid longer than after instillation of a solution.[5] Dissolution occurs gradually to a concentration governed by the drug's solubility in tear film and the size and quantity of particles. With smaller particles, the dissolution rate into the tear film is more elevated because of the increased surface area of exposed drug at the tear–drug interface.[2] Thus, the advantage of suspensions over solutions diminishes with reduced particle size.[14] In addition, suspensions formulations actually show enhanced ocular bioavailability over solutions if the dissolution rate of the particles is greater than their rate of clearance from the precorneal area.[79]

Due to the rapid clearance from the ocular surface, only a small fraction of the instilled drug becomes available for absorption into the eye. It is generally considered that for topically applied drugs, less than 1% to no more than 10% of the dose applied enters the anterior chamber.[30,80] Some examples, documented by experimental studies in rabbits, indicate that as little as 2% of pilocarpine, 1.6% of clonidine, and 7 to 10% of flurbiprofen is absorbed after topical application.[1]

Strategies to Improve Ocular Bioavailability

Because only a very small fraction of the drug applied to the eye can be absorbed into the inner eye, many ideas have been developed to improve ocular bioavailability of medications delivered to the eye. The main effort in ocular drug delivery during the two past decades has been in the design of systems to prolong the precorneal retention time or to facilitate drug penetration across the cornea of topically applied drugs. The challenge in this effort was to improve drug bioavailability from less than 10% to at least 15% to 20%.[81]

Improvement of Precorneal Retention

Ophthalmic Ointments In the past, ointments were the only answer to achieving prolonged delivery. The thick, oleaginous bases of ophthalmic ointments are primarily mixtures of white petrolatum and mineral oil, with or without a water-miscible agent such as lanolin.[4] The mineral oil is added to the petrolatum to allow the vehicle to melt at eye temperature, while the lanolin is added to the nonemulsive ointment base in order to absorb water and allow for water-soluble drugs to be retained in the delivery systems.[4] Hydrophilic drugs are dispersed in the base as particles, like in suspensions, while lipid-soluble drugs are dissolved in the ointment base.[3] Ophthalmic ointments must contain preservatives in order to prevent bacterial contamination during use, and effects of pH and tonicity should be controlled as previously discussed for ophthalmic solutions and suspensions.[3]

After application to the eye, the ointment is retained in the cul-de-sac until the base melts and exposes drug particles, thereby delivering the drug to the tear fluid.[5] Although these preparations melt at the temperature of the ocular surface and disperse with tear fluid, studies in humans and rabbits have clearly shown that petrolatum-based ointment is retained longer than certain viscous vehicles such as methylcellulose or polyvinyl alcohol.[82] A first explanation is that the large molecules of the petrolatum–mineral oil base ointment are not easily removed by the lacrimal drainage system, and a second factor of prolonged retention is the physicochemical relationship between the ointment base and the tear film. The fact that ointment bases and the tear film both have nonpolar oil components may allow oil bases to be readily absorbed by the preocular tear film.[82] The overall result is that the precorneal disappearance rate of drugs administered in an ointment has been reported to be as low as 0.5% per minute,[2] and gamma scintigraphic studies confirmed that significant amounts of ointment are retained 4 hours after dosing.[83]

The fact that the ointment must first melt and dissolve at the ocular surface implies peak drug concentration (Cmax) in the tear fluid to be lower and time at which peak concentration (Tmax) is achieved in ocular tissues to be later than when a drop of solution or suspension is applied.[35] Total bioavailability, however, is significantly greater than that from aqueous solution or suspensions, since less drug is immediately lost to drainage.[14] The prolonged residence time of ophthalmic ointment is particularly suitable when frequent instillations of

solutions or suspensions are impractical. Ointment formulations are usually administered in dosage frequencies of twice daily, but depending on the response to therapy, they may be administered as often as every few hours. When both drops and ointments should be used, it is suggested from experimental data that the eye drop should be given either before the ointment or at least 2 hours after ointment application to obtain the highest intraocular drug concentrations.[84] Ointment preparations are usually nonirritating and safe to use on the external eye.[10] Although it has been repeatedly stated that the use of ointment delays corneal wound healing, ointment vehicles presently used do not appear to interfere with corneal or conjunctival wound healing. Ointment use, however, should be avoided in eyes with impending corneal perforations or deep or flaplike corneal lacerations before or during intraocular surgery because of the irritative properties of white petrolatum and mineral oil.[3,4,10] Disadvantages of ophthalmic ointment application include imprecise dosing and formation of a film on the cornea, which partially obstructs vision.[4]

Viscous Eye Drops and Gels In the early 1970s, it appeared that the limited preocular residence time of aqueous ophthalmic solutions could be corrected at least in part by increasing the viscosity of the vehicle with the addition of methylcellulose, a hydrophilic polymer.[85] Then, attempts to increase ocular residence time of eye drop formulations via enhanced viscosity became a popular strategy in the early research stages of ophthalmic drug delivery, and science developed around the use of viscosity enhancers that were often hydrophilic polymers, such as various cellulose derivatives, polyvinyl alcohol, and polyvinyl pyrrolidone. These research efforts led to a significant body of literature demonstrating that these polymers can prolong precorneal residence time and improve ocular bioavailability of hydrophilic drugs.[3] Experimentally, it was determined that the improvement in ocular drug delivery reached a maximum level at a viscosity of about 12 to 15 cps and that higher viscosity formulations caused ocular irritation with an increase in reflex tears and blinks leading to rapid elimination of the instilled drug.[2,86] Today, viscosity enhancers such as hydroxypropylcellulose and polyvinyl alcohol continue to be included in some ophthalmic solutions and suspensions, but their function is more for patient or reasons of bioadhesion than for viscosity enhancement.[36,87]

Gel formation is an extreme case of viscosity enhancement through the use of natural gums, hyaluronic acid, polyacrylic acids, or cellulosic components such as sodium carboxymethylcellulose.[3] Polyacrylic acid derivatives, including carbopols and polycarbophils, are appropriate for use as vehicles in ophthalmic formulations. Both are polymers of acrylic acid, but carbopols are cross-linked with allyl sucrose, while polycarbophils are cross-linked with divinyl glycol.[39] An example is carbopol 934P, which has a molecular weight of 3,000,000 Da and is readily soluble in aqueous solutions.[88] The use of ophthalmic gels as a vehicle for hydrophilic drugs can enhance drug penetration and reduce the frequency of administration. The improvement of drug retention at the ocular surface is due to both the increased viscosity and the bioadhesive properties of these high-molecular weight molecules. In addition, hyaluronic acid and polyacrylic acid derivatives exhibit a pseudoplastic behavior and do not influence the viscosity characteristics of the precorneal tear film.[39] Today, fusidic acid formulated with a carbopol is commercialized as an ophthalmic gel to give a long-lasting antibiotic efficiency. Ophthalmic gels have also been accepted as tear substitutes because of their prolonged residence time on the ocular surface.

The concept of bioadhesion to enhance the maintenance of topically applied hydrophilic drugs at the ocular surface became a strategy during the last decade when some polymers used in viscous vehicles were recognized to attach to the mucin layer of the tear film, a property that further improves their retention in the preocular area.[89] The mucin layer of the tear film can be considered as a diffusional barrier for charged molecules and macromolecules, and typical bioadhesive polymers have the following characteristics to adhere to mucin-epithelial surfaces: (a) strong hydrogen-bonding groups, such as carboxyl, hydroxyl, amide, and sulfate groups; (b) strong anionic charges; (c) high molecular weight; (d) sufficient chain flexibility; and (e) surface energy properties favoring spreading onto mucus.[2,89] Negatively charged polymers have been found capable of good mucoadhesive performances, presumably attributable to formation of strong noncovalent bonds with the carbohydrate pendant chains of the mucin molecule.[90] Polymers commonly used in ophthalmic formulations for their bioadhesive properties include hydroxypropyl methylcellulose, hyaluronic acid, carboxymethylcellulose, and polyacrylic acid derivatives.[39] The preocular residence of a radiolabeled polyacrylic acid-based gel was compared in humans with that of saline control, using lacrimal dacryoscintigraphy. At 8 minutes postdosing, the label levels retained in the precorneal area were 7% and 42% for saline and carbomer, respectively. At 35 minutes, approximately 20% of the labeled carbomer was retained at the ocular surface, suggesting stabilization of tear film for a considerable time.[91] The mucoadhesion value determined for sodium hyaluronate is close to that obtained with a standard mucin-mucin and was found to be higher than those of Gellan, sodium alginate, and dextran respectively.[92,93] The high mucoadhesive capacity of sodium hyaluronate is explained by its molecular similarity to ocular mucus glycoprotein.[92] Xyloglucan is a recently identified polysaccharide from tamarind seed that displays mucoadhesive properties comparable to those of polyacrylic acid. Used as an ophthalmic adjuvant, it prolonged the precorneal residence time of timolol and increased its ocular bioavailability as efficiently as Gelrite, the reference in situ gelling vehicle.[94]

In Situ Gel-Forming Systems In situ gel-forming systems are ophthalmic solutions that undergo gelation on contact with the ocular surface. Such a change in viscosity can be triggered by changes in external factors such as temperature, pH, or

electrolyte concentration. A gel-forming preparation of timolol (timolol XE) was introduced in clinical ophthalmology in the early 1990s. It uses a polysaccharide (Gelrite) derived from gellan gum, which forms a clear gel in the presence of mono or divalent cations found in the tear fluid.[95] The corneal contact time of Gelrite was evaluated in healthy human patients by gamma scintigraphy using Technetium-99m as a radioactive label. Twenty-one minutes after instillation, Gelrite maintained 39% of the tracer on the ocular surface, whereas only 12% and 17% remained at the ocular surface when the tracer was added to a reference solution containing no viscosity enhancer and to a hydroxyethylcellulose solution, respectively.[96] Thus, Gelrite is a suitable vehicle because it leads to an increase in residence time of topically applied timolol and allows a once-a-day administration. Gelation activated by the tear pH of 7.2 to 7.4 or by the temperature of the ocular surface (~32–34°C) was also investigated experimentally.[3] Recently, a reversibly thermo-gelling timolol, which changes from a solution to a gel at the temperature of the human eye, was studied in healthy volunteers.[97] This formulation was better retained at the ocular surface than was conventional aqueous timolol.

Colloidal Systems and Emulsions Liposomes and nanoparticles are drug carrier systems evaluated for sustained drug release. Liposomes are small vesicles (0.01–10 (m) that consist of phospholipid bilayers separated by an aqueous compartment. Lipophilic drugs can be trapped in the lipid layer and hydrophilic medications in the aqueous compartment, allowing both types of medication to be delivered to the eye. By varying the phospholipid composition of liposomes or incorporating into liposomes ligands for which receptors are present at the ocular surface, the degree of liposome accumulation at the site of absorption, and hence the rate of drug release from these liposomes, can be controlled.[2,98] Almost every class of topically or subconjunctivally applied ophthalmic drug has been studied in liposomal form with promising preliminary penetration and pharmacokinetic results. Antibiotics, antifungals, antivirals, antiinflammatories, and immunosuppressives have been intercalated into liposomes of various composition for anterior segment use.[99] The results of these studies showed the potential of liposomes as ocular drug delivery systems for both hydrophobic and hydrophilic drugs, but it also appeared that the clinical applicability of liposomes would be curtailed by their limited drug-loading capacity and stability as well as by the expense of their large-scale manufacture.

Nanoparticles are polymeric colloidal particles ranging in size from 10 to 1000 nm (1μm). They consist of nanospheres or nanocapsules in which drugs may be entrapped or onto which drugs can be encapsulated or adsorbed and are made of various polymers such as polyacrylamide and polymethylmethacrylate.[87,88] The potential use of nanoparticles as an ophthalmic drug delivery system has been evaluated for various hydrophilic and hydrophobic drugs, including pilocarpine, amikacin, betaxolol, carteolol, cyclosporine, and indomethacin, loaded into or on nanospheres of different polymers. These studies showed that the formulations were maintained longer and generally produced an enhanced ocular absorption and pharmacological effect. One of the reasons for the efficiency of nanoparticles was their bioadhesive properties.[88] Recently, solid lipid nanoparticles (SLN) have been elaborated as possible carriers for various hydrophobic and hydrophilic drugs, which are incorporated into SLN as ion-pair complexes. Experimentally, topical application of tobramycin-loaded SLN to rabbit eyes significantly improved ocular bioavailability of the drug compared to standard eye drops.[100]

Oil-in-water emulsions are particularly useful in the delivery of water-insoluble drugs. They consist of an aqueous phase, a lipophilic phase, and a surfactant phase with sometimes a cosurfactant to act on the homogeneity and stability of the dispersed system. In the emulsion, the hydrophobic drug is solubilized in the internal oil phase thereby remaining in the preferred solution state. Ophthalmic emulsions are transparent (blurred vision caused by oils is minimized by the water in the external phase) and are not very viscous because of the high level of dispersion of oil and water droplets.[34,87,98] The in vitro studies of diffusion kinetics and preliminary results in healthy patients have shown a delayed drug release and an increased ocular bioavailability of the drugs which would result from the quick adsorption of the nanodroplets, representing the internal phase of the microemulsification, on the ocular surface membranes.[101] A newly formulated cyclosporine ophthalmic emulsion demonstrated excellent pharmacokinetic properties and safety, and has recently been approved by the U.S. FDA for treatment of dry eye in humans.[102]

Solid Delivery Devices Soft contact lenses used for the treatment of a variety of corneal diseases as a support bandage can also serve as nonerodible vehicles for progressive drug release in the tear pool. A contact lens is made with hydrophilic polymers and 50% to 75% water, and when soaked in a drug solution, it absorbs the drug, which is then released slowly in the tear film when the lens is placed on the cornea.[2,3,7] Although some studies demonstrated the improved delivery of certain medications via presoaked contact lenses, these devices still represent "pulse-dose" drug delivery system. In addition, the amount of time the lens soaks, the drug concentration in the soaking solution, and the different properties of the soft lenses (polymer composition, degree of cross-linking, and lens thickness) markedly affect the amount and rate of drug delivery, which cannot be adequately controlled. Moreover, delivering high concentrations of drugs and any associated preservatives may also expose treated eyes and patients to a greater risk of toxic effects.[3]

The collagen corneal shield, originally developed for use as a corneal bandage, began to be evaluated as a drug delivery system in the early 1990s. The shield is currently fabricated from porcine scleral tissue or bovine dermal collagen and contains mainly collagen type I and some collagen type III.[103]

Upon hydration, it softens and forms a clear, thin (~0.1 mm in thickness) film that conforms to the corneal surface. The shield undergoes hydrolysis while in place on the cornea, within 12, 24, 48, or 72 hours depending on the degree of collagen cross-linking determined by titrating the exposure to ultraviolet radiation during the manufacturing process. A collagen shield with dissolution time of 72 hours is currently available for veterinary use (Vet Shield, Oasis, Glendora, CA). The natural absorptive capacity and biodegradability of collagen have led to the use of collagen shields as sustained-drug delivery devices. Collagen shields have been studied extensively, and a number of investigators have, for instance, verified their usefulness as an alternative to intensive, fortified topical treatment in infectious keratitis using rabbit models of staphylococcal, *Pseudomonas* or *Candida albicans* keratitis.[103,104] While the pharmacokinetics of collagen shield drug delivery are better understood than those of drug-soaked soft contact lenses, shields still have the potential to cause ocular toxic reactions on the basis of their pulse-dose drug delivery profile.[28,103] In addition, the potential role of this device in the treatment of certain ocular diseases remains to be assessed by controlled trials. Despite this lack of clinical data, a 72-hour shield presoaked in ciprofloxacin (3 mg/mL) is currently in use with satisfying results for the treatment of bacterial keratitis in humans.[103]

Ophthalmic inserts are solid or semisolid devices, the size and shape of which are designed for application in the lower fornix. Their main objective is to deliver medication at the ocular surface by sustained-release mechanisms.[105] They have been classified as erodible (soluble) or nonerodible (insoluble) inserts. The best known nonerodible ocular insert is the Ocusert, a diffusional system designed for controlled release of pilocarpine for 7 days in humans, but it is presently withdrawn from the market.[105] Soluble inserts are made from biodegradable polymers, the physicochemical characteristics of which are described in the current literature.[105,106] Drug release occurs by gradual dissolution of the polymer matrix, which takes place by either hydrolysis or enzymatic erosion, eliminating the need for removing the implant after complete drug release.[105] From a pharmacokinetic standpoint, the advantages of an ocular insert delivery system include constant delivery rate, which means zero-order pharmacokinetics (see Fig.7.1.3), and prolonged drug residence time in the tear fluid. These properties were illustrated by studies in rabbits showing that the precorneal residence time of gentamicin varied from 5.1 to 21.9 hours when the drug was administered with different soluble ophthalmic inserts made of various cellulose derivatives, compared to 0.08 hours when the drug was instilled as standard eye drops.[107] Similarly, an experimental gelatin-based (Gelfoam) ocular insert containing phenylephrine (1.7 mg) and tropicamide (0.6 mg) induced a larger and longer-lasting mydriatic response than that produced by eye drops with equivalent amounts of both drugs.[108] Ocular bioerodible minitablets containing cipofloxacin have been recently evaluated in human patients. The formulation had prolonged drug release properties and was considered advantageous for the therapy of bacterial keratitis in people.[109] A PVA/EVA/silicone-coated drug reservoir–type system has also been evaluated in horses for sustained release of ciprofloxacin. It was well tolerated, and the predicted length of drug delivery to the ocular surface was approximately 14 days.[110] As discussed previously, ocular inserts might favor the intraocular absorption of some topically applied drugs, such as the β-blockers, via the noncorneal route.[111] The disadvantages of ocular inserts include difficulty of placement, risks of loss, and mechanical irritation.

Improvement of Corneal Absorption

There are two main approaches for enhancing corneal transfer of topically applied drugs. The first approach is to modify the physicochemical properties of the drug through prodrug derivatization, and the second is to increase transiently the permeability of the corneal epithelium. The latter can be accomplished by exposing the epithelium to appropriate substances known as penetration enhancers or absorption promoters.[34,39]

Ophthalmic Prodrugs To overcome the resistance to transport of hydrophilic drugs across the corneal epithelium, a prodrug approach can be considered. Prodrugs are defined as pharmacologically inactive derivatives of drug molecules that are chemically or enzymatically converted to the active parent drugs.[87] Ophthalmic prodrugs are usually lipophilic esters or diesters of parent drugs that easily penetrate the corneal epithelial barrier, where they are enzymatically converted by esterases to permit access of the active moiety to the anterior chamber.[34,112] An ideal ocular prodrug should be stable and soluble in aqueous solutions to enable formulation, sufficiently lipophilic to pass the corneal barrier, well tolerated, and capable of releasing the active moiety within the eye at a rate corresponding to the therapeutic need.[34]

Steroids were perhaps the first class of ophthalmic drugs to which prodrug concept was applied, since the acetate prodrugs of dexamethasone and prednisolone were designed to improve corneal absorption and were found to increase the antiinflammatory efficiency by a factor of 1.5 to 2.0 compared to their parent drugs.[34] Dipivalyl epinephrine (or dipivefrin), developed as an epinephrine prodrug in the late 1970s, is formed by esterification of the hydroxyl groups of the epinephrine molecule. The major advantage of dipivefrin is that a 10-fold lower dose has a therapeutic effect comparable to that produced by epinephrine, with a significant lowering of systemic side effects and reduction of dose.[34] Recently, various prodrugs of prostaglandin $F_{2\alpha}$ ($PGF_{2\alpha}$) for topical use have been developed to improve corneal penetration and decrease side effects associated with the autacoid activity of the PGs. These ester prodrugs readily penetrate the corneal epithelium, where they are hydrolyzed to a free-acid moiety that reaches the anterior segment of the eye to exert a potent ocular hypotensive effect.[114]

Penetration Enhancers Several promoters have been developed to enhance the absorption of topically applied drugs through the cornea. Surface-active absorption enhancers, including preservative agents and medium-chain fatty acids, are

believed to increase the permeability of the epithelial cell membranes, while calcium chelators act principally on the tight junctions. However, most penetration enhancers have been shown to affect both transcellular and paracellular penetration.[34,39] As discussed previously, a number of preservatives are included in ophthalmic solutions and suspensions for sterility reasons. Benzalkonium chloride, a quaternary ammonium, is the prototype of the surfactant-type preservatives; it is the most frequently used in commercial eye drops because of its rapid bactericidal efficacy and low toxicity under properly controlled conditions, and it shows the highest promoting effect on corneal drug penetration of currently used preservatives.[114] Benzalkonium chloride at concentrations as low as 0.001% enlarges intercellular spaces in the superficial layers, thereby facilitating the corneal absorption of drugs that utilize the paracellular route but also form polar defects in the lipid layer of the cell membranes leading to increased penetration of drugs.[28,34] The surfactant effect of benzalkonium chloride accounts for these effects but also for its potential epithelial toxicity. Electron microscopical studies revealed that even after short-term application, 0.01% benzalkonium chloride impairs the cell membranes of the outer layer of the corneal epithelium, inducing focal exfoliation of the superficial cells.[115] This is in agreement with in vitro experiments showing that benzalkonium chloride is cytotoxic to rabbit and canine corneal epithelial cultured cells at concentrations of 0.01 to 0.0003%.[116,117] When used on a chronic basis, benzalkonium inhibits epithelium adhesion, causes loss of superficial epithelial layers, delays the healing of epithelial defects, and induces significant histopathologic and inflammatory changes in the ocular surface and possibly in deeper ocular structures.[118] The space between corneal epithelial cells with intercellular junctions, which represents the barrier for the paracellular route, can also be transiently expanded by chelating agents, such as edetic acid (EDTA), and by sodium salts of medium-chain fatty acids, such as caprylate and caprate that enhance the corneal penetration of hydrophilic compounds.[34,119] Capric acid, which affects both cell membranes and tight junctions and forms ion-pair complexes with cationic drugs, was reported to significantly increase the corneal permeability of hydrophilic β-blockers such as atenolol, tilisolol, and carteolol.[120] Other compounds evaluated as potential ocular penetration enhancers included sodium dodecyl sulfate, saponin, bile salts, and cyclodextrins.[34,39] As discussed previously, cyclodextrins were initially evaluated to increase the solubility of a wide variety of hydrophobic compounds in order to formulate these drugs as ophthalmic solutions.[20] Because a decrease in toxicity of the drug–cyclodextrin complex was observed in parallel, cyclodextrin complexation was further proposed as to enhance corneal permeability and improve ocular bioavailability of hydrophobic drugs. For instance, complexation of a poorly water-soluble drug such as dexamethasone with 2-hydroxypropyl-β-cyclodextrin was associated with a large increase in the drug bioavailability in human eyes compared with the commercially available 0.1% dexamethasone.[121] In light of current data, it seems that this approach would be beneficial to enhance ocular penetration of poorly water-soluble drugs but does not seem to afford a real improvement for hydrophilic drugs.[122] A recent strategy for the formulation of ocular delivery systems is to associate a penetration enhancer and a viscosity enhancer to overcome both the corneal epithelial barrier and the lacrimal drainage. For instance, sustained-release formulations of ciprofloxacin with dodecylmaltoside as penetration enhancer and hydroxymethylcellulose or carbopol as viscous vehicle delivered 10-fold more drug into the aqueous humor than the standard solution formulation.[123]

Periocular and Ocular Injections

Subconjunctival Injection

Subconjunctival administration may be indicated for infectious or inflammatory conditions of the cornea and anterior segment because of the expected high and/or sustained drug levels that can be achieved in these ocular structures. Whether a high level or a sustained effect is achieved depends on the drug formulation. This route of administration provides therapeutic drug levels for 8 to 12 hours after a single injection of a water-soluble drug and for up to 2 to 3 weeks with drugs in suspension, such as the acetate formulations of corticosteroids.[1] Depending on the nature of the ocular disorder, subconjunctival injections may be used as a supplement to frequent eye drop dosing or to reduce the need for frequent instillation of drops. They are also indicated during the immediate postoperative period of some intraocular surgical procedures. Generally, the subconjunctival route is more relevant for hydrophilic drugs because they have not to pass through the cornea and conjunctiva, which are rate-limiting barriers for these drugs.[1,3] Subconjunctival injections should be administered below the bulbar conjunctiva or Tenon's capsule for optimal efficacy.

Several mechanisms have been proposed to explain the movement of drugs from the subconjunctival injection site to the anterior segment of the eye: (a) the drug may diffuse directly into the cornea and sclera and penetrate the anterior chamber or underlying tissues; (b) the drug may regurgitate through the conjunctival hole produced by injection and then mix with tears before entering the eye transcorneally, and (c) the drug may be absorbed into conjunctival blood vessels and enter the general circulation before returning to anterior uvea.[124] Studies in rabbits suggest that a significant amount of the drug injected by the subconjunctival route is absorbed by the conjunctival vasculature and is systemically available.[125] In dogs, the systemically available fraction of methylprednisolone acetate is sufficient to develop systemic effects such as adrenal suppression.[126] Although it is generally assumed that subconjunctival administration delivers higher drug concentrations to anterior ocular structures than to posterior structures,[35] recent data suggest that effective intravitreal drug concentrations can be achieved after subconjunctival injection and most likely result from direct diffusion through the sclera.[127]

Subconjunctival administration of liposome-entrapped drugs, such as 5-fluorouracil, cyclosporine, gentamicin, and

tobramycin, has been experimented by various investigators in order to provide prolonged residence time of therapeutic drug levels in the anterior segment of the eye. Although promising results were observed in animals, this method of drug delivery to the eye is not clinically applied so far.[128] In animal studies, liposomal agents were detectable in the cornea, sclera, retina, and choroid for as long as 7 days after subconjunctival injection, a finding that might result in less frequent dosing.[99]

Retrobulbar and Peribulbar Injections

Retrobulbar and peribulbar injections are used to introduce a drug into the orbital cavity. The drug then diffuses rapidly through the orbital tissues and the back of the eye.[4] Several techniques have been proposed and compared.[129]

Nowadays, retrobulbar or peribulbar injection is used only for regional anesthesia in veterinary ophthalmology.[130] Retrobulbar anesthesia is used as an adjunctive procedure in ocular surgery to reduce nystagmus and enophthalmos.[130] Lidocaine 0.2% and bupivacaine 0.5% can be combined for rapid and long-lasting effects.[131] Potential complications of retrobulbar block include globe perforation, optic nerve injury, extraocular muscle injury, and orbital hemorrhage.[132] When retrobulbar injection is used to produce exophthalmia for increased surgical exposure of the globe, it may result in increased intraocular pressure.[130]

Intracameral Injection

Injection or irrigation of the anterior chamber is mainly indicated in two situations: during surgery to control hemorrhage or pupil size and in the management of advanced intraocular infection. Tissue plasminogen activator (tPA) and carbachol can also be administered intracamerally at the completion of cataract surgery in the dog. Local intolerance results in corneal endothelial damage with corneal edema and damage to the iris and lens.[4]

Intravitreal Injection

The vitreous body is an avascular gel-like medium in which drug delivery by the vascular route is generally low because of the blood–ocular barriers and tight junctions of the retinal pigment epithelium, which severely restrict the passage of drugs from the blood flow to the vitreous humor. Similarly, therapeutic drug levels cannot be achieved into the posterior pole of the eye after topical application because drug transfer from the anterior segment is slow and reduced.[133] Consequently, direct administration of a drug into the vitreous cavity can provide effective concentrations at the target site and is generally required in threatening posterior segment diseases in humans, such as bacterial endophthalmitis, macular edema, and intraocular proliferation.[134] In veterinary ophthalmology, the potential hazards of the procedure have actually limited its use to the chemical ablation of the ciliary epithelium in end-stage glaucomatous eyes and less frequently to the treatment of infectious endophthalmitis. The safety of the drug and its concentration reaching the retina must be taken into account to avoid toxicity. Common clinical practice is to deliver the desired dose of the drug in 0.05 to 0.10 mL of solution, using a microsyringe.[135] After placement in the midvitreous, drugs diffuse readily through the vitreous humor following a brief initial equilibration period, and then are lost by first-order kinetics via the anterior or the posterior route.[136] Elimination of intravitreal drugs by the anterior route follows a diffusion pattern that moves the drug around the lens to the anterior chamber, whereas a retinal pump mechanism has been described for active transport of drugs out of the retina and then direct elimination into the systemic circulation. Drugs that leave the vitreous humor via the anterior chamber, such as the aminoglycoside antibiotics, exhibit vitreal half-life of about 20 to 30 hours.[137] In contrast, posterior-route drugs, such as cephalosporins, are transported actively across the retina by a peptide carrier and have a short half-life that ranges from 2 to 10 hours.[35,138] In fact, the half-life varies with the molecular weight of the compound, and as most of the intravitreally administered drugs in solution have a molecular weight less than 500 Da, their half-life is likely to be shorter than 3 days.[136] The half-life of drugs in vitreous humor may be affected by factors such as the presence of inflammation and infection, the presence or absence of lens, and the lipophilicity of the administered drug.[35,139]

Because intravitreal injections in humans are painful and not convenient for frequent administration, an approach for prolonged delivery of intraocular drugs is administration of crystalline formulations, or systems such as liposomes, microspheres, or implantable devices. These delivery systems have been in evaluation for the last 15 years to provide constant (zero-order kinetics) and sustained release of the drug within the vitreous cavity with a single administration, and they offer an alternative to multiple intravitreous injections. It has been reported that incorporating drugs into liposomes increases half-life, and because fewer intravitreal injections are required, the toxicity is diminished.[140] Triamcinolone acetonide, which is in a suspension form, has a half-life of approximately 19 days after intravitreal injection in human eyes that have undergone vitrectomy.[141] Numerous animal studies have shown that when drugs entrapped within liposomes are injected, therapeutic vitreous concentrations are achieved during a longer period, with less toxicity and superior clinical efficacy than free-drug administration. This was notably demonstrated for liposomal preparations of penicillin, gentamicin, clindamycin, amphotericin B, and ganciclovir.[99] The potential usefulness of microspheres made of polymers of lactic acid or copolymers of lactic and glycolic acid and loaded with drugs for delivery by intravitreous injection has been investigated in animal models of diverse human vitreoretinal diseases and offered promising results.[142,143] Furthermore, because liposomes and microspheres can be phagocytosed by the retinal pigment epithelium (RPE) cells

when injected into the subretinal space, the possibility of targeting drugs to RPE cells is presently being assessed.[99,143]

Implantable Devices

Some implantable matrices and devices have been specifically designed to deliver drug to intraocular structures. Systems investigated were implanted beneath the bulbar conjunctiva into the anterior chamber or vitreous cavity. In the horse, nonerodible microosmotic pumps implanted subconjunctivally were well tolerated and allowed effective delivery of atropine during the 7 days they were in place.[144] The Oculex Drug Delivery System (DDS; Oculex Pharmaceuticals, Sunnydale, CA) is a biodegradable drug delivery system to which any variety of drugs can be bound; it provides sustained drug release after it is inserted into the eye at the completion of intraocular surgery. It consists of a drug plus a matrix of lactic acid and glycolic acid copolymer, which is extensively used as a resorbable suture material under the trade name of Vicryl. Surodex is a DDS formulation containing 60 μg of dexamethasone designed to be implanted into the anterior chamber. This device was experimentally shown to deliver drug in the anterior chamber at constant rate (zero-order pharmacokinetics) over 7 days.[145] Inserted in the anterior chamber or the ciliary sulcus of human eyes undergoing phacoemulsification, the system was found safe and clearly superior to 0.1% dexamethasone eye drops in reducing postsurgical inflammation.[145,146] A recent experiment in rabbits, using a DDS formulation containing 0.5 mg of cyclosporine, demonstrated that following implantation of the device in the anterior chamber, the drug was recovered at high concentrations in all layers of the cornea over a 3-month period.[147]

Various implantable devices were considered as promising delivery systems to be used in the treatment of posterior segment ocular diseases. Initially, the devices were implanted in the vitreous cavity, but recently it became apparent that transscleral delivery could be an effective method of achieving therapeutic drug concentrations in the posterior segment of the eye.[148]

An intravitreally implanted system has been used clinically in humans with severe uveitis.[149,150] This biodegradable device is implanted into the vitreous through the pars plana to produce constant (zero-order pharmacokinetics) and long-lasting drug levels that diffuse into the vitreous body and are delivered to the retina-choroid. It was calculated that with such a system containing either 2 mg or 15 mg of fluocinolone acetonide and with a constant drug release of approximately 2 μg/day, the duration of drug delivery to the posterior segment will be 2.5 and 18 years, respectively.[150]

Biodegradable implant or scleral plugs, as well as nonbiodegradable implant designed to be inserted in a scleral pocket, are currently under investigation to deliver corticosteroid, antiviral drugs, or immunosuppressive agents to the posterior segment. These systems were shown to be effective in different animal models of human vitreo-retinal diseases and might represent useful systems for sustained drug delivery to the retina-choroid.[151–155]

Devices for sustained release of cyclosporine into intraocular tissues have been developed for long-term control of equine recurrent uveitis (ERU) with minimal owner maintenance.[156] A polyvinyl alcohol/silicone-coated intravitreal cyclosporine implant was first evaluated,[157] but owing to some side effects, a new device to be inserted suprachoroidally is presently under development and seems promising in the management of ERU.[156]

Systemic Administration

Diffusion of drugs present in the systemic circulation to intraocular sites is severely curtailed by the blood–ocular barriers. A large number of studies in humans and rabbits that measured drug concentrations in aqueous and vitreous humor after systemic administration indicated that lipophilicity, molecular weight, and protein binding are determinants of drug penetration through the blood–ocular barriers.[4] These studies were mostly dedicated to the research of intraocular penetration of systemic antibiotics and corticosteroids. Hydrophilic drugs such as penicillins and cephalosporins are thought to penetrate poorly into the aqueous humor of noninflamed eyes,[158,159] while lipophilic drugs, such as chloramphenicol, may achieve high levels in the eye after systemic administration.[158] It should be noted that protein binding is not an absolute determinant of drug penetration into the ocular tissues, since many drugs that have low protein binding in serum penetrate poorly across the blood–eye barrier, and others that are highly protein-bound in serum may diffuse more easily into the eye. For example, penicillins show low protein binding in serum (20%–30%), yet ocular penetration is poor with normal doses. In contrast, chloramphenicol serum protein binding is about 50% to 60%, yet ocular penetration is far superior.[160] In fact, it is more accurate to state that the rate of drug transfer from the serum across the blood–eye barrier is enhanced as the free fraction in the serum increases, while the extent to which the drug will ultimately penetrate is determined by pharmacokinetic parameters related to its systemic distribution. Factors that induce breakdown of the blood–ocular barriers, such as ocular inflammation, ocular infection, and ocular trauma, promote intraocular penetration of systemically administered drugs.[35] Induction of a low intraocular pressure by compression with an ocular reducer balloon is also able to induce temporary changes in the blood–aqueous barrier and was experimentally found to improve the intraocular penetration of systemic drugs.[161]

REFERENCES

1. Schoenwald RD. Ocular drug delivery: Pharmacokinetic considerations. *Clin Pharmacokin* 1990; 18: 255–269.
2. Sasaki H, Yamamura K, Nishida K, Nakamura J, Ichikawa M. Delivery of drugs to the eye by topical application. *Prog Ret Eye Res* 1996; 15: 583–620.

3. Bar-Ilan A, Neumann R. Basic considerations of ocular drug-delivery systems. In: Zimmerman TJ, Kooner KS, Sharir M, Fechtner R, eds. *Textbook of Ocular Pharmacology,* Philadelphia: Lippincott-Raven, 1997: 139–150.
4. Bartlett JD, Cullen AP. Clinical administration of ocular drugs. In: Bartlett JD, Jaanus SD, eds. *Clinical Ocular Pharmacology,* Boston: Butterworth Publishers, 1984: 365–418.
5. Frangie JP. Clinical pharmacokinetics of various topical ophthalmic delivery systems. *Clin Pharmacokin* 1995; 29: 130–138.
6. Malmberg GJ, Lupo R. Compounding in veterinary ophthalmology. *Vet Clin of N Am: Sm Anim Pract* 2004; 34: 825–838.
7. Miller TR. Principles of therapeutics. *Vet Clin N Am: Eq Pract* 1992; 8: 479–497.
8. Wilson CG. Assessing ocular drug delivery with lacrimal scintigraphy. *Pharm Sci Tech Today* 1999; 2: 321–326.
9. Davies NM, Wang G, Tucker IG. Evaluation of a hydrocortisone/hydroxypropyl-β-cyclodextrin solution for ocular drug delivery. *Intern J Pharmaceut* 1997; 156: 201–209.
10. Baggot JD, Brown SA. Basis for selection of the dosage form. In: Hardee GE, Baggot JD, eds. *Development and Formulation of Veterinary Dosage Forms.* New York: Marcell Deker, 1998; 7–144.
11. Kwon K, Diestelhorst M, Süverkrüp R. Dose uniformity problems of suspension eye drops. *Klinische Monatsblatter fur Augenheilkunde* 1996; 209: 144–149.
12. Oldham GB, Andrews V. Control of microbial contamination in unpreserved eye drops. *Br J Ophthalmol* 1996; 80: 588–591.
13. Maurice D. The effect of low blink rate in rabbits on topical drug penetration. *J Ocular Pharm Therap* 1995; 11: 297–304.
14. Shell J. Pharmacokinetics of topically applied ophthalmic drugs. *Surv Ophthalmol* 1982; 26: 207–218.
15. Lederer C, Harold R. Drop size of commercial glaucoma medications. *Am J Ophthalmol* 1986; 101: 691–694.
16. Van Santvliet L, Ludwig A. Determinants of eye drop size. *Surv Ophthalmol* 2004; 49: 197–213.
17. Mishima S, Gasset A, Klyce SD, Baum JL. Determination of tear volume and tear flow. *Invest Ophthalmol* 1966; 5: 264–276.
18. Hegeman SL, Bosin TR, Harrison SD. Fundamental concepts in ocular pharmacology. In: Bartlett JD, Jaanus SD, eds. *Clinical Ocular Pharmacology.* Boston: Butterworth Publishers, 1984; 3–35.
19. Wilson CG. Assessing ocular drug delivery with lachrimal scintigraphy. *Pharm Sci Technology Today* 1999; 2: 321–326.
20. Davies NM. Biopharmaceutical considerations in topical ocular drug delivery. *Clin Exp Pharm Physiol* 2000; 27: 558–562.
21. Friedrich SW, Cheng Y-L, Saville B. Theoretical corneal permeation model for ionizable drugs. *J Ocular Pharm* 1993; 9: 229–250.
22. Chrai SS, Patton TF, Mehta A, Robinson JR. Lacrimal and instilled fluid dynamics in rabbit eyes. *J Pharm Sci* 1973; 62: 1112–1121.
23. Patton T. Pharmacokinetic evidence for improved ophthalmic drug delivery by reduction of instilled volume. *J Pharm Sci* 1977; 66: 1058–1059.
24. Weiss M, Hendrickson J. Information on drop size needs to be eyed closely. *Am J Hosp Pharm* 1994; 51: 2969–2970.
25. Chrai S, Makoid M, Eriksen S, Robinson J. Drop size and initial dosing frequency problems of topically applied ophthalmic drugs. *J Pharm Sci* 1974; 63: 333–338.
26. Whitson JT, Love R, Brown RH, Lynch MG, Schoenwald RD. The effect of reduced eye drop size and eyelid closure on the therapeutic index of phenylephrine. *Am J Ophthalmol* 1993; 115: 357–359.
27. Petursson G, Cole R, Hanna C. Treatment of glaucoma using mini-drops of clonidine. *Arch Ophthalmol* 1984; 102: 1180–1181.
28. Lee VHL. Topical ocular drug delivery: Recent advances and future perspectives. *Pharmacy Intern* 1985; 6: 135–138.
29. Doane MG, Jensen AD, Dohlman CH. Penetration routes of topically applied eye medications. *Am J Ophthalmol* 1978; 85: 383–386.
30. Lee VHL, Robinson JR. Topical ocular drug delivery: Recent developments and future challenges. *J Ocular Pharm* 1986; 2: 67–108.
31. Grass GM, Robinson JR. Mechanisms of corneal drug penetration I: In vitro and in vivo kinetics. *J Pharm Sci* 1988; 77: 3–14.
32. Grass GM, Robinson JR. Mechanisms of corneal drug penetration II: Ultrastructural analysis of potential pathways for drug movement. *J Pharm Sci* 1988; 77: 15–23.
33. Grass GM, Cooper ER, Robinson JR. Mechanisms of corneal drug penetration III: Modeling of molecular transport. *J Pharm Sci* 1988; 77: 24–26.
34. Sasaki H, Yamamura, Mukai T, et al. Enhancement of ocular drug penetration. *Crit Reviews Therap Drug Carrier Syst* 1999; 16: 85–146.
35. Maurice DM, Mishima S. Ocular pharmacokinetics. In: Sears ML, ed. *Pharmacology of the Eye.* Berlin: Springer-Verlag, 1984; 19–116.
36. Grass GM, Robinson JR. Relationship of chemical structure to corneal penetration and influence of low-viscosity solution on ocular bioavailability. *J Pharm Sci* 1984; 73: 1021–1027.
37. Sasaki H, Ichikawa M, Yamamura K, Nishida K, Nakamura J. Ocular membrane permeability of hydrophilic drugs for ocular peptide delivery. *J Pharm Pharmaco* 1997; 49: 135–139.
38. Prausnitz MR, Noonan JS. Permeability of cornea, sclera, and conjunctiva: A literature analysis for drug delivery to the eye. *J Pharm Sci* 1998; 87: 1479–1487.
39. Kaur IP, Smitha R. Penetration enhancers and ocular bioadhesives: Two new avenues for ophthalmic drug delivery. *Drug Develop Indust Pharm* 2002; 28: 353–369.
40. Patil PN. Some factors which affect the ocular drug response. *Pharm Sci* 1984; 5: 201–204.
41. Johnson DA, Johns KJ, Robinson RD, Head WS, O'Day DM. The relationship of corneal epithelial defect size to drug penetration. *Arch Ophthalmol* 1995; 113: 641–644.
42. Ahmed I, Patton TF. Importance of the noncorneal absorption route in topical ophthalmic drug delivery. *Invest Ophthalmol Vis Sci* 1985; 26: 584–587.
43. Maurice DM, Polga J. Diffusion across the sclera. *Exp Eye Res* 1977; 25: 577–582.
44. Ashton P, Podder SK, Lee VHL. Formulation influence on conjunctival penetration of four beta-blockers in the pigmented rabbit. *Pharm Res* 1991; 8: 1166–1174.
45. Wang W, Sasaki H, Chien D-S, Lee VHL. Lipophilicity influence on conjunctival drug penetration in the pigmented rabbit: A comparison with corneal penetration. *Curr Eye Res* 1991; 6: 571–579.
46. Hämäläinen KM, Kanasen K, Auriola S, Kontturi K, Urtti A. Characterization of paracellular and aqueous penetration routes in cornea, conjunctiva and sclera. *Invest Ophthalmol Vis Sci* 1997; 38: 627–634.
47. Sasaki H, Ichikawa M, Kawakami S, Yamamura K, Nishida K, Nakamura J. In situ ocular absorption of tilisolol through

ocular membranes in albino rabbits. *J Pharm Sci* 1996; 85: 940–943.
48. Prausnitz MR, Noonan JS. Permeability of cornea, sclera, and conjunctiva: A literature analysis for drug delivery to the eye. *J Pharm Sci* 1998; 87: 1479–1488.
49. Geroski DH, Edelhauser HF. Transscleral drug delivery for posterior segment disease. *Advan Drug Del Reviews* 2001; 52: 37–48.
50. Ahmed I, Patton TF. Importance of the noncorneal absorption route in topical ophthalmic drug delivery. *Invest Ophthalmol Vis Sci* 1985; 26: 584–587.
51. Cruysberg LPJ, Nuijts RMMA, Geroski DH, Gilbert JA, Hendrikse F, Edelhauser HF. The influence of intraocular pressure on the transscleral diffusion of high-molecular-weight compounds. *Invest Ophthalmol Vis Sci* 2005; 46: 3790–3794.
52. Achim H-P, Woodward DF. Update on the mechanism of action of bimatoprost: A review and discussion of new evidence. *Surv Ophthalmol,* 2004; 49(suppl. 1): S5–S11.
53. Kim JW, Lindsey JD, Weinreb RN. Increased human scleral permeability with prostaglandin exposure. *Invest Ophthalmol Vis Sci* 2001; 42: 1514–1521.
54. Aihara M, Lindsey JD, Weinreb RN. Enhanced FGF-2 movement through human sclera after exposure to latanaprost. *Invest Ophthalmol Vis Sci* 2001; 42: 2554–2559.
55. Schoenwald RD, Deshpande GS, Rethwisch DG, Barfknecht CF. Penetration into the anterior chamber via the conjunctival/scleral pathway. *J Ocular Pharm Therap* 1997; 13: 41–59.
56. Friedrich SW, Saville BA, Cheng Y-L, Rootman DS. Pharmacokinetic differences between ocular inserts and eyedrops. *J Ocular Pharm Therap* 1996; 12: 5–14.
57. Lehr C-M, Lee Y-H, Lee VL. Improved ocular penetration of gentamicin by mucoadhesive polymer polycarbophil in the pigmented rabbit. *Invest Ophthalmol Vis Sci* 1994; 35: 2809–2814.
58. Paulsen FP, Föge M, Thale AB, Tillmann BN, Mentlein R. Animal model for the absorption of lipophilic substances from tear fluid by the epithelium of the nasolacrimal ducts. *Invest Ophthalmol Vis Sci* 2002; 43: 3137–3143.
59. Pascoe PJ, Ilkiw JE, Stiles J, Smith EM. Arterial hypertension associated with topical ocular use of phenylephrine in dogs. *J Am Vet Med Assoc* 1994; 205: 1562–1564.
60. Mealey K. Systemic absorption of topically administered drugs. *Compend Cont Ed Pract Vet* 2000; 22: 649–657.
61. Zimmerman TJ, Kooner KS, Kandarakis AS, Ziegler LP. Improving the therapeutic index of topically applied ocular drugs. *Arch Ophthalmol* 1984; 102: 551–553.
62. Ellis PP, Wu PY, Pfoff DS. Effect of nasolacrimal occlusion on timolol concentrations in the aqueous humor of the human eye. *J Pharm Sci* 1992; 81: 219–220.
63. Whitson JT, Love R, Brown RH, Lynch MG, Schoenwald RD. The effect of reduced eye drop size and eyelid closure on the therapeutic index of phenylephrine. *Am J Ophthalmol* 1993; 115: 357–359.
64. Urtti A. Delivery of antiglaucoma drugs: Ocular vs systemic absorption. *J Ocular Pharm* 1994; 10: 349–357.
65. Järvinen K, Urtti A. Duration and long-term efficacy of phenylephrine-induced reduction in the systemic absorption of ophthalmic timolol in rabbits. *J Ocular Pharm* 1992; 8: 91–98.
66. Chiou GCY. Systemic delivery of polypeptide drugs through ocular route. *J Ocular Pharm* 1994; 10: 93–99.
67. Chiou GCY, Li BHP. Chronic systemic delivery of insulin through the ocular route. *J Ocular Pharm* 1993; 9: 85–90.
68. Morgan RV. Delivery of systemic regular insulin via the ocular route in cats. *J Ocular Pharm* 1995; 11: 565–573.
69. Morgan RV, Huntzicker MA. Delivery of systemic regular insulin via the ocular route in dogs. *J Ocular Pharm* 1996; 12: 515–526.
70. Pillion DJ, Wang P, Yorks J, McCann P, Meezan E. Systemic absorption of insulin and glucagon applied topically to the eyes of rats and a diabetic dog. *J Ocular Pharm Therap* 1995; 11: 283–295.
71. Salazar M, Shimada K, Patil PN. Iris pigmentation and atropine mydriasis. *J Pharm Exp Therap* 1976; 197: 79–88.
72. Salminen L, Urtti A, Periviita L. Effect of ocular pigmentation on pilocarpine pharmacology in the rabbit eye. I. Drug distribution and metabolism. *Intern J Pharm* 1984; 18: 17–24.
73. Urtti A, Salminen L, Kujari H, Jäntti V. Effect of ocular pigmentation on pilocarpine pharmacology in the rabbit eye. II. Drug response. *Intern J Pharm* 1984; 19: 53–61.
74. Eiferman RA, Stagner JI. Intraocular penetration of amikacin: Iris binding and bioavailability. *Arch Ophthalmol* 1982; 100: 1817–1819.
75. Tabbara KF, Ghosheh R, O'Connor R. Ocular tissue absorption of minocycline in the rabbit. *Arch Ophthalmol* 1983; 101: 1426–1428.
76. Fukuda M, Sasaki K. Different iris coloration and uptake of a fluoroquinolone agent into the iris ciliary body of rabbit eyes. *Ophthal Res* 1994; 26: 137–140.
77. Katz IM, Berger ET. Effect of iris pigmentation on response of ocular pressure to timolol. *Surv Ophthalmol* 1979; 23: 395–398.
78. Zemel E, Loewenstein A, Lei B, Lazar M, Perlman I. Ocular pigmentation protects the rabbit retina from gentamicin-induced toxicity. *Invest Ophthalmol Vis Sci* 1995; 36: 1875–1884.
79. Sieg JW, Robinson JR. Vehicle effects on ocular drug bioavailability. I. Evaluation of fluorometholone. *J Pharm Sci* 1975; 64: 931–936.
80. Patton F, Robinson R. Quantitative precorneal disposition of topically applied pilocarpine nitrate in rabbits. *J Pharm Sci* 1976; 65: 1295–1301.
81. Lee VHL. Review: New directions in the optimization of ocular drug delivery. *J Ocular Pharm* 1990; 6: 157–164.
82. Hardberger R, Hanna C, Boyd CM. Effects of drug vehicles on ocular contact time. *Arch Ophthalmol* 1975; 93: 42–45.
83. Greaves JL, Wilson CG, Birmingham AT. Assessment of the precorneal residence of an ophthalmic ointment in healthy subjects. *Br J Clin Pharm* 1993; 35: 188–192.
84. Ellis PP, Riegel M. Influence of ophthalmic ointments on the penetration of pilocarpine drops. *J Ocular Pharm* 1989; 5: 119–125.
85. Chrai SS, Robinson JR. Ocular evaluation of methylcellulose vehicle in albino rabbits. *J Pharm Sci* 1974; 63: 1218–1223.
86. Patton TF, Robinson JR. Ocular evaluation of polyvinyl alcohol vehicle in rabbits. *J Pharm Sci* 1975; 64: 1312–1316.
87. Ding S. Recent developments in ophthalmic drug delivery. *Pharm Sci Technol Today* 1998; 1: 328–335.
88. Le Bourlais C, Acar L, Zia H, Sado PA, Needham T, Leverge R. Ophthalmic drug delivery systems—Recent advances. *Prog Ret Eye Res* 1998; 17: 33–58.
89. Greaves JL, Wilson CG. Treatment of diseases of the eye with mucoadhesive delivery systems. *Adv Drug Del Rev* 1993; 11: 349–383.
90. Saettone MF, Monti D, Tilde Torracca M, Chetoni P. Mucoadhesive ophthalmic vehicles: Evaluation of polymeric low-viscosity formulations. *J Ocular Pharm* 1994; 10: 83–92.

91. Wilson CG, Zhu YP, Frier M, Rao LS, Gilchrist P, Perkins AC. Ocular contact time of a carbomer gel (GelTears) in humans. *Br J Ophthalmol* 1998; 82: 1131–1134.
92. Herrero-Vanrell R, Fernandez-Carballido A, Frutos G, Cadórniga R. Enhancement of the mydriatic response to tropicamide by bioadhesive polymers. *J Ocular Pharm Therap* 2000; 16: 419–428.
93. Hartmann V, Keipert S. Physico-chemical, in vitro and in vivo characterisation of polymers for ocular use. *Pharmazie* 2000; 55: 440–443.
94. Burgalassi S, Chetoni P, Panichi L, Boldrini E, Saettone MF. Xyloglucan as a novel vehicle for timolol: Pharmacokinetics and pressure lowering activity in rabbits. *J Ocular Pharm Therap* 2000; 16: 497–509.
95. Laurence J, Holder D, Vogel R, et al. A double-masked, placebo-controlled evaluation of timolol in a gel vehicle. *J Glaucoma* 1993; 2: 177–182.
96. Meseguer G, Buri P, Plazonnet B, Rozier A, Gurny R. Gamma scintigraphic comparison of eyedrops containing pilocarpine in healthy volunteers. *J Ocular Pharm Therap* 1996; 12: 481–488.
97. Ishibashi T, Yokoi N, Bron AJ, Tiffany JM, Komuro A, Kinoshita S. Retention of reversibly thermo-gelling timolol on the human ocular surface studied by video meniscometry. *Curr Eye Res* 2003; 27: 117–122.
98. Le Bourlais CA, Treupel-Acar L, Rhodes CT, Sado PA, Leverge R. New ophthalmic drug delivery systems. *Drug Devel Indust Pharm* 1995; 21: 19–59.
99. Ebrahim S, Peyman GA, Lee PJ. Applications of liposomes in ophthalmology. *Surv Ophthalmol* 2005; 50: 167–182.
100. Cavalli R, Gasco MR, Chetoni P, Burgalassi S, Saettone MF. Solid lipid nanoparticles (SLN) as ocular delivery systems for tobramycin. *Intern J Pharm* 2002; 238: 241–245.
101. Vandamme ThF. Microemulsions as ocular drug delivery systems: Recent developments and future challenges. *Prog Ret Eye Res* 2002; 21: 15–34.
102. Tang-Liu DD, Acheampong A. Ocular pharmacokinetics and safety of ciclosporin, a novel topical treatment for dry eye. *Clin Pharmacokin* 2005; 44: 247–261.
103. Willoughby CE, Batterbury M, Kaye SB. Collagen corneal shields. *Surv Ophthalmol* 2002; 47: 174–182.
104. Sawusch MR, O'Brien TP, Dick JD, Gottsch JD. Use of collagen corneal shields in the treatment of bacterial keratitis. *Am J Ophthalmol* 1988; 106: 279–281.
105. Gurtler F, Gurny R. Patent literature review of ophthalmic inserts. *Drug Develop Indust Pharm* 1995; 21: 1–18.
106. Deshpande AA, Heller J, Gurny R. Bioerodible polymers for ocular drug delivery. *Crit Rev Therap Drug Carrier Sys* 1998; 15: 381–420.
107. Bayens V, Kaltsatos V, Boisrame B, Fathi M, Gurny R. Evaluation of soluble bioadhesive ophthalmic drug inserts (BODI®) for prolonged release of gentamicin. *J Ocular Pharm Therap* 1998; 14: 263–272.
108. Lee Y-C, Millard JW, Negvesky GJ, Butrus SI, Yalkowsky SH. Formulation and in vivo evaluation of ocular insert containing phenylephrine and tropicamide. *Intern J Pharm* 1999; 182: 121–126.
109. Weyenberg W, Vermeire A, Dhondt MMM, et al. Ocular bioerodible minitablets as strategy for the management of microbial keratitis. *Invest Ophthalmol Vis Sci* 2004; 45: 3229–3233.
110. Gilger BC, Valentine V, Papich M, Wang B, Allen JB. Long-term release of antibiotic to the ocular surface of horses by a cirpofloxacin-containing drug delivery device: Preliminary evaluation. 31st Meeting of the Am Coll Vet Ophthalmol (abstract). 2000; 32.
111. Urtti A, Sendo T, Pipkin JD, Rork G, Repta AJ. Application site dependent ocular absorption of timolol. *J Ocular Pharm* 1988; 4: 335–343.
112. Urtti A. Delivery of antiglaucoma drugs: Ocular vs systemic absorption. *J Ocular Pharm* 1994; 10: 349–357.
113. Alm A. Prostaglandin derivatives as ocular hypotensive agents. *Prog Ret Eye Res* 1998; 17: 291–312.
114. Sasaki H, Nagano T, Yamamura K, Nishida K, Nakamura. Ophthalmic preservatives as absorption promoters for ocular drug delivery. *J Pharm Sci* 1995; 47: 703–707.
115. Dormans JMA, van Logten MJ. The effects of ophthalmic preservatives on corneal epithelium of the rabbit: A scanning electron microscopical study. *Toxicol Applied Pharma* 1982; 62: 251–261.
116. Simmons SJ, Jumblatt MM, Neufeld AH. Corneal epithelial wound closure in tissue culture: An vivo model of ocular irritancy. *Toxicol Applied Phar* 1987; 88: 13–23.
117. Hendrix DVH, Ward DA, Barnhill MA. Effects of anti-inflammatory drugs and preservatives on morphologic characteristics and migration of canine corneal epithelial cells in tissue culture. *Vet Ophthalmol* 2002; 5: 127–135.
118. Baudoin C, Pisella P-J, Fillacier K, et al. Ocular surface inflammatory changes induced by topical antiglaucoma drugs: Human and animal studies. *Ophthalmology* 1999; 105: 556–563.
119. Morimoto K, Nakamura T, Morisaka K. Effect of medium-chain fatty acid salts on penetration of a hydrophilic compound and a macromolecular compound across the rabbit cornea. *Arch Intern Pharmacodyn Thérap* 1989; 302: 18–26.
120. Sasaki H, Igarashi Y, Nagano T, Nishida K, Nakamura J. Different effects of absorption promoters on corneal and conjunctival penetration of ophthalmic beta-blockers. *Pharm Res* 1995; 12: 1146–1150.
121. Kristinsson JK, Fridriksdóttir H, Thóristóttir S, Sigurdartóttir AM, Stefánsson E, Loftsson T. Dexamethasone-cyclodextrin-polymer co-complexes in aqueous eye drops. *Invest Ophthalmol Vis Sci* 1996; 37: 1199–1203.
122. Loftsson T, Stefánsson E. Effect of cyclodextrins on topical drug delivery to the eye. *Drug Develop Indust Pharm* 1997; 23: 473–481.
123. Ke T-L, Cagle G, Schlech B, Lorenzetti OJ, Mattern J. Ocular bioavailability of ciprofloxacin in sustained release formulations. *J Ocular Pharm Therap* 2001; 17: 555–563.
124. Conrad JM, Robinson JR. Mechanisms of anterior segment absorption of pilocarpine following subconjunctival injection in albino rabbits. *J Pharm Sci* 1980; 69: 875–884.
125. Barza M, Kane A, Baum J. The difficulty of determining the route of intraocular penetration of gentamicin after subconjunctival injection in the rabbit. *Invest Ophthalmol Vis Sci* 1981; 20: 509–514.
126. Regnier A, Toutain PL, Alvinerie M, Periquet B, Ruckebusch Y. Adrenocortical function and plasma biochemical values in dogs after subconjunctival treatment with methylprednisolone acetate. *Res Vet Sci* 1982; 32: 306–310.
127. Lee TW, Robinson JR. Drug delivery to the posterior segment of the eye: Some insights on the penetration pathways after

subconjunctival injection. *J Ocular Pharm Therap* 2001; 17: 565–572.
128. Niesman MR. The use of liposomes as drug carriers in ophthalmology. *Crit Rev Therap Drug Carr Sys* 1992; 9: 1–38.
129. Munger RJ. Retrobulbar injections in the dog: A comparison of three techniques. *J Am Anim Hosp Assoc* 1978; 14: 490–498.
130. Severin GA. *Severin's Ophthalmology Notes,* 3rd ed. Fort Collins, CO: Digital Imaging & Layout, 1996.
131. Kanemaki N, Ono K, Suga T, Wada Y. Retrobulbar anesthesia of both bupivacaine and lidocaine for intraocular surgery. 31st Annual Meeting of the American College of Veterinary Ophthalmology (abstract) 2000; 10.
132. Dutton JJ. Editorial: Anatomical considerations in ophthalmic anesthesia. *Surv Ophthalmol* 2001; 46: 172–178.
133. Meredith TA. Antimicrobial pharmacokinetics in endophthalmitis treatment: Studies of ceftazidime. *Trans Am Ophthalmol Soc* 1994; 91: 653–699.
134. Jonas JB, Sofker A. Intraocular injection of crystalline cortisone as adjunctive treatment of diabetic macular edema. *Am J Ophthalmol* 2001; 135: 425–427.
135. Raju JR, Weinberg DV. Accuracy and precision of intraocular injection volume. *Am J Ophthalmol* 2002; 133: 564–566.
136. Maurice D. Review: Practical issues in intravitreal drug delivery. *J Ocular Pharm Therap* 2001; 17: 393–401.
137. Miglioli PA, Dorigo MT. Antibiotic levels in aqueous and vitreous humor after intraocular administration. *Chemotherapy* 1989; 35: 406–409.
138. Macha S, Mitra AK. Ocular pharmacokinetics of cephalosporins using microdialysis. *J Ocular Pharm and Therap* 2001; 17: 485–498.
139. Ben-Nun J, Joyce DA, Cooper RL, Cringle J, Constable IJ. Pharmacokinetics of intravitreal injection: Assessment of a gentamicin model by ocular dialysis. *Invest Ophthalmol Vis Sci* 1989; 30: 1055–1061.
140. Peyman GA, Ganiban GJ. Delivery systems for intraocular routes. *Adv Drug Del Rev* 1995; 16: 107–123.
141. Beer PM, Bakri SJ, Singh RJ, Liu W, Peters GB III, Miller M. Intraocular concentration and pharmacokinetics of triamcinolone acetonide after a single intravitreal injection. *Ophthalmology* 2003; 110: 681–686.
142. Moritera T, Ogura Y, Honda Y, Wada R, Hyon S-H, Ikada Y. Microspheres of biodegradable polymers as a drug-delivery system in the vitreous. *Invest Ophthalmol Vis Sci* 1991; 32: 1785–1790.
143. Herrero-Vanrell R, Refojo MF. Biodegradable microspheres for vitreoretinal drug delivery. *Adv Drug Del Rev* 2001; 52: 5–16.
144. Blair MJ, Gionfriddo JR, Polazzi LM, Sojka JE, Pfaff AM, Bingaman DP. Subconjunctivally implanted micro-osmotic pumps for continuous ocular treatment in horses. *Am J Vet Res* 1999; 60: 1102–1105.
145. Tan DTH, Chee S-P, Lim l, Theng J, Van Ede M. Randomized clinical trial of surodex steroid drug delivery system for cataract surgery. Anterior versus posterior placement of two surodex in the eye. *Ophthalmology* 2000; 2001; 108: 2172–2181.
146. Chang DF, Garcia IH, Hunkeler JD, Minas T. Phase II results of an intraocular steroid delivery system for cataract surgery. *Ophthalmology* 1999; 106: 1172–1177.
147. Theng JTS, Ei TS, Zhou L, Lam K-W, Chee SP, Tan D. Pharmacokinetics and toxicity study of an intraocular cyclosporine DDS in the anterior segment of rabbit eyes. *Invest Ophthalmol Vis Sci* 2003; 44: 4895–4899.
148. Geroski DH, Edelhauser HF. Transscleral drug delivery for posterior segment disease. *Adv Drug Deliver Reviews* 2001; 52: 37–48.
149. Jaffe GJ, Pearson PA, Ashton P. Dexamethasone sustained drug delivery implant for the treatment of severe uveitis. *Retina* 2000; 20: 402–403.
150. Jaffe GJ, Ben-nun J, Guo H, Dunn JP, Ashton P. Fluocinolone acetonide sustained drug delivery device to treat severe uveitis. *Ophthalmology* 2000; 107: 2024–2033.
151. Okabe J, Kimura H, Kunou N, Okabe K, Kato A, Ogura Y. Biodegradable intrascleral implant for sustained intraocular delivery of bethamethasone phosphate. *Invest Ophthalmol Vis Sci* 2003; 44: 740–744.
152. Okabe K, Kimura H, Okabe J, Kato A, Kunou N, Ogura Y. Intraocular tissue distribution of betamethasone after intrascleral administration using a non-biodegradable sustained drug delivery device. *Invest Ophthalmol Vis Sci* 2003; 44: 2702–2707.
153. Yasukawa T, Kimura H, Tabata Y, Ogura Y. Biodegradable sclera plugs for vitreoretinal drug delivery. *Adv Drug Del Rev* 2001; 52: 25–36.
154. Sakurai E, Matsuda Y, Ozeki H, Kunou N, Nakajima K, Ogura Y. Scleral plug of biodegradable polymers containing ganciclovir for experimental cytomegalovirus retinitis. *Invest Ophthalmol Vis Sci* 2001; 42: 2043–2048.
155. Sakurai E, Nozaki M, Okabe K, Kunou N, Kimura H, Ogura Y. Scleral plug of biodegradable polymers containing tacrolimus. *Invest Ophthalmol Vis Sci* 2003; 44: 4845–4852.
156. Dwyer A, Gilger BC. Equine recurrent uveitis. In: Gilger BC, ed. *Equine Ophthalmology.* St. Louis: Elsevier Saunders, 2005.
157. Gilger BC, Wilkie DA, Davidson MG, Allen JB. Use of an intravitreal sustained-release cyclosporine delivery device for treatment of equine recurrent uveitis. *Am J Vet Res* 2001; 62: 1892–1896.
158. Barza M. Factors affecting the intraocular penetration of antibiotics: The influence of route, inflammation, animal species and tissue pigmentation. *Scand J Infect Dis Supplementum* 1978; 14: 151–159.
159. Walstad RA, Blika S. Penetration of ceftazidime into the normal rabbit and human eye. *Scand J Infect Dis Supplementum* 1985; 44: 63–67.
160. Rolinson GN. The significance of protein binding of antibiotics in antibacterial chemotherapy. *J Antimicro Chemotherapy* 1980; 6: 311–317.
161. Murube J, Castillo TR, Coronado A, Cabrera F. Previous ocular compression increases intraocular penetration of systemic drugs. *Ophthalmic Res* 1994; 26: 202–206.

Chapter 7

Clinical Pharmacology and Therapeutics

Part 2: Antimicrobials, Antiinflammatory Agents, and Antiglaucoma Drugs

Alain Regnier

ANTIMICROBIALS

Antibacterial Agents

Periocular and ocular structures are uniquely predisposed to infection by a variety of bacteria. Although some ocular infections may be self-limiting, most should be treated to shorten the clinical course of the infection and reduce the likelihood of complications that may lead to irreversible ocular damage.

General Considerations

The first principle of antibacterial therapy is that the use of antibacterial agents must be restricted to situations in which they are necessary. It is clear that indiscriminate use of antibacterials encourages the development of drug-resistant bacteria.[1] Thus, selection of the cases requires a thorough diagnostic evaluation in order to decide if the encountered disease will benefit from antibacterial therapy. Rational antibacterial therapy depends on the choice of an agent with appropriate spectrum of activity and ability to penetrate the site of infection in concentrations effective against the causative bacteria. The decision to use an antibiotic in a given situation must also take into account its potential risk of toxicity. Result of the therapy depends on effective treatment modalities, including early initiation of treatment and adequate administration route and treatment duration. Antibiotics can be chosen empirically or specifically. Empirical use of an antibiotic should be reserved for minor ocular infections that may not warrant the expense of laboratories analyses. For those infections that may threaten the vision, there is no substitute for isolation and sensitivity testing. Antibiotics are divided into bactericidal agents that destroy bacteria and bacteriostatic agents that inhibit bacterial multiplication. Many bacteriostatic drugs may become bactericidal when present in high concentrations, as may occur with fortified topical ophthalmic medications.[2] Bactericidal agents must be preferred for the treatment of patients with impaired host defenses because efficacy of bacteriostatic agents is more dependent on the natural defense mechanisms. The sulfonamides, trimethoprim, the tetracyclines, chloramphenicol, and the macrolides are bacteriostatic agents, while all others antibiotics are bactericidal agents. The simultaneous administration of two antibacterial agents may provide an additive or synergistic effect and may therefore be necessary for treatment of mixed bacterial infections, enhancement of therapeutic activity, and therapy of severe infections. However, combination of two antibiotics may also produce the opposite effect. Should a combination of antibiotics not commercially available be used, they must be carefully chosen because some combinations are antagonistic when systemically administered or are incompatible when topically used in the same container.

Antibiotic Classes

Penicillins

The penicillins are bactericidal, and their spectrum of activity is largely determined by their molecular structure. Natural penicillins (G and K) are mainly active against Gram-positive and Gram-negative cocci and some Gram-positive bacilli. Efficacy of the penicillinase-resistant penicillins (oxacillin, cloxacillin) is aimed directly against penicillinase-producing strains of Gram-positive cocci, particularly *Staphylococcus* spp., whereas aminopenicillins and carboxypenicillins (ampicillin, amoxycillin, carbenicillin, ticarcillin) have a more extended bacterial spectrum against Gram-negative microorganisms than do the natural penicillins. Combination with penicillinase inhibitors such as clavulanic acid and sulbactam extend their spectrum of activity to many penicillinase-producing isolates of *Staphylococcus.*

The poor liposolubility of penicillin G restricts its passage through blood–ocular barriers, whether given intramuscularly or injected subconjunctivally in the noninflamed canine eye.[2,3] In humans, penicillin G is used in the form of fortified drops for treating corneal ulcers caused by penicillin-sensitive staphylococci, streptococci, and micrococci.[4] In cattle, therapeutic drug concentrations can be achieved for 32 to 56 hours at the ocular surface after topical application of sodium benzylpenicillin, procaine penicillin, or benethamine penicillin ointment preparation,

as well as after a single application of a slow-release ophthalmic formulation of procaine benzylpenicillin.[5,6] Although subconjunctival injection of procaine penicillin can maintain therapeutic concentrations in the bovine tear fluid for 40 to 67 hours, it was reportedly not able to control spontaneous infectious bovine keratoconjunctivitis (IBK) caused by *Moraxella bovis.*[7,8] In sheep, low drug levels were detected in tears after subcutaneous administration of procaine penicillin.[9] Although studies on the preocular residence time of topical benzathine cloxacillin led to divergent results in cattle,[6,10] application of intramammary forms was reported to be clinically effective for treating naturally occurring IBK.[11] Penicillin G and ampicillin can be used topically and/or subconjunctivally in horses for the prophylaxis or treatment of streptococcal keratitis.[12] In cats, oral clavulanic acid-potentiated amoxicillin was found to be as effective as oral doxycycline in the treatment of the acute chlamydial conjunctivitis, using an experimental model of the disease.[13] Ticarcillin, a carboxypenicillin with extended Gram-negative bacterial spectrum, has shown high in vitro efficacy against Gram-positive bacteria isolated from equine eyes with bacterial keratitis.[14] Ticarcillin may be formulated for topical or subconjunctival use.[12]

Cephalosporins

The cephalosporins are broad-spectrum antibiotics closely related in structure to penicillins and similar in their mechanism of action. First-generation cephalosporins, including cefazolin, cefadroxil, cephalexin, and cephalothin, are active against most Gram-positive pathogens.[4,15] Cefazolin is used in veterinary ophthalmology for treatment of bacterial corneal ulcers either as part of a broad-spectrum approach or as a more specific action against Gram-positive cocci.[4] Ophthalmic topical cefazolin is prepared by diluting the parenteral solution (100 mg/ml) in a tear substitute to a final concentration of 50 mg/ml.[16] Cefazolin penetrates the anterior chamber of the noninflamed eye in bactericidal concentrations after subconjunctival injection in humans and rabbits[17] and after intravenous administration (20 mg/kg) in the dog.[18] Therapeutic concentrations against most Gram-positive bacteria are achieved in the human aqueous humor with systemic cephradine or cefoxitin, which are first- and second-generation cephalosporins, respectively.[19,20] Third-generation cephalosporins, such as cefatoxamine,[21] ceftriaxone,[22,23] ceftazidime,[24,25] and ceftriaxone,[26] penetrate the human vitreous after parenteral administration and are used for prophylaxis and treatment of postoperative endophthalmitis.[26] It is usually difficult to justify the use of third-generation cephalosporins in veterinary ophthalmology because of their cost and their limited spectrum relative to bacteria present in most intraocular infections in animals.

Aminoglycosides

The aminoglycosides are bactericidal agents active against aerobic Gram-negative and aerobic Gram-positive bacteria, and their activity may be additive or synergistic with penicillin or cephalosporin antibiotics.[16] Gentamicin and tobramycin have very similar antibacterial and pharmacokinetic properties. They are primarily used by topical routes, subconjunctival routes, or both, and are best recommended for treatment of bacterial corneal infections, particularly those caused by *Pseudomonas aeruginosa.* Netilmicin, a derivative of gentamicin available as an ocular formulation in some countries, has an antibacterial activity similar to that of gentamicin and tobramycin.[27] Topical aminoglycosides are indicated for established infection rather than prophylaxis in order to limit the emergence of bacterial resistance. Conflicting results have been published regarding the prevalence of antibiotic resistance found in microbial isolates associated with equine bacterial keratitis. In a first retrospective study, results indicated that resistance to gentamicin and tobramycin of *Streptococcus equi* and *Pseudomonas aeruginosa,* isolated from cases of equine bacterial keratitis, had significantly increased over the past 10 years,[28] whereas a more recent investigation documented no resistance to gentamicin and tobramycin among the isolates of *Pseudomonas aeruginosa* identified between 1993 and 2004 in horses with bacterial keratitis.[29] Gentamicin and tobramycin are available as topical ophthalmic solutions (3 mg/ml), but tobramycin is also presented as an ophthalmic ointment.[4] Topical application of concentrated preparations (13.6 mg/ml) of gentamicin can achieve corneal concentrations that may be bactericidal for almost all *Pseudomonas* strains[30,31] but is unable to produce therapeutic levels in aqueous of noninflamed eyes.[30,31] Similarly, fortified eye drops of tobramycin (14.5 mg/ml) can be prepared for treatment of severe bacterial keratitis.[32] Effective drug concentrations in both cornea and anterior chamber can be achieved after subconjunctival administration of gentamicin and tobramycin.[33–36] After subconjunctival injection of 20 to 40 mg gentamicin, therapeutic concentrations are achieved in human aqueous humor within 2 hours and for 24 hours.[34,35] Systemic absorption of the drug is not reported after topical application but has been observed after subconjunctival injection.[35,37] This finding should be taken into account when treating very small animals, particularly if they are old and possibly have renal problems. Penetration of gentamicin into inflamed vitreous after subconjunctival injection also has been attributed to direct penetration through the sclera as well as to hematogenous carriage.[33] Conjunctival hyperemia, edema, or both, are sometimes associated with subconjunctival injection of gentamicin. Parenteral administration of gentamicin or tobramycin achieves only low drug concentrations in the anterior segment[30,38,39] and is not potentially useful for treating bacterial infections of the cornea. When using gentamicin, clinicians should be aware of incompatibility with sulfonamides and chloramphenicol.

Kanamycin is effective against *Moraxella bovis,* and its subconjunctival administration may be considered to treat IBK despite the short duration of therapeutic concentration in tear fluid observed after drug administration.[40]

Neomycin is a common component of topical ophthalmic preparations because it is bactericidal against many staphylococci and Gram-negative microorganisms. Topically applied, neomycin penetrates the canine cornea only if the epithelium barrier is altered.[3] Allergic reaction of the conjunctiva may occur with its prolonged use.

Amikacin is effective against most gentamicin-and tobramycin-resistant Gram-negative bacilli.[4] Topical application may provide therapeutic corneal levels but achieve only subtherapeutic concentrations in the anterior chamber.[74] Subconjunctival injection produces the highest levels in aqueous humor but is unable to achieve consistent bactericidal concentrations.[74] After parenteral administration, amikacin does not penetrate aqueous humor and vitreous sufficiently to reach therapeutic concentrations.[41,42] Because amikacin is the least toxic aminoglycoside to the retina, its intravitreal administration was suggested as a component of bacterial endophthalmitis therapy.[43]

Tetracyclines

Tetracyclines are bacteriostatic antibiotics with a wide spectrum of activity against Gram-positive and Gram-negative organisms, including *Moraxella bovis* as well as most strains of *Mycoplasma* and *Chlamydia.* By contrast, *Pseudomonas aeruginosa* is rarely responsive to tetracycline, and resistance of staphyloccoci and streptococci is increasing. Tetracycline suspension and ointment, oxytetracycline (combined with polymixin B) ointment, chlortetracycline ointment, and tetracycline hydrochloride ointment are available for topical ocular use.[4] In cattle, a single subconjunctival injection of a long-acting oxytetracycline formulation may produce therapeutic concentrations in tears for 72 hours.[44] Although the long-acting oxytetracycline formulation administered intramuscularly to calves did not achieve therapeutic levels in tears,[44] it was found relatively successful in treating IBK caused by *Moraxella bovis.*[45,46] The modified tetracyclines, doxycycline and minocycline, are more lipophilic than the parent tetracycline and penetrate relatively well the eye after systemic administration.[47–49] Using experimental models of *Chlamydia psittaci* infection in cats, different studies have demonstrated that oral administration of doxycycline (5 mg/kg every 12 hours or 10 mg/kg once a day) is clinically and microbiologically more efficient to control the disease[50] than is topical 1% chlortetracycline ointment or 1% fusidic acid viscous drops.[51] Presently, oral doxycycline is the preferred treatment of chlamydial conjunctivitis in cats not only because of its efficiency but also because the systemic therapy can eliminate the organisms from extraocular sites (gastrointestinal and urogenital tracts), which act as reservoirs for *Chlamydia.*[51] Oral administration of doxycycline in cats should be accompanied either by a water or food swallow to minimize the risk of oesophagitis and oesophageal stricture, which is a complication of this therapy.[52] In the dog, intravenous infusion of 10 mg/kg doxycycline hyclate diluted in 60 mL of lactated Ringer, and infused over 30 minutes, can give intraocular levels that might be therapeutic against Rickettsial infections for at least 6 hours.[53] The potential for intraocular penetration of doxycycline has also been recently evaluated in horses.[54] In this experiment, doxycycline was given orally to healthy horses at a dose of 10 mg/every 12 hours, and drug concentrations were measured in aqueous and vitreous samples. At steady-state serum concentration (<1 μg/mL) achieved with repeated administrations, the drug concentrations observed in the aqueous and vitreous humors were very low and considered ineffective against most leptospiral isolates.[54]

Chloramphenicol

Chloramphenicol is effective against a wide variety of Gram-positive and Gram-negative organisms, including most strains of *Mycoplasma* and *Chlamydia,* but *Pseudomonas* spp. are usually resistant to this antibiotic. After topical administration, chloramphenicol readily diffuses in the canine anterior chamber only if there is disruption of the epithelial barrier.[3] In vitro studies on enucleated ovine eyes indicated that among topical formulations, ophthalmic ointment appears to provide higher chloramphenicol levels in the cornea and aqueous humor than does an eye drop preparation.[55] It seems from results of a recent investigation that the prevalence of chloramphenicol resistance found in strains of *Streptococcus equi* isolated from cases of equine bacterial keratitis is still very low.[29] Although systemic absorption of the drug has been documented after topical administration in cats, it did not produce aplastic anemia over a 3-week period of treatment.[56] Chloramphenicol is antagonistic to erythromycin.

Polypeptide Antibiotics

Polymyxin B, bacitracin, gramicidin, and vancomycin have a narrow antibacterial spectrum. The primary activity of bacitracin, gramicidin, and vancomycin is against Gram-positive bacteria, while the antibacterial spectrum of polymyxin B is restricted to Gram-negative bacteria. The combination polymyxin B-bacitracin-neomycin is widely used for treatment of nonspecific infections of the ocular surface because it is bactericidal, inexpensive, and available under numerous trade names as both ointments and solutions. Polymyxin B and bacitracin do not penetrate the anterior segment of the intact canine eye following topical administration.[2] Vancomycin is not currently available as an ophthalmic preparation, but a topical solution can be prepared by diluting the parenteral solution 1:4 in a tear substitute to a final concentration of 50 mg/ml.[16] Administered by the intravitreal and/or parenteral routes, vancomycin is considered a drug of choice in the initial treatment of acute endophthalmitis caused by Gram-positive pathogens.[57]

Fluoroquinolones

Fluoroquinolones are bactericidal against a wide range of Gram-negative and a number of Gram-positive aerobes. They also possess significant activity against *Mycoplasma* spp. and *Chlamydia* spp.[58] The fluoroquinolones initially available for topical administration included norfloxacin, ciprofloxacin, ofloxacin, and levofloxacin ophthalmic solutions. Ciprofloxacin is also available as an ointment.[59] The topical fourth-generation fluoroquinolones moxifloxacin and gatifloxacin were approved in 2003 for ocular indications.[60] Because of their spectrum of activity and apparent lack of toxicity, the topical fluoroquinolones have become first-line

antibiotics for the initial treatment of bacterial keratitis in people.[61] Their microbiologic efficacy has been demonstrated in experimental models of pseudomonal and staphylococcal keratitis.[16,62] Topically applied, ofloxacin has higher corneal penetration and ability to exceed the MIC_{90} of ocular pathogens than topical ciprofloxacin, as demonstrated in humans,[63] and more recently in dogs.[64] Norfloxacin ophthalmic solution also demonstrated high potency to penetrate the nonulcerated human cornea after topical application.[65] Topical fluoroquinolones are mostly indicated in dogs and horses for the treatment of severe corneal infections due to sensitive organisms, particularly aminoglycoside-resistant *Pseudomonas* spp. and should be dictated by susceptibility testing results.[66] In a recent in vitro experiment, all *Streptococcus equi* and *Pseudomonas aeruginosa* isolated from bacterial equine keratitis were susceptible to ciprofloxacin.[29] A serious complication observed in human bacterial keratitis treated with topical ofloxacin is an increase in corneal perforation, but to our knowledge this side effect has not been reported in veterinary ophthalmology.[67] The cause is unknown, but experimentally ofloxacin, ciprofloxacin, and norfloxacin have been shown to have significant antiproliferative and cytotoxic effects on stromal keratocytes.[68] As widespread use of antibiotics facilitate the emergence of resistant bacteria, routine use of topical fluoroquinolones in animals for treating superficial ocular infections that are not vision-threatening conditions (e.g., conjunctivitis) should be discouraged. Several studies in humans have demonstrated that systemic fluoroquinolones, such as ciprofloxacin, ofloxacin, pefloxacin, and levofloxacin, are able to achieve therapeutic levels in ocular fluids.[69–72] In the dog, intravenous administration of marbofloxacin (4–5 mg/kg) may lead to aqueous drug concentrations that are above the MIC_{90} for most pathogens with the exception of *Streptococcus* spp.[73]

Parenteral enrofloxacin may be associated with generalized retinal degeneration in some cats when the drug is administered at a dosage higher than that recommended by the manufacturer (5 mg/kg q 24 hours). Older cats (>12 years) appear to be more often affected than younger cats (<9 years) by this side effect. The estimated incidence is 0.0008%, which means one out of 122,414 cats.[74] Clinically, blindness often results, but some subjects may regain vision with discontinuation of the drug.[74] Fundoscopic abnormalities are characterized by gray discoloration with tapetal hyperreflectivity, initially observed in the area centralis and then by generalized attenuation of retinal blood vessels.[74] Changes in the electroretinogram with significant decrease in a- and b-wave amplitudes are present and may precede fundoscopic changes.[75] Histological examination of affected retinas revealed that rod photoreceptors first degenerate before atrophy of the outer retina develops.[76] Following the report on the possible association between enrofloxacin and retinal atrophy in cats, other veterinary-labeled fluoroquinolones were evaluated in postapproval studies for their potential to induce retinal degeneration in cats.[77] When a 3% oral liquid formulation of orbifloxacin was given to cats at doses ranging from 15 to 75 mg/kg every 24 hours for 30 days, retinal changes characterized by focal tapetal hyperreflectivity and minimal photoreceptor degeneration on histology were identified only in subjects receiving 45 and 75 mg/kg, which are dosages largely exceeding the approved dose range of 2.5 to 7.5 mg/kg.[78] Marbofloxacin was also evaluated at doses up to 20 times the recommended dose, and no clinical and histologic lesions were found in the eyes of the treated animals.[77]

Lincosamides and Macrolides

Although structurally distinct, clindamycin, a lincosamide antibiotic, and erythromycin, a macrolide antibiotic, have the same action on the 50S ribosomal subunit, and their spectrum of action is mainly Gram-positive bacteria. Clindamycin is a chlorinated analogue of lincomycin; its activity against *Toxoplasma gondii*[2,4] is of particular interest in ophthalmology. Although a possible clindamycin-induced decrease in the antitoxoplasmic activity of phagocytic cells has been suggested by experimental data in cats,[79] oral clindamycin at a dosage of 25 mg/kg daily, for 14 to 42 days, is currently recommended in the treatment of ophthalmic signs of toxoplasmosis in cats.[80] Erythromycin, available in some countries as a 0.5% ophthalmic ointment, is active against *Chlamydia* and *Mycoplasma* spp. A high efficiency against Gram-positive organisms isolated from infected equine eyes was demonstrated and suggests that erythromycin might be an appropriate first-choice antibiotic for treating equine keratitis caused by Gram-positive pathogens.[81] Azithromycin is structurally related to erythromycin but has a better activity against Gram-negative pathogens and some other pathogens, notably *Borrelia burgdorferi* and *Bartonella henselae*.[82] It is administered to cats at a usual dosage of 50 mg daily for 21 days to treat the ocular forms of *Bartonella henselae* infection.[83] The drug, available in 250-mg tablets and in a 40-mg/mL fruit-flavored oral suspension, should be prepared in a liver- or fish-flavored suspension, in capsules or palatable chewable treats, in a 50-mg dose to be administered to cats.[6]

Sulfonamides

Topical ophthalmic preparations of sulfonamides include sodium sulfacetamide and sulfisoxazole. They are uncommonly used in veterinary ophthalmology because of effective and readily available alternative topical antibiotics. They are indicated for treating staphylococcal blepharitis in humans, but local hypersensitivity and photosensitivity reactions may occur with their topical application.[4,84] Trimethoprim-sulfadiazine administered orally in the dog can maintain concentrations in aqueous humor and vitreous greater than the MIC of many susceptible microorganisms and may be indicated to begin empirical treatment of bacterial endophthalmitis.[85] Keratoconjunctivitis sicca (KCS) is a side effect observed in about 4% of dogs taking systemic sulfonamides.[86] There is no significant association between the type, dosage, and duration of sulfonamide treatment.[86] In horses, no significant decrease in tear production was identified in animals treated with 30 mg/kg of trimethoprim-sulfadiazine for 8 weeks.[87]

Fusidic Acid

Fusidic acid is a steroidal antibiotic effective against a wide range of Gram-positive organisms and particularly staphylococci. It is available as a 1% ophthalmic gel. Pharmacokinetic studies in the cat eye have shown that a single topical application of this formulation results in drug concentrations in the tear fluid above the MIC_{90} for *Staphylococcus* species for 24 hours.[88] In addition, experimental data in the rabbit indicate that topical fusidic acid penetrates the intact and abraded cornea, resulting in corneal levels well above the MIC for staphylococci and streptococci.[89] Good corneal penetration and absence of local toxicity make this topical preparation suitable for the control of Gram-positive infections of the ocular surfaces.

Routes of Administration

After an antibiotic has been selected for use, based on its spectrum of activity and pharmacologic behavior within the eye, the clinician must determine which route of administration will best ensure an effective concentration of drug at the site of infection. Antibiotics can be administered topically, subconjunctivally, intraocularly, and systemically. Selection of one or more methods of drug delivery is determined by the site and severity of the infection.

Topical Administration

Topical application of antibiotics is the route of choice for treating most palpebral, conjunctival, and corneal infections, as well as infections of the nasolacrimal system. The topical treatment of ocular surface infections is preferred because the antiinfective agent may be given in a relatively small dose while achieving therapeutic drug concentrations at the site of infection. For instance, there is experimental evidence that topical application of ophthalmic antibiotic solutions or ointments is more effective in eliminating bacteria from the cornea than are periocular and intravenous routes of administration.[90] In contrast, topical medication alone is unable to improve or cure intraocular infections and must be used in conjunction with a subconjunctival, intraocular, or systemic antibiotherapy.

Bacterial conjunctivitis and mild superficial keratitis are usually responsive to empirical treatment involving topical broad-spectrum antibacterials such as polymyxin-bacitracin-neomycin, chloramphenicol, tetracycline, or gentamicin applied 3 to 4 times daily.[91] The antibiotic concentration of commercial eye drops is usually effective for treatment of these ocular infections but may be insufficient for progressive bacterial ulcers of the cornea that require aggressive antimicrobial chemotherapy based on knowledge of the identity of the infecting bacteria and susceptibility to available antimicrobials.[91] In these cases, initial topical therapy may be oriented by the Gram stain of corneal smears, as illustrated in Table 7.2.1. To be efficient, the specific antibiotherapy should produce high concentrations in the cornea by frequent applications of highly concentrated solutions.[92,93] In horses, a subpalpebral tube delivery system is necessary to provide such a frequent topical administration.[94,95] For antibiotics not available as ophthalmic drops or ointment, topical solutions may be prepared by mixing the parenteral preparation of the drug with artificial tears.[4] Topical delivery of "fortified" concentrations of antibiotics is also a common practice when a severe bacterial ulcer of the cornea is present.[91] Fortified antibiotic ophthalmic solutions are prepared by adding a small volume of a parenteral antibiotic preparation to the dropper bottle of the equivalent topical antibiotic. Suggested concentrations of fortified antibiotics used for topical treatment of infectious ulcerative keratitis in small animals and horses are presented in Table 7.2.2. The potential for local toxicity should also be considered before administration is decided, since some data suggest that frequent administration of commercial or fortified antibiotic solutions may cause toxic conjunctivitis, punctate superficial keratopathy, or delay corneal re-epithelialization.[96] The effects of gentamicin, tobramycin, chloramphenicol, ofloxacine, and ciprofloxacine on corneal epithelium have been determined using rabbit and dog corneal epithelial cultures.[97–98] In these studies, gentamicin was found more toxic to corneal epithelium than tobramycin was at similar concentrations of 0.05 to 2.0 mg/L.[97–98] The effects of gentamicin on corneal epithelium are often tolerated for the therapeutic benefit derived from its use, but because it causes slower healing rates, the possibility that it may delay corneal epithelium healing after topical application should be considered when using commercial preparations in the prophylactic treatment of corneal epithelial defects and fortified formulations in the curative treatment of

Table 7.2.1. Selection of Initial Antibiotics on the Basis of Smear Morphology

Gram Stain	Suggested Antibiotics
Gram-positive cocci *Staphylococcus* spp. *Streptococcus* spp.	Bacitracin 500U/g, chloramphenicol 0.5%, gentamicin 0.3%, cefazolin 3.3%, erythromycin, vancomycin 3%
Gram-positive rods *Corynebacterium* spp. *Bacillus cereus*	Chloramphenicol 0.5%, bacitracin 500U/g, erythromycin 0.5%, carbenicillin
Gram-negative cocci *Neisseria* spp.	Bacitracin 500U/g, penicillin G (100,000 U/mL)
Gram-negative rods *Pseudomonas aeruginosa* *Escherichia coli* *Proteus* spp.	Gentamicin 1.0 to1.4%, tobramycin 1.4%, amikacin 3.3%, ciprofloxacin 0.3%, ofloxacin 0.3%, norfloxacin 0.3%

Table 7.2.2 Fortified and Noncommercial Antibiotic Solutions for Topical Ophthalmic Use

Antibiotic	Concentrations of Commercial Eye Solutions	Concentrations of Formulated Eye Solutions	Shelf Life
Amikacin	N/A	10 mg/mL	30 days
Carbenicillin	N/A	4–8 mg/mL	3 days
Cefazolin	N/A	50 mg/mL	4 days
Gentamicin	3 mg/mL	14 mg/mL	30 days

corneal bacterial ulcers.[98] Data from in vitro studies also showed that ofloxacin was more toxic to the corneal epithelium than were the aminoglycosides,[97] and conversely that ciprofloxacin was less toxic to the corneal epithelium than were the aminoglycosides and the other fluoroquinolones.[99] At the opposite of the in vitro data, an in vivo evaluation of the kinetics of corneal epithelium regeneration in rabbits demonstrated that gentamicin at a concentration of 3 mg/mL did not delay the healing of experimental epithelial ulcers.[100]

Subconjunctival Injection

The ability to deliver effective concentrations of antibiotics to the anterior segment of the eye (cornea, iris, aqueous humor) by subconjunctival injections is supported by experimental data.[93] A comparison of topical and subconjunctival routes of treatment for bacterial corneal ulcers has shown that subconjunctival administration produces transiently high antibiotic levels in the cornea and that concentrations after 8 hours are similar to those achieved by hourly topical applications.[101] Thus, subconjunctival injection may be indicated when there is a need to obtain high tissue concentrations of antibiotics in emergency management of acute anterior segment infection, and as such, it may be used as part of the antimicrobial therapy in ulcerative and nonulcerative bacterial keratitis in conjunction with topical antibiotic administration.[92] The subconjunctival route was found equivalent to retrobulbar injection in penetrating inflamed vitreous humor and may be considered as an adjunctive therapy in the treatment of bacterial endophthalmitis.[93] Subconjunctival injections of antibiotic are recommended every 12 to 24 hours, but repeated injections expose the conjunctiva to an inflammatory reaction.[91] Parenteral formulations of chloramphenicol and tetracycline are not well tolerated by the subconjunctival route and should be avoided. Table 7.2.3 presents the recommended dosages for subconjunctival antibiotics.

Intravitreal Injection

Injection of antibiotics in the vitreous cavity is a mainstay in treatment of bacterial endophthalmitis in human patients. In veterinary ophthalmology, this technique has not gained wide acceptance because it requires expertise and carries the risk of iatrogenic lesion to the retina. Most often, it is used as a salvage procedure when response from subconjunctival and systemic routes of administration is poor.[91] Antibacterial concentrations in the vitreous humor can be maintained for 48 hours after a single intravitreal injection of netilmicin (500 μg/0.1 ml), piperacillin (2,000 μg/0.1 ml), and ampicillin (2,000 μg/0.1 ml).[102]

Table 7.2.3 Suggested Dosages for Subconjunctival Antibiotics

Antibiotic	Dosage (mg)
Amikacin	25–125
Ampicillin	50–100
Carbenicillin	100
Cephalotin	100
Cefazolin	100
Gentamicin	10–40
Methicillin	20–100
Tobramycin	20–40
Vancomycin	25

Systemic Administration

In small animals, systemic antibiotics are given primarily for infections of palpebral soft tissue, bacterial orbital cellulitis, and retrobulbar abscess. Bacterial ulcers with contamination of the anterior segment should also be treated with adjunctive systemic antibiotherapy. The dosages are the same as for other severe infections. Orbital cellulitis and abscess formation require systemic antibiotic administration with adjunctive removal of the initiating factor and establishment of surgical drainage. Most animals respond favorably to a systemic broad-spectrum antibiotic such as amoxicillin-clavulanic acid administered for 10 days. The parenteral administration of a carefully selected antibiotic can also be helpful in bacterial endophthalmitis. As a general rule, those antibiotics with low protein binding and high lipid solubility penetrate better the intraocular tissue and humors following systemic administration.[93] By altering permeability of the blood–ocular barriers, intraocular inflammation enhances penetration of systemic antibiotics into the eye.[93] Pharmacokinetic data indicate trimethoprim-sulfadiazine as a drug of choice in the dog.[85] In reference to human data, it appears that parenteral administration of cephalotin or cefamandole is potentially useful in

Gram-positive infections.[103] For Gram-negative infections, the intravenous drugs of choice may be ceftazidime and ceftizoxime.[103] In food animals, the systemic administration of sulfonamides or the long-acting oxytetracycline formulation may be considered for the treatment of infectious keratoconjunctivitis.[104]

Antiviral Agents

Nucleoside analogues and interferons are currently used in veterinary ophthalmology, chiefly for treating feline herpesvirus ocular disease. These compounds operate on the viral replication cycle, and nucleosides analogues have a common target: viral DNA polymerases. Drugs currently used are virostatic in nature and are unable to eradicate latent viral infection.

Drug Outline

Pyrimidine Nucleoside Analogues

Idoxuridine, trifluridine (or trifluorothymidine), and bromovinyldeoxyuridine belong to the pyrimidine nucleoside analogue class of compounds. Structurally, they all are 5-substitutes analogues of 2-deoxythymidine, the natural precursor of DNA synthesis.[105] Idoxuridine is no longer commercially available as an ophthalmic preparation but can be compounded as a 0.1% ophthalmic solution or a 2.5% ophthalmic ointment.[106] Trifluridine is marketed as 1% ophthalmic drops. Both drugs have low solubility, and their intraocular penetration is low unless the epithelial barrier is altered.[107] Idoxuridine and trifuridine were found highly effective against some strains of feline herpesvirus-1 (FHV-1) in vitro.[109]

Purine Nucleoside Analogues

Vidarabine, or adenine arabinoside, is effective against several DNA viruses, notably the herpesviruses. Administered topically as a 3% ointment, vidarabine has been reported to be as effective as idoxuridine in the treatment of herpetic keratitis in humans[105] but does not show cross-resistance to idoxuridine.[107] The commercial formulations are no longer available, but a 3% ophthalmic ointment and a 1% ophthalmic suspension can be compounded.[106]

Acyclovir is a guanine derivative of vidarabine that is selectively phosphorylated by herpesvirus thymidine kinase and then acts as a competitive inhibitor of the incorporation of deoxyguanosine triphosphate into DNA. Preferential inhibition of the synthesis of viral DNA, as opposed to normal cellular DNA, results in minimum toxicity to uninfected normal cells.[107] In vitro testing has shown that acyclovir is less active against FHV-1 than idoxuridine, trifluridine, and the new purine analogue compounds (ganciclovir, cidofovir, penciclovir).[108,109] Acyclovir is available as a 5% ophthalmic ointment in polyethylene base and as oral and parenteral preparations.[110] In the cat, administration of acyclovir at 50 mg/kg does not achieve plasma concentrations susceptible to inhibit FHV-1.[111] Such therapeutic concentrations can be obtained with repeated administrations of valacyclovir (60 mg/kg), a prodrug of acyclovir, with 2.3 times greater systemic availability than the parent drug in cats. However, this dosage regimen can be toxic to the kidneys and bone marrow[111] and was unable to suppress viral replication in cats experimentally infected with FHV-1.[112]

Ganciclovir, cidofovir, and penciclovir are new compounds. Ganciclovir and penciclovir are closely related to acyclovir, while cidofovir is a cytosine analogue. Their in vitro antiviral efficacy was recently assessed using cultured feline kidney cells infected with FHV-1.[113] By comparing the mean inhibitory concentration 50 (IC_{50}) of the drugs, it was concluded that the antiviral effect of ganciclovir and idoxuridine is equivalent and is about twice that of cidofovir and penciclovir.[113] Efficacy of cidofovir against FHV-1 was further confirmed in vitro using feline corneal epithelial cells for viral cultures, but cytotoxic effects were observed at all drug concentrations tested.[114] Although cidofovir could represent an interesting compound for treating cats with ocular-induced FHV-1 disease, its long half-life of elimination, which could allow less frequent application than other antiviral drugs,[113] necessitates further study to evaluate the clinical relevance of the cytopathic effect observed in vitro.[114]

Foscarnet

The pyrophosphate analogue, foscarnet, inhibits the herpesviruses, including cytomegalovirus, by selective inhibition of the DNA polymerase without requiring phosphorylation to achieve this effect.[115] Foscarnet is used as monotherapy or combined with ganciclovir for the treatment of cytomegalovirus retinitis in human patients with acquired immunodeficiency syndrome.[116] Its in vitro activity against FHV-1 is very limited: approximately four times less than that of acyclovir.[113]

Interferons

Interferons (IFNs) are a group of related glycoproteins that form part of the cytokine family. They differ in biological and chemical properties, cell origin, inducing agent, and antigenicity, and are divided into two major classes: the type I and type II IFNs. Type I IFNs are subdivided into four subfamilies, termed IFN-α, IFN-β, IFN-ω, and IFN-τ (trophoblast IFN).[117] Members of the type I IFN superfamily are related to each other structurally, while IFN-γ, the only type II interferon, has no structural homology with type I IFNs. Virus, bacteria, and protozoa are common biological causes of type I IFN induction in a large number of cell types, while antigens, bacteria, and protozoa can lead to IFN-γ production by T lymphocytes or NK cells.[117] Type I IFNs bind to the same basal receptor but exhibit different patterns of receptor interaction and signal transduction that lead to different biologic activities, among which are the actions on virus replication cycle.[118] In cells exposed to IFNs, the antiviral effects are primarily mediated by IFN-induced proteins, which, depending on the virus and host cell, interact with various steps in the virus life cycle. For instance, IFNs affect transcription and release of mature

virions of herpes simplex virus.[117–119] In addition to their induction of antiviral proteins at the cellular level, IFNs also stimulate the immunological defenses, notably the immune cell–mediated lysis of virus-infected cells.[117]

Because they represent components of the natural defense to virus infections, IFNs offer a potential approach to treatment of viral disease. Preparations of recombinant human IFN-α and IFN-β are currently available for parenteral administration, and a recombinant feline IFN-ω has recently been marketed for veterinary use.[120] At concentrations ranging from 10^2 to 10^6 UI/mL, human recombinant IFN-α did not manifest cytotoxic effects on feline corneal epithelial cells cultured in vitro.[121] A modest but significant reduction in replication and spread of FHV-1 within infected feline corneal epithelial cells was observed when the concentration of 10^5 UI of recombinant IFN-α/mL was added to the culture medium.[121] Human recombinant IFN-α was found to be synergistic with acyclovir against FHV-1 in cell cultures.[122] The activity of the recombinant feline IFN-ω was recently assessed on healthy cats using expression of the Mx-protein in conjunctival and white blood cells. The Mx-protein is induced at the transcription level by IFN-ω and confers resistance to the viral infection. Mx-protein expression in conjunctival cells was observed after topical application in the eyes but not after oral administration of the IFN. After topical application, the biologic effect was apparently dose-dependent and long-lasting for a concentration of 500,000 U of IFN-ω/mL.[123]

L-Lysine

Current recommendation of oral supplementation with lysine in cats with FHV-1 ocular disease was initially transposed from early reports claiming that the supplement lysine could prevent or relieve herpes simplex infection.[124] This recommendation was recently supported by results of in vitro and in vivo experiments with FHV-1.[125–127] In cell cultures, arginine has a growth-promoting effect on FHV-1, but attenuation of virus replication can be obtained by supplementing viral culture medium with lysine. The effect of lysine on FHV-1 replication in vitro appeared dependent of the lysine–arginine ratio available to the virus and was optimally observed when lysine was added to media containing low concentrations of arginine.[125] The clinical applicability of arginine reduction in the diet is not advised in cats because it results in increased blood levels of ammonia, so oral administration of lysine has been proposed as a logical means of controlling FHV-1 infection.[126,127] Using experimental models of FHV-1 infection, it was observed that oral administration of 500 mg of lysine every 12 hours lessened the severity of herpetic conjunctivitis in cats[127] and that a once-daily dose of 400 mg given to cats latently infected with FHV-1 reduced viral shedding secondary to changes in housing and husbandry but not to corticosteroid administration.[127] The current recommendation of using dietary lysine supplementation in an attempt to suppress FHV-1 infection and reactivation is based on these experimental data but has not been assessed by controlled clinical trials.

Other Potential Antiviral Agent or Formulation

Lactoferrin is one of the substances secreted in tears to protect the ocular surface against infection. This is a mammalian iron-binding glycoprotein with antibacterial, antifungal, antiviral, and antiprotozoal properties.[128] In a recent experiment, bovine lactoferrin manifested a significant inhibitory effect on in vitro replication of FHV-1, presumably resulting from effects on FHV-1 adsorption to the cell surface, penetration into the cells, or both.[128] The potential for lactoferrin to be used as a topical treatment in cats with FHV-1 ocular disease warrants further studies. The use of liposomes to deliver antiviral drugs to the eye is still in the development stages, but in vitro studies demonstrated a high efficacy of liposomal formulations containing 2.5% or 5% polividone iodide against herpes simplex virus type 1 and a better tolerance than the aqueous solutions.[129]

Guidelines for Ophthalmic Uses

In veterinary ophthalmology, antiviral drugs are primarily used to treat feline herpetic ocular disease. An in-depth overview of the management of ocular FHV-1 infection is presented in Chapter 24, "Feline Ophthalmology." Idoxuridine, trifluridine, and ganciclovir are considered as useful first-line antiviral agents for the treatment of FHV-1 epithelial keratitis on the basis of in vitro data.[130] Their clinical usefulness is currently considered questionable in acute conjunctivitis without corneal involvement,[130] although a 2- to 3-week course of their topical application may help to improve conjunctival inflammation in severe cases.[131] It has been assumed that trifluridine should be preferred in herpetic keratitis owing to better corneal penetration. However, neither drug is predictably effective, and clinical trials concluded that the efficacies of trifluridine and idoxuridine were similar.[132] Trifluridine, idoxuridine, and ganciclovir are virostatic; therefore, to be effective, they must be applied frequently to the affected cornea until the corneal ulcers heal. Local irritation manifested by blepharospasm and conjunctival hyperemia may develop during treatment with every drug. In these cases, topical medication must be changed. Vidarabine ointment is less irritating and may be applied every 3 to 4 hours.

Although in vitro data do not militate in favor of the use of acyclovir for the treatment of FHV-1 ocular manifestations, a recent clinical trial showed that when the 0.5% acyclovir ophthalmic ointment is applied 5 times daily, it may improve the clinical signs of FHV-1 conjunctivitis and keratitis.[133] In refractory and severe cases, combined therapy with topical antiviral medication, human recombinant IFN-α, and oral lysine is currently used.[130,131] INF-α can be instilled as a 10^3 to 10^6 U/mL solution, 2 to 3 times daily, or administered orally at a once-daily dose of 25 UI.[130] Based on current information, a dose of 500 mg lysine given twice daily with food, is recommended as a complementary therapy for both cats with acute FHV-1 disease and those with chronic conjunctivitis or stromal keratitis.[130,131] Cats with recrudescent disease episodes can be maintained indefinitely on 500 mg of oral lysine twice

daily as a long-term prophylactic measure.[131] Lysine therapy is inexpensive and usually well tolerated. Experimentally, lysine supplementation to a commercial-type cat diet was increased to evaluate the safety of excess lysine in cats.[134] As a result of increasing dietary lysine intake, mean plasma lysine concentration increased, while plasma arginine concentration did not change, nor were clinical signs of arginine deficiency observed in these animals.[134]

In the horse, topical application of idoxuridine is used in the treatment of the two clinical forms of the superficial punctate keratitis, which is attributed to equine herpesvirus-2 (EHV-2) infection.[135,136] Vidarabine and trifluridine may represent alternatives if idoxuridine is not available,[135,136] but use of acyclovir is more questionable due to lack of in vitro efficacy against EHV-1.[135]

Antifungal Agents

Occurrence of keratomycoses and systemic mycoses is strongly influenced by locality, species of the patient, degree of exposure, and individual susceptibility. Horses seem to develop keratomycosis more frequently than do other species, and intraocular mycoses tend to be more prevalent in dogs than in cats, except for cryptococcosis.[137] Although treatment of systemic mycoses has advanced substantially with the introduction of new azole agents, chemotherapy of keratomycosis is hampered by the lack of antifungal preparations designed for ophthalmic use. Therefore, medical treatment of equine keratomycosis is based on use of compounded ophthalmic preparations or medications approved for humans.[137]

In domestic animals, ocular mycoses may present as dermatophytic infections of the eyelids (mycotic blepharitis), keratomycosis, or intraocular diseases (retinochoroiditis, endophthalmitis) secondary to a systemic mycotic infection. These disorders bear no resemblance to each other, and the organisms involved in them are quite dissimilar. Species of *Microsporum* and *Trichophyton* are most frequently isolated from mycotic blepharitis in dogs and cats. A wide variety of fungi may be involved in fungal keratitis, but early and recent surveys have shown that the most frequent is *Aspergillus* in horses[138–140] and dogs.[141] *Fusarium, Penicillium, Cylindrocarpon, Scytalidium,* and *Torulopsis* may also be responsible of corneal infection in horses.[140] At the opposite, *Candida albicans,* a common cause of human keratomycosis, seems to be rare in equine and canine cases of keratomycosis. Coccidiodomycosis, blastomycosis, cryptococcosis, and histoplasmosis are the most common systemic mycoses that can present with intraocular lesions in small animals.

Although treatment of systemic mycoses has advanced substantially as more drugs become available, chemotherapy of keratomycosis is still hampered by the lack of antifungal preparations designed for ophthalmic use. The principal topical antifungals used for corneal diseases are derived, with the exception of natamycin, from systemically administered compounds. The three main groups of antifungals currently used in nondermatophyte infections (polyene antibiotics, pyrimidines, and imidazole derivatives) can be considered for treatment of oculomycoses. An extensive review of the pharmacological and clinical properties of antifungal agents currently available for veterinary ophthalmology has been published recently.[137]

Antifungal Classes

Currently, there are three main chemical groups of drugs for use in fungal eye infections: polyenes, azoles (as derivatives of imidazoles), and 5-fluorocytosine.[142]

Polyene Antibiotics

The antifungal activity of polyene antibiotics relates to their ability to bind to a sterol moiety present in the fungal cell membrane and form a polyene-sterol complex that alters the selective permeability of the membrane and results in leakage of essential intracellular components, notably potassium efflux. Oxidative damage to the cells also seems to be involved.[143] Of the polyenes, amphotericin B, natamycin, and nystatin are of clinical ophthalmic use. Amphotericin B, produced by *Streptomyces nodosus,* exhibits a broad spectrum of activity against systemic fungal infections (e.g., cyptococcosis, histoplasmosis, blastomycosis, coccidioidomycosis), and several *Candida* species.[143,144] Some strains of *Mucor* and filamentous fungi, such as *Aspergillus,* are resistant.[143,144] The drug is either fungistatic or fungicidal, depending on drug concentration and susceptibility of the fungus.[110] For treatment of deep-seated mycoses, amphotericin B is administered systemically, but potential renal toxicity precludes widespread use in small animals.[145] In addition, its value in intraocular fungal infections is restricted by poor intraocular penetration following parenteral administration and potential retinal toxicity when administered intravitreally.[4] Topically applied, amphotericin B penetrates the intact corneal epithelium poorly because of its high molecular weight (924.11 Da) but can reach high levels in the corneal stroma after removal of the epithelium.[142,146] Topical application of a 1% solution, made from the commercial intravenous preparation, may produce toxic effects such as conjunctival hyperhemia, corneal edema, and iritis, and may delay closure of epithelial defects.[146] This is linked to the combined effect of amphotericin B and of desoxycholate present as a solubilizer in the preparation. Concentrations from 0.075% to 0.20% amphotericin B were found to be better tolerated and effective in treating human and experimental keratomycoses.[4,147] In horses, concentrations above 0.30% can be irritating to the eye.[148] The solution must be prepared with sterile water, because amphotericin B is incompatible with saline, refrigerated, and kept in a dark bottle to avoid photodegradation. Natamycin (pimaricin) has a better spectrum of activity than amphotericin B and is particularly effective against *Fusarium.*[144,145] Natamycin is used as a 5% topical ophthalmic suspension and is not parenterally administered due to systemic toxicity. Like amphotericin B, natamycin penetrates the cornea only if the corneal epithelium is altered.[146] The suspension often adheres to areas of epithelial defects, but topical

application is usually well tolerated.[4] Nystatin may be topically applied as an ophthalmic compounded formulation.[137]

Azole Agents

Currently, there are two major types of azoles in use for treatment of fungal ocular infections: the imidazoles (i.e., miconazole, ketoconazole, econazole), with two nitrogen atoms in the five-membered ring structure, and the triazoles (i.e., fluconazole, itraconazole, voriconazole), which were more recently introduced and contain three nitrogen atoms in the five-membered ring.[142] Azole agents have a common mode of action, which relates mainly to their ability to increase fungal cell membrane permeability by interfering with the cytochrome P450-dependent lanosterol C14 demethylase, which leads to accumulation of 14-methylated ergosterol precursors in the membrane.[143,144] In addition, azole agents inhibit mitochondrial oxidative and peroxidative enzymes, resulting in accumulation of toxic intracellular products and cell death.[110,144] At higher concentrations, they interact with the phospholipids present in the fungal cell wall, causing direct damage to the cell membrane.[143] The imidazoles are also effective against some Gram-positive bacteria and anaerobes.[110] Miconazole, in addition to having activity against fungi, including *Aspergillus, Candida, Fusarium, Penicillium,* and *Alternaria* organisms, is also active against Gram-positive cocci.[4] Miconazole has been used topically, subconjunctivally, and intravenously to treat fungal infection of the cornea in humans,[4] although some studies failed to demonstrate benefit against experimental keratomycoses.[147,149,150] A 1% solution, prepared from the commercial intravenous preparation, is safe for topical application.[151] Subconjunctival injection usually is 5 to 10 mg daily in humans.[4] Miconazole is also marketed as a 2% dermatologic cream and a 2% vaginal cream, and it has been suggested these preparations may be used topically to treat canine keratomycosis.[141] Ketoconazole penetrates the cornea and aqueous humor well when given orally, topically, or subconjunctivally but penetrates the vitreous poorly after systemic administration.[147,152] A 1% solution did not significantly retard closure of experimentally produced corneal epithelial defects in the rabbit and was not irritating to conjunctiva or cornea.[151] Ketoconazole has been successfully used topically and orally in human patients with fungal keratitis.[153,154] *Aspergillus* isolates associated with equine keratomycosis have been found similarly sensitive to ketoconazole and miconazole.[139] Ketoconazole-related cataractogenesis was recently reported in dogs treated for extended period of time (up to 37 months) and with dosages ranging from 6 to 30 mg/kg daily.[155] In a recent randomized clinical trial, topical 2% econazole and 5% natamycin appeared similarly effective in the management of human fungal keratitis.[156] Fluconazole orally administered was shown to achieve high corneal concentrations in the rabbit[157] and concentrations exceeding MICs for pathogenic fungi in feline aqueous humor.[158] Conflicting results have been published on the efficacy of its oral administration to control fungal infection in experimental *Aspergillus* keratitis.[159,160] Topical application of the 2 mg/mL intravenous solution was found effective for treating a case of equine *Histoplasma* keratitis[161] and to lessen the severity of corneal lesions in a rabbit model of *Aspergillus* keratitis.[160] In humans, the topical application of this formulation was demonstrated to lead to concentrations in aqueous humor that satisfy MICs for most of the *Candida* strains.[162] Itraconazole has a broader spectrum of activity than fluconazole and is fungicidal against *Aspergillus* spp.[143] Available in oral and intravenous formulations,[143] itraconazole is used for the treatment of histoplasmosis, blastomycosis, and certain forms of aspergillosis in humans.[143] Oral treatment with itraconazole has been ineffective in reducing *Aspergillus fumigatus* infection in a rabbit model of keratomycosis.[159] In the dog, 42% of cases with ocular blastomycosis responded favorably to itraconazole given orally (10 mg/kg daily) for 60 days.[163] Histopathologic evaluation of canine eyes unresponsive to therapy revealed that intraocular inflammation and number of *Blastomyces dermatitidis* were not significantly different from those observed in untreated eyes.[164] On the basis of an experimental trial in the horse, it may be assumed that topical application of a 1% itraconazole/30% dimethyl sulphoxide petroleum-based ointment is well tolerated and can achieve high drug concentrations in the cornea.[165]

Voriconazole, a representative of the third generation of azole agents, is available in oral and intravenous formulations. It presents a better and broader antifungal activity than fluconazole and is primarily used for treatment of opportunistic fungal infections in immunocompromised patients.[143] Administered intravitreally at a concentration up to 25 μg/mL, it did not induce electrophysiological and histological changes of the retina and therefore may be indicated for the treatment of fungal endophthalmitis.[166]

5-Fluorocytosine

Flucytosine (5-fluorocytosine, 5FC), derived from a fluorinated pyrimidine derivative, is enzymatically converted inside fungal cells to 5-fluorouracil that is subsequently metabolized to 5-fluorodeoxyuridine monophosphate, a potent inhibitor of DNA synthesis, and to 5FUMP, which is incorporated into the RNA.[143] Conversion of 5FC to 5-fluorouracil is limited in mammalian cells, and toxicity of the drug is low. The main effectiveness of 5FC is restricted to *Cryptococcus neoformans* and some strains of *Candida* and *Aspergillus.*[142] In vitro testing has shown that 5FC was the least active antifungal compound against most filamentous fungi isolated from equine fungal keratitis,[139] but when dictated by culture and sensitivity analyses, the drug may be formulated for topical use by dissolving contents of oral capsules in sterile water to form 1% solution.[66] Topically applied as a 1% solution, 5FC appeared less effective than amphotericin B and natamycin in a rabbit model of *Candida albicans* keratitis.[147]

Other Antifungals

Antiseptics such as iodides and chlorhexidine have antifungal properties in addition to their antibacterial activity and may be used when specific antifungal agents are not available.[145,167]

The mechanism of action of iodides is not clearly identified but may be related to enhancement of host immune response.[144] Povidone-iodine solution or Lugol's iodine solution has been recommended for treatment of equine fungal keratitis.[168] Chlorhexidine digluconate at concentrations ranging from 0.02 to 0.2% in vitro exhibited a dose-related antifungal activity against a wide range of *Fusarium* and *Aspergillus* isolates.[167] Applied to human patients with fungal keratitis, a 0.2% chlorexhidine digluconate solution was found almost as effective as a 1% econazole preparation in arachis oil.[167] Silver sulfadiazine with a broad antibacterial and antifungal activity is available in several countries as a 1% dermatologic cream and has proved useful against keratomycosis in humans[169] and horses.[12,137,170] Fungal cell walls are made of some specific components that are not found in mammalian cells, such as chitin, 1,3-β-glucan, and mannan. Targeting these components by interfering with their synthesis represents a new approach to treat fungal infections. For instance, lufenuron, a chitin-synthesis inhibitor marketed for control of fleas in cats and dogs, was found effective for treating cutaneous fungal infections in small animals.[171] In vitro, this compound failed to inhibit growth of an equine corneal *Aspergillus* isolate at concentrations ranging up to 64 μg/mL.[172]

Ocular Uses

Equine Keratomycosis

Conventional therapies for horses with keratomycosis have been presented in several publications.[12,168,170,173] Data on the in vitro susceptibility of fungi isolated from horses with keratomycosis suggest that natamycin, miconazole, itraconazole, or ketoconazole can be used for therapy.[140] Natamycin may be recommended for the initial treatment of corneal infections caused by filamentous fungi (i.e., *Aspergillus, Fusarium*), although it is costly, and miconazole may be a first-line choice to treat keratomycosis caused by *Candida* spp.[12] Natamycin is available as a 5% ophthalmic suspension, while 1% miconazole solution and 1–2% ketoconazole solution should be compounded to be administered topically or through a subpalpebral lavage system. Miconazole may have limited effectiveness against *Fusarium,*[170] *Candida albicans,*[174] and *Cylindrocarpon destructans.*[175] As stated previously, itraconazole may be applied as a 1% itraconazole-30% dimethyl sulfoxide petrolatum-based ophthalmic ointment.[176] Alternatives may be amphotericin B or silver sulfadiazine. Different drugs may be combined to enhance the therapeutic effect but should be administered separately to avoid chemical incompatibility.[170] Frequency of administration is as important as drug selection. Antifungal medications should be applied every 2 to 4 hours initially, with the frequency reduced to 6 times daily once clinical improvement is seen. Duration of treatment may vary from 3 to 8 weeks depending on response. Antifungal therapy is often combined with a broad-spectrum topical antibiotic, such as gentamicin, to treat or prevent secondary bacterial infection,[177] and atropine is used for its mydriatic-cycloplegic properties. Experimentally, it has been shown that in vitro activity of gentamicin and tobramycin is not altered when these antibiotics are combined with miconazole, atropine, or both.[178] Surgical procedures to debride diseased tissue and protect the cornea may also be necessary.

Canine Keratomycosis

In dogs, clinical experience of topical antifungal ocular therapy is limited by the relatively low prevalence of the disease and the lack of controlled trials of efficacy. A recent publication reported that natamycin and miconazole gave best results in dogs with corneal fungal infection. Miconazole has been used as topical solution (0.5% to 1%), subconjunctival injection (2 to 3 mg daily), or topical ointment (2% vaginal preparation).[141] Topical applications were repeated every 2 to 4 hours until corneal lesions were healed, and adjunctive therapy included topical broad-spectrum antibiotic, atropine, and possibly surgical treatment. The authors suggested combined therapy with a topical polyene, such as natamycin, and a systemic imidazole, such as miconazole, might be most effective for canine keratomycosis.[141]

ANTIINFLAMMATORY AGENTS

Glucocorticoids

Subcellular Effects

It has been widely accepted that physiological and therapeutic effects of glucocorticoids are mediated through the cytosolic glucocorticoid receptor complex, which consists of one molecule of receptor protein (glucocorticoid receptor, or GR) and several other proteins. These receptors are present in almost all body cells, such as cells involved in the inflammatory reaction and those of the sclera, cornea, conjunctiva, iris, choroid, and retina.[179,180] On binding of the glucocorticoids, the complex dissociates; the GR and its ligand form a dimmer that translocates to the nucleus, where it binds to specific hormone responsive elements (HREs) in the genomic DNA to subsequently act as a transcription factor that turns genes on or off.[181,182] A positive modulation of gene transcription leads to expression of regulatory proteins bringing about the therapeutic properties of the glucocorticoids. Accordingly, a major part of the antiinflammatory action has been attributed to the liberation by cells under glucocorticoid influence of a protein termed lipocortin (lipomodulin, macrocortin), which inhibits phospholipase A_2 and prevents release of arachidonic acid.[183] This results in suppression of the biosynthesis of eicosanoids produced by cyclooxygenase (COX) and lipoxygenase pathways. Recent data also suggest glucocorticoids may induce local expression of somatostatin, which may account for their antiinflammatory action.[184] In contrast, the glucocorticoid-receptor complex may negatively regulate the transcription of genes encoding for proinflammatory molecules, such as cytokines, metalloproteases, or nitric oxide synthase, which is an enzyme expressed in macrophages and involved in

cytotoxic effects and pathological vasodilatation.[185] Expression of COX activity is depressed in glucocorticoid-treated cells, suggesting glucocorticoids inhibit prostaglandin synthesis not only at the level of phospholipase A_2 but also at the level of the COX pathway.[186] Interaction of the glucocorticoid-receptor complex with specific target DNAs likely explains why these agents diminish the expression of adhesive molecules for leukocytes on the surface of endothelial cells.[187] The result is a decrease of endothelial cell ability to direct leukocyte traffic into inflamed tissues. Lysosomal membrane stabilization is a well-known, yet not clearly explained, subcellular action of glucocorticoids. This effect blocks degranulation of neutrophils, mast cells, and basophils and prevents release of proinflammatory substances such as proteases, histamine, and bradykinin. It has been suggested that glucocorticoids may stabilize lysosomes by interfering with the cyclic adenosine monophosphate (cAMP) pathway.[188]

Tissue Effects

The effects of glucocorticoids on inflammatory mediators account for their actions on the vascular and cellular manifestations of the inflammatory process. Because these actions are nonspecific, they impair almost all types of inflammation. Glucocorticoids not only inhibit the vascular and cellular responses characteristic of early inflammation but also suppress the persistent, nonresolving changes of chronic inflammation. In acute inflammation, they achieve their vascular effect by decreasing vasodilation and reducing capillary permeability, which result in less hyperemia and fluid exudation. When used for the treatment of uveitis, glucocorticoids reduce iris hyperemia and inhibit the passage of proteins and leukocytes into aqueous humor. The decrease in vasodilation may be partly due to a vasoconstrictor action on small blood vessels[189] or to inhibition of the vasodilator effect of nitric oxide synthase.[185] Glucocorticoids are also able to inhibit the growth of limbal blood vascular cells that are involved in corneal neovascularization observed in various clinical situations.[190] As they inhibit the ability of inflammatory cells to elaborate chemotactic mediators, glucocorticoids also markedly reduce leukocyte recruitment into inflamed areas. Experimental studies have illustrated that local administration of glucocorticoids in eyes with corneal or uveal inflammation significantly reduces inflammatory cell migration to the site.[188,191] Glucocorticoids also suppress the later stages of inflammation by inhibiting formation of fibroblasts and their collagen-forming activity as well as by reducing postinflammatory neovascularization. As a result, glucocorticoids are topically administrated for treatment of nonulcerative keratitis to suppress or prevent neovascular ingrowth and scar tissue formation in an attempt to preserve the structure and transparency of the cornea.[192]

Routes of Administration

In the treatment of ocular inflammation, glucocorticoids may be administered topically, subconjunctivally, or systemically. Topical application is a simple and direct method of glucocorticoid administration to the eye. This route is effective in treating many external ocular inflammatory diseases and inflammations of the anterior segment. Topical glucocorticoid preparations are available as solutions, suspensions, or ointments. Phosphate derivatives provide a clear solution in contrast to acetate and alcohol derivatives, which are less water soluble and are in suspensions. Experimental and human studies have shown that the greatest barrier to intraocular penetration of topical glucorticoids is the lipid-rich corneal epithelium, so that the lipophilic acetate and alcohol corticosteroid preparations penetrate the cornea better than polar preparations such as sodium salts of the steroid phosphate.[193,194] Subconjunctival injections of glucocorticoids are effective in achieving high drug levels in the anterior segment of the eye and are selected to reduce the need for frequent instillation of eye drops. Subconjunctivally injected glucocorticoid may penetrate the eye via the sclera, but it appears that much of the dose enters the anterior chamber by diffusing through the puncture site in the conjunctiva into the tear film and thereafter via passage through the cornea.[195] Drug release is primarily regulated by the biochemical composition of the glucocorticoid. Phosphate esters are water-soluble products, rapidly absorbed from the injection site, and short acting. Acetate and diacetate esters are poorly water-soluble and form depots when injected under the conjunctiva. A methylprednisolone acetate depot, the triamcinolone acetonide and diacetate suspensions, as well as the betamethasone acetate-sodium phosphate suspension may be administered by the subconjunctival route for prolonged release of steroid.

Absorption from these suspensions is slow, thereby maintaining therapeutic levels for 2 to 3 weeks.[196] However, data in humans suggest that a significant amount of active glucocorticoid may remain up to 13 months in subconjunctival depots.[197] Peribulbar injection is used in humans to deliver glucocorticoids to the posterior segment of the eye. After peribulbar injection of 5 mg of dexamethasone disodium phosphate, drug levels with antiinflammatory potency are reached in the vitreous body.[198] Intravitreal administration of triamcinolone acetonide has recently been recommended as a possible treatment for diabetic macular edema, proliferative diabetic retinopathy, chronic pre-phthisical ocular hypotony, chronic uveitis, and exudative retinal detachment in humans.[199,200] In humans having received a 20 to 25 mg intravitreal injection of triamcinolone acetonide, the drug can be present in measurable concentrations in the vitreous for up to 1.5 years after the application.[199] To the author's knowledge, the clinical relevance of this procedure has not been evaluated in veterinary ophthalmology. Systemic administration of glucocorticoids is mainly employed to treat inflammation of orbital tissues and posterior segment of the eye, which are difficult to reach by other routes.[188] In humans, oral administration of dexamethasone (7.5 mg) was shown to result in an average intravitreal drug concentration with an antiinflammatory potency, although it is approximately 25% of that achieved after peribulbar injection.[201]

Ophthalmic Uses

Glucocorticoids are beneficial in various nonpyogenic inflammatory disorders of the adnexa and globe, and their popularity sometimes leads to indiscriminate use. Although various topical corticosteroid preparations have been formulated to provide a beneficial therapeutic effect, it is possible that one compound may be preferred over another, depending on the location of the inflammation in the eye. Dexamethasone sodium phosphate 0.1% or bethametasone sodium phosphate 0.1%, which are poorly absorbed by the cornea and have an antiinflammatory effect that is five to seven times that of prednisolone,[195] may be the drugs of choice for the treatment of superficial ocular inflammations, such as blepharitis, conjunctivitis, episcleritis, and noninfectious/nonulcerative keratitis. Prednisolone acetate 1.0% or dexamethasone alcohol 0.1% should be preferred for treating anterior uveitis owing to better intraocular diffusion. The clinical efficacy of topical glucocorticoid preparations is improved by adjusting the frequency of application to the severity of the inflammation. Severe inflammations may require hourly treatment, whereas mild, external inflammatory conditions may be controlled with two or three daily administrations.[188,202] The dose is then slowly decreased based on clinical improvement, since abrupt cessation of glucocorticoid administration is likely to lead to an acute rebound inflammation.[202] Subconjunctival injection of glucocorticoid may be used to control certain forms of noninfectious keratoconjunctivitis, anterior episcleritis or scleritis, and anterior uveitis. Based on their estimated duration of action, long-acting glucocorticoids may be repeated 2 to 3 weeks apart by this route of administration. One potential problem with the subconjunctival administration of repository glucocorticoids is that a granuloma may develop at the injection site and may require surgical excision.[203,204] Systemic administration of glucocorticoids may either be combined with topical or subconjunctival therapy for treatment of severe or refractory anterior uveitis or used alone for the control of chorioretinitis, optic neuritis, or noninfectious orbital inflammation. Parenteral glucocorticoids are currently combined with nonsteroidal antiinflammatory agents in horses with uveitis. In small animals, oral or parenteral therapy with preparations of short- or intermediate-acting glucocorticoids such as prednisone, prednisolone, or methylprednisolone may be used. Conventional protocols for systemic glucocorticoid therapy in small animals have been reviewed.[205]

Adverse Effects and Contraindications

Effects on Corneal Healing Treatment of certain corneal wounds or ulcers with topical glucocorticoids occasionally results in rapid stromal melting in affected areas. In vitro studies demonstrate that glucocorticoids increase the lytic action of corneal collagenase, suggesting that this effect might be responsible for corneal destruction in clinical conditions.[206] Therefore, topical glucocorticoids are generally considered contraindicated in the presence of corneal ulceration. However, systemic glucocorticoids have little effect on corneal healing processes and may be used in patients with active corneal ulcer.[202] Topical glucocorticoids are routinely used after intraocular surgery in an attempt to reduce postoperative inflammation. Experimental data suggest that topical glucocorticoid may delay corneal healing by affecting corneal epithelial healing rates,[207] stromal keratocyte proliferation, and collagen deposition.[208] In vitro, dexamethasone manifested less cytopathic effects than prednisolone on cultured canine epithelial cells[209] but was found to induce significant increase in proliferation, apoptosis, and necrosis of human cultured corneal keratocytes.[210] Whether these effects are important or not in veterinary ocular surgery is unknown. Nevertheless, postoperative corneal wound disruptions have been reported in small animals given glucocorticoids subconjunctivally.[211] Based on the aforementioned finding, dexamethasone would be the drug of choice when a glucocorticoid is indicated in a dog with a corneal epithelial defect.[209]

Effects on Ocular Infections

Glucocorticoids interfere with defense mechanisms by decreasing leukocyte movement from vessels to the site of infection and depressing macrophage phagocytosis of microbes.[212] Depression of the ingestive ability of monocytes and macrophages might result from changes in the number of receptors on their cell membranes and from a decreased activation of macrophages by lymphokines and nitric oxide synthase.[185,213] As a result, glucocorticoids can potentially activate or exacerbate ocular bacterial, viral, or fungal infections, and their use in management of ocular infections is still debated. For instance, controversy abounds over the role of topical glucocorticoids in the treatment of bacterial keratitis. Experimental models of bacterial keratitis suggested that glucocorticoid therapy does not enhance bacterial replication if administered concurrently with an effective bactericidal antibiotic.[214] If these drugs are considered in clinical settings, they should be used only after the causative agent has been identified and specifically treated. In viral infection, such as feline herpesvirus ocular disease, the unpredictable efficacy of most available antiviral agents appears to argue against using topical or systemic glucocorticoid therapy with antiviral medication. It has been advocated that glucocorticoid therapy would be justified only in the presence of severe stromal keratitis, although it is considered very risky.[215] For fungal infections, most authors agree that glucocorticoid should be avoided. They enhance corneal fungal infections when administered topically or subconjunctivally, and if combined with an antifungal, their deleterious effects are inversely related to the efficacy of the antifungal agent.[216,217] In horses with fungal keratitis or stromal abscess, the use of topical or systemic glucocorticoids, or both, is generally contraindicated.[95,218] Long-term topical use of glucocorticoids is believed to predispose to keratomycosis in horses by interfering with local host immune defenses. Previous corticosteroid use was identified in 76% of 53 equine eye with fungal keratitis.[218] It was recently documented that the topical application of corticosteroid-antibiotic

combinations for 2 weeks in horses has no adverse effect on the ocular bacterial and fungal flora known to be pathogenic, suggesting that the role of glucocorticoids in infectious keratitis is probably not related to direct increase in the prevalence of known or opportunistic pathogens.[220] In small animals, systemic glucocorticoids are contraindicated or must be used cautiously in conjunction with specific antiinfective therapy in cases of intraocular fungal infection (blastomycosis, histoplasmosis, etc.) and evolutive inflammation of the posterior segment associated with parasitic or infectious diseases such as toxoplasmosis or erhlichiosis.[202]

Other Ocular Complications

Glaucoma, posterior subcapsular cataract, mydriasis, and calcific band keratopathy are clinically significant ocular complications of topical ocular corticosteroid therapy in humans.[221] Secondary open-angle glaucoma is most likely to occur after prolonged topical therapy with potent antiinflammatory steroids. Human corticosteroid-induced glaucoma appears to have a genetic basis and is related to a decrease in outflow facility resulting from an accumulation of extracellular material, resembling basement membranes, in the trabecular meshwork.[222] Increased expression of laminin and myocilin has been identified in the trabecular meshwork cells in the presence of glucocorticoids and might play a pathogenic role in the accumulation of extracellular matrix material in the trabecular meshwork.[223,224] An in-depth overview of this topic has been published in the last few years.[225] The hypertensive effect of corticosteroids has recently been documented in Beagles with primary open-angle glaucoma and in normal cats and cattle. In Beagles with primary open-angle glaucoma, IOP increased by a mean 5 mm Hg in the treated eyes within 2 weeks of topical application of 0.1% dexamethasone and returned to normal when the treatment was discontinued.[226] Healthy cats treated with topical 0.1% dexamethasone or 1.0% prednisolone acetate, as well as normal cows receiving topical 1% prednisolone acetate, manifested a significant increase in IOP within 2 to 3 weeks of treatment.[227–229] These feline and bovine models of steroid-induced ocular hypertension were developed to provide clues to elucidate the role and mechanisms of steroids in developing primary open-angle glaucoma. Steroid-induced cataract, although not documented in small animals, has been produced experimentally in cats by topical administration of dexamethasone or prednisolone. In these animals, cataract development consisted in subcapsular opacities, observed after at least 40 days of corticosteroid treatment and showing progressive opacification on continuing treatment.[227] The mechanisms responsible for the cataractous changes are not clearly identified, mostly because of the difficulties in developing suitable in vivo and in vitro models for steroid cataract.[230] Decrease in lens enzymes, alteration in lens hydration by modulation of the Na^+,K^+-adenosine triphosphatase (Na^+,K^+-ATPase), alteration in the systems involved in protection of the lens from oxidative stress, and protein adduct formation might be involved in the pathogenesis of glucocorticoid-induced cataracts.[230] Posterior subcapsular cataract, rise in IOP, and accumulation of subretinal fluid at the posterior pole of the fundus (central serous chorioretinopathy) have also been reported in humans in response to systemically administered glucocorticoids.[231,232] An increase in IOP was not observed in healthy dogs given hydrocortisone by the oral route at a dose of 3.3 mg/kg every 8 hours for 5 weeks.[233] In calves receiving parenteral administration of dexamethasone (30 μg/kg subcutaneously twice daily) for experimental purpose, bilateral exophthalmos was observed after approximately 28 days of treatment.[234] Protrusion of the globes was the result of adipose tissue deposition in the retrobulbar area. Excess body fat was not detected elsewhere in the body, and the mechanism by which dexamethasone induced this side effect was not determined.[234]

Systemic Adverse Effects

Systemic complications after topical or subconjunctival administration of corticosteroids have been recognized in the dog but are less likely than after systemic therapy.[235–239] Their occurrence is both dose and duration dependent. Signs of glucocorticoid-induced hepatopathy, marked reduction in corticosteroid production, and eventually alopecia may develop in dogs with long-term topical ocular glucocorticoid therapy.[235–239] Repeated topical administration of dexamethasone ophthalmic ointment in horses was also found to induce detectable corticosteroid concentrations in serum and urine. Because the drug was detectable in urine and serum for up to 1 day after the final application, the authors recommended discontinuing topical administration of dexamethasone at least 24 hours before competition to avoid drug detection in postrace samples.[240] Another illustration of systemic side effects caused by topically applied glucocorticoids is the possible occurrence of abortion in llamas when dexamethasone-containing ophthalmic ointment is given during late gestation.[241]

Soft Steroids for the Treatment of Ocular Inflammation

The need for topical glucocorticoids with efficacy comparable to that of currently available formulations but with fewer ocular side effects led to the concept of "soft steroids" as safe antiinflammatory agents.[242] As discussed previously, soft drugs are designed to act exclusively at the desired target receptors and undergo a predictable transformation to an inactive metabolite. Loteprednol etabonate 0.5%, structurally similar to other corticosteroids, is an example of a soft steroid. It has high liposolubility, good intraocular penetration, and an improved therapeutic index due to its predictable metabolic inactivation.[243] In clinical trials, topical loteprednol etabonate was effective in controlling postoperative intraocular inflammation in people who underwent cataract surgery[244] and was less prone to elevate intraocular pressure than was prednisolone acetate.[245] There are no data on its potential efficiency and usefulness in veterinary ophthalmology.

Nonsteroidal Antiinflammatory Drugs

Aspirin and aspirinlike drugs, commonly grouped as nonsteroidal antiinflammatory drugs (NSAIDs), have been used for a long time to treat a wide variety of inflammatory disorders, and their clinical indications in ophthalmology have

been rapidly expanding during the last decade. Since their discovery by Vane in 1971, we know that these agents exert their antiinflammatory effects by inhibiting prostaglandin synthesis.

Mechanism of Action

Arachidonic acid, released from cell membrane phospholipids by phospholipase A_2, is converted to prostaglandins via the COX pathway. Prostaglandin endoperoxide synthase, or cyclooxygenase (COX), is the enzyme that catalyzes the committed step in the synthesis of prostaglandins (PGE_2, PGD_2, $PGF_{2\alpha}$, and PGI_2) and thromboxane A_2 from the precursor arachidonic acid. The enzyme is a membrane-bound glycoprotein, and recent studies have found that there are actually two prostaglandin endoperoxide synthase isoenzymes, referred to as COX-1 and COX-2. COX-1 is present in most tissues and promotes release of prostaglandins that regulate normal cell activity.[246] In contrast, little or no COX-2 is found in resting cells, and the enzyme is expressed only in response to noxious stimuli.[246] However, cardiovascular side effects observed in human patients taking COX-2 selective NSAIDs seem to indicate that certain organ systems require COX-2 activity for physiologic function.[247] Prostaglandins found in inflamed areas are initially derived from the injured tissues, and as the response proceeds, prostaglandin production is increased by the invasion of inflammatory cells. Almost all ocular tissues, with the exception of lens, have the ability to convert arachidonic acid to prostaglandins, and PGE_2 is predominant in inflammatory conditions. Atropine-resistant miosis, rise in intraocular pressure, disruption of the blood–aqueous barrier, vasodilation associated with vascular permeability in the conjunctiva and iris, and possibly corneal neovascularization are inflammatory effects caused by prostaglandins in the eye.[248] Leukocyte infiltration of ocular tissues and fluids is mediated by leukotrienes rather than prostaglandins.[248] When involved in inflammation of ocular tissues, prostaglandins may act directly as well as indirectly by synergizing with other mediators. For instance, PGE_2 and bradykinin have a potentiating effect on the breakdown of the blood–aqueous barrier, and PGE_2 produces more severe conjunctival edema when instilled with histamine.[249]

The inhibition of COX is the enzymatic basis of the antiinflammatory effect of NSAIDs. These agents specifically block the synthesis of prostaglandins from arachidonic acid by competing with arachidonate for binding to the COX active site of prostaglandin endoperoxide synthase. Aspirin, indomethacin, flurbiprofen, and possibly flunixin meglumine cause irreversible inactivation of the enzyme, while interaction with ibuprofen is reversible.[250] It has been proposed that COX-2, the inductible isoenzyme, is the relevant target for the antiinflammatory effects of NSAIDs, whereas inhibition of COX-1, the constitutive isoenzyme, results in the side effects of these compounds.[246,251] Many common NSAIDs, such as aspirin, indomethacin, diclofenac, and ibuprofen, inhibit both COX-1 and COX-2, but NSAIDs with COX-2 inhibitory selectivity, including carprofen, meclofenamic acid, meloxicam, and nimesulide, have been licensed for veterinary use in North America and Europe during the last few years.[251,252] Recent in vitro experiments have established that meloxicam, tolfenamic acid, and carprofen have a potent selective activity on COX-2 isoenzyme in dogs.[253,254]

Routes of Administration and Products Available

Topical NSAIDs have been developed to improve the ocular bioavailability of these compounds and diminish their systemic side effects. The NSAIDs available as topical preparations for ophthalmic use include 1.0% indomethacin, 0.03% flurbiprofen, 1% suprofen, 0.1% diclofenac sodium, and 0.5% ketorolac tromethamine. Indomethacin 0.1% has also been marketed in some countries.[255] After topical application of diclofenac, high drug levels are reached in the normal as well as inflamed cornea, but diffusion in the aqueous humor is poor when the cornea is inflamed.[256] Flurbiprofen is not ocularly metabolized, and approximately 10% of the dose enters the anterior chamber when topically applied.[257] Ocular pharmacokinetic data in humans indicate that after topical application, aqueous humor levels of flurbiprofen and diclofenac are similar and reach a maximum in about 2 hours, and that diclofenac remains in the anterior chamber for longer than flurbiprofen (7.4 hrs vs. 3.7 hrs).[258] In the dog, topical application of 0.03% flurbiprofen prior to laser anterior capsulotomy significantly diminishes the anterior chamber inflammation and prevents the miotic response.[259,260] However, comparative study of topical 1.0% suspensions of flurbiprofen, diclofenac, tolmedin, and suprofen offered evidence that diclofenac is more effective than the others in stabilizing the blood–aqueous barrier in canine eyes.[261] Studies in humans and dogs reported that topical indomethacin readily penetrates the cornea and enters the aqueous humor sufficiently to prevent in situ prostaglandin synthesis and blood–aqueous breakdown.[262,263] Topical 0.1% indomethacin solution was as effective as topical 1% indomethacin suspension in preventing the increase in permeability of the blood–aqueous barrier and the miotic response induced by aqueous paracentesis in the dog.[264] In people, administration of 0.5% ketorolac tromethamine eyedrops significantly reduces ocular inflammation following cataract surgery.[265]

Although subconjunctival injection of flunixin meglumine was found to inhibit local prostacyclin accumulation in a model of ocular inflammation,[266] this route of administration should be avoided because it causes severe inflammation at the injection site.[267]

Oral aspirin,[268] sulindac,[269] and carprofen[270] as well as parenteral lysine acetylsalicylate,[271] phenylbutazone,[271] flunixin meglumine,[272,273] and tolfenamic acid[274] have been evaluated for their ability to control surgical inflammation in the canine eye. All these agents, with the exception of sulindac, significantly inhibited the disruption of the blood–aqueous barrier induced by various experimental procedures. Parenteral flunixin meglumine also limited miosis associated with the irritative response of the

eye.[275] Combined administration of parenteral flunixin meglumine and dexamethasone has an additive effect at reducing the blood–aqueous barrier breakdown in the dog.[273]

Ophthalmic Uses and Side Effects

Ophthalmic uses of NSAIDs include prophylactic and therapeutic indications. Because the ocular inflammatory response associated with intraocular surgical procedures is partially dependent on local release of prostaglandins,[276] topical or systemic NSAIDs, or both, are routinely administered before cataract surgery to maintain full mydriasis during surgery and reduce the increase in aqueous humor protein secondary to blood–aqueous barrier breakdown. Based on the aforementioned data, one could speculate that topical diclofenac, ibuprofen, or indomethacin would be preferred for preoperative management of cataract surgery. Many protocols involving different agents and routes of administration are suggested in the veterinary literature. Adding glucocorticoid, topically or intravenously, to the regimen significantly enhances the inhibition of surgical inflammation.[273,277] For instance, one protocol consists of administering topical 1% prednisolone acetate four times daily, beginning 24 hours prior to surgery. Two hours prior to surgery, 1% prednisolone acetate and 0.03% flurbiprofen are instilled every 30 minutes, and then flunixin meglumine (0.5 mg/kg) is administered intravenously after anesthetic induction.[278] The possible side effects associated with the preoperative use of topical NSAIDs include ocular irritation and tendency to increase intraocular hemorrhage during surgery.[202] They also have the potential to increase intraocular pressure postoperatively and should be used with caution in dogs predisposed to glaucoma.[279] Topical NSAIDs are also recommended during the postoperative period to reduce the postsurgical inflammation, avoiding the potential undesirable side effect of corticosteroids on corneal healing. In early reports, ketorolac and suprofen were described as not affecting postoperative corneal wound healing,[280,281] while topical flurbiprofen was shown to decrease stromal wound strength.[282] In the last few years, corneal ulceration with stromal melting and perforation was, however, associated with topical diclofenac sodium and ketorolac tromethamine use in human patients who have had recent ocular surgery.[283,284] The mechanisms underlying this side effect are still unknown, but corneal ulceration and keratolysis induced by the generic diclofenac product (diclofenac sodium ophthalmic solution, Falcon) was shown to be associated with overexpression of matrix metalloproteinase-8 in the corneal epithelium of the treated cornea.[285] To our knowledge, such corneal problems associated with perioperative use of topical NSAIDs have not been reported in veterinary ophthalmology. Recent data suggest, however, that topical NSAID use in dogs may be associated with delayed epithelial healing.[209] Systemic NSAIDs given pre- or postoperatively may also induce undesirable side effects, including gastrointestinal intolerance, hemorrhage, renal failure, and liver injury.[255] Among the new generation NSAIDs, carprofen has the least effect on renal function and integrity compared with ketorolac or ketoprofen when administered to dogs before general anesthesia and hence might be the NSAID of choice before cataract surgery.[286]

Although topical NSAIDs may be potent inhibitors of corneal neovascularization,[287] their clinical usefulness for treatment of keratitis is not well established in human and veterinary ophthalmology. Experimental data suggest that topical 1.0% indomethacin is more effective than 0.1% diclofenac and 0.03% flurbiprofen in controlling acute corneal inflammation.[288] In humans, noninfectious keratitis may represent indications for topical application of NSAID, as it has been observed that they may exacerbate bacterial corneal infections.[289] Topical NSAIDs should not be considered as ideal substitutes for topical glucocorticoids in cases of infectious keratitis because of their variable effects on ocular infection. For instance, flurbiprofen is comparable to dexamethasone in its ability to worsen experimental acute herpetic keratitis,[290] whereas ketorolac tromethamine does not exacerbate the course of herpetic ocular infection.[291] In the clinical setting, ketorolac was not found consistently effective for treating the inflammation associated with ocular FHV-1 infection.[215] Investigators recently observed that suprofen induces cytopathic changes and dose-dependent retardation of epithelial defect closure when applied on cultured canine corneal epithelial cells, advising to use this drug with caution in dogs with corneal ulceration.[209]

Although the role of prostaglandins in spontaneous animal uveitis remains to be determined, parenteral NSAIDs (phenylbutazone, flunixin meglumine) have been recommended in equine patients with anterior uveitis for a long time.[292] The role of NSAIDs in the management of small animal uveitis has not been investigated, but combined administration of systemic NSAID and glucocorticoid is recommended for treatment of severe iridocyclitis in dogs and cats.[267] Experimental studies have found that in some forms of uveitis, leukocyte infiltration of the inflamed areas is potentiated by NSAID treatment.[293] This is most important because it implies that NSAIDs may be detrimental in treating some forms of ocular inflammation, such as granulomatous uveitis. It has been suggested that selective inhibition of the COX pathway may shift more arachidonic acid toward the lipoxygenase pathway and thereby increase the synthesis of leukotrienes.[293]

Dual COX/Lipoxygenase Inhibitors

The search for potent antiinflammatory compounds devoid of steroidal side effects has prompted the development of nonsteroidal agents with combined lipoxygenase and COX inhibitory activity. Potency of some compounds to inhibit the inflammatory process was assessed in rabbit and dog models of experimental ocular inflammation.[294–296] Tepoxalin, a novel inhibitor of COX and 5-lipoxygenase, is approved for relief of musculoskeletal pain and inflammation in dogs. Its preoperative oral administration did not cause a significant reduction of intraocular inflammation induced by aqueocentesis in dogs.[297]

Immunosuppressive and Antiallergic Agents

In the eye, immune-mediated hypersensitivity reactions play essential roles in the pathogenesis of a number of ocular disorders such as chronic superficial keratitis (pannus), uveitis, keratoconjunctivitis sicca, episcleritis, and corneal graft rejection. Immunomodulation to affect or manipulate the immune system at its critical points causes a change in the expression of the disease and can provide effective strategies for the therapy of immune-mediated ocular disorders. Corticosteroids have long been used for the treatment of such conditions, but newer immunomodulatory agents have also been introduced over the last decade. Recent papers review the mechanisms of action and clinical applications of immunosuppressants in veterinary patients with immune-mediated ophthalmic diseases.[298,299]

Glucocorticosteroids

Glucocorticoids are the most widely used drugs in the treatment of ocular immune-mediated disease. Their immunosuppressive and antiinflammatory effects overlap to some extent because they are based upon a common subcellular action and are manifested against mediators and cells implicated in both inflammatory and immune responses. These responses are dose-related, with immunosuppressive effects requiring higher steroid dosages than the antiinflammatory effects. Corticosteroids directly or indirectly affect humoral immunity and cell-mediated immunity through effects on the immune system that can be divided into effects on cell movement and on cell functional capacity. Glucocorticoid administration causes neutrophilia, monocytosis, lymphopenia, and eosinopenia. Neutrophilia and monocytosis result from decreased margination of these cells and reduction of access to sites of inflammation. Macrophages result from the transformation of circulating monocytes, and in addition to phagocytic function, they serve as antigen-presenting cells. A major effect of glucocorticoids is to prevent the influx of leukocytes at the sites of inflammation; hence there are fewer monocytes and macrophages in inflamed areas to process antigens and present them to T lymphocytes. Glucocorticoids also lead to transient lymphopenia resulting from lymphocyte movement to the lymphatics, spleen, and bone marrow. Redistribution of lymphocytes from circulation may result in fewer T lymphocytes to be exposed to antigens and become activated. Therefore, there are fewer stimuli for a humoral or a cell-mediated response.[205,300] Corticosteroid attenuation of cell-mediated and humoral immune responses also results from a decrease in effective antigen presentation to T cells. Factors contributing to diminished antigen presentation include reduced phagocytosis by antigen-presenting macrophages, decreased production of macrophage-elaborated cytokines that influence lymphocytes, and reduced expression of the surface major histocompatibility complex molecules necessary for antigen presentation. At high enough dose, glucocorticoids have the potential to directly inhibit capacity of lymphocytes to produce various immune cytokines, such as the T cell autocrine-acting lymphokine, interleukin-2 (IL-2), and the paracrine-acting accessory cell cytokines IL-1 and IL-6.[301] Such cytokines have profound effects on proliferation and differentiation of activated lymphocytes. Corticosteroids also induce apoptosis in immature T- and B-cell precursors. This latter effect may be one of the major mechanisms through which corticosteroids exert their effects on lymphocytes.[302,303]

Glucocorticoids are used as immunosuppressant agents for controlling ocular inflammation where immunopathogenic processes are supposed to be involved. Immune-mediated blepharitis, such as atopic blepharitis, bilateral ulcerative blepharitis, and autoimmune blepharitis, may require topical or systemic glucocorticoid therapy, or both. Ocular superficial disorders such as allergic conjunctivitis, eosinophilic keratoconjunctivitis, chronic superficial keratitis, and superficial punctate keratitis most often respond favorably to topically applied or subconjunctivally injected glucocorticoid. Nodular granulomatous episclerokeratitis, with a presumed immune-mediated cause, is best treated with topical or systemic glucocorticoid therapy, or both. Poorly responsive cases require immunosuppression with azathioprine. Immune mediated uveitis, such as lens-induced uveitis, is treated with immunosuppressive glucocorticoids by topical, subconjunctival, and/or systemic routes. Optic neuritis associated with granulomatous meningoencephalitis may improve with immunosuppressive doses of systemic glucocorticoid.[205,304]

Calcineurin Inhibitors

Cyclosporine, tacrolimus (formerly FK 506), pimecrolimus, and rapamycin (sirolimus) belong to a family of natural products that are inhibitors of specific signal transduction pathways that lead to T lymphocyte activation. The cyclic polypeptide cyclosporine was isolated from the fungus *Tolypocladium inflatum* in 1972. Tacrolimus, pimecrolimus, and rapamycin are macrolide antibiotics isolated from *Streptomyces tsukubacusis* and *Streptomyces hygroscopicus* respectively.[305] All three compounds are small molecules that bind to intracytosolic receptors termed *immunophilins* (immunosuppressant-binding proteins) and therefore are designed immunophilin ligands.[306,307]

In T lymphocytes, cyclosporine predominantly binds to cyclophilin, while tacrolimus and rapamycin bind to a separate group of receptors, termed FK-binding proteins (FKBPs). Cyclophilin is distinct from FKBP, though both have a similar enzymatic activity.[306] Cyclophilin/cyclosporine and FKBP/FK-506 complexes interact with the calcium-activated protein phosphatase, calcineurin, leading to inhibition of transcription factors required for lymphokine mRNA expression. Accordingly, production of lymphokines, such as IL-2 or interferon-gamma, involved in the process of helper T lymphocyte activation is blocked, resulting in inhibition of the initiation of specific B- and T-cells responses.[305,308] Rapamycin has no effect on the production of lymphokines and acts by blocking signal transduction pathways emanating from lymphokine receptors such as the

IL-2 receptor. Thus, rapamycin inhibits the proliferation of T cells induced by lymphokines and particularly IL-2.[309] Studies on effect of cyclosporine on type I hypersensitivity have led to contradictory results. Data indicate that cyclosporine inhibits mast cell degranulation and suppresses mast cell–mediated cytokine production,[310,311] and in accordance with these findings a recent experimental study in an animal model has shown that topical cyclosporine inhibits the development of mast cell–mediated allergic conjunctivitis.[312] At the opposite, other investigators report that cyclosporine has no modulatory effect on mast cells and does not suppress IgE-mediated immediate hypersensitivity responses.[313,314]

Topical cyclosporine was first tested in dogs with keratoconjunctivitis sicca[315] and presently has gained widespread acceptance among veterinary ophthalmologists. Compounded solutions in corn or olive oil (1% or 2%) or the commercial 0.2% ophthalmic ointment can be used. A 0.05% ophthalmic emulsion has recently been approved for treatment of human patients with keratoconjunctivitis sicca.[316] A commercial ophthalmic form of tacrolimus for veterinary use does not exist, but the drug can be compounded.[106] Cyclosporine is a neutral hydrophobic peptide that easily penetrates the corneal epithelium after topical application. Once in the stroma, the drug accumulates and only a small part of the administered dose enters the anterior segment. Experimental data in the rabbit demonstrate that a dose-dependent corneal storage of cyclosporine can be achieved following topical application of this drug.[317] Increase in the frequency and duration of topical application leads to higher corneal concentrations of cyclosporine. Topically applied cyclosporine also penetrates into the lacrimal gland in concentration high enough to produce an immunosuppressive effect.[318] At the opposite, topical application produces only subtherapeutic drug concentrations in the aqueous humor.[319] Systemic absorption may exist after topical application and has been reported in rabbits[317] and dogs.[320] In the dog, the blood concentration of cyclosporine observed after long-term topical administration of the 2% solution is high enough to suppress cellular immunity as measured by lymphocyte proliferation assays and $CD4^+/CD8^+$ lymphocyte subset analysis.[320,321] Idiopathic KCS in dogs, a presumed immune-disease involving the lacrimal glands, has become the major indication of topical cyclosporine in veterinary ophthalmology. Since the first report by Kaswan in 1989,[315] other clinical investigations have established that this medication is a first-choice treatment for canine idiopathic KCS.[322–324] It appears that topical cyclosporine improves the signs and symptoms of KCS by increasing lacrimation and reversing inflammatory lesions of the cornea.[325] The increase in tear production most likely results from the local and possibly peripheral immunosuppressant effect of cyclosporine on the immunogenic lesions of the lacrimal glands[320,325] and from an independent lacrimogenic effect.[325] A clinical experiment in dogs with KCS suggested topical cyclosporine therapy can regenerate the atrophied lacrimal acinar lobules and restore secretory function.[326] The lacrimogenic effect of cyclosporine would result from an inhibition of local secretion of lymphokines including the prolactin protein, which is an inhibitor of lacrimal acini secretion.[325] Improvement of the superficial corneal inflammatory lesions may, at least in part, result from the property of cyclosporine to reduce corneal vascularization.[325] In experimental models of corneal neovascularization, systemic or topical cyclosporine was able to block corneal angiogenesis.[327,328] The mechanism whereby cyclosporine inhibits vessel growth is unclear but may involve its ability to inhibit lymphokines, and particularly IL-2, which is a known factor of corneal angiogenesis.[327,328] Synthetic analysis of the clinical data shows that topical administration of 1% or 2% cyclosporine ophthalmic solution as well as 0.2% ophthalmic ointment leads to an increase in tear production in approximately 80% of canine KCS cases.[315,322–324,329,330] However, in advanced cases (initial Schirmer tear test <2 mm), the rate of success is no more than 60%.[324] Improved lacrimation is characterized by an increase of at least 5 mm of the Schirmer tear test and is apparent within the first month of treatment in most cases. Some dogs may require 2 to 3 months of therapy before improvement of Schirmer tear test is observed.[324] Partial to complete clearing of cornea was reported in 67% to 100% of the cases.[322,324] Reduction of corneal vascularization and pigmentation may take from 1 to 12 months to become apparent. Corneal improvement may occur even in dogs without increased lacrimation.[322,324] Twice-daily application of one drop 1% or 2% cyclosporine solution or one application 0.2% cyclosporine ointment is used for management of KCS in most dogs. Frequency of administration can be reduced to once daily if Schirmer tear test increases to 20 mm or more.[325] Periocular irritation is seen in 2% to 10% of dogs who receive oral cyclosporine diluted in oil vehicle.[325] Immediate discomfort on application (blinking, squinting, and pawing the eyes) may be associated with use of the 0.2% ophthalmic ointment.[330] Long-term use of topical cyclosporine for treating KCS is apparently safe, although local and systemic immunosuppression are potential risk factors that may predispose dogs to opportunistic infection.[320,325]

The use of topical cyclosporine has been extended to treatment of other ocular diseases that seem to involve immunogenic mechanisms and/or that poorly respond to more conventional immunosuppressant such as glucocorticoids. Cyclosporine has proved useful in controlling chronic superficial keratitis in dogs,[331] and response to therapy monitored over a 6-week period showed that topical 0.2% cyclosporine ointment was as effective as 0.1% dexamethasone eye drops.[332] The efficacy of topical cyclosporine for treating nictitans plasmacytic conjunctivitis has also been demonstrated.[333] Topical cyclosporine may be an alternative to glucocorticoid therapy in poorly responsive cases of eosinophilic keratoconjunctivitis, episcleritis, scleritis, and superficial punctate keratitis.[334] Treatment consists of twice-daily application until improvement of lesions is achieved, with tapering of therapy over weeks. Some forms of equine keratitis and keratouveitis have been reported to respond favorably to topical cyclosporine.[334,335] Devices for sustained release of cyclosporine into intraocular tissues have been developed for long-term control of equine recurrent

uveitis (ERU) with minimal owner maintenance.[336] A polyvinyl alcohol/silicone-coated intravitreal cyclosporine implant, releasing 4 μg/day of cyclosporine, was first evaluated.[337] Although intravitreal implantation of this device was reported as a successful treatment for ERU, complications in the immediate as well as long-term postsurgical period (i.e., intraocular hemorrhage, progressing cataract, and retinal detachment) were encountered with its use.[338] A new device to be inserted suprachoroidally has been developed as an alternative to the intravitreally implanted system, and preliminary results seem encouraging.[338] A toxicological evaluation of a subconjunctival cyclosporine implant designed for long-term treatment of chronic immune-mediated keratopathies in dogs has been performed recently.[339] The device inserted beneath the dorsal bulbar conjunctiva was well tolerated for 6 months and did not induce any ocular clinical, electrophysiologic, or pathologic changes.[339] Further studies are needed to prove its clinical efficacy.

Topical tacrolimus has been evaluated for its potential to treat canine KCS.[340,341] A 0.03% solution in olive oil applied twice daily was safe in healthy dogs and gave clinical results similar to those observed with topical 2% cyclosporine in KCS-affected dogs.[340] Used as a 0.02% aqueous suspension, tacrolimus also increased tear secretion in dogs with KCS and was well tolerated.[341] Topical pimecrolimus, another macrolide immunomodulator, was recently evaluated in a pilot study including 14 dogs with either KCS or chronic superficial keratitis.[342] A satisfactory response to treatment was observed in about 70% (10/14) of all the cases.[342] Further, larger controlled studies are warranted to determine the definite role of pimecrolimus in the treatment of these immune-mediated ocular diseases. Systemic administration of tacrolimus or rapamycin has proved effective for the treatment of uveitis in people.[343,344] In vivo and in vitro experiments have determined that rapamycin can inhibit corneal graft rejection and corneal neovascularization.[500,501]

Cytotoxic Agents

Purine and folic acid analogs as well as alkylating agents form the cytostatic drugs, all of which have been used in chemotherapy of cancer. They are known to block cellular invasion and thereby inhibit the proliferation of immunocompetent cells. Owing to their unrestricted cytotoxicity these drugs may produce severe side-effects.

Methotrexate, the most commonly used folic acid analog, binds to dihydrofolate reductase and prevents the conversion of dihydrofolic acid to tetrahydrofolic acid which is essential for nucleic acid synthesis and hence for cell division.[347] Methotrexate suppresses B and T cell functions and is used for treatment of steroid-resistant ocular inflammatory disease in humans.[347–349] Injected by subconjunctival route in the dog, methotrexate (12.5 mg) enters the anterior segment and achieves therapeutic levels for 6 hours in the anterior chamber.[350] There is no report on its potential usefulness for managing ocular immune-mediated disorders in animals.

Azathioprine is a purine analogue, activated in the liver, that interferes with the synthesis of purine bases and thereby inhibits nucleic acid synthesis. The drug is relatively selective in its cytotoxic effect to helper T lymphocytes.[348] Azathioprine was one of the first immunosuppressive agent used in human ophthalmology. It is recommended as a steroid-sparing agent for the treatment of uveitis and scleritis.[348] In veterinary ophthalmology, azathioprine is indicated for control of nodular granulomatous episclerokeratitis in dogs.[351,352] The drug is given orally, alone or in combination with topical glucocorticoid. Treatment is initiated at a dosage of 2 mg/kg once daily for 10 to 15 days and as lesions regress the dose is tapered to the lowest efficacious dose possible. Monitoring of the blood cell count is essential since bone marrow suppression may occur. Some dogs may suffer bouts of vomiting and diarrhea. Acute hepatic necrosis is also an occasional adverse side-effect.[352] Azathioprine may also be recommended for treatment of steroid-resistant uveitis in dogs, such as the uveitis associated with uveo-dermatologic syndrome.[202]

Interferon-Alpha

Among its many cellular effects, interferon-α (IFN-α) has been shown to display immunomodulatory activity by affecting B and T cell function.[119] Human recombinant IFN-α has been used experimentally in KCS-affected dogs which were given 20 to 80 UI every day for 12 weeks.[353] Only 55% (11/20) of all dogs treated responded favorably to this treatment. No local or systemic side effects were observed during the trial period.[353] The potential efficacy of oral IFN-α has also been evaluated for management of nodular granulomatous episcleritis when other modalities were ineffective or intolerable.[354] A marked improvement was noted after one month of treatment with IFN-α given at an empirical dose of 80 IU/dog/day, and all lesions resolved after 2 months of treatment.[354]

Megestrol Acetate

Mainly known as a potent progestogen, megestrol acetate has also glucocorticoid-like properties which are poorly understood.[355] Alone or in combination with topical glucocorticoid, megestrol acetate has proven effective in treating eosinophilic keratoconjunctivitis in cats. Oral induction doses ranging from 2.5 mg daily to 5 mg daily are given until clinical response is favorable, and then dosing is reduced to 2.5 mg or 5 mg once every 7 to 14 days.[202,355] Side effects of megestrol acetate include polyphagia/weight gain, polydipsia, mammary hyperplasia, pyometra, diabetes mellitus, adrenocortical suppression and behavioral changes.[355]

Antiallergic Agents

Ocular allergy has received little attention in veterinary ophthalmology and use of anti-allergic agents seldom has been reported.[356,357] Allergy corresponds to Type I (immediate)

hypersensitivity which is mediated by IgE-mast cell interaction. When allergens bind to the IgE attached to mast cells, a series of events is initiated that eventually culminates in mast cell degranulation and release of histamine, slow reacting substance of anaphylaxis (SRS-A) and other proinflammatory mediators. Ocular expression of this type of hypersensitivity may be manifested in dogs and cats as atopic blepharitis and conjunctivitis.[304] Substances that inhibit degranulation by stabilizing mast cell membrane or compete for histamine receptor sites are clinically useful to prevent the consequences of the inflammatory reaction resulting from allergy.

Mast cell stabilizing agents, antihistamines, and dual-acting (multiple-acting) agents are the drugs most commonly used for management of allergic ocular disease in people, including hay fever conjunctivitis, vernal keratoconjunctivitis and atopic keratoconjunctivitis.[358,359] The sodium cromoglycate is the prototypic of the mast cell stabilizer agents, also represented by the lodoxamide tromethamine which is experimentally 2500 times more potent than sodium cromoglycate.[359] Clinically, topical lodoxamide tromethamine appeared more effective than topical sodium cromoglycate for alleviating the clinical signs of ocular allergy in people.[358,359] Anecdotal reports mention the use of mast cell stabilizers for treating ocular allergy in companion animals but they do not draw conclusion in support of clinical usefulness.[304,357] Sodium cromoglycate and lodoxamide tromethamine are also recommended as adjuvant therapy for equine eosinophilic keratitis.[360] Dual-acting agents, including olopatadine, ketotifen, azelastine, and nedocromil, have mast cell stabilizing effects, H_1 receptor antagonism, and/or other antimediator properties.[359] Available topical antihistamines for treatment of ocular allergy are classified as H_1-receptor antagonists and include levocabastine and emedastine. Levocabastine was reported to be effective for treating seasonal allergic conjunctivitis in children.[361] Topical antihistamine/vasoconstrictor combinations, known as ocular decongestants, are used for relief of symptoms in mild human allergic conjunctivitis. Commercial available combinations include pyrilamine/phenylephrine, pheniramine/naphazoline and antazoline/naphazoline. They have been recommended as substitutes for glucocorticoids in management of allergic conjunctivitis in small animals but their efficacy remains to be determined.[358] Ketorolac which proved to be effective in reducing conjunctival induced allergic reaction in people by inhibition of mast cell degranulation, ICAM-1 (an adhesion molecule) expression and prostaglandin release,[362] is the only topical NSAID approved by the FDA for use in patients with acute seasonal allergic conjunctivitis.[359]

ANTIGLAUCOMA DRUGS

Control of elevated intraocular pressure (IOP) associated with glaucoma can be achieved through medical and/or surgical therapy. Medical treatment of glaucoma is important in the management of the disease and relies on topical or systemic administration of pharmacologic agents which can be grouped into three categories on the basis of their IOP lowering effect: (1) those that reduce the rate of aqueous humor secretion, (2) those that increase aqueous humor outflow without affecting its formation, and (3) those that affect both aqueous humor outflow and formation. They include parasympathomimetic and adrenergic agents, as well as carbonic anhydrase inhibitors, prostaglandins and osmotic diuretics which form the different classes of compounds that are used to decrease IOP in animals.[363,364]

Drugs Acting at Cholinergic Receptors

This class of agents is divided into direct-acting and indirect-acting parasympathomimetics. Drugs in the former class stimulate cholinergic receptors directly, while drugs in the latter class are inhibitors of acetylcholinesterase, permitting acetylcholine to accumulate at the cholinoreceptive sites.

Effects on the Eye

Topical application of a parasympathomimetic compound on the eye results in miosis and lowering of IOP. In human and primate eyes, contraction of the longitudinal fibers of the ciliary muscle with widening of the scleral spur is the likely mechanism by which parasympathomimetics decrease resistance of aqueous humor passage through outflow pathway.[365] In primate and human eyes, increase in the number of giant vacuoles in the endothelium of Schlemm's canal may also participate in improved aqueous outflow.[365] In small animals, the contribution that contraction of ciliary muscle makes on aqueous removal has not been determined, and thus the mechanism by which parasympathomimetics lower the IOP is not established. Nevertheless, a cholinergic activity has been identified in the ciliary body musculature of the canine eye, indicating that there is the potential for modulation of outflow facility by the cholinergic nervous system.[366] Further evidence supporting such a hypothesis were observations that either intracameral injection of pilocarpine or N-demethylated carbachol,[367] as well as topical application of pilocarpine in canine eyes,[368] induce a substantial increase in outflow facility.

Direct-Acting Parasympathomimetics

Pilocarpine is a natural alkaloid obtained from the leaves of South Africa shrubs of the genus *Pilocarpus*. The drug is used as a nitrate or a hydrochloride and is available in concentrations of 0.5 to 8% in methylcellulose or polyvinyl alcohol vehicles. Most commercial pilocarpine eye drops are in solutions with a pH range of 4.5 to 5.5 to preserve the drug from hydrolysis. Pilocarpine hydrochloride 4% in a high-viscosity acrylic gel has been introduced to prolong drug–eye contact time.[365] Studies in glaucomatous (open-angle) and normotensive Beagles indicate that a single instillation of 0.5 to 8.0% pilocarpine hydrochloride reduces IOP by 30% to 40% for at least 6 hours.[369,370] In these animals, a single-drop instillation of pilocarpine (1%, 2%, or 4%) increased the coefficient of tonographic outflow facility from 0.33 μl/min/mmHg prior

treatment to 0. 61 μl/min/mmHg after treatment in normal eyes and from 0.15 μl/min/mmHg prior treatment to 0.38 μl/min/mmHg after treatment in glaucomatous eyes.[368] Glaucomatous Beagles responded with a greater reduction of IOP than normotensive dogs, and no significant difference in the hypotensive response was found among the different concentrations. Miosis occurred within 10 to 15 minutes and lasted for 6 to 8 hours.[369] Therapeutic additivity of pilocarpine with adrenergic agents, or carbonic anhydrase inhibitors, has been demonstrated in human eyes.[365] The combination of 1% epinephrine and pilocarpine hydrochloride (1%, 2%, 3%, 4%, and 6%) produced a significant IOP-lowering effect in glaucomatous (open-angle) and normotensive Beagles. Following a single instillation of these combinations, the drop in IOP lasted for at least 8 hours and was not dose-related.[371] Surprisingly, combined administration of 1% epinephrine with either 1%, 2%, or 4% pilocarpine did not increase tonographic outflow facility in these eyes in comparison to pilocarpine 4% used alone.[368]

Carbachol is the carbamyl ester of choline. Because the drug is not lipid-soluble at any pH and penetrates the intact corneal epithelium poorly, it must be combined with a surfactant, such as benzalkonium chloride, to facilitate its penetration through the corneal epithelium.[365] Carbachol is stable in solution and is available for topical use in concentrations of 0.75% to 3%. A 0.01% solution is used for intracameral administration at completion of an intraocular surgery to induce rapid miosis and inhibit postoperative ocular hypertension.[365] At concentrations of 0.75%, 1.5%, 2.25%, and 3%, carbachol reduced IOP in normotensive and early glaucomatous (open-angle) Beagles. The reduction in IOP was clearly evident within 1 hour and peaked 2 to 7 hours after instillation.[372] A minimum concentration of 0.75% carbachol was recommended in the management of open-angle glaucoma in the Beagle.[372] The 0.01% solution injected into the anterior chamber of dogs at the end of cataract surgery can prevent the postoperative increase in IOP associated with phacoemulsification.[373]

Indirect-Acting Parasympathomimetics

The anticholinesterases are divided into the carbamate inhibitors, which bind to the acetylcholinesterase in a reversible manner, and the organophosphorus inhibitors, which irreversibly inhibit the enzyme by forming a stable complex.

Demecarium bromide is a potent carbamate inhibitor, no longer commercially available, which can be compounded in 0.125% and 0.25% solutions for veterinary use.[106] The drug remains stable for extended periods and does not require refrigeration.[365] A single drop of demecarium bromide in a human eye provided a significant reduction of IOP starting a few hours after instillation and lasting for more than 3 days.[374] The accompanying miosis lasted for up to 10 days.[374] Investigations using single-drop application of either 0.125% or 0.25% topical demecarium bromide and conducted in normal and glaucomatous (open-angle) Beagles revealed that both formulations induce long-term miosis (up to 77 hours) and IOP lowering effect that lasts up to 55 hours.[375] The mean decrease in IOP is about the same magnitude as that observed with pilocarpine solution and gel as well as with carbachol solution, but it is more prolonged.[375] Echothiophate iodide (or phospholine iodide) is another long-acting organophosphorus compound, available in 0.03%, 0.125%, and 0.25% solutions.[376] The refrigerated solution remains stable for at least 1 month after reconstitution. Instillation of one drop echothiophate iodide 0.125% or 0.25% results in decrease in IOP of about 10 mmHg and about 13 mmHg in normotensive and glaucomatous (open-angle) Beagle eyes respectively.[375] Reduction in IOP persists for 25 to 53 hours. Associated miosis becomes maximal within 1 to 3 hours and persists for 49 to 55 hours.[375] Thus, echothiophate iodide appears as potent as demecarium bromide in the dog.

Clinical Use

The major use of parasympathomimetic drugs has been the long-term treatment of open-angle glaucoma in the dog. Use of these agents in combination with adrenergic drugs or carbonic anhydrase inhibitors would also be of help for initial therapy in most early glaucomas. However, once glaucoma is advanced, parasympathomimetic therapy has little beneficial effect because the filtration angle is usually obliterated by extensive peripheral anterior synechiae.[377] Parasympathomimetic agents should be avoided in secondary glaucoma associated with iridocyclitis because the miosis predisposes to synechia formation, and they should be used with caution in dogs with subluxated or luxated lens because they may induce a pupillary block. Pilocarpine solution should be prescribed 3 to 4 times daily,[377] while pilocarpine gel, which reduced IOP by 25% to 30% for at least 24 hours in glaucomatous canine eyes, is applied once daily.[378] Although demecarium bromide is a long-acting hypotensive ocular agent, its instillation has been recommended in the dog on a twice-daily basis to regulate IOP and avoid occasional peaks that may be destructive for the glaucomatous eye.[375] In order to determine the ability of prophylactic antiglaucoma treatment to prevent or delay onset of glaucoma in the second eye of dogs with unilateral closed-angle glaucoma, a combination of 0.25% demecarium bromide and a topical corticosteroid (DB/GB) was compared to topical 0.5% betaxolol in a multicenter clinical trial.[379] Untreated control eyes developed glaucoma significantly sooner (median 8 months) than eyes treated either with betaxolol (median 30.7 months) or DB/GB (median 31 months). Although both treatment protocols similarly delayed the onset of glaucoma in the fellow eye, DB/GB would be preferable to betaxolol in preventing closed-angle glaucoma because of less frequent dosing.[379] Pilocarpine is also used in small animal ophthalmology to stimulate tear production in patients with keratoconjunctivitis sicca and to improve the ocular and digestive signs of feline dysautonomia.

Side Effects

Because of the low pH (4.5–5.5) of its ophthalmic solutions, pilocarpine may cause local irritation manifested by

blepharospasm, prolapsed nictitans, epiphora, and conjunctival hyperemia, which are observed within the first 15 minutes and may last for up to 6 hours.[370,380] These signs are most prominent for the first 72 hours of treatment. Use of a special droptainer with a buffer system in its tip to adjust the pH of the pilocarpine solution to a level close to the physiological pH was evaluated in glaucomatous Beagles.[381] Pilocarpine in 1% and 2% solutions instilled by buffer-tip droptainer (pH 7) showed excellent pharmacological effects determined by miosis and ocular hypotension and were well tolerated.[381] Topical application of pilocarpine transiently increases the permeability of the blood–aqueous barrier but does not result in short- or long-term changes.[382] In the dog, systemic side effects are unlikely after topical administration of pilocarpine 0.5% to 8% solution or 4% gel.[370,378]

Ocular and systemic side effects may occur with topical application of indirect-acting parasympathomimetics. Since they potentiate the action of acetylcholine on muscles, they produce more severe ciliary and iridal spasms than does pilocarpine. Decreased vision resulting from miosis and induced myopia is the most adverse reaction reported in human ophthalmology.[365] A transient increase in blood–aqueous barrier permeability occurs in the canine eye after topical application of demecarium bromide.[382] Systemic toxicity may develop with any cholinesterase inhibitor and may include salivation, vomiting, diarrhea, and abdominal cramps. In order to minimize the risk of toxicity, indirect-acting parasympathomimetics should be avoided in subjects treated with flea preparations containing organophosphates.[375] When signs are severe, atropine (0.2 mg/kg IV or IM) and pralidoxime chloride (20 mg/kg IV) are administered to block the action of acetylcholine. In humans, their long-term use may result in cataract formation, disruption of the blood–aqueous barrier, retinal detachment, and, in children, development of iris cysts.[365,376]

Drugs Acting at Adrenoceptors

Drugs that stimulate or block the activity of the ocular sympathetic nervous system may be used to lower IOP. Pharmacologically, their mechanisms of action are still unresolved and continue to be the subject of considerable study.

Epinephrine and Dipivefrin

Epinephrine, or adrenaline, is classified as a nonspecific adrenergic agonist that stimulates α and β types of membrane receptors. Dipivefrin, or dipivalyl epinephrine, is an epinephrine prodrug produced by the addition of two pivalic acid groups to the parent compound. The lipophilic prodrug penetrates the epithelium barrier, where it is converted by esterases (acetylcholinesterase, cholinesterase, and arylesterase) to its parent drug, epinephrine, which is absorbed in the anterior segment.[383,384] Epinephrine has been used for many years to treat glaucoma in humans, but knowledge of its mechanism of action is still incomplete. Currently, it is believed that its ability to lower IOP is manifested both by reduction in the formation of aqueous humor and increase in aqueous outflow. Investigations in monkeys and humans indicate that epinephrine and dipivefrin reduce aqueous humor formation, most likely by decreasing blood flow in the ciliary body, through their vasoconstrictive action upon the vasculature of the ciliary body.[385,386] Improvement in facility of aqueous outflow by adrenergic drugs has also been clearly identified in primate and human eyes.[283–285,387–389] It was also found in human eyes that increase in aqueous outflow is mediated by β-2 adrenergic receptors and is correlated with increased cyclic AMP production by the trabecular meshwork.[388,389]

At concentrations of 1% and 2%, topical epinephrine was effective in reducing IOP in glaucomatous (open-angle) and normotensive Beagles.[390] In these animals, the 0.5% solution of dipivefrin manifested hypotensive and mydriatic effects similar to those of the 2% solution of epinephrine.[390] Topical epinephrine or dipivefrin, alone or in combination with other antiglaucomatous drugs such as direct-acting parasympathomimetics, β-blockers, and carbonic anhydrase inhibitors, has its main indication in the management of open-angle glaucoma. Various local and systemic side effects have been reported in humans with the ocular instillation of epinephrine and dipivefrin.[391] The most common side effects include local intolerance, formation of adrenochrome deposits in the conjunctiva and cornea, loss of eyelashes, and macular edema in aphakic eyes.[391] Incidence of conjunctival and corneal staining in veterinary ophthalmology in unknown. Local irritation consisting of mild conjunctivitis and tearing has been reported in the dog with the 0.5% solution of dipivefrin.[390] Since some of the corneal esterases that convert dipivefrin to epinephrine are inhibited by anticholinesterase drugs, combined use of these long-acting miotics and dipivefrin is contraindicated.[392]

Alpha$_2$-Adrenergic Agonists

The mechanism by which α_2-adrenergic agonists lower IOP is not fully understood. Studies in human eyes have clearly demonstrated that these drugs decrease aqueous formation, but conflicting results regarding their effect on outflow facility have been reported.[392,393] From different investigations, it appears that α_2-adrenergic agonists most likely decrease aqueous humor formation by interfering with presynaptic (nerves) and postsynaptic (nonpigmented epithelial cells) α_2-adrenoceptors at the sympathetic nerve–ciliary body junction.[393–395] Activation of the presynaptic α_2-receptors inhibits norepinephrine release, thereby blocking the tonic adrenergic stimulation of the secretory ciliary epithelium by endogenous norepinephrine. Activation of the postsynaptic ciliary body α_2-receptors, coupled to a G_i protein, suppresses the activity of adenylate cyclase and reduces the intracellular concentration of cAMP in the ciliary epithelium. The net effect is also a decrease in aqueous humor formation.[395]

Apraclonidine (p-aminoclonidine), a derivative of clonidine with comparable IOP-lowering effect and minimal cardiovascular effects, has been developed for use in humans. It is available as a topical 0.5% solution. The IOP-lowering ability of apraclonidine has been evaluated in dogs and cats. Single topical

administration of 0.5% apraclonidine in the canine eye resulted in a 3.0 mmHg (16%) IOP decrease 8 hours after treatment.[396] In the cat, apraclonidine-treated eyes showed mean IOP decrease of 4.8 mmHg (24%) 6 hours after treatment.[397] The topical application of apraclonidine resulted in ocular and nonocular side effects both in dogs and cats. Mydriasis occurred in 29% of the treated canine eyes and at the opposite pupillary diameter was reduced a mean 46% in the feline treated eyes.[396,397] Reduction in heart rate was more marked in cats than in dogs, and undesirable gastrointestinal effects, such as salivation and vomiting, occurred in most cats.[396,397] Thus, it appears that apraclonidine is not a first-line antiglaucomatous agent in the dog and is too toxic to be used in the cat. Nonocular side effects most likely result from systemic absorption of the topical drug. This is consistent with the finding that conjunctival–scleral route is the main pathway for apraclonidine absorption after topical application.[398] Brimonidine tartrate, a highly selective α_2-agonist, has been introduced for treating acute and chronic elevations of IOP in human beings.[399] Its hypotensive effect in human glaucoma patients was found to be similar to that of timolol and was not associated with any systemic side effects.[400] Current data indicate that brimonidine reduces IOP in human eyes by a dual mechanism, decreasing aqueous inflow and increasing uveoscleral outflow.[401] Ocular effects of single and multiple doses of topical 0.2% brimonidine were recently evaluated in glaucomatous Beagles.[402] After application, a trend to reduction in IOP was observed but not at statistical significance.[402] As a result, the authors advised to use brimonidine as additive therapy and not as monotherapy in glaucomatous dogs. Side effects observed with brimonidine treatment in dogs included miosis and decrease in heart rate.[402] A survey conducted in a poison control center documented the clinical signs associated with ingestion of brimonidine ophthalmic solution by dogs.[403] Severe cardiovascular effects (hypotension, bradycardia) and central nervous system depression can ensue the ingestion of brimonidine depending on the amount of drug ingested. Supportive care and yohimbine or atipamezole as α_2-antagonist are helpful to reverse the signs of the toxicosis.[403]

Beta-Blockers

Topical β-blockers have become the most widely used medications for the control of ocular hypertension in humans. In 1967, it was observed that propranolol caused a reduction in IOP after intravenous or topical administration. A number of other β-blockers used for cardiovascular disease (i.e., practolol, oxprenolol, and atenolol) then were investigated as antiglaucoma agents, but adverse side effects limited their ocular use. It was not until 1977 that timolol was found to be a safe and effective agent for lowering IOP in human glaucoma patients. Since the drug was first marketed in 1978, levobunolol, betaxolol, metipranolol, and more recently carteolol have been released as antiglaucoma medications. All but betaxolol are nonspecific β-blocking agents (i.e., they block both β_1 and β_2 receptors). Betaxolol is a β_1-selective ophthalmic β-blocker. Carteolol is the only compound that possesses intrinsic sympathetic activity when bound to the β-adrenergic receptors.[404–406] Many investigations have convincingly demonstrated that topical β-blockers reduce IOP by decreasing formation of aqueous humor.[407–410] A single drop of 0.5% timolol solution suppresses aqueous formation in the range of 13% to 48% in normal human eyes.[408] In cat eyes, the rate of aqueous humor formation is reduced 28%, 56%, and 71% by 0.005%, 0.025%, and 0.15% intracamerally injected timolol solution respectively.[409] Topical 0.5% timolol given to normal rabbit eyes decreases aqueous flow by 35% as measured by sulfacetamide clearance from aqueous humor.[410] However, their mechanism of action is still uncertain, and three possibilities have been suggested: (a) they may block β-receptors in the ciliary processes; (b) they may inhibit active transport and ultrafiltration related to Na^+,K^+-ATPase; or (c) they may act through a vasoactive mechanism. According to the classical view, β-blocking agents lower aqueous humor flow by altering the adrenergic neuronal control of aqueous humor formation by blockade of the β-receptors in the ciliary processes.[405] β_2-adrenergic receptors seem to be predominant in the ciliary processes,[411,412] and experimental findings indicate that β-adrenergic receptors mediating pressure changes in the anterior segment of the cat eye are predominantly β_2.[413] It has been postulated that occupation of the β-adrenoceptors of the ciliary epithelium inhibits the tonic influence of norepinephrine released by the sympathetic nerves, thereby inducing a decrease of cAMP levels in the ciliary epithelium and hence a reduction of the secretory function of the ciliary epithelium.[406] However, in vivo and in vitro findings indicated that the correlation between aqueous humor formation and ciliary epithelial cAMP content was unclear and that β-blocking drugs might act through mechanisms unrelated to β-adrenergic blockade in the ciliary epithelium.[414,415] Since plasma membrane ATPases of the ciliary epithelium are involved in aqueous humor formation, the potential relationship between inhibition of ciliary ATPases and the IOP-lowering effect of the β-blockers was investigated. Studies provided support to a mechanism for β-adrenergic antagonists inhibition of ciliary Na^+,K^+-ATPase activity in vitro and in vivo.[416,417] At the opposite, other studies in rabbits demonstrated that neither Na^+,K^+-ATPase nor Mg^{++}-ATPase was inhibited by timolol and showed that the IOP-lowering effect of the drug was related to a significant reduction of blood flow in the iris root-ciliary body, related to a significant reduction in dopamine concentrations in this tissue.[418] Beta-blockers have no effect on aqueous outflow.[406]

Topical timolol maleate is available as solution and gel-forming solution in 0.25% and 0.50% concentrations. In normotensive dogs and cats, a single application of 0.5% solution induced a mean reduction in IOP of 2.5 mmHg (16%) and 4.1 mmHg (22%) respectively.[419,420] Maximum IOP reduction occurred within 2 to 4 hours in dogs[419] and within 6 to 12 hours in cats.[420] A contralateral decrease in IOP also occurred in nontreated eyes.[419,420] A dose-response study of timolol maleate employing single- and multiple-drop instillations in

normotensive and glaucomatous (open-angle) Beagles found that 0.25% and 0.5% timolol were ineffective in normotensive eyes but lowered IOP in glaucomatous eyes by approximately 4 to 5 mmHg.[421] A dose-related reduction in IOP was observed in normotensive dogs, with concentrations of 2% to 8%.[422] In eyes with open-angle glaucoma, decrease in IOP ranging from 8 to 14 mmHg was observed for up to 6 hours after administration of 4%, 6%, and 8% concentrations.[422] The effect of topical application of timolol on IOP has been evaluated in females horses with normotensive eyes.[423] A significant mean decrease of approximately 4 to 5 mmHg was observed 8 hours after single-dose application, and the pressure-lowering effect was present throughout the 5-day multiple-dose study with a maximum reduction in IOP of 27%.[423] No ocular side effects were noted with the exception of 11% reduction in the pupil size. These results indicate that timolol could be of benefit in the management of glaucoma in horses.[423]

In people, carteolol, metipranolol, and levobunolol have similar potency to that of timolol for decreasing IOP (approximately 20% to 30%).[404] The IOP-lowering effect of β-blockers in man is generally additive to that of the other antiglaucomatous agents, such as parasympathomimetics, epinephrine, and dipivefrin.[406] Typically, such combinations provide an additive effect by using two drugs that together affect aqueous inflow and outflow. For instance, pilocarpine is often used in combination with β-blockers. In glaucomatous (open-angle) Beagles, the response to either 4% or 6% timolol was enhanced by combination with 2% pilocarpine.[423] When two topical antiglaucomatous medications are combined during the same dosing episode, at least 5 minutes should pass between applying the two formulations because coadministration reduces their ocular bioavailability. Pharmacokinetics data in rabbits demonstrate that when timolol is coadministered with either pilocarpine or epinephrine, its ocular absorption is reduced by 20% to 70%.[424] In people, the topical β-blockers are indicated in primary glaucoma (open-angle and closed-angle), many types of secondary glaucomas, and various conditions with ocular hypertension.[404,406] They are also commonly used in small animal veterinary ophthalmology, although their effectiveness has never been documented by controlled clinical trials. Nevertheless, experimental data suggest that topical timolol is potentially effective for controlling glaucoma when applied twice daily at a concentration of 0.5% in cats and at concentrations ranging from 4% to 8% in dogs. The latter are not available commercially and would probably induce systemic side effects. Combination of timolol and pilocarpine also may be useful in some glaucomatous dogs. As stated previously, topical 0.5% betaxolol is an alternative to demecaruim bromide to prevent or delay the onset of hypertension in an eye predisposed to primary closed-angle glaucoma.[379] The most common ocular side effect of topical β-blocking agents is local intolerance (i.e., stinging, burning) on ocular instillation.[406] Photophobia, ptosis, blepharoconjunctivitis, and superficial keratitis are other potential ocular side effects of these drugs.[406] Changes of the ocular surface observed during treatment with timolol has been associated with a significant reduction in tear production and turnover.[425] It seems that carteolol has better ocular tolerability than the other compounds.[404] In humans, topical timolol has minimal effect on pupillary diameter. On the contrary, significant reduction in the pupil size is observed in the canine and feline treated eyes.[419,420,422] Reduction of pupillary diameter is more marked in cats than in dogs with a maximum duration of one week after treatment.[419,420] Timolol has been shown to be more toxic to regenerating corneal epithelium than levobunolol and betaxolol in rabbit eyes[426] and therefore may not be the drug of choice in animals with glaucoma and corneal epithelial defects. In people, topical β-blockers are contraindicated in those with severe heart failure and bronchial asthma because of their potential cardiopulmonary adverse effects resulting from systemic absorption. It is possible that the partial agonist activity of carteolol may reduce its cardiovascular and bronchopulmonary adverse effects by lessening systemic β-blockade effect.[404,405] Significant decrease in pulse rate was observed in normotensive and glaucomatous Beagles treated with topical timolol at concentrations ranging from 2% to 8%.[421,422] A contralateral effect on IOP and pupillary diameter was also identified in the nontreated eyes when timolol was topically given to dogs and cats.[419,420] These effects likely result from systemic uptake via transconjunctival route and nasolacrimal duct pathway. A systemic activity of topically applied timolol has been demonstrated in an experimental dog model.[427] To prevent occurrence of deleterious cardiovascular effects secondary to systemic absorption, the literature suggests using 0.25% timolol in cats as well as dogs weighing less than 20 lbs, and 0.5% timolol in dogs with body weight above 25 lbs.[364]

Carbonic Anhydrase Inhibitors

Carbonic anhydrase inhibitors (CAIs), which belong to the class of nonbacteriostatic sulfonamide-related compounds, were used in ophthalmology as early as 1954 with the introduction of acetazolamide. Methazolamide and dichlorphenamide were released subsequently. These agents have been widely used ever since, but because their clinical usefulness is limited by various systemic side effects, topical carbonic anhydrase inhibitors have been developed in the last decade.

Mechanism of Action

The ciliary process epithelium contains enzyme systems, such as NA^+,K^+-ATPase and carbonic anhydrase, that are involved in aqueous humor formation. Carbonic anhydrase is a ubiquitous enzyme for which seven isoenzymes have been identified. CA I, CA II, and CA III are located in the cytosol, CA IV is membrane bound, CA V is present in mitochondria, and CA VI and CA VII are found only in salivary glands.[428] Only CA II, CA III, and CA IV are present in significant amounts in pigmented and nonpigmented epithelial cells to catalyze the reversible hydration of carbon dioxide.[428] Newly formed

bicarbonate ions are neutralized by sodium and other cations and transferred to the intercellular channels and the posterior chamber (Fig. 7.2.1). Water is then osmotically attracted from the vessels of the ciliary stroma to aqueous humor formation: $H_2O + CO_2 \leftrightarrow HCO_3^- + H^+$.[429] The common feature of CAIs is a sulfonamide group ($-So_2NH_2$) attached to an aromatic ring. Competition of the sulfonamide group with carbonic acid for its site on carbonic anhydrase, to make it inactive, is the basis of the pharmacological action of these drugs.[430] It is known that 98% inhibition of CA II must be achieved in ciliary epithelium by systemic or topical inhibitors for full IOP reduction.[431] In parallel to the decreased appearance of bicarbonate into the posterior chamber, the rate of sodium transport is decreased by equimolar amount, and entry of water into the posterior chamber is reduced. Accordingly, aqueous humor formation is suppressed by 40% to 60%.[432] In the dog, carbonic anhydrase inhibition by acetazolamide lowers aqueous flow from 9 μl/minute prior treatment to 6.4 μl/minute after treatment.[432] Although systemic CAIs are diuretics, it is currently believed that their ocular hypotensive effect does not depend on diuresis. There is, however, some indication that the systemic acidosis induced by these agents also inhibits aqueous humor formation and enhances their pressure-lowering effect.[432]

Systemic Carbonic Anhydrase Inhibitors

Acetazolamide, the first drug in this group to be synthesized, can be administered either orally or intravenously. It is supplied in tablets of 125 and 500 mg as well as in time-release capsules of 500 mg. A single oral administration of a dose

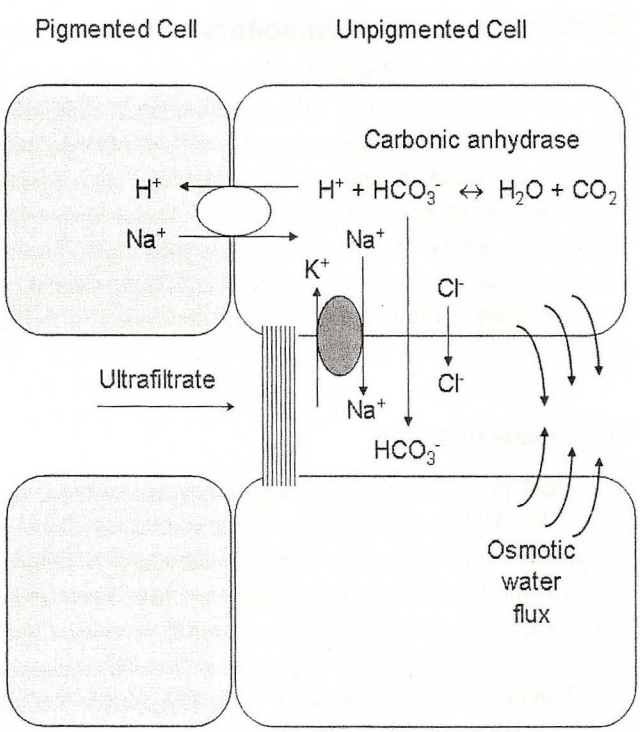

Figure 7.2.1. Contribution of carbonic anhydrase to aqueous humor formation in the unpigmented and pigmented ciliary body epithelium.

ranging from 10 to 75 mg/kg significantly lowers IOP in normotensive and glaucomatous Beagles for at least 8 hours.[433] A dosage of 4 to 8 mg/kg 2 to 3 times daily is usually recommended for treatment of canine glaucoma.[378] In the cat, doses ranging from 10 to 25 mg/kg are effective in lowering the IOP in glaucomatous animals. The hypotensive effect lasts about 5 hours.[434] Acetazolamide is also available for intravenous injection as a lyophilized powder (500 mg/vial). Intravenous acetazolamide at a dose of 5 to 10 mg/kg is useful as adjunctive therapy in the management of acute glaucoma.

Dichlorphenamide has been withdrawn from the market but is available in generic forms in United States. The oral dose rate in the dog ranges from 2 to 4 mg/kg 2 to 3 times daily.[377] In glaucomatous Beagles, the maximal effect occurs 3 hours after administration of a dose of 10 mg/kg.[433] Single oral administration of dichlorphenamide in the cat in doses ranging from 0.5 to 2 mg/kg significantly reduced IOP for 4 hours.[434]

Methazolamide is supplied in 50 mg tablets. After oral administration of 25 or 50 mg methazolamide to healthy Beagle dogs, a significant IOP decrease of 18% to 21% was observed 3 to 6 hours after administration depending on the dose, but thereafter IOP increased to levels above the control baseline values.[435] The lowering effect on IOP was accounted for by a mean 28% reduction in aqueous humor formation.[435] The rebound effect was ascribed to a possible upregulation of CA after treatment ceased, and it should be kept in mind in clinical settings when administration of methazolamide is stopped.[435] In a study of the systemic CAIs in normal and glaucomatous dogs, results suggested that methazolamide decreases IOP at dosage levels lower than acetazolamide, dichlorphenamide, and ethoxzolamide.[433] In glaucomatous dogs, the IOP-decreasing effect of oral metazolamide (5mg/kg twice daily) was comparable to that achieved with topical dorzolamide instilled twice or three times daily.[436] When co-administered, the drugs did not produce an additional reduction in IOP.[436]

Topical Carbonic Anhydrase Inhibitors

In the last few years, a large number of studies have focused on the development of topical CAIs as potent systemic agents with fewer systemic adverse effects. The history of the design and development of the topical CAIs has been extensively reviewed.[430,437]

Topical CAIs that are currently approved for the treatment of glaucoma in humans include dorzolamide (formerly MK-507), marketed in 1995, and brinzolamide, which was recently developed. Dorzolamide and brinzolamide are most potent against CA II, with less activity against CA IV.[438,439] Experimental data in rabbits indicate that topical dorzolamide and brinzolamide readily penetrate the eye by both the corneal and scleral routes.[438,439] After topical application on canine eyes, the dorzolamide concentrations achieved in the ciliary body were much higher than those reached in the aqueous humor, suggesting that in the dog the cornea–scleral route has also a

role in the intraocular penetration of the drug.[440] In healthy dogs, administration of a single dose of 2% dorzolamide was associated with a mean reduction in IOP of 3.1 mmHg (18%) from 30 minutes to 6 hours after treatment.[441] Mean aqueous flow rate decreased from 43% in treated eyes.[441] In a short-term study in normal dogs, a maximum decrease in IOP of about 6 mmHg was reached after 5 days of treatment at 8-hour intervals.[442] Topical dorzolamide was also found to lower IOP when applied to normotensive feline eyes every 12 hours.[443] The amplitude of IOP decrease observed in cats after twice daily applications of dorzolamide was almost the same as that observed previously in dogs with 3 times daily applications.[443] Topical dorzolamide seems to influence IOP in horses less than it does in small animals, since its twice-daily application to normotensive equine eyes reduced IOP only by an average of 2 mmHg.[444] In light of these findings, the authors' suggestion was that topical dorzolamide can be recommended only as adjunctive therapy in glaucomatous horses.

The 1% ophthalmic solution of brinzolamide applied to normotensive canine eyes induced a reduction in IOP the amplitude of which was similar to that induced by topical dorzolamide but lower than that resulting from oral administration of 5 mg/kg of methazolamide.[445] By contrast, topical dorzolamide was unable to significantly influence IOP of normotensive feline eyes.[446]

Clinical Use

Because they diminish aqueous humor formation, CAIs can be employed in the treatment of practically all types of glaucoma. Short-term administration of systemic or topical CAIs may be effective in the management of acute increases in IOP resulting from primary or secondary glaucoma. On the basis of findings in normal and glaucomatous dogs, combined administration of topical and systemic CAI has no additional IOP-decreasing effects over dorzolamide or brinzolamide alone that would warrant its use in dogs with acute glaucoma.[436,445] Topical CAIs also represent a valuable substitute for oral methazolamide in the long-term treatment of chronic glaucoma in dogs, since their effects on IOP are comparable and systemic side effects are less likely.[436,445] Theoretically, CAIs can be used in combination with other antiglaucoma agents because their effect is usually additive, reducing IOP more than any single agent. In the dog, the combined use of dorzolamide and latanoprost may be appropriate for the management of chronic glaucoma, since dorzolamide given every 8 hours and latanoprost instilled once in the morning were demonstrated to have an additive effect on decreasing IOP.[447] A commercial combination of 2% dorzolamide and 0.5% timolol is available. Its administration twice daily in humans with glaucoma has an IOP-lowering effect similar to that obtained with dorzolamide alone instilled 3 times daily.[448] Combined use of dorzolamide and timolol has not been evaluated in small animals so far, but recent findings indicate that in horses this combination may not have additional IOP-lowering effects over dorzolamide alone.[444]

Adverse Effects

No ocular side effects have been described in relation to the systemic administration of CAIs, but acute overdosage or long-term therapy may result in a variety of clinical and biochemical disorders. The side effects of the various agents of this class are similar, with dichlorphenamide appearing to cause the fewest and being considered the drug of choice for prolonged treatment in small animals.[377] Common transient side effects associated with oral or parenteral CAIs include increased diuresis, gastrointestinal disturbances (anorexia, vomiting, diarrhea), and possibly increased respiratory rate secondary to metabolic acidosis. Cats appear to be more susceptible to these drugs and should be observed very closely. The dose should be decreased or therapy discontinued if signs of toxicity are observed. Except for acetazolamide, little is known about either the short- or long-term effects of the other CAIs on blood chemistry in the dog. In this species, the intravenous and oral administrations of acetazolamide were found to cause significant metabolic acidosis that achieved a steady state after 1 to 5 days of treatment.[449,450] This effect, attributed to increased bicarbonaturia, was associated with an increase in PO_2 and a decrease in PCO_2, indicative of compensatory hyperventilation. All dogs given acetazolamide had an increase in plasma chloride. A decrease in plasma potassium also develops, reaching its maximum between the second and fifth day of treatment, presumably as a result of increased kaliuresis. Normal food intake usually obviates any serious potassium depletion, but care must be taken in patients with anorexia or preexisting hypokalemia.[449,450] When acetazolamide administration is discontinued, complete recovery of acid-base and blood electrolyte disorders occurs within 36 hours because of the short half-life of the drug.[450] The ophthalmic formulation of 2% dorzolamide has a pH of 5.6, and its instillation may be associated with symptoms of ocular discomfort on instillation in people.[451] By comparison, 1% brinzolamide, which is formulated as an ocular suspension with a pH of 7.5, is better tolerated by human patients.[452] In dogs, topical administration of 2% dorzolamide has been associated with blepharitis, which resolved following discontinuation of the drug.[363] In short-term studies of topical CAIs in the dog, cat, and horse, no local or systemic side effects were reported.[441,443,444]

Prostaglandin Analogues

History and Chemistry

The prostaglandins (PGs) are a family of biologically active lipids with a wide spectrum of possible pharmacologic activity. Since early studies showed that low doses of $PGF_{2\alpha}$ can decrease IOP, it has been established that most of the naturally occurring PGs, as well as some of their analogues and esters, are potent ocular hypotensive agents in both animals and humans.[453,454] The PG derivatives currently approved for the reduction of IOP in humans and animals were developed through chemical modification of $PGF_{2\alpha}$. Latanoprost (formerly PhXA41) and isopropyl unoprostone first emerged as a

result of active screening programs, and new PG analogues, including travoprost and bimatoprost, have recently been introduced onto the market.[453–455] They all are esterified prodrugs of the $PGF_{2\alpha}$, designed to facilitate penetration through the ocular membranes by increased lipid solubility. Latanoprost is the right-handed epimer of a phenyl-substituted analogue of $PGF_{2\alpha}$, while unoprostone is an isopropyl ester of the 20-ethyl derivative of $PGF_{2\alpha}$. Travoprost and bimatoprost are structurally similar to other $PGF_{2\alpha}$ analogues (Fig. 7.2.2). After topical application, the prodrug is enzymatically hydrolyzed during its passage through the corneal epithelium to release the active form, which is then delivered to the anterior segment of the eye.[456,457] The major intraocular metabolite that is expected to act on target tissues is 17-phenyl-$PGF_{2\alpha}$ for latanoprost, bimatoprost, and travoprost[457,458] and a free acid of isopropyl unoprostone for unoprostone.[459] It has been established that human and canine ocular tissues have a similar profile of $PGF_{2\alpha}$ prodrug hydrolysis.[460]

Mechanism of Action

A common feature of the biologically active forms of latanoprost, bimatoprost, travoprost, and unoprostone is the high affinity and selectivity for the prostanoid FP receptors, and investigation revealed that the IOP-lowering action of these PG derivatives is mediated through their binding to FP receptors in humans,[461] monkeys,[462] and presumably in dogs.[463] The pivotal role of FP receptors in the ocular hypotensive effects of the $PGF_{2\alpha}$ analogues has also been demonstrated with the use of FP-receptor deficient (FPKO) mice.[464] By contrast, the IOP-lowering action of PGs in the feline species is mediated by EP_1, and not by FP receptors, unlike in humans and dogs.[462,465]

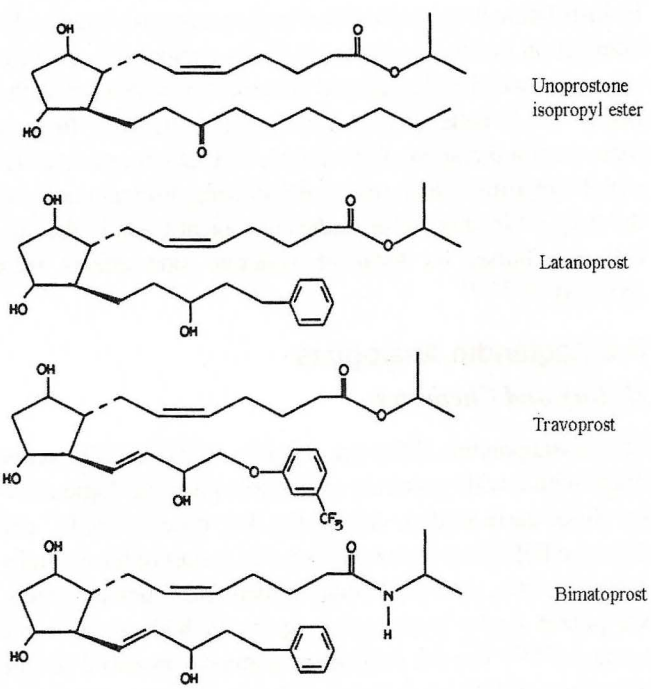

Figure 7.2.2. Chemical structures of the four commercially available prostaglandins in veterinary ophthalmology.

In humans and in animal species studied so far, it has been well established that increase in uveoscleral outflow is the primary mechanism by which PGs reduce IOP.[466] Increased uveoscleral outflow has been reported in humans, monkeys, rabbits, and dogs treated with $PGF_{2\alpha}$ or its analogues[463,467–469] and in cats treated with PGA_2.[470] However, data in the current literature indicate that latanoprost, bimatoprost, and unoprostone also affect the pressure-dependent conventional outflow pathway.[471,472] The mechanisms by which activation of FP receptors lead to an increased uveoscleral outflow are still under investigation, but there is scientific evidence that matrix metalloproteinase (MMP) mediated alterations in the extracellular matrix (ECM) of the ciliary muscle contribute to this pharmacological effect. This concept is based on in vitro and in vivo observations that after several days of treatment with $PGF_{2\alpha}$, the MMP-1, -2, and -3 are increased within uveoscleral outflow tissues,[473,474] while collagen types I, III, and IV are decreased.[475] The amount of myocilin, an intra- and extracellular protein of the ciliary muscle, which may contribute to outflow resistance, also is reduced after topical $PGF_{2\alpha}$ treatment.[476] Ultrastructurally, remodeling of ECM components within the uveoscleral outflow pathway was characterized as lysis of ECM between ciliary muscle bundles and widening of the intermuscular spaces in monkey eyes treated with $PGF_{2\alpha}$,[477] latanoprost, or bimatoprost.[472] In addition to the changes induced within the uveoscleral outflow pathway, long-term treatment with latanoprost or bimatoprost also led to morphologic changes in the trabecular meshwork, perhaps in agreement with increased conventional outflow.[472] Experiments in humans, monkeys, and rabbits suggest that in addition to its IOP-reducing effect, latanoprost increases blood velocity in the optic nerve head or dilates the vessels supplying the optic nerve head because of its pharmacologic effect on the vessels.[478] Increased nerve head perfusion may be important for preservation of visual function in glaucomatous eyes.

Clinical Pharmacology

Experimental studies have demonstrated that topical application of 0.005% latanoprost significantly reduces IOP in normotensive and glaucomatous canine eyes.[479] In normotensive canine eyes, 0.005% latanoprost instilled in the evening, morning, as well as twice daily induced an average decline in IOP of about 25%, while in glaucomatous eyes, it produced a mean decline in IOP of about 50%.[479,480] In glaucomatous dogs, a comparable IOP-lowering action was observed with once- or twice-daily application of 0.03% bimatoprost[481] and 0.004% travoprost.[482] In normal dogs, the amplitude and duration of the IOP-lowering effect of a single application of 0.12% unoprostone isopropyl were found to be similar to those observed after a single application of 0.005% latanoprost.[479,483] By contrast, neither once-daily application of 0.005% latanoprost[479] and 0.03% bimatoprost[484] nor twice-daily applications of 0.03% bimatoprost[485] and 0.12% unoprostone[484] significantly lowered the IOP of normal cats.

These observations illustrate that FP receptor signaling does not play a crucial role in the IOP response to PGs or PG analogues in cats.[462,465] The potential of 0.005% latanoprost for lowering IOP has also been evaluated in normotensive equine eyes.[486] In clinically normal horse, a once-daily application of 0.005% latanoprost resulted in a mean decrease in IOP of 1.03 mmHg or about 5% in males, and 3.01 mmHg or about 17% in females.[486] The reason for the gender effect in the response of the equine eye to topical 0.005% latanoprost has not been determined.[486]

Clinical Use

In a short time, PG derivatives have reached extensive clinical use in human beings with ocular hypertension and primary open-angle glaucoma.[487] Several studies documented their IOP-lowering effect in people, but latanoprost has mostly been evaluated as either monotherapy or an adjunctive agent added to another antiglaucoma agent.[454] In patients with either ocular hypertension or primary open-angle glaucoma, latanoprost, bimatoprost, and travoprost administered once daily in the evening induce a higher reduction in IOP than 0.5% timolol applied twice daily.[488–490] Latanoprost twice daily is less effective than once daily in humans with glaucoma.[491] This reduction of efficacy possibly results from development of subsensitivity at the level of the FP receptor with twice-daily administrations.[491] In people with glaucoma who are no longer regulated on one antiglaucomatous drug alone, a combination of two drugs is common. Latanoprost proved efficacious when added either to timolol or pilocarpine.[492,493] When added to β-blockers, latanoprost compared favorably in IOP-lowering efficacy and was similar in safety to brimonidine and dorzolamide.[492] In the dog, the PG derivatives are mostly indicated for the treatment of primary glaucoma and may replace mannitol, acetazolamide, or both, as first-line drugs in the emergency management of acute closed-angle primary glaucoma.[364] Recent investigations using high resolution imaging of the anterior segment of dogs with primary glaucoma suggested that latanoprost may rapidly lower IOP in primary closed-angle glaucoma by inducing miosis, which breaks the pupillary block, and by opening the collapsed ciliary cleft in primary open-angle glaucoma.[494] Although latanoprost, bimatoprost, and travoprost are instilled once daily in humans, experimental data in glaucomatous dogs suggest that twice-daily instillation of these drugs should be recommended in the dog to decrease daily IOP fluctuations.[481,482]

Side Effects

Side effects most commonly encountered in glaucomatous human eyes treated with $PG_{2\alpha}$ analogues include conjunctival hyperemia, iris darkening, and eyelash changes. Cystoid macular edema, iritis, herpes simplex reactivation, periocular skin darkening, and headaches are other potential complications of this therapy.[495] Several PG derivatives used for the treatment of glaucoma cause increased pigmentation of the iris in humans, but most of the data have been obtained with latanoprost.[496] Increased iris pigmentation was observed in about 5% of the patients during 2 years of treatment with latanoprost, and it appeared that individuals with hazel or heterochromic eye color were at risk of developing this side effect. Because $PGF_{2\alpha}$ analogues are selective agonists of FP receptors, it is likely that FP-receptor activation is involved in this phenomenon. Results of different studies suggest that latanoprost can stimulate tyrosinase gene transcription in the iris[497] and that latanaprost-induced melanogenesis most likely results from stimulation of iridal melanogenesis rather than melanocyte proliferation.[488,496] Endogenous PGE_2 produced by iridal melanocytes exposed to latanoprost might also contribute to the increased melanogenesis.[498] Iris darkening in humans has raised concerns about the possibility of development of precancerous lesions or pigmentary glaucoma in some individuals, but presently no evidence of harmful consequences of this phenomenon has been reported.[496,499] As reported in humans, conjunctival hyperemia has been observed in dogs treated with latanoprost,[479] which also induced epiphora, blepharospasm, and blepharedema when instilled in equine eyes.[486] A moderate to marked miosis is usually present in dogs treated with the $PGF_{2\alpha}$ derivatives.[479–481] The pupillary constriction is more limited when the drug is instilled only in the evening.[480,481] The occurrence of miosis reflects the sensitivity of the canine sphincter muscle to the $PGF_{2\alpha}$, which appears to act directly rather than through the release of adrenergic neurotransmitters.[500] Reports have also described miosis in cats and horses receiving latanoprost,[479,486] as well as in cats treated with bimatoprost.[485] A consequence of the miotic effect of PG derivatives in companion animals is their contraindication in glaucoma secondary to subluxation or anterior luxation of the lens because of the potential pupillary block that may result from vitreous entrapment.[364] In addition, PG derivatives should be used cautiously in glaucomatous dogs with intraocular inflammation[364] and also in aphake or pseudophake subjects because they may lead to disruption of the blood–aqueous barrier in these subjects.[501] Because most horses with secondary glaucoma appear to be at risk for recurrent uveitis, PG analogues have the potential to exacerbate the inflammatory process and should be used with caution in these animals.[486]

Osmotic Agents

Mechanism of Action

After oral or intravenous administration, osmotic agents (also called hyperosmotic agents) are distributed in the extracellular fluids (primarily plasma), thereby contributing to a substantial increase in their osmolality. This increase creates an osmotic gradient in which the extracellular fluids are hypertonic to intraocular fluids (i.e., aqueous and vitreous humors), from which they are separated by semipermeable membranes (i.e., blood–aqueous and blood–vitreous barriers). This osmotic gradient favors the diffusion of water from the intraocular

fluids back into the plasma.[502,503] This fluid shift has two effects on the eye. First, it inhibits the ultrafiltration process that contributes to aqueous humor formation, and second, it reduces the volume of the vitreous body. Shrinkage of the vitreous displaces the iris–lens plane posteriorly and subsequently opens the iridocorneal angle, allowing for better drainage.[495] As a final result, IOP is reduced. For the pharmacologic effects of osmotic agents to occur, they should not cross the blood–aqueous and blood–vitreous barriers. If for any reason integrity of either barrier is compromised, as in ocular inflammation, the osmotic agent may leak into the intraocular fluids, and the extent of osmosis as well as of ocular hypotension will be reduced.[505] Because of its large molecular weight, mannitol penetrates in the eye less than other osmotic agents in presence of ocular inflammation.[506] Other factors important in the establishment of an adequate osmotic gradient between plasma and intraocular fluids include the dosage of the drug, its molecular weight, and its systemic bioavailability (rate of absorption for oral route and rate of elimination). Water deprivation for up to 4 hours following the use of an osmotic agent will reduce the extracellular fluid volume and enhance the increase in blood osmolality and the resulting hypotensive ocular effect.[503]

Products Available

Mannitol, a six-carbon sugar, is poorly absorbed from the gastrointestinal tract and must therefore be administered intravenously. It is available in concentrations of 5% to 25%, but the 20% solution is most often used in ophthalmology.[502] The dose for the lowering of IOP in dogs ranges from 1 to 2 g/kg infused over a period of 20 to 30 minutes.[504,507] To increase the effectiveness of the drug, one fifth of the total dose can be administered rapidly over the first 2 to 5 minutes.[504]

Following intravenous administration of 1.5 g/kg mannitol, IOP of normal canine eyes decreases from baseline values in times ranging from 0.25 to 5.5 hours. A mean maximal depression of 9 mmHg occurs 1.5 hours after administration.[507] It has been assumed that in patients with acute glaucoma, mannitol is a most effective hyperosmotic agent, reducing intraocular pressure within 0.5 to 1 hour, with the effect lasting for some 6 to 10 hours.[508] Mannitol is not metabolized but is filtered across the glomerulus and excreted in the urine without reabsorption by the renal tubules, causing a marked diuresis. If mannitol is infused during surgery, bladder catheterization is advisable to prevent uncontrolled urination during the recovery period.

Glycerin, or glycerol, is a trihydric alcohol that is rapidly absorbed from the gastrointestinal tract after oral administration. The drug is marketed as flavored commercial preparations of 50% and 75% glycerin. Glycerin USP, which contains approximately 1.25 g of glycerin per milliliter, may also be used and mixed in milk or syrup to improve palatability.[506] Glycerin is administered perorally or in food in a daily dose of 1 to 2 g/kg.[504] Occasionally, animals may experience nausea or vomiting after ingestion of the drug. The incidence of vomiting appears to be dose dependent, occurring most frequently with doses higher than 2g/kg.[504,507] Administrations of 1.44 g/kg glycerin in healthy dogs led to a significant ocular hypotensive effect, occurring within 1 hour and lasting about 10 hours.[507] Glycerin is metabolized into glucose, so hyperglycemia and glycosuria may ensue.[503] Weight gain may be another consequence of glycerin metabolism if the drug is administered for a prolonged period. Because this agent is readily metabolized, it induces less diuresis than mannitol.

Isosorbide is a dihydric alcohol that resembles mannitol in chemical structure and can be given orally. It is available as a 45% flavored solution.[506] Unlike glycerin, it is totally inert and does not produce elevated blood glucose. In humans, a dose of 1.5 to 2.0 g/kg induces an ocular hypotensive effect similar to that of 1 to 1.5 g/kg glycerin.[502] A daily dose of 1.5 g/kg is recommended in the dog,[503] although there is currently no published study documenting its effect on IOP in this species.

Clinical Use

Osmotic agents are used mainly in the emergency treatment of acute glaucoma.[377,504,505] These compounds are employed for short-term control of IOP; they are not practical for prolonged therapy.[506] Rapid reduction of intraocular pressure is usually achieved with mannitol rather than with glycerin. Both drugs, however, can be used in combination for maintenance of normal intraocular pressure. Mannitol is infused first; 6 to 8 hours later, glycerin can be administered and repeated as necessary for maintenance.[505] Osmotic agents are also indicated to reduce intraocular pressure in patients with hyphema, but their value in facilitating the resorption of anterior chamber hemorrhage is not clearly established. Mannitol may be employed preoperatively or intraoperatively to lower IOP and reduce vitreous volume.[506] This drug may also be used both before and during surgical procedures on the lens (i.e., cataract surgery, removal of a luxated or subluxated lens), because shrinkage of the vitreous body reduces the incidence and severity of vitreous prolapse. Finally, osmotic agents are indicated after intraocular surgery to relieve ciliary block glaucoma.[506]

Side Effects and Contraindications

The major potential toxicity of intravenous osmotic agents is related to their effect on the volume and distribution of body fluids. Mannitol may quickly expand extracellular fluid volume and subsequently overload the cardiovascular system.[502,503,506] This acute expansion of extracellular fluid volume may precipitate pulmonary edema in patients with cardiac failure or who are under general anesthesia. Deaths due to pulmonary edema occurred in a few dogs and cats that underwent ophthalmic surgery and were given mannitol while anesthetized with methoxyflurane in oxygen.[509] Subsequent studies have shown that infusion of 2.2 g/kg of 20% mannitol in healthy dogs, under the same anesthetic regimen of methoxyflurane with oxygen maintenance, increases central

venous pressure enough to produce pulmonary perivascular and interstitial edema.[510] Infusion of a lower dose (0.25 g/kg) of 25% mannitol in dogs anesthetized with halothane does not induce significant changes in cardiovascular variables but has no effect on IOP.[511] Mannitol does not cross the blood–brain barrier and thus extracts water from cerebral fluid and tissue. Cerebral dehydration induced during the phase of maximal plasma hyperosmolization has been found in association with side effects such as nausea, vomiting, and changed consciousness. Shrinking the brain could also promote subdural hematoma.[502] Mannitol should be avoided in patients with renal failure. Glycerin should be avoided in patients with diabetes mellitus because the drug is converted to glucose.[506]

Neuroprotective Therapy of Glaucomatous Optic Neuropathy

Glaucoma is characterized by loss of retinal ganglion cells (RGCs) and their axons in the optic nerve, referred to as glaucomatous optic neuropathy (GON). There is no doubt that IOP is an important risk factor for the development of optic nerve damage at the level of the lamina cribrosa, but other factors may act in combination to cause atrophy and loss of RGCs.[512,513] The goal of glaucoma treatment in humans is to preserve the visual field and prevent the loss of visual function associated with the disease. The conventional treatment of glaucoma has been directed toward controlling IOP, because scientific evidence shows that lowering IOP in patients with glaucoma is beneficial to decrease the rate of RGC loss.[514] However, clinical trials showed that even with excellent control of IOP, some patients have worsening visual field resulting from progressive RGC loss. The rationale for a therapeutic strategy directed at keeping RGCs alive and functional when lowering IOP is not enough, or is difficult to achieve, therefore derived from these clinical observations. The current understanding of the pathophysiology of the GON indicates that RGCs die in glaucoma via apoptosis, which might have several causes, including compromised blood flow to the optic nerve, blockade of retrograde axonal transport of trophic factors that facilitate RGC survival, and excitotoxic injury to the nerve cell.[512–516] Treatments that aim to directly protect the RGC against glaucomatous damage, therefore, may be achievable through correction of compromised blood flow through the use of vasoactive agents or reduction of IOP, use of neurotrophic factors to influence the survival of injured RGCs, and prevention of excitotoxic RGC death. Excitotoxicity refers to the pathophysiologic condition in which excitatory amino acids (EAAs), such as glutamate and aspartate, excite the neurons excessively, resulting in neurotoxicity and neural death.[512] A variety of findings in humans with glaucoma and animals with experimental hypertension have suggested that an increase in glutamate levels may be involved in glaucomatous RGC loss by overactivation of N-methyl-D-aspartate (NMDA) receptors on RGC cell bodies.[517] A large variety of agents may potentially prevent excitotoxicity such as Ca^{++} channel blockers, EAA receptor antagonists, nitric oxide inhibitors, and free radical scavengers.[512–517] Neuroprotection also has been demonstrated in animal models of glaucoma with conventional antiglaucoma agents such as brimonidine, timolol, and dorzolamide.[518–519] Pharmacologic neuroprotection is now being tested in clinical trials and probably will take more place in the management of human primary open-angle glaucoma in the next few years.

REFERENCES

1. Dunny GM. Bacterial antibiotic resistance. In: Kirk RW, ed. *Current Veterinary Therapy IX: Small Animal Practice.* Philadelphia: WB Saunders, 1986: 1084–1087.
2. Mauger TF. Antibacterials. In: Mauger TF, Graig EC, eds. *Havener's Ocular Pharmacology,* 6th ed. St. Louis: Mosby, 1994: 234–297.
3. Rowley RA, Rubin LF. Aqueous humor penetration of several antibiotics in the dog. *Am J Vet Res* 1970; 31: 43–49
4. Yolton DP. Anti-infective drugs. In: Bartlett JD, Jaanus SD, eds. *Clinical Ocular Pharmacology,* 3rd ed. Boston: Butterworth-Heinemann, 1995: 249–302.
5. Abeynayake P, Cooper BS. The concentration of penicillin in bovine conjunctival sac fluid as it pertains to the treatment of *Moraxella bovis* infection (II). Topical Application. *J Vet Pharm Therap* 1989; 12: 31–36.
6. Binkhorst GJ. Antibiotic levels in bovine lacrimal fluid after single application of ointments containing procaine benzyl penicillin plus dihydrostreptomycin and benzathine cloxacillin. *Vet Rec* 1987; 121: 124–125.
7. Abeynayake P, Cooper BS. The concentration of penicillin in bovine conjunctival sac fluid as it pertains to the treatment of *Moraxella bovis* infection (I). Subconjunctival injection. *J Vet Pharm Therap* 1989; 12: 25–30.
8. Allen LJ, George LW, Willith NH. Effect of penicillin or penicillin and dexamethasone in cattle with infectious bovine keratoconjunctivitis. *J Am Vet Med Assoc* 1995; 206: 1200–1203.
9. Nouws JFM, König CDW. Penetration of some antibiotics into the lacrimal fluid of sheep. *Vet Q* 1983; 5: 114–122.
10. Daigneault J, George LW, Baggot JD. Ocular and serum disposition kinetics of cloxacillin after topical administration of benzathine cloxacillin and intravenous administration of sodium cloxacillin to calves. *Am J Vet Res* 1990; 51: 381–385.
11. George LW, Keefe T, Daigneault J. Effectiveness of two benzathine cloxacillin formulations for treatment of naturally occurring infectious bovine keratoconjunctivitis. *Am J Vet Res* 1989; 50: 1170–1174.
12. Hamor RE. Equine infectious keratitis. *Vet Clin N Am Eq Pract* 1999; 15: 623–646.
13. Sturgess CP, Gruffydd-Jones TJ, Harbour DA, Jones RL. Controlled study of the efficacy of clavulanic acid-potentiated amoxicillin in the treatment of *Chlamydia psittaci* in cats. *Vet Rec* 2001; 149: 73–76.
14. Moore CP, Collins BK, Fales WH. Antibacterial susceptibility patterns for microbial isolates associated with infectious keratitis in horses: 63 cases (1986–1994). *J Am Vet Med Assoc* 1995; 207: 928–933.
15. Caprile KA. The cephalosporin antimicrobial agents: A comprehensive review. *J Vet Pharm Therap* 1988; 11: 1–32.
16. Callegan MC, Hobden JA, Hill JM, Insler MS, O'Callaghan RJ. Topical antibiotic therapy for the treatment of experimental

staphylococcus aureus keratitis. *Invest Ophthalmol Vis Sci* 1992; 33: 3017–3023.
17. Saunders JH, McPherson SD. Ocular penetration of cefazolin in humans and rabbits after subconjunctival injection. *Am J Ophthalmol* 1980; 89: 564–566.
18. Whelan NC, Richardson RJ, Kinyon JM, Pace A, Welch PM, Brienza CA. Ocular and serum pharmacokinetics of intravenous cefazolin in dogs. 31st Annual Meeting of the American College of Veterinary Ophthalmology 2000: 13.
19. Axelrod JL, Kochman RS. Cephradine levels in human aqueous humor. *Arch Ophthalmol* 1981; 99: 2034–2036.
20. Axelrod JL, Kochman RS. Cefoxitin levels in human aqueous humor. *Am J Ophthalmol* 1980; 90: 388–393.
21. Busse H, Seeger K, Wreesmann P. Concentrations of cefoxatine in the anterior chamber of the eye in rabbits and humans. *J Antimicrob Chemother* 1980; 6: 143–145.
22. Axelrod JL, Newton JC, Sarakhun C, et al. Ceftriaxone: A new cephalosporin with aqueous humor levels effective against enterobacteriaceae. *Arch Ophthalmol* 1985; 103: 71–72.
23. Gobeaux D, Ambart L, Couderc JL, Renard Ph, De Charnace B, Lokiec F. Ceftriaxone diffusion from blood to aqueous humor in man. *Br J Ophthalmol* 1989; 73: 574–575.
24. Clements DB, Tailor V. A study of aqueous and serum levels of ceftazidime following subconjunctival administration. *Br J Ophthalmol* 1987; 71: 433–435.
25. Mochizuki K, Yamashita Y, Torisaki M, Komatsu M, Tanahashi T, Kawasaki K. Intraocular kinetics of ceftazidime (Modacin). *Ophthal Res* 1992; 24: 150–154.
26. Sharir M, Triester G, Kneer J, Rubinstein E. The intravitreal penetration of ceftriaxone in man following systemic administration. *Invest Ophthalmol Vis Sci* 1989; 30: 2179–2183.
27. Bonfiglio G, Scuderi AC, Russo G. Netilmicin: In vitro activity, time-kill evaluation and postantibiotic effect on microorganisms isolated from ocular infections. *Chemother* 2001; 47: 117–122.
28. Sauer P, Andrew SE, Lassaline M, Gelatt KN, Denis HM. Changes in antibiotic resistance in equine bacterial ulcerative keratitis (1991–2000): 65 horses. *Vet Ophthalmol* 2003; 6: 309–313.
29. Keller RL, Hendrix DV. Bacterial isolates and antimicrobial susceptibilities in equine bacterial ulcerative keratitis (1993–2004). *Eq Vet J* 2005; 37: 207–211.
30. Insler MS, Helm CJ, George WJ. Topical vs systemic gentamicin penetration into the human cornea and aqueous humor. *Arch Ophthalmol* 1987; 105: 922–924.
31. Rootman DS, Willoughby RPN, Blindish R, Avaria M, Basu PK, Krajden M. Continuous flow contact lens delivery of gentamicin to rabbit cornea and aqueous humor. *J Ocul Pharm* 1992; 8: 317–323.
32. Gilbert ML, Wilhelmus KR, Osato MS. Comparative bioavailability and efficacy of fortified topical tobramycin. *Invest Ophthalmol Vis Sci* 1987; 28: 881–885.
33. Barza M, Kane A, Baum J. The difficulty of determining the route of intraocular penetration of gentamicin after subconjunctival injection in the rabbit. *Invest Ophthalmol Vis Sci* 1981; 20: 509–514.
34. Hillman JS, Jacobs SI, Garnett AJ, Kheskani MB. Gentamicin penetration and decay in the aqueous humor. *Br J Ophthalmol* 1979; 63: 794–796.
35. Mathalone MBR, Harden A. Penetration and systemic absorption of gentamicin after subconjunctival injection. *Br J Ophthalmol* 1972; 56: 609–612.
36. Gorden TB, Cunningham RD. Tobramycin levels in aqueous humor after subconjunctival injection in humans. *Am J Ophthalmol* 1982; 93: 107–110.
37. Trope GE, Lawrence JR, Huid VMD, Everden A. Systemic absorption of topical and subconjunctival gentamicin. *Br J Ophthalmol* 1979; 63: 692–693.
38. Woo FL, Johnson AP, Insler MS, George WJ, LaCorte WS. Gentamicin, tobramycin, amikacin and netilmicin levels in tears following intravenous administration. *Arch Ophthalmol* 1985; 103: 216–218.
39. Petounis A, Papaparos G, Karagerogiou-Makromihelaki C. Penetration of tobramycin sulphate into the human eye. *Br J Ophthalmol* 1978; 62: 660–662.
40. George LW, Reina-Guerra M, Baggot JD, Mihalhi J. Distribution of kanamycin in ocular tissues of calves. *J Vet Pharm Therap* 1986; 9: 183–191.
41. Radda TM, Gnad HD, Graninger W, Rameis H. Amikacin levels in human aqueous humor. *Arzneimittelforschung* 1983; 33: 1607–1608.
42. El-Massry A, Meredith TA, Aguilar HE, et al. Aminoglycoside levels in the rabbit vitreous cavity after intravenous administration. *Am J Ophthalmol* 1996; 122: 684–689.
43. D'Amico DJ, Caspers-Velu L, Libert J, et al. Comparative toxicity of intravitreal aminoglycoside antibiotics. *Am J Ophthalmol* 1985; 100: 264–275.
44. George LW, Smith JA, Kaswan R. Distribution of oxytetracycline into ocular tissues and tears of calves. *J Vet Pharm Therap* 1985; 8: 47–54.
45. George LW, Smith JA. Treatment of *Moraxella bovis* infections in calves using a long-acting oxytetracycline formulation. *J Vet Pharm Therap* 1985; 8: 55–61.
46. Smith JA, George LW. Treatment of acute ocular *Moraxella bovis* infections in calves with a parenterally administered long-acting oxytetracycline formulation. *Am J Vet Res* 1985; 46: 804–807.
47. Tsacopoulos M. The penetration of vibramycin (doxycycline) in human aqueous humor. *Ophthalmologic* 1969; 159: 413–429.
48. Tabbara KF, Gosheh R, O'Connor GR. Ocular tissue absorption of minocycline in the rabbit. *Arch Ophthalmol* 1983; 101: 1426–1428.
49. Salminen L. Penetration of ocular compartments by tetracyclines, II. An experimental study with doxycycline. *Albrecht Von Graefes Archiv fur Klinische und Experimentelle Ophalmologie* 1977; 204: 201–207.
50. Sykes JE, Studdert VP, Browning GF. Comparison of the polymerase chain reaction and culture for the detection of feline *Chlamydia psittaci* in untreated and doxycycline-treated experimentally infected cats. *J Vet Intern Med* 1999; 13: 146–152.
51. Sparkes AH, Caney SMA, Sturgess CP, Gruffydd-Jones TJ. The clinical efficacy of topical and systemic therapy for the treatment of feline ocular chlamydiosis. *J Feline Med Surg* 1999; 1: 31–35.
52. German AJ, Cannon MA, Dye C, et al. Oesophageal strictures in cats associated with doxycycline therapy. *J Feline Med Surg* 2005; 7: 33–41.
53. Whelan NC, Richardson RJ, Kinyon JM. Ocular and serum pharmacokinetics of intravenous doxycyclin in the dog. 31st Annual Meeting of the American College of Veterinary Ophthalmologists 2000: 33.
54. Gilmour MA, Clarke CR, MacAllister CG, et al. Ocular penetration of oral doxycycline in the horse. *Vet Ophthalmol* 2005; 8: 331–335.

55. Ismail S, Morton DJ. Ophthalmic uptake of chloramphenicol from proprietary preparations using an in vitro method of evaluation. *Int J Pharmaceut* 1987; 37: 11–13.
56. Conner GH, Gupta BN. Bone marrow blood and assay levels following medication of cats with chloramphenicol ophthalmic ointment. *Vet Med Sm Anim Pract* 1973; 68: 895–899.
57. Meredith TA, Aguilar HD, Shaarawy A, Kuicaid M, Dick J, Niesman MR. Vancomycin levels in the vitreous cavity after intravenous administration. *Am J Ophthalmol* 1995; 119: 774–778.
58. El Bahri L, Blouin A. Fluoroquinolones: A new family of antimicrobials. *Comp Cont Educ Pract Vet* 1991; 13: 1429–1433.
59. Kern T. Antibacterial agents for ocular therapeutics. *Vet Clin N Am Sm Anim Pract* 2004; 34: 655–668.
60. McGee DH, Holt WF, Kastner PR, Rice RL. Safety of moxifloxacin as shown in animal and in vitro studies. *Surv Ophthalmol* 2005; 50 (suppl 1): S46–S54.
61. Daniell M, Mills R, Morlet N. Microbial keratitis: What's the preferred initial therapy? *Br J Ophthalmol* 2003; 87: 1167–1174.
62. Hobden JA, O'Callaghan RJ, Hill JM, Hagenah M, Insler MS, Reidy JJ. Ciprofloxacin and prednisolone therapy for experimental *Pseudomonas* keratitis. *Curr Eye Res* 1992; 3: 259–266.
63. Donnenfeld ED, Schrier A, Perry HD, Aulicino T, Gombert ME, Snyder R. Penetration of topically applied ciprofloxacin, norfloxacin and ofloxacin into the aqueous humor. *Ophthalmol* 1994; 101: 902–905.
64. Yu-Speight AW, Kern TJ, Erb HN. Ciprofloxacin and ofloxacin aqueous humor concentrations after topical administration in dogs undergoing cataract surgery. *Vet Ophthalmol* 2005; 8: 181–187.
65. Bron AM, Péchinot A, Garcher C, Guyonnet G, Kazmierczak A. Ocular penetration of topically applied norfloxacin 0.3% in the rabbits and in humans. *J Ocular Pharm* 1992; 8: 241–246.
66. Moore CP, Collins BK, Fales WH, Halenda RM. Antimicrobial agents for treatment of infectious keratitis in horses. *J Am Vet Med Ass* 1995; 207: 855–862.
67. Mallari P, McCarty D, Daniell M, et al. Increased incidence of corneal perforation after topical fluoroquinolone treatment for microbial keratitis. *Am J Ophthalmol* 2001; 131: 131–133.
68. Seitz B, Hayashi S, Wee W, et al. In vitro effects of aminoglycosides and fluoroquinolones on keratocytes. *Invest Ophthalmol Vis Sci* 1996; 37: 656–665.
69. Keren G, Alhalel A, Bartou E, et al. The intravitreal penetration of orally administered ciprofloxacin in humans. *Invest Ophthalmol Vis Sci* 1991; 32: 2388–2392.
70. Giamarellou H, Kanellas D, Kavouklis E, Petrikkos G, Gabriel L. Comparative pharmacokinetics of ciprofloxacin, ofloxacin and pefloxacin in human aqueous humour. *Europ J Clinic Microbiol Infect Dis* 1993; 12: 293–297.
71. Herbert EN, Pearce IA, McGalliard J, Wong D, Groenewald C. Vitreous penetration of levofloxacin in the uninflamed phakic human eye. *Br J Ophthalmol* 2002; 86: 387–389.
72. Morlet N, Graham GG, Gatus B, McLachlan J, Salonikas C, Naidoo D, Goldberg I, Lam CM. Pharmacokinetics of ciprofloxacin in the human eye: A clinical study and population pharmacokinetic analysis. *Antimicrobial Agents Chemother* 2000; 44: 1674–1679.
73. Regnier A, Concordet D, Schneider M, Boisramé B, Toutain PL. Population pharmacokinetics of marbofloxacin in aqueous humor after intravenous administration in dogs. *Am J Vet Res* 2003; 64: 889–893.
74. Gelatt KN, van der Woerdt A, Ketring KL, et al. Enrofloxacin-associated retinal degeneration in cats. *Vet Ophthalmol* 2001; 4: 99–106.
75. Ford MM, Narfström K, Giuliano EA, Moore CP. Enrofloxacin and the feline retina: Ophthalmoscopic and electroretinographic effects. 34th Annual Meeting of the American College of Veterinary Ophthalmologists 2003: 58.
76. Dubiezig RR, Ford MM, Narfström K. Enrofloxacin and the feline retina: Histologic effects. 34th Annual Meeting of the American College of Veterinary Ophthalmologists 2003: 5.
77. Wiebe V, Hamilton P. Fluoroquinolone-induced retinal degeneration in cats. *J Am Vet Med Assoc* 2002; 221: 1568–1571.
78. Kay-Mugford PA, Ramsey DT, Dubielzig RR. Ocular effects of orally administered orbifloxacin in cats. 32nd Annual Meeting of the American College of Veterinary Ophthalmologists 2001: 56.
79. Davidson MG, Lappin MR, Rottman JR, et al. Paradoxical effects of clindamycin in experimental, acute toxoplasmosis in cats. *Antimicrobial Agent Chemother* 1996; 40: 1352–1359.
80. Lappin MR, Greene CE, Winston S, et al. Clinical feline toxoplasmosis: Serologic diagnosis and therapeutic management of 15 cases. *J Vet Intern Med* 1989; 3: 139–143.
81. Hinkle KM, Gerding PA, Kakoma I, Schaeffer DJ. Evaluation of activity of selected ophthalmic antimicrobial agents in combination against common ocular microorganisms. *Am J Vet Res* 1999; 60: 316–318.
82. Peters DH, Friedel HA, McTavish D. Azithromycin. A review of its antimicrobial activity, pharmacokinetic properties and clinical efficacy. *Drugs* 1992; 44: 750–799.
83. Ketring KL, Zuckerman EE, Hardy WD Jr. Bartonella: A new etiological agent of feline ocular disease. *J Am Anim Hosp Assoc* 2004; 40: 6–12.
84. Flach A. Photosensitivity to sulfisoxazole ointment. *Arch Ophthalmol* 1981; 99: 609–610.
85. Sigel CW, Macklin AW, Grace ME, Tracy CH. Trimethoprim and sulfadiazine concentrations in aqueous and vitreous humors of the dog. *Vet Med Sm Anim Clin* 1981; 76: 991–993.
86. Diehl KJ, Roberts SM. Keratoconjunctivitis sicca in dogs associated with sulfonamide therapy: 16 cases (1980–1990). *Prog Vet Comp Ophthalmol* 1991; 4: 276–282.
87. Rothschild CM, Sellon DC, Bryan GM, Gay JM, Hines MT. Effects of trimethoprim-sulfadiazine on tear production and the fluctuations of Schirmer tear test values in horses. *Vet Ophthalmol* 2004; 7: 385–390.
88. McLellan GJ, Cobb MA, Lybaert P, McLaren IM. Determination of the concentration of sodium fusidate in feline tear fluid and ocular tissues following topical application of fusidic acid. 33rd Annual Meeting of the American College of Veterinary Ophthalmologists 2002: 1.
89. Taylor PB, Burd EM, Tabbara K. Corneal and intraocular penetration of topical and subconjunctival fusidic acid. *Br J Ophthalmol* 1987; 71: 598–601.
90. Leibowitz HM, Ryan WJ, Kupferman A. Route of antibiotic administration in bacterial keratitis. *Arch Ophthalmol* 1981; 99: 1420–1423.
91. Stanz KM. Antibiotic therapy of the eye. In: Bonagura JD, ed. *Kirk's Current Veterinary Therapy XII: Small Animal Practice.* Philadelphia: WB Saunders, 1995: 1211–1218.
92. Callegan MC, O'Callaghan O, Hill JM. Pharmacokinetic considerations in the treatment of bacterial keratitis. *Clin Pharmacokinetics* 1994; 27: 129–149.
93. Barza M. Animal models in the evaluation of chemotherapy of ocular infections. In: Zak O, Sande MA, eds. *Experimental*

Models in Antimicrobial Chemotherapy. Vol. 1. London: Academic Press, 1986; 187–211.
94. Miller TR. Principles of therapeutics. *Vet Clin N Am Eq Pract* 1992; 8: 479–497.
95. Nasisse MP, Nelms S. Equine ulcerative keratitis. *Vet Clin N Am Eq Pract* 1992; 8: 537–555.
96. Abrams KL. Ocular drug reactions and toxicities. In: Bonagura JD, ed. *Kirks's Current Veterinary Therapy XII: Small Animal Practice.* Philadelphia: WB Saunders, 1995: 1223–1226.
97. Nelson JD, Silverman V, Lima PH, Beckman G. Corneal epithelial wound healing: A tissue culture assay on the effect of antibiotics. *Curr Eye Res* 1990; 9: 277–285.
98. Hendrix DVH, Ward DA, Barnhill MA. Effects of antibiotics on morphologic characteristics and migration of canine corneal epithelial cells in tissue culture. *Am J Vet Res* 2001; 62: 1664–1669.
99. Cutarelli PE, Lass JH, Lazarus HM, Putman SC, Jacobs MR. Topical fluoroquinolones: Antimicrobial activity and in vitro corneal epithelial toxicity. *Curr Eye Res* 1991; 10: 557–563.
100. Petroutsos G, Guimaraes R, Giraud J, Pouliquen Y. Antibiotics and corneal epithelial wound healing. *Arch Ophthalmol* 1983; 101: 1775–1778.
101. Baum J, Barza M. Topical *vs* subconjunctival treatment of bacterial corneal ulcers. *Ophthalmol* 1983; 90: 162–168.
102. Miglioli PA, Dorigo MT. Antibiotic levels in aqueous and vitreous humor after intraocular administration. *Chemother* 1989; 35: 406–409.
103. Axelrod JL. The eye. In: Ristuccia AM, Cumba BA, eds. *Antimicrobial Therapy.* New York: Raven Press, 1984: 415–420.
104. Moore CP, Miller RB. Infectious and parasitic eye diseases of cattle. In: Howard JL, ed. *Current Veterinary Therapy* 3: Food Animal Practice. Philadelphia: WB Saunders Company, 1993: 834–839.
105. Furman PA. Chemotherapy of herpesvirus infections. *Curr Eye Res* 1987; 6: 213–219.
106. Malmberg GJ, Lupo R. Compounding in veterinary ophthalmology. *Vet Clin of N Am Sm Anim Pract* 2004; 34: 825–838.
107. Lass JHM. Antiviral. In: Lamberts DW, Potter DE, eds. *Clinical Ophthalmic Pharmacology,* 1st ed. Boston: Little Brown, 1987: 107–155.
108. Nasisse MD, Guy JS, Davidson MG, Sussman W, De Clercq E. In vitro susceptibility of feline herpesvirus-1 to vidarabine, idoxuridine, trifluridine, acyclovir, or bromovinyldeoxyuridine. *Am J Vet Res* 1989; 50: 158–160.
109. Maggs DJ, Clarke HE. In vitro efficacy of ganciclovir, cidofovir, penciclovir, foscarnet, idoxuridine, and acyclovir against feline herpesvirus type-1. *Am J Vet Res* 2004; 65: 399–403.
110. Sande MA, Mandell GL. Antifungal and antiviral agents. In: Gilman AG, Goodman LA, Gilman A, eds. *The Pharmacological Basis of Therapeutics.* 7th ed. New York: MacMillan Publishing, 1985: 1219–1239.
111. Owens JG, Nasisse MP, Tadepalli SM, Dorman DC. Pharmacokinetics of acyclovir in the cat. *J Vet Pharmacol Therap* 1996; 19: 488–490.
112. Nasisse MP, Dorman DC, Jamison KC, Weigler BJ, Hawkins EC, Stevens JB. Effects of valacyclovir in cats infected with feline herpesvirus 1. *Am J Vet Res* 1997; 58: 1141–1144.
113. Glaze MB, Gelatt KN. Feline Ophthalmology. In, Gelatt KN. ed. *Veterinary Ophthalmology*, 3rd ed. Philadelphia: Lippincott, Williams and Wilkins, 1999: 997–1053.
114. Sandmeyer LS, Keller CB, Bienzle D. Effects of cidofovir on cell death and replication of feline herpesvirus-1 in cultured feline corneal epithelial. *Am J Vet Res* 2005; 66: 217–222.
115. Galle LE. Antiviral therapy for ocular viral disease. *Vet Clin N Am Sm Anim Pract* 2004; 34: 639–654.
116. Jabs DA. Treatment of cytomegalovirus retinitis in patients with AIDS. *Ann Inter Med* 1996; 125: 144–145.
117. Vilcek J, Sen GC. Interferons and other cytokines. In: Fields BN, Knipe DM, Howley PM, eds. *Fields Virology,* 3rd ed., Vol. 1. Philadelphia: Lippincott-Raven Publishers, 1996: 375–399.
118. Pestka S. The interferon receptors. *Semin Oncol* 1997; 24 (suppl 9): S9–S40.
119. Nathan C. Interferon and inflammation. In: Gallin JI, Goldstein IM, Synderman R, eds. *Inflammation: Basic Principles and Clinical Correlates.* 2nd ed. New York: Raven Press, 1992: 265–290.
120. de Mari K, Maynard L, Sanquer A, Lebreux B, Eun H-M. Therapeutic effects of recombinant feline interferon-α on feline leukemia virus (FeLV)-infected and FeLV/feline immunodeficiency virus (FIV)-coinfected symptomatic cats. *J Vet Intern Med* 2004; 18: 477–482.
121. Sandmeyer LS, Keller CB, Bienzle D. Effects of interferon-α on cytopathic changes and titers for feline herpesvirus-1 in primary cultures of feline corneal epithelial cells. *Am J Vet Res* 2005; 66: 210–216.
122. Weiss RC. Synergistic antiviral activities of acyclovir and recombinant human leukocyte (alpha) interferon on feline herpesvirus replication. *Am J Vet Res* 989; 10: 1672–1677.
123. Bäcklein T, Speier S, Metzler A, Spiess B, Richter M. Activity of topically and orally applied interferon omega in cats indicated by Mx-protein expression in conjunctival and white blood cells. 34th Annual Meeting of the American College of Veterinary Ophthalmologists 2003: 41.
124. Griffith RS, Norins AL, Kagan C. A multicentered study of lysine therapy in Herpes simplex infection. *Dermatologica* 1978; 156: 257–267.
125. Maggs DJ, Collins K, Thorne JG, Nasisse MP. Effects of L-and lysine and L-arginine on in-vitro replication of feline herpesvirus type-1. *Am J Vet Res* 2000; 31: 1474–1478.
126. Stiles J, Townsend WM, Rogers QR, Krohne SG. Effect of oral administration of L-lysine on conjunctivitis caused by feline herpesvirus in cats. *Am J Vet Res* 2002; 63: 99–103.
127. Maggs DJ, Nasisse MP, Kass PH. Efficacy of oral supplementation with L-lysine in cats latently infected with feline herpesvirus. *Am J Vet Res* 2003; 64: 37–42.
128. Beaumont SL, Maggs DJ, Clarke HE. Effects of bovine lactoferrin on in vitro replication of feline herpesvirus. *Vet Ophthalmol* 2003; 3: 245–250.
129. Wutzler P, Sauerbrei A, Klöcking R, et al. Virucidal and chlamydicidal activities of eye drops with povidone-iodine liposome complex. *Ophthal Res* 2000; 32: 118–125.
130. Nasisse MP. Ocular feline herpesvirus-1 infection. In: Bonagura JD, ed. *Kirk's Current Veterinary Therapy XIII; Small Animal Practice.* Philadelphia: WB Saunders, 2000: 1057–1060.
131. Stiles J. Feline herpesvirus. *Clin Tech Sm Anim Pract* 2003; 18: 178–185.
132. Stiles J. Treatment of cats with ocular disease attributable to herpesvirus infection: 17 cases (1983–1993). *J Am Vet Med Assoc* 1995; 207: 599–603.

133. Williams DL, Robinson JC, Lay E, Field H. Efficacy of topical aciclovir for the treatment of feline herpetic keratitis: Results of a prospective clinical trial and data from in vitro investigations. *Vet Rec* 2005; 157: 254–257.
134. Fascetti AJ, Maggs DJ, Kanchuk ML, Clarke HE, Rogers QR. Excess dietary lysine does not cause lysine-arginine antagonism in adult cats. *J Nutr* 2004; 134: S2042–S2045.
135. Maggs D. Ocular manifestations of equine herpesviruses. In: Robinson NE, ed. *Current Therapy in Equine Medicine* 5. Philadelphia: Saunders, 2003: 473–476.
136. Matthews AG. Cornea. In: Barnett KC, Crispin SM, Lavach JD, Matthews AG, eds. *Equine Ophthalmology. An Atlas and Text,* 2nd ed. Edinburgh: Saunders, 2004: 107–147.
137. Ford MM. Antifungals and their use in veterinary ophthalmology. *Vet Clin N Am Sm Anim Pract* 2004; 34: 669–691.
138. Moore CP, Fales WH, Whittington P, Baner L. Bacterial and fungal isolates from equidae with ulcerative keratitis. *J Am Vet Med Assoc* 1983; 182: 600–603.
139. Coad CT, Robinson NM, Wilhelmus KR. Antifungal sensitivity testing for equine keratomycosis. *Am J Vet Res* 1985; 46: 676–678.
140. Brooks DE, Andrew SE, Dillavou CL, Ellis G, Kubilis PS. Antimicrobial susceptibility patterns of fungi isolated from horses with ulcerative keratomycosis. *Am J Vet Res* 1998; 59: 138–142.
141. Marlar AB, Miller PE, Canton DE, Scagliotti R, Murphy CJ. Canine keratomycosis: A report of eight cases and literature review. *J Am Anim Hosp Assoc* 1994; 30: 331–340.
142. Manzouri B, Vafidis GC, Wyse RKH. Pharmacotherapy of fungal eye infections. *Expert Opin Pharmacotherapy* 2001; 2: 1849–1857.
143. Polak A. Antifungal therapy-state of the art at the beginning of the 21st century. In: Jucker E, ed. *Antifungal Agents–Advances and Problems.* Basel: Birkhäuser Verlag, 2003.
144. Prescott JF, Baggott JD. Antifungal chemotherapy. In: *Antimicrobial Therapy in Veterinary Medicine.* Boston: Blackwell Scientific Publications, 1988: 267–285.
145. Huber WG. Antifungal and antiviral agents. In: Booth NH, McDonald LE, eds. *Veterinary Pharmacolgy and Therapeutics.* 6th ed. Ames: Iowa State University Press, 1988: 849–860.
146. O'Day DM, Ray WA, Head WS, Robinson RD. Influence of the corneal epithelium on the efficacy of topical antifungal agents. *Invest Ophthalmol Vis Sci* 1984; 25: 855–859.
147. O'Day DM, Robinson R, Head WS. Efficacy of antifungal agents in the cornea. I. A comparative study. *Invest Ophthalmol Vis Sci* 1983; 24: 1098–1102.
148. Bistner SI, Riis RC. Clinical aspects of mycotic keratitis in the horse. *Cornell Vet* 1979; 69: 364–372.
149. Segal E, Romano A, Barishak YR. Miconazole activity in experimental aspergillus ocular infections. *Ophthalmic Res* 1981; 13: 12–19.
150. O'Day DM, Head WS, Robinson RD, Williams TE, Gedde SJ. Anomalous effect of subconjunctival miconazole on *Candida albicans* keratitis in rabbits. *Am J Ophthalmol* 1991; 112: 562–566.
151. Foster CS, Lass JH, Moran-Wallace K, Giovanoni R. Ocular toxicity of topical antifungal agents. *Arch Ophthalmol* 1981; 99: 1081–1084.
152. Chu W, Foster CS, Moran K, Giovanoni R. Intraocular penetration of ketoconazole in rabbits (Abstract). *Invest Ophthalmol Vis Sci* 1979; 20(suppl): 133.
153. Ishibashi Y. Oral ketoconazole therapy for keratomycosis. *Am J Ophthalmol* 1983; 95: 342–345.
154. Torres MA, Mohamed J, Cavados-Adame H, Martinez LA. Topical ketoconazole for fungal keratitis. *Am J Ophthalmol* 1985; 100: 293–298.
155. DaCosta PD, Merideth RE, Sigler RL. Cataracts in dogs after long-term ketoconazole therapy. *Vet Comp Ophthalmol* 1996; 6: 176–180.
156. Prajna NV, John RK, Nirmalan PK, Lahita P, Srinivasan M. A randomised clinical trail comparing 2% econazole and 5% natamycin for the treatment of fungal keratitis. *Br J Ophthalmol* 2003; 87: 1235–1237.
157. O'Day M, Foulds G, Williams TE, Robinson RD, Allen RH, Head WS. Ocular uptake of fluconazole following oral administration. *Arch Ophthalmol* 1990; 108: 1006–1008.
158. Vaden SL, Heit MC, Hawkins EC, Manaugh C, Riviere JE. Fluconazole in cats: Pharmacokinetics following intravenous and oral administration and penetration into cerebrospinal fluid, aqueous humour and pulmonary epithelial lining fluid. *J Vet Pharmacol Therap* 1997; 20: 181–186.
159. O'Day DM, Head WS, Robinson RD, Williams TE, Gedde S. The evaluation of therapeutic responses in experimental keratomycosis. *Curr Eye Res* 1992; 11: 35–44.
160. Avunduk AM, Beuerman RW, Warnel ED, Kaufman HE, Greer D. Comparison of efficacy of topical and oral fluconazole treatment in experimental Aspergillus keratitis. *Curr Eye Res* 2003; 26: 113–117.
161. Richter M, Hauser B, Kaps S, Spiess B. Keratitis due to Histoplasma spp. in a horse. *Vet Ophthalmol* 2003; 6: 99–103.
162. Abbasoglu OE, Hosal BM, Sener B, Erdemoglu N, Gursel E. Penetration of topical fluconazole into human aqueous humor. *Exp Eye Res* 2001; 72: 147–151.
163. Brooks DE, Legendre AM, Gumm GG, Laratta LJ, Abrams KL, Morgan RV. The treatment of canine ocular blastomycosis with systemically administered itraconazole. *Prog Vet Comp Ophthalmol* 1991; 1: 263–268.
164. Hendrix DVH, Bochsler PN, Rohrbach BW. Effect of itraconazole therapy on the histopathologic findings in the eyes of dogs with blastomycosis (abstract). 31st Annual Meeting of the American College of Veterinary Ophthalmologists 2000: 30.
165. Ball MA, Rebhun WC, Trepanier L, Gaarder J, Schwark WS. Corneal concentrations and preliminary toxicological evaluation of an itraconazole/dimethyl sulphoxide ophthalmic ointment. *J Vet Pharm Therap* 1997; 20: 100–104.
166. Gao H, Pennesi ME, Shah K, et al. Intravitreal voriconazole: An electroretinographic and histopathologic study. *Arch Ophthalmol* 2004; 122: 1687–1692.
167. Martin MJ, Rahman MR, Johnson GJ, Srinivasan M, Clayton YM. Mycotic keratitis: Susceptibility to antiseptic agents. *International Ophthalmology* 1996; 19: 299–302.
168. McLaughlin SA, Gilger BC, Whitley RD. Infectious keratitis in horses: Evaluation and management. *Comp Cont Ed Pract Vet* 1992; 3: 372–380.
169. Mohan M, Gupta SK, Kalra VK, et al. Topical silver sulfadiazine. A new drug for ocular keratomycosis. *Br J Ophthalmol* 1988; 72: 192–195.
170. Nasisse MP, Nelms S. Equine ulcerative keratitis. *Vet Clin N Am Eq Pract* 1992; 8: 537–555.
171. Ben-Ziony Y, Arzi B. Use of lufenuron for treating fungal infections of dogs and cats: 297 cases (1997–1999). *J Am Vet Med Assoc* 2000; 217: 1510–1513.

172. Scotty NC, Johnson PJ, Giuliano EA, et al. Determination of antifungal activity in vitro and measurement of blood concentrations following oral administration in horses. 34th Annual Meeting of the American College of Veterinary Ophthalmologists 2003: 3.
173. Kern TJ, Brooks DE, White MM. Equine keratomycosis: Current concepts of diagnosis and therapy. *Eq Vet J* 1983: (suppl)33–38.
174. Hendrix DV, Ward DA, Guglick MA. Disseminated candidiasis in a neonatal foal with keratomycosis as the initial sign. *Vet Comp Ophthalmol* 1997; 7: 10–13.
175. Hendrix DVM, Chmielenski NT, Smith PJ, Brooks DE, Gelatt KN, Whittaker C. Keratomycosis in four horses caused by *cyclindrocarpon-destructans*. *Vet Comp Ophthalmol* 1996; 6: 252–257.
176. Ball MA, Rebhun WC, Gaarder JE, Patten V. Evaluation of itraconazole-dimethyl sulfoxide ointment for treatment of keratomycosis in nine horses. *J Am Vet Med Assoc* 1997; 211: 199–203.
177. Grahn B, Wolfer J, Keller C, et al. Equine keratomycosis: clinical and laboratory findings in 23 cases. *Prog Vet Comp Ophthalmol* 1993; 3: 2–6.
178. Hinkle KM, Gerding PA, Kakoma I, Schaeffer DJ. Evaluation of activity of selected ophthalmic antimicrobial agents in combination against common ocular microorganisms. *Am J Vet Res* 1999; 60: 316–318.
179. Tchernitchin A, Wenk EJ, Hernandez MR, et al. Glucocorticoid localization by radioautography in the rabbit eye following systemic administration of ^{3}H-dexamethasone. *Invest Ophthalmol Vis Sci* 1980; 19: 1231–1236.
180. Hernandez MR, Weng EJ, Weinstein BI, Gordon GI, Dunn W, Southren AL. Corneal-conjunctival uptake of topical ^{3}H-dexamethasone in the rabbit eye. *Invest Ophthalmol Vis Sci* 1981; 20: 120–123.
181. Burnstein, KL, Cidlowski JA. Regulation of gene expression by glucocorticoids. *Ann Rev Physiol* 1989; 51: 683–689.
182. Muller M, Renkawitz R. The glucocorticoid receptor. *Biochimica et Biophysica Acta* 1991; 1088: 171–182
183. Flower RJ. Lipocortin and the mechanism of action of the glucocorticoids. *Br J Pharm* 1988; 94: 987–1015.
184. Karalis K, Mastorakos G, Sano H, Wilder RL, Chrousos GP. Somatostatin may participate in the antiinflammatory action of glucocorticoids. *Endocrinol* 1995; 136: 4133–4138.
185. Moncada S, Plamer RM. Inhibition of the induction of nitric oxide synthase by glucocorticoids: Yet another explanation for their anti-inflammatory effects? *Trends Pharmacol Sci* 1991; 12: 130–131.
186. Goppelt-Struebe M, Wolter D, Resch K. Glucocorticoids inhibit prostaglandins synthesis not only at the level of phospholipase A2 but also at the level of cyclo-oxygenase/PGE isomerase. *Br J Pharmacol* 1989; 98: 1287–1295.
187. Cronstein BN, Kimmel SC, Levin RI, Martiniuk F, Weissmann G. A mechanism for the antiinflammatory effects of corticosteroids: The glucocorticoid receptor regulates leukocyte adhesion to endothelial cells and expression of endothelial-leukocyte adhesion molecule 1 and intercellular adhesion molecule 1. Proceedings of the National Academy of Sciences of the United States of America 1992; 89: 9991–9995.
188. Pappa KS. Antiinflammatory agents: Corticosteroid drug. In: Mauger TF, Craig EL, eds. *Havener's Ocular Pharmacology*. 6th ed. St Louis: Mosby, 1994: 364–428.
189. Friedburg D, Meissner B. Fluorescein angiography of the corneal limbus. Drug effects on the capillary blood flow. *Graefe's Arch Clin Exp Ophthalmol* 1978; 207: 213–219.
190. Boneham GC, Collin HB. Steroid inhibition of limbal blood and lymphatic vascular cell growth. *Curr Eye Res* 1995; 14: 1–10.
191. Bassu PK, Avaria M, Jandie R. Effect of hydrocortisone on the mobilization of leukocytes in corneal wounds. *Br J Ophthalmol* 1981; 65: 694–698.
192. Boneham GC, Collin HB. Steroid inhibition of limbal blood and lymphatic vascular cell growth. *Curr Eye Res* 1995; 14: 1–10.
193. McGhee CNJ, Watson DG, Midgley JM, Noble MJ, Dutton GGN, Fern AI. Penetration of synthetic corticosteroids into human aqueous humour. *Eye* 1990; 4: 526–530.
194. Musson DG, Bidgood AM, Olejnik O. An in vitro comparison of the permeability of prednisolone, prednisolone sodium phosphate and prednisolone acetate across the NZW rabbit cornea. *J Ocular Pharm* 1992; 8: 139–150.
195. McGee CNJ. Pharmacokinetics of ophthalmic corticosteroids. *Br J Ophthalmol* 1992; 76: 681–684.
196. Castrén JA, Raitta C, Laamanen A. Uber das eindringen eines depot-corticosteroids in die vorderkammer und den glaskörper, und die verweildauer des steroids im auge. *Acta Ophthalmologica* 1964; 42: 680–683.
197. Kalina PH, Erie JC, Rosenbaum L. Biochemical quantification of triamcinolone in subconjunctival depots. *Arch Ophthalmol* 1995; 113: 867–869.
198. Weijtens O, van der Sluijs A, Schoemaker RC, et al. Peribulbar corticosteroid injection: Vitreal and serum concentrations after dexamethasone disodium phosphate injection. *Am J Ophthalmol* 1997; 123: 358–363.
199. Jonas JB. Intravitreal triamcinolone acetonide as treatment for extensive exudative retinal detachment. *Br J Ophthalmol* 2004; 88: 587–588.
200. Spandau UHM, Derse M, Schmitz-Valckenberg P, Papoulis C, Jonas JB. Dosage dependency of intravitreal triamcinolone acetonide as treatment for diabetic macular oedema. *Br J Ophthalmol* 2005; 89: 999–1003.
201. Weijtens O, Schoemaker RC, Cohen AF, et al. Dexamethasone concentration in vitreous and serum after oral administration. *Am J Ophthalmol* 1998; 125: 673–679.
202. Wilkie DA. Control of ocular inflammation. *Vet Clin N Am Sm Anim Pract* 1990; 20: 693–713.
203. Fischer GA. Granuloma formation associated with subconjunctival injection of a corticosteroid in dogs. *J Am Vet Med Assoc* 1979; 174: 1086–1088.
204. Hakanson N, Shively JN, Merideth RE. Granuloma formation following subconjunctival injection of triamcinolone in two dogs. *J Am Anim Hosp Assoc* 1991; 27: 89–92.
205. Behrend EN, Kemppainen RJ. Glucocorticoid therapy: Pharmacology, indications and complications. *Vet Clin N Am Sm Anim Pract* 1997; 27: 187–213.
206. Brown SI, Weller CA, Vidrich AM. Effect of corticosteroids on corneal collagenase of rabbits. *Am J Ophthalmology* 1970; 70: 744–747.
207. Petroutsos G, Guimaraes R, Giraud JP, Pouliquen Y. Corticosteroids and corneal epithelial wound healing. *Br J Ophthalmol* 1982; 66: 705–708.
208. Phillips K, Arffa R, Cintron C, et al. Effects of prednisolone and medroxyprogesterone on corneal wound healing, ulceration and neovascularization. *Arch Ophthalmol* 1983; 101: 640–643.

209. Hendrix DVH, Ward DA, Barnhill MA. Effects of anti-inflammatory drugs and preservatives on morphologic characteristics and migration of canine corneal epithelial cells in tissue culture. *Vet Ophthalmol* 2002; 5: 127–135.
210. Bourcier T, Borderie V, Forgez P, Lombet A, Rostène W, Laroche L. In vitro effects of dexamethasone on human corneal keratocytes. *Invest Ophthalmol Vis Sci* 1999; 40: 1061–1070.
211. Wyman M. Contemporary ocular therapeutics. In: Kirk RW, ed. *Current Veterinary Therapy IX: Small Animal Practice.* Philadelphia: WB Saunders, 1986: 684–696.
212. Cohn LA. The influence of corticosteroids on host defense mechanisms. *J Vet Intern Med* 1991; 5: 95–104.
213. Dannenberg AM. The anti-inflammatory effects of glucocorticoids. *Inflammation* 1979; 3: 329–343.
214. Leibowitz HM, Kupferman A. Topically administered corticosteroids: Effect on antibiotic treated bacterial keratitis. *Arch Ophthalmol* 1980; 98: 1287–1290.
215. Nasisse MP. Anti-inflammatory therapy in herpesvirus keratoconjunctivitis. *Prog Vet Comp Ophthalmol* 1991; 1: 63–65.
216. O'Day DM, Ray WA, Robinson R, Head WS. Efficacy of antifungal agents in the cornea: II. Influence of corticosteroids. *Invest Ophthalmol and Vis Sci* 1984; 25: 331–335.
217. O'Day DM, Ray WA, Head S, Robinson RD, Williams TE. Influence of corticosteroid on experimentally induced keratomycosis. *Arch Ophthalmol* 1991; 109: 1601–1604.
218. Hendrix DVH, Brooks DE, Smith PJ, et al. Corneal stromal abscesses in the horse: A review of 24 cases. *Eq Vet J* 1995; 27: 440–447.
219. Gaarder JE, Rebhun WC, Ball MA, Patten V, Shing S, Herb H. Clinical appearances, healing patterns, risk factors, and outcomes of horses with fungal keratitis: 53 cases (1978–1996). *J Am Vet Med Assoc* 1998; 213: 105–112.
220. Gemensky-Metzler AJ, Wilkie DA, Kowalski JJ, Schmall LM, Willis AM, Yamagata M. Changes in bacterial and fungal ocular flora of clinically normal horses following experimental application of topical antimicrobial or antimicrobial-corticosteroid ophthalmic preparations. *Am J Vet Res* 2005; 66: 800–811.
221. Taravella MJ, Stulting RD, Mader TH, Weisenthal RW, Forstot SL, Underwood LD. Calcific band keratopathy associated with the use of topical steroid-phosphate preparations. *Arch Ophthalmol* 1994; 112: 608–613.
222. Johnson D, Gottanka J, Flügel C, Hoffmann F, Futa R, Lütjen-Drecoll E. Ultrastructural changes in the trabecular meshwork of human eyes treated with corticosteroids. *Arch Ophthalmol* 1997; 115: 375–383.
223. Dickerson JE, Steely HT, English-Wright SL, Clark AF. The effect of dexamethasone on integrin and laminin expression in cultured human trabecular meshwork cells. *Exp Eye Res* 1998; 66: 731–738.
224. Clark AF, Steely HT, Dickerson JE, et al. Glucocorticoid induction of the glaucoma gene *MYOC* in human and monkey trabecular meshwork cells and tissues. *Invest Ophthalmol Vis Sci* 2001; 42: 1769–1780.
225. Wordinger RJ, Clark AF. Effects of glucocorticoids on the trabecular meshwork: Towards a better understanding of glaucoma. *Prog Retinal Eye Res* 1999; 18: 629–667.
226. Gelatt KN, Mackay EO. The ocular hypertensive effects of topical 0.1% dexamethasone in beagles with inherited glaucoma. *J Ocular Pharm Therapeut* 1998; 14: 57–66.
227. Zhan G-L, Miranda OC, Bito LZ. Steroid glaucoma: Corticosteroid-induced ocular hypertension in cats. *Exp Eye Res* 1992; 54: 211–218.
228. Bhattacherjee P, Paterson CA, Spellman JM, Graff G, Yanni JM. Pharmacological validation of a feline model of steroid-induced ocular hypertension. *Arch Ophthalmol* 1999; 117: 361–364.
229. Gerometta R, Podos SM, Candia OA, et al. Steroid-induced ocular hypertension in normal cattle. *Arch Ophthalmol* 2004; 122: 1492–1497.
230. Jobling AI, Augusteyn RC. What causes steroid cataracts? A review of steroid-induced posterior subcapsular cataracts. *Clin Exp Optometry* 2002; 2: 61–75.
231. Carnahan MC, Goldstein DA. Ocular complications of topical, peri-ocular, and systemic corticosteroids. *Curr Opin Ophthalmol* 2000; 11: 478–483.
232. Bouzas EA, Karadimas P, Pournaras CJ. Central serous chorioretinopathy. *Surv Ophthalmol* 2002; 47: 431–448.
233. Herring IP, Herring ES, Ward DL. Effect of orally administered hydrocortisone on intraocular pressure in nonglaucomatous dogs. *Vet Ophthalmol* 2004; 7: 381–384.
234. Townsend WM, Renninger M, Stiles J, Townsend JR, Krohne SG. Dexamethasone-induced exophthalmos in a group of Holstein calves. *Vet Ophthalmol* 2003; 6: 265–268.
235. Regnier A, Toutain PL, Alvinerie M, Periquet B, Ruckebusch Y. Adrenocortical function and plasma biochemical values in dogs after subconjunctival treatment with methylprednisolone acetate. *Res Vet Sci* 1982; 32: 306–310.
236. Roberts SM, Lavach JD, Macy DW, Severin GA. Effect of ophthalmic prednisolone acetate on the canine adrenal gland and hepatic function. *Am J Vet Res* 1984; 45: 1711–1714.
237. Eichenbaum JD, Macy DW, Severin GA, Paulsen ME. Effect in large dogs of ophthalmic prednisolone acetate on adrenal gland and hepatic function. *J Am Anim Hosp Assoc* 1988; 24: 705–709.
238. Glaze MB, Crawford MA, Nachreiner RF, Casey HW, Nafe LA, Kearney MT. Ophthalmic corticosteroid therapy: Systemic effects in the dog. *J Am Vet Med Assoc* 1988; 192; 73–75.
239. Murphy CJ, Feldman E, Bellhorn R. Iatrogenic Cushing's syndrome in a dog caused by topical ophthalmic medications. *J Am Anim Hosp Assoc* 1990; 26: 640–642.
240. Spiess BM, Nyikos S, Stummer E, Sahin A, Naegeli H. Systemic dexamethasone concentration in horses after continued topical treatment with an ophthalmic preparation of dexamethasone. *Am J Vet Res* 1999; 60: 571–576.
241. Graham BP, Powell CC, Gionfriddo JR, et al. Evaluation of neomycin, polymyxin B, dexamethasone ophthalmic ointment as a cause of abortion in llamas (abstract). 33rd Annual Conference of the American College of Veterinary Ophthalmologists, 2002: 67.
242. Kulkarni PS. Steroids in ocular therapy. In: Zimmerman TJ, Kooner KS, Sharir M, Fechtner RD, eds. *Textbook of Ocular Pharmacology.* Philadelphia: Lippincott-Raven Publishers, 1997: 61–74.
243. Whitcup SM, Ferris III FL. New corticosteroids for the treatment of ocular inflammation. *Am J Ophthalmol* 1999; 127: 597–599.
244. Stewart RS, Horwitz B, Howes J, Novack GD, Hart K, Loteprednol Etabonate Postoperative Inflammation Study Group 1. Double-masked, placebo-controlled evaluation of loteprednol etabonate 0.5% for postoperative inflammation. *J Cataract Refract Surg* 1998; 24: 1480–1489.

245. Novack GD, Howes J, Crockett RS, Sherwood MB. Change in intraocular pressure during long-term use of loteprednol etabonate. *J Glaucoma* 1998; 7: 266–269.
246. Vane JR, Botting RM. Overview: Mechanisms of action of anti-inflammatory drugs. In: Vane J, Botting J, Botting R, eds. *Improved Non-steroid Anti-inflammatory Drugs: Cox-2 Enzyme Inhibitors.* Dordrecht: Kluwer Academic Publishers, 1995: 1–27.
247. Mamdani M, Juurlink DN, Lee DS, et al. Cyclo-oxygenase-2 inhibitors versus non-selective non-steroidal anti-inflammatory drugs and congestive heart failure outcomes in elderly patients: A population-based cohort study. *Lancet* 2004; 363: 1751–1756.
248. Millichamp NJ, Dziezyc J. Mediators of ocular inflammation. *Prog Vet Comp Ophthalmol* 1991; 1: 41–58.
249. Bhattacherjee P. Prostaglandins and inflammatory reactions in the eye. *Method Find Exp Clin* 1980; 2: 17–31.
250. Smith WL, DeWitt DL, Shimokawa T, Kraemer SA, Meade EA. Molecular basis for the inhibition of prostanoid biosynthesis by nonsteroidal anti-inflammatory agents. *Stroke* 1990; 21: (suppl IV)24–28.
251. Livingston A. Mechanism of action nonsteroidal anti-inflammatory drugs. *Vet Clin N Am Sm Anim Pract* 2000; 30: 773–781.
252. Frolich JC. A classification of NSAIDs according to the relative inhibition of cyclooxygenase isoenzymes. *Trends Pharmacol Sci* 1997; 18: 30–34.
253. Ricketts AP, Lundy KM, Seibel SB. Evaluation of selective inhibition of canine cyclooxygenase 1 and 2 by carprofen and other nonsteroidal anti-inflammatory drugs. *Am J Vet Res* 1998; 59: 1441–1446.
254. Kay-Mugford P, Benn SJ, LaMarre J, Conlon P. In vitro effects of nonsteroidal anti-inflammatory drugs on cyclooxygenase activity in dogs. *Am J Vet Res* 2000; 61: 802–810.
255. Giuliano EA. Nonsteroidal anti-inflammatory drugs in veterinary ophthalmology. *Vet Clin N Am Sm Anim Pract* 2004; 34: 707–723.
256. Palmero M, Bellot JL, Alcoriza N, Garcia-Cabanes C, Orts A. The ocular pharmacokinetics of topical diclofenac is affected by ocular inflammation. *Ophthalmic Res* 1999; 31: 309–316.
257. Tang-Liu DD-S, Liu SS, Weinkam RJ. Ocular and systemic bioavailability of ophthalmic flurbiprofen. *J Pharmacokinet Biop* 1984; 12: 611–626.
258. Ellis PP, Pfoff DS, Bloedow DC, Riegel M. Intraocular diclofenac and flurbiprofen concentrations in human aqueous humor following topical application. *J Ocular Pharmacol* 1994; 10: 677–682.
259. Dziezyc J, Millichamp NJ, Smith WB. Effect of flurbiprofen and corticosteroids on the ocular irritative response in dogs. *Vet Comp Ophthalmol* 1995; 5: 42–45.
260. Millichamp NJ, Dziezyc JD. Comparison of flunixin meglumine and flurbiprofen for control of ocular irritative response in dogs. *Am J Vet Res* 1991; 52: 1452–1455.
261. Ward DA. Comparative efficacy of topically applied flurbiprofen, diclofenac, tolmetin, and suprofen for the treatment of experimentally induced blood–aqueous barrier disruption in dogs. *Am J Vet Res* 1996; 57: 875–878.
262. Sanders DR, Goldstick B, Kraff C, Hutchins R, Bernstein MS, Evans MA. Aqueous penetration of oral and topical indomethacin in humans. *Arch Ophthalmol* 1983; 101: 1614–1616.
263. Spiess BM, Mathis GA, Franson KL, Leber A. Kinetics of uptake and effects of topical indomethacin application on protein concentration in the aqueous humor of dogs. *Am J Vet Res* 1991; 52: 1159–1163.
264. Regnier AM, Dossin O, Cutzach EE, Gelatt KN. Comparative effects of two formulations of indomethacin eyedrops on the paracentesis-induced inflammatory response in the canine eye. *Vet Comp Ophthalmol* 1995; 5: 242–246.
265. Flach AJ, Kraff MC, Sander DR, Tanenbaum L. The quantitative effect of 0.5% ketorolac tromethamine solution and 0.1% dexamethasone sodium phosphate solution on postsurgical blood–aqueous barrier. *Arch Ophthalmol* 1988; 106: 480–483.
266. Cooley PL, Milvae R, Riis RC, Laratta LJ. Effect of flunixin meglumine on prostacyclin accumulation in the equine eye. *Am J Vet Res* 1984; 45: 1383–1385.
267. Krohne SG, Vestre WA. Ophthalmic usage on nonsteroidal anti-inflammatory agents. In: Kirk RW, ed. *Current Veterinary Therapy X: Small Animal Practice.* Philadelphia: WB Saunders, 1989: 642–644.
268. Brightman AH, Helper LC, Hoffman WE. Effect of aspirin on aqueous protein values in the dog. *J Am Vet Med Assoc* 1981; 178: 572–573.
269. Ward DA, Ferguson DC, Ward SL, Green K, Kaswan RL. Comparison of the blood–aqueous barrier stabilizing effects of steroidal and nonsteroidal anti-inflammatory agents in the dog. *Prog Vet Comp Ophthalmol* 1992; 2: 117–124.
270. Krohne SG, Blair MJ, Bingaman D, Gionfriddo JR. Carprofen inhibition of flare in the dog measured by laser flare photometry. *Vet Ophthalmol* 1998; 1: 81–84.
271. Regnier A, Bonnefoi M, Lescure F. Effect of lysine-acetylsalicylate and phenylbutazone premedication on the protein content of secondary aqueous humour in the dog. *Res Vet Sci* 1984; 37: 26–29.
272. Regnier A, Whitley RD, Benard P, Bonnefoi M. Effect of flunixin meglumine on the breakdown of the blood–aqueous barrier following paracentesis in the canine eye. *J Ocular Pharmacol* 1986; 2: 165–170.
273. Krohne SDG, Vestre WA. Effect of flunixin meglumine and dexamethasone on aqueous protein values after intraocular surgery in the dog. *Am J Vet Res* 1987; 48: 420–422.
274. Roze M, Thomas E, Davot JL. Tolfenamic acid in the control of ocular inflammation in the dog: Pharmacokinetics and clinical results obtained in an experimental model. *J Sm Anim Pract* 1996; 37: 371–375.
275. Millichamp NJ, Dziiezyc J, Rohde BH, Chiou GCY, Smith WB. Acute effects of anti-inflammatory drugs on neodymium: Vttrium aluminum garnet laser-induced uveitis in dogs. *Am J Vet Res* 1991; 52: 1279–1284.
276. Dziezyc J, Millichamp NJ, Keller CB, Smith WB. Effects of prostaglandin F2α and leukotriene on pupil size intraocular pressure, and blood–aqueous barrier in dogs. *Am J Vet Res* 1992; 53: 1302–1304.
277. Sanders DR, Kraff M. Steroidal and nonsteroidal anti-inflammatory agents. Effect on postsurgical inflammation and blood–aqueous humor barrier breakdown. *Arch Ophthalmol* 1984; 102: 1453–1456.
278. Nasisse MP, Davidson MG, Jamieson VE, English RV, Olivero DK. Pharmacoemulsification and intraocular lens implantation: A study of technique in 182 dogs. *Prog Vet Comp Ophthalmol* 1991; 1: 225–232.
279. Millichamp NJ, Dziezyc J, Olsen JW. Effect of flurbiprofen on facility of aqueous outflow in the eyes of dogs. *Am J Vet Res* 1991; 52: 1448–1451.

280. Waterbury L, Kunysz EA, Beuerman R. Effects of steroidal and non-steroidal anti-inflammatory agents on corneal wound healing. *J Ocular Pharmacol* 1987; 3: 43–54.
281. Lee BP, Kupperman A, Leibowitz HM. Effect of suprofen on corneal wound healing. *Arch Ophthalmol* 1985; 103: 95–97.
282. Miller D, Gruenberg P, Miller R, Bergamini MVW. Topical flurbiprofen or prednisolone effect on corneal wound healing in rabbits. *Arch Ophthalmol* 1981; 99: 681–682.
283. Lin JC, Rapuano CJ, Laibson PR, Eagle RC, Cohen EJ. Corneal melting associated with use of topical nonsteroidal anti-inflammatory alter ocular surgery. *Arch Ophthalmol* 2000; 118: 1129–1132.
284. Guidera AC, Luchs JI, Udell IJ. Keratitis, ulceration, and perforation associated with topical nonsteroidal anti-inflammatory drugs. *Ophthalmol* 2001; 108: 936–944.
285. O'Brien TP, Li Qj, Sauerburger F, Reviglio VE, Rana T, Ashraf MF. The role of matrix metalloproteinases in ulcerative keratolysis associated with perioperative diclofenac use. *Ophthalmol* 2001; 108: 656–659.
286. Lobetti RG, Joubert KN. Effect of administration of nonsteroidal anti-inflammatory drugs before surgery on renal function in clinically normal dogs. *Am J Vet Res* 2000; 61: 1501–1506.
287. Cooper CA, Bergamini MVW, Leopold IH. Use of flurbiprofen to inhibit corneal neovascularization. *Arch Ophthalmol* 1980; 98: 1102–1105.
288. Alio JL, Ayala MJ, Mulet ME, Artola A, Ruiz JM. Topical treatment of experimental acute corneal inflammation by dexamethasone and nonsteroidal drugs. *Ophthalmic Res* 1994; 26: 87–94.
289. Opremcak EM. Nonsteroidal antiinflammatory drugs. In: Mauger TF, Craig EL, eds. *Havener's Ocular Pharmacology,* 6th ed. St Louis: Mosby, 1994: 351–364.
290. Trousdale MD, Dunkel EC, Nesburn AB. Effect of flurbiprofen on herpes simplex keratitis in rabbits. *Invest Ophthalmol Vis Sci* 1980; 19: 267.
291. Fraser-Smith EB, Matthews TR. Effect of ketoralac on herpes simplex virus type on ocular infection in rabbits. *J Ocular Pharmacol* 1988; 4: 321–326.
292. Lavach JD, Roberts SM, Severin GA. Current concepts in equine ocular therapeutics. *Vet Clin N Am Large Anim Pract* 1984; 6: 435–449.
293. Rao NA, Patchett R, Fernandez MA, Sevanian A, Kunkel SL, Marak GE. Treatment of experimental granulomatous uveitis by lipoxygenase and cyclo-oxygenase inhibitors. *Arch Ophthalmol* 1987; 105: 413–415.
294. Chiou GCY, Yao QS, Varma RS. Inhibition of ocular inflammation by chalcone derivatives and prednisolone. *J Ocular Pharmacol* 1992; 8: 213–223.
295. Chiou GCY, Yao QS, Chang MS, Okawara T. Prevention and treatment of ocular inflammation with a new class of nonsteroidal anti-inflammatory agents. *J Ocular Pharmacol* 1994; 10: 335–347.
296. Dziezyc J, Millichamp NJ, Rohde BH, Smith WB. Comparison of prednisone and RMI-1068 in the ocular irritative response in dogs. *Invest Ophthalmol Vis Sci* 1992; 33: 460–465.
297. Gilmour MA, Kennard G. Effects of oral meloxicam, deracoxib, tepoxalin and carprofen in reducing intraocular inflammation in the dog (abstract). 35th Annual Conference of the American College of Veterinary Ophthalmologists, 2004: 62.
298. Moore CP. Immunomodulating agents. *Vet Clin N Am Sm Anim Pract* 2004; 34: 725–737.
299. Grahn BH, Storey ES. Lacrimostimulants and lacrimomimetics. *Vet Clin N Am Sm Anim Pract* 2004; 34: 739–753.
300. Andronopoulos AP, Moutsopoulos HM. Immune consequences of glucocorticoid therapy. In: Lüdecke DK, Chrousos GP, Tolis G, eds. *ACTH, Cushing's Syndrome and Other Hypercortisolemic States.* New York: Ravens Press, 1990: 177–181.
301. Guyre PM, Girard MT, Morganelli PM, Manganiello PD. Glucocorticoid effects on the production and actions of immune cytokines. *J Ster Biochem* 1988; 30: 89–93.
302. Marx J. How the glucocorticoids suppress immunity. *Science* 1995; 270: 232–233.
303. Wilckens T. Glucocorticoids and immune function: Physiological relevance and pathogenic potential of hormonal dysfunction. *Trends Pharm Sci* 1995; 16: 193–197.
304. Bistner S. Allergic and immunologic: Mediated diseases of the eye and adnexae. *Vet Clin N Am Sm Anim Pract* 1994; 24: 711–734.
305. Baumann GG. Molecular mechanism of immunosuppressive agents. *Transplant Proceed* 1992; 24: 4–7.
306. Schreiber SL. Chemistry and biology of the immunophilins and their immunosuppressive ligands. *Science* 1991; 251: 283–287.
307. Mochizuki M, De Smet M. Use of immunosuppressive agents in ocular diseases. *Prog Retinal Eye Res* 1994; 13: 479–506.
308. Siekierka JJ, Sigal NH. FK-506 and cyclosporin A: Immunosuppressive mechanism of action and beyond. *Curr Opin Immunol* 1992; 4: 548–552.
309. Dumont FJ, Su Q. Mechanism of action of the immunosuppressant rapamycin. *Life Sciences* 1996; 58: 373–395.
310. Stellato C, De Paulis A, Ciccarelli A, et al. Anti-inflammatory effect of cyclosporin A on human skin mast cells. *J Invest Dermatol* 1992; 98: 800–804.
311. Wershil BK, Furuta GT, Lavigne JA, Choudhury AR, Wang ZS, Galli SJ. Dexamethasone or cyclosporin: A suppress mast cell-leukocyte cytokine cascades. *J Immunol* 1995; 154: 1391–1398.
312. Whitcup SM, Chan CC, Luyo DA, Bo P, Li Q. Topical cyclosporine inhibits mast cell-mediated conjunctivitis. *Invest Ophthalmol Vis Sci* 1996; 37: 2686–2693.
313. Munro CS, Higgins EM, Marks JM, Daly BM, Friedmann PS, Shuster S. Cyclosporin A in atopic dermatitis: Therapeutic response is dissociated from effects on allergic reactions. *Br J Dermatol* 1991; 124: 43–48.
314. Abu El-Asrar AM, Tabbara KF, Geboes K, Missoten L, Desmet V. An immunohistochemical study of topical cyclosporine in vernal keratoconjunctivitis. *Am J Ophthalmol* 1996; 121: 156–161.
315. Kaswan RL, Salisbury MA, Ward DA. Spontaneous canine keratoconjunctivitis sicca, a useful model for human keratoconjunctivitis sicca: Treatment with cyclosporine eye drops. *Arch Ophthalmol* 1989; 107: 1210–1216.
316. Stonecipher K, Perry HD, Gross RH, Kerney DL. The impact of topical cyclosporine A emulsion 0.05% on the outcomes of patients with keratoconjunctivitis sicca. *Curr Med Res Opin* 2005; 21: 1057–1063.
317. Bellot JL, Alio JL, Ruiz Moreno JM, Artola A. Corneal concentration and systemic absorption of cyclosporin-A following its topical application in the rabbit eye. *Ophthalmic Res* 1992; 24: 351–356.
318. Kaswan RL. Intraocular penetration of topically applied cyclosporine. *Transp Proceed* 1988; 209: 650–655.

319. Diaz-Llopis M, Menezo JL. Penetration of 2% cyclosporine eyedrops into human aqueous humour. *Br J Ophthalmol* 1989; 73: 600–603.
320. Gilger BC, Andrews J, Wilkie DA, Lairmore MD. Lymphocyte proliferation and blood drug levels in dogs with keratoconjunctivitis sicca receiving long-term topical ocular cyclosporine. *Vet Comp Ophthalmol* 1996; 6: 125–130.
321. Gilger BC, Andrews J, Wilkie DA, Wyman M, Lairmore MD. Cellular immunity in dogs with keratoconjunctivitis sicca before and after treatment with topical 2% cyclosporine. *Vet Immunol Immunopathol* 1995; 49: 199–208.
322. Salisbury MA, Kaswan RL, Ward DA, Martin CL, Ramsey JM, Fischer CA. Topical application of cyclosporine in the management of keratoconjunctivitis sicca in dogs. *J Am Anim Hosp Assoc* 1990; 26: 269–279.
323. Olivero DK, Davidson MG, English RV, Nasisse MP, Janieson VE, Gerig TM. Clinical evaluation of 1% cyclosporine for topical treatment of keratoconjunctivitis sicca in dogs. *J Am Vet Med Assoc* 1991; 199: 1039–1042.
324. Morgan RV, Abrams KL. Topical administration of cyclosporine for treatment of keratoconjunctivitis sicca in dogs. *J Am Vet Med Assoc* 1991; 199: 1043–1046.
325. Kaswan RL, Salisbury MA. A new perspective on canine keratoconjunctivitis sicca: Treatment with ophthalmic cyclosporine. *Vet Clin N Am Sm Anim Pract* 1990; 20: 583–613.
326. Bounous DI, Carmichael KP, Kaswan RL, Hirsh S, Stiles J. Effects of ophthalmic cyclosporine on lacrimal gland pathology and function in dogs with keratoconjunctivitis sicca. *Vet Comp Ophthalmol* 1995; 5: 5–12.
327. Lipman RM, Epstein RJ, Hendricks RL. Suppression of corneal neovascularization with cyclosporine. *Arch Ophthalmol* 1992; 110: 405–407.
328. Benelli U, Ross JR, Nardi M, Klintworth GK. Corneal neovascularisation induced by xenografts or chemical cautery: Inhibition by cyclosporin A. *Invest Ophthalmol Vis Sci* 1997; 38: 274–282.
329. Christmas R. Cyclosporine ophthalmic ointment in dogs with keratoconjunctivitis sicca. *Canine Pract* 1995; 20: 6–9.
330. Sansom J, Barnett KC, Neumann W, et al. Treatment of keratoconjunctivitis sicca in dogs with cyclosporine ophthalmic ointment: European clinical field trial. *Vet Rec* 1995; 137: 504–507.
331. Jackson PA, Kaswan RL, Merideth RE, Barrett PM. Chronic superficial keratitis in dogs: A placebo controlled trial of topical cyclosporine treatment. *Prog Vet Comp Ophthalmol* 1991; 1: 269–275.
332. Williams DL, Hoey AJ, Smitherman P. Comparison of topical cyclosporin and dexamethasone for the treatment of chronic superficial keratitis in dogs. *Vet Rec* 1995; 137: 635–639.
333. Read RA. Treatment of canine nictitans plasmacytic conjunctivitis with 0.2% percent cyclosporin ointment. *J Sm Anim Pract* 1995; 36: 50–56.
334. Read RA, Barnett KC, Sansom J. Cyclosporin-responsive keratoconjunctivitis in the cat and horse. *Vet Rec* 1995; 137: 170–171.
335. Gratzek AT, Kaswan RL, Martin CL, Champagne ES, White SL. Ophthalmic cyclosporine in equine keratitis and keratouveitis: 11 cases. *Eq Vet J* 1995; 25: 327–333.
336. Dwyer A, Gilger BC. Equine recurrent uveitis. In: Gilger BC, ed. *Equine Ophthalmology.* St. Louis: Elsevier Saunders, 2005: 285–322.
337. Gilger BC, Wilkie DA, Davidson MG, Allen JB. Use of an intravitreal sustained-release cyclosporine delivery device for treatment of equine recurrent uveitis. *Am J Vet Res* 2001; 62: 1892–1896.
338. Gilger BC, Malok E, Stewart T, Ashton P, Smith T, Jaffe GJ, Allen JB. Long-term effect on the equine eye of an intravitreal device used for sustained release of cyclosporine A. *Vet Ophthalmol* 2000; 3: 105–110.
339. Beale AB, Salmon J, Robinson MR, Gilger BC. Ocular toxicity of subconjunctival sustained release cyclosporine delivery devices in dogs (abstract). 35th Annual Conference of the American College of Veterinary Ophthalmologists, 2004: 12.
340. Adkins EA, Hendrix DVH, Stuffle JL, Ward DA, Skorobohach BJ. An investigation of the safety and efficacy of topical ophthalmic application of tacrolimus in dogs (abstract). 34th Annual Meeting of the American College of Veterinary Ophthalmologists, 2003: 42.
341. Berdoulay A, English RV, Nadelstein B. Effect of topical 0.02% tacrolimus aqueous suspension on tear production in dogs with keratoconjunctivitis sicca. *Vet Ophthalmol* 2005; 8: 225–232.
342. Nell B, Walde I, Billich P, Vit P, Meingassner JG. The effect of topical pimecrolimus on keratoconjunctivitis sicca and chronic superficial keratitis in dogs: Results from an exploratory study. *Vet Ophthalmol* 2005; 8: 39–46.
343. Ishioka M, Ohno S, Nakamura S, et al. FK506 treatment of noninfectious uveitis. *Am J Ophthalmol* 1994; 118: 723–729.
344. Shanmuganathan VA, Casely EM, Raj D, et al. The efficacy of sirolimus in the treatment of patients with refractory uveitis. *Br J Ophthalmol* 2005; 89: 666–669.
345. Olsen TW, Benegas NM, Joplin AC, Evangelista T, Mindrup EA, Holland EJ. Rapamycin inhibits corneal allograft rejection and neovascularization. *Arch Ophthalmol* 1994; 112: 1471–1475.
346. Kwon YS, Hong HS, Kim JC, Shin JS, Son Y. Inhibitory effect of rapamycin on corneal neovascularization in vitro and in vivo. *Invest Ophthalmol Vis Sci* 2005; 46: 454–460.
347. Mochizuki M, De Smet M. Use of immunosuppressive agents in ocular diseases. *Prog Retin Eye Res* 1994; 13: 479–506.
348. Hemady R, Tauber J, Foster CJ. Immunosuppressive drugs in immune and inflammatory ocular disease. *Surv Ophthalmol* 1991; 35: 369–385.
349. Shah SS, Lowder CY, Schmitt MA, Wilke WS, Komorsky GS, Meisler DM. Low-dose methotrexate therapy for ocular inflammatory disease. *Ophthalmol* 1992; 99: 1419–1423.
350. Bussanich MN, Rootman J, Kumi C, Gudauskas G. Ocular absorption and toxicity of methotrexate in the dog. *Canad Vet J* 1985; 26: 263–266.
351. Schadler HJ. Azathioprine in treatment for ocular nodular espiscleritis. *Vet Med* 1985; 80: 64–67.
352. Paulsen ME, Lavach JD, Snyder SP, Severin GA, Eichenbaum JD. Nodular granulomatous episclerokeratitis in dogs: 19 cases (1973–1985). *J Am Vet Med Assoc* 1987; 190: 1581–1587.
353. Gilger BC, Rose PD, Davidson MG, Roberts SM, Miller T. Low-dose oral administration of interferon-alpha for the treatment of immune-mediated keratoconjunctivitis sicca in dogs. *J Interferon Cytokine Res* 1999; 19: 901–905.
354. Riis RC. Interferon treatment of idiopathic ocular granulomatous disease of collies (abstract). 31st Annual Meeting of the American College of Veterinary Ophthalmologists, 2000: 1.
355. Romatowski J. Use of megestrol acetate in cats. *J Am Vet Medical Assoc* 1989; 194: 700–702.
356. Abbot RN. Ocular allergies in dogs. *Vet Med Sm Anim Clin* 1975; 70: 1085–1089.

357. Glaze MB. Ocular allergy. Seminars in Veterinary Medicine and Surgery Small Animal 1991; 6: 296–302.
358. Trocme SD, Raizman MB, Bartley GB. Medical therapy for ocular allergy. *Mayo Clin Proceed* 1992; 67: 557–565.
359. Bielory L. Ocular allergy guidelines: A practical treatment algorithm. *Drugs* 2002; 62: 1611–1634.
360. Brooks DE. Equine stromal and endothelial keratopathies: Medical management of stromal abscesses, eosinophilic keratitis, calcific band keratopathy striate band opacities, and endothelitis in the horse. *Clin Techn Eq Pract* 2005; 4: 21–28.
361. Caldwell DR, Verin P, Hartwich-Young R, Meyer SM, Drake MM. Efficacy and safety of lodoxamide 0.1% vs cromolyn sodium 4% in patients with vernal keratoconjunctivitis. *Am J Ophthalmol* 1992; 113: 632–637.
362. Leonardi A, Busato F, Fregona I, Plebani M, Secchi A. Anti-inflammatory and antiallergic effects of ketorolac tromethamine in the conjunctival provocation model. *Br J Ophthalmol* 2000; 84: 1228–1232.
363. Willis AM, Diehl KA, Robbin TE. Advances in topical glaucoma therapy. *Vet Ophthalmol* 2002; 5: 9–17.
364. Willis AM. Ocular hypotensive drugs. *Vet Clin N Am Sm Anim Pract* 2004; 34: 755–776.
365. Kaufman PL, Gabelt BT. Direct, indirect, and dual-action parasympathetic drugs. In: Zimmerman TJ, Kooner KS, Sharir M, Fechtner RD, eds. *Textbook of Ocular Pharmacology.* Philadelphia: Lippincott-Raven, 1997: 221–238.
366. Gwin RM, Gelatt KN, Chiou CY. Adrenergic and cholinergic innervation of the anterior segment of the normal and glaucomatous dog. *Invest Ophthalmol Vis Sci* 1979; 18: 674–682.
367. Chiou CY, Trzeciakowski J, Gelatt KN. Reduction of intraocular pressure in glaucomatous dogs by a new cholinergic drug. *Invest Ophthalmol Vis Sci* 1980; 19: 1198–1203.
368. Gum GG, Metzger KJ, Gelatt KJ, Gilley RL, Gelatt JK. Tonographic effects of pilocarpine and pilocarpine-epinephrine in dogs. *J Sm Anim Pract* 1993; 34: 112–116.
369. Gwin RM, Gelatt KN, Gum GG, Peiffer RL, Williams LW. The effect of topical pilocarpine on intraocular pressure and pupil size in the normotensive and glaucomatous beagle. *Invest Ophthalmol Vis Sci* 1977; 16: 1143–1148.
370. Whitley RD, Gelatt KN, Gumm GG. Dose response of topical pilocarpine in the normotensive and glaucomatous beagle. *Am J Vet Res* 1980; 41: 417–424.
371. Gelatt KN, Gum GG, Brooks DE, Wolf DW, Bromberg NM. Dose response of topical pilocarpine-epinephrine combinations in normotensive and glaucomatous beagles. *Am J Vet Res* 1983; 44: 2018–2027.
372. Gelatt KN, Gum GG, Wolf ED, White NM. Dose response of topical carbamylcholine chloride (carbachol) in normotensive and early glaucomatous beagles. *Am J Vet Res* 1984; 45: 547–554.
373. Stuhr CM, Miller PE, Murphy CJ, Schoster JV, Thomas CB. Effect of intracameral administration of carbachol on the postoperative increase in intraocular pressure in dogs undergoing cataract extraction. *J Am Vet Med Assoc* 1998; 212: 1885–1888.
374. Shihab ZM. Antiglaucoma therapy. In: Lamberts DW, Potter DE, eds. *Clinical Ophthalmic Pharmacology,* 1st ed. Boston: Little Brown, 1987: 193–256.
375. Gum GG, Gelatt KN, Gelatt JK, Jones J. Effect of topically applied demecarium bromide and echothiophate iodide on intraocular pressure and pupil size in beagles with normotensive eyes and beagles with inherited glaucoma. *Am J Vet Res* 1993; 54: 287–293.
376. Ellis FD. Antoglaucoma medications. In: Zimmerman TJ, Kooner KS, Sharir M, Fechtner RD, eds. *Textbook of Ocular Pharmacology.* Philadelphia: Lippincott-Raven, 1997: 795–799.
377. Gaarder J. Canine glaucoma. In: Bonagura JD, ed. *Kirk's Current Veterinary Therapy XIII; Small Animal Practice.* Philadelphia: WB Saunders, 2000: 1075–1081.
378. Carrier M, Gum GG. Effects of 4% pilocarpine gel on normotensive and glaucomatous canine eyes. *Am J Vet Res* 1989; 50: 239–244.
379. Miller PE, Schmidt GM, Vainisi SJ, Swanson JF, Herrmann MK. The efficacy of topical prophylactic antiglaucoma therapy in primary closed angle glaucoma in dogs: A multicenter clinical trial. *J Am Anim Hosp Assoc* 2000; 36: 431–438.
380. Martin CL, Wyman M. Primary glaucoma in the dog. *Vet Clin N Am Sm Anim Pract* 1978; 8: 257–286
381. Gelatt KN, Mackay EO, Gelatt JK, Stengard-Ollies K, Aza J. Effects on intraocular pressure and pupil size in glaucomatous beagles after topical pilocarpine instilled with standard (pH 5) and buffer-tip (pH 7) droptainer. *J Ocular Pharmacol Therapeut* 1997; 13: 95–104.
382. Krohne SG. Effect of topically applied 2% pilocarpine and 0.25% demecarium bromide on blood–aqueous barrier permeability in dogs. *Am J Vet Res* 1994; 55: 1729–1733.
383. Wei C, Anderson JA, Leopold I. Ocular absorption and metabolism of topically applied epinephrine and a dipivalyl ester of epinephrine. *Invest Ophthalmol Vis Sci* 1978; 17: 315–321.
384. Nakamura M, Shirasawa E, Hikida M. Characterization of esterases involved in the hydrolysis of dipivefrin hydrochloride. *Ophthal Res* 1993; 25: 46–51.
385. Alm A. The effect of topical 1-epinephrine on regional ocular blood flow in monkeys. *Invest Ophthalmol Vis Sci* 1980; 19: 487–491.
386. Michelson G, Groh MJM. Dipivefrin reduces blood flow in the ciliary body in humans. *Ophthalmol* 1994; 101: 659–664.
387. Neufeld AH. The mechanisms of action of adrenergic drugs in the eye. In: Drance SM, ed. *Glaucoma: Applied Pharmacology in a Medical Treatment.* Orlando: Grune & Stratton. 1984: 277–301.
388. Erickson-Lamy KA, Nathanson JA. Epinephrine increases facility of outflow and cyclic AMP content in the human eye in vitro. *Invest Ophthalmol Vis Sci* 1992; 33: 2672–2678.
389. Erickson K, Liang LL, Shum P, Nathanson JA. Adrenergic regulation of aqueous outflow. *J Ocular Pharmacol* 1994; 10: 241–252.
390. Gwin RM, Gelatt KN, Gum GG, Peiffer RL. Effects of topical 1-epinephrine and dipivalyl epinephrine on intraocular pressure and pupil size in the normotensive and glaucomatous beagle. *Am J Vet Res* 1978; 39: 83–86.
391. Fang EN, Kass MA. Epinephrine and dipivefrin. In: Zimmerman TJ, Kooner KS, Sharir M, Fechtner RD, eds. *Textbook of Ocular Pharmacology.* Philadelphia: Lippincott-Raven, 1997: 239–246.
392. Abramovsky J, Mindel JS. Dipivefrin and echothiophate: Contraindications to combined use. *Arch Ophthalmol* 1979; 97: 1937–1940.
393. Lee DA, Topper JE, Brubaker RF. Effect of clonidine on aqueous humor flow in normal human eyes. *Exp Eye Res* 1984; 38: 239–246.
394. Toris CB, Tafoya ME, Camras CB, Yablonski ME. Effects of apraclonidine on aqueous humor dynamics in human eyes. *Ophthalmol* 1995; 102: 456–461.

395. Ogidigben M, Chu TC, Potter D. Alpha-2 adrenoceptor mediated changes in aqueous dynamics: Effect of pertussis toxin. *Exp Eye Res* 1994; 58: 729–736.
396. Miller PE, Nelson NJ, Rhaesa SL. Effect of topical administration of 0.5% apraclonidine on intraocular pressure, pupil size, and heart rate in clinically normal dogs. *Am J Vet Res* 1996; 57: 79–82.
397. Miller PE, Rhaesa SL. Effects of topical administration of 0.5% apraclonidine on intraocular pressure, pupil size, and heart rate in clinically normal cats. *Am J Vet Res* 1996; 57: 83–86.
398. Chien DS, Homsy JJ, Gluchowski C, Tang-Liu DDS. Corneal and conjunctival/scleral penetration of p-aminoclonidine, AGN 190342, and clonidine in rabbit eyes. *Curr Eye Res* 1990; 9: 1051–1059.
399. Walters TR. Development and use of brimonidine in treating acute and chronic elevations of intraocular pressure. A review of safety, efficacy, dose-response, and dosing studies. *Surv Ophthalmol* 1996; 41: (suppl 1)S19–S26.
400. Katz LJ. Brimonidine tartrate 0.2% twice daily vs. timolol 0.5%: 1- year results in glaucomatous patients. Brimonidine Study Group. *Am J Ophthalmol* 1999; 127: 20–26.
401. Toris CB, Camras CB, Yablonski ME. Effects of brimonidine on aqueous humor dynamics in human eyes. *Arch Ophthalmol* 1995; 113: 1514–1517.
402. Gelatt KN, MacKay EO. Effects of single and multiple doses of 0.2% brimonidine tartrate in the glaucomatous beagle. *Vet Ophthalmol* 2002; 5: 253–262.
403. Welch SL, Richardson JA. Clinical effects of brimonidine ophthalmic drops ingestion in 52 dogs. *Vet Human Toxicol* 2002; 44: 34–35.
404. Zimmerman TJ. Topical ophthalmic beta blockers: A comparative review. *J Ocular Pharmacol* 1993; 9: 373–384.
405. Frishman WH, Fuksbrumer MS, Tannenbaum M. Topical ophthalmic β-adrenergic blockade for the treatment of glaucoma and ocular hypertension. *J Clin Pharmacol* 1994; 34: 795–803.
406. Juzych MS, Zimmerman TJ. Beta-blockers. In: Zimmerman TJ, Kooner KS, Sharir M, Fechtner RD, eds. *Textbook of Ocular Pharmacology.* Philadelphia: Lippincott-Raven, 1997: 261–275.
407. Helal J Jr, Macri FJ, Cevario SJ. Timolol inhibition of aqueous humor production in the cat. *Gen Pharmac* 1979; 10: 377–380.
408. Coakes RL, Brubaker RF. The mechanism of timolol in lowering intraocular pressure: In the normal eye. *Arch Ophthalmol* 1978; 96: 2045–2048.
409. Liu HK, Chiou GCY, Garg LC. Ocular hypotensive effects of timolol in cats' eyes. *Arch Ophthalmol* 1980; 98: 1467–1469.
410. Vogh BP, Godman DR, Maren TH. Measurement of aqueous humor flow following scleral injection of sufacetamide as marker: Effect of methazolamide, timolol, and pilocarpine. *J Ocular Pharmacol* 1989; 5: 293–302.
411. Nathanson JA. Human ciliary process adrenergic receptor: Pharmacological characterization. *Invest Ophthalmol Vis Sci* 1981; 21: 798–804.
412. Trope GE, Clark B. Beta adrenergic receptors in pigmented ciliary processes. *Br J Ophthalmol* 1982; 66: 788–792.
413. Colasanti BK, Trotter RR. Effects of selective $beta_1$- and $beta_2$-adrenoreceptor agonists on intraocular pressure in the cat. *Invest Ophthalmol Vis Sci* 1981; 20: 69–76.
414. Boas RS, Messenger MJ, Mittag TW, Podos SM. The effects of topically applied epinephrine and timolol on intraocular pressure and aqueous humor cyclic-AMP in the rabbit. *Exp Eye Res* 1981; 32: 681–690.
415. Shahidullah M, Wilson Ws, Millar C. Effects of timolol, terbutaline and forskolin on IOP, aqueous humour formation and ciliary cyclic AMP levels in the bovine eye. *Curr Eye Res* 1995; 14: 519–528.
416. Whikehart DR, Montgomery B, Sorna DH. The inhibition of Na, K-ATPase, and Mg-ATPase by timolol maleate in cultured non-pigmented epithelial cells of the ciliary body. *J Ocular Pharmacol* 1992; 8: 107–114.
417. Rittenhouse KD, Pøllack GM. Pharmacodynamics of beta-blocker modulation of aqueous humor production. *Exp Eye Res* 1999; 70: 429–439.
418. Watanabe K, Chiou GCY. Action mechanism of timolol to lower the intraocular pressure in rabbits. *Ophthal Res* 1983; 15: 160–167.
419. Wilkie DA, Latimer CA. Effects of topical administration of timolol maleate on intraocular pressure and pupil size in dogs. *Am J Vet Res* 1991; 52: 432–435.
420. Wilkie DA, Latimer CA. Effects of topical administration of timolol maleate on intraocular pressure and pupil size in cats. *Am J Vet Res* 1991; 52: 436–439.
421. Gum GG, Larocca RD, Gelatt KN, Mead JP, Gelatt JK. The effect of topical timolol maleate on intraocular pressure in normal beagles and beagles with inherited glaucoma. *Prog Vet Comp Ophthalmol* 1991; 1: 141–150.
422. Gelatt KN, Larocca RD, Gelatt JK, Strubbe T, Mac Kay EO. Evaluation of multiple doses of 4 and 6% timolol, and timolol combined with 2% pilocarpine in clinically normal beagles and beagles with glaucoma. *Am J Vet Res* 1995; 56: 1325–1331.
423. Van der Woerdt A, Wilkie DA, Gilger BC, Strauch SM, Orczeck SM. Effect of single- and multiple-dose 0.5% timolol maleate on intraocular pressure and pupil size in female horses. *Vet Ophthalmol* 2000; 3: 165–168.
424. Lee VHL, Li S, Podder SK, Chang JCS, Ohdo S, Grass GM. Pharmacokinetic basis for nonadditivity of intraocular pressure lowering in timolol combinations. *Invest Ophthalmol Vis Sci* 1991; 32: 2948–2957.
425. Shimazaki J, Hanada K, Yagi Y, et al. Changes in ocular surface caused by antiglaucomatous eyedrops: Prospective, randomised study for the comparison of 0.5% timolol *v* 0.12% unoprostone. *Br J Ophthalmol* 2000; 84: 1250–1254.
426. Trope GE, Lin GS, Basu PK. Toxic effects of topically administered betagan, betoptic and timoptic on regenerating corneal epithelium. *J Ocular Pharmacol* 1988; 4: 359–366.
427. Svec AL, Strosberg AM. Therapeutic and systemic side effects of ocular ß-adrenergic antagonists in anesthetized dogs. *Invest Ophthalmol Vis Sci* 1986; 27: 401–405.
428. Jampel HD, Chen X, Chue C, Zack D. Expression of carbonic anhydrase isoenzyme III in the ciliary processes and lens. *Invest Ophthalmol Vis Sci* 1997; 38: 539–543.
429. Derick RJ. Carbonic anhydrase inhibitors. In: Mauger TF, Graig EL, eds. *Havener's Ocular Pharmacology,* 6th ed. St Louis: Mosby, 1994: 172–180.
430. Higginbotham EJ. Topical carbonic anhydrase inhibitors. *Ophthalmol Clin N Am* 1989; 2: 113–130.
431. Brechue WF, Maren TH. A comparison between the effects of topical and systemic carbonic anhydrase inhibitors on aqueous humor secretion. *Exp Eye Res* 1993; 57: 67–78.
432. Friedland BR, Maren TH. Carbonic anhydrase: Pharmacology of inhibitors and treatment of glaucoma. In: Sears ML, ed. *Pharmacology of the Eye.* Berlin: Springer-Verlag,1984: 279–309.
433. Gelatt KN, Gum GG, Williams LW, Gwin RM. Ocular hypotensive effects of carbonic anhydrase inhibitors in

normotensive and glaucomatous beagles. *Am J Vet Res* 1979; 40: 334–345.

434. Othman GM, Samy MT. Can carbonic anhydrase inhibitors relieve intraocular pressure in cats with glaucoma? *Vet Med* 1987; 82: 498–509.
435. Skorobohach BJ, Ward DA, Hendrix DVH. Effect of oral administration of methazolamide on intraocular pressure and aqueous humor flow rate in clinically normal dogs. *Am J Vet Res* 2003; 64: 183–187.
436. Gelatt KN, MacKay O. Changes in intraocular pressure associated with topical dorzolamide and oral methazolamide in glaucomatous dogs. *Vet Ophthalmol* 2001; 4: 61–67.
437. Kass MA. Topical carbonic anhydrase inhibitors. *Am J Ophthalmol* 1989; 107: 280–282.
438. Maren TH, Conroy CW, Wynns GC, Levy NS. Ocular absorption, blood levels, and excretion of dorzolamide, a topically active carbonic anhydrase inhibitor. *J Ocular Pharmacol Therapeut* 1997; 12: 23–30.
439. De Santis L. Preclinical overview of brinzolamide. *Surv Ophthalmol* 2000; 44: (suppl 2) S119–S129.
440. Ward DA, Cawrse MA, Cox SK, Hendrix DVH. Blood and ocular tissue levels of topical dorzolamide in dogs (abstract). 34th Annual Meeting of the American College of Veterinary Ophthalmologists 2003: 43.
441. Cawrse MA, Ward MA, Hendrix DVH. Effects of topical application of a 2% solution of dorzolamide on intraocular pressure and aqueous humor flow rate in clinically normal dogs. *Am J Vet Res* 2001; 62: 859–863.
442. Kennard G, Whelan NC. The additive effect of dorzolamide and latanoprost in reducing intraocular pressure in normal dogs (abstract). 32nd Annual Meeting of the American College of Veterinary Ophthalmologists 2001: 49.
443. Rainbow ME, Dziezyc J. Effects of twice daily application of 2% dorzolamide on intraocular pressure in normal cats. *Vet Ophthalmol* 2003; 6: 147–150.
444. Willis AM, Robbin TE, Hoshaw-Woodard S, Wilkie DA, Schmall ML. Effect of topical administration of 2% dorzolamide hydrochloride or 2% dorzolamide hydrochloride-0.5% timolol maleate on intraocular pressure in clinically normal horses. *Am J Vet Res* 2001; 61: 709–713.
445. Whelan NC, Welch P, Pace A, Brienza CA. A comparison of the efficacy of topical brinzolamide and dorzolamide alone and in combination with oral methazolamide in decreasing normal canine intraocular pressure (abstract). 30th Annual Meeting of the American College of Veterinary Ophthalmologists 1997: 80.
446. Gray HE, Willis AM, Morgan RV. Effects of topical administration of 1% brinzolamide on normal cat eyes. *Vet Ophthalmol* 2003; 6: 285–290.
447. Kennard G, Whelan NC. The additive effect of dorzolamide and latanoprost in reducing intraocular pressure in normal dogs (abstract). 32nd Annual Meeting of the American College of Veterinary Ophthalmologists 2001: 49.
448. Hutzelmann J, Owens S, Shedden A, Adamsons I, Vargas E. Comparison of the safety and efficacy of the fixed combination of dorzolamide/timolol and the concomitant administration of dorzolamide and timolol: A clinical equivalence study. *Br J Ophthalmol* 1998; 82: 1249–1253.
449. Rose RJ, Carter J. Some physiological and biochemical effects of acetazolamide in the dog. *J Vet Pharmacol Therapeut* 1979; 2: 215–221.
450. Haskins SC, Munger RJ, Helphrey MG, et al. Effects of acetazolamide on blood acid-base and electrolyte values in dogs. *J Am Vet Med Assoc* 1981; 179: 792–796.
451. Strahlman E, Tipping R, Vogel R. Dorzolamide Dose-Response Study Group. A 6-week dose-response study of the ocular hypotensive effect of dorzolamide with a one-year extension. *Am J Ophthalmol* 1996; 122: 183–192.
452. Silver LH, Brinzolamide Comfort Study Group. Ocular comfort of brinzolamide 1% ophthalmic suspension compared with dorzolamide 2% ophthalmic solution: Results from two multicenter comfort studies. *Surv Ophthalmol* 2000: 44(suppl 2): S141–S145.
453. Bito LZ. Prostaglandins, other eicosanoids, and their derivatives as potential antiglaucoma agents. In: Drance SM, ed. *Glaucoma: Applied Pharmacology in Medical Treatment.* Orlando: Grune and Stratton, 1984: 477–505.
454. Alm A. Prostaglandin derivatives as ocular hypotensive agents. *Prog Retin Eye Res* 1998; 17: 291–312.
455. Eisenberg DL, Toris CB, Camras CB. Bimatoprost and travoprost: A review of recent studies of two new antiglaucoma drugs. *Surv Ophthalmol* 2002; 47(suppl 1): S105–S115.
456. Bito LZ. Prostaglandins and other eicosanoids: Their ocular transport, pharmacokinetics and therapeutic effects. *T Ophthal Soc UK* 1986; 105: 162–170.
457. Bito LZ, Baroody RA. The ocular pharmacokinetics of eicosanoids and their derivatives. 1. Comparison of ocular eicosanoid penetration and distribution following the topical application of $PGF_{2\alpha}$, $PGF_{2\alpha}$-1-methyl ester, and $PGF_{2\alpha}$-1-isopropyl ester. *Exp Eye Res* 1987; 44: 217–226.
458. Davies SS, Ju W-K, Neufeld AH, Abran D, Chemtob S, Roberts II LJ. Hydrolysis of bimatoprost (Lumigan) to its free acid by ocular tissue in vitro. *J Ocular Pharm Therap* 2003; 19: 45–54.
459. Numaga J, Koseki N, Kaburaki T, Kawashima H, Tomita G, Araie M. Intraocular metabolites of isopropyl unoprostone. *Curr Eye Res* 2005; 30: 909–913.
460. Woodward DF, Chan MF, Cheng-Bennet A, et al. In-vivo activity and enzymatic hydrolysis of novel prostaglandin $F_{2\alpha}$ prodrugs in ocular tissues. *Exp Eye Res* 1996; 63: 411–423.
461. Anthony TL, Pierce KL, Stamer WD, Regan JW. Prostaglandin $F_{2\alpha}$ receptors in the human trabecular meshwork. *Invest Ophthalmol Vis Sci* 1998; 39: 315–321.
461. Lee P-Y, Podos SM, Severin C. Effect of prostaglandin $F_{2\alpha}$ on aqueous humor dynamics of rabbit, cat, and monkey. *Invest Ophthalmol Vis Sci* 1984; 25: 1087–1093.
463. Gum GG, Kingsburry S, Whitley RD, Garcia A, Gelatt KN. Effect of topical prostaglandin PGA_2, PGA_2 isopropyl ester, $PGF_{2\alpha}$ isopropyl ester on intraocular pressure in normotensive and glaucomatous canine eyes. *J Ocular Pharmacol* 1991; 7: 107–116.
464. Ota T, Aihara M, Narumiva S, Araie M. The effects of prostaglandin analogues on IOP in prostanoid FP-receptor-deficient mice. *Invest Ophthalmol Vis Sci* 2005; 46: 4159–4163.
465. Bhattacherjee P, Williams BS, Paterson CA. Responses of intraocular pressure and the pupil of feline eyes to prostaglandins EP_1 and FP receptor agonists. *Invest Ophthalmol Vis Sci* 1999; 40: 3047–3053.
466. Hurwitz LM, Kaufman PL, Robin AL, Weinreb RN, Crawford K, Shaw B. New developments in the drug treatment of glaucoma. *Drugs* 1991; 41: 514–532.
467. Gabelt BT, Kaufman PL. The effect of prostaglandin on trabecular outflow facility in cynomolgus monkeys. *Exp Eye Res* 1990; 51: 87–91.
468. Payer JF, Gabelt BT, Kaufman PL. The effect of topical $PGF_{2\alpha}$ on uveoscleral outflow and outflow facility in the rabbit eye. *Exp Eye Res* 1992; 54: 277–283.

469. Toris CB, Camras CB, Yablouski ME. Effect of a new $PGF_{2\alpha}$ analog on aqueous humor dynamics in human eyes. *Ophthalmol* 1993; 100: 1297–1304.
470. Toris CB, Yablonski ME, Wang YL, Hayashi M. Prostaglandin A_2 increases uveoscleral outflow and trabecular outflow facility in the cat. *Exp Eye Res* 1995; 61: 649–657.
471. Taniguchi T, Haque MSR, Sugiyama K, Hori N, Kitazawa Y. Ocular hypotensive mechanism of topical isopropyl unoprostone, a novel prostaglandin metabolite-related dug, in rabbits. *J Ocular Pharmacol Therapeut* 1996; 12: 489–498.
472. Richter M, Kraus A H-P, Woodward DF, Lütjen-Drecoll E. Morphological changes in the anterior eye segment after long-term treatment with different receptor selective prostaglandin agonists and a prostamide. *Invest Ophthalmol Vis Sci* 2003; 44: 4419–4426.
473. Weinreb RN, Kashiwagi K, Kashiwagi F, Tsukahara S, Lindsey JD. Prostaglandins increase matrix metalloproteinase release from human ciliary smooth muscle cells. *Invest Ophthalmol Vis Sci* 1997; 38: 2772–2780.
474. Gaton DD, Sagara T, Lindsey JD, Gabelt BT, Kaufman PL, Weinreb RN. Increased matrix metalloproteinases 1, 2, and 3 in the monkey uveoscleral outflow pathway after topical prostaglandin $F_{2\alpha}$-isopropyl ester treatment. *Arch Ophthalmol* 2001; 119: 1165–1170.
475. Sagara T, Gaton DD, Lindsey JD, Gabelt BT, Kaufman PL, Weinreb RN. Topical prostaglandin F_2alpha treatment reduces collagen types I, III, and IV in the monkey uveoscleral outflow pathway. *Arch Ophthalmol* 1999; 117: 794–801.
476. Lindsey JD, Gaton DD, Sagara T, Polansky JR, Kaufman PL, Weinreb RN. Reduced TIGR/myocilin protein in the monkey ciliary muscle after topical prostaglandin $F_{2\alpha}$ treatment. *Invest Ophthalmol Vis Sci* 2001; 42: 1781–1786.
477. Lütjen-Drecoll E, Tamm E. Morphological study of the anterior segment of cynomolgus monkey eyes following treatment with prostaglandin $F_{2\alpha}$. *Exp Eye Res* 1988; 47: 761–769.
478. Ishii K, Tomidokoro A, Nagahara M, et al. Effects of topical latanoprost on optic nerve head circulation in rabbits, monkeys, and humans. *Invest Ophthalmol Vis Sci* 2001; 42: 2957–2963.
479. Studer ME, Martin CL, Stiles J. Effects of 0.005% latanoprost solution on intraocular pressure in healthy dogs and cats. *Am J Vet Res* 2000; 61: 1220–1224.
480. Gelatt KN, MacKay EO. Effects of different dose schedules of latanoprost on intraocular pressure and pupil size in the glaucomatous beagle. *Vet Ophthalmol* 2001; 4: 283–288.
481. Gelatt KN, MacKay EO. Effects of different dose schedules of bimatoprost on intraocular pressure and pupil size in the glaucomatous beagle. *J Ocular Pharmacol Therapeut* 2002; 18: 525–534.
482. Gelatt KN, MacKay EO. Effects of different dose schedules of travoprost on intraocular pressure and pupil size in the glaucomatous beagle. *Vet Ophthalmol* 2004; 7: 53–57.
483. Ofri R, Raz D, Kass PH, Lambrou GN, Percicot CL. The effect of 0.12% unoprostone isopropyl (Rescula) on intraocular pressure in normotensive dogs. *J Vet Med Sci* 2000; 62: 1313–1315.
484. Bartoe JT, Davidson HJ, Horton MT, Jung Y, Brightman AH. The effects of bimatoprost and unoprostone isopropyl on the intraocular pressure of normal cats. *Vet Ophthalmol* 2005; 8: 247–252.
485. Regnier A, Lemagne C, Ponchet A, Cazalot G, Concordet D, Gelatt KN. Ocular effects of topical 0.03% bimatoprost solution in normotensive feline eyes. *Vet Ophthalmol* 2006; 9: 39–43.
486. Willis AM, Diehl KA, Hoshaw-Woodward S, Kobayashi I, Vitucci MP, Schmall M. Effect of topical administration of 0.005% latanoprost solution on eyes of clinically normal horses. *Am J Vet Res* 2001; 62: 1945–1951.
487. Soltau JB. Changing paradigms in the medical treatment of glaucoma. *Surv Ophthalmol* 2002; 47(suppl 1): S2–S5.
488. Alm A, Stjernschantz J, the Scandinavian Latanaprost study group. Effects on intraocular pressure and side effects of 0.005% latanoprost applied once daily, evening or morning : a comparison with timolol. *Ophthalmol* 1995; 102: 1743–1752.
489. Mishima HK, Masuda K, Kitazawa Y, Azuma I, Araie M. A comparison of latanoprost and timolol in primary open-angle glaucoma and ocular hypertension. *Arch Ophthalmol* 1996; 114: 929–932.
490. Sherwood M, Brandt J, for the bimatoprost study groups 1 and 2. Six-month comparison of bimatoprost once-daily and twice-daily with timolol twice-daily in patients with elevated intraocular pressure. *Surv Ophthalmol* 2001; 45(suppl 4): S361–S368.
491. Lindén C, Alm A. Latanoprost twice daily is less effective than once daily: Indicator of receptor sunsensitivity. *Curr Eye Res* 1998; 17: 567–572.
492. Stewart WC, Sharpe ED, Day DG, et al. Comparison of the efficacy and safety of latanoprost 0.005% compared to brimonidine 0.2% or dorzolamide 2% when added to topical β-adrenergic blocker in patients with primary open-angle glaucoma or ocular hypertension. *J Ocular Pharmacol Therapeut* 2000; 16: 251–260.
493. Toris CB, Zhan G-L, Zhao J, Camras CB, Yablonski ME. Potential mechanism for the additivity of pilocarpine and latanoprost. *Am J Ophthalmol* 2001; 131: 722–728.
494. Miller PE, Bentley E, Diehl KA, Carter R. High resolution ultrasound imaging of the anterior segment of dogs with primary glaucoma prior to and following the topical application of 0.005% latanoprost (abstract). 34th Annual Meeting of the American College of Veterinary Ophthalmologists 2003: 53.
495. Schumer RA, Camras CB, Mandahl AK. Putative side effects of prostaglandin analogs. *Surv Ophthalmol* 2002; 47(suppl 1): S219–S230.
496. Stjernschantz JW, Albert DA, Hu D-N, Drago F, Wistrand PJ. Mechanism and clinical significance of prostaglandin-induced iris pigmentation. *Surv Ophthalmol* 2002; 47(suppl 1): S162–S175.
497. Lindsey JD, Hewitt EG, Angert M, Weinreb RN. Induction of tyrosinase gene transcription in human iris organ cultures exposed to latanoprost. *Arch Ophthalmol* 2001; 119: 853–860.
498. Bergh K, Wentzel P, Stjernschantz J. Production of prostaglandin E2 by iridial melanocytes exposed to latanoprost acid, a prostaglandin $F_{2\alpha}$ analogue. *J Ocular Pharmacol Therapeut* 2002; 18: 391–400.
499. Grierson I, Pfeiffer N, Cracknell KPB, Appleton P. Histology and fine structure of the iris and outflow system following latanoprost therapy. *Surv Ophthalmol* 2002; 47 (suppl 1): S176–S184).
500. Yoshitomi T, Ito Y. Effects of indomethacin and prostaglandins on the dog iris sphincter and dilator muscles. *Invest Ophthalmol Vis Sci* 1988; 29: 127–132.
501. Arcieri ES, Santana A, Rocha FN, Guapo GL, Costa VP. Blood–aqueous barrier changes after the use of prostaglandin analogues in patients with pseudophakia and aphakia. *Arch Ophthalmol* 2005; 123: 186–192.
502. Craig EL. Osmotic agents. In: Manger TF, Craig EL, eds. *Havener's Ocular Pharmacology,* 6th ed. St Louis: Mosby, 1994: 180–189.

503. Dugan SJ, Roberts SM, Severin GA. Systemic osmotherapy for ophthalmic disease in dogs and cats. *J Am Vet Med Assoc* 1989; 194: 115–118.
504. Gwin RM. Current concepts in small animal glaucoma: Recognition and treatment. *Vet Clin N Am Sm Anim Pract* 1980; 10: 357–376.
505. Brooks DE. Glaucoma in the dog and cat. *Vet Clin N Am Sm Anim Pract* 1990; 20: 775–797.
506. Singh K, Krupin T. Hyperosmotic agents. In: Zimmerman TJ, Kooner KS, Sharir M, Fechtner RD, eds. *Textbook of Ocular Pharmacology.* Philadelphia: Lippincott-Raven, 1997: 291–296.
507. Lorimer DW, Hakanson NE, Pion PD, Merideth RE. The effect of intravenous mannitol or oral glycerol on intraocular pressure in dogs. *Cornell Vet* 1989; 79: 249–258.
508. Bedford PGC. The treatment of canine glaucoma. *Vet Rec* 1980; 107: 101–104.
509. Brock KA, Thurmon JC. Pulmonary edema associated with mannitol administration. *Canine Pract* 1979; 6: 31–34.
510. Brock DA, Thurmon JC, Benson GJ, et al. Selected hemodynamic and renal effects of intravenous infusions of hypertonic mannitol in dogs anesthetized with methoxyflurane in oxygen. *J Am Anim Hosp Assoc* 1985; 21: 207–214.
511. Gilroy BA. Intraocular and cardiopulmonary effects of low-dose mannitol in the dog. *Vet Surg* 1986; 15: 342–344.
512. Abbasoglu OE, Kooner KS. Future role of neuroprotective agents in glaucoma. In: Zimmerman TJ, Kooner KS, Sharir M, Fechtner RD, eds. *Textbook of Ocular Pharmacology.* Philadelphia: Lippincott-Raven, 1997: 329–339.
513. Quigley HA. Neuronal death in glaucoma. *Prog Retin Eye Res* 1998; 18: 39–57.
514. Goldberg I. Relationship between intraocular pressure and preservation of visual field in glaucoma. *Surv Ophthalmol* 2003; 48(suppl 1): S3–S7.
515. Levin LA. Retinal ganglion cells and neuroprotection for glaucoma. *Surv Ophthalmol* 2003; 48(suppl 1): S21–S24.
516. Naskar RN, Dreyer EB. New horizons in neuroprotection. *Surv Ophthalmol* 2001; 45(suppl 3): S250–S255.
517. Osborne NN, Ugarte M, Chao M, et al. Neuroprotection in relation to retinal isscuemia and relevance to glaucoma. *Surv Ophthalmol* 1999; 43(suppl 1) S102–S128.
518. WoldeMussie E, Ruiz G, Wijono M, Wheeler LA. Neuroprotection of retinal ganglion cells by brimonidine in rats with laser-induced chronic ocular hypertension. *Invest Ophthalmol Vis Sci* 2001; 42: 2849–2855.
519. Seki M, Tanaka T, Matsuda H, et al. Topically administered timolol and dorzolamide reduce intraocular pressure and protect retinal ganglion cells in a rat experimental glaucoma model. *Br J Ophthalmol* 2005; 89: 504–507.

Chapter 7

Clinical Pharmacology and Therapeutics

Part 3: Mydriatics/Cycloplegics, Anesthetics, Ophthalmic Dyes, Tear Substitutes and Stimulators, Intraocular Irrigating Fluids, Topical Disinfectants, Viscoelastics, Fibrinolytics and Antifibrinolytics, Antifibrotic Agents, Tissue Adhesives, and Anticollagenase Agents

Ian P. Herring

MYDRIATICS/CYCLOPLEGICS

Pharmacological agents used to achieve pupillary dilation, relieve ciliary spasm, or both, have a variety of ophthalmic diagnostic and therapeutic applications. The agent of choice is generally dictated by the goal of the practitioner. In a diagnostic setting, mydriasis is commonly induced to facilitate visual examination of the posterior segment of the eye, in which case a short-acting agent with or without significant cycloplegic effect may be chosen. While cycloplegia is important to refraction in humans and primates, refraction by retinoscopy is reportedly unaffected by cycloplegia in dogs.[1,2] In the management of iridocyclitis, more prolonged mydriasis and significant cycloplegia are often desired. In such cases, the mydriasis will help prevent posterior synechia between the iris and lens surface, and relaxation of the ciliary body will relieve some of the discomfort associated with uveitis. Mydriasis is also required for cataract extraction surgery and other surgeries of the posterior segment.

Mydriatic agents achieve pupillary dilation by either paralysis of the pupillary sphincter (e.g., cholinergic antagonists) or stimulation of the iris dilator muscle (e.g., sympathomimetics). Generally speaking, drugs that induce pupillary sphincter paralysis also cause some degree of cycloplegia, while those that stimulate the iris dilator musculature do not. While mydriatic/cycloplegic medications are generally applied topically, reports on the use of intracameral mydriatics during phacoemulsification have recently appeared.[3,4]

With regard to speed of onset, completeness of effect, and duration of effect, the effects of mydriatic/cycloplegic medications vary by species. In addition, certain ophthalmic disease states (e.g., uveitis) will also affect these parameters. Results from various studies of mydriatic and cycloplegic agents conducted in companion animal species are summarized in Tables 7.3.1, 7.3.2, 7.3.3, and 7.3.4.

Cholinergic Antagonists

Mechanism of Action

Cholinergic antagonists act through a reversible blockade of cholinergic receptors in smooth muscle and secretory glands.

Clinical Indications

Cholinergic antagonists are used clinically to facilitate visualization during ophthalmic examination and surgery of the lens and posterior segment. They also have therapeutic indications in the management of iridocyclitis.

Side Effects/Contraindications

Mydriatic agents should be avoided in cases of glaucoma, where pupillary dilation may cause a severe rise in intraocular pressure. Dilation of the pupil may also allow an unstable lens to fall anteriorly, potentially resulting in pupillary block glaucoma. Topical application of some anticholinergic agents may induce a substantial reduction in aqueous tear production.[5] Salivation (sometimes profound) is noted frequently and vomiting occasionally seen following topical administration of some anticholinergics, presumably due to their bitter taste.[6–8] Systemic side effects are a particular concern in horses because of their potential for inducing colic. Decreases in gastrointestinal myoelectric activity, decreased borborygmi, and abdominal pain have been documented following topical and subconjunctival administration of atropine in this species.[9,10]

Tropicamide

Tropicamide is available as a 0.5% and 1.0% solution. It is a rapid-acting drug, producing complete mydriasis within 30 minutes in dogs, where its effects begin to wane as quickly as

Table 7.3.1 Mydriatics and Mydriatic/Cycloplegics in the Dog

Drug	Time until		
	Maximum Dilation (hours)	Duration (hours)	Extent of Dilation
Parasympatholytics			
1% Atropine	1.0	96–120	Maximal
4% Atropine	0.75	96–120	Maximal
0.25% Scopolamine	0.75	96–120	Maximal
1% Cyclopentolate	0.75	60	Maximal
1% Tropicamide	0.5	12	Maximal
2% Homatropine	0.75	48	Moderate
5% Homatropine	0.75	48	Moderate
Sympathomimetics			
10% Phenylephrine	2.0	12–18	Maximal
0.1% Epinephrine	—	—	None
1% Epinephrine	1.0	9	Maximal
2% Epinephrine	0.75	6	Moderate

Data from Rubin LF, Wolfes RL. Mydriatics for canine ophthalmoscopy. *J Am Vet Med Assoc* 1962;140:137–141; and Gwin RM, Gelatt KN, Gum GG, Peiffer RL. Effects of topical L-epinephrine and dipivalyl epinephrine on intraocular pressure and pupil size in the normotensive and glaucomatous beagle. *Am J Vet Res* 1978;39:83–86.

Table 7.3.2 Mydriatics and Mydriatic/Cycloplegics in the Cat

Drug	Time until		
	Maximum Dilation (hours)	Duration (hours)	Extent of Dilation
Parasympatholytics			
1% Atropine	1.0	60	Maximal
4% Atropine	0.5	144	Maximal
1% Cyclopentolate	0.5[a]	66	Maximal
2% Cyclopentolate	0.5[a]	108	Maximal
0.5% Tropicamide	0.75[a]	8–9	Maximal
1% Tropicamide	0.75[a]	8–9	Maximal
2% Homatropine	0.75	7	Moderate
Sympathomimetics			
10% Phenylephrine	—	—	None
2% Epinephrine	—	—	None
Parasympatholytic/sympathomimetic combinations			
1% Atropine/10% phenylephrine	1.0	120	Maximal
1% Cyclopentolate/10% phenylephrine	0.5	108	Maximal
2% Homatropine/10% phenylephrine	1.0	24	Moderate

Adapted with permission from Gelatt KN, Boggess TS, Cure TH. Evaluation of mydriatics in the cat. *J Am Anim Hosp Assoc* 1973;9:283–287.
[a]Reached ~80% of maximal dilation in 0.25 hours.

2 hours following instillation.[6] In cats, mydriasis occurs within 15 minutes and lasts approximately 10 hours.[8] Because of its rapid onset, completeness of mydriasis and relatively short duration of action, it is well suited for diagnostic mydriasis. Tropicamide is also useful for inducing mydriasis prior to cataract extraction surgery; multiple doses are commonly applied in the hours preceding the procedure. In this setting, the relatively short duration of action may provide additional benefit because it is perhaps less likely to exacerbate postoperative intraocular pressure spikes than longer acting agents such as atropine.

While excellent mydriasis can be achieved with tropicamide, its cycloplegic effect is not as pronounced as that of atropine, homatropine, or cyclopentolate, somewhat limiting

Table 7.3.3 Mydriatics and Mydriatic/Cycloplegics in the Cow

Drug	Time until		
	Maximum Dilation (hours)	Duration (hours)	Extent of Dilation
Parasympatholytics			
1% Atropine	0.75	24	Moderate
3% Atropine	2	168	Maximal
0.25% Scopolamine	2[a]	144	Maximal
1% Cyclopentolate	12	48	Moderate
2% Cyclopentolate	12	96	Maximal
0.5% Tropicamide	3[b]	3	Moderate
1% Tropicamide	3[b]	8	Moderate
2% Homatropine	2[a]	48	Moderate
Sympathomimetics			
10% Phenylephrine	—	—	None
Parasympatholytic/sympathomimetic combinations			
1% Atropine/10% phenylephrine	2	24	Moderate

Adapted with permission from Gelatt KN, Gum GG, MacKay EO. Evaluation of mydriatics in cattle. *Vet Comp Ophthalmol* 1995;5:45–49.
[a]Reached ~50% of maximal dilation in 0.75 hours.
[b]Reached ~50% of maximal dilation in 0.50 hours.

Table 7.3.4 Mydriatics and Mydriatic/Cycloplegics in the Horse

Drug	Time until		
	Maximum Dilation (hours)	Duration (hours)	Extent of Dilation
Parasympatholytics			
1% Atropine	10	132	Maximal
3% Atropine	12	264	Maximal
0.25% Scopolamine	4	108	Maximal
1% Cyclopentolate	12	96	Maximal
2% Cyclopentolate	12	120	Maximal
0.5% Tropicamide	1	5	Maximal
1% Tropicamide	5[a]	12	Maximal
2% Homatropine	3	8	Moderate
Sympathomimetics			
10% Phenylephrine	—	—	None
Parasympatholytic/sympathomimetic combinations			
1% Atropine/10% phenylephrine	8	84	Maximal

Adapted with permission from Gelatt KN, Gum GG, MacKay EO. Evaluation of mydriatics in horses. *Vet Comp Ophthalmol* 1995;5:104–108.
[a]Reached ~95% of maximal dilation in 0.75 hours.

its usefulness in the treatment of discomfort associated with uveitis.[11–14] However, tropicamide has been shown to reduce blood–aqueous barrier permeability.[15,16] With regard to potential effects on aqueous tear production, a single application of tropicamide does not cause a reduction in STT values in normal dogs but causes a transient STT decline in cats.[17]

Atropine

Atropine sulfate is available as a 0.5% to 2.0% solution as well as a 1% ointment. Because of its potent mydriatic and cycloplegic effects and long duration of action, atropine is often the cycloplegic agent of choice in cases of iridocyclitis.

Onset and duration of action varies somewhat by species. Maximal pupillary dilation occurs in 30 to 60 minutes in normal dogs, cats, and cattle.[6,8,18] In dogs, using 1% solution, maximum mydriasis is noted in 1 hour and mydriasis lasts 96 to 120 hours,[6] whereas in cats mydriasis occurs in 30 to 45 minutes and persists for 60 hours.[8] In the horse, 1% atropine sulfate begins to take effect within approximately 45 minutes, but mydriasis does not become maximal until 10 to 48 hours postadministration.[19,20] Duration of action in horses may extend beyond 14 days, with

female and Arabian breeds being potentially more sensitive to the mydriatic effects of the drug.[20] Iridal melanin binding of atropine is well documented in humans and rabbits,[21–23] where it subsequently acts as a slow-release depot and extends atropine's duration of action in eyes with heavily pigmented irides.

Side effects of topical atropine in dogs and cats are common and include profuse salivation and occasional vomiting.[6,8] These side effects are likely related to the bitter taste of the drug, which is ingested after exiting the nasolacrimal duct and can be minimized to some degree by the use of ointment instead of solution. Contact allergic periocular dermatitis associated with ophthalmic atropine has been documented in the human literature, and the author has occasionally noted it in animals. It is important to recognize this potential problem so that it is not confused with exacerbation of the disease under treatment. Delirium has been reported following topical atropine administration in humans[24] and is also noted occasionally in older dogs, where it is usually manifest as compulsive circling and resolves when the drug is discontinued.[25]

Homatropine

In dogs and cats, homatropine acts more slowly than atropine and does not achieve complete mydriasis.[6,8] Mydriasis generally subsides within 10 hours in cats[8] and 24 hours in dogs.[6] In horses, homatropine is a less effective mydriatic with a shorter duration of action than atropine but somewhat longer than tropicamide.[19]

Scopalamine

Scopalamine is a potent mydriatic with a rapid onset of action and long duration in dogs, horses, and cattle.[6,18,19]

Cyclopentolate

Cyclopentolate is an effective mydriatic/cycloplegic with a duration of action comparable to that of atropine in dogs, cats, horses, and cattle.[6,8,18,19] Maximal pupillary dilation in dogs and cats occurs within approximately 45 minutes and persists for over 24 hours in dogs[6] and over 60 hours in cats.[8] Conjunctival edema has been reported as a common side effect of topical application of cyclopentolate in dogs[6] but not cats.[8] Intracameral administration of cyclopentolate has recently been reported as a safe and effective method of achieving mydriasis during phacoemulsification in humans.[3,4]

Sympathomimetics

Mechanism of Action

Sympathomimetic effects on the iris include direct stimulation of α-adrenergic receptors in the iris dilator musculature.

Clinical Indications

Sympathomimetics are useful in potentiating the effects of other mydriatic medications in some species and in providing adjunct mydriasis and vasoconstriction during ocular surgery. Adrenergic agents are also useful in the diagnosis of sympathetic ocular denervation (Horner's syndrome).[26]

Side Effects/Contraindications

Side effects following ophthalmic application of sympathomimetic medications are rare. Arterial hypertension has been described in a series of dogs receiving topical phenylephrine in preparation for cataract extraction surgery, although none of those cases experienced recognized clinical complications related to the hypertension.[27] Topical administration of 10% phenylephrine in research dogs elicited a dose-dependent arterial hypertensive response and associated bradycardia.[28] While they are unlikely to cause clinical complications in routine clinical use, it is advisable to use caution regarding ophthalmic administration of sympathomimetics in dogs with known or suspected arterial hypertension. Due to myocardial sensitization to epinephrine induced by halothane anesthesia and the attendant risk of inducing cardiac arrhythmias, it is prudent to avoid intracameral epinephrine in animals undergoing halothane anesthesia[29–31] or receiving thiobarbiturates.[32–35] Similar concerns may be valid when using propofol anesthesia.[36]

Phenylephrine

Ophthalmic phenylephrine hydrochloride is available in 2.5% and 10% solutions. A direct-acting α_1-adrenergic agonist, phenylephrine causes local ocular effects of mydriasis and conjunctival vasoconstriction following topical ophthalmic administration. It is commonly used in conjunction with other medications to maximize pupillary dilation for diagnostic and therapeutic purposes and alone to help localize the site of sympathetic denervation in Horner's syndrome.[26] Because of the absence of cycloplegic effects from phenylephrine, its usefulness in treatment of iridocyclitis is limited to helping achieve mydriasis when posterior synechia is present. While it does achieve complete pupillary dilation in the dog, the time to complete mydriasis is too slow (approximately 2 hours) for the drug to be practical as the sole agent in achieving diagnostic mydriasis.[6] It is an ineffective sole mydriatic agent in the cat but prolongs the action of parasympatholytics.[8] Phenylephrine has no significant mydriatic effect in horses when applied alone or in combination with tropicamide[19,37] and may shorten the duration of mydriasis achieved with atropine.[19] Because phenylephrine appears to potentiate the mydriatic effect of other medications in some species, it is often considered a useful adjunct medication to facilitate mydriasis in preparation for intraocular surgery.

Epinephrine

Applied topically, 0.1% epinephrine is an ineffective mydriatic,[6] but at 1% to 2% concentrations, incomplete mydriasis of short duration occurs.[38] Topical 2% epinephrine is an ineffective mydriatic in the cat.[8] Intracameral epinephrine is

commonly used to help achieve maximal pupillary dilation during intraocular surgery, where it is instilled by itself as a dilute solution (1:10,000) or added to irrigating fluids (1:1,000,000). Several clinical trials have confirmed the efficacy of this latter approach.[39–41] Intracameral epinephrine may also help provide intraocular hemostasis through its vasoconstrictive properties. It is imperative that epinephrine introduced into the anterior chamber be preservative-free and bisulfate-free because of endothelial toxicity associated with these additives.[42,43]

Indirect-Acting Sympathomimetics

Cocaine and hydroxyamphetamine are indirect-acting sympathomimetic agents with applications predominantly related to the localization of nerve lesions causing ocular sympathetic denervation (Horner's syndrome). Cocaine has sympathomimetic activity through prevention of norepinephrine reuptake by the nerve terminus, resulting in a buildup of norepinephrine at the synapse. In humans, cocaine is an effective mydriatic in the normal eye and can be used to confirm (but not localize) Horner's syndrome by virtue of the fact that an iris with sympathetic denervation will not dilate. In normal dogs, 4% cocaine exerts no mydriatic effect.[6] However, it has been suggested that 6% cocaine applied topically is useful in confirming Horner's syndrome in dogs and cats,[44] as it is in people. Hydroxyamphetamine elicits release of norepinephrine from sympathetic nerve endings. When applied topically in animals with Horner's syndrome, it causes pupillary dilation in those with preganglionic sympathetic disruption but not in those with a postganglionic lesion.[44]

LOCAL ANESTHETICS

The applications of local anesthetic agents in veterinary ophthalmology are numerous. Pertinent routes of administration include topical application and intracameral, intravenous and regional injection.

All local anesthetics act by impeding sodium ion entrance to the axon interior, thereby preventing nerve depolarization.[45] Local anesthetics share a common general structure, which consists of a hydrophilic amino group (a secondary or tertiary amine) linked by an amide or ester linkage to a lipid-soluble aromatic residue. Many of the pharmacological differences between the various local anesthetics are determined by the nature of this amide–ester linkage.[46]

Topical

Topical anesthetics facilitate many veterinary ophthalmic diagnostic and therapeutic procedures, including tonometry, corneal and conjunctival scrapings, corneal suture and foreign body removal, nasolacrimal canalicular manipulations, and intracameral injection. Topical anesthetics are sometimes employed in a modification of the Schirmer tear test to investigate basal tear production, wherein the anesthetic causes a substantial reduction in Schirmer values.[47,48] Topical ophthalmic anesthetics can also be used intraoperatively to increase corneal analgesia and may thereby allow maintenance of a lower plane of anesthesia. However, due to their toxic effects on corneal epithelium, repeated application of such agents may be injurious.[49,50] The effects of topical anesthetics on precorneal tear film stability have been evaluated with variable results. Topical oxybuprocaine has no effect on precorneal tear film stability,[51] while topical proparacaine reportedly destabilizes the tear film.[52]

Because of their toxic effects on corneal epithelium, topical anesthetics should never be used as therapeutic agents.[49,50] Numerous reports in the human ophthalmic literature highlight the potentially devastating ocular consequences of topical anesthetic abuse. It should also be kept in mind that topical anesthetics have demonstrated antimicrobial activity, so corneoconjunctival cultures should be obtained prior to applying these agents.[53,54]

Cocaine was the first drug utilized for corneal anesthesia,[55] but deleterious effects on the corneal epithelium as well as unnecessary sympathomimetic pupillary effects have rendered it a historical footnote in this application. Currently, the two compounds most commonly used for topical ophthalmic anesthesia in veterinary ophthalmology are proparacaine and tetracaine.

Proparacaine

Available as a 0.5% solution, proparacaine hydrochloride is a well-tolerated and effective topical ophthalmic anesthetic. In humans, proparacaine reportedly causes less discomfort and exerts a longer anesthetic effect than tetracaine following ophthalmic instillation.[56–58] In dogs, using Cochet-Bonnet esthesiometry as a measurement tool, a single application of topical proparacaine results in a significant anesthetic effect lasting 45 minutes, with maximal effect lasting approximately 15 minutes.[59] Application of a second drop extended the detectable duration of effect to 55 minutes.[59] In cats, the duration of corneal anesthesia induced by topical proparacaine is approximately 25 minutes.[60] Total duration of action of proparacaine in rabbits has been reported as 63 minutes.[61] As topical anesthetic drug effects begin to wane, recovery of corneal sensation follows a steep curve in all species that have been studied.

Tetracaine

Tetracaine is available as an ophthalmic ointment and solution and is an effective topical anesthetic. In humans, discomfort upon instillation of tetracaine is significantly more prolonged with tetracaine than proparacaine,[57,58] and duration of corneal anesthesia is slightly shorter.[57] Ocular sensitivity manifest by symptoms of acute conjunctival hyperemia, chemosis, and nictitans protrusion has been reported in dogs following topical application.[62] The duration of effect of topical tetracaine has not been reported for companion animal species.

Intracameral

Intracameral anesthetics have been recently employed as an adjunct method of pain control in humans undergoing cataract extraction surgery. Studies have shown preservative-free lidocaine at concentrations of 1% or less to be safe with regard to short-term endothelial toxicity.[63–65] In dogs, intracameral administration of 0.1 ml 1% and 2% preservative-free lidocaine caused no clinically detectable adverse effects on corneal endothelial density or morphology, corneal thickness, or IOP.[66] Preservative-free 0.5% bupivacaine, which is more potent and longer-acting than lidocaine, has also been shown effective for intracameral anesthesia in people but may carry additional concerns for endothelial toxicity.[67] Studies on the clinical effectiveness and utility of intracameral anesthesia during phacoemulsification or other intraocular procedures in companion animals have yet to be reported.

Regional Injection

Regional injection of anesthetic agents may be applied to achieve eyelid akinesia (via auriculopalpebral nerve block), local analgesia through local infiltration or line blocks, or globe akinesia and analgesia via peribulbar and retrobulbar injection. The local anesthetic agents with the widest ophthalmic application include lidocaine and bupivacaine. Lidocaine, an intermediate-acting local anesthetic, has a rapid onset of action and provides approximately 45 minutes to 1 hour of clinical effect.[68] Bupivacaine is approximately 4 times more toxic than lidocaine but is also four times more potent and thereby provides significantly longer anesthetic effect, lasting approximately 5 to 10 hours when used as a 0.5% solution.[69]

Lidocaine 2% appears to be the most popular local anesthetic used for auriculopalpebral nerve block in animals. Although numerous local anesthetics and combinations have been used for retrobulbar or peribulbar injection in human ophthalmic practice, a combination of lidocaine and bupivacaine is perhaps most popular, with lidocaine providing rapid onset and bupivacaine providing prolonged duration of effect.[70] The duration of effect of certain local anesthetics, particularly lidocaine, can be prolonged with the addition of epinephrine (5 μg/ml) to the injection.[46] The addition of hyaluronidase to peribulbar or retrobulbar anesthetic injection is reported to improve the speed and quality of the block.[71,72]

Retrobulbar and peribulbar injection of local anesthetic can be a useful adjunct to general anesthesia during ophthalmic surgery in animals.[73] In addition to providing akinesia and analgesia, reported benefits include abolishing the oculocardiac reflex.[74,75] Postoperative comfort may also be improved. A recent study in humans revealed improved hemodynamics and a near-significant trend of decreased immediate postoperative pain when preemptive retrobulbar anesthetics were used during enucleation.[76] In domestic animal species, retrobulbar anesthetic blocks have been described in cattle, horses, and dogs.[73,77,78] Anecdotally, peribulbar and retrobulbar injection of local anesthetics is being performed with increasing frequency for enucleation in veterinary patients, but clinical effectiveness studies have yet to be described.

Significant reported complications of peribulbar and retrobulbar injections in humans include globe perforation,[79,80] anesthetic myotoxicity,[81–83,84] and brain stem anesthesia. Numerous less significant complications, such as orbital hemorrhage[5] and chemosis, may also occur. In humans, central nervous system complications of retrobulbar anesthesia are rare but well documented.[84,86,87] This complication is most commonly believed related to penetration of the optic nerve sheath and subarachnoid injection of the anesthetic agent.[84,86] With increasing amounts of anesthetic agent placed in the retrobulbar space, risk of respiratory arrest increases via mechanisms not related to direct CNS or vascular injection.[88] Though it is poorly documented in animals, the author has witnessed sudden death in a calf during a Peterson block. Anesthetic extraocular myotoxicity has been blamed for postoperative strabismus and diplopia following local ophthalmic anesthesia in humans.[81–83] There appear to be differences in the extraocular myotoxic effects of local anesthetic agents depending on the species studied and the site of injection (i.e., within or adjacent to muscle).[89–92] This complication has not been reported in veterinary patients. In many regards, peribulbar anesthesia is reportedly as effective as and safer than the retrobulbar route.[93,94] Finally, sub-Tenon's (episcleral) anesthesia appears to be gaining popularity in human ophthalmic surgery as a safer and equally effective method of achieving eyelid and globe akinesia and analgesia.[95,96]

Intravenous

Intravenous lidocaine appears to be gaining popularity in veterinary anesthesia, and systemic lidocaine infusion has been recently shown to be as effective as morphine in provision of intraoperative analgesia during phacoemulsification in dogs.[97]

OPHTHALMIC DYES

Several dyes have diagnostic application in veterinary ophthalmology. While fluorescein dye is undoubtedly in widest use, rose bengal and trypan blue are also employed by veterinary ophthalmologists. Based upon its reported characteristics, lissamine green might have potential application in veterinary ophthalmology as well.

Fluorescein

Sodium fluorescein (mw 376 daltons) is a water-soluble hydroxyxanthene dye with a number of diagnostic applications. It is undoubtedly the most widely used dye in veterinary ophthalmology and is available as a 2% alkaline solution or as dye impregnated paper strips.

Topical application of fluorescein is perhaps most commonly utilized to help determine the integrity of the corneal epithelium. Following application, the ocular surface is rinsed thoroughly with eyewash solution. Dye will not adhere to an intact epithelial surface, but if a corneal ulcer is present, the dye will stain the exposed hydrophilic corneal stroma. Corneal erosions (which by definition do not penetrate the basement membrane of the epithelium) and disruptions in

superficial epithelial intercellular junctions will stain only very lightly because of the small amount of exposed hydrophilic substance. The sensitivity of this test is increased with the use of a cobalt blue light source (wavelength 465–490 nm), which causes bright green fluorescence of the dye. Because presence of fluorescein may interfere with interpretation of fluorescent antibody–based testing for infectious agents, samples for such should be collected prior to the topical application of fluorescein.[98] Topically applied fluorescein can also be used to investigate for leakage of aqueous humor from corneal incisions or wounds (Seidel test). To perform the Seidel test, highly concentrated fluorescein is applied to the corneal surface without flushing. At high concentrations, fluorescein solution appears orange on the ocular surface. Leaking aqueous humor will dilute the fluorescein locally and produce a brightly fluorescing stream from the leakage site. Tear film stability can be evaluated with the tear film breakup time, which utilizes topical fluorescein as an indicator dye. Following application to the corneal surface, the eyelids are maintained open until dark spots appear in the stained tear film, which are indicators of dispersion of the tear film. Patency of the nasolacrimal system can be investigated by confirming the passage of topically applied fluorescein to the nares or pharynx. During this test, called the Jones test, the dye should not be rinsed, and normal blinking is allowed to occur. More specialized veterinary ophthalmic applications of fluorescein dye include its use in retinal angiography and fluorophotometry. Fluorescein angiography is useful in the diagnosis and characterization of retinal and choroidal disease states. Measurement of ocular fluorescein concentrations via fluorophotometry allows in vivo determination of several important physiologic parameters, including tear film turnover and aqueous humor flow rate, and is a valuable technique for evaluating the blood–ocular barriers.

Adverse Effects of Fluorescein

Topical application of fluorescein is nonirritating but may cause temporary destabilization of the precorneal tear film.[99,100] When administered intravenously in humans, side effects including nausea, vomiting, and urticaria are not uncommon.[101–103] Apparent nausea and occasional vomiting are also noted in some dogs administered intravenous fluorescein. Photosensitivity has also been reported in humans.[104,105] The most serious consequence of intravenous fluorescein administration is potentially fatal anaphylaxis, which has been reported in humans and animals.[106] While anaphylaxis caused by fluorescein is rare, investigators should be aware of this potential.

Rose Bengal

Rose bengal is a halide derivative of fluorescein and is available as a 1% solution and in impregnated paper strips. Ophthalmic application via paper strip is reported to be much less irritating than application of solution.[107]

Rose bengal is commonly employed to detect dendritic corneal epithelial ulcers caused by herpesviruses[108,109] and has recently been suggested to be useful in the diagnosis of corneal microerosions associated with equine keratomycosis.[110] Although rose bengal has classically been considered a vital stain, staining only dead or devitalized epithelial cells, it has been more recently demonstrated to stain healthy corneal epithelium when there is poor coverage of the surface epithelium by the preocular tear film or its components.[111,112] Rose bengal is therefore commonly employed in the diagnosis of keratoconjunctivitis sicca (KCS).

Rose bengal has dose-dependent toxic effects on corneal epithelial cells.[112,113] In humans with KCS, corneal application of rose bengal in eyes preinstalled with fluorescein resulted in the appearance of fluorescein-positive microdots, likely related to disruption of superficial epithelial intercellular junctions allowing fluorescein penetration.[114] However, the clinical significance of these induced changes is unclear. Rose bengal also has toxic effects against bacteria[115,116] and viruses.[117,118] Activity against herpesvirus appears to be light dependent, and while rose bengal use can interfere with virus isolation, it appears to have no therapeutic effect in vivo.[119] However, its use prior to collection of samples for herpesvirus isolation may produce negative results.[118,120] Herpesvirus detection by polymerase chain reaction (PCR) is not affected by prior rose bengal staining.[120]

Lissamine Green

Lissamine green is a synthetic organic acid dye reported to have a staining profile similar to that of rose bengal.[121] It has been characterized as a true vital dye because it does not stain healthy cells even in the absence of the preocular tear film but does stain membrane-damaged cells.[122] It has been suggested that lissamine green is equally as useful as rose bengal in the evaluation of the ocular surface in KCS patients, yet is better tolerated by patients.[123] Additionally, lissamine green is noncytotoxic to corneal epithelial cells.[113] Lissamine green has been reported to stain herpetic corneal epithelial lesions,[121,122] but it does not interfere with herpesvirus replication or PCR results.[120,122] Despite these apparently appealing characteristics of this vital stain, its utility in veterinary ophthalmology has yet to be defined.

Trypan Blue

The azo dye trypan blue is seeing increasingly common use in human cataract surgery to stain the anterior lens capsule and facilitate its visualization during capsulorrhexis,[124,125] and it is used by many veterinary ophthalmologists for this purpose. It can be particularly helpful when complete cataract and lack of fundic reflex impair visualization of the anterior capsule. Various methods of dye application have been reported, including injection under air and injection under viscoelastic or mixed with viscoelastic.[126–129] While concentrations of 0.1% are most commonly used, concentrations as low as 0.0125% reportedly achieve satisfactory capsular staining.[127] Based upon published in vitro studies, corneal endothelial toxicity

from 0.1% trypan blue should not be a concern under normal usage conditions.[130–132]

TEAR SUBSTITUTES AND STIMULATORS

Tear Substitutes

Tear replacement solutions and ointments are widely used in the management of quantitative and qualitative tear film disorders in animals; the most common of these is canine immune-mediated KCS. Tear substitutes serve a host of purposes in these diseases, the most obvious being provision of lubrication to improve comfort levels in affected animals. Additionally, optical aberrations induced by poor tear film quality[133] are improved with artificial tear supplementation, potentially resulting in improved vision.[134,135] A wide array of products of varying compositions are commercially available, some of which contain preservatives while others are preservative free. The recommended frequency of application depends upon the agent used and severity of disease. Because of corneal epithelial toxicity associated with preservatives, particularly benzalkonium chloride, use of preservative-free medications is often advocated for people with severe KCS in whom frequent application of solutions is indicated.[136–139] Clinical trials to assess for clinically deleterious effects of artificial tears with preservatives have not been performed in companion animals. Preservative-free tear substitutes are provided in single-dose packaging and are generally considerably more costly than products containing preservatives.

Limitations to the use of tear substitutes include intermittent application (as opposed to the continuous flow of natural tears) and the inability of tear substitutes to replicate the specific molecular composition and trilaminar nature of the normal tear film. In order to improve tear substitute efficacy, improved corneal adhesion and prolonged corneal contact are desirable. Common agents included in tear replacement solutions include polyvinyl alcohol, cellulose polymers (e.g., methylcellulose, carboxymethylcellulose, hydroxypropyl methylcellulose), polyethylene glycol, dextran, polyvinylpyrrolidone, and hyaluronate. With their prolonged action relative to solutions, artificial tear ointments are also commonly utilized in the management of KCS. Due to the hypertonic nature of the tear film in KCS, most appropriate tear replacement products are hypotonic or isotonic. Studies have not been reported for companion animals, and human studies conflict somewhat on the ideal tonicity of artificial tears in the management of dry eye. It has been reported that isotonic and hypotonic tear replacement solutions are equally beneficial in humans with mild KCS,[140] whereas hypotonic solutions are a more effective treatment in people with severe dry eye, where it results in improved tear film stability, corneal staining, and conjunctival cytology compared to isotonic solutions.[141]

As implied in the preceding text, the ideal tear replacement solution has yet to be identified. Hyaluronate solution appears to pose a number of potential therapeutic advantages as a tear replacement agent. Its relatively high viscosity leads to prolonged ocular retention, yet reduced viscosity under the shear stress of eyelid closure (due to its pseudoplasticity) facilitates natural blinking. Sodium hyaluronate has been shown to suppress breakup of the tear film in humans.[142,143] Specifically, tear film stability is prolonged with hyaluronate at concentrations of 0.1% or higher.[142] Controlled studies comparing 0.1% hyaluronate with 1.4% polyvinyl alcohol and 0.9% NaCl solution in humans with dry eye showed significant benefits from hyaluronate with regard to clinical symptoms and reduction in rose bengal staining.[144,145] Sodium hyaluronate has also been demonstrated to exert a positive influence on corneal epithelial migration in vitro and in vivo,[146–148] which may provide an additional benefit in patients with KCS because of the common occurrence of corneal ulceration in this population.

Autologous Serum

The composition of tears and serum closely resemble each other in a number of respects, with some exceptions including serum containing more vitamin A, lysozyme, fibronectin, and TGF-B1, and less IgA, EFG, and vitamin C than tears.[149] Improvement in tear film breakup times, corneal vital staining, pain scores, and impression cytology have been documented in humans with KCS who were treated with topical autologous serum.[150–153]

Lacrimostimulants

Cyclosporine

Cyclosporine (CSA), a naturally occurring fungal metabolite, exhibits immunosuppressive mechanisms related to the binding of nuclear proteins required for initiation of T-cell activation, preventing T-cell production of specific inflammatory cytokines such as interleukin (IL)-2 and IL-4 and thereby disrupting immune-mediated processes.[154] Because of its highly specific inhibition of T-cell activation, CSA has been used to treat a number of immune-mediated ocular disorders in animals, including KCS.

In early studies using a 1% to 2% solution of CSA in an oil base, 75% to 82% of idiopathic canine KCS cases showed significant improvement in aqueous tear production and clinical signs, although positive responses sometimes required 2 to 3 months of treatment.[155–158] A 0.2% ointment product was subsequently shown to be similarly efficacious.[159] Increased aqueous tear production is more likely to result in dogs with initial STT values higher than 2 mm/min than in dogs with STT values of 0 to 2 mm/min, presumably because of more extensive and irreversible lacrimal acinar destruction in the latter group.[155,159] Tear production in dogs with neurogenic KCS is not likely to improve with CSA treatment.[155] Beyond improvements in tear production, other clinical benefits of CSA therapy in KCS-affected animals include reduction of corneal vascularization and pigmentation.[160,161] This improvement in keratitis occurs even in dogs whose tear production does not increase.[155,159] In the treatment of KCS, twice-daily treatment is generally recommended for control of disease,

although once-daily administration appears clinically adequate in some dogs. However, it is not known whether or not low-grade lacrimal adenitis persists during low-frequency administration of CSA in KCS-affected dogs.

Multiple mechanisms of action are likely responsible for the therapeutic efficacy of CSA. T-cell suppression by CSA undoubtedly plays a major role in restoring tear production in dogs affected with immune-mediated lacrimal adenitis in which lymphocytic infiltration of lacrimal gland acini and ducts has been documented as a hallmark of the disease.[160] Improvement in conjunctival mucin stores in KCS-affected dogs has also been documented with CSA treatment, which may contribute to its therapeutic effect in this disease.[162] In dogs with spontaneous chronic idiopathic KCS, topical CSA suppresses lacrimal acinar and conjunctival epithelial cell apoptosis and facilitates lymphocytic apoptosis, leading to reestablishment of the normal apoptotic balance in affected dogs.[163] Considering the reversible increase in lacrimation that occurs in normal dogs treated with topical CSA, a direct lacrimal stimulant effect is also likely.[155] Some of its effects may also be related to stimulation of neurotransmitter release,[164] which appears to be impaired in KCS-affected animals.[165]

The primary side effect of topical CSA administration is ocular irritation, which occurs in a proportion of treated dogs and improves with continued treatment and resolution of disease.[157,159] In this author's experience, ocular irritation appears to be more common with compounded oil-based preparations than with the commercially available ointment-based product. However, dogs also on occasion will not tolerate the latter. Although reduction in blood lymphocyte counts and suppression of lymphocyte proliferation has been demonstrated in dogs receiving topical CSA,[166–168] adverse clinical sequelae linked to these findings have not been reported.

While topical CSA has been the treatment of choice for dogs with immune-mediated KCS, other similar drugs are beginning to emerge as effective therapeutic agents. Topical 0.02% tacrolimus has been recently documented to significantly increase tear production and improve clinical signs in dogs with naturally occurring KCS, including some animals that were nonresponsive to topical CSA treatment.[169] Additionally, a recent study evaluating pimecrolimus in eight dogs with KCS documented improvement in STT values and clinical signs in treated dogs.[170] These agents appear promising additions in the management of KCS, but their long-term safety is unknown. Of note are concerns regarding the carcinogenic potential of tacrolimus and pimecrolimus that have recently been raised.[171,172]

Pilocarpine

Topical and oral pilocarpine have long been recommended for the medical management of KCS,[173,174] but controlled studies involving KCS-affected animals are lacking. Applied topically, pilocarpine produces no detectable effect on tear production in normal dogs.[175] Oral pilocarpine has been described as efficacious in a case series of normal and KCS-affected animals, but signs of systemic toxicity (e.g., salivation, vomiting, inappropriate defecation, diarrhea) are common with this route of administration.[173] While largely supplanted in the treatment of KCS by drugs such as CSA, pilocarpine remains a viable treatment in dogs with neurogenic KCS wherein loss of parasympathetic innervation is the presumed cause of impaired lacrimal secretion. There is anecdotal support for this mode of therapy in such cases, but substantiating clinical trials have not been reported.

Other Potential Lacrimostimulants

In a recent limited study of three English Bulldogs with KCS induced by surgical removal of the gland of the nictitans, treatment with topical nerve growth factor resulted in significant improvements in Schirmer tear test, conjunctival goblet cell density, tear mucous, corneal haze, corneal sensitivity, and impression cytology.[176] Based upon these findings, further investigation of this treatment is warranted.

An open-label clinical trial evaluating the efficacy of oral α-interferon in dogs with chronic KCS found a favorable response in STT values in 55% of dogs.[177] The increase in STT values was modest, but posttreatment STT values in responders were significantly greater than their pretreatment STT values.[177] The exact role of these treatments as primary or adjunctive therapeutic measures in the management of KCS remains to be determined.

INTRAOCULAR IRRIGATING FLUIDS

Irrigating fluids are used during intraocular surgical procedures for several purposes, including maintenance of a formed anterior chamber, flushing of residual viscoelastic and other materials from the eye, cooling of phacoemulsification handpieces, and aiding in the removal of emulsified lens material during phacoemulsification. Many surgeons routinely utilize a variety of additives in their irrigating solutions, including heparin, epinephrine, antibiotics, and anesthetics, in an attempt to facilitate surgical procedures and enhance their outcomes. It is imperative that irrigating solutions and additives be nontoxic to the eye in general and the corneal endothelium in particular. In order to minimize adverse effects on the corneal endothelium, irrigating solutions and additives should approximate aqueous humor with regard to pH, osmolality, and ionic composition.

Commonly used irrigating solutions include lactated Ringer's solution (LRS), balanced salt solution (BSS), BSS-Plus (which contains oxidated glutathione and bicarbonate as well as dextrose), and 0.9% NaCl. There has been considerable study and debate about the ideal constitution of irrigating solutions with regard to preservation of corneal endothelium. In vitro work has shown that additives, particularly glutathione, help to preserve corneal endothelial cell junctions and pumping function.[178–182] Some,[283,184] but not all,[185] in vivo

studies in humans have supported this finding. In those in vivo studies in which a benefit has been attributed to glutathione, it appeared to benefit the corneal endothelium predominantly in the short term with no significant differences found over the long term. However, it would seem logical that individuals with preexisting corneal endothelial dysfunction would be most likely to benefit from such solutions.[184]

Studies evaluating various surgical irrigation fluids in companion animals are limited. Comparison of the corneal effects of irrigation with 0.9% NaCl, BSS, and BSS-Plus (100 ml over 22 minutes) in dogs revealed no significant differences between these fluids on corneal endothelial morphology or cell density.[186] A mild (4%) increase in corneal thickness was detected in saline-treated eyes in this study, but this was transient and not associated with detectable corneal edema.[186] A study comparing the effects of anterior chamber irrigation with BSS and BSS-Plus in cats revealed increased endothelial polymegathism and pleomorphism in BSS-treated eyes compared to BSS-Plus treatment.[187] However, 1 month later there were no detectable differences between treatment groups.[187]

Following evidence that free-radical formation during phacoemulsification contributes substantially to corneal endothelial damage,[188] addition of 0.001 M ascorbic acid to irrigating solution was recently evaluated and shown to protect corneal endothelium from such damage.[189] To be certain, investigators will continue to explore additives that may benefit surgical outcomes, but potential untoward effects of irrigating solution additives and preservatives on corneal endothelial function must always be considered.

Effects of irrigating fluid temperature have also been investigated. Use of cooled irrigating solution has been shown safe for the corneal endothelium in cats[190] and humans[184] and shown to decrease postoperative ocular inflammation in a rabbit model.[191] In humans undergoing phacoemulsification, early postoperative inflammation was decreased by use of cooled irrigating solution, but the beneficial effects were transient, with the cooled solution actually resulting in a more persistent low-grade disruption of the blood–aqueous barrier than room temperature solution.[192]

TOPICAL DISINFECTANTS

Appropriate presurgical preparation of the ocular surface is considered to play an important role in the prevention of postsurgical infection-related complications such as endophthalmitis. Dilute (1:10 to 1:50) povidone-iodine 10% solution is a widely used and effective topical antiseptic for veterinary ophthalmic surgical preparation and can be safely applied to the eyelids and corneoconjunctival surfaces.[193,194] When preparing a perforated eye, care should be taken to prevent introduction of concentrated povidone-iodine into the anterior chamber because it has been demonstrated to exhibit severe endothelial toxicity at 5% and 10% concentrations,[195] although concentrations of 0.1% or less are safe.[196] While the ideal regimen for prevention of postoperative endophthalmitis remains unclear, a recent manuscript reviewing relevant human ophthalmic literature concluded that preoperative povidone-iodine antisepsis is important in preventing postsurgical endophthalmitis, while other commonly utilized prophylactic methods, including subconjunctival antibiotic injection, lash trimming, preoperative topical antibiotics, and antibiotic-containing irrigation solutions, appear less so.[197] Additionally, povidone-iodine 5% applied topically at the conclusion of ocular surgery has been shown to provide residual antibacterial activity for at least 24 hours, while a single topical application of broad-spectrum antibiotic does not.[198] While povidone-iodine appears to be the standard disinfectant for ocular surface application, other compounds have also received some attention. In dogs, a comparison of chlorhexidine diacetate, chlorhexidine gluconate, and povidone-iodine solutions used for ocular surface antisepsis revealed 0.05% chlorhexidine gluconate and 0.2% povidone-iodine solutions to be well tolerated and similarly efficacious in reducing conjunctival bacterial numbers.[199] However, chlorhexidine diacetate was toxic to corneal epithelium and should not be utilized for ocular surface disinfection.[199] A study evaluating topical chlorhexidine gluconate in rabbits revealed no delay in corneal healing with concentrations less than or equal to 1%, but higher concentrations were found detrimental to epithelial regeneration.[200] Due to concerns of local toxicity, surgical scrubs should never be used on or near the conjunctival or corneal surface.[201]

VISCOELASTICS

The routine use of viscoelastic materials during ophthalmic surgery has increased the ease and success of many procedures. They are routinely employed during intraocular surgical procedures to help maintain anterior chamber depth during surgical manipulations, to assist in mobilization and dissection of tissues, to assist in control of hemorrhage, and to provide corneal endothelial protection from ultrasonic, mechanical, and irrigation[202] trauma as well as free-radical damage[203] during phacoemulsification procedures. Viscoelastics are also useful in the closure of full-thickness corneal wounds and in keratoplasty procedures, as well as a wetting agent to maintain corneal clarity during intraocular surgery. Their indispensable role as a surgical tool has led to the increasingly common use of the phrase ophthalmic viscosurgical devices, or OVDs, when referring to viscoelastic agents.

Ophthalmic viscoelastic agents must be biocompatible with the eye in all regards. A variety of suitable agents are commercially available, the physical properties of each being dictated by such physicochemical variables as molecular chain length and intramolecular and intermolecular interactions.[204] Familiarity with the specific rheologic properties of a variety of viscoelastic agents allows the ophthalmic surgeon to choose the most appropriate agent to suit the surgical situation. The rheologic properties of importance are viscosity, pseudoplasticity, elasticity, cohesiveness, and coatability.[204]

Viscosity is the primary determinant of a substance's resistance to flow. At a given temperature, viscosity is a function of

the substance's molecular weight and concentration. Because physiologic osmolarity must be maintained, increases in the viscosity of an ophthalmic viscoelastic are made by increasing the molecular weight of its constituent agent. The higher the viscosity of a solution, the less likely it is to displace from the anterior chamber and the more useful it is in the dissection of tissues. *Pseudoplasticity* is the behavior of a substance the viscosity of which changes in relation to shear rate. With substances exhibiting pseudoplasticity, viscosity decreases as shear rate increases, and vice versa. This property allows a substance that is extremely viscous at rest to be extruded through a thin cannula. Ophthalmic viscoelastics vary significantly with regard to pseudoplasticity, with chondroitin sulfate demonstrating no pseudoplasticity, HPMC being intermediate, and sodium hyaluronate demonstrating high pseudoplasticity. *Elasticity* is the ability of a substance to regain its original shape following deformation. It is this property of ophthalmic viscoelastic substances that provides protection from mechanical insults such as the high frequency vibrations associated with phacoemulsification. *Cohesiveness* is the degree to which a substance adheres to itself and is a function of molecular length, weight, and elasticity. Highly cohesive viscoelastics, such as hyaluronate, are easily aspirated as a single mass, whereas those that are less cohesive leave the eye in fragments. Cohesive viscoelastics are therefore removed from the eye quickly by the vacuum employed during phacoemulsification and provide little to no endothelial protection during this portion of the procedure. The *coatability* of a viscoelastic refers to its ability to adhere to other materials. Coatability is related to the surface tension and molecular charge of the viscoelastic and surface tension of the tissue, implant, or instrument that the viscoelastic is surrounding.

From a clinical standpoint, viscoelastics can be thought of in terms of higher-viscosity cohesive agents and lower-viscosity dispersive agents.[205] Cohesive agents are best at creating and preserving space, while dispersive agents are more readily maintained in the anterior chamber (e.g., adjacent to the corneal endothelium during phacoemulsification) and are capable of partitioning spaces. Newer viscoelastic agents have been formulated to be viscoadaptive, reportedly possessing the advantages of dispersive and cohesive agents depending on the flow rate and turbulence within the eye.[206] At steady state or low shear rates, these viscoadaptive substances are very cohesive, but at mid to high shear rates, they fracture and become pseudodispersive.[207]

While new developments are on the horizon, currently available ophthalmic viscoelastic substances include sodium hyaluronate, hydroxypropylmethylcellulose, and chondroitin sulfate. Sodium hyaluronate is commercially available in several concentrations and molecular weights. It is an exceptionally cohesive substance and excels at maintaining a formed anterior chamber during intraocular manipulations that do not involve aspiration (e.g., during capsulorrhexis). However, this cohesive property also results in rapid removal of the substance once vacuum is applied, thus reducing its ability to protect the corneal endothelium during phacoemulsification. In one study, low-molecular-weight hyaluronate was shown to afford better endothelial protection than high-molecular-weight sodium hyaluronate.[208] Hydroxypropylmethylcellulose is available as a 2% product at various molecular weights. It is less cohesive and less viscous than sodium hyaluronate but exhibits better coatability. Chondroitin sulfate is combined with sodium hyaluronate for ophthalmic use because it is not sufficiently viscous to permit its use as a sole agent. Chondroitin sulfate-hyaluronate combination viscoelastic has been shown to provide superior coating of the corneal endothelium,[209] and some studies have demonstrated an advantage of this product with regard to endothelial protection during phacoemulsification.[210,211] However, other studies have found no difference between chondroitin sulfate-hyaluronate and other viscoelastics in this regard.[212–214] The disparity in these results may be related to study design and different surgical techniques employed in the studies.

The primary drawback to the use of viscoelastic agents in ophthalmic surgery is their potential to contribute to postoperative ocular hypertension. This problem is particularly pronounced if the substance is left in the anterior chamber at the conclusion of surgery. The use of hyaluronidase has been shown to minimize ocular hypertension associated with viscoelastics in human cataract surgery,[215,216] but similar reports do not exist in animals. It has also been suggested that prolonged viscoelastic contact with the corneal endothelium can result in endothelial toxicity,[217] but there is no substantial supportive documentation of this.[218,219] While the benefits of surgical viscoelastics clearly outweigh these risks, the ophthalmic surgeon recognize the potential complication of postoperative ocular hypertension and take appropriate measures to minimize it.

FIBRINOLYTICS AND ANTIFIBRINOLYTICS

Fibrinolytics

Ophthalmic application of fibrinolytic agents is directed at preventing or reducing the complications associated with intraocular fibrin formation, including synechia, pupillary seclusion, glaucoma valve implant occlusion, and retinal traction band formation, among others. Of the various fibrinolytic agents available, tissue plasminogen activator (tPA) is the only one with widespread ophthalmic application. Tissue plasminogen activator is a serine protease that converts plasminogen to plasmin in the presence of fibrin, resulting in rapid fibrinolysis. Indications for ophthalmic tPA administration include postoperative, postinflammatory, and posttraumatic intraocular fibrin and blood clot formation. When used following hyphema, there is a potential for rebleeding to occur.[220]

The intracameral tPA dose most commonly used in veterinary ophthalmology is 25 μg.[221] Because of its considerable expense, a vial of tPA is generally diluted to 250 μg/ml, divided into multiple small aliquots of 0.1 to 1.0 ml, and

frozen for future use. Because the product does not contain an antibacterial preservative,[222] preparation must be performed under strictly aseptic conditions, preferably under a sterile hood.[223] Despite concerns cited by the manufacturer,[222] product diluted in this manner has been documented to retain fibrinolytic activity for over a year when stored at –70°C.[223] Intracameral administration results in rapid fibrinolysis, often beginning within 15 to 30 minutes. Completeness of fibrinolysis depends largely on the duration that the fibrin has been present in the eye.

Administration of tPA for intracameral fibrinolysis has been investigated in companion animal species. Experimentally in dogs, intracameral administration of 25 μg tPA resulted in rapid anterior chamber fibrinolysis and was nontoxic to corneal endothelium.[224,225] However, intracameral administration of 50 μg resulted in mild endothelial toxicity.[225] While topical administration results in detectable levels of tPA in aqueous humor,[226] it does not achieve significant fibrin clot resolution in dogs.[227] A published series of cases in companion animals has documented the efficacy of tPA in a variety of clinical scenarios in several species.[221]

Toxicity of intravitreal tPA injection has been studied experimentally in cats and rabbits.[228–230] In cats, intravitreal injection of 25 μg/0.1 ml did not result in detectable toxicity, but dose-dependent toxicity was noted with injections of 50 μg or greater.[230] Toxic changes in affected cats included anterior segment inflammation, visible fundic alterations, histologic photoreceptor loss, and electroretinographic changes.[230] Similar toxic changes in rabbits were attributed to the L-arginine vehicle of the commercial product tested rather than to tPA itself.[228] Retinal toxicity following intravitreal tPA injection has also been described in human case reports.[231,232]

Other fibrinolytics with much more limited ophthalmic applications include streptokinase and urokinase. Ophthalmic applications of novel fibrinolytics such as tenecteplase and lanoteplase have not been reported.

Antifibrinolytics

Optimal medical management of traumatic hyphema remains controversial, but antifibrinolytics such as aminocaproic acid (ACA) have been utilized to reduce the potential for rebleeding following traumatic hyphema in humans, with many clinical trials supporting its effectiveness.[233–235] Due to numerous side effects associated with systemic ACA administration, including nausea, dizziness, and hypotension, efficacy of topical ACA administration has also been evaluated. Topical ACA has been shown to reduce the incidence of rebleeding following traumatic hyphema in some studies[236–238] but not others.[239] Some human studies have also shown tranexamic acid to be effective in reducing rebleeding following traumatic hyphema.[240,241] The use and effectiveness of antifibrinolytic medications in the management of hyphema in companion animals has not been reported.

Recently, topical ophthalmic application of antifibrinolytic agents has been advocated as potentially beneficial in the promotion of corneal epithelialization through the preservation of fibronectin in the corneal wound bed. Experimental studies in rats and rabbit models have demonstrated benefit of topical ACA and tranexamic acid administration on corneal epithelization.[242,243] A recent clinical study in dogs with nonhealing corneal ulcers showed a 94% cure rate with topical ACA (35.7 mg/ml; applied 3 times daily) following debridement versus a 41% cure rate with topical gentamicin treatment following debridement.[244]

ANTIFIBROTIC AGENTS

Mitomycin C

Mitomycin C (MMC) is an antibiotic compound isolated from the fungus *Streptomyces caespitosus.* It is a potent inhibitor of DNA synthesis and fibroblast proliferation commonly used during glaucoma valve implant surgery to reduce collagen deposition and thereby suppress fibrosis surrounding the implant. It is generally applied using a Weck-cell sponge soaked in 0.4 to 0.5 mg/ml MMC with a contact time of 5 minutes, followed by copious saline lavage. Several reports describe its use during valve implant surgery in glaucomatous dogs.[245–247] Two experimental studies evaluating the effectiveness of MMC as an adjunct treatment for glaucoma valve implant surgery in normal dogs revealed that while its use significantly decreased fibrosis associated with filtering blebs, no differences in facility of outflow were found between MMC-treated eyes and saline controls.[248,249] There are conflicting reports in the human ophthalmic literature regarding the effectiveness of MMC in glaucoma valve surgery. Perhaps most significantly, a recent randomized controlled prospective study involving human glaucoma patients undergoing valve implant surgery found no difference in outcome between MMC-treated eyes and BSS controls.[250] While most clinical trials in dogs have suggested the addition of MMC to filtering or valve procedures is safe, a prospective randomized controlled study is required to determine its clinical effectiveness in the management canine glaucoma.

There is considerable evidence of toxic effects on the ciliary body and resultant suppression of aqueous flow associated with episcleral application of MMC,[251–254] but such effects have not been investigated in companion animals.

5-Fluorouracil

A pyrimidine analog, 5-fluorouracil (5-FU) inhibits RNA and DNA synthesis, culminating in cell death. It is particularly effective against rapidly dividing cells, such as fibroblasts, and is employed during glaucoma surgery to minimize fibrosis and subsequent bleb failure. As with mitomycin, there are clinical reports of its use in dogs with glaucoma.[247] Repeated subconjunctival injections are recommended, which makes use of this medication less attractive than MMC for canine patients. Subconjunctival administration of 5-FU has been shown to cause toxic changes in the ciliary body similar to what has been reported for mitomycin.[254] Prospective controlled studies using adjunctive 5-FU in glaucoma surgery have yet to be reported in dogs.

TISSUE ADHESIVES

The use of tissue adhesives in ophthalmology was first reported for the management of corneal disease.[255,256] Although corneal disease remains the most common ophthalmic indication for tissue adhesives, their reported use in human ophthalmology has grown to encompass temporary tarsorrhaphy, conjunctival closure, punctal occlusion, strabismus surgery, and retinal detachment surgery. Adhesives currently in common ophthalmic use include cyanoacrylate adhesives, of which there are several derivatives, and fibrin-based glues, with the former being much more commonly utilized. Recent veterinary ophthalmic clinical reports document the utility of cyanoacrylate adhesives for such conditions as refractory corneal ulceration, corneal stromal ulceration, corneal laceration, and descemetocele.[257,258]

Cyanoacrylate Adhesives

In addition to their adhesive properties, cyanoacrylates have demonstrated antibacterial properties, but only against Gram-positive organisms.[259–261] Despite demonstrated antibacterial properties, microbial keratitis has been associated with prolonged presence of glue on the corneal surface.[262,263] Cyanoacrylate adhesives also appear beneficial in halting corneal stromal melting, especially when applied early in the disease process, perhaps by preventing neutrophil access to the ulcer site.[262,263]

Cyanoacrylate derivatives with short side chains polymerize faster than those with long side chains. However, tissue toxicity from cyanoacrylate is related to the release of breakdown products, such as formaldehyde, and is less pronounced in those derivatives with butyl or longer side chains.[262] Minimizing the applied dose will also reduce toxicity.[255] As a compromise between fast polymerization, good tensile strength, and reduced toxicity, adhesives with butyl side chains appear to be in the greatest favor for ophthalmic application. A veterinary butyl derivative (Vetbond) was recently shown to be well tolerated by the rabbit cornea in an experimental model.[264]

Strict attention to application technique improves success with cyanoacrylate adhesives in the management of corneal disease.[255] The surface to be glued should be thoroughly dry at the time of application, which can be accomplished using cellulose sponges, and epithelium covering the surface to be glued should be debrided. Importantly, a minimal amount of adhesive should be used. The latter objective can be accomplished by using a small gauge (25–30 gauge) needle to apply a thin layer of adhesive over the affected surface. Blinking must be avoided until the glue polymerizes. Some advocate the use of a bandage contact lens postoperatively to minimize conjunctival reaction. Vote and Elder described an application method for corneal perforations that incorporates a patch (using Steri-Drape material) to provide a smooth surface and increased repair strength.[265]

Fibrin-Based Adhesives

Fibrin-based adhesives have not seen the widespread use in ophthalmology that cyanoacrylate adhesives have. However, reported human clinical ophthalmic application of fibrin-base adhesives has included persistent corneal surface defects,[266,267] corneal perforation,[266–269] conjunctival closure,[270–272] and corneal stem cell transplantation.[273] Fibrin glue is considerably more complex to prepare and apply, takes longer to polymerize, and has lower tensile strength than cyanoacrylate. However, because it is biologic, it may be covered by tissue such as conjunctiva, amniotic membrane, or cornea. To this author's knowledge, the ophthalmic use of fibrin glue has yet to be reported in the veterinary literature.

ANTICOLLAGENASE AGENTS

It is well recognized that under normal conditions the strictly coordinated activities of corneal proteinases, particularly matrix metalloproteinases (MMPs) and serine proteinases, play a central role in the maintenance of normal corneal architecture. Under pathologic conditions, however, dysregulation of these endogenous corneal proteinases as well as contributions from proteinases of microbial origin may result in progressive corneal stromal degradation.[274–276] Neutrophils arriving via the tear film or through the corneal stroma are another important source of collagenase.[274,277,278] Factors secreted by collagen-stimulated neutrophils augment collagen degradation by corneal fibroblasts through a stimulatory effect on MMP synthesis.[279]

Over the years, a number of antiproteinases have been employed clinically in an attempt to control corneal stromal degradation associated with these enzymatic processes. Compounds that have received particular attention in veterinary ophthalmic application include N-acetylcysteine, tetracyclines, ethylenediaminetetraacetic acid (EDTA), autogenous serum, and, to a lesser extent, synthetic inhibitors of MMPs (e.g., Galardin). Although many such agents have been demonstrated to have good in vitro activity against proteinases, thereby providing sound rationale for their use, evidence of their clinical effectiveness remains largely anecdotal. Following is a brief summary of the scientific evidence relating to these particular compounds and their respective potentials to provide corneal protection in the face of corneal proteolytic degradation. Because of the differing mechanisms of action of these various compounds, it is reasonable to expect that additive or potentially synergistic effects may be obtained by using them in combination.

Acetylcysteine

Acetylcysteine has been shown to reduce proteolytic activity in numerous in vitro studies,[280–283] and it has been recommended for use in the management of corneal disease in companion animals at concentrations ranging from 1% to 10%.[284,285] However, confirmatory in vivo work has been limited. In one study, treatment with acetylcysteine had no significant effect on gelatinolytic activity or stromal collagenase levels after keratoprosthesis implantation in rabbits.[281]

Investigation of the influence of acetylcysteine on corneal epithelial healing rates in dogs showed more rapid epithelialization with 3% acetylcysteine, but not with 10% or 20%

concentrations, compared to controls.[286] While one study demonstrated that 10% and 20% acetylcysteine did not inhibit re-epithelialization in rabbits,[287] another demonstrated corneal epithelial necrosis following topical application of 20% acetylcysteine.[288]

EDTA

Presumably through binding of zinc and calcium, EDTA has been shown to strongly inhibit MMP activity in vitro,[283] which suggests that it may be useful in clinical scenarios as well.[289–291] However, there is little documentation of its clinical effectiveness.

Tetracyclines

Tetracycline antibiotics concentrate in the cornea following topical or systemic administration,[292–295] and their antiproteolytic properties have been well documented.[280,283,296] Systemic tetracycline (50 mg/kg/day) was shown to significantly reduce corneal perforation in a rabbit *Pseudomonas* model[297] and to inhibit ulceration in an alkali-burn–induced ulceration model.[298] Systemic doxycycline (5 mg/kg/day) also promotes corneal re-epithelialization in the rabbit alkali-burn model.[299] Human case reports highlight the potential clinical utility of tetracyclines in the management of melting ulcers.[300,301] Systemic tetracycline has also been shown to assist healing in persistent corneal epithelial defects in humans.[302,303]

Multiple mechanisms, independent of their antimicrobial effects, are likely for the antiprotease activity of tetracyclines. Included among their potential mechanisms are chelation of cations necessary for enzyme activity (i.e., zinc and calcium),[291] inhibition of gene expression,[304] and inhibition of α_1-antitrypsin degradation.[305,306] Inhibition of leukotaxis[307] may be another element in the purported effectiveness of tetracyclines in the management of melting ulcers. Based upon evidence that tetracyclines more readily inhibit collagenase produced by neutrophils than that produced by fibroblasts,[308] it has been suggested that inhibition of neutrophil collagenase can likely be achieved clinically, while inhibition of collagenase from fibroblasts is less likely.[309]

Serum

Autologous serum is purportedly beneficial in managing corneal ulcers because of its antiproteolytic properties,[291] which has been well documented through in vitro studies.[282,283] Antiproteolytic activity in serum is accounted for by the presence of α_2-macroglobulin and α_1-antitrypsin.[310,311] In addition to antiproteolytic properties, serum has epitheliotrophic properties that may promote corneal healing.[312] Serum has been shown to be superior to plasma with regard to stimulation of corneal epithelial growth, migration, and differentiation, presumably because of higher concentrations of epithelial growth factor and platelet-derived growth factor and vitamin A in the former.[313]

Although serum is commonly used in the treatment of a number of corneal diseases, including in the management of melting corneal ulcers, the methods of preparing serum for clinical use have varied widely. A recent investigation into the optimal method of processing of serum for ophthalmic use suggests allowing blood clotting for 120 minutes or longer at room temperature, centrifugation at 3000x*g* for 15 minutes, and dilution to 25% with BSS.[312] This recommendation is based upon assayed serum epitheliotrophic factor levels and in vitro corneal epithelial growth patterns using serum prepared according this protocol compared to several others.[312] In contrast to this recommendation of using diluted serum, others have suggested that 100% serum may be preferred on the basis of in vitro evidence of diminished cellular toxicity compared to 50% serum.[314] Fortunately, serum factors are stable at –4°C for at least 1 month and at –20°C for at least 3 months,[151] so harvested serum can be stored easily and effectively for future use. Because serum is an excellent microbial growth medium, strict attention to asepsis during preparation and use is of paramount importance.

Synthetic Protease Inhibitors (Galardin, Ilomostat)

Synthetic thiol-containing MMP inhibitors have been shown to strongly inhibit protease activity in vitro.[279,283] In vivo experimental studies in rabbits have also been promising, with demonstrated benefit from MMP inhibition in a variety of corneal injury models.[315,316]

Multiple mechanisms are likely responsible for the beneficial effects of synthetic MMP inhibitors. In vitro work has shown that these agents reduce collagen degradation by *Pseudomonas aeuruginosa* through direct inhibition of active MMPs, and also prevent the conversion of proMMPs to active MMPs.[317,318] It has also been demonstrated that inflammatory cytokine expression is suppressed by synthetic MMP inhibitors, which may reduce corneal destruction indirectly through diminished cytokine-mediated chemotaxis of neutrophils to the ulcer site.[319] Based upon the evidence thus far, synthetic protease inhibitors may have a role in the management of proteolytic corneal degradation in companion animals.

REFERENCES

1. Nowak MR, Neumann W. Refraction of the dog eye. *Klin Monatsbl Augenheilkd* 1987; 191: 81–83.
2. Murphy CJ, Zadnik K, Mannis MJ. Myopia and refractive error in dogs. *Invest Ophthalmol Vis Sci* 1992; 33: 2459–2463.
3. Lundberg B, Behndig A. Intracameral mydriatics in phacoemulsification cataract surgery. *J Cataract Refract Surg* 2003; 29: 2366–2371.
4. Behndig A, Eriksson A. Evaluation of surgical performance with intracameral mydriatics in phacoemulsification surgery. *Acta Ophthalmol Scand* 2004; 82: 144–147.
5. Hollingsworth SR, Canton DD, Buyukmihci NC, Farver TB. Effect of topically administered atropine on tear production in dogs. *J Am Vet Med Assoc* 1992; 200: 1481–1484.
6. Rubin LF, Wolfes BS. Mydriatics for canine ophthalmoscopy. *J Am Vet Med Assoc* 1962; 140: 137–141.

7. Lynch R, Rubin LF. Salivation induced in dogs by conjunctival instillation of atropine. *J Am Vet Med Assoc* 1965; 147: 511–513.
8. Gelatt KN, Boggess TS, Cure TH. Evaluation of mydriatics in the cat. *J Am Anim Hosp Assoc* 1973; 9: 283–287.
9. Zekas LJ, Lester GB, Brooks DE. The effect of ophthalmic atropine on intestinal transit and myoelectric activity in normal adult horses. Proceedings of the 29th Annual Conference of the American College of Veterinary Ophthalmologists. Seattle, WA, 1998: 28.
10. Williams MM, Spiess BM, Pascoe PJ, O'Grady M. Systemic effects of topical and subconjunctival ophthalmic atropine in the horse. *Vet Ophthalmol* 2000; 3: 193–199.
11. Gettes BC, Bellmont O. Tropicamide. Comparative cycloplegic effects. *Arch Ophthalmol* 1961; 66: 336–340.
12. Hiatt RL, Jerkins G. Comparison of atropine and tropicamide in esotropia. *Ann Ophthalmol* 1983; 15: 341–343.
13. Lovasik JV. Pharmacokinetics of topically applied cyclopentolate HCl and tropicamide. *Am J Optom Physiol Opt* 1986; 63: 787–803.
14. Egashira SM, Kish LL, Twelker JD, Mutti DO, Zadnik K, Adams AJ. Comparison of cyclopentolate versus tropicamide cycloplegia in children. *Optom Vis Sci* 1993; 70: 1019–1026.
15. Mori M, Araie M, Sakurai M, Oshika T. Effects of pilocarpine and tropicamide on blood-aqueous barrier permeability in man. *Invest Ophthalmol Vis Sci* 1992; 33: 416–423.
16. Petternel V, Findl O, Kruger A, Schauersberger J, Amon M. Effect of tropicamide on aqueous flare before and after cataract surgery. *J Cataract Refract Surg* 2000; 26: 382–385.
17. Margadant DL, Kirkby K, Andrew SE, Gelatt KN. Effect of topical tropicamide on tear production as measured by Schirmer's tear test in normal dogs and cats. *Vet Ophthalmol* 2003; 6: 315–320.
18. Gelatt KN, Gum GG, MacKay EO. Evaluation of mydriatics in cattle. *Vet Comp Ophthalmol* 1995; 5: 46–49.
19. Gelatt KN, Gum GG, MacKay EO. Evaluation of mydriatics in horses. *Vet Comp Ophthalmol* 1995; 5: 104–108.
20. Davis JL, Stewart T, Brazik E, Gilger BC. The effect of topical administration of atropine sulfate on the normal equine pupil: Influence of age, breed and gender. *Vet Ophthalmol* 2003; 6: 329–332.
21. Salazar M, Patil PN. An explanation for the long duration of mydriatic effect of atropine in eye. *Invest Ophthalmol* 1976; 15: 671–673.
22. Salazar M, Shimada K, Patil PN. Iris pigmentation and atropine mydriasis. *J Pharm Exp Ther* 1976; 197: 79–88.
23. McGregor MLK. Anticholinergic agents (parasympatholytics). In: Mauger TF, Craig EL, eds. *Havener's Ocular Pharmacology,* 6th ed. St. Louis: Mosby, 1994: 140–171.
24. Summers WK, Reich TC. Delirium after cataract surgery: Review and two cases. *Am J Psychiatry* 1979; 136: 386–391.
25. Ward DA. Clinical Pharmacology and Therapeutics. Part 3. In: Gelatt KN, ed. *Veterinary Ophthalmology,* 3rd ed. Philadelphia: Lippincott Williams and Wilkins, 1999: 336–354.
26. Boydell P. The accuracy of denervation hypersensitivity testing with 10% phenylephrine eyedrops in Horner's syndrome in the dog. Proceedings of the 30th Annual Conference of the American College of Veterinary Ophthalmologists. Chicago, IL, 1999: 49.
27. Pascoe PJ, Ilkiw JE, Stiles J, Smith EM. Arterial hypertension associated with ocular use of phenylephrine in dogs. *J Am Vet Med Assoc* 1994; 205: 1562–1564.
28. Herring IP, Jacobson JD, Pickett JP. Cardiovascular effects of topical ophthalmic 10% phenylephrine in dogs. *Vet Ophthalmol* 2004; 7: 41–46.
29. Katz RL, Matteo RS, Papper EM. The injection of epinephrine during general anesthesia. II. Halothane. *Anesthesiology* 1962; 23: 597–600.
30. Rubin LF. Applications of adrenergic drugs in ophthalmology. *J Am Anim Hosp Assoc* 1968; 4: 250–255.
31. Zink J, Sasyniuk BI, Dresel PE. Halothane-epinephrine-induced cardiac arrhythmias and the role of heart rate. *Anesthesiology* 1975; 43: 548–555.
32. Muir WW, Werner LL, Hamlin RL. Arrhythmias in dogs associated with epinephrine and thiamylal anesthesia. *Am J Vet Res* 1975; 36: 1291–1297.
33. Atlee JL, Malkinson CE. Potentiation by thiopental of halothane-epinephrine-induced arrhythmias in dogs. *Anesthesiology* 1982; 57: 285–288.
34. Bednarski RM, Muir WW. Arrhythmogenicity of dopamine, dobutamine, and epinephrine in thiamylal-halothane anesthetized dogs. *Am J Vet Res* 1983; 44: 2341–2343.
35. Bednarski RM, Majors LJ, Atlee JL. Epinephrine-induced ventricular arrhythmias in dogs anesthetized with halothane: Potentiation by thiamylal and thiopental. *Am J Vet Res* 1985; 46: 1829–1831.
36. Kamibayashi T, Hayashi Y, Sumikawa K, Yamatodani A, Kawabata K, Yoshiya I. Enhancement by propofol of epinephrine-induced arrhythmias in dogs. *Anesthesiology* 1991; 75: 1035–1040.
37. Hacker DV, Buyukmihci NC, Franti CE, Bellhorn RW. Effect of topical phenylephrine on the equine pupil. *Am J Vet Res* 1987; 48: 320–322.
38. Gwin RM, Gelatt KN, Gum GG, Peiffer RL Jr. Effects of topical 1-epinephrine and dipivalyl epinephrine on intraocular pressure and pupil size in the normotensive and glaucomatous Beagle. *Am J Vet Res* 1978; 39: 83–86.
39. Elliott A, Carter C. Pupil size after extracapsular cataract extraction and posterior chamber lens implantation: A prospective randomized trial of epinephrine and acetylcholine. *Ophthalmic Surg* 1989; 20: 591–594.
40. Corbett MC, Richards AB. Intraocular adrenaline maintains mydriasis during cataract surgery. *Br J Ophthalmol* 1994; 78: 95–98.
41. Liou SW, Yang CY. The effect of intracameral adrenaline infusion on pupil size, pulse rate, and blood pressure during phacoemulsification. *J Ocul Pharmacol Ther* 1998; 14: 357–361.
42. Edelhauser HF, Hyndiuk RA, Zeeb A, Schultz RO. Corneal edema and the intraocular use of epinephrine. *Am J Ophthalmol* 1982; 93: 327–333.
43. Slack JW, Edelhauser HF, Helenek MJ. A bisulfate-free intraocular epinephrine solution. *Am J Ophthalmol* 1990; 110: 77–82.
44. Scagliotti RH. Comparative Neuro-ophthalmology. In: Gelatt KN, ed. *Veterinary Ophthalmology.* Philadelphia: Lippincott Williams and Wilkins, 1999: 1307–1400.
45. Strichartz G. Molecular mechanisms of nerve block by local anesthetics. *Anesthesiology* 1976; 45: 421–441.

46. Catterall WA, Mackie CM. Local anesthetics. In: Hardman JG, Limbird LE, eds. *Goodman and Gilman's The Pharmacological Basis of Therapeutics*, 10th ed. New York: McGraw-Hill, 2001: 367–384.
47. Gelatt KN, Peiffer RL, Jr, Erickson JL, Gum GG. Evaluation of tear formation in the dog, using a modification of the Schirmer tear test. *J Am Vet Med Assoc* 1975; 166: 368–370.
48. Hamor RE, Roberts SM, Severin GA, Chavkin MJ. Evaluation of results for Schirmer tear tests conducted with and without application of a topical anesthetic in clinically normal dogs of 5 breeds. *Am J Vet Res* 2000; 61: 1422–1425.
49. Gunderson T, Liebman SD. Effect of local anesthetics on regeneration of corneal epithelium. *Arch Ophthalmol* 1944; 31: 29–33.
50. Behrendt T. Experimental study of corneal lesions produced by topical anesthesia. *Am J Ophthalmol* 1956; 41: 99–105.
51. Mengher LS, Pandher KS, Bron AJ. Topical anaesthetic and tear film stability. *Acta Ophthalmol Copenh* 1986; 64: 79–82.
52. Lemp MA, Hamill JR Jr. Factors affecting tear film breakup in normal eyes. *Arch Ophthalmol* 1973; 89: 103–105.
53. Badenoch PR, Coster DJ. Antimicrobial activity of topical anesthetic preparations. *Br J Ophthalmol* 1982; 66: 364–367.
54. Mullin GS, Rubinfeld RS. The antibacterial activity of topical anesthetics. *Cornea* 1997; 16: 662–665.
55. Koller C. Preliminary report on local anesthesia of the eye. *Arch Ophthalmol* 1934; 12: 473–474.
56. Boozan CW, Cohen IJ. Ophthaine, a new topical anesthetic for the eye. *Am J Ophthalmol* 1953; 36: 1619–1621.
57. Bartfield JM, Holmes TJ, Raccio-Robak N. A comparison of proparacaine and tetracaine eye anesthetics. *Acad Emerg Med* 1994; 1: 364–367.
58. Shafi T, Koay P. Randomised prospective masked study comparing patient comfort following the instillation of topical proxymetacaine and amethocaine. *Br J Ophthalmol* 1998; 82: 1285–1287.
59. Herring IP, Bobofchak MA, Landry MP, Ward DL. Duration of effect and effect of multiple doses of topical ophthalmic 0.5% proparacaine hydrochloride in clinically normal dogs. *Am J Vet Res* 2005; 66: 77–80.
60. Binder DR, Herring IP, Ward DL. Duration of effect of topical ophthalmic application of 0.5% proparacaine hydrochloride on corneal sensitivity in clinically normal cats. Proceedings of the 36th Annual Conference of the American College of Veterinary Ophthalmologists. Nashville, TN, 2005: 81.
61. Liu JC, Steinemann TL, McDonald MB, Thompson HW, Beuerman RW. Topical bupivacaine and proparacaine: A comparison of toxicity, onset of action, and duration of action. *Cornea* 1993; 12: 228–232.
62. Koch SA, Rubin LF. Ocular sensitivity of dogs to topical tetracaine HCl. *J Am Vet Med Assoc* 1969; 154: 15–16.
63. Carino NS, Slomovic AR, Chung F, Marcovich AL. Topical tetracaine versus topical tetracaine plus intracameral lidocaine for cataract surgery. *J Cataract Refract Surg* 1998; 24: 1602–1608.
64. Kadonosono K, Ito N, Yazama F, et al. Effect of intracameral anesthesia on the corneal endothelium. *J Cataract Refract Surg* 1998; 24: 1377–1381.
65. Heuermann T, Hartmann C, Anders N. Long-term endothelial cell loss after phacoemulsification: Peribulbar anesthesia versus intracameral lidocaine 1%: Prospective randomized clinical trial. *J Cataract Refract Surg* 2002; 28: 639–643.
66. Gerding PA Jr, Turner TL, Hamor RE, Schaeffer DJ. Effects of intracameral injection of preservative-free lidocaine on the anterior segment of the eyes in dogs. *Am J Vet Res* 2004; 65: 1325–1330.
67. Anderson NJ, Nath R, Anderson CJ, Edelhauser HF. Comparison of preservative-free bupivacaine vs. lidocaine for intracameral anesthesia: A randomized clinical trial and in vitro analysis. *Am J Ophthalmol* 1999; 127: 393–402.
68. Craig EL. Anesthesia. In: Mauger TF, Craig EL, eds. *Havener's Ocular Pharmacology,* 6th ed. St. Louis: Mosby, 1994: 201–233.
69. Laaka V, Nikki P, Tarkkanen A. Comparison of bupivacaine with and without adrenalin and mepivacaine with adrenalin in intraocular surgery. *Acta Ophthalmol Copenh* 1972; 50: 229–239.
70. Wong DH. Regional anaesthesia for intraocular surgery. *Can J Anaesth* 1993; 40: 635–657.
71. Dempsey GA, Barrett PJ, Kirby IJ. Hyaluronidase and peribulbar block. *Br J Anaesth* 1997; 78: 671–674.
72. Kallio H, Paloheimo M, Maunuksela EL. Hyaluronidase as an adjuvant in bupivacaine-lidocaine mixture for retrobulbar/peribulbar block. *Anesth Analg* 2000; 91: 934–937.
73. Raffe MR, Bistner SI, Crimi AJ, Ruff J. Retrobulbar block in combination with general anesthesia for equine ophthalmic surgery. *Vet Surg* 1986; 15: 139–141.
74. Kirsch RE, Samet P, Kugel V, Axelrod S. Electrocardiographic changes during ocular surgery and their prevention by retrobulbar injection. *AMA Arch Ophthalmol* 1957; 58: 348–356.
75. Mendelblatt FI, Kirsch RE, Lemberg L. A study comparing methods of preventing the oculocardiac reflex. *Am J Ophthalmol* 1962; 53: 506–512.
76. Yeatts RP, Doneyhue W, Scuderi PE, Brasington CR, James R. Effect of preemptive retrobulbar analgesia on perioperative hemodynamics and postoperative pain after enucleation. *Ophthal Plast Reconstr Surg* 2004; 20: 226–231.
77. Peterson DR. Nerve block of the eye and associated structures. *J Am Vet Med Assoc* 1951; 118: 145–148.
78. Accola PJ, Bentley E, Smith LJ, Forrest LJ, Baumel C, Murphy CJ. Retrobulbar injection technique and anesthesia in dogs. Proceedings of the 35th Annual Conference of the American College of Veterinary Ophthalmologists. Washington, D.C., 2004: 45.
79. Ramsay RC, Knobloch WH. Ocular perforation following retrobulbar anesthesia for retinal detachment surgery. *Am J Ophthalmol* 1978; 86: 61–64.
80. Mount AM, Seward HC. Scleral perforations during peribulbar anaesthesia. *Eye* 1993; 7(Pt 6): 766–767.
81. Rainin EA, Carlson BM. Postoperative diplopia and ptosis. A clinical hypothesis based on the myotoxicity of local anesthetics. *Arch Ophthalmol* 1985; 103: 1337–1339.
82. Salama H, Farr AK, Guyton DL. Anesthetic myotoxicity as a cause of restrictive strabismus after scleral buckling surgery. *Retina* 2000; 20: 478–482.
83. Han SK, Kim JH, Hwang JM. Persistent diplopia after retrobulbar anesthesia. *J Cataract Refract Surg* 2004; 30: 1248–1253.
84. Javitt JC, Addiego R, Friedberg HL, Libonati MM, Leahy JJ. Brain stem anesthesia after retrobulbar block. *Ophthalmol* 1987; 94: 718–724.

85. Cionni RJ, Osher RH. Retrobulbar hemorrhage. *Ophthalmol* 1991; 98: 1153–1155.
86. Nicoll JM, Acharya PA, Ahlen K, Baguneid S, Edge KR. Central nervous system complications after 6000 retrobulbar blocks. *Anesth Analg* 1987; 66: 1298–1302.
87. Hamilton RC. Brain-stem anesthesia as a complication of regional anesthesia for ophthalmic surgery. *Can J Ophthalmol* 1992; 27: 323–325.
88. Wittpenn JR, Rapoza P, Sternberg P, Jr., Kuwashima L, Saklad J, Patz A. Respiratory arrest following retrobulbar anesthesia. *Ophthalmol* 1986; 93: 867–870.
89. Carlson BM, Rainin EA. Rat extraocular muscle regeneration. Repair of local anesthetic-induced damage. *Arch Ophthalmol* 1985; 103: 1373–1377.
90. Porter JD, Edney DP, McMahon EJ, Burns LA. Extraocular myotoxicity of the retrobulbar anesthetic bupivacaine hydrochloride. *Invest Ophthalmol Vis Sci* 1988; 29: 163–174.
91. Okland S, Komorowski TE, Carlson BM. Ultrastructure of mepivacaine-induced damage and regeneration in rat extraocular muscle. *Invest Ophthalmol Vis Sci* 1989; 30: 1643–1651.
92. Carlson BM, Emerick S, Komorowski TE, Rainin EA, Shepard BM. Extraocular muscle regeneration in primates. Local anesthetic-induced lesions. *Ophthalmol* 1992; 99: 582–589.
93. Davis DB 2nd, Mandel MR. Posterior peribulbar anesthesia: An alternative to retrobulbar anesthesia. *J Cataract Refract Surg* 1986; 12: 182–184.
94. Davis DB 2nd, Mandel MR. Efficacy and complication rate of 16,224 consecutive peribulbar blocks. A prospective multicenter study. *J Cataract Refract Surg* 1994; 20: 327–337.
95. Briggs MC, Beck SA, Esakowitz L. Sub-Tenon's versus peribulbar anaesthesia for cataract surgery. *Eye* 1997; 11(Pt5): 639–643.
96. Ripart J, Lefrant JY, Vivien B, et al. Ophthalmic regional anesthesia: Medial canthus episcleral (sub-tenon) anesthesia is more efficient than peribulbar anesthesia: A double-blind randomized study. *Anesthesiology* 2000; 92: 1278–1285.
97. Smith LJ, Bentley E, Shih A, Miller PE. Systemic lidocaine infusion as an analgesic for intraocular surgery in dogs: A pilot study. *Vet Anaesth Analg* 2004; 31: 53–63.
98. da Silva Curiel JMA, Nasisse MP, Hook RR, Wilson HH, Collins K, Mandell CP. Topical fluorescein dye: Effects on immunofluorescent antibody test for feline herpesvirus keratoconjunctivitis. *Prog Vet Comp Ophthalmol* 1991; 1: 99–104.
99. Mengher LS, Bron AJ, Tonge SR, Gilbert DJ. Effect of fluorescein instillation on the pre-corneal tear film stability. *Curr Eye Res* 1985; 4: 9–12.
100. Patel S, Murray D, McKenzie A, Shearer DS, McGrath BD. Effects of fluorescein on tear breakup time and on tear thinning time. *Am J Optom Physiol Opt* 1985; 62: 188–190.
101. Karhunen U, Raitta C, Kala R. Adverse reactions to fluorescein angiography. *Acta Ophthalmol Copenh* 1986; 64: 282–286.
102. Kwiterovich KA, Maguire MG, Murphy RP, et al. Frequency of adverse systemic reactions after fluorescein angiography. Results of a prospective study. *Ophthalmol* 1991; 98: 1139–1142.
103. Jennings BJ, Mathews DE. Adverse reactions during retinal fluorescein angiography. *J Am Optom Assoc* 1994; 65: 465–471.
104. Danis RP, Stephens T. Phototoxic reactions caused by sodium fluorescein. *Am J Ophthalmol* 1997; 123: 694–696.
105. Danis RP, Wolverton S, Steffens T. Phototoxicity from systemic sodium fluorescein. *Retina* 2000; 20: 370–373.
106. Davidson MG, Baty KKT. Anaphylaxis associated with intravenous sodium fluorescein administration in a cat. *Prog Vet Comp Ophthalmol* 1991; 1: 127–128.
107. Scott PM. Rose bengal strips. *Am J Ophthalmol* 1979; 87: 572.
108. Marsh RJ, Fraunfelder FT, McGill JI. Herpetic corneal epithelial disease. *Arch Ophthalmol* 1976; 94: 1899–1902.
109. Nasisse MP, Guy JS, Davidson MG, Sussman WA, Fairley NM. Experimental ocular herpesvirus infection in the cat. Sites of replication, clinical features and effects of corticosteroid administration. *Invest Ophthalmol Vis Sci* 1989; 30: 1758–1768.
110. Brooks DE, Andrew SE, Denis H, et al. Rose bengal positive epithelial microerosions as a manifestation of equine keratomycosis. *Vet Ophthalmol* 2000; 3: 83–86.
111. Feenstra RP, Tseng SC. Comparison of fluorescein and rose bengal staining. *Ophthalmol* 1992; 99: 605–617.
112. Feenstra RP, Tseng SC. What is actually stained by rose bengal? *Arch Ophthalmol* 1992; 110: 984–993.
113. Kim J, Foulks GN. Evaluation of the effect of lissamine green and rose bengal on human corneal epithelial cells. *Cornea* 1999; 18: 328–332.
114. Tabery HM. Toxic effect of rose bengal dye on the living human corneal epithelium. *Acta Ophthalmol Scand* 1998; 76: 142–145.
115. Banks JG, Board RG, Carter J, Dodge AD. The cytotoxic and photodynamic inactivation of micro-organisms by Rose Bengal. *J Appl Bacteriol* 1985; 58: 391–400.
116. Dahl TA, Midden WR, Neckers DC. Comparison of photodynamic action by Rose Bengal in gram-positive and gram-negative bacteria. *Photochem Photobiol* 1988; 48: 607–612.
117. Roat MI, Romanowski E, Araullo-Cruz T, Gordon YJ. The antiviral effects of rose bengal and fluorescein. *Arch Ophthalmol* 1987; 105: 1415–1417.
118. Chodosh J, Banks MC, Stroop WG. Rose bengal inhibits herpes simplex virus replication in vivo and human corneal epithelial cells in vitro. *Invest Ophthalmol Vis Sci* 1992; 33: 2520–2527.
119. Brooks SE, Kaza V, Nakamura T, Trousdale MD. Photoinactivation of herpes simplex virus by rose bengal and fluorescein. In vitro and in vivo studies. *Cornea* 1994; 13: 43–50.
120. Stroop WG, Chen TM, Chodosh J, et al. PCR assessment of HSV-1 corneal infection in animals treated with rose bengal and lissamine green B. *Invest Ophthalmol Vis Sci* 2000; 41: 2096–2102.
121. Norn MS. Lissamine green. Vital staining of cornea and conjunctiva. *Acta Ophthalmol Copenh* 1973; 51: 483–491.
122. Chodosh J, Dix RD, Howell RC, Stroop WG, Tseng SC. Staining characteristics and antiviral activity of sulforhodamine B and lissamine green B. *Invest Ophthalmol Vis Sci* 1994; 35: 1046–1058.
123. Manning FJ, Wehrly SR, Foulks GN. Patient tolerance and ocular surface staining characteristics of lissamine green versus rose bengal. *Ophthalmol* 1995; 102: 1953–1957.
124. Melles GR, de Waard PW, Pameyer JH, Houdijn Beekhuis W. Trypan blue capsule staining to visualize the capsulorhexis in cataract surgery. *J Cataract Refract Surg* 1999; 25: 7–9.
125. Jacob S, Agarwal A, Agarwal A, et al. Trypan blue as an adjunct for safe phacoemulsification in eyes with white cataract. *J Cataract Refract Surg* 2002; 28: 1819–1825.

126. Kayikicioglu O, Erakgun T, Guler C. Trypan blue mixed with sodium hyaluronate for capsulorhexis. *J Cataract Refract Surg* 2001; 27: 970.
127. Yetik H, Devranoglu K, Ozkan S. Determining the lowest trypan blue concentration that satisfactorily stains the anterior capsule. *J Cataract Refract Surg* 2002; 28: 988–991.
128. Caporossi A, Balestrazzi A, Alegente M, Casprini F, Caporossi T. Trypan blue staining of the anterior capsule: The one-drop technique. *Ophthalmic Surg Lasers Imaging* 2005; 36: 432–434.
129. Wong VW, Lai TY, Lee GK, Lam PT, Lam DS. A prospective study on trypan blue capsule staining under air vs under viscoelastic. *Eye* 2005.
130. van Dooren BT, de Waard PW, Poort-van Nouhuys H, Beekhuis WH, Melles GR. Corneal endothelial cell density after trypan blue capsule staining in cataract surgery. *J Cataract Refract Surg* 2002; 28: 574–575.
131. van Dooren BT, Beekhuis WH, Pels E. Biocompatibility of trypan blue with human corneal cells. *Arch Ophthalmol* 2004; 122: 736–742.
132. Chang YS, Tseng SY, Tseng SH, Chen YT, Hsiao JH. Comparison of dyes for cataract surgery. Part 1: Cytotoxicity to corneal endothelial cells in a rabbit model. *J Cataract Refract Surg* 2005; 31: 792–798.
133. Tutt R, Bradley A, Begley C, Thibos LN. Optical and visual impact of tear break-up in human eyes. *Invest Ophthalmol Vis Sci* 2000; 41: 4117–4123.
134. Liu Z, Pflugfelder SC. Corneal surface regularity and the effect of artificial tears in aqueous tear deficiency. *Ophthalmol* 1999; 106: 939–943.
135. Montes-Mico R, Caliz A, Alio JL. Changes in ocular aberrations after instillation of artificial tears in dry-eye patients. *J Cataract Refract Surg* 2004; 30: 1649–1652.
136. Lopez Bernal D, Ubels JL. Quantitative evaluation of the corneal epithelial barrier: Effect of artificial tears and preservatives. *Curr Eye Res* 1991; 10: 645–656.
137. Berdy GJ, Abelson MB, Smith LM, George MA. Preservative-free artificial tear preparations. Assessment of corneal epithelial toxic effects. *Arch Ophthalmol* 1992; 110: 528–532.
138. Gobbels M, Spitznas M. Corneal epithelial permeability of dry eyes before and after treatment with artificial tears. *Ophthalmol* 1992; 99: 873–878.
139. Palmer RM, Kaufman HE. Tear film, pharmacology of eye drops, and toxicity. *Curr Opin Ophthalmol* 1995; 6: 11–16.
140. Papa V, Aragona P, Russo S, Di Bella A, Russo P, Milazzo G. Comparison of hypotonic and isotonic solutions containing sodium hyaluronate on the symptomatic treatment of dry eye patients. *Ophthalmologica* 2001; 215: 124–127.
141. Aragona P, Di Stefano G, Ferreri F, Spinella R, Stilo A. Sodium hyaluronate eye drops of different osmolarity for the treatment of dry eye in Sjogren's syndrome patients. *Br J Ophthalmol* 2002; 86: 879–884.
142. Hamano T, Horimoto K, Lee M, Komemushi S. Sodium hyaluronate eyedrops enhance tear film stability. *Jpn J Ophthalmol* 1996; 40: 62–65.
143. Johnson ME, Murphy PJ, Boulton M. Effectiveness of sodium hyaluronate eyedrops in the treatment of dry eye. *Graefes Arch Clin Exp Ophthalmol* 2004: 1–4.
144. Condon PI, McEwen CG, Wright M, Mackintosh G, Prescott RJ, McDonald C. Double blind, randomised, placebo controlled, crossover, multicentre study to determine the efficacy of a 0.1% (w/v) sodium hyaluronate solution (Fermavisc) in the treatment of dry eye syndrome. *Br J Ophthalmol* 1999; 83: 1121–1124.
145. McDonald CC, Kaye SB, Figueiredo FC, Macintosh G, Lockett C. A randomised, crossover, multicentre study to compare the performance of 0.1% (w/v) sodium hyaluronate with 1.4% (w/v) polyvinyl alcohol in the alleviation of symptoms associated with dry eye syndrome. *Eye* 2002; 16: 601–607.
146. Miyauchi S, Sugiyama T, Machida A, et al. The effect of sodium hyaluronate on the migration of rabbit corneal epithelium. I. An in vitro study. *J Ocul Pharmacol* 1990; 6: 91–99.
147. Nishida T, Nakamura M, Mishima H, Otori T. Hyaluronan stimulates corneal epithelial migration. *Exp Eye Res* 1991; 53: 753–758.
148. Sugiyama T, Miyauchi S, Machida A, Miyazaki K, Tokuyasu K, Nakazawa K. The effect of sodium hyaluronate on the migration of rabbit corneal epithelium. II. The effect of topical administration. *J Ocul Pharmacol* 1991; 7: 53–64.
149. Tsubota K, Higuchi A. Serum application for the treatment of ocular surface disorders. *Int Ophthalmol Clin* 2000; 40: 113–122.
150. Fox RI, Chan R, Michelson JB, Belmont JB, Michelson PE. Beneficial effect of artificial tears made with autologous serum in patients with keratoconjunctivitis sicca. *Arthritis Rheum* 1984; 27: 459–461.
151. Tsubota K, Goto E, Fujita H, et al. Treatment of dry eye by autologous serum application in Sjogren's syndrome. *Br J Ophthalmol* 1999; 83: 390–395.
152. Noble BA, Loh RS, MacLennan S, et al. Comparison of autologous serum eye drops with conventional therapy in a randomised controlled crossover trial for ocular surface disease. *Br J Ophthalmol* 2004; 88: 647–652.
153. Kojima T, Ishida R, Dogru M, et al. The effect of autologous serum eyedrops in the treatment of severe dry eye disease: A prospective randomized case-control study. *Am J Ophthalmol* 2005; 139: 242–246.
154. Hess AD. Mechanisms of action of cyclosporine: Considerations for the treatment of autoimmune diseases. *Clin Immunol Immunopathol* 1993; 68: 220–228.
155. Kaswan RL, Salisbury MA, Ward DA. Spontaneous canine keratoconjunctivitis sicca. A useful model for human keratoconjunctivitis sicca: Treatment with cyclosporine eye drops. *Arch Ophthalmol* 1989; 107: 1210–1216.
156. Salisbury MA, Kaswan RL, Ward DA, et al. Topical application of cyclosporine in the management of keratoconjunctivitis sicca in dogs. *J Am Anim Hosp Assoc* 1990; 26: 269–274.
157. Morgan RV, Abrams KL. Topical administration of cyclosporine for treatment of keratoconjunctivitis sicca in dogs. *J Am Vet Med Assoc* 1991; 199: 1043–1046.
158. Olivero DK, Davidson MG, English RV, Nasisse MP, Jamieson VE, Gerig TM. Clinical evaluation of 1% cyclosporine for topical treatment of keratoconjunctivitis sicca in dogs. *J Am Vet Med Assoc* 1991; 199: 1039–1042.
159. Sansom J, Barnett KC, Neumann W, et al. Treatment of keratoconjunctivitis sicca in dogs with cyclosporine ophthalmic ointment: A European clinical field trial. *Vet Rec* 1995; 137: 504–507.
160. Kaswan RL, Martin CL, Chapman WL. Keratoconjunctivitis sicca: Histopathologic study of nictitating membrane and lacrimal gland from 28 dogs. *Am J Vet Res* 1984; 45: 112–118.

161. Kaswan RL, Salisbury MA. A new perspective on canine keratoconjunctivitis sicca. Treatment with ophthalmic cyclosporine. *Vet Clin North Am Small Anim Pract* 1990; 20: 583–613.
162. Moore CP, McHugh JB, Thorne JG, Phillips TE. Effect of cyclosporine on conjunctival mucin in a canine keratoconjunctivitis sicca model. *Invest Ophthalmol Vis Sci* 2001; 42: 653–659.
163. Gao J, Schwalb TA, Addeo JV, Ghosn CR, Stern ME. The role of apoptosis in the pathogenesis of canine keratoconjunctivitis sicca: The effect of topical Cyclosporin A therapy. *Cornea* 1998; 17: 654–663.
164. Yoshida A, Fujihara T, Nakata K. Cyclosporin A increases tear fluid secretion via release of sensory neurotransmitters and muscarinic pathway in mice. *Exp Eye Res* 1999; 68: 541–546.
165. Zoukhri D, Kublin CL. Impaired neurotransmitter release from lacrimal and salivary gland nerves of a murine model of Sjogren's syndrome. *Invest Ophthalmol Vis Sci* 2001; 42: 925–932.
166. Gilger BC, Andrews J, Wilkie DA, Wyman M, Lairmore MD. Cellular immunity in dogs with keratoconjunctivitis sicca before and after treatment with topical 2% cyclosporine. *Vet Immunol Immunopathol* 1995; 49: 199–208.
167. Gilger BC, Andrews J, Wilkie DA, Larimore MD. Lymphocyte proliferation and blood drug levels in dogs with keratoconjunctivitis sicca receiving long-term topical ocular cyclosporine. *Vet Comp Ophthalmol* 1996; 6: 125–130.
168. Izci C, Celik I, Alkan F, et al. Histologic characteristics and local cellular immunity of the gland of the third eyelid after topical ophthalmic administration of 2% cyclosporine for treatment of dogs with keratoconjunctivitis sicca. *Am J Vet Res* 2002; 63: 688–694.
169. Berdoulay A, English RV, Nadelstein B. Effect of topical 0.02% tacrolimus aqueous suspension on tear production in dogs with keratoconjunctivitis sicca. *Vet Ophthalmol* 2005; 8: 225–232.
170. Nell B, Walde I, Billich A, Vit P, Meingassner JG. The effect of topical pimecrolimus on keratoconjunctivitis sicca and chronic superficial keratitis in dogs: Results from an exploratory study. *Vet Ophthalmol* 2005; 8: 39–46.
171. Niwa Y, Terashima T, Sumi H. Topical application of the immunosuppressant tacrolimus accelerates carcinogenesis in mouse skin. *Br J Dermatol* 2003; 149: 960–967.
172. U.S. Food and Drug Administration. FDA Issues Public Health Advisory Informing Health Care Providers of Safety Concerns Associated with the Use of Two Eczema Drugs, Elidel and Protopic. Talk Paper T05-06. Rockville, MD, 2005.
173. Rubin LF, Aguirre G. Clinical use of pilocarpine for keratoconjunctivitis sicca in dogs and cats. *J Am Vet Med Assoc* 1967; 151: 313–320.
174. Severin GA. Keratoconjunctivitis sicca. *Vet Clin North Am* 1973; 3: 407–422.
175. Smith EM, Buyukmihci NC, Farver TB. Effect of topical pilocarpine treatment on tear production in dogs. *J Am Vet Med Assoc* 1994; 205: 1286–1289.
176. Coassin M, Lambiase A, Costa N, et al. Efficacy of topical nerve growth factor treatment in dogs affected by dry eye. *Graefes Arch Clin Exp Ophthalmol* 2005; 243: 151–155.
177. Gilger BC, Rose PD, Davidson MG, Roberts SM, Miller T. Low-dose oral administration of interferon-alpha for the treatment of immune-mediated keratoconjunctivitis sicca in dogs. *J Interferon Cytokine Res* 1999; 19: 901–905.
178. Edelhauser HF, Van Horn DL, Hyndiuk RA, Schultz RO. Intraocular irrigating solutions. Their effect on the corneal endothelium. *Arch Ophthalmol* 1975; 93: 648–657.
179. Edelhauser HF, Van Horn DL, Schultz RO, Hyndiuk RA. Comparative toxicity of intraocular irrigating solutions on the corneal endothelium. *Am J Ophthalmol* 1976; 81: 473–481.
180. Edelhauser HF, Gonnering R, Van Horn DL. Intraocular irrigating solutions. A comparative study of BSS Plus and lactated Ringer's solution. *Arch Ophthalmol* 1978; 96: 516–520.
181. Wiederholt M, Koch M. Effect of intraocular irrigating solutions on intracellular membrane potentials and swelling rate of isolated human and rabbit cornea. *Invest Ophthalmol Vis Sci* 1979; 18: 313–317.
182. Nuyts RM, Edelhauser HF, Holley GP. Intraocular irrigating solutions: A comparison of Hartmann's lactated Ringer's solution, BSS and BSS Plus. *Graefes Arch Clin Exp Ophthalmol* 1995; 233: 655–661.
183. Benson WE, Diamond JG, Tasman W. Intraocular irrigating solutions for pars plana vitrectomy. A prospective, randomized, double-blind study. *Arch Ophthalmol* 1981; 99: 1013–1015.
184. Joussen AM, Barth U, Cubuk H, Koch H. Effect of irrigating solution and irrigation temperature on the cornea and pupil during phacoemulsification. *J Cataract Refract Surg* 2000; 26: 392–397.
185. Puckett TR, Peele KA, Howard RS, Kramer KK. Intraocular irrigating solutions. A randomized clinical trial of balanced salt solution plus and dextrose bicarbonate lactated Ringer's solution. *Ophthalmol* 1995; 102: 291–296.
186. Nasisse MP, Cook CS, Harling DE. Response of the canine corneal endothelium to intraocular irrigation with saline solution, balanced salt solution, and balanced salt solution with glutathione. *Am J Vet Res* 1986; 47: 2261–2265.
187. Glasser DB, Matsuda M, Ellis JG, Edelhauser HF. Effects of intraocular irrigating solutions on the corneal endothelium after in vivo anterior chamber irrigation. *Am J Ophthalmol* 1985; 99: 321–328.
188. Holst A, Rolfsen W, Svensson B, Ollinger K, Lundgren B. Formation of free radicals during phacoemulsification. *Current Eye Research* 1993; 12: 359–365.
189. Rubowitz A, Assia EI, Rosner M, Topaz M. Antioxidant protection against corneal damage by free radicals during phacoemulsification. *Invest Ophthalmol Vis Sci* 2003; 44: 1866–1870.
190. Mannis MJ, Miller RB, Carlson EC, Hinds D, May DR. Effect of hypothermic perfusion on corneal endothelial morphology. *Br J Ophthalmol* 1983; 67: 804–807.
191. Jabbour NM, Schepens CL, Buzney SM. Local ocular hypothermia in experimental intraocular surgery. *Ophthalmol* 1988; 95: 1687–1690.
192. Findl O, Amon M, Kruger A, Petternel V, Schauersberger J. Effect of cooled intraocular irrigating solution on the blood-aqueous barrier after cataract surgery. *J Cataract Refract Surg* 1999; 25: 566–568.
193. Isenberg SJ, Apt L, Yoshimori R, Khwarg S. Chemical preparation of the eye in ophthalmic surgery. IV. Comparison of povidone-iodine on the conjunctiva with a prophylactic antibiotic. *Arch Ophthalmol* 1985; 103: 1340–1342.

194. Roberts SM, Severin GA, Lavach JD. Antibacterial activity of dilute povidone-iodine solutions used for ocular surface disinfection in dogs. *Am J Vet Res* 1986; 47: 1207–1210.
195. Alp BN, Elibol O, Sargon MF, et al. The effect of povidone iodine on the corneal endothelium. *Cornea* 2000; 19: 546–550.
196. Naor J, Savion N, Blumenthal M, Assia EI. Corneal endothelial cytotoxicity of diluted povidone-iodine. *J Cataract Refract Surg* 2001; 27: 941–947.
197. Ciulla TA, Starr MB, Masket S. Bacterial endophthalmitis prophylaxis for cataract surgery: An evidence-based update. *Ophthalmol* 2002; 109: 13–24.
198. Apt L, Isenberg SJ, Yoshimori R, Chang A, Lam GC, Wachler B, Neumann D. The effect of povidone-iodine solution applied at the conclusion of ophthalmic surgery. *Am J Ophthalmol* 1995; 119: 701–705.
199. Fowler JD, Schuh JCL. Preoperative chemical preparation of the eye: A comparison of chlorhexidine diacetate, chlorhexidine gluconate, and povidone-iodine. *J Am Anim Hosp Assoc* 1992; 28: 451–457.
200. Hamill MB, Osato MS, Wilhelmus KR. Experimental evaluation of chlorhexidine gluconate for ocular antisepsis. *Antimicrob Agents Chemother* 1984; 26: 793–796.
201. Mac Rae SM, Brown B, Edelhauser HF. The corneal toxicity of presurgical skin antiseptics. *Am J Ophthalmol* 1984; 97: 221–232.
202. Dua HS, Benedetto DA, Azuara-Blanco A. Protection of corneal endothelium from irrigation damage: A comparison of sodium hyaluronate and hydroxypropylmethylcellulose. *Eye* 2000; 14(Pt1): 88–92.
203. Artola A, Alio JL, Bellot JL, Ruiz JM. Protective properties of viscoelastic substances (sodium hyaluronate and 2% hydroxymethylcellulose) against experimental free radical damage to the corneal endothelium. *Cornea* 1993; 12: 109–114.
204. Liesegang TJ. Viscoelastic substances in ophthalmology. *Surv Ophthalmol* 1990; 34: 268–293.
205. Arshinoff SA. Dispersive-cohesive viscoelastic soft shell technique. *J Cataract Refract Surg* 1999; 25: 167–173.
206. Mamalis N. OVDs. Viscosurgical, viscoelastic, and viscoadaptive. What does this mean? *J Cataract Refract Surg* 2002; 28: 1497–1498.
207. Dick HB, Krummenauer F, Augustin AJ, Pakula T, Pfeiffer N. Healon5 viscoadaptive formulation: Comparison to Healon and Healon GV. *J Cataract Refract Surg* 2001; 27: 320–326.
208. Miyata K, Maruoka S, Nakahara M, et al. Corneal endothelial cell protection during phacoemulsification: Low- versus high-molecular-weight sodium hyaluronate. *J Cataract Refract Surg* 2002; 28: 1557–1560.
209. McDermott ML, Hazlett LD, Barrett RP, Lambert RJ. Viscoelastic adherence to corneal endothelium following phacoemulsification. *J Cataract Refract Surg* 1998; 24: 678–683.
210. Behndig A, Lundberg B. Transient corneal edema after phacoemulsification: Comparison of 3 viscoelastic regimens. *J Cataract Refract Surg* 2002; 28: 1551–1556.
211. Kim EK, Cristol SM, Kang SJ, Edelhauser HF, Kim HL, Lee JB. Viscoelastic protection from endothelial damage by air bubbles. *J Cataract Refract Surg* 2002; 28: 1047–1053.
212. Lane SS, Naylor DW, Kullerstrand LJ, Knauth K, Lindstrom RL. Prospective comparison of the effects of Occucoat, Viscoat, and Healon on intraocular pressure and endothelial cell loss. *J Cataract Refract Surg* 1991; 17: 21–26.
213. Miller KM, Colvard DM. Randomized clinical comparison of Healon GV and Viscoat. *J Cataract Refract Surg* 1999; 25: 1630–1636.
214. Maar N, Graebe A, Schild G, Stur M, Amon M. Influence of viscoelastic substances used in cataract surgery on corneal metabolism and endothelial morphology: Comparison of Healon and Viscoat. *J Cataract Refract Surg* 2001; 27: 1756–1761.
215. Calder IG, Smith VH. Hyaluronidase and sodium hyaluronate in cataract surgery. *Br J Ophthalmol* 1986; 70: 418–420.
216. Harooni M, Freilich JM, Abelson M, Refojo M. Efficacy of hyaluronidase in reducing increases in intraocular pressure related to the use of viscoelastic substances. *Arch Ophthalmol* 1998; 116: 1218–1221.
217. Hyndiuk RA, Schultz RO. Overview of the corneal toxicity of surgical solutions, drugs and clinical concepts in corneal edema. *Lens Eye Toxic Res* 1992; 9: 331–350.
218. Nguyen LK, Yee RW, Sigler SC, Ye HS. Use of in vitro models of bovine corneal endothelial cells to determine the relative toxicity of viscoelastic agents. *J Cataract Refract Surg* 1992; 18: 7–13.
219. Zhu SN, Nolle B, Duncker G. Effects of viscoelastics on bovine corneal endothelial cells in vitro. *Acta Ophthalmol Scand* 1997; 75: 155–158.
220. Williams DF, Han DP, Abrams GW. Rebleeding in experimental traumatic hyphema treated with intraocular tissue plasminogen activator. *Arch Ophthalmol* 1990; 108: 264–266.
221. Martin CL, Kaswan R, Gratzek A, Champagne E, Salisbury MA, Ward D. Ocular use of tissue plasminogen activator in companion animals. *Prog Vet Comp Ophthalmol* 1993; 3: 29–36.
222. Ward C, Weck S. Dilution and storage of recombinant tissue plasminogen activator (Activase) in balanced salt solutions. *Am J Ophthalmol* 1990; 109: 98–99.
223. Jaffe GJ, Green GD, Abrams GW. Stability of recombinant tissue plasminogen activator. *Am J Ophthalmol* 1989; 108: 90–91.
224. Gerding PA, Jr., Essex-Sorlie D, Vasaune S, Yack R. Use of tissue plasminogen activator for intraocular fibrinolysis in dogs. *Am J Vet Res* 1992; 53: 894–896.
225. Gerding PA, Jr., Essex-Sorlie D, Yack R, Vasaune S. Effects of intracameral injection of tissue plasminogen activator on corneal endothelium and intraocular pressure in dogs. *Am J Vet Res* 1992; 53: 890–893.
226. Gerding PA, Jr., Eurell TE. Evaluation of intraocular penetration of topically administered tissue plasminogen activator in dogs. *Am J Vet Res* 1993; 54: 836–839.
227. Gerding PA, Jr., Hamor RE, Ramsey DT, Vasaune S, Schaeffer DJ. Evaluation of topically administered tissue plasminogen activator for intraocular fibrinolysis in dogs. *Am J Vet Res* 1994; 55: 1368–1370.
228. Johnson MW, Olsen KR, Hernandez E, Irvine WD, Johnson RN. Retinal toxicity of recombinant tissue plasminogen activator in the rabbit. *Arch Ophthalmol* 1990; 108: 259–263.
229. Irvine WD, Johnson MW, Hernandez E, Olsen KR. Retinal toxicity of human tissue plasminogen activator in vitrectomized rabbit eyes. *Arch Ophthalmol* 1991; 109: 718–722.
230. Hrach CJ, Johnson MW, Hassan AS, Lei B, Sieving PA, Elner VM. Retinal toxicity of commercial intravitreal tissue

plasminogen activator solution in cat eyes. *Arch Ophthalmol* 2000; 118: 659–663.
231. Hesse L, Schmidt J, Kroll P. Management of acute submacular hemorrhage using recombinant tissue plasminogen activator and gas. *Graefes Arch Clin Exp Ophthalmol* 1999; 237: 273–277.
232. Chen SN, Yang TC, Ho CL, Kuo YH, Yip Y, Chao AN. Retinal toxicity of intravitreal tissue plasminogen activator: Case report and literature review. *Ophthalmol* 2003; 110: 704–708.
233. Crouch ER, Jr., Frenkel M. Aminocaproic acid in the treatment of traumatic hyphema. *Am J Ophthalmol* 1976; 81: 355–360.
234. McGetrick JJ, Jampol LM, Goldberg MF, Frenkel M, Fiscella RG. Aminocaproic acid decreases secondary hemorrhage after traumatic hyphema. *Arch Ophthalmol* 1983; 101: 1031–1033.
235. Wilson TW, Jeffers JB, Nelson LB. Aminocaproic acid prophylaxis in traumatic hyphema. *Ophthalmic Surg* 1990; 21: 807–809.
236. Allingham RR, Crouch ER, Jr., Williams PB, Catlin JC, Loewy DM, Jacobson J. Topical aminocaproic acid significantly reduces the incidence of secondary hemorrhage in traumatic hyphema in the rabbit model. *Arch Ophthalmol* 1988; 106: 1436–1438.
237. Crouch ER, Jr., Williams PB, Gray MK, Crouch ER, Chames M. Topical aminocaproic acid in the treatment of traumatic hyphema. *Arch Ophthalmol* 1997; 115: 1106–1112.
238. Pieramici DJ, Goldberg MF, Melia M, et al. A phase III, multicenter, randomized, placebo-controlled clinical trial of topical aminocaproic acid (Caprogel) in the management of traumatic hyphema. *Ophthalmol* 2003; 110: 2106–2112.
239. Karkhaneh R, Naeeni M, Chams H, Abdollahi M, Mansouri MR. Topical aminocaproic acid to prevent rebleeding in cases of traumatic hyphema. *Eur J Ophthalmol* 2003; 13: 57–61.
240. Deans R, Noel LP, Clarke WN. Oral administration of tranexamic acid in the management of traumatic hyphema in children. *Can J Ophthalmol* 1992; 27: 181–183.
241. Rahmani B, Jahadi HR. Comparison of tranexamic acid and prednisolone in the treatment of traumatic hyphema. A randomized clinical trial. *Ophthalmol* 1999; 106: 375–379.
242. Crouch ER, 3rd, Crouch ER, Jr., Williams PB. Aminocaproic acid and tranexamic acid increase the rate of acute corneal reepithelialization in Sprague Dawley rats. *J Ocul Pharmacol Ther* 1998; 14: 109–118.
243. Williams PB, Crouch ER, Jr., Crouch ER, Mazaheri M. Topical aminocaproic acid facilitates reepithelialization of persistent epithelial defects. *Curr Eye Res* 1999; 18: 150–157.
244. Regnier A, Cazalot G, Cantaloube B. Topical treatment of non-healing corneal epithelial ulcers in dogs with aminocaproic acid. *Vet Rec* 2005; 157: 510–513.
245. Bentley E, Nasisse MP, Glover T, Nelms S. Implantation of filtering devices in dogs with glaucoma: Preliminary results in 13 eyes. *Vet Comp Ophthalmol* 1996; 6: 243–246.
246. Bentley E, Miller PE, Murphy CJ, Schoster JV. Combined cycloablation and gonioimplantation for treatment of glaucoma in dogs: 18 cases (1992–1998). *J Am Vet Med Assoc* 1999; 215: 1469–1472.
247. Sapienza JS, van der Woerdt A. Combined transscleral diode laser cyclophotocoagulation and Ahmed gonioimplantation in dogs with primary glaucoma: 51 cases (1996–2004). *Vet Ophthalmol* 2005; 8: 121–127.
248. Glover TL, Nasisse MP, Davidson MG. Effects of topically applied mitomycin-C on intraocular pressure, facility of outflow, and fibrosis after glaucoma filtration surgery in clinically normal dogs. *Am J Vet Res* 1995; 56: 936–939.
249. Tinsley DM, Niyo Y, Tinsley LM, Betts DM. In vivo clinical trial of perioperative mitomycin-C in combination with a drainage device implantation in normal canine globes. *Vet Comp Ophthalmol* 1995; 5: 231–241.
250. Costa VP, Azuara-Blanco A, Netland PA, Lesk MR, Arcieri ES. Efficacy and safety of adjunctive mitomycin C during Ahmed Glaucoma Valve implantation: A prospective randomized clinical trial. *Ophthalmol* 2004; 111: 1071–1076.
251. Mietz H, Addicks K, Diestelhorst M, Krieglstein GK. Extraocular application of mitomycin C in a rabbit model: Cytotoxic effects on the ciliary body and epithelium. *Ophthalmic Surg* 1994; 25: 240–244.
252. Kee C, Pelzek CD, Kaufman PL. Mitomycin C suppresses aqueous human flow in cynomolgus monkeys. *Arch Ophthalmol* 1995; 113: 239–242.
253. Mietz H, Addicks K, Bloch W, Krieglstein GK. Long-term intraocular toxic effects of topical mitomycin C in rabbits. *J Glaucoma* 1996; 5: 325–333.
254. Levy J, Tessler Z, Rosenthal G, et al. Toxic effects of subconjunctival 5-fluorouracil and mitomycin C on ciliary body of rats. *Int Ophthalmol* 2001; 24: 199–203.
255. Refojo MF, Dohlman CH, Ahmad B, Carroll JM, Allen JC. Evaluation of adhesives for corneal surgery. *Arch Ophthalmol* 1968; 80: 645–656.
256. Webster RG Jr., Slansky HH, Refojo MF, Boruchoff SA, Dohlman CH. The use of adhesive for the closure of corneal perforations. Report of two cases. *Arch Ophthalmol* 1968; 80: 705–709.
257. Bromberg NM. Cyanoacrylate tissue adhesive for treatment of refractory corneal ulceration. *Vet Ophthalmol* 2002; 5: 55–60.
258. Watte CM, Elks R, Moore DL, McLellan GJ. Clinical experience with butyl-2-cyanoacrylate adhesive in the management of canine and feline corneal disease. *Vet Ophthalmol* 2004; 7: 319–326.
259. Eiferman RA, Snyder JW. Antibacterial effect of cyanoacrylate glue. *Arch Ophthalmol* 1983; 101: 958–960.
260. Howell JM, Bresnahan KA, Stair TO, Dhindsa HS, Edwards BA. Comparison of effects of suture and cyanoacrylate tissue adhesive on bacterial counts in contaminated lacerations. *Antimicrob Agents Chemother* 1995; 39: 559–560.
261. Quinn JV, Osmond MH, Yurack JA, Moir PJ. N-2-butylcyanoacrylate: Risk of bacterial contamination with an appraisal of its antimicrobial effects. *J Emerg Med* 1995; 13: 581–585.
262. Weiss JL, Williams P, Lindstrom RL, Doughman DJ. The use of tissue adhesive in corneal perforations. *Ophthalmol* 1983; 90: 610–615.
263. Leahey AB, Gottsch JD, Stark WJ. Clinical experience with N-butyl cyanoacrylate (Nexacryl) tissue adhesive. *Ophthalmol* 1993; 100: 173–180.
264. Ollivier F, Delverdier M, Regnier A. Tolerance of the rabbit cornea to an n-butyl-ester cyanoacrylate adhesive (Vetbond). *Vet Ophthalmol* 2001; 4: 261–266.
265. Vote BJ, Elder MJ. Cyanoacrylate glue for corneal perforations: A description of a surgical technique and a review

of the literature. *Clin Experiment Ophthalmol* 2000; 28: 437–442.
266. Sumich PM, Cook SD, Tole DM. Fibrin tissue-filler glue for persistent epithelial defects. *Clin Experiment Ophthalmol* 2003; 31: 267–269.
267. Hick S, Demers PE, Brunette I, La C, Mabon M, Duchesne B. Amniotic membrane transplantation and fibrin glue in the management of corneal ulcers and perforations: A review of 33 cases. *Cornea* 2005; 24: 369–377.
268. Duchesne B, Tahi H, Galand A. Use of human fibrin glue and amniotic membrane transplant in corneal perforation. *Cornea* 2001; 20: 230–232.
269. Sharma A, Kaur R, Kumar S, et al. Fibrin glue versus N-butyl-2-cyanoacrylate in corneal perforations. *Ophthalmol* 2003; 110: 291–298.
270. Zauberman H, Hemo I. Use of fibrin glue in ocular surgery. *Ophthalmic Surg* 1988; 19: 132–133.
271. Biedner B, Rosenthal G. Conjunctival closure in strabismus surgery: Vicryl versus fibrin glue. *Ophthalmic Surg Lasers* 1996; 27: 967.
272. Dadeya S, Ms K. Strabismus surgery: Fibrin glue versus vicryl for conjunctival closure. *Acta Ophthalmol Scand* 2001; 79: 515–517.
273. Pfister RR, Sommers CI. Fibrin sealant in corneal stem cell transplantation. *Cornea* 2005; 24: 593–598.
274. Fini ME, Parks WC, Rinehart WB, et al. Role of matrix metalloproteinases in failure to re-epithelialize after corneal injury. *Am J Pathol* 1996; 149: 1287–1302.
275. Strubbe DT, Brooks DE, Schultz GS, et al. Evaluation of tear film proteinases in horses with ulcerative keratitis. *Vet Ophthalmol* 2000; 3: 111–119.
276. Ollivier FJ, Brooks DE, Van Setten GB, et al. Profiles of matrix metalloproteinase activity in equine tear fluid during corneal healing in 10 horses with ulcerative keratitis. *Vet Ophthalmol* 2004; 7: 397–405.
277. Robertson PB, Ryel RB, Taylor RE, Shyu KW, Fullmer HM. Collagenase: Localization in polymorphonuclear leukocyte granules in the rabbit. *Science* 1972; 177: 64–65.
278. Smith VA, Rishmawi H, Hussein H, Easty DL. Tear film MMP accumulation and corneal disease. *Br J Ophthalmol* 2001; 85: 147–153.
279. Li Q, Fukuda K, Lu Y, et al. Enhancement by neutrophils of collagen degradation by corneal fibroblasts. *J Leukoc Biol* 2003; 74: 412–419.
280. Burns FR, Stack MS, Gray RD, Paterson CA. Inhibition of purified collagenase from alkali-burned rabbit corneas. *Invest Ophthalmol Vis Sci* 1989; 30: 1569–1575.
281. Fitton JH, Ziegelaar BW, Hicks CR, et al. Assessment of anti-collagenase treatments after insertion of a keratoprosthetic material in the rabbit cornea. *Cornea* 1998; 17: 108–114.
282. Haffner JC, Fecteau KA, Eiler H. Inhibition of collagenase breakdown of equine corneas by tetanus antitoxin, equine serum and acetylcysteine. *Vet Ophthalmol* 2003; 6: 67–72.
283. Ollivier FJ, Brooks DE, Kallberg ME, et al. Evaluation of various compounds to inhibit activity of matrix metalloproteinases in the tear film of horses with ulcerative keratitis. *Am J Vet Res* 2003; 64: 1081–1087.
284. Rebhun WC. Bacterial ulcers of the equine cornea. *Equine Pract* 1981; 3: 40–49.
285. Severin GA. *Severin's Veterinary Ophthalmology Notes,* 3rd ed. Fort Collins, CO: 1995: 123.
286. Aldavood SJ, Behyar R, Sarchahi AA, et al. Effect of acetylcysteine on experimental corneal wounds in dogs. *Ophthalmic Res* 2003; 35: 319–323.
287. Petroutsos G, Guimaraes R, Giraud JP, Renard G, Pouliquen Y. Effect of acetylcysteine (Mucomyst) on epithelial wound healing. *Ophthalmic Res* 1982; 14: 241–248.
288. Thermes F, Molon-Noblot S, Grove J. Effects of acetylcysteine on rabbit conjunctival and corneal surfaces. A scanning electron microscopy study. *Invest Ophthalmol Vis Sci* 1991; 32: 2958–2963.
289. Brown SI, Akiya S, Weller CA. Prevention of the ulcers of the alkali-burned cornea. Preliminary studies with collagenase inhibitors. *Arch Ophthalmol* 1969; 82: 95–97.
290. Brown SI, Weller CA. Collagenase inhibitors in prevention of ulcers of alkali-burned cornea. *Arch Ophthalmol* 1970; 83: 352–353.
291. Berman MB. Collagenase inhibitors: Rationale for their use in treating corneal ulceration. *Int Ophthalmol Clin* 1975; 15: 49–66.
292. Hardberger RE, Hanna C, Goodart R. Effects of drug vehicles on ocular uptake of tetracycline. *Am J Ophthalmol* 1975; 80: 133–138.
293. Salminen L. Penetration of ocular compartments by tetracyclines. I. An experimental study with tetracycline. *Albrecht Von Graefes Arch Klin Exp Ophthalmol* 1977; 204: 189–199.
294. Salminen L. Penetration of ocular compartments by tetracyclines. II. An experimental study with doxycycline. *Albrecht Von Graefes Arch Klin Exp Ophthalmol* 1977; 204: 201–207.
295. Tabbara KF, Ghosheh R, O'Connor GR. Ocular tissue absorption of minocycline in the rabbit. *Arch Ophthalmol* 1983; 101: 1426–1428.
296. Golub LM, Lee HM, Lehrer G, et al. Minocycline reduces gingival collagenolytic activity during diabetes. Preliminary observations and a proposed new mechanism of action. *J Periodontal Res* 1983; 18: 516–526.
297. Levy JH, Katz HR. Effect of systemic tetracycline on progression of *Pseudomonas aeruginosa* keratitis in the rabbit. *Ann Ophthalmol* 1990; 22: 179–183.
298. Seedor JA, Perry HD, McNamara TF, Golub LM, Buxton DF, Guthrie DS. Systemic tetracycline treatment of alkali-induced corneal ulceration in rabbits. *Arch Ophthalmol* 1987; 105: 268–271.
299. Perry HD, Hodes LW, Seedor JA, Donnenfeld ED, McNamara TF, Golub LM. Effect of doxycycline hyclate on corneal epithelial wound healing in the rabbit alkali-burn model. Preliminary observations. *Cornea* 1993; 12: 379–382.
300. Perry HD, Golub LM. Systemic tetracyclines in the treatment of noninfected corneal ulcers: A case report and proposed new mechanism of action. *Ann Ophthalmol* 1985; 17: 742–744.
301. McElvanney AM. Doxycycline in the management of pseudomonas corneal melting: Two case reports and a review of the literature. *Eye Contact Lens* 2003; 29: 258–261.
302. Perry HD, Kenyon KR, Lamberts DW, Foulks GN, Seedor JA, Golub LM. Systemic tetracycline hydrochloride as adjunctive therapy in the treatment of persistent epithelial defects. *Ophthalmol* 1986; 93: 1320–1322.
303. Dursun D, Kim MC, Solomon A, Pflugfelder SC. Treatment of recalcitrant recurrent corneal erosions with inhibitors of matrix metalloproteinase-9, doxycycline and corticosteroids. *Am J Ophthalmol* 2001; 132: 8–13.

304. Uitto VJ, Firth JD, Nip L, Golub LM. Doxycycline and chemically modified tetracyclines inhibit gelatinase A (MMP-2) gene expression in human skin keratinocytes. *Ann N Y Acad Sci* 1994; 732: 140–151.
305. Sorsa T, Konttinen YT, Lindy O, et al. Doxycycline protects serum alpha-1-antitrypsin from human neutrophil collagenase. *Agents Actions Suppl* 1993; 39: 225–229.
306. Sorsa T, Lindy O, Konttinen YT, et al. Doxycycline in the protection of serum alpha-1-antitrypsin from human neutrophil collagenase and gelatinase. *Antimicrob Agents Chemother* 1993; 37: 592–594.
307. Elewski BE, Lamb BA, Sams WM Jr., Gammon WR. In vivo suppression of neutrophil chemotaxis by systemically and topically administered tetracycline. *J Am Acad Dermatol* 1983; 8: 807–812.
308. Suomalainen K, Halinen S, Ingman T, et al. Tetracycline inhibition identifies the cellular sources of collagenase in gingival crevicular fluid in different forms of periodontal diseases. *Drugs Exp Clin Res* 1992; 18: 99–104.
309. Ingman T, Sorsa T, Suomalainen K, et al. Tetracycline inhibition and the cellular source of collagenase in gingival crevicular fluid in different periodontal diseases. A review article. *J Periodontol* 1993; 64: 82–88.
310. Berman MB, Barber JC, Talamo RC, Langley CE. Corneal ulceration and the serum antiproteases. I. Alpha 1-antitrypsin. *Invest Ophthalmol* 1973; 12: 759–770.
311. Berman M, Gordon J, Garcia LA, Gage L. Corneal ulceration and the serum antiproteases. II. Complexes of corneal collagenases and alpha-macroglobulins. *Exp Eye Res* 1975; 20: 231–244.
312. Liu L, Hartwig D, Harloff S, Herminghaus P, Wedel T, Geerling G. An optimised protocol for the production of autologous serum eyedrops. *Graefes Arch Clin Exp Ophthalmol* 2005; 243: 706–714.
313. Hartwig D, Herminghaus P, Wedel T, et al. Topical treatment of ocular surface defects: Comparison of the epitheliotrophic capacity of fresh frozen plasma and serum on corneal epithelial cells in an in vitro cell culture model. *Transfus Med* 2005; 15: 107–113.
314. Geerling G, Daniels JT, Dart JK, Cree IA, Khaw PT. Toxicity of natural tear substitutes in a fully defined culture model of human corneal epithelial cells. *Invest Ophthalmol Vis Sci* 2001; 42: 948–956.
315. Schultz GS, Strelow S, Stern GA, et al. Treatment of alkali-injured rabbit corneas with a synthetic inhibitor of matrix metalloproteinases. *Invest Ophthalmol Vis Sci* 1992; 33: 3325–3331.
316. Barletta JP, Angella G, Balch KC, et al. Inhibition of pseudomonal ulceration in rabbit corneas by a synthetic matrix metalloproteinase inhibitor. *Invest Ophthalmol Vis Sci* 1996; 37: 20–28.
317. Hao JL, Nagano T, Nakamura M, Kumagai N, Mishima H, Nishida T. Effect of galardin on collagen degradation by *Pseudomonas aeruginosa*. *Exp Eye Res* 1999; 69: 595–601.
318. Hao JL, Nagano T, Nakamura M, Kumagai N, Mishima H, Nishida T. Galardin inhibits collagen degradation by rabbit keratocytes by inhibiting the activation of pro-matrix metalloproteinases. *Exp Eye Res* 1999; 68: 565–572.
319. Sotozono C, He J, Tei M, Honma Y, Kinoshita S. Effect of metalloproteinase inhibitor on corneal cytokine expression after alkali injury. *Invest Ophthalmol Vis Sci* 1999; 40: 2430–2434.

Chapter 8

Fundamentals of Veterinary Ophthalmic Pathology

Bruce H. Grahn and Robert L. Peiffer

INTRODUCTION AND PRINCIPLES

Few would argue that understanding disease processes on cellular and subcellular levels facilitates clinical management, and a thorough understanding of ocular pathology is essential for the practicing veterinary ophthalmologist. The organization of an ocular pathology chapter within the context of a largely clinical text is a daunting challenge given the merging of clinical ophthalmology and pathology. An important objective of this chapter is to facilitate understanding of ocular pathology with minimal duplication of material that is covered in the other chapters of this book. We have purposefully limited the discussion of clinical ophthalmology, anatomy, and embryology; we emphasize the gross, subgross, and light microscopic descriptions and illustrations to this aim.

This chapter is organized into introduction, fixation and processing of ocular tissues for light and electron microscopy, and basic principles of ocular pathology. The discussions of pathologic conditions are organized as congenital, inherited developmental, and acquired disorders. Congenital conditions are organized by those that affect organogenesis and those that affect tissue differentiation. Inherited developmental disorders in this chapter are breed-specific ocular diseases that are most common in dogs. These disorders either are confirmed as inherited or are breed-specific bilateral conditions that are likely induced by a genetic mutation. They are further categorized by the affected tissues. The acquired disease section is categorized into degenerative, inflammatory, and neoplastic conditions.

The transparency of the dioptric system of the eye allows the veterinary clinician observation (with indirect and direct ophthalmoscopic and biomicroscopic examination) of gross and subgross pathology in varied ocular tissues with resolution that approaches that of the light microscope. Additional specialized techniques, including spectral microscopy, electroretinography, fluorescein and indocyanine green angiography, and optical coherence tomography have allowed clinicians to examine varied ocular disorders noninvasively at a near cellular level. Additionally, ultrasonography, magnetic resonance imaging, computed tomography, and nuclear scintigraphy provide the veterinary ophthalmologist with enhanced views of most of the intraocular structures when the transparencies of ocular tissues are limited. These examination techniques and the submission of ocular biopsies, eviscerated samples, and whole globes for light microscopic examination unify clinical and pathologic disciplines and refute the axiom that pathology of the tissues of the eye and adnexa are unique: they are, in fact, very similar to those occurring in other organs.

FIXATION AND PROCESSING OF OCULAR TISSUE

Fixed ocular tissues are submitted in the form of whole globes with orbital tissues from exenteration or transpalpebral enucleations, globes without orbital tissues (transconjunctival enucleations), eviscerated specimens, excisional or incisional biopsies, cytology of exfoliate preparations, or fine needle aspirates. Each of these samples has unique fixation and preparation requirements in order to optimize the pathologist's examination. It is important that globes be fixed promptly at the time of removal from the orbit to ensure as rapid a fixation of the internal structures of the eye as possible and minimize autolytic changes.

The most common method of fixation for light microscopic evaluation of exenterated tissues is immersion in 10% buffered formaldehyde or Bouin's fluid. Several other fixatives have specific advantages and disadvantages (Table 8.1), including preservation of specific ocular tissues and compatibility with immunohistochemical and ultrastructural techniques. Ocular tissues are usually immersed at a ratio of 1 part tissue to 10 parts fixative and the container placed on a rotary mixer for 24 to 48 hours. To enhance fixation of retina, all globes that are immersion fixed in buffered formaldehyde should also receive an intravitreous formaldehyde injection (0.5–1 ml) via 25 gauge needle inserted through the sclera near the optic nerve prior to immersion to compensate for limited formaldehyde penetration of the fibrous ocular tunic. The globes are then hardened by immersion into graduated concentrations of alcohol from 60% to 80% for 24 to 48 hours. The alcohol dehydrates and hardens the globe and allows for easier sectioning.

Table 8.1 Ocular Fixatives and Their Advantages and Disadvantages

	Formaldehyde	Bouin's Fluid	Gluteraldehyde	Triple fixatives: Paraformaldehyde, Gluteraldehyde Formaldehyde, and Osmium	Zenker's Fluid	Davidsons Fixative
Maintenance of tissue relationships (re neurosensory retina–RPE)	Marginal	Good	Poor by immersion of the globe because penetration is marginal so globes must be sectioned and then small pieces immersed	Excellent; however, globe is typically opened	Good	Excellent
Preservation of membranes for ultrastructure	Poor	Poor	Excellent	Excellent	Good	Very good
Immuno-compatability	Good	Good; however, different epitope retrieval is required	Good	Good; however, different epitope retrieval is required	Good; however, different epitope retrieval is required	Good
Advantages and disadvantages	Cost, availability	Better penetration of globe	Excellent fixation of small tissue sections or small globes with thin sclera (mice, rats) destined for electron microscopy	Uncommonly used except in research; osmium is toxic and expensive	Uncommonly used because of mercury toxicity	Very good immersion fixative

Exenterations are performed as a surgical therapy for orbital neoplasia. These neoplasms are often malignant, and the determination of clean surgical margins is critical for prognosis and to determine the need for adjunctive therapy. It is important that the ophthalmic surgeon clearly identify any margins that must be examined in detail. The volume of tissue removed by an exenteration is large, and the orbital tissues should be incised every 0.5 to 1 cm through to the sclera to allow fixation penetration (Fig. 8.1). Alternatively, exenterated tissues may then be trimmed carefully from the globe and identified by sutures and labeled tabs, or by dye on specific surfaces, to provide the pathologist with adequate orientation for sectioning and margins to confirm the extent of the orbital neoplasm. After trimming, the globe, cornea, and attached optic nerve are measured with calipers and recorded. The globe should be transilluminated with a bright light to assist in determining intraocular masses or foreign bodies before orientating and sectioning. The globe for most species is orientated by identification of the shape of the cornea; extraocular muscle insertion; and location of the vortex veins, long posterior ciliary arteries, and optic nerve. This method allows the pathologist to transect the globe in a vertical plane from dorsal (twelve o'clock) to ventral (six o'clock), which allows examination of both tapetal and nontapetal fundus for animals. Exceptions include globes from animals with a macula (primates and birds). These eyes should be sectioned horizontally to allow examination of the macula. The globe is then transected with a brain knife, razor blade, or long scalpel blade, and the sections are examined with a dissecting microscope and gross findings recorded and photographed (Fig. 8.2). The hemispheres are then placed cut-surface down and sectioned approximately 2 cm into the hemisectioned globe with a brain knife or blade. The calotte is placed in an embedding chamber of appropriate size. An alternative to hemisection (which may dislocate the lens) is the removal of a cap, cutting

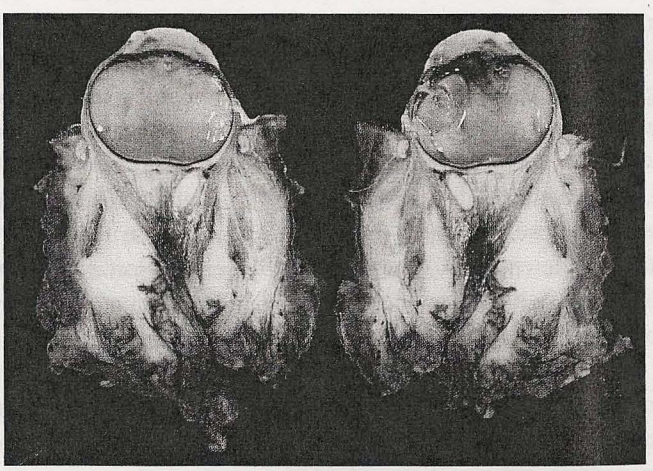

Figure 8.1. An exenterated bovine eye that was immersion fixed in Bouin's fluid for 72 hours and sectioned. Note the incomplete fixation of the orbital and ocular tissues. To ensure adequate fixation of globes that are exenterated, or removed by transpalpebral enucleation, the orbital tissues should be trimmed, removed, and labeled prior to immersion in fixatives; or multiple incisions should be placed circumferentially to the level of the episclera at 0.5 to 1-cm intervals through the attached orbital tissues to allow fixatives to penetrate adequately.

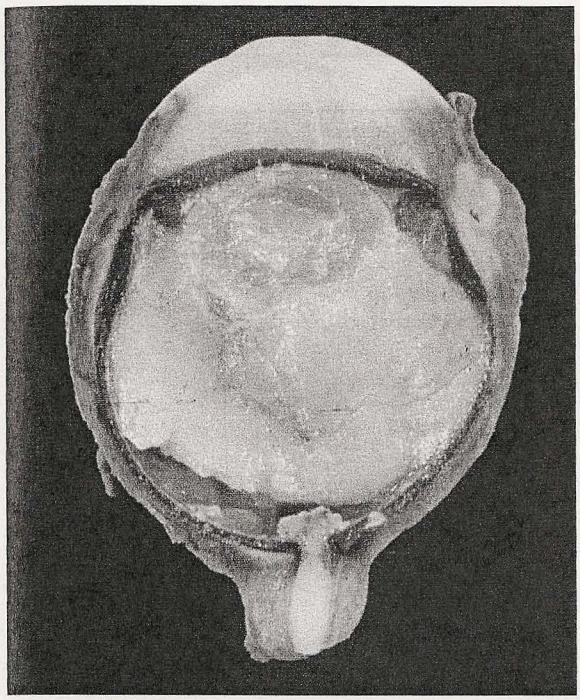

Figure 8.2. A Bouin's fluid–fixed globe from a dog diagnosed with a chronic lens rupture; the globe was enucleated via a transconjunctival approach. Note the lack of extraocular tissues and adequate fixation. Several gross lesions are evident, including plasmoid aqueous and vitreous, an exudative retinal detachment, and a lens capsule rupture, all synonymous with the gross diagnoses of endophthalmitis and phacoclastic uveitis.

from just inside the limbus to adjacent to the optic disc on the same side, followed by subgross intraocular examination and making a cut parallel to the first to end up with a central section and two calottes. The main section is embedded with the initial cut down to minimize the need for rough-cutting to obtain a section containing both pupil and optic nerve.

Transpalpebral enucleated globes are handled very similarly to exenterated globes. The indication for a transpalpebral enucleation is extensive neoplasia of the conjunctiva and eyelids, most commonly squamous cell carcinoma in the bovine and equine species. The orbital tissues attached to these globes are not as extensive as with exenterations, and the specimen is usually adequately fixed by immersion in either Bouin's fluid or 10% buffered formaldehyde with or without and an intravitreous formaldehyde injection. These globes are trimmed and, where necessary, extraocular tissues are labeled and margins inked. Globes are examined grossly, transilluminated to detect intraocular lesions, and processed as described previously for exenterated globes.

Blind and painful globes, globes with untreatable intraocular neoplasia, glaucoma, uveitis, and occasionally eyes enucleated for diagnostic evaluations, are usually surgically removed via a transconjunctival approach. These globes are routinely immersion fixed in Bouin's fluid or 10% buffered formaldehyde and have minimal attached orbital tissues, which limits the amount of trimming required by the pathologist. Examination and processing proceed as for the exenterated globes.

Rodent and other small globes are fixed by immersion, oriented appropriately for embedding, and processed whole and stained similarly to eyes from other animals. Multiple sections of these globes are taken until the appropriate area in the eye is located. Fetal rodents have very small globes that are difficult to remove intact because of their relative size and thin sclera. Fixation of the whole body in Bouin's fluid, and then serial sections of the skull horizontally to view both globes, are most appropriate for research.

Biopsies of eyelid skin, conjunctiva, and adnexa are common submissions. They are routinely fixed in buffered formaldehyde. It is important to identify cut surfaces with India ink or sutures and labels to alert the pathologist for orientation and margin evaluation.

Paraffin embedding and sectioning are performed routinely for all globes and biopsies. Some histotechnologists prefer sectioning the lens in a separate block to improve the quality of the section, and they will remove the lens prior to embedding the globe.

Fine needle aspirates of intraocular and scrapings of orbital and eyelid masses and exudates are occasionally submitted. Usually the fine needle aspirates are submitted as smears on glass slides and are stained routinely with Wright-Geimsa and examined by clinical pathologists. When a liquid aspirate is attained, it is placed in an EDTA (purple-topped) tube and submitted for cytospin analysis.

The recommended stains for routine light microscopic examination of ocular tissues are hematoxylin and eosin, periodic acid-Schiff (PAS), and luxol fast blue. These stains allow the pathologist a thorough examination of the cellular morphology, basement membranes, and optic nerve. Additional special stains for evaluating infectious organisms and infiltrates are listed in Table 8.2. Special stains and immunohistochemistry have several applications in ophthalmic pathology to allow identification of tissues and structures, identification of infectious organisms, and determination of cellular lineage. Commonly utilized immunohistochemical antibodies are listed in Table 8.3. Tagging the antibody with a red marker instead of the common yellow-brown marker enhances the examiner's ability to identify positive labeling in the often heavily pigmented ocular tissues.

Transmission and occasionally scanning electron microscopy are useful in veterinary ophthalmology to identify cells of origin of poorly differentiated neoplasms, to identify specific infectious agents, and as research tools. Specimens from the eye and adnexa destined for electron microscopy have specific fixation, embedding, sectioning, and staining requirements to obtain optimal electron microscopic evaluation. Small biopsies of eyelid skin, conjunctiva, sclera, or cornea may be adequately fixed by immersion in gluteraldehyde. Although biopsies of the intraocular tissues from globes that are routinely immersion fixed can be prepared for Epon embedding and sectioning for electron microscopy, the subcellular details are limited. For optimal fixation of intraocular tissues, specialized fixation techniques are used. Several techniques are available, and most involve prompt fixation of the enucleated globe. These globes are immersed in chilled fixative immediately after enucleation for several minutes, then removed, and the globe is opened with a pars plana incision to enhance exposure of the intraocular tissues to other fixatives and buffers. For optimal fixation of the outer segments and

Table 8.2 The Common Histochemical Stains Used in Ophthalmic Pathology

Target	Stain	Result
General purpose	Hematoxylin and eosin	Proteins: pink Nucleic acid: purplish blue Calcium: blue
Basement membranes (mucopolysaccharides and glycoproteins)	Periodic acid-Schiff (PAS)	Dark pink
Collagen/muscle	Masson's trichrome	Collagen: blue Muscle: red
Acid mucopolysaccharides	Alcian blue Colloidal iron	Blue
Mucin	Mucicarmine	Pink to red
Iron	Perl's Prussian blue	Blue
Calcium	Von Kossa	Black
	Alizarin red	Red
Myelin	Luxol fast blue	Aqua to blue
Axons	Bodian	Black
Lipid (fresh frozen tissue only)	Oil red O Sudan black	Red Black
Amyloid	Congo red Thioflavin T Crystal violet	Red (yellow-green birefringence with polarization) Fluorescent white Violet to purple
Elastic tissue	Verhoeff-Van Gieson	Black
Melanin	Fontana-Masson	Black
Fungi	PAS Gomori methenamine silver	Purple-pink Black
Acid-fast organisms	Ziehl-Neelsen	Red
	Fite-Faraco	Red
Acanthomoeba	Calcaflour white Acridine orange	Fluorescent white Fluorescent orange
Chlamydia	Giemsa	Pink inclusions

Table 8.3 Common Immunohistochemical Markers Used in Ophthalmic Pathology

Tissue	Antibody
Melanocytes	S-100, melanin A, tyrosinase, HMSA 45
Glial cells	GFAP
Vascular endothelium	Factor VII
Epithelial cells	Cytokeratin
Smooth muscle cells	Actin
Hematopoietic cells	Leukocyte common antigen

retinal pigment epithelium (RPE), osmium is often added to these specialized fixation protocols. These protocols provide excellent fixation and intracytoplasmic and cellular membrane detail of the outer and inner retinal segments (Fig. 8.3). Occasionally, methodologies such as histochemistry for lipids and some cell markers require fresh rather than fixed tissue

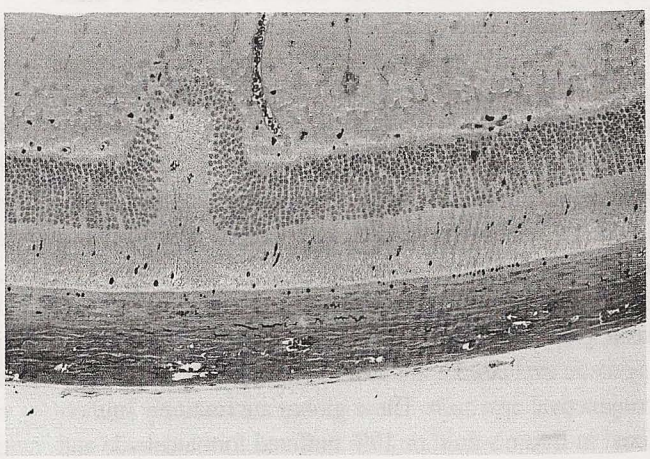

Figure 8.3. This is a section of the posterior segment from a Sprague-Dawley rat with a retinal fold. Note the excellent fixation and minimal artifacts present in this Epon-embedded tissue. This globe was triple fixed, plastic embedded, and sectioned. (Stain toluidine blue, original magnification 50X.)

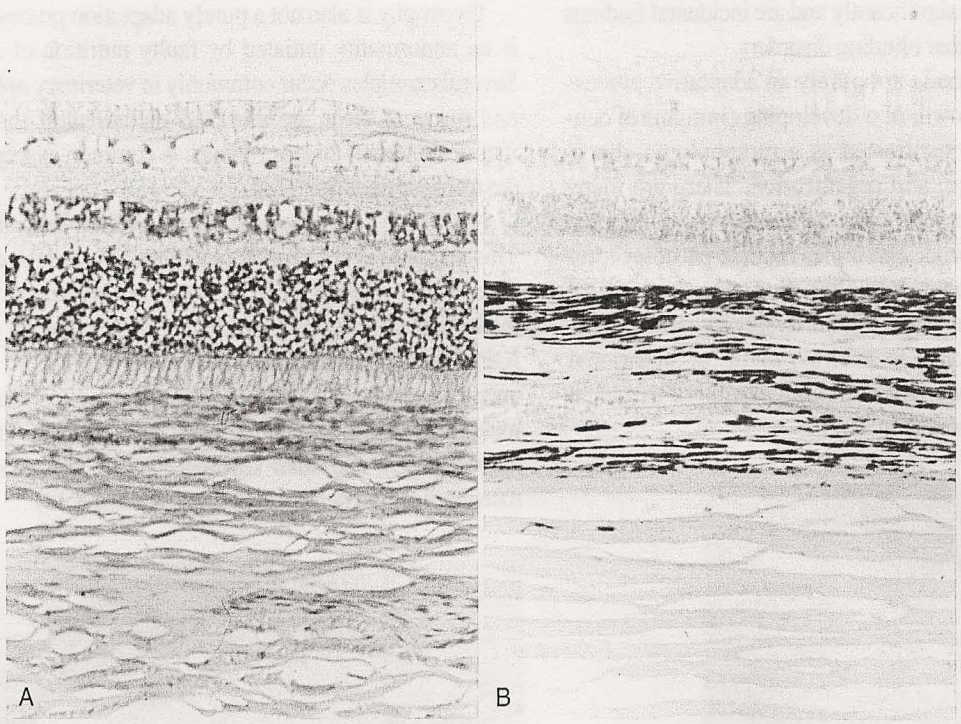

Figure 8.4A and B. The universal lesion in all dogs with Collie eye anomaly is choroidal hypoplasia. It is not a visually striking lesion and sometimes requires comparison to age- and site-matched controls. Note that the poorly pigmented choroid is less than half the thickness that normally approximates the retinal thickness. (Hematoxylin and eosin stain original magnification 100X.)

or special fixation and freezing. We encourage preoperative communication between clinician and pathologist to identify and address these specialized fixation and processing issues.

FUNDAMENTAL PATHOLOGY

The eye is a relatively closed system, and the injury to one ocular tissue often induces bystander injury to adjacent tissues. Many of the ocular tissues are postmitotic, which limits the capacity for pristine repair. Most ocular tissues must therefore adapt to injury in relatively limited ways, and many of these adaptations are sequential. The cellular responses of ocular tissues occur from development to maturity and include hypoplasia, aplasia, atrophy, dysplasia, hypertrophy, hyperplasia, metaplasia, necrosis, apoptosis, degeneration and calcification, and neoplasia.

Hypoplasia is defined as diminished cell proliferation due to inadequate cytokine stimulation, lack of progenitor cells, or specific cellular receptors. Hypoplasia is occasionally associated with inadequate conjunctival epithelial cell turnover. However, it is most commonly associated with restricted development of an ocular tissue. The most common example occurs in the subalbinotic animals in which the uvea is hypoplastic (Fig. 8.4B). Hypoplasia may be induced by decreased neural crest induction or migration.

Aplasia is a lack of development of a tissue and is not an adaptation response but a lack of induction of cellular development. Aplasia is usually focal, thereby affecting only a small area of the ocular tissues. Absence of tissue creates a defect called a coloboma. Colobomata of the optic nerve, uvea, and lens are only occasionally diagnosed (Fig. 8.5). Most ocular colobomata do

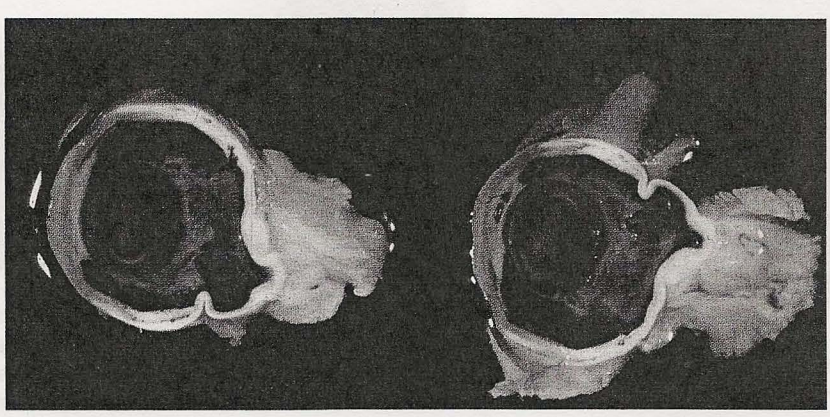

Figure 8.5. A gross section of a formalin-fixed eye from a blind Collie puppy. Note the peripapillary coloboma, staphyloma, and retinal detachment.

not affect ocular function significantly and are incidental findings in globes submitted for other blinding disorders.

Dysplasia by definition is not purely an adaptative process but rather an atypical growth of a developing (immature) ocular tissue. Dysplasia is manifested as a morphologic abnormality in cell size, shape, and organization. There are many examples of dysplasia in veterinary ophthalmology, and most are inherited genetic defects. Examples include photoreceptor dysplasias, retinal pigment epithelial dysplasia, and retinal dysplasia (Fig. 8.6). However, retinal dysplasia is occasionally an adaptation response to a virus, toxin, or nutritional deficiency that induces necrosis and degeneration of tissues in the eye during development (Fig. 8.7).

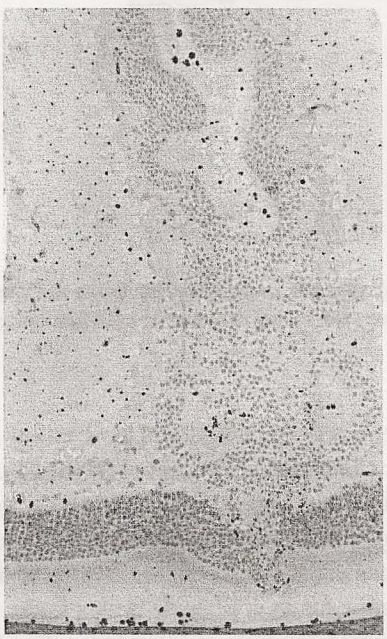

Figure 8.6. A section of retina from a Miniature Schnauzer dog with inherited retinal dysplasia. Note the prominent rosettes with incomplete photoreceptor development in the center and the discontinuous outer limiting membrane. (Toluidine blue stain, original magnification 200X.)

Figure 8.7. A hematoxylin- and eosin-stained section of a retina of a calf that survived in utero bovine virus diarrhea (BVD) infection. Note the retinal dysplasia, glial proliferation, and retinal degeneration (Original magnification 100X).

Dystrophy is also not a purely adaptation process. Dystrophy is an abnormality initiated by faulty nutrition of mature cells. Several examples occur commonly in veterinary ophthalmology, and many of these are inherited mutations of the cornea that manifest in many breeds of dogs. A common example is corneal dystrophy (Fig. 8.8).

Atrophy is a reduction of tissue mass after the cells are mature. This response is common in ocular tissues, and the etiologies are diverse and include genetic mutations, ischemia, denervation, inadequate nutrition, advanced age, and prolonged elevations of IOP. These conditions may induce degeneration, necrosis, or apoptosis, and subsequently a loss of tissues. Common examples include senile iris atrophy, glaucomatous uveal, retinal and optic nerve atrophy, and outer segment atrophy associated with neurosensory retinal detachment (Figs. 8.9 and 8.10).

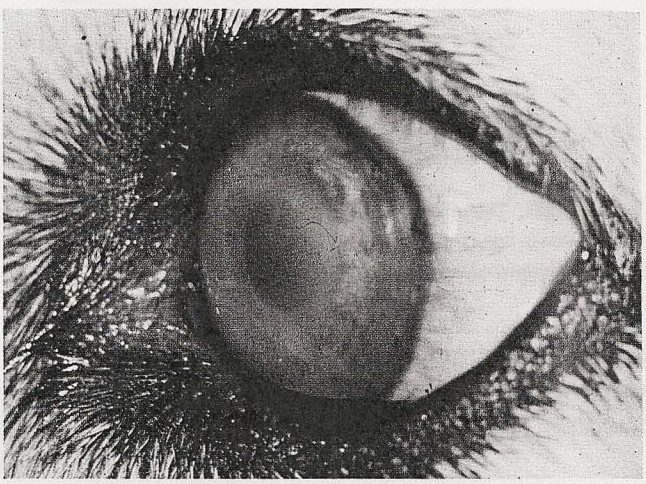

Figure 8.8. A clinical photograph of inherited corneal dystrophy in an Alaskan Malamute dog. Note the opalescent circular ring in cornea.

Figure 8.9. Optic disc and nerve degeneration that developed secondary to chronic primary glaucoma in a Basset Hound. Note the prominent optic disc cupping, papillary gliosis, and optic nerve degeneration. Also note the inner retinal degeneration that is more extreme on the nontapetal side (right side) than the tapetal area (tapetal sparing.) (Hematoxylin and eosin stain, original magnification 20X.)

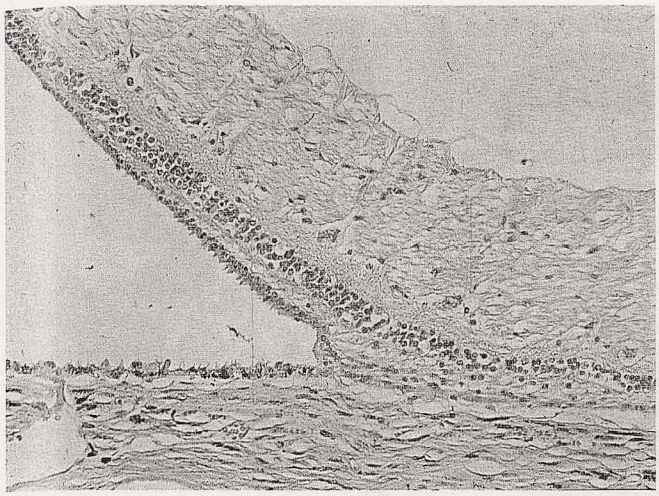

Figure 8.10. A histologic section of a chronically detached retina. Note the retinal detachment, outer retinal atrophy, and retinal pigment epithelial hypertrophy and pigmentation. (Hematoxylin and eosin stain, original magnification 100X.)

Figure 8.11. Retinal pigment epithelial hypertrophy is a common and acute adaptational response to retinal detachment in domestic animals. (Toluidine blue stain, Epon embedded, original magnification 400X.)

Hypertrophy is an increase in cell size and therefore cellular mass. A few ocular tissues adapt to stress by hypertrophy, which is often a prelude to hyperplasia. Common examples within the eye include retinal pigment, lens, iris, and vascular endothelial hypertrophy (Fig. 8.11).

Hyperplasia also increases cellular mass and commonly occurs with hypertrophy. However, hyperplasia results in increased mass by an increase in the number of cells. Hyperplasia is an efficient adaptation response within ocular tissues that are capable of mitotic replication (i.e., retinal pigment, lens and corneal epithelium, and uveal melanocytes) (Fig. 8.12).

Metaplasia is an adaptation response to stress in which a mature tissue changes or transforms into another. This is an important response in the eye, and examples include fibrous and osseous metaplasia of the corneal, lens, uveal, and RPE (Fig. 8.13).

These adaptational cellular responses, whether congenital, developmental, or acquired, leave a footprint that is often unique in its gross, subgross, and light microscopic appearance. This facilitates diagnosis by the ophthalmologist and confirmation of such by the pathologist. When the ocular cells or tissue can no longer adapt to the insult, an irreversible cellular event develops (i.e., cell death). Cells die by two basic mechanisms: necrosis or apoptosis.

Necrosis is cell death that often affects multiple cells within the eye, and it is characterized with light microscopy by increased

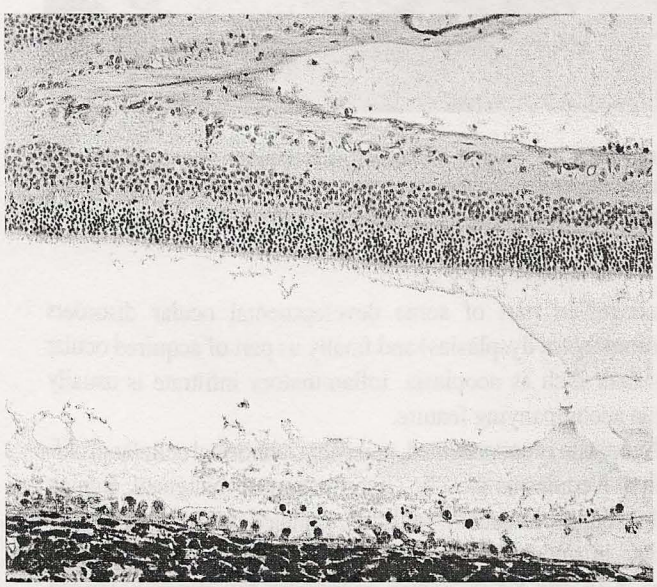

(a)

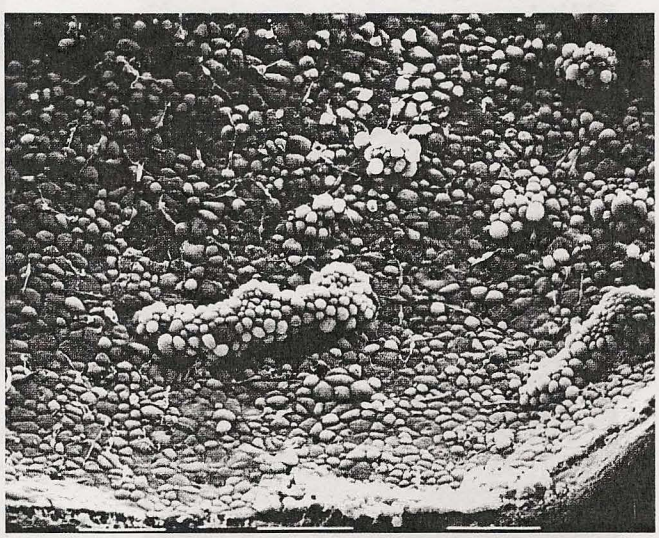

(b)

Figure 8.12. A. Serous retinal detachment in a dog. Note the retinal pigment epithelial hypertrophy, hyperplasia, and migration into the detachment where they perform macrophage duties. Note also the degeneration of the outer and inner segments and outer nuclear layer. (Periodic acid-Schiff stain, original magnification 300X.) **B.** A scanning electron micrograph of the RPE under a detached retina in a dog. The retina has been removed. Note the retinal pigment epithelial hypertrophy and hyperplasia. (Bars = 0.1mm.)

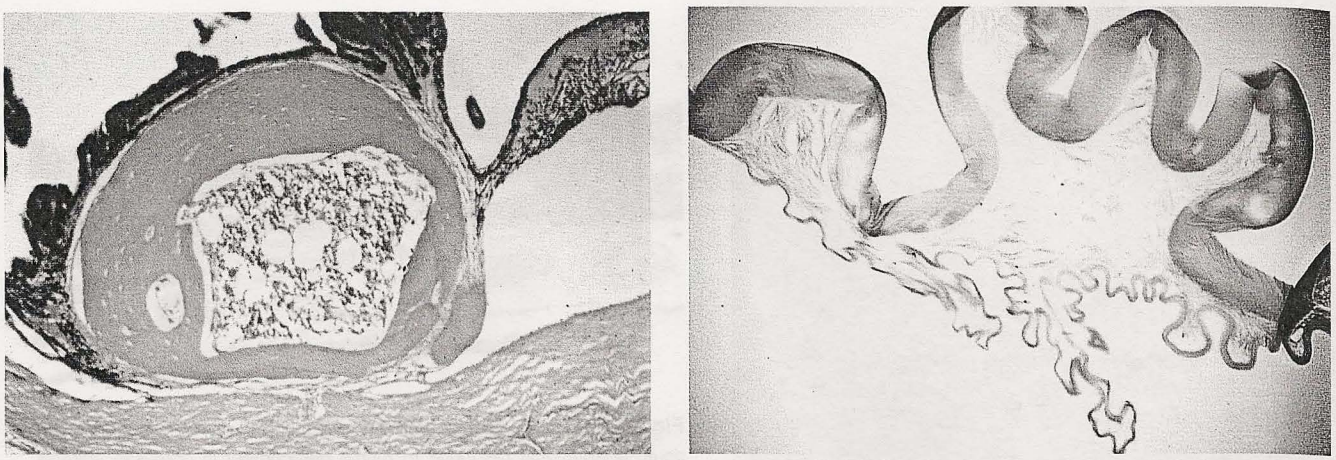

(a) (b)

Figure 8.13. **A.** Osseous metaplasia of the anterior segment of an eye from a Guinea pig. (Hematoxylin and eosin stain, original magnification 100X.) **B.** Fibrous metaplasia of lens epithelial cells in this hypermature cataract in a dog. The metaplastic lens epithelium extends throughout the folded lens capsule as multiple spindle cells. (PAS, original magnification 100X.)

cellular cytoplasmic eosinophilia and nuclear changes of pyknosis (nuclear shrinkage), karyolysis (nuclear fragmentation), and karyorrhexis (nuclear disappearance). Several types of necrosis are recognized; in coagulative necrosis, cell morphology is retained somewhat, contrasted to liquefactive necrosis in which enzymes destroy the cellular architecture (Fig. 8.14). Necrosis is usually accompanied by an inflammatory infiltrate.

In contrast, apoptosis is programmed cell death that often affects individual cells. Morphological clues for diagnosis of apoptosis include cell shrinkage, detachment from neighboring cells, development of cell surface blebs, and frequently phagocytosis of the affected cell (Fig. 8.15). Apoptosis is recognized as an efficient method of physiologic cell removal and remodeling of ocular tissues during development. Apoptosis is also

Figure 8.14. Choroiditis and retinal necrosis in a septic calf. (Hematoxylin and eosin stain, original magnification 200X.)

Figure 8.15. Progressive retinal atrophy in a middle-aged collie. Note the organelle swelling and cone nuclei exhibiting apoptotic changes. (Transmitting electron micrograph 3600X.)

a recognized part of some developmental ocular disorders (photoreceptor dysplasias) and finally as part of acquired ocular disorders such as neoplasia. Inflammatory infiltrate is usually not an accompanying feature.

Neoplasia is uncontrolled, persistent, abnormal cellular proliferation. Neoplasms may be either benign or malignant. Benign ocular neoplasms contain well-differentiated cells that are usually similar in appearance to the tissues from which they derive (Figs. 8.16 and 8.17). Benign neoplasms are generally termed by adding the suffix *-oma* to the name of the cell of origin: melanocytoma, tarsal gland adenoma, and so on. Benign neoplasms are slowly expansile, are usually encapsulated, and induce damage by compression of adjacent tissues. Malignant neoplasms are signified by attaching *sarcoma* or *carcinoma* to the

Figure 8.16. Tarsal gland adenoma is a common, benign eyelid neoplasm of dogs. Note the well-differentiated glandular structure. (Hematoxylin and eosin stain, original magnification 100X.)

Figure 8.18. A subgross view of a malignant intraocular sarcoma in a cat. Note the complete invasion of the vitreous, choroid, ciliary body, and iris. In several areas, the sarcoma is invading the sclera. (Periodic acid-Schiff stain, original magnification 2X.)

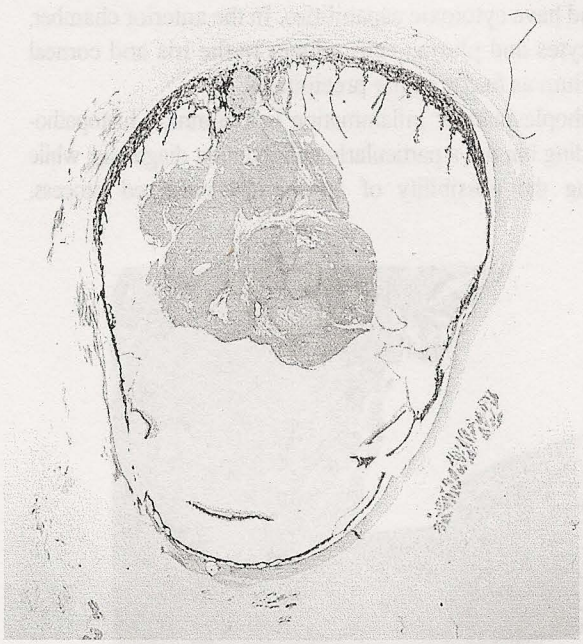

Figure 8.17. A well-differentiated ciliary adenoma from a cat. Notice the endophytic growth and lack of ocular tissue invasion of this benign neoplasm. (Periodic acid-Schiff stain, magnification 2X.)

tissue of origin: intraocular sarcoma, squamous cell carcinoma. Malignant ocular neoplasms may be categorized into four groups: carcinomas, sarcomas, melanomas, and lymphoreticular (round cell) neoplasms. These malignant neoplasms range from poorly differentiated to well differentiated and are characterized best by their invasive characteristics of tissues. Histological features of malignant neoplasms include cellular pleomorphism, increased nucleocytoplasmic ratio, high mitotic index, atypical mitotic figures, destruction and invasion of cellular architecture, and necrosis (Fig. 8.18).

OCULAR INFLAMMATION

Ocular inflammation results from a variety of insults, including accidental or surgical trauma; exposure to toxic substances, infectious agents, noninfectious immunogenic stimuli, and physical agents; and neoplasia. The unique anatomic and physiologic properties of the eye render it exquisitely sensitive to inflammation and its sequelae, and the clinician dedicates significant resources to tempering the inflammatory response. These properties include ocular functional dependence on tissue transparency and precise intertissue physical relationships; inflammation resolves with fibrosis, and scars are not transparent; they distort tissue relationships as they mature and contract. Likewise, because the eye is largely composed of a voluminous extracellular fluid compartment with a relatively slow turnover, the vitreous, the chemical mediators and products of inflammation exert an exaggerated and prolonged effect on the ocular tissues, whereas elsewhere in the body they are metabolized, diluted, and carried away by the vasculature in a more efficient manner.

The eye is an immunologically privileged site related to the isolation and avascularity of many of its component tissues and the absence of lymphatics; the conjunctiva does have some lymphatics, and their presence in the orbit is somewhat controversial. These features largely dictate how a particular ocular tissue responds to inflammatory stimuli. Anterior chamber–associated immune deviation

(ACAID) has implications for the modulation of the ocular inflammatory response, as discussed in detail in Chapter 5.

Ocular inflammation should be regarded as a series of events occurring over time; the pathologist is thus limited to viewing a single frame in an orchestrated sequence of events (the clinician has an advantage in this regard). Inflammation is largely regulated by a vast array of chemical mediators that are primarily endogenous but may be exogenous in origin, such as from venoms and microbial products. Acute inflammation is of rapid onset and short duration in terms of days. The initial events are vascular and exudative, mediated by plasma factors (the kinin, clotting, and complement systems) and tissue factors (vasoactive amines, prostaglandins, lysosomal products, and lymphocyte products). Vascular changes include dilation with congestion and increased vascular permeability, with disruption of the blood–ocular barrier and the egress of intravascular fluid and protein into adjacent tissues. Fibrin, the smallest of the plasma proteins, is the primary proteinaceous component; fibrinous inflammation is commonly associated with bacterial infection, septicemia, or surgical or accidental trauma. Clinically, these changes manifest as conjunctival and uveal edema, aqueous flare, and plasmoid vitreous. If the blood–ocular barrier of the RPE is compromised by these mediators, serous or exudative retinal detachment results. If the tight intercellular junctions of the ciliary epithelium remain intact, edema of the ciliary processes may occur.

Subsequent events are characterized and defined by the attraction and recruitment of the cells of inflammation. Neutrophils are the hallmark of acute inflammation (Fig. 8.19); note that this is the pathologist's definition of acute, which may differ from that of the clinician's. Neutrophils are produced in the bone marrow, are rapidly mobilized in response to injury, and have a short life span of 1 to 2 days in tissues. They are phagocytic cells whose granules contain substances that degrade nonviable substances; neutrophils possess direct antimicrobial capacity as well. External degranulation can occur and may contribute to tissue damage, as is the case in the pathogenesis of the type III hypersensitivity reaction to canine adenovirus, type I, where the antigen–antibody complexes that form within the corneal endothelium subsequently fix a neutrophil-chemotaxin complement. If infiltration is accompanied by liquifactive necrosis, the inflammation is described as purulent and suppurative. In the anterior chamber, neutrophils gravitate inferiorly to present clinically as hypopyon.

Inflammation becomes chronic in the presence of persistence of the original stimulus, significant tissue destruction or a foreign body, or a poor blood supply. Chronic inflammation is both exudative and proliferative, occurs over weeks, and is superimposed on the process of repair. Lymphocyte and plasma cell infiltrates are the hallmark of chronic disease, with implications of an immune-mediated process (Fig. 8.20). Lymphocytes are either (thymus T-lymphocytes) or nonthymus-derived lymphocytes (B-lymphocytes). The former are involved with cell-mediated immune responses and include subpopulations that are specifically cytotoxic, secretors of lymphokines, immunomodulatory, and carriers of immune memory. B-lymphocytes are capable of transforming into plasma cells, which secrete class-specific antibodies to a specific antigen. Inspissation of plasma cells leads to the evolution of plasmacytoid and Russell body cells. Some lymphocytes, referred to as null cells, lack both T and B characteristics, and have cytotoxic capabilities. In the anterior chamber, lymphocytes and plasma cells adhere to the iris and corneal endothelium as fine granular precipitates.

Lymphoplasmacytic inflammation is a common histopathologic finding but not a particularly enlightening diagnosis; while suggesting the possibility of an immune-mediated process,

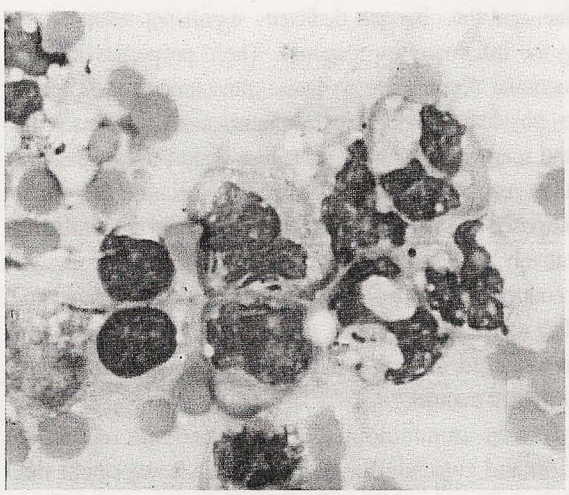

Figure 8.19. Neutrophils are the first-responder inflammatory cells. Note the toxic neutrophils, which contain intracytoplasmic bacteria, and the red blood cells and mononuclear cells. This was a fine-needle aspirate from the vitreous of a dog with septic endophthalmitis. (Wrights-Giemsa stain, magnification 400X.)

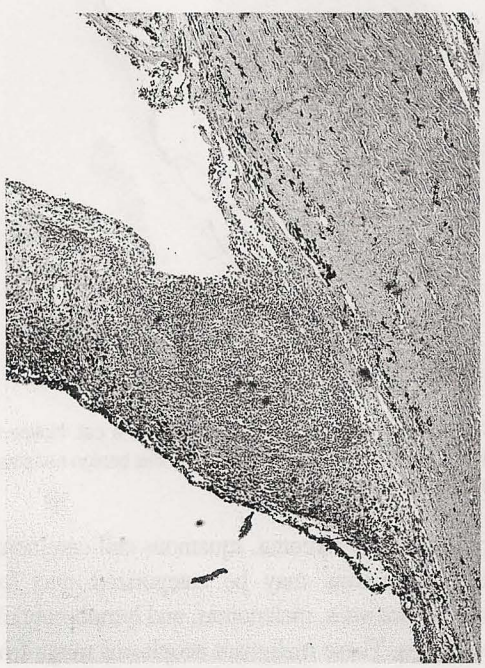

Figure 8.20. Idiopathic lymphocytic plasmacytic uveitis in a cat. Note the diffuse infiltration of lymphocytes and the lymphoid follicle at the anterior base of the iris. (Hematoxylin and eosin stain, original magnification 200X.)

practically it portrays the limitations of the pathologist in providing a diagnosis of greater clinical value. Many infectious diseases can present with such an infiltrate and "the torch is returned" to the clinician to pursue additional diagnostic modalities (serology, cultures, IFA, PCR).

Eosinophils are produced in the bone marrow and are present in both acute and chronic inflammation; their granules contain arginine-rich basic protein, peroxidase, arylsulfatase, and phospholipase. They are attracted by antibody–antigen complexes, modulate the inflammatory response by inhibiting mast cell products, and demonstrate a killer function toward parasites, and thus are associated with allergic reactions and parasitic infestation. Mast cells granules contain heparin, histamine, and serotonin, among other factors; are found in abundance in the conjunctiva and uvea; and play an initiating role in hypersensitivity responses (Fig. 8.21). Cytoplasmic metachromatic granules, not seen on routinely stained preparations, are readily evident when stained with toluidine blue, or Duffies stain (Figs. 8.21 and 8.22).

The presence of a resistant or replicating stimulus leads to the activation of the macrophage system and is referred to as granulomatous inflammation, which is always chronic. It can be initiated by specific organism, immunologic reactions, or foreign bodies. Its hallmark is the epithelioid cell, a specialized histiocyte characterized by abundant cytoplasm and a large, pale nucleus (with an appearance reminiscent of a squamous epithelial cell). Fusion of epithelioid cells form multinucleated giant cells that differ in appearance depending on the inciting stimulus (Fig. 8.23). Foreign-body giant cells possess multiple nuclei dispersed throughout the cytoplasm; the nuclei of Langerhans giant cells array around the periphery of the cell and are usually associated with infectious granulomas; and Touton giant cells are encountered in xanthomatous and lipogranulomatous disease with cytoplasmic lipid vacuoles and the nuclei concentrically arranged in the midperiphery.

Granulomatous inflammation is described as discrete, zonal, or diffuse, dependent upon the organization of the macrophages within the tissues. In the discrete form, distinct compact granulomas develop; there may or may not be central necrosis. Discrete granulomas may form in virtually any of the ocular tissues and require distinction both clinically and histopathologically from nodular or follicular lymphoplasmacytic infiltrates. In zonal granulomatous inflammation, the epithelioid cells surround the stimulus; chalazion, phacoclastic uveitis (in some species), and scleritis exemplify, with sebaceous secretion, lens protein, and

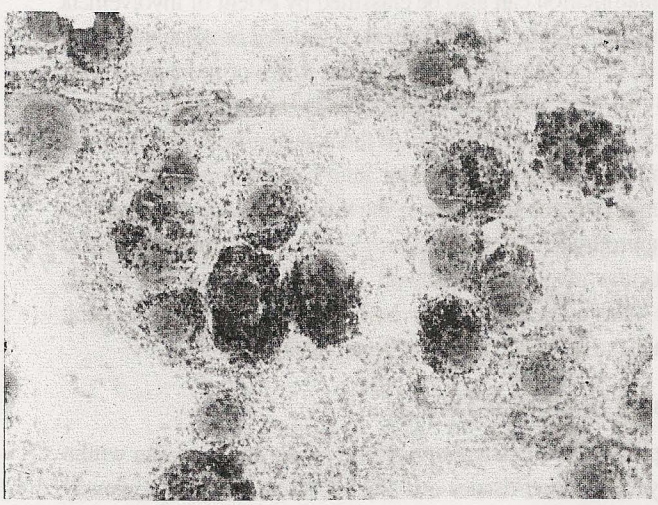

Figure 8.21. Mast cells are normal inhabitants of the conjunctival and episcleral tissues, and their prominent granules contain heparin, histamine, and serotonin. This cytology specimen was a fine-needle aspirate from an episclera mast cell tumor. (Toluidine blue stain, original magnification 400X.)

Figure 8.22. Mast cells are readily identified by several histochemical stains, including Duffies stain. Note the blue-stained mast cells and red stained eosinophils in this palpebral conjunctival biopsy from a cat. (Duffies stain, original magnification 250X.)

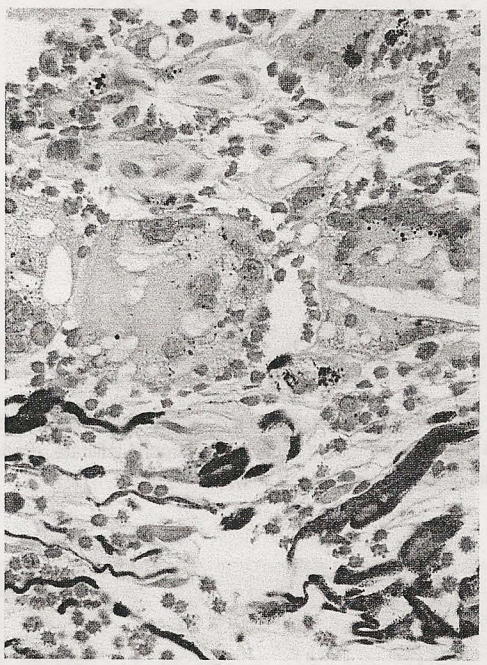

Figure 8.23. Multiple coalescing epithelioid macrophages within a fibrovascular membrane on the iris of dog with chronic retinal detachment and uveitis. Some of these giant cells have peripheral nuclei typical of Langerhans giant cells. (Hematoxylin and eosin stain, original magnification 400X.)

collagen the respective stimuli. Epithelioid cells intermixed with lymphocytes and plasma cells are broadly distributed in diffuse granulomatous inflammation, with uveodermatologic syndrome providing a prototypic example. In the anterior chamber, macrophages will congregate and adhere to the corneal endothelial surface as large "mutton-fat" precipitates.

Regardless, the pathologist attempts to identify what the cells are phagocytizing to arrive at an etiologic diagnosis, and stains for fungi (PAS or Gimori's methenamine silver), mycobacteria (Ziehl-Neelsen, Fite's, or auramine-rhodamine fluorescence), and spirochetes (silver stains) are useful in this regard (Figs. 8.24, 8.25, and 8.26).

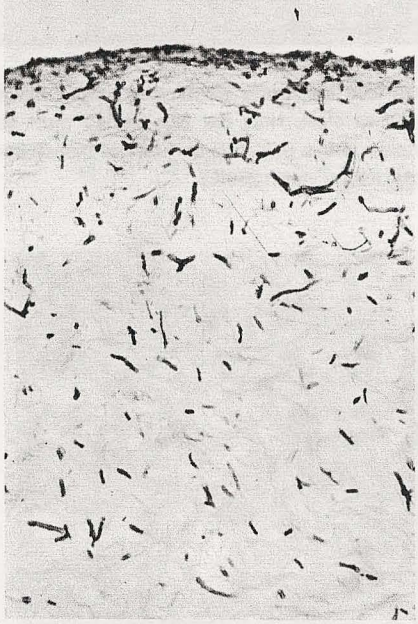

Figure 8.24. Diffuse mycotic keratitis in a horse. Note the fungal hyphae throughout the cornea stroma and a diffuse neutrophil infiltrate. (Periodic acid-Schiff stain, original magnification 350X.)

Figure 8.25. A vitreous aspirate from a dog with systemic blastomycosis and endophthalmitis. There are five *Blastomyces dermatitidis* organisms, degenerate neutrophils, and plasmoid vitreous. (Periodic acid-Schiff stain, original magnification 400X).

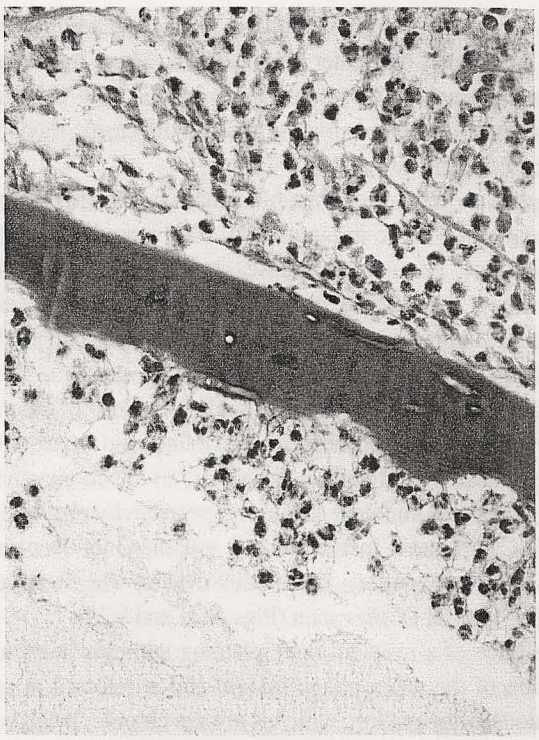

Figure 8.26. Mycotic keratitis in horse. Note the fungal hyphae within Descemet's membrane, the erosions on this basement membrane, and the dense infiltration of neutrophils nearby. (Periodic acid-Schiff stain, original magnification 350X.)

Granulomatous inflammation may have an acute neutrophilic component; this type of response is typical in mycotic infection. Pyogranulomatous blepharitis (presumed an immune-mediated disease) and the pyogranulomatous uveitis that accompanies feline coronavirus infection are additional examples. Note that the terminology is not precise in that there is not necessarily necrosis and suppuration in these processes.

From the preceding, it is evident that inflammation can be described as acute or chronic and as nongranulomatous or granulomatous on the basis of the nature of the cellular infiltrate. Ocular inflammation can also be classified by extent of involvement of the ocular tissues. Involvement of isolated or adjacent tissues may be described with the suffix *-itis;* if two or more tissues are involved, that which is most directly or primarily involved comes first in the terminology. If there is significant involvement of one of the large extracellular fluid compartments—the anterior and posterior chambers or the vitreous—*endophthalmitis* is the appropriate descriptor. *Panophthalmitis* implies extensive intraocular involvement as well as involvement of the fibrous coats—the cornea, sclera, or both; extension to adjacent orbit and adnexa often accompanies panophthalmitis.

Repair of Ocular Tissue

The principles of tissue healing and repair are the same within the eye as in other tissues and are discussed in detail previously in this chapter. However, in addition to the anatomic and functional interdependence of the ocular tissues and the relationship of function to transparency of the dioptric system, the limited mitotic potential of critical tissues (the corneal endothelium in some species and retinal neurons) as well as the proliferative and

metaplastic capabilities of the lens and neuroectodermal epithelium dictate that functional repair is indeed the exception rather than the rule, and the clinician struggles to create an environment in which functional repair prevails. This perspective is important in considering the sequelae of inflammation.

Sequelae and Complications of Ocular Inflammation

In general, the sequelae and consequences of intraocular inflammation are proportional to the severity and duration of the inflammatory process. Fibrinous exudation initially with subsequent organization (fibrosis) can lead to adhesions and membranogenesis. Adhesions may form between iris and cornea (anterior synechiae) and iris and lens (posterior synechiae) (Fig. 8.27). Adhesions between iris root and peripheral cornea (peripheral anterior synechiae) result in angle closure. Anterior chamber fibrinous exudation (Fig. 8.28) with subsequent organization is a common feature of immune-mediated pigmentary dispersion uveitis in Golden Retrievers. Membranes that organize retrolentally (frequently with condensation of a posteriorly detached vitreous as a scaffold) incorporate the ciliary processes and are referred to as cyclitic membranes (Fig. 8.29); they can be devastating to the eye by virtue of ciliary and retinal traction with resultant ciliary detachment and hypotony and tractional retinal detachment; phthisis bulbus is a common outcome. Vitreal and periretinal membranes, uncommon in animal eyes in contrast to humans, may also result in retinal detachment as they mature and contract.

Secondary cataracts may occur as a result of perturbation of the nourishing fluids of aqueous and vitreous by the products of inflammation with associated effects on lens metabolism. The lens epithelial cells are particularly susceptible with anterior subcapsular fibrous plaques and posterior migration with bladder cell formation common associations. Membranes may adhere to the anterior lens capsule with focal cataract formation. Inflammatory cells and products may weaken the zonulae with resultant lens dislocation; these sequelae are seen most commonly in the cat and occasionally in the dog.

Ocular membranogenesis is an important sequel to inflammation that can occur with exuberance especially in the canine eye. While one may refer to specific tissues, such as retrolental corneal membranes, pupillary membranes, and cyclitic membranes, it is important conceptually that these membranes frequently exist as an anatomic continuum as they extend along the tissue surfaces of the anterior and posterior segment. They may be caused by fibrous ingrowths through a corneal or scleral wound, organization of fibrinous exudation or hemorrhage, or granulation responses by the uveal tissue, or they may arise from metaplastic epithelium; phacoclastic uveitis, which occurs following breach of the lens capsule, is largely the result of the proliferation of metaplastic lens epithelium.

Figure 8.27. Pupillary occlusion due to posterior synechiae. There is a fibrous adhesion of the iris leaflets to the anterior lens capsule in this domestic chicken. (Hematoxylin and eosin stain, original magnification 40X.)

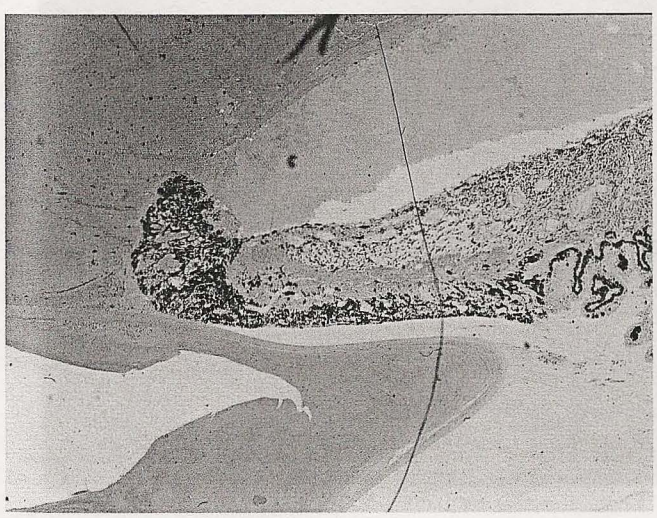

Figure 8.28. Plasmoid aqueous, cataract, posterior synechiae, and a mild preiridal fibrovascular membrane inducing ectropion uvea in calf with endophthalmitis secondary to septicemia. (Hematoxylin and eosin stain, original magnification 40X.)

Figure 8.29. A ruptured lens capsule with a perilenticular fibrous membrane and diffusely thickened iris and ciliary body in a cat. (Periodic acid-Schiff stain, original magnification 2X.)

The formation of fibrovascular membranes on the anterior iris (Fig. 8.30), retina, or optic disc, as a consequence of the effects of soluble vasogenic proteins (predominantly vascular endothelial growth factor [VEGF]), is a common and consequential event in the eyes of domestic animals and can occur as a result of chronic retinal detachment, retinal ischemia from glaucoma or hypertension, chronic uveitis, and intraocular tumors. The sources of these proteins may be retinal neurons, inflammatory cells, or neoplastic cells. In domestic animals, the iris is much more commonly affected than the posterior segment tissues, again in contrast to human eyes. While clinically the process is described as rubeosis irides, or "red iris," in human eyes, clinical manifestations are more difficult to detect in animals, and the term *preiridal fibrovascular membrane* (PIFM) is preferred. These membranes may proliferate over the pectinate ligaments and lead to angle closure or obstructive glaucoma, may bleed as a common cause of spontaneous hyphema, and may extend as pupillary, retroiridal, or anterior lens capsular membranes.

Secondary glaucoma occurs as common and significant sequelae of inflammation by a variety of possible mechanisms. Extensive peripheral anterior synechiae with angle closure may occur with or without iris bombé or pupillary membranes; in the latter instance, not only is aqueous circulation inhibited at the pupil but the pressure differential between anterior and posterior chambers leads to anterior bowing of the iris with angle closure that will mature into peripheral anterior synechiae. As mentioned previously, iridocorneal angle (ICA) obstruction or closure can occur as a result of PIFMs or other anterior chamber membranes. In phacolytic glaucoma, lens protein escaping through the intact lens capsule is ingested by macrophages that are of significant dimension to physically obstruct the trabecular meshwork. In chronic lymphoplasmacytic uveitis, notably in cats, accumulations of inflammatory cells within the ciliary cleft can block access to the trabecular meshwork. Lastly, the chemical by-products of chronic inflammation may have a deleterious effect on trabecular endothelial cells.

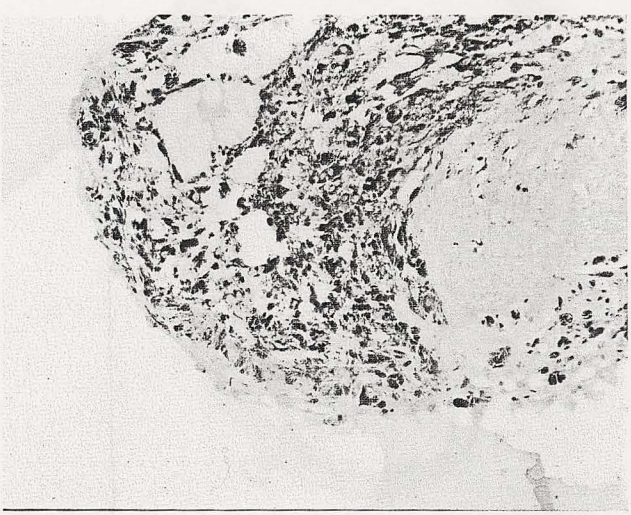

Figure 8.30. Entropion uvea in dog. Note the small preiridal fibrovascular membrane (PFM) that envelops the iris leaflet and pulls the tip inward toward the lens. (Hematoxylin and eosin stain, original magnification 200X.)

Retinal detachment may occur as the result of exudation from the choroid as the retinal pigment epithelial barrier is compromised (Fig. 8.31) or as a result of traction by cyclitic, vitreal, or preretinal membranes (Fig. 8.32).

Atrophy develops as postinflammatory sequelae to cell and tissue loss in the uvea, retina, and optic nerve (Fig. 8.33). Less significant uveal changes include a melanocytic hyperplasia with resultant hyperpigmentation and the formation of inflammatory iridociliary cysts.

Phthisis bulbus (wasted eye) occurs when severe inflammation and its sequelae result in cessation of aqueous production. The clinical definition of this end-stage process is a shrunken eye; to the pathologist, the hallmarks are an atrophic and disorganized globe that is usually characterized by a cyclitic membrane and variable degrees of chronic inflammation. Fibrous or osseous metaplasias of the ocular epithelium are commonly encountered, necessitating decalcification in order to process the globe.

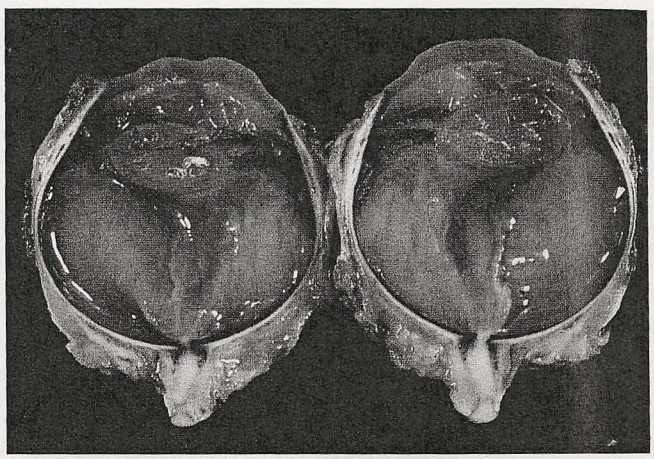

Figure 8.31. Gross section of canine eye with septic endophthalmitis. Note the opaque plasmoid aqueous and vitreous and the exudative retinal detachment.

Figure 8.32. Gross section of a formalin-fixed dog's eye with a rhegmatogenous retinal detachment. Note the giant tears in the peripheral retina and the retinal scrolling. Focal vitreous traction bands induced the scrolling and contraction of the retina.

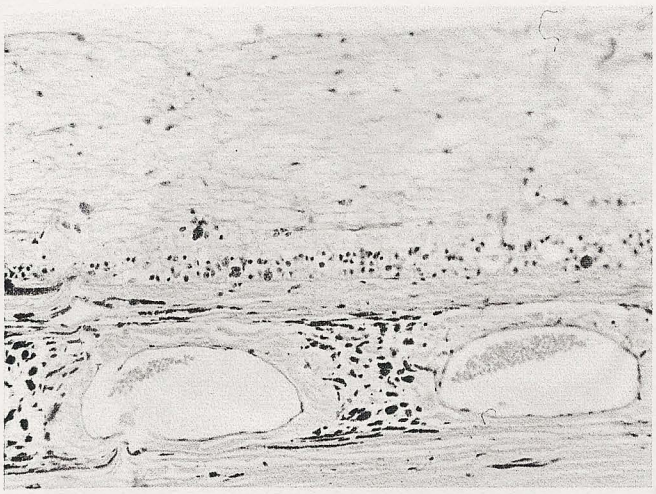

Figure 8.33. Retinal and choroidal degeneration with intraretinal migration of retinal pigmented epithelial cells. (Hematoxylin and eosin stain, original magnification 300X.)

PATHOLOGY OF CONGENITAL DISORDERS

All diseases may be classified into congenital, inherited developmental, and acquired conditions. The congenital disorders are those that manifest at birth and include those that are idiopathic (induced by exposure of the embryo to nutritional deficiencies, toxins, or infectious agents) and those induced by genetic mutations. To avoid duplication, we have included the inherited conditions that manifest at birth in the congenital section. The section on inherited developmental ocular disease includes all known inherited or suspected genetic disorders that manifest after birth.

There are many ways to categorize congenital anomalies. Many congenital disorders involve multiple ocular tissues, while others affect single tissues, differences that may create confusion for the novice pathologist and ophthalmologist. We have categorized congenital disorders into those that occur during organogenesis (anophthalmos, cystic globe, cyclopia, synophthalmia, microphthalmia, coloboma); disorders of tissue differentiation that affect all or most of the globe after organogenesis (multiple ocular anomalies, anterior segment dysgenesis, congenital glaucoma); and those that affect only specific ocular tissues (surface ectoderm, mesoderm, neural crest, and neuroectoderm tissues). To avoid redundancy, we do not review the developmental biology of the eye. A thorough knowledge of embryology is a prerequisite for understanding congenital anomalies, and a review of Chapter 1 of this text is recommended.

Defective Organogenesis

Anophthalmos is a total absence of ocular tissue. This is a rare condition that results from failure of the primary optical vesicle to develop or from a complete regression of the optic vesicle. This condition is usually bilateral; concurrent anomalies of skeletal and central nervous system anomalies are common and, in swine, are associated with maternal deficiencies of vitamin A.[2-4] Most often, there is a histologic evidence of a globe not identifiable on clinical examination of the neonate—hence the term clinical anophthalmos. When the contents of the orbit are removed, fixed and sectioned, and examined histologically, remnants of primordial ocular tissues are usually evident on serial section. These are more appropriately termed either cystic eyes or microphthalmia.

Cystic eyes are rare and manifest as small, round, scleral-wrapped structures lined with a single layer of undifferentiated neuroectoderm (Fig. 8.34). The lens and cornea are absent, and development has been arrested at the optic vesicle stage, with failure of invagination to form the optic cup. The differential diagnosis is microphthalmia, which mandates that the globe should contain remnants of surface ectoderm (lens), evidence of neural crest migration (uvea), and differentiation of neuroectoderm into a bilayered structure.

Microphthalmia is diagnosed commonly by the clinical ophthalmologist (Fig. 8.35), and occasionally these small globes

Figure 8.34. A cystic eye from a foal. The globe is lined by a single layer of neuroectoderm, confirming a lack of embryonic invagination of this eye. A large piece of cartilage of undetermined origin is present also. (Hematoxylin and eosin stain, original magnification 1X.)

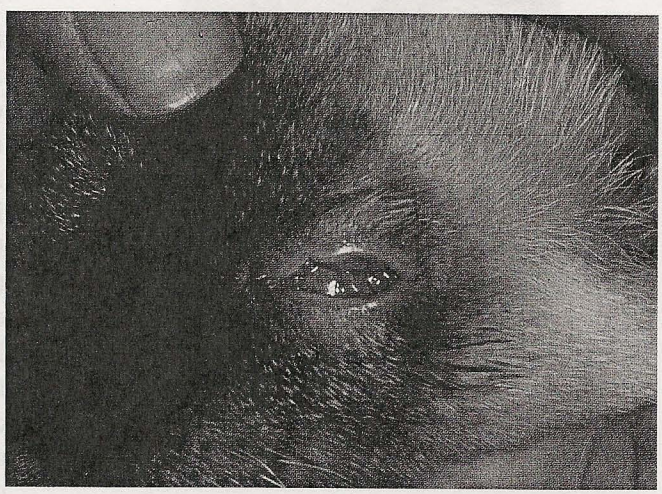

Figure 8.35. Microphthalmia in a Siamese kitten. Note the lack of an obvious globe that is inducing the third eyelid prolapse and mild ectropion.

are examined by the pathologist (Fig. 8.34). When the orbital contents are available for examination histologically, the eyelids, conjunctiva, and associated goblet cells, tarsal glands, lacrimal glands, and extraocular muscles are usually normal. There is considerable variation in extent of microphthalmia, and the palpebral fissure and the orbit are usually smaller. The eye may be slightly smaller and require calipers to confirm the diagnosis or so extreme that only a small, disorganized, spherical remnant is present. Phthisis bulbus is the major differential diagnosis, and the histologic features of inflammation allows accurate differentiation of these postinflammatory or traumatized globes. Microphthalmia is usually accompanied with microphakia, suggesting arrested development at the optic cup stage. Evidence of retinal differentiation is identified with light microscopy. Microphthalmia occurs early in development because of deficiencies in the optic vesicle or later because of a lack induction of ocular tissues.

Cyclopia manifests as a single orbit and globe that is located centrally in the forehead and is occasionally documented in domestic animals (Fig. 8.36). True cyclopia is exceedingly rare, and usually this midline anomaly represents fusion of the developing globes with partial or complete duplication of intraocular structures and is properly referred to as synophthalmos (Fig. 8.37). Synophthalmos and cyclops are usually accompanied by several cranial anomalies, including cleft palate, hydrocephaly, microcephaly, hydrencephaly, median proboscis, and cranioschisis. Cyclopia has been induced by feeding ewes *Veratum californica*.[5,6] This plant contains jervine, cyclopamine, and cyoposine, and these steroid alkaloids damage the neural groove of the fetal lamb at day 14 and 15. Prolonged gestation is common with these deformed lambs, and considerable variation in anomalies occurs in outbreaks of toxin exposure of flocks. Exposure of the fetal lamb after day 15 may induce skeletal anomalies but not cyclopia. Similarly, synophthalmia has been induced in mice by exposure of pregnant dams to Ochratoxin. Numerous rodent models have been investigated to further unravel the pathogenesis of such congenital anomalies that develop early in embryogenesis.[7]

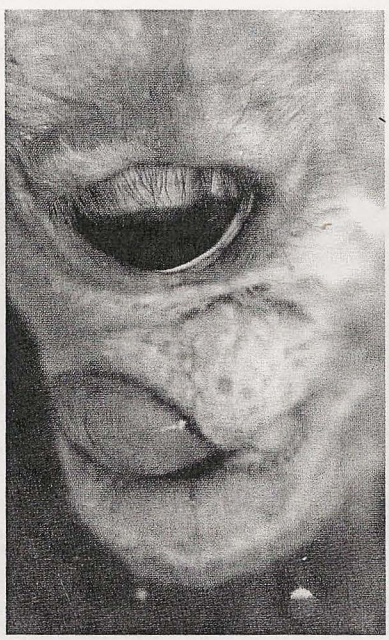

Figure 8.36. A bovine cyclops. Note the single central eye and lack of nasal and maxillary development.

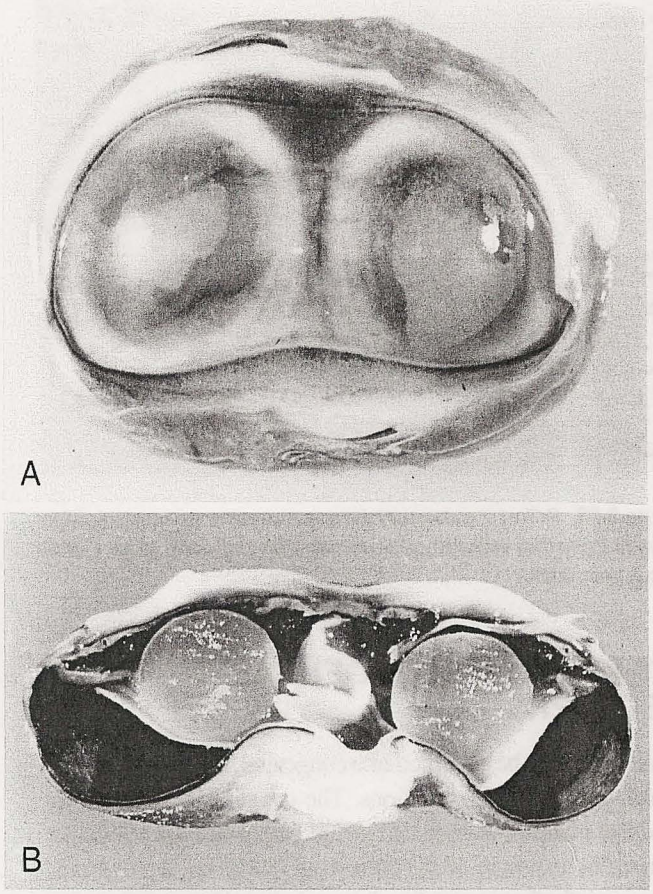

Figure 8.37. **A.** Synophthalmos in a newborn kid. **B.** Sagittal section of the synophthalmos reveals paired lenses, partial separation of the anterior segments, and sharing of a posterior segment.

Coloboma is an absence of tissue that is normally present. Colobomata are classified as typical (orientated along the embryonic fissure) and atypical (orientated along all other planes). Typical colobomata develop because of incomplete fusion of the embryonic fissure; atypical colobomata develop because of a lack induction or impaired proliferation of the affected tissues. Colobomata may affect the eyelids and conjunctiva, cornea, sclera, uvea, retina, and/or optic nerve; lens colobomata manifest as consequences of ciliary body and zonular colobomata. When the coloboma is extensive and involves the sclera, there is often a thinning of the fibrous layer (ectasia) without pouching of the uvea and retina (staphyloma). Occasionally, a cystic scleral coloboma is present with neurocrest and neuroectoderm within orbital tissues. Defective differentiation of the neurocrest (uveal hypoplasia) and neuroectoderm (retinal dysplasia) along the staphyloma is common. Colobomata of ocular tissues occur in all domestic animals; choroidal and optic nerve colobomata are common in dogs with Collie eye anomaly (Fig. 8.38), and optic nerve colobomata and staphylomas are frequent in Charolais cattle.[8–12]

Figure 8.38. A peripapillary coloboma, staphyloma, retinal detachment, and retinal dysplasia in a Collie puppy with Collie eye anomaly. (Hematoxylin and eosin stain, original magnification 100X.)

Defective Tissue Differentiation

After the optic cup is formed, ocular development involves differentiation of neuroectoderm into retina, ciliary, and iridal epithelium; neural crest and mesenchymal differentiation into vascular and fibrous tunics of the eye; and surface ectoderm into the lens, corneal, and conjunctival epithelium and lacrimal, eyelid, and conjunctival glands. Anomalies of differentiation of neuroectoderm, neural crest, and mesenchymal tissues and surface ectoderm are frequently diagnosed.

Defective Neuroectoderm Differentiation

Retinal Dysplasia

Retinal dysplasia is an abnormal differentiation of retinal layers and is identified by multiple rosettes and glial proliferation (Figs. 8.6, 8.38, and 8.39). Rosettes are pathognomic for retinal dysplasia and are composed of a central lumen containing dysplastic photoreceptor inner and outer segments surrounded by multiple layers of neuroblasts and axons, and the external limiting membrane is discontinuous in the fetal retina. The pathogenesis of retinal dysplasia is complex and largely unknown. Four mechanisms have been postulated that may induce retinal dysplasia: proliferative outgrowth of the retina, retinal detachment, congenital absence of RPE, and retinal dysplasia in situ.[13]

Retinal dysplasia is induced by multiple etiologies. The most common etiologies are genetic mutations, and many are reported in dogs.[14] To date the mutations have not been identified, although the mode of inheritance has been confirmed in numerous breeds of dogs, and other organ systems are occasionally reported.[15–18]

Figure 8.39. Retinal dysplasia in a dog. Note the outer nuclear rosettes and complete disorganization of the retina. (Hematoxylin and eosin stain, original magnification 300X.)

Retinal dysplasia is also induced by in utero virus infections in cattle, cats, and sheep. These lesions are characterized by cellular necrosis and scarring, and retinal rosettes are induced by virus infections, including BVD, feline panleukopenia, feline leukemia, canine herpes virus, blue tongue, and others.[19–21] The histologic lesion is similar in all diseases. The acute lesions induced by these viruses are a nonsuppurative endophthalmitis with multifocal chorioretinal necrosis. Chronic lesions include multifocal chorioretinal scarring, atrophy, and retinal rosettes. The RPE is commonly affected with multifocal hyperplasia and degeneration. Other neural tissues are commonly affected, and cerebellar atrophy, hydrocephalus, and hydrancephaly are noted.

Retinal dysplasia has been reported secondary to maternal toxin exposure[22] and nutritional deficiencies (vitamin A, zinc, taurine).[3,23]

Retinal folds represent uncoordinated growth of retina and the outer coats of the eye such that excess retina is present; while folds may be encountered as a component of retinal dysplasia as a secondary consequence of the altered growth rate of the dysplastic retina, they are distinct in terms of pathogenesis and significance (Figs. 8.3 and 8.40). The antithesis is a developing retina that grows less than normal with resultant stretching, peripheral tearing, and congenital nonattachment.

Optic Nerve Hypoplasia and Ganglion Cell Hypoplasia

Optic nerve hypoplasia develops secondary to either ganglion cell hypoplasia or atrophy as the axons of these ganglion cells form the majority of the optic nerve. The clinical diagnosis of optic nerve hypoplasia is limited to morphologic estimation and records on eye certification examinations confirm this disorder in some purebred dogs.[14] However, the ganglion cell and optic nerve morphology is seldom documented histologically in these dogs. Some or most of these conditions are inherited and most likely involve ganglion cell hypoplasia.[24–27]

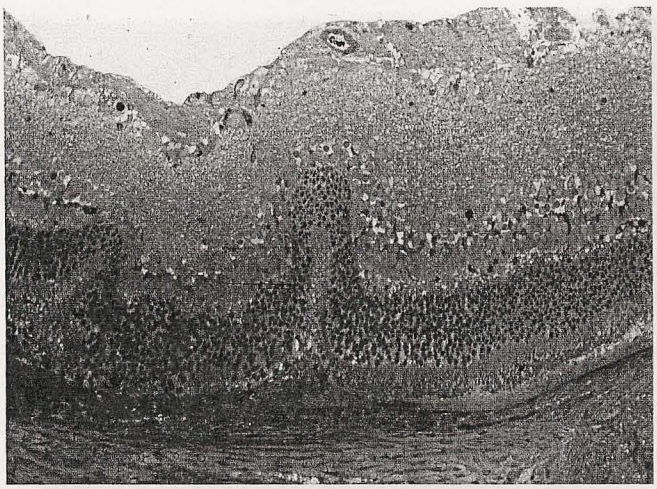

Figure 8.40. A retinal fold (central) and retinal dysplasia on the left side of this photo. (Toluidine blue stain, original magnification 200X.)

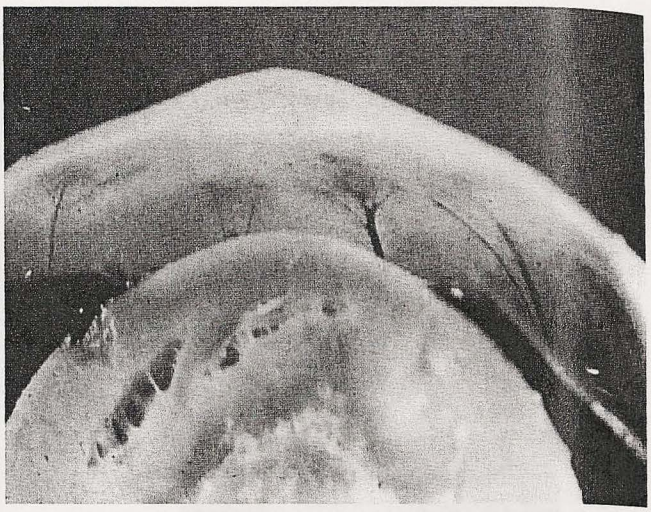

Figure 8.41. Iris-to-cornea persistent pupillary membranes.

Optic nerve and ganglion cell atrophy are induced in young cattle by deficiency of vitamin A. The pathogenesis includes failed remodeling of the optic nerve foramen, which results in stenosis and optic nerve compression and atrophy.[28] Vitamin A deficiency induces optic nerve hypoplasia and retinal dysplasia and multiple systemic anomalies in piglets.[2,3] Griseofulvin toxicity induces cyclopia, anophthalmia, and aplastic optic nerves in kittens from queens medicated at 500 to 1000 mg orally.[29]

Defective Neurocrest and Mesenchymal Differentiation

After the optic cup is formed and the lens vesicle separates from the surface ectoderm, the periocular mesenchyme and neural crest cells undergo a series of migrations, differentiations, and atrophies to form the anterior segment and vitreous, and errors in these developments may induce anterior or posterior segment anomalies. Anterior segment dysgenesis includes multiple anomalies of the cornea, lens, and anterior uvea (Fig. 8.41). Affected globes are often microphthalmic, and the lens is small (microphakia). The anterior uvea is hypoplastic, and persistent pupillary membranes are often present. The cornea is occasionally hypoplastic. Anterior segment dysgenesis is due to either a primary lack of induction and differentiation of neural crest tissues or a lack of induction of these tissues by surrounding tissues. The lens is consistently small and is likely directly involved in the development of these anomalies.

Congenital glaucoma has many similar anomalies to anterior segment dysgenesis except for the effects on the retina, optic nerve, and the buphthalmos. The uvea is consistently hypoplastic, and microphakia is always present (Fig. 8.42A).[30,31] The filtration angle is also primitive, and the uvea is hypoplastic (Fig. 8.42B). Examination of the retina and optic nerve will reveal degeneration of the ganglion cells, nerve fiber layer, optic nerve, and inner plexiform and inner nuclear layers. Considerable confusion surrounds the congenital and primary glaucomas of dogs in the veterinary literature. Congenital glaucoma is confirmed by documenting a buphthalmic globe with microphakia and a hypoplastic uvea at birth. The IOPs in these globes may be elevated, normotensive, or even hypotensive. Primary glaucoma associated with goniodysgenesis and primary glaucoma in dogs associated with open angles are inherited developmental anomalies of dogs. However, goniodysgenesis should be regarded as a focal anterior segment dysgenesis, and it is not the etiology of the primary glaucoma but a marker for this disease. Mice are particularly prone to congenital glaucoma associated with anterior segment dysgenesis that occurs spontaneously with variable incidence among strains. Experimental glaucoma models can also be induced with specific teratogens, and glaucomas of variable pathogeneses have been described in transgenic strains.

Persistent pupillary membranes are incomplete atrophy of the perilenticular vasculature (Figs. 8.41, 8.43). These remain as pigmented strands that arise and insert on the iris collarette and may span the pupil. If the membrane inserts on the lens or cornea, it is not only persistent but dysplastic as well. In normal development, such relationships do not occur. This condition is common and, in some breeds of dogs, an inherited congenital condition.[14] Horses are perhaps the most commonly affected animal, and iris-to-iris persistent pupillary membranes are present in most if not all horses.

Uveal hypoplasia is also a common anomaly. All animals with poorly pigmented uvea have a hypoplastic vascular tunic in their eyes. The extreme of this hypoplasia is albinism in which all the uvea pigment is missing. The mildest form is focal hypoplasia of the uvea. When this focal hypoplasia involves the irides, the condition is termed *heterochromia.* The tapetum is usually poorly developed or absent. Iridal aplasia, or aniridia, is a congenital anomaly in horses and is occasionally encountered in other species.

Collie eye anomaly is an inherited congenital condition in Collie dogs. Ophthalmic and gross examination will reveal a variety of ocular anomalies, including microphthalmia, choroidal hypoplasia that is focal and located temporal to the optic disc, and peripapillary colobomata and scleral ectasia,

(a)

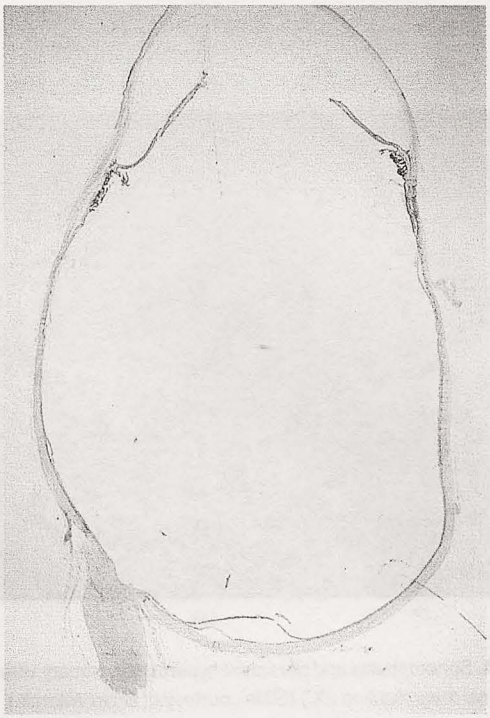

(b)

Figure 8.42. A. Congenital glaucoma in a llama (*Llama glama*). Note the microphakia, corneal striae, and dilated pupil. (Reprinted with permission, Cullen CL, Grahn BH. Congenital glaucoma in a llama (*Llama glama*). *J Vet Comp Ophthalmol* 1997;7:253–257.) **B.** Subgross section of the same eye. Note the buphthalmia, uveal hypoplasia, and mild optic disc cupping. The microphakic lens was removed from the anterior chamber during sectioning. (Periodic acid-Schiff stain, original magnification 2X.)

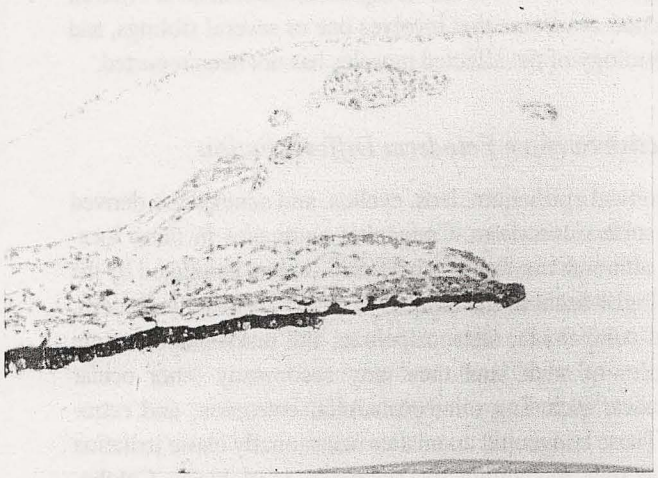

Figure 8.43. Iris-to-iris persistent pupillary membranes in a dog. These hollow mesenchymal tubes originate near the iris collarette and may bridge the pupil and insert on the iris leaflet or the anterior lens capsule. (Hematoxylin and eosin stain, original magnification 100X.)

and retinal detachment. Light microscopic examination will confirm the focal choroidal hypoplasia, which manifests with thinning and hypopigmentation (Fig. 8.44), optic nerve and peripapillary colobomata, and scleral ectasia and staphyloma. When the retina is detached focally or entirely, the outer segments and inner segments will be degenerate, and when the detachment is chronic, the outer and inner nuclear and plexiform layers will also be atrophied. The RPE will be hyperplastic, pigmented, and hypertrophied juxtaposed to the areas of retinal detachment.

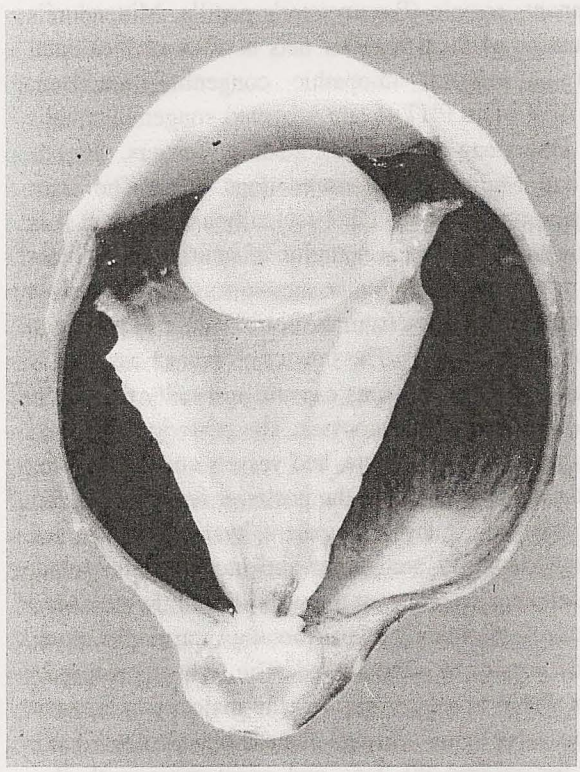

Figure 8.44. Collie eye anomaly with choroidal hypoplasia, retinal detachment, and peripapillary coloboma.

Persistent hyperplastic primary vitreous (PHPV), persistent hyperplastic tunica vasculosa lentis (PHTVL), and patent hyaloid artery (PHA) are disorders that involve retention and persistence of vascular supply to the lens (Fig. 8.45). During

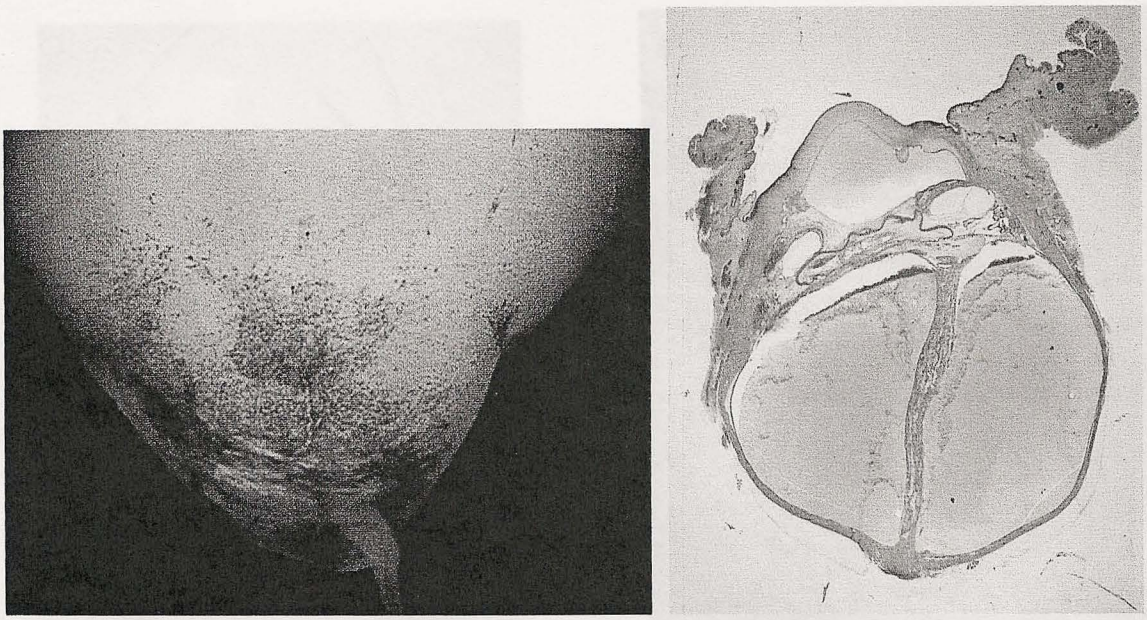

(a) (b)

Figure 8.45. A. Spherophakia and persistent hyperplastic primary vitreous in a dog. **B.** Persistent hyperplastic primary vitreous in a dog. (Hematoxylin and eosin stain, original magnification 2X.) (Slide courtesy of Brian Wilcock.)

ocular development, the hyaloid artery extends from the optic disc to the lens and anastamoses with a capillary net from the anterior uvea (tunica vasculosa lentis). During normal development in domestic animals, these vessels atrophy and only focal remnants remain (Bergmeister's papilla, Mittendorf's dot). Retention of these vascular nets is often an incidental unilateral or bilateral idiopathic congenital condition, although PHPV and PHTVL are inherited congenital conditions in Doberman dogs, Staffordshire Terriers, Bloodhounds, and Miniature Schnauzer dogs.[18,32–35] The light microscopic anomalies of PHPV (actually a misnomer: it is metaplastic as well) include retention of multiple blood vessels and primitive perilenticular mesoderm and neurocrest cells in a core that extends from the optic disc to the posterior lens capsule (Fig. 8.45B). The lens often has an associated cataract, and the posterior lens capsule is usually thickened with spindle cells and melanocytes. The posterior lens capsule is occasionally incomplete, and vessels and fibrous and pigmented tissues extend into the posterior lens cortex. The light microscopic finding with patent hyaloid arteries are similar; however, they are milder and include only patent blood vessels that extend from the optic disc to the posterior lens capsule. Occasionally, choristomatous cartilaginous or adipose tissue may be encountered. The light microscopic findings of PHTVL are similar, but the majority of vessels and pigment from neurocrest and mesodermal tissues extend from the iris around the lens and anastomose with the retained primary vitreous core and extend to the optic disc. Persistent pupillary membranes, PHA, PHTVL, and PHPV may be referred to individually or collectively as persistent embryonic vasculature (PEV).

Congenital anomalies of extraocular muscles are rare in animals. The clinical manifestations are often a bilateral strabismus. The neurologic system is usually intact and normal. The affected extraocular muscles are either hypoplastic or more commonly misplaced, and their insertions are inconsistent with the other extraocular muscles, a malalignment that induces the strabismus. Congenital strabismus is often an incidental syndrome that involves one or several siblings, and the histology of the affected muscles has not been reported.

Defective Surface Ectoderm Differentiation

The corneal epithelium, lens, eyelids, and adnexal are derived from surface ectoderm. Congenital anomalies in these locations, although not rare clinically, are seldom examined by the pathologist because the clinical diagnosis is usually obvious. Eyelid colobomata, micropalpebrae, and macropalpebrae are examples of such, and they may accompany other ocular anomalies, including microphthalmia, entropion, and ectropion. These congenital anomalies occasionally cause irritation of the cornea and conjunctiva secondary to trichiasis. Colobomata and micropalpebrae are examples of defective ectodermal induction and differentiation.

Anomalies involving the cilia and tarsal glands of dogs are commonly diagnosed by ophthalmologists and are seldom examined histologically. Ectopic cilia, distichiae, and districhiasis develop because of dysplasia of the tarsal glands (Fig. 8.46). They may manifest as congenital or developmental anomalies, and they may be inherited in some dogs. Trichiasis and trichomegaly are similar congenital anomalies of the eyelids that occur because of misdirected normal hair follicles and excessively large cilia respectively. Unless they induce corneal or conjunctival irritation, they are not significant.

Lacrimal gland and duct aplasia or hypoplasia are potential etiologies for congenital keratoconjunctivitis sicca. This is an

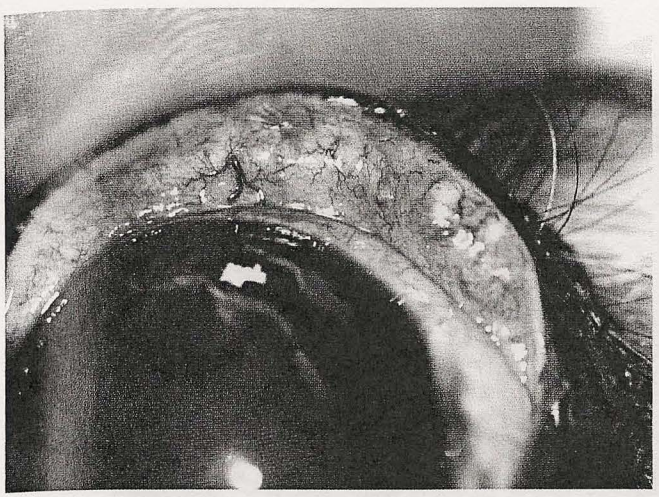

Figure 8.46. Multiple dysplastic eyelid tarsal glands with ectopic cilia in a dog. Note the multiple ectopic cilia present on the palpebral conjunctival surface. The yellow swollen tarsal glands are chalazion.

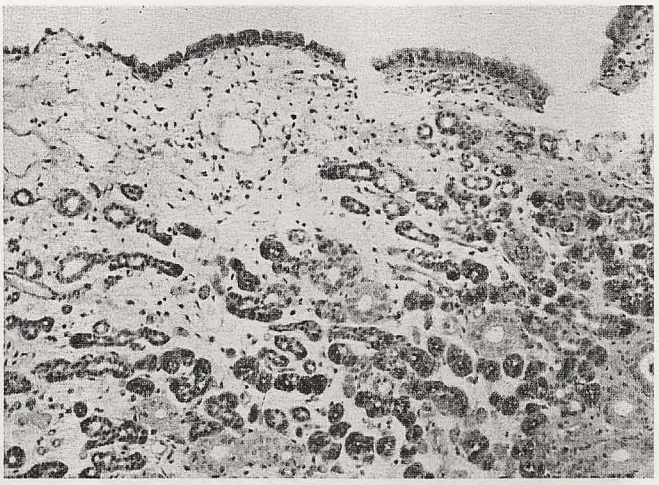

Figure 8.47. Dacryops in a dog. Note the glandular structure and ducts that are reminiscent of lacrimal tissue. (Periodic acid-Schiff, original magnification 200X.)

uncommon congenital anomaly that is rarely if ever examined histologically. Ipsilateral micropalpebral fissure is a common association. Congenital lacrimal gland disorders may develop because of a lack of induction of the gland, or secondary to duct atresia, or a lack of neurogenic stimuli.

Punctal, canalicular, and nasolacrimal duct atresia are also seen in dogs,[36] camelids, cattle, and horses occasionally, but histologic examination of these tissues is not reported. The clinical manifestation is epiphora, and the etiology is atresia. Occasionally, ectopic and supernumerary nasolacrimal duct openings are noted in cattle, horses, and dogs. The etiology is usually unknown, and the pathogenesis is thought to be a lack of canalization of surface ectoderm into a patent duct.

Dacryops, canaliculops, and orbital cysts are uncommon congenital anomalies of dogs, cats, and horses.[37,38] These cysts arise from abnormal development of the lacrimal glands, glands of the third eyelid, and nasolacrimal drainage ducts and canaliculi. The clinical manifestation is a tumor in the periocular tissue in the first months of life. Light microscopic examinations of these anomalies are similar and include a thin-walled cuboidal epithelium surrounding a serous to hemorrhagic fluid (Fig. 8.47).

Dermoids are congenital lesions of the cornea, conjunctiva, and eyelid. Dermoids are choristomas that are misplaced normal tissues (Fig. 8.48). They most likely develop because of defective induction or differentiation of surface ectoderm. Corneal and conjunctival dermoids are commonly removed when trichiasis induces ocular irritation. Histologic examination reveals stratified and squamous epithelium that is keratinized and variably pigmented. The associated dermis contains sebaceous and sweat glands, adipose tissue, and hair follicles (Fig. 8.48B). Occasionally, cartilage and bone are encountered. The edges of the dermoid blends into the corneal and conjunctiva epithelium and stroma.

Microcorneas and macrocorneas are uncommon clinical entities that have no apparent histologic abnormality. Their clinical significance is limited, and the etiology is likely defective induction. Congenital corneal opacities are frequently diagnosed in domestic animals; however, they are seldom examined histologically. Those that involve the endothelium and are white or pigmented are often remnants of the embryonic vasculature (see earlier discussion of persistent pupillary membranes). Transient subepithelial opacities are frequently seen in puppies. The etiology and histologic appearance are unknown. Rarely, the differentiation of cornea and sclera is indistinct, and the limbus is misshapen. These congenital defects are not significant and are rarely examined histologically. These anomalies most likely arise from defective ectodermal differentiation.

Congenital anomalies of the lens include cataracts, aphakia, microphakia, spherophakia, lenticonus, and lenticular coloboma (Fig. 8.49). These disorders may be isolated anomalies, but they are commonly associated with anterior segment dysgenesis, congenital glaucoma, and anomalies of the embryonic vasculature. Most if not all of these anomalies develop secondary to defective induction and differentiation of surface ectoderm.

Cataracts are the most common congenital lenticular anomaly. The light microscopic manifestations are lens fiber–protein alteration, fiber cell membranolysis, and lens epithelial cell dysplasia or metaplasia, hypertrophy, posterior migration, and occasionally mineralization (Figs. 8.13 and 8.50). Congenital cataracts may be unilateral or bilateral and may be the only anomaly of the lens; however, many are associated with microphakia, lenticonus and spherophakia, and anterior segment dysgenesis.

Aphakia is complete absence of a lens, and it is a rare anomaly.[39] The lack of differentiation of a lens from surface ectoderm does occur (Fig. 8.51). Occasionally, in conjunction with congenital glaucoma or anterior segment dysgenesis, the ophthalmologist is unable to detect a lens. However, most of these globes have a small lens embedded within the sclera, cornea, or anterior uvea, and careful sectioning and histologic examination will identify a part of a lens capsule, lens epithelium, and dysplastic lens fibers (Fig. 8.51).

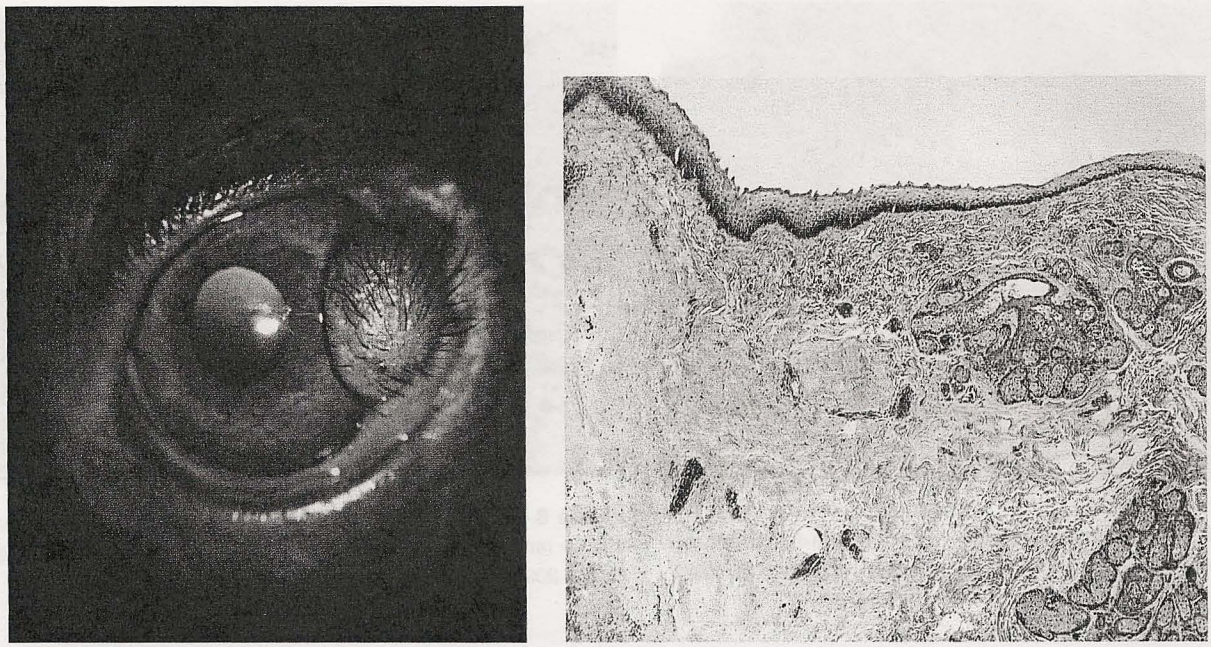

(a) (b)

Figure 8.48. **A.** A corneal dermoid in a puppy. **B.** Histologic section of the same corneal dermoid of the dog after keratectomy. Note the dermal components including hair, sebaceous glands, fat, and keratinized and pigmented epithelium. (Hematoxylin and eosin stain, original magnification 200X.)

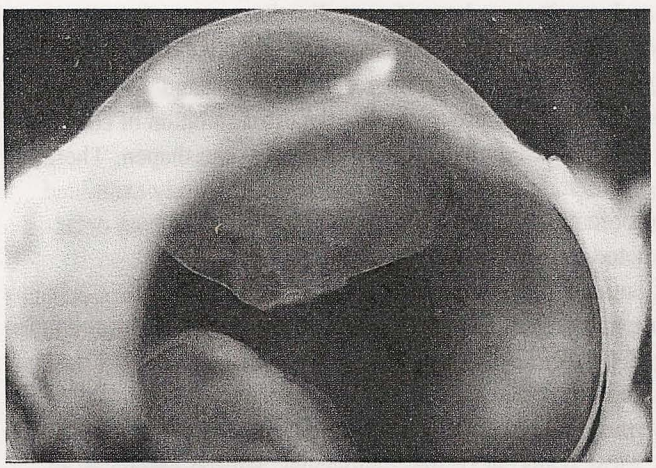

Figure 8.49. Gross hemisection of a rabbit globe. Note the posterior lenticonus in this gross specimen.

Figure 8.50. A histologic section of the posterior lens capsule and subcapsular cortex of a lens with a mature cataract. Note the posterior migration of the lens epithelium and metaplastic lens epithelium (bladder cells). (Hematoxylin and eosin stain, original magnification 400X.) (Reprinted with permission, Kuiken T, Grahn BH, Wobeser G. Pathology of ocular lesions in free-living moose (*Alces alces*) from Saskatchewan. *J Wildlife Dis* 1997;33:87–94.

Microphakia is common in most domestic animals. This congenital anomaly is commonly associated with congenital cataracts and often as part of anterior segment dysgenesis or congenital glaucoma (Fig. 8.42A). Most microphakic lenses are not examined histologically. Lens measurement either in the clinic using ultrasound or following intracapsular extraction using calipers confirms a small lens. Many breeds of dogs with microphakia also have microphthalmia, and the condition is bilateral and is often inherited.

Spherophakia is an uncommon congenital anomaly that manifests with a round lens in contrast to the normal ellipsoid shape. This is readily apparent on gross and histologic examinations. Spherophakia is most often caused by lack of development of the embryonic lens, which is sphere shaped, and further development was most likely arrested. Spherophakic lenses are smaller than normal lenses. This anomaly may manifest as a unilateral or bilateral disorder. While it may be a singular anomaly, most commonly it is one of the multiple lesions of anterior segment dysgenesis or congenital glaucoma (Fig. 8.42A). Cataracts may be present with this anomaly, and many cases of spherophakia have circumferential lens epithelium consistent with posterior migration of lens epithelium and failed differentiation of the primary lens fiber cells.

Lenticonus is an uncommon anomaly in animals. It is a misshaped lens, and it may manifest as a posterior or more

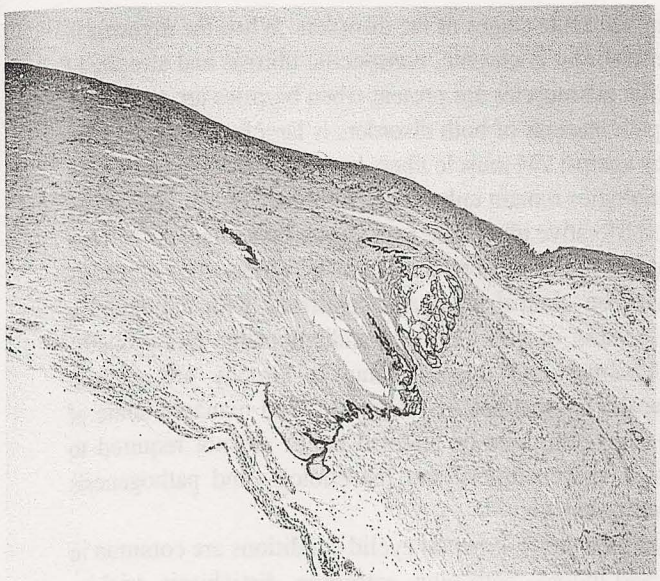

Figure 8.51. Histologic section of a cornea of a puppy with congenital glaucoma and aphakia and multiple ocular anomalies. Note the periodic acid-Schiff–positive basement membrane of varied thickness embedded in the corneal. The epithelial cells within the membrane were reminiscent of lens epithelium, although misplaced corneal endothelium and Descemet's membrane is also a consideration. Incomplete lens separation and development is a common accompaniment to congenital glaucoma and multiple ocular anomalies in many animals. (Periodic acid-Schiff stain, original magnification 200X.)

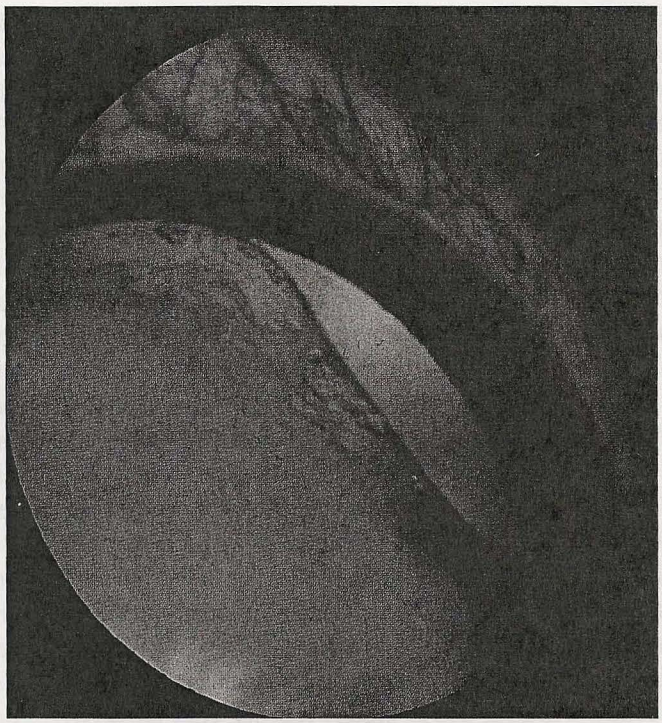

Figure 8.52. A clinical photograph of a lenticular coloboma in a dog. Note the flattened equatorial region and lack of zonulae in this area and the generalized nuclear and focal cortical cataracts.

rarely an anterior capsular anomaly. Posterior lenticonus is often associated with the developmental condition of persistent embryonic vasculature and is the manifestation of posterior capsule dysplasia. Anterior lenticonus is most often associated with anterior segment dysgenesis and occasionally congenital glaucoma and reflects delayed separation of the lens vesicle from surface ectoderm. When these anomalies are examined with light microscopy, the lens capsule is distorted in either an anterior or posterior direction, and subcapsular cataract is usually present. When the condition is associated with developmental anomalies of the vitreous, a posterior retrolental fibrovascular membrane is present, the posterior lens capsule is often incomplete, and these abnormal tissues extend into the lens cortex (Fig. 8.45). Lenticular colobomata are actually pseudocolobomata, as they occur secondary to zonular aplasia of the lens. These are rare anomalies that manifest as an equatorial lens flattening where the zonulae are absent (Fig. 8.52). Other than the misshapen equator, lens morphology is normal. If multiple colobomata are present around the lens equator, lens subluxation may develop due to lack of zonular support. The light microscopic findings with this disorder may include focal zonular aplasia associated with ciliary body coloboma.

Inherited Developmental Disorders

Inherited ocular disorders of dogs, cats, and laboratory rodents are common and only occasionally diagnosed in horses and cattle. Inherited disorders may be congenital (manifest at birth) or developmental (manifest postnatally). Inherited developmental disorders manifest variably from the first few months of age to later in life. This inconsistency in the age of initial presentation has led to considerable confusion in the classification of inherited congenital developmental disorders, inherited breed-specific developmental disorders, and some acquired ocular conditions. Inherited congenital disorders are categorized in the previous section. These lesions are identifiable at birth or at eyelid opening and therefore are easily classified as congenital.

However, it is critical for the ophthalmologist and the pathologist to differentiate inherited developmental disorders from acquired disorders. To accurately diagnose inherited ocular developmental disorders, the ophthalmologist and pathologist require knowledge of breed predispositions, ages of onset, clinical manifestations, and a thorough understanding of ocular pathology. For example, the differentiation of glaucoma secondary to primary lens luxation from primary glaucoma and buphthalmos with a secondary lens luxation can be very challenging for the novice pathologist. However, an accurate diagnosis is critical to the ophthalmologist advising the owner of the breeding animal. This is an important part of veterinary ocular pathology that has commanded only marginal documentation in veterinary ophthalmic pathology references. We emphasize the histologic features and the signs and clinical manifestations that aid in differentiating these conditions from acquired ocular disorders.

To consider a condition inherited, a breed predisposition should be noted. Occasionally, a sex predisposition is also present. To confirm that a condition is inherited, it needs to be

reproduced by test breeding and confirmed by histology. A pedigree analysis will usually document the mode of inheritance. Finally, examination of DNA, RNA, and proteins at a molecular level are required to document the mutation inducing the anomaly and then the pathogenesis of the condition can be gradually unraveled and completely documented. Ophthalmologists have been categorizing many disorders as inherited on the basis of breed predisposition and pedigree analysis where the basic molecular research is still lacking. As further research is completed, many new inherited developmental conditions will be documented. We have limited our descriptions to inherited developmental disorders that have a unique breed predisposition, a consistent bilateral clinical manifestation, and histologic examination findings most consistent with genetic etiology. These inherited disorders of the eye include dysplasias, dystrophies, atrophies, and some immune-mediated and degenerative disorders. Some of these disorders affect other ocular tissues and induce inflammation, especially when they are chronic, and they are easily misdiagnosed as acquired ocular disorders. These developmental anomalies are most common in dogs and laboratory rodents. They are occasionally reported in cats and other species and involve all ocular tissues. We have categorized these by the tissues affected. Where multiple breeds within the species manifest with similar disorders, we have summarized the data into tables.

Developmental Orbital, Eyelid, Third Eyelid, and Lacrimal Disorders

Inherited development conditions of the orbital tissues in animals have not been reported. However, shallow orbits, and large eyelid fissures predominate in brachycephalic dogs, have a multifactorial inheritance, and predispose to keratitis and conjunctivitis and occasionally ocular proptosis. The clinical manifestations of the secondary corneal disease induced by the shallow orbits, large eyelid fissures, and exposure are common clinical disorders, but they are seldom examined histologically. When the cornea and conjunctiva are examined histologically, chronic inflammation, scarring, and pigmentation are expected. Proptosed globes induce significant orbital cellulitis and extraocular myositis. As the lesions become chronic, lymphocytic plasmacytic cellulitis and scarring of orbital tissues will be noted on light microscopic examination of orbital biopsies.

Extraocular myositis of Golden Retriever dogs, eosinophilic masticatory myositis of German Shepherd dogs and Weimaraners, and craniomandibular osteopathy of West Highland White and Scottish Terriers are bilateral, immune-mediated, predominantly breed-specific conditions that may have a genetic etiology or predisposition. Reproduction of these disorders with test breeding or pedigree analysis of related dogs has not been reported. Eosinophilic myositis and extraocular polymyositis are confirmed by biopsy and light microscopic examination, which reveals eosinophilic (Fig. 8.53) and lymphocytic plasmacytic myositis respectively during the acute stages of the disorders. When the myositis in either disorder is chronic, nonspecific fibrosis and atrophy of the affected muscles are present when biopsies are examined. The pathogenesis of both disorders is largely unknown. Antibodies against 2M muscle fibers have been detected, although the etiologies remain unknown. Craniomandibular osteopathy is a proliferative idiopathic mandibular bone disorder of West Highland White Terriers and Scottish Terriers. The diagnosis is based on clinical signs and confirmed with radiographic identification of proliferative mandibulopathy. Occasionally, exophthalmos and temporal muscle atrophy are present; hence, the ophthalmologist diagnoses and manages some of these dogs. Biopsies of affected bones are not required to diagnose the condition, and the etiology and pathogenesis remains unknown.

Inherited developmental eyelid conditions are common in dogs and include entropion, ectropion, distichiasis, trichiasis, and ectopic cilia. Fortunately, they are diagnosed clinically, and the pathogenesis involves abnormalities in eyelid fissure length, associated eyelid muscles, and adnexa. The light microscopic findings of secondary conjunctivitis and keratitis are due to exposure secondary to the primary eyelid anomaly.

Inherited developmental disorders of the third eyelid of dogs are also common and include prolapsed glands of the nictitating membrane and keratoconjunctivitis sicca. The diagnosis of these is also clinical, and histologic examination is not usually required. The pathogenesis of third eyelid gland prolapse includes a suspected lack of ligamentous attachment to the third eyelid cartilage. Secondary lymphocytic plasmacytic adenitis and conjunctivitis are noted histologically on biopsies of prolapsed glands or lacrimal gland biopsies.

Immune-mediated lacrimal gland and nictitans gland atrophy are common and likely inherited in several breeds of dogs, including American Cocker Spaniels and American Bulldogs.

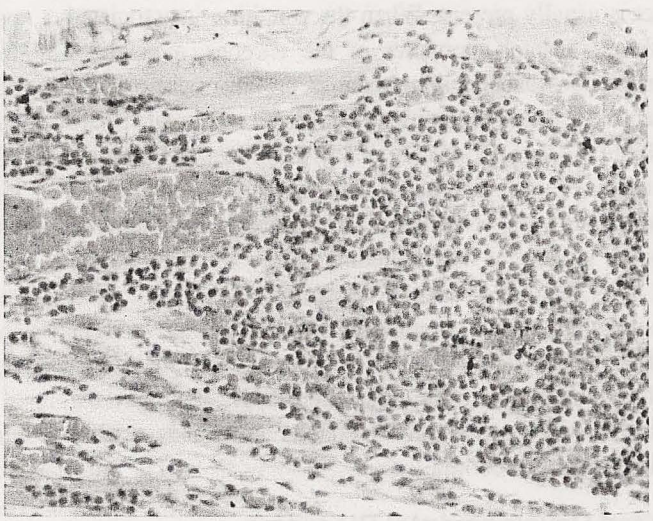

Figure 8.53. Extraocular myositis in a young Golden Retriever. There are dense infiltrations of lymphocytes and plasma cells within the rectus muscles. (Hematoxylin and eosin stain, original magnification 100X.)

The lacrimal gland atrophy induces the keratoconjunctivitis sicca. The histologic findings of lacrimal gland biopsies include a diffuse lymphocytic glandular infiltrate with loss of acini and glandular atrophy.[40–43] The lack of tear film induces multiple secondary nonspecific corneal and conjunctival changes, such as ulcerative keratitis or nonulcerative keratitis with mixed inflammatory cell infiltrate, including neutrophils, lymphocytes and plasma cells. The epithelium will be hyperplastic and may be keratinized and pigmented when the condition is chronic.

Inherited Corneal, Conjunctival, and Sclera Disorders

Corneal stromal dystrophies are inherited stromal metabolic defects that induce the accumulation of lipid extracellular and intracellular in many breeds of dogs between 6 months to 5 years of age (Figs. 8.8 and 8.54).[14,44–48] The light microscopic findings are subtle and easily missed. Small spherical to elliptical clefts are detected between the collagen fibers in the superficial and midstroma, less commonly in the deep stroma of the cornea. Stromal keratocytes in affected corneas may appear degenerate, necrotic, or normal. Frozen sections of affected cornea that are stained with lipid stains, including oil red O, reveal the extracellular and intracellular lipid accumulations. Special fixatives that preserve the lipid accumulations also allow routine histologic sectioning and staining to identify these deposits. The mutations responsible for the many types of corneal dystrophy in dogs and cats are currently unknown. The pathogenesis involves a metabolic defect in the stromal keratocytes, which induces the intracellular and extracellular lipid accumulation.

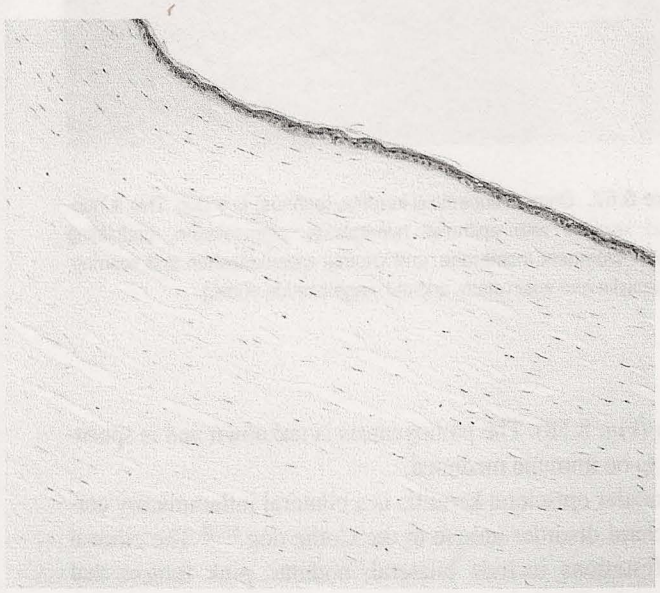

Figure 8.54. Histologic section of a cornea of a young American Cocker Spaniel diagnosed with inherited corneal dystrophy. A band of subepithelial clefts are present where lipid was present. The lipid has leached out of the clefts during processing, and this anomaly is easily mistaken for artifactual corneal stroma; however, the clefts are symmetric and larger than the artifactual separations of fixation. (Periodic acid-Schiff stain, original magnification 50X.)

Corneal endothelial dystrophy is an inherited condition, which may be sex linked in the Boston Terriers.[49,50] Several other breeds of dogs may also be affected with this condition, including the Poodle, Chihuahua, Shih Tzu, and others (Fig. 8.55A).[14] The histologic features include atrophy of the corneal endothelium, corneal stromal and epithelial edema, and ulceration, vascularization and scarring. The Manx cat is also affected by an inherited endothelial dystrophy that, unlike affected dog breeds, which manifests late in life; affected Manx cats develop corneal edema at 4 to 5 months of age.[51] The pathogenesis is poorly understood and appears to involve endothelial apoptosis that allows the pressure gradient of IOP to overwhelm the remaining endothelial pump function, and corneal decompensation and edema develop. The edema often begins in the paracentral or temporal areas and progresses across the entire cornea. The histologic features include extensive corneal edema, detected by the presence of intra- and intercellular edema and subepithelial bullae, thickening of the corneal stroma with dampening of tinctorial quality, and notable decreases in common artifactual fixation–induced intercollagenous clefts, thickening of Descemet's membrane, and depletion and flattening or metaplasia of endothelial cells (Fig. 8.55B). Ulceration, subepithelial pigmentation, stromal scarring, and vascularization are advanced changes. Gutatta, the hallmark of Fuch's endothelial dystrophy in humans, has not been documented in the dog.

Corneal subepithelial dystrophy is also known as epithelial erosion syndrome and superficial punctuate keratopathy. This condition is likely inherited in the Shetland Sheepdog and is occasionally diagnosed in other dog breeds.[14] The pathogenesis of this subepithelial dystrophy is largely unknown but appears to involve a metabolic defect that induces a lipid deposit around the epithelial cells. This condition manifests with focal corneal rings and spots with associated corneal erosions and ulcers. Histologic examination reveals corneal erosions and ulcers, vascularization, scarring, and dyskeratotic and degenerate corneal epithelium.

An inherited bilateral corneal epithelial basement membrane dystrophy is diagnosed in Boxer dogs.[52,53] Surgical keratectomies are occasionally submitted for histologic examination. The light microscopic findings on these submissions include corneal ulceration and associated edema and occasional neutrophil infiltration into the stroma. The epithelium is often nonadherent at the periphery and is elevated off the stroma. A clear acellular band is usually present in the superficial stroma (Fig. 8.56). The pathogenesis is poorly understood and may be the result of a lack of hemidesmosomes and an accumulation of basement membranelike material.[52,53]

Chronic superficial keratitis (pannus) is a bilateral, symmetrical inflammatory keratitis that is inherited in the German Shepherd and several other large-breed dogs.[14] The clinical manifestations of focal temporal limbal or generalized vascularized and pigmented keratitis are pathognomonic and

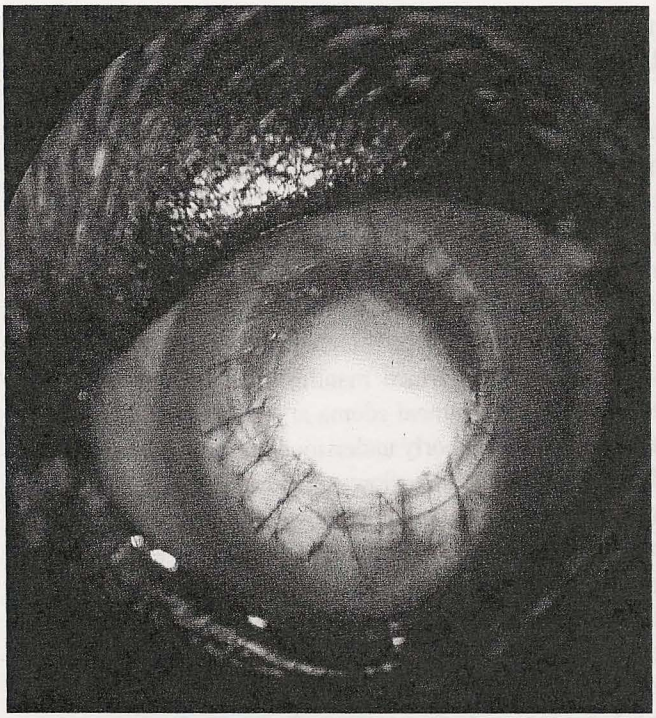

(a)

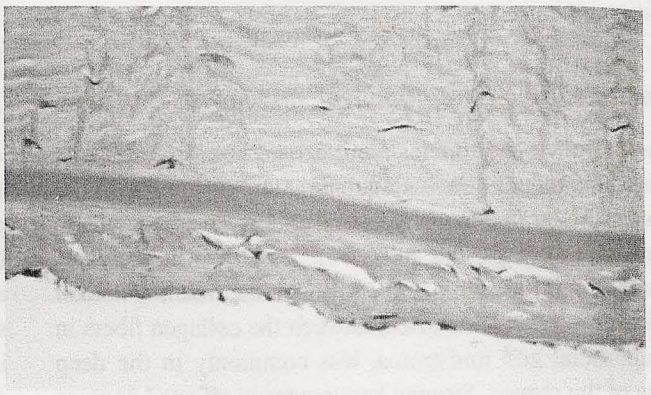

(b)

Figure 8.55. **A**. Clinical photograph of a dog after a corneal transplantation. Note the central clear button and the peripheral diffuse corneal edema secondary to corneal endothelial degeneration. **B**. A biopsy of the corneal button after penetrating keratoplasty and corneal transplantation of the dog in A. Note the fibrous metaplasia of the corneal endothelium (Periodic acid-Schiff stain, original magnification 300X.)

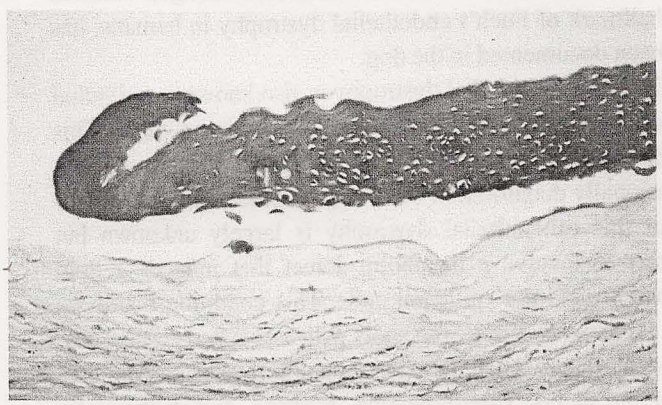

Figure 8.56. An indolent corneal ulcer in a Boxer dog. Note the epithelial nonadherence, irregular thickened basement membrane, corneal edema, and relatively acellular subepithelial stromal layer. (Hematoxylin and eosin stain, original magnification 200X.)

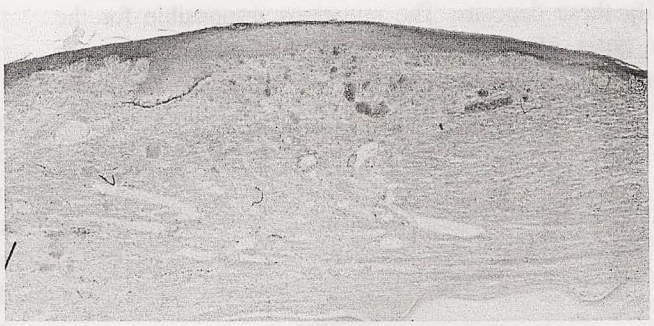

Figure 8.57. Chronic superficial keratitis (pannus) in a dog. This is nonspecific keratitis with epithelial hyperplasia, pigmentation, undulating epithelial basement membrane, and stromal vascularization and scarring. (Hematoxylin and eosin stain, original magnification 100X.)

histologic examination is seldom completed. When the cornea is examined histologically, there is edema, vascularization, pigmentation, and mineralization (Fig. 8.57). The inflammatory cell infiltrate is mixed and includes lymphocytes and plasma cells that often line up in the superficial stroma.

Ligneous conjunctivitis is an idiopathic, perhaps inherited conjunctivitis of Doberman Pinscher dogs.[54] The clinical presentation is dramatic with proliferative conjunctivitis and ocular discharge. Biopsies examined with light microscopy reveal an amorphous conjunctival hyaline-like membrane in the substantia propria and diffuse lymphocyte infiltration. The surface of the conjunctiva is often encased in purulent debris and fibrin (Fig. 8.58). The pathogenesis is unknown and is speculated to be immune mediated.

Nodular episcleral keratitis is a bilateral inflammatory corneoscleral disorder unique to the Collie dog.[55,56] The clinical manifestations include bilateral, nodular, pink tumors that commonly develop near the temporal limbus (Fig. 8.59A). Excisional biopsies submitted for light microscopic examination reveal a diffuse mixed inflammatory infiltrate with lymphocytes, plasma cells, macrophages, and fibroblasts (Fig. 8.59B). The pathogenesis is unknown and assumed to be immune-mediated on the basis of the response to immune modulators. The etiology is also unknown. However, because it is a unique bilateral condition of Collie dogs, it may be

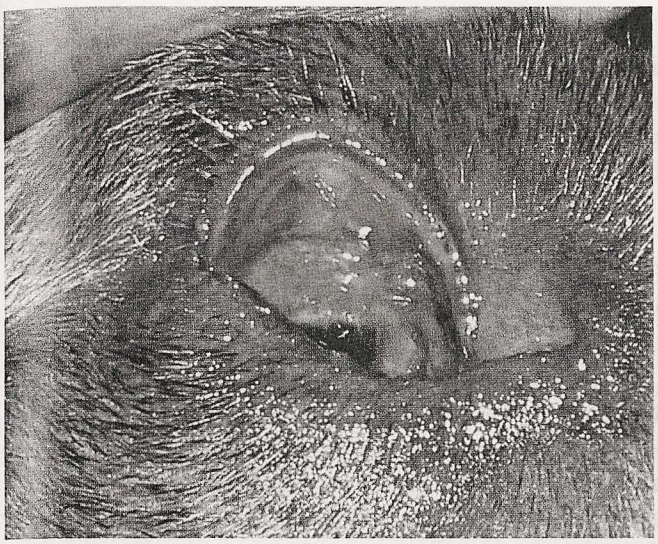

Figure 8.58. Ligneous conjunctivitis in a Doberman Pinscher. Note the conjunctivitis and fibrinous conjunctival discharge and adherent membranes. (Photo courtesy of Dr. Lynne Sandmeyer.)

inherited. Bilateral episcleritis is also diagnosed commonly in American Cocker Spaniels. The diagnosis is confirmed with light microscopic examination of biopsies, which reveal a diffuse mixed inflammatory cell infiltrate that targets the episcleral tissues similarly to nodular episcleral keratitis in Collie dogs. The etiology and pathogenesis remains unknown and is assumed to be immune-mediated on the basis of response to immune suppression and the cellular infiltrate noted histologically. Given the increased frequency of diagnosis of this bilateral condition in American Cocker Spaniels, a genetic etiology may be considered.

Inherited Developmental Glaucoma

Open-Angle Glaucoma of Beagle Dogs

Primary open-angle glaucoma is an inherited autosomal-recessive condition in the Beagle dog.[57–60] This disorder manifests with increased IOP, corneal edema, buphthalmos, and blindness between 2 and 4 years. The mutation responsible for the development is unknown, and the pathogenesis is poorly understood. The glaucoma may be associated with glycosaminoglycan (GAG) accumulation around the pectinate ligaments in the ciliary cleft. The filtration angle is open and appears normal early in the disease. Light microscopic examination of enucleated globes reveals ganglion cell and nerve fiber layer degeneration and optic nerve cupping due to axon loss, and in chronic glaucoma, the inner plexiform and inner nuclear layers are degenerate. With time, the entire retina will be reduced to a glial scar. The filtration angle will become recessed and appear narrow in the chronic stages of the disease as buphthalmos develops.

Primary Glaucoma and Goniodysgenesis in Purebred Dogs

Primary glaucoma associated with goniodysgenesis is the most common of the developmental glaucomas of purebred dogs.[61] It is reported in American Cocker Spaniels, Bouvier des Flandres, Siberian Huskies, Bassett Hounds, Shar Pei, and many other breeds of dogs and is most likely inherited in all breeds affected, although the disorder is difficult to reproduce. The gross clinical manifestations of acute primary glaucoma include corneal edema and conjunctival and episcleral congestion. The onset of glaucoma is variable, and many affected dogs are middle-aged to older. This is a malignant form of glaucoma that is very difficult to treat, and many eyes are enucleated or eviscerated because of blindness and lack of response to most therapies.

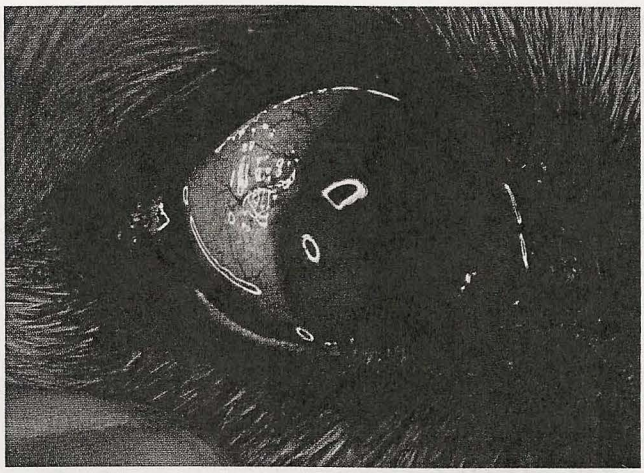

(a)

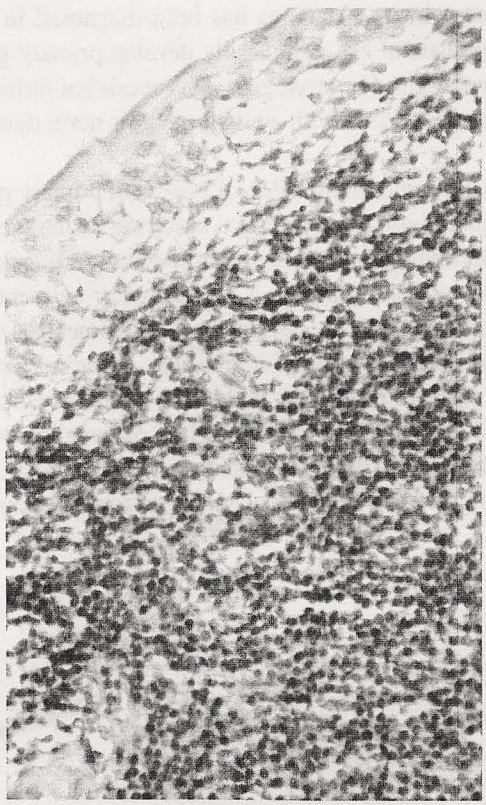

(b)

Figure 8.59. **A.** Nodular episclerokeratitis in a young Collie dog. **B.** Episcleritis is a mixed inflammatory infiltrate with lymphocytes, plasma cells, and macrophages. (Hematoxylin and eosin stain, original magnification 400X.)

There has been considerable confusion regarding the classification of open and closed angles in veterinary medicine in recent years. To clarify this, an angle is closed when peripheral anterior synechiae, or the base of the iris, swells over the filtration angle and occludes it. Goniodysgenesis is an open angle with a lack of development of the uveal meshwork. Goniodysgenesis is caused by failed rarefaction of primitive uveal neurocrest tissues that span the filtration angle that normally occurs shortly after birth. The histologic confirmation of goniodysgenesis includes nodular thickening of Descemet's membrane, thickened and shortened pectinate ligaments, and an accompanying periodic acid-Schiff–positive basement membrane material within the trabecular meshwork (Figs. 8.60 and 8.61). Goniodysgenesis is only a marker for the idiopathic glaucoma in the previously mentioned dog breeds. Once primary glaucoma has been diagnosed in one eye, the contralateral eye will usually develop primary glaucoma within months. However, goniodysgenesis has little predictive value. Many dogs with goniodysgenesis never develop glaucoma.

Light microscopic examination of eyes with primary glaucoma and goniodysgenesis reveals a spectrum of intraocular pathology depending on the length of time that the glaucoma has been present before the eye is enucleated or eviscerated. Acute (<4 days) histologic lesions include corneal edema, mixed inflammatory neutrophil infiltrations in the trabecular meshwork, pigment dispersion within the anterior segment, and retinal degeneration that includes loss of ganglion cells, nerve fiber layer, and focal full-thickness retinal necrosis.[62,63] Chronic primary glaucoma associated with goniodysgenesis is manifested histologically by optic nerve degeneration, retinal degeneration, uveal atrophy, pigment dispersion, preiridal fibrovascular membranes, corneal degeneration and ulceration, striae, lens luxation, cataract formation, and buphthalmos and scleral thinning (Figs. 8.9 and 8.62).

Melanocytosis of Dogs

Melanocytosis, also known as pigmentary glaucoma, pigmentary dispersion and glaucoma syndrome, is most likely an inherited, intraocular melanocytic proliferation disorder of the Cairn Terrier.[64] Recently, this syndrome has also been reported in the Boxer and Golden Retriever dogs.[65] Occasionally, melanocytosis develops as a unilateral condition in dogs other than Cairn Terriers. Melanocytosis induces secondary glaucoma by dispersion of pigment, melanocytes, and pigment-laden macrophages in the anterior uvea, filtration angle, and ciliary body and choroid. The light microscopic examination reveals a diffusely thickened anterior uvea with a normal-appearing population of melanocytes, and macrophages laden with pigment (Fig. 8.63). These cells and pigment accumulate throughout the uvea, anterior and posterior chambers, vitreous, and into the filtration angle, around the episcleral-collecting veins, and within the episcleral tissues. Accompanying secondary ocular pathology includes retinal, uveal, and vitreous degeneration consistent with sustained glaucoma. The etiology and pathogenesis are unknown, and melanocytosis is categorized in this section because most cases are bilateral and the condition predominates in middle-aged Cairn Terriers.

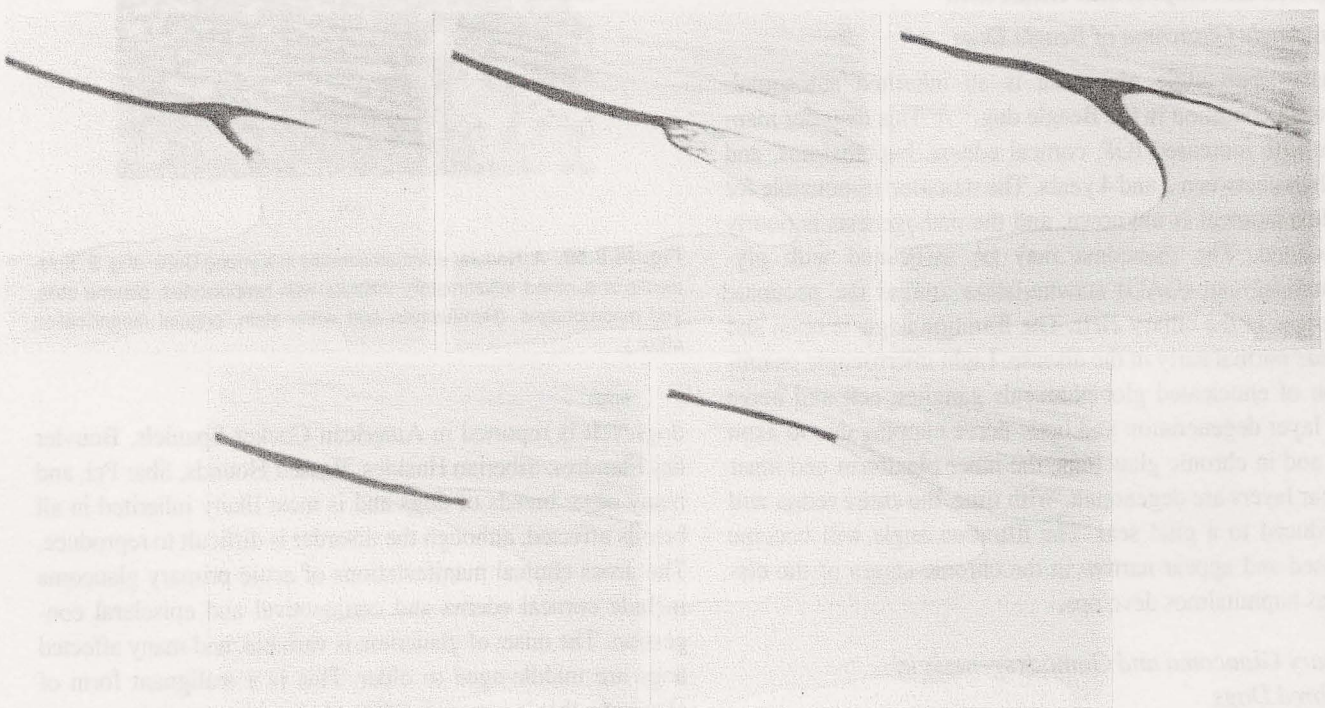

Figure 8.60. Schematic illustrations of the spectrum of irregular thickening, fimbriation, scrolling, and extension of Descemet's membrane that commonly occur in the syndrome of goniodysgenesis and primary glaucoma in dogs.

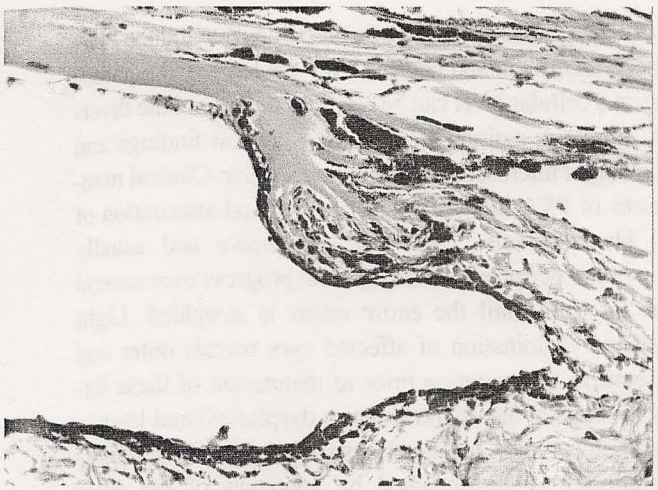

Figure 8.61. Goniodysgenesis in an American Cocker Spaniel. The pectinate ligament is shortened and thickened, and the termination of Descemet's membrane is fimbriated. (Hematoxylin and eosin stain, original magnification 200X.)

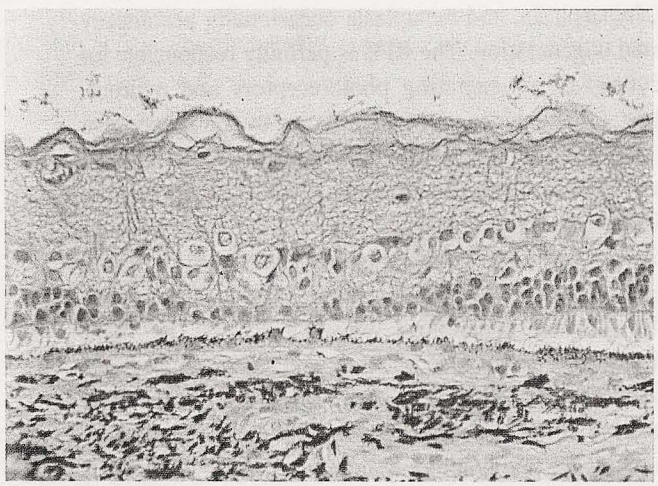

Figure 8.62. Retinal degeneration consistent with chronic glaucoma. Note the loss of nerve fiber, ganglion cell, and inner plexiform layers. In addition, the inner nuclear layer and outer plexiform layers are reduced, and centrally there is a focal full-thickness retinal degeneration and two hyperplastic retinal pigment epithelial cells. (Hematoxylin and eosin stain, original magnification 300X.)

Primary Glaucoma in Rabbits

The New Zealand white rabbit is subject to a recessively inherited goniodysgenesis that manifests early in life as buphthalmos, a result of the elasticity of the thin lapine corneosclera. Interestingly, because the rabbit lacks a lamina cribrosa, it is a good model to compare and contrast mechanisms of posterior segment changes associated with elevated IOP.

Inherited Developmental Lenticular Disorders

Inherited developmental lenticular disorders include lens luxations and cataracts. These are most common in the dog.[14] Inherited lens luxations are limited to a few breeds of dogs, including the Terrier breeds, German Shepherd, Border Collie, Shar Pei, and Tibetan Terrier.[66–70] The clinical diagnosis of

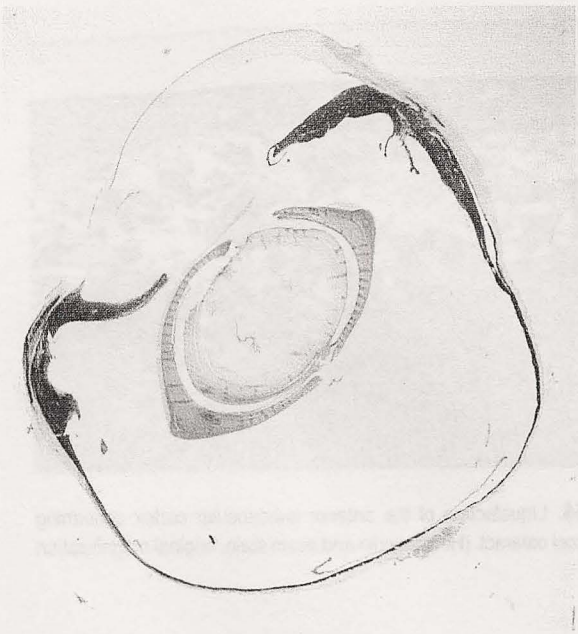

Figure 8.63. Ocular melanocytosis in a Cairn Terrier. Note the heavily pigmented irides and ciliary body with extension of pigment into the episcleral tissues around the aqueous collecting veins and choroid. Glaucoma was present prior to enucleation and confirmed with light microscopic examination of the retina and optic nerve. (Hematoxylin and eosin stain, original magnification 2X.)

lens luxation is relatively easy and is confirmed by biomicroscopic confirmation of lens dislocation and zonular rupture. However, confirmation of the etiology (i.e., inherited [primary] versus secondary to glaucoma and buphthalmos or uveitis and secondary zonular degeneration) is more difficult.[67,71] Recently, light microscopic examination of Terrier breeds and Shar Pei dogs with zonular dysplasia confirmed distinctive lamellar and cross-hatched patterns, and strong periodic acid-Schiff and Mason's trachoma staining and negative elastin staining.[72] The mutations responsible for zonular dysplasia and the pathogenesis remain unknown. Uveitis, secondary glaucoma, cataracts, and vitreous and retinal degeneration are common with chronic anterior or posterior primary lens luxation and confirmed with light microscopy.

In contrast, inherited cataracts may develop in most, if not all, purebred dog breeds.[14] Genetic mutations for all cataracts remain unknown, and the diagnosis of most inherited cataracts occurs after biomicroscopic examination that documents the breed-specific bilateral cataract morphology and age of onset. The gross appearance of cataracts is limited to white opacification of the lens. Light microscopic examination of inherited cataracts in all animals reveal nonspecific findings, including liquefaction of lens fibers, lens epithelial hyperplasia, metaplasia, and migration, which occur in diabetic, traumatic, nutritional, and toxic cataracts (Figs. 8.64 and 8.65). The pathogenesis of cataract formation despite varied etiologies is limited to protein, metabolic, and fluid abnormalities.

Inherited Development Retinal and Vitreous Disorders

Inherited retinopathies are common in dogs, cats, and rodents, and they are only occasionally diagnosed in other animals. We

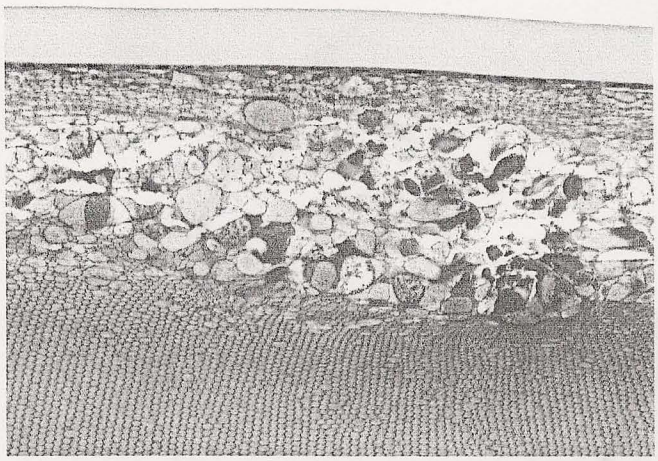

Figure 8.64. Liquefaction of the anterior subcapsular cortex confirming anterior cortical cataract. (Hematoxylin and eosin stain, original magnification 200X.)

Figure 8.65. Posterior lens cortex liquefaction and lens epithelial migration. (Hematoxylin and eosin stain, original magnification 200X.)

limit our discussion to those of the dog and cat because most of the gross, light, and electron microscopic changes are similar in all animals. Progressive retinal atrophy (PRA) is a collective term that includes an aggregate of multiple genetic defects in the dog and cat that manifest clinically in a similar fashion. These include photoreceptor dysplasias (*rcd1, rcd2, rd, erd*), rod cone degenerations (*prcd, xlpra*), cone degeneration (*cd*), congenital stationary night blindness (*csb*), rod cone dysplasia in Abyssinian cats (*Rdy*), and rod cone degeneration in Abyssinian cats (*rdAc*). All of these conditions are inherited as autosomal-recessive conditions except X-linked PRA in Siberian Huskies. All the clinical diagnoses can be confirmed with scotopic and photopic electroretinography by 18 months of age. The onset of clinical signs (nyctalopia, day blindness, retinal atrophy) is quite variable, manifesting between 6 months and 8 years of age.[73] Retinal pigment epithelial dystrophy[73] and multifocal retinopathies[74–76] have unique clinical features and are discussed separately.

PRA in Dogs Some of the genetic mutations that induce PRA have been identified, and because they are known, the pathogenesis at a cellular level can be confirmed. Despite the diversity of unique mutations for PRA, the clinical findings and gross and light microscopic findings are similar. Clinical manifestations of PRA include retinal atrophy and attenuation of retinal blood vessels. These are progressive and usually develop at the periphery of the retina to progress over several months to years until the entire retina is atrophied. Light microscopic examination of affected eyes reveals outer and inner segment degeneration prior to maturation of these tissues at 8 weeks of age (photoreceptor dysplasias) and later in life for photoreceptor degenerations (Fig. 8.15). The photoreceptor atrophy is accompanied by apoptosis of the outer nuclear and outer plexiform layers, and eventually the inner nuclear and inner plexiform layers. Several variations include rod dysplasias, rod-cone dysplasias, and cone dysplasias. Despite variations in the photoreceptor affected, light microscopic findings are similar, and with time the retina is reduced to glial scar. The RPE is marginally involved and mild hypertrophy, hyperplasia, and metaplasia occasionally accompany the retinal degeneration. The RPE is partially responsible for phagocytosis of degenerating photoreceptors and neurons. With time, other ocular tissues are affected by the progressive retinal degeneration, including the vitreous, which degenerates and liquefies. Clumped collagen strands will be floating in liquid vitreous in the dependent posterior segment. Asteroid hyalosis is a common accompaniment also. Asteroid bodies are acellular, light purple, dense vitreous structures composed of lipid mineral concretions when examined by light microscopy. The lens is also affected, and subcapsular liquefaction and bladder cells and posterior migration of metaplastic lens epithelium are often present. These cataracts are usually extensive and commonly induce a mild to moderated lymphocytic plasmacytic uveitis. In addition, zonular degeneration may be present and manifests grossly with an aphakic crescent and vitreous prolapse into the anterior chamber. Preiridal fibrovascular membranes are also occasionally noted in globes affected with chronic photoreceptor dysplasias. Similarly, secondary glaucoma may be noted in these globes. The histologic confirmation of chronic PRA is difficult because the complete retinal degeneration is nonspecific. The differential diagnoses that warrant consideration when diagnosing PRA histologically include nutritional deficiencies (taurine, vitamin E, vitamin A), toxins (numerous drugs such as fluoroquinolones, aminoglycosides, and antimalarial), plant toxicoses (including Bracken fern [*Pterdium* sp.] and locoweed [*Astragulus* sp.]), light toxicity, radiation, sudden acquired retinal degeneration, and others (see acquired retinal diseases).[77–85]

PRA in Cats Three early-onset photoreceptor degenerations have been reported in cats: mixed breed retinal degeneration,[86] Persian retinal degeneration,[87] and Abyssinian retinal dysplasia.[88,89] Only the Persian retinal degeneration is an autosomal-recessive condition,[87] while the other two are

autosomal-dominant conditions.[86,88] These three rod-cone degenerations all manifest with clinical signs (retinal degeneration, tapetal hyperreflectivity, retinal vascular attenuation) within a few months of age. Light microscopic examination confirms both rod and cone degeneration that extends from the outer segment to the inner segment and gradually through all the layers of the retina. The Abyssinian cats with photoreceptor dysplasia fail to develop rod and cone outer segments, there is incomplete synaptogenesis, and degeneration begins near the central retina and progresses to the periphery by about 7 months. Eventually, the RPE, choriocapillaris, and tapetum also atrophy.

A late-onset autosomal-recessive photoreceptor degeneration is also reported in Abyssinian cats.[90,91] Light microscopic examination reveals disorientation of the rod outer segments initially, then degeneration of the outer segment in affected cats at approximately 6 months of age. Over the next year, the rods, their axons and associated nuclei, and axons in the outer plexiform, inner nuclear, and inner plexiform layers degenerate (Fig. 8.66). The cones remain normal till the affected cats are 2 to 3 years of age.

Retinal Pigment Epithelial Disorders At least two inherited retinal degenerations have been linked to the RPE: congenital stationary night blindness in Briard dogs[92,93] and retinal pigment epithelial dystrophy as reported in several breeds of dogs.[94,95] In addition, multifocal serous retinal detachments are inherited in Great Pyrenees, Coton de Tulear, and Mastiff dogs[74–76] and are most likely directly related to mutations that alter retinal pigment epithelial function.

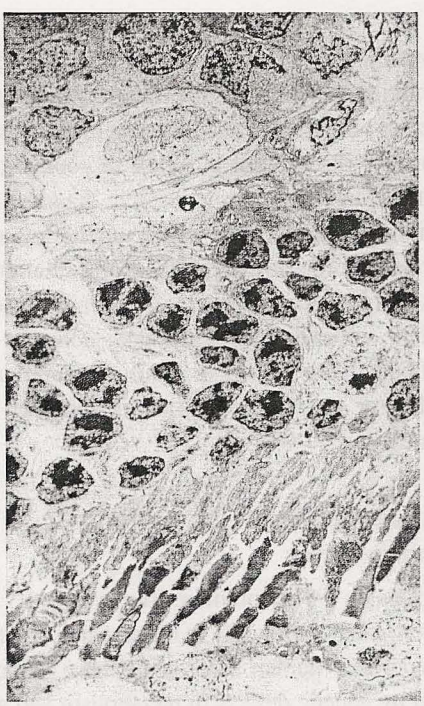

Figure 8.66. Transmitting electron micrograph of the retina of a 6-month-old Abyssinian cat with progressive retinal degeneration. Note the degenerating outer and inner segments of the photoreceptors (Magnification 4000X.) (Micrograph courtesy of Kristina Narfstrom.)

Congenital Stationary Night Blindness in Briard Dogs Congenital stationary night blindness has been reported in the Briard dog. This disorder is a slowly progressive blinding disorder caused by a mutation in the RPE 65 gene. The gross manifestations include retinal atrophy. Light microscopic abnormalities include apoptosis and degeneration of the photoreceptors and a progressive loss of the nuclear and plexiform layers and retinal pigment epithelial vacuoles and pigmentation.

Central Retinal Atrophy Central retinal atrophy is a rare disorder of dogs in North America, and multiple etiologies have been reported, including genetic mutations and nutritional deficiency of vitamin E.[96–100] Some dog breeds manifest with central progressive retinal atrophy resulting from mutations that alter vitamin E metabolism.[99,100] These defects induce lipofuscin accumulation in the RPE. The outer segment degeneration is slow and progressive between 2 and 6 years of age. The hallmark histologic finding is lipofuscin accumulation within the RPE and degeneration of the outer and inner segments, and if chronic, the outer and inner nuclear and associated plexiform layers will also be degenerate. Unlike progressive retinal atrophy and photoreceptor dysplasias, secondary intraocular diseases such as cataracts and vitreous degeneration are uncommon with central retinal atrophy.

Multifocal Retinopathies in Dogs Multifocal retinal detachments most likely develop secondary to retinal pigment epithelial dysplasias that affect RPE function. These disorders are inherited in the Great Pyrenees, Coton de Tulear, and Bull Mastiff dogs. They manifest as bullous retinal detachments at approximately 11 to 17 weeks (Fig. 8.67). There is progressive enlargement of most focal retinal and RPE detachment

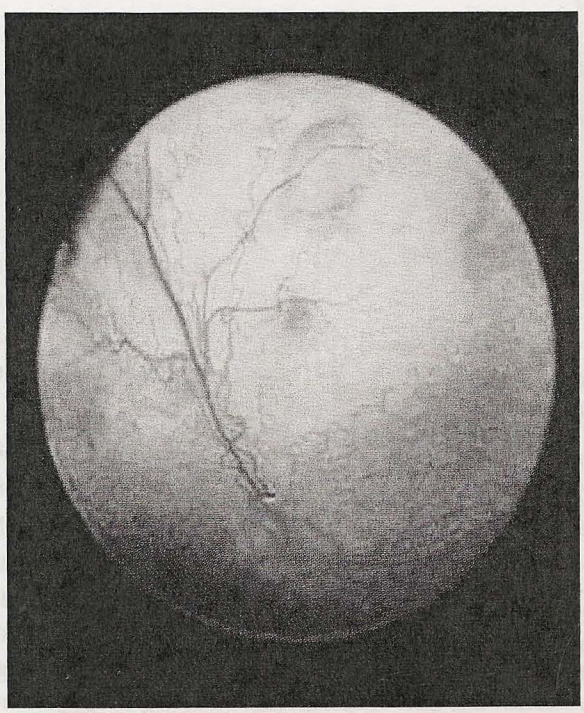

Figure 8.67. Inherited multifocal retinopathy of a Great Pyrenees dog.

and development of new lesions until the affected dogs are approximately 6 to 10 months of age. Light microscopic examinations confirm multifocal bullous retinal detachments with associated retinal pigment epithelial hypertrophy, hyperplasia, and pigmentation (Fig. 8.68). In addition, there are focal areas of degeneration of the outer nuclear and plexiform layers associated with each detachment. The RPE also develops focal detachment from Bruch's membrane (Fig. 8.69). The mutations responsible for and the pathogenesis of these multifocal anomalies are unknown.

Inherited Choroidal and Vitreous Anomalies Inherited disorders of the choroid and vitreous are uncommon, and reports are limited to the dog and cat. Inherited tapetal anomalies have been reported in Beagles[101,102] and cats[103,104]; multifocal choroidal retinopathy has been reported in Borzoi dogs[105]; and although no published reports are available, inherited vitreous degeneration is suspected in Whippets, Italian Greyhounds, and other dogs.

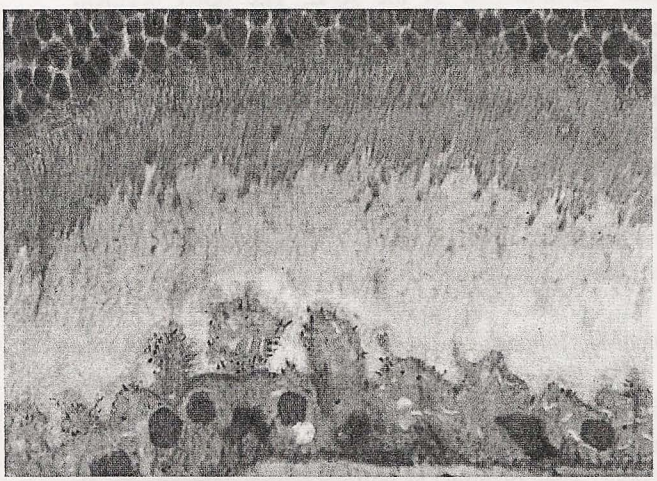

Figure 8.68. Retinal pigment epithelial hypertrophy, vacuolation, and pigmentation that developed near the edge of a focal inherited retinal detachment in a Great Pyrenees dog. (Toluidine blue stain, original magnification 300X.)

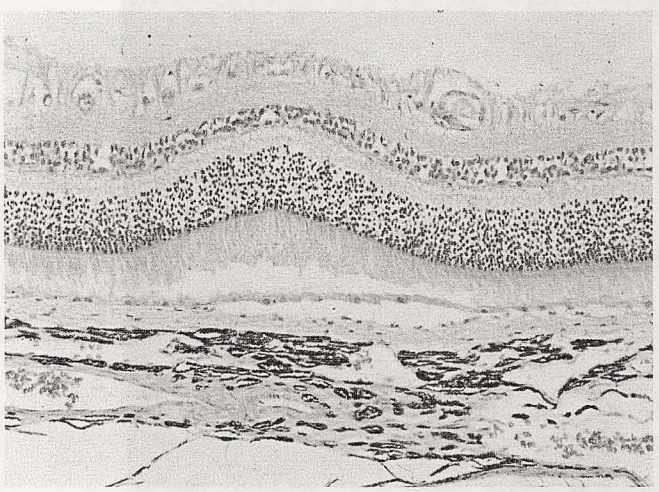

Figure 8.69. Histologic section of the retina of a 4-month-old Great Pyrenees dog with inherited multifocal retinopathy. Note the focal retinal and retinal pigment epithelial detachments. (Hematoxylin and eosin stain, original magnification 200X.) (Reprinted with permission, Grahn BH, Philibert H, Cullen CL, Houston DM, Schmutz S. Multifocal retinopathy of Great Pyrenees. *Vet Ophthalmol* 1999;1:211–221.)

Tapetal Degeneration in Dogs and Cats Inherited tapetal degeneration in Beagles is an autosomal-recessive condition in which the number of tapetal cells is normal at birth. The clinical manifestations include loss of the normal reflective tapetum due to progressive degeneration. This degeneration begins at approximately 2 months after birth, and by about 3 months, the tapetal cells have lost all their rodlets and are packed with membranous inclusions.[101,102]

A similar disorder develops in Siamese cats with Chediak-Higashi syndrome. The tapetum in these cats is also normal at birth and is completely degenerate by 2 months of age when the eyes are examined with light microscopy. Macrophages are absent in both of these disorders.[103–104]

Borzoi Chorioretinopathy Multifocal choroidal retinal lesions have been reported in Borzoi dogs (Fig. 8.70A).[14,105–107] The lesions have been reproduced in test-bred Borzoi dogs, although the mode of inheritance is unknown.[105] Initial reports speculated that this disorder was part of PRA.[106,107] PRA has been excluded as part of this disorder by electroretinography and light microscopy.[105] The light microscopic findings of Borzoi retinopathy include focal choroidal atrophy, loss of choriocapillaris, focal hypertrophy and pigmentation of the RPE, and focal degeneration of associated photoreceptors (Fig. 8.70B).

Vitreous Degeneration Vitreous degeneration is suspected to be an inherited condition in Whippets and Italian Greyhounds given the development of syneresis and prolapse of tendrils of degenerate vitreous into the anterior chamber in young dogs (6 months to 4 years of age). Light microscopic diagnosis of vitreous degeneration is nonspecific in regard to etiology, and the lesions are subtle. Thorough light microscopic examination of the vitreous will reveal condensed vitreous fibers and a lack of fine fibrillary vitreous collagen and detachment of these condensed fibers from the inner limiting membrane (Fig. 8.71). Whether or not this condition is inherited is unknown at this time.

Inherited Storage Disorders and Amino Acid and Lipid Peroxidation Disorders

Metabolic storage diseases are uncommon. However, many of these have been investigated thoroughly in the research laboratory as models for similar human disorders. These storage disorders are caused by genetic defects in metabolism and are generally the result of a deficient degratory pathway. These metabolic defects result in accumulation of complex lipids, glycoproteins, or polysaccharides within specific types of cell

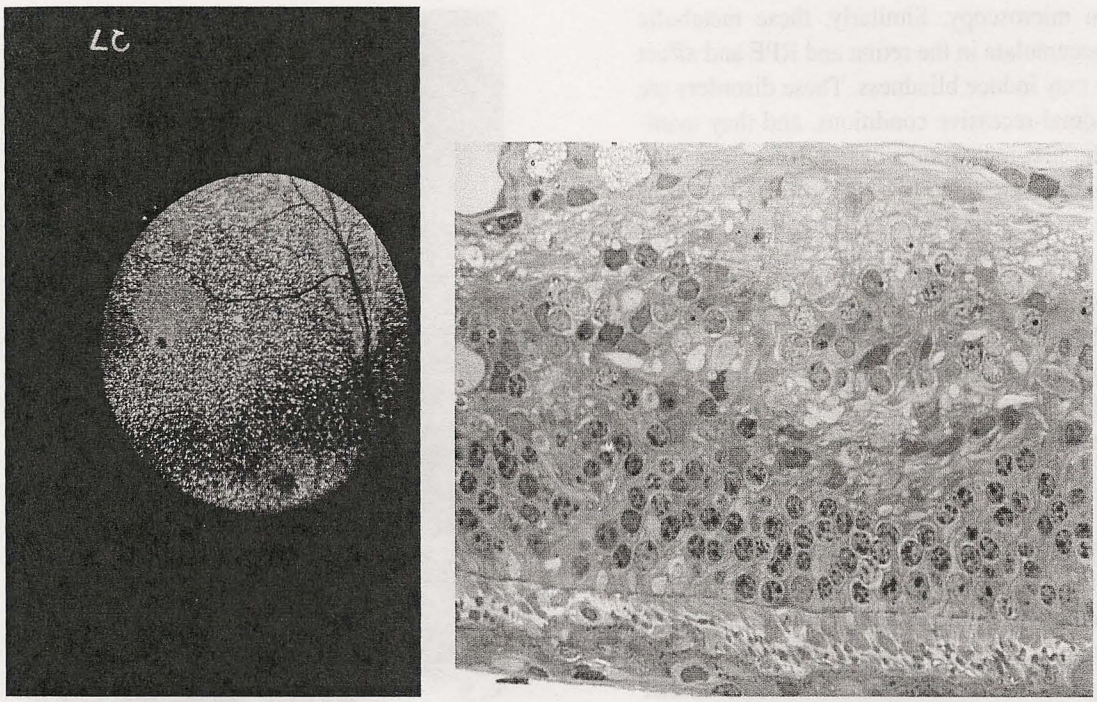

(a) (b)

Figure 8.70. **A.** A mature Borzoi dog with a characteristic lesion of Borzoi retinopathy. Note the focal hyperpigmented and hyperreflective lesions. **B.** Histologic lesion of Borzoi retinopathy. Note the retinal pigment epithelial hypertrophy, hyperplasia and pigmentation, and the outer and inner segment photoreceptor degeneration and loss of outer nuclear, outer plexiform, and inner nuclear layers. Occasional mononuclear cells are present within this focal lesion. The retina on either side of this lesion was normal morphologically. (Toluidine blue stain, original magnification 400X.)

Figure 8.71. Vitreous degeneration in a dog with secondary glaucoma and retinal detachment. The vitreous strands are congealed and therefore appear thickened and bunched together, and they are apposed to the inner limiting membrane of the ventral nontapetal retina. Plasma proteins are also present around the thickened vitreous tendrils. Note the characteristic retinal degeneration of the inner retina (glaucoma) and loss of photoreceptors and outer nuclear layer (detachment). (Periodic acid-Schiff stain, original magnification 200X.)

within the eye. These cells may include keratocytes, ganglion cells, and RPE. Histopathologic signs may be subtle when the sole diagnostic examination is light microscopy. These systemic metabolic conditions are best defined by histochemistry and transmission electron microscopy. The typical clinical presentation is that of a young animal with neurologic and frequently ocular signs. A variety of inherited developmental disorders that affect systemic lysosomal enzymes (gangliosidosis, mucopolysaccaridoses, mannosidosis), lipid peroxidation defect (neuronal ceroid lipofuscinosis), and amino acid metabolism (ornithinuria) have been reported in several animals.

Lysosomal Storage Disorders That Affect the Cornea and Retina Gangliosidosis (G_{m1} and G_{m2}) and mucopolysaccaridoses (MPSI, VI, VII) induce a cloudy cornea in affected cats.[108–112] Dogs with mucopolysaccaridoses types I and VII also manifest clinically with a cloudy cornea.[113–114] Gangliosidosis has also been reported in cattle.[115,116] Mannosidosis has been reported in cats[117] and in sheep and goats.[118,119] In all species affected by G_{m1} and G_{m2}, MPSI, VI, VII, and mannosidosis, the clinical signs are diverse and involve multiple organ systems including the eyes. Cloudy corneas are a common clinical manifestation, which develops secondary to accumulation of glycosaminoglycans and glycoproteins within membranous inclusions in the corneal stromal keratocytes and endothelium. These inclusions will be noted on

light and electron microscopy. Similarly, these metabolic by products will accumulate in the retina and RPE and affect their function and may induce blindness. These disorders are inherited as autosomal-recessive conditions, and they manifest clinically in the first few months of life. Neurologic disease predominates and is progressive, and affected animals die at a young age.

Fucosidisis Fucosidisis has been reported in English Springer Spaniels with alpha-L-fucosidase deficiency and manifested histopathologically as vacuolated ganglion cells, astrocytes, and RPE. Affected dogs were visually impaired and exhibited generalized progressive neurologic disease.[120,121] This condition is inherited as an autosomal-recessive condition.

Amino Acid Metabolic Disorders Ornithinuria is an inherited disorder in the cat associated with a deficiency of ornithinuria transferase.[122] The clinical manifestation is bilateral retinal atrophy that occurs in older cats. The histopathologic lesion is generalized and includes retinal, retinal pigment epithelial, and choriocapillaris and choroidal atrophy. Choroidal vascular atrophy is the unique histologic finding with this disorder. The diagnosis is confirmed by documenting elevated levels of ornithine in the urine or plasma.

Lipid Peroxidation Defects Neuronal ceroid lipofuscinoses are inherited autosomal-recessive conditions in dogs and cats,[123–127] cattle,[128] sheep,[129,130] and goats.[131] Decreased peroxidase activity is associated with the development of ceroid lipofuscinosis. Clinical manifestations include blindness and mental deterioration, seizures, ataxia, and tremors. Stacked membranous inclusions in RPE (Fig. 8.72) and ganglion cells are noted with light and electron microscopy and are associated with visual and ophthalmoscopic abnormalities noted. These are progressive neurologic diseases that lead to paralysis and death.

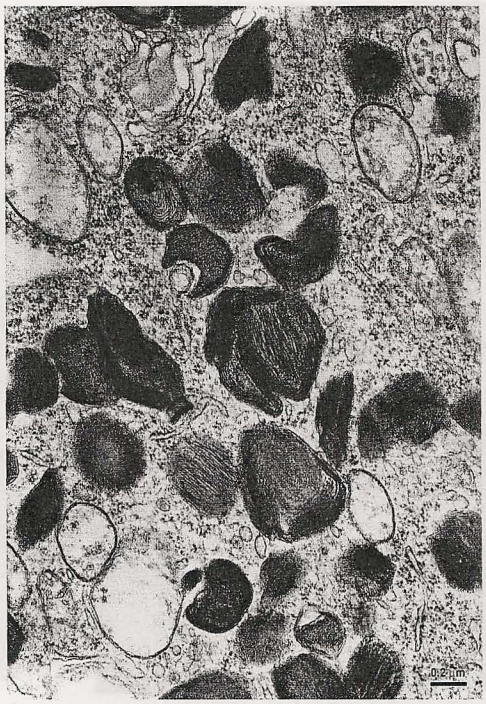

Figure 8.72. These cytoplasmic inclusions are characteristic of neuronal ceroid lipofuscinosis. (Courtesy of Kristina Narfstrom.) (Micrometer bar = 0.2mm.)

ACQUIRED OCULAR DISORDERS

The pathology of acquired ocular disorders is diverse. We have categorized this section into noninfectious ocular disorders, infectious ocular disease, and neoplasia. Within these categories, we have subcategorized disorders by the specific tissues affected and generally when all ocular tissues are affected.

Noninfectious Inflammatory Ocular Disease

Ocular Trauma

Traumatic disease is almost always accompanied by inflammation; the importance of the posttraumatic inflammatory component in relation to the damage created directly by the trauma and the outcome varies from insignificant (uncomplicated traumatic hyphema) to greatly important (phacoclastic uveitis following lens capsule rupture). Mechanical trauma includes accidental perforating and penetrating wounds of the globe, with or without the introduction of microbes and foreign bodies; contusion injuries; and surgical trauma. Physical trauma includes chemical and thermal burns and those changes induced by electromagnetic radiation.

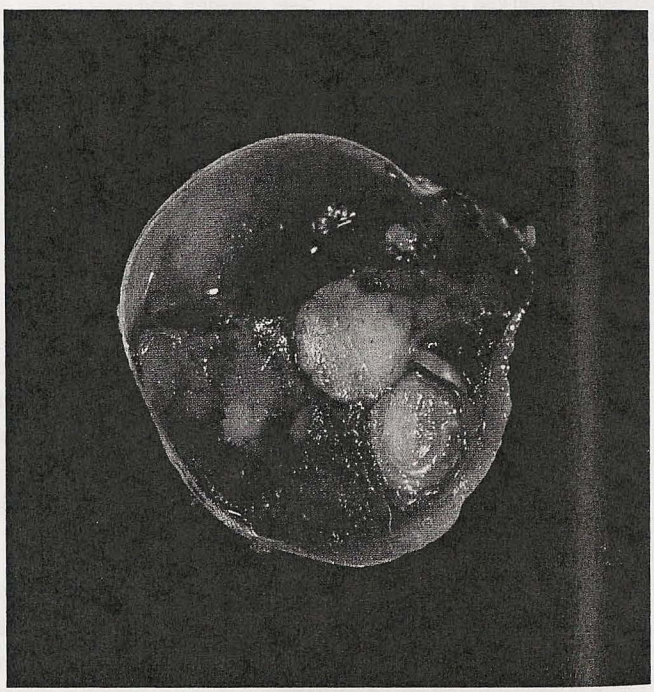

Figure 8.73. This cat eye sustained penetrating trauma. Note the thin, discontinuous sclera with the uveal plug, the ruptured lens, and major disruption of the intraocular contents.

A penetrating wound is one that extends only partway through the tissue of reference; a perforating wound has both an entrance and exit site in the tissue of reference (Figs. 8.73 and 8.74). Thus, a perforating injury to the cornea may be either a penetrating wound in the globe, depending whether or not it is

accompanied by a scleral perforation as well. With either, the sudden decompression of the globe leads to a breakdown of the blood–ocular barrier and protein exudation into the extracellular fluid compartments—the paracentesis effect—which is largely prostaglandin mediated. Uveal tissue is drawn into the defect with inflammatory exudates (Fig. 8.75), which it may effectively seal; if not (dependent largely on size), extrusion of lens, vitreous, and retina may follow. Shearing of the ciliary vessels as they pass from sclera to choroid may occur with expulsive subchoroidal hemorrhage that hastens the extrusion of globe contents.

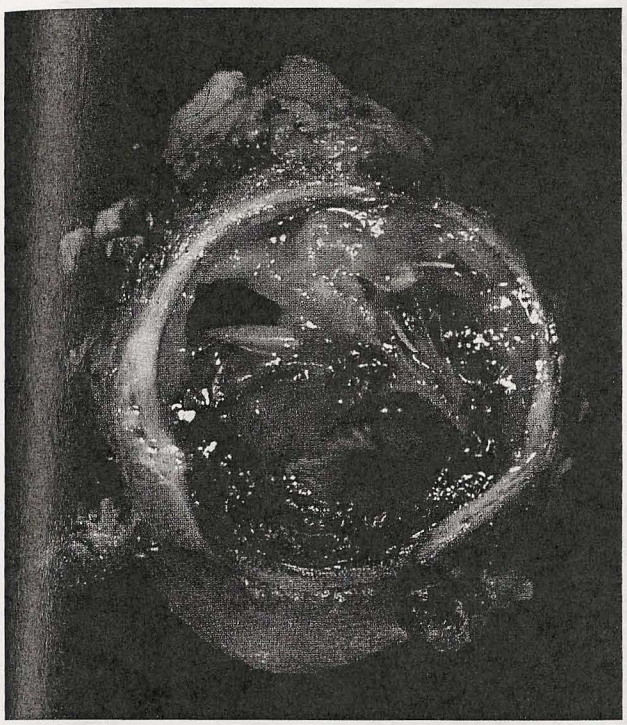

Figure 8.74. Plant foreign bodies within the vitreous of this dog's eye. Spear grass seeds will occasionally penetrate the sclera and induce a fulminant endophthalmitis.

Figure 8.75. Endophthalmitis and scleral perforation in a dog with penetrating trauma and septic endophthalmitis. Note the streaming of inflammatory exudates through the choroidal and scleral perforation. (Hematoxylin and eosin stain, original magnification 200X.)

While small hemorrhages usually resorb without significant sequelae, large and recurrent hemorrhages may be a stimulus for synechiae and membranogenesis as they organize; they can lead to hemoglobin-staining of the cornea in the presence of endothelial compromise and elevated IOP; and they can leave behind hemosiderin and cholesterol residues. The specific lesions that may be related to both concussive and penetrating/perforating wounds are listed in Table 8.4.

Table 8.4 Ocular Lesions Associated with Accidental or Surgical Trauma

Tissue	Lesions
Orbit	Edema, hemorrhage
	Orbital bone fractures
Adnexa	Edema, hemorrhage
	Laceration
Globe	Corneoscleral perforation
	Epithelial of fibrous ingrowth (late)
Conjunctiva	Erythema, chemosis, and hemorrhage
	Laceration
Cornea	Epithelial erosion
	Blood-staining (with hyphema, endothelial damage, elevated IOP)
	Penetration/perforation
Anterior uvea	Hyphema
	Trabecular fracture
	Iris sphincter muscle rupture
	Iridodialysis
	Iridoschisis (separation of pigmented epithelium)
	Post-contusion angle deformity
	Cyclodialysis
Lens	Capsular rupture
	Luxation/subluxation with zonular disinsertion
	Cataract
Vitreous	Detachment
	Prolapse (if zonules ruptured)
	Hemorrhage (from retinal vessels)
Retina	Edema
	Hemorrhage
	Necrosis
	Tear/peripheral dialysis
Optic nerve	Avulsion

Acquired Orbital Disorders

Idiopathic Orbital Inflammatory Syndrome

Historically described in the ophthalmic pathology of humans literature as *pseudotumor,* this poorly defined process has been described and probably does occur in animal species, albeit rarely; by definition, it is a benign nongranulomatous, noninfectious inflammatory process. It is characterized by a diffuse lymphocytic plasmacytic orbital cellulitis when biopsies are examined with light microscopy.

Orbital Cellulitis Abscess

Orbital cellulitis/abscess is most commonly seen in young, growing dogs related to sharp foreign bodies that penetrate the oral cavity behind the upper last molar teeth. Occasionally, the foreign body penetrates the orbit through the conjunctiva or eyelids, or it migrates, as is the case with porcupine quills.[132] The injury sometimes results from sepsis extended into the orbit from surrounding tissues (orbit, nasal, or sinus cavities),[134] or, in the case of hedgehogs, it is self-inflicted.[133] Occasionally, fine-needle aspirates and orbital biopsies are submitted for examination and to confirm the diagnosis of orbital cellulitis. During the acute stage, the inflammatory cell infiltrates are neutrophilic. With time, the infiltrate becomes more mixed, with macrophages, lymphocytes, and plasma cells predominating.

Extraocular Myositis

While the orbit may be involved secondarily in eosinophilic myositis of the masticatory muscles (Fig. 8.53) (initially with exophthalmos related to compression of the orbital contents, and chronically with enophthalmos caused by atrophy of orbital and masticatory tissues), extraocular myositis is likely a primary perhaps inherited condition of the orbit and masticatory muscles.[135] Occasionally, other breeds of dogs are affected.[136] The orbital tissues are edematous and infiltrated diffusely with lymphocytes and plasma cells. Muscle degeneration is seen initially, with muscle atrophy the sequelae in chronic, uncontrolled cases. Other breeds, notably the Shar Pei, may be affected unilaterally or bilaterally (see previous discussion of inherited developmental orbital disorders).

Orbital Cysts

Cysts in or around the orbit are occasionally removed and submitted for histologic examination.[137,138] The diagnosis is confirmed by light microscopic examination that reveals a thin, epithelial-lined, fluid-filled structure that likely originates from the nasolacrimal, lacrimal, or other periocular tissue (Figs. 8.76 and 8.77). Zygomatic mucocoeles are also occasionally removed and submitted for light microscopy. The diagnosis is confirmed with light microscopic identification of cysts associated with the zygomatic salivary tissue.

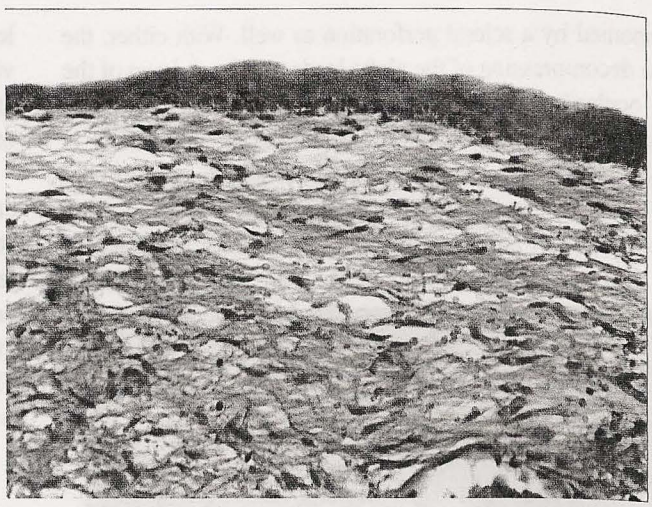

Figure 8.76. Lacrimal gland cyst lining. (Hematoxylin and eosin stain, original magnification 200X.)

Figure 8.77. Lacrimal gland cyst lining from a dog with attached lacrimal gland. (Hematoxylin and eosin stain, original magnification 200X.)

Acquired Conjunctiva Disorders

Conjunctivitis

Conjunctivitis is characterized acutely by vascular dilation, edema, neutrophilic infiltration, and exudation (Fig. 8.78) manifested as ocular discharge. Pseudomembranes composed of necrotic cells, protein, and fibrin may form; true membranes result from epithelial necrosis, and removal results in an ulcerative, frequently hemorrhagic lesion (Fig. 8.58). With chronicity, the nature of the inflammatory infiltrate changes, and lymphoid follicles may form on the surface (Fig. 8.79). Although there are many primary etiologies for conjunctivitis in animals (bacterial, viral, parasitic, toxic, immune mediated, etc.), the light microscopic changes are generally nonspecific. Conjunctival biopsies are harvested to differentiate conjunctival neoplasms, eosinophilic conjunctivitis, and ligneous conjunctivitis and to assess goblet cells numbers.

Figure 8.78. Acute conjunctivitis in a dog. Note the subepithelial congestion and neutrophil infiltration. (Hematoxylin and eosin stain, original magnification 200X.)

Figure 8.79. Chronic conjunctivitis in a dog. Note the conjunctival epithelial exudates, hyperplastic epithelium, diffuse mononuclear cell infiltrate, and vascular congestion. (Hematoxylin and eosin stain, original magnification 200X.)

Eosinophilic Keratoconjunctivitis in Cats

Eosinophilic keratoconjunctivitis is an idiopathic, chronic ocular condition of cats (Fig. 8.22). This condition has been associated with *Herpes felis* infections.[139–141] The clinical manifestations include conjunctival hyperemia with multifocal white to yellow granular foci. The diagnosis is confirmed with light microscopic examination of biopsies confirming a mixed inflammatory infiltrate with eosinophils predominating and a mix of lymphocytes, plasma cells, and mast cells.

Lipogranulomatous Conjunctivitis

Nodular white cystic masses have been reported on the conjunctival surfaces of cats.[142,143] The light microscopic findings include lipogranulomas with giant cells, macrophages, and a sparse number of neutrophils and lymphocytes. The condition is idiopathic and assumed to be related to tarsal gland rupture.

Miscellaneous Conjunctival Disorders Including Goblet Cell Atrophy, Conjunctival Overgrowth, and Conjunctival Sequestrums

Deficiency of tear film mucin has been reported in both dogs and cats.[144–146] The clinical manifestations include indolent corneal ulcers, nonspecific conjunctivitis, and keratitis. The light microscopic examination of bulbar conjunctival biopsies reveals reduced numbers of goblet cells in all quadrants and a mild, nonspecific lymphocytic plasmacytic conjunctivitis (Fig. 8.80). Periodic acid-Schiff–stained sections facilitate goblet cell assessment, and ratios of goblet cells to basal epithelial cells have been reported by quadrant.[145,146]

Conjunctival overgrowth is an unusual idiopathic condition of rabbits that manifests clinically with a proliferative conjunctival growth that develops circumferentially across the cornea (Fig. 8.81A). Light microscopic findings include a normal-appearing conjunctival epithelium that extends across the cornea (Fig. 8.81B). The epithelium on the leading edges of the overgrowth and the cornea are occasionally noted to be hyperplastic (Fig. 8.81B). A mild lymphocytic plasmacytic cell infiltrate is present and is considered not significant.

Rarely, conjunctival sequestrums in cats are diagnosed. These sequestrums are similar histologically to corneal sequestrum; the section "Corneal Sequestrae" provides a more complete description.

Keratitis

Inflammatory disease of the cornea can be most meaningfully classified as either ulcerative or nonulcerative and superficial or deep (interstitial).

Nonulcerative Keratitis

Acute inflammation is characterized by edema associated with loss of epithelial integrity and neutrophilic infiltrate from the conjunctiva via the tear film or migration from scleral and episcleral vessels. With chronicity, the nature of the infiltrate changes, neovascularization from limbal blood vessels occurs, and scarring and epithelial pigmentation may develop (Figs. 8.82 and 8.83).

Occasionally, corneal epithelium will become displaced by trauma into the corneal or conjunctival stroma and rarely into the eye (Fig. 8.84A). The epithelium will then grow and become trapped. Its continual growth results in an inclusion cyst with keratin debris being continually deposited in the center of the cyst. The diagnosis is made by light microscopic confirmation of an epithelial lined cyst within the cornea (Fig. 8.84B) or the presence of epithelium growing across intraocular surfaces.

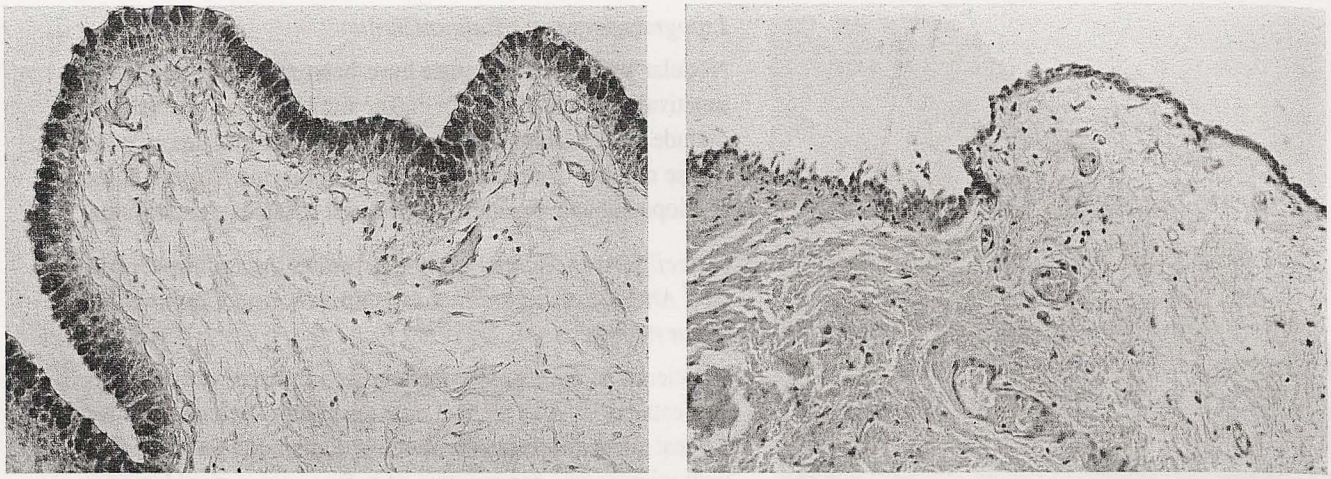

(a) (b)

Figure 8.80. **A.** A conjunctival biopsy from the conjunctival fornix of a normal cat. (Periodic acid-Schiff stain, original magnification 50X.) **B.** A conjunctival biopsy from a cat with goblet cell atrophy. Compare this photo with an age-matched control cat (**A**). (Periodic acid-Schiff stain, original magnification 50X.) (Reprinted with permission, Cullen CL, Njaa BL, Grahn BH. Ulcerative keratitis associated with qualitative tear film abnormalities in cats. *Vet Ophthalmol* 1999;2:197–204.)

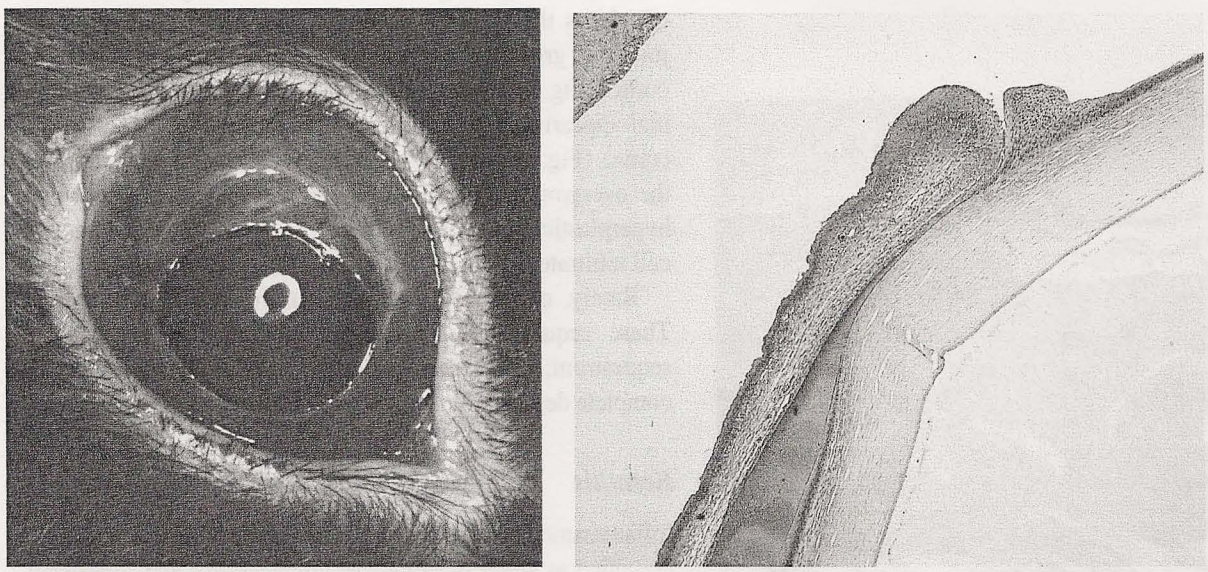

(a) (b)

Figure 8.81. **A.** Conjunctival overgrowth in a rabbit. **B.** Histologic appearance of conjunctival overgrowth in a rabbit. Note the exuberant growth of a leaf of conjunctiva over the cornea, and the hyperplastic corneal epithelium and conjunctival epithelium at the edge. (Hematoxylin and eosin stain, original magnification 100X.)

Ulcerative Keratitis

It is also useful to classify ulcerative keratitis as simple, indolent, and complex. Simple ulcers are focal, and they are seldom examined histologically unless they are incidental to another globe-threatening disorder. The histologic findings include superficial corneal ulceration and an associated edema and sparse neutrophil infiltrate. Indolent corneal ulcers are best categorized as primary (idiopathic) or secondary to a known cause, such as tear film abnormality, conjunctival or eyelid foreign body, or cilia, or they may be inherited (see "Inherited Developmental Disorders") (Fig. 8.56). The histologic features of indolent corneal ulcers are similar despite the varied etiologies and include nonadherent epithelial margins, stromal edema and mild inflammatory cell infiltrate, and a dense, pale staining acellular zone in the superficial stroma under the ulcer (Fig. 8.56). Complex corneal ulcers are deep stromal ulcers that may be infected (Fig. 8.85A). They typically involve collagenolysis and loss of stroma, and infectious agents may be identified with special stains (Fig. 8.85B).

Episcleritis and Scleritis

Inflammation of the sclera and epicslera may be classified by location (anterior or posterior), diffuse or nodular, and granulomatous or nongranulomatous. Episcleritis is clinically and histologically categorized into bilateral nodular disorder of

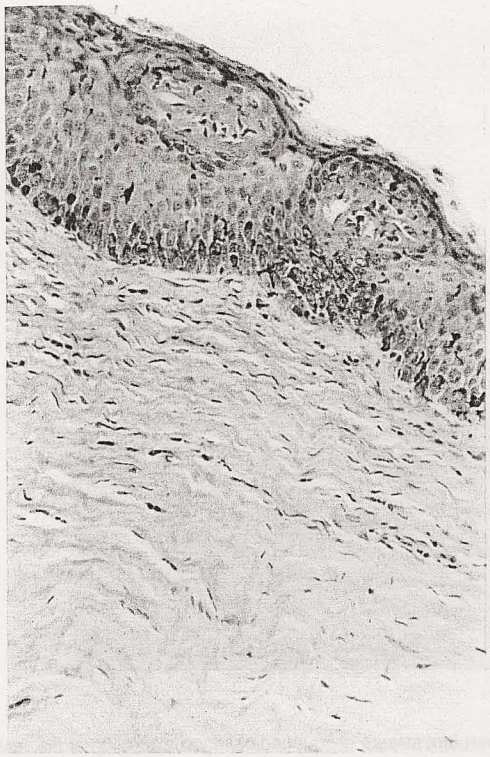

Figure 8.82. Chronic keratitis in any species can induce chronic changes in the cornea to the extent that the cornea begins to resemble skin. The epithelium thickens and pigments. There are multiple squamous eddies, which are foci of dyskeratosis. The underlying stroma is fibrotic. (Hematoxylin and eosin stain, original magnification 100X.)

Figure 8.83. Pigmentary keratitis is common in small brachycephalic dogs. It develops in a medial to temporal progression, and light microscopy will reveal epithelial and subepithelial melanocyte hypertrophy and hyperplasia as well as subepithelial scarring and vascularization. (Hematoxylin and eosin stain, original magnification 400X.)

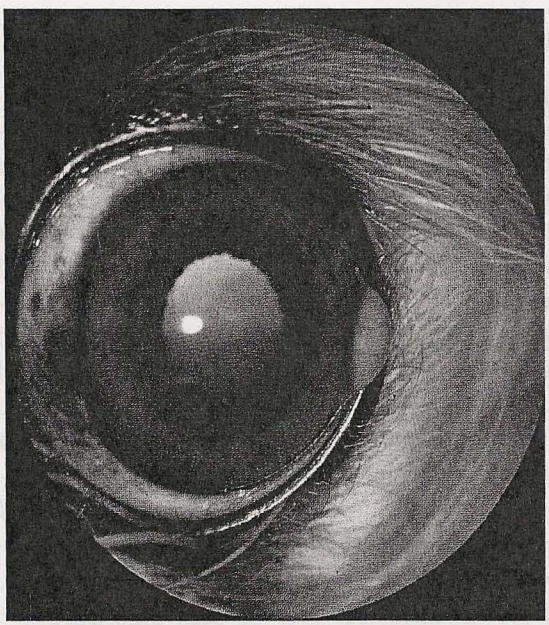

(a)

(b)

Figure 8.84. **A.** A corneal epithelial inclusion cyst in a Miniature Poodle. **B.** Histologic section of the same corneal epithelial inclusion cyst. Epithelial inclusion cysts are an epithelial-lined space that contains epithelial debris. (Hematoxylin and eosin stain, original magnification 100X.)

Collie dogs (see "Inherited Developmental Disorders," Fig. 8.59A and B), a unilateral or bilateral diffuse superficial episcleritis (Fig. 8.86) and scleritis, and necrotic scleritis (Fig. 8.87). Specific morphologic and cellular differences are noted in these conditions.[147,148]

Scleritis typically is characterized by macrophages palisading about degenerating collagen fibrils and may be accompanied by discrete uveal granulomas or extend to involve adjacent uvea in a diffuse inflammatory process. Scleral necrosis (degeneration is a more appropriate term) and

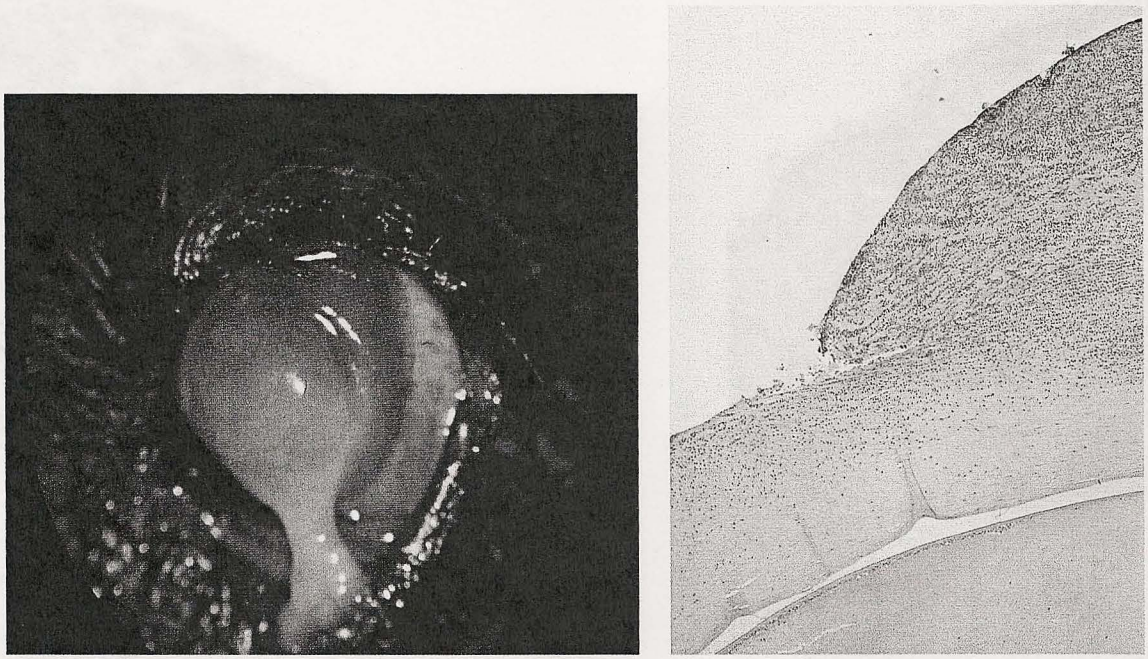

(a) (b)

Figure 8.85. **A.** Collagenolysis of the cornea in a dog. Note the large, deep ulcer with mucopurulent stream of liquefied collagen extending of the ventral edge. **B.** Histological section of a melting corneal ulcer in a dog. Note the lack of corneal epithelium, neutrophil infiltration throughout the corneal stroma, and loss of stroma secondary to collagenolysis. (Hematoxylin and eosin stain, original magnification 250X.)

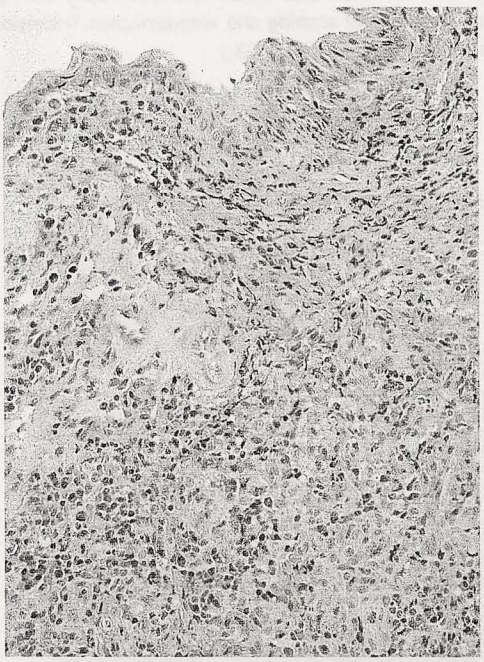

Figure 8.86. Focal episcleritis lesion in an American Cocker Spaniel. Note the mixed inflammatory infiltrate that includes lymphocytes, plasma cells, macrophages, and occasional neutrophils. Plump, proliferating fibroblasts are also present. (Hematoxylin and eosin stain, original magnification 400X.)

malacia with perforation may occur and when present confirms the diagnosis necrotic scleritis (Fig. 8.87B). The majority of cases are immune-mediated processes localized to the eye—that is, not associated with systemic collagen-vascular disease. The diversity of clinical presentations, frequent unilaterality, and variable response to treatment are difficult to explain in light of current understanding of etiopathogenesis; perhaps we are dealing with a spectrum of specific diseases that share similar clinical and histopathologic features.

Acquired Inflammatory Uveal Disorders

Lymphoplasmacytic uveitis is a common, nonspecific histologic diagnosis in animals, and establishing an etiologic diagnosis can be difficult. The classic histologic features include diffuse or nodular infiltrates of lymphocytes and plasma cells in the anterior uvea (Fig. 8.88) and occasionally the posterior uvea (choroid). Less commonly, granulomatous uveitis will be diagnosed (Fig. 8.89). Several accompanying ocular disorders may be present, including glaucoma, ulcerative and nonulcerative keratitis, hyalitis, vitreous degeneration, and cataracts. Equine recurrent uveitis and feline lymphocytic uveitis are common idiopathic conditions. Equine recurrent uveitis (periodic ophthalmia) in its acute form manifests histologically as a predominantly lymphocytic anterior uveal and peripapillary choroidal infiltrate with exudation into the aqueous and vitreous (Fig. 8.90). With chronicity and recurrence, crystallin protein inclusions may be seen ultrastructurally within the ciliary epithelium, and the basal layer of the inverted nonpigmented ciliary epithelial cells are enveloped by amyloid. An accompanying mononuclear perivascular infiltrate will be evident in uvea, retina, and optic nerve.[149,150]

In feline lymphoplasmacytic uveitis, two variants, one with and the other without anterior uveal lymphoid nodules, exist (Figs. 8.20 and 8.88).[151,152] These nodules are largely lymphocytic without follicular differentiation. Many cases will demonstrate a granulomatous component with mutton-fat keratic precipitates that, with chronicity, can lead to endothelial

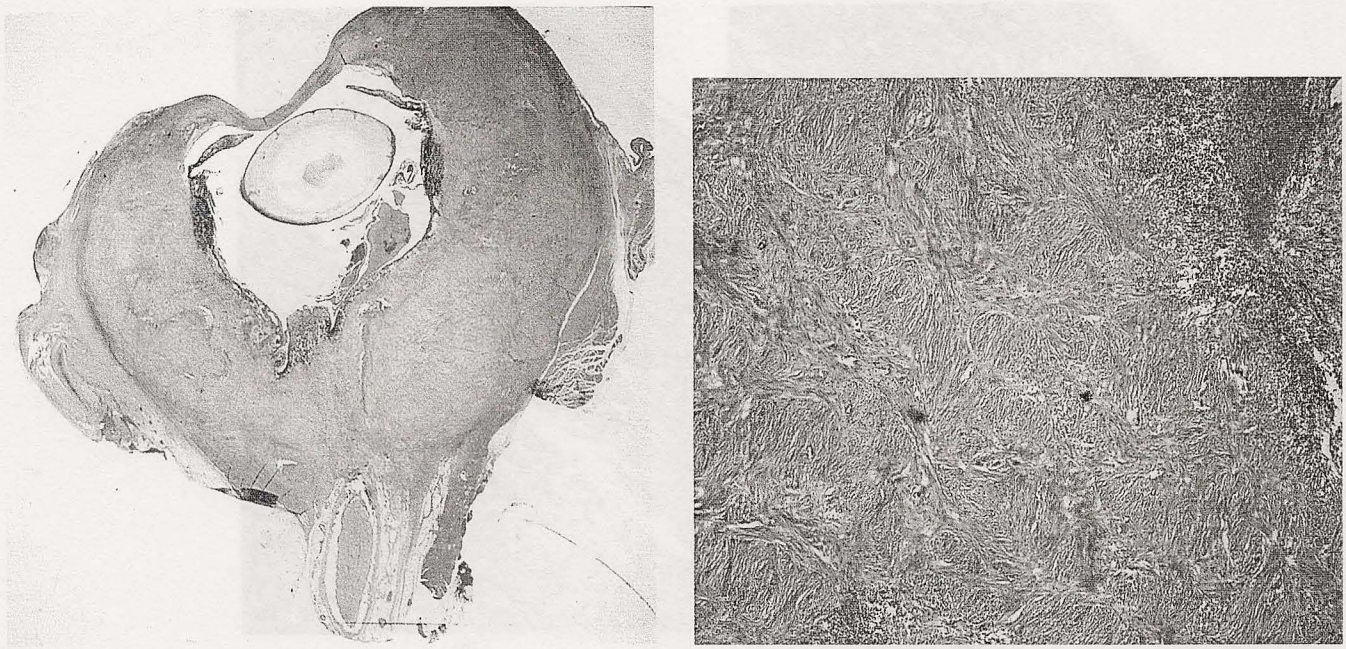

(a) (b)

Figure 8.87. A. Subgross section of a dog's globe with necrotizing scleritis. Note the extensively thickened sclera and eosin-stained patches characteristic of collagen degeneration. (Hematoxylin and eosin stain, original magnification 2X.) (Slide courtesy of Brian Wilcock.) **B.** Collagen degeneration that is characteristic of necrotic scleritis. Note the eosinophilic staining of the collagen fibers of the sclera and the lack of scleracyte nuclei and the bands of dark blue inflammatory cells near the edges. Examination at higher magnification revealed lymphocytes, plasma cells, macrophages, and occasional neutrophils. (Hematoxylin and eosin stain, original magnification 100X.)

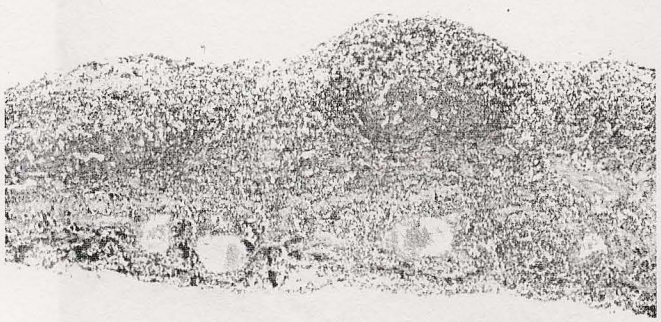

Figure 8.88. Lymphocytic plasmatic uveitis in a cat diagnosed with secondary glaucoma and idiopathic uveitis. (Hematoxylin and eosin stain, original magnification 250X.)

damage and bullous keratopathy; however, epithelioid cells are rarely a prominent feature of the uveal infiltrate. Lymphoid aggregates may obstruct the ciliary cleft and trabecular meshwork, and secondary glaucoma is common. Inflammatory cells and proteinaceous globules may localize retrolentally and within the peripheral anterior vitreous in a "snowbanking" effect; clinicians have erroneously described this condition as pars planitis or intermediate uveitis when in fact the pars plana is not involved in the inflammatory process; rather, the vitreous cells migrate from the retina where mononuclear perivascular infiltrates are common. The condition may be unilateral or bilateral and has been associated with FIV, FHV-1, FeLV, toxoplasmosis, and bartonellosis, but many cases remain idiopathic and are presumed immune mediated in spite of exhaustive diagnostics.

Bovine malignant catarrhal fever is characterized by the accumulation of lymphocytes and lymphoblasts within the subendothelial and adventitial regions of blood vessels with arterial, arteriolar, and venular necrosis and hemorrhage (Fig. 8.91). The lymphoid cells may have frequent mitoses. Conjunctiva, uvea, retina, and optic nerve meninges may be involved. The reaction has been classified as a type IV hypersensitivity reaction.

Uveodermatologic syndrome is an immune-mediated condition of young dogs whose ophthalmic manifestations of severe and relentless granulomatous panuveitis may or may not be associated with whitening of the hair coat (poliosis), dermal depigmentation (vitiligo), and/or mucus membrane ulceration.[153,154] Akitas, Siberian Huskies, and Samoyeds are predisposed. Dispersion and phagocytosis of melanin is a histologic feature of both dermal and ocular lesions, and if skin lesions are present, they can be biopsied to confirm the ocular diagnosis. Extensive granulomatous panuveitis and exudative retinal detachment are frequent presenting features, and glaucoma is a common blinding sequelae (Fig. 8.92).

Lens-Induced Uveitis

Phacolytic Uveitis Phacolytic uveitis manifests in two variants: a mild lymphoplasmacytic uveitis responsive to topical corticosteroids and a severe granulomatous anterior uveitis that is generally nonresponsive to even the most aggressive antiinflammatory therapy and requires lens removal to salvage the eye (Fig. 8.93).[155,156] The pathogenesis

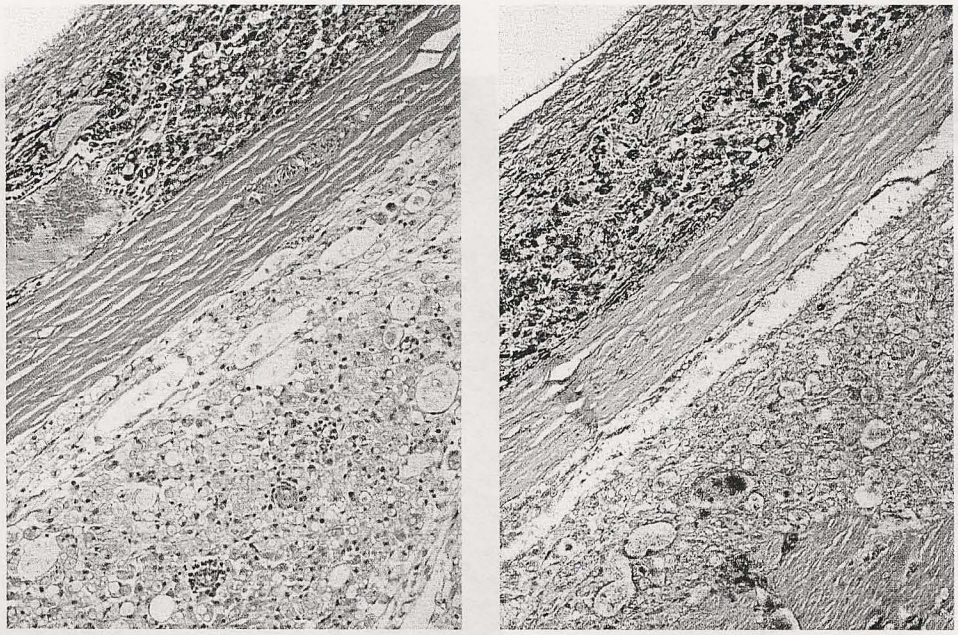

(a) (b)

Figure 8.89. A. Granulomatous panophthalmitis in cat. Note the predominance of large foamy macrophages in the episcleral tissues and within the choroid and scattered lymphocytes and plasma cells around episcleral and scleral vessels and within the choroid. (Hematoxylin and eosin stain original magnification 300X.) **B.** Confirmation of acid fast bacilli (ocular tuberculosis) in the same eye. Note the filamentous pink bacilli within the macrophages. (Fite's stain, original magnification 300X.)

Figure 8.90. Histologic section of acute equine recurrent uveitis. Note the infiltrate of neutrophils and lymphocytes into the ciliary process and vitreous and fibrin accumulation. (Periodic acid-Schiff stain, original magnification 300X.)

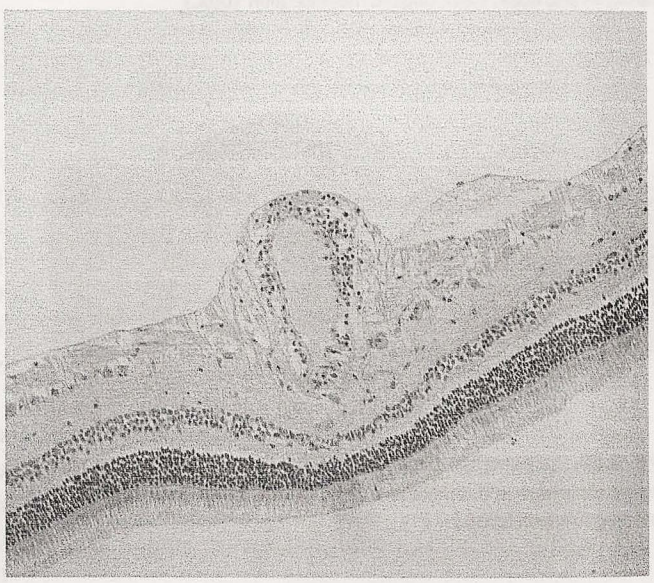

Figure 8.91. Vasculitis in the retina of a cow with malignant catarrhal fever. (Hematoxylin and eosin stain, original magnification 250X.)

of both is likely similar; liquefied cataractous lens proteins leak through an intact capsule to initiate the inflammatory response. The light microscopic findings of the mild form include minimal anterior uvea lymphocytic plasmacytic infiltrate and a cataract. The granulomatous version also includes a cataractous lens; however, the uveitis is more severe and keratitic precipitates and plasmoid aqueous, and mixed inflammatory uveal infiltrates include macrophages, lymphocytes, and neutrophils. The reason for the difference is unknown; the granulomatous variant occurs most commonly in diabetic cataracts with a predisposition for Miniature Schnauzers.

Phacoclastic Uveitis Phacoclastic uveitis is the granulomatous lens-induced uveitis that follows rupture of the lens capsule with resultant exposure of large amounts of lens protein (Figs. 8.94 and 8.95).[156] The capsular rupture can occur following blunt or penetrating (including surgical) trauma or spontaneously with an intumescent cataract (usually diabetic), or it can be associated with infectious agents (*Encepalitizoon caniculi* in rabbits). The nature of the response is dependent

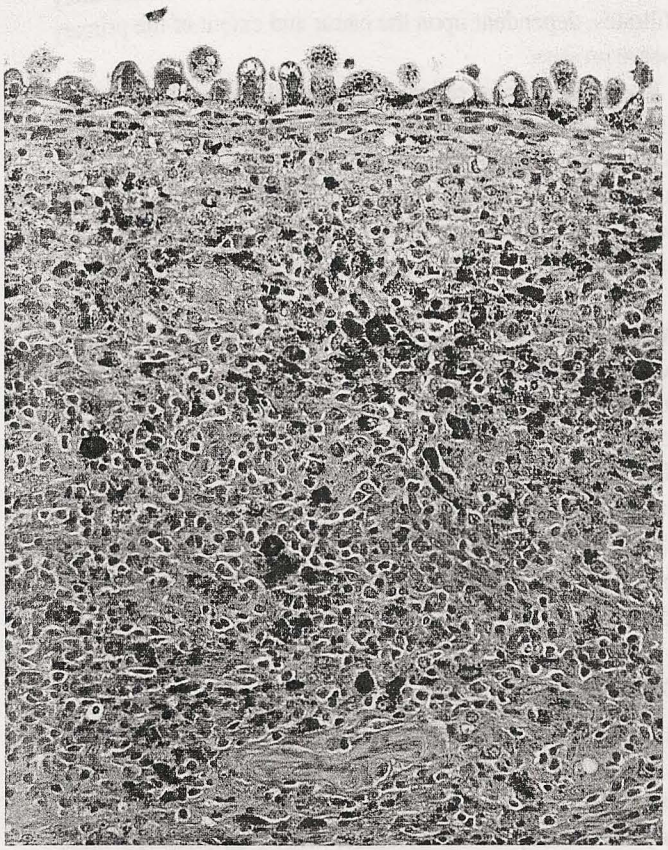

Figure 8.92. Vogt Koyanagic Harada–like syndrome in a dog. Note the extensive choroiditis with lymphocytes plasma cells and macrophage that are targeting the choroidal melanocytes. The retina was detached, and the RPE is hypertrophied. (Hematoxylin and eosin, original magnification 400X.)

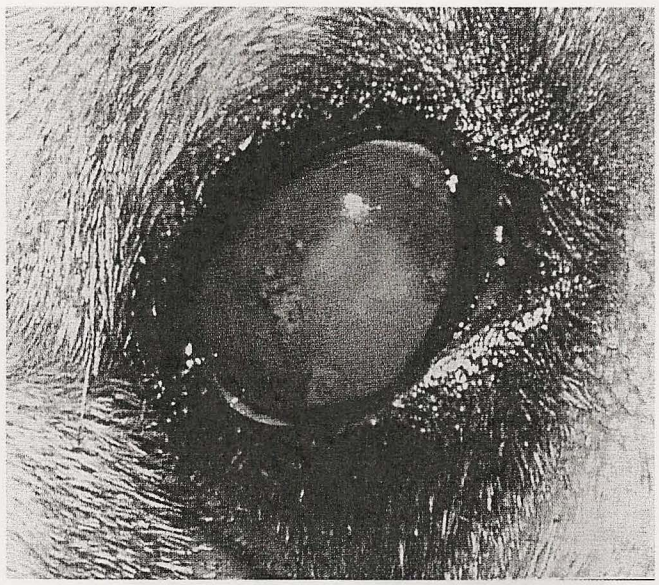

Figure 8.93. The clinical manifestations of phacolytic uveitis in a dog are varied from mild uveitis with episcleral congestion to fulminant uveitis. Note the keratitic precipitates and hypopyon in this dog with fulminant phacolytic uveitis.

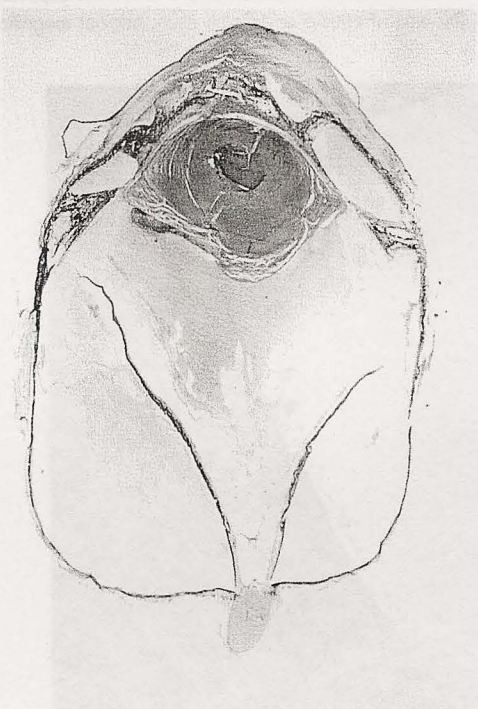

Figure 8.94. Phacoclastic uveitis in a dog. Note the discontinuous lens capsule, keratitis, posterior and anterior synechiae, retinal detachment, and plasmoid aqueous and vitreous. These gross findings are usually synonymous with penetrating ocular trauma. (Hematoxylin and eosin stain, original magnification 2X.) (Slide courtesy of Brian Wilcock.)

upon species, the age of the animal, the amount and nature of the lens protein exposed, the presence of concurrent microbial endophthalmitis, and duration. The resulting lesion represents a combination of the effects of the initial insult, the immunologic response to the released lens protein, a reparative fibrometaplastic proliferation of the lens epithelium, membranogenesis of proximal tissues, sepsis, and not infrequently secondary glaucoma (Figs. 8.94 and 8.95). The inflammatory response is zonal, being most severe at the site of capsular rupture; the edges of the ruptured capsule may be fimbriated, retracted, and/or coiled. Response in the dog eye is intense with a prominent neutrophilic component acutely; the inflammation can extend throughout the eye. The response of the rabbit eye to capsular rupture is localized, measured, and largely granulomatous, with the cat eye somewhere between. Spontaneous and small traumatic lens capsule ruptures in young animals of any species can occur without any inflammatory response at all.

Acquired Retinal Disorders

Retinal Detachment The lateral junctions of the RPE (along with the tight endothelial junctions of the retinal vascular endothelium) form the posterior blood–aqueous barrier; when compromised by inflammation or ischemia, the choroidal blood vessels will leak serous to protein-rich fluid, which will collect in the potential space between retina and RPE with resultant neurosensory retinal detachment (Figs. 8.2, 8.12, 8.31, and 8.96). Separated from the nutrition of the choriocapillaris, the outer segments initially, with the photoreceptors themselves following, will atrophy. Exudative retinal detachment, then, is a nonspecific response to a variety

Figure 8.95. An equatorial lens capsule rupture in a dog. Note the discontinuous and coiled lens capsule, fibrous tissue that spans the capsular tear and envelopes the lens. (Periodic acid-Schiff stain, original magnification 250X.)

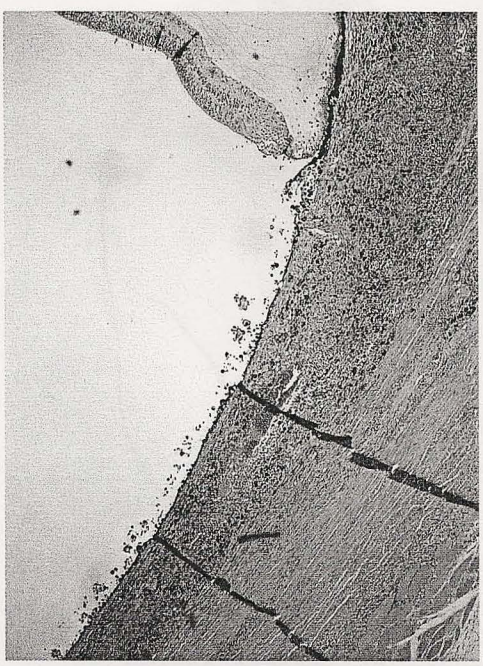

Figure 8.96. Exudative retinal detachment in a dog with Vogt Koyanagi Harada-like syndrome. Note the diffuse inflammatory infiltrate in the choroid and pars plana and the detached retina and retinal pigment epithelial hypertrophy. (Hematoxylin and eosin stain, original magnification 100X.)

of (a) infectious or noninfectious inflammatory diseases of the posterior sclera and choroid or (b) ischemia of the RPE, as encountered in systemic hypertension or choroidal neoplasia with choriocapillaris obliteration. The neurosensory retina remains attached at the ora ciliaris retinae and the optic disc, with the fluid in the subretinal space varying from serous to protein-rich to hemorrhagic, with or without inflammatory infiltrates, dependent upon the cause and extent of the primary disease process.

Rhegmatogenous retinal detachments develop secondary to holes or tears. Retinal tears develop secondary to trauma or involve vitreous traction bands (Figs. 8.5, 8.10, and 8.32). These detachments are often focal initially and then extend under the retina and eventually spread. The histologic lesion of retinal degeneration is similar to exudative detachments.

Sudden Acquired Retinal Degeneration Syndrome (SARDS)

SARDS is a unique retinal disorder in dogs, characterized clinically by its acute-onset, permanent blindness and its occurrence in middle-aged often overweight dogs.[157–159] The light microscopic findings in SARDS is a generalized photoreceptor apoptosis, with minimal inflammation except a few macrophages that engulf the photoreceptor debris. The etiology and pathogenesis remain unknown. There is evidence that ongoing photoreceptor apoptosis occurs after blindness.[158]

Ocular Degenerative Diseases

Let it clearly be stated from the outset that the topics covered in this section were selected somewhat arbitrarily, with nebulous overlap with the earlier section on congenital and inherited developmental diseases, which emphasized those disorders present at birth, and developmental conditions with an inherited basis. Degeneration is strictly defined as a deterioration of, relative to a tissue, a change to less actively functional form, without reference to cause. In some circles, the definition has been extended as a contrast to a dystrophic process, which generally has a genetic basis and occurs as a primary condition, usually early in life, while a degeneration occurs as a secondary manifestation of some primary disease. In this text, we define it broadly to include those diseases associated with a nutritional basis, toxic conditions, aging changes, changes that occur associated with systemic disease; and those diseases of unknown etiology that may be suspected to have a genetic basis but lack adequate scientific evidence and remain somewhat equivocal in regard to cause. Degenerative conditions are common and include orbital atrophy, corneal degeneration, cataract, secondary glaucoma, and vitreous degeneration.

Degenerative Orbit Disorders

Enophthalmos secondary to atrophy of periorbital muscles/adipose tissue is a common sequel to chronic extraocular myositis and orbital cellulitis. Light microscopic examination reveals extraocular muscle fibrosis and adnexal atrophy and lymphocytic orbital cellulitis.

Degenerative Lacrimal Gland Disorders

Lacrimal gland degeneration develops most commonly secondary to immune-mediated or inflammatory adenitis and

also toxins (Fig. 8.97). During the acute stages, lymphocytic infiltration of the gland is noted most commonly. When septic orbital cellulitis has involved the gland, neutrophils will predominate (Fig. 8.97B). When the lesions are chronic, the glands will be atrophied and minimal inflammation is present. This loss of glandular tissue induces keratoconjunctivitis sicca.[40–42]

Degenerative Corneal Disorders

Several corneal degenerations are noted clinically and include pigmentary keratitis, corneal calcific degeneration (Fig. 8.98A), and corneal lipid degeneration (Fig. 8.98B) in dogs, horses, and cats. All corneal degenerations are the product of chronic keratitis, and often the primary etiology is not evident.

Corneal Sequestrae

Corneal sequestrae are most commonly diagnosed in cats and occasionally in horses. In the cat, these are impressive black to brown corneal or occasionally conjunctival lesions, which are idiopathic. The histologic features are bland but pathognomonic and include a loss of keratocytes and an amber–pink color on hematoxylin- and eosin-stained sections (Fig. 8.99). Periodic acid-Schiff stains will identify granules in the degenerate keratocyte and suggest an autolytic process. The source of the brown color is debated and is most likely some stain and

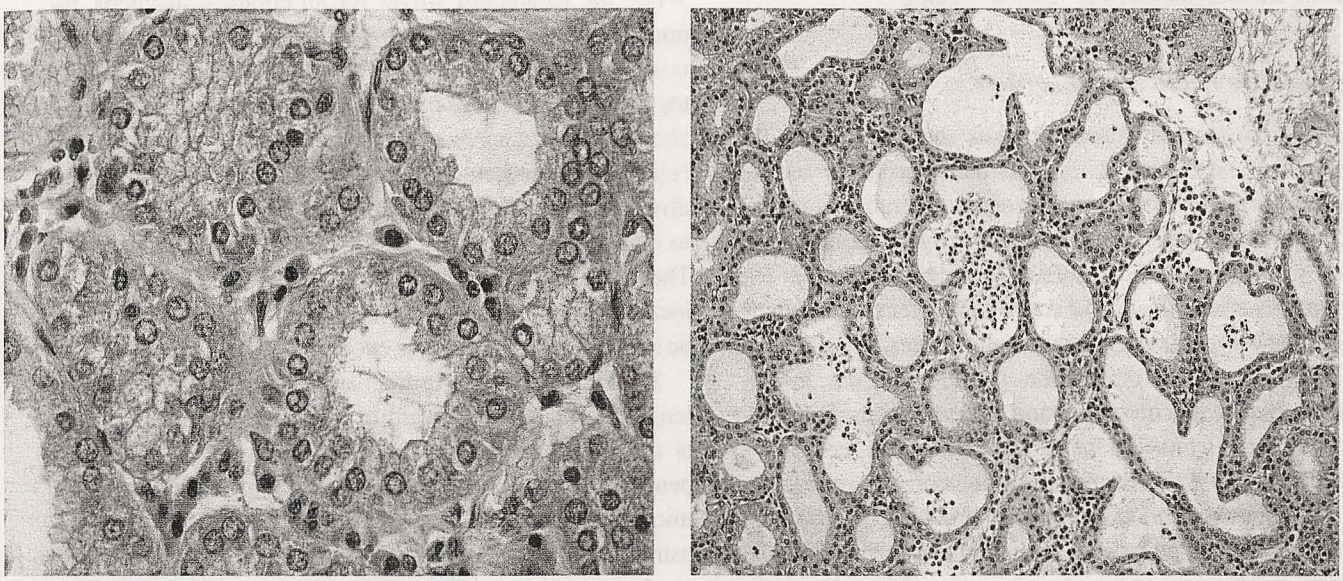

(a) (b)

Figure 8.97. **A.** Normal canine lacrimal gland. Note the acinar structure and periacinar accumulation of lymphocytes and plasma cells. (Hematoxylin and eosin stain, original magnification 400X.) **B.** Lacrimal gland adenitis with neutrophil infiltration. (Hematoxylin and eosin stain original magnification 300X.)

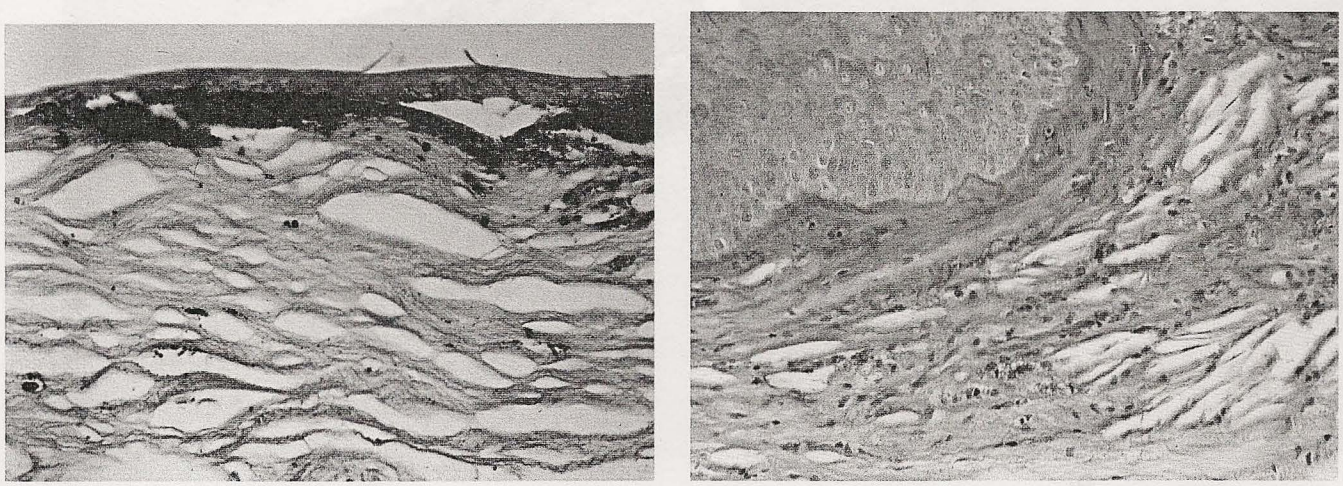

(a) (b)

Figure 8.98. **A.** Calcific corneal degeneration in a dog. Calcium is present and demonstrated as a granular subepithelial deposit. (Von Kossa stain, original magnification 250X.) **B.** Lipid corneal degeneration in a dog. Note stromal clefts where lipid was present before processing, the diffuse infiltration of lymphocytes and plasma cells, and epithelial hypertrophy and undulating epithelial basement membrane. (Periodic acid-Schiff stain, original magnification 250 X.)

porphyrins.[160–161] Although melanin has recently been suggested,[162] there is minimal evidence at an ultrastructural level of melanosomes or their dispersed contents in sufficient quantity to account for the entire lesion. The etiology and the pathogenesis of these lesions remain unknown. When the lesions are chronic, light microscopy reveals vascularization and mild inflammatory infiltrates under the sequestrum (Fig. 8.99B).

Uveal Atrophy

Uveal atrophy is nonspecific and occurs secondary to chronic glaucoma, uveitis, and old age. The iris, ciliary body, and choroid are decreased in thickness secondary to a loss of pigment, smooth muscle, and vascular tissues.

Degenerative Lenticular Disorders

A basic discussion of cataractogenesis should reference the biochemical and metabolic changes that precede or accompany the morphologic changes that occur. Alterations in nutrition, metabolism, and osmotic balance can lead to alterations in cell membranes and/or proteins that define cataract. The lens consists predominantly of water and protein, with minute amounts of inorganic ions, organic phosphates, nucleic acid, and lipid. The proteins include the soluble crystallins, insoluble albuminoids, mucoproteins, and nucleoproteins. Differentiation of lens epithelial cells into lens fiber cells is a continuing process that occurs at the equator; this process, as well as transcapsular transport, is provided by Na^+,K^+-ATPase–dependent pump located within the lens epithelium. Oxygen needs are minimal, and anaerobic glycolysis, which converts glucose to lactic acid, provides most of the energy required. Glucose enters the lens by both diffusion and facilitated transport; transport mechanisms play a role in cation and amino acid influx as well. Alterations in substrate or enzymatic activity can alter the homeostatic equilibrium of the lens with increased hydration and associated protein alterations. Cataractogenesis is also associated with increases in lens glutathione, insoluble proteins, and hydrolytic enzymes. There is increasing evidence that oxidative damage is a common final pathway for a variety of cataracts.

The time frame of cataract development is large and includes congenital, developmental, and age-related factors. Other features facilitating classification include location, stage of development (incipient/immature/mature/hypermature), location within the lens, morphologic alterations, and etiology. While the pathologist strives for an etiologic diagnosis, the nonspecificity of cataract morphology frequently limits diagnosis to morphologic description. Histopathologically, cataractogenesis is manifested by a limited number of morphological alterations in the lens capsule, epithelial cells, and/or lens fiber cells, which represent the common end stage of a spectrum of diverse insults, be they genetic, traumatic, toxic, or secondary to ocular or systemic disease (Figs. 8.50, 8.100, and 8.101). The histopathologist can readily classify these changes by location and morphology but in the absence of other clues may be hard pressed to determine etiology.

Distinction between artifact and real change may be challenging, especially in regard to cortical alterations. The lens is dense and sequestered within the globe; thus, fixatives penetrate poorly, and shattering and fragmentation under the microtome blade occurs frequently. Both fixative and osmotic factors may distort size and shape and contribute to the appearance of vacuoles that resemble pathologic alterations.

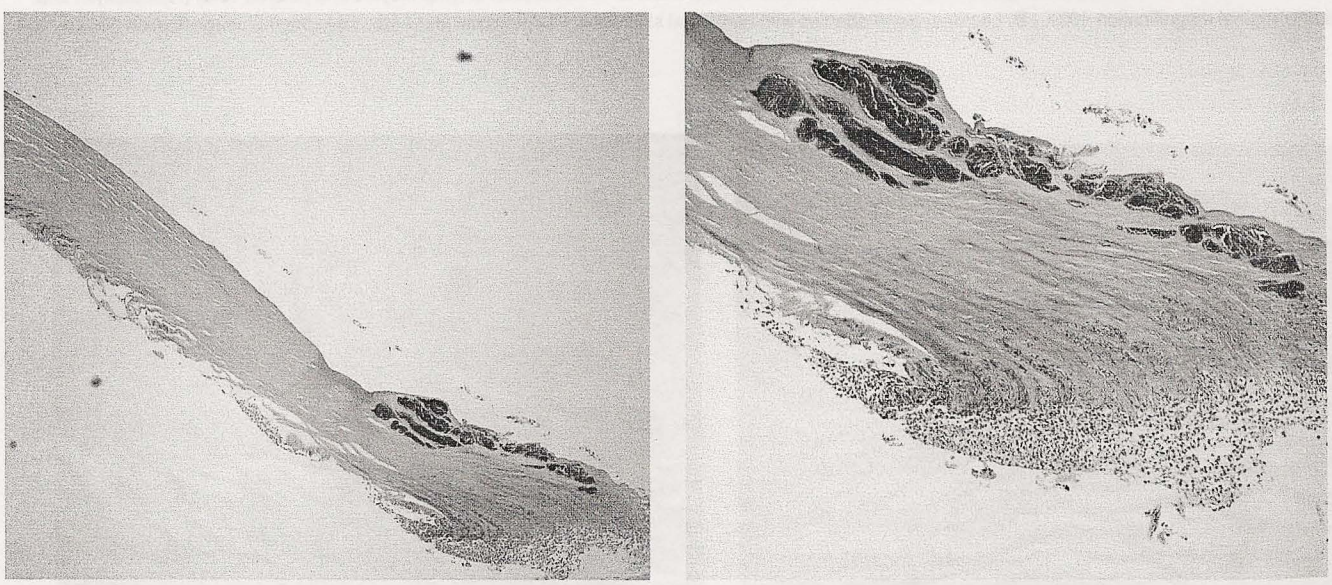

(a) (b)

Figure 8.99. A. A feline corneal sequestrum that was removed many months after it was diagnosed. Note the characteristic amber color and acellularity of most of the sequestrum. (Hematoxylin and eosin stain, original magnification 50X.) **B.** The edge of the same sequestrum. There are many degenerating neutrophils invading the edge and several large colonies of bacteria present near the surface of this sequestrum. (Hematoxylin and eosin stain, original magnification 200X.)

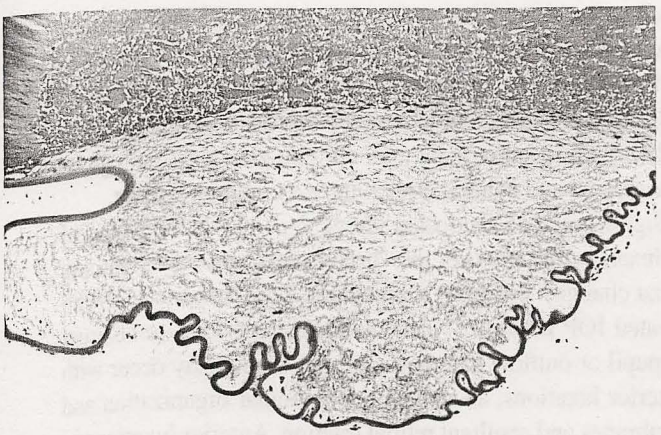

Figure 8.100. Fibrous metaplasia of lens epithelium that have migrated under the posterior lens capsule of a dog. (Periodic acid-Schiff stain, original magnification 100X.)

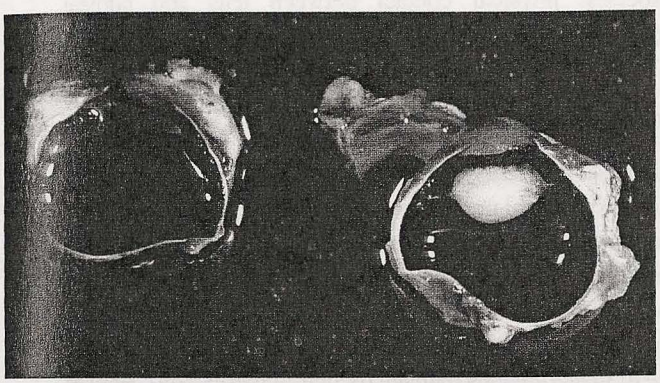

Figure 8.101. A mature cataract is present in this sectioned dog's eye.

The capsular changes of delamination seen with heat and/or infrared exposure and pseudoexfoliation have not been described in animal eyes; however, anterior capsular thickness may increase in response to excess basement membrane production by stressed lens epithelial cells. Capsular opacification associated with persistence of the fetal vasculature and spontaneous congenital capsular rupture were discussed in the section "Congenital Disorders," and the features of traumatic or spontaneous acquired capsular rupture in the section "Phacoclastic Uveitis."

Lesions affecting the lens epithelium may involve the anterior or equatorial epithelial cells. These cells may demonstrate degeneration, fibrous metaplasia, posterior migration, hypertrophy, and/or hyperplasia in response to disease (Figs. 8.50, 8.100, and 8.101). Excess or ectopic basement membrane may be produced. Epithelial cells may transform from cuboidal to flattened fusiform cells, frequently forming a multilayered plaque; while fibrous in appearance by light microscopy, ultrastructurally these cells maintain intercellular macula adherens and are surrounded by basement membrane, maintaining characteristics of epithelial cells. When epithelial cells migrate posteriorly, they follow the posterior capsule where they may undergo metaplasia or migrate into the posterior cortex where they hypertrophy, perhaps as an abortive attempt at repair, with production of lens proteins. These cells maintain their nuclei and are known as bladder cells (Fig. 8.50).

Cortical cataracts can be described by virtue of their location. By morphology, they are characterized by changes in cell membranes, lens proteins, or both. Intercellular fluid accumulation will manifest as clefts and fissures between cells. Intercytoplasmic swelling imparts enlarged profiles and a granular cytoplasm; as lens proteins denature, they become more eosinophilic and homogeneous. Fiber cell membranolysis will result in extracellular pools or distinct spherules of altered protein; the latter are referred to as Morgagni globules. Increased fluid intake leads to swelling of the lens with stretching of the capsule (spontaneous rupture, usually of the posterior capsule, may occur). As the osmotic pressure with the aqueous humor equalizes across the lens capsule due to altered metabolism and loss of transcapsular transport mechanisms, soluble proteins migrate from the lens, with resultant shrinkage and capsular wrinkling. Cholesterol deposits or dystrophic calcification may occur.

Interpretation of changes in the lens nucleus are somewhat problematic for the pathologist. As mentioned, the etiologies and pathomechanisms of cataract formation are diverse. The role of altered carbohydrate metabolism, in particular glucose and galactose, have been studied extensively. In diabetes mellitus, excessive levels of glucose enter the lens, the rate-limiting enzymes of the Emben-Meyerhoff pathway are saturated, and the sorbitol pathway and aldose reductase are activated, with the sugar being metabolized to polyalcohols with resultant osmotic imbalance and water influx.[163] Elevation of galactose levels related to excessive dietary intake or genetic enzymatic defects follows a similar pattern[164,165]; neonatal marsupials supplemented with cow's milk, which is high in galactose that these animals are unable to properly metabolize, will develop cataractogenesis. The pivotal role that glucose plays in lens metabolism is further demonstrated in that low glucose levels can also lead to cataract formation.

Hypocalcemia can cause cataracts in dogs and cats, and numerous toxins, chemicals, and pharmaceutical agents have been shown to cause both experimental and spontaneous disease. Glucocorticoids administered both topically and systemically in humans can result in posterior subcapsular cataracts that continue to progress after treatment is discontinued. Heavy metals, including lead and silver, can induce cataracts. A cholinesterase inhibitor used to control sea lice in Atlantic salmon has been implicated in cataractogenesis. Dinitrophenol in dogs and hygromycin B in swine have also been shown to be cataractogenic.[166–170]

Radiant energy can cause cataractogenesis; light energy may be cataractogenic in fish. The lens is quite sensitive to radiation, which results in increases in membrane permeability and alters protein synthesis and metabolism. Younger animals are more susceptible; birds are remarkably resistant. A period of latency follows exposure with vacuoles forming at the posterior pole and progressing to cortical involvement.[171–174]

Nutritional factors other than carbohydrates may be cataractogenic, including amino acid deficiencies of tryptophan, phenylalanine, valine, and histidine; arginine deficiency causes cataracts in wolf pups.[175–180]

Other intraocular diseases such as uveitis, glaucoma, and retinal degeneration cause cataracts by altering the ocular milieu and thus lens nutrition. Turkeys and chickens with avian encephalomyelitis and Marek's disease develop cataracts. In fish, phacotropism is demonstrated by trematode (diplostomun) larvae with associated cataract, and encephalitizoon has been associated with cataract and lens capsule rupture in rabbits.[181,182]

In many cases, including cataracts in pinnepeds, etiologies remain undefined; various dietary, environmental, genetic, and traumatic factors have been postulated. Likewise, the cellular and subcellular mechanisms of inherited cataracts in domestic animals is largely unknown.

Acquired Lens Luxations

The lens is anchored by the zonular fibers, which blend with the anterior and posterior lens capsule and extend to the ciliary body. Disruption usually occurs at the site of capsular insertion, with resultant subluxation or luxation (Fig. 8.102). Congenital abnormalities in zonular insertion and/or physical properties in connective tissue disorders predisposes to dislocation, and bilateral lens luxation has been described in a dog with Ehler-Danlos syndrome. There are heritable conditions in certain breeds of dogs (notably terriers) in which the zonules appear normal initially but are of reduced tensile strength and rupture easily after a certain age. The inherited lens luxations are discussed in the "Inherited Developmental Disorders" section. Chronic inflammation will also result in zonulysis and lens luxation in cats and dogs. Physical trauma to the globe of sufficient magnitude can dislodge the lens and, as described in subsequent text, chronic glaucoma with globe enlargement and zonular stretching is a common finding.

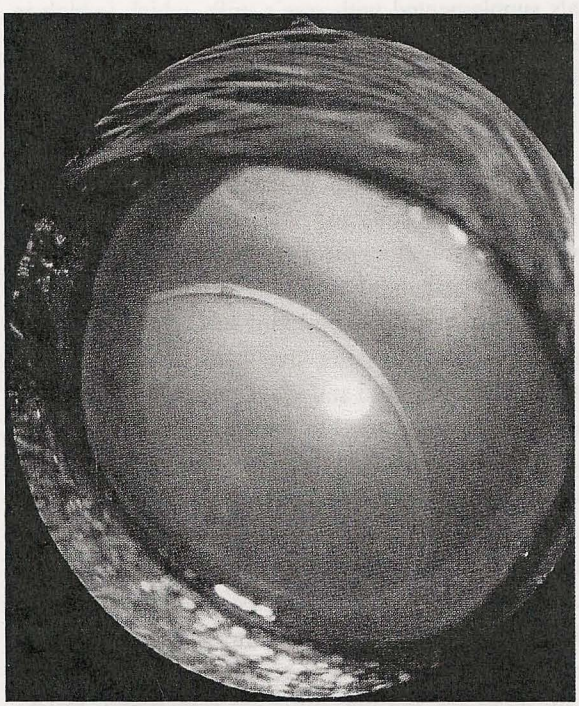

Figure 8.102. A clinical photograph of an inherited posterior lens luxation in a Jack Russell terrier. Note the prominent aphakic crescent and the edge of the ventral and posterior luxated lens.

Significance of dislocated lenses depends on the nature of the luxation, the status of the vitreous, and associated lens and ocular changes. Posterior subluxations may be associated with elevated IOP if formed vitreous moves anteriorly to obstruct the pupil or outflow pathways; similar events may occur with posterior luxations, as well as perilenticular organization and membranes and resultant retinal traction. Anterior luxations in the dog are accompanied by glaucoma as the lens and/or adherent vitreous obstruct the pupil and outflow pathway; this is less frequently the case in cats because of their deep anterior chamber and, as luxations in this species usually accompany chronic uveitis, the associated vitreous syneresis. Regardless of species, physical contact between lens and corneal endothelium may compromise the latter.

Acquired Glaucoma

Glaucoma is a generic term used to describe a variety of pathophysiological processes in which the IOP reaches a level sufficient to cause damage to the eye. In humans, glaucoma can occur in individuals whose IOP falls in or close to normal range (normotensive glaucoma); alternatively, a population is recognized with IOP above normal values but without evidence of glaucomatous damage (ocular hypertension). Neither of these conditions has been unequivocally demonstrated to occur in eyes of other animal species. Pathologic elevation of the IOP is the consequence of obstruction or misdirection of aqueous flow or outflow anywhere along its course from the posterior chamber through the pupil, into the ciliary cleft (CC), across the trabecular meshwork (TM), and into the peripheral vasculature of the scleral venous plexus.

In terms of classification, glaucoma should foremost be classified as being primary or secondary. The former is a genetic and bilateral (although not always concurrently so) condition that occurs in the absence of antecedent ocular disease associated with the elevation of IOP. The latter, in contrast, occurs as a direct result of antecedent or concurrent ocular disease that results in impaired aqueous circulation or outflow. Either primary or secondary glaucoma that manifests at birth should be labeled congenital (see "Pathology of Congenital Disorders" in this chapter). Although seemingly simplistic, this scheme is somewhat ambiguous; for example, the primary glaucoma most commonly encountered in the dog is associated with congenital goniodysgenesis, although it manifests later in life see Inherited Development Disorders in this Chapter.

Because of the unique morphology of the subprimate outflow pathway, a morphologic classification of glaucoma in animals should consider those changes that occur within the ciliary cleft distinct and separate from those that occur at the ICA. With an open ICA, normal anatomic relationships exist

between iris root, pectinate ligament, and the inner surface of the peripheral cornea. An ICA can be open but dysplastic, with abnormalities of the pectinate ligament (to be elaborated upon shortly). An ICA can be open but obstructed, for instance by the proliferation of a fibrovascular membrane from the iris root across the surface of the pectinate ligament. The ICA is closed when the anterior surface of the iris root is displaced anteriorly to come in contact with the anterior surface of the pectinate ligament and/or peripheral cornea. The ciliary cleft may be open, narrowed, or collapsed. It is quite possible to have an open ICA with a collapsed ciliary cleft; in fact, this is the most common manifestation associated with both primary glaucoma and glaucoma associated with lens luxation in the dog. As the cleft collapses, access of the aqueous fluid to the ciliary cleft and trabecular meshwork is impaired, outflow decreases, with subsequent elevation of IOP. Because of the anatomic relationships, angle closure is always associated with narrowing and collapse of the ciliary cleft. Collapse of the ciliary cleft may be one of the key events that leads to acute elevation of IOP in the majority of animal glaucomas; unfortunately, the mechanism(s) that maintain and control ciliary cleft width have yet to be defined. While determining shallowing of the anterior chamber related to anterior displacement of the iris leaflet can be problematic for the pathologist, both the status of the ICA and the width of the cleft can be assessed with reasonable accuracy in histopathologic sections.

Gonioscopic appearance can readily be correlated with the above morphologic classification scheme; if the ICA is open, but the cleft is collapsed, the iris root will be in direct apposition with the outer pigment band; the pectinate ligament and cleft will not be observable. With angle closure, the iris root is displaced anteriorly to obscure visualization of the outer pigmented band.

Species Characteristics of Acquired Glaucoma

Canine Acquired Glaucoma In the dog, secondary glaucomas occur two to three times as frequently as primary glaucoma (see "Inherited Developmental Disorders"). Congenital glaucoma occurs rarely, and when it does it is usually associated with anterior segment dysgenesis; the histopathology has been detailed in the Doberman Pinscher in which it occurs as an inherited disease. The condition occurs sporadically in any breed, with a spectrum of changes including uveal hypoplasia and microphakia (see "Pathology of Congenital Disorders").

A recessively inherited primary open-angle glaucoma has been developed as a model for human glaucoma in the Beagle dog; there is no evidence of goniodysgenesis at the time of insidious elevation of IOP, which first appears at about a year of age, and the ICA and ciliary cleft are open (see "Inherited Developmental Disorders").

The most common primary glaucoma seen in dogs is an inherited condition associated with goniodysgenesis. Goniodysgenesis is a broad term that implies abnormal development of the pectinate ligament, ciliary cleft, and/or trabecular meshwork. The condition in the Bouvier is associated with pectinate ligament dysplasia; similar changes have been noted in the American and English Cocker Spaniels, Basset Hound, Welsh Springer Spaniel, Chow Chow, Shar Pei, Samoyed, and Norwegian Elkhound, among others (see "Inherited Developmental Disorders") (Figs. 8.9, 8.60, 8.61, and 8.62).

Secondary glaucoma in dogs occurs in association with lens luxation, intraocular neoplasia, and retinal detachment. These processes are discussed in a subsequent section.

Acquired Glaucoma of Cats The majority of glaucomas that occur in cats are those that develop secondary to chronic lymphoplasmacytic uveitis or diffuse iris melanoma, with occasional congenital cases associated with anterior segment dysgenesis. Narrow-angle glaucoma is a somewhat enigmatic condition that occurs unilaterally (more commonly) or bilaterally in middle-aged domestic cats that present with anterior displacement of lens and iris with resultant shallowing of the anterior chamber. Vitreous displacement ciliovitreal block with posterior misdirection of aqueous flow is the most likely explanation, but the pathogenesis is poorly understood. By light microscopy, the TEM and lens appear normal.[183–186]

Acquired Glaucoma in Horses The majority of equine glaucoma cases likely occur secondary to chronic uveitis; the prominence of uveoscleral outflow in this species may render these beasts somewhat resistant to IOP elevations caused by conventional pathway alterations.[187–191] Histopathologically, preiridal fibrovascular membranes are frequent findings.

Pathogenesis of Secondary Glaucoma

Secondary glaucoma occurs because of obstruction of the circulation of aqueous at the ciliary process diaphragm, the pupil, the ICA, the ciliary cleft, or the trabecular meshwork. Ciliovitreal block was described earlier as a primary mechanism in the cat and may play a role in the IOP elevation that occurs with anteriorly luxated lenses or following lens extraction and partial vitrectomy. In all of these situations, anterior displacement of vitreous prevents flow of aqueous through the pupil and results in posterior chamber aqueous accumulation.

Obstruction of aqueous flow through the pupil may occur as an intumescent cataract swells anteriorly to increase resistance at the lens–iris diaphragm (phacomorphic glaucoma); by an anteriorly luxated lens acting as a cork to obstruct the pupil; as a result of vitreous that is displaced into the posterior chamber in association with a posteriorly subluxated lens, or more commonly, of vitreous that is pulled into the pupil by an anteriorly luxated lens; with the formation of occlusive fibrovascular pupillary membranes; or with total anterior synechiae and associated iris bombé. Pupillary membranes and posterior synechiae generally are a consequence of inflammation or preiridal fibrovascular membrane formation.

Closure of the ICA can occur as a result of either total or peripheral anterior synechiae. Peripheral anterior synechiae can develop secondary to pupillary obstruction associated with any of the factors discussed previously; space occupying lesions of the posterior chamber or segment, including neoplasms and ciliary cysts; uveitis; or preiridal fibrovascular membranes that span the ICA. Broad anterior synechiae typically form following corneal perforation, for iris adheres to adjacent structures, be it lens capsule or cornea. Two criteria are required: the first is proximity, and the second the presence of fibrin, which acts as a tissue adhesive. Transient fibrinous adhesions rather quickly organize to become irreversible and permanent.

Preiridal fibrovascular membranes can cause glaucoma in the absence of peripheral anterior synechiae simply by spanning the pectinate ligament in a solid fibrovascular sheet or on occasion can extend into the ciliary cleft. The significance of these membranes can be somewhat problematic for the pathologist to determine because they may be encountered in primary glaucoma as well, presumably related to the release of vasogenic factors by hypoxic retina. In early rubeosis iridis, hypertrophy of the vascular endothelium in vessels in the anterior iris stroma is noted, and spindle-shaped cells migrate onto the anterior iris surface, anterior to the pigmented margin. The cells differentiate into vascular channels, and with maturity a fibrous component develops (Fig. 8.103). Contraction of these surface membranes results in distortion of the pupillary margin (entropion or ectropion uveae) with characteristic bending of the normally linear sphincter muscle. These membranes may span the pupil or extend onto the posterior surface of the iris and indeed may extend posteriorly to incorporate the ciliary processes and contribute to cyclitic membrane formation. The vessels are fragile and give rise to the spontaneous hyphema that occurs in end-stage globes with retinal detachment, uveitis, and/or secondary glaucoma.

Figure 8.103. A preiridal fibrovascular membrane in a cat. Note the iridal vessels that extend through the anterior iridal surface and across the filtration angle, and the plasmoid aqueous and mononuclear cell infiltrate. (Periodic acid-Schiff stain, original magnification 250X.)

Obstruction of an open iridocorneal angle may also be seen with epithelial or fibrous ingrowth following accidental or surgical perforating trauma; less commonly, obstruction results from proliferating corneal endothelium or, following lens capsule disruption, lens epithelium.

Secondary glaucoma can occur as a result of acquired alterations of the ciliary cleft; with lens luxation, the ciliary cleft collapses, which likely plays a contributory role in the associated glaucoma. In chronic uveitis, the ciliary cleft may be densely infiltrated with inflammatory cells that obstruct outflow by their physical presence or produce cytokines that adversely affect trabecular endothelium; this is the most common mechanism of glaucoma secondary to feline lymphoplasmacytic uveitis or uveodermatologic syndrome in dogs. Macrophages are too large to readily pass through the trabecular pores and on occasion accumulate within the cleft to cause an obstructive secondary glaucoma; this is an uncommon condition in domestic animals. These glaucomas are identified by the suffix *-lytic,* with the prefix designating the ingested material. For instance, *phacolytic* glaucoma describes an elevation of IOP related to obstruction by macrophages filled with ingested lens protein, and *hemolytic* glaucoma is caused by macrophages filled with ingested erythrocytes or their breakdown products. With a ruptured lens capsule, denatured lens proteins may be seen obstructing the ciliary cleft; this condition is labeled lens particle glaucoma. In addition, the ciliary cleft may be obliterated by primary or secondary intraocular neoplasia, most commonly melanocytomas or iridociliary adenocarcinomas. Secondary glaucoma can occur as a result of damage to the trabecular meshwork itself by inflammation, trauma, or destruction by tumor.

Effects of Elevated IOP

The changes that occur secondary to elevated IOP can be attributed to one of four mechanisms: direct or indirect physical effects of the elevated pressure on cells and tissues; vascular effects as the IOP exceeds the luminal pressure of the capillary beds, creating a state of hypoxia; and stagnation of aqueous flow. In glaucoma, the avascular tissues that are dependent on aqueous circulation are deprived of both nutrition and waste removal. While the mechanism (or mechanisms) that stimulate release of neuroexcitotoxins is not well understood, these substances (notably glutamate) likely contribute to posterior segment changes (Table 8.5).

Enlargement of the globe occurs as a result of direct pressure on the collagen of the cornea and sclera; this effect is species and age dependent, related to the elasticity of the connective tissue. In general, young animals have a greater tendency than older animals for enlargement of the globe. In the cat, the anterior segment enlarges in greater proportion than the posterior segment. The intercalary sclera is thinner than that posterior to the equator and is a common location for localized ectasia and staphyloma formation.

Table 8.5 Pathophysiology of Ocular Changes in Glaucoma

Tissue	Effect	Result
Globe	Direct pressure	Globe enlargement
		Scleral ectasia/staphyloma
		Exposure keratitis
Conjunctiva/episclera	Indirect pressure (compression of vasculature with resultant increased venous pressure)	Vascular injection/hyperemia
	Aqueous stagnation	
Corneal endothelium	Tissue hypoxia	Corneal edema
Uvea	Tissue hypoxia	Aqueous flare
		Muscle dysfunction
		Atrophy
Lens	Indirect pressure (zonular stretching with globe enlargement)	Cataract
		Subluxation/luxation
Vitreous	Direct pressure (?)	
	Direct pressure	
	Indirect pressure	Syneresis
Retina	Tissue hypoxia	
	Neuroexcitotoxicity	Retinal atrophy
	Direct pressure	
	Indirect pressure (compression of ganglion cell axons at lamina cribrosa with disruption of axoplasmic flow)	
Optic nerve	Hypoxia	Optic atrophy +/− cupping, demyelination

As the globe enlarges, exposure keratitis may occur and manifest with a spectrum of possible changes from ulceration to epidermidalization. Diffuse corneal edema results as a consequence of direct pressure effects (including hydrostatic pressure) and aqueous stagnation. Descemet's membrane is less elastic than stroma and with stretching can fracture and become edematous (Fig. 8.104A) to produce striae that represent focal scarring (Fig. 8.104B).

Acutely, hypoxia of iris endothelial cells may result in the leakage of protein into the aqueous, and iris musculature hypoxia contributes to a fixed moderate pupil. With chronicity, uveal atrophy develops. Stagnation of aqueous predisposes to cataract formation; acute lens epithelial cell necrosis, the histologic correlate of glaucomflecken as described in humans, has not been documented in animals. As the globe enlarges, the zonules stretch and rupture, leading to secondary lens dislocation. Vitreous syneresis occurs.

The most critical changes that occur are those involving the neurosensory retina and optic nerve. Fascinating and somewhat enigmatic species differences in susceptibility to and patterns of posterior segment changes exist. A variety of factors are at play in the pathogenesis of these changes. The first is a direct pressure effect on the cells of the retina. The second is a vascular effect on both the retinal and choroidal circulation with hypoxia. Third, there is an indirect physical effect as the ganglion cell axons are compressed at the level of the lamina cribrosa with resultant disruption of axoplasmic flow. Lastly, affected retinal neurons may release neuroexcitotoxins that adversely affect neighboring neurons. In human eyes, classical glaucomatous degeneration is limited to the inner retina (ganglion cell and nerve fiber layer), and the cat eye largely follows this pattern. In the dog, degenerative changes frequently involve all of the retinal layers, and there is a geographic sensitivity whereby the superior retina is somewhat more resistant to IOP-mediated degenerative change (Fig. 8.9). Cat retinas experience less severe effects when compared to dogs with equivalent extent and duration of elevated IOP.

Optic nerve changes include atrophy with or without cupping of the optic disc and associated posterior bowing of the lamina cribrosa. Cupping occurs in approximately 50% of glaucomatous canine eyes as a result of the physical effects of

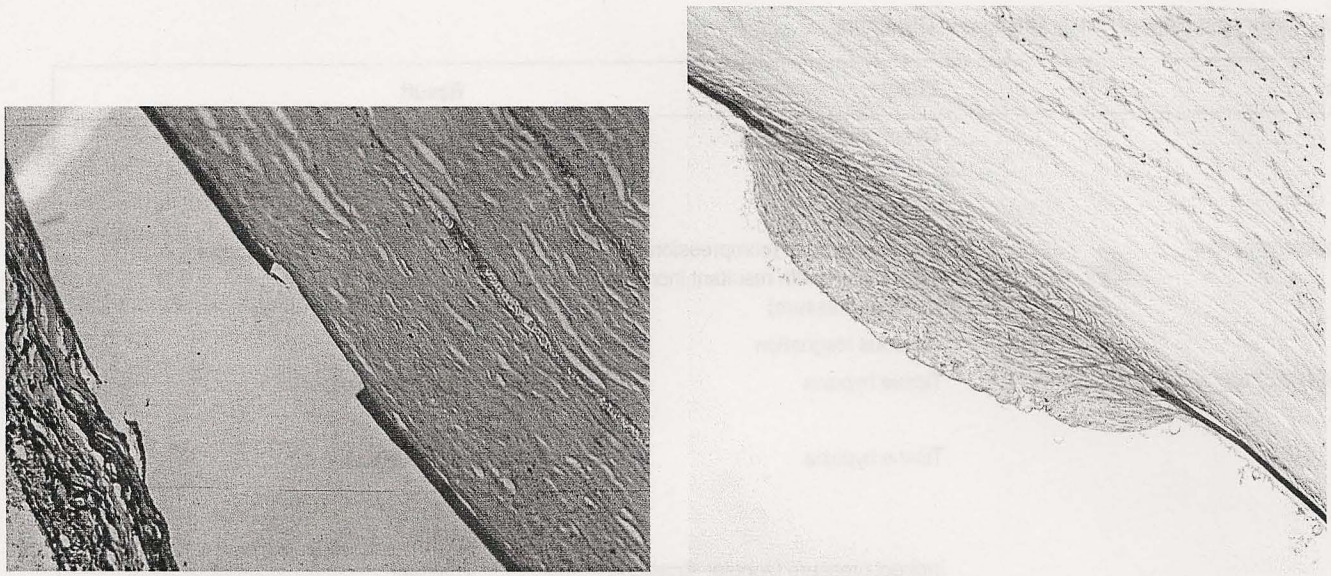

(a) (b)

Figure 8.104. A. A light microscopic section of an acute corneal stria that develops secondary to buphthalmos and corneal stretching. Note the break in Descemet's membrane and the corneal vascularization. Light microscopic examination confirmed glaucoma. (Periodic acid-Schiff stain, original magnification 300X) **B.** With time, a striae will change in histologic appearance as metaplastic endothelium reduplicates multiple thin layers of Descemet's membrane. (Periodic acid-Schiff stain, original magnification 200X.)

elevated IOP on this relatively weak area of sclera as well as the loss of axons and glial cells from the optic disc (Fig. 8.9). Large-diameter ganglion cells and their axons seem more susceptible to glaucomatous injury. Postlaminar liquifactive necrosis, or cavernous atrophy, is seen occasionally in glaucomatous canine eyes (Fig. 8.105).

Figure 8.105. Liquefactive necrosis of the optic nerve will occasionally develop in glaucoma, and hyaluronic acid–positive material that is presumed to be vitreous may be detected within the optic nerve. (Alcian blue plus hyaluronidase, original magnification 200X.)

Acquired Vitreous Disorders

While vitreous syneresis (liquefaction) and detachment are considered consequences of normal aging, they may also occur as a result of pathologic processes, including inflammation and glaucoma, that cause depolymerization of vitreous hyaluronic acid and collagenolysis (Fig. 8.106). Clinical diagnosis of either condition may be problematic; however, it is facilitated by posterior segment biomicroscopy. Syneresis is generally regarded as innocuous. Detachment of the posterior hyaloid membrane from the internal limiting membrane of the retina occurs in domestic animals, but incidence and relation to age has not been studied. Significance may involve traction on the retina at the leading edge of the vitreous detachment with the theoretical consequences of retinal tears, hemorrhage, folds, and cystoid degeneration of underlying retina. Posterior vitreous detachment can be diagnosed in paraffin-embedded sections with optimal processing, with protein condensation delineating the posterior hyaloid membrane. Syneresis is a gross pathologic diagnosis made upon qualitative evaluation of vitreous viscosity upon opening the globe (Fig. 8.107).

Asteroid hyalosis is the formation of 0.01 to 0.1 mm, roughly spherical bodies suspended within formed vitreous. Their nature is thought to be a calcium and phosphorous–containing lipid and they may arise from degenerated vitreous collagen fibrils (Figs. 8.106 and 8.108). Asteroid bodies are weakly basophilic with hematoxylin and eosin stains with the suggestion of lamellar arrangement, and they stain positively for lipid, although they resist fat solvents. They are mucopolysaccharide positive and hyaluronidase resistant. With polarized light, birefringent spicules are observed. Asteroid hyalosis is not an uncommon finding in older dogs and has not been reported in cats or other domestic animals. It may be unilateral or bilateral, and even in its densest presentation, does not seem to effect vision appreciably. In dogs there is an association with iridociliary neoplasia.

Cholesterolosis bulbi is an uncommon condition that results from incomplete resolution of intraocular hemorrhage and syneresis. The refractile cholesterol crystals settle to the bottom of the vitreous chamber (and/or the anterior chamber in aphakic eyes) when the eye is at rest. Other significant

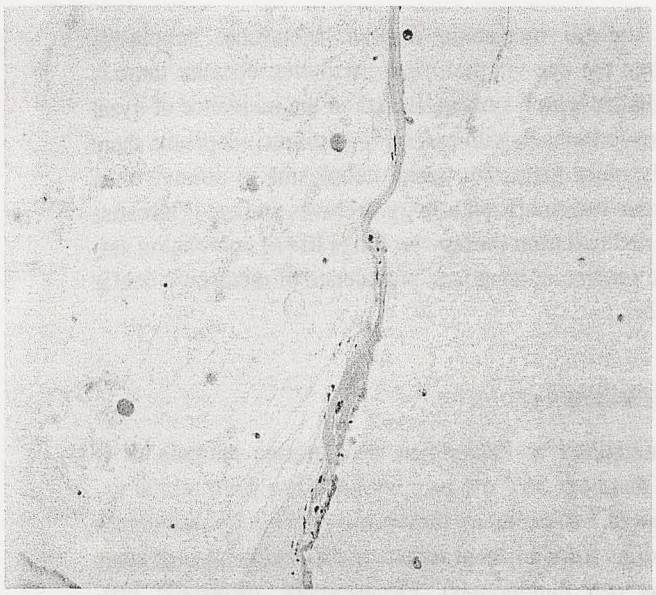

Figure 8.106. Vitreous degeneration is easily overlooked during light microscopic examination of eyes. Note the congealed strands of vitreous in this section. Asteroid hyalosis bodies and areas of clear fluid are also present in this photograph. (Periodic acid-Schiff stain, original magnification 200X.)

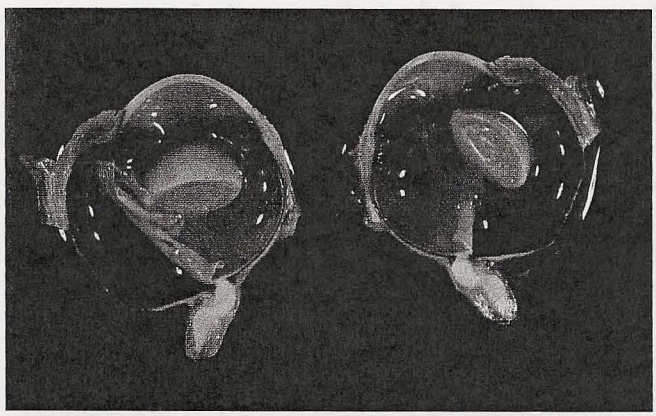

Figure 8.107. This is a gross section of a Bouin's-fixed dog eye. Note the retinal detachment, scrolling of the retinal edge, and vitreous strands.

ocular lesions usually accompany this condition. In paraffin-embedded sections, the cholesterol esters have been dissolved in processing and their location is seen as slitlike spaces, occasionally with an associated granulomatous inflammatory response, and hemosiderosis may be present and is demonstrated nicely with stains for iron.

Optic Nerve Degeneration

Optic nerve degeneration or atrophy is a common pathologic diagnosis. The etiologies include optic nerve trauma, glaucoma, optic nerve neoplasia, optic neuritis, progressive retinal atrophy, retinal detachment, and others. The gross clinical signs include a cavitation of the optic nerve, and histologic findings include decreased axons, gliosis, and fibrosis (Fig. 8.5).

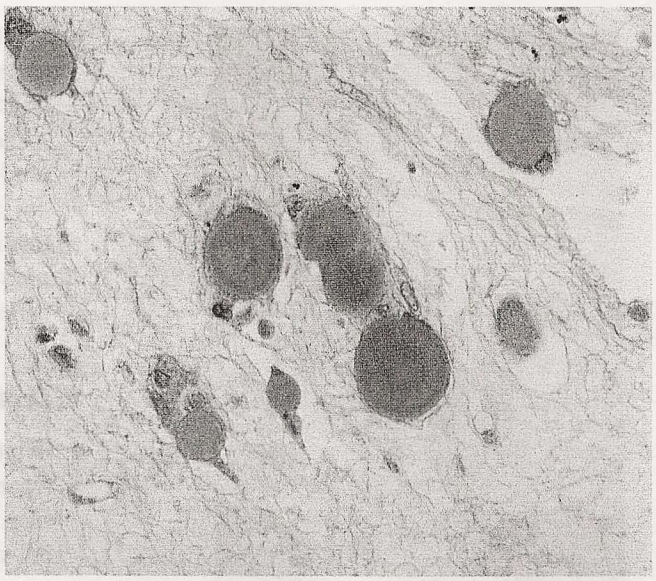

Figure 8.108. Asteroid hyalosis in a dog. Note the amorphous pink granular bodies associated with dark, small hyalocyte nuclei. (Periodic acid-Schiff stain, original magnification 400X.)

Metabolic Diseases That Affect the Eye

Diabetes Mellitus

The ocular manifestations of diabetes mellitus other than cataracts have not been systematically studied in animal species; in human eyes, these include glycogenic vacuolization of the iris pigmented epithelium; thickening of the ciliary body basement membrane; and ischemic retinopathy with retinal and optic disc neovascularization, with secondary ramifications of vitreous hemorrhage, tractional retinal detachment, rubeosis irides, and neovascular glaucoma. The canine and feline posterior segments are spared the ravages of vasoproliferative disease, perhaps simply as a consequence of disease duration—these changes take many years to develop in humans. Diabetic cataracts in dogs are osmotic in nature related to polyalcohol accumulation; are rapid in onset, accompanied by intumesence; and are frequently associated with lens-induced uveitis. Ultrastructural changes have been described by Taylor, Peiffer, and Costella.[192] There are species differences in regard to propensity for diabetic cataractogenesis related to differences in enzyme levels and thus sugar metabolism; diabetic cataracts in cats have been reported only rarely.[193]

Systemic Hypertension

The ophthalmic pathology of systemic hypertension in the dog and cat include vascular lesions, including fibrinoid necrosis and occlusion of choroidal and retinal arterioles with nonperfusion of the choriocapillaris; ischemic atrophy of the RPE; retinal ischemia with detachment, exudation, hemorrhage, and necrosis; and papilledema (Fig. 8.109).

Infectious Ocular Diseases

A myriad of infectious agents may affect the orbital, adnexal, or ocular tissues, either as a result of vascular seeding or direct

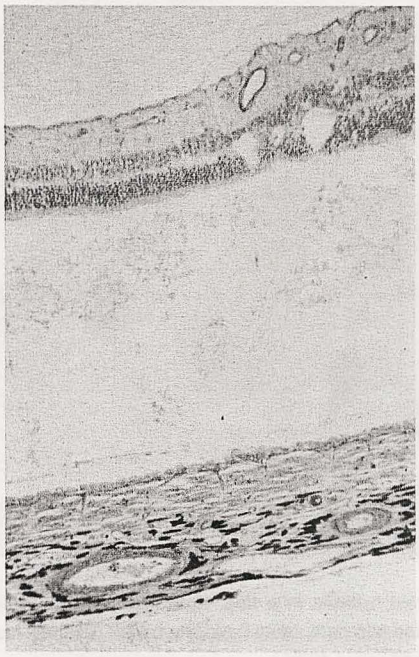

Figure 8.109. Systemic hypertension will induce significant intraocular disease, including retinal detachment, retinal edema and hemorrhage, and fibrinoid necrosis of retina and choroidal vessels. When the hypertension is not controlled, the retina will degenerate, and thickened retinal and choroidal arteries eventually develop. (Periodic acid-Schiff stain, original magnification 250X.)

extension of endogenous infectious disease or as a consequence of inoculation of endogenous agents caused by trauma. The visibility of the eye, the importance of vision as a cognitive sense, and anatomic and physiologic factors contribute to the fact that ocular signs are frequently the reason for presentation of systemic infectious disease. Infectious agents, their morphology, and common features are summarized in Table 8.6.

Ocular Neoplasia

We have categorized ocular neoplasia in this chapter by the tissue involved (orbital, adnexal, conjunctival and corneal, uvea, retina, and optic nerve). Ocular neoplasms are primary (originate in the eye); or they are metastatic and gain access into the ocular tissues via the vascular system; or they invade the orbit and then the globe by extension from adjacent tissue (e.g., nasal carcinoma). Most primary ocular neoplasms are benign in behavior, often despite histologic evidence of malignancy. However, their expansive growth induces significant alterations within the eye or orbit or ocular surface that may necessitate enucleation. Examples include melanocytomas of the eyelids, limbus, and uvea and iridociliary epithelial neoplasms. Malignant primary neoplasms, although small in number, are important because metastasis of these is common. Examples of malignant primary ocular neoplasms include feline intraocular sarcoma, feline diffuse iris melanoma, conjunctival melanoma, and many of the spindle cell neoplasms of the orbit. Virtually any systemic neoplasm can metastasize to the eye. Indeed, the rich vascularity of the uvea and the eyes' sequestration from the immune system may mark it as a favored site for metastatic disease. Metastatic neoplasms extend into the eye via the uveal circulation because there is no intraocular lymph system. Based on the incidence of uveal metastasis in humans with extensive systemic neoplasia, there are likely more metastatic uveal neoplasms in animals than our current veterinary pathology archives indicate. Because medical and radiation therapy prolongs life of companion animals, we predict an increased prevalence of metastatic ocular neoplasia.

Orbital Neoplasia

Orbital neoplasia is uncommon in domestic animals. It is reported that over 56% are primary and arise from orbital tissues. Most of the secondary tumors are either lymphosarcomas or extensions from adjacent tissues (nasal carcinomas or sinus squamous cell carcinomas). Occasionally, metastatic neoplasms, most commonly lymphosarcomas, localize in the orbit. There are no breed or sex predispositions, and most affected animals are middle-aged and older. Unfortunately, most orbital neoplasms are malignant. There are many reported primary orbital neoplasms in animals, including flat bone osteosarcoma (Figs. 8.112 and 8.113), chondrosarcoma, hemangiosarcoma, neurofibrosarcoma, lacrimal gland adenoma and adenocarcinoma, third eyelid adenoma and adenocarcinoma, zygomatic salivary adenoma and adenocarcinoma, Harderian gland adenoma, granular cell myoblastoma, and fibrosarcoma.[194–203] The distinctive gross and light microscopic appearances of these primary neoplasms are described in Table 8.7.

Reported metastatic neoplasms and those that extend into the orbit from adjacent tissues include nasal adenocarcinoma, lymphosarcoma (Fig. 8.114a), and squamous cell carcinoma.[194–197,203–207] Their histologic features are listed in Table 8.8. The histories that accompany the biopsies of these metastatic orbital neoplasms are valuable to the pathologist in identifying the potential tissues of origin of anaplastic neoplasms.

The immunohistochemical staining patterns and electron microscopic ultrastructure are often required to confirm a tissue-specific diagnosis with anaplastic orbital neoplasia. The choice of available immunohistochemical staining is extensive, and a thorough knowledge of embryology and tissue derivations aids the selection. Briefly, cytokeratin markers help identify epithelial neoplasms; vimentin is expressed on most neoplasms that arise from neurocrest tissues; synatophysin and neurospecific enolase help identify most neoplasms that are neuroectoderm in origin; actin is expressed on some mesenchymal neoplasms; and S100, tyrosinase, and melanin A are useful in identifying poorly pigmented melanomas. With the exception of meningiomas, lipomas, and adenomas, most orbital neoplasms are malignant and metastasis is common and the prognosis is poor.

Eyelid and Conjunctival Neoplasms

Eyelid and conjunctival neoplasms occur commonly in dogs (tarsal gland adenomas), cattle (squamous cell carcinoma), and

Table 8.6 Common Endogenous Infectious Causes of Ocular Inflammatory Disease with Key Histopathologic Features

Organism/Disease	Morphologic Features of Organism	Classification of Inflammation
Feline immunodeficiency virus	—	Lymphoplasmacytic uveitis Retinal perivasculitis
Feline coronavirus	—	Variable neutrophilic infiltrate Lymphoplasmacytic vasculitis/endophthalmitis with prominent exudation.
Feline herpesvirus	Intranuclear inclusions	Lymphoplamacytic keratoconjunctivitis/ uveitis
Bovine malignant catarrhal fever	—	Lymphoblastic perivascular and intramural accumulation with vascular necrosis, +/− hemorrhage (Fig. 8.91) Corneal endothelialitis
Canine distemper	Inclusions in glial and other cells	Nongranulomatous lacrimal adenitis, chorioretinitis, optic neuritis
Canine adenovirus-1	Inclusions in corneal endothelial cells	Nongranulomatous anterior uveitis, neutrophilic endothelialitis
Rickettsia	—	Mononuclear perivasculitis
Borrelia burgdorferi	—	Nongranulomatous uveitis
Equine recurrent uveitis	Silver-positive spirochetes, *Onchocerca microfilaria* (both rarely identified)	Lymphoplasmacytic uveitis Amyloid envelopment of ciliary processes (Fig. 8.90)
Histoplasma capsulatum	Intracytoplasmic (macrophage), 2–4 μm PAS+ yeasts with central density and a clear capsule (Figure 8.111)	Diffuse granulomatous to pyogranulomatous
Cryptococcus neoformans	Focal-multifocal ellipsoidal yeasts 4–40 μm in diameter, thin-walled PAS+ yeasts, thick mucicarmine+ capsule	Minimal pyogranulomatous host reaction, neurotrophic
Coccidioides immitis	Large coalescing pyogranulomas with PAS + endospore-containing spherules	Discrete pyogranulomatous
Blastomyces dermatitidis	5–20 μm PAS+ thick-walled, broad-based budding organisms	Diffuse pyogranulomatous (Fig. 8.25)
Aspergillus	PAS and silver + septated hyphae within vitreous, oriented perpendicular to retinal surface	Pyogranulomatous +/− necrosis
Protrotheca (zophi most common)	2–20 μm refractile, PAS+, argyrophilic wall; unicellular or multiple daughter cells within a single parent cell	Lymphoplasmacytic to diffuse granulomatous
Nocardia asteroids	Branching, filamentous gm+ bacteria, vitreous predisposition	Pyogranulomatous +/− necrosis
Tuberculosis	Acid-fast organisms within macrophages	Discrete granulomatous uveitis/ panophthalmitis (Fig. 8.89)
Leishmaniasis	Protozoa within macrophages	Granulomatous uveitis/panophthalmitis
Toxoplasmosis	Rare merozoites or cysts	Lymphoplasmacytic uveitis distant from organism +/− focal necrotizing retinitis
Hapatozoon canis	Protozoan–intracytoplasmic gametes or schizonts in tissue (muscle biopsy)	
Toxocara canis, Baylisascaris procyonis	+/− nematode fragments	Zonal eosinophilic granulomatous
Bartonella	Gram-negative bacteria	Lymphoplasmacytic uveitis, conjunctivitis
Candida albicans	Periodic acid-Schiff positive yeast (Fig. 8.110)	Lymphoplasmacytic uveitis

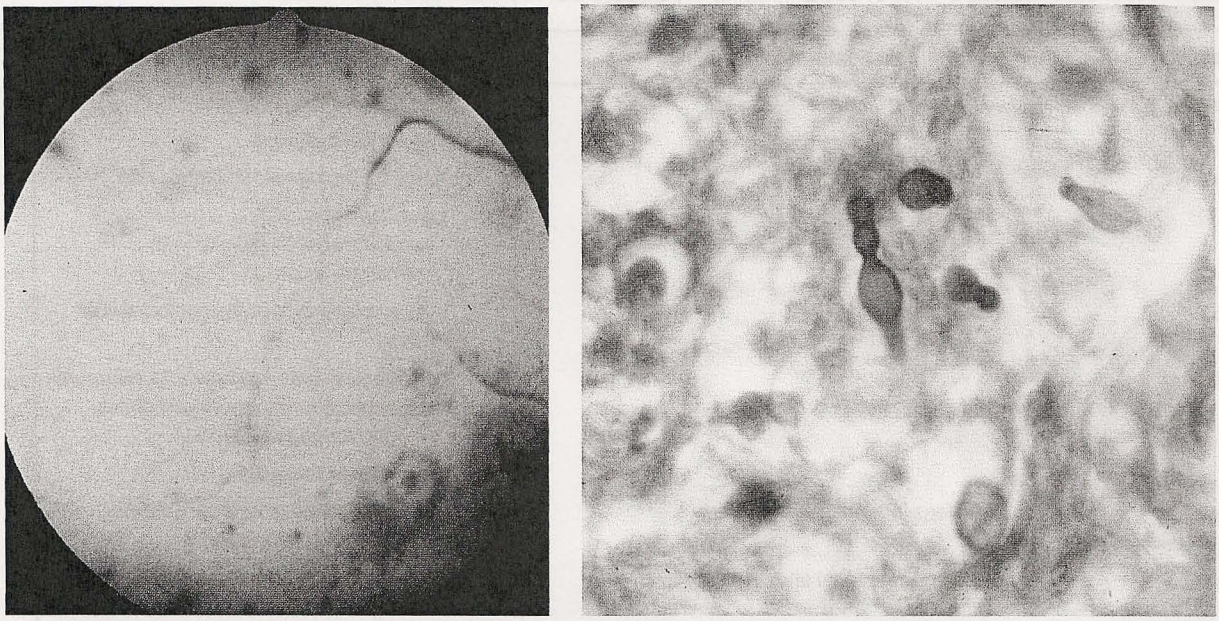

(a) (b)

Figure 8.110. **A.** A fundus photograph of a cat with systemic candidiasis. **B.** Histologic appearance of *Candida albicans.* (Periodic acid-Schiff stain, original magnification 400X.)

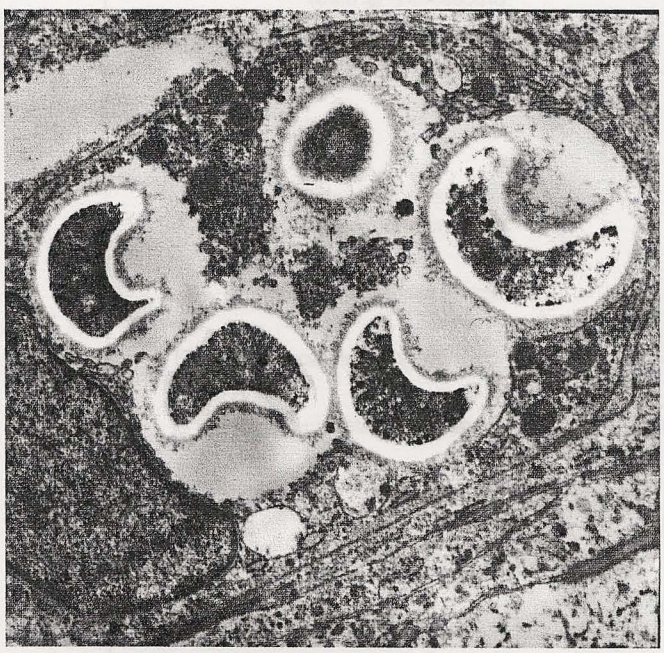

Figure 8.111. *Histoplasma capsulatum* will induce a significant chorioretinitis. Transmitting electron microscopy will confirm the characteristic shape and size of this organism. (Original magnification 6300X.)

Figure 8.112. A firm mass that was attached to orbital bones is evident temporal to the right eye of this dog.

horses (sarcoids and squamous cell carcinomas), and less frequently in other domestic animals. The characteristics of the common eyelid neoplasms of dogs are provided in Table 8.9. Most eyelid neoplasms of dogs are benign, or even if histologic features of malignance exist, they usually behave in a benign fashion. The tarsal gland adenoma accounts for approximately 40% of the reported eyelid tumors in dogs, and melanoma and papilloma accounts for 20% and 17% respectively.[208–210] In contrast, in the cat and cow, squamous cell carcinoma is the most common eyelid and conjunctival neoplasm.[211–214] Many, if not all, eyelid and conjunctival neoplasms have multiple predisposing factors, including ultraviolet exposure, lack of protective pigmentation, and species susceptibility.

Tarsal gland adenomas are sebaceous gland neoplasms that develop most commonly in older dogs (>10 years). Grossly, these adenomas are lobulated, usually pigmented, and friable (Fig. 8.116A). As a result, hemorrhage and fibrin crusts are often present. In any given tumor, the ductal or secretory cells may predominate (Fig. 8.116B and C); in the older literature, ductal adenomas were confused with basal cell carcinomas, which are rarely encountered in domestic animals. Hemorrhage, necrosis, pigmentation, and chalazion are commonly noted. The lipid secretion is often extruded from the tarsal

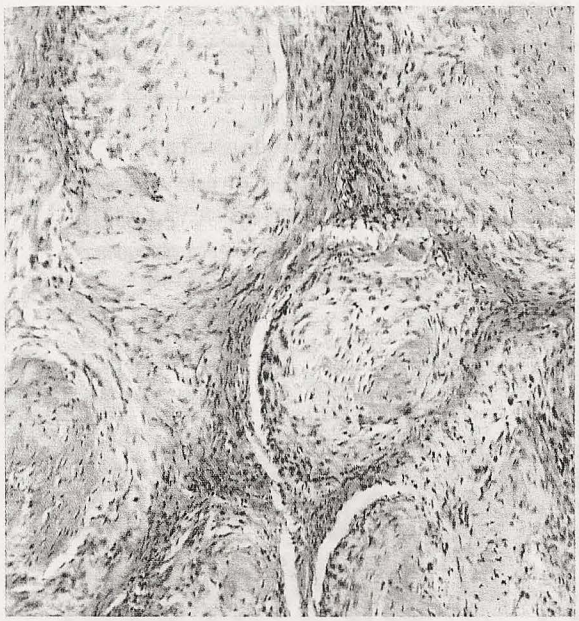

Figure 8.113. Flat bone osteosarcoma was confirmed after orbital biopsy of the dog in Figure 8.112. (Hematoxylin and eosin stain, original magnification 250X.)

gland during the progressive neoplastic expansion, which induces a significant granulomatous response. Rarely, hyperchromatism and increased mitotic activity warrant the diagnosis of tarsal gland adenocarcinoma. Fortunately, even these diseases behave as benign neoplasms and respond to excision or varied therapies, including cryosurgery or laser ablation.

Squamous cell carcinoma is a common eyelid and conjunctival neoplasm of the horse, cow, and cat. Poorly pigmented eyelids and conjunctiva in these species predispose to precancerous changes, including plaques, papillomas, keratin horns (Fig. 8.117A), and carcinoma in situ (Fig. 8.117B). These preneoplastic lesions may be erythematous, scaly, crusty, or even hornlike. The preneoplastic lesions may regress spontaneously or slowly develop into squamous cell carcinoma. In the cat, horse, and cow, squamous cell carcinoma may manifest as a friable, salmon-pink mass or as an ulcerative lesion. The diagnosis is confirmed with biopsy and light microscopic examination. Broder's classification may be utilized to establish the prognosis: grade 1 squamous cell carcinomas are well differentiated with large, round epithelial cells with prominent intercellular bridges, abundant pink cytoplasm, homogenous nuclear patterns, and only a few mitotic figures (Fig. 8.117C). Keratin pearls are prominent features, as are neutrophils, within these well-differentiated neoplasms. Grade II squamous cell carcinomas display prominent epithelial characteristics with fewer keratin pearls and increased mitotic figures. Grade III squamous cell carcinomas are similar; however, the mitotic index is higher and there is more evidence of tissue invasion, which creates multiple neoplastic islands (Fig. 8.117D). Grade IV are poorly differentiated carcinomas with no keratin pearls, amolphilic cytoplasm with pleomorphic, and hyperchromatic nuclei (Fig. 8.117E). The mitotic index is high, and tissue invasion is obvious. Metastatic potential increases with each grade of squamous cell carcinoma, and although uncommon, they do spread via the lymphatics to the regional lymph nodes (mandibular, retropharyngeal, and mediastinal). Papilloma virus may play a role in the development of squamous cell carcinomas. Solar radiation and lack of pigment in the eyelids are predisposing factors in the cow, cat, and horse.

Table 8.7. Gross and Histologic Characteristics of Primary Orbital Neoplasms

Neoplasm	Gross Features	Histologic Features
Osteoma and osteosarcoma	Firm, white, and gritty on cross section	Trabecular bone with fibrous tissue and cartilage (Fig. 8.113)
Chondrosarcoma	Translucent gray	Cartilage and poorly differentiated mesenchymal cells
Rhadbomyosarcoma	Gray to red in color and nodular	Ribbon and strap cells with cross striations
Neurofibrosarcoma	Gray to white and firm	Bundles and fascicles of spindle cells
Lacrimal gland adenomas and adenocarcinomas	Pink, friable, lobulated mass located in dorsolateral orbital quadrant	Sheets of epithelial cells with variable gland and duct formation
Zygomatic gland adenomas and adenocarcinomas	Pink, friable, lobulated mass located in ventral orbit (Fig. 8.115)	Sheets of epithelial cells with variable gland and duct formation
Third eyelid adenomas and adenocarcinomas	Pink, friable, lobulated mass located in ventromedian orbital quadrant	Sheets of epithelial cells with variable gland and duct formation
Mast cell neoplasms	Edematous, red, friable mass without distinct borders	Diffuse round cell neoplasm with granules and eosinophils
Melanoma	Usually pigmented and arising from conjunctiva	Variable spindle to plump cells with pigment (usually)
Meningioma	White to gray and often round or oval	Multiple nests and whorls of spindle-shaped cells (Fig. 8.136)

Table 8.8 Gross and Histologic Features of Common Metastatic Orbital Neoplasms of Animals

Neoplasm	Gross Features	Histologic Features
Nasal or sinus adenocarcinoma	Gray, friable, well vascularized; may have mucin and will extend into orbit from the nasal cavity or sinus	Basal epithelial cells with variable adenomatous development
Squamous cell carcinoma	Salmon-pink, friable mass that extends into orbit from the conjunctiva	Sheets of epithelial cells with tight junctions and variable keratin production (Fig. 8.117)
Lymphosarcoma	Gray, friable mass that lacks distinct borders	Diffuse round-cell tumor with a large nuclei and minimal cytoplasm (Fig. 8.114B)

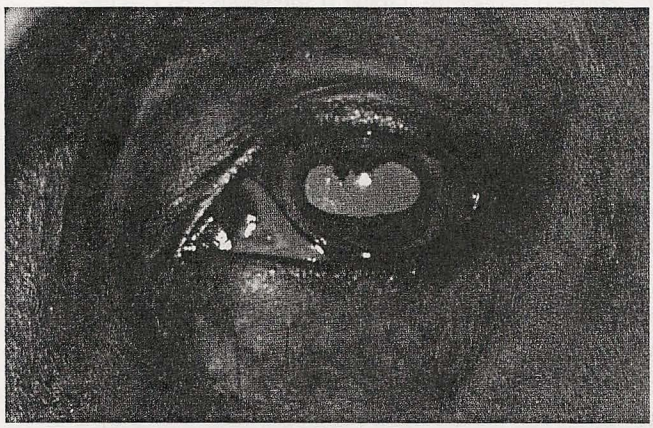

(a)

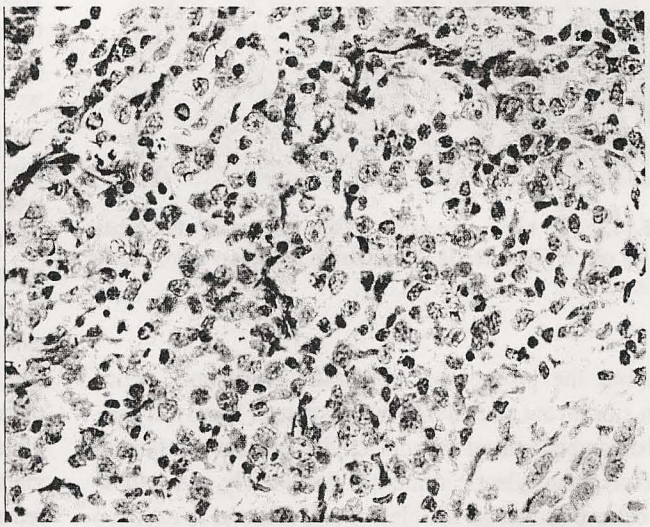

(b)

Figure 8.114. A. A medial canthal tumor that is inducing third eyelid prolapse in a horse. **B.** Histology confirmed orbital lymphosarcoma after biopsy. (Hematoxylin and eosin, original magnification 300X.)

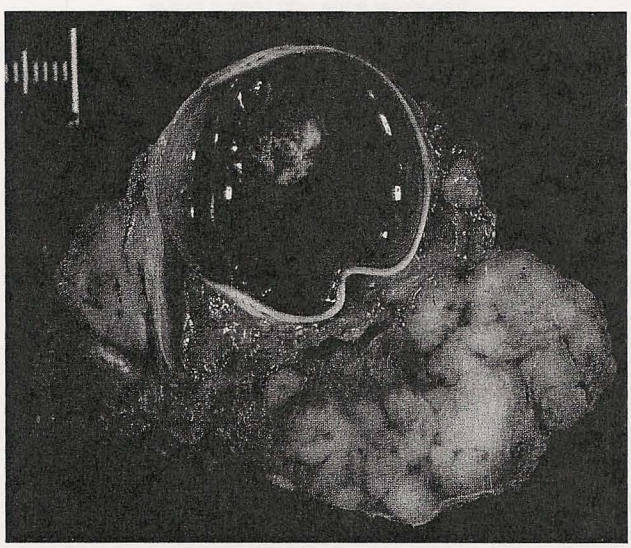

Figure 8.115. Orbital tumor that is consistent in appearance with a glandular neoplasm. Light microscopy confirmed the diagnosis of zygomatic adenocarcinoma.

Papillomas of the eyelids are common in dogs, horses, and ruminants (Fig. 8.118A). Grossly, papillomas are often pedunculated, and their surfaces are rough and papillary. Light microscopic examination of these tumors reveals hyperplastic squamous epithelium that envelops a core of rich fibrovascular tissue (Fig. 8.118B). The papilloma variations of squamous cell carcinomas are very similar in appearance; however, the carcinoma invades deeper tissues and is usually only lightly pigmented. Papillomas are induced by papilloma viruses, and they manifest in young animals (<1year of age).

Histiocytomas are occasionally diagnosed and are similar to papillomas; they are benign and occur in young animals. They are, however, round and smooth and manifest as sessile smooth pink tumors on eyelid skin. Often the center of the tumor is depressed and may be ulcerated. Light microscopy features include a mass of large round to polyhedral histiocytes that extend through the epidermis and into the dermis (Figs. 8.119A and B). These neoplasms are benign and resolve spontaneously.

Table 8.9. Common Eyelid and Conjunctival Neoplasms

Neoplasm	Species Most Commonly Affected	Gross Characteristics	Histologic Features
Tarsal gland adenoma	Dogs	Variably pigmented, friable nodular mass associated with the tarsal glands (Fig. 8.116A)	Multilobular arrangement with large, vacuolated epithelial cells or basal cells usually arranged in distinctive glandular pattern with variable pigment and often with chalazion and associated foamy macrophages and lymphocytes (Fig. 8.116B & C)
Squamous cell carcinoma	Cattle, horses, cats	Pale salmon-pink, friable, flat eyelid skin or conjunctival mass	Large, pale pink–staining epithelial cells with intercellular bridges, abundant cytoplasm, keratin pearls, and hyperplastic projections into the substantia propria (Fig. 8.117B, C, D, & E)
Histiocytic tumors	Dogs, cats	Firm, nodular, pale masses (Fig. 8.119A)	Large, pale macrophagelike cells (Fig. 8.119B)
Papillomas	Dogs, horses, cattle	Pedunculated, roughened, friable, cauliflowerlike, often pigmented eyelid mass of younger animals (Fig. 8.118A)	Hyperplastic squamous epithelial fronds with central fibrovascular cores (Fig. 8.118B)
Eyelid melanomas	Dogs, horses	Pigmented, often pedunculated masses on the eyelid skin and flat, black conjunctival masses (Fig. 8.122A)	Variable mix of spindle to plump, more epithelial-like cells with prominent nucleoli, usually pigmented (Fig. 8.122B)
Conjunctival melanoma	Dogs	Flat, variably pigmented conjunctival masses; commonly occur on the third eyelid (Fig. 8.123A)	Variable pigmentation with a mix of plump and spindle cells with prominent nucleoli and noted junctional activity (Fig. 8.123B)
Sarcoid	Horses	Firm, pale, pedunculated or intradermal masses	Spindle to spiral cells that form interlacing bundles with overlying hyperplastic epithelium with extensive rete pegs (Fig. 8.121)
Mast cell tumors	Dogs, cats	Edematous and hyperemic diffuse eyelid masses	Large, round cells with cytoplasmic granules (Fig. 8.21)
Lymphosarcoma	Any species	Firm, infiltrative eyelid mass	Round cells with large nuclei and sparse, dark cytoplasm
Peripheral nerve sheath neoplasms	Cats, horses	Firm, pink eyelid mass	Sheets and fascicles of spindle cells
Hemangioma, hemangiosarcoma	Dogs, horses	Vascular mass that originates in the conjunctiva and extends into the cornea	Vascular mass with dilated, thin-walled vascular channels (hemangioma); hemangiosarcomas are more cellular with evidence of invasion (Fig. 8.125A, B, & C)

Basal cell epitheliomas are uncommon, benign, multilobulated, often pigmented neoplasms of eyelids of animals.[215] These neoplasms are either benign histologically and called basal cell papillomas or more invasive and termed basal cell carcinomas. The latter is a misnomer given their benign clinical nature. These neoplasms arise from the basal cells of the epithelium and adnexa. Light microscopic examination reveals basal cell papillomas are pigmented masses of acanthotic epithelium with prominent intercellular bridges. Basal cell carcinomas are a uniform population of basophilic epithelial cells with oval nuclei, and the mitotic index is often greater than 5 per high-power field. Sebaceous differentiation of these neoplasms is not uncommon, and nests of neoplastic cells resembling glands are noted.

Mast cell neoplasms will occasionally arise in the eyelids and conjunctiva.[216–218] The clinical manifestations include hyperemia, edema, and swelling. The diagnosis is confirmed with light microscopy confirming a diffuse population of round cells with basophilic granular cytoplasm (Fig. 8.21). When a mast cell neoplasm is confirmed histologically, it should be staged by aspirating the draining lymph nodes and the primary source of the neoplasm determined. Mast cell

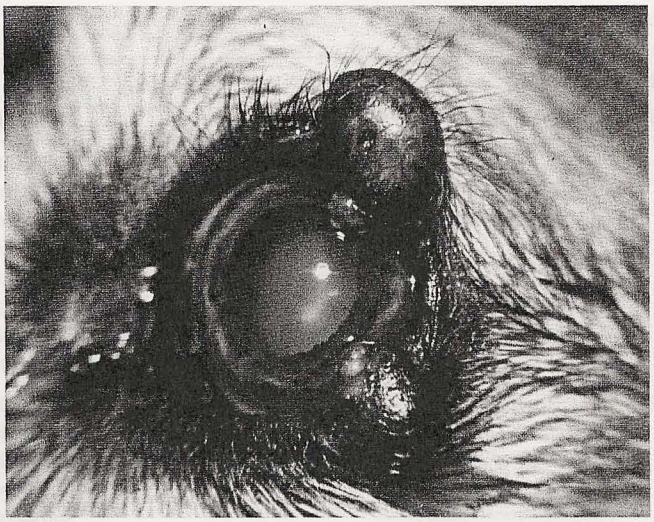

(a)

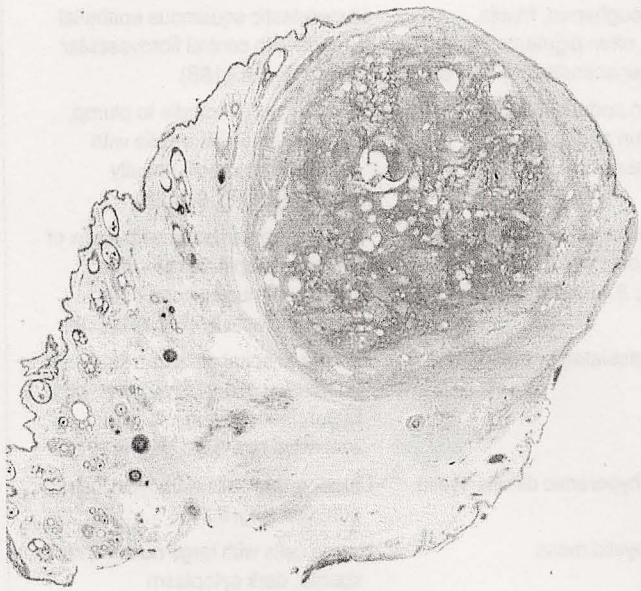

(b)

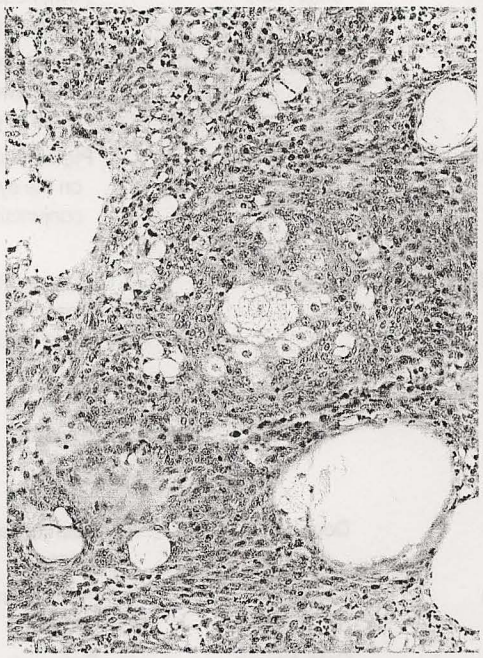

(c)

Figure 8.116. **A.** Multiple tarsal gland adenomas on the eyelid margin of an old dog. **B.** Subgross appearance of one of the tarsal gland adenomas from the eyelid of the same dog. (Hematoxylin and eosin stain, original magnification 2X.) **C.** Histologic features of a tarsal gland adenoma. Note the darkly staining basal cells with focal sebaceous differentiation and a mild diffuse neutrophil and macrophage infiltration. The neutrophil and often macrophage infiltration is a common inflammatory response to lipid extrusion and chalazion (clear vacuoles) that accompany these adenomas. (Hematoxylin and eosin stain, original magnification 300X.)

neoplasms are graded by differentiation of the cells, mitotic activity, nuclear and nucleolar size, and tissue invasion. Eosinophils and collagen degeneration are common accompaniments in mast cell neoplasms. Despite these efforts, mast cell neoplasia are often unpredictable in their biologic behavior in most species.

Eyelid and conjunctival lymphosarcoma are occasionally diagnosed after biopsy (Figs. 8.120A and B). The clinical manifestations are diffuse or focal swollen eyelids with or without inflammation.[219–220] Most, if not all, eyelid lymphosarcomas are a manifestation of systemic malignant lymphosarcomas. Lymphosarcoma is diagnosed on the basis of morphology, which includes either follicular or diffuse architecture. Diffuse lymphosarcomas are categorized by nuclear size (small, mixed, and large). Follicular lymphosarcomas are categorized into floral, mantle cell, marginal cell, and large cell variants. Immunohistochemistry is useful in diagnosing T cell, B cell, and leukemic variants of lymphosarcomas.

Peripheral nerve sheet neoplasms of the eyelids are reported in cats and horses.[221–222] These are locally aggressive eyelid neoplasms that are firm on palpation. Histologic characteristics include interlacing fascicles of spindle cells with Antoni A patterns with elongated, plump nuclei arranged in rows and palisades and Antoni B patterns in which the spindle cells are arranged in a loose, interlacing pattern and the nuclei are smaller.

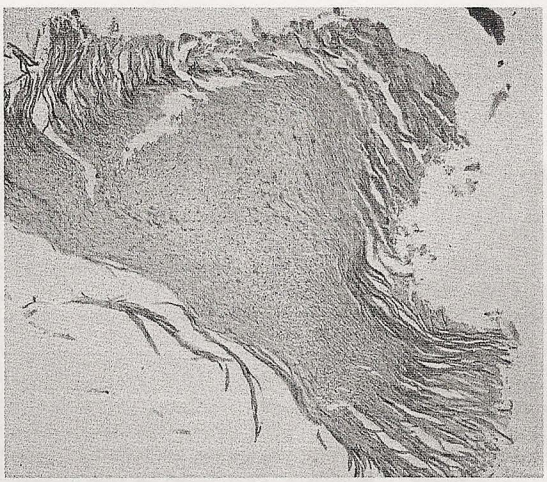

(a)

(b)

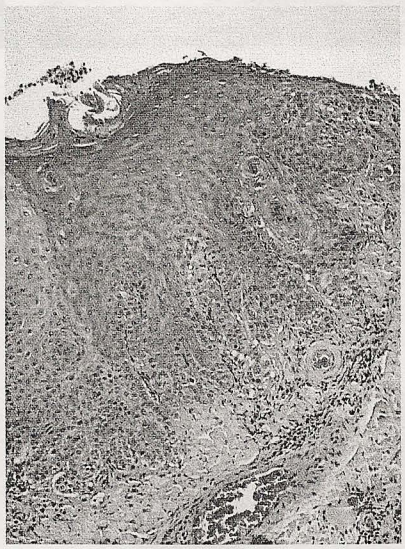

(c)

(d)

(e)

Figure 8.117. **A.** A keratin horn that was removed from the limbus of a Hereford bull. (Hematoxylin and eosin stain, original magnification 200X.) **B.** Carcinoma in situ in the cornea epithelium of a cow. Note the carcinoma is limited to the epithelium and has not crossed the basement membrane and invaded the stroma. The surface is keratinized and contains a focal keratin pearl. (Hematoxylin and eosin stain, original magnification 300X.) **C.** A well-differentiated squamous cell carcinoma from the conjunctiva of a Hereford bull. Note the invasion into the subconjunctiva and keratin pearls. (Hematoxylin and eosin, original magnification 300X.) **D.** An invasive squamous cell carcinoma that is invading the orbital tissues. Note the keratin pearls and diverse epithelial morphology. (Hematoxylin and eosin stain, original magnification 400X.) **E.** A malignant squamous cell carcinoma that has replaced the cornea of this cow. (Hematoxylin and eosin stain. Original magnification 300X.)

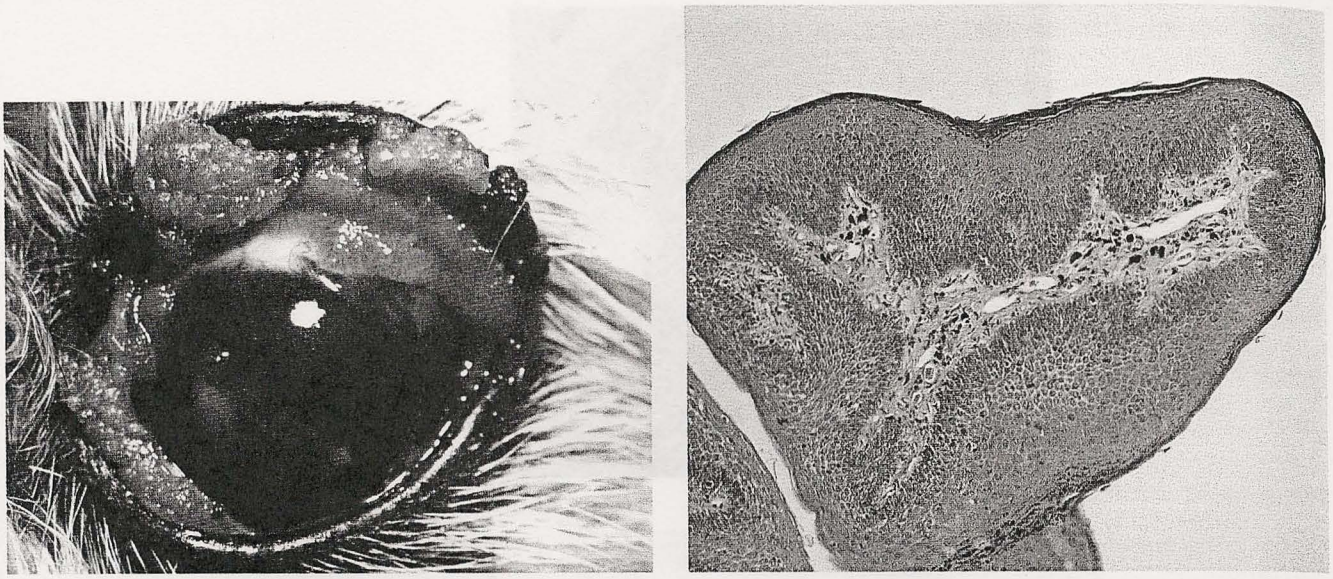

(a) (b)

Figure 8.118. **A.** Conjunctival papillomatosis in dog. **B.** Histological section of a conjunctival papilloma. Note the characteristic vascular core and prominent epithelial hyperplasia and keratinized surface. (Hematoxylin and eosin stain, original magnification 200X.)

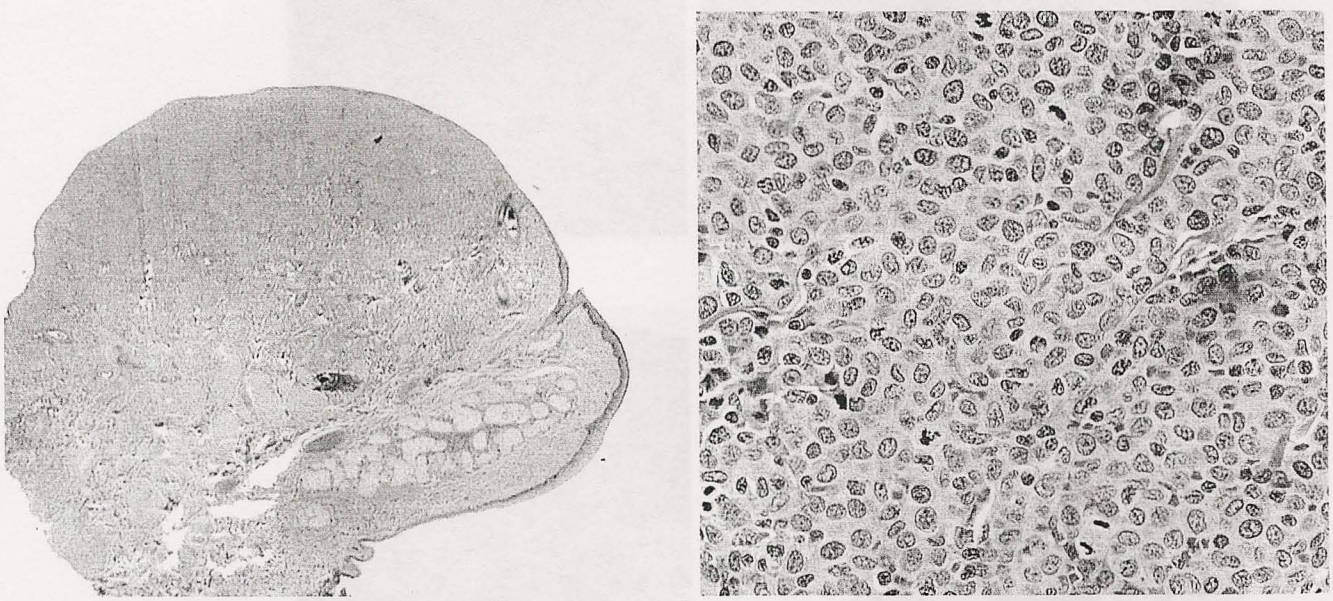

(a) (b)

Figure 8.119. **A.** Subgross section of eyelid histiocytoma. (Hematoxylin and eosin stain, original magnification 50X.) **B.** Note the large, pale polyhedral cells that are characteristic of a histiocytoma. (Hematoxylin and eosin stain, original magnification 300X.)

Sarcoids are common tumors of the eyelids of horses.[223–225] Thoroughbred horses may be predisposed to developing this condition, and younger horses are commonly affected with these benign fibroblastic tumors. Sarcoids have been categorized into three groups based on their gross appearance: (a) large fibroblastic tumors measuring larger than 20 cm; (2) verrucous or wartlike tumors that are smaller and less than 6 cm in diameter; and (3) a mixed type with features of both verrucous and fibroblastic. Light microscopic examination reveals a monotonous population of fascicles of spindle cells that are woven together (Fig. 8.121). These spindle cells extend through the dermis, and the overlying epithelium extends deep into the sarcoid as rete pegs. The etiology is most likely a virus, and bovine papilloma virus and a C type retrovirus have been reported.[226–228] Sarcoids are viral-induced benign fibromas that will respond to several therapies, and the prognosis is generally good with effective therapy.

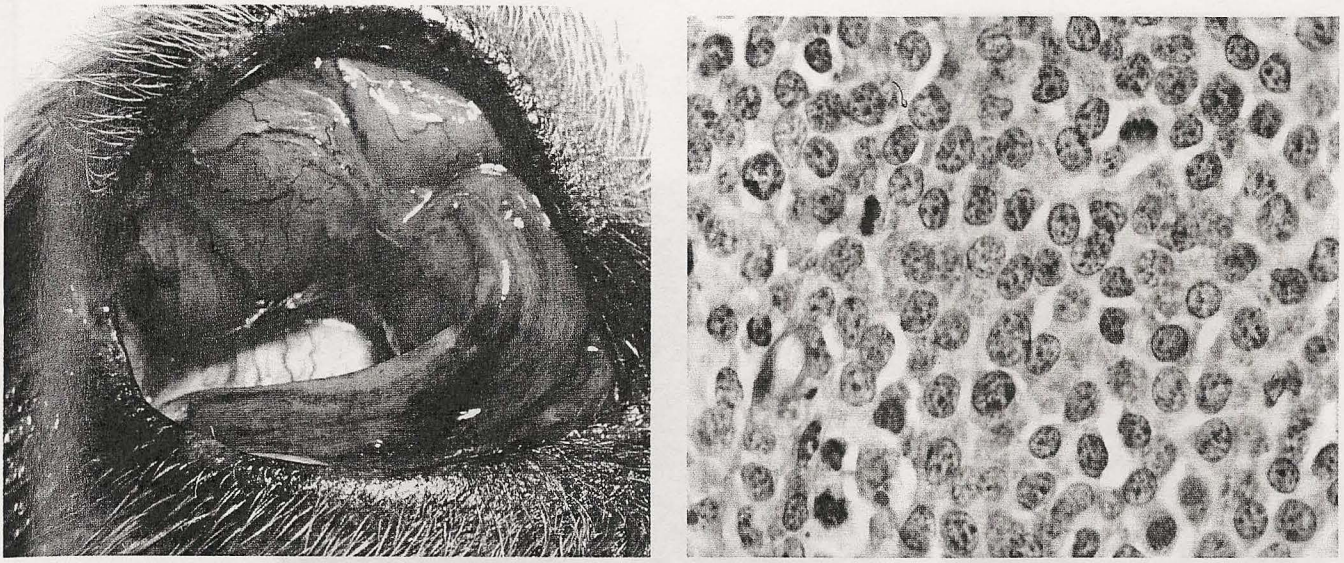

(a) (b)

Figure 8.120. A. The clinical manifestation of conjunctival lymphosarcoma in a dog. **B.** A conjunctival biopsy of the same dog reveals a diffuse population of round cells with scant cytoplasm and nuclei characteristic of lymphosarcoma. (Hematoxylin and eosin stain, original magnification 400X.)

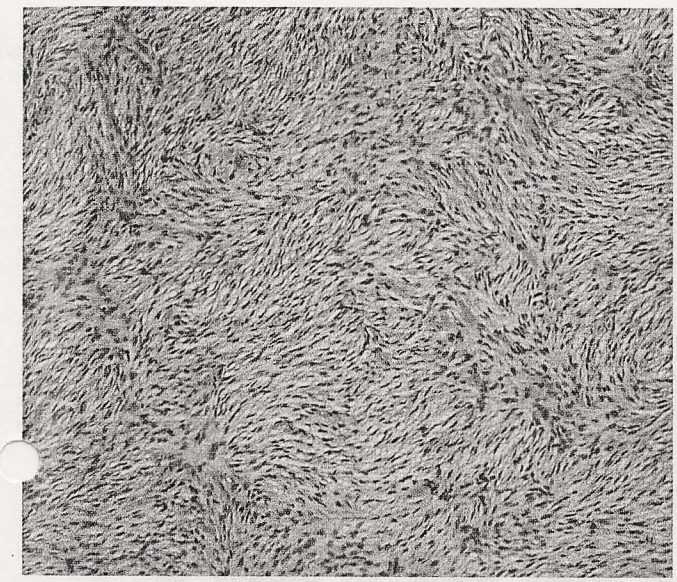

Figure 8.121. A histologic section of an equine eyelid sarcoid. Note the prominent spindle cells and characteristic interlacing pattern. (Hematoxylin and eosin, original magnification 300X.)

Eyelid melanomas are round to oval, black to brown tumors that involve eyelid skin of older animals (Fig. 8.122A). Light microscopic features include variable, pigmented, round- to spindle-shaped melanocytes with prominent nucleoli (Fig. 8.122B). Most eyelid melanomas are benign and should be termed melanocytomas. Occasional eyelid melanomas are malignant based on the pleomorphic cells with mitotic index greater than 2 per high-power field with evidence of invasive growth into the dermis and subcutaneous tissues. Malignant melanomas are often accompanied by ulceration and inflammation. Poorly pigmented melanomas can be difficult to diagnosis on the basis of morphology, and immunohistochemical stains, including S-100, tyrosinase, HMSA5, and melanin A, may be useful to confirm the diagnosis.

Conjunctival melanoma, in contrast, is usually malignant, and without effective therapy, these neoplasms are invasive and prone to metastasize.[229–232] Gross examination reveals a black to brown, flat to nodular mass that grows through the conjunctiva (Fig. 8.123). The bulbar surface of the third eyelid is the most common site of origin. Light microscopic examination of biopsies or enucleation or exenteration specimens confirms the diagnosis. The neoplastic melanocytes are usually heavily pigmented and vary from round- (epithelial) to spindle-shaped cells. One of the characteristics of these melanomas is junctional activity in which nests of neoplastic melanocytes extend out from the primary neoplasm at the border epithelium and substantia propria (Fig. 8.124). Conjunctival melanomas invade the subconjunctiva and orbit, and although a large prospective study is still lacking, these neoplasms should be considered malignant, and they may recur and metastasize when incompletely removed.

Conjunctival hemangioma and hemangiosarcomas are occasionally diagnosed in dogs, horses, and other domestic animals.[233–240] Clinical features include a vascular mass that often develops in the bulbar conjunctiva and extends into the cornea (Fig. 8.125). Light microscopic features confirm the diagnosis. Hemangiomas are characterized with well-differentiated capillaries, pleomorphic hyperchromatic spindle cells, and prominent hyalinized collagen beams (Fig. 8.125c). Hemangiosarcomas have poorly differentiated endothelial cells, lack well-developed capillaries, and are consistently invasive. The poorly differentiated hemangiosarcomas may require immunohistochemistry to confirm the diagnosis. Hemangiosarcomas are malignant,

(a) (b)

Figure 8.122. A. Eyelid melanoma in a Golden Retriever. Note the black, pedunculated eyelid tumor. **B.** Plump melanocytes arranged in bundles with hyperplastic epithelium typical of eyelid melanomas. These eyelid melanomas are usually benign, and excisional biopsies are curative. (Hematoxylin and eosin stain, original magnification 300X.)

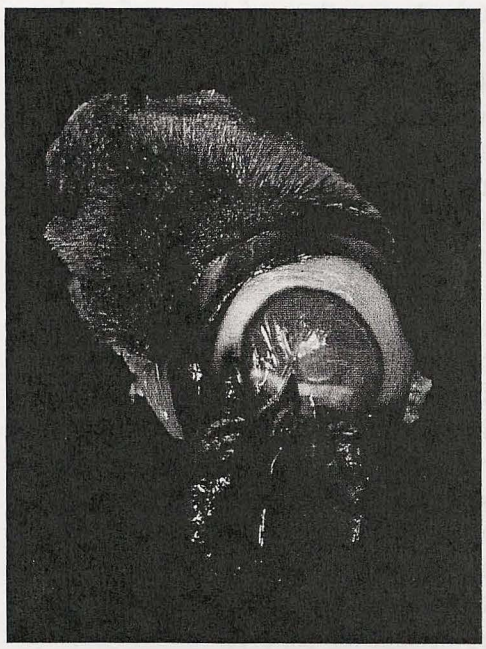

Figure 8.123. Conjunctival melanoma, when ignored, can invade and metastasize. Note the involvement of the conjunctiva, third eyelid, and cornea in this exenteration specimen.

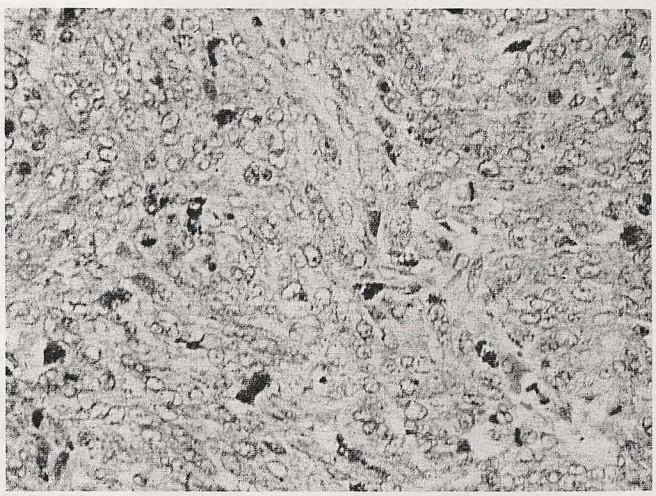

Figure 8.124. Conjunctival melanoma with anisocytosis and anisokaryosis and several mitotic figures. The malignant melanomas will grow in tendrils and establish small packets of neoplastic cells, often away from the apparent edges of the tumor. (Hematoxylin and eosin stain, original magnification 300X.)

and recurrence at the original site and metastasis, especially in horses, are reported,[237–240] while hemangiomas are benign.

Corneal and Scleral Neoplasia

Although the cornea is commonly invaded by squamous cell carcinoma, and occasionally by vascular neoplasms, conjunctival melanoma, and peripheral nerve sheath tumors, the primary neoplasms of the cornea are limited to limbal melanocytoma[241–244] and occasionally primary corneal squamous cell carcinoma.[245–246] There are no primary scleral neoplasms reported, although several primary conjunctival and intraocular neoplasms invade the sclera; the orbital, conjunctival, and intraocular neoplasia discussions in this chapter provide further detail.

Limbal melanocytoma is a relatively common primary neoplasm of the cornea and sclera of the dog, and it occasionally occurs in other species (cats).[244] Limbal melanocytomas

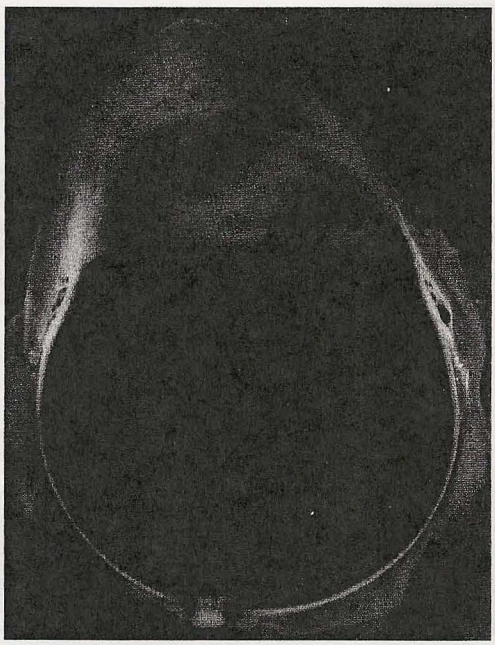

(a)

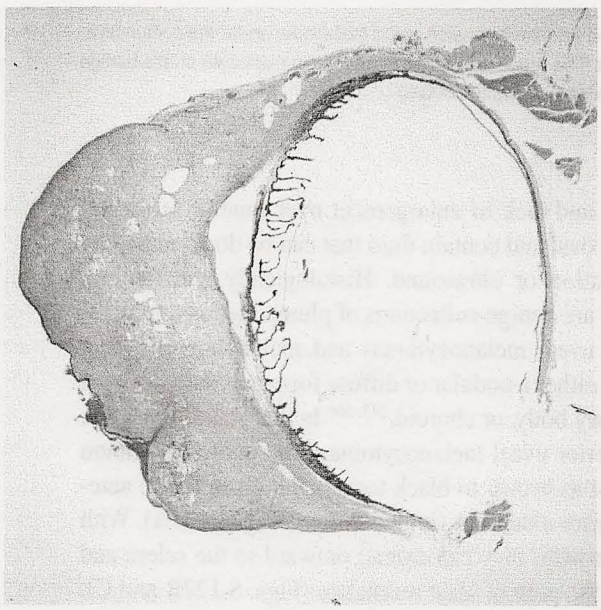

(b)

(c)

Figure 8.125. **A.** Gross section of a mature dog with a vascularized corneal tumor. **B.** Subgross section of this tumor reveals corneal and scleral invasion and multiple channels within the neoplasm. (Original magnification 2X.) **C.** Light microscopy of the tumor in A and B confirms the diagnosis conjunctival hemangiosarcoma. Note the well-differentiated vascular channels containing red blood cells. (Hematoxylin and eosin stain, original magnification 350X.)

are benign neoplasms that arise from a band of melanocytes located deep in the cornea apposed Descemet's membrane. Their gross appearance is pathognomonic with a rainbow-shaped band of variably pigmented neoplastic cells that extend into the deep corneal stroma and a mass of similar cells that extend outward toward the limbus and into the episclera, Tenon's capsule, superficial cornea, and conjunctiva (Fig. 8.126A). Light microscopy reveals a bland population of often well-pigmented melanocytes that preclude examination of cellular morphology without bleaching (Fig. 8.126B). Once the melanin is bleached, the cellular morphology confirms the benign nature of these neoplasms. The melanocytes manifest with mild anisocytosis, variably sized nucleoli, and minimal mitotic figures and tissue invasion; two cell types are present, a bland spindle cell and a large, noncohesive, melanin-laden cell, with the intercytoplasmic pigment displacing the nucleus to the periphery of the cell. Limbal melanomas occur in two age groups of dogs: young animals in which limbal melanomas manifest clinically with continued local growth into the limbal tissues, necessitating removal to prevent ongoing ocular involvement; and dogs older than 8 years in which the limbal melanomas are slow to enlarge and can be observed

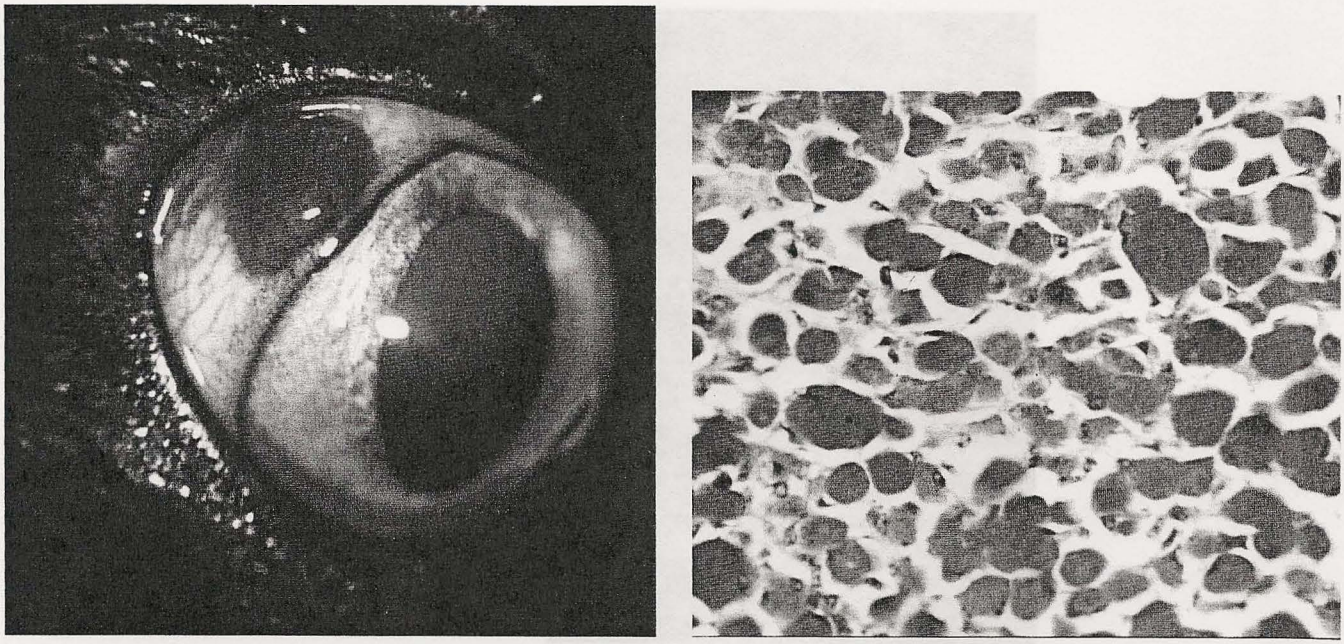

(a) (b)

Figure 8.126. **A.** Limbal melanoma in cat. Note the small, fan-shaped, deep corneal extension and the extension of the melanoma under the conjunctiva. No intraocular melanoma was present in this eye. **B.** Histology from a limbal melanoma in a cat. The predominate cell is a plump melanocyte of this benign neoplasm. Occasional pigmented spindle cells are present. (Hematoxylin and eosin stain, original magnification 300X.)

without therapy. Regardless of growth, these melanocytomas do not metastasize, and local invasion of limbal tissues are the extent of damage of these neoplasms. In cats, the tumors are usually benign and tend to be slow-growing.

Primary corneal squamous cell carcinoma is uncommon in all animals.[246] The gross manifestations include a friable, pink corneal mass that is not attached to the limbus. The light microscopic findings are similar to that described for conjunctival squamous cell carcinoma and include epithelial atypia, hyperchromasia, mitoses, anaplasia, and invasion of the stroma. The differential diagnoses of corneal squamous cell carcinoma include extension from a primary conjunctival site, corneal carcinoma in situ, corneal papilloma, and conjunctival inclusion cysts. Chronic corneal exposure is reported as a predisposing cause.[246]

Intraocular Neoplasia

Intraocular neoplasia includes a variety of primary neoplasms of the uvea and its lining epithelium and many metastatic neoplasms. Most of the primary neoplasms are benign; however, their growth and induction of vascular tissues and inflammation often contribute to eye-threatening complications. The clinical and histologic features of common primary and metastatic intraocular neoplasms reported are listed in Table 8.10.

Uveal Neoplasia

Uveal melanomas are the most common intraocular neoplasms. The differentials that should be considered during the clinical examination include iridal nevi and freckles and uveal cysts. The former are common in all species and can be differentiated from uveal melanomas by their sessile nature, flat appearance, and lack of enlargement over time. Uveal cysts are round to oval and contain fluid that can be documented by retroillumination or ultrasound. Histologically, the freckles and the nevi are benign collections of plump melanocytes.

Anterior uveal melanocytomas and melanomas manifest clinically in either a nodular or diffuse form and develop from the iris, ciliary body, or choroid.[247–266] In dogs and horses, the nodular anterior uveal melanocytomas are the most common and manifest as brown to black tumors that extend into anterior or posterior chambers or the vitreous (Fig. 8.127A). With continued growth, they can extend outward to the sclera and grow along the path of least resistance (Figs. 8.127B and C). They commonly extend out of the globe along the aqueous collecting veins at the limbus, along the choroid, and out by the optic nerve. Anterior uveal melanomas vary considerably in pigmentation, and poorly pigmented and amelanotic types are often misdiagnosed clinically as ciliary epithelial neoplasms. Anterior uveal melanomas are typically a benign neoplasm that extend into ocular tissues and induce inflammation and preiridal fibrovascular membranes. Malignant variants do occur; however, enucleation before the melanoma extends beyond the globe is usually curative. When melanomas are examined with light microscopy, the two cell types described for limbal melanocytomas are observed: (a) the more common, plump, overdistended pigmented melanocytic cell represents the end-stage postmitotic cell, and (b) the germinal melanocytic cell, which is less pigmented, is fusiform in shape, and contains a prominent central nucleus (Fig. 8.127D). Mitotic figures are uncommon except in the occasional more malignant variety that account for less than 5% of the total population of these neoplasms.[250–260]

Table 8.10 Gross and Histologic Characteristics of the Primary Intraocular Neoplasms and Some Metastatic Neoplasms

Neoplasm	Species	Gross Appearance	Histologic Features
Nodular uveal melanoma	Dog, horse, cat	Nodular variably pigmented iridal tumor, or ciliary mass (Fig. 8.127A & B)	Variably pigmented spindle to ovoid cells with small, round, or slightly elongated nuclei and large, round, heavily pigmented cells (Fig. 8.127C & D)
Diffuse iris melanoma	Cat, occasionally seen in dogs	Diffuse brown iridal thickening (Fig. 8.129A)	Iris is thickened by spindle to oval, often lightly pigmented cells with prominent nucleoli; usually mitotic figures are rare and extend out through sclera around the aqueous collecting veins (Fig. 8.129B)
Choroidal melanoma	Dog	Brown choroidal mass (Fig. 8.128A)	Choroidal location is key to diagnosis, variably pigmented spindle to polyhedral cells with eccentric nuclei and single nucleoli, will invade the sclera often extending into the orbit around the optic nerve (Fig. 8.128B & C)
Ciliary adenoma	Dog, cat	Pink to light brown mass that grows into the vitreous behind the lens or into the posterior chamber and through the pupil or into the anterior chamber through the iris (Fig. 8.132A)	Tumor is composed of sheets and cords of pale-staining cuboidal columnar cells with eosinophillic or cytoplasm that may contain a few melanin granules and distinct basement membranes (Fig 8.132B & C)
Ciliary adenocarcinoma	Cat, dog, occasionally other species	Ciliary, iridal to anterior choroidal tumors often accompanied by inflammation	Solid sheets of epithelial cells with less differentiation and prominent mitotic figures, pleomorphism, and invasion of the ciliary body, choroid, and iris (Fig. 8.133)
Medulloepithelioma	Dog, cat, occasionally other species	Young animal with leucocoria, hyphema, or a white mass arising from the ciliary body and extending into the vitreous (Fig. 8.134A)	Nonteratoid: contain cells that resemble RPE and ciliary epithelium and neuroglia (Fig. 8.134B & C) Teratoid: contain hyaline cartilage, bone rhabdomyoblasts, neuroglia, and mesenchymal cells
Retinoblastoma	Dog, llama (single reports); rare in any species	Retinal–choroidal mass in a young animal	Small, neuroblastic cells with hyperchromatic nuclei and scant cytoplasm with rosettes and pseudorosettes formation
Feline intraocular sarcomas	Reports limited to cats	Yellow-tan-white, rapidly growing intraocular mass (Fig. 8.131A)	Cell types are variable and include plump spindle cells to round cells, to giant cells (Fig. 8.131B & C)
Intraocular nerve sheath tumors	Rare; dog, cat	Pale gray iridal or ciliary tumors	Interlacing bundles of spindle cells with Antoni A or B patterns
Intraocular leiomyosarcoma	Rare; dog	Gray iridal, anterior or posterior tumor	Spindle cells resembling smooth muscle
Hemangiomas of the iris and ciliary body	Rare in any species	Vascularized mass in iris or ciliary body	Vascular cords and sinuses with plump, endothelial-like cells
Optic nerve meningioma	Most common optic nerve neoplasm in any species	Pale gray mass that extends from the orbit into the optic disc uncommonly (most induce exophthalmos) (Fig. 8.136A)	Whorls and nests of spindle cells that arise from the meninges; calcification is common (Fig. 8.136B)
Other optic nerve neoplasms	Gliomas, astrocytomas, etc.; rare in all species	Gray optic nerve mass	Small, round cells with prominent nuclei (Fig. 8.135)
Extraskeletal intraocular osteosarcoma	Rare (single report in dog)	Uveitis	Pleomorphic spindle cells with osteoid production

(continued)

Table 8.10 Gross and Histologic Characteristics of the Primary Intraocular Neoplasms and Some Metastatic Neoplasms *(continued)*

Metastatic intraocular neoplasms	May occur in all species with chronic systemic metastatic neoplasia	Uveitis (hyphema, aqueous, and vitreous flare), retinal detachment, secondary glaucoma, cataract	Variable depending on the primary neoplasms (mesenchymal: Fig. 8.137A & B; round cell: Fig. 8.138; epithelial: Fig. 8.139); most invade the ciliary body and choroid

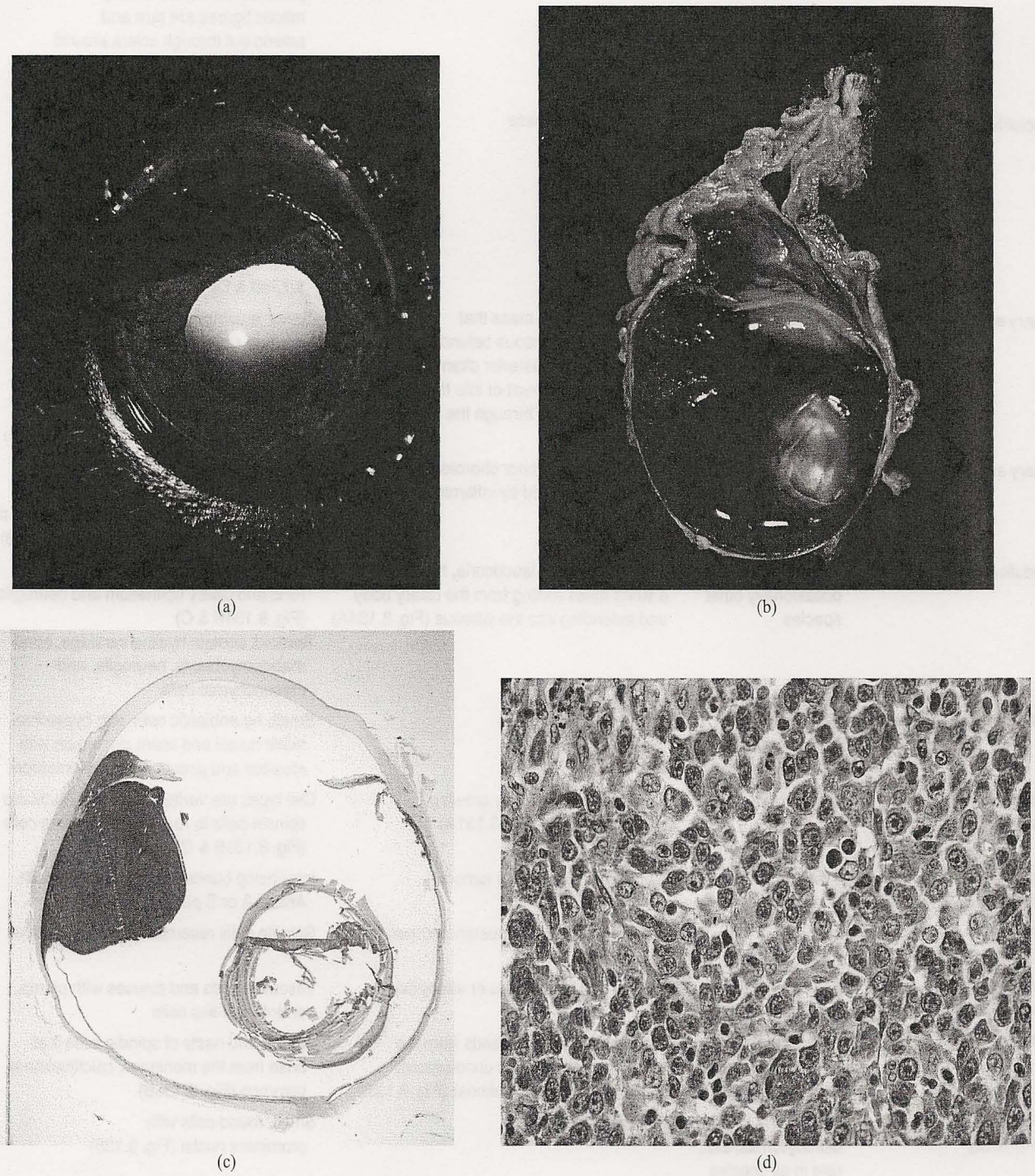

Figure 8.127. **A.** Clinical appearance of a nodular uveal melanoma in a dog. **B.** Gross section of a dog's eye with a nodular uveal melanoma. Note the black nodular mass extends throughout the anterior uvea. **C.** Subgross section of a dog's eye with nodular uveal melanoma noted in B. Note the involvement of the ciliary body and iris. (Hematoxylin and eosin stain, original magnification 2X.) **D.** Histologic section of a nodular melanoma noted in B and C. Note the anisocytosis, anisokaryosis, prominent distinctive nucleoli, and cytoplasm with occasional pigment granules. (Hematoxylin and eosin stain, original magnification 400X.)

Choroidal melanocytomas are much less common in domestic animals than in humans. Choroidal melanocytomas originate in the choroid (Fig. 8.128A) and display morphology and behavior similar to that of anterior uveal melanomas.[259–266] They are typically diagnosed later in their course of disease because of their hidden location. They manifest grossly as heavily pigmented choroidal tumors; if they extend through the basement membrane of the RPE, they will extend under the retina, induce detachment, and extend into the vitreous (Fig. 8.128B). Choroidal melanocytomas also grow slowly and follow the path of least resistance and usually extend out of the globe into the orbit around the optic nerve. Poorly pigmented choroidal melanocytomas are uncommon. The pigmented choroidal melanomas must be bleached to allow the pathologist to evaluate the cellular detail. The histologic appearance is typical of most uveal melanomas and includes variably pigmented, round to polyhedral cells, which vary from plump cells with pyknotic nuclei to plump or slender spindle cells or even small, epitheliod cells (Fig. 8.128C). Mitotic figures vary from none to significant numbers. Only occasional malignant versions of these choroidal melanomas will metastasize.

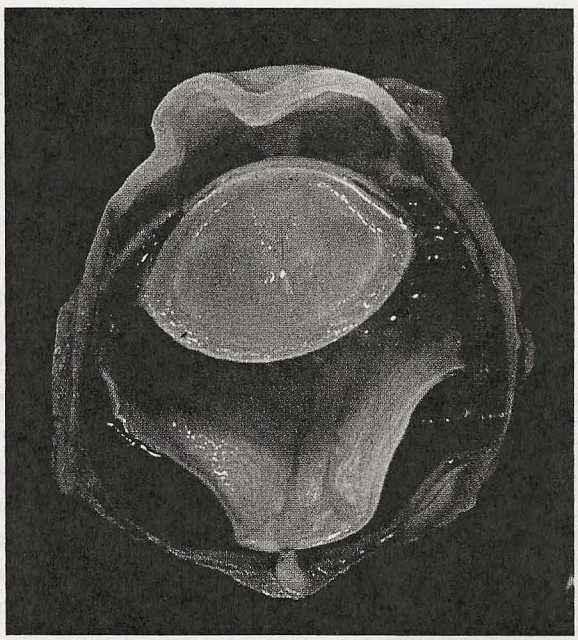

(a)

(b)

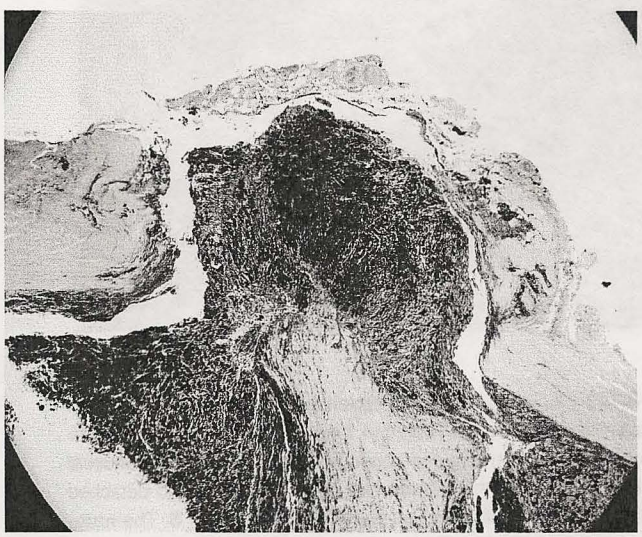

(c)

Figure 8.128. **A.** Gross section of a Bouin's-fixed eye from a dog with a brown choroidal tumor that extends into the sclera and through the choroid. **B.** Subgross appearance of a choroidal melanoma in a dog. This melanoma is invading the orbit, and a large preiridal fibrovascular membrane is present. (Hematoxylin and eosin stain, original magnification 2X.) **C.** The light microscopic features of choroidal melanoma are similar to other uveal melanomas. They commonly exit the globe along a path of least resistance orbit around the optic nerve. (Hematoxylin and eosin stain, original magnification 100X.)

Diffuse iris melanomas occur in cats as a variably brown pigmented neoplasm that originates in the anterior iridal border, and as these neoplastic cells proliferate, they obliterate the iris architecture and extend out the filtration angle (Fig. 8.129A).[267–278] The cells are noncohesive and may be seen within the aqueous, on the anterior lens capsule, and seeding the outflow pathway. The light microscopic appearance includes a pleomorphic bland population of oval to round epithelial cells that contain prominent, small, round nuclei that are usually displaced to the periphery (Fig. 8.129B). The intracytoplasmic pigmentation is variable, and amelanotic forms are not uncommon. These melanomas will extend into the ciliary body and commonly exit the filtration angle and grow into the sclera and cornea. Secondary intraocular changes include glaucoma and mild uveitis. These melanomas are generally more malignant than the nodular melanocytoma, and some will metastasize; involvement of the scleral venous plexus with melanoma cells within the aqueous collecting veins warrants a poor prognosis. The percentage of cases that metastasize is unknown but may approach 20% of the total cases. This neoplasm is also induced as an animal model with intracameral feline sarcoma virus injections.[279–280] The presence of these viral particles in spontaneous clinical cases is unknown. However, PCR for this virus in two studies of a few naturally occurring feline diffuse iris melanomas has been inconclusive.[281–282]

Primary intraocular spindle cell neoplasms are uncommon in all animals, and the reports are limited to a few miscellaneous spindle cell neoplasms of the uvea of dogs[283–285] and posttraumatic sarcomas of cats.[281–282]

Iridal tumors of blue-eyed dogs are unique, uncommon, low-grade spindle cell neoplasms that develop in dog breeds such as the Siberian Husky. These neoplasms manifest clinically as a flat or nodular vascularized iridal mass that will extend into the anterior chamber and ciliary body (Fig. 8.130). Light microscopic examination reveals a pleomorphic spindle cell population that most likely originates from iridal nerves. Metastasis of these spindle cell neoplasms has not been reported. Other incidental spindle cell uveal neoplasms include osteosarcoma,[285] peripheral nerve sheath neoplasms,[284] and smooth muscle

(a)

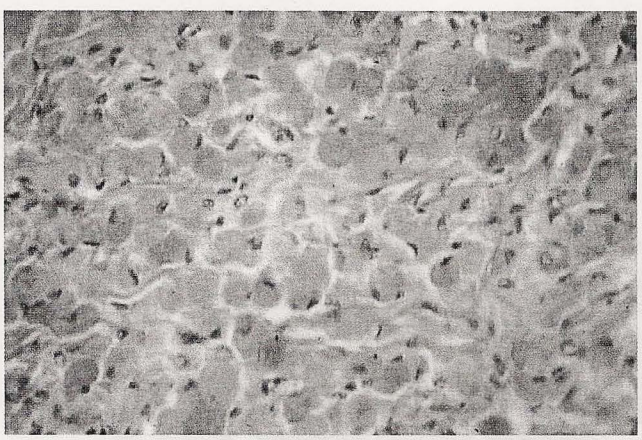

(b)

Figure 8.129. A. The subgross characteristics of a malignant feline diffuse iridal melanoma. Note the thickened, heavily pigmented iris and extension through the sclera around the aqueous collecting veins. The unusual findings in this eye were the anterior lens capsule rupture and detached retina. (Periodic acid-Schiff stain, original magnification 2X.) **B.** The histologic characteristics of diffuse iris melanoma in cats are varied; however, most of the neoplastic melanocytes are a bland population of plump cells with a displaced peripheral nucleus and limited numbers of spindle cells. Mitotic figures are usually uncommon, and nucleoli are inconspicuous. (Hematoxylin and eosin stain, original magnification 250X.)

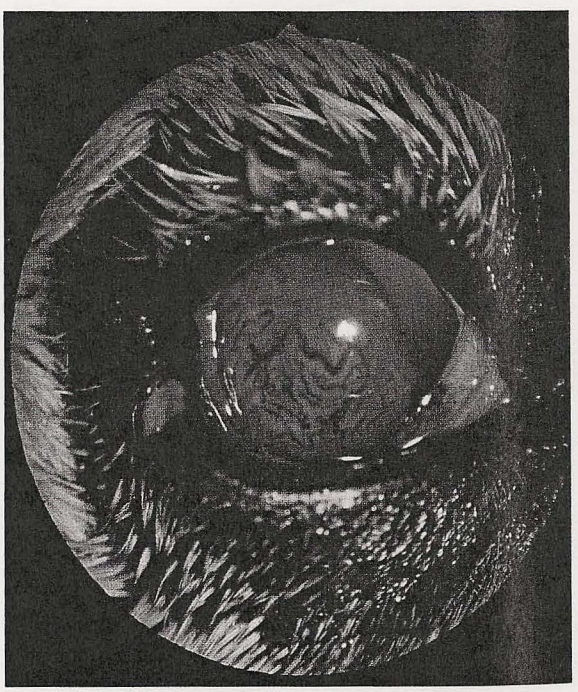

Figure 8.130. A well-vascularized iridal spindle cell neoplasm of a blue-eyed Siberian Husky.

leiomyomas.[283] The prognoses for these rare uveal spindle cell neoplasms are unknown.

However, feline intraocular sarcomas are malignant and were originally reported as posttraumatic sarcomas. Most, or perhaps all, of these spindle cell sarcomas are associated with a ruptured lens.[291, 296] The clinical manifestations include leucocoria and evidence of a rapidly growing white mass. These neoplasms are malignant and invade the sclera and commonly exit the globe into the orbit around the optic nerve and at the filtration angle (Fig. 8.131A). Most, if not all, of these sarcomas probably develop from neoplastic changes in metaplastic lens epithelium, sometimes years after a lens capsule rupture. Light microscopy reveals a variable spindle cell neoplasm with many phenotypes. These may resemble osteosarcomas, fibrosarcomas, chondrosarcomas, and even giant cell varieties (Figs. 8.131B, C, and D). These pleomorphic neoplasms can resemble other intraocular neoplasms, including ciliary adenocarcinomas and some metastatic sarcomas and carcinomas, and immunohistochemical staining is warranted in some cases.[296] When these spindle cells exit the globe, they may extend into the orbit and cranial vault and metastasize to the lung, liver, and other organs.

Ocular Neuroectodermal Neoplasms

Neoplasia of neuroectoderm of animals are considered uncommon (ciliary adenomas and adenocarcinomas) and rare (medulloepithelioma, retinoblastoma, astrocytomas, and gliomas). Several neoplasms of the neuroectoderm are reported in a variety of species: iridociliary adenomas and adenocarcinomas[297–302]; retinoblastoma[303, 304]; medulloepitheliomas[305–314]; and gliomas, astrocytomas, oligodendrocytomas, and glioblastomas.[315, 316] With the exception of some ciliary adenocarcinomas, these neoplasms are considered benign, and metastasis is uncommon.

Iridociliary adenomas are the most common of these neuroectodermally derived neoplasms. The clinical manifestations include a variably pigmented, usually pink to white endophytic tumor that displaces the iris forward or grows into the posterior chamber and through the pupil in front of the lens or into the vitreous behind the lens (Fig. 8.132A). Signs of uveitis, including hyphema and aqueous flare, occur with larger adenomas because preiridal fibrovascular membranes are commonly present. Light microscopic examination reveals variably pigmented papillary or solid tumors composed of neuroectoderm that is very similar in appearance to anterior uveal epithelium (Figs. 8.132B and C). Many cells are cuboidal, and they usually secrete prominent basement membranes. These neoplasms grow slowly, and metastasis has not been reported.

Iridociliary adenocarcinomas are also rare neoplasms that manifest as a diffuse enlargement of the ciliary body and iris, and they may extend into the choroid. Uveitis is a common clinical manifestation. Light microscopy reveals sheets of epithelial-like cells with numerous mitotic figures, anisocytosis, and anisokaryosis with active invasion of intraocular tissues (Fig. 8.133). These poorly differentiated neoplasms often require histochemical and immunohistochemical stains to differentiate them from intraocular sarcomas, metastatic carcinomas, lymphosarcomas, and melanomas in many species. Differentiating stains include positive staining with periodic acid-Schiff, neurospecific enolase, vimentin, and no staining with cytokeratin, melanocytic, and lymphosarcoma markers.[296] Asteroid hyalosis and preiridal fibrovascular membranes are commonly associated with both benign and malignant iridociliary neoplasia.

Medulloepitheliomas are primitive neuroectodermal neoplasms that are congenital, although they may not manifest clinically until the affected animal is several months to years old. They have been reported in horses, dogs, and llamas.[305–314] The clinical manifestations include a leucocoria due to a pink to white endophytic papillary mass that extends into the vitreous or, less commonly, the posterior chamber (Figs. 8.134A and B). These neoplasms develop from primitive pluripotential neuroectoderm destined to become iridociliary epithelium. Light microscopic examination reveals sheets and rosettes of primitive neuroblasts with elongated cells with prominent basement membranes (Fig. 8.134C). These neoplasms often contain islands of muscle, cartilage, bone, and primitive vitreous and neurogenic tissue—hence the common term *teratoid medulloepithelioma*. Medulloepitheliomas are easily misdiagnosed as retinoblastoma, which is not surprising given the origin of both from neuroectoderm that lines the primitive optic cup.

Retinoblastomas are very rare in domestic animals,[303–304] although it is the most common primary intraocular neoplasm in humans. The clinical manifestations are leucocoria caused by an endophytic vitreous tumor that is variably pigmented. Histologic features include rosettes and fluerettes of primitive neuroblast cells that were destined to become retina.

Primary neoplasia of the neuroectoderm of the optic nerve is uncommon and includes gliomas and astrocytomas. These neoplasms are rare, and the clinical manifestations and light microscopic descriptions and features are limited to a few reports.[315–321] Clinical manifestations of gliomas of the optic nerve and retina include pale masses that extend from the optic nerve into the vitreous. Light microscopy reveals a mass of glial cells. There are varied types, including astrocytomas (Fig. 8.135), oligodendroglioma, ependymoma, and astrocytoma. To differentiate these gliomas, immunohistochemistry is required.[315, 316] The prognosis for these rare neuroectodermal neoplasms is unknown.

Neoplasia of the Neural Crest Tissues of the Optic Nerve

Meningiomas arise from the meninges that envelope the optic nerve and brain.[322–327] When meningiomas extend into orbital tissues (Fig. 8.136A) or the eye, the clinical manifestations include exophthalmos and third eyelid prolapse. Histologic features include epithelioid cells arranged in nests (Fig. 8.136B). Other cellular variations include more primitive mesenchymal cells with prominent cytoplasm, and often

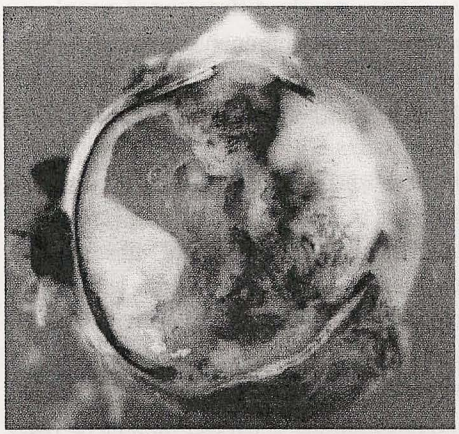

(a)

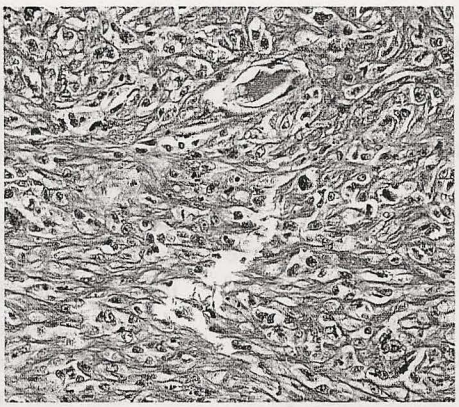

(b)

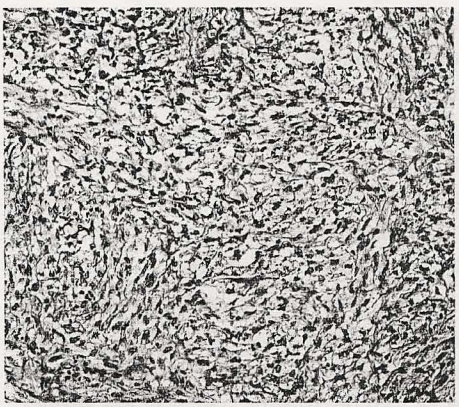

(c)

(d)

Figure 8.131. A. Feline intraocular sarcomas are aggressive neoplasms that will often encircle the inside of a eye and obliterate the anterior and posterior segment and extend out through the sclera. **B.** A mixed neoplastic cell type of feline intraocular sarcoma. There is bone production and marked anisocytosis and anisokaryosis. (Periodic acid-Schiff stain, original magnification 300X.) **C.** A foamy spindle cell variant of feline intraocular sarcoma. (Periodic acid-Schiff stain, original magnification 300X.) **D.** Feline intraocular sarcomas are malignant, and extension through the sclera is common. Note the neoplastic cells invading the sclera and extension into the episclera. (Periodic acid-Schiff, original magnification 250X.)

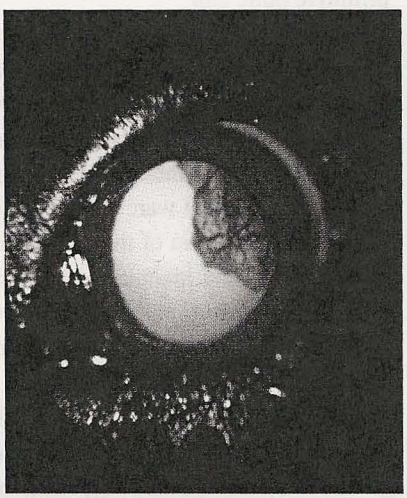

(a)

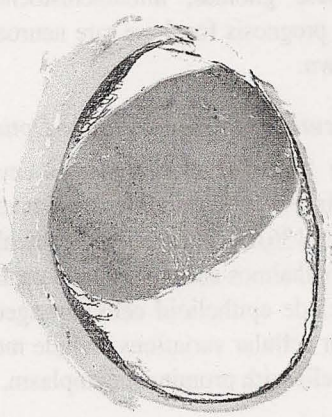

(b)

(c)

Figure 8.132. A. Ciliary adenomas are usually pink-colored masses that grow around the lens and become visible through the pupil, as present in this American Cocker Spaniel. **B.** A dense, cellular tumor has grown into the vitreous off the ciliary processes and has the typical subgross appearance of a ciliary adenoma in this cat. **C.** A histologic section of the ciliary adenoma noted in B. Note the characteristic cords of epithelial cells with pale blue cytoplasm and prominent basement membranes. There are many similarities to the normal nonpigmented ciliary epithelium on the ciliary process, confirming a well-differentiated benign adenoma. (Periodic acid-Schiff stain, original magnification 300X.)

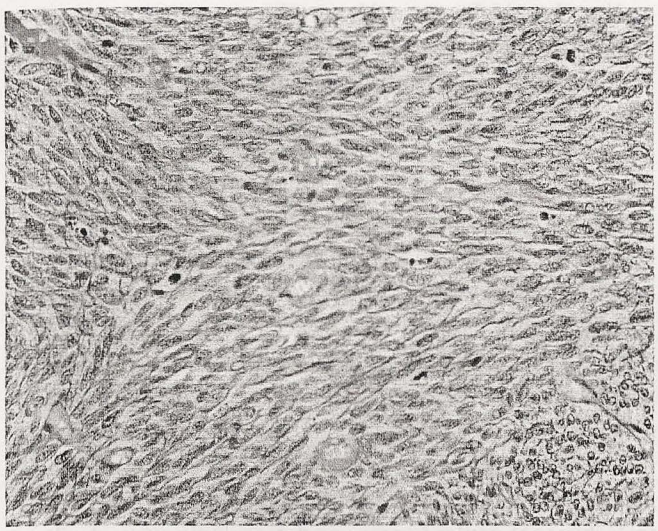

Figure 8.133. Ciliary adenocarcinomas are variable in appearance and can resemble intraocular sarcomas and even medulloepitheliomas. They produce prominent basement membranes and grow in sheets. They usually have some of the characteristics of ciliary epithelium, including the round to oval nucleus, as noted in this globe. (Periodic acid-Schiff stain, original magnification 400X.)

there are areas of osseous or cartilaginous metaplasia that account for the calcification noted on imaging studies of these neoplasms. Meningiomas are usually benign, although they will grow into adjacent orbital tissues. Metastasis has been reported,[324] but many are slow growing and relatively benign neoplasms.

Metastatic Ocular Neoplasia

Metastatic neoplasia to the eye does occur, and as radiation therapy and chemotherapy extends life expectancy, an increased number of metastatic ocular neoplasms would be expected. All malignant neoplasms could metastasize to the ocular tissues given the prominent vascular supply to the eye and orbit. Lymphosarcoma is the most common metastatic ocular neoplasm.

The clinical manifestations of metastatic ocular disease are nonspecific and include exophthalmos if the metastases are in the orbit or uveitis when the ocular tissues are invaded. We limit our description to general histologic features of metastatic ocular neoplasms. Most intraocular metastatic neoplasms manifest clinically as an anterior uveal tumor

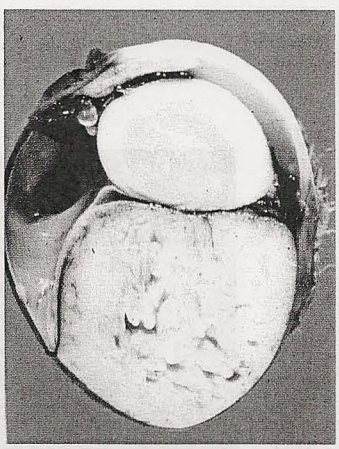

(a)

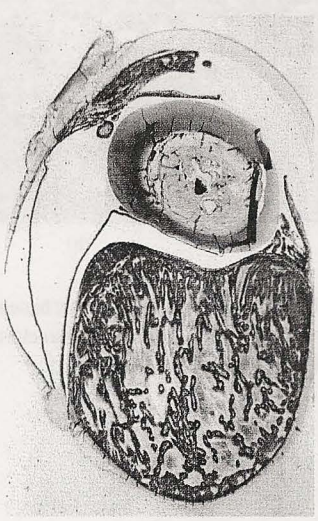

(b)

(c)

Figure 8.134. **A.** A gross section of an ocular medulloepithelioma. **B.** Subgross section of a medulloepithelioma. These neoplasms originate from the immature ciliary epithelium and extend into the vitreous or, as in this specimen, under the retina and through the iris. (Periodic acid-Schiff stain, original magnification 2X.) **C.** Rosettes are one of the characteristics of medulloepitheliomas. (Hematoxylin and eosin stain, original magnification 300X.)

Figure 8.135. Subgross section of a dog's eye containing an optic nerve astrocytoma. Note the neoplasm is centered on the optic disc and extends into the vitreous cavity. (Hematoxylin and eosin stain, original magnification 2X.) (Reprinted with permission, Caswell J, Curtis C, Gibbs B. Astrocytoma arising at the optic disc in dog. *Can Vet J* 1999;40:427–428.)

and/or choroidal mass with or without retinal detachment. These neoplasms induce significant uveitis with aqueous flare and hyphema. These metastatic neoplasms extend into the uvea via the ciliary and choroidal arteries and extend into the ocular tissues (Fig. 8.137A). The cellular characteristic of epithelial cells, mesenchymal (Fig. 8.137B), and round cell malignant neoplasms assist the pathologist in the selection of appropriate histochemical and immunohistochemical differentiating labels. These metastatic neoplasms are often anaplastic and easy to misdiagnose as malignant primary intraocular neoplasms. Lymphosarcomas are round cell neoplasms that invade anterior uveal tissues and choroid (Fig. 8.138). They are also the most common metastatic neoplasms to the orbit and eyelid tissues. They are easily identified by common lymphocytic markers. Carcinomas will also metastasize to ocular tissues, most commonly choroid, ciliary body, and iris. These include renal, respiratory, mammary, and gastrointestinal carcinomas that are often so anaplastic that the original tissue of origin is not discernable. These carcinomas often grow in sheets on the surfaces of intraocular tissues (Fig. 8.139). They also produce prominent basement membranes and most will stain readily with cytokeratins markers.[296]

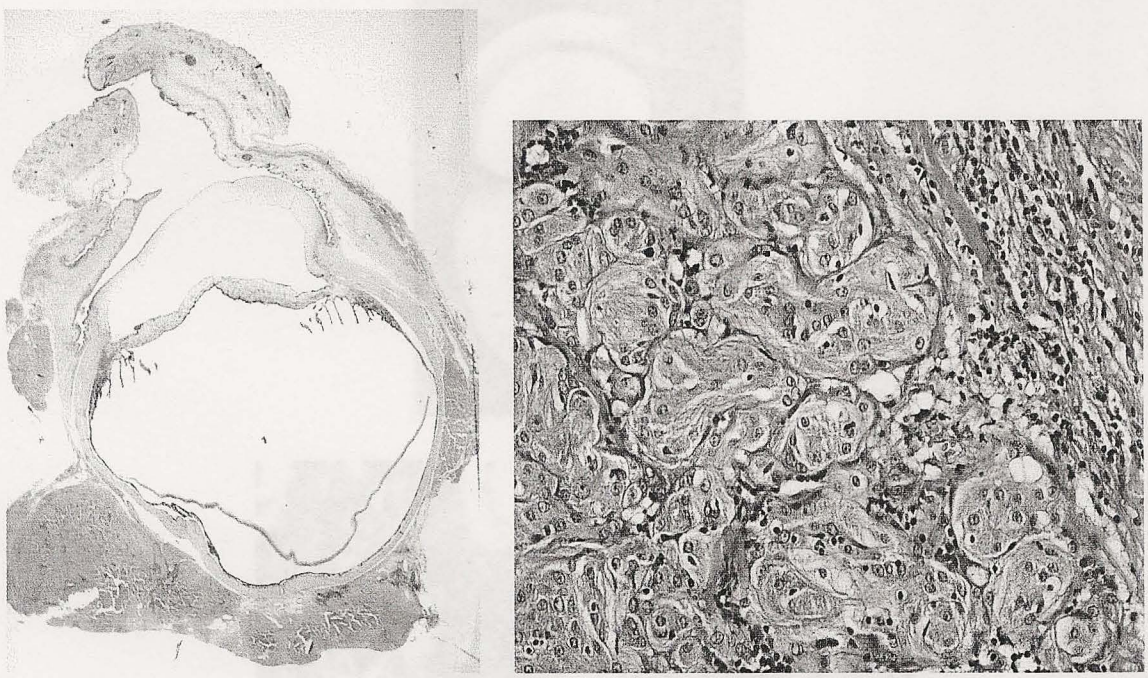

(a) (b)

Figure 8.136. **A.** Subgross section of a dog's eye with an orbital meningioma. Note the invasion of the orbital tissues by this neoplasm. (Hematoxylin and eosin stain, original magnification 2X.) **B.** Histologic section of the optic nerve meningioma in A. Note the characteristic pale pink cytoplasm, small, dark-staining nuclei and packets of neoplastic cells. (Hematoxylin and eosin stain, original magnification 400X.)

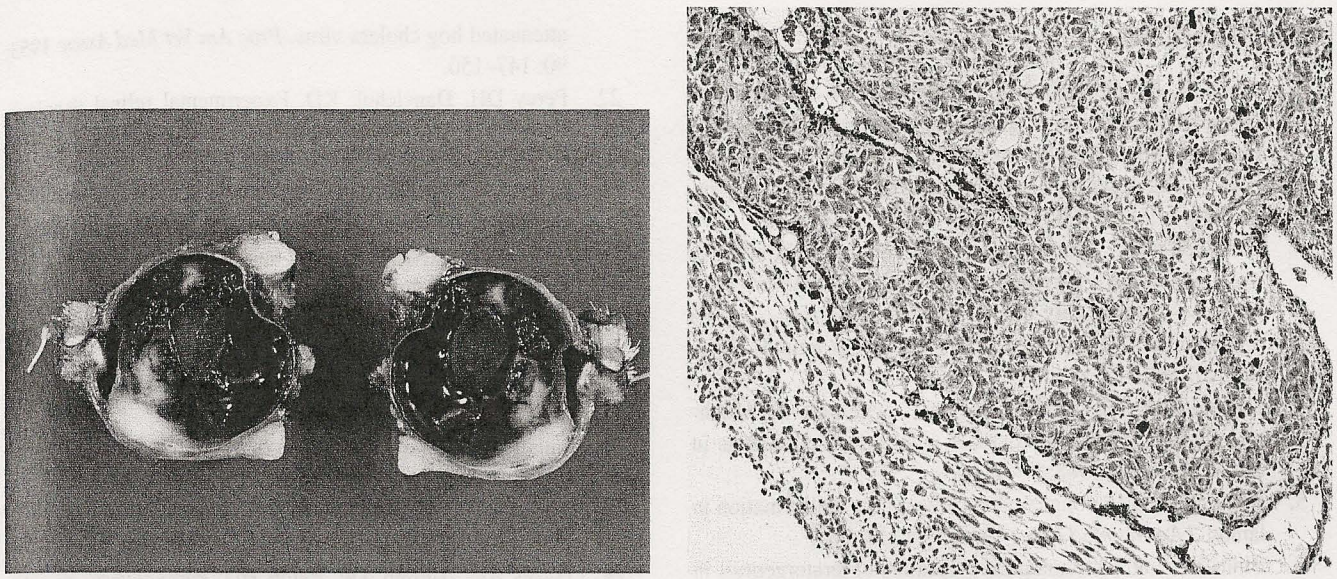

(a) (b)

Figure 8.137. A. Metastatic uveal neoplasia in a dog. The white tissue is the neoplasm and is in a location consistent with many metastatic intraocular tumors. These metastatic neoplasms enter the globe by blood vessels and invade the uveal tissues, often growing in the ciliary body and choroid initially. (Original magnification 1X.) **B.** Histologic section of a ciliary process from a dog's eye with a poorly differentiated metastatic sarcoma. Note how this metastatic sarcoma distends the ciliary process and extends into the vitreous. (Hematoxylin and eosin stain, original magnification 300X.)

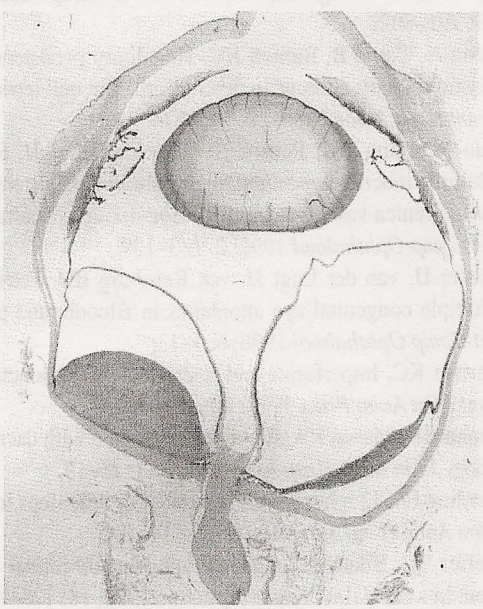

Figure 8.138. Metastatic choroidal lymphosarcoma in a cat. (Hematoxylin and eosin stain, original magnification 2X.)

Figure 8.139. Metastatic carcinoma extending in sheets over the ciliary body of a cat. (Periodic acid-Schiff stain, original magnification 300X.)

REFERENCES

1. Sasoh M, Ma N, Yoshida S, Semba R, Uji Y. Immunocytochemical localization of glutamate in normal and detached cat retina. *Invest Ophthalmol Vis Sci* 1998; 39: 786–792.
2. Hale F. The relation of vitamin A to anophthalmos in pigs. *Am J Ophthalmol* 1935; 18: 1087–1093.
3. Bendixen HC. Littery occurrence of anophthalmia or microphthalmia together with other malformations in swine—presumably due to vitamin A deficiency of the maternal diet. *Acta Pathol Microbiol Scand* (suppl) 1944; 54: 161–179.
4. Leipold HW, Huston K. Congenital syndrome of anophthalmia-microphthalmia together with associated defects in cattle. *Vet Pathol* 1968; 5: 407–418.
5. Binns W, et al. A congenital cyclopean-like malformation in lambs. *J Am Vet Med Assoc* 1959; 134: 180–183.
6. Binns W, et al. Chronological evaluation of teratorgenesis in sheep fed *Veratrum californicum*. *J Am Vet Med Assoc* 1963; 147: 839–842.
7. Robinson MS, Holmgren A, Dewey MJ. Genetic control of ocular morphogenesis: Defective lens development associated with ocular abnormalities in C57BL/6 mouse. *Exp Eye Res* 1993; 56: 7–16.
8. Brown GC, Sheilds JA, Patty BE, Goldberg RE. Congenital pits of the optic nerve head. *Arch Ophthalmol* 1979; 97: 1341–1344.
9. Roberts SR, Dellaporta A, Winter FC. The collie ectasia syndrome. *Am J Ophthalmol* 1966; 62: 728–752.
10. Roberts SR. Congenital posterior ectasia in the sclera of collie dogs. *Am J Ophthalmol* 1960; 50: 451–465.
11. Roberts SR, Dellaporta A, Winter FC. Pathologic alterations in the eyes of puppies one to fourteen days of age. *Am J Ophthalmol* 1966; 61: 1458–1466.
12. Roberts SR, Dellaporta A, Winter FC. Pathologic alterations in the eyes of young and adult dogs. *Am J Ophthalmol* 1966; 62: 728–752.
13. Silverstein AM, Osburn BI, Prendergast RA. The pathogenesis of retinal dysplasia. *Am J Ophthalmol* 1971; 72: 13–21.
14. Rubin LF. *Inherited Eye Diseases of Purebred Dogs*. Baltimore: Williams and Wilkins, 1989.
15. Carrig CB, Sponenberg DP, Schmidt GM, Tvedten HW. Inheritance of associated ocular and skeletal dysplasia in Labrador retrievers. *J Am Vet Med Assoc* 1988; 193: 1269–1272.
16. Meyers VN, Jezyk PF, Aguirre GD, Patterson DF. Short-limbed dwarfism and ocular defects in Samoyed dog. *J Am Vet Med Assoc* 1983; 183: 975–978.
17. Whiteley HE. Dysplastic canine retinal morphogenesis. *Invest Ophthalmol Vis Sci* 1991; 32: 1492–1498.
18. Grahn BH, Storey ES, McMillan C. Inherited retinal dysplasia and persistent hyperplastic primary vitreous in miniature Schnauzer dogs. *Vet Ophthalmol* 2004; 7: 151–158.
19. Albert DM, Lahav M, Carmichael LE, Percy DH. Canine herpes-induced retinal dysplasia and associated ocular anomalies. *Invest Ophthalmol Vis Sci* 1976; 15: 267–278.
20. Bistner SI, Rubin LF, Saunders LZ. The ocular lesions of bovine viral diarrhea-mucosal disease. *Pathol Vet* 1970; 7: 275–286.
21. Kilman JH, Young GA, Luedke AJ, Kitchell RC. The experimental production of malformations in fetal pigs by means of attenuated hog cholera virus. *Proc Am Vet Med Assoc* 1953; 90: 147–150.
22. Percy DH, Danylchuk KD. Experimental retinal dysplasia due to cytosine arabinoside. *Invest Ophthalmol Vis Sci* 1977; 16: 353–364.
23. Gottschall-Pass KT, Grahn BH, Gorecki DKJ, Paterson PG. Oscillatory potentials and light microscopic changes demonstrate an interaction between zinc and taurine in the developing rat retina. *J Nutr* 1997; 127: 1206–1213.
24. Barnett KC, Grimes TD. Bilateral aplasia of the optic nerve in a cat. *Brit J Ophthalmol* 1974; 58: 663–667.
25. Ernest JT. Bilateral optic nerve hypoplasia in a pup. *J Am Vet Med Assoc* 1976; 168: 125–128.
26. Gelatt KN, Leipold HW. Bilateral optic nerve hypoplasia in two dogs. *Can Vet J* 1971; 12: 91–96.
27. Kern TJ, Riis RC. Optic nerve hypoplasia in three miniature poodles. *J Am Vet Med Assoc* 1981; 178: 49–54.
28. Hayes KC, Nielsen SW, Eaton HD. Pathogenesis of optic nerve lesion in vitamin A-deficient calves. *Arch Ophthalmol* 1968; 80: 777–787.
29. Scott FW, de LaHunta A, Schultz RD, Bistner SI, Riis RC. Teratogenesis in cats associated with griseofulvin therapy. *Teratology* 1974; 11: 79–86.
30. Cullen CL, Grahn BH. Congenital glaucoma in a Llama (*Llama glama*). *Vet Comp Ophthalmol* 1997; 7: 253–257.
31. Halenda RM, Grahn BH, Sorden SD, Collier LL. Congenital equine glaucoma: Clinical and light microscopic findings in two cases. *Vet Comp Ophthalmol* 1997; 7: 105–109.
32. Van der Linde-Sipman JS, Stades FC, de Wolff-Rouendaal D. Persistent hyperplastic tunica vasculosa lentis and persistent hyperplastic primary vitreous in the Doberman pinscher: Pathologic aspects. *J Am Anim Hosp Assoc* 1983; 13: 791–802.
33. Leon A, Curtis B, Barnett KC. Hereditary persistent hyperplastic primary vitreous in the Staffordshire bull terrier. *J Am Anim Hosp Assoc* 1986; 22: 765–774.
34. Van Rensburg IBJ, Petrick SW, van der Lugt JJ, Smit M. Multiple inherited eye anomalies including persistent hyperplastic tunica vasculosa lentis in Bouvier des Flandres. *Prog Vet Comp Ophthalmol* 1992; 2: 133–139.
35. Venter IJ, van der Lugt JJ, van Rensburg IBJ, Petrick SW. Multiple congenital eye anomalies in Bloodhound puppies. *Vet Comp Ophthalmol* 1996; 6: 9–13.
36. Barnett KC. Imperforate and micro-lachrymal puncta in the dog. *J Sm Anim Pract* 1979; 20: 481–490.
37. Grahn BH, Mason RA. Epiphora associated with dacryops in a dog. *J Am Anim Hosp Assoc* 1995; 31: 15–19.
38. Gerding PA. Epiphora associated with canaliculops in a dog. *J Am Anim Hosp Assoc* 1991; 27: 424–426.
39. Peiffer RL. Bilateral congenital aphakia and retinal detachment in a cat. *J Am Anim Hosp Assoc* 1982; 18: 128–130.
40. Kaswan RL, Martin CL, Chapman WL. Keratoconjunctivitis sicca: Histopathologic study of nictitating membrane and lacrimal gland from 28 dogs. *Am J Vet Res* 1984; 45: 112–117.
41. Kern TJ, Erb HN, Schaedler JM, Dougherty EP. Scanning electron microscopy of experimental keratoconjunctivitis sicca in dogs: Cornea and bulbar conjunctiva. *Vet Pathol* 1988; 25: 468–474.
42. Martin CL, Munnell J, Kaswan R. Normal ultrastructure and histochemical characteristics of canine lacrimal glands. *Am J Vet Res* 1988; 49: 1566–1572.

43. Powell CC, Martin CL. Distribution of cholinergic and adrenergic nerve fibers in the lacrimal glands of dogs. *Am J Vet Res* 1989; 50: 2084–2088.
44. MacMillan AD, Waring GO, Spangler WL, Roth AM. Crystalline corneal opacities in the Siberian husky. *J Am Vet Med Assoc* 1979; 175: 829–832.
45. Ekins MB, Waring GO, Harris RR. Oval lipid corneal opacities in Beagles: Part II. *J Am Anim Hosp* 1980; 16: 601–605.
46. Morrin A, Waring GO, Spangler W. Oval lipid corneal opacities in Beagles: Ultrastructure of the abnormal Beagle cornea. *Am J Vet Res* 1982; 43: 443–453.
47. Spangler WL, Waring GO, Morrin LA. Oval lipid corneal opacities in Beagles. V Ultrastructure. *Vet Pathol* 1982; 19: 150–159.
48. Waring GO, MacMillan A, Reveles P. Inheritance of crystalline corneal dystrophy in Siberian Huskies. *J Am Anim Hosp Assoc* 1986; 22: 655–658.
49. Gwin RM, Polack FM, Warren JK, Samuelson DA, Gelatt KN. Primary canine corneal endothelial cell dystrophy: Specular microscopic evaluation, diagnosis and therapy. *J Am Anim Hosp Assoc* 1982; 18: 471–479.
50. Martin CL, Dice PF. Corneal endothelial dystrophy in the dog. *J Am Anim Hosp* 1982; 18: 327–336.
51. Bistner SI, Aguirre G, Shively JN. Hereditary corneal dystrophy in the Manx cat: A preliminary report. *Invest Ophthalmol Vis Sci* 1976; 15: 15–26.
52. Gelatt KN, Samuelson DA. Recurrent corneal erosions and epithelial dystrophy in the Boxer dog. *J Am Anim Hosp Assoc* 1982; 18: 453–460.
53. Kirschner SE, Niyo Y, Betts DM. Idiopathic persistent corneal erosions: Clinical and pathological findings in 18 dogs. *J Am Anim Hosp Assoc* 1989; 25: 84–90.
54. Ramsey D, Ketring K, Glaze M, Render J. Ligneous conjunctivitis in four Doberman pinschers. *J Am Anim Hosp Assoc* 1996; 32: 439–447.
55. Paulsen ME, Lavach JD, Snyder SP, Severin GA, Eichenbaum JD. Nodular granulomatous episclerokeratitis in dogs: 19 cases (1973–1985). *J Am Vet Med Assoc* 1987; 190: 1581–1587.
56. Deykin AR, Guandalini A, Ratto A. A retrospective histopathologic study of primary episcleral and scleral inflammatory disease in dogs. *Vet Comp Ophthalmol* 1997; 7: 245–248.
57. Gelatt KN, Peiffer RL, Gwin RM, Gum GG, Williams LW. Clinical manifestations of inherited glaucoma in the beagle. *Invest Ophthalmol Vis Sci* 1977; 16: 1135–1142.
58. Gelatt KN, Gum GG. Inheritance of primary glaucoma in the Beagle. *Am J Vet Res* 1981; 42: 1691–1693.
59. Samuelson DA, Gum GG, Gelatt KN. Ultrastructural changes in the aqueous outflow apparatus of Beagles with inherited glaucoma. *Invest Ophthalmol Vis Sci* 1989; 30: 550–561.
60. Gum GG, Gelatt KN, Knepper PA. Histochemical localization of glycosaminoglycans in the aqueous outflow pathways in normal Beagles and Beagles with inherited glaucoma. *Prog Vet Comp Ophthalmol* 1993; 3: 52–57.
61. Gelatt KN, McKay EO. Prevalence of the breed-related glaucomas in pure-bred dogs in North America. *Vet Ophthalmol* 2004; 7: 97–111.
62. Smedes SL, Dubielzig RR. Early degenerative changes associated with spontaneous glaucoma in dogs. *J Vet Diagn Invest* 1994; 6: 459–263.
63. Reilly CM, Morris R, Dubielzig RR. Canine goniodysgenesis-related glaucoma: A morphologic review of 100 cases looking at inflammation and pigment dispersion. *Vet Ophthalmol* 2005; 8: 253–258.
64. Petersen-Jones SM. Abnormal ocular pigment deposition associated with glaucoma in the Cairn Terrier. *J Sm Anim Pract* 1991; 32: 19–22.
65. van de Sandt RROM, Boeve MH, Stades FC, Kik MJL. Abnormal ocular pigment deposition and glaucoma in the dog. *Vet Ophthalmol* 2003; 6: 273–278.
66. Lazarus JA, Pickett PJ, Champagne ES. Primary lens luxation in the Chinese Shar Pei: Clinical and hereditary characteristics. *Vet Ophthalmol* 1998; 1: 101–107.
67. Gwin RM, Samuelson DA, Powell GN, et al. Primary lens luxation in the dog associated with lenticular zonulae degeneration and its relationship to glaucoma. *J Am Anim Hosp* 1982; 18: 485–491.
68. Foster SJ, Curtis R, Barnett KC. Primary lens luxation in the Border Collie. *J Sm Anim Pract* 1986; 27: 1–6.
69. Curtis R, Barnett KC. Clinical and pathological observations concerning the etiology of primary lens luxation in the dog. *Vet Rec* 1983; 112: 238–246.
70. Curtis R. Aetiopathological aspects of inherited lens dislocation in the Tibetan Terriers. *J Comp Path* 1983; 93: 151–163.
71. Martin CL. Zonular defects in the dog: A clinical and scanning electron microscopic study. *J Am Anim Hosp Assoc* 1978; 14: 571–579.
72. Morris RA, Dubielzig RR. Light microscopic evaluation of zonular fiber morphology in dogs with glaucoma secondary to lens displacement. *Vet Ophthalmol* 2005; 8: 81–84.
73. Narfstrom K, Ekesten B. Diseases of the canine ocular fundus. In: Gelatt KN, ed. *Veterinary Ophthalmology.* 3rd ed. Baltimore: Lippincott, Williams and Wilkins, 1999.
74. Grahn BH, Philibert H, Cullen CL, et al. Multifocal retinopathy of Great Pyrenees dogs. *Vet Ophthalmol* 1998; 1: 221–231
75. Grahn BH, Cullen CL. Retinopathy of Great Pyrenees dogs: Fluorescein angiography, light microscopy, and transmitting and scanning electron microscopy. *Vet Ophthalmol* 2001; 4: 191–199.
76. Grahn BH, Sandmeyer LS, Breaux CB. Retinopathy of Coton de Tulear dogs. *Proc Am Coll Vet Ophthalmol* 2005; 36: 20.
77. van der Woerdt A, Nasisse MP, Davidson MG. Sudden acquired retinal degeneration in the dog. Clinical and laboratory findings in 36 cases. *Prog Vet Comp Ophthalmol* 1991; 1: 11–18.
78. Miller PE, Galbreath EJ, Kehren JC, Steinberg H, Dubielzig RR. Photoreceptor cell death by apoptosis in dogs with sudden acquired retinal degeneration syndrome. *Am J Vet Res* 1998; 59: 149–152.
79. Lanum J. The damaging effects of light on the retina. Empirical findings, theoretical and practical implications. *Surv Ophthalmol* 1978; 22: 221–249.
80. Sadda SR, Yu YS, de Yuan E, Rencs EV, Green WR, Gottsch JD. Photosensitization-induced retinopathy in the newborn Beagle. *Invest Ophthalmol Vis Sci* 1994; 35: 1202–1211.
81. Buyukmichi N. Photic retinopathy in the dog. *Exp Eye Res* 1981; 33: 95–109.
82. Kuwabora T, Gorn RA. Retinal damage by visible light. *Arch Ophthalmol* 1968; 79: 69–78.
83. Jamieson VE, Davidson MG, Nasisse MP, English RV. Ocular complications following cobalt 60 radiotherapy of

neoplasms in the canine head region. *J Am Anim Hosp Assoc* 1991; 27: 51–60.
84. Roberts SM, Lavach JD, Severin GA, Withrow SJ, Gillette EL. Ophthalmic complications following megavoltage irradiation of the nasal and paranasal cavities in dogs. *J Am Vet Med Assoc* 1987; 190: 43–47.
85. Peiffer RL, Wright W, Steinbok P, Mahaley MS. Long-term study of the ocular effects of orthovoltage irradiation in rats. *Am J Vet Res* 1981; 42: 1598–1605.
86. West-Hyde L, Buyukmihci N. Photoreceptor degeneration in a family of cats. *J Am Vet Assoc* 1982; 181: 243–248.
87. Rubin LF, Lipton DE. Retinal degeneration in kittens. *J Am Vet Med Assoc* 1973; 162: 467–469.
88. Barnett KC, Curtis R. Autosomal dominant progressive retinal atrophy in Abyssinian cats. *J Hered* 1985; 76: 168–170.
89. Leon A, Curtis R. Autosomal dominant rod-cone dystrophy in the *rdy* cat. 1. Light and electron microscopic findings. *Exp Eye Res* 1990; 51: 361–381.
90. Narfstrom K, Nilsson SE. Progressive retinal atrophy in the Abyssinian cat. *Invest Ophthalmol Vis Sci* 1986; 27: 1569–1576.
91. Narfstrom K, Nilsson SE. Morphological findings during retinal development and maturation in hereditary rod cone degeneration in Abyssinian cats. *Exp Eye Res* 1989; 49: 611–628.
92. Narfstrom K, Wrigstad A, Nilsson SEG. The Briard dog: A new animal model of congenital stationary night blindness. *Br J Ophthalmol* 1989; 73: 750–756.
93. Narfstrom K, Wrigstad A, Ekesten B, Nilsson SEG. Hereditary retinal dystrophy in the Briard dog: Clinical and hereditary characteristics. *Vet Comp Ophthalmol* 1994; 4: 85–92.
94. Aguirre GD, Laties A. Pigment epithelial dystrophy in the dog. *Exp Eye Res* 1976; 23: 247–256.
95. Bedford PGC. Retinal pigment epithelial dystrophy (CPRA): A study of the disease in the Briard. *J Sm Anim Pract* 1984; 25: 129–138.
96. Barnett KC. The diagnosis of central progressive retinal atrophy in the Labrador retriever. *J Sm Anim Pract* 1967; 8: 631–632.
97. Watson P, Bedford PGC. The pigments of retinal pigment epithelial dystrophy in dogs. *Vet Pathol* 1992; 29: 5.
98. Riis RC, Sheffy BE, Loew E, Kern TJ, Smith JS. Vitamin E deficiency retinopathy of dogs. *Am J Vet Res* 1981; 42: 74–86.
99. Davidson MG, Geoly FJ, Gilger BC, McLellan GJ, Whiteley W. Retinal degeneration associated with vitamin E deficiency in hunting dogs. *J Am Vet Med Assoc* 1998; 213: 645–651.
100. McLellan GJ, Elks R, Lybaert P, Watte C, Moore DL, Bedford PGC. Vitamin E deficiency in dogs with retinal pigment epithelial dystrophy. *Vet Rec* 2002; 151: 663–667.
101. Bellhorn RW, Bellhorn MB, Swarm RL, Impellizzer CW. Hereditary tapetal abnormality in the Beagle. *Ophthalmic Res* 1975; 7: 250–260.
102. Wen Gy, Sturman JA, Wisniewski HM, MacDonald A, Niemann WH. Chemical and ultrastructural changes in the tapetum of Beagles with a hereditary abnormality. *Invest Ophthalmol Vis Sci* 1982; 23: 733–742.
103. Collier LL, King EJ, Prieur DJ. Tapetal degeneration in cats with Chediak-Higashi syndrome. *Curr Eye Res* 1985; 4: 767–773.
104. Wen GY, Wisniewski HM, Sturman JA. Hereditary abnormality in the tapetum lucidum of the Siamese cats: A histochemical and quantitative study. *Histochemistry* 1982; 75: 1–9.
105. Storey ES, Grahn BH, Alcorn J. Multifocal chorioretinal lesions in Borzoi dogs. *Vet Ophthalmol* 2005; 8: 337–347.
106. MacMillan AD, Scagliotti RH. Retinal degeneration in the Borzois. *The Borzoi Quarterly* 1977.
107. Chaudieu G. Study of the inheritance of focal retinal degeneration in a population of 160 Borzois. *Pratique Med et Chirugurgicale de L'animal de Compagnie* 1995; 30: 461–472.
108. Cowell K, Jezyk P, Haskins M, Patterson D. Mucopolysaccharidosis in a cat. *J Am Vet Med Assoc* 1976; 169: 334–339.
109. Langweiler M, Haskins M, Jezyk P. Mucopholysaccharidosis in a litter of cats. *J Am Anim Hosp Assoc* 1978; 14: 748–751.
110. Collins L Munnell J, Lorenz M. The pathology of feline GM_2 gangliosidosis. *Am J Path* 1978; 90: 723–730.
111. Breton L, Guerin P, Morin M. A case of mucopolysaccharidosis VI in a cat. *J Am Anim Hosp Assoc* 1983; 19: 891–896.
112. Haskins M, Jezyk P, Desnick R, McDonough S, Patterson D. Mucopolysaccharidosis in a domestic shorthaired cat: A disease distinct from that seen in the Siamese cat. *J Am Vet Med Assoc* 1979; 175: 384–387.
113. Shull R, Munger R, Spellacy E, Hall C, Constantopoulos G, Neufeld E. Canine alpha-L-iduronidase deficiency: A model for mucopolysaccharidosis I. *Am J Pathol* 1982; 109: 244–248.
114. Haskins M, Desnick R, Diferrant N, Jezyk P, Patterson D. β-glucuronidase deficiency in a dog: A model of human mucopolysaccharidosis VII. *Ped Res* 1984; 18: 980–984.
115. Donnelly WHC, Sheahan BJ, Rogers TA. G_{m1} gangliosidosis in Friesian calves. *J Path* 1973; 111: 173–179.
116. Donnelly WHC, Sheahan B, Kelly M. Beta-galactosidase deficiency in G_{m1} gangliosidosis of Friesen calves. *Res Vet Sci* 1973; 15: 139–141.
117. Jezyk P, Haskins M, Newman L. Alpha mannosidosis in a Persian cat. *J Am Vet Med Assoc* 1986; 189: 1483–1485.
118. Murnane R, Prieur D, Ahern-Rindell A, Parish S, Collier L. The lesions of an ovine lysosomal storage disease. *Am J Pathol* 1989; 134: 263–270.
119. Lovell K. Caprine Beta mannosidosis: Development of glial and myelin abnormalities in the optic nerves and corpus callosum. *Glia* 1990; 3: 26–32.
120. Hartley WJ, Canfield PJ, Donnelly TM. A suspected new canine storage disease. *Acta Neuropathol* 1982; 56: 225.
121. Kelly WR, Clague AE, Barns RJ, Bates MJ, Mackay BM. canine a-l-fucosidosis: A storage disease of Springer spaniels. *Acta Neruopathlo* 1983; 60: 9.
122. Valle D, Boison A, Jezyk P, Aguirre G. Gyrate atrophy of the choroid and retina in a cat. *Invest Ophthalmol Vis Sci* 1981; 20: 251–254.
123. Siakotos A, Armstrong D, Koppang N, Connole E. Studies on the retina and pigment epithelium in hereditary canine ceroid lipofuscinosis. II. The subcellular distribution of lysosomal hydrolases and other enzymes. *Invest Ophthalmol Vis Sci* 1978; 17: 618–633.
124. Berson E, Watson G. Electroretinograms in English Setters with neuronal ceroid lipofuscinosis. *Invest Ophthalmol Vis Sci* 1980; 19: 87–90.

125. Sisk D, Levesque D, Wood P, Styer E. Clinical and pathologic features of ceroid lepofuscinosis in two Australian Cattle dogs. *J Am Vet Med Assoc* 1990; 197: 361–364.
126. Smith RE, Sutton RH, Jolly RD, Smith KR. A retinal degeneration associated with ceroid lipofuscinosis in adult miniature Schnauzers. *Vet Comp Ophthalmol* 1996; 6: 187–191.
127. Minatel L, Underwood SC, Carfagnini JC. Ceroid lipofuscinosis in a Cocker Spaniel dog. *Vet Pathol* 2000; 37: 488–490.
128. Read WK, Bridges CH. Neuronal lipodystrophy. Occurrence in an inbred strain of cattle. *Pathol Vet* 1969; 6: 235–238.
129. Graydon FJ, Jolly RD. Ceroid-lipofuscinosis (Batten's disease). *Invest Ophthalmol Vis Sci* 1984; 25: 294.
130. Edwards JF, Storts RW, Joyce JR, et al. Juvenile-onset neuronal ceroid-lipofuscinosis in Rambouillet sheep. *Vet Path* 1994; 31: 48–54.
131. Fiske RA, Storts RW. Neuronal ceroid-lipofuscinosis in Nubian goats. *Vet Pathol* 1988; 25: 171–173.
132. Grahn BH, Szentimrey D, Pharr JW, Farrow CS, Fowler JD. Ocular and orbital porcupine quills in the dog. A review and case series. *Can Vet J* 1995; 36: 488–493.
133. Wheler CL, Grahn BH, Pocknell AN. Proptosis and orbital cellulitis in eight African hedgehogs (*Atelerix albiventris*). *J Zoo Wildlife Med* 2002; 32: 236–241.
134. Grahn BH, Szentimrey D, Battison A, Hertling R. Exophthalmos associated with frontal sinus osteomyelitis in a puppy. *J Am Anim Hosp* 1995; 31: 397–401.
135. Carpenter JL, Schmidt GM, Moore FM, Albert DM, Abrams KL, Elner VM. Canine bilateral extraocular polymyositis. *Vet Pathol* 1989; 26: 510–512.
136. Allgoewer I, Blair M, Basher T, et al. Extraocular muscle myositis and restrictive strabismus in 10 dogs. *Vet Ophthalmol* 2000; 3: 21–26.
137. Martin CL, Kaswan RL, Doran CC. Cystic lesions of the periorbital region. *Comp Cont Ed Pract* 1987; 9: 1022–1029.
138. Grahn BH, Mason R. Epiphora associated with Dacryops in a dog. *J Am Anim Hosp Assoc* 1995; 31: 15–19.
139. Pentlarge V. Eosinophilic conjunctivitis in five cats. *J Am Anim Hosp Assoc* 1991; 27: 21–28.
140. Allgoewer I, Schaffer E, Stockhaus C, Vogtlin A. Feline eosinophillic conjunctivitis. *Vet Ophthalmol* 2001; 4: 69–74.
141. Larocca R. Eosinophilic conjunctivitis, herpesvirus, and mast cell tumor of the third eyelid in a cat. *Vet Ophthalmol* 2000; 3: 221–225.
142. Read RA, Lucas J. Lipogranulomatous conjunctivitis of cats: Clinical findings from 21 eyes of 13 cats. *Vet Ophthalmol* 2001; 4: 93–98.
143. Kerlin RL, Dubielzig RR. Lipogranulomatous conjunctivitis in cats. *Vet Comp Ophthlmol* 1997; 7: 177–179.
144. Moore CP, Wilsman NJ, Nordheim EV, et al. Density and distribution of canine conjunctival goblet cells. *Invest Ophthalmol Vis Sci* 1987; 28: 1925–1932.
145. Cullen CL, Njaa BL, Grahn BH. Ulcerative keratitis associated with qualitative tear film abnormalities in cats. *Vet Ophthalmol* 1999; 2: 197–204.
146. Grahn BH, Sisler S, Storey ES. Qualitative tear film and conjunctival goblet cell assessment of cats with corneal sequestra. *Vet Ophthalmol* 2005; 8: 167–170.
147. Breaux CB, Grahn BH, Sandmeyer LS. Retrospective immunohistochemical and clinical investigation of episcleritis. *Proc Am Coll Vet Ophthalmol* 2005; 36: 1.
148. Williams CO, Dietrich UM, Moore PA, Dubielzig RR, Carmichael KP. The immunopathogenesis of canine nodular ocular episcleritis. *Proc Am Coll Vet Ophthalmol* 2005; 36: 37.
149. Dubielzig RR, Render JA, Morreale RJ. Distinctive morphologic features of the ciliary body in equine recurrent uveitis. *Vet Comp Ophthalmol* 1997; 7: 163–167.
150. Cooley PL, Wyman M, Kindig O. Pars plicata in equine recurrent uveitis. *Vet Pathol* 1990; 27: 138–140.
151. Peiffer RL, Wilcock BP. Histopathologic study of uveitis in cats: 139 cases (1978–1988). *J Am Vet Med Assoc* 1991; 198: 135–138.
152. Davidson MG, Nasisse MP, English RV, Wilcock BP, Jamieson VE. Feline anterior uveitis: A study of 53 cases. *J Am Anim Hosp Assoc* 1991; 27: 77–83.
153. Lindley DM, Boosinger TR, Cox NR. Ocular histopathology of Vogt-Koyanagi-Harada-like syndrome in the Akita dog. *Vet Pathol* 1990; 27: 294–296.
154. Kern T, Walton DK, Riis RC, Manning TO, Laratta LJ, Dziezyc J. Uveitis associated with poliosis and vitiligo in six dogs. *J Am Vet Med Assoc* 1985; 187: 408–414.
155. Van der Woerdt A, Nasisse MP, Davidson MG. Lens-induced uveitis in dogs: 151 cases (1985–1990). *J Am Vet Med Assoc* 1992; 201: 921–926.
156. Wilcock BP, Peiffer RL. The pathology of lens-induced uveitis in dogs. *Vet Pathol* 1987; 24: 549–553.
157. Van der Woerdt A, Nasisse MP, Davidson MG. Sudden acquired retinal degeneration in the dog: Clinical and laboratory findings in 36 cases. *Prog Vet Comp Ophthalmol* 1991; 1: 11–18.
158. Miller PE, Galbreath EJ, Kehren JC, Steinberg H. Dubielzig RR. Photoreceptor cell death by apoptosis in dogs with sudden acquired retinal degeneration syndrome. *Am J Vet Res* 1998; 59: 149–152.
159. Mattson A, Roberts SM, Isherwood JME. Clinical features suggesting hyperadrenocorticism associated with sudden acquired retinal degeneration syndrome in a dog. *J Am Anim Hosp Assoc* 1992; 28: 199–202.
160. Morgan RV. Feline corneal sequestration: A retrospective study of 42 cases (1987–1991) *J Am Anim Hosp Assoc* 1994; 30: 24–28.
161. Featherstone HJ, Sansom J. Feline corneal sequestra: A review of 64 cases (80 eyes) from 1993–2000. *Vet Ophthalmol* 2004; 7: 213–227.
162. Featherstone HJ, Franklin VJ, Sansom J. Feline corneal sequestrum: Laboratory analysis of ocular samples from 12 cats. *Vet Ophthalmol* 2004; 7: 229–238.
163. Beam S, Correa MT, Davidson MG. A retrospective-cohort study on the development of cataracts in dogs with diabetes mellitus: 200 cases. *Vet Ophthalmol* 1999; 2: 169–172.
164. Sato S, Takahashi Y, Wyman M, Kador PF. Progression of the sugar cataract in the dog. *Invest Ophthalmol Vis Sci* 1991; 32: 1925–1931.
165. Wyman M, Sato S, Akagi Y, Terubayashi H, Datiles M, Kador PF. The dog as a model for ocular manifestations of high concentrations of blood sugars. *J Am Vet Med Assoc* 1988; 193: 1153–1156.
166. Martin CL, Chambreau T. Cataract production in experimentally orphaned puppies fed a commercial replacement for bitch's milk. *J Am Anim Hosp Assoc* 1982; 18: 115–119.

167. Glaze MC, Blanchard Gl. Nutritional cataracts in a Samoyed litter. *J Am Anim Hosp Assoc* 1983; 19: 951–954.
168. Bunce GE, Kinoshita J, Horwitz J. Nutritional factors in cataract. *Ann Rev Nutr* 1990; 10: 233–254.
169. Brightman AH, Brogdon JD, Helper LC, Everds N. Electric cataracts in the canine: A case report. *J Am Anim Hosp Assoc* 1984; 20: 895–898.
170. Martin CL. The formation of cataracts in dogs with disophenol: Age susceptibility and production with chemical grade 2,6-diiodo-4-nitrophenol. *Can Vet J* 1975; 16: 228–232.
171. Brown D, Magrane W, Cross F, Reynolds R. Clinical observations of eyes of cattle, swine, and burros surviving exposure to gamma and mixed neutron-gamma radiation. *Am J Vet Res* 1972; 33: 309–315.
172. Jamieson V, Davidson M, Nasisse M, English R. Ocular complications following cobalt 60 radiotherapy of neoplasms in the canine head region. *J Am Anim Hosp Assoc* 1991; 27: 51–55.
173. Roberts S, Lavach J, Severin G, Withrow S. Gillette E. Ophthalmic complications following megavoltage irradiation of the nasal and paranasal cavities of dogs. *J Am Vet Med Assoc* 1987; 190: 43–47.
174. Lipman R, Tripathi B, Tripathi R. Cataracts induced by microwave and ionizing radiation. *Surv Ophthalmol* 1988; 33: 200–210.
175. Vainisi S, Edelhauser H, Wolf D, Cotlier E, Reesere F. Nutritional cataracts in Timber wolves. *J Am Vet Med Assoc* 1981; 179: 1175–1180.
176. Anderson RS, Trune DR, Shearer TR. Histologic changes in selenite cortical cataract. *Invest Ophthalmol Vis Sci* 1988; 29: 1418–1427.
177. Poston HA, Riis RC, Rumsey GL, Ketola HG. The effect of supplemental dietary amino acids, minerals, and vitamins on salmonids fed cataractogenic diets. *Cornell Vet* 1977; 67: 472–509.
178. Ketola HG. Influence of dietary zinc on cataracts in rainbow trout (*Salmo gairdneri*). *J Nutr* 1979; 109: 965–969.
179. Hughes SF, Riis RC, Nickum JG, Rumsey GL. Biomicroscopic and histologic pathology of the eye in riboflavin deficient rainbow trout (*Salmo gairdneri*). *Cornell Vet* 1981; 71: 269–279.
180. Poston HA, Rumsey GL. Factors affecting dietary requirements and deficiency signs of L-tryptophan in rainbow trout. *J Nutr* 1983; 113: 2568–2577.
181. Shariff M, Richards RH, Sommerville C. The histopathology of acute and chronic infections of rainbow trout (*Salmo gairdneri*) with eye flukes (*Diplostomum spp*). *J Fish Dis* 1980; 3: 455–457.
182. Wolfer J, Grahn BH, Wilcock B, Percy D. Phacoclastic uveitis in the rabbit. *Vet Comp Ophthalmol* 1992; 3: 92–97.
183. Wilcock BP, Peiffer RL. The causes of glaucoma in cats. *Vet Path* 1990; 27: 35–40.
184. Ridgway MD, Brightman AH. Feline glaucoma: A retrospective study of 29 clinical cases. *J Am Anim Hosp Assoc* 1989; 25: 485–490.
185. Blocker T, van der Woerdt A. The feline glaucomas: 82 cases (1995–1999). *Vet Ophthalmol* 2004; 4: 81–85.
186. Czederpiltz JMC, La Croix NC, van der Woerdt A, Bentley E, Dubielzig RR, Murphy CJ, Miller PE. Putative aqueous humor misdirection syndrome as a cause of glaucoma in cats: 32 cases (1997–2003). *J Am Vet Med Assoc* 2005; 227: 1434–1441.
187. Wilcock BP, Brooks DE, Latimer CA. Glaucoma in horses. *Vet Pathol* 1991; 28: 74–78.
188. Samuelson D, Smith P, Brooks D. Morphologic features of the aqueous humor drainage pathways in horses. *Am J Vet Res* 1989; 50: 720–727.
189. Brooks DE. Histomorhometry of the optic nerves of normal horses and horses with glaucoma. *Vet Comp Ophthalmol* 1995; 5: 193–210.
190. Miller TR, Brooks DE, Gelatt KN, King TC, Smith PJ, Sapienza JS, Pellicane CP. Equine glaucoma: Clinical findings and response to treatment in 14 horses. *Vet Comp Ophthalmol* 1995; 5: 170–181.
191. Cullen CL, Grahn BH. Equine glaucoma: A retrospective study of 13 cases presented at the Western College of Veterinary Medicine from 1992–1999. *Can Vet J* 2000; 41: 470–480.
192. Taylor VL, Peiffer RL, Costella MJ. Ultrastructural analysis of normal and diabetic cataracts in the dog. *Vet Comp Ophthalmol* 1997; 7: 117–125.
193. Thoresen SI, Bjerkas E, Aleksandersen M, Peiffer RL. Diabetes mellitus and bilateral cataracts in a kitten. *J Fel Med Surg* 2002; 4: 115–122.
194. Gilger BC, McLaughlin SA, Whitley RD. Wright J. Orbital neoplasms in cats: 21 cases (1974–1990). *J Am Vet Med Assoc* 1992; 201: 1083–1086.
195. Kern TJ. Orbital neoplasia in 23 dogs. *J Am Vet Med Assoc* 1985; 186: 489–491.
196. Attali-Soussay K, Jegou JP, Clerc B. Retrobulbar tumors in dogs and cats: 25 cases. *Vet Ophthalmol* 2001; 4: 19–27.
197. Mauldin EA, Deehr AJ, Hertzke D, Dubielzig RR. Canine orbital menigiomas: A review of 22 cases. *Vet Ophthalmol* 2000; 3: 11–16.
198. Rebhun WC, Edwards NJ. Two cases of orbital adenocarcinoma of probable lacrimal gland origin. *J Am Anim Hosp Assoc* 1977; 13: 691–694.
199. Pletcher JM, Koch SA, Stedham MA. Orbital chondroma rodens in a dog. *J Am Vet Med Assoc* 1979; 175: 187–190.
200. O'Brien MG, Withrow SJ, Straw RC, Powers BE, Kirpensteijn JK. Total and partial orbitectomy for the treatment of periorbital tumors in 24 dogs and 6 cats: A retrospective study. *Vet Surg* 1996; 25: 471–479.
201. Basher AW, Severin GA, Chavkin MJ, Fran AA. Orbital neuroendocrine tumors in three horses. *J Am Vet Med Assoc* 1997; 210: 668–671.
202. Goodhead AD, Venter IJ, Nesbit JW. Retrobulbar extra-adrenal paraganglioma in a horse and its surgical removal by orbitotomy. *Vet Comp Ophthalmol* 1997; 7: 96–100.
203. Rebhun W. Orbital lymphosarcoma in cattle. *J Am Vet Med Assoc* 1982; 180: 149–152.
204. Cullen CL, Grahn BH, Wolfer J. Diagnostic Ophthalmology: Orbital, nasal and frontal sinus neoplasia in a 2-year old Shetland sheepdog. *Can Vet J* 2000; 41: 723–724.
205. Wolfer J, Grahn, BH. Diagnostic Ophthalmology: Exophthalmos in a cat secondary to an orbital round cell tumor. *Can Vet J* 1995; 36: 518–519.
206. Rebhun W, Piero F. Ocular lesions in horses with lymphosarcomas: 21 cases (1977–1997). *J Am Vet Med Assoc* 1998; 212: 852–854.
207. Van Maanen C, Klein WR, Dik KJ. Three cases of carcinoid in the equine nasal cavity and maxillary sinuses: Histological and immunohistochemical features. *Vet Path* 1996; 33: 92–95.

208. Krehbiel JD, Langham RF. Eyelid neoplasms in dogs. *Am J Vet Res* 1975; 36: 115–119.
209. Roberts S, Severin G. Prevalence and treatment of palpebral neoplasms in the dog. *J Am Vet Med Assoc* 1986; 189: 1355–1359.
210. Gelatt KN. Meibomian adenoma in a dog. *Vet Med Small Anim Clin* 1980; 10: 962–963.
211. Williams LW, Gelatt KN, Gwin RM. Ophthalmic neoplasms in the cat. *J Am Anim Hosp Assoc* 1981; 17: 999–1008.
212. Monlux A, Anderson W, Davis C. The diagnosis of squamous cell carcinoma of the eye (cancer eye) in cattle. *Am J Vet Res* 1957; 28: 5–34.
213. Anderson D, Lush J, Chambers D. Studies of bovine ocular squamous carcinoma (cancer eye) II. Relationship between eyelid pigmentation and occurrence of cancer eye lesions. *J Anim Sci* 1957; 16: 739–746.
214. Kaps S, Richter M, Philipp M, Bart M, Eule C, Speiss BM. Primary invasive ocular squamous cell carcinoma in a horse. *Vet Ophthalmol* 2005; 8: 193–197.
215. Gelatt KN. Basal cell carcinoma of the eyelid of dog. *Vet Clin North Am Small Anim Clin* 1971; 10: 847.
216. Johnson B, Brightman AH, Whiteley HE. Conjunctival mast cell tumor in two dogs. *J Am Anim Hosp Assoc* 1988; 24: 439–441.
217. Hallstrom M. Mastocytomas in the third eyelid of a dog. *J Small Anim Pract* 1970; 11: 469–471.
218. Grahn BH, Wolfer J, Randall J. Diagnostic Ophthalmology: Exophthalmos in a dog secondary to mastocytoma. *Can Vet J* 1994; 35: 730–731.
219. Blodi FC, Ramsey FK. Ocular tumors in domestic animals. *Am J Ophthalmol* 1967; 50: 109–115.
220. Krohne SG, Henderson NM, Richardson RC, Vestre WA. Prevalence of ocular involvement in dogs with multicentric lymphoma: Prospective evaluation of 94 cases. *Vet Comp Ophthalmol* 1994; 4: 127–134.
221. Hoffman A, Blocker T, Dubielzig RR, Ehrhar EJ. Feline periocular peripheral nerve sheath tumor: A case series. *Vet Ophthalmol* 2005; 8: 153–158.
222. Strubbe TD. Periocular neurofibrosarcoma in a horse. *Vet Ophthalmol* 2001; 4: 237–241.
223. Tarwid J, Fretz P, Clark E. Equine sarcoids: A study with emphasis on pathologic diagnosis. *Comp Cont Ed Pract Vet* 1985; 7: S293–S300.
224. Knottenbelt DC, Kelly DF. The diagnosis and treatment of periorbital sarcoid in the horse: 445 cases from 1974–1999. *Vet Ophthalmol* 2000; 3: 169–191.
225. Piscopo SE. The complexities of sarcoid tumors. *Equine Pract* 1999; 21: 14–18.
226. Cheevers W, Robertson S, Brassfield A, Davis WC, Crawford TD. Isolation of a retrovirus from cultured equine sarcoid tumor cells. *Am J Vet Res* 1982; 43: 804–806.
227. Trenfield K, Spradbrow P, Vanselow B. Sequences of papillomavirus DNA in equine sarcoids. *Equine Vet J* 1985; 17: 449–452.
228. Nasir L, Reid SW. Bovine papilloma viral gene expression in equine sarcoid tumors. *Vir Res* 1999; 61: 171–175.
229. Collins BK, Collier LL, Miller MA, Linton LL. Biologic behavior and histologic characteristics of canine conjunctival melanoma. *Prog Vet Comp Ophthalmol* 1993; 3: 135–140.
230. Croxatto JO. Malignant melanoma arising from primary acquired melanosis in a dog. *Can Pract* 1992; 17: 22–24.
231. Levene A. Precancerous and cancerous melanosis of the canine conjunctiva. *J Comp Path* 1973; 83: 253–257.
232. Cook CS, Rosenkrantz W, Peiffer RL, Macmillan A. Malignant melanoma of the conjunctiva in a cat. *J Am Vet Med Assoc* 1985; 186: 505–506.
233. Mughannam AJ, Hacker DV, Spangler WL. Conjunctival vascular tumors in six dogs. *Vet Comp Ophthalmol* 1997; 7: 56–59.
234. Summer GG. Angiokeratoma: A benign vascular tumor of the dog. *J Sm Anim Pract* 1990; 31: 390–392.
235. Murphy CJ, Bellhorn RW, Buyukmihci NC. Bilateral conjunctival masses in two dogs. *J Am Vet Med Assoc* 1989; 195: 225–227.
236. Buyukmihci NC. Canine conjunctival angiokeratomas. *J Am Vet Med Assoc* 1981; 178: 1279–1282.
237. Vestre WA, Turner TA, Carlton WW. Conjunctival hemangiosarcoma in horse. *J Am Vet Med Assoc* 1982; 180: 1481–1482.
238. Moore PF, Jacker DV, Buyukmihci NC. Ocular angiosarcoma in the horse: Morphological and immunohistochemical studies. *Vet Path* 1986; 23: 240–244.
239. Crawley GR, Bryan GM, Gogolewski RP. Ocular hemangioma in a horse. *Equine Pract* 1987; 9: 9–13.
240. Hacker D, Moore P, Buyukmihci N. Ocular angiosarcoma in four horses. *J Am Vet Med Assoc* 1986; 189: 200–203.
241. Martin C. Canine epibulbar melanomas and their management. *J Am Anim Hosp Assoc* 1981; 17: 83–90.
242. Diter SR, Dubielzig RR, Aguirre G, Acland G. Primary ocular melanomas in dogs. *Vet Path* 1983; 20: 379–395.
243. Ryan A, Diter SR. Clinical and pathologic features of canine ocular melanomas. *J Am Vet Med Assoc* 1984; 184: 60–67.
244. Harling D, Peiffer RL, Cook C. Feline limbal melanoma: Four cases. *J Am Vet Med Assoc* 1986; 22: 795–802.
245. Bernays ME, Flemming D, Peiffer RL. Primary corneal papilloma and squamous cell carcinoma associated with pigmentary keratitis in four dogs. *J Am Vet Med Assoc* 1999; 214: 215–217.
246. Latimer KS, Kaswan RL, Sundberg JP. Corneal squamous cell carcinoma in the dog. *J Am Vet Med Assoc* 1987; 190: 1430–1432.
247. Ryan AM, Diters RW. Clinical and pathologic features of canine ocular melanomas. *J Am Vet Med Assoc* 1984; 184: 60–67.
248. Wilcock BP, Peiffer RL. Morphology and behavior of primary ocular melanomas in 91 dogs. *Vet Path* 1986; 23: 418–424.
249. Freidman DS, Miller I, Dubielzig RR. Malignant canine anterior uveal melanoma. *Vet Path* 1989; 26: 523–525.
250. Giuliano EA, Chappell R, Fischer B, Dubielzig RR. A matched observation study of canine survival with primary intraocular melanocytic neoplasia. *Vet Ophthalmol* 1999; 2: 185–190.
251. Diters R, Dubielzig RR, Aguirre GD, Acland GM. Primary ocular melanoma in dogs. *Vet Path* 1983; 20: 379–395.
252. Render JA, Ramsey DT, Ramsey CC. Contralateral uveal metastasis of malignant anterior uveal melanoma in a dog. *Vet Comp Ophthalmol* 1997; 7: 263–266.
253. Bussanich NM, Dolman PJ, Rootman J, Dolman CL. Canine uveal melanomas: Series and literature review. *J Am Anim Hosp Assoc* 1987; 23: 415–422.
254. Minami T, Patnaik AK. Malignant anterior uveal melanoma with diffuse metastasis in a dog. *J Am Vet Med Assoc* 1992; 201: 1894–1896.
255. Truska RC, Mclean IW, Quinn AJ. Intraocular canine melanocytic neoplasms. *J Am Anim Hosp Assoc* 1985; 21: 85–88.

256. Mays MB, Nguyen HT, Wolf ED, Samuelson DA, Bloomberg NM. A xanthomatous lesion resembling balloon cell melanoma of the iris and ciliary body of a dog. *J Comp Path* 1985; 95: 217–225.
257. Roperto F, Restucci B, Crovace A. Bilateral ciliary body melanomas in a dog. *Prog Vet Comp Ophthalmol* 1993; 3: 149–151.
258. Rovesti GL, Guandalini A, Peiffer RL. Suspected latent vertebral metastasis of uveal melanoma in a dog: A case report. *Vet Ophthalmol* 2001; 4: 75–77.
259. O'Toole D, Murphy J. Spindle B cell melanoma in the choroid in a dog. *J Small Anim Pract* 1983; 24: 561–567.
260. Aguirre GD, Brown G, Shields JA, Dubielzig RR. Melanoma of the choroid of a dog. *J Am Anim Hosp Assoc* 1984; 20: 471–476.
261. Dubielzig RR, Aguirre GD, Gross SL, Diters RW. Choroidal melanomas in dogs. *Vet Path* 1985; 22: 582–585.
262. Weisse K, Frese K, Meyer D. Benign melanoma of the choroid in a beagle: Ophthalmologic, light and electron microscopic investigations. *Vet Path* 1985; 22: 586–591.
263. Morgan RV, Patton CS. Choroidal melanoma in a dog. *Cornell Vet* 1993; 83: 211–217.
264. Schoster JV, Dubielzig RR, Sullivan L. Choroidal melanoma in a dog. *J Am Vet Med Assoc* 1993; 203: 89–91.
265. Collison PN, Peiffer RL. Clinical presentation, morphology and behavior of primary choroidal melanomas in eight dogs. *Prog Vet Comp Ophthalmol* 1993; 3: 158–164.
266. Hyman JA, Koch SA, Wilcock BP. Canine choroidal melanoma with metastases. *Vet Ophthalmol* 2002; 5: 113–117.
267. Cordy RH. Primary intraocular malignant melanoma in a Siamese cat. *Vet Path* 1977; 14: 648–649.
268. Peiffer RL, Seymour WG, Williams LW. Malignant melanoma of the iris and ciliary body in a cat. *Mod Vet Pract* 1977; 58: 853–856.
269. Souri E. Intraocular melanoma in a cat. *Fel Pract* 1978; 8: 43–45.
270. Acland GM, Mclean IW, Aguirre FD, Trucksa R. Diffuse iris melanoma in cats. *J Am Vet Med Assoc* 1980; 176: 52–56.
271. Ducan DE, Peiffer RL. Morphology and prognostic indicators of anterior uveal melanomas in cats. *Prog Vet Comp Ophthalmol* 1991; 1: 25–32.
272. Harris BP, Dubielzig RR. A typical primary ocular melanoma in cats. *Vet Ophthalmol* 1999; 2: 121–124.
273. Kalishman JB, Chappell R, Flood LA, Dubielzig RR. A matched observational study of survival in cats with enucleation due to diffuse iris melanoma. *Vet Ophthalmol* 1998; 1: 25–29.
274. Bjerkas E, Arnesen K, Peiffer RL. Diffuse amelanotic iris melanoma in a cat. *Vet Comp Ophthalmol* 1997; 7: 190–191.
275. Bertroy RW, Brightman AH, Regan K. Intraocular melanoma with multiple metastases in a cat. *J Am Vet Med Assoc* 1988; 192: 87–88.
276. Schwink K, Betts DM. Malignant melanoma of the iris in a cat. *Comp Anim Pract* 1988; 2: 35–41.
277. Patnaik AK, Mooney S. Feline melanoma: A comparative study of ocular, oral, and dermal neoplasms. *Vet Pathol* 1988; 25: 105–112.
278. Bellhorn RW, Henkind P. Intraocular malignant melanoma in domestic cats. *J Sm Anim Pract* 1970; 10: 631–637.
279. Niederkorn JY, Shadduck JA, Albert D. Enucleation and the appearance of second primary tumors in cats bearing a virally induced intraocular tumors. *Invest Ophthalmol Vis Sci* 1982; 23: 719–725.
280. Albert DM, Shadduck JA, Craft JL, Niederkorn JY. Feline uveal melanoma model induced with feline sarcoma virus. *Invest Ophthalmol Vis Sci* 1981; 20: 606–623.
281. Stiles J, Biensle D, Render JA, Buyukmihci NC, Johnson EC. Use of nested polymerase chain reaction (PCR) for detection of retroviruses from formalin-fixed, paraffin-embedded uveal melanomas in cats. *Vet Ophthalmol* 1999; 2: 113–116.
282. Cullen CL, Haines DM, Jackson ML, Grahn BH. Lack of detection of feline leukemia and feline sarcoma viruses in diffuse iris melanomas of cats by immunohistochemistry and polymerase chain reaction. *J Vet Diag Invest* 2002; 14: 340–343.
283. Billson FM, Mould JRB, Lee WR. Myxoid leiomyoma of the iris in a dog. *Vet Ophthalmol* 2003; 6: 173–176.
284. Sato T, Yamamoto A, Shibuya H, Sudo H, Shiriai W, Amemori T. Intraocular peripheral nerve sheath tumor in a dog. *Vet Ophthalmol* 2005; 8: 283–286.
285. Heath S, Rankin AJ, Dubielzig RR. Primary ocular osteosarcoma in a dog. *Vet Ophthalmol* 2003; 6: 85–87.
286. Stoltz JH, Carpenter JL, Albert DM, Vainisi SJ, Munn RJ. Histologic, immunohistological and ultrastructural features of an intraocular sarcoma of a cat. *J Vet Diag Invest* 1994; 6: 114–116.
287. Peiffer RL, Monticello T, Bouldin TW. Primary ocular sarcomas in the cat. *J Sm Anim Pract* 1988; 29: 105–116.
288. Cullen CL, Haines DM, Jackson ML, Peiffer RL, Grahn BH. The use of immunohistochemistry and polymerase chain reaction for detection of feline leukemia virus and feline sarcoma virus in six cases of feline ocular sarcoma. *Vet Ophthalmol* 1998; 1: 189–193.
289. Dubielzig RR, Hawkins KL, Toy KA, Rosebury WS, Mazur M, Jasper TG. Morphologic features of feline ocular sarcomas in 10 cats: Light microscopy, ultrastructure, and immunohistochemistry. *Vet Comp Ophthalmol* 1994; 4: 7–12.
290. Dubielzig RR, Everitt J, Shadduck JA, Albert DM. Clinical and morphologic features of post-traumatic ocular sarcomas in cats. *Vet Pathol* 1990; 27: 62–65.
291. Zeiss CJ, Johnson EM, Dubielzig RR. Feline intraocular tumors may arise from transformation of lens epithelium. *Vet Pathol* 2003; 40: 355–362.
292. Dubielzig RR. Ocular sarcoma following trauma in three cats. *J Am Vet Med Assoc* 1984; 184: 578–581.
293. Miller WW, Boosinger TR. Intraocular osteosarcoma in a cat. *J Am Anim Hosp Assoc* 1987; 23: 317–320.
294. Hakanson N, Shively JN, Reed RE, Merideth RE. Intraocular spindle cell sarcoma following ocular trauma in a cat: Case report and literature review. *J Am Anim Hosp Assoc* 1990; 26: 63–66.
295. Barrett PM, Meredith RE, Alarcon F. Central amaurosis induced by an intraocular posttraumatic fibrosarcoma in a cat. *J Am Anim Hosp Assoc* 1995; 31: 242–245.
296. Grahn BH, Peiffer RL, Cullen CL, Haines DM. Immunohistochemical evaluation of 75 intraocular neoplasms from cats. *Vet Ophthalmol* 2006 (at press).
297. Peiffer RL. Ciliary body epithelial tumours in the dog and cat: A report of thirteen cases. *J Sm Anim Pract* 1983; 24: 347–370.
298. Dubielzig RR, Steinberg H, Garvin H, Deehr AJ, Fischer B. Iridociliary epithelial tumors in 100 dogs and 17 cats: A morphological study. *Vet Ophthalmol* 1998; 1: 223–231.

299. Clerc B. Surgery and chemotherapy for the treatment of adenocarcinoma of the iris and ciliary body in five dogs. *Vet Comp Ophthalmol* 1996; 6: 265–270.
300. Whittemore JC, Gionfriddo JR, Steyn P, Ehrhart EJ. Indium-111 labeled vitamin b12 imaging of a ciliary adenoma with a concurrent grade 2 soft tissue sarcoma of the leg in a Labrador. *Vet Ophthalmol* 2004; 7: 209–212.
301. Lavach JD. Iridociliary adenoma in a dog. *J Am Anim Hosp Assoc* 1984; 20: 468–470.
302. Barron CN, Saunders LZ. Intraocular tumors in animals II. Primary nonpigmented intraocular tumors. *Cancer Res* 1959; 19: 1171–1174.
303. Syed NA, Nork TM, Poulsen GL, Riis RC, George C, Albert DM. Retinoblastoma in a dog. *Arch Ophthalmol* 1997; 115: 758–763.
304. Fugaro MN, Kiupel M, Montiani-Ferreira F, Hawkins JF, Janovitz EB. Retinoblastoma in the eye of a llama (*Llama glama*). *Vet Ophthalmol* 2005; 8: 287–290.
305. Bistner SI. Medullo-epithelioma of the iris and ciliary body in a horse. *Cornell Vet* 1974; 64: 588–595.
306. Lahav M, Albert DM, Kircher CH, Percy DH. Malignant teratoid medulloepithelioma in a dog. *Vet Pathol* 1976; 13: 11–16.
307. Aleksandersen M, Bjerkas E, Heiene R, Heegaard S. Malignant teratoid medulloepithelioma with brain and kidney involvement in a dog. *Vet Ophthalmol* 2004; 7: 407–411.
308. Bras ID, Gemensky-Metzler AJ, Colitz CMH, Wilkie DA. Immunohistochemical characterization of a malignant intraocular teratoid medulloepithelioma in a cockatiel. *Vet Ophthalmol* 2005; 8: 59–65.
309. Wilcock BP, Williams MM. Malignant intraocular medulloepithelioma in a dog. *J Am Anim Hosp Assoc* 1980; 16: 617–619.
310. Langloss JM, Zimmerman LE, Krehbiel JD. Malignant intraocular teratoid medulloepithelioma in three dogs. *Vet Path* 1976; 13: 343–352.
311. Lahav M, Albert DM. Medulloepithelioma of the ciliary body in the goldfish. *Vet Path* 1978; 15: 208–212.
312. Symanski CM. Malignant teratoid medulloepithelioma in a horse. *J Am Vet Med Assoc* 1987; 190: 301–302.
313. Riis RC, Scherlie PH, Rebhun WC. Intraocular medulloepithelioma in a horse. *Equine Vet J* 1990; 10: 66–68.
314. Eagle RC, Font RL, Swercsek TW. Malignant medulloepithelioma of the optic nerve in a horse. *Vet Path* 1978; 15: 488–494.
315. Stone SF, Ehrhart EJ, Dubielzig RR, Zeiss CJ, Powell CC, Charles B. Tumors of the canine optic nerve head and peripapillary retina. *Proc Am Col Vet Ophthalmol* 2005; 36: 6.
316. Ehrhart EJ, Stone SG, Dubielzig RR, Zeiss CJ, Powell CC, Charles B. Tumors of the canine ciliary body and retina. *Proc Am Col Vet Ophthalmol* 2005; 36: 44.
317. Barnett KC, Grimes TD. Retrobulbar tumour and retinal detachment in a dog. *J Sm Anim Pract* 1972; 13: 315–317.
318. Spiess BM, Wilcock BP. Glioma of the optic nerve with intraocular and intracranial involvement in a dog. *J Comp Path* 1987; 97: 79–81.
319. Brooks DE, Patton CS. An ocular ganglioneuroblastoma in a dog. *Prog Vet Comp Ophthalmol* 1991; 1: 299–302.
320. Caswell J, Curtis C, Gibbs B. Astrocytoma arising at the optic disc in dog. *Can Vet J* 1999; 40: 427–428.
321. Jensen OA, Kaarsholm S, Prause JU, Heegaard S. Neuroepithelial tumor of the retina in a dog. *Vet Ophthalmol* 2003; 6: 57–60.
322. Patnaik AK, Kay WJ, Hurvitz AI. Intracranial meningioma: A comparative pathologic study of 28 dogs. *Vet Pathol* 1986; 23: 369–373.
323. Paulsen ME, Severin GA, LeCouteur RA, Young S. Primary optic nerve meningioma in a dog. *J Am Anim Hosp Assoc* 1989; 25: 147–152.
324. Dugan SJ, Schwartz PD, Roberts SM, Ching SV. Primary optic nerve meningioma and pulmonary metastasis in a dog. *J Am Anim Hosp Assoc* 1993; 29: 11–16.
325. Andrews EJ. Clinicopathologic characteristics of meningiomas in dogs. *J Am Vet Med Assoc* 1973; 163: 151–157.
326. Nafe LA. Meningiomas in cats: A retrospective clinical study of 36 cases. *J Am Vet Med Assoc* 1979; 174: 1224–1227.
327. Lawson DC, Burk RL, Prata RG. Cerebral meningioma in the cat: Diagnosis and surgical treatment of ten cases. *J Am Anim Hosp Assoc* 1984; 20: 333–342.

Chapter 9

Ophthalmic Examination and Diagnostics

Part 1: The Eye Examination and Diagnostic Procedures

Franck J. Ollivier, Caryn E. Plummer, Kathleen P. Barrie

Because most ocular structures can be visualized either directly or indirectly, a thorough ophthalmic examination can provide a rapid and accurate diagnosis for many ophthalmic diseases. Furthermore, the eye lends itself to numerous simple and efficient diagnostic procedures, many of which can be performed during a routine examination. This chapter describes examination techniques, diagnostic procedures, and modalities available to veterinarians interested in ophthalmology and, in particular, to veterinary ophthalmologists. Most of these procedures are noninvasive, and a thorough understanding of them can facilitate the identification and diagnosis of many ocular disorders.[1–26]

ANAMNESIS/HISTORY

When combined with a veterinarian's observations, a thorough history will support and often, determine an appropriate course of action. Therefore, the history should not be minimized, but it does not need to be exhaustive. The history should include signalment, primary complaint, current treatment, concurrent disease, and additional medications being used. Further information may be required depending on the specific complaint.

Signalment can provide an important clue to the cause of many ophthalmic conditions. For example, some diseases occur only in a particular species (e.g., corneal sequestrum in felids), whereas others occur more commonly in association with a particular coat color (e.g., multiple ocular anomalies in the homozygous Merle dog). Furthermore, many diseases are inherited or otherwise common to certain breeds (e.g., Collie eye anomaly, hereditary cataract in Morgan horses).

The primary complaints from the owners are usually among the following: ocular discharge, ocular color changes, pain, opacity, pupillary changes, decreased vision or blindness, and enlargement of the eye. Obvious historical concerns include characterization, onset, progression, and duration of the primary ocular complaint. The role of concurrent diseases or secondary complaints should not be underestimated. Many ophthalmic diseases are manifestations of a systemic disease (e.g., diabetic cataracts, mycotic chorioretinitis, hypertensive retinopathy), and some primary ophthalmic diseases may have systemic concerns (e.g., iris melanoma). Concurrent diseases may affect treatment recommendations as well. For example, because of the respiratory implications of its β-blocking effects, timolol should be used with caution (or even avoided altogether) in severely asthmatic cats with glaucoma.

Existing medical therapy can greatly influence findings on ophthalmic examination. For example, topical atropine inhibits the pupillary light reflex (topical atropine has been demonstrated to produce mydriasis for up to 14 days in horses[27]), and sulfonamides and related compounds can potentially induce KCS.[28] Treatment options may also be influenced by existing medical therapy. For example, methazolamide should be used with caution (or not at all) in animals receiving aspirin therapy for chronic arthritis. Veterinary studies are lacking, but in humans, methazolamide and aspirin have both been implicated in severe gastroenteritis, coma, and even death when used together.[29] Knowledge of drug interactions and side effects helps the veterinarian to avoid such complications and occasionally assists in making a diagnosis.

Questions concerning vision can be difficult for animal owners to answer, and the veterinarian must be cautious to avoid "leading" his or her clients. Specific questions should be asked regarding the animal's ability to see in a variety of conditions. For example, night vision may be reduced (e.g., progressive retinal atrophy [PRA]), day vision may be primarily affected (e.g., axial lens opacity obstructing vision when the pupil is constricted), or the animal may have problems visualizing stationary or moving objects (i.e., central versus peripheral retinal disease).

The history should never replace the complete examination, but it will provide valuable information that supports the findings of an ophthalmic examination.

GENERAL EXAMINATION

The basic equipment necessary to perform a proper ocular examination includes the following:

a bright, focal light source (a Finhoff transilluminator is ideal)
Schirmer tear test (STT) strips

a variety of ocular stains
a topical anesthetic
a mydriatic agent
eye wash
sterile culture swabs
forceps
surgical blades
glass slides
cannulas for nasolacrimal duct irrigations
some form of ophthalmoscope for examination of the fundus

The variety of animals that present for ocular examination necessitates a variety of examination facilities to accommodate the different animal species. Small animals can usually be examined on a table in a closed room; large animals require more specialized facilities. Horses may be examined in stocks or stalls, cattle in chutes or stanchions, and other large animals with appropriate restraint that is safe for both animal and examiner; in some cases, this means general anesthesia. Regardless of the species or the state of the animal's ophthalmic health, it is absolutely necessary to have an initially well-lit environment with the ability to darken the area as necessary to allow the examination of specific structures and reflexes of the eye. A proper examination area reduces stress on both the patient and the veterinarian, which facilitates and expedites the ophthalmic examination.

The initial portion of the ophthalmic examination should be performed from a distance. The animal's attitude, overall symmetry and body condition, and ability to navigate in an unfamiliar environment are carefully evaluated. This may provide some insight into the patient's general health and visual acuity. A general physical examination and thorough ophthalmic examination then follow. Because of the close relationship of the eye with the central nervous system, a complete neurologic examination is indicated in patients suspected of having neuro-ophthalmic disease. The neuro-ophthalmic examination can provide a rapid assessment of the integrity of cranial nerves II through VIII.

RESTRAINT

The best method of restraint for any given situation varies with the species involved, the patient's temperament, and the desired effect. Generally, however, the best restraint for the ophthalmic examination is the least amount possible. Methods of restraint include manual, mechanical, and chemical. The health of the animal, extent and duration of the ophthalmic examination, and needs of the client must be considered before a method is chosen, and the client should be informed of any potential risk, especially if sedation or general anesthesia is necessary for completion of the ocular examination.

Most dogs and cats require only manual restraint for ophthalmic examinations. Fractious animals, however, may require additional restraint. Muzzles can be employed with aggressive or fearful dogs, but fractious cats are more difficult to restrain. Towels, especially in the form of the "kitty burrito," or cat bags usually reduce the risk of injury to both the owner and examiner, but chemical restraint may be necessary if a detailed ophthalmic examination is desired. If sedation or general anesthesia is necessary, it is important to consider the effects of pharmacologic agents on the ocular examination.[29] Many anesthetic agents and sedatives decrease tear production or alter IOP. In most dogs, sedation and general anesthesia frequently make the ophthalmic examination more difficult because the eyes tend to roll downward (infraversion) and the nictitating membrane tends to protrude. Ketamine with or without diazepam in combination for brief sedation of cats results in a loss of the blink reflex, which can lead to corneal drying, and mydriasis, which alters the pupillary light reflexes. It can cause nystagmus and in some species will elevate IOP. Opiates may alter pupil size, reactivity, and IOP. Butorphanol may induce miosis in the dog.[30] Acepromazine may cause nictitans protrusion, which obscures the globe during evaluation.

In small animals, protrusion of the nictitating membrane is frequently a challenge to the thorough ophthalmic examination. This problem can be averted by keeping the animal alert with movements or interesting noises, moving the patient's head in different directions, positioning the animal over the edge of a table or otherwise keeping it off balance, and by limiting the length of time and intensity of the light to which the patient's eye is exposed. Experienced clinicians can complete most examinations quickly by using these maneuvers. Practice of the essential components of the ophthalmic examination facilitate its completion even in uncooperative patients.

Chemical restraint greatly facilitates a complete ophthalmic examination of the horse. Xylazine, 0.3 to 0.4 mg/kg intravenously, is usually adequate for examination. Especially difficult equine patients may require either a higher dose of xylazine (1.1 mg/kg intravenously) or a switch to detomidine, 0.02 to 0.04 mg/kg intravenously, or romifadine. If more invasive diagnostic or treatment procedures are to be performed, such as corneal scrapings or conjunctival biopsies or placement of a subpalpebral lavage system, most animals will require the more potent detomidine with or without the addition of butorphanol, 0.01 to 0.02 mg/kg intravenously.[31–33] Detomidine or romifadine at an appropriate dose usually results in rapid sedation without an excitation phase and with a steady head position (without movement such as the jerks that are frequently observed with xylazine and butorphanol sedation) that is necessary when performing any procedure near an eye with impaired corneal integrity.[10] Difficult horses should be restrained in stocks, and a twitch may be used in conjunction with chemical restraint during the examination. As with small animals, the use of restraint and sedation in the horse depends on the animal's temperament, the experience of the handlers and examiner, and the facilities.

Dairy cattle can usually be adequately restrained in a stanchion, with the head pulled laterally by an assistant using a nose lead. Beef cattle may be more difficult to restrain, and squeeze chutes with special head restraints may be necessary. Tilt tables are especially useful with ruminants when lateral

positioning is required or for better immobilization without general anesthesia. Sheep and goats can usually be restrained manually with the help of an assistant. Goats can be examined standing, and sheep can be examined seated on their rumps to avoid excessive movements. Llamas and alpacas may need to be supported in a chute or a sling.

Rodents, rabbits, birds, and small exotics can usually be restrained manually. Mice and rats are sometimes challenging to examine because of their small size and inherently fast and agile movements. Restraint of rodents is best achieved by grasping the animal in the palm of the hand with the heel of the hand gently tucked under the trunk and tail and then gently stabilizing the head by holding the base of the skull between the thumb and the forefinger.[34] Alternatively, an open syringe case or other thin, rigid tube may be utilized so that the rodent's head is sticking out one end and is stabilized, again with the thumb, while the tail is gently grasped from the other end of the tube.[34] Rabbits are usually adequately restrained on a table with a handler's hands supporting the hind limbs with one hand and the back or neck with the other. Difficult rabbits may be restrained in special box devices, and xylazine, 2 to 5 mg/kg intramuscularly, can be used if necessary.[35] Nonhuman primates can be similarly restrained in special devices or seats, and ketamine, 5 to 40 mg/kg intramuscularly, may be used for additional restraint.[35] Most small to medium-sized birds can be examined safely when properly restrained with a hand about the neck and feet, with wings tucked in or wrapped within a towel. Leather working gloves facilitate handling of raptors and other large birds. Ferrets are usually adequately restrained for the ocular examination by simply scruffing the animal by the back of the neck and suspending it, allowing its legs to dangle.

Fish present a different challenge because their removal from water must be for an extremely limited period (no more than 3–5 minutes). Most require heavy sedation or anesthesia, which is usually accomplished by adding a species-specific dose of tricaine methanesulfonate to a small container of clean water and placing the fish in this bath.[36] The fish should be immobilized within 5 minutes and then is very carefully removed from the water and either restrained manually or placed gently on a smooth, padded, plastic surface. The fish should be kept moist and handled only with powder-free latex gloves because its skin is very easily injured.[36]

Whenever an exotic species is to be examined, the clinician should have a strong working knowledge of the species-specific sedation and anesthetic protocols and their potential risks; otherwise, the clinician should defer to an experienced exotic animal specialist. Many wild species require sedation or anesthesia for the ocular examination in order to secure the safety of the examiner and any handlers and to minimize stress for the patient.

Akinesia

The orbicularis oculi muscle closes the eyelids and thus can impair or even prevent ocular examination, especially in large animals. Akinesia of this muscle is routine in the horse, occasionally required in cattle, but only rarely performed in small animals. Eyelid akinesia may be performed for routine eye examination, diagnostic procedures (e.g., corneal cytology, electroretinography [ERG]), treatments (e.g., subconjunctival injections), and to augment anesthesia during surgery. Most horses require an auriculopalpebral block in order for the veterinarian to fully examine their eyes, especially if the horse is afflicted with a painful disease process or if the structural integrity of the globe (usually the cornea) is compromised.

The palpebral nerve, which arises from the auriculopalpebral branch of the facial nerve, innervates the orbicularis oculi muscle. These motor fibers may be blocked at any point between the origin of the auriculopalpebral nerve and the palpebral nerve branch. There are three main points at which the auriculapalpebral or palpebral nerves can be blocked in the horse (Fig. 9.1.1). The first is just anterior to the base of the ear where the auriculopalpebral nerve emerges from the parotid salivary gland and becomes subcutaneous on the lateral aspect of the coronoid process. Here local anesthetic may be injected into the depression just caudal to the ramus of the mandible at the ventral edge of the temporal portion of the zygomatic arch.[19,20,37–39] The rostral auricular artery and vein should be avoided. The second is just lateral to the highest point of the caudal zygomatic arch where the palpebral nerve can be "strummed" under the skin over the dorsal border of the bone.[10,40] The third is where the palpebral nerve lies on the zygomatic arch caudal to the bony process of the frontal bone. Considering the branching of the motor fibers, more proximal blocks generally are preferred because they affect more of the orbicularis oculi muscle (Fig. 9.1.1).[5] A 25-gauge, 5/8-inch needle is used to inject the 1 to 5 mL (usually 1 to 2 mL is sufficient) of anesthetic subfascially adjacent to the nerve, and the injection site is massaged to facilitate drug diffusion about the nerve.[5] Lidocaine is most often employed for this procedure because of its rapid onset and reasonably long duration; however, procaine, bupivacaine, and mepivacaine can be used.[41] With effective akinesia, ptosis, narrowing of the palpebral fissure, and occasionally lower-lid ectropion result. These effects typically last from 45 minutes to 1 hour.[5] A hospitalized horse receiving repeated auriculopalpebral nerve blocks occasionally becomes resistant, thereby taking longer to achieve akinesia and sometimes, requiring higher doses of anesthetic. It appears that local tissues become resistant to drug penetration and that accurate needle placement for injections thus becomes increasingly important.[5]

Akinesia may be achieved in a similar fashion among cattle. The auriculopalpebral nerve can sometimes be palpated as it passes over a palpable notch in the zygomatic arch at the level of the temporomandibular joint.[42] If the nerve cannot be palpated, anesthetic may be injected subcutaneously along the zygomatic arch, starting at the supraorbital process and continuing approximately 3.75 cm caudally.[43] The needle is directed caudally, dorsally, and medially until it contacts the zygomatic arch. The needle is then advanced over the dorsal border of the zygomatic arch, and the area is infiltrated with 5 to 10 mL of anesthetic.

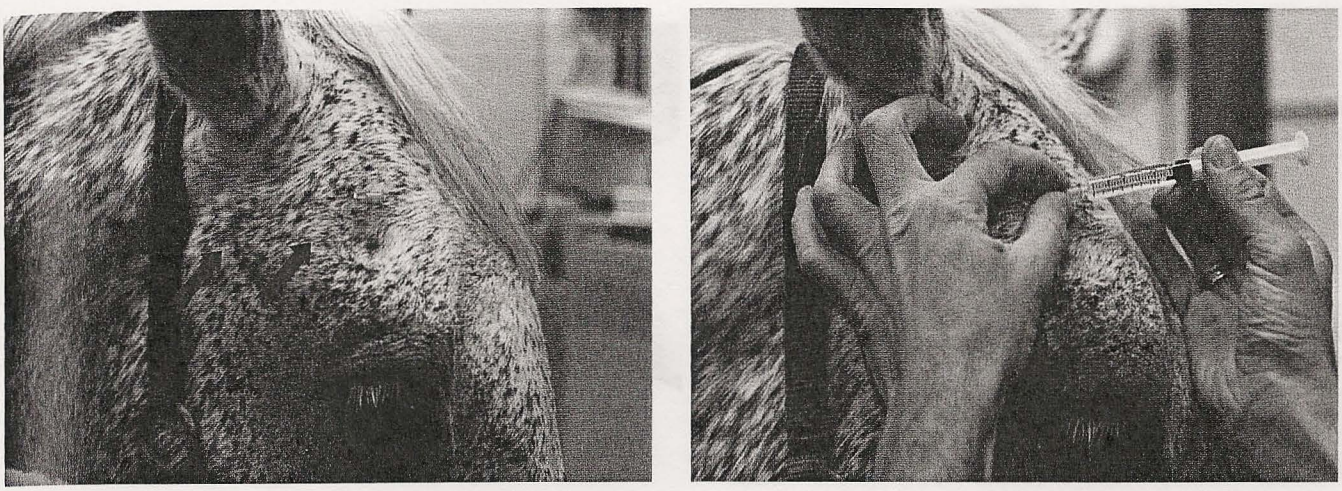

(a) (b)

Figure. 9.1.1. The auriculopalpebral nerve block in a horse facilitates examination of the eye and is crucial when the cornea is fragile and near perforation. This figure illustrates the proximal placement of the block with the needle, while the arrows mark alternative locations that will elicit a similar response.

In the dog, the auriculopalpebral nerve can be found and blocked along the most lateral part of the zygomatic arch, at the midpoint of the caudal third of the bone.[44] Alternatively, terminal palpebral nerve fibers may be blocked as they pass over the orbital rim. In this case, the orbital rim is palpated, and a small-gauge, 5/8- or 1-inch needle is inserted 2-cm lateral to the lateral canthus. The needle is directed medially along the dorsal orbital rim, and then the procedure is repeated along the ventral orbital rim, injecting a total of between 1 and 3 mL of anesthetic throughout the region.[5] This more distal block can also provide some anesthesia through blocking local sensory as well as motor nerves.

Regional Anesthesia/Analgesia

Sensation to the eyelids is provided by the ophthalmic and maxillary divisions of the trigeminal nerve (i.e., cranial nerve V). In most domestic animals, the frontal, lacrimal, and infratrochlear nerves arise from the ophthalmic division of cranial nerve V, whereas the zygomatic nerve arises from the maxillary division.[45,46] In the horse, cow, and dog, the frontal nerve innervates most of the central upper lid, the lacrimal nerve innervates the lateral upper lid, the zygomatic nerve innervates most of the lateral lower lid, and the infratrochlear nerve innervates the medial canthus.[20,40,43,47] Anesthesia of these nerves is occasionally necessary for eyelid and conjunctival biopsies and for subpalpebral lavage placement, especially in the horse. Most often, any diagnostic or surgical procedure that requires blockage of the sensory nerves to the eyelids in small animals is performed while the patient is under general anesthesia, making usage of sensory blocks of the face very infrequently necessary. The risks of general anesthesia to large animal patients and the accurate placement of local anesthesia that is possible in them with adjunctive sedation make these sensory blocks very useful and common in large animal practice.

Several different sensory blocks may be employed in large animals depending on the location of the eyelid lesion to be addressed. The central two-thirds of the upper eyelid is innervated by the frontal or supraorbital nerve and is blocked by injecting 2 mL of 2% lidocaine into the supraorbital foramen.[40] This foramen can be identified as a small depression in the supraorbital process of the frontal bone, medial to its most narrow aspect (Fig. 9.1.2). The lateral upper eyelid and lateral canthus are innervated by the lacrimal nerve and can be blocked with a line block along the lateral third of the dorsal orbital rim. A block of the zygomatic nerve will anesthetize the lateral lower lid and is achieved with a line block along the ventrolateral orbital rim. The medial canthal region is innervated by the infratrochlear nerve and is desensitized by injecting anesthetic through the bony trochlear notch on the dorsal rim of the orbit near the medial canthus.[9,20,40,43,47]

Analgesia of the eye and orbit and immobilization of the globe have many indications, including analgesia for enucleation, as an adjunctive to general anesthesia to reduce nystagmus (especially in horses) and enophthalmos for intraocular surgery, and to facilitate standing diagnostic and treatment procedures of the eyelids, globe, or orbit, most frequently in large animals. In small animals, retrobulbar injections are most commonly used to augment analgesia for enucleation procedures or for better positioning or exposure of the globe for testing and sampling in the research setting. For enucleations in small animals, either lidocaine, bupivicaine, or a combination thereof is injected behind the globe by means of a spinal needle that has been bent into a mild semicircular shape and inserted through the conjunctival fornix between the globe and the bony orbital wall and carefully walked along the orbit until it is positioned behind the globe. The placement in small animals is usually one injection laterally or two injections, one medially and one laterally. Before injection of the anesthetic, the stylet of the needle is removed and the syringe is connected and aspirated. If blood enters the syringe, the needle should be repositioned so that the agent is not injected into a blood vessel. Systemic absorption of an agent placed in

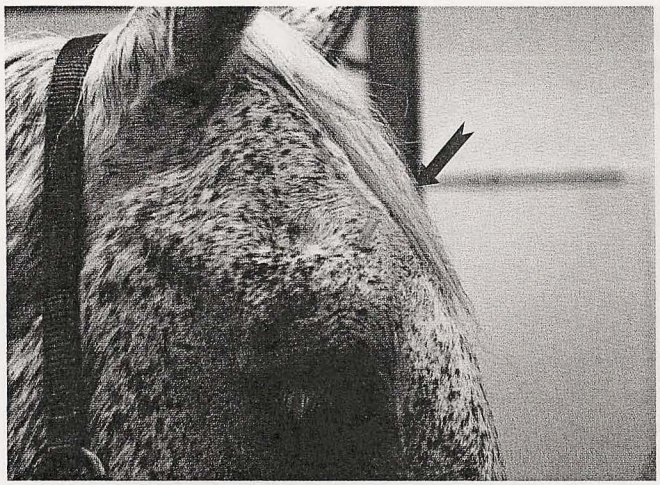

Figure 9.1.2. The supraorbital nerve block is performed at the level of the supraorbital foramen (directly within the foramen if possible, in the region if not) and is useful for anesthesia of the upper eyelid.

the retrobulbar space is significant, so careful dosing of the anesthetic is crucial. This is especially true in cats, in which the toxic systemic dose of lidocaine should never be approximated or exceeded. The volume of anesthetic required for effectiveness varies depending on the size of the animal.

In large animals, retrobulbar anesthesia is commonly employed. In the horse, several methods are described, including the four-point block, the modified Peterson block, and direct injection into the orbital cone above or below the zygomatic arch.[10] The site above the zygomatic arch and caudal to the temporal process of the malar bone requires only a single injection, and because it is not located near either the globe or the optic nerve, it is relatively safe. In this technique, a 22-gauge, 2.5-inch spinal needle is directed through the skin perpendicular to the skull in the orbital fossa, just posterior to the posterior aspect of the dorsal orbital rim. The needle is advanced until it enters the cone, evidenced by the slight "popping" sensation as the eye releases into its normal position.[10] After aspiration, 10 to 12 mL of 2% lidocaine, mepivicaine, or bupivicaine is injected into the space so that the globe is pushed externally.

The four-point block is a local muscle block in which 5 to 10 mL of anesthetic agent is placed in each of four spots (dorsal, lateral, ventral, and medial) with a 20-gauge, 3-inch spinal needle through either skin or bulbar conjunctiva following the curve of the globe posteriorly into the extraocular muscles and orbit. The ventral injection should be directed slightly nasally to avoid the optic nerve.[10] Frequently, only one or two injections are necessary (usually laterally and medially) if the anesthetic is placed with a curved needle to the retrobulbar space, as in small animals (Fig. 9.1.3). This technique should not be used when intraocular surgery is to be performed because it may place pressure on the globe.

In ruminants, retrobulbar anesthesia is accomplished either by retrobulbar injections or the Peterson nerve block or its modification. With retrobulbar injection in cows or small ruminants, the slightly bent needle is either placed laterally

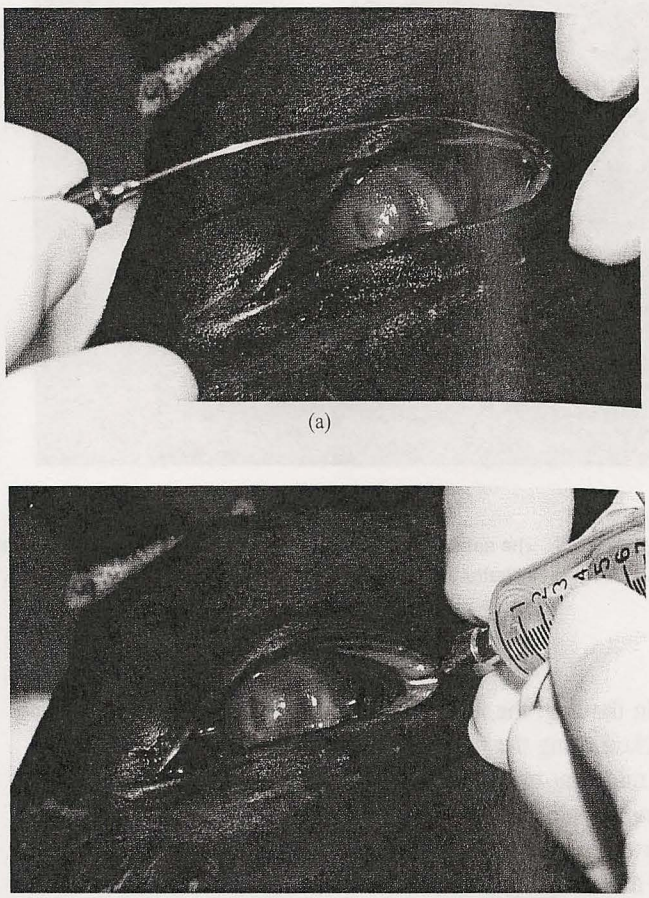

(a)

(b)

Figure 9.1.3. A retrobulbar block is performed with a mixture of lidocaine, bupivicaine, and epinephrine through a 22-gauge, 2.5-inch spinal needle that has been bent to follow the curve of the globe and the orbit prior to enucleation.

and medially at the canthi or dorsally and ventrally through the eyelids or conjunctival fornices and directed along the orbital walls in to the orbit.[42,43] In cattle, 10 to 15 mL of 2% lidocaine is injected through an 18-gauge, 6-inch needle. In small ruminants, a smaller volume is injected through a 22-gauge, 3-inch needle.[42] Many practitioners find that a single injection (as opposed to the paired injections) is sufficient to achieve the desired result of relative exophthalmos, analgesia, and immobilization.

The Peterson nerve block is performed by placing an 18-gauge, 6-inch needle through the notch formed by the supraorbital process cranially and the zygomatic arch ventrally. It is advanced horizontally and slightly caudally until it hits the coronoid process of the mandible. It is then walked off the rostral border and advanced to the pterygopalatine fossa where 7 to 15 mL of 2% lidocaine is injected.[43,47]

OPHTHALMIC EXAMINATION

The objectives of the signalment and anamnesis and the eye examination are to identify the cause of the ocular disease in order to install an appropriate treatment; to determine the severity of the ocular diseases; and to choose the right treatment,

either etiologic and/or symptomatic, medical and/or surgical.[5,17,48,49] The important steps of the ophthalmic examination are discussed in this section.

The eye examination must be complete, organized, and conducted in a timely manner. In addition, certain tests and observations must precede others to avoid interference or complications. If indications for microbiological sampling are present, samples are taken on moistened sterile swabs before instillation of any diagnostic drugs (stains, mydriatics, local anesthetics) because they contain preservatives that may prevent the bacterial growth.[8,50] If a keratoconjunctivitis sicca (KCS) is suspected to be the primary cause of the corneal condition, the Schirmer tear test (STT) may be indicated and should also be done early in the ophthalmic examination: it must be performed before excessive ocular manipulation and instillation of any ophthalmic solutions or ointments.[5,17] The pupillary light reflexes should be evaluated before mydriatics or miotics are used. Similarly, measurement of intraocular pressure (IOP) should precede instillation of mydriatics. The eye lends itself to examination from the anterior (superficial) structures to the posterior (deep) tissues: examination should proceed in this order: lids, orbital structures, conjunctiva and nictitating membrane, cornea and sclera, anterior chamber and iris, lens, vitreous and retina. An orderly, well-planned examination saves time and facilitates both the diagnosis and treatment of ocular disease (Table 9.1.1).

A bright and focal source of light such as a Finhoff transilluminator is directed at various angles, using direct illumination and retroillumination techniques, and may be used in conjunction with magnification to examine the eye. Additional equipment needed to perform a more accurate examination of the adnexa and anterior segment (slitlamp biomicroscope) or the posterior segment (direct and indirect ophthalmoscope) is described in the section "Ophthalmic Diagnostic Procedures."

Distance Examination and Assessment of Vision

The ophthalmic examination begins with an indirect assessment of vision and comfort and can be performed in an adequate illumination prior to tranquilization or nerve blocks if either of those procedures is necessary for the next steps of the examination. How does the animal navigate in an unfamiliar environment? Does it rub or paw at its eyes?

The distance evaluation assesses the size (i.e., microphthalmia or macrophthalmia, buphthalmia or phthisis bulbi) and the position of the globe (i.e., enophthalmos or exophthalmos), as well as the direction of the globes (i.e., strabismus) and their movement (i.e., nystagmus). Any ocular discharge, ptosis, swelling, or muscle atrophy should also be noted. It is important to examine each eye consecutively and to assess ocular and adnexal structures for symmetry. For example, a subtle enophthalmos or exophthalmos may not be obvious when facing the patient but may become apparent when viewing from above the animal's head. Evaluation of ocular movements can be achieved by turning the animal's head from side to side. Normal saccadic and optokinetic movements are noted as the eyes move back and forth in synchronicity, with the fast phase occurring in the direction of head movement. Abnormalities may suggest extraocular muscle, nerve, orbital, or central nervous system (CNS) disease.

Vision, which requires functioning of both the central and peripheral ophthalmic systems, may be roughly assessed with a menace test. The menace test evaluates the optic nerve (afferent way, i.e., cranial nerve II) and the facial and abducens nerve (efferent way, i.e., cranial nerves VII and VI). It is performed by making a menacing gesture with the hand toward the eye, taking care not to touch the vibrissae or cause excessive air currents, which may induce a false-positive

Table 9.1.1 Diagnostic Sequence of the Basic Eye Examination

I. History
Signalment, primary complaint, concurrent disease, current treatment
II. Assessment of the vision and distance examination
Observation of the animal's movement in its environment
Visual testing: menace response, cotton ball test, visual placing, dazzle reflex, maze test
Palpebral reflex
Observation of symmetry, ocular discharge
Eyeball (position, size, direction, movements, retropulsion)
Observation of the pupil: static (symmetry, size, shape) and dynamic (pupillary light reflexes, swinging flash light)
III. Tear test and corneoconjunctival culture
Corneoconjunctival culture
Schirmer tear test
IV. Adnexa and anterior segment examination prior pupillary dilation
Orbit/globes
Eyelids (skin, palpebral fissure, eyelid margin position, abnormal structure: cilia, abscess, neoplasia)
Nasolacrimal apparatus
Conjunctiva (color, surface, foreign body)
Nictitating membrane (position, palpebral side, margin, corneal side: search for foreign bodies)
Cornea (transparency, shine, surface)
Anterior chamber (transparency ,depth)
Iridocorneal angle if indicated (gonioscopy)
Iris (color, aspect, pupil size, pupil shape)
V. Intraocular pressure measurement and pupil dilation
Topical anesthesia and applanation tonometry
Instillation of mydriatic (usually tropicamide 1%)
VI. Anterior segment examination after pupillary dilation
Lens (position, size, shape, surface, transparency)
VII. Posterior segment examination after papillary dilation
Vitreous (transparency)
Fundus (tapetal color, nontapetal color, retinal vessels, optic nerve head size, color and shape)
VIII. Additional diagnostic techniques as indicated

result. If the animal can see, it should blink or move its head away from the stimulus. The menace response is an acquired cortical reflex; therefore, some healthy young animals, particularly puppies, kittens, and foals, may not demonstrate a positive menace response. The menace response can be absent during the first 9 days postpartum in foals[51] and should be acquired by 2 weeks of age.[3,9,52] The menace test should be performed on horses before eyelid akinesia. The response to a menace is also inconsistent in birds.[4] If a patient does not cooperate for the menace test, which is a problem common in the cat, a cotton ball may be thrown across the animal's line of sight. An animal with vision (afferent way, cranial nerve II) will usually follow this stimulus, so oculomotor nerves are also evaluated with this test (efferent way, i.e. cranial nerves III, IV, and VI). Multiple attempts may be required to attract the animal's attention, however, which may desensitize the animal to the stimulus.

The visual placing can also be performed in small animals to test motor function and mental status. The animal is held in space and supported under the chest and head while approaching a flat surface such as a table. The normal response is to extend and raise the legs in anticipation of standing on the surface. If the expected response is not forthcoming, then tactile stimulation should be used to establish the normalcy of proprioception and the efferent way of the reflex.

The palpebral reflex or blink reflex should be tested in animals that fail to blink completely. The medial or lateral canthus (or both) is gently touched, which normally stimulates a blink reflex. If cranial nerves V (afferent way, i.e., trigeminal nerve) or VII (efferent way, i.e., facial nerve) are not functioning or the eyelids are physically unable to close (e.g., buphthalmia), the animal may not blink completely.

The pupils should be observed for asymmetry (i.e., anisocoria) in both light and dark settings. An animal with unilateral Horner's syndrome, for example, may have symmetrically constricted pupils in bright light. In dim light, however, only the normal pupil dilates. The examiner may more accurately assess pupil asymmetry by looking through a direct ophthalmoscope from a distance of 3 to 5 feet. The ophthalmoscope is set at zero or a positive diopter setting, and the examiner observes the patient's pupils while directing the light source toward the bridge of the patient's nose. The pupillary light reflex (PLR) can then be tested using a focal light source. This subcortical reflex requires functioning of the retina, cranial nerves II (afferent way, i.e., optic nerve) and III (efferent way, i.e., parasympathetic fibers along the oculomotor nerve), midbrain, and iris sphincter muscle, which explains why cortically blind animals can have a normal PLR. Both direct and consensual (i.e., constriction of the contralateral pupil) PLRs should be tested. Because all optic nerve fibers decussate at the optic chiasm in nonmammalian vertebrates, these animals are not expected to have a true consensual PLR.[4] A false consensual PLR, however, may be noted in avian species related to direct passage of an intense light through the illuminated eye, across the thin septum dividing the orbits, and onto the contralateral retina.

The "swinging flashlight" technique is a modification of the PLR test. A focal light source is passed repeatedly from one eye to the other, which normally stimulates the pupil under direct illumination to constrict slightly more than the contralateral pupil. A unilateral lesion of the retina or a prechiasmal optic nerve will often result in a pupil that constricts when the fellow eye is illuminated but subsequently dilates when illuminated directly. Fearful animals with excessive release of epinephrine and norepinephrine from the adrenal medulla as well as animals under the effects of topical or systemic drugs inducing mydriasis or miosis may have abnormal pupillary reflexes. Anisocoria and abnormalities of the pupillary reflexes are discussed in detail in Chapter 29.

The "dazzle" reflex is a subcortical reflex that requires functioning of the retina and cranial nerves II (afferent way, i.e., optic nerve) and VII (efferent way, i.e., facial nerve). A bright, focal light source must be used, particularly in animals with lesions obstructing the visual axis. Blinking or squinting represents a normal response.

In animals suspected of blindness, an obstacle course or "maze test" may be used to determine clinical vision. Gray foam cylinders are used to create a maze in the examination room through which the patient must navigate. In the absence of such equipment, chairs, tables, and garbage cans will suffice. The test should be performed in both light and dim illuminations, thereby allowing the animal time to adjust to the darkness, and obstacles may be readjusted to avoid memorization. For the dark-adapted test, a red light is ideal. The maze test is particularly useful in animals with suspected retinal degenerations.

Tear Tests and Microbiological Sampling

At this point in the examination, or even before some of the aforementioned tests are conducted, the STT should be performed (see "Tear Tests" under "Ophthalmic Diagnostic Procedures"). Excessive manipulation of the eye and orbit before tear testing may prematurely stimulate reflex tearing, which could falsely elevate the STT values as well as the instillation of any diagnostic eye drops (stains, mydriatics, local anesthetics). If a microbiological culture is indicated for any conjunctival or corneal condition, it should be performed before the STT and before the instillation of any diagnostic eye drops.[53]

Adnexa and anterior segment examination is performed before pupil dilation. The orbit itself is then evaluated by observation, palpation of the bony orbital rim, retropulsion of the globe through a closed eyelid, and manipulation of the mandible. As the coronoid process of the mandible ramus impinges on the lateral orbit, jaw manipulation may reveal pain or resistance associated with orbital infections, neoplasia, and trauma. In such instances, the roof of the mouth should be examined for any abnormalities, with particular focus on the soft palate caudal to the last upper molar on the affected side. The eyeball itself is observed for any change in symmetry, size, position, direction, and movements. Diagnostic procedures for the orbit and globe may include survey radiography, orbital arteriography and venography, special

radiographic contrast procedures (i.e., air and radiopaque materials), B-scan ultrasonography, biopsy, and orbitotomy.

Eyelids should then be examined for position, movement, and conformation as well as for dermatologic lesions. The eyelids should be manually everted to examine the conjunctival surfaces as well as the external surfaces and eyelid margins for evidence of abnormal eyelashes or hair (trichiasis, distichiasis, ectopic ciliae), foreign bodies, tumors, or infections. The eyelids differ between species to a considerable extent. The upper eyelid is more mobile in mammals whereas the lower eyelid is more mobile in many lower vertebrates. Larval amphibians and most fish lack eyelids. Metamorphosed amphibians have poor lid development. Most reptiles have mobile lower eyelids, although crocodilians have well-developed upper lids with bony tarsal plates. Birds have a tarsal plate in the lower eyelid and an almost transparent nictitating membrane. The complete fusion of the upper and lower eyelids forms the spectacle in snakes and geckos.[4] The eyelids normally follow the curvature of the cornea, with the meibomian gland openings exposed and the palpebral conjunctiva unexposed. Many species are susceptible to eyelid and eyelash abnormalities. If the eyelid margin is rolled either outward (i.e., ectropion) or inward (i.e., entropion), discomfort, epiphora, conjunctivitis, and even keratitis may develop. Keratitis-induced blepharospasm can further exacerbate entropion because of orbicularis oculi muscle hypertrophy, thus necessitating use of topical anesthesia or even a palpebral nerve block to evaluate the degree of anatomic defect.

The nictitating membrane should be observed for the conjunctival appearance on the palpebral (outer) and bulbar (inner) surfaces (discussed later in this chapter), its protrusion, any abnormal masses (tumors, granulomas, proptosis of the nictitating membrane gland), foreign bodies, and eversion of the cartilage. Manual retropulsion of the globe will cause protrusion of the nictitating membrane to facilitate examination of the anterior surface of the membrane and the leading edge that is usually pigmented. With chronic conjunctivitis, the bulbar surface of the nictitating membrane in particular should be examined for lymphoid follicles or trapped foreign bodies. Topical tetracaine or proparacaine is instilled, and the nictitating membrane is protracted with Van Graefe's forceps (Fig. 9.1.4). In lightly pigmented animals, particularly ungulate species, the external surface of the nictitating membrane is a common site for squamous cell carcinoma, and digital palpation under topical anesthesia is indicated if abnormalities are noted. There is a lack of nictitating membrane in nonhuman primates and in species with spectacles (snakes and geckos).

The nasolacrimal system is then assessed, and any excessive tearing or hypofunction of the tear secretion is noted. The excessive tearing can be caused by a partial or complete obstruction of the drainage apparatus or an increased lacrimation resulting from ocular irritation and uveitis. The drainage apparatus is evaluated by noticing the presence of abnormal discharge (i.e., epiphora, crusty, mucoid, or mucopurulent discharge) and by examining the dorsal and ventral lacrimal puncta. These lacrimal puncta are located 2- to 5-mm lateral of the nasal canthus and 1- to 3-mm bulbar to the eyelid margins in the canine. In some animals, pigment around the margin of the opening facilitates localization. The rabbit lacks a superior punctum, and the pig lacks an inferior punctum. In addition, the entire nasolacrimal apparatus is absent in aquatic, lower vertebrates including fish, amphibians, and chelonians.[4] The lacrimal sac, which is located subcutaneously just ventral to the medial canthus, may become infected (i.e., dacryocystitis) and swollen. The nasolacrimal duct itself may similarly become obstructed, especially as it passes through the bony maxilla, where there is little room for dilation. Patency of this apparatus is tested by placing fluorescein dye in each eye and then observing its passage at the nares. If an obstruction of the nasolacrimal drainage apparatus is suspected, a nasolacrimal flush can be performed to determine the type and degree of obstruction. In cases of infection, obstruction, or both, debris may be collected for culture and cytology. Contrast radiography (i.e., dacryocystorhinography) may also be useful in cases of chronic obstruction or suspected neoplasia. These procedures are discussed in more detail under Part 2 of this chapter.

Figure 9.1.4. Examination of the bulbar surface of the nictitating membrane is performed after instillation of a topical anesthetic and using thumb forceps (Von Graefe's forceps).

The quality and quantity of the tear secretion is indirectly assessed by the observation of the normal preocular tear film (PTF). The PTF is a three-layered structure with both protective and nutritional roles. The middle, or aqueous, layer is produced primarily by the lacrimal and nictitans glands in mammals, and deficiencies may be identified via the STT. The inner, or mucin, layer is produced primarily by conjunctival goblet cells, and deficiencies may produce signs of KCS in animals with normal STT values. Tear breakup times, discussed under "Ophthalmic Diagnostic Procedures," aid in the identification of these mucin deficiencies. Finally, the outer, or lipid, layer of the tear film is produced primarily by the meibomian glands, and deficiencies may occur with inflammations and

congenital defects of the eyelid margins. Tear breakup times are also useful in the diagnosis of this disorder. Slitlamp biomicroscopy may be useful in characterizing the microscopic details of the PTF by observing its specular reflections. An additional test used to detect tear film abnormalities is the rose Bengal dye or lissamine green dye test (see "External Ophthalmic Stains"), which primarily evaluates the integrity of the mucin layer of the PTF.

The palpebral, bulbar, and nictitating membrane conjunctiva should be examined for evidence of inflammation (hyperemia, chemosis, symblepharon), trauma, foreign bodies, aberrant cilia (palpebral surface), petechiae, lymphoid follicles, and abnormal growths (tumors). The conjunctiva can be used to assess the presence of icterus or anemia. The caruncle, which is a small, irregular nodule located in the medial canthus, is larger in ungulates than in carnivores, and it may also be a common site of squamous cell carcinoma. Additional tests for conjunctival diseases include culture, cytology, biopsy, immunofluorescent antibody (IFA) tests, and polymerase chain reaction (PCR) tests (mainly for detection of feline herpesvirus). Scrapings for IFA tests should be obtained before administration of fluorescein dye because the dye will yield false-positive results.[54]

The cornea is examined next. Most mammalian corneas are oval, with a horizontal diameter larger than the vertical diameter. The normal cornea is an avascular, nonpigmented, convex structure. The presence of surface irregularities (growth or defects), blood vessels, pigment, or other opacities indicates disease. Corneal integrity is most readily evaluated with fluorescein dye. The dye is hydrophilic, binding readily to exposed corneal stroma when ulcers are present. The dye will not bind to intact healthy corneal epithelium, however, or to the endothelium and Descemet's membrane.

Corneal sensation may be demonstrated by touching the cornea gently with a thin wisp of cotton while holding open the eyelids. When touched from the periphery to avoid a menace response, the normal corneal reflex is retraction of the globe, with protraction of the nictitating membrane. This corneal reflex tests cranial nerves V, VI, and VII. The degree of corneal sensation can be semiquantified in different areas of the cornea using an esthesiometer, which is discussed later.

Slitlamp biomicroscopy may be useful in characterizing the microscopic details and exact depth of corneal lesions. Specular microscopy may elucidate the cellular abnormalities and densities of the corneal endothelium. Additional tests for corneal disease include culture, cytology, STT, and rose Bengal or lissamine green stains.

The anterior chamber is observed for its transparency and depth. The anterior chamber depth shows more variation in exotic species than in domestic animals, which is partly a reflection of the size and shape of the lens. In fish, the lens may appear to almost touch the cornea. The anterior chamber depth may decrease because of intumescent cataracts, iris bombé, or mass in or behind the iris, or it may appear to be unusually deep in animals with the loss of lens support in cases of aphakia or pseudophakia, reabsorbing cataracts, or lens luxations. A slit beam, as may be found on many direct ophthalmoscopes, pen lights, and slitlamp biomicroscopes, may be useful in evaluating the depth of the anterior chamber. The aqueous humor of the anterior chamber should be transparent, therefore free of blood (i.e., hyphema), cells (i.e., hypopyon), fibrin, cysts, parasites, tumors and other foreign bodies, and protein (i.e., aqueous flare). Aqueous flare can similarly be detected with a slit beam. In a dark room, a slit or tiny circular beam is focused on the cornea and viewed from an angle perpendicular to the beam. Containing only 10 to 50 mg/1 dL protein, the normal aqueous humor is clear.[55,56] With inflammation, however, this protein content can reach 5 to 7 g/dL, which is a condition called plasmoid aqueous.[55,57] Under these conditions, both protein and cells suspended in the aqueous humor reflect the focused beam, thus creating the Tyndall effect. An otoscope head or slitlamp biomicroscope can provide magnification for characterizing microscopic debris such as keratic precipitates or aqueous floaters.

If the anterior chamber cannot be visualized because of corneal opacification, B-scan ultrasonography may prove useful for evaluating chamber depth and consistency. Aqueous paracentesis, described under "Ophthalmic Diagnostic Procedures," may provide useful information via culture, serology, or cytology. Laser cell fluorophotometry or flaremetry, a recently developed diagnostic technique, can also measure protein and cellular debris levels in the aqueous humor.[58]

Because of the presence of the scleral shelf, the canine iridocorneal angle and ciliary cleft cannot be visualized without special lenses. The direct goniolens and indirect gonioprism allow observation of the filtration angle for congenital defects, abnormal narrowing, peripheral anterior synechiae, extension of iris or limbal neoplasms, and foreign bodies. Any animal with glaucoma should be repeatedly evaluated gonioscopically to characterize the iridocorneal angle and ciliary cleft conformation as either open, narrow, or closed. If glaucoma is unilateral, the fellow eye should be examined for abnormalities that may indicate predisposition to developing bilateral disease. Furthermore, animals with anterior uveitis known to be predisposed to angle abnormalities and glaucoma should be evaluated periodically by gonioscopy. This will allow improved decisions regarding prophylactic antiglaucoma therapy and prognosis. The gonioscopy instruments and techniques are described in detail later in this chapter. Though still experimental, ultrasonic biomicroscopy using probes from 40 to 60 MHZ permits high-resolution imaging of the aqueous outflow pathways.

The iris is evaluated for color, consistency, pupillary membranes strands, pupil size and pupil shape, and stability. Multiple colors within an iris may occur congenitally, as with heterochromia irides, or may be acquired, as with chronic inflammation or neoplasia. Blue irises occur in some lightly pigmented breeds, whereas albino animals have pink to white irises. Iris darkening or thickening (or both) may occur with chronic inflammation and neoplasia. Hypoplastic and atrophic

irises are thin, and they usually transilluminate; focal holes may be present as well, especially near the pupil margin.

The major arterial circle of the iris is often visible as an elevated, wavy line near the iris base. A similar structure, the minor arterial circle of the iris, may occasionally be seen near the pupil margin. Strands of pigmented tissue on the iris collarette, which are occasionally seen extending to contact the lens, cornea, or other sites of the iris collarette, are abnormal remnants called persistent pupillary membranes. Strands of iridal tissue not arising from the collerette and extending to the cornea and lens are called anterior and posterior synechia, respectively. Adhesions of the peripheral iris to the peripheral posterior cornea and across the opening of the ciliary cleft are called peripheral anterior synechiae.

The pupil may be abnormally dilated with iris atrophy, glaucoma, retinal disease, or optic nerve disease, or it may be abnormally small with Horner's syndrome or anterior uveitis. Abnormalities of pupil shape may occur with lens luxations, posterior synechiae, iris neoplasia, trauma, or iris atrophy. With reabsorbing cataracts, lens luxations and subluxations, and pseudophakia, the iris may be observed to tremor (i.e., iridodonesis) during eye movement, which is caused by the lack of lens support. The pupil is round in dogs, a vertical slit in cats, and a horizontal ellipse in horses and cattle. Most ungulate species have nodular extensions of the posterior pigmented epithelium of the iris (i.e., granula iridica or corpora nigra), which protrude along the dorsal and ventral pupillary margins. Similar structures are not typically seen in small animals. Pupillary masses in small animals should be retroilluminated to determine whether they are hollow (i.e., cystic) or solid (i.e., neoplasia). Details of iris lesions may be seen through an otoscope head or, preferably, slitlamp biomicroscope. A slit beam can be used to determine if an iris lesion is elevated. Further diagnostic procedures include transillumination, retroillumination, gonioscopy, ultrasonography, brush cytology, and biopsy.

Intraocular Pressure Measurement and Pupil Dilation

Before administration of mydriatics, all animals presented for ophthalmic examination should have the IOP evaluated by instrumental tonometry. Eyes with IOP elevations to between 25 and 40 mmHg may not demonstrate overt signs of glaucoma. IOP may be measured with the TonoPen, the pneumatonograph, the Mackay-Marg tonometer, or less preferably, the Schiotz tonometer (see "Tonometry" in this chapter).

In the absence of glaucoma, pupils are chemically dilated. Tropicamide (1%) is preferred in most mammals because of its rapid onset (10–20 minutes) and relatively short duration (6–8 hours in dogs and 8–12 hours in horses).[59,60] Atropine (1%) is preferred in the rat, and tubocurare derivatives such as vecuronium (0.5% in raptors) must be used in nonmammalian vertebrates because of the presence of striated muscle fibers in the pupillary sphincter muscle. Atropine is usually not used for diagnostic purposes in dogs and horses because it lasts up to 3 days in dogs and 5 to 14 days in horses.[61,27] It is also not used in cats because it may stimulate profuse salivation due to the bitter taste. Inflamed irides usually resist mydriasis and often require multiple doses of tropicamide (1%), atropine (1%), or the addition of phenylephrine (10%) and scopolamine (0.3%). Complete mydriasis is essential for thorough cataract evaluations as well as for peripheral fundic examinations.

Anterior Segment Examination after Pupil Dilation: Lens Examination

The lens is evaluated with both direct illumination and retroillumination for its position, size, shape, surface irregularities, and transparency. Size and shape of the lens in different species varies tremendously. A slit beam is often useful in characterizing cataracts. While directing the beam onto the lens and looking from an oblique angle, the examiner observes a cross-section of that lens. Cataracts should be classified both anatomically and by stage of maturity. The presence of wrinkling in the anterior lens capsule and visibility of a tapetal reflex can help with staging cataract maturity. Cataract appearance and location may give clues as to the cause. Diabetic cataracts and some inherited cataracts (e.g., in Afghan Hounds and Standard Poodles) often begin as equatorial vesicles or clefts. Posterior axial cataracts may occur with persistent hyperplastic primary vitreous or progressive retinal atrophy.

When using the slitlamp biomicroscope, higher magnifications may help to distinguish lens imperfections from true cataractous changes. Lens imperfections appear as irregularities of the anterior and posterior Y-sutures or as multiple linear areas in the lens nucleus. These abnormalities are translucent, and they may regress with age. Nuclear sclerosis, which is an aging change that leads to a hazy, gray-blue appearance in the center of the lens, must be distinguished from a senile cataract. The lens may appear to be cataractous at a glance, but retroillumination and ophthalmoscopy demonstrate that nuclear sclerosis does not actually obstruct the passage of light or prevent visualization of the ocular fundus. Other methods of lens evaluation include both A- and B-scan ultrasonography and magnetic resonance imaging (MRI).

Posterior Segment Examination

The vitreous is normally a clear and homogenous gel that fills the space between the posterior axial lens capsule, posterior chamber, and ocular fundus. In prenatal animals, the hyaloid artery extends from the center of the optic disc to the posterior lens capsule. In very young animals, and especially ruminants, a persistent hyaloid artery may be visible postnatally for several weeks. In cattle, a proximal remnant of this artery can be seen extending a short distance from the optic disc (i.e., Bergmeister's papilla). Visualization of a proximal hyaloid remnant requires either direct or indirect fundoscopy (see "Direct Ophthalmoscopy and Indirect Ophthalmoscopy"), or slitlamp biomicroscopy using the Hruby and Goldmann lenses.

Abnormalities of the anterior vitreous may be observed with direct illumination and slitlamp biomicroscopy. The vitreous should be examined for extensions of uveal or retinal

hemorrhages, neoplasia, parasites, retinal detachment, infection, and inflammation. Degenerative changes appear as suspended crystalline formations (i.e., asteroid hyalosis), shifting "snowflakes" (i.e., synchysis scintillans), or accumulations of collagen and cells (i.e., vitreal floaters). Ultrasonic examination of the vitreous may prove useful if direct visualization is impaired. Another diagnostic procedure, vitreous paracentesis (i.e., hyalocentesis), is particularly useful with inflammatory lesions of the vitreous space and is discussed under "Ophthalmic Diagnostic Procedures."

Successful examination of the ocular fundus requires intimate knowledge of the normal variations within each species. The fundus is a complicated structure that can suffer a variety of pathologic conditions, so it should be thoroughly examined in a systematic manner. Structures or areas to be evaluated include the optic nerve head (i.e., optic disc or optic papilla: shape, color, and topography), retinal vasculature (number and size), tapetal fundus in species with a tapetum (reflectivity, pigmentation, depigmentation, hemorrhage, exudates), and nontapetal fundus. Diagnostic procedures to evaluate the ocular fundus include both direct and indirect ophthalmoscopy, slitlamp biomicroscopy with the Hruby lens, fluorescein angiography, electroretinography (ERG; i.e., flash and pattern), ultrasonography, biopsy, scanning laser tomography, and optical coherence tomography. Direct and indirect ophthalmoscopy are the primary means to visualize and evaluate the ocular fundus. Fluorescein angiography permits analysis of the retinal and choroidal blood vessels, their permeability, and the integrity of the retinal pigment epithelium (RPE). Flash ERG, discussed in Part 4 of Chapter 9, evaluates the function of the outer retinal layers and is most useful in the diagnosis and investigation of retinal degenerations. Though still experimental, the pattern ERG is indicated for those diseases affecting the inner retinal layers (e.g., glaucoma). The newer imaging procedures, such as scanning laser tomography and optical coherence tomography, permit high-resolution topographic and full-thickness visualization of the retinal layers (see Chapter 9, Part 2).

OPHTHALMIC DIAGNOSTIC PROCEDURES

Slitlamp Biomicroscopy

Slitlamp biomicroscopy permits improved direct visualization of surface lesions of the eyelids, conjunctiva, sclera, and iris. More importantly, it enables the examiner to identify and localize even the most subtle lesions of the cornea, anterior chamber, lens, and anterior vitreous. When combined with special lenses, the slitlamp biomicroscope can also be used to evaluate the iridocorneal angle and ciliary cleft, pars plana, and ocular fundus.[63] The slitlamp biomicroscope remains the instrument of choice for the examination of the ocular anterior segment.

In 1911, Gullstrand developed the first slitlamp biomicroscope, combining a corneal microscope with a slit lamp that used a magnesium oxide light.[63,64] After years of refinement and modifications,[63] the slitlamp biomicroscope saw its first publications in veterinary medicine when Uberreiter described its use in the evaluation of both normal and diseased animal eyes between 1953 and 1959.[65–68] Later, Martin published a series of papers on slitlamp biomicroscopy of the normal dog eye.[69–71]

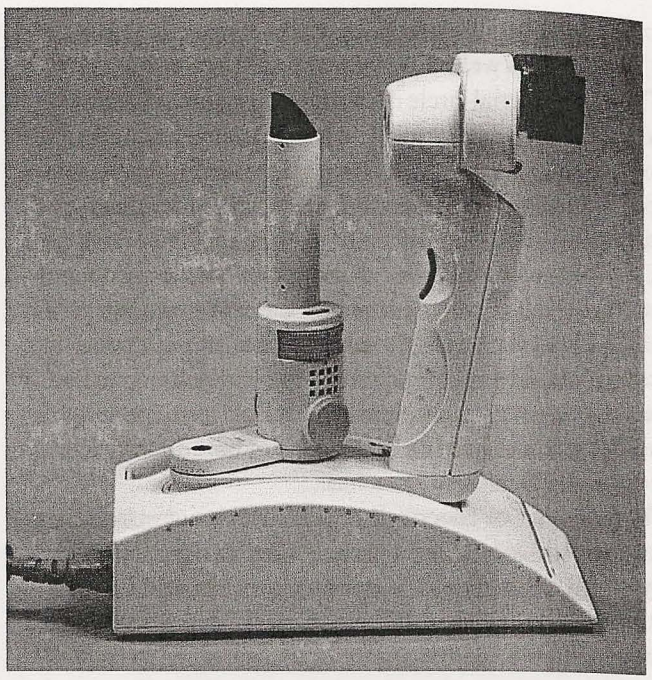

Figure 9.1.5. The portable binocular Kowa SL15 slitlamp biomicroscope with an external, pivoting, and adjustable light source. The strong white focal light can be modified by a series of diaphragms and filters that adjust the light shape (diffuse or focused beam); the light intensity; and the light-beam width, length, orientation, and color (cobalt blue or red free). In addition, the entire housing of the light source pivots to change the direction of the beam. Returning light is focused through the objective lenses of the binocular microscope and can be adjusted from x5 to x40, depending on the model.

A binocular microscope with an external, pivoting, and adjustable light source forms the basic design of the slitlamp biomicroscope (Fig. 9.1.5).[63] The strong white focal light can be modified by a series of diaphragms and filters that adjust the light shape (diffuse or focused beam); light intensity; and light-beam width, length, orientation, and color (cobalt blue or red-free). In addition, the entire housing of the light source pivots to change the direction of the beam. Returning light is focused through the objective lenses of the binocular microscope, and magnification can be adjusted from x5 to x40, depending on the model. It is interesting to keep in mind the optic properties of the examined eye because it adds magnification to the biomicroscope's magnification. Therefore, the magnification of the biomicroscope remains unchanged at the surface of the cornea but is multiplied by 1.1, 1.3, 1.5, and 1.7 inside of the cornea, at the anterior capsule, in the center of the lens, and at the posterior lens capsule, respectively (numbers valid for human).[63,65–71]

Both table-mounted and portable slitlamp biomicroscopes are available.[63,69] Table-mounted models are more expensive and delicate, but they offer a wider range of magnifications, greater variability of slit-beam width and orientation, and the potential for photography. They are useful for both laboratory

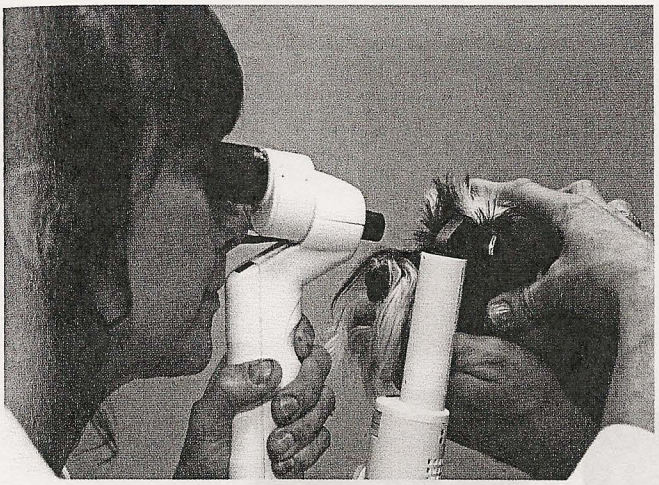

Figure 9.1.6. The use of the slitlamp biomicroscope in a dog.

and small animal patients. Table-mounted slitlamp biomicroscopes are manufactured by Haag Streit, Marco, Nikon, Reichert, Topcon, and Zeiss. Portable units are less expensive and can be used on both small- and large-animal patients in any position (Fig. 9.1.6). These factors have made handheld slitlamp biomicroscopes the models of choice among veterinary ophthalmologists (Fig. 9.1.6). Portable models are available from Clement-Clark, Kowa, Nippon, and Zeiss. Kowa has produced several portable models, the newest of which is the SL-15 (Fig. 9.1.5). This lightweight, durable model is powered by a rechargeable battery, thereby improving its portability. Slit-beam widths are preselected at 0.1, 0.2, and 0.8 mm; ocular magnifications of x10 and x16 are included. Older models, which are no longer manufactured, include the SL-1, SL-2, and SL-5. The SL-2 has a continuously variable slit-beam width of 0 to 10 mm and a zoom magnification system ranging from x5 to x20. The SL-5 has preselected slit-beam widths of 0.1, 0.2, and 0.8 mm and ocular magnifications of x10 and x20. The Zeiss model has a fixed magnification of x12. Because the portable models are most commonly used in veterinary ophthalmology, additional details are provided.

Before performing slitlamp biomicroscopy, the oculars (i.e., eyepieces) should be adjusted to accommodate the interpupillary distance and to correct the refractive error of the examiner's eyes.[63,64,72] This is done by focusing on a target rod (i.e., focusing bar) that attaches to the instrument at a fixed distance from the objective (i.e., the focal distance of the slit beam) or on small print or small parallel lines present in the periphery of the viewing field as seen through the slitlamp.[72] The animal's head is restrained by an assistant or the examiner's free hand (Fig. 9.1.6). In the sedated or anesthetized patient, an eyelid speculum may be useful; in such cases, the cornea must be kept moist with normal saline or ocular flush to prevent optical distortion as well as corneal damage. The light beam is angled at 20 to 45 degrees from the axis of the microscope, usually away from the muzzle to avoid interference, and the oculars are rested against the examiner's brow. The focal distance of the instrument is 7 to 10 cm, at the intersection of the light beam axis with the microscope axis, and the fine focus is achieved by moving either toward or away from the eye within this range. Following this first part of the biomicroscopic examination (i.e., eyelids, conjunctiva, cornea, anterior chamber, and iris), 1% tropicamide (1% atropine in the rat) can be instilled to induce mydriasis in order to perform the biomicroscopic examination of the lens.[59,60]

The slitlamp biomicroscope allows many ways of illumination according to the goal of the examination (Fig. 9.1.7): direct illumination when the light is focused directly onto the object of interest, retroillumination when the light is directed behind the object of interest, and specular reflections when the surface is evaluated by these reflections. Direct illumination can be diffuse (i.e., unfocused) or focal (i.e., focused); retroillumination can be direct (i.e., the object is viewed directly against the illuminated light-reflecting surface) or indirect (i.e., the object is viewed against a dark background beside the illuminated light-reflecting surface).[63]

Initially, diffuse illumination is used to locate the eye and to inspect the surface of the eyelids, cornea, conjunctiva, and iris, but no localization in depth is possible with this method. This technique is performed using a wide, low-intensity slit beam. The examination then continues with a direct focal illumination. Using low magnification, a broad slit beam is focused on the cornea creating a parallelpiped or "optical block" (i.e., three-dimensional section) of illuminated tissue; this method is used to examine transparent media (cornea and lens) and allows localization of the lesions in depth (Fig. 9.1.8).[63] This method allows visualization of the cornea, including an anterior surface seen as a bright sharp line (tear film) with a dark zone underneath (epithelium); an intervening stroma seen as a wide, diffuse, gray (translucent) zone; and the posterior surface (Descemet's membrane and endothelium) seen as a bright, sharp, deep line. The lens can be similarly evaluated in three dimensions with a sharp convex line (i.e., anterior capsule), a less sharp concave line (i.e., posterior capsule), and a wide diffuse, gray zone in between (i.e., lens nuclei, lens cortex, lens sutures). The anterior chamber is normally invisible, but abnormal presence of red blood cells, white cells, or protein (i.e., aqueous flare or Tyndall effect) can also be seen using this method. However, nontransparent structures such as the iris yield only a magnified, two-dimensional view. The slit beam is then narrowed and intensified to reveal a two-dimensional cross-section (called "optic section") of the cornea and lens, thereby allowing the examiner to accurately determine lesion depth and axial positioning. The thinner the slit-beam, the better the definition and the depth localization of the lesions. This property of the narrow beam (i.e., permitting visualization and localization by means of optic sections, analogous to the serial sections in histology) is of the greatest importance.[63]

Direct and indirect retroillumination is performed by reflecting the slit beam from deeper structures while focusing on more superficial structures. This technique improves detection of opacities in the cornea, anterior chamber, lens, and vitreous, because they reflect, refract, or obstruct returning light.

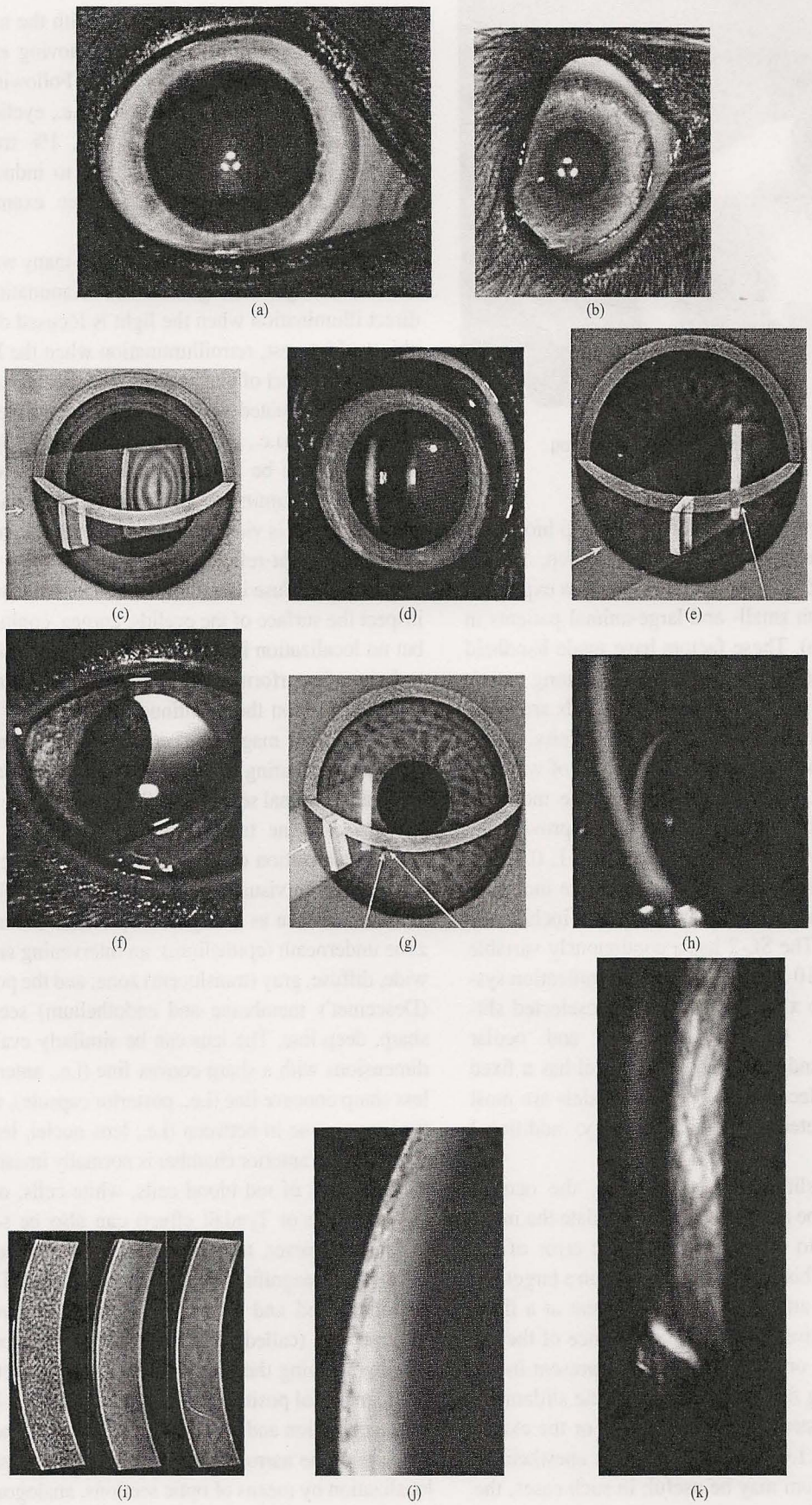

Figure 9.1.7. The slitlamp biomicroscope allows many ways of illumination according to the goal of the examination: direct illumination when the light is directed directly onto the object of interest (**A, B, C,** & **D**) and retroillumination when the light is directed behind the object of interest (**E, F, G,** & **H**), and specular reflections when the surface is evaluated by these reflections (**I, J,** & **K**). Direct illumination can be diffuse (i.e., unfocused) (**A** & **B**) or focal (i.e., focused) (**C** & **D**); retroillumination can be direct (i.e., the object is viewed directly against the illuminated light-reflecting surface) (**E** & **F**) or indirect (i.e., the object is viewed against a dark background beside the illuminated light-reflecting surface) (**G** & **H**). *Yellow arrows:* direction of the light beam. *Black arrows:* direction of the observer (*full line:* direct observation; *dotted line:* indirect observation). **A:** blue iris of a horse, **B:** blue iris of a dog, **D:** eye of an owl, **F:** ciliary body cyst in a cat, **H:** iris cyst in a dog, **J:** corneal edema in a horse, **K:** normal view of the dog cornea, anterior, chamber and iris.

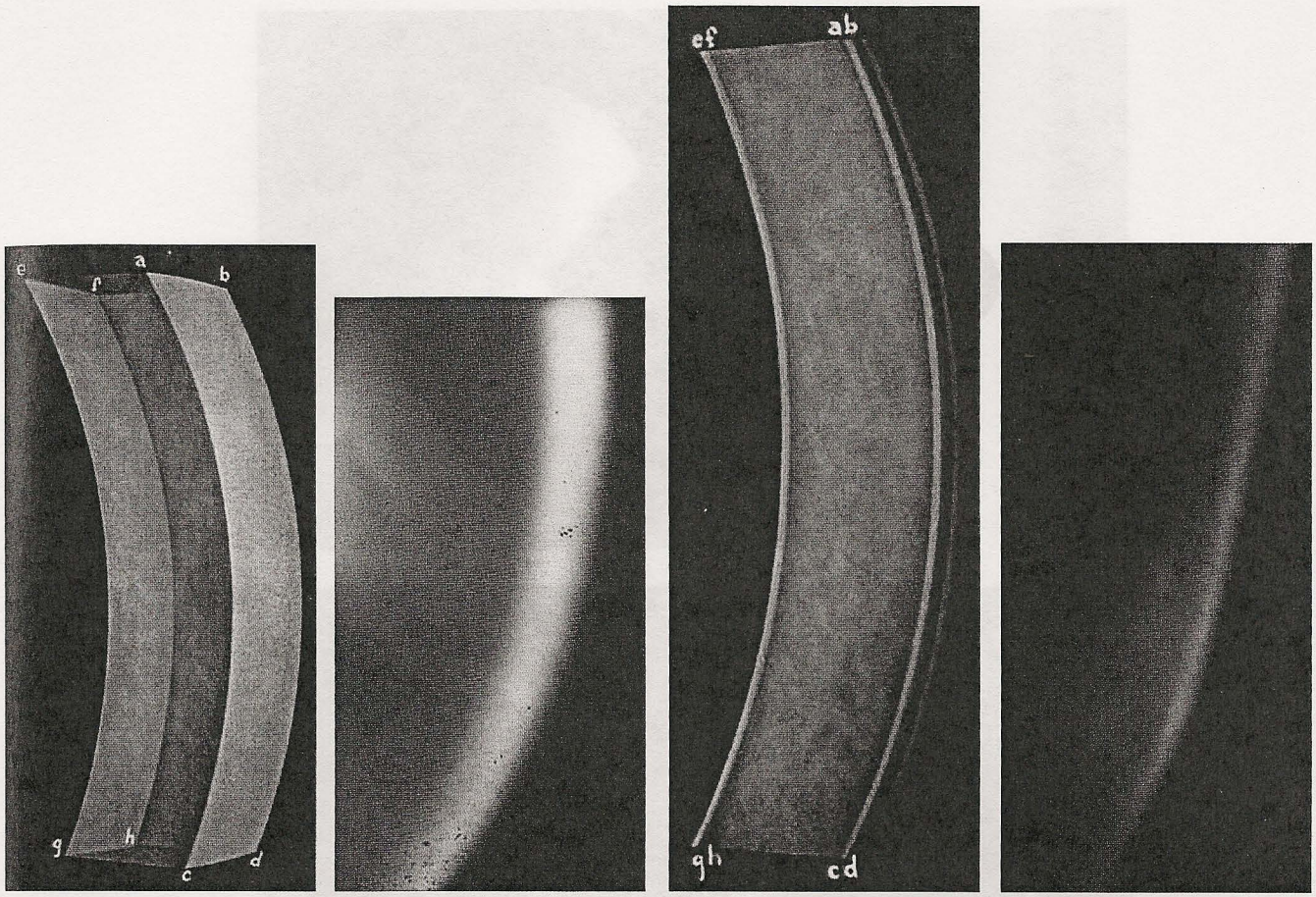

Figure 9.1.8. Focal illumination with the slitlamp: importance of the thickness of the beam. To perform an examination with a direct focal illumination, a broad slit beam is focused on the cornea, creating a parallelpiped or "optical block" (i.e., three-dimensional section) of illuminated tissue (**A** & **B**). This method is used to examine transparent media (cornea and lens) and allows localization of the lesions in depth as well as visualization of the cornea, including an anterior surface seen as a bright sharp line (tear film) with a dark zone underneath (epithelium); an intervening stroma seen as a wide, diffuse, gray (translucent) zone; and posterior surface (Descemet's membrane and endothelium) seen as a bright, sharp, deep line. The lens can be similarly evaluated in three dimensions with a sharp convex line (i.e., anterior capsule), a less sharp concave line (i.e., posterior capsule), and a wide, diffuse, gray zone in between (i.e., lens nuclei, lens cortex, lens sutures). The anterior chamber is normally invisible, but abnormal presence of red blood cells, white cells or protein (i.e., aqueous flare or Tyndall effect) can also be seen using this method. However, nontransparent structures such as the iris yield only a magnified, two-dimensional view. The slit beam is then narrowed and intensified to reveal a two-dimensional cross-section (called "optic section") of the cornea and lens (**C** & **D**), thereby allowing the examiner to accurately determine lesion depth and axial positioning. The thinner the slit-beam, the better the definition and the depth localization of the lesions. **B:** corneal edema in a dog, **D:** superficial corneal edema and deep corneal stromal abscess in a horse.

Direct retroillumination is performed by placing the objectives in the path of the reflected light, which causes opaque lesions to appear dark against a light background and transparent lesions to appear clear within a dark halo. Indirect retroillumination allows improved detection of transparent lesions by taking advantage of differences between their refractive indices and those of the surrounding tissues. Lesions are observed against a darker background because the reflected light is directed away from the objectives.[63]

Using the direct and retroillumination methods, three basic types of lesions can be defined (Fig. 9.1.9): obstructive lesions (i.e., block the light) such as pigment, blood clot, dense scar, dense cataract, and tissues masses; translucent lesions (i.e., some light may pass through the lesion but is scattered) such as corneal edema, keratic precipitates, fibrin, mild cataract, and thin scars; and refractile lesions (i.e., light passes freely through the lesion but is refracted) such as the lens equator, lens vacuoles, lens wrinkles, distorted tear film, and corneal bullae.[63]

Specular reflections are seen in cases of an imperfect reflective surface (Fig. 9.1.7). For example, a perfect mirror does not generate specular reflections because it does not scatter the light, whereas an imperfect mirror does scatter the light. With direct focal illumination using a narrow slit-beam width directed at the limbus, a bright reflection (i.e., specular reflex) results from the curved internal and external surfaces of the cornea. This reflex can be used to evaluate the continuity of the PTF and the corneal endothelium, with defects appearing as breaks in the linear reflex.[63] Polarized light has even been used to evaluate the precorneal tear film (PTF) in dogs and cats.[73,74] Because even slight ocular movements make this technique difficult or even impossible, sedation or general anesthesia is often employed.

Slitlamp biomicroscopy is also useful for assessment of corneal thickness (i.e., pachymetry), anterior chamber depth, and aqueous flare. With direct and indirect goniolenses, the slitlamp biomicroscope allows for a magnified and stereoscopic

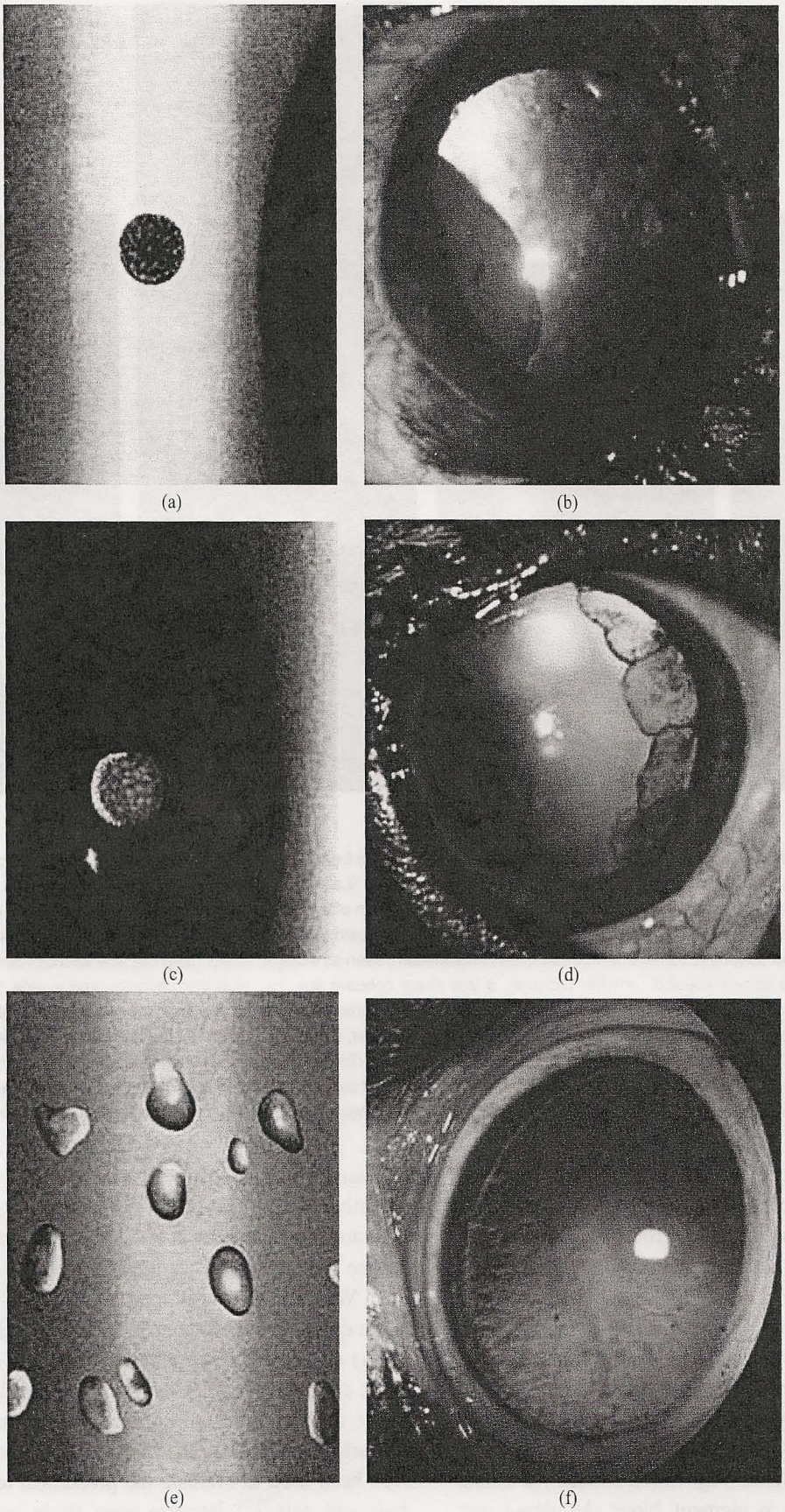

Figure 9.1.9. Types of lesions observed with the slitlamp biomicroscope. Using the direct and retroillumination methods, three basic types of lesions can be defined: obstructive lesions (**A**) (i.e., block the light) such as pigment, blood clot, dense scar, dense cataract, and tissues masses (**B:** ciliary body tumor); translucent lesions (**C**) (i.e., some light may pass through the lesion but is scattered) such as corneal edema, keratic precipitates, fibrin, mild cataract, thin scars, and cysts (**D:** ciliary body cysts), and refractile lesions (**E**) (i.e., light passes freely through the lesion but is refracted) such as the lens equator, lens vacuoles (**F**), lens wrinkles, distorted tear film, and corneal bullae.

view of the iridocorneal angle and ciliary cleft.[64] Special contact and noncontact lenses are also available for use with the slitlamp biomicroscope, thus allowing visualization of the vitreous chamber, ciliary body, and fundus. Examples of such lenses are the Goldmann 3, Hruby, and Rosen lenses.[64]

Direct Ophthalmoscopy

In 1704, Méry described direct visualization of the feline ocular fundus when the eye was immersed in water.[62,75] De la Hire later explained this phenomenon, stating that the water neutralized the reflective and refractive effects of the corneal curvature. In 1846, William Cumming reported his findings of the fundus reflex in humans. Charles Babbage subsequently developed the first ophthalmoscope, using a mirror with a hole in its center. This crude device reflected light at the eye, with the central hole allowing visualization of the fundus by the examiner. In 1854, Thomas Wharton Jones publicized Babbage's device, and Von Helmholtz reported his ophthalmoscope several years later.[62] Constructed of pasteboard, cover glasses, and a lens, this device permitted visualization of an image of the patient's ocular fundus. Reynat is credited as being the first to use direct ophthalmoscopy for veterinary ophthalmology in 1858.[76] Van Biervliet and van Rooy in Belgium and Guerineau in France subsequently reported equine ocular abnormalities observed by direct ophthalmoscopy in 1861. Three decades later, in 1892, Bayer of Vienna published the first atlas of comparative ophthalmoscopy.

Ophthalmoscopy is a difficult but very important procedure for the clinician to master. With diligence and practice, practice, practice, this technique can be mastered and will give the veterinarian yet another tool with which to examine and investigate the patient and its problems. Direct ophthalmoscopy is the classic form of ophthalmoscopy with which most clinicians are familiar since it is commonly available in a set with an otoscope. The direct ophthalmoscope consists of a power source and a halogen coaxial optical system. Light is directed via a mirror or prism into the patient's eye and then reflected back through a lens in the ophthalmoscope to the examiner.[5] Direct ophthalmoscopes take advantage of the refractive power of the patient's cornea and lens. Therefore, refractive errors in both the patient and examiner affect the ability to focus on the ocular fundus. Refractive errors of most animals appear to be reasonably static with the exceptions of the nonhuman primate and the cat, in which some accommodation may occur. Most ocular fundi are in focus at 0 to −2 D if the examiner is emmetropic.[5] The resultant image is real, erect, and magnified several times above normal depending on the species being evaluated (Table 9.1.2). The size of the eye being examined, thus the working distance from the examiner to the lesion of interest, will affect magnification, so it is important to compare any lesions with the size or diameter of the optic disc rather than with any units of measurement.

In order for the clinician to perform direct ophthalmoscopy, animals must be either reasonably cooperative or adequately restrained. Most small animals can be restrained on the examination table by an assistant; some fractious animals or large animals require some measure of sedation and/or an auriculopalpebral nerve block to facilitate the examination. Before examination, the pupils are usually dilated with a short-acting mydriatic such as 0.5% to 1% tropicamide (or 1% atropine in the rat).[59,60] Eyes with dark-colored irides require the stronger concentration of the mydriatic agent than eyes with lighter colored irides and frequently take longer to dilate. The fundi of large animals such as the horse can be visualized without dilation, but mydriasis will ensure a thorough examination. Following adequate mydriasis, the examiner places the direct ophthalmoscope snugly against his or her brow and identifies the patient's fundic reflex from a distance of approximately 0.5

Table 9.1.2 Optical Changes of Direct Ophthalmoscopy in Animals

Species	Fundus Magnification	mm Equivalent per/ Diopter Change
Dog	17.2	0.28
Cat	19.5	0.22
Horse	7.9	1.33
Cow	10.6	0.74
Sheep	13.9	0.43
Pig	15.2	0.36
Rabbit	25.3	0.13
Rat	77.2	0.01
Iguana	38.8	0.06
Great Horned Owl	9.6	0.9
Pigeon	31.6	0.08
Monkey	20.7	0.19
Human	14.7	0.39

Modified from Murphy CJ, Howland HC. The optics of comparative ophthalmoscopy. *Vis Res* 1987; 27: 599–607.

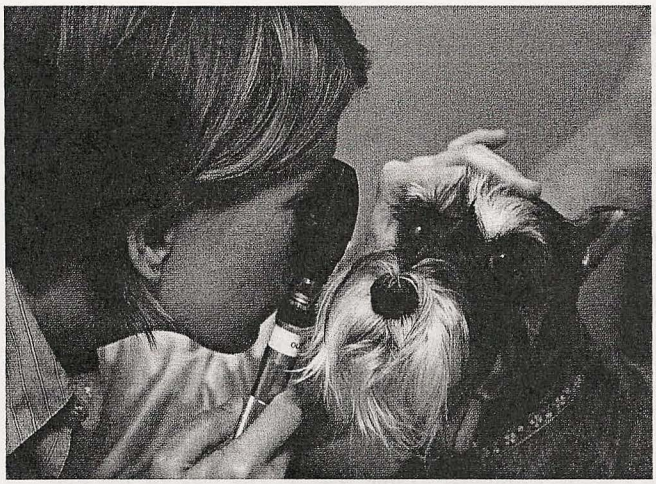

Figure 9.1.10. For direct ophthalmoscopy performed in a dog, the examiner uses the right eye to examine the patient's right eye and the left eye to examine the patient's left eye. The examiner must be quite close to the patient to have the optimal view of the fundus.

Figure 9.1.11. Use of a panoptic ophthalmoscope in a dog. This instrument is a good compromise between the direct and indirect methods of ophthalmoscopy. The image obtained is real (neither inverted or reversed) and intermediate in magnification between the two.

to 0.75 m (Figs. 9.1.10 and 9.1.11). Ideally, the examiner's right eye should be used to examine the patient's right eye, and vice versa. This is especially important in patients with frontal eyes and long noses because this position minimizes contact between the examiner's nose and the patient's muzzle. Alternating eyes takes practice sometimes because most people have a dominant eye that they prefer to use. Once the fundic reflex is identified, the examiner moves toward the patient to a point approximately 2 to 3 cm from the eye. If the direct ophthalmoscope is positioned too far from the cornea, the entire fundus cannot be visualized, and even the slightest movements will cause most of the fundic image to be lost. The constant head and eye movements of our veterinary patients will frequently cause the examiner to lose the image. If this happens, the quickest way to regain alignment is to back up, find the tapetal reflection once more, and then move close again. Once the fundus is visualized, ophthalmoscopy should proceed in a timely and orderly fashion. If the examiner has an established order or pattern to his or her examination, fewer lesions will be missed and it will be easier to properly describe and localize any lesions or areas of interest. The optic nerve is typically identified and examined first. Afterward, the remainder of the fundus is thoroughly examined in quadrants, making sure that the tapetal regions of the fundus, the nontapetal regions of the fundus, the fundic periphery, and the retinal vasculature are closely examined.

A circular dial on the direct ophthalmoscope holds a series of concave and convex lenses that can be rotated through the viewing aperture.[77–80] Green or black numbers on the circular dial represent convex or converging lenses, while red numbers represent concave or diverging lenses. A separate dial or switch adjusts the size, shape, and color of the light beam. Options include large and small spots, slit, graticule, red-free filter (which appears green), and blue filter. The red-free light is used to evaluate retinal vessels and the nerve fiber layer. It is also useful for differentiating hemorrhage, which appears black, from normal pigment and pigmented lesions such as melanomas, which appear brown. The graticule consists of a grid (often of 16 squares) used to estimate the size of fundic lesions. This is most useful for ophthalmologists who deal with human eyes, which are of very similar size. The slit beam aids in detection of elevations or depressions in the ocular fundus. The blue filter can be used to examine the nerve fiber layer of the retina and to augment the external examination of fluorescein dye uptake in any corneal defects. Distances between the normal retina and the surface of such abnormalities can be estimated by changing the dioptric power of the ophthalmoscope. For example, if the retina is in focus at 0 D, and the surface of a lesion is in focus at +3 D (green or black), the lesion is elevated. If the surface of the lesion is in focus at −3 D (red), however, it is depressed. The size of the circular spot of white light should be adjusted to the patient's pupil size to minimize light reflections from the corneal surface. The intensity of the illuminating light is controlled by a rheostat and is generally adjusted for the comfort of both the patient and examiner. If for some reason the pupil is not dilated, it is best to have the illuminating light dim to minimize the pupillary constriction that will result when the light is directed on the eye. It is also important to perform the fundic examination in a dim room to optimize the conditions for a thorough and complete examination.

The direct ophthalmoscope can also be used to pick up any central opacities in the clear media anterior to the fundus by retroillumination. Once the fundic reflex is identified by the examiner looking through the ophthalmoscope at a distance, a dark spot detected against the fundus reflection indicates that an opacity is blocking the return of light to the observer. The depth of this opacity, whether in the cornea, anterior chamber, lens, or vitreous, cannot be determined, but the examiner will be alerted to its presence and will know to go back and more closely examine and localize the lesion. There are ways, however, of localizing a lesion with the direct ophthalmoscope. By using the diopter settings on the ophthalmoscope as previously

described, the clinician can determine whether a lesion is raised or depressed relative to the rest of the fundus. Also, examination of a lesion's shape or morphology, as in the shape of a fluid lesion or hemorrhage in the back of the eye, can be helpful in determining a lesion's position.[6] Fluid lesions must conform to the anatomy and shape of normal structures present. Intraretinal hemorrhages tend to be small and round because of confinement by axon, dendrites, and Müller cell processes occupying the area. Hemorrhages in the nerve fiber layer of the retina tend to form flame-shaped shapes with flat and feathered borders because the blood has oozed between the fibers. Preretinal hemorrhages within a formed vitreous are usually large and red and tend to form flat tops due to the effects of gravity causing the red blood cells to settle out. If the vitreous is liquefied and a preretinal hemorrhage is present, the blood will diffuse within the liquid vitreous. Lesions may also be localized by comparing them to the position of a known structure such as a blood vessel or the tapetum. Another method of determining a lesion's location is to take advantage of the phenomenon of parallax in which a structure of interest is looked at against the background from two different observation points and determining if the structure moves in relation to the background.[6] This determines whether the two points are separated or apposed and whether they are located on or in front of the retina. This method is particularly useful when examining inferior retinal detachments.[6]

The advantages of direct over indirect ophthalmoscopy include greater magnification, availability of options such as the slit and grid, and ability to alter the dioptric power of the ophthalmoscope. Disadvantages include a small field of view that can result in lesions being missed, short working distance between examiner and patient, lack of stereopsis, difficulty in examining the peripheral fundus, and greater distortion when the visual axis is not completely transparent (Fig. 9.1.14).

Indirect Ophthalmoscopy

Ruete first conceived of the indirect ophthalmoscope in 1853.[62] Despite several advantages over direct ophthalmoscopy, however, it did not gain wide acceptance in the United States until 1947, when Schepens and Bahn[81] developed a high-intensity light that improved visualization of the fundus. In 1960, Rubin[82] published the first study describing use of indirect ophthalmoscopy in dogs. In 1966, Vierheller[83] published his clinical experiences with the device. Indirect ophthalmoscopy has since become a routine part of the veterinary ophthalmic examination.

Indirect ophthalmoscopy, in contrast to direct ophthalmoscopy, allows the clinician to view a larger portion of the fundus (larger field of view) at one time and to do so from a larger and safer working distance from the patient (Figs. 9.1.12 and 9,1.13). The image generated with indirect ophthalmoscopy may be a bit confusing to the novice examiner because it is inverted and reversed (upside down and backwards), but once the technique is mastered, it is an indispensable tool for a thorough evaluation (Fig. 9.1.14).[84] Since there is much less magnification of the image perceived with indirect ophthalmoscopy than with direct ophthalmoscopy, a better overview of the fundus can be achieved (Fig. 9.1.14; Table 9.1.3). The two methods often complement each other nicely, particularly if a lesion is detected with the indirect method and then examined more closely, at greater magnification, with the direct method. The necessary components of indirect ophthalmoscopy are a strong, focal light source and a converging lens.

Indirect ophthalmoscopy has additional advantages over direct ophthalmoscopy when a binocular indirect ophthalmoscope is utilized, including stereopsis and the ability to use both hands for patient manipulation. Binocular indirect ophthalmoscopy uses a light source, a mirror to direct light into the patient's eye, a handheld converging lens to magnify the

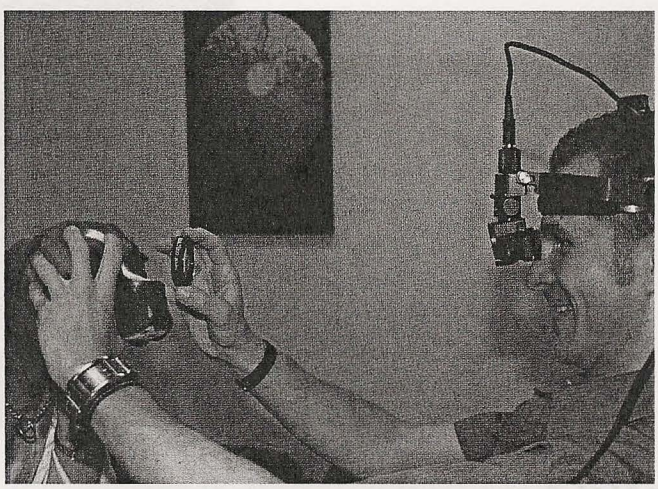

Figure 9.1.12. In bilateral indirect ophthalmoscopy in a dog, this method of fundoscopy allows the examiner to look at the fundus from a distance and benefit from the advantage of stereopsis, or depth perception. The view of the fundus will be inverted and reversed, but it gives a good overview or survey view of the back of the eye.

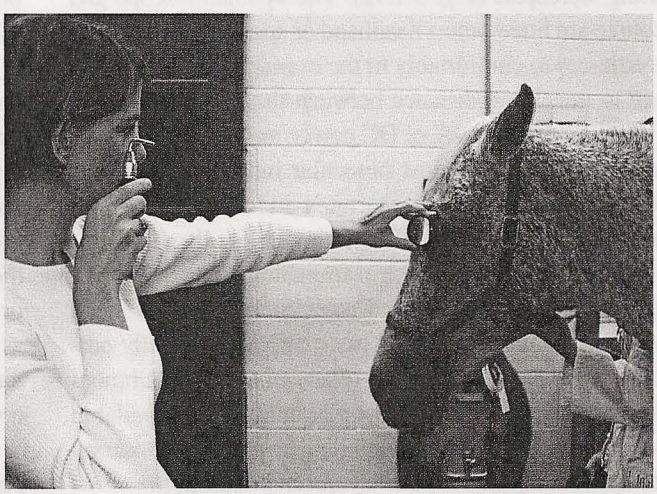

Figure 9.1.13. Monocular indirect ophthalmoscopy with a transilluminator in a horse. This method gives a similar view to that obtained with the indirect headset but without the stereopsis.

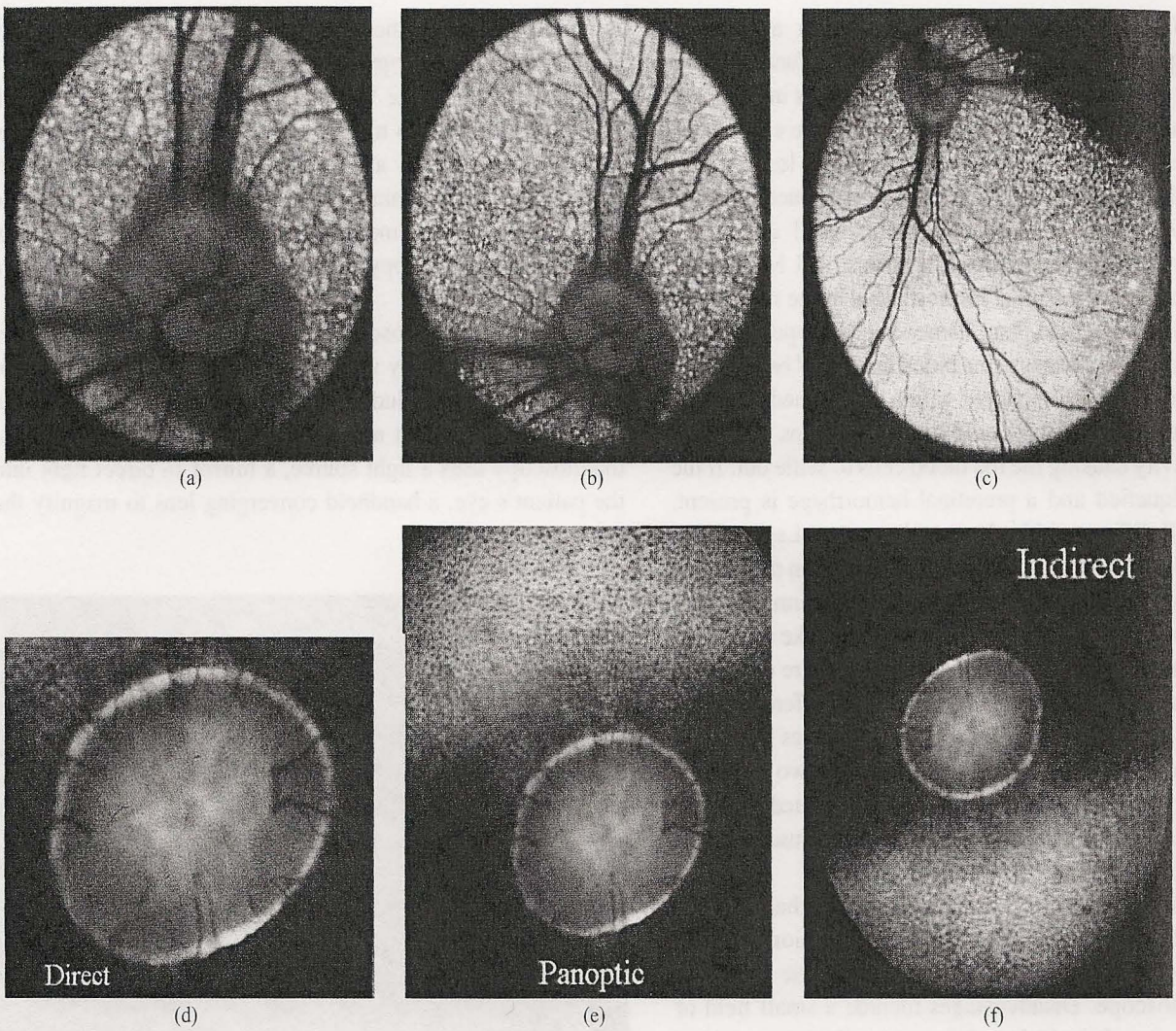

Figure 9.1.14. Comparison of direct, panoptic, and indirect ophthalmoscopy. These photos illustrate the different appearances in terms of magnification and orientation of the canine and equine fundus with each of the three methods of ophthalmoscopy: direct (**A** & **D**), panoptic (**B** & **E**), and indirect (**C** & **F**) ophthalmoscopy.

reflected image, and two prisms to split the reflected light so that it can be directed into both of the examiner's eyes, thereby permitting stereopsis (Fig. 9.1.12). The ophthalmoscope and light source are fitted onto a headband or spectacle frames that can be adjusted to comfortably fit the examiner. Eyepieces are adjusted to match the distance between the examiner's eyes. Light sources use either AC or DC power, and light intensity is altered with a rheostat. Most binocular indirect ophthalmoscopes have interchangeable apertures and filters as well as permanent or detachable teaching mirrors. The headset provides the light necessary for the examination, frees the operator's hands to hold the lens and position the patient's head (frequently without the aid of an assistant), and optically narrows the examiner's interpupillary distance to permit a binocular view and stereopsis. If a binocular headset is unavailable or cost-prohibitive for the clinician, indirect ophthalmoscopy can be performed quite ably and adequately without it.

Monocular indirect ophthalmoscopy employs only a bright, handheld light source (e.g., transilluminator, direct ophthalmoscope or strong otoscope, fiberoptic bundle, penlight) and a handheld lens (Fig. 9.1.13). This method does not allow for stereopsis and requires an assistant to restrain the patient and position the head, but it gives a wonderful overall picture of the fundus.

To perform the fundic examination following mydriasis, the examiner grasps the patient's muzzle with one hand and stabilizes the head. The other hand is used to hold the eyelids open and to position the lens from 2 to 4 cm in front of the patient's cornea. When a binocular headset is not available, an assistant positions the head and holds the eyelids open while the examiner uses one hand to hold the light source against his or her temple so that both the head and the light source move as a unit and the other hand to hold and position the lens. If a direct ophthalmoscope is used as the light source for indirect ophthalmoscopy, the dioptric power should be adjusted to +4 or +6.[5] The lens is held with the thumb and forefinger and positioned so that the strongest convex surface is facing the examiner (or flatter surface toward patient) for the best image. From a distance of approximately 0.50 to 0.75 m, the examiner then directs the light into the patient's eye and identifies

Table 9.1.3 Lateral and Axial Magnification in Indirect Ophthalmoscopy

	Lateral Magnification				Axial Magnification			
Species	**14-D Lens**	**20-D Lens**	**30-D Lens**	**40-D Lens**	**14-D Lens**	**20-D Lens**	**30-D Lens**	**40-D Lens**
Dog	2.57	1.72	1.11	0.82	8.85	3.97	1.65	0.9
Cat	2.91	1.95	1.26	0.93	11.31	5.08	2.11	1.15
Horse	1.18	0.79	0.51	0.38	1.86	0.84	0.35	0.19
Cow	1.58	1.06	0.68	0.5	3.34	1.5	0.62	0.34
Sheep	2.07	1.39	0.9	0.66	5.74	2.58	1.07	0.58
Great-horned owl	1.43	0.96	0.62	0.46	2.75	1.23	0.51	0.28
Tawny owl	2.16	1.45	0.94	0.69	6.26	2.81	1.17	0.64
Pigeon	4.72	3.16	2.04	1.51	29.84	13.4	5.58	3.04
Pig	2.26	1.52	0.98	0.72	6.83	3.07	1.28	0.7
Human	2.19	1.47	0.95	0.7	6.39	2.87	1.19	0.65
Monkey	3.09	2.07	1.34	0.99	12.79	5.74	2.39	1.3
Rabbit	3.77	2.53	1.63	0.2	18.99	8.53	3.55	1.93
Gecko	4.19	2.81	1.81	1.34	23.48	10.54	4.39	2.39
Iguana	5.79	3.88	2.5	1.85	44.71	20.07	8.35	4.55
Flying fox	5.38	3.6	2.32	1.72	38.62	17.34	7.22	3.93
Opossum	7.3	4.89	3.16	2.33	71.24	31.98	13.31	7.25
Frog	9.15	6.13	3.95	2.92	111.9	50.24	20.91	11.39
Rat	11.52	7.72	4.98	3.68	177.44	79.65	33.15	18.06
Bat	36.23	24.27	15.66	11.56	1753.33	787.07	327.6	178

Modified from Murphy CJ, Howland HC. Optics of comparative ophthalmoscopy. Transactions of the Annual Scientific Program of the College of Veterinary Ophthalmologists, 1985; 16: 132–157.

the fundic reflex. The light should be adjusted so that its intensity permits adequate, but not excessive, illumination of the ocular fundus. Excessively bright light can obscure details and cause patient discomfort and thus lack of cooperation. Anesthetized patients that cannot move may develop retinal burns when the light utilized for the examination is too strong. In animals that have a tapetum, the light should be decreased for examination of that region and may need to be increased for examination of the nontapetal fundus.[6] Reflections from the surface of the handheld lens occasionally obscure part of the fundic image, but this can be easily corrected by slightly tilting the lens.

Once the fundic reflex is identified, opacities of the cornea, lens, and vitreous can be seen in front of the reflection. Opacities anterior to the posterior lens nucleus in the dog and cat, and opacities anterior to the posterior lens capsule in the horse, will move in the same direction as the eye rotates. Opacities posterior to these landmarks will move in the direction opposite that of the eye rotation. Opacities in the anterior chamber or vitreous may oscillate or float with eye movement. Lesions anterior to the retina or optic nerve (e.g., persistent hyaloid artery) will change position with respect to their background when viewed from a different angle, an example of the parallax phenomenon. Slight manipulations of the handheld lens itself can reveal subtle hyperreflectivity or streaking in the tapetal fundus. Examination of the fundus with indirect ophthalmoscopy should proceed in an orderly fashion, as in direct ophthalmoscopy, taking care to examine the optic nerve, the retinal vasculature, and the tapetal and nontapetal fundus, even the periphery. The extreme peripheral retina at the ora ciliaris can be visualized with practice and good mydriasis, especially ventrally and temporally.

There are many different lenses available for use with indirect ophthalmoscopy, ranging in diopter strength from +5.5 to +90 D. The choice of a lens will vary depending on the amount of magnification and size of the field of view desired, the amount of stereopsis desired, and the size of the patient's pupil. Fundic magnification varies with lens and species.[85] The magnification of the image is equal to the diopter strength of the eye divided by the diopter strength of the lens,[6,86] so the smaller the diopter rating of the lens, the greater the magnification of the image (smaller number, bigger image). It is important to take into account that additional magnification is built into the binocular headset, so that the image perceived with its use will be even more magnified than that with the lens alone. The strength of the lens also affects the depth perception of the examiner. The higher the diopter strength of the lens, the less stereopsis there will be (larger number, less stereopsis).[6] Also, it is important to consider the size of the animal's pupil when selecting a lens. The higher the diopter strength of the lens, the easier it will be for the examiner to see through a small pupil (smaller pupil, higher number).[86] In general, the higher the diopter strength of the lens, the smaller the image will be, but the larger the field of view, the smaller

the pupil through which an examination can be performed, and the less the stereopsis.[6,86] The +20 D lens is the most versatile, providing a fundus view of approximately 40 degrees, and probably the best choice and compromise for the clinician who wishes to purchase only one lens.[5] However, a PanRetinal 2.2 lens is also available that provides a nice, accurate view of the fundus in its natural concave position.

Various models of binocular indirect ophthalmoscopes are available from Heine, Keeler, Propper, Topcon, Xonix, and Zeiss.[5] Camera and video attachments are available for some models, thus allowing the examiner to display and record findings for teaching and research purposes. Commercial monocular indirect ophthalmoscopes are manufactured by Reichert and the American Optical Corporation.[5] These instruments use an internal lens to magnify the reflected fundic image. The American Optical monocular scope is useful for looking through small pupils and produces an erect image.

Indirect ophthalmoscopy can also be used to semiqualify the refractive error of an animal. By slowly withdrawing the handheld lens from the eye and observing any change in magnification of the image, the clinician can roughly estimate the refractive power of the patient. If the fundic image becomes larger, then the animal is somewhat myopic; if it becomes smaller, then the patient is hyperopic; and if the size of the image remains static, then the animal is emmetropic.[82] Indirect ophthalmoscopy is a useful technique, and its main disadvantage is the cost of the head-mounted binocular equipment.

Retinoscopy

Retinoscopy, also known as skiascopy, is the objective determination of the dioptric state or refractive error of the eye. Commonly used in human ophthalmology and optometry, this technique has also found use in veterinary ophthalmology, particularly to define the normal, pathologic, and surgically induced refractive state of the eyes and in the evaluation and improvement of intraocular lens implants.[87–95]

When light rays are projected onto an eye from infinity, they emerge from an emmetropic eye as parallel rays, from a myopic eye as converging rays, and from a hyperopic eye as diverging rays. The location at which these emergent light rays form a focal point or plane is called the far point. The far point is at infinity, in front of infinity, and beyond infinity for the emmetropic, myopic, and hyperopic eye, respectively. The procedure of retinoscopy utilizes a lens placed in front of the eye to modify the image produced (Fig. 9.1.15). The power of the lens that corrects the image, or neutralizes the movement of the fundic reflex, permits an estimation of the dioptric power of the patient's eye and its difference from emmetropia. Retinoscopy allows veterinary ophthalmologists to determine quantitatively the refractive error of the eye to within 0.25 to 0.50 D of its true refractive state.

The retinoscope, either streak or spot, consists of a tungsten bulb filament, a condensing lens, a circular or linear aperture, and an angulated, plane mirror. Streak retinoscopes produce a linear band of light, whereas spot retinoscopes produce a circular beam. Streak retinoscopes are more commonly

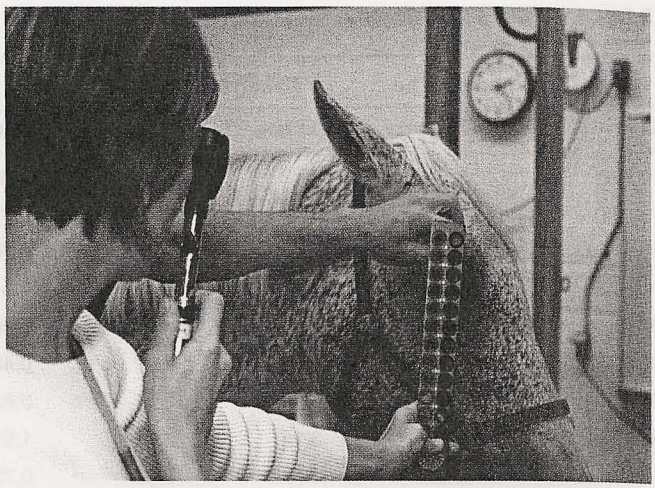

Figure 9.1.15. Retinoscopy performed in a horse. Retinoscopy allows the examiner to determine the refractive power of the patient's eye compared to emmetropia.

employed in veterinary ophthalmology. A sleeve in the handle of the streak retinoscope is moved up and down to change the orientation of the mirror and bulb, thus affecting the vergence of the emitted light. Rotating the sleeve clockwise or counterclockwise affects the orientation of the streak itself. Both streak and spot retinoscopes are available from Copeland, Heine, Keeler, Propper, Reichert, and Welch Allyn.[5] Plus or minus spherical lenses, which are available in increments of 0.25 D, are placed between the retinoscope and the patient to quantitate the refractive error of the eye. A skiascopy bar or rack, which contains a series of plus and minus spherical lenses in increments of 0.5 to 1.0 D, is a simple, convenient, and inexpensive tool for quantifying the refractive error of an animal's eye (Fig. 9.1.15).

Mydriasis prior to retinoscopy is often unnecessary and can even make the procedure more difficult. And because of the limited accommodative ability of most domestic animals, the cycloplegia afforded by the mydriatic agents is not necessary.[91] With the retinoscope resting against the brow, the examiner is positioned 0.67 m (about arm's length) from the patient's eye (a measured 0.67-m string attached to the retinoscope is useful for maintaining this working distance) (Fig. 9.1.15). The sleeve is moved either down (i.e., Heine and Welch Allen retinoscopes) or up (i.e., Copeland retinoscope) such that the projected light rays are very slightly divergent (i.e., plane-mirror effect), and the streak is positioned vertically. Purkinje images from the patient's cornea and lens are superimposed, and the streak is swept horizontally across the animal's pupil. The streak is then rotated horizontally and is swept vertically across the pupil. Finally, a trial lens or skiascopy bar is placed 1 to 2 cm from the patient's cornea, and the process is repeated (Fig. 9.1.15). As the streak is slowly swept across the pupil, the fundic reflex will move in either the same or the opposite direction, depending on the refractive error of the patient. With no refractive lens, the fundic reflex will move in the same direction as the sweep with emmetropic and hyperopic eyes ("with motion") and in the opposite direction of the sweep with less than 1.5-D myopic eyes ("against

motion"). If a "with motion" is observed, plus lenses of increasing dioptric strength are placed in front of the patient's eye until an "against motion" is observed or neutralization is reached. Neutralization is characterized by a fundic reflex that completely fills the pupil without any notable direction of movement. If an "against motion" is observed, minus lenses of increasing dioptric strength are used to achieve neutrality. At a working distance of 0.67 m, a +1.5-D lens is needed to achieve neutralization with an emmetropic eye; therefore, the refractive error of an eye is determined by subtracting 1.5 D from the gross refraction needed to achieve neutrality.

Retinoscopy in the canine reveals that most phakic dogs are within 1.0 D of emmetropia.[87,91,92] Attempts to correlate refractive error with animal size and environment have yielded variable results. Results of one study[90] suggest that indoor dogs and small to medium breeds show a tendency toward myopia, whereas outdoor and large-breed dogs show a tendency toward hyperopia. Breed predispositions to refractive errors also occur, with slight myopia occurring in some populations of German Shepherds, Rottweilers, Miniature Schnauzers, and Labrador Retrievers.[91,92] Retinoscopic results of aphakic canine eyes suggest the mean refractive errors range from +14.0 to +15.2 D and that a +41.5 D lens will usually correct this error to within 1.0 D of emmetropia.[87,90,93] Refractive error in normal horses has been reported to range from −3 to +3 D,[96–98] but most appear to be within 1 D of emmetropia.[99,100] After cataract surgery, the aphakic equine eye has been reported to be hyperopic at +9.94 D.[101] Currently, intraocular lens implants are not commonly employed in horses after cataract surgery, and in one case in which a 25 D lens was implanted, the correction achieved was to only +8 D.[101]

Applications for retinoscopy are presently limited in veterinary ophthalmology, and considerable practice is necessary to produce consistent results with retinoscopy in animals. For that reason, model eyes are available for teaching and practice purposes.[102] With increased use, retinoscopy may continue to improve our selection of intraocular lens implants for patients undergoing cataract surgery and assist with evaluating performance problems in working animals.

Corneoconjunctival Culture

Culture and sensitivity testing provide useful information for the diagnosis and determination of appropriate antimicrobial therapy in many corneal and conjunctival diseases. They should be obtained very carefully from any deep and progressive corneal ulcers, particularly melting ulcers.[8,50,103–108] Cultures may also be taken from purulent or granulomatous conjunctival lesions or from animals with chronic conjunctivitis that does not respond to therapy. Additionally, mycoplasmal or chlamydial cultures (or both) may be desirable in certain species with conjunctivitis, including the cat, cow, sheep, goat, and pig.

Both corneal and conjunctival cultures should be obtained early in the ophthalmic examination, before administration of topical solutions or ointments (Fig. 9.1.16). Most topical ophthalmic preparations contain preservatives that may impair culture results, and some topical drugs (e.g., proparacaine, tetracaine, benoxinate) inhibit bacterial growth experimentally.[53,109] One study, however, demonstrated that a single application of topical anesthetic is unlikely to inhibit culture results.[110] To obtain a culture, the eyelids are gently retracted, and a sterile moistened swab is passed back and forth on the area of the cornea or the conjunctiva to be cultured. Care should be taken not to contaminate the sample by inadvertently touching the eyelid margins, hair, skin, and other nearby structures (Fig. 9.1.16). The swab is then placed in transport broth for shipping or is inoculated either directly onto or into the appropriate culture medium and incubated for isolation and organisms identification.[5,111]

In many animals with external ocular diseases, treatment may be initiated before results of the microbial culture and susceptibility testing are known. Therefore, it seems desirable to

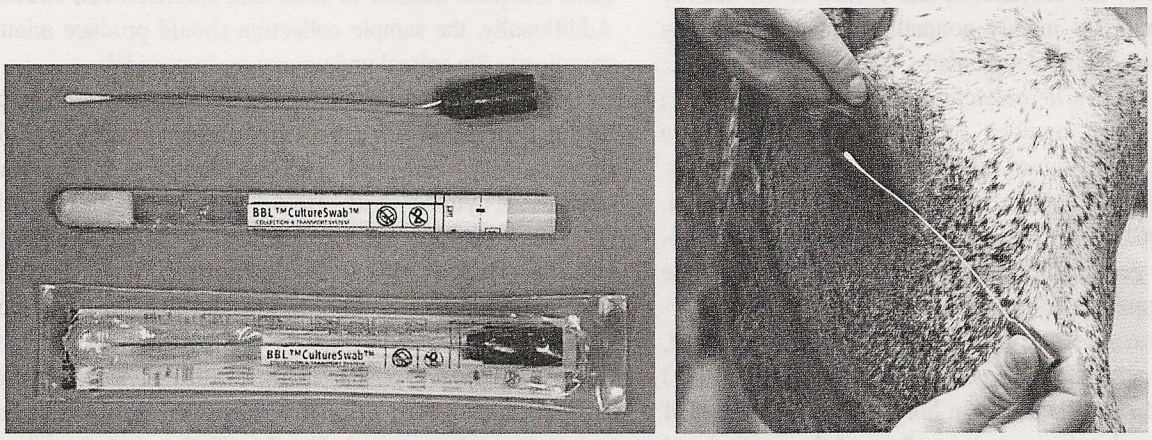

(a) (b)

Figure 9.1.16. Corneoconjunctival culture. **A.** One type of culture medium. **B.** Corneoconjunctival culture in a horse. Both corneal and conjunctival cultures should be obtained early in the ophthalmic examination, before administration of topical solutions or ointments. To obtain a culture, the eyelids are gently retracted, and a sterile moistened swab is passed back and forth on the area of the cornea or the conjunctiva to be cultured. Care should be taken not to contaminate the sample by inadvertently touching the eyelid margins, hair, skin, and other nearby structures. The swab is then placed in transport broth for shipping or is inoculated either directly onto or into the appropriate culture medium and incubated for isolation and organisms identification.

know the most commonly isolated pathogenic microorganisms when choosing a therapeutic antimicrobial agent and also the typical flora of the eye in various species.[112] Comparison of normal eyes and eyes with clinical signs of external ocular diseases indicate that prevalence rates of microorganisms' species varied according to season, geographic location, climate, breed, and sampling technique.[111–115]

Positive bacterial cultures were recovered from 70% to 94% of normal canine eyes and 35% to 54% of normal feline eyes.[112,116,117] Low frequency of normal ocular bacteria in cats may reflect efficient natural host defense mechanisms of tears. Gram-positive organisms most commonly isolated in the normal flora of the canine and feline eye are *Staphylococcus* spp., *Streptococcus* spp., *Corynebacterium* spp., *Bacillus* spp., *Pseudomonas aeruginosa, Escherichia coli, Klebsiella,* and *Neissaria* spp. *Fusobacterium* spp. are the only anaerobic bacteria that can be sometimes found in the normal canine eye, whereas no anaerobic bacteria are present in the healthy feline eye.[111,112,118] The pathogenic organisms (*Staphylococcus aureus, Streptococcus β-hemolyticus, Pseudomonas aeruginosa*) involved in bacterial corneal disease are usually part of the ubiquitous and indigenous microflora of the corneal and conjunctival surface; the defense mechanisms of the cornea are not always effective enough to prevent the bacterial invasion from these organisms.[118] Furthermore, opportunistic bacteria (*Staphylococcus epidermidis, Escherichia coli, Corynebacterium* spp., *Klebsiella, Bacillus* spp.) that are either nonpathogenic or generically considered to be weakly pathogenic may cause disease in an immunocompromised host or present as a coinfection.[111] These opportunistic organisms may colonize tissue after gaining entry into an unusual anatomic site via trauma or other insult. Positive fungal cultures, including *Penicillium* sp. and *Seratia* sp., were recovered from 4% to 13% of normal canine eyes.[112,119]

In Florida, positive microbial cultures were recovered from the conjunctiva of 95% of normal equine eyes. Many bacterial and fungal organisms normally found in the equine conjunctival flora are potential ocular pathogens.[8] The microbial population of the conjunctiva and cornea of the healthy equine eye comprises mainly nonpathogenic or potentially pathogenic Gram-positive organisms (*Staphylococcus* spp., *Streptococcus* spp., *Corynebacterium* spp., *Bacillus* spp.) along with a few number of Gram-negative bacteria (*Pseudomonas aeruginosa, Escherichia coli, Klebsiella, Neissaria* spp.), and varying numbers of filamentous fungi, (*Aspergillus* spp., *Penicillium* spp., *Alternaria* spp.) depending on the geographic area.[8,12,103–107,111,115,120–122] The pathogenic organisms (*Staphylococcus aureus, Streptococcus β-hemolyticus,* nutritionally variant *Streptococci, Pseudomonas aeruginosa, Fusarium* sp., *Aspergillus* spp.) involved in ulcerative keratitis in horses are usually part of the ubiquitous and indigenous microflora of the corneal and conjunctival surface; the defense mechanisms of the cornea are not always effective enough to prevent the bacterial invasion from these organisms.[49,104,106,115,120,121,123–126]

The microbial population of the conjunctiva and cornea of the healthy bovine eye comprises mainly nonpathogenic or potentially pathogenic bacteria (*Staphylococcus* spp., *Streptococcus* spp., *Corynebacterium* spp., *Bacillus* spp.) along with varying numbers of fungi depending on the geographic area.[12]

The inflammatory cells (e.g., polymorphonuclear neutrophils [PMNs]), corneal cells (e.g. fibroblasts), and some bacteria and fungi are associated with the release of highly destructive proteinases that can result in rapid corneal stromal melting and perforation in many species. *Streptococcus β hemolyticus* and *Pseudomonas aeruginosa* are commonly found in cases of melting corneal ulcers, and a mixed bacterial and fungal infection can also be present.[8,106.114,123,127,128] It is also important to note that a melting ulcer can be sterile, especially in foals.[8,114]

Corneoconjunctival cytology may give immediate information about the causative organisms: the examination of Gram-stained slides allows detection of intracellular or extracellular organism, approximation of the quantity of organisms present, determination of the number of species of organism present, and identification of some of these organisms by their morphological aspects (Gram-positive/Gram-negative, cocci/rods). However, corneoconjunctival cultures are more sensitive than cytology, and therefore culture speciation, and susceptibility testing is very often essential to successful management of bacterial corneal diseases.[5] (Additional information concerning clinical ophthalmic microbiology is found in Chapter 6.)

Corneoconjunctival Cytology

Cytology is used either alone or in combination with culture techniques to provide rapid results that may influence the immediate course of therapy.[48,129–132] Conditions for which cytology is indicated include deep melting, or progressive, corneal ulcers; corneal or conjunctival abscesses; chronic or severe keratitis or conjunctivitis; keratitis or conjunctivitis that does not respond to therapy; and proliferative masses of the cornea, conjunctiva, and nictitating membrane.[17] The ideal corneal and/or conjunctival sample provides a monolayer of cells, adequate number of cells, and unaltered cell structure. Additionally, the sample collection should produce minimal irritation to the animal undergoing evaluation.[133]

Instruments for collecting cytologic samples include cotton or Dacron swabs, cytobrushes, spatulas (Kimura platinum spatula), and even the blunt end of a scalpel blade. Impression cytology may also be used for sample collection (Fig. 9.1.17). Most of the collection techniques described hereafter require topical anesthesia (i.e., 0.5% tetracaine or 0.5% proparacaine), and care must be taken to avoid ocular trauma.

The cotton or Dacron swab provides the least traumatic method of retrieving exfoliative samples; topical anesthetic may not even be required (Fig. 9.1.17).This technique is recommended when excessive manipulation is contraindicated, such as with deep or extremely malacic corneal ulcers. Although this technique is minimally irritating, easily obtainable, and inexpensive, it can produce inadequate samples because the cells appear to have affinity for the cotton fibers.

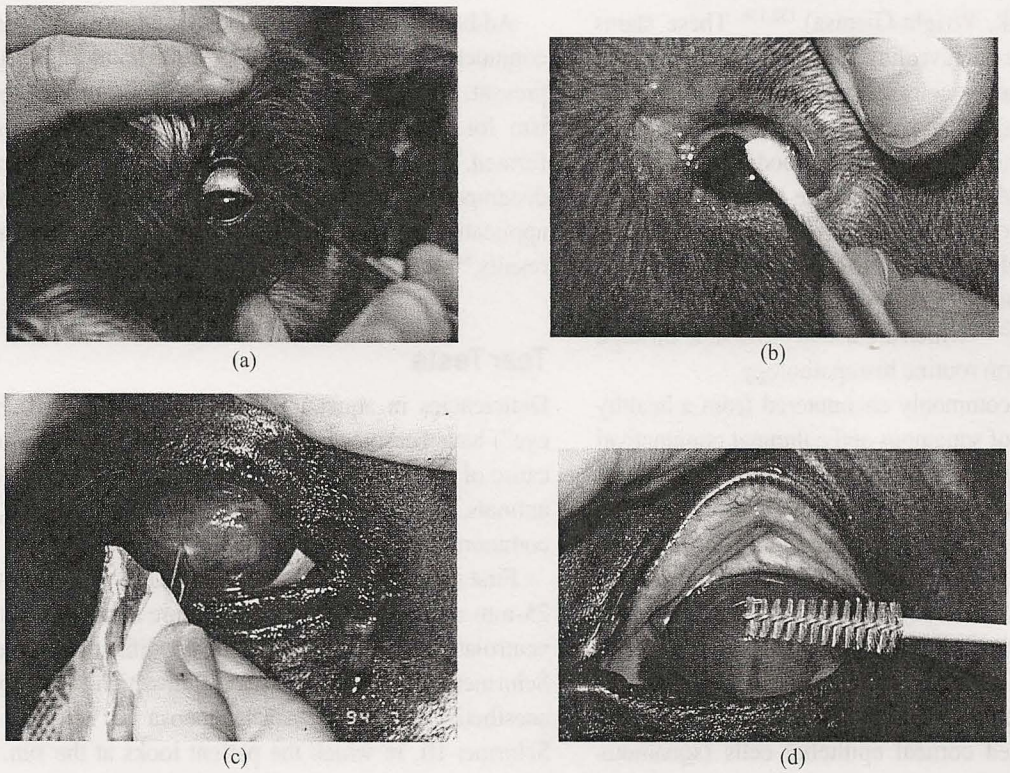

Figure 9.1.17. For corneoconjunctival cytology, scrapings are obtained using the Kimura platinum spatula (**A**), a Dacron swab (**B**), the blunt end of a beaver blade (**C**), or cytobrushes (**D**). Many collection techniques require topical anesthesia, and care must be taken to avoid ocular trauma. Spatulas (Kimura spatula, beaver blades, and chemistry measuring spatulas) provide a more precise method of collecting cells from specific areas, and greater numbers of deeper cells can be obtained. This technique remains the standard technique in diagnostic veterinary ophthalmology. Unfortunately, this method may lead to greater damage among harvested cells, and care must be taken to avoid ocular trauma. The blunt end of a scalpel blade functions similarly to the spatula but with a slightly greater incidence of trauma. This method of cell collection requires topical anesthesia. The cotton or Dacron swab provides the least traumatic method of retrieving exfoliative samples; topical anesthetic may not even be required. The cytobrush provides superior diagnostic samples compared with other methods of cell collection. Care must be taken to gently roll the cytobrush both when collecting samples and when transferring those samples to a glass slide. As with the spatula, this technique requires topical anesthesia and should be used with caution in compromised corneas. The advantages of this technique over the scraping include an increase in sample cellularity.

The more tightly the cotton wool is attached to the shaft, the better the quality of the smear.[134] Samples should be gently rolled onto glass slides to avoid cell damage.

Spatulas (Kimura spatula, beaver blades, and chemistry measuring spatulas) provide a more precise method of collecting cells from specific areas, and greater numbers of deeper cells can be obtained. This technique remains the standard in diagnostic veterinary ophthalmology (Fig. 9.1.17). Unfortunately, this method may lead to greater damage among harvested cells, and care must be taken to avoid ocular trauma. It may also be difficult to evaluate cellular morphologic details because of overlapping of cells and crushing artifact.[133] The blunt end of a scalpel blade functions similarly to the spatula but with a slightly greater incidence of trauma. This method of cell collection requires topical anesthesia (i.e., 0.5% tetracaine or 0.5% proparacaine).

The cytobrush provides superior diagnostic samples compared with the previously discussed methods of cell collection (Fig. 9.1.17).[133,134] This nylon-bristled brush is an 8-cm long plastic instrument with a tapered tip containing a nest of 3- to 4-mm long, nonabsorbent, soft nylon bristles at its distal end. Care must be taken to gently roll the cytobrush both when collecting samples and when transferring those samples to glass slides. One disadvantage of the cytobrush is its size, which makes collecting samples difficult from small puppies, kittens, and birds. This can be overcome by trimming part of its bristles. As with the spatula, this technique requires topical anesthesia and should be used with caution in compromised corneas. The advantages of this technique over the scraping include an increase in sample cellularity, acquisition of cells from deeper layers with less intervention, and the improved morphologic appearance of each cell due to a decrease in the cell overlap.[133]

Impression cytology with cellulose acetate strips or the Biopore membrane device can be used and provides a good cell number; however, cellular clumping is common and application of this technique may not be practical for the clinician.[133,135]

Subsequent to collection, slides can be fixed with heat, acetone, special cytologic fixative sprays, or some combination thereof. If possible, several slides containing adequate sample volume should be prepared to permit the use of different stains if indicated. Staining methods most commonly used include the Gram stain and various Romanowsky-type

stains (e.g., Dif-Quick, Wright-Giemsa).[132,136] These stains are generally adequate for revealing morphologic characteristics of cells (inflammatory cells and neoplastic cells), organisms (bacteria, fungal hyphae, yeast bodies, viral, mycoplasmal, or chlamydial inclusion bodies) and other structures. Giemsa and Gram stains make the best combination for examination of cell detail, possible inclusions, and bacterial or mycotic elements.[132] More specialized stains for fungal elements include periodic acid-Schiff and Gomori's methenamine-silver,[132,137] which are usually available through laboratories that perform routine histopathology.

The types of cells commonly encountered from a healthy conjunctiva are sheets of squamous and columnar conjunctival epithelial cells that may contain cytoplasmic melanin granules and goblets cells that have a large amount of mucus in the cytoplasm and a nucleus at the periphery. Occasional bacteria may be present, and lymphocytes, PMNs, monocytes, and plasma cells are rarely seen. Mastocytes and polymorphonuclear eosinophils (PMEs) should not be seen in normal conjunctiva.[130,132,136,138–141]

The types of cells commonly encountered from a healthy cornea are noncornified corneal epithelial cells (squamous and intermediate), lymphocytes, and PMNs. Mastocytes and eosinophils are absent in the healthy cornea. Nuclei, keratin debris, mucus and bacteria are also observed. In the presence of bacterial corneal disease, PMNs are the predominant cells observed, and bacteria are seen as well.[113,136,138–141]

Results of culture are often more sensitive than cytology, but examination of Gram-stained slides may give immediate information about the causative organisms, thus allowing prompt, focused therapy. With the proper equipment and practice, exfoliative cytology is a very rewarding and useful tool for the practicing clinician.

Additional tests that can be conducted on corneal and conjunctival scrapings or swabs include the PCR and IFA. At present, feline herpesvirus type-1 (FHV-1) is the only organism for which corneoconjunctival PCR is commonly performed. IFAs are available for FHV-1, chlamydia, and canine distemper. Samples for IFA should be collected before the application of fluorescein stain, which can yield false-positive results.[54]

Tear Tests

Deficiencies in aqueous tear production (i.e., KCS or "dry eye") have been recognized for several decades as a frequent cause of corneal and conjunctival lesions in both humans and animals. Several tests aid in the diagnosis of dry eye, the most common of which is the Schirmer tear test.

First described by Schirmer in 1903,[142] this test uses a 5 × 25-mm strip of filter paper to measure aqueous tears from the ventrolateral conjunctival fornix. Modifications developed by Schirmer include the Schirmer II, in which the conjunctiva is anesthetized and the nasal mucosa is irritated, and the Schirmer III, in which the patient looks at the sun. In 1961, Halberg and Berens introduced a standardized test kit containing 5 × 35 mm strips of Whatman no. 41 filter paper with a rounded tip notched at 5 mm for bending. Some commercial strips available now are impregnated with blue dye at the 5 mm point that marks tear fluid migration and a millimeter scale beginning at the 2-mm point, thereby allowing a fast and easy reading of the results (Fig. 9.1.18).[143,144] Also available is a modified test strip, which is less expensive and is not impregnated with dye; it is 5-mm wide for the first 10 mm and approximately 7 mm wide beyond that. The reference values are different for this test strip.[145]

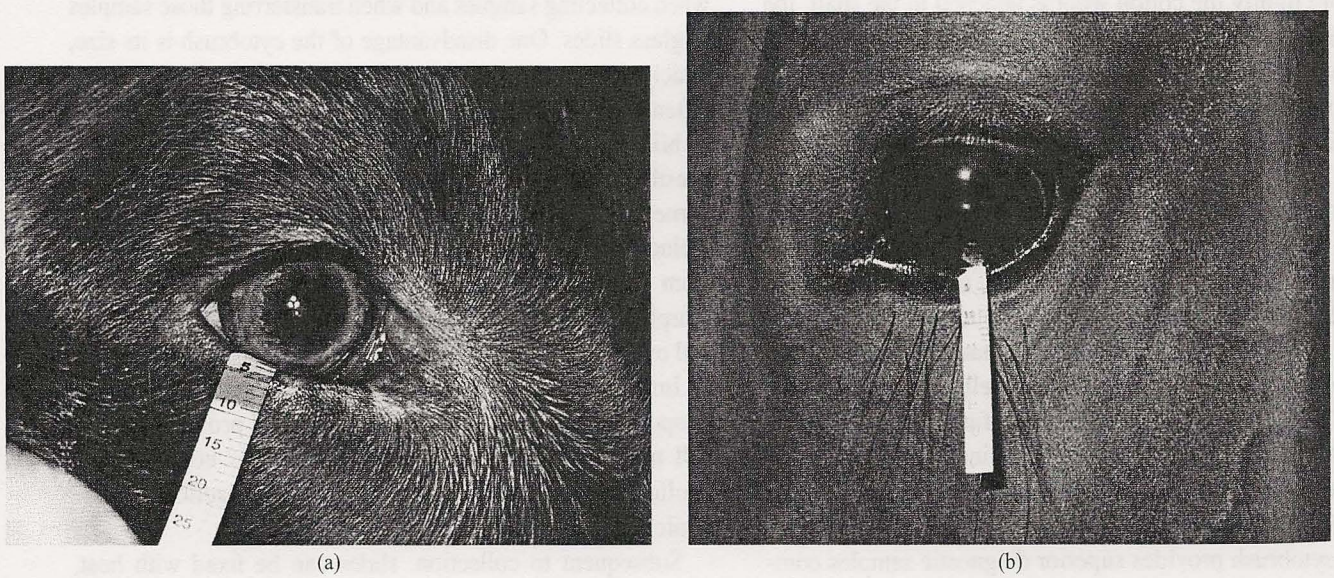

(a) (b)

Figure 9.1.18. Schirmer tear test (STT) in a dog (**A**) and a horse (**B**). This test is performed on most small animals with use of minimal restraint and should be performed prior to application of other ocular medications or stains. The standard test strip is a 5 × 35-mm no. 41 filter paper strip. Test strips are bent at the notch, preferably while the strip is still in its packing, to avoid absorption of oils from the examiner's skin. The folded end is inserted in the lower conjunctival fornix, in contact with the cornea, near the junction of the middle and temporal thirds of the eyelids, where it should remain for 1 minute. Tears are measured from the fold in millimeters per minute, immediately at removal. The values obtained in the second eye are apparently not affected by the stimulation of basal secretion in the first eye.

Roberts and Erickson described use of the STT in the dog in 1962, and additional reports followed.[146–149] In 1975, Gelatt and colleagues[150] described use of the canine Schirmer I and canine Schirmer II tear tests. In 1970, Veith and colleagues[151] established parameters for the STT in cats. The STT has been extensively used to evaluate the relative contributions of the lacrimal and nictitans glands and to determine the adverse effects of systemic and topical eye medications (atropine sulfate, tropicaine, trimethoprim-sulfadiazine) as well as general anesthesia on the tear production in the dog, cat, and horse.[28,150,152–157]

Despite criticism of its poor repeatability and inconstancy, the STT remains the standard means for quantifying the aqueous tear production.[158] This test is performed on most small animals with use of minimal restraint and should be performed prior to application of other ocular medications or stains. The reference values listed in the following text were determined with the standard strip (5 × 35 mm no. 41 filter paper). Test strips are bent at the notch, preferably while the strip is still in its packing, to avoid absorption of oils from the examiner's skin. The folded end is inserted in the lower conjunctival fornix, in contact with the cornea, near the junction of the middle and temporal thirds of the eyelids, where it should remain for 1 minute (Fig. 9.1.18).[158] Tears are measured from the fold in millimeters per minute, immediately at removal. The values obtained in the second eye are apparently not affected by the stimulation of basal secretion in the first eye.[159] This test (STT I), performed without any topical anesthetic, measures the trigeminal–facial reflex tearing in addition to the basal secretion. Reported means for the normal canine STT I vary from 18.64 ± 4.47 mm/min to 23.90 ± 5.12 mm/min.[143,144,149–150,157–160] The reported mean value for the feline Schirmer I tear test vary from 14.3 ± 4.7 mm/min to 16.92 ± 5.73 mm/min.[151,153,154,157] Normal STT values in the rabbit are 5.30 ± 2.96 mm/min.[161] In the dog, values less than 10 mm/min are suspicious if combined with clinical signs of KCS, and values less than 5 mm/min are considered to be diagnostic. Low STT values in the cat must be carefully interpreted in light of clinical signs, because clinically normal cats can have values as low as 5 mm/min. Equine tear production is often copious and may overwhelm commercial strips in less than a 1 minute period.[159a,162,163] STT I values varying from 20.6 ± 6.5 mm/min to 24.8 ± 4.8 mm/min[152, 162–164] have been reported in conscious normal adult horses using a 5 × 35 mm tear test strip. Fluctuations in STT values on both daily and weekly bases have been reported in dogs but not in horses.[164] No difference in the STT I values were found between the left and right eye of 100 healthy horses or between males and females.[164] Beech and colleagues[162] confirmed that gender, age, housing, and season had no effect and reported an STT II value of 20 ± 5 mm/min that was not significantly different from the STT I value. STT I values of less than 10 mm/min in the horse are diagnostic for a tear deficiency.[159] Finally, an STT I value of 24.18 ± 6.5 mm per 30 seconds has been reported in cows.[12]

A Schirmer II tear test (STT II) can be performed similarly except that the cornea and conjunctiva are topically anesthetized. The STT II estimates only basal tear secretion, eliminating any contribution from reflex tears. For the STT II, the lower conjunctival fornix is gently dried with a cotton-tipped applicator 1 minute after the instillation of the topical anesthetic, and the test strip is inserted as previously described. Mean wetting in clinically normal canine eyes includes 3.8 ± 2.7 mm/min, 11.66 ± 6.1 mm/min, and 13.95 ± 4.40 mm/min.[150,156,160] Schirmer II results in clinically normal cats have been reported to be approximately 80% of the Schirmer I results.[156]

The phenol red thread tear test has also been described as an accurate assessment of tear production in both humans and animals.[159,165] Kurihashi first described use of a thread to measure tear production in 1975. In 1982, Hamano refined this method by impregnating the thread with phenol red, which is a pH-sensitive indicator. The thread is 75 mm in length, with a 3-mm indentation at one end. The folded end is placed in the lower conjunctival fornix for 15 seconds. As the slightly alkaline tears wick along the thread, a color change from pale yellow to orange occurs. Mean length of absorption for this test is 34.15+/–4.45 and 23.04+/–2.23 mm per 15 seconds in the dog and the cat respectively, with no significant effect of topical anesthesia on the test.[159] The main advantage of this method is the rapid result. Further studies are necessary, however, to determine the efficacy of this test in the diagnosis of dry eye.

Dissatisfaction with the STT, particularly in human ophthalmology, has led some investigators to pursue alternative methods of assessing PTF. As a result, the tear film meniscus has become a focus of attention, and attempts have been made to correlate its height, width, cross-sectional area, and radius of curvature with both normal and dry-eye conditions.[166] Further research is needed, however, to establish parameters in domestic animals.

External Ophthalmic Stains

External ophthalmic stains facilitate the diagnosis of corneal, conjunctival, lacrimal, and nasolacrimal diseases.[167,168] Stains commonly used in veterinary ophthalmology include sodium fluorescein and rose Bengal dyes.[169–172] Lissamine green has found limited use in human and veterinary ophthalmology, and Alcian blue, methylene blue, and Trypan blue have been used experimentally (Table 9.1.4).[173–178]

Fluorescein dye is used to detect corneal and conjunctival defects, aqueous humor leakage with the Seidel test, and PTF deficiencies (mucin and lipid deficiencies) by the tear breakup time (TBUT), and to assess the nasolacrimal duct patency (Fig. 9.1.19). It has also been used in measurement of IOP with the Goldmann, Perkins, Draeger, and Halberg tonometers and in determining aqueous humor flow rates by fluorophotometry.[179,180]

Sodium fluorescein is a weak, dibasic acid of the xanthene group that is detectable in solution at concentrations as low as 1 ppm. Its absorption spectrum peaks at 490 nm (i.e., blue light). Sodium fluorescein converts almost 100% of absorbed light to emitted fluorescent light with a peak wavelength of 520 nm (i.e., green light). Fluorescence is most intense at alkaline pH; at acid pH, sodium fluorescein appears yellow or orange. Fluorescein is available as a 0.5% to 2.0% alkaline solution or as an impregnated paper strip.[8,50,109,111,181,182] In small animals, the paper strip

Table 9.1.4 External Ophthalmic Stains

Characteristics	Fluorescein	Rose Bengal	Lissamine
Staining	Stroma	Healthy and degenerated cells	Degenerated cells
Intrinsic toxicity	Limited	Yes	No
Increased staining of dead cells	Yes	Yes	Yes
Staining blockable by tear component	No	Yes	Yes
Stromal diffusion	Rapid	Limited	Unknown
Staining increased	Disrupts cell–cell junctions	Insufficient protection of PTF	
Clinical use	Corneal abrasions nasolacrimal patency	KCS	KCS

is moistened with sterile 0.9% saline or ocular flush and touched to the dorsal bulbar conjunctiva. For topical use in horses, the strips are mixed in tear solutions immediately before use to ensure sterility. Contaminated solutions readily grow bacteria such as *Pseudomonas aeruginosa.* Commonly used preservatives such as benzalkonium chloride and chlorobutanol are inactivated by fluorescein.[183] In large animals, it is convenient to immerse the paper strip in 0.5 ml of 0.9% sterile saline or eye flush within a syringe and needleless hub and use it to gently squirt the cornea (Fig. 9.1.19).

The most common use of sodium fluorescein is the detection of corneal and conjunctival epithelial defects. All red, inflamed, or painful eyes should be routinely stained with fluorescein, including eyes with suspected KCS that may be associated with corneal ulceration.[5,127] After the instillation of fluorescein on the conjunctiva, the eyelids are closed or the patient is allowed to blink. The stain is subsequently distributed across the corneal and conjunctival surfaces. Direct contact between the paper strip and the cornea can deposit excess stain, which may be misinterpreted as a corneal defect. Gently flushing the eye after staining will remove any excess fluorescein and simplify the diagnosis of both corneal and conjunctival lesions. Corneal integrity is evaluated with fluorescein dye, a hydrophilic chemical that is absorbed by exposed corneal stroma when corneal epithelial defects (ulcers) are present (Fig. 9.1.19). Fluorescein also stains intercellular spaces, but does not bind to intact healthy corneal epithelium or to Descemet's membrane (Table 9.1.4).[5] Fluorescein will also stain conjunctival ulcers and abrasions (e.g., those occurring with FHV-1 infection). The use of a direct ophthalmoscope or slitlamp biomicroscope with a cobalt-blue filter enhances fluorescence and facilitates identification of ulcers.[5]

Fluorescein may similarly be used to detect the leakage of aqueous humor through deep corneal ulcers, lacerations, puncture wounds, and suture sites (i.e., the Seidel test).[50,107] To perform the Seidel test, sodium fluorescein is liberally applied undiluted to the cornea without subsequent flushing. At this high concentration (2%), the dye fluoresces at wavelengths closer to the yellow and orange spectra. If the corneal integrity is compromised, a minute volume of green fluorescence appears at the site of the leak because of local dilution of the dye.

The TBUT is a noninvasive ocular diagnostic test that may be used to support a presumptive diagnosis of a qualitative tear abnormality: it is a measure of the stability of the PTF that involves recording the time it takes for the fluorescein dye, and hence the tear film, to dissociate from the corneal surface.[154,181] Abnormalities of the mucin and/or lipid layers in PTF can thus be evaluated using TBUT. To perform this test, 1% to 2% fluorescein is applied to the eye, the animal is allowed to blink, and the lids are then maintained in the open position until the fluorescent tear film begins to disassociate: the dry spot will appear as a dark, round spot in the fluorescent tear film. Slitlamp biomicroscopy using a cobalt-blue filter facilitates this procedure. In the dog, the average normal time between the first blink and development of the first dry spot is approximately 20 seconds (19.7 ± 5secs).[181,184] In cats, Cullen and colleagues recently estimated the average TBUT to be 16.7 ± 4.5 secs.[154] In horses, Harling found the TBUT to be over 13 seconds.[163] Normal eye movements can interfere with accurate analysis of the TBUT. Xylazine and ketamine may be used to minimize such movements. In affected animals, TBUT is usually less than 5 seconds.[184] The TBUT is relatively easy to perform, and its use is encouraged when qualitative PTF dysfunction is a differential diagnosis. A conjunctival biopsy to enumerate goblet cells may be performed to confirm mucin deficiency.[163,181]

Patency of the nasolacrimal apparatus is tested by applying sodium fluorescein to the eye and timing the passage of fluorescein through the system to the external nares (i.e., the Jones test).[185] Each side is tested, and passage times are compared. Fluorescein normally traverses the nasolacrimal apparatus within 5 minutes in the dog and cat, and in less than 10 minutes in the horse.[163] The amount of fluorescein, rate of tear production, and length of the nasolacrimal duct all influence this time. Thus, longer times or failure of passage may indicate partial or complete obstruction, respectively. False-negative results may occur in the cat or dog that frequently licks its nares, thereby removing the stain before it is visualized. False-negative results may also occur in brachycephalic breeds, in which the stain drains caudally into the nasopharynx rather than through the external nares. Examination of the caudal tongue and pharynx with blue light can confirm passage in these animals.

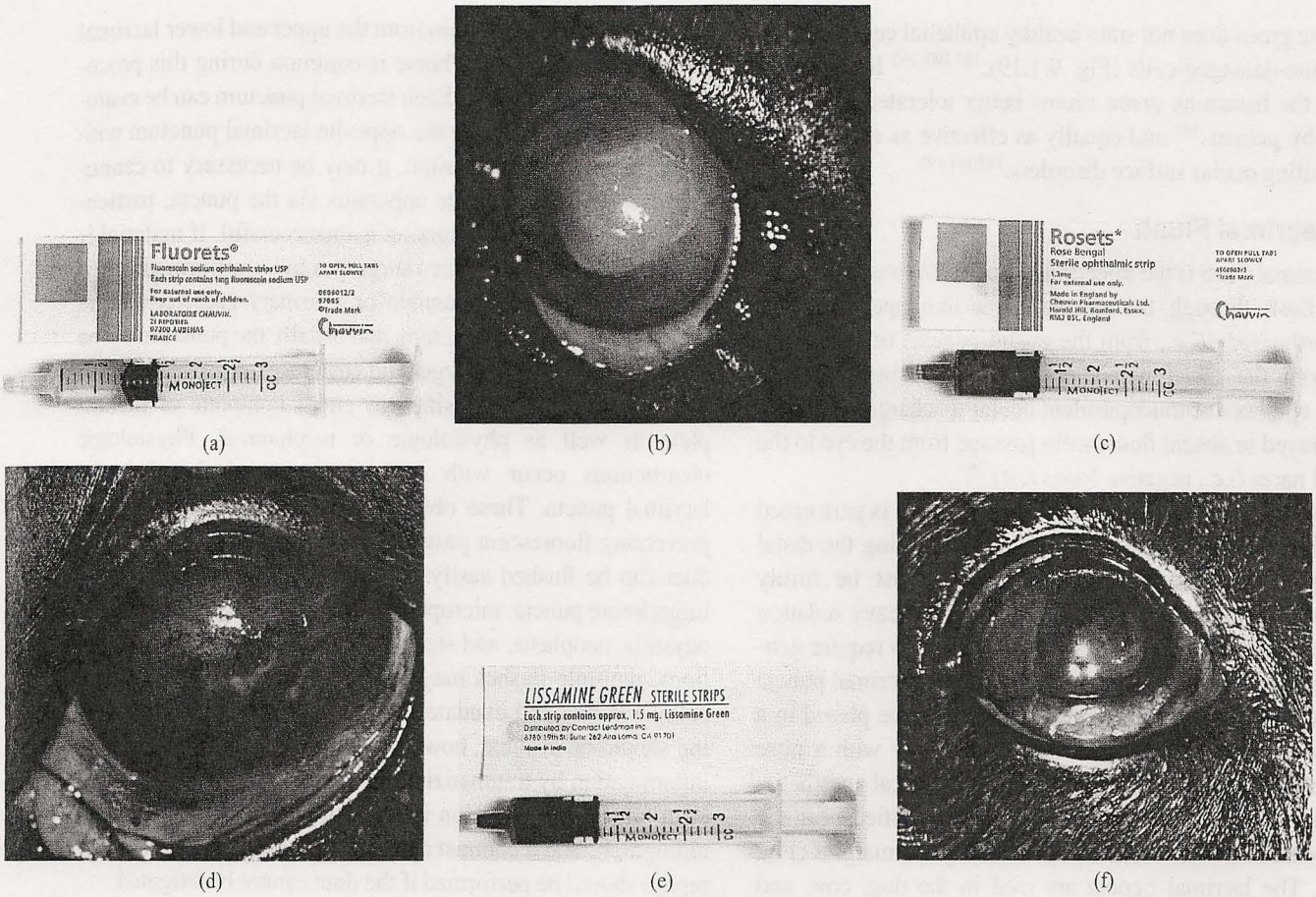

Figure 9.1.19. Ophthalmic stains. Fluorescein dye (**A** & **B**) is used to detect corneal and conjunctival defects, aqueous humor leakage with the Seidel test, and precorneal tear film (PTF) deficiencies (mucin and lipid deficiencies) by the tear break-up time (TBUT), and to assess the nasolacrimal duct patency. Rose Bengal (**C** & **D**) is used to assist diagnosis of PTF disorders (KCS, mucin deficiency), and superficial corneal epithelial abnormalities. For adequate visualization of rose Bengal stain retention, slitlamp biomicroscopy is recommended. In a clinical setting, the lissamine green (**E** & **F**) seems better tolerated than rose Bengal by patients and equally as effective as rose Bengal in evaluating the ocular surface disorders.

Rose Bengal (i.e., tetrachloro-tetraiodofluorescein) is available as an impregnated paper strip and a solution.[169,172] The solution can be irritating, but use of the 0.5% or lower concentrations versus the 1.0% solution appears to minimize this irritation.[172] In animals, rose Bengal is used to assist diagnosis of PTF disorders (KCS or mucin deficiency) and superficial corneal epithelial abnormalities (Fig. 9.1.19). For adequate visualization of rose Bengal stain retention, slitlamp biomicroscopy is recommended.

Rose Bengal was previously thought to stain only dead and degenerating cells and mucus. Recent work, however, suggests that rose Bengal has a dose-dependent ability to also stain healthy corneal epithelial cells; it also has a toxic effect on these cells in a dose-dependent fashion. This dye is actually toxic to corneal epithelium at routine concentrations and certainly more toxic and irritating than the lissamine green (Table 9.1.4).[168,169,186–188] Normal tear film components such as mucin appear to block absorption of rose Bengal, thus suggesting that stain uptake is not dictated by the lack of cell vitality but rather represents poor stability of the PTF and inadequate protection of the corneal epithelium.[186–188]

Besides being used to assess the integrity of the PTF, rose Bengal may also be used to demonstrate very small superficial ulcers and erosions such as the punctate corneal lesions often present in early stages of keratomycosis, punctate keratitis in the dog, and dendritic lesions caused by FHV-1 infection in the cat (Fig. 9.1.19).[187] These lesions frequently do not retain fluorescein, but they will stain an intense red with rose Bengal.[189] If indicated, the Rose Bengal and the fluorescein stains can be conveniently administered at the same time because the stain properties are not affected by the mixing.[172] Rose Bengal and lissamine green are bactericidal and vivacidal, and therefore any swab for microbiology culture or virus identification (i.e., by PCR) should be performed prior to staining.

Lissamine green is a synthetically produced organic acid dye with two aminophenyl groups.[187] Although lissamine green is used clinically in Europe (rose Bengal is not available in some European countries), it has not been widely adopted in the United States. The lissamine green has been tested on cultured rabbit and human corneal epithelial cells,[187] and the cell viability was much greater for 1% and 0.5% lissamine green than for rose Bengal at the same concentrations. No difference in cell viability was seen for the lissamine green and the rose Bengal at 0.1% (see Table 9.1.4).[187] Norn showed that lissamine green has a staining profile nearly identical to rose Bengal, and Chodosh and colleagues showed that

lissamine green does not stain healthy epithelial cells but only membrane-damaged cells (Fig. 9.1.19).[187,190–192] In a clinical setting, the lissamine green seems better tolerated than rose Bengal by patients[191] and equally as effective as rose Bengal in evaluating ocular surface disorders.[187,191,192]

Nasolacrimal Flush

Nasolacrimal flush is the injection of normal saline solution or ocular flush through the nasolacrimal drainage apparatus either orthograde (i.e., from the eyelid puncta) or retrograde (i.e., from the distal nare's opening). Indications include chronic epiphora or mucopurulent ocular discharge combined with delayed or absent fluorescein passage from the eye to the external nares (i.e., negative Jones test).[25]

In the dog, cat, and cattle, nasolacrimal flush is performed orthograde because of the difficulty in identifying the distal opening of the nasolacrimal duct. Dogs must be firmly restrained, and resistant animals may require heavy sedation or even light, general anesthesia. Cats may also require general anesthesia (e.g., ketamine), because their lacrimal puncta are small and difficult to cannulate. Cattle can be placed in a chute or stanchion, their heads pulled laterally with a nose lead. Following one or more instillations of topical anesthetic, the upper and lower lacrimal puncta are identified near the medial canthus, 1- to 2-mm bulbar to the eyelid margins (Fig. 9.1.21). The lacrimal puncta are oval in the dog, cow, and horse, and they are round in the cat. In some animals, a small amount of pigment along the margins of the lacrimal puncta facilitates identification. With the upper lid everted to expose the upper lacrimal punctum, a cannula or blunt-tipped hypodermic needle (in the cow, 20–21-gauge; in the dog, 22–23-gauge; in the cat, 24–25-gauge) is gently inserted in a medial direction (Fig. 9.1.21). Sterile saline is then slowly injected until it flows from the lower lacrimal punctum. This establishes patency of the upper and lower lacrimal puncta, upper and lower canaliculi, and lacrimal sac. If the lower lacrimal punctum is imperforate, a small bleb rises under the conjunctiva in that area. Pressure is then applied to occlude the lower punctum, and 2 to 10 mL of sterile saline or ocular flush are injected through the nasolacrimal duct. Resistance to passage (or failure of passage) is noted, and any debris exiting the duct may be collected for cytology and possible culture. Care must be taken to hold the muzzle down during this procedure; otherwise, the flush may drain caudally into the nasopharynx.

In the standing horse, a retrograde nasolacrimal flush is usually performed (Fig. 9.1.20). The animal is placed in stocks, and a lower lip twitch is applied. Many horses also require sedation with xylazine or detomidine for adequate restraint. The distal opening of the nasolacrimal duct is usually visible at the ventral mucocutaneous junction of the external nares. Topical anesthetic ointment is applied around this opening, and a short polyethylene tube is inserted proximally after its tip has been coated with lidocaine gel (4- to 6-French urinary catheter, tomcat catheter, or 5-French feeding tube). Approximately 10 to 15 mL of sterile saline are injected; fluid should be observed to drain from the upper and lower lacrimal puncta. Sneezing by the horse is common during this procedure and may be violent. Each lacrimal punctum can be evaluated in turn by occluding the opposite lacrimal punctum with digital pressure. On occasion, it may be necessary to cannulate nasolacrimal drainage apparatus via the puncta, particularly if the retrograde irrigation is unsuccessful, if material is required for culture, or when surgery is to be performed in this area. A suitably sized cannula or a urinary catheter can be used to cannulate the punctum, and usually the punctum of the lower eyelid is slightly larger and easier to cannulate.[10,163,193]

Obstructions are classified as either complete or incomplete as well as physiologic or mechanical. Physiologic obstructions occur with entropion and misplaced lower lacrimal puncta. These obstructions may be complete, thus preventing fluorescein passage entirely, but the nasolacrimal duct can be flushed easily. Mechanical obstructions include imperforate puncta, micropuncta, canalicular agenesis, dacryocystitis, neoplasia, and stenosis. With inflammatory obstructions, multiple flushes may be required to loosen and expel cellular debris and exudate. Excessive pressure during flushing should be avoided, however, because this may exacerbate inflammation by traumatizing the nasolacrimal apparatus and even forcing the infection into the surrounding tissues. Skull radiographs and a contrast dye study (i.e., dacryocystorhinography) should be performed if the duct cannot be irrigated.

Corneal Esthesiometry

The corneal epithelium is the most densely innervated and exquisitely sensitive surface epithelium of the body. The corneal sensitivity is essential for the maintenance of the normal corneal physiologic process. The corneal sensation is derived from the ophthalmic division of the trigeminal ganglion in dogs, humans, cats, horses, and rabbits. A gradation appears to exist in the sensitivity of the cornea, with the sensitivity inversely proportional to the total number of corneal stromal nerve fibers present. Human corneas have the most sensitive, and the cat, dog, and rabbit corneas have less sensitivity.[194,195] Corneal sensitivity in animals is most acute in the central cornea, with the cornea most sensitive along the horizontal meridian and the least sensitive in the vertical meridian.[196,197]

Corneal sensation may be demonstrated by touching the cornea gently with a thin wisp of cotton while holding open the eyelids. When touched from the periphery to avoid a menace response, the normal reflex is retraction of the globe, with protraction of the nictitans. This reflex tests cranial nerves V and VI.

The degree of corneal sensation can also be semiquantified in different areas of the cornea using a corneal esthesiometer (Fig. 9.1.22). This instrument evaluates the corneal sensitivity by measuring the corneal touch threshold (CTT). These instruments contain a small-diameter (0.12 mm), adjustable from 6.0 to 0.5 cm (pressure varying from 11 to 200 mg/0.0113mm^2), platinum (Larson-Millodot esthesiometer) or nylon (Cochet-Bonnet esthesiometer) filament. Pressure from the tip of the

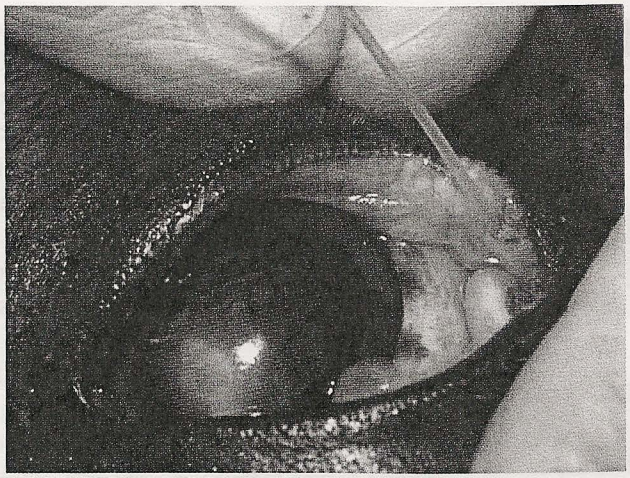

(a)

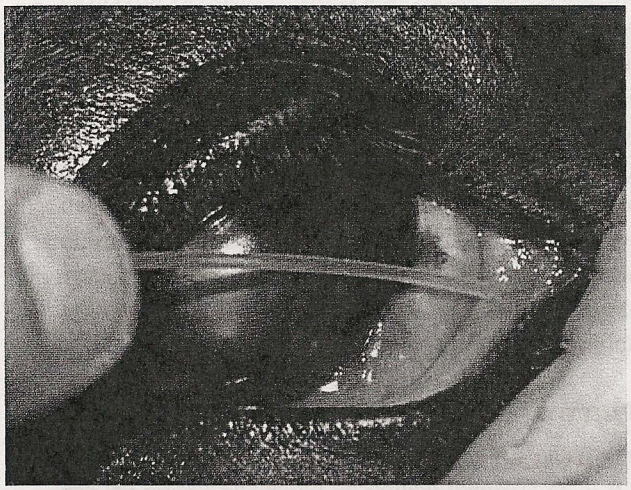

(b)

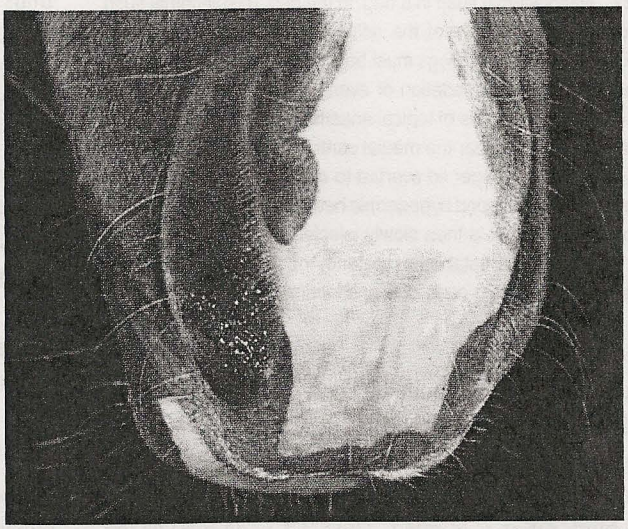

(c)

(d)

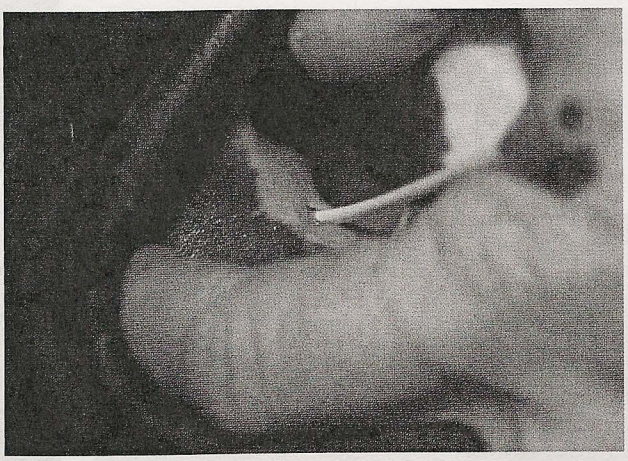

(e)

Figure 9.1.20. Nasolacrimal flush in a horse (**A–E**). In the standing horse, a retrograde nasolacrimal flush is usually performed. The animal is placed in stocks, and a lower lip twitch is applied. Many horses also require sedation with xylazine or detomidine for adequate restraint. The distal opening of the nasolacrimal duct is usually visible at the ventral mucocutaneous junction of the external nares (**D**). Topical anesthetic ointment is applied around this opening, and a short polyethylene tube is inserted proximally after its tip has been coated with lidocaine gel (**E**). Approximately 10 to 15 mL of sterile saline are injected; fluid should be observed to drain from the upper and lower lacrimal puncta (**A, B, C**). Sneezing by the horse is common during this procedure and may be violent. Each lacrimal punctum can be evaluated in turn by occluding the opposite lacrimal punctum with digital pressure.

Figure 9.1.21. Nasolacrimal flush in a dog. In the dog, nasolacrimal flush is performed orthograde because of the difficulty in identifying the distal opening of the nasolacrimal duct. Dogs must be firmly restrained, and resistant animals may require heavy sedation or even light, general anesthesia. Following one or more instillations of topical anesthetic, the upper and lower lacrimal puncta are identified near the medial canthus, 1- to 2-mm bulbar to the eyelid margins. With the upper lid everted to expose the upper lacrimal punctum, a cannula or blunt-tipped hypodermic needle is gently inserted in a medial direction. Sterile saline is then slowly injected until it flows from the lower lacrimal punctum. This establishes patency of the upper and lower lacrimal puncta, upper and lower canaliculi, and lacrimal sac.

filament is able to stimulate about 100 nerve endings over 4 to 10 epithelial cells. The shorter the filament, the more pressure is applied to the cornea, and vice versa (Fig. 9.1.22). When the CTT pressure to stimulate corneal sensory nerve endings is reached, the blink reflex is elicited. The CTT is defined as the pressure at which the majority of touch stimuli cause a blink response. Therefore, the CTT and the corneal sensitivity are inversely proportional: the lower the CTT, the higher the corneal sensitivity. The test should be performed in a quiet environment with a minimal of head restraint or eyelid manipulation. The test should begin with the esthesiometer monofilament length at maximal length (6.0 cm); the length is then decreased at regular increments until the animal demonstrates consistent corneal blink reflexes in response to the stimulus. The CTT has been measured in humans, rabbits, dogs, cats, and horses.[194,195,198] The reported CTT in standardized unit (mg/0.0113mm^2) include 87 to 167 in albino rabbit,[195] 96 in dogs,[194] 45 in pigmented rabbits, 43 in cats,[199] 15 in adult horses,[198,200] 13 in foal,[198] and 10 to 14 in humans.[196] The equine cornea is thus very sensitive compared to the other animals. The corneal sensitivity has been shown to depend on the corneal region tested: the greatest corneal sensitivity level in all these species was confined to the central cornea. The corneal sensitivity differs among breeds of dogs, depending on their skull type: the brachycephalic dogs have the least sensitive corneas (i.e., CTT higher in brachycephalic than in dolichocephalic dogs).[194] Similarly, the cornea of brachycephalic cats is less sensitive than that of Domestic Short-haired cats.[201] No difference in CTT was found according to the sex and age in dogs and horses,[194,198,200] whereas variations exist in normal human corneal sensitivity depending on the age, gender, and pigmentation of the iris.[202]

Tonometry

Tonometry is the indirect measurement or estimation of IOP or tension. It is an essential diagnostic procedure during the eye examination in animals, particularly of any eye that is red or

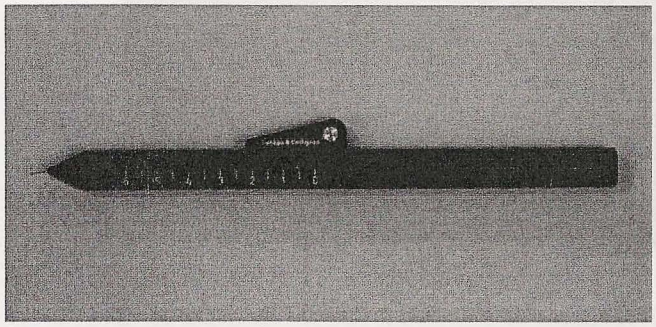

(a)

(b)

Figure 9.1.22. Corneal esthesiometry. The degree of corneal sensation can also be semiquantified in different areas of the cornea using a corneal esthesiometer such as the Cochet-Bonnet esthesiometer (**A**). This instrument evaluates the corneal sensitivity by measuring the corneal touch threshold (CTT). These instruments contain a small-diameter, adjustable from 6.0 to 0.5 cm, platinum (Larson-Millodot esthesiometer) or nylon (Cochet-Bonnet esthesiometer) filament. Pressure from the tip of the filament is able to stimulate about 100 nerve endings over 4 to 10 epithelial cells. The shorter the filament, the more pressure is applied to the cornea, and vice versa.

painful or that has focal or diffuse corneal edema, mydriasis, orbital trauma, lens luxation, or a history of glaucoma, either of the eye of interest or the fellow eye. Tonometry may be performed via digital palpation, indentation, or applanation techniques. It is relatively quick and simple and provides crucial information to the clinican.[5] This noninvasive procedure allows the examiner to evaluate IOP (either hypertension or hypotension) and to intermittently monitor glaucomatous eyes for progression or response to therapy. The procedure can be performed with minimal discomfort to the patient, and the results can significantly determine prognosis and guide decisions regarding treatment regimens. The normal IOP of most animals is usually somewhere between 15 and 25 mmHg due to the conservation between species. Generally, the difference in IOP between fellow eyes should be less than 8 mmHg.[203] If this is not the case, a thorough examination should be performed to identify any pathology that may be responsible for the difference.

Digital tonometry was reported as early as pre-Hippocratic times, and it is still practiced by some human and veterinary ophthalmologists. The first indentation tonometer was reported by von Grafe in 1862. This was followed by reports of a similar device from Donders in 1863. In 1905, Schiotz developed and described an indentation tonometer that eventually became the most widely used instrument in the world. Maklakoff engineered the first applanation tonometer in 1885, and a modification of this device (i.e., Tonomat) was created by Posner and Inglima in 1964. Verhoeff developed the Souter applanation tonometer in 1916, reporting its use for optical estimations of IOP, and in 1954, Goldmann developed a slit-lamp-mounted applanation tonometer, which has become the standard for applanation tonometry in human ophthalmology.[5]

To perform digital tonometry, the index and middle fingers are placed against the patient's closed upper eyelid, and slight pressure is applied with one finger while the globe is stabilized with the other (Fig. 9.1.24).[5] Digital tonometry requires considerable practice, but it may be necessary when instrumental tonometers are unavailable or considerable corneal pathology is present. The accuracy of digital tonometry varies widely between clinicians and generally does not approach that obtained by indentation and applanation tonometers (Fig. 9.1.24). However, a study in humans comparing digital with Goldmann tonometry showed that glaucoma specialists could digitally identify most eyes with an IOP of greater than 30 mmHg.[204] Digital tonometry basically differentiates between soft and hard eyes and is not a substitute for a more objective measurement.

Instrumental tonometry has since been reported for many animal species, including laboratory species, companion animal species, nonhuman primates, and many captive exotic species.[205–227] The Schiotz tonometer is the primary indentation tonometer used today. Various models are available; they consist of a convex corneal footplate attached to a 3-mm diameter, jewel-mounted plunger, a holding bracket, a recording scale, and either a 7.5 or 10.0 g weight. The footplate approximates the curvature of the human cornea, and the low-friction plunger protrudes slightly from its concave surface. Depending on the corneal rigidity, the plunger is variably depressed such that each 0.05 mm of depression moves the stylet one scale unit. The instrument measures the amount of corneal indentation produced by a given weight. Scale readings are converted to mmHg via the instrument's calibration or conversion table. Conversion tables have been calculated for the dog and the cat from invasive manometry, but these tables result in higher IOPs than the comparable scale readings on the human conversion table, perhaps because of differences between corneal and scleral rigidity, and may not be as accurate.[206,210,211,228]

In order for the examiner to achieve the most accurate reading possible with Schiotz tonometry, the patient must be restrained with the head and eyes directed upward nearly vertical and the eyelids held open against the orbital rim.[5] Care must be taken to avoid pressure being placed against the entire globe rather than strictly against the cornea, because pressure on the globe may artifactually elevate the IOP. Pressure on the jugular veins from excessive restraint or a tight-fitting collar may also elevate the IOP, particularly in brachycephalic dogs.[5] Schiotz tonometry is impractical in the horse and other large species with laterally positioned globes because of the difficulties encountered in properly positioning these animals while they are awake. General anesthesia is required in large animals in order to place them in lateral recumbency and in any other animal whose head cannot safely be directed upward.[10] However, despite this complicated process, normal Schiotz values have been reported in the horse as between 14 and 22 mmHg.[229] Following instillation of topical anesthetic, the footplate of the instrument is rested on the central cornea, with the instrument held vertically, and scale readings are recorded. Three separate readings are taken, and the closest two results are averaged. Because of the weight of the instrument pressing on the globe, consecutive readings become progressively lower.

Before and after its use, the Schiotz tonometer should be cleaned to prevent debris from entrapping the plunger. The Schiotz tonometer should also be checked with a stainless steel calibration surface just before each use to ensure the plunger is functioning properly. The footplate of the Schiotz tonometer is designed to match the human corneal curvature; therefore, its accuracy may vary in veterinary patients. Large eyes with flatter corneas generally give falsely low readings, whereas small eyes with greater corneal curvature tend to give falsely high readings.[5] Eye movement may affect the results as well. Readings taken at the limbus yield higher values compared with more accurate, central corneal readings.[5] Nictitans protrusion can interfere with Schiotz tonometry, but this can be overcome by inserting the instrument's footplate beneath the third eyelid or by retracting the nictitans with thumb forceps. Results of studies comparing the Schiotz instrument with the 5.5- and 7.5-g weights and the Mackay-Marg or TonoPen applanation tonometers, however, suggest that reasonable correlations are possible with the Schiotz tonometer.[230,231] It can provide a reasonable estimation of IOP (probably ± 4 to 5 mmHg) but still is not as accurate as the

applanation tonometers and is not as easy to employ.[5] Schiotz tonometry is not recommended in patients with weakened or diseased corneas. Its results may be inaccurate following scleral buckling and glaucoma filtration procedures or any other procedure that alters the rigidity of the fibrous coat of the eye.

Applanation tonometers measure the force required to flatten, or applanate, a constant area of cornea, or by measuring the surface area flattened by a predetermined force. A variety of instruments are available that utilize this technique to estimate IOP. A 3- to 4-mm diameter planosurface on the contact probe flattens an area of the cornea, and applied forces are evaluated either optically with a split-field prism and fluorescein or electronically with linear transducers, gas-suspended probes, or air-pulse noncontact sensors. Available applanation tonometers include the Goldmann, Draeger, Perkins, Halberg, Maklakoff, Mackay-Marg, TonoPen, TonoVet, and pneumatonograph tonometers. The TonoPen is currently the most widely used form in veterinary medicine because of its ease of use and portability (Fig. 9.1.23).

The Goldmann, Draeger, Perkins, and Halberg applanation tonometers estimate IOP by aligning a corneal contact prism with a hand dial or small motor to calculate the force of applanation. The Goldmann tonometer is affixed to a table-mounted slitlamp biomicroscope and is the most accurate applanation tonometer in human ophthalmology. It requires that the eye remain stationary for several seconds to obtain an accurate reading. The Draeger, Perkins, and Halberg applanation tonometers are handheld instruments, and similar to the Goldmann tonometer, they require the eye to remain stationary for several seconds. These instruments have been used in sedated rabbits and nonhuman primates, but they are not useful for clinical veterinary ophthalmology.[5]

Electronic applanation instruments became available after the advent of the Mackay-Marg tonometer. Of these, however, only the TonoPen and TonoVet models remain commercially available today. The Mackay-Marg tonometer relies on a ceramic actuating rod suspended within the tip of a stainless-steel probe that activates a position transducer.[5] The high-frequency, alternating current supplied to the transducer by an amplifier-recorder unit is subsequently modified and returned to the recorder.[5] The lowest repeatable measurements represent the IOP. Most laboratory studies have found the Mackay-Marg tonometer demonstrates superior accuracy over other available applanation tonometers.

The TonoPen is an 18 × 2 cm, handheld, battery-operated instrument that functions similarly to the Mackay-Marg tonometer. The footplate of the instrument contains the plunger, which achieves applanation of the cornea and is covered by a disposable latex membrane that protects the sensitive plunger and prevents disease transmission. Light tapping of the instrument on the central two thirds of the cornea perpendicular to the point of contact will produce accurate readings (Fig. 9.1.23).[232] Recoil of the ceramic plunger following corneal contact produces a signal that is amplified, digitized, and passed through a single-chip microprocessor. IOP measurements are displayed on a liquid-crystal screen. Prior to use of the TonoPen, topical anesthetic is instilled into the eye, and the eyelids are retracted. The probe tip is used to gently and repeatedly contact the central cornea without indenting it. Brief clicks indicate when individual readings have been recorded, and a sustained tone indicates when a mean IOP has been calculated. The mean IOP is then displayed along with the coefficient of variance (i.e., 5%, 10%, 20%, or >20%). The TonoPen is very accurate in the normal range of IOPs but tends to overestimate IOP in the low range and underestimate IOP in the high range in dogs, cats, and humans.[227,230,231,233] Because of its portability, reliability, and cost, the TonoPen has become the most popular instrument among veterinary ophthalmologists for measurement of IOP.

The TonoVet is the latest model of tonometer to be produced and distributed to the veterinary market. It utilizes a novel induction-impaction method to determine IOP, essentially measuring rebound action of the magnetic probe as it contacts the eye and bounces back.[234] It has the advantage of not requiring topical anesthesia prior to its use; however, it must be held upright during measurement, which may make its

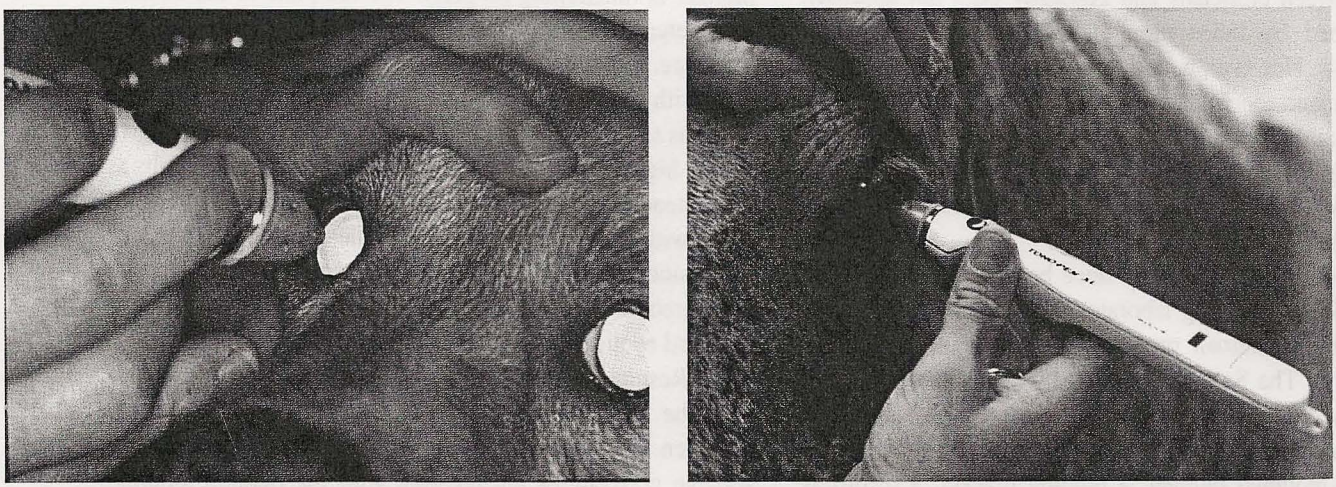

(a) (b)

Figure 9.1.23. Applanation tonometry in a dog **(A)** and a horse **(B)** using the TonoPen tonometer.

Figure 9.1.24. Digital tonometry in a dog. Although not a precise measurement of IOP, digital tonometry can often provide a useful estimate, although subjective, of the intraocular tension, particularly when instruments that would allow a more precise measurement to be made are unavailable.

use difficult in recalcitrant or recumbent patients. Preliminary studies report that its accuracy is comparable to that of the TonoPen.[234]

The pneumatonograph is an applanation tonometer-tonographer that measures IOP via a gas-suspended plunger. Compressed air is directed into a sensor housing that contains a hollow, metal plunger with a silicone sensor membrane at its tip. Part of the gas supports the plunger, thereby allowing it to move in a near-frictionless state; the rest of the gas passes through the hollow plunger (i.e., measurement chamber), gently pressing the sensor against the cornea during applanation.[5] Pressure from the eye restricts the flow of gas between the sensor membrane and the plunger tip, thus increasing the pressure within the measurement chamber.[5] To record IOP with the pneumatonograph, the patient's cornea is anesthetized, and the eyelids are gently retracted. With the plunger extended, the silicone footplate contacts the central cornea. Pressure is then applied until the plunger is depressed approximately halfway into the sensor housing, as indicated by red and green marks on the plunger, and contact is maintained for several seconds.[5] Although very accurate in other species, the pneumatonograph may give falsely reduced pressure readings in the horse and the cow.[235]

It is important to consider the effects any sedation or anesthesia may have on your tonometric estimations. In small, cooperative patients, the main factors affecting the measurement of IOP, aside from those already discussed such as excessive restraint, improper positioning, or excessive pressure on the globes, include improper or inexperienced use of equipment or a disease process affecting one or both globes. In larger animals, such as horses, sedation must often be administered in order to achieve a thorough ophthalmic examination. Many common sedatives, such as xylazine or acepromazine, may significantly decrease IOP, even by as much as 23% in the case of xylazine.[219,236] There is debate about whether or not an auriculopalpebral nerve block affects IOP in the horse. Some studies report that animals that have not received an auriculopalpebral block prior to tonometry will have an elevated IOP caused by the pressure of the eyelids on the globe.[229,237] Other studies failed to support this finding.[236,238] General anesthesia will frequently affect IOP, usually by decreasing it.

Gonioscopy

Gonioscopy is the examination of the iridocorneal angle (ICA), or filtration angle, and ciliary cleft of the eye. Examination of this region is crucial for evaluating the aqueous outflow pathways and also for insight into the pathogenesis of a glaucomatous state. The angle should be examined for width (open, closed, or narrow), presence and character of the pectinate ligaments that traverse the space between the cornea and the base of the iris, presence of synechia (especially peripheral anterior synechia), peripheral iris cysts, foreign bodies, neoplasia, granulomas, traumatic iridal dialyses or other injuries, and anterior segment colobomas.[203,239–242] Gonioscopy can also be used to identify potential intraocular extension of limbal masses, such as melanomas.

Trantas reported direct visualization of the human iridocorneal angle in 1907 and again in 1918.[243] Later, Salzmann constructed the first goniolens from a modified Fick keratoconus contact lens.[243] Between 1919 and 1920, Koeppe described gonioscopy using a slitlamp and a special steeper contact lens. Troncoso modified the Koeppe goniolens in 1920, using a monocular instrument called a gonioscope to magnify the angle by a power of 13 to 21. In 1938, Barken described gonioscopy as a diagnostic aid for human primary glaucoma,[243] and in that same year, Goldmann introduced the indirect goniolens that allowed visualization of all 360 degrees of the iridocorneal angle simply by rotating the mirror of the goniolens. In 1942, Troncoso introduced the binocular gonioscope, which was a handheld instrument allowing stereoscopic visualization of the iridocorneal angle.[244] In 1936, Troncoso and Castroviejo[245] published the comparative gonioscopic anatomy of the rabbit, pig, cat, dog, and nonhuman primate. In 1960, Calkins[246] published a phylogenetic study of the iridocorneal angle in a variety of species, and Magrane[247] and Lovekin[203] also briefly described gonioscopy in 1957 and 1964, respectively. Lescure[248] photographed the canine ICA and ciliary cleft in 1963 using the Goldmann lens. In 1969, Gelatt published photographs of the normal canine ICA and ciliary cleft using the Koeppe lens and Kowa fundus camera.[25]

The ICA of most animals, including humans, cannot be directly visualized because the scleral shelf obscures the view. Some animals with very large and deep anterior chambers, such as felids, have ICAs and ciliary clefts that are somewhat visible to the unaided eye. In most species, however, light directed at the ICA cannot return from the eye to allow examination of the structures of interest because of the angle of incidence of the light as it exits and the difference between the refractive indices of cornea (1.376) and air (1.000). Usually, in

small animals, light coming from the ICA is reflected back into the anterior chamber.[249] In order to appreciate the angle, a contact lens must be placed on the cornea to bend light in such a way that it exits the cornea toward the observer. After the lens is placed on the cornea, the light can exit the eye because the curvature of the lens is different from that of the cornea, and the refractive index of the lens (either plastic or glass) is different from that of the air (the difference between the cornea and the lens is less than that between the cornea and the air).[5,239]

Many different goniolenses are available commercially, and they fall into two categories: direct or indirect. Direct goniolenses allow the examiner to look across the anterior chamber to the opposite ICA segment. The image perceived with direct gonioscopy is magnified and real, but it is difficult to examine the entire 360 degrees of the angle, and the examiner must be quite physically close to the patient for an effective examination (Fig. 9.1.26). The observer must change positions to examine the entire ICA. Examples include small lenses such as the Cardona, Hoskins-Barkan, Layden, and Swan-Jacob models, which are useful in small eyes; Barkan and Koeppe lenses, which are held in place with a finger or instrument; and Franklin and Troncoso models, which have silicone flanges and tube-handles, respectively (Fig. 9.1.25). There are goniolenses that use vacuum created by a small syringe to improve attachment to the cornea.

Indirect goniolenses use mirrors or prisms that allow the ICA and opening of the ciliary cleft to be visualized from directly in front of the patient. The entire circumference of the angle can be observed simply by changing focus from mirror to mirror; therefore, minimal manipulation is necessary and safe working distances are possible. However, indirect goniolenses or prisms are designed for human corneas, which are significantly smaller and have a more acute curvature than canine corneas. When they are used in our small animals, they have a tendency to distort the image of the angle, producing an artifactual narrowing of the iridocorneal angle. The Karickhoff diagnostic lens, Posner gonioprisms, and Sussman gonioscope are examples. There are various other single-, two-, and three-mirrored forms as well.

After the lens is in place, a light source is utilized to illuminate the ICA (Fig. 9.1.26). A portable slitlamp biomicroscope is ideal for providing magnification and stereopsis, but an otoscope with the speculum removed, a Heine or Barkan gonioscope, or a handheld fundus camera can also be used. While the most difficult animals may require sedation for a thorough examination, most small animals can usually be examined with only topical anesthetic. In rare cases, a temporary palpebral nerve block may be necessary. If a lesion or area of interest is located in a particularly difficult area to examine, such as at twelve o'clock, and the patient must be placed in dorsal recumbency for the examination, sedation or even general anesthesia may be required. After the topical anesthetic is instilled, a 1.0% to 2.5% methylcellulose solution is placed on the contact surface of the goniolens, and the lens is then applied to the cornea. Less viscous solutions, such as 0.9% saline, are not as effective at preventing air from getting between the lens and the cornea. Air bubbles should be avoided because they will distort light and prevent adequate visualization of the ICA. Gonioscopy is performed after examination of the rest of the interior of the eye because the coupling gel necessary to affix the contact goniolens to the cornea will obscure the view for ophthalmoscopy.

The entire ICA and opening of the ciliary cleft are systematically evaluated, with special attention given to width, pectinate ligament conformation, inner and outer pigment zones, and uveoscleral trabecular meshwork (Fig. 9.1.27). Gonioscopy is most often used to evaluate glaucoma in small animals, particularly dogs and cats. The ICA and ciliary cleft are classified as open, narrow, or closed, and any abnormalities are noted during the examination. Indentation or dynamic gonioscopy may be used to differentiate reversible iridocorneal angle apposition

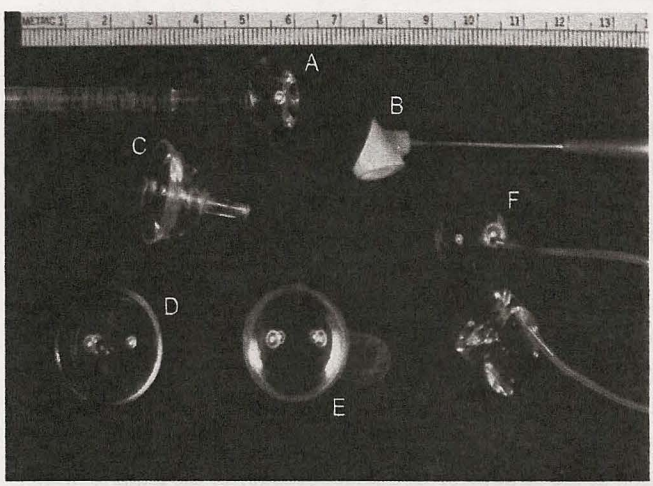

Figure 9.1.25. Selected goniolenses used in animals. **A.** Franklin; **B.** Koeppe; **C.** Troncoso; **D.** Lovac; **E.** Cardona; **F.** Swan-Jacob.

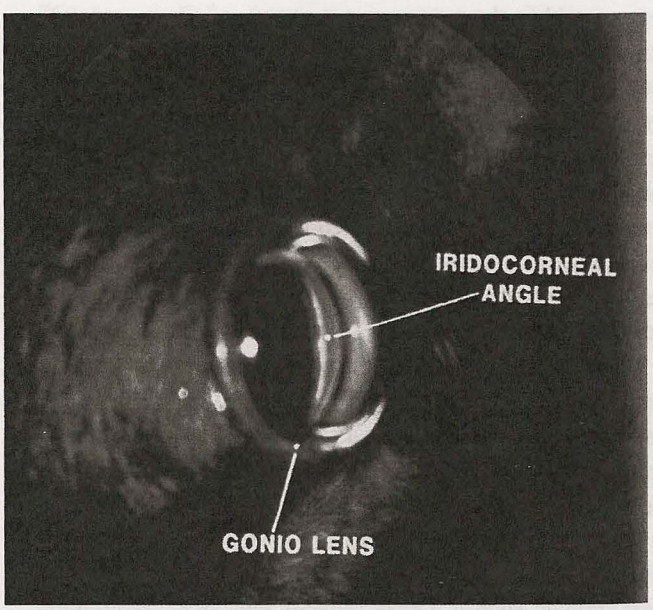

Figure 9.1.26. The direct Franklin goniolens in place on a canine cornea.

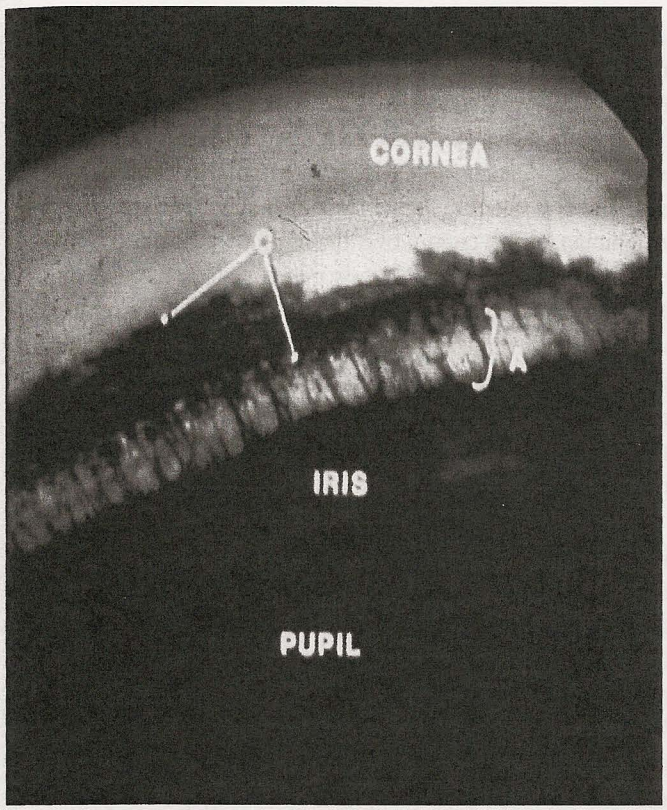

Figure 9.1.27. The normal ICA seen by gonioscopy using a Franklin goniolens. Note the pectinate ligament (**A**) and inner and outer pigmented layers (**C**). In this figure, the cornea appears in the dorsal aspect and the iris below the angle.

from angle closure associated with peripheral anterior synechiae by applying slight pressure at the peripheral cornea to achieve separation if it is possible.

In the horse, the ICA can be examined without the use of a specifically designed goniolens. The entire circumference of the angle in the foal and portions of the nasal and temporal angle at the limbus in the adult horse are visible through the cornea. The portions of the angle seen in the adult horse are generally representative of the entire angle (Michau, personal communication, 2005). Fortunately, abnormalities of the ICA are rare in the horse.

Tonography

Tonography is the use of continuous tonometry to estimate noninvasively the facility of conventional aqueous humor outflow.[250,251] In this technique, a tonometer is allowed to rest on the cornea for a set time period, usually 2 or 4 minutes. Its weight forces fluid out of the eye, and the resultant pressure rate of decay is recorded. In theory, the weight of the tonograph probe on the cornea increases both the IOP and the rate of aqueous humor outflow without changing the rate of aqueous humor formation. The subsequent decline in IOP is measured over a period of minutes, thereby allowing the examiner to estimate the pressure-sensitive conventional (i.e., corneoscleral trabecular outflow) facility of aqueous humor outflow. The unconventional (i.e., uveoscleral outflow) aqueous humor outflow is pressure-independent and thus is not estimated by tonography.

Schiotz first described reduction of IOP through repeated tonometry in 1905, noting that pressure reduction occurred to a greater degree in normal than in glaucomatous eyes. In 1911, Polak-van Gelda reported similar results using intermittent Schiotz tonometry over a period of 1 to 2 minutes. The following year, Schoenberg described the application of continuous tonometry on the human eye, recording the rate of decline in IOP for both normal and glaucomatous eyes. By the 1960s, tonography had become a routine part of the diagnostic regimen for human glaucoma. Sole reliance on tonography to detect glaucoma should be avoided, however, because misinterpretation and misdiagnosis may occur as a result of some overlap between the facility of aqueous outflow in normal versus early glaucomatous eyes.[252–254] Nevertheless, tonography remains an important, noninvasive, and repeatable clinical diagnostic procedure for the estimation of conventional aqueous humor outflow.

The results of tonography have been reported in the rabbit, cat, dog, horse, and nonhuman primates.[255–258] It has further been used to compare the facility of aqueous humor outflow in normal and glaucomatous Beagles.[259,260] Tonography has established that there is increased resistance to aqueous humor outflow in dogs with glaucoma.[259,260] The technique appears to be very accurate when compared with the traditional, invasive, constant-pressure, and two-step perfusion techniques of measuring aqueous humor outflow.[261] The typical tonogram waveform is a gradually descending line with only slight fluctuations, which reflect pulse and respiration. The descending line represents decreasing IOP. The slope of the line is greater with normal than with glaucomatous eyes. Human tonography tables have been used to calculate the coefficient of aqueous humor outflow in the dog, cat, and horse. Using either the Schiotz tonograph or the pneumatonograph, the facility of aqueous humor outflow is 0.24 ± 0.07 μL/mmHg/min to 0.297 ± 0.149 μL/mmHg/min for the normal dog eye, 0.27 to 0.32 μL/mmHg/minute for the normal cat eye, and 0.88 ± 0.65 μL/mmHg/min for the normal horse eye.[260,262,263]

Two types of tonographs are available: those that utilize indentation and those that utilize applanation to estimate changes in IOP.[264–267] The Schiotz tonograph is an indentation-type instrument, consisting of an electronic Schiotz tonometer connected to a transducer. Readings are displayed on a console. The Schiotz probe is large, covering most of the corneal surface, and has all the mechanical problems associated with this type of tonometer. Applanation tonography is performed with a pneumatonograph or a modified Mackay-Marg tonometer. The pneumatonograph uses a compressed air–supported, silicone-tipped plunger to flatten or applanate a focal area of the cornea, thus displaying both digital and waveform results in a manner similar to the Schiotz tonograph. The pneumatonograph probe is smaller than the Schiotz instrument and is more easily maintained on the center of the cornea.

Sedation or general anesthesia is necessary when performing tonography because the eye must be immobile for 2 to 4 minutes during the procedure, and most veterinary patients are unwilling or unable to cooperate for that long

without pharmacological intervention. The agents for sedation or anesthesia must be chosen carefully, however, because many drugs can cause significant changes in venous blood pressure, IOP, and pupil size and thereby potentially affect the facility of aqueous humor outflow. Gelatt described a protocol using acepromazine (0.5 mg/kg IV) followed 5 minutes later by ketamine (10 mg/kg IM),[259,260] but the general health status of each individual patient must be considered carefully before choosing any one particular protocol. The use of halothane anesthesia has also been reported for patient anesthesia prior to pneumatonography, which may be more useful clinically.[268,269] Topical anesthetic is applied to the corneas, and if necessary to permit probe placement and prevent blinking, auriculopalpebral nerve blocks may be performed. Regardless of the method of restraint, the patient is placed in dorsal recumbency, and the eyelids are held open manually or with an eyelid speculum. The speculum should not be so tight-fitting as to put direct pressure on the globe, and the cornea should be kept moist to avoid damage to the epithelium. The contact surface of the tonograph probe is carefully placed against the central cornea, and measurements are continuously recorded for a period of 2 to 4 minutes. During this time, the contact probe should remain in a fixed position to minimize artifacts, which may result from probe movement, probe malfunction, nystagmus, blinking, sneezing, and hyperventilation.

Even though this technique has tremendous potential for quantifying conventional or pressure-sensitive aqueous humor outflow and may be helpful in defining the clinical significance of anatomical aberrations of the ICAs as viewed with gonioscopy, tonography is not commonly utilized in clinical veterinary ophthalmology. Lack of consistency and the difficulties associated with recording data in untrained animals and the need for either heavy sedation or anesthesia make this tool most useful in the research setting.

Anterior Chamber Paracentesis

The aqueous humor that occupies the anterior chamber may be quite easily sampled for diagnostic or therapeutic purposes.[55,57,138,270–273] Depending on the temperament and the overall health status of the patient, the procedure can be performed either with sedation and topical anesthesia or under short-acting general anesthesia. Some clinicians opt to do aqueous paracentesis with topical anesthesia alone, but the risk of injuring the eye and jeopardizing vision is much higher if the animal is awake. The bulbar conjunctiva should be cleaned prior to the sampling with a dilute (5%) Betadine solution and then rinsed with normal saline.[5] After the instillation of a topical anesthetic (it is sometimes helpful to hold a cotton-tipped applicator soaked with the topical anesthetic agent on the site of insertion for a moment for better anesthesia) and placement of an eyelid speculum, the bulbar conjunctiva is grasped with small forceps near the site of entry and a small needle (25 to 30 gauge) is inserted with its bevel up in a gentle twisting, drilling motion through the clear cornea near the limbus or the subconjunctival limbus parallel and anterior to the iris (Fig. 9.1.28). It is important to visualize the tip of the needle during insertion and centesis so as to avoid puncturing either the iris or the lens capsule.[5] If a syringe is attached to the needle, a small amount of aqueous is aspirated. Alternatively, the aqueous that fills the hub of the needle may be wicked into a capillary tube. This second method, without the cumbersome attached syringe, offers the clinician greater control over the needle's position.[274] If it is available, an aqueous paracentesis pipette, which consists of a 30-gauge needle mounted on a plastic tube with a removable bulb on the end, may be used to collect the fluid.[275] The procedure is similarly performed in large animals (e.g., equines) as in small animals, except for the site of aspiration, which should be either dorsal or temporal to take advantage of the scleral extension beyond the iris base.

Aqueous humor centesis may be used to acquire a sample for microbiologic culture or cytology, especially in cases of infectious anterior uveitis or intraocular neoplasia. Aqueous may also be submitted for protein measurement, antibody titers (e.g., *Leptospira* spp, *Toxoplasma gondii*), or PCR analysis for minute quantities of DNA from infectious agents.[58,276–283] When aqueous humor antibody titer levels are compared to serum levels, a determination can be made as to whether or not there has been local antibody production against a specific agent. The Goldmann-Witmer coefficient or C value indicates local antibody production if it is greater than 1. The formula for the C value is [specific IgG in AqH/specific IgG in serum] × [total IgG in serum/total IgG in AqH].[277,281] The procedure is also useful for aspirating cystic lesions or vacuuming cells off lesions of the iris.[6] If IOP is elevated, aqueous paracentesis may be used to alleviate the hypertension, especially if the animal is not systemically healthy enough to handle mannitol or glycerol. Also, paracentesis can be performed to instill drugs, such as tissue plasminogen activator for the dissolution of fibrin clots, into the anterior chamber.[10]

While in most instances this procedure is safe, it does carry with it a certain amount of risk, especially if it is being performed in eyes with opaque corneas or marked iris bombé. Potential complications for this procedure include hyphema, lens capsule rupture with subsequent phacoclastic uveitis, endothelial damage and corneal edema, anterior uveitis, endophthalmitis, choroidal hemorrhage and edema, and glaucoma (secondary to the previously mentioned complications).[5] Protein levels in the aqueous humor will increase following this procedure due to the sudden hypotension experienced by the eye and a release of prostaglandins.[276,284–288] To prevent or dilute this prostaglandin release and the resultant uveitis from a diagnostic tap, an equal amount of normal saline or balanced salt solution can be injected into the anterior chamber, especially when the aspirated volume exceeds 0.3 mL.[5,10]

Vitreous Paracentesis

Vitreous paracentesis, also called hyalocentesis, is the aspiration of material from the vitreous chamber. This procedure, when properly performed and utilized, can provide a definitive diagnosis for posterior segment diseases or endophthalmitis.

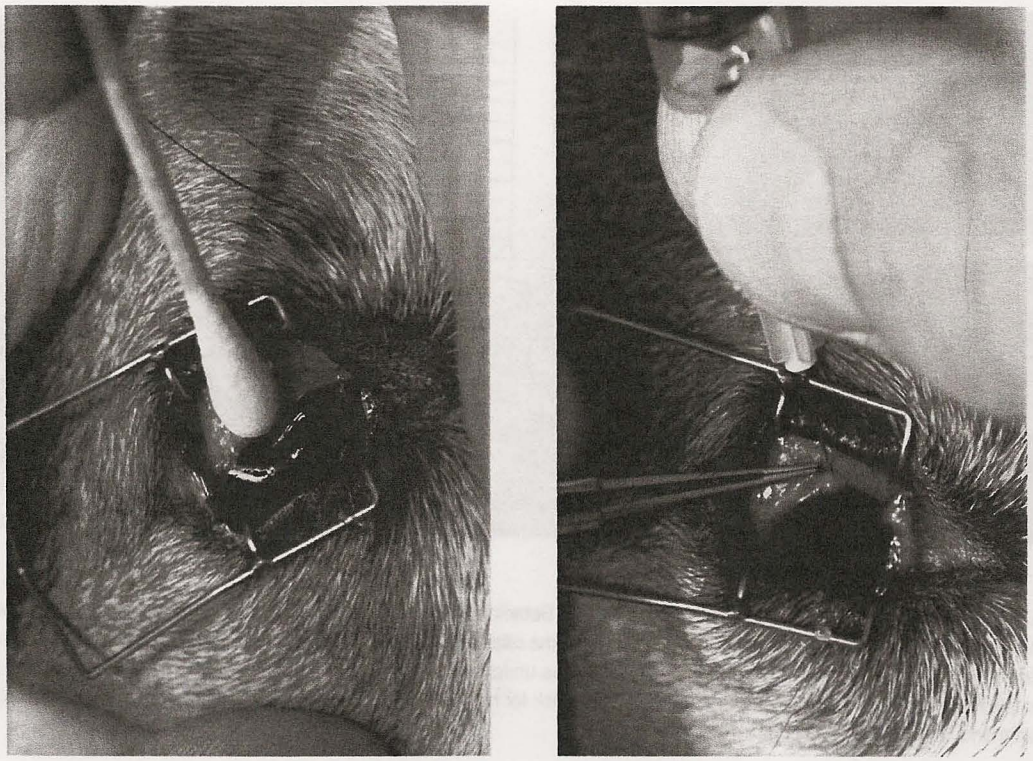

(a) (b)

Figure 9.1.28. Aqueous centesis in a dog. After cleansing with a dilute Betadine solution and the application of a topical anesthetic agent (**A**), an hypodermic needle (usually 22 gauge) is introduced through the limbus and beneath the bulbar conjunctiva into the anterior chamber (**B**) at such an angle as to avoid contact with both the iris and interior cornea.

Samples taken from the vitreal chamber can be submitted for cytology, culture and sensitivity, protein measurement, specific antibody titers (e.g., toxoplasmosis, leptospirosis), or PCR.[282,283] Additionally, vitreous paracentesis can be performed toward therapeutic aims, such as to instill antimicrobial agents in the case of endophthalmitis or to instill gentamicin or other ocular toxic agents in the case of end-stage, medically refractive glaucoma.

Vitreous paracentesis is usually performed with the patient under general anesthesia, or at least very heavily sedated. Short-acting anesthetic agents, such as propofol (6 to 8 mg/kg intravenously without premedication; 2 to 4 mg/kg intravenously with premedication), work well for this relatively quick procedure.[30] If the anterior segment is clear and allows visualization of the posterior segment, it will behoove the surgeon to dilate the pupil with mydriatic agents (if they are not contraindicated) prior to performing the procedure to further improve the visualization. The globe and adnexa are prepared as for any other aseptic procedure with an antiseptic solution, such as a dilute povidone-iodine solution, and rinsed with 0.9% sterile saline. An eyelid speculum will facilitate exposure. The globe is stabilized by grasping the lateral bulbar conjunctiva with forceps, and a 22-gauge hypodermic needle is inserted approximately 6 to 8 mm behind the limbus in the dog (Fig. 9.1.29).[289] The pars plana ciliaris is widest in the lateral and dorsolateral portions of the globe, so it is there that insertion is initiated. The needle is directed toward the center of the globe through the sclera and pars plana ciliaris, taking care to avoid penetrating the lens anteriorly or the retina posteriorly. Once the needle is situated, 0.10 to 0.3 mL of fluid are slowly aspirated (sometimes more in the end-stage, glaucomatous eye) and replaced with an equal volume of sterile 0.9% saline unless one of the goals of the centesis is to lower IOP by decreasing the volume within the globe. The needle frequently needs to be repositioned to find areas of more liquefied vitreous. Aged and diseased vitreous is usually liquefied; therefore, aspiration is usually easy. Granulomatous or neoplastic material and normal vitreous, however, may require more aggressive aspiration and, in some cases, a larger-gauge hypodermic needle is necessary to remove an adequate sample. This procedure can also be performed under the operating microscope or with ultrasound guidance to improve the accuracy of needle placement within the vitreous chamber. Vitreous centesis in the horse is performed similarly, but because of the larger size of the equine eye, the needle is introduced through the conjunctiva and sclera 10 mm behind the limbus at the dorsal aspect of the globe.[290]

Dilute cytology samples can be concentrated by ultracentrifugation. Vitreous samples are frequently more reliable than aqueous samples for yielding infectious agents responsible for endophthalmitis.[6] The procedure is not without risk, however. Potential complications include choroidal or ciliary body hemorrhage, hyphema, retinal tear or detachment (or both), lens subluxation, cataract formation, uveitis (anterior, posterior, or

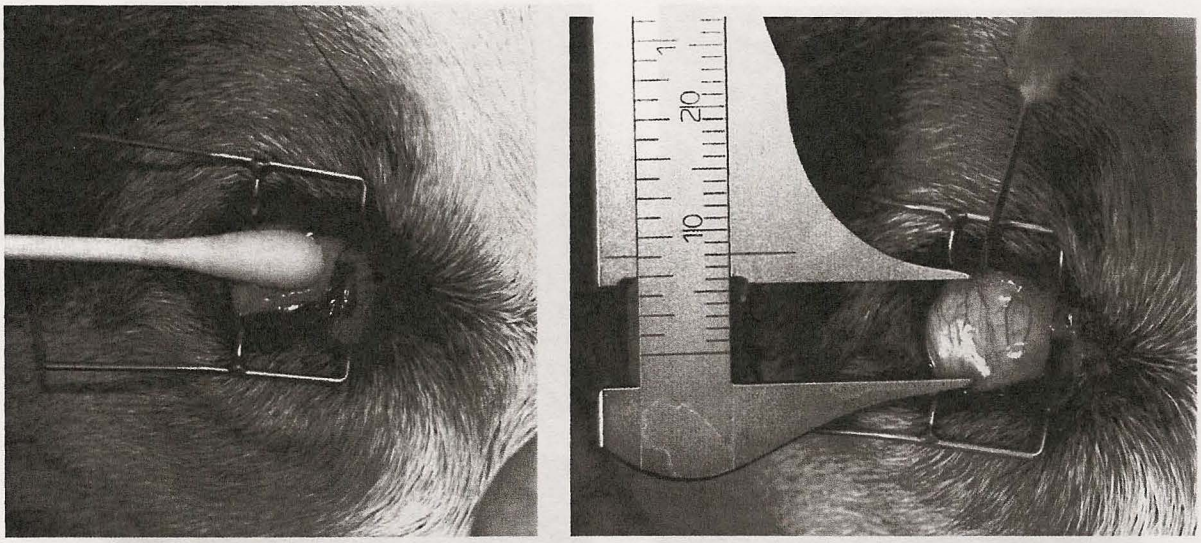

(a) (b)

Figure 9.1.29. Vitreous paracentesis in a dog. After cleansing with a dilute Betadine solution and the application of a topical anesthetic agent (**A**), an hypodermic needle (usually 22 gauge) must be inserted through the sclera behind the ciliary body (7–8 mm behind the limbus) (**B**) and directed in a posterior direction to avoid contacting and traumatizing the lens. This injection should not be undertaken lightly and is performed in order to either inject an agent into the vitreous or obtain sample material from the vitreal chamber. With it comes risk for hemorrhage, inflammation, lenticular damage and its associated consequences, retinal detachments, and the introduction of infectious agents.

both), and endophthalmitis (septic or otherwise). Patients may require postprocedural treatment with mydriatics, topical and systemic antibiotics, systemic or topical antiinflammatory agents, or some combination thereof.

REFERENCES

1. Parker J. Examination of the equine eye as part of the examination of the horse for purchase. *Equine Vet J* 1983; 2(suppl): 3–6.
2. Merideth RE, Wolf ED. Ophthalmic examination and therapeutic techniques in the horse. *Compend Cont Ed* 1981; 3: 426–433.
3. Latimer CA, Wyman M. Neonatal ophthalmology. *Vet Clin North Am Equine Pract* 1985; 1: 235–259.
4. Millichamp NJ. Ophthalmic disease in exotic species. *Vet Clin North Am Exotic Anim* 2002; 5: 223–242.
5. Strubbe TD, Gelatt KN. Ophthalmic examination and diagnostic procedures. In: Gelatt KN, ed. *Veterinary Ophthalmology,* 3rd ed. Philadelphia: Lippincott Williams and Wilkins, 1999: 427–466.
6. Martin CL. Anamnesis and the ophthalmic examination. In: Martin CL, ed. *Ophthalmic Disease in Veterinary Medicine.* London: Manson Publishing Ltd., 2005: 41–70.
7. Koch SA. Ophthalmic examination of the horse. *Equine Vet J* 1983; 2(suppl): 7–8.
8. Brooks DE. Corneal ulceration. In: Brooks DE, ed. *Equine Ophthalmology for Equine Practitioner.* Jackson: Teton Newmedia, 2004: 58–87.
9. Carastro SM. Equine ocular anatomy and ophthalmic examination. *Vet Clin North Am Equine Pract* 2004; 20: 285–299.
10. Michau TM. Equine ocular examination: Basic and advanced diagnostic techniques. In: Gilger BC, ed. *Equine Ophthalmology.* St. Louis: Elsevier Saunders, 2005: 1–62.
11. Barnett KC, Crispin SM, Lavach JD, Matthews AG, ed. *Feline Ophthalmology,* 1st ed. London: Saunders, 2002: 1–10.
12. Whitley RD, Moore CP. Ocular diagnostic and therapeutic techniques in food animals. *Vet Clin North Am Large Anim Pract* 1984; 6: 553–575.
13. Morales RJ. Corneal diagnostic procedures. *Clinical Tech in Small Anim Pract* 2003; 18: 145–151.
14. Mould J. Approach to an ophthalmic examination. In: Peterson-Jones SM, Crispin SM, eds. *Manual of Small Animal Ophthalmology.* Shurdington: B.S.A.V.A, 1993: 11–26.
15. Cottrell B, Peterson-Jones SM. Special examination techniques. In: Peterson-Jones SM, Crispin SM, eds. *Manual of Small Animal Ophthalmology.* Shurdington: B.S.A.V.A, 1993: 27–36.
16. Hopper C, Crispin SM. Laboratory examination techniques. In: Peterson-Jones SM, Crispin SM, eds. *Manual of Small Animal Ophthalmology.* Shurdington: B.S.A.V.A, 1993: 37–44.
17. Slatter D, ed. *Fundamentals of Veterinary Ophthalmology,* 2nd ed. Philadelphia: W.B. Saunders Company, 1990.
18. Barnett KC, Crispin SM, Lavach JD, Matthews AG, eds. *Canine Ophthalmology,* 1st ed. London: Saunders, 2002: 1–8.
19. Gelatt KN, Peiffer RL, Gwin RM, Williams LW. The status of equine ophthalmology. *J Equine Med Surg* 1977; 1: 13–19.
20. Wilkie DA. Ophthalmic procedures and surgery in the standing horse. *Vet Clin North Am Equine Pract* 1991; 7: 535–547.
21. Gelatt KN. Examination of the eye. *Am Anim Hosp Assoc Proc* 1970; 37: 326–331.
22. Krawitz L. Clinical examination of the canine and feline eye. *J Am Vet Med Assoc* 1965; 147: 33–37.
23. Bistner SI. Examination of the eye. *Vet Clin North Am* 1971; 1: 29–52.
24. Cooley PL. Normal equine ocular anatomy and eye examination. *Vet Clin North Am Equine Pract* 1992; 8: 427–449.
25. Gelatt KN. *Diagnostic Procedures in Comparative Ophthalmology,* 2nd ed. Elkland: American Animal Hospital Association, 1974.

26. Keeney AH. *Ocular Examination: Basis and Technique,* 2nd ed. St. Louis: CV Mosby, 1976.
27. Davis JL, Stewart T, Brazik E, Gilger BC. The effect of topical administration of atropine sulfate on the normal equine pupil: Influence of age, breed and gender. *Vet Ophthalmol* 2003; 6: 329–332.
28. Berger SL, Scagliotti RH. A quantitative study of the effects of Tribrissen on canine tear production. *J Am Anim Hosp Assoc* 1995; 31: 236–41.
29. Collins BK, Gross ME, Moore CP, Branson KR. Physiological, pharmacological, and practical considerations for anesthesia of domestic animals with eye diseases. *J Am Vet Med Assoc* 1995; 207: 220–230.
30. Thurmon JC, Tranquilli WJ, Benson GJ, eds. *Lumb and Jones' Veterinary Anesthesia,* 3rd ed. Baltimore: Williams & Wilkins, 1996.
31. Millichamp NJ. Principles of ophthalmic surgery. In: Auer JA, ed. *Equine Surgery,* Philadelphia: WB Saunders, 1992: 588–598.
32. Millichamp NJ. Ocular trauma. *Vet Clin North Am Equine Pract* 1992; 8: 521–536.
33. Thurmon JC, Benson GJ. Injectable anesthetics and anesthetic adjuncts. *Vet Clin North Am Equine Pract* 1987; 3: 15–36.
34. Beaumont SL. Ocular disorders of pet mice and rats. *Vet Clin North Am Exotic Anim Pract* 2002; 5: 311–324.
35. Marx KL, Roston MA. *The Exotic Animal Drug Compendium.* Trenton, NJ: Veterinary Learning Systems, 1996.
36. Jurk I. Ophthalmic disease of fish. *Vet Clin North Am Exotic Anim Pract* 2002; 5(2): 243–260.
37. Maksimovic B. Innere und aussere Ohrmuskelanasthesie beim Pferd. *Acta Vet Belgrade* 1952; 2: 80–81.
38. Rubin LF. Auriculopalpebral nerve block as an adjunct to the diagnosis and treatment of ocular inflammation in the horse. *J Am Vet Med Assoc* 1964; 144: 1387–1388.
39. Rubin LF, Gelatt KN. Analgesia of the eye. In: Soma LR, ed. *Veterinary Anesthesia.* Baltimore: Williams & Wilkins, 1971.
40. Manning JP. Palpebral, frontal, and zygomatic nerve blocks for examination of the equine eye. *Vet Med Small Anim Clin* 1976; 71: 187–189.
41. Havener. *Ocular Pharmacology,* 6th ed. St. Louis: CV Mosby, 1994.
42. Skarda R. Techniques of local anesthesia in ruminants and swine. *Vet Clin North Am Food Anim Pract* 1986; 2: 623–663.
43. Welker B. Ocular surgery. *Vet Clin North Am Food Anim Pract* 1995; 11: 149–157.
44. Gelatt KN. *Veterinary Ophthalmic Pharmacology and Therapeutics,* 2nd ed. Bonner Springs, Kansas: VM Publishing, 1978: 9–28.
45. Cyce KM, Sack WO, Wensing CJG. *Textbook of Veterinary Anatomy.* Philadelphia: WB Saunders, 1987: 310–311.
46. Evans HE, Christensen GC. *Miller's Anatomy of the Dog.* Philadelphia: WB Saunders, 1979: 913–916.
47. Peterson DR. Nerve block of the eye and associated structures. *J Am Vet Med Assoc* 1951; 18: 145–148.
48. Bistner S. Clinical diagnosis and treatment of infectious keratitis. *Compend Contin Educ Pract Vet* 1981; 3: 1056–1066.
49. Severin GA, ed. *Veterinary Ophthalmology Notes,* 2nd ed. Fort Collins: Colorado State University, 1976.
50. Crispin SM. Examination of the eye and adnexa. In: Barnett KC, Crispin SM, Lavach JD, Matthews AG, eds. *Equine Ophthalmology,* 2nd ed. London: Saunders, 2004: 1–13.
51. Enzerink E. The menace response and pupillary light reflex in neonatal foals. *Eq Vet J* 1998; 30: 546–548.
52. Adams R, Mayhew IG. Neurological examination of newborn foals. *Eq Vet J* 1984; 16: 306–312.
53. Kleinfeld J, Ellis PP. Effects of topical anesthetics on growth of microorganisms. *Arch Ophthalmol* 1966; 76: 712–715.
54. Da Silva Curieal JMA, Nasisse MP, Hook RR. Topical fluorescein dye: Effects on immunofluorescent antibody test for feline herpesvirus keratoconjunctivitis. *Prog Vet Comp Ophthalmol* 1991; 1: 99–104.
55. Olin DD. Examination of the aqueous humor as a diagnostic aid in anterior uveitis. *J Am Vet Med Assoc* 1977; 171: 557–559.
56. Blogg JR, Coles EH. Aqueous humor proteins: A review. *Vet Bull* 1970; 40: 347–351.
57. Hogan MJ, Wood IS, Godfrey WA. Aqueous humor cytology in uveitis. *Arch Ophthalmol* 1973; 89: 217–220.
58. Krohne SG, Krohne DT. Use of laser flaremetry to measure aqueous humor protein concentration in dogs. *J Am Vet Med Assoc* 1995; 206: 1167–1172.
59. Rubin LF, Wolfes RL. Mydriatics for canine ophthalmoscopy. *J Am Vet Med Assoc* 1962; 140: 137–141.
60. Gelatt KN, Boggess TS, Cure TH. Evaluation of mydriatics in the cat. *J Am Anim Hosp Assoc* 1973; 9: 283–287.
61. Gelatt KN, Gum GG, Mackay EO. Evaluation of mydriatics in horses. *Vet Comp Ophthalmol* 1995; 5: 104–107.
62. Albert DM, Edwards DD. *The History of Ophthalmology.* Cambridge: Blackwell Science, 1998.
63. Berliner ML. *Biomicroscopy of the eye: Slit lamp biomicroscopy of the living eye,* Vol 1. New York: Paul B Hoeber, 1943.
64. Schmidt TA. On slit-lamp microscopy. *Coc Ophthalmol* 1975; 39: 117–153.
65. Überreiter O. Augenuntersuchungs methoden mit besonderer berucksichtigung der Mikroskopie am lebenden Tierange. *Wien Tierarztl Monatsschr* 1956; 43: 1–13.
66. Überreiter O. Augenuntersuchungs methoden. *Wien Tierarztl Monatsschr* 1954; 41: 767–780.
67. Überreiter O. Die Mikroskopie am lebenden Tierange. *Wien Tierarztl Monatsschr* 1956; 43: 77–82.
68. Überreiter O. Examination of the eye and eye operations in animals. *Adv Vet Sci* 1959; 5: 1–80.
69. Martin CL. Slit lamp examination of the normal canine anterior ocular segment. Part I: Introduction and technique. *J Small Anim Pract* 1969; 10: 143–149.
70. Martin CL. Slit lamp examination of the normal canine anterior ocular segment. Part II: Description. *J Small Anim Pract* 1969; 10: 151–162.
71. Martin CL. Slit lamp examination of the normal canine anterior ocular segment. Part III: Discussion and summary. *J Small Anim Pract* 1969; 10: 163–169.
72. Blumenthal E. Adjusting the slit-lamp oculars: An unnecessary burden or a must? *Surv Ophthalmol* 1995; 50: 225–228.
73. Carrington SD, Bedford PGC, Guillon JP, Woodward EG. Polarised light microscopic observations on the precorneal tear film. 3. The normal tear film of the cat. *J Small Anim Pract* 1987; 28: 821–826.
74. Carrington SD, Bedford PGC, Guillon JP, Woodward EG. Polarised light microscopic observations on the precorneal tear film. 3. The normal tear film of the dog. *J Small Anim Pract* 1987; 28: 605–622.

75. Enbaugh JK. *Principles of Ophthalmoscopy.* Springfield, IL: Charles C. Thomas, 1958.
76. Rubin LF. *Atlas of Veterinary ophthalmoscopy.* Philadelphia: Lea & Febiger, 1974.
77. Catcott EH. Ophthalmoscopy in canine practice. *J Am Vet Med Assoc* 1952; 121: 35–37.
78. Bunce DF. The use of the ophthalmoscope in veterinary practice. *Vet Med* 1955; 50: 599–604.
79. Barnett KC. Principles of ophthalmoscopy. *Vet Med* 1967; 62: 56–57.
80. Bistner SI. Techniques and advances in ophthalmology. *Vet Med Small Anim Clin* 1983; 78: 489–491.
81. Schepens CL, Bahn GC. Examination of the ora serrata: Its importance in retinal detachment. *Arch Ophthalmol* 1950; 44: 677–690.
82. Rubin LF. Indirect ophthalmoscopy. *J Am Vet Med Assoc* 1960; 137: 648–651.
83. Vierheller RC. Clinical experience with indirect ophthalmoscopy. *Mod Vet Pract* 1966; 47: 41–44.
84. Havener WH, O'Dair RB. The indirect ophthalmoscope. *Eye, Ear, Nose & Throat Monthly* 1963; 42: 41–52.
85. Murphy CJ, Howland JC. Optics of comparative ophthalmoscopy. Transactions of the Sixteenth Annual Scientific Program of the College of Veterinary Ophthalmologists, 1985; 16: 132–157.
86. Goldbaum M, Joondeph H, Huamonte F, Peyman G. Retinal examination and surgery. In: Peyman G, Sanders D, Goldberg M, eds. *Principles and Practice of Ophthalmology,* Vol. II. Philadelphia: WB Saunders, 1980: 988–1097.
87. Pollet L. Refraction of normal and aphakic canine eyes. *J Am Anim Hosp Assoc* 1982; 18: 323–326.
88. Miller TR, Priehs DR. Refraction in the normal dog. 21st Program of the American College of Veterinary Ophthalmology 1990.
89. Murphy CJ, Zadnik K, Mannis M, Campbell L. The refractive state of the phakic, pseudophakic and aphakic canine eye. 21st Program of the American College of Veterinary Ophthalmology 1990.
90. Gaiddon J, Nathalie B, Lallement P. Refraction by retinoscopy of normal, aphakic, and pseudophakic canine eyes: Advantage of a 41-diopter intraocular lens. *Vet Comp Ophthalmol* 1996; 6: 121–124.
91. Murphy CJ, Zadnik K, Mannis MJ. Myopia and refractive error in dogs. *Invest Ophthalmol Vis Sci* 1992; 33: 2459–2463.
92. Nelson MJ, Mutti DO, Zadnik K, Murphy CJ. A naturally occurring model of myopia in the Labrador Retriever. *Invest Ophthalmol Vis Sci* 1996; (suppl): 1485.
93. Davidson MG, Murphy CJ, Nasisse MP, et al. Refractive state of aphakic and pseudophakic eyes of dogs. *Am J Vet Res* 1993; 54: 174–177.
94. Sivak JG, Allen DB. An evaluation of the ramp retina in the horse eye. *Vis Res* 1975; 15: 1353–1356.
95. Davidson MG. Clinical retinoscopy for the veterinary ophthalmologist. *Vet Comp Ophthalmol* 1997; 7: 128–137.
96. Stuhr CM. The normal refractive state of the equine (abstract). *Vet Ophthalmol* 1999; 2: 265.
97. Hamori D. Notes of hereditary myopia in horses (abstract). *Vet Bull* 1943; 13: 136.
98. Miller PE. A limited review of feline and equine vision. *Proc Am Coll Vet Ophthalmol* 1996; 26: 94–102.
99. Ramsey DT, Mutti DO, Zadnik C, et al. Refractive error in Rocky Mountain horses with cornea globosa and with normal corneas (abstract). *Invest Ophthalmol Vis Sci* 2000; 41: S135.
100. Roberts SM. Equine vision and optics. *Vet Clin North Amer Equine Pract* 1992; 8: 451–457.
101. Millichamp NJ, Dziezyc J. Cataract surgery in horses. *Invest Ophthalmol Vis Sci* 1996; 37: S763.
102. Wessels GF, Oeinck C, Guzek JP, Wessels IF. A home-made model eye for teaching retinoscopy. *Ophthalmic Surg Lasers* 1995; 26: 489–491.
103. Massa KL, Murphy CJ, Hartmann FA, et al. Usefulness of aerobic microbial culture and cytologic evaluation of corneal specimens in the diagnosis of infectious ulcerative keratitis in animals. *J Am Vet Med Assoc* 1999; 15: 1671–1674.
104. Hamor RE, Whelan NC. Equine infectious keratitis. *Vet Clin North Am Equine Pract* 1999; 15: 623–646.
105. Cullen CL, Grahn BH. Diagnostic ophthalmology. Corneal ulcer with severe secondary anterior uveitis in a pony. *Can Vet* 2000; 41: 887–889.
106 McLaughlin SA, Gilger BC, Whitley RD. Infectious keratitis in horses: Evaluations and management. *The Compendium Equine* 1992; 14: 372–379.
107. Nasisse MP, Nelms S. Equine ulcerative keratitis. *Vet Clin North Am Equine Pract* 1992; 8: 537–555.
108. Nasisse MP. Canine ulcerative keratitis. *Compend Contin Educ Pract Vet* 1986; 7: 686–701.
109. Ward D. Ocular pharmacology. In: Gelatt KN, ed. *Veterinary Ophthalmology,* 3rd ed. Philadelphia: Lippincott Williams & Wilkins, 1999: 336–354.
110. Champagne ES, Pickett JP. The effect of topical 0.5% proparacaine HCL on corneal and conjunctival culture results. *Trans Am Coll Vet Ophthalmol* 1995; 26: 144–145.
111. Moore CP. Diseases and surgery of the lacrimal secretory system. In: Gelatt KN, ed. *Veterinary Ophthalmology,* 3rd ed. Philadelphia: Lippincott Williams & Wilkins, 1999: 583–607.
112. Gerding PA, Kakoma I. Microbiology of the canine and feline eye. *Vet Clin North Am Small Anim Pract* 1990; 20: 615–625.
113. Murphy JM, Lavach JD, Severin GA. Survey of conjunctival flora in dogs with clinical signs of external diseases. *J Am Vet Med Assoc* 1978; 172: 66–68.
114. Matthews AG. Cornea. In: Barnett KC, Crispin SM, Lavach JD, Matthews AG, eds. *Equine Ophthalmology,* 2nd ed. London: Saunders, 2004: 107–148.
115. Andrew SE, Nguyen A, Jones GL. Seasonal effects on the aerobic bacterial and fungal conjunctival flora of normal thoroughbred brood mares in Florida. *Vet Ophthalmol* 2003; 6: 45–50.
116. Gaskin JM. Microbiology of the canine and feline eye. *Vet Clin North Am Small Anim Pract* 1980; 10: 303–316.
117. Campbell LH, Fox JG, Snyder SB. Ocular bacteria and mycoplasma of the clinically normal cat. *Feline Pract* 1973; 3: 10–12.
118. Whitley RD. Canine and feline primary ocular bacterial infections. *Vet Clin North Am Small Anim Pract* 2000; 30: 1151–1167.

119. Samuelson DA, Andresen TL, Gwin RM. Conjunctival fungal flora in horses, cattle, dogs, and cats. *J Am Vet Med Assoc* 1984; 184: 1240–1242.
120. Moore CP, Collins BK, Fales WH. Antibacterial susceptibility patterns for microbial isolates associated with infectious keratitis in horses: 63 cases (1986–1994). *J Am Vet Med Assoc* 1995; 207: 928–933.
121. Moore CP, Fales WH, Whittington P, et al. Bacterial and fungal isolates from Equidae with ulcerative keratitis. *J Am Vet Med Assoc* 1983; 182: 600–603.
122. Gaarder JE, Rebhun WC, Ball MA, et al. Clinical appearances, healing patterns, risk factors, and outcomes of horses with fungal keratitis: 53 cases (1978–1996). *J Am Vet Med Assoc* 1998; 213: 105–112.
123. Sweeney CR, Irby NL. Topical treatment of Pseudomonas sp-infected corneal ulcers in horses: 70 cases (1977–1994). *J Am Vet Med Assoc* 1996; 209: 954–957.
124. Da Silva Curiel JM, Murphy CJ, Jang SS, et al. Nutritionally variant streptococci associated with corneal ulcers in horses: 35 cases (1982–1988). *J Am Vet Med Assoc* 1990; 197: 624–626.
125. Chmielewski NT, Brooks DE, Smith PJ, et al. Visual outcome and ocular survival following iris prolapse in the horse: A review of 32 cases. *Equine Vet J* 1997; 29: 31–39.
126. Keller RL, Hendrix DV. Bacterial isolates and antimicrobial susceptibilities in equine bacterial ulcerative keratitis (1993–2004). *Equine Vet J* 2005; 37: 207–211.
127. Brooks DE. Equine ophthalmology. In: Gelatt KN, ed. *Veterinary Ophthalmology,* 3rd ed. Philadelphia: Lippincott Williams & Wilkins; 1999: 1053–1116.
128. Lavach JD. Cornea. In: Lavach JD, ed. *Large Animal Ophthalmology,* 1st ed. St. Louis: Mosby, 1990: 101–149.
129. Cello RM. The use of conjunctival scrapings in the diagnosis and treatment of external diseases of the eye. *6th Gaines Vet Symposium* 1956: 22–25.
130. Lavach JD, Thrall MA, Benjamin MM, Severin GA. Cytology of normal and inflamed conjunctivas in dogs and cats. *J Am Vet Med Assoc* 1977; 170: 722–727.
131. Roszel JF. Exfoliative cytology in diagnosis of malignant canine neoplasms. *Vet Scope* 1967; 12: 14–20.
132. Murphy JM. Exfoliative cytologic examination as an aid in diagnosing ocular diseases in the dog and cat. *Semin Vet Med Surg Small Anim* 1988; 3: 10–14.
133. Wills M, Bounous DI, Hirsh S, et al. Conjunctival brush cytology: Evaluation of a new cytological collection technique in dogs and cats with a comparison to conjunctival scraping. *Vet Comp Ophthalmol* 1997; 7: 74–81.
134. Bauer GA, Spiess BM, Lutz H. Exfoliative cytology of conjunctiva and cornea in domestic animals: A comparison of four collecting techniques. *Vet Comp Ophthalmol* 1996; 6: 181–186.
135. McKelvie P. Ocular surface impression cytology. *Adv Anat Pathol* 2003; 10(6): 328–37.
136. Gerding PA, McLaughlin SA, Troop MW. Cytology of normal and inflamed conjunctivas in dogs and cats. *J Am Vet Med Assoc* 1988; 193: 242–244.
137. Forster RK, Wirta MG, Solis M, Rebell G. Methenamine-silver stained corneal scrapings in keratomycosis. *Am J Ophthalmol* 1976; 82: 261–265.
138. Naib ZM, Clepper AS, Elliott SR. Exfoliative cytology as an aid in the diagnosis of ophthalmic lesions. *Acta Cytol* 1967; 11: 295–303.
139. Prasse KW, Winston SM. The eyes and associated structures. In: Cowell RL, Tyler RD, Meinktoh JH, eds. *Diagnostic Cytology and Hematology of the Dog and Cat,* 2nd ed. St. Louis: Mosby, 1999: 68–82.
140. Raskin RE. Eyes and adnexa. In: Raskin RE, Meyer DJ, eds. *Atlas of the Canine and Feline Cytology.* Philadelphia: WB Saunders Co., 2001: 367–384.
141. Giuliano EA, Moore CP. Eyes and ocular adnexa. In: Cowell RL, Tyler RD, eds. *Diagnostic Cytology and Hematology of the Horse,* 2nd ed. St. Louis: Mosby, 2002: 43–64.
142. Schirmer O. Studien zur Physiologie und Pathologie der Tranenabsonderung und Tranenabfuhr. *Graefe's Arch Ophthalmol* 1903; 56: 197–291.
143. Hirsh SG, Kaswan RL. A comparative study of Schirmer tear test strips in dogs. *Vet Comp Ophthalmol* 1995; 5: 215–217.
144. Wyman M, Gilger B, Mueller P, Norris K. Clinical evaluation of a new Schirmer tear test in the dog. *Vet Comp Ophthalmol* 1995; 5: 211–214.
145. Van der Woerdt A, Adamcak A. Comparison of absorptive capacities of original and modified Schirmer tear test strips in dogs. *J Am Vet Med Assoc* 2000; 216: 1576–1577.
146. Roberts SR, Erickson OF. Dog tear secretion and tear proteins. *J Small Anim Pract* 1962; 3: 1–5.
147. Roberts SR. Abnormal tear secretion in the dog. *Mod Vet Pract* 1962; 43: 37–41.
148. Rubin LF, Lynch RK, Stockman WS. Clinical estimation of lacrimal function in dogs. *J Am Vet Med Assoc* 1965; 147: 946–947.
149. Harker DB. A modified Schirmer tear test technique. *Vet Rec* 1970; 86: 196–199.
150. Gelatt KN, Peiffer RL Jr., Erickson JL, Gum GG. Evaluation of tear formation in the dog, using a modification of the Schirmer tear test. *J Am Vet Med Assoc* 1975; 166: 368–370.
151. Veith LA, Cure TH, Gelatt KN. The Schirmer tear test in cats. *Mod Vet Pract* 1970; 51: 48–49.
152. Brightman AH, Manning JP, Benson GJ, Musselman EE. Decreased tear production associated with general anesthesia in the horse. *J Am Vet Med Assoc* 1983; 182: 243–244.
153. Arnett BD, Brightman AH, Musselman EE. Effect of atropine sulfate on tear production in the cat when used with ketamine hydrochloride and acetylpromazine maleate. *J Am Vet Med Assoc* 1984; 185: 214–215.
154. Cullen CL, Lim C, Sykes J. Tear film breakup times in young healthy cats before and after anesthesia. *Vet Ophthalmol* 2005; 8: 159–165.
155. Williams RD, Manning JP, Peiffer RL. The Schirmer tear test in the equine: Normal values and the contribution of the gland of the nictitating membrane. *J Eq Med Surg* 1979; 3: 117–119.
156. McLaughlin SA, Brightman AH, Helper LC, Primm ND, Brown MG, Greeley S. Effect of removal of lacrimal and third eyelid glands on Schirmer tear test results in cats. *J Am Vet Med Assoc* 1988; 193: 820–822.
157. Margadant DL, Kirkby K, Andrew SE, Gelatt KN. Effect of topical tropicamide on tear production as measured by Schirmer's tear test in normal dogs and cats. *Vet Ophthalmol* 2004; 7: 385–390.

158. Hawkins EC, Murphy CJ. Inconsistencies in the absorptive capacities of Schirmer tear test strips. *J Am Vet Med Assoc* 1986; 188: 511–513.
159. Brown MH, Galland JC, Davidson HJ, Brightman AH. The phenol red thread tear test in dogs. *Vet Comp Ophthalmol* 1996; 6: 274–277.
159a. Crispin SM. Tear-deficient and evaporative dry eye syndromes of the horse. *Vet Ophthalmol* 2000; 3: 87–92.
160. Hamor RE, Roberts SM, Severin GA, Chavkin MJ. Evaluation of results for Schirmer tear tests conducted with and without application of a topical anesthetic in clinically normal dogs of 5 breeds. *Am J Vet Res* 2000; 61: 1422–1425.
161. Abrams KL, Brooks DE, Funk RS, Theran P. Evaluation of the Schirmer tear test in clinically normal rabbits. *Am J Vet Res* 1990; 51: 1912–1913.
162. Beech J, Zappala RA, Smith G, Lindborg S. Schirmer tear test results in normal horses and ponies: Effect of age, season, environment, sex time of the day and placement of strips. *Vet Ophthalmol* 2003; 6: 251–254.
163. Harling DE. Epiphora and lacrimal system dysfunction in the horse. *Equine Practice* 1988; 10: 27–38.
164. Regnier JM. Le test de Schirmer chez le cheval: Valeurs usuelles et fluctuations journalieres et hebdomadaires. These de doctorat veterinaire. *Ecole Nationale Veterinaire de Toulouse* 2002: 1–50.
165. Sakamoto R, Bennett ES, Henry VA, et al. The phenol red thread tear test: A cross-cultural study. *Invest Ophthalmol Vis Sci* 1993; 34: 3510–3514.
166. Mainstone JC, Bruce AS, Golding TR. Tear meniscus measurement in the diagnosis of dry eye. *Curr Eye Res* 1996; 15: 653–660.
167. Cohen IJ. Use of fluorescein in eye injuries. *J Occup Med* 1963; 5: 540–541.
168. Feenstra RPG, Tseng SCG. Comparison of fluorescein and rose Bengal staining. *Ophthalmology* 1992; 99: 605–617.
169. Gelatt KN. Vital staining of the canine cornea and conjunctiva with rose Bengal. *J Am Anim Hosp Assoc* 1972; 8: 17–22.
170. Khurana AK, Chaundhary BK, Gupta S. Tear film profile in dry eye. *Acta Ophthalmol* 1991; 69: 79–86.
171. Laroche RR, Campbell RC. Quantitative rose Bengal staining technique for external ocular diseases. *Ann Ophthalmol* 1988; 20: 274–276.
172. Slatter DH. Differential vital staining of the canine cornea and conjunctiva with fluorescein-rose Bengal and Alcian blue. *J Small Anim Pract* 1972; 14: 291–296.
173. Franck C, Boge I. Break-up time and lissamine green epithelial damage in "office eye syndrome." *Acta Ophthalmol* 1993; 71: 62–64.
174. Khurana AK, Sunder S, Ahluwalia KC. Tear film profiles in Grave's ophthalmopathy. *Acta Ophthalmol* 1992; 70: 346–349.
175. Norn MS. Lacrimal apparatus tests. *Acta Ophthalmol* 1965; 43: 557–566.
176. Norn MS. Methylene blue (methylthionine) vital staining of the cornea and conjunctiva. *Acta Ophthalmol* 1967; 45: 347–358.
177. Norn MS. Trypan blue-vital staining of cornea and conjunctiva. *Acta Ophthalmol* 1967; 45: 380–389.
178. Norn MS. Vital staining of the canaliculus lacrimalis and the palpebral border (Marx's line). *Acta Ophthalmol* 1966; 44: 948–959.
179. Brubaker RF. Flow of aqueous humor in man. *Invest Ophthalmol Vis Sci* 1991; 32: 3145–3166.
180. Ward DA, Cawrse MA, Hendrix DV. Fluorophotometric determination of aqueous humor flow rate in clinically normal dogs. *Am J Vet Res* 2001; 62(6): 853–858.
181. Moore CP. Qualitative tear film disease. *Vet Clin North Am Small Anim Pract* 1990; 20: 565–581.
182. Kimura SJ. Fluorescein paper: Simple means of insuring use of sterile fluorescein. *Am J Ophthalmol* 1951; 34: 446–447.
183. Cello RM, Lasmanis J. Pseudomonas infection of the eye of the dog resulting from the use of contaminated fluorescein solution. *J Am Vet Med Assoc* 1958; 132: 297–299.
184. Moore CP, Wilsman NJ, Nordheim EV, et al. Density and distribution of canine conjunctival goblet cells. *Invest Ophthalmol Vis Sci* 1987; 28: 1925–1932.
185. Jones LT. An anatomical approach to problems of the eyelids and lacrimal apparatus. *Arch Ophthalmol* 1961; 66: 111–124.
186. Feenstra RPG, Tseng CG. What is actually stained by rose Bengal? *Arch Ophthalmol* 1992; 110: 984–993.
187. Kim J. The use of vital dyes in corneal disease. *Curr Opin Ophthalmol* 2000; 11: 241–247.
188. Tseng SC, Zhang SH. Interaction between rose Bengal and different protein components. *Cornea* 1995; 14: 427–435.
189. Brooks DE, Andrew SE, Denis H, et al. Rose Bengal positive epithelial microerosions as a manifestation of equine keratomycosis. *Vet Ophthalmol* 2000; 3: 83–86.
190. Chodosh J, Dix RD, Howell RC, Stroop WG, Tseng SC. Staining characteristics and antiviral activity of sulforhodamine B and lissamine green B. *Invest Ophthalmol Vis Sci* 1994; 35: 1046–1058.
191. Manning FJ, Wehrly SR, Foulks GN. Patient tolerance and ocular surface staining characteristics of lissamine green versus rose bengal. *Ophthalmology* 1995; 102: 1953–1957.
192. Norn MS. Lissamine green. Vital staining of cornea and conjunctiva. *Acta Ophthalmol Copenh* 1973; 51: 483–491.
193. Crispin SM. Nasolacrimal cannulation in the horse. *In Practice* 1988: 154–156.
194. Barrett PM, Scagliotti RH, Merideth RE, Jackson PA, Alarcon FL. Absolute corneal sensitivity and corneal trigeminal anatomy in normal dogs. *Prog Vet Comp Ophthalmol* 1991; 1: 245–254.
195. Millodot M. The influence of age on the sensitivity of the cornea. *Invest Ophthalmol Vis Sci* 1977; 16: 240–242.
196. Millodot M, Larson W. New measurements of corneal sensitivity: A preliminary report. *Am J Optom Arch Am Acad Optom* 1969; 46: 261–265.
197. Millodot M. Objective measurement of corneal sensitivity. *Acta Ophthalmol Copenh* 1973; 51: 325–334.
198. Brooks DE, Clark CK, Lester Cochet GD. Bonnet aesthesiometer-determined corneal sensitivity in neonatal foals and adult horses. *Vet Ophthalmol* 2000; 3: 133–137.
199. Chan-Ling T. Sensitivity and neural organization of the cat cornea. *Invest Ophthalmol Vis Sci* 1989; 30: 1075–1082.
200. Kaps S, Richter M, Spiess BM. Corneal esthesiometry in the healthy horse. *Vet Ophthalmol* 2003; 6: 151–155.
201. Blocker T, van der Woerdt A. A comparison of corneal sensitivity between brachycephalic and Domestic Short-haired cats. *Vet Ophthalmol* 2003; 4: 127–130.
202. Millodot M. The influence of age on the sensitivity of the cornea. *Invest Ophthalmol Vis Sci* 1977; 16: 240–242.

203. Lovekin LG. Primary glaucoma in dogs. *J Am Vet Med Assoc* 1964; 145: 1081–1091.
204. Baum J, Chaturvedi N, Netland PA, Dreyer EB. Assessment of intraocular pressure by palpation. *Am J Ophthalmol* 1995; 119: 650–651.
205. Bryan GM. Tonometry in the dog and cat. *J Small Anim Pract* 1965; 6: 117–120.
206. Peiffer RL Jr, Gum GG, Gelatt KN. Calibration of the Schiotz tonometer for the normal canine eye. *Am J Vet Res* 1977; 38: 1881–1889.
207. Heywood R. Intraocular pressure in the Beagle dog. *J Small Anim Pract* 1971; 12: 119–121.
208. Vainisi SJ. Tonometry and gonioscopy in the dog. *J Small Anim Pract* 1970; 11: 231–240.
209. Magrane WG. Tonometry in ophthalmology. *North Am* Vet 1951; 32: 413–414.
210. Peiffer RL Jr, Gelatt KN, Gwin RM. Schiotz calibration table for the canine eye. *J Canine Pract* 1977; 4: 49–52.
211. Pickett JP, Miller PE, Majors LJ. Calibration of the Schiotz tonometer for the canine and feline eye. *Trans Am Coll Vet Ophthalmol* 1988; 19: 47–53.
212. Vareilles P, Conquet P, LeDouarec J. A method for the routine intraocular pressure (IOP) measurement in the rabbit: Range of IOP variations in this species. *Exp Eye Res* 1977; 24: 369–375.
213. Gelatt KN, Peiffer RL Jr., Gum GG, Gwin RM, Erickson JL. Evaluation of applanation tonometers for the dog eye. *Invest Ophthalmol* 1977; 16: 963–968.
214. Gelatt KN, Gum GG, Barrie KP. Tonometry in glaucomatous globes. *Invest Ophthalmol Vis Sci* 1981; 20: 683–688.
215. Gelatt KN, Gum GG. Evaluation of electronic tonometers in the rabbit eye. *Am J Vet Res* 1981; 42: 1778–1781.
216. McMillian F, Forster RK. Comparison of Mackay-Marg, Goldmann, and Perkins tonometers in abnormal corneas. *Arch Ophthalmol* 1975; 93: 420–424.
217. Moses RA, Marg E, Oechsli R. Evaluation of the basic validity and clinical usefulness of the Mackay-Marg tonometer. *Invest Ophthalmol* 1962; 1: 78–85.
218. Bito LZ, Merritt SQ, DeRousseau CJ. Intraocular pressure of rhesus monkeys (Macaca mulatta). *Invest Ophthalmol Vis Sci* 1979; 18: 785–793.
219. McClure JR, Gelatt KN, Manning JP, Gum GG. The effect of parenteral acepromazine and xylazine on intraocular pressure in the horse. *Vet Med Small Anim Clin* 1976; 71: 1727–1730.
220. Dziezyc J, Millichamp NJ, Smith WB. Comparison of applanation tonometers in dogs and horses. *J Am Vet Med Assoc* 1992; 201: 430–433.
221. Miller PE, Pickett JP, Majors LJ. In vivo and in vitro comparison of MacKay-Marg and TonoPen applanation tonometers in the dog and cat. *Trans Am Coll Vet Ophthalmol* 1988; 19: 53–58.
222. Priehs DR, Gum GG, Whitley RD, Moore LE. Evaluation of three applanation tonometers in dogs. *Am J Vet Res* 1990; 51: 1547–1550.
223. Sapienza JS, Procher D, Collins BR, Gum GG, Brooks DE. Tonometry in clinically normal ferrets. *Prog Vet Comp Ophthalmol* 1991; 1: 291–294.
224. Stiles J, Buyukmichi NC, Farver TB. Tonometry of normal eyes in raptors. *Am J Vet Res* 1994; 55: 477–479.
225. Whittaker CJ, Heaton-Jones TG, Kubilis PS, et al. Intraocular pressure variation associated with body length in young American alligators. *Am J Vet Res* 1995; 56: 1380–1383.
226. Mermoud A, Baerveldt G, Minckler DS, Lee MB, Rao NA. Intraocular pressure in Lewis rat. *Invest Ophthalmol Vis Sci* 1994; 35: 2455–2460.
227. Plummer CE, Ramsey DT, Hauptmann JG. Assessment of corneal thickness, intraocular pressure, optical corneal diameter, and axial globe dimensions in Miniature horses. *Am J Vet Res* 2003; 64: 661–665.
228. Gelatt KN, Gum GG. Comparisons of anterior chamber manometric recordings (mmHg) and Schiotz tonometer scale-units in normal and glaucomatous dogs. *Anim Eye Res* 1995; 14: 49–58.
229. Severin GA. *Veterinary Ophthalmology Notes,* 3rd ed. Fort Collins: College of Veterinary Medicine and Biomedical Sciences, Colorado State University, 1995.
230. Miller PE, Pickett JP. Comparison of the human and canine Schiotz tonometry conversion tables in clinically normal cats. *J Am Vet Med Assoc* 1992; 201: 1017–1020.
231. Miller PE, Pickett JP. Comparison of the human and canine Schiotz tonometry conversion tables in clinically normal dogs. *J Am Vet Med Assoc* 1992; 201: 1021–1025.
232. Khan JA, Davis M, Graham CE, Trank J, Whitacre MM. Comparison of oculab Tono-Pen readings obtained from various corneal and scleral locations. *Archives of Ophthalmology* 1991; 109: 1444–1446.
233. Boothe W, Lee D, Panek W, Pettit T. The TonoPen: A manometric and clinical study. *Archives of Ophthalmology* 1988; 106: 1214–1217.
234. Knollinger AM, La Croix NC, Barrett PM, Miller PE. A clinical and manometric evaluation of the TonoVet rebound tonometer in dogs and horses. Proceedings of the American College of Veterinary Ophthalmology (abstract) 2004: 8.
235. Kotani T, Tuzuki K, Izumisawa Y, Yamashita K, Oukuma N, Tamura S. Which are the optimal tonometers for different animal species? *Anim Eye Res* 1993; 12: 55–61.
236. Van der Woerdt A. Effect of auricle-palpebral nerve block and intravenous administration of xylazine on intraocular pressure and corneal thickness in horse. *Am J Vet Res* 1995; 56: 155–158.
237. Trim CM, Colbern GT, Martin CL. Effects of xylazine ad ketamine on intraocular pressure in horse. *Vet Rec* 1985; 117: 442–443.
238. Miller PE, Pickett JP, Majors LJ. Evaluation of two applanation tonometers in horses. *Am J Vet Res* 1990; 51: 935–937.
239. Martin CL. Gonioscopy and anatomical correlations of the drainage angle of the dog. *J Sm Anim Prac* 1969; 10: 171–184.
240. Vainisi SJ. Tonometry and gonioscopy in the dog. *J Sm Anim Prac* 1970; 11: 231–240.
241. Gelatt KN, Ladds PW. Gonioscopy in dogs and cats with glaucoma and ocular tumors. *J Sm Anim Prac* 1971; 12: 105.
242. Bedford PGC. Gonioscopy in the dog. *J Sm Anim Prac* 1977; 18: 615–629.
243. Becker SC. *Clinical Gonioscopy.* St. Louis: CV Mosby, 1972.
244. Troncoso MU. Comparative anatomy of the angle of the anterior chamber in mammalia. In: *Treatise on Gonioscopy.* Philadelphia: FA Davis, 1948.
245. Troncoso MU, Castroviejo R. Microanatomy of the eye with the slit-lamp biomicroscope: Comparative anatomy of the

angle of the anterior chamber in living and sectioned eyes of mammalia. *Am J Ophthalmol* 1936; 19: 371–384.
246. Calkins LL. The aqueous filtration angle: A phylogenetic and ontogenetic comparative histoanatomic study of mammalian eyes. *Trans Am Ophthalmol Soc* 1960; 58: 364–391.
247. Magrane WG. Canine glaucoma. I. Methods of diagnosis. *J Am Vet Med Assoc* 1957; 131: 311–314.
248. Lescure F. L'angle camerulaive du chien etude goniophotographique. *World Vet Cong Proc* 1963; 17: 1001–1004.
249. Shaffer R, Tour R. A comparative study of gonioscopic methods. *Trans Am Ophthalmol Soc* 1955; 53: 189–208.
250. Garner LL. *Tonography and the Glaucomas.* Springfield, IL: Charles C. Thomas, 1965.
251. Drews RC. *Manual of Tonography.* St. Louis: CV Mosby, 1971.
252. Podos SM, Becker B. Tonography—Current thoughts. *Am J Ophthalmol* 1973; 75: 733–735.
253. Becker B, Constant MA. Experimental tonography. *Arch Ophthalmol* 1955; 54: 321–329.
254. Hetland-Eriksen J, Odberg T. Experimental tonography on enucleated human eyes. I. The validity of Grant's tonography formula. *Invest Ophthalmol* 1975; 14: 199–204.
255. Kornbluth W, Linner E. Experimental tonography in rabbits. *Arch Ophthalmol* 1955; 54: 717–724.
256. Helper LC, et al. Preliminary studies of tonography in the dog. *4th Proc Am Coll Vet Ophthalmol* 1974; 4: 34–45.
257. Eakins K. A comparative study of intraocular pressure and gross outflow facility in the cat eye during anesthesia. *Exp Eye Res* 1969; 8: 106–115.
258. Bill A, Barany EH. Gross facility, facility of conventional routes and pseudofacility at aqueous humor outflow in the cynomologus monkey. *Arch Ophthalmol* 1966; 75: 665–673.
259. Gelatt KN, Gwin RM, Peiffer RL Jr., Gum GG. Tonography in the normal and glaucomatous Beagle. *Am J Vet Res* 1977; 38: 515–520.
260. Gelatt KN, Gum GG, Mackay EO. Estimation of aqueous humor outflow facility by pneumatonography in normal, genetic carrier, and glaucomatous Beagles. *Vet Comp Ophthalmol* 1996; 6: 148–151.
261. Peiffer RL Jr, Gelatt KN, Gum GG. Determination of the facility of aqueous humor outflow in the dog, comparing in vivo and in vitro tonographic and constant pressure perfusion techniques. *Am J Vet Res* 1976; 37: 1473–1477.
262. Toris CB, Yablonski ME, Wang YL, et al. Prostaglandin A2 increases uveoscleral outflow and trabecular outflow facility in the cat. *Exp Eye Res* 1995; 61: 649–657.
263. Smith PJ, Gum GG, Whitley RD, Samuelson DA, Brooks DE, Garcia-Sanchez GA. Tonometric and tonographic studies on the normal pony eye. *Equine Vet J* 1990; (suppl 10): 36–38.
264. Moses RA. Constant pressure applanation tonography with the Mackay-Marg tonometer I. A preliminary report. *Arch Ophthalmol* 1966; 76: 20–24.
265. Moses RA. Constant pressure applanation tonography with the Mackay-Marg tonometer II. Limits of the instrument. *Arch Ophthalmol* 1967; 77: 45–49.
266. Moses RA, Grodzki WJ. Constant-pressure tonography based on the electronic Schiotz tonometer. *Invest Ophthalmol* 1972; 11: 585–592.
267. Feshall JG, Azar DT, Kaufman PL. Comparative aqueous outflow facility measurements by pneumatonography and Schiotz tonography. *Invest Ophthalmol Vis Sci* 1986; 27: 1776–1780.
268. Spiess BM. Tonographie beim Hund: Methodik und Normalwerte. *Wien Tierarztl Mschr* 1995; 82: 245–250.
269. Glover MS, Nasisse MP, Davidson MG. Effects of topically applied mitomycin-C on intraocular pressure, facility of outflow, and fibrosis after glaucoma filtration surgery in clinically normal dogs. *Am J Vet Res* 1995; 56: 936–940.
270. Hazel SJ, Thrall MA, Severin GA, Lauerman LH, Lavach JD. Laboratory evaluation of aqueous humor in the healthy dog, cat, horse, and cow. *Am J Vet Res* 1985; 46: 657–659.
271. Bussanich MN. Don't overlook fine-needle aspiration biopsy to differentiate intraocular tumors. *Vet Med Small Anim Clin* 1984; 79: 1055–1061.
272. Howard DR. Canine anterior chamber paracentesis. *Southwest Vet* 1968; 21: 299–302.
273. Goldberg MF. Cytological diagnosis of phacolytic glaucoma utilizing millipore filtration of the aqueous. *Br J Ophthalmol* 1967; 51: 847–853.
274. May DR, Noll FG. An improved approach to aqueous paracentesis. *Ophthalmic Surg* 1988; 19: 821–822.
275. O'Rourke J, Taylor DM, McDonald P, Kreutzer DL. An aqueous paracentesis pipette. *Ophthalmic Surg* 1991; 22: 166–167.
276. Blogg JR, Coles EH. Clinicopathological aspects of canine aqueous humour proteins. *Res Vet Sci* 1971; 12: 95–100.
277. Chavkin MJ, Lappin MR, Powell CC, Cooper CM, Munana KR, Howard LH. Toxoplasma gondii specific antibodies in the aqueous humor of cats with toxoplasmosis. *Am J Vet Med Res* 1994; 55: 1244–1249.
278. Wurster U, Riese K, Hoffman K. Enzymatic activities and protein concentration in the intraocular fluids of ten mammals. *Acta Ophthalmol Copenh* 1982; 60: 729–741.
279. Matthews AG, Poulter T. Albumin and immunoglobulins G, A, and M in aqueous humor from clinically normal equine eyes. *Equine Vet J* 1986; 18: 117–120.
280. Faber NA, Crawford M, LeFebvre RB, et al. Detection of *Leptospira* spp. in the aqueous humor of horses with naturally acquired recurrent uveitis. *J Clin Microbiol* 2000; 38: 2731–2733.
281. van der Voet JCM, Liem A, Otto AJ, Kijlstra A. Intraocular antibody synthesis during experimental uveitis. *Invest Ophthalmol Vis Sci* 1988; 30: 316–322.
282. Wollanke B, Rohrbach BW, Gerhards H. Serum and vitreous humor antibody titers in and isolation of Leptospira interrogans from horses with recurrent uveitis. *J Am Vet Med Assoc* 2001; 219: 795–800.
283. McLaughlin BG, McLaughlin PS. Equine vitreous humor chemical concentrations: Correlation with serum concentrations, and postmortem changes with time and temperature. *Can J Vet Res* 1988; 52: 476–480.
284. Stjernschantz J, Uusitalo R, Palkama A. The aqueous proteins of the rat in normal eye and after aqueous withdrawal. *Exp Eye Res* 1973; 16: 215–221.
285. Spiess BM, Mathis GA, Franson KL, Leber A. Kinetics of uptake and effects of topical indomethacin application on

protein concentration in the aqueous humor of dogs. *Am J Vet Res* 1991; 52: 1159–1163.

286. Ward DA, Ferguson DC, Kaswan RL, et al. Leukotrienes and sensory innervation in blood-aqueous barrier disruption in the dog. *J Ocul Pharmacol* 1992; 8: 69–76.
287. Regnier AM, Dossin O, Cutzach EE, Gelatt KN. Comparative effects of two formulations of indomethacin eyedrops on the paracentesis-induced inflammatory response of the canine eye. *Vet Comp Ophthalmol* 1995; 5: 242–246.
288. Ward DA. Comparative efficacy of topically applied flurbiprofen, diclofenac, tolmetin, and suprofen for the treatment of experimentally induced blood-aqueous barrier disruption in dogs. *Am J Vet Res* 1996; 57: 875–878.
289. Smith PJ, Pennea L, MacKay EO, Mames RN. Identification of ideal sites for sclerotomies in surgery for rhegmatogenous retinal detachments in the dog. *Vet Comp Ophthalmol* 1997; 7: 180–191.
290. Miller TL, et al. Description of ciliary body anatomy and identification of sites for transscleral cyclophotocoagulation in the equine eye. *Vet Ophthalmol* 2001; 4: 183–190.

Chapter 9

Ophthalmic Examination and Diagnostics

Part 2: Ocular Imaging

Maria E. Källberg

Imaging is essential in the diagnosis and clinical management of a wide variety of diseases involving the face, eye, orbit, and brain. Improvements in both imaging hardware and software have made possible accurate visualization of the anatomic detail of the eye to a degree previously available only through a combination of surgery, gross dissection, histopathology, and laboratory evaluation. The abilities to reconstruct multidimensional views of the globe and orbit and to noninvasively evaluate visually inaccessible areas from a variety of views provide imaging techniques important to the ophthalmologist's ability to make accurate diagnoses. They also have contributed to improved patient care. Optimal examination of the ocular tissues requires familiarity with the anatomy and pathology of the visual system as well as knowledge of the various imaging techniques available.

RADIOGRAPHY

Radiographic examination of the skull can be used to evaluate the animal patient with ocular or orbital disease. The skull is one of the most complex and specialized parts of the skeleton,[1] and there is considerable variation in normal anatomy both between and within species.[2] Radiography is useful in those diseases associated with bony destruction of the nasal cavity and orbit and in orbital fractures (Fig. 9.2.1).[1,3] Plain-film and computed radiographs also demonstrate opacification of normally radiolucent structures, such as the sinus cavities and retrobulbar space.[4] Soft tissue swelling and areas of hemorrhage can be demonstrated following ocular trauma.[4] Radiographs can aid in localizing foreign bodies depending on the size and composition of the foreign body. Highly malignant primary orbital tumors and invasive metastatic neoplasms may result in bony wall destruction; sinus or nasopharyngeal tumors may expand or erode bone and invade the orbit.

The limitations of radiographs include exposure to high levels of ionizing radiation, superimposition of bony structures, lack of aetiological specificity, and the inability to differentiate between the various intraocular structures and the soft tissue and fat opacities in the retrobulbar region. In a study comparing magnetic resonance imaging (MRI) and radiography in small animals with orbital diseases, radiography was found to be helpful only in cases in which neoplastic disease extended markedly beyond the orbit into the nasal chamber and paranasal sinuses.[5] Radiographic changes other than soft tissue swelling were not evident in other orbital disease processes.

General anesthesia is recommended in the dog and cat to obtain precise lateral, dorsoventral, ventrodorsal, and oblique views of the orbit. Due to the complex nature of the skull, positioning of the animal is essential.[1] Descriptions of the normal orbital radiographic anatomy and positioning of the dog, cat, and horse have been published elsewhere.[6–12] Aspirations, biopsies, and nasal or sinus lavage techniques should be performed following radiographic study of the orbital region so as not to introduce artifactual changes into the radiographic image.

Special Radiographic Techniques

Exophthalmos is the most important indication for zygomatic sialography. The zygomatic salivary gland empties lateral and posterior to the last upper molar tooth. The duct is cannulated, and a nonionic iodinated contrast medium is administered by retrograde infusion.[13]

The entire nasolacrimal drainage apparatus can be outlined through dacryocystorhinography.[13–15] First described in animals in 1961, this technique has since been used to characterize the anatomy and to identify obstructive lesions of the nasolacrimal duct in the dog, cat, horse, cow, sheep, llama, and rabbit.[16–23]

Dacryocystorhinography is performed with the patient under general anesthesia. The nasolacrimal duct is first flushed with 0.9% sterile saline to clear loose debris and to determine patency. The upper punctum (or lower punctum in the rabbit) is then cannulated, and radiopaque contrast material is injected until it emerges from the lower punctum, external nares (unless the duct is completely obstructed), or both (Fig. 9.2.2). In the dog, cat, and rabbit, 0.5 to 1.0 mL of contrast is injected; in the horse, cow, and llama, 3.0 to 5.0 mL of contrast is usually needed. Ionic or nonionic iodinated contrast agents may be

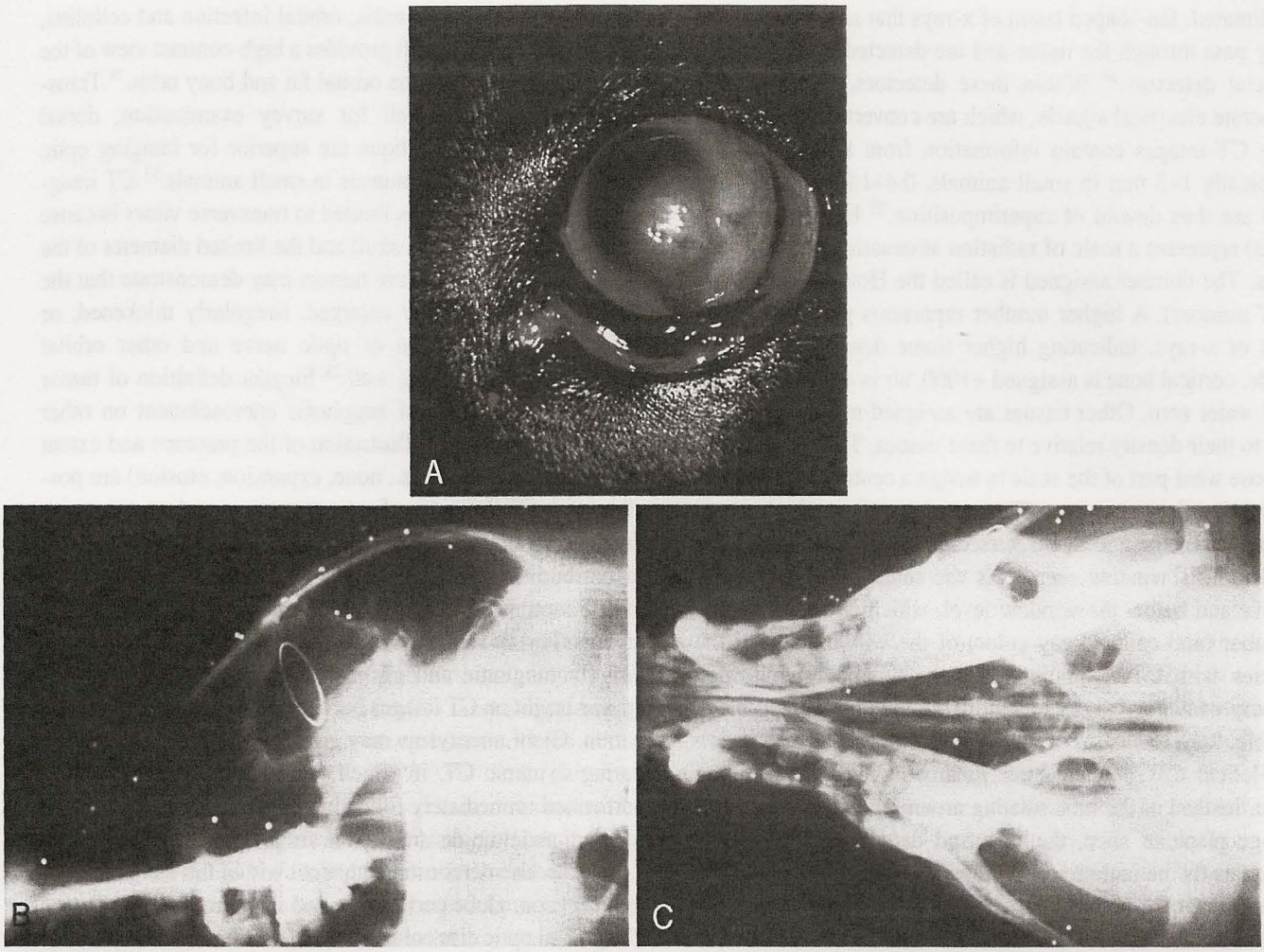

Figure 9.2.1. **A.** Traumatic corneal perforation with anterior chamber hemorrhage in a dog. **B.** Lateral skull radiograph with a Flieringa ring placed on the cornea of the traumatized eye indicates multiple metallic pellets. **C.** Ventrodorsal view indicates metallic foreign bodies close to the globe but does not localize them to an intraocular location.

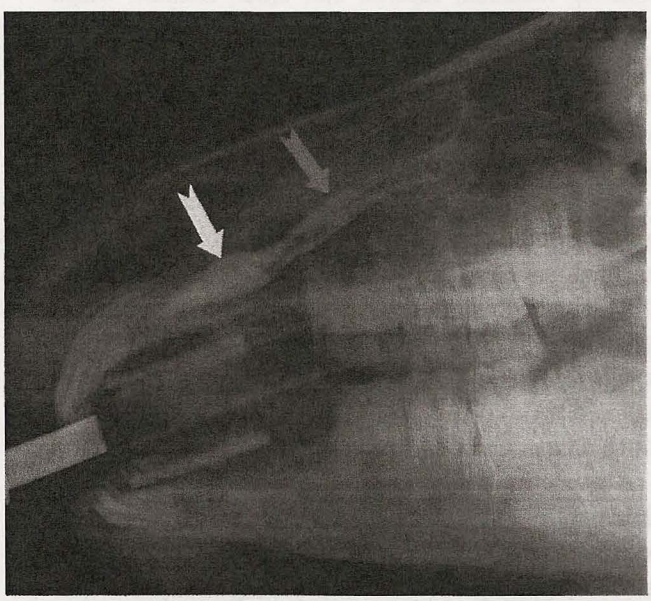

Figure 9.2.2. Dacryocystorhinogram of a young horse with bilateral nasolacrimal duct atresia. The last 4 cm of the ducts are moderately dilated in a blind end with fimbriated margins. *Arrows* indicate the blind end of the distal-dilated nasolacrimal duct (*yellow*); nasolacrimal duct within the turbates (*red*); and proximal-restricted nasolacrimal duct within its intraosseous portion (*blue*).

used. Following contrast injection, lateral, dorsoventral, and oblique radiographs are recommended.

Dacryocystorhinography outlines the nasolacrimal drainage apparatus, thereby revealing dilatation and osteolysis associated with chronic inflammation and exposing both the site and extent of nasolacrimal duct obstructions. It can also reveal lacrimal sac dilatation and osteolysis associated with dacryocystitis, thus helping to differentiate this condition from maxillary sinusitis and carnassial tooth root abscesses.[17,18] In addition, nasal neoplasms that obstruct or deviate the nasolacrimal duct can be delineated with this procedure, whereas those that invade the nasolacrimal duct may lead to spillage of contrast material into the nasal cavity. Dacryocystorhinography can also be used to confirm the absence of a canaliculus in animals with congenital epiphora.

COMPUTED TOMOGRAPHY AND MAGNETIC RESONANCE IMAGING

Computed tomography (CT) has improved the diagnosis and management of ocular and orbital diseases. The x-ray tube of the CT machine sits within a gantry and emits a thin,

collimated, fan-shaped beam of x-rays that are attenuated as they pass through the tissue and are detected by an array of special detectors.[24] Within these detectors, x-ray photons generate electrical signals, which are converted into images. The CT images contain information from thin slices only (typically 1–3 mm in small animals, 0.4–1.0 cm in horses) and are thus devoid of superimposition.[25] Hounsfield units (HU) represent a scale of radiation attenuation values of tissues. The number assigned is called the Hounsfield number (CT number). A higher number represents greater attenuation of x-rays, indicating higher tissue density.[24,26] In this scale, cortical bone is assigned +1000, air is assigned −1000, and water zero. Other tissues are assigned numbers according to their density relative to these tissues. The operator can choose what part of the scale to assign a central color gray to maximize tissue contrast. The range of CT numbers represented by the gray scale is referred to as a window or window width. This window represents the range of CT numbers above and below the window level, which is the center CT number (and central gray color) of the window. All of the tissues with CT numbers above the upper window edge appear white, and those below the lower edge appear black (Table. 9.2.1).

Helical CT scanners have greatly reduced the imaging time. Instead of the tube rotating around the patient for each image plane or slice, the tube and detectors continuously rotate as the patient moves progressively through the gantry. Images can be reconstructed at any position within the scanned volume.[27]

The anatomy of the orbit is an ideal subject for CT, though use of CT in this area has been somewhat upstaged by MRI.[28–30] The relatively dense nerves, globe, and extraocular muscles, which are surrounded by lucent orbital fat and encased in dense bone, provide a tissue of high contrasts for CT, which provides anatomic detail of orbital bone, soft tissue, and foreign bodies superior to that of radiography.[28,31] CT also provides much better visualization of bony orbital structures than does MRI.[28,32] CT is used in the analysis of orbital trauma, optic neuritis, orbital infection and cellulitis, and orbital neoplasia.[28] It provides a high-contrast view of the optic nerve relative to the orbital fat and bony orbit.[28] Transverse images work well for survey examination; dorsal oblique and sagittal oblique are superior for imaging optic nerves and extraocular muscle in small animals.[33] CT imaging of the equine skull is limited to transverse views because of the size of the equine skull and the limited diameter of the gantry.[34] CT of optic nerve tumors may demonstrate that the optic nerve is diffusely enlarged, irregularly thickened, or fusiform.[28] Calcification of optic nerve and other orbital tumors may be noted as well.[28] Elegant definition of tumor boundaries, appraisal of neoplastic encroachment on other orbital structures, and illustration of the presence and extent of bone involvement (i.e., none, expansion, erosion) are possible with CT.[28] A case of cavernous sinus enlargement was detected by CT in a dog.[35] Evaluation of optic chiasma and extraorbital extensions of orbital tumors is facilitated by the use of contrast enhancement. It also helps with defining vascular and cystic lesions as well as optic nerve lesions, particularly meningioma and glioma.[24] Iodinated contrast agents appear bright on CT images because of increased x-ray attenuation. Giant aneurysms may be distinguished from tumors during dynamic CT, in which rapid sequential scanning is performed immediately following bolus injection of contrast medium and time-density curves are plotted.[35]

CT can also demonstrate changes within the globe, such as lens luxation, globe perforation, and intravitreal hemorrhage.[4] Congenital optic disc colobomas can be identified[36] and multiple intraocular and orbital foreign bodies larger than 0.5 mm can be accurately localized with CT (Fig. 9.2.3).[4]

In comparison with CT, MRI has several advantages and disadvantages (Table 9.2.2).[34,37] Advantages include absence of ionizing radiation; superior soft tissue contrast, which yields detailed soft tissue anatomy and highlight areas of pathologic findings; and direct multiplanar imaging that does not require changes in position of the patient or gantry. Some disadvantages include longer acquisition times and poorer spatial resolution.

MRI represents the unstable portion of an animal's own magnetic field. Nuclei with an odd number of electrically charged particles (protons and neutrons) are measured with MRI with hydrogen (^{1}H) being the most common atom contributing to the MRI image. Nuclei with an even number protons and neutron such as carbon (^{12}C), oxygen (^{16}O), and calcium (^{40}Ca) do not line up with the magnetic field of the MRI. That is, tissue with high hydrogen content such as water and fat are imaged; regions of bone or air appear as signal void or black.

Magnetic resonance images of the globe and orbit are obtained by placing the head within a highly uniform and strong, static magnetic field. The patient's hydrogen atoms align themselves with the axis of the magnetic field. The hydrogen nuclei are stimulated with radiofrequency (RF) energy pulses. The energy from the RF pulses is absorbed by the protons, causing them to shift in their axial

Table 9.2.1 Hounsfield Numbers of Some Important Tissues and Orbital Structures[24]

Tissue	Hounsfield Number (HU)
Air	*−1000*
Fat	*−100*
Water	*0*
CSF	*+5*
Optic nerve	*+5 to +10*
Vitreous	*+5 to +15*
Soft tissue	*+30 to +40*
Hemorrhage	*+70 to +80*
Calcification	*+100 and above*
Cortical bone	*+300 to +1000*
Metal	*>+1000*

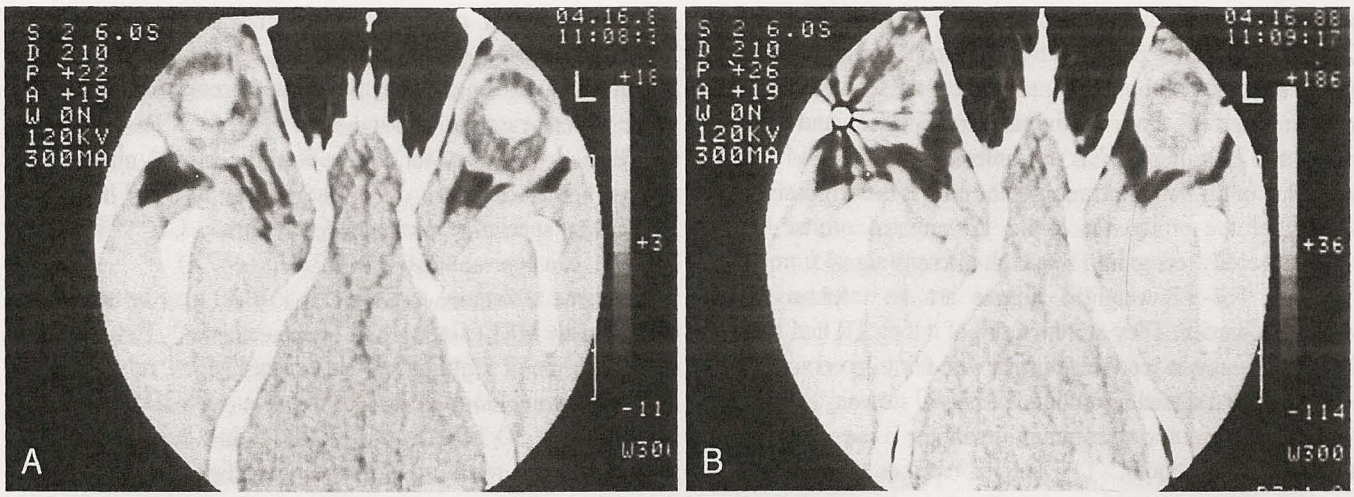

Figure 9.2.3. **A.** CT scan shows increased vitreal density and exophthalmos in the affected left eye from Figure 9.2.1. **B.** CT scan shows "starburst" effect from a metallic object in the eye.

Table 9.2.2 Comparative Characteristics of MR Imaging *versus* CT

Advantages
I. CT scans are produced with ionizing radiation, whereas MR images depend on magnetic fields and radiofrequency waves. The lack of the potential side effects from radiation exposure makes MR imaging the modality of choice if repeated studies are required. No serious adverse biologic effects of MR imaging have been reported to date.
II. Sectional MR images in axial, coronal, sagittal, and oblique planes can be obtained directly, without moving patients. CT scans, however, require additional patient positioning.
III. Soft-tissue differentiation is better with MR imaging than CT because of the distinct, inherent properties, such as proton density and relaxation rates, of normal and pathologic tissues. Instrument parameters and use of paramagnetic contrast agents further contribute to MR imaging contrast sensitivity.
IV. Artifacts caused by the high density of cortical bone on CT scans obscure the details of soft tissues surrounded by bone. Because cortical bone emits a low radiofrequency signal, the orbital apex, intracanalicular optic nerve, and structures in the parasellar and posterior fossa areas are particularly well depicted on MR images.
V. Intravenous administration of Gd-DTPA is safer than iodinated radiographic contrast agents.
VI. MR imaging is the modality of choice to evaluate the central nervous system because of its multiplanar capabilities and excellent contrast resolution.
Disadvantages
I. Cortical bone is only indirectly delineated by MR imaging; thus, CT is the modality of choice for examination of bony details in conditions such as orbital fractures and tumor-induced hyperostosis. Tumor invasion of bone, however, is depicted on MR images by the bright tumor signal replacing the dark signal void of the cortical bone.
II. Longer scanning times of MR imaging can lead to problems with motion artifacts.
III. MR imaging is contraindicated in animals with intraocular metallic foreign bodies.
IV. MR imaging may cost more than comparable CT.

alignment perpendicular to the magnetic field.[27,29–40] After the pulse is turned off, the stimulated protons realign longitudinally with the main magnetic field (T1 relaxation) and lose coherence in the perpendicular plane (T2 relaxation). Because hydrogen atoms are held together differently in each tissue, their relaxation rates differ. Rapid flow of blood or cerebrospinal fluid (CSF) creates a signal void[41,42] because the hydrogen-containing components of the fluid, present at the time for the radiofrequency pulse in the slice being imaged, do not remain within the slice long enough to encounter both the 90° and 180° pulses and therefore do not produce a signal.

The most-often used magnetic pulse sequence for imaging is the spin echo pulse sequence, which includes T1-, T2-, and proton density (PD)–weighted images.[42] The magnetic pulse is initially applied to rotate the nuclear field 90° and, after a specified time, a second pulse produces a 180° rotation. A delay occurs before the next 90° pulse, and during the delay the radiofrequency waves are sampled by the coil. The time between the 90° pulse and detection of the radiofrequency waves by the coil is termed the echo time, or TE. The time lapse between each pulse sequence is termed the repetition time or TR. An image is considered T1-weighted when the TR and TE are short. Tissue with shorter T1 times is brighter (more intense), and tissue with

longer T1 times is darker (less intense) (Table 9.2.3). The T2-weighted image is produced by a longer TR and a longer TE and has the best soft tissue contrast of the three sequences. Tissue with longer T2 times is brighter (more intense), and tissue with shorter T2 times is darker (less intense) (Table 9.2.3).[42] The hallmark of a T1-weighted image of the orbit is the bright signal intensity of the orbital fat, while T2-weighted orbital MR images are easily recognized by a high-intensity signal from the vitreous.[27] The PD-weighted images are an intermediate-weighted sequence. They are the result of a long TR and short TE.[27] This sequence produces images with fair to good soft tissue contrast and spatial resolution. The signal intensity is based on the hydrogen ion concentration within the tissue. With fat-suppression techniques, T1-weighted images demonstrate increased gray scale and intensity of extraocular muscles and lacrimal glands.[34] The FLAIR sequence suppresses the signal from selected fluids, enabling the distinction of hyperintense solid tissues from cystic lesions, and may differentiate between certain fluids.

The intraocular structures of the dog and cat visible on PD-weighted, T1-weighted, and T2-weighted MR images include the cornea, anterior chamber, posterior chamber, iris, lens, ciliary body, choroid, retina, and sclera.[37,41] The orbital structures of the dog and cat visible on PD-weighted, T1-weighted, and T2-weighted MR images include the optic nerve and chiasm, extraocular muscles, orbital fat, zygomatic salivary gland, ophthalmic artery and vein, and orbital bones.[37,41]

Contrast agents, such as the paramagnetic agent gadolinium-diethylenetriamine pentaacetic acid (Gd-DTPA), will appear bright on T1-weighted images because of their ability to shorten the relaxation time of adjacent hydrogen protons.[40] In small animals, an intravenous dose of Gd-DTPA at a rate 0.1 mmol/kg is recommended.[34] An optimal dose of Gd-DTPA has not been reported in horses. MRI can be used to identify uveal and choroidal melanomas as well as chiasmal and retrochiasmal neoplastic and inflammatory lesions.[43] MRI can also be used to exclude mass lesions causing optic neuritis and to diagnose optic nerve tumors, retrobulbar tumors, and vascular anomalies.[5,28,29,35,41,43] MRI is contraindicated, however, for intraocular and orbital magnetic foreign bodies. Because of the large body mass of horses, MRI in that species has the same limitations as CT.[44,45] Foals, however, can be evaluated with MRI (Fig. 9.2.4).

Magnetic resonance angiography (MRA) may be accomplished with MRI using one of three methods.[40] Two of the methods, time of flight and phase contrast MRA, rely on the fact that flowing blood enters a tissue slice (with 2D MRA) or volume (with 3D MRA) after the tissue has been rendered signal-free, thus resulting in images with high-signal vessels

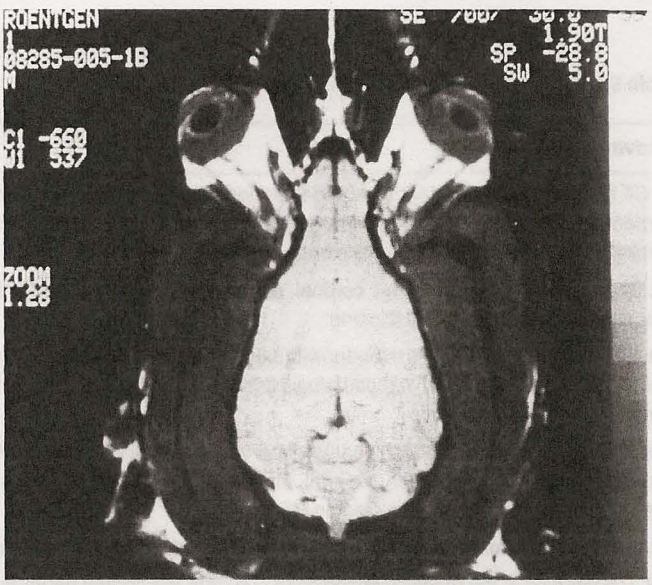

Figure 9.2.4. T1-weighted MR image from a normal horse. Both intraocular and orbital contents are readily identified.

Table 9.2.3 The Relative Order of Signal Intensity in Ocular Tissues [27]

Signal Intensity	T1-weighted	T2-weighted	Proton Density Weighted
High (white)	Fat	Vitreous and aqueous	Vitreous and aqueous
Intermediate	Cornea	Brain	Extraocular muscles
	Lens capsule	Extraocular muscles	Optic nerve
	Iris	Optic nerve	
	Retina/choroid	Iris	
	Brain	Fat	
	Extraocular muscles		
	Optic nerve		
	Vitreous and aqueous		
Low (black)	Lens	Bone	Fat
	Sclera	Sclera	Sclera
	Bone	Lens	

against a low-signal background. The third method, contrast enhanced or Gad-enhanced MRA, imparts vessels with a high signal because of the shortening effects on T1 relaxation caused by the gadolinium–blood mixture.

Functional imaging studies that show physiology and metabolic function are useful for cases in which structural imaging might be normal.[31,46] Functional MRI is based on changes in T2 signals caused by deoxyhemoglobin. This signal change is termed the blood oxygenation level–dependent mechanism. A local increase in neuronal activity leads to increased cerebral blood flow and a decrease in deoxyhemoglobin. Positron emission tomography and single-photon emission CT both use radiolabeled molecules to image metabolism, including regional blood flow and glucose metabolism.

PHOTOGRAPHY

External Photography

Most ophthalmic lesions are easily photographed. Lesions can be documented to evaluate progression and response to therapy, for teaching purposes, and for publication. In addition, many veterinarians appreciate the value of photographs for consultation, discussion purposes, client relations and education, and professional development.

An impressive arsenal of cameras is available for external photography, and the choices are often limited only by the operator's level of photographic knowledge and the cost of the equipment.[47–51] Several moderately priced cameras are available for close-up photography, and many of these can be easily operated by the novice. Single-lens reflex(SLR) cameras are better adapted for close-up photography but can be significantly more expensive. Single-lens reflex cameras also require a more extensive knowledge of photography.

Macrolenses are useful for external, close-up photography. Designed with small apertures, these lenses avoid the aberrations normally inherent in close-up focusing, and they can provide a 1:1 reproduction ratio (i.e., image size–object size) from distances as close as 0.25 m. Macro-zoom lenses often have poorer resolution and can provide only a 1:3 or 1:4 reproduction ratio. Close-up lenses can be attached to the front of most lenses like a filter, thereby producing images of 1/10 to 4/5 life-size. Aberration is a significant problem with these lenses, however, and they should not be used with any camera lens having a focal length of more than 50% the focal length of the close-up lens. Extension tubes can be used between the camera body and the lens to produce images of 50% to 175% life-size without the aberration inherent in close-up lenses. Capable of producing a 1:1 reproduction ratio, these tubes provide excellent photographs when combined with a macro lens. Teleconverters can effectively double or triple the focal length of the primary lens, but these converters also tend to soften the final image.

Electronic flashes may be top-mounted, side-mounted, handheld, or lens-mounted. Lens-mounted ring flashes are available for most macrolenses, but these tend to produce horseshoe corneal reflection artifacts when the lens is positioned too close to the cornea. Side- or top-mounted flashes can create shadow artifacts when used with lens-extension tubes. Automatic exposure systems are available as either a sensor in the flash unit or a built-in light meter in the camera. These may greatly simplify photography, but they tend to give inconsistent results at distances of less than 0.5 to 0.7 m. External photography units complete with strobe flash are available for ophthalmic use (e.g., Nikon and Yashica eye cameras). The camera-mounted flash, especially when using a single-lens reflex (SLR) camera, enables the photographer to adequately illuminate the subject even when the object being photographed cannot be seen. This is especially useful when photographing internal structures of the eye (e.g., lens luxation, synechiae, cataracts). The photographer need only to ensure that the corneal surface is in focus and the flash illuminates the internal structures.

Several cameras are available for digital imaging of the ocular adnexa and anterior segment. Several features unique to the digital camera affect the camera use.[52] The camera's buttons, features, and display should be easy to use and understand. Transferring data should be simple and straightforward. Removable storage disks or storage in addition to the internal memory increases the number of images that can be taken and decreases the transfer time to a computer. SLR digital cameras allow the user to see the subject through the same lens that will capture the image, and these cameras therefore offer an excellent preview capability. Viewfinders are offset from the camera's lens and do not provide a perfect preview of the final image. Liquid crystal display (LCD) screens can display the image as seen through the camera's lens, but the refresh rate of the monitor has to be fast to avoid misaligned photographs. A fast capture time (the time between depressing the shutter button and capturing the image) is important for the captured image to resemble the intended image. Correct alignment with what you see and what is ultimately captured is facilitated by an SLR camera or an LCD monitor that is fast, a camera that has macro-flash capability, and a macrolens. Digital cameras have a unique feature called digital zoom—a digital enlargement of the image. This feature is not an optical zoom (i.e., generated from the lens), and therefore the image will not be as crisp as an optical close-up photo.

Other important features are waiting time for file writing, focal range, and ability to delete photos.[53] The main differences between the quality of images produced by four different digital cameras imaging the ocular adnexa and anterior segment in small animals were related to the inherent camera resolution, the ease and speed of achieving focus, and the effect of flash illumination and artifacts on the image.[54] Higher resolution SLR cameras with ring-flash options provided the best quality images.

Two major considerations with digital imaging are the resolution needed to image the object of interest and the compression that can be utilized to minimize the space needed to store the image.[55] Resolution is the ability to distinguish between two adjacent points. Image compression is a technique to reduce file

size by removing redundant information. In some compression methods, such as TIFF (tagged image file format), the full information can be retrieved, but in others, such as JPEG (Joint Photographic Experts Group), the information is permanently deleted. If all images are taken at maximum quality, storage and archiving can become an issue. A camera that lets you choose the compression ratios will give you the greatest flexibility in either preserving disk space or maintaining high photo quality. Subjective grading of anterior eye images taken by four digital cameras attached to a slitlamp, stored as TIFF files, and then compressed to various sizes showed that it is appropriate to store images at between 1280 × 811 and 767 × 569 pixel resolution and at up to 1:70 JPEG compression.[55]

Fundus Photography

Fundus photography has proved to be invaluable in the documentation of posterior segment diseases among animals, thus contributing significantly to the advancement of veterinary ophthalmology. Additional uses of the fundus camera, particularly the handheld models, include photography of the iridocorneal angle and ciliary cleft, iris, posterior chamber, lens, and vitreous.

In 1899, Dimmer presented human fundic photographs to the Ninth International Congress of Ophthalmology. Twenty-three years later, Nordenson presented his compact, table-top fundic camera, which was subsequently marketed in 1926.[56] Fundus photography in animals was first reported by Leonardi in 1930, and Huber later used the Nordenson camera to photograph the canine fundus in 1937. In 1947, Saurer published photographs of the canine, bovine, and caprine fundi, noting the need for mydriasis.[57] Catcott used a modified Nordenson camera and color film to photograph the canine fundus in 1952,[56] and Luginbuhl published color photographs of canine and feline fundi in 1958.[58] In 1964, Donovan and Wyman described fundus photography in the cat and dog using the Noyori portable fundus camera.[59] In 1968, Barnett published color photographs of both normal and abnormal fundi in fully conscious dogs using the Zeiss, OPL, and Krahn fundus cameras.[60]

Both table-mounted and handheld fundus cameras are available. Table-mounted cameras take excellent photographs, but they are useful only in tranquilized or anesthetized small animals.[61] Different models are manufactured by Canon, Kowa, Topcon, and Zeiss. Handheld models are more frequently used in veterinary ophthalmology; they are portable, less expensive than table-mounted models, and relatively easy to use. Examples of handheld models include the Kowa RC-1, RC-2, RC-3 (only available as used models) and the Genesis model. The Kowa Genesis features several improvements over earlier models (Fig. 9.2.5). It is less bulky than the RC-2 and RC-3 models, and it easily fits the hand. Focus is adjusted by pressing an electronic switch located where the index finger rests, and a foot pedal is provided as an alternative to digitally triggering the shutter. Film advancement and rewinding are motorized. Primarily because of cost, however, the older Kowa RC-2 and RC-3 models remain the most commonly used handheld fundus cameras in veterinary ophthalmology throughout the United States. Consisting of a 35-mm camera, base power unit, and flash strobe, these cameras can be adapted with a larger power unit, motorized 35-mm film base for fluorescein angiography, stereo prism, and Polaroid film back. Focus is adjusted from –20 to +20 D with the camera's eyepiece, and a variable-intensity, 12-V, 10-W light illuminates the patient's fundus. Fundus magnification varies with the patient, averaging X19 at 0-D focus and X38 with the X2 adjustment. The strobe flash lasts 1/750 second, and the flash intensity is adjusted from 50 to 100 W/sec in increments of 10 W/sec. With use, the strobe flash gradually reduces in intensity, thus necessitating adjustments in the flash-intensity settings and, eventually, strobe replacement. Each camera flash strobe tends to have its own identity as well, so exposure tables should be used only as a guide (Table 9.2.4).

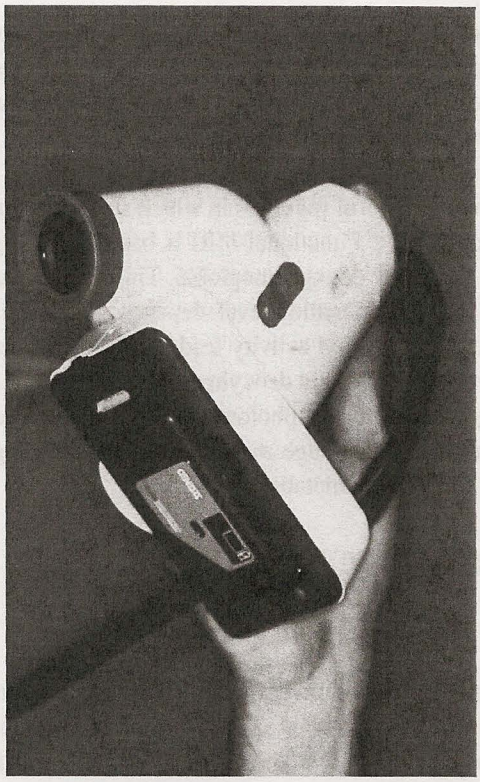

Figure 9.2.5. The Kowa Genesis fundus camera.

Direct digital acquisition of images using an electronic camera offers several advantages over conventional photography. These images can be easily analyzed, enhanced, archived, and transferred electronically. Digital table-mounted cameras are manufactured by various companies such as Canon, Kowa, Topcon, Optos, CMT Medical Technologies, and Zeiss. The field angles range from 20° to 200°, and the light source is either white light or multifrequency laser light (532 nm and 633 nm). Digital fundus images have been shown to be superior to film-based images.[62] Important features to test for in the charge-coupled device (CCD) image sensor in electronic cameras are resolution, light sensitivity, linearity, and the response to fast changes in light sensitivity (step response).[63]

Digital handheld fundus cameras have been developed. The Nidek camera (Model NM-200D, Nidek Inc., Fremont, CA) provides high-resolution 30° images with a digital progressive-scan

Table 9.2.4 Exposure Guidelines for the Flash Strobe of the RC-2 Kowa Fundus Cameras for Different Species of Animals

	External Eye/ Strobe Intensity		Fundus/Strobe Intensity	
Animal Species	**ISO 25**	**ISO 64**	**ISO 25**	**ISO 64**
Dog	7[a]	4–5	2–3 T	1–2 T[b]
		3–4 TR	3–4 NT	2 NT[b]
Cat	7	4	1–2 T	1 T[b]
		3 TR	2–3 NT	2 NT[b]
Horse	7[a]	4–5	3–4 T	1 T
		3–4 TR	4 NT	1–2 NT
Cow	7[a]	4–5	3–4 T	1 T
		3–4 TR	4 NT	2 NT
Sheep	7[a]	4–5	3–4 NT	1 T
		3–4 TR	4 NT	2 NT
Swine	7[a]	4–5	6–7	2–3
Nonhuman primate	7[a]	4–5	6–7	3
Albino rabbit	6–7	3–4	3–4	1
Pigmented rabbit	7[a]	4–5	6–7	3

NT, nontapetal fundus; *T*, tapetal fundus; *TR*, tapetal reflex.
[a]May be slightly underexposed.
[b]Using a 50% neutral-density filter.

CCD camera. The working distance from camera to cornea is 8 mm and the required pupil diameter is 4 mm. Photographed images are displayed on a monitor in color and can be saved in a TIFF format. The system was reported to be easy to use on dogs.[64] The Kowa Genesis-D is a lightweight (1070 g) digital handheld fundus camera that looks and works more like the RC-2 (Fig. 9.2.6). Focus is adjusted by turning a wheel with the index finger, and the shutter is triggered by the thumb as with the RC-2. The images are displayed on a 6.4-cm LCD monitor and can be saved on a compact flash card in JPG or BMP format. The 30° horizontal and 25° vertical field-of-view can be increased by the use of a +28 D aspheric lens in a lens holder that is mounted on the front of the camera.

Another digital handheld device, introduced in 1997, is the RetCam II (Massie Laboratories, CA), which by the use of various lenses (130°, 120°, 80°, and 30° field-of-view, and portrait) can visualize the fundus, anterior segment, and adnexa. The imaging probe fits on the cornea interfaced with an ophthalmic gel similar to an ultrasound probe. The RetCam has an instant digital video clip capture (up to 20 seconds of real-time video) and instant digital image capture. The image is displayed on a monitor and can be printed by an inkjet color printer or a dye sublimation color printer or saved in a standard bitmap format. The RetCam also has fluorescein angiography as an optional feature.

The pupils are dilated with 1% tropicamide (1% atropine in the rat), and the eyelids are held open manually by the examiner. In the sedated or anesthetized animal, an eyelid speculum may be preferred; under these conditions, the cornea must be intermittently moistened to maintain its transparency and to prevent injury. The fundus camera is positioned within 1 cm of the cornea, and the photographs are taken. If the camera is too close to the eye, accidental contact may induce globe retraction and nictitans protrusion. If the camera is too far from the eye, corneal reflectivity may produce flash artifacts. In addition, if the camera is not centered on the pupil, part of the photograph will be black (from the obstructing iris). Nictitans protrusion may be overcome by coaxing the conscious patient. In sedated or anesthetized patients, the nictitans may be retracted by an assistant using a moist, cotton-tipped applicator.

DiLoreto and colleagues described a new method of fundus photography in small laboratory animals.[65] A 2.2 Volk Panretinal lens is held in apposition to a Topcon TRC SOFT fundus camera lens via a home-made metal sleeve. This procedure is reported to improve definition and to increase the field of observation in small laboratory animal fundus photography. It remains to be seen, however, whether a similar adaptation will work for handheld models.

Unlike the static images created by fundus photography, fundus videography creates continuous, dynamic images that can be replayed immediately after recording. Fundus videography is particularly useful in fluorescein angiography, allowing real-time analysis of the phases of vascular filling.

A scanning digital video ophthalmoscope (Fig. 9.2.7) has been developed by WILD Medtec GmbH (Wien, Austria). The Scanning-Video-Ophthalmoscope unites the advantages of classical indirect ophthalmoscopy with those of the scanning laser ophthalmoscope. A strip of the retina is illuminated by the insertion of a slit-aperture into the illumination beam path. A second slit-aperture in front of the picture level in the observation beam path is arranged so that only a part of the reflecting light at the retina is let through, suppressing, as the confocal aperture of the SLO, the unwanted reflexes. The slit-apertures are mechanically coupled and oscillate together in a time synchronized fashion so that the retina is scanned sequentially by a beam of light. The WILD camera works with real-time capture and video tracking enabling optimal image choice. The image is captured as a single picture, picture-sequence, or video sequence (Fig. 9.2.8). For documentation of the fundus, it has a 25°, a 50°, and a 50° field-angle objective lens with a central ring to determine cup–disk ratio. Wide angle image capture is possible with a Volk lens. Sectional image capture of the anterior eye segment is possible using slitlamp illumination. It is available with a color camera as well as an integrated black-and-white camera (the latter in the fluorescein angiography version). Fluorescein angiography can be captured in real time, in sequence, or as single images. Handheld use and mobile operation using a laptop is possible.

Retinal Imaging

Confocal Scanning Laser Ophthalmoscopy/Tomography

To attain a perfectly sharp representation of a single spot in a specimen, one would ideally collect only the light reflected directly from the plane of the specimen. In standard light

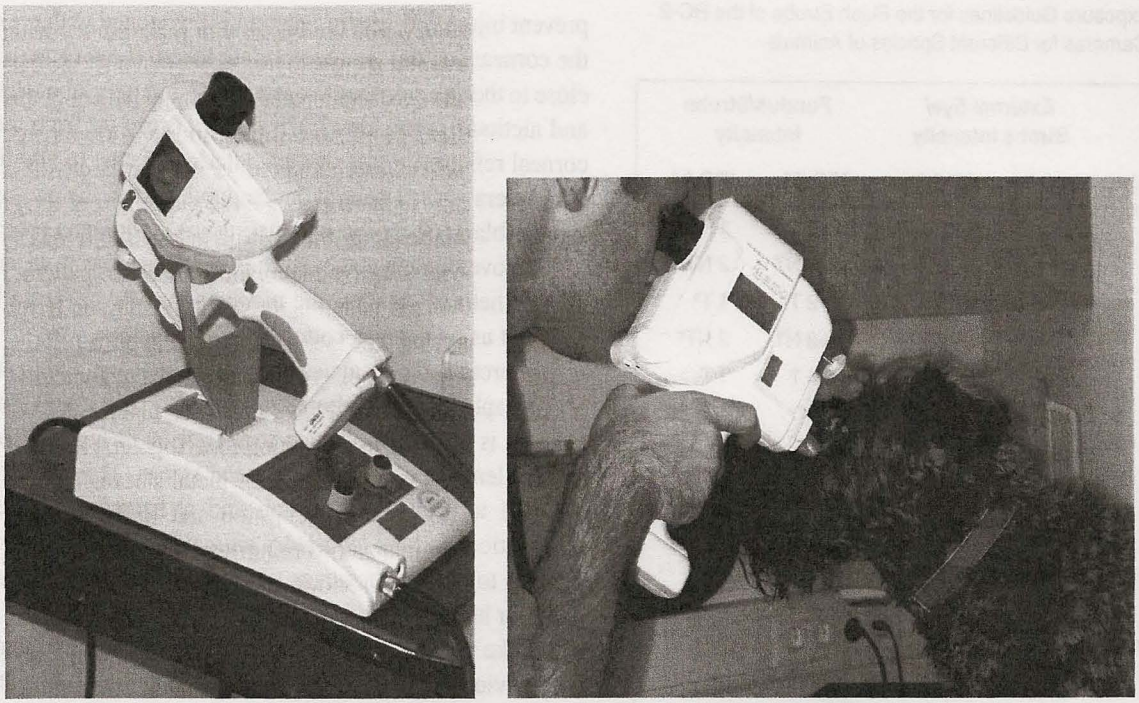

(a) (b)

Figure 9.2.6. The Kowa Genesis-D fundus camera. **A.** Camera and base. **B.** Fundus photography in a dog.

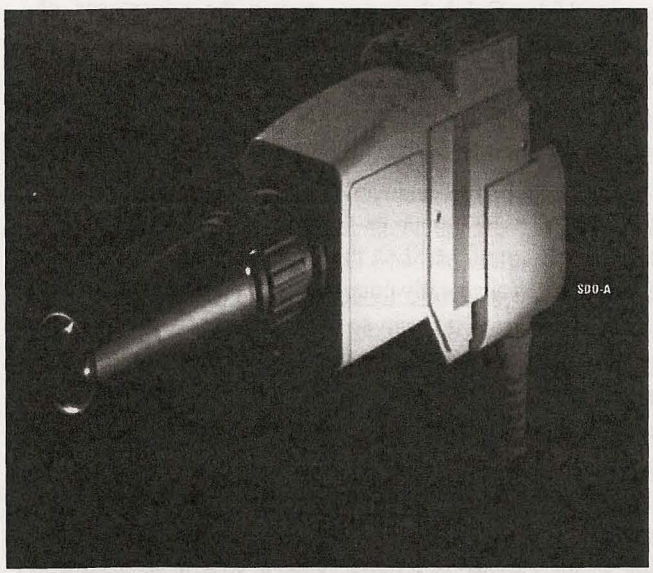

Figure 9.2.7. The WILD Scanning-Video-Ophthalmoscope.

microscopy, however, material both above and below the plane of the specimen also returns light, which results in blurring of the image.[66] Light scattering, which arises when light randomly strikes minute particles in a specimen and then rebounds into other particles before reaching a detecting surface, also reduces image contrast. Confocal scanning microscopes minimize blurring and enhance contrast by illuminating only focal spots of tissue at selected depths of the specimen; this is accomplished by using a pinhole aperture to filter out the signals arising from the tissues above and below the brightly illuminated spot and rapidly scanning the specimen in a raster pattern to ensure that every spot in the desired plane is examined. Reflections from out-of-focus planes and scattered light do not come into focus at the aperture and are suppressed.[66]

The confocal scanning laser ophthalmoscope (CSLO) has been developed for the diagnosis and monitoring of optic nerve head (ONH) changes in human glaucoma. It provides true, three-dimensional optical sections of the ONH.[66–69] Confocal optics assure that only a thin "slice" of optic nerve tissue is in focus on the image plane; thus, high-resolution tomographic optic nerve images are obtained. The ability to detect small changes in optic disc topography may be important for detecting damage and monitoring change in glaucoma. The lateral and axial resolutions with CSLO are 20 and 300 μm, respectively.[67]

The Rodenstock CSLO (Rodenstock Instruments; Danbury, CT) obtains each focal plane image, in 1/30 second, as a 525-horizontal-line analog video signal.[67] A helium-neon or argon laser is used to obtain real-time images, which are stored on a videocassette recorder. Layered viewing of the retina as well as viewing of deeper, scatter-sensitive tissue are possible. The Rodenstock CSLO has obtained incredible in vivo images of the photoreceptor layer and retinal blood flow of the optically powerful, small eyes of snakes with retinal damage.[70,71] These images correlate with measures of histopathologic retinal sections in this species.

The Heidelberg Retinal Tomograph (HRT) (Heidelberg Engineering; Heidelberg, Germany) is a scanning laser tomograph that produces three-dimensional images of optic disc topography.[67,72,73] The HRT uses a diode laser beam (670 nm) that is projected onto the retina with a confocal system.[68,72] The instrument automatically performs 32 evenly spaced, consecutive, 256 × 256 measuring points, two-dimensional tomographic scans perpendicular to the optic axis (i.e., z-axis) in 1.6

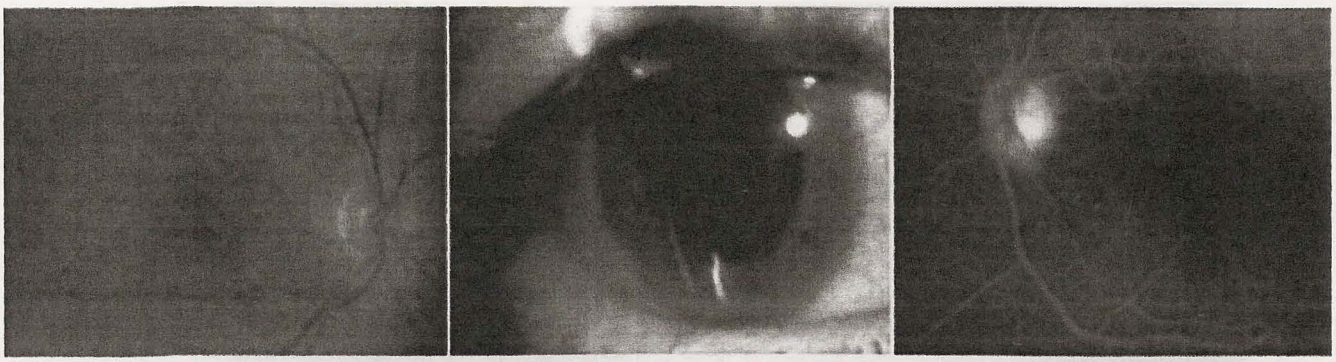

Figure 9.2.8. Images of human fundus, anterior segment, and fluorescein with the WILD Scanning-Video-Ophthalmoscope.

seconds over a section of ONH varying between 0.5- and 4.0-mm deep. The sum of the reflectance values along the z-axis for each aligned pixel is used to generate a reflectivity image, and the location along the z-axis at which the maximum reflectance occurred is used to generate a topographic image.[72] The integrated computer constructs a single mean topographic image in three dimensions (i.e., x, y, and z) from the 32 topographic section images using a preset reference plane located 50 μm below the retinal surface temporal to the optic disk. The margin of the ONH must be defined by the operator for determination of three-dimensional measures. Optic nerve topographic indices such as optic disc area, optic cup area, cup-to-disc area ratio, cup shape and depth, neuroretinal rim area and volume, retinal height, and mean retinal nerve fiber layer (NFL) thickness are readily obtained from reproducible and accurate tomographic images.[73] Mean values as determined with the HRT in the normal adult cat at a mean IOP of 17.2 mmHg are 1.31 ± 0.47 mm^2 for disc area, 0.68 ± 0.28 mm^2 for cup area, 0.52 ± 0.14 for cup-to-disc area ratio, 0.14 ± 0.04 mm for cup depth, 0.35 ± 0.11 mm for maximum cup depth, and 0.08 ± 0.04 mm for mean retinal thickness (Fig. 9.2.9).[74] The temporal NFL, rim area, and rim volume are less than the nasal areas of the optic nerve head of rhesus monkeys.[75] The cSLO (I + Tech CSLO, Clermont-Ferrand, France) was used to generate excellent images of the fundi of dogs, monkeys, and minipigs.[76] Heidelberg Engineering has recently developed a second-generation HRT machine (HRT II).[77] This device is essentially a small, lightweight, portable, and automated version of the original HRT (Fig. 9.2.10). The transverse field is fixed to 15 × 15 degrees with a 384 × 384 measuring point grid in each of the scanned planes. The number of scanned planes ranges from 16 to 64 depending on the optic disk depth. This version uses an internal fixation target and automatically acquires three consecutive series of scans, shortening the duration of the image scans.[78] The cSLO is probably appropriate for scanning the optic nerve head only. The physical limitations of axial resolution for cSLO preclude useful quantitative thickness measurements of the retina and the NFL.

Nerve Fiber Analyzer

A reduction in thickness of the NFL caused by retinal ganglion cell death may precede visual-field loss in glaucoma.[68] Because these axons are readily evident and less compacted in the NFL than in the ONH, quantification of NFL thickness has been investigated as a means of detecting and following glaucomatous damage. The nerve fiber analyzers, Gdx variable corneal compensator (VCC) (Laser Diagnostic Technologies; San Diego, CA) and Retina Thickness Analyzer (RTA) II (Talia Technology Ltd., Lod, Israel) are scanning laser polarimeters that use form birefringence to measure NFL thickness.[67,68] The arrangement of microtubules in retinal ganglion cell axons within the NFL changes the polarization of near-infrared diode laser light (780 nm) passing through it. The amount of change in the polarization (i.e., phase shift) is called retardation and is linearly correlated with NFL thickness.[67,79] The RTA operates on the assumptions that the NFL is the main source of retinal birefringence, that most of the light is reflected from the outer retina and double passes the full NFL thickness, and that NFL birefringence is homogeneous. The lens and cornea may also demonstrate form birefringence independent of the NFL.[67,68] The VCC has increased the diagnostic accuracy of scanning laser polarimetry by better elimination of the portion of the signal resulting from anterior segment birefringence for an individual eye compared to the fixed corneal compensation in older models. The in vitro resolution of the NFA is 13 μm.[67,68] HRT and GDx are both able to measure peripapillary NFL but use different methods and locations for their measurements. The HRT assesses NFL on the outer edge of the optic nerve head using a reference plane; the GDx assesses NFL around the optic disk from 1.1 to 2.5 disk diameters. A study comparing these two techniques showed significantly higher variability in NFL measurements acquired with the HRT than with the GDx.[80] Table 9.2.5 shows comparisons of Optical Coherence Tomography, Retina Thickness Analyzer, and Confocal Scanning Laser Ophthalmoscope.

Optical Coherence Tomography

Optical coherence tomography (OCT) is an imaging technology that can obtain micron-resolution cross-sectional or tomographic images of the eye.[67,68] OCT is analogous to A-mode ultrasonography except that optical or light tissue reflectivity rather than acoustic tissue reflectivity is used. Optical imaging techniques function by measuring the time delay when light is reflected from various intraocular

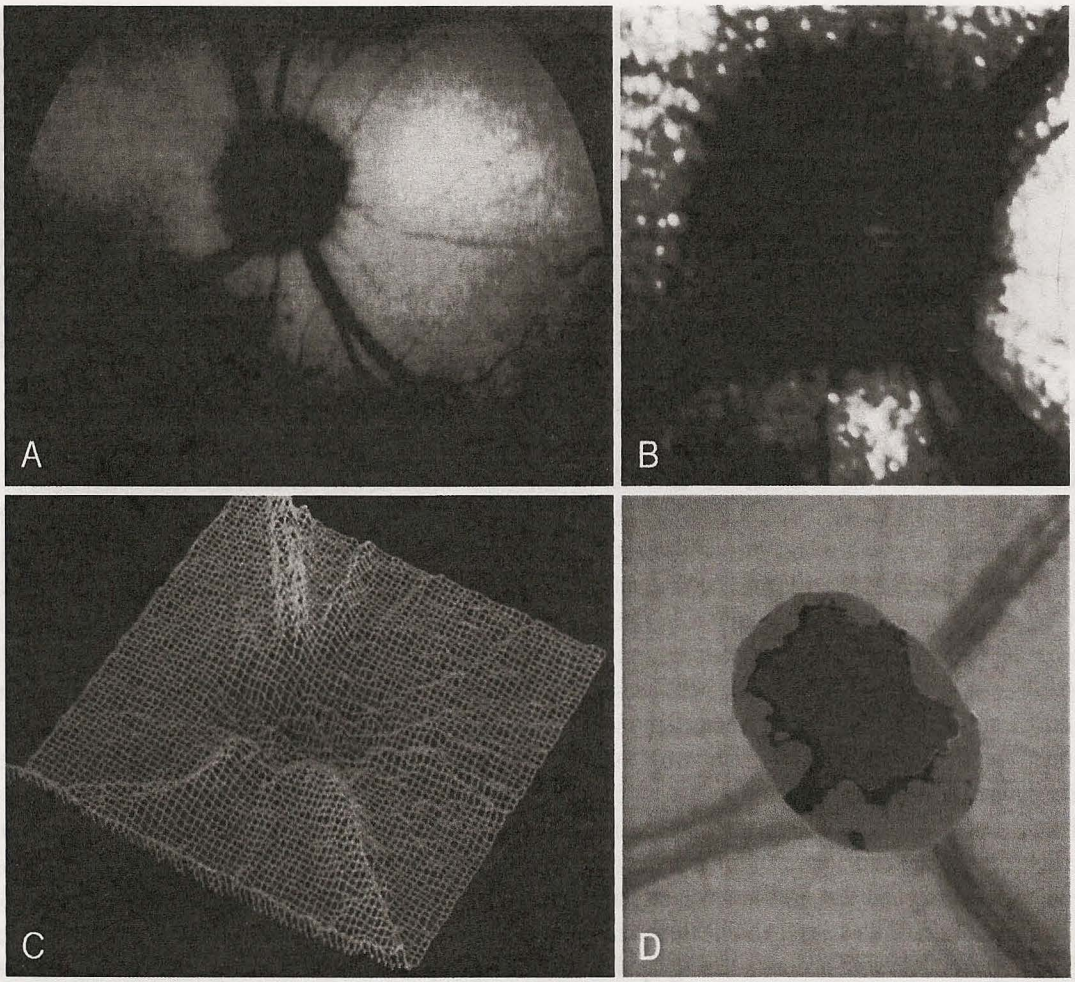

Figure 9.2.9. **A.** Normal fundus photograph obtained in a normal cat. **B.** Scanning laser image obtained with the Heidelberg Retinal Tomograph (HRT) in a normal cat. **C.** Topographic image obtained with the HRT in a normal cat. **D.** Pixel-intensity image obtained with the HRT in the same cat. *Blue* and *green* indicate more superficial areas of the ONH; *orange* indicates the deeper portion of the optic cup.

Figure 9.2.10. The Heidelberg Retinal Tomograph II is a confocal scanning ophthalmoscope used to evaluate ONH topography.

Table 9.2.5 Resolutions at the Z-Axis (Axial) and X- and Y-Axis (Lateral or Transverse) of Various Ophthalmic Imaging Techniques

Imaging Method	Axial Resolution (μm)	Lateral Resolution (μm)
OCT	10–20	20–50
Ultrasonography	200	500–600
UBM	20–50	
NFA	13	20
HRT/CSLO	300	20

Data from Schuman JS, Noecker RJ. Imaging of the optic nerve head and nerve fiber layer in glaucoma. *Ophthalmol Clin North AM* 1995; 8: 259–279; and Schuman JS. Imaging of the optic nerve head and nerve fiber layer in glaucoma. In: Epstein DL, Allingham RR, Schuman JS, eds. *Chandler and Grant's glaucoma*, 4th ed. Baltimore: Williams & Wilkins, 1997: 104–119.

structures, and these techniques have higher spatial resolution than ultrasound (10–20 μm versus 150 μm).[67,68,81] OCT uses short pulses (10^{-15} seconds) of coherent (i.e., same phase)

light to perform high-resolution measurements and imaging of the ocular microanatomy. An optical beam from a diode laser (830 nm) is directed onto a 50/50 beam splitter, which splits the light such that one beam is directed into the eye and is reflected from intraocular structures of varying depths (i.e., z-axis) and the second beam is reflected from a reference mirror of known spatial positions. A confocal fiberoptic interferometer measures the time delays of optical tissue echoes of different intraocular structures by comparing the reflected light beam with the reference beam. When two light pulses of the same coherence length coincide, they produce a phenomenon known as constructive interference, which can be measured by a photodetector. For all practical purposes, the OCT signal may be considered to be composed of light that has undergone a single backscattering event at the tissue layer of interest. The OCT signal from a particular tissue layer is a combination of its reflectivity and the absorption and scattering properties of the overlying layers.[67,68,81]

Tomographic or cross-sectional imaging of ocular tissues is achieved by performing rapid, successive, axial or longitudinal scans of the eye while scanning the optical beam in the transverse direction. A single OCT scan is similar to one-dimensional, A-scan ultrasonography. It requires 0.7 seconds to acquire a complete axial scan series of 512 scans, which provide a cross-sectional map of the reflection and backscatter of the ocular tissue. Images may be displayed in logarithmic gray scale or in pseudocolor. White or red represent thick regions, and dark gray or black-blue represent thin areas.[67,68,81,82] Axial resolution (i.e., z-axis) is determined by the light-source pulse duration and is around 10 μm. Transverse resolution (i.e., x-and y-axes) is determined by the size of the focused beam, limited by the pupillary aperture, and is typically 10 to 50 μm.

The NFL, retinal pigment epithelium (RPE), and choriocapillaris are highly backscattering, and they appear red in pseudocolor.[81] Intermediate reflectivity is observed for the yellow outer and inner plexiform layers, both of which are more reflective than the outer and inner nuclear layers. The photoreceptor layer exhibits minimal reflectivity and appears dark blue. Retinal blood vessels are identified by their increased reflectivity and by their shadowing of reflections from the RPE and choriocapillaris. Larger choroidal vessels appear as dark spaces.[67,68,81]

Macular holes, retinal vessel occlusion, diabetic retinopathy, chorioretinitis, age-related macular degeneration, and retinal degeneration have all been evaluated by OCT in humans.[81] Thickness of the NFL as measured with OCT was thin and correlated with visual-field defects in humans with glaucoma.[67,83] OCT can also be used to accurately image the cornea, iridocorneal angle, lens, and anterior segment.[81]

Most tissue layers of the retina and optic nerve, including the NFL, inner nuclear layer, photoreceptor layer, RPE, optic cup, and choriocapillaris, can be imaged in the dog[84] and rabbit (Fig. 9.2.11). The ventral rim of the ONH in the dog is thicker than the dorsal rim. Tilting of the disc is found in Beagles with primary open-angle glaucoma in advanced stages, with anterior movement of the lamina cribrosa being noted in Beagles with early glaucoma. NFL thickness near the ONH in both normal Beagles and Beagles with early glaucoma was 278 to 361 μm, with Beagles suffering from advanced glaucoma having an NFL thickness of 161 ± 35 μm. Histopathologic measurement of mean canine NFL thickness was 242 ± 58 μm in normal dogs and 90 ± 59 μm in glaucomatous dogs. Cup depth as measured by OCT in normal Beagles averaged 300 μm, compared with 100 to 200 μm in Beagles with early glaucoma.[84]

Ultrahigh-resolution OCT research scanners with an ultrabroad spectral bandwidth centered at about 800 nm and an axial resolution of 2 to 3 μm have been developed. This enhanced resolution enables the visualization and detection of numerous retinal layers, including the retinal ganglion cell

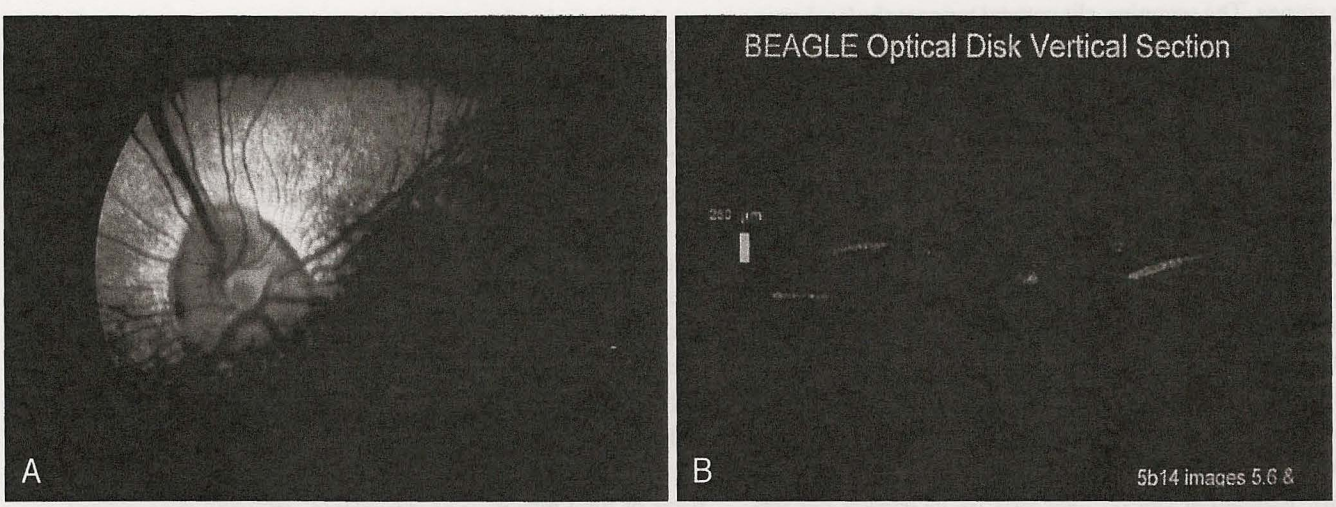

Figure 9.2.11. A. Normal fundus appearance of a young Beagle dog. **B.** Vertical OCT image of the same dog. The optic cup depth is 305 μm. Scan is from dorsal to ventral (i.e., left to right). The dorsal rim of the optic nerve head is more anterior than the ventral rim in this dog. The red linear region on the right is deep retinal backscatter by the dark circular region. (Courtesy of WW Dawson and A Sergeev.)

layer.[78,85] The 800 nm wavelength employed for retinal scanning is close to visible wavelengths and cannot directly visualize angle structures owing to scattering loss through the limbus. High-speed OCT prototypes have been developed using a longer wavelength of 1300 nm, which decreases scattering through turbid tissues and allows visualization of angle structures.[78,86,87] The scan width was 4 to 15 mm and scan depths 3.25 to 6 mm. Eight image frames were acquired and displayed per second in real time, each with 500 axial scans. The axial resolution was 14 μm full-width-half-maximum in cornea. An ultrahigh-resolution OCT system with a spatial resolution of 1.3 μm was used to image the corneal layers of New Zealand rabbits.[88] The epithelial thickness centrally was 45.8 μm ± 2.2 μm and 37.6 ± 1.4 μm at the limbus.

CORNEAL IMAGING

Pachymetry and Specular Microscopy

Central Corneal Thickness (CCT) is a sensitive indicator of the state of deturgescence of the cornea and a wide range of disorders that may affect the anterior segment in general or the cornea in particular. Optical pachymeter, optical slitlamp, ultrasound, and specular microscopy pachymetry are used to measure corneal thickness. Measurements can be obtained after reflection of light or ultrasound from the anterior and posterior surface of the cornea. Other instruments developed for the determination of corneal thickness include optical coherence tomography, confocal microscopy, and ultrasonic biomicroscopy. Scanning-slit topography/pachymetry, and noncontact specular microscopy have been introduced to evaluate corneal status and to determine thickness.[89] Corneal optical pachymetry is the measurement of the thickness of the optical cross-section of the cornea viewed in a slitlamp. The slitlamp, using oblique illumination, observes an oblique slice of cornea. The apparent thickness is a physical measurement made by moving an optical marker from the front to the back of the cornea. The scanning-slit corneal topography/pachymetry system (e.g., Orbscan II, Orbtek, Bausch and Lomb Surgical) scans the cornea from limbus to limbus, capturing 40 independent images, acquiring up to 240 points per slit. It is used to assess anterior and posterior corneal curvature, surface regularity, and thickness in different disorders.

Ultrasound pachymetry uses a pulse of ultrasonic energy that is sent toward the cornea, and the returning echoes are detected. The time between these returning echoes is measured and multiplied by the speed of sound in the cornea (1,636 m/s) to give the corneal thickness. The first-generation digital pachymeters used a free-running 50 MHz clock as a "ruler" to convert time between echoes into corneal thickness. This method gives a basic resolution of a single measurement of 33 microns. Resolution can be increased by increasing the frequency of the probe or by using an analog instead of a digital technology.

Specular microscopy evaluates endothelial morphology but is also reliable in measuring corneal thickness. It uses near-infrared light that is projected as an angled split beam onto the cornea, and the light reflected by the anterior and posterior layers of the cornea is detected by a line sensor. CCT is calculated by measuring the distance interval between the anterior and posterior reflection images on the line sensor. There are two types of specular microscopes: contact and noncontact. Both microscopes can be used interchangeably to evaluate endothelial cell morphology and density.[90] The pachymetry differences may derive from their slightly distinct image-grabbing principles. During contact specular microscopy, the ocular surface is indented with a 3.0 mm diameter cone with the possibility of generating excessive corneal tissue for measurement. In contrast, noncontact specular images are affected by the anterior corneal refractive power and the variation in air–corneal refractive indices.

Confocal Biomicroscope

The confocal biomicroscope works according to the same principle as described for the confocal scanning laser ophthalmoscope/tomography in which light from the illumination source passes through a pinhole aperture and is focused at a spot within the specimen by an objective lens. Light reflected back from the specimen is then focused at the detector by passage through a pinhole aperture, whereas out-of-focus light is blocked. By changing the position of the focal plane, it is possible to obtain images at different depths of the specimen. Scanning of all the pinpoint images then provides sectional views of the specimen in a single plane. An alternative to point scanning uses a slit of illumination that is scanned over the back focal plane of the microscope objective.[91] The clinical utility of noncontact specular microscopy and that of confocal microscopy are similar for examination of the normal transparent cornea, but confocal biomicroscopy appears superior to noncontact specular microscopy for evaluation of the endothelium of the diseased cornea.[92]

A further development of the confocal microscopy is the confocal laser microscopy (HRT II + Rostock Cornea Module, Heidelberg Engineering, Inc, Vista, CA), which uses a diode laser of 670 nm wavelength as its light source. This instrument can be used for pachymetry as well as imaging of the corneal layers and conjunctiva (Fig. 9.2.12).

Several studies have compared measurements of corneal thickness obtained with various instruments.[93–95] Optical methods including slitlamp and specular microscopy are widely used for corneal pachymetry but provide less measurement reproducibility than ultrasonic measurements.[96] Because optical pachymetry is dependent on measurements of reflected light beams through the corneal tissue, when the corneal medium is not clear or has optical interfaces, the pathways of light rays may be interrupted, affecting the measurements.[94] There are several advantages and disadvantages of the different instruments. The most important is to use one specific instrument for long-term patient follow-up because they cannot simply be used interchangeably.

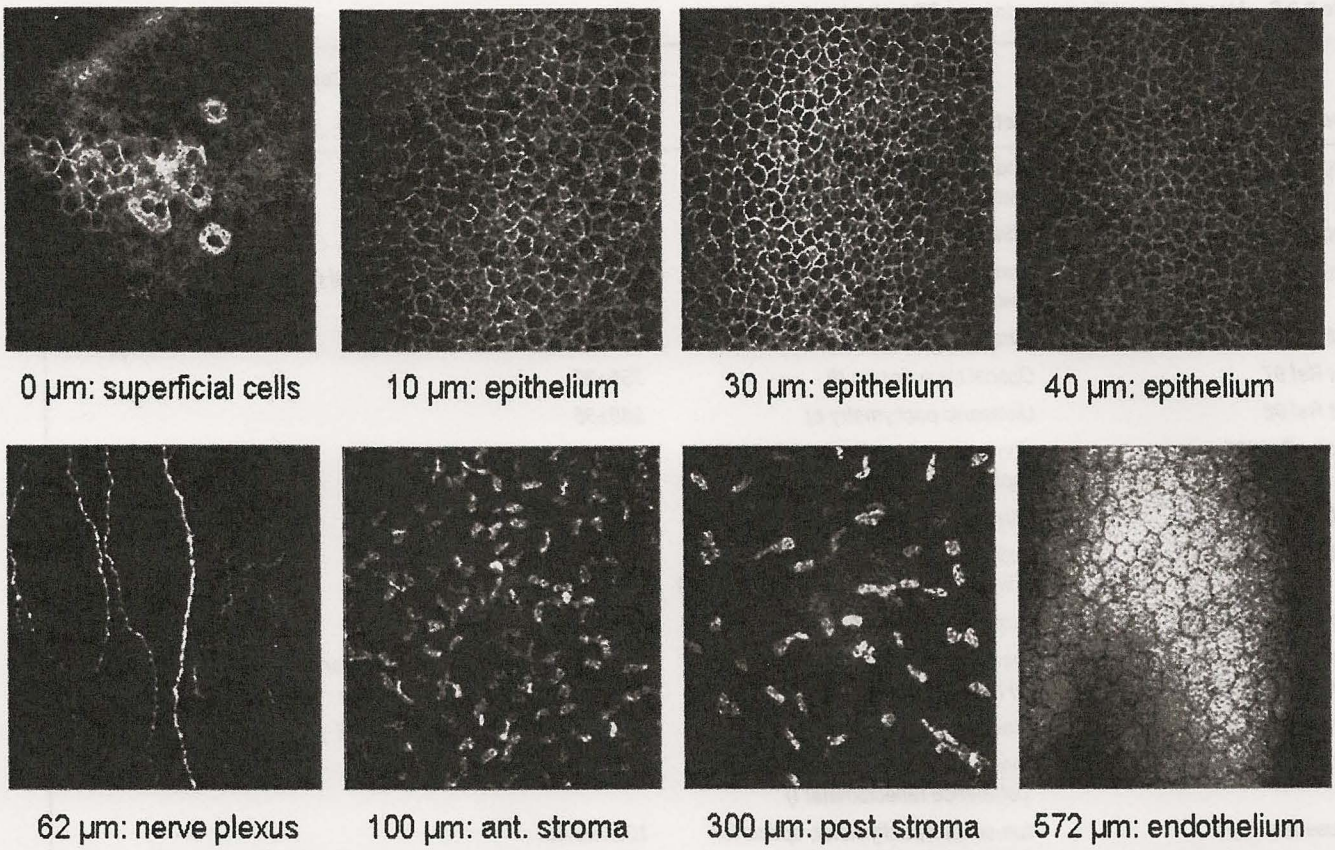

Figure 9.2.12. Specular microscopy of the human cornea with the HRT II + Rostock Cornea Module, Heidelberg Engineering. Depth of focus indicated in µm.

Numerous studies have been done to determine corneal thickness and corneal endothelial cell density in various species (Tables 9.2.6 and 9.2.7).[97–110] Postnatal development and age-related changes of endothelial cells and corneal thickness have been studied in cats, dogs, and chicks.[111–116] Following eyelid opening in dogs, there is an initial decrease in CCT until approximately 6 weeks of age.[114] There is a similar decrease in CCT in chicks until approximately 12 days of age.[116] Following the postnatal period, CCT increases with age in the dog, cat, and chick, while there is a discrepancy in the results for horses.[103,105,106] The density of corneal endothelial cells decreases with age in dogs, horses, cats, and llamas.[101,103,112,115,117]

Differences in corneal endothelial repair after endothelial wounding have been shown, with the young adult dog, rabbit, and rat having a marked regenerative potential, while the cat and humans showing very poor regenerative capabilities.[118–124] Specular microscopy has shown that the endothelium of induced diabetic dogs shows differences in cell morphology.[125,126] A decrease in endothelial cell density has been shown after phacoemulsification and extracapsular lens removal in dogs,[127] after injection of air in the anterior chamber of cats,[128] and by tissue plasminogen activator injection in the anterior chamber in dogs.[129] Rhesus macaques with laser-induced ocular hypertension also have a significant loss of endothelial cells in the central cornea.[107] No effect on endothelial cell density was shown by intracameral injections of viscoelastic solutions in dogs[130] or irrigation of the anterior chamber in dogs with saline, balanced-salt solution, and balanced-salt solution with glutathione.[131]

BLOOD FLOW ASSESSMENT

Fluorescein Angiography

Fluorescein angiography has been used experimentally since 1957, when Chao and Flocks first described the use of several intravenous dyes to study retinal circulation times in the cat. In 1972, serial fluorescein photography was described in the pigmented rabbit by Harris and colleagues.[132] The following year, Bellhorn[133] described fluorescein angiography in laboratory animals. Gelatt and coworkers compared restraint, film types, and fluorescein doses for fluorescein angiography in the dog in 1976, and Peruccio described fluorescein angiography in the cat in 1982.[134,135] Fluorescein angiography has since been used both clinically and experimentally to characterize normal and abnormal vascular conditions of the human and animal fundus.[136–139] This method has also been adapted to evaluate the iris vasculature in both humans and animals.[140,141]

Sodium fluorescein is a weak acid that maximally fluoresces in response to light at a wavelength of 485 nm, emitting light with a peak wavelength of 530 nm. In blood, 60% to 80% of fluorescein is protein-bound, mainly to albumin, thus limiting the amount of free fluorescein available for excitation. The absorption and emission spectra of the dye are altered in

Table 9.2.6 Mean Corneal Thickness in μm± SD in Adult Animals

			Site on Cornea	
Species	***Methods***	***Central***	***Dorsal***	***Lateral***
Dog Ref 109	*Endothelial specular microscope with pachometer a)*	*620±47*		
Dog Ref 104	*Ultrasonic pachymetry b)*	*560±5.2*	*612±4.5*	*581±6.4*
Dog Ref 115	*Contact optical specular microscope with digital pachometer c)*	*610±9 S.E.*	*Peripheral 670±10 S.E.*	
Cat Ref 102	*Ultrasonic pachymetry b)*	*578±64*	*601±65*	*584±60*
Cat Ref 97	*Optical slit scanning d)*	*755±33*		
Cat Ref 98	*Ultrasonic pachymetry e)*	*569±36*		
Rabbit Ref 100	*Non-contact pachymeter, optical low coherence reflectometer f)*	*356.11±14.34*		
Rabbit Ref 99	*Ultrasonic pachmetry e)*	*407±20*		
Rabbit Ref 108	*Optical slit scanning specular microscope with digital pachometer a)*	*380±20*		
Horse Mini Ref 106	*Ultrasonic pachymetry g)*	*785±2.98*		
Horse Euthanized 5 sites measured Ref 103	*Specular microscopy h) and ultrasonic pachymetry g)*	*858.5 mean OD/OS*	*932.5 mean OD/OS*	*879.5 mean OD/OS*
Horse Rocky Mountain Ref 105	*Ultrasonic pachymetry g)*	*770.0±7.5*	*827.2±9.3*	*783.0±9.2*
Rat Ref 100	*Non-contact pachymeter, optical low coherence reflectometer f)*	*159.08±14.99*		
Mouse Ref 100	*Non-contact pachymeter, optical low coherence reflectometer f)*	*106.0±3.45*		
Llama Ref 101	*Ultrasonic pachymetry g)*	*630±5*		
Alpaca Ref 101	*Ultrasonic pachymetry g)*	*595±9*		
AChick ref 116	*Ultrasonic pachymetry g)*	*242±0.2*		
Rhesus macaques Ref 107	*Non-contact specular microscopy h) and ultrasonic pachymetry g)*	*468±20 h) 480±30 g) (no sign diff)*		

a) HS-CEM3 Endothelial Microscope System, Heyer-Schulte Medical Optics Center, Irvine, CA

b) Corneo-Scan II, CS2000 Storz Surgical Inc, St. Louis, MO

c) Bio-Optics contact LSM-2000B, Bio-Optics, Arlington, MA

d) Modification of Haag-Streit 900 slit lamp

e) VIDA 55, Visual Instruments Distribution Associates: South Laguna, CA

f) Optical low coherence reflectometer, Haag-Streit, Bern, Switzerland

g) DGH500, DGH Technology Inc, Exton, PA

h) Topcon SP-2000P, Topcon America, Paramus, NJ

whole blood, with optimum excitation point at 485 nm and peak emission at 530 nm. Other dyes available for angiography include indocyanine green (peak absorption, 790 nm; peak emission, 820 nm), pyranine (peak absorption, 455 nm; peak emission, 520 nm), and rhodamine (peak absorption, 555 nm; peak emission, 585 nm).

Once injected into the jugular, tail, or cephalic vein, sodium fluorescein appears in the eye within 5 to 15 seconds in most species.[142,143] After entering the choriocapillaris, unbound fluorescein readily passes into the choroidal interstitium via numerous, large fenestrae. Movement of dye into the retina is prevented by the tight junctions between RPE cells. Fluorescein entering the retinal vasculature is retained within the lumen of these vessels by tight junctions and the lack of fenestrae between the endothelial cells. Breakdown of either the RPE or retinal vascular barrier allows fluorescein to enter the retina.

A blue excitation filter in the light pathway (e.g., Kodak Wratten 47A blue filter) induces maximal fluorescence, and a yellow filter in the optical pathway (e.g., Kodak Wratten 15 yellow filter) provides maximal contrast. Further contrast is provided by the retina through a yellow pigment (i.e., xanthophyll)

Table 9.2.7 Mean ± SD Corneal Endothelial Cell Density in Cells/mm^2

Species	Methods	Central	Site on Cornea		
			Periphery	Dorsal	Lateral
Dog Ref 109	*Contact specular microscope a)*	*2,816*			
Dog Ref 110	*Contact specular microscope b)*	*2,555*	*2,875*		
Dog Ref 115	*Contact specular microscope c)*	*2,335*	*2,310*		
Cat Ref 117	*Specular microscopy c)*	*2,991±236*			
Cat Ref 112	*Specular microscope*	*2,403±177*			
Rabbit Ref 108	*Contact slit scanning microscope d)*	*2,998±326*			
Horse euthanized 5 sites measured Ref 103	*Non-contact specular microscope e)*	*3,216*		*3,086*	*3,250*
Llama Ref 101	*Non-contact specular microscope e)*	*2,669*			
Alpaca Ref 101	*Non-contact specular microscope e)*	*2,275*			
Rhesus monkey Ref 107	*Non-contact specular microscope e)*	*3,990*			

a) HS-CEM3 Endothelial Microscope System, Heyer-Schulte Medical Optics Center, Irvine, CA

b) Bio-Optics LSM-2100C, Arlington, MA

c) Bio-Optics LSM-2000B, Arlington, MA

d) Heyer-Schulte Medical Center, Irvine, USA

e) Topcon SP-2000P, Topcon America, Paramus, NJ

in the outer nuclear and outer plexiform layers. This pigment absorbs the blue excitation frequencies, thus allowing the retina to act as its own optical filter.

Either black-and-white or color high-speed film may be used for fluorescein angiography as well as video systems. The tapetal reflection in many species, however, limits the value of this procedure for tapetal abnormalities. Custom processing may enhance the photograph or slide quality. Animals should be sedated for fluorescein angiography, because even the slightest movement can disrupt the photographic sequence. Short-term, general anesthesia may also be performed, but the resultant changes in globe position often make this undesirable. Drugs and drug combinations that have been used successfully in this procedure include acepromazine, 0.5 mg/kg intravenously, and ketamine, 10 mg/kg intramuscularly, in the dog; ketamine, 40 mg/kg and 30 mg/kg, in the cat and rabbit, respectively; and intraperitoneal ketamine, 30 mg/kg, and pentobarbital, 30 mg/kg, in the rat and hamster. The horse and pig require general anesthesia.[144] Fluorescein is administered rapidly via the cephalic or jugular veins in the dog and cat, the jugular veins in the horse, the ear veins in the rabbit, the tail veins in the rat and hamster, the cephalic or saphenous vein in pigs, and the wing veins in birds. Doses are chosen to maximize vascular fluorescence while minimizing side effects. Reported doses include 10% sodium fluorescein, 20 mg/kg, in the dog, up to 5 mL in nonhuman primates, up to 2 mL in the cat, 1 to 2 mL in the rabbit, 0.5 mL (0.03 ml/100g) in the rat, 0.25 ml in the hamster, and 2.5 ml in the miniature pig.[133–135,144–146] Reported side effects at these doses include emesis in approximately 5% of small animals and anaphylaxis in one cat.[136] The lethal dose of fluorescein in the rabbit is 2.5 g/kg. The low toxicity of fluorescein is attributed, at least in part, to its negligible tissue binding.

Once the animal is sedated and the pupils dilated, the eye and camera are aligned, and control (i.e., prefluorescein injection) photographs are taken. Fluorescein is then injected as a rapid bolus via an intravenous catheter, and photography is initiated. Photographs are taken at a rate of at least one every 2 seconds, beginning 5 seconds after the injection. After 20 seconds, photographs are taken at 1, 5, and 10 minutes following the injection.

Phases of the fluorescein angiogram include prefilling, choroidal, retinal arteriolar, retinal capillary, retinal venous, and recirculation. The choroidal phase is characterized by a central-to-peripheral progression of fluorescence behind the RPE (i.e., choroidal flush). With incomplete pigmentation of the nontapetal fundus or absence of the tapetal zone, the choroidal phase may be visualized. Cilioretinal arteries also fill during this phase, and as fluorescein leaks into the optic nerve from the choroid (via the border tissue of Elschnig), the optic nerve begins to fluoresce. In humans, it takes approximately 6 to 8 seconds after injection for the dye to reach the retinal circulation.[147] The retinal arteriolar phase begins 0.5 to 1.0 second after the choroidal phase, spreading outward from the optic disc. With careful focusing, the retinal capillary phase can subsequently be seen radiating from the optic disc. The retinal venule phase is characterized by laminar flow, with the venous margins fluorescing first. With optimal fluorescein doses, a second retinal arteriolar phase (i.e., recirculation phase) can be observed as well. Sodium fluorescein is rapidly eliminated via the kidneys and stains the urine.

Abnormalities of the fluorescein angiogram are described as either hyper- or hypofluorescent. Hyperfluorescence occurs with leakage of fluorescein into the vitreous or the subretinal space (i.e., retinal detachment), staining of tissue from leaky retinal or choroidal blood vessels, RPE defects (i.e., increased choroidal visibility), and increased accumulation associated with tumors, active hemorrhages, and vascular abnormalities (e.g., neovascularization, aneurysm, shunts). Hypofluorescence results from vascular attenuation or occlusion and from visual obstructions such as pigment, hemorrhage, edema, and exudates. Pseudofluorescence can occur with poor matching of excitation and barrier filters. Autofluorescence occurs in the tapetal fundus of the cat, lemur, and many other tapetal species. Drusen formation in the optic nerve, lipofuscin in the retina, and normal sclera can produce autofluorescence as well. Control photographs taken before fluorescein injection will help to minimize any misinterpretations caused by these latter two phenomena.

Indocyanine green angiography is an alternative to fluorescein angiography.[148] Indocyanine green is a water-soluble, tricarbocyanine dye with emission and excitation peaks in the near-infrared spectrum.[150] These longer wavelengths pass more readily than the shorter emission wavelengths of fluorescein through the RPE, thereby allowing better visualization of the underlying choroidal vasculature.

The protocol described above is ideal for identifying abnormal vessels. Ophthalmic disorders such as diabetic retinopathy and glaucoma may give rise to, or result from, ocular circulatory pathologies. Measurements of the time required for fluorescein dye to pass through the retinal circulation, quantitative fluorescein angiography, have been done in several animal models.[150] The introduction of the scanning laser ophthalmoscope has greatly improved quantitative fluorescein angiography. There are two commercial scanning laser systems: the analog Rodenstock SLO, which records data on an S-VHS video recorder or in a digital format, and the more recently developed Heidelberg retina angiograph (HRA) system, which digitally records data on a computer system. SLO allows imaging of the retina with a very high temporal resolution (Fig. 9.2.13). The Rodenstock SLO records at a speed of 30 frames per second and the HRA at 20 frames per second. The times between the first appearance of fluorescein in a retinal artery and corresponding retinal vein (AVP times) recorded with the SLO have ranged between 1.45s and 1.74s in humans.[150] The SLO used for angiography works according to the same principle as the tomograph. The difference lies in the wavelength of the laser used to excite the dye and having a fully open aperture. A blue laser (488 nm) and an infrared laser (795 nm) are used to excite fluorescein and indocyanine green, with barrier filters at 500 nm and 810 nm. The SLO is a confocal device that minimizes blurred and reflected images and enhances contrast by illuminating only a very small amount of tissue at selected depths in the retina.[150] It is used to explore the effects of diabetes, ischemia, and inflammatory processes of induced uveitis.[76,151,152] Confocal SLO was used to record retinal blood velocity parameters in dogs, monkeys, and minipigs.[153] Arteriovenous filling times, in seconds, for cynomolgus monkeys and Göttingen minipigs were 2.82 ± 0.15 and 2.4 ± 0.04 respectively.

Measurement of leukocyte velocity may indicate the relative blood flow through retinal tissue.[150] It is possible to stain leukocytes and track their movement through the circulation using SLO and any of fluorescent dyes such as acridine orange, fluorescein isothiocyanate, sodium fluorescein, and carboxyfluorescein diactate.[154,155,156] Acridine orange stains

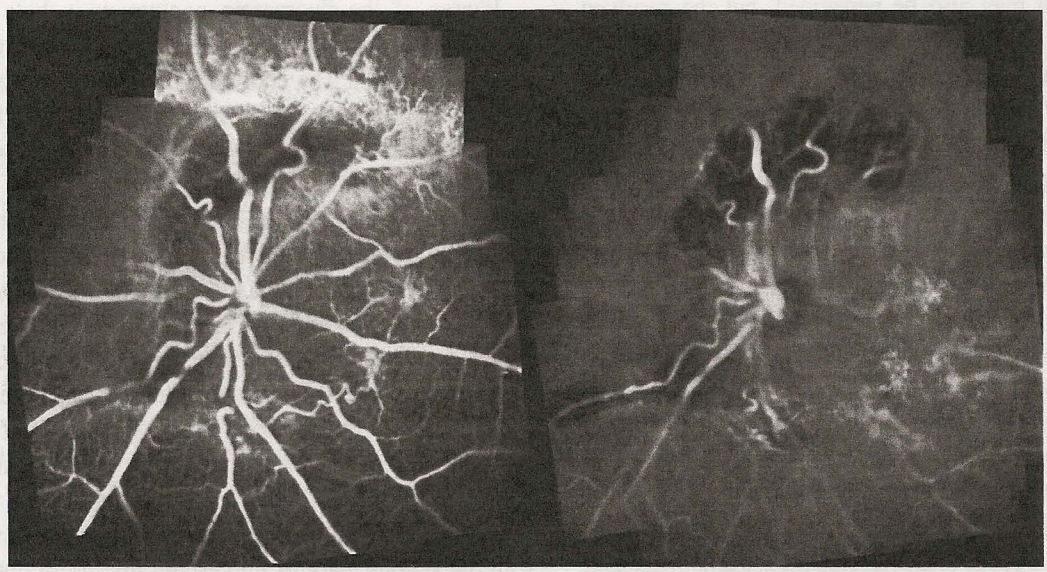

Figure 9.2.13. Simultaneous acquisition of both fluorescein (left image) and indocyanine green (right image) from rat retinas taken with the montaging mode of the HRA giving a field of view of about 73 × 73 degrees. The images are captured by moving the camera horizontally with a speed of two to three images per second. Images to be included are selected manually, and then the montage image is done automatically by the computer.

all subsets of leukocytes and is the most frequently used dye in rodents. It is carcinogenic and phototoxic to cellular lysosomes, and therefore has no applications in human research.[150]

Laser Flowmetry

Laser Doppler techniques are used to measure blood velocity or blood flow. Laser Doppler velocimetry (LDV) measures the maximum blood cell velocity present in larger retinal vessels. The velocity is calculated from an analysis of Doppler shifts observed in light scattered by moving red blood cells. The LDV was later developed to be able to measure velocity of blood in the capillaries of the ONH.[157] Experiments with the method in minipigs and cats have shown changes in ONH blood flow in response to varied blood carbon dioxide levels, carotid occlusion, hyperoxia, flicker stimulation, and increased IOP.[157] The Heidelberg retina flowmeter (HRF, Heidelberg Gmbh, Heidelberg, Germany) combines laser Doppler flowmetry and scanning laser technology.[150] HRF images consist of a 2560 × 2560 μm area of retina or ONH with a scanning 785-nm diode laser. The HRF computer extracts the individual frequency components of the reflected light. The results are displayed as a color-coded two-dimensional perfusion map with low perfusion values displayed as light colors and high perfusion values displayed as dark colors (Fig. 9.2.14). The reflectance image and three two-dimensional perfusion maps showing the values for the parameters volume, flow, and velocity in arbitrary units are displayed from top to bottom. Beagles with advanced primary open-angle glaucoma showed no change in ocular blood flow after administration of amlodipine, as measured with the HRF.[158] The capillary microcirculation, measured with HRF, of the temporal neuroretinal rim (NRR) of the Rhesus monkey ONH with laser-induced glaucoma had significantly increased blood flow, and the nasal NRR significantly reduced blood flow, compared to blood flow in the NRR of normal normotensive monkey eyes.[75] No blood flow changes were detected with the HRF in the optic nerve head in the Rhesus monkey model of ONH ischemia.[159]

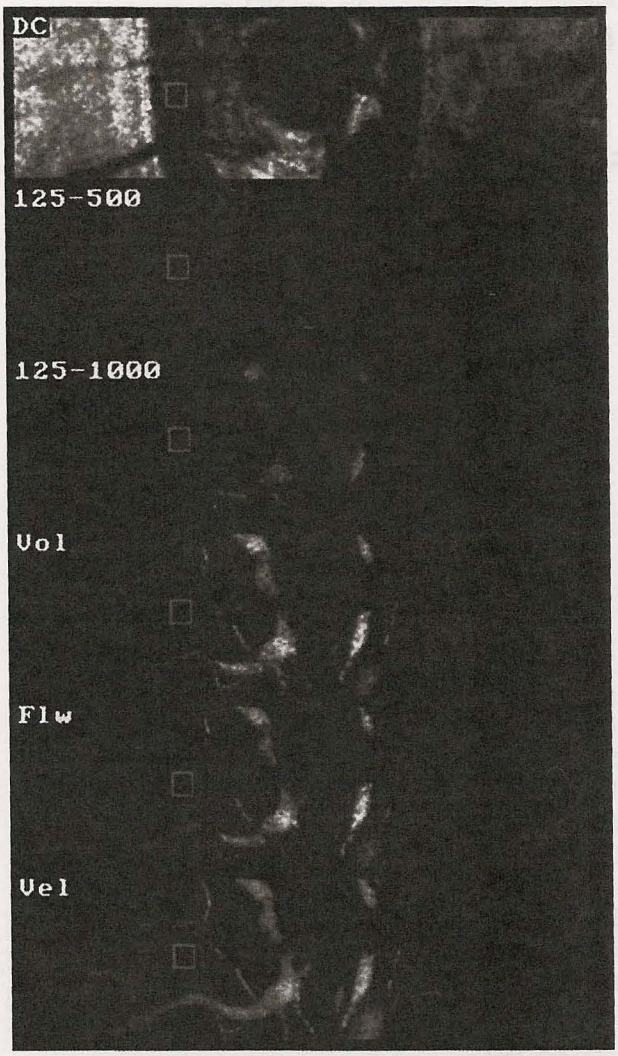

Fig. 9.2.14. Images from a monkey fundus taken with the Heidelberg retina flowmeter. The reflectance image and three two-dimensional perfusion maps showing the values for the parameters volume, flow, and velocity in arbitrary units are displayed from top to bottom.

Color Doppler OCT

Color Doppler optical coherence tomography (CDOCT) is a functional application of OCT and is the first technique to simultaneously record, with micron-scale resolution, the depth, diameter, flow rate, and flow dynamics of blood vessels within the living retina.[150] Conventional OCT records the amplitude of reflected light as a function of depth within the tissue being imaged. CDOCT differs from conventional OCT by measuring Doppler shifts in the reflected light using interferometric phase information, much like LDV. CDOCT provides superior axial resolution and depth localization. It also decreases the spatial resolution to approximately 10 to 20 μm, resulting in a higher signal-to-noise ratio than confocal detection alone. Thus far, limitations in both spatial and velocity resolution have permitted use of CDOCT only for imaging of large retinal vessels. Because the spatial resolution is inversely related to the optical bandwidth of the source, it can be improved by using a broader bandwidth source, as demonstrated for ultrahigh-resolution (2 to 3 μm) structural imaging in the human retina.

A practical algorithm for ocular imaging in veterinary medicine is as follows: B-scan ultrasonography is the initial imaging modality to assess intraocular abnormalities and the immediate retrobulbar space. Ultrasound biomicroscopy (UMB) has the best resolution for examination of the anterior segment. CT is the most appropriate imaging modality to evaluate orbital trauma and neoplastic involvement of the orbit. MRI is helpful in orbital mass localization and identification. Plain-film and computed radiography is more often used in veterinary medicine than are CT and MRI to examine orbital and nasal cavity disease. For disorders affecting the chiasmal and retrochiasmal pathways, MRI is the modality of choice. OCT and CSLO are beneficial in serial

examination of the optic nerve and NFL topography in dogs with glaucoma.

REFERENCES

1. Myer W. The cranial vault and associated structures. In: Thrall DE, ed. *Textbook of Veterinary Diagnostic Radiology,* 2nd ed. Philadelphia: WB Saunders, 1994: 23–39.
2. Thrall DE, ed. *Textbook of Veterinary Diagnostic Radiology,* 2nd ed. Philadelphia: WB Saunders, 1994.
3. Lattimer JC. Equine nasal passages and sinuses. In: Thrall DE, ed. *Textbook of Veterinary Diagnostic Radiology,* 2nd ed. Philadelphia: WB Saunders, 1994: 73–86.
4. Weiss RA, Haik BG, Saint-Louis LA, Ellsworth RM. Advance diagnostic imaging techniques in ophthalmology. *Adv Ophthal Plastic Reconstruct Surg* 1987; 6: 207–263.
5. Dennis R. Use of magnetic resonance imaging for the investigation of orbital disease in small animals. *J Small Anim Pract* 2000; 41: 145–155.
6. Hare WCD. Radiographic anatomy of the feline skull. *J Am Vet Med Assoc* 1959; 134: 349–355.
7. Stickle R. The equine skull. In: Thrall DE, ed. *Textbook of Veterinary Diagnostic Radiology,* 2nd ed. Philadelphia: WB Saunders, 1994: 66–72.
8. Caron JP, Barber SM, Bailey JV, et al. Periorbital skull fractures in five horses. *J Am Vet Med Assoc* 1986; 188: 280–284.
9. Smallwood JE, Spaulding KA. Radiographic anatomy of the dog and horse. In: Thrall DE, ed. *Textbook of Veterinary Diagnostic Radiology,* 2nd ed. Philadelphia: WB Saunders, 1994: 556–603.
10. Diesem C. Organs of vision. In: Getty R, ed. *Sisson and Grossman's the Anatomy of the Domestic Animals,* 5th ed. Philadelphia: WB Saunders, 1975: 703–719.
11. Diesem C. Gross anatomic structures of equine and bovine orbit and its contents. *Am J Vet Res* 1968; 29: 1769–1781.
12. Schebitz H, Wilkens H. *Atlas of Radiographic Anatomy of the Horse.* 3rd ed. Philadelphia: WB Saunders, 1978.
13. Johnston GR, Feeney DA. Radiology in ophthalmic diagnosis. *Vet Clin North Am Small Anim Pract* 1980; 10(2): 317–337.
14. Campbell W. The radiography of the lacrimal system. *Br J Radiol* 1964; 37: 1–26.
15. Iba GB, Hanafee WN. Distention dacryocystography. *Br J Radiol* 1968; 90: 1020–1022.
16. Gelatt KN, Guffy MM, Boggess TS III. Radiographic contrast techniques for detecting orbital and nasolacrimal tumors in dogs. *J Am Vet Med Assoc* 1970; 156: 741–746.
17. Yakely WL, Alexander JE. Dacryocystorhinography in the dog and cat. *J Am Vet Med Assoc* 1971; 159: 1417–1421.
18. Gelatt KN, Cure TH, Guffy MM, Jessen C. Dacryocystorhinography in the dog and cat. *J Small Anim Pract* 1972; 13: 381–397.
19. Latimer CA, Wyman M, Diesem CD, Burt JK. Radiographic and gross anatomy of the nasolacrimal duct of the horse. *Am J Vet Res* 1984; 45: 451–458.
20. Gilanpour H. Anatomic and radiographic studies of the lacrimal drainage system in sheep (*Ovis aries*). *Am J Vet Res* 1979; 40: 1177–1179.
21. Heider L, Wyman M, Burt J, Root C, Gardner H. Nasolacrimal duct anomaly in calves. *J Am Vet Med Assoc* 1975; 167: 145–147.
22. Sapienza JS, Isaza R, Johnson RD, Miller TR. Anatomic and radiographic study of the lacrimal apparatus of llamas. *Am J Vet Res* 1992; 53: 1007–1009.
23. Marini RP, Foltz CJ, Kersten D, Batchelder M, Kaser W, Li X. Microbiologic, radiographic, and anatomic study of the nasolacrimal duct apparatus in the rabbit. *Lab Anim Sci* 1996; 46: 656–662.
24. Naik MN, Tourani KL, Sekhar GC, Honavar SG. Interpretation of computed tomography imaging of the eye and orbit. A systemic approach. *Indian J Ophthalmol* 2002; 50: 339–353.
25. Daniel GB, Mitchell SK. The eye and orbit. *Clin Tech Small Anim Pract* 1999; 14(3): 160–169.
26. Hathcock JT, Russ LS. Principles and concepts of computed tomography. *Vet Clin North Am Small Anim Pract* 1993; 23(2): 399–415.
27. Penninck D, Daniel GB, Brawer R, Tidwell AS. Cross-sectional imaging techniques in veterinary ophthalmology. *Clin Tech Small Anim Pract* 2001; 16(1): 22–39.
28. Leib MC. The continuing utility of computed tomography in ophthalmology. *Ophthalmol Clin North Am* 1994; 7: 271–276.
29. Ketonen LM, Valanne LK, Berman EL. Current status of magnetic resonance imaging. *Ophthalmol Clin North Am* 1994; 7: 289–300.
30. Guy JR, Mancuso AA, Quisling R. The role of magnetic resonance imaging in optic neuritis. *Ophthalmol Clin North Am* 1994; 7: 449–458.
31. Karesh JW, Schnitzer DB, Chirico PA, Barrett CP. Advanced neuroimaging techniques for the demonstration of normal orbital, periorbital, and intracranial anatomy. In: Duane's Ophthalmology on CD-ROM. Foundation. Vol 1 Chapter 35. Philadelphia: Lippincott–Raven, 1998.
32. Dortzbach RK, Kronish JW, Gentry LR. Magnetic resonance imaging of the orbit. Part II. Clinical application. *Ophthalmol Plast Reconstr Surg* 1989; 5: 160–170.
33. Boroffka SA, Voorhout G. Direct and reconstructed multiplanar computed tomography of the orbits of healthy dogs. *Am J Vet Res* 1999 Dec; 60(12): 1500–1507.
34. Ramirez S, Tucker RL. Ophthalmic imaging. *Vet Clin North Am Large Anim Pract* 2004; 20: 441–457.
35. Tidwell AS, Ross LA, Kleine LJ. Computed tomography and magnetic resonance imaging of cavernous sinus enlargement in a dog with unilateral exophthalmos. *Vet Radiol Ultrasound* 1997 Sep-Oct; 38(5): 363–370.
36. Mafee MF, Jampol LM, Langer BG, Tso M. Computed tomography of optic nerve colobomas, morning glory anomaly, and colobomatous cyst. *Radiol Clin North Am* 1983; 25: 693–700.
37. Morgan RV, Daniel GB, Donnell RL. Magnetic resonance imaging of the normal eye and orbit of the dog and cat. *Vet Radiol Ultrasound* 1994; 35(2): 102–108.
38. Dortzbach RK, Kronish JW, Gentry LR. Magnetic resonance imaging of the orbit. Part 1. Physical principles. *Ophthalmic Plast Reconstr Surg* 1989; 5: 151–159.
39. Kronish JW, Dortzbach RK. Magnetic resonance imaging of the orbit. In: Duane's Ophthalmology on CD-ROM. Clinical. Vol 2 Chapter 25. Philadelphia: Lippincott–Raven, 1998.

40. Tidwell AS, Jones JC. Advanced imaging concepts: A pictorial glossary of CT and MRI technology. *Clin Tech Small Anim Pract* 1999 May; 14(2): 65–111.
41. Grahn BH, Stewart WA, Towner RA, Noseworthy MD. Magnetic resonance imaging of the canine and feline eye, orbit, and optic nerves and its clinical application. *Can Vet J* 1993; 34: 418–424.
42. Shores A. Magnetic resonance imaging. *Vet Clin North Am Small Anim Pract* 1993; 23(2): 437–459.
43. Davis PC, Newman NJ. Advances in neuroimaging of the visual pathways. *Am J Ophthalmol* 1996; 121: 690–705.
44. Morgan RV, Daniel GB, Donnell RL. Magnetic resonance imaging of the normal eye and orbit of the horse. *Prog Vet Comp Ophthalmol* 1993; 3: 127–133.
45. Boroffka S, van den Belt A. CT/ultrasound diagnosis—retrobulbar hematoma in a horse. *Vet Radiol Ultrasound* 1996; 37: 441–443.
46. Lee AG, Brazis PW, Garrity JA, White M. Imaging for neuro-ophthalmic and orbital disease. *Am J Ophthalmol* 2004; 138: 852–862.
47. Snyder WE. Veterinary medical photography: Close-up lenses. *Vet Med* 1968; 63: 898–899.
48. Patton DR. Photography of the external eye. *J Am Anim Hosp Assoc* 1973; 9: 278–282.
49. Jensen HE. Photographic techniques in small animal ophthalmology. *Vet Clin North Am* 1973; 3: 335–344.
50. Mandell AI, Foster CW, Luther JD. External photography of the eye. *Int Ophthalmol Clin* 1976; 16: 133–143.
51. Roberts SM, Kilminster A. Clinical photography. Proceedings of the American College of Veterinary Ophthalmology 1990: 30–37.
52. Miller PJ, Light J. A comparison of digital cameras. *Facial Plast Surg* 1999; 15(2): 111–117.
53. Vedantham V. Digital ophthalmic photography. *Indian J Ophthalmol* 2004; 52(1): 83–84.
54. Millichamp NJ, Wadsworth L, Dziezyc J, Yu-Speight A, Harris J, Sisley DR. Evaluation of digital imaging to document the adnexa and anterior segment in veterinary ophthalmology. In Proceedings. *35th Annual Conf Am Coll Vet Ophthalmol* 2004; 48.
55. Peterson RC, Wolffsohn JS. The effect of digital image resolution and compression on anterior eye imaging. *Br J Ophthalmol* 2005; 89: 828–830.
56. Rubin LF. *Atlas of Veterinary Ophthalmoscopy.* Philadelphia: Lea & Febiger, 1974.
57. Saurer H. Beitrag zur Photographie des Augenhintergrunde bei Haustieren. *Schweiz Arch Tierheilkd* 1947; 89: 199–205.
58. Luginbuhl H. Die Farbphotographische Darstellung des Augenhintergrundes bei ver sheidenen Haustieren. *Schweiz Arch Tierheilkd* 1958; 100: 187–195.
59. Donovan EF, Wyman M. Fundus photography of the dog and cat by means of the Noyori hand fundus camera. *Am J Vet Res* 1964; 25: 865–870.
60. Barnett KC, Keeler CR. Retinal photography in animals. *Br J Ophthalmol* 1968; 52: 200–201.
61. Barnett KC, Keeler CR. Fundus photography. *Vet Rec* 1967; 80: 624–627.
62. Rapkin JS, Rapkin KM, Wilson GW. Digital fundus imaging. *Ann Ophthalmol* 1991; 23: 46–53.
63. Kopp O, Markert S, Tornow RP. Comparing light sensitivity, linearity and step response of electronic cameras for ophthalmology. *Biomed Tech* 2002; 47(2): 602–605.
64. Hoang HD, Brant LM, Jaksetic MD, Lake SG, Stuart BP. Electronic imaging system incorporating a hand-held fundus camera for canine ophthalmology. *Contemp Top Lab Anim Sci* 2001; 40(6): 41–42.
65. DiLoreto D Jr, Grover DA, del Cerro C, del Cerro M. A new procedure for fundus photography and fluorescein angiography in small laboratory animal eyes. *Curr Eye Res* 1992; 24(suppl 1): 3–9.
66. Lichtman JW. Confocal microscopy. *Sci Am* 1994; 271: 40–45.
67. Schuman JS, Noecker RJ. Imaging of the optic nerve head and nerve fiber layer in glaucoma. *Ophthalmol Clin North Am* 1995; 8: 259–279.
68. Schuman JS. Imaging of the optic nerve head and nerve fiber layer in glaucoma. In: Epstein DL, Allingham RR, Schuman JS, eds. *Chandler and Grant's Glaucoma,* 4th ed. Baltimore: Williams & Wilkins, 1997: 104–119.
69. Fitzke FW. Imaging the optic nerve and ganglion cell layer. *Eye* 2000; 14(3B): 450–453.
70. Zwick H, Lund DJ, Elliot R, Schuschereba ST. Confocal spectral ophthalmoscopic imaging of retinal laser damage in small vertebrate eyes. *Proc Soc Photo-Optical Instrum Eng* 1995; 2393: 182–188.
71. Zwick H, Lund DJ, Elliot R, Schuschereba ST, Edsall PR. Small eye confocal scanning laser ophthalmoscopy and assessment of retinal damage. *Proc Soc Photo-Optical Instrum Eng* 1996; 2674: 80–88.
72. Chauhan BC, MacDonald CA. Influence of time separation on variability estimates of topographic measurements with confocal scanning laser tomography. *J Glaucoma* 1995; 4: 189–193.
73. Rohrschneider K, Burk R, Kruse FE, Völcker HE. Reproducibility of the optic nerve head topography with a new laser tomographic scanning device. *Ophthalmol* 1994; 101: 1044–1049.
74. Chmielewski NT, Brooks DE, MacKay EO, Dawson WW. Feline optic nerve head analysis using confocal laser tomography. *Invest Ophthalmol Vis Sci Abstract* 1996; 37: S1095.
75. Brooks DE, Kallberg ME, Komaromy AM, Ollivier FJ, Lambrou GN. Optic nerve head neuroretinal rim blood flow differences in monkeys with laser-induced glaucoma. *Vet Ophthalmol* 2005 Mar-Apr; 8(2): 113–119.
76. Rosolen SG, Saint-Macary G, Gautire V, LeGargasson J-F. Ocular fundus images with confocal scanning laser ophthalmoscopy in the dog, monkey and minipig. *Vet Ophthalmol* 2001; 4: 41–45.
77. Comer MG, Ciulla TA. Diagnostic imaging of retinal disease. *Int Ophthalmol Clin* 2004 Fall; 44(4): 1–15.
78. Stein DM, Wollstein G, Schuman JS. Imaging in glaucoma. *Ophthalmol Clin North Am* 2004; 17: 33–52.
79. Tjon-Fo-Sang M, van Strik R, de Vries J, Lemij HG. Improved reproducibility of measurements with the nerve fiber analyzer. *J Glaucoma* 1997; 6: 203–211.
80. Iester M, Mermoud A. Retinal NFL measured by Heidelberg retina tomography and nerve fiber analyzer. *Eur J Ophthalmol* 2005 Mar-Apr; 15(2): 246–254.
81. Puliafito CA, Hee MR, Schuman JS, Fujimoto JG. *Optical Coherence Tomography of Ocular Diseases.* Thorofare, NJ: Slack, 1996.
82. Jaffe GJ, Caprioli J. Optical coherence tomography to detect and manage retinal disease and glaucoma. *Am J Ophthalmol* 2004; 137: 156–169.

83. Schuman JS, Hee MR, Puliafito CA, et al. Quantification of nerve fiber layer thickness in normal and glaucomatous eyes using optical coherence tomography. *Arch Ophthalmol* 1995; 113: 586–596.
84. Dawson WW, Moores MD, Reitze DH, Brooks DE, Sergeev A, Gelatt KN. Comparison of optical coherence tomography (OCT) and histology at the neural rim in glaucoma. *Invest Ophthalmol Vis Sci Abstract* 1996; 37: S1152.
85. Wollstein G, Paunescu LA, Ko TH, et al. Ultrahigh-resolution optical coherence tomography in glaucoma. *Ophthalmology* 2005; 112: 229–237.
86. Huang D, Li Y, Radhakrishnan S. Optical coherence tomography of the anterior segment of the eye. *Ophthalmol Clin North Am* 2004; 17: 1–6.
87. Radhakrishnan S, Rollins AM, Roth JE, et al. Real-time optical coherence tomography of the anterior segment at 1310 nm. *Arch Ophthalmol* 2001; 119: 1179–1185.
88. Reiser BJ, Ignacio TS, Wang Y, et al. In vitro measurement of rabbit corneal endothelial thickness using ultrahigh resolution optical coherence tomography. *Vet Ophthalmol* 2005; 8(2): 85–88.
89. Modis L, Langenbucher A, Seitz B. Scanning-slit and specular microscopic pachymetry in comparison with ultrasonic determination of corneal thickness. *Cornea* 2001; 20(7): 711–714.
90. Modis Jr L, Langenbucher A, Seitz B. Corneal endothelial cell density and pachymetry measured by contact and noncontact specular microscopy. *J Cataract Refract Surg* 2002; 28: 1763–1769.
91. Masters BR, Bohnke M. Confocal microscopy of the human cornea in vivo. *Int Ophthalmol* 2001; 23: 199–206.
92. Hara M, Morishige N, Chikama T-I, Nishida T. Comparison of confocal biomicroscopy and noncontact specular microscopy for evaluation of the corneal endothelium. *Cornea* 2003; 6: 512–515.
93. Giraldez Fernandez MJ, Diaz Rey A, Cervino A, Yebra-Pimentel E. A comparison of two pachymetric systems: Slit-scanning and ultrasonic. *CLAO J* 2002; 28(4): 221–223.
94. Kawana K, Tokunaga T, Miyata K, Okamoto F, Kiuchi T, Oshika T. Comparison of corneal thickness measurements using Orbscan II, non-contact specular microscopy, and ultrasonic pachymetry in eyes after laser in situ keratomileusis. *Br J Ophthalmol* 2004; 88: 466–468.
95. Ogbuehi KC, Almubrad TM. Limits of agreement between the optical pachymeter and a noncontact specular microscope. *Cornea* 2005; 24(5): 545–549.
96. Pierro L, Conforto E, Giordano RA, Lattanzio R. High-frequency ultrasound biomicroscopy versus ultrasound and optical pachymetry for the measurement of corneal thickness. *Ophthalmologica* 1998; 212(suppl 1): 1–3.
97. Carrington SD. Woodward EG. Corneal thickness and diameter in the domestic cat. *Ophthal Physiol Opt* 1986; 6(4): 385–389.
98. Chan-Ling T, Efron N, Holden BA. Diurnal variation of corneal thickness in the cat. *Invest Ophthalmol Vis Sci* 1985 Jan; 26(1): 102–105.
99. Chan T, Payor S, Holden BA. Corneal thickness profiles in rabbits using an ultrasonic pachometer. *Invest Ophthalmol Vis Sci* 1983 Oct; 24(10): 1408–1410.
100. Schulz D, Iliev M E, Frueh BE, Goldblum D. In vivo pachymetry in normal eyes of rats, mice and rabbits with the optical low coherence reflectometer. *Vision Research* 2003; 43: 723–728.
101. Andrew SE, Willis AM, Anderson DE. Density of corneal cells, corneal thickness, and corneal diameters in normal eyes of llamas and alpacas. *Am J Vet Res* 2002 Mar; 63(3): 326–329.
102. Gilger BC, Wright JC, Whitley D, McLaughlin SA. Corneal thickness measured by ultrasonic pachymetry in cats. *Am J Vet Res* 1993; 54(2): 228–230.
103. Andrew SE, Ramsey DT, Hauptman JG, Brooks DE. Density of corneal endothelial cells and corneal thickness in eyes of euthanized horses. *Am J Vet Res* 2001 Apr; 62(4): 479–482.
104. Gilger BC, Whitley RD, McLaughlin SA, Wright JC, Drane JW. Canine corneal thickness measured by ultrasonic pachymetry. *Am J Vet Res* 1991 Oct; 52(10): 1570–1572.
105. Ramsey DT, Hauptman JG, Peterson-Jones SM. Corneal thickness, intraocular pressure, and optical corneal diameter in Rocky Mountain horses with cornea globosa or clinically normal corneas. *Am J Vet Res* 1999 Oct; 60(10): 1317–1321.
106. Plummer CE, Ramsey DT, Hauptman JG. Assessment of corneal thickness, intraocular pressure, optical corneal diameter, and axial globe dimensions in Miniature horses. *Am J Vet Res* 2003 Jun; 64(6): 661–665.
107. Ollivier FJ, Brooks DE, Komaromy AM, et al. Corneal thickness and endothelial cell density measured by noncontact specular microscopy and pachymetry in Rhesus macaques (Macaca mulatta) with laser-induced ocular hypertension. *Exp Eye Res* 2003; 76: 671–677.
108. Sailstad DM, Peiffer RL Jr. Specular microscopic observations of the corneal endothelium in the normal rabbit. *Lab Anim* 1981 Oct; 15(4): 393–395.
109. Stapleton S, Peiffer RL Jr. Specular microscopic observations of the clinically normal canine corneal endothelium. *Am J Vet Res* 1979 Dec; 40(12): 1803–1804.
110. Pigatto JAT, Laus JL, Abib FC, Pereira GT. Density and mean cell area of corneal endothelial cells in normal adult dogs using contact specular microscopy in vitro. 27 WSAVA Congress 2002.
111. Moodie KL, Hashizume N, Houston DL, et al. Postnatal development of corneal curvature and thickness in the cat. *Vet Ophthalmol* 2001; 4(4): 267–272.
112. MacCallum DK, Bahn CF, Lillie JH, Meyer RF, Martonyi CL. Evidence for corneal endothelial hypertrophy during postnatal growth of the cat cornea. *Invest Ophthalmol Vis Sci* 1983 Feb; 24(2): 247–250.
113. Tailoi CL, Curmi J. Changes in corneal endothelial morphology in cats as a function of age. *Curr Eye Res* 1988 Apr; 7(4): 387–392.
114. Montiani-Ferreira F, Peterson-Jones S, Cassotis N, Ramsey DT, Gearhart P, Cardoso F. Early postnatal development of central corneal thickness in dogs. *Vet Ophthalmol* 2003; 6(1): 19–22.
115. Gwin RM, Lerner I, Warren JK, Gum G. Decrease in canine corneal endothelial cell density and increase in corneal thickness as functions of age. *Invest Ophthalmol Vis Sci* 1982 Feb; 22(2): 267–271.
116. Montiani-Ferreira F, Cardoso F, Peterson-Jones S. Postnatal development of central corneal thickness in chicks of Gallus gallus domesticus. *Vet Ophthalmol* 2004; 7(1): 37–39.
117. Chan-Ling T, Curmi J. Changes in corneal endothelial morphology in cats as a function of age. *Curr Eye Res* 1988 Apr; 7(4): 387–392.

118. Befanis PJ, Peiffer RL Jr, Brown D. Endothelial repair of the canine cornea. *Am J Vet Res* 1981 Apr; 42(4): 590–595.
119. Matsuda M, Sawa M, Edelhauser HF, Bartels SP, Neufeld AH, Kenyon KR. Cellular migration and morphology in corneal endothelial wound repair. *Invest Ophthalmol Vis Sci* 1985 Apr; 26(4): 443–449.
120. Tuft SJ, Williams KA, Coster DJ. Endothelial repair in the rat cornea. *Invest Ophthalmol Vis Sci* 1986 Aug; 27(8): 1199–1204.
121. Ling TL, Vannas A, Holden BA. Long-term changes in corneal endothelial morphology following wounding in the cat. *Invest Ophthalmol Vis Sci* 1988 Sep; 29(9): 1407–1412.
122. Bourne WM, Nelson LR, Buller CR, Huang PT, Geroski DH, Edelhauser HF. Long-term observation of morphologic and functional features of cat corneal endothelium after wounding. *Invest Ophthalmol Vis Sci* 1994 Mar; 35(3): 891–899.
123. Huang PT, Nelson LR, Bourne WM. The morphology and function of healing cat corneal endothelium. *Invest Ophthalmol Vis Sci* 1989 Aug; 30(8): 1794–1801.
124. Brogdon JD, McLaughlin SA, Brightman AH, Helper LC. Effect of epidermal growth factor on healing of corneal endothelial cells in cats. *Am J Vet Res* 1989 Aug; 50(8): 1237–1243.
125. Neuenschwander H, Julia C, Wyman M, Kador PF. Endothelial changes in galactose-fed dogs. *Curr Eye Res* 1995 Apr; 14(4): 319–322.
126. Yee RW, Matsuda M, Kern TS, Engerman RL, Edelhauser HF. Corneal endothelial changes in diabetic dogs. *Curr Eye Res* 1985 Jul; 4(7): 759–766.
127. Gwin RM, Warren JK, Samuelson DA, Gum GG. Effects of phacoemulsification and extracapsular lens removal on corneal thickness and endothelial cell density in the dog. *Invest Ophthalmol Vis Sci* 1983 Feb; 24(2): 227–236.
128. Olson RJ. Air and the corneal endothelium: An in vivo specular microscopy study in cats. *Arch Ophthalmol* 1980 Jul; 98(7): 1283–1284.
129. Gerding PA Jr, Essex-Sorlie D, Yack R, Vasaune S. Effects of intracameral injection of tissue plasminogen activator on corneal endothelium and intraocular pressure in dogs. *Am J Vet Res* 1992 Jun; 53(6): 890–893.
130. Gerding PA Jr., McLaughlin SA, Brightman AH, Essex-Sorlie D, Laing RA, Hirokawa K. Effects of intracameral injection of viscoelastic solutions on corneal endothelium in dogs. *Am J Vet Res* 1990 Jul; 51(7): 1086–1088.
131. Nasisse MP, Cook CS, Harling DE. Response of the canine corneal endothelium to intraocular irrigation with saline solution, balanced salt solution, and balanced salt solution with glutathione. *Am J Vet Res* 1986 Oct; 47(10): 2261–2265.
132. Harris LS, Toyofuku H, Shimmyo M. Fluorescein iris angiography in the albino rabbit. *Arch Ophthalmol* 1972; 88: 193–195.
133. Bellhorn RW. Fluorescein fundus photography in veterinary ophthalmology. *J Am Anim Hosp Assoc* 1973; 9: 227–233.
134. Gelatt KN, Henderson JD Jr, Steffen GR. Fluorescein angiography of the normal and diseased ocular fundi of the laboratory dog. *J Am Vet Med Assoc* 1976; 169: 980–984.
135. Peruccio C, Helper LC, Monti F, Brightamn AH. Fundus fluoroangiography in the cat. *J Am Anim Hosp Assoc* 1982; 18: 939–945.
136. Davidson MG, Baty KT. Anaphylaxis associated with intravenous sodium fluorescein administration in a cat. *Prog Vet Comp Ophthalmol* 1991; 1: 127–128.
137. Guyer DR, Puliafito CA, Mones JM, et al. Digital indocyanine-green angiography in chorioretinal disorders. *Ophthalmol* 1992; 99: 287–291.
138. Weinhaus RS, Burke JM, Delori FC, et al. Comparison of fluorescein angiography with microvascular anatomy of macaque retinas. *Exp Eye Res* 1995; 61: 1–16.
139. De Schaepdrijver L, Simoens P, Lauwers H. Fluorescein angiography of the canine retina. *Vet Comp Ophthalmol* 1996; 6: 111–119.
140. Rumelt MB. A simplified technique for anterior segment fluorescein angiography. *Am J Ophthalmol* 1974; 78: 1029–1031.
141. Bergstrom JJ, Roth M, Martonyi CL. Pigmented iris angiography. *Arch Ophthalmol* 1976; 94: 1180–1182.
142. Hill DW, Young S. Arterial fluorescence angiography of the fundus oculi of the cat: Appearances and measurements. *Exp Eye Res* 1973; 16: 457–465.
143. Newsom WA, Levereh SD Jr, Kirkland VE. Retinal fluorescence angiography of the rhesus monkey. *Arch Ophthalmol* 1968; 79: 768–774.
144. Gasthuys F, Pollet L, Simoens P, Lauwers H, De Laey JJ. Anesthesia for fluorescein angiography of the ocular fundus in the miniature minipig. *Vet Res Commun* 1990; 14: 393–402.
145. De Shaepdrijver L, Simoens P, Pollet L, Lauwers H, De Laey JJ. Morphologic and clinical study of the retinal circulation in the miniature pig. B: Fluorescein angiography of the retina. *Exp Eye Res* 1992 Jun; 54(6): 975–985.
146. Satoh T, Yamaguchi K. Ocular fundus abnormalities detected by fluorescein and indocyanine green angiography in the Royal College of Surgeons dystrophic rat. *Exp Anim* 2000; 49(4): 275–280.
147. Chopdar A. *Fundus Fluorescein Angiography.* Oxford: Butterworth-Heinemann Ltd, 1996.
148. O'Brart DPS, de Souza Lima M, Bartsch DU, Freeman W, Weinreb RN. Indocyanine green angiography of the peripapillary region in glaucomatous eyes by confocal scanning laser ophthalmoscopy. *Am J Ophthalmol* 1997; 123: 657–666.
149. Yannuzzi LA, Flower RW, Slakter JS. *Indocyanine Green Angiography.* St. Louis: Mosby, 1997.
150. Rechtman E, Harris A, Kumar R, et al. An update on retinal circulation assessment technologies. *Curr Eye Res* 2003; 27(6): 329–343.
151. Nishijima K, Kiryu J, Tsujikawa A, et al. In vivo evaluation of platelet-endothelial interactions after transient retinal ischemia. *Invest Ophthalmol Vis Sci* 2001 Aug; 42(9): 2102–2109.
152. Hamada M, Ogura Y, Miyamoto K, Nishiwaki H, Hiroshiba N, Honda Y. Retinal leukocyte behavior in experimental autoimmune uveoretinitis of rats. *Exp Eye Res* 1997 Sep; 65(3): 445–450.
153. Rosolen SG, Saint-Macary G, Gautier, LeGargasson. SLO angiography: Arterio-venous filling times in monkey and minipig. *Vet Ophthalmol* 2002; 5(1): 19–22.
154. Khoobehi B, Peyman GA. Fluorescent labeling of blood cells for evaluation of retinal and choroidal circulation. *Ophthalmic Surg Lasers* 1999 Feb; 30(2): 140–145.

155. Fillacier K, Peyman GA, Luo Q, Lhoobehi B. Study of lymphocyte dynamics in the ocular circulation: Technique of labeling cells. *Curr Eye Res* 1995 Jul; 14(7): 579–584.
156. Kim J, Yang Y, Cho C. Visualization and flow of platelets and leukocytes in vivo in rat retinal and choroidal vessels. *Ophthalmic Res* 1997; 29(6): 374–380.
157. Harris A, Kagemann L, Cioffi GA. Assessment of human ocular hemodynamics. *Surv Ophthalmol* 1998 May-June; 42(6): 509–533.
158. Cutler TJ, Brooks DE, Kallberg ME, Komaromy AM, Miyabayashi, Gelatt KN. Effect of amlodipine on ocular blood flow in Beagles with POAG. *Invest Ophthalmol Vis Sci* 2001; 42, S415.
159. Brooks DE, Kallberg ME, Cannon RL, et al. Functional and structural analysis of the visual system in the rhesus monkey model of optic nerve head ischemia. *Invest Ophthalmol Vis Sci* 2004 Jun; 45(6): 1830–1840.

Chapter 9

Ophthalmic Examination and Diagnostics

Part 3: Diagnostic Ultrasonography

Ursula M. Dietrich

PHYSICS AND BASIC PRINCIPLES

Ultrasonography is a noninvasive imaging technique used for the qualitative and quantitative evaluation of intraocular and orbital lesions.[1–16] It is a safe and rapid method, relatively easy to learn, and can be performed in an awake animal. Ultrasonography is indicated in eyes with opaque ocular media when an ophthalmic examination can no longer be performed (corneal edema, hyphema, cataract, vitreous hemorrhage)[1–13] and in eyes with ocular trauma[8] or suspected orbital disease.[14–16] Other indications involve biometric measurements of intraocular and orbital structures[17–19] and determination of axial eye length for artificial lens power calculations.[20–23]

The ultrasonic beam is a series of acoustic waves with a frequency greater than 20 KHz (20,000 oscillations/sec) and is therefore inaudible to humans. Ultrasound frequencies used in ocular diagnostics usually range from 7.5 to 50 MHz.[24] A piezoelectric crystal, which is built into the front of the ultrasound transducer, responds to an electrical stimulus with mechanical deformation and the emission of ultrasound waves.[24–26] Sound waves require a medium, such as liquids, tissue, or gas, for their transmission and are propagated as longitudinal waves. Particles (molecules) in the medium oscillate in the direction of wave propagation and transfer energy to the neighboring molecules.[25] Travel velocity of ultrasound in a medium depends on the density and compressibility of this medium. A liquid medium is more compressible than a solid medium, so, for example, sound waves pass through vitreous much more slowly than through the lens.[24] This medium-specific resistance to sound propagation is called the acoustic impedance, which is the product of density and sound velocity within this medium. The wave nature of ultrasound is similar to optical radiation and obeys the same fundamental laws of reflection and refraction.[23] If the sound waves strike an acoustic interface, which is the junction of two ocular media with different acoustic impedances (e.g., lens–vitreous, vitreous–retina), an echo occurs and part of the wave is reflected back to the transducer. The piezoelectric crystal receives this echo, processes it, and displays the signal on the screen.[24–26]

Echo strength is largely dependent on the physical structure of the medium; the angle of sound incidence; and the size, shape, and smoothness of the acoustic interface.[24] If the ultrasound beam strikes a smooth surface (e.g., lens capsule) perpendicularly, almost all of the wave is reflected back to the transducer and a maximal echo is produced on the screen. The sharper the angle of the sound wave that hits the interface, the more sound energy is diverted away and weaker the returning echoes.[24] On very rough interfaces, the sound waves are scattered, and the returning echoes are very weak. Likewise, intense scattering occurs on very small structures and with increasing ultrasound frequency.[24] Ultrasound energy is gradually absorbed as the ultrasound waves propagate through tissue.[26] Absorption of sound energy is measured in decibel (dB) and is dependent on the frequency of the sound waves. Depth of sound wave penetration in tissue is directly proportional to the wavelength. For example, the ultrasound waves of a low-frequency, 7.5-MHz ultrasound transducer provide poor ocular near-field visualization but better tissue penetration. Therefore, this type of transducer is best used for examination of the orbit and retrobulbar area. On the other hand, high-frequency ultrasound waves (20–50 MHz) penetrate only a few millimeters into tissue and therefore allow excellent imaging of the anteriorly located structures of the eye.[24]

A-MODE

A-mode (amplitude modulation) is the most original of all ultrasound methods. Echoes received by the transducer are displayed one-dimensionally and time-dependent as vertical spikes (amplitudes) from a baseline.[24–26] The height of the spike reflects the intensity of the echo. The distance between individual spikes depends on the time required for the ultrasound waves to reach a given acoustic interface and for their echo to return to the transducer. Spacing of spikes on the horizontal baseline also reflects the spatial distribution of the structures being examined.[24] Diagnostic A-mode was standardized for use in human ophthalmology by Karl Ossoinig.[27] It requires specific instrumentation and a nonfocused, 8-MHz

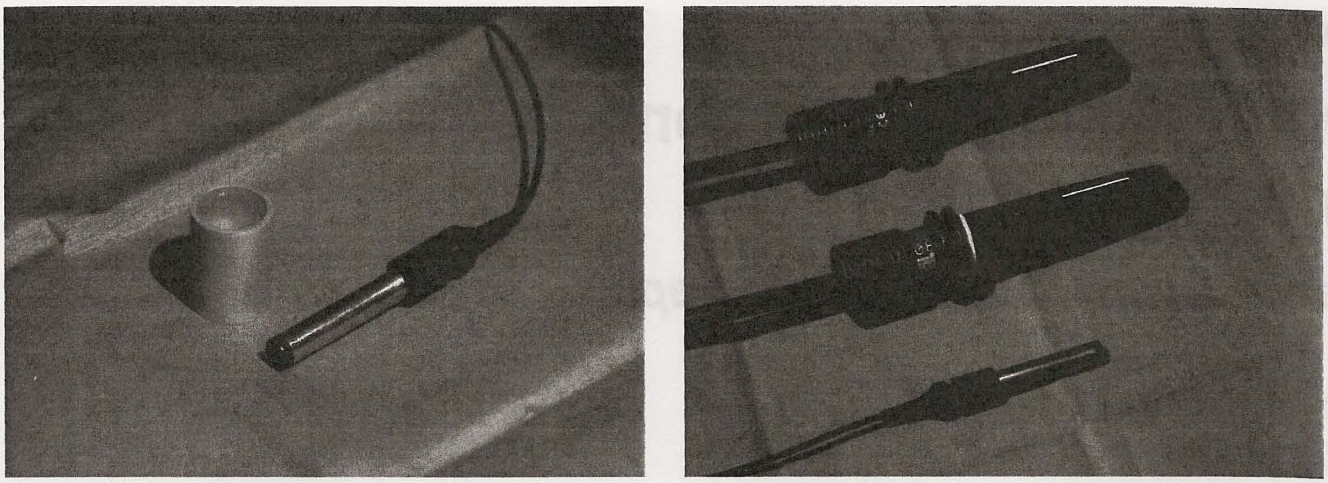

(a) (b)

Figure 9.3.1. A. Standardized diagnostic A-mode probe with tissue model for external calibration. **B.** Ocular ultrasound probes. *Top:* Diagnostic 10 MHz B-mode probe. The white marker on the probe tip designates upper portion of the echogram. *Middle:* High-frequency (20 MHz) diagnostic B-mode probe. *Bottom:* Standardized diagnostic 8 MHz A-mode probe. (Courtesy of University of Georgia and the University of Munich.)

transducer, which is externally calibrated with a tissue model[27] (Fig. 9.3.1A). If used in combination with a B-mode scan, standardized diagnostic A-mode provides objective and accurate information about the internal reflectivity of ocular lesions and is the most reliable method for the diagnosis of retinal detachment in humans.[24,27] The use of diagnostic A-mode is somewhat limited in veterinary ophthalmology because the interpretation of the spike pattern in a moving eye is difficult. However, earlier reports document the successful diagnosis of retinal detachment and vitreous hemorrhage in dogs with A-mode ultrasound.[2] Many ophthalmic ultrasound machines incorporate a vector A-scan within the B-mode picture.

Although this vector-A-scan method is different from diagnostic A-scan, it may greatly improve the diagnostic accuracy of ocular ultrasound and is especially useful in veterinary ophthalmology. Whereas B-mode may yield information about the topography of an ocular or orbital lesion, the vector A-scan may provide objective information on a lesion's character and size.[28,29] Also, ocular measurements can be performed with the B-mode guided vector A-scan and were shown to be as accurate as measurements performed with a biometric A-mode probe.[30]

Biometric A-scan is commonly used for axial eye length measurements in both human and veterinary ophthalmology and requires a special biometric A-mode transducer.[24] It is the method of choice for in vivo measurement of intraocular distances, such as anterior chamber depth, axial lens thickness, vitreous body, and axial globe length.[17–19] Measurements of the anterior–posterior axial globe length for calculation of intraocular lens dioptric strength have been performed in dogs and cats.[20–23]

B-MODE

In B-mode (brightness modulation) ultrasound, echoes are displayed two-dimensionally as light dots of different intensity and brightness on the screen. The coalescence of multiple dots forms a picture that reassembles a histological "slice" of the examined tissue.[24] The quality of the B-mode picture largely depends on the technical characteristics of the ultrasound machine, such as signal processing, gray scale, and speed of transducer oscillation.[24–26] Most B-mode transducers are real-time sector scanners with a very fast frame rate of 10 to 60 frames/second, allowing visualization of movement during the scanning process.[24]

B-scan ultrasonography is the most commonly used echographic method for evaluation of intraocular and orbital lesions in veterinary ophthalmology.[1,3–16] A standard 10-MHz transducer with a focal range of 3 to 4 cm is the most suitable ophthalmic transducer, allowing visualization of anterior and posterior segment abnormalities as well as orbital lesions.[8] However, structures very close to the transducer tip (cornea, anterior chamber, iris) are more difficult to image with a 10-MHz transducer because of near-field reverberation artifacts.[8] For an improved examination of the anterior segment, a water-bath technique is helpful and may consist of a water-filled glove placed between the closed eyelids and the transducer.[5] Ultrasound probes with higher frequencies between 20 and 35 MHz (high-frequency ultrasound) and 50 and 100 MHz (ultrasound biomicroscopy) have been developed and allow a highly magnified examination of the cornea, sclera, anterior chamber, iris, iridocorneal angle, ciliary body, and anterior lens capsule.[31,32] With high-frequency ultrasound, tissue resolutions between 20 and 80 microns can be achieved with pictures comparable to a low-power microscopic view of ocular structures.[31,32]

EXAMINATION TECHNIQUE

The ultrasound transducer is placed directly onto the cornea after a topical anesthetic (e.g., proparacaine) has been instilled into the eye. Ocular transducers have a small scan head, which

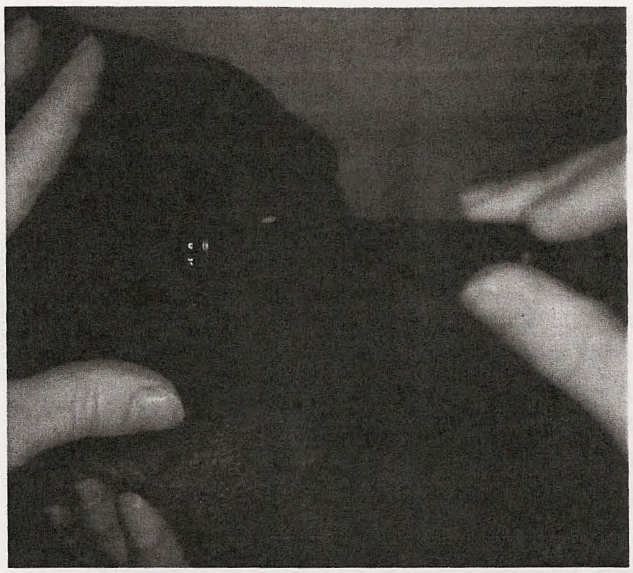

Figure 9.3.2. Vertical axial scan: the white marker on the probe tip points dorsally. (Modified with permission from Dietrich U. Ultrasonographic examination of the eyes of dogs with cataracts using the combined B-mode/vector A-scan system. Inaugural dissertation. Ludwig-Maximilians-University, Munich, Germany 1996.)

Figure 9.3.3. Horizontal axial scan: the white marker on the probe tip points nasally. (Courtesy of University of Georgia and the University of Munich.)

facilitates positioning on the cornea. The corneal contact method is the preferred examination technique and allows the best possible imaging of the globe and orbit.[5–8] Scanning of the eye through the closed lids is less desirable because of sound attenuation produced by the lid tissues.[24] However, it is the recommended examination technique in case of a corneal injury, ocular trauma, or after intraocular surgery to avoid further damage to the cornea.[23,27] It is very important to use a large amount of coupling gel, such as methylcellulose, on the cornea or lids to decrease near-field reverberation artifacts.[23]

Ultrasound examination is performed in a vertical and horizontal plane and initially in an axial direction,[1,5,8] with the lens being a landmark for orientation within the globe.[24] A white marker on the tip of the transducer indicates the plane of scanning and the side of the transducer, which is represented on the upper portion of the B-scan screen[24] (Fig. 9.3.1B). In vertical axial direction (the marker points dorsally), the meridian of the opposite fundus between twelve o'clock and six o'clock is examined (Fig. 9.3.2). If the probe is directed in horizontal axial direction (the marker points nasally), the meridian between three o'clock to nine o'clock can be evaluated[24] (Fig. 9.3.3). In each plane, the transducer is slightly shifted dorsally and ventrally, so the most peripheral areas of the opposite fundus dorsally and ventrally can be assessed.[5] Examination of the opposite normal eye and orbit is highly recommended as a "normal" control for comparison purposes.

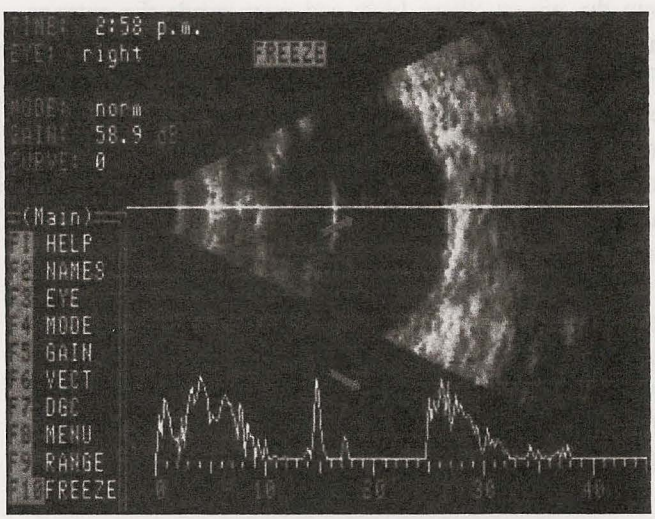

Figure 9.3.4. Normal B-mode/vector A-scan echogram of a canine eye. The integrated vector A-scan is displayed on the bottom half of the screen. Echoes appear as bright lines or dots of different intensity on B-mode and as vertical spikes from a horizontal baseline on the A-scan vector. In axial vertical direction (white marker points dorsally), the posterior lens capsule produces a strong echo on B- and A-mode (*arrows*). The strong posterior eye wall echo contrasts against the acoustically empty vitreous. (Modified with permission from Dietrich U. Ultrasonographic examination of the eyes of dogs with cataracts using the combined B-mode/vector A-scan system. Inaugural dissertation. Ludwig-Maximilians-University, Munich, Germany 1996.)

NORMAL ULTRASONOGRAPHIC FINDINGS ON A- AND B-MODE

Structures in the globe and orbit are described as hyperechoic, hypoechoic, or anechoic, depending on the presence and strength of the returning echo. In a normal eye, and by using a 10-MHz sector scanner, strong single echoes are received from the cornea, anterior and posterior lens capsule, and posterior eye wall.[8] Those echoes appear as vertical spikes on the A-mode axis or as bright, reflective lines on B-mode (Fig. 9.3.4). With a water-bath technique, the anterior chamber can be visualized as an anechoic, black area on B-mode. The iris may be more difficult to visualize in dogs and cats, but the iris

and corpora nigra are easily recognized in the horse.[8] The normal lens is translucent, and only the posterior lens capsule can be visualized as a highly reflective, concave line on B-mode. Anterior chamber and vitreous are clear and anechoic and appear as a homogenous black area on B-mode or a horizontal line on A-mode. The vitreous is bordered posteriorly by the eye posterior eye wall echo. This strong echo is composed of retina, choroid, and sclera, which cannot be differentiated from each other echographically.[24] The adjacent orbital soft tissue, composed of fat, connective tissue, nerves, and blood vessels, is depicted as a highly reflective and heterogenous area on B-mode and represented by a series of multiple, gradually declining echoes of different height on A-mode.[24] The optic nerve can be visualized as a cone-shaped, elongated, hyporeflective area in the medioventral part of the orbit.[1,5,8] Retrobulbar muscles are recognized as thin, elongated hypoechoic structures with attachments at the globe.[1,5]

Anterior segment lesions

Neoplasia

Neoplasia in the anterior segment typically present as circumscribed, echodense, masslike structures. They usually arise from the iris or ciliary body and may invade the anterior chamber or vitreous, causing lens luxation or subluxation[3,4] (Fig. 9.3.5). Iris melanoma is the most common type of iris neoplasia. In the dog, it usually arises as a densely pigmented structure from the iris surface and requires differentiation from iris cysts. On ultrasound, iris melanoma appears acoustically dense and solid, whereas iris cysts have an anechoic, fluid-filled center, surrounded by a thin cyst wall (Fig. 9.3.6). It may be advantageous to use a water-bath standoff or high-frequency ultrasound for better anterior segment resolution, especially if the neoplasia is very small. Hyphema and hypopyon may appear as rather echodense, pointlike lesions, whereas fibrin in the anterior chamber produces single hyperreflective strands.[8]

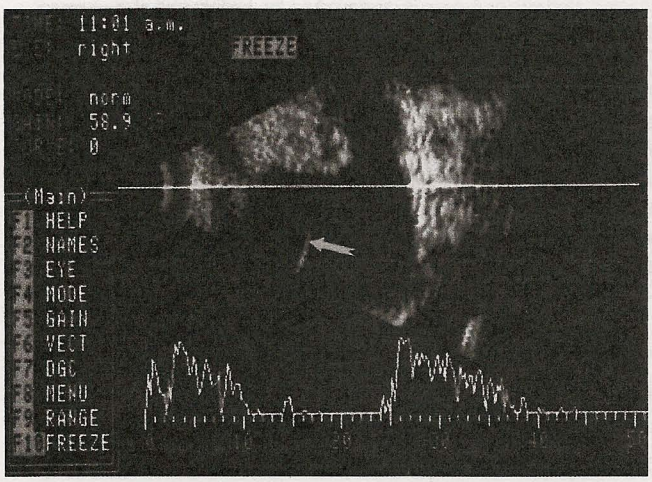

Figure 9.3.5. Ciliary body tumor (*T*) invading the vitreous and causing a lens subluxation (*arrow*). (Courtesy of University of Georgia and the University of Munich.)

Lens

Nucleus sclerosis or cataract formation increases the internal reflectivity of the lens, which is normally an anechoic structure. Depending on the distribution, density, and maturity of the cataract, single or multiple echoes may be received from within the lens, and the equatorial regions of the lens become clearly outlined[8,24] (Fig. 9.3.7). The more mature and calcified the lens is, the stronger and brighter the echoes within the lens become. Lens thickness may be increased in a mature cataract[13] or decreased in a hypermature or resorbing cataract[8] (Fig. 9.3.8). Ocular ultrasound is an important part of the preoperative evaluation process for cataract surgery, and lens anomalies, embryonal remnants in the vitreous, vitreous degeneration, or retinal detachment may be detected prior to

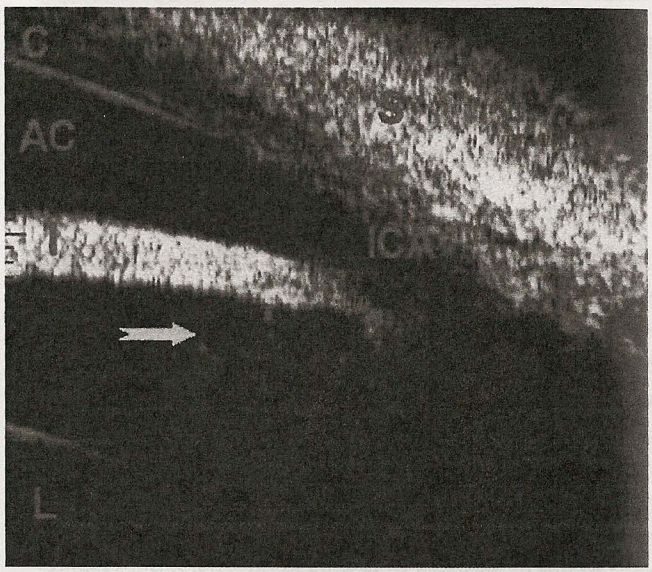

Figure 9.3.6. Ultrasound biomicroscopy (50 MHz) of an iris cyst (*arrow*) in a Boston Terrier. The cyst is behind the iris, has no internal reflectivity, and is surrounded by a thin cyst wall. *S,* sclera; *C,* cornea; *ICA,* iridocorneal angle; *I,* iris; *AC,* anterior chamber; *L,* lens. (Courtesy of University of Georgia and the University of Munich.)

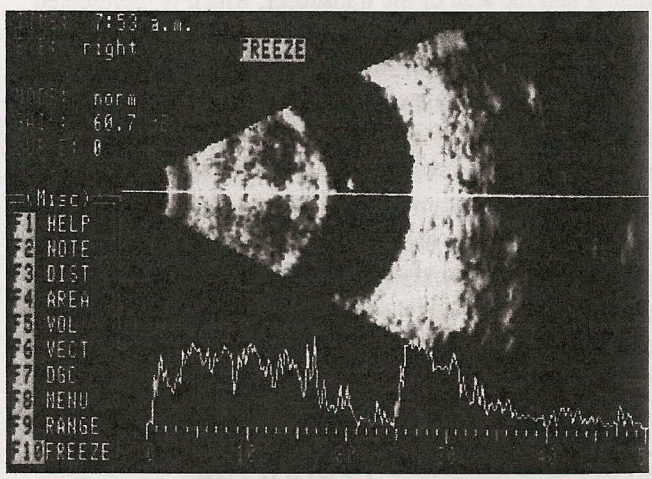

Figure 9.3.7. B-mode ultrasound of a mature cataract in a diabetic dog. The internal reflectivity of the lens is increased (strong echoes on B- and A-mode), and both the anterior and posterior lens capsules are well outlined. The lens is intumescent and larger in size. (Courtesy of University of Georgia and the University of Munich.)

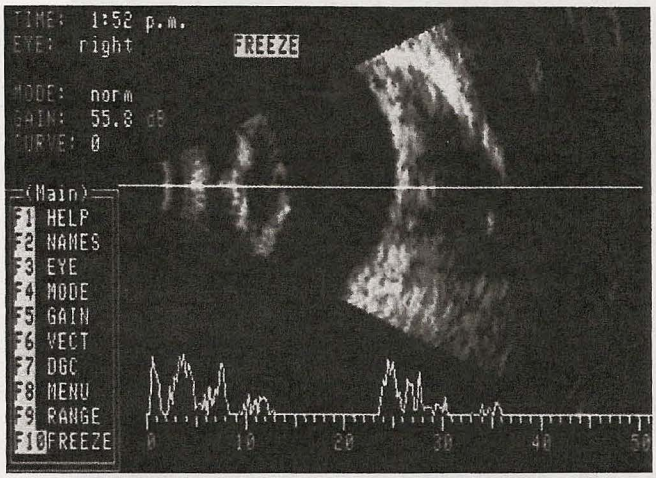

Figure 9.3.8. Hypermature cataract. The lens has decreased in size and has a wrinkled and irregular anterior and posterior lens capsule. (Courtesy of University of Georgia and the University of Munich.)

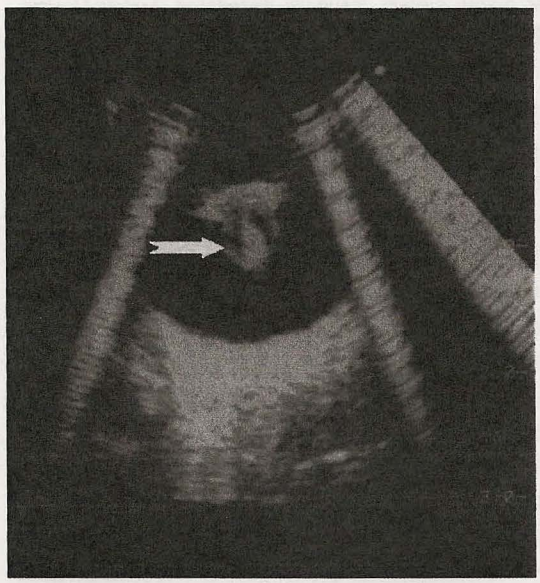

Figure 9.3.9. Posterior lenticonus (*arrow*) in a young Bloodhound puppy. (Courtesy of University of Georgia and the University of Munich.)

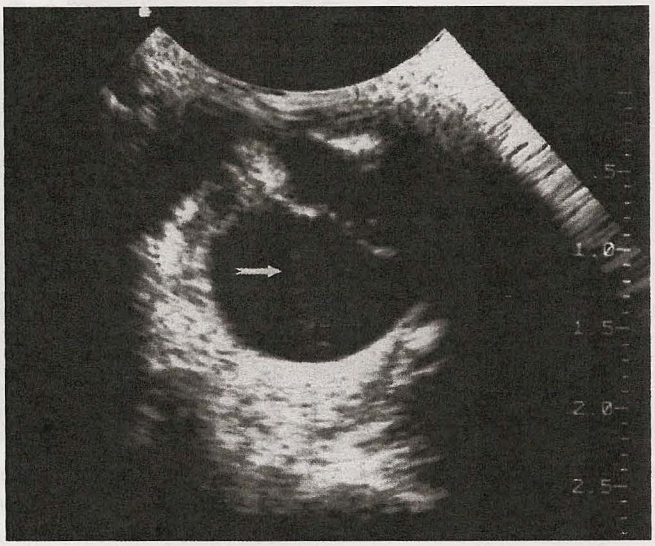

Figure 9.3.10. Persistent hyperplastic primary vitreous/persistent tunica vasculosa lentis (PHPV/PHTVL) in a Doberman Pinscher. The hyaloidea is attached to the posterior lens capsule (*arrow*) and appears as a linear, highly reflective structure on the B-mode echogram. (Courtesy of University of Georgia and the University of Munich.)

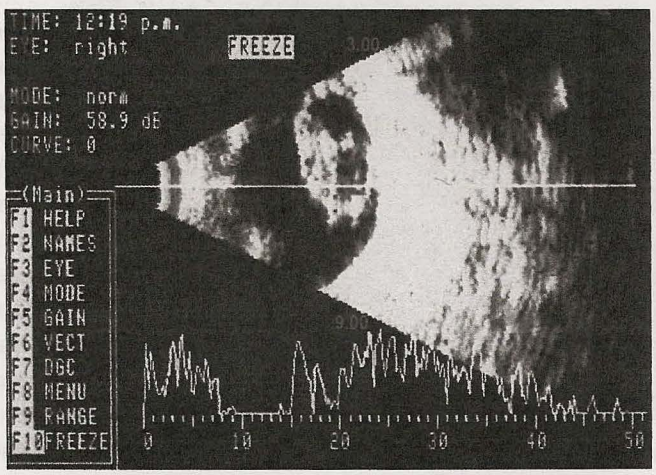

Figure 9.3.11. Horizontal B-mode/vector A-scan echogram of a posterior lens luxation in a Shi Tzu. The lens is recognized as a round structure in the vitreous with high internal reflectivity and a smooth, highly reflective capsule. (Courtesy of University of Georgia and the University of Munich.)

surgery[8–12,29] (Figs. 9.3.9 and 9.3.10). In an anterior or posterior lens luxation, the lens can be visualized as a spherical structure with smooth, very highly reflective borders[8] (Fig. 9.3.11). A lens subluxation may be more difficult to detect but is suspected if the echoes of the anterior and posterior lens capsule are not aligned in an axial scan (Fig. 9.3.12). A lens subluxation can also result in an increased or decreased anterior chamber depth.[8]

Posterior Segment Lesions

Posterior segment lesions appear as pointlike, membranelike, or masslike structures on B-mode.[24] The vitreous is acoustically empty in the normal eye and recognized as a homogenous, black area on B-mode or as a horizontal, flat line on A-mode. Pathologic changes in the vitreous include hemorrhage, inflammation, membrane formation, degeneration, and embryologic remnants. Fresh hemorrhage and inflammatory cells produce very diffuse, pointlike echoes of low or medium reflectivity. In severe ocular hemorrhage, the posterior eye wall echo is very weak, and the lens may appear as a clear anechoic structure with distinct capsule echoes (Fig. 9.3.13). Organized hemorrhage and blood clots have an increased reflectivity and masslike appearance, and they may be falsely interpreted as an intraocular neoplasia. Degeneration (syneresis) of the vitreous creates multifocal dots or linear structures in the vitreous cavity of medium to high reflectivity.[8,9] It is important to increase the gain setting during the examination of the vitreous in order to detect very fine echoes that may otherwise go unnoticed.[24] The calcium lipid deposits in asteroid hyalosis produce very strong, multifocal bright echoes on B-mode, and they appear clustered in the center of the vitreous.[8] On A-mode, asteroid hyalosis produces multiple echoes of medium to high amplitude, and typically, an anechoic zone is

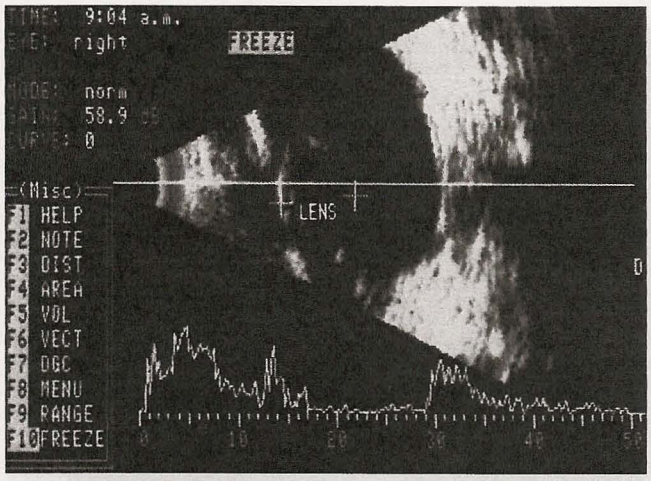

Figure 9.3.12. B-mode/vector A-mode ultrasound of a lens subluxation in a dog. Echoes of the anterior and posterior lens capsule are no longer aligned in an axial scan. The lens has shifted ventrally. (Courtesy of University of Georgia and the University of Munich.)

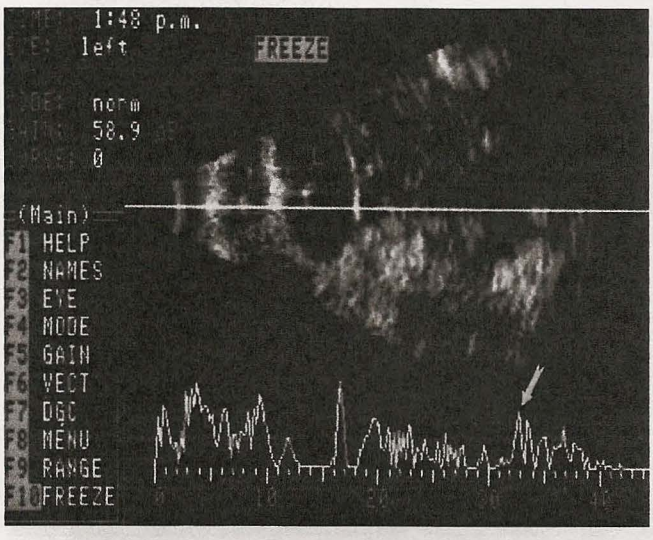

Figure 9.3.13. B-mode/vector A-scan echogram of an eye with ocular hemorrhage after blunt trauma. The hemorrhage is fresh and provides multiple, diffuse echoes in the vitreous and anterior chamber. The corresponding echoes on the A-scan vector are of low to medium amplitude. The lens (*L*) can be identified as an anechoic structure on B-mode and produces strong anterior and posterior lens capsule echoes on A-mode. A distinct posterior eye wall echo is no longer visible on B-mode but can easily be detected on the A-scan (*arrow*). (Courtesy of University of Georgia and the University of Munich.)

observed between the vitreous opacities and the posterior eye wall[29] (Fig. 9.3.14). In fresh posterior uveitis or endophthalmitis, inflammatory debris in the vitreous is recognized as finely distributed bright echoes[7] on B-mode or multiple spikes on the horizontal axis on A-mode (Fig. 9.3.15). In long-standing hemorrhage or inflammation, membrane formation in the vitreous may be observed.[4]

Diagnosis of a complete retinal detachment is facilitated by its typical appearance on ultrasound. The detached retina is seen as a highly reflective, continuous, linear structure with attachments at the optic disc posteriorly and ora ciliaris retina anteriorly, resembling the wings of a seagull[1,4,7–9] (Fig.

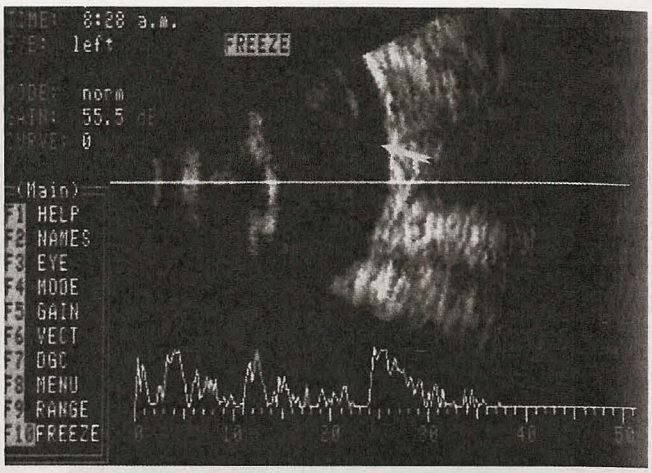

Figure 9.3.14. Asteroid hyalosis. The calcium-phosphate crystals are diffusely distributed throughout the vitreous but leave an anechoic zone between opacities and posterior eye wall (*arrow*). This is a typical finding in asteroid hyalosis. (Modified with permission from Dietrich U. Ultrasonographic examination of the eyes of dogs with cataracts using the combined B-mode/vector A-scan system. Inaugural dissertation. Ludwig-Maximilians-University, Munich, Germany 1996.)

9.3.16A). On A-mode, a 100% high spike is produced when the ultrasound beam is directed perpendicular to the detachment[24,27] (Fig. 9.3.16B). In a fresh retinal detachment, undulating movement of the retina during real-time scanning may be observed.[24] In long-standing retinal detachment, the retina often takes the form of a funnel-shaped membrane that can be open or closed[24] (Fig. 9.3.17). Other differential diagnoses for linear, highly reflective structures include dense vitreous membranes (sequelae to long-standing intraocular inflammation or vitreous hemorrhage) or giant retinal tears in a rhegmatogenous detachment. In both cases, the linear structure may have an unusual insertion at the optic disc.[24] A careful B-mode examination in different planes, combined with standardized A-mode, should be performed in all vitreoretinal diseases.

Orbital Lesions

Most orbital lesions (neoplasia, abscess) have a more homogenous composition than normal orbital tissue, and if they are large enough to produce clinical symptoms, they can be easily detected.[8,14–16] Depending on the type of lesion, the affected area may exhibit higher or lower reflectivity. An abscess can be identified as a cystlike, well-circumscribed area of a very low internal reflectivity (Fig. 9.3.18), whereas an orbital neoplasia is characterized by increased reflectivity and a more invasive growth pattern.[16]

For orbital scans, the scan head is placed directly onto the cornea, or alternatively, the transducer can be placed on the shaved skin caudal to the orbital ligament.[15] This allows improved scanning of the optic nerve, orbital fissure, optic canal, and extraocular muscles because these structures are oriented perpendicular to the ultrasound beam.[15] In some cases, computed tomography (CT) and magnetic resonance imaging (MRI) were found to provide better information

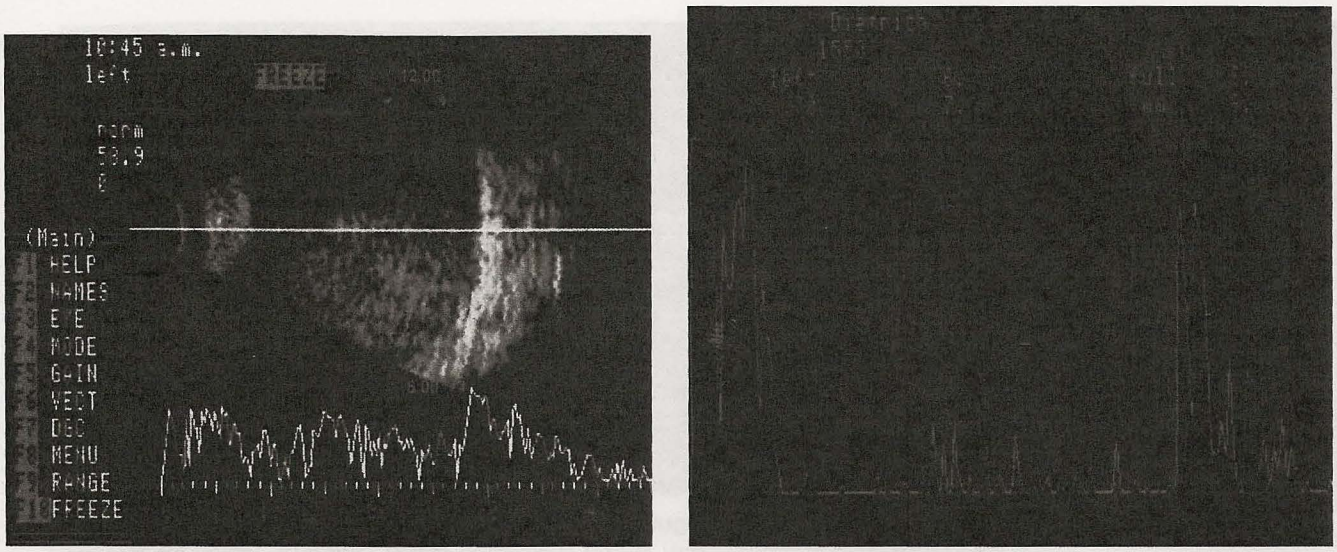

(a) (b)

Figure 9.3.15. **A.** B-mode/vector A-scan echogram of an eye with endophthalmitis caused by a systemic fungal infection with *Aspergillus* spp. In this vertical axial scan, pointlike opacities of medium reflectivity are diffusely distributed in the ventral part of the vitreous. **B.** Corresponding diagnostic A-mode echogram. Multiple spikes of low to medium reflectivity are observed along the horizontal baseline axis. (Courtesy of University of Georgia and the University of Munich.)

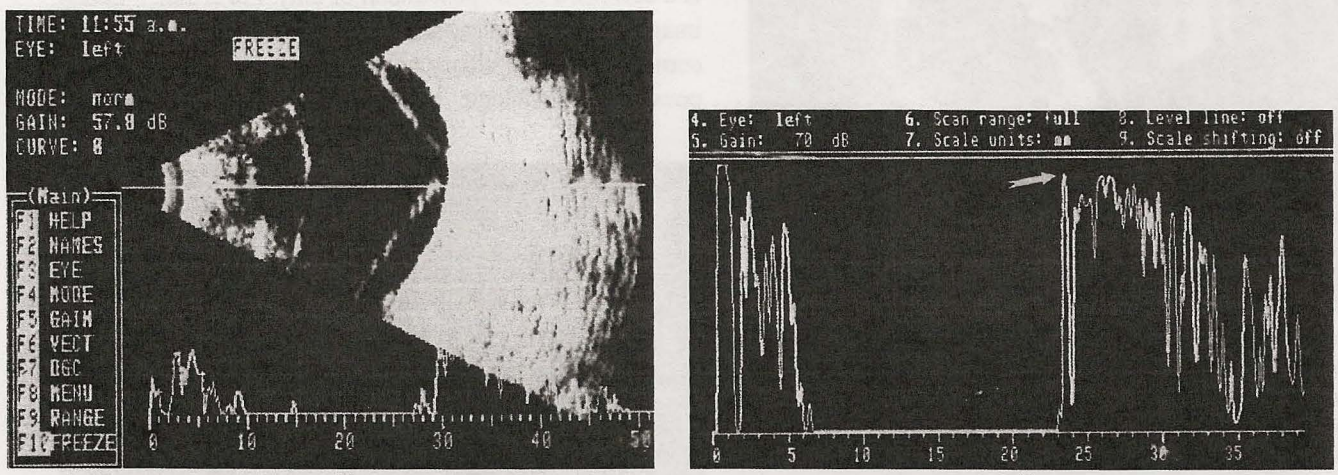

(a) (b)

Figure 9.3.16. **A.** B-mode echogram of a complete retinal detachment. A highly reflective membranelike structure extends in the vitreous in the shape of a seagull wing. This characteristic pattern is caused by tight attachments of the retina around the optic disc and ora serrata retinae. In real-time ultrasound, undulating movements of the retina may be observed during scanning procedure. **B.** Corresponding diagnostic A-scan of a complete retinal detachment. The sound wave strikes the detached retina perpendicularly and causes a single spike of almost 100% reflectivity on the horizontal A-mode axis (*arrow*). (Courtesy of University of Georgia and the University of Munich.)

about the extent of an orbital lesion compared with other imaging techniques such as radiography and ultrasound.[33,34] However, ultrasonography can be used as an excellent first choice in orbital diagnostic because it is the least expensive and the most widely available method, and it does not require the patient to be anesthetized.[16]

Artifacts

During ultrasound examination, it is important to recognize acoustic artifacts that may interfere with accurate interpretations of ultrasound findings. In many cases, reverberation artifacts (multiple signals) occur because of entrapped air between the transducer tip and the eye; they can be avoided by using a large amount of coupling gel or by simply by changing the probe position.[24] Reverberation artifacts usually occur between two highly reflective interfaces or between the probe tip and a highly reflective structure, such as a lens capsule, an artificial lens, or orbital bone. Metallic foreign bodies produce a typical reverberation artifact ("comet tail artifact"), which may actually help the examiner in the interpretation of the echogram[23] (Fig. 9.3.19).

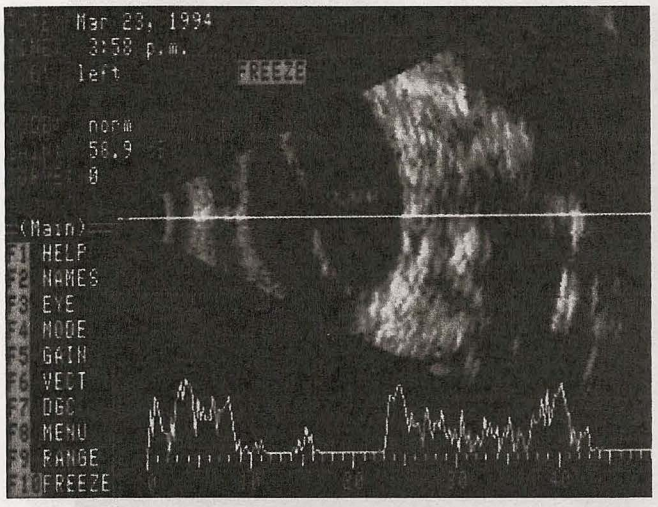

Figure 9.3.17. B-mode ultrasound of a long-standing retinal detachment, which appears as a T-shaped membrane (closed funnel). (Courtesy of University of Georgia and the University of Munich.)

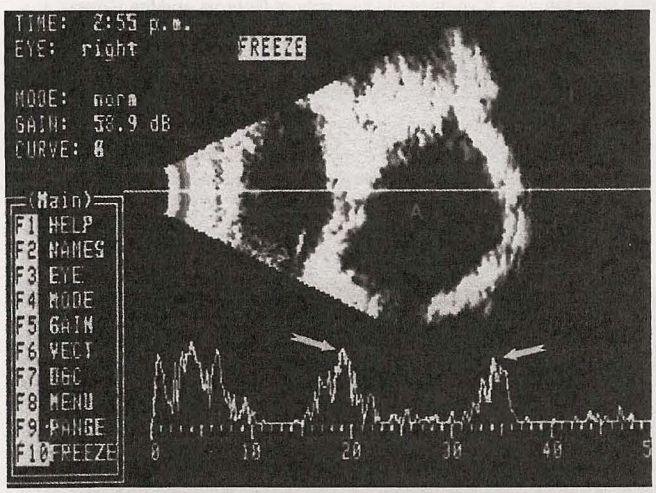

Figure 9.3.18. B-mode/vector A-scan echogram of a retrobulbar abscess in a Miniature Schnauzer. The abscess is anechoic in the center and surrounded by a thick, highly reflective wall. It can be clearly distinguished from the surrounding orbital tissue. The corresponding vector A-scan shows the low echogenicity within the cystic structure and the high posterior surface echo (*arrows*). (Courtesy of University of Georgia and the University of Munich.)

Shadowing is caused by a very strong sound attenuation at a dense interface (e.g., bone, large foreign body) and produces the absence of echoes behind the interface. This may also help to diagnose a lesion in the eye or orbit.[24]

HIGH FREQUENCY ULTRASOUND BIOMICROSCOPY (UBM)

The pioneer work of Charles Pavlin and Stuart Foster led to the development of ultrasound biomicroscopy (UBM), which allows the observation of living tissue at microscopic resolution.[32] This high-frequency ultrasound imaging technique is similar to conventional B-scan ultrasonography but uses frequencies between 50 and 100 MHz. Tissue resolution is increased by approximately 10 times compared with a 10 MHz probe and allows discrimination of structures as small as 50 μm. This corresponds to a lateral tissue resolution between 20 and 50 μm compared to 500 to 600 μm achieved with a 10-MHz probe.[32] The trade-off for the higher resolution is a decreased tissue penetration of only 4 to 5 mm.[32] Ocular imaging of the cornea, sclera, anterior chamber, iris, iridocorneal angle, and ciliary processes is comparable to a low-power histopathologic section. The layers of the cornea

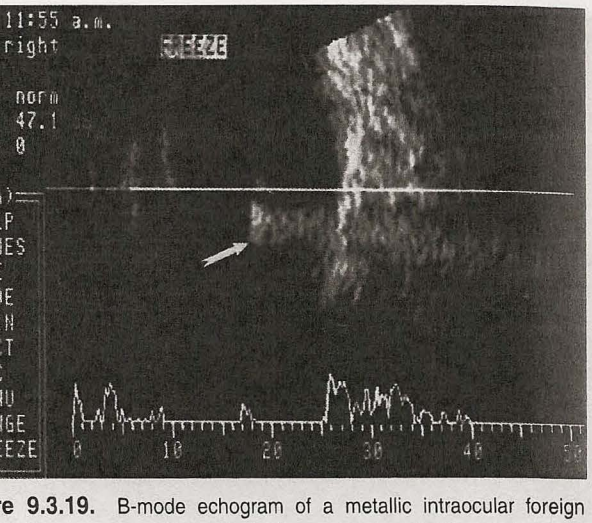

Figure 9.3.19. B-mode echogram of a metallic intraocular foreign body. Multiple reverberation artifacts ("comet tail artifact") are observed behind the object as the sound waves are reflected back and forth between the probe and the highly reflective metallic object (*arrow*). (Courtesy of University of Georgia and the University of Munich.)

Figure 9.3.20. Ultrasound biomicroscopic image (50 MHz) of a normal canine eye. Epithelium (*E*) and Descemet's membrane (*D*) provide strong echoes at the interfaces with air or aqueous humor. The corneal stroma (*S*) shows weaker echogenicity. Other areas identified on this picture include limbal/scleral region (*LS*), anterior chamber (*AC*), and iris (*I*). The anterior region of the lens (*L*) and the highly reflective anterior lens capsule (*ALC*) can further be demonstrated. (Courtesy of University of Georgia and the University of Munich.)

(epithelium, stroma, Descemet's membrane, and endothelium) can be easily differentiated (Fig. 9.3.20).

In humans, UBM is extremely useful in the diagnosis of pupillary block glaucoma, iris-plateau syndrome, and the visualization of iris and ciliary body tumors.[32,35–37] It is further possible to evaluate the functional status of glaucoma-filtering devices[37] and the position of intraocular lenses.[38]

The clinical value of UBM has been demonstrated in veterinary ophthalmology.[40–42] The depth and extension of corneal lesions (such as corneal sequestrum in the cat and squamous cell carcinoma in horses), and the thickness and size of limbal melanoma and iris melanoma, can be determined with UBM[41] (Figs. 9.3.21 and 9.3.22). This information is very helpful for the planning and performance of the intended surgical treatment and cannot be obtained with other diagnostic methods.

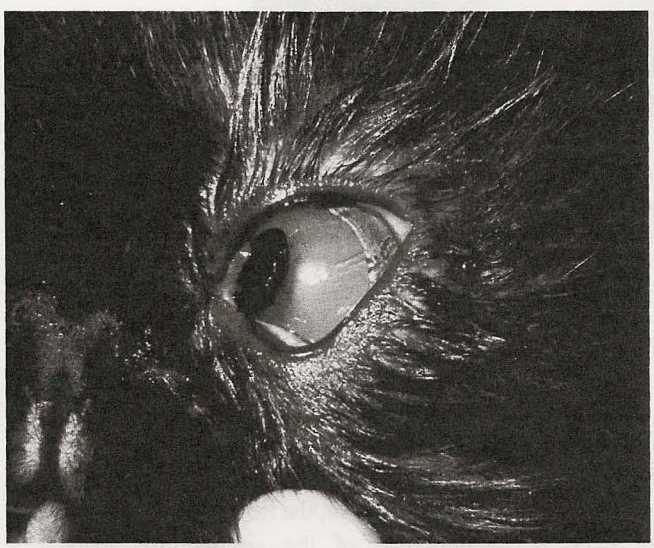

(a)

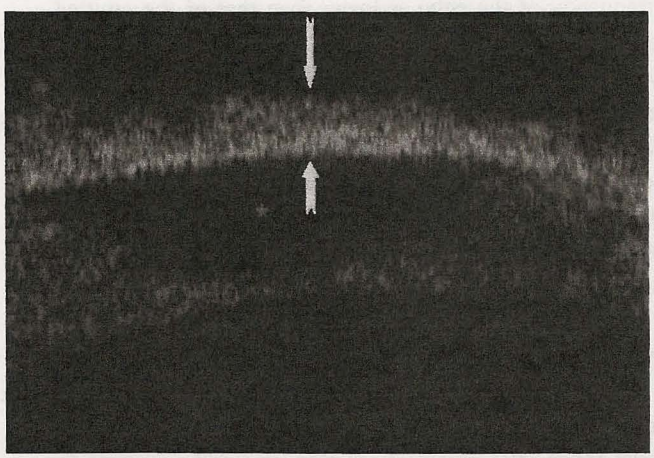

(b)

Figure 9.3.21. **A.** Corneal sequestrum in a 5-year-old Persian cat. Depth of the sequestrum cannot be determined by clinical examination only. **B.** Corresponding ultrasound biomicroscopic picture of the corneal sequestrum in A. Notice the highly reflective sequestrum invading about one third of the corneal stroma (*arrows*). However, corneal necrosis also involves deeper corneal layers, indicated by areas or low echogenicity (*). The ultrasound examination was helpful in planning the surgery, and a lamellar keratoplasty was performed in this cat. (Courtesy of University of Georgia and the University of Munich.)

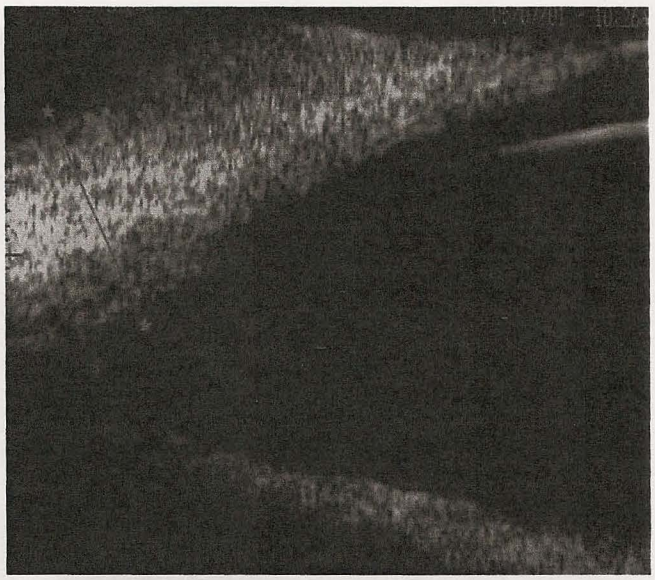

Figure 9.3.22. Ultrasound biomicroscopic picture of a limbal melanoma in a German Shepherd dog. Depth and extension of the mass can be easily determined with this high of a magnification and is helpful in planning the surgery. (Courtesy of University of Georgia and the University of Munich.)

The high resolution of the iridocorneal angle and ciliary cleft allows accurate measurement and assessment of angle width,[39,40,41,42] which renders UBM a useful method for the diagnosis of early glaucoma in the dog and may give additional information on angle-closure mechanisms.[40] Quantitative measurements of the anterior segment were performed in enucleated cat eyes with UBM, and the mean values for axial corneal thickness (0.47 mm), anterior chamber depth (4.20 mm), angle recess (0.38 mm), angle opening distance (1.05 mm), and iris width (base 0.38 mm, middle 0.52 mm) were established.[42] UBM scanning requires a water bath in form of a methylcellulose and saline–filled eyecup, which is placed between the eyelids (Fig. 9.3.23A). The transducer tip is then placed in the water bath opposite to the area of interest and close to the eye (Fig. 9.3.23B). Stay sutures placed at the limbus may facilitate globe position. The patient position is critical in obtaining a good-quality image, and anesthesia or heavy sedation of the animal is required, which, together with the relative higher costs of this machine, may be one of the biggest limitations for the use of UBM in a clinical setting.

Recently developed high-frequency ultrasound probes operate with lower frequencies (20–35 MHz) than are used in UBM but also allow an exceptionally detailed examination of the anterior segment[31] (Fig. 9.3.24). Those probes have an integrated offset device and do not require an external water bath. General anesthesia is not required, which makes the use of those probes more practical in a clinical setting.

COLOR DOPPLER ULTRASOUND

Color Doppler imaging (CDI) combines conventional B-mode ultrasound with a color Doppler instrument and allows the simultaneous evaluation of vascular velocity patterns. The technique of the Doppler instrument is based on the Doppler

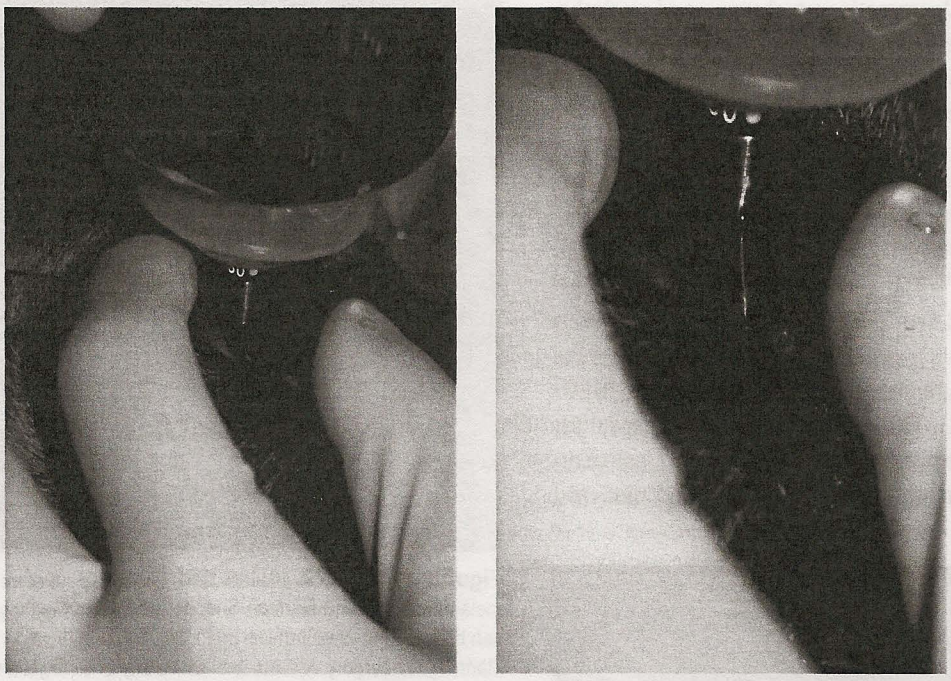

(a) (b)

Figure 9.3.23. **A.** Ultrasound biomicroscopic examination technique. The examination requires the animal to be under general anesthesia. An eyecup is placed between the lids and filled with methylcellulose and saline. Stay sutures are placed at the medial and lateral limbus to facilitate positioning of the globe. **B.** The transducer tip is placed in the water bath opposite the lesion and close to the eye. Stay sutures help to bring the area of interest into focus. (Courtesy of University of Georgia and the University of Munich.)

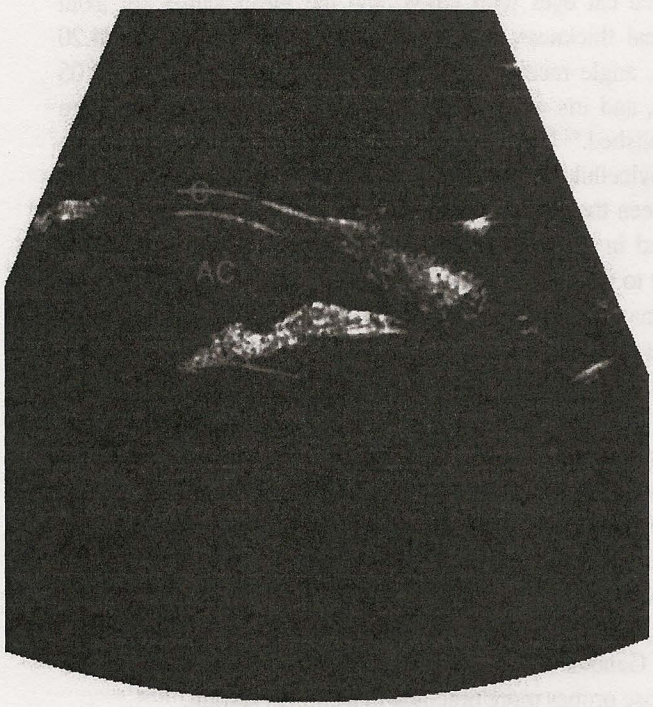

Figure 9.3.24. High-frequency ultrasound (20 MHz) picture of a normal canine eye. This method highly magnifies the anterior segment and allows a detailed examination of ocular structures. The 20-MHz transducer is flexible, and in contrast to an ultrasound biomicroscopic examination, the animal can be examined while awake. *C,* cornea; *S,* sclera; *AC,* anterior chamber; *I,* iris. (Slide courtesy of Xavier Lescure; courtesy of University of Georgia and the University of Munich.)

principle, which is a change in the perceived frequency of the sound emitted by a moving echo source.[43] If motion of the echo source is toward the transducer, the frequency of the perceived echo is greater than of the emitted frequency. Conversely, if reflector motion is away from the transducer, the frequency of the echo is lower than that of the emitted sound. The greater the velocity of the blood cells in the blood vessels, the greater the Doppler shift, that is, the greater the difference between the reflected and emitted frequencies.[43]

Doppler color flow imaging allows visualization of blood vessels and their flow characteristics within the eye and orbit.[43,44] The best resolution is achieved for evaluation of blood vessels greater than 200 μm in diameter. By definition, blood flow toward the transducer is colored in red, and blood flow away from the transducer is colored in blue. Spectral analysis can be used to quantify the velocity of the blood flow. The velocity waveform of an artery has a high peak systolic velocity (PSV) and a low end diastolic velocity (EDV). The resistive index (RI) or Pourcelot ratio is a measurement to interpret the shape of the waveform or a vessel and can be calculated as follows:

$$RI = (PSV - EDV)/PSV$$

The RI ranges from 0 to 100%, with 0% representing no resistance and 100% representing high resistance.[43] A high RI correlates with increased distal vascular resistance and

decreased perfusion. Determination of the RI helps to evaluate the functional variables of the orbital vascular bed, such as blood flow velocities and vascular resistance patterns, which may be altered during the course of ocular disorders in humans and animals.[43,45] In order to determine specific normal orbital and ocular blood velocity parameters in the dog, CDI was performed in normal Beagle dogs.[45] The external and internal ophthalmic artery and vein, external ethmoid artery, dorsal and ventral external ophthalmic veins, long posterior ciliary arteries, major retinal artery, and short posterior ciliary arteries could consistently be imaged.[45] When compared to values obtained from Beagles with primary open-angle glaucoma,[46] significant differences in blood flow velocities and RIs were detected in the external ethmoidal artery, internal ophthalmic artery, external ophthalmic artery, anterior ciliary artery, and short posterior ciliary arteries (Fig. 9.3.25).[46] In dogs with glaucoma, EDV was significantly decreased (5.55 cm/sec) and RI significantly increased (0.57) in the short posterior ciliary arteries (the primary blood supply to the canine optic disc) compared with normal dogs (EDV, 7.48 cm/sec; RI 0.44). Those changes in blood velocity parameters occurred before large elevations in IOP were observed, suggesting that glaucoma in the dog is mainly associated with vascular flow changes that are either primary or secondary to the disease process.

A CDI study was performed in the normal Beagle to evaluate the effects of L-type calcium channel blockers (amlodipine) on the hemodynamics of orbital arteries.[47] Calcium channel blockers have been found to be beneficial in preventing visual field loss in humans with normal tension glaucoma.[48] In the normal Beagle, systemic amlodipine (given at a dose of 0.625 mg/5kg SID) was found to significantly increase blood flow velocities and to decrease RI in the short posterior ciliary artery, long posterior ciliary artery, and ophthalmic artery. Those changes may suggest a beneficial effect of calcium channel blockers in the treatment of vascular disturbances in the glaucomatous dog eye.[47]

CDI has been successfully applied in clinical settings for the diagnosis of ocular and orbital disease.[10,12,49] Hypervascularity on CDI was detected in two dogs and a cat with acute proptosis, in a dog with orbital cellulitis, and in two dogs with iris neoplasia.[49] A hypovascular CDI pattern was observed in a dog with acute head trauma and periorbital swelling, in a dog with chronic glaucoma and buphthalmus, and in two cats with traumatic proptosis. Normal CDI patterns were found in a dog with optic nerve hypoplasia and in a dog and cat with complete retinal detachments.[49] CDI facilitated the diagnosis of PHPV/PTVL in a Bloodhound puppy, as blood flow was found in the lens and hyperechoic strand in the vitreous.[10]

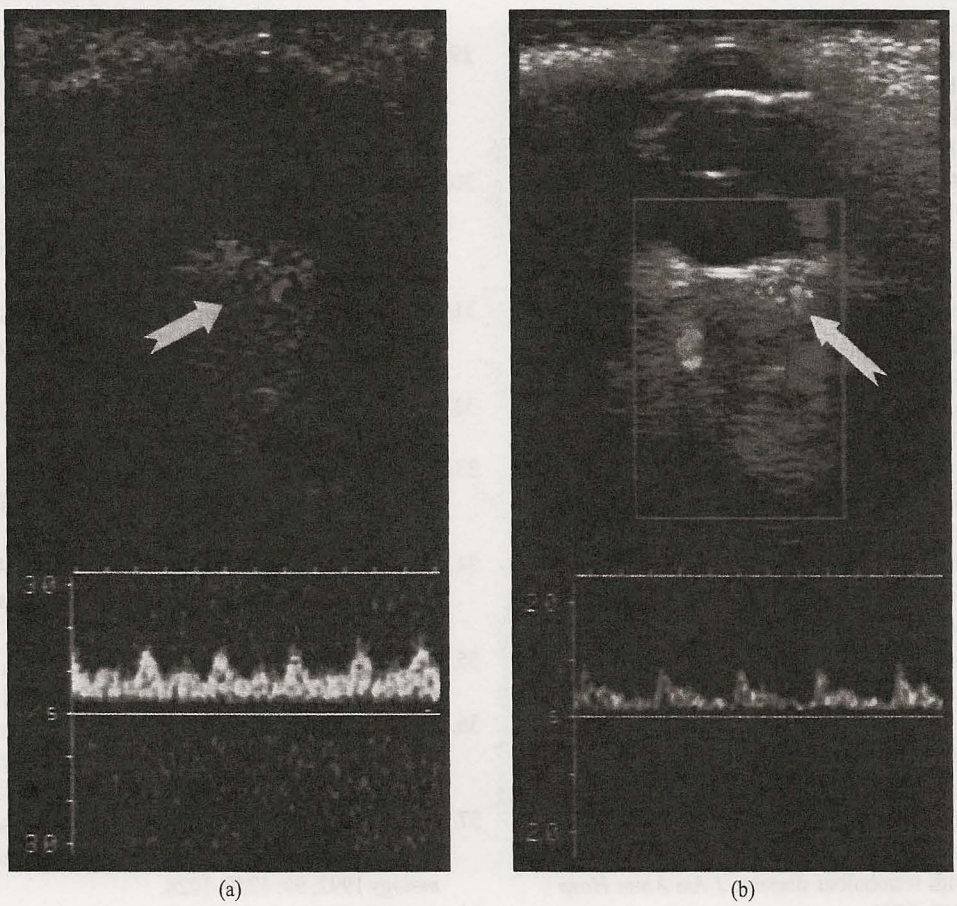

(a) (b)

Figure 9.3.25. Color Doppler images (*top*) and pulse waveforms (*bottom*) of the short posterior ciliary arteries (*SPCA;* see *arrows*) of a normal (**A**) and (**B**) glaucomatous Beagle. Comparisons of the normal to the glaucomatous Beagle's SPCA Doppler blood flow parameters indicated decreased end diastolic velocities (EDV) and increased resistive indexes(RI) compared to the normal dogs. (Photos courtesy of Kathleen Gelatt-Nicholson.)

A persistent hyaloid artery was diagnosed with CDI in a mixed-breed dog.[12]

Although CDI is frequently performed in humans, this technique has some limitations for the use in veterinary practice because sedation or anesthesia is routinely required. In one study, CDI was attempted in the awake dog.[50] Artifacts caused by eye and head movements limited the number of vessels that could be accurately examined, and numerous attempts were necessary to obtain the best quality waveforms.

REFERENCES

1. Eisenberg HM. Ultrasonography of the eye and orbit. *Vet Clin N Am: Sm Anim Pract* 1985; 15: 1263–1274.
2. Rubin LF, Koch SA. Ocular diagnostic ultrasonography. *J Am Vet Med Assoc* 1968; 153: 1706–1716.
3. Miller WW, Cartee RE. B-scan ultrasonography for the detection of space-occupying ocular masses. *J Am Vet Med Assoc* 1985; 187: 66–68.
4. Dziezyc J, Hager DA, Millichamp NJ. Two-dimensional real-time ocular ultrasonography in the diagnosis of ocular lesions in dogs. *J Am Anim Hosp Assoc* 1987; 32: 501–507.
5. Hager DA, Dziezyc J, Millichamp NJ. Two-dimensional real-time ocular ultrasonography in the dog. Technique and normal anatomy. *Vet Radiol* 1987; 28: 60–65.
6. Mettenleiter EM. Sonographische Diagnostik (B-mode Verfahren) am Auge des Pferdes. Teil I: Methodik und Normalbefunde. *Tierdärztl Praxis* 1995; 32: 481–488.
7. Mettenleiter EM. Sonographisch Diagnostik (B-mode Verfahren) am Auge des Pferdes. Teil II: Pathologische Fdälle. *Tierdärztl Praxis* 1995; 23: 588–595.
8. Williams J, Wilkie DA. Ultrasonography of the eye. *Compend Cont Ed Vet Med* 1996; 18: 667–676.
9. Van der Woerdt A, Wilkie DA, Myer W. Ultrasonographic abnormalities in the eyes of dogs with cataracts: 147 cases (1986–1992). *J Am Vet Med Assoc* 1993; 203: 838–841.
10. Boroffka S, Verbruggen AM, Boeve MH. Ultrasonographic diagnosis of persistent hyperplastic tunica vasculosa lentis/persistent hyperplastic primary vitreous in two dogs. *Vet Radiol & Ultrason* 1998; 39: 440–444.
11. Ori JI, Yoshikai T, Yoshimur S, Ujino H, Takase K. Posterior lenticonus with congenital cataract in a Shih Tzu dog. *J Vet Med Sci* 2000; 62: 1201–1203.
12. Bayon A, Tovar MC, Fernandez MJ, Agut A. Ocular complications of persistent hyperplastic primary vitreous in three dogs. *Vet Ophthalmol* 2001; 4: 35–40.
13. Williams DL. Lens morphometry determined by B-mode ultrasonography of the normal and cataractous canine lens. *Vet Ophthalmol* 2004; 7: 91–95.
14. Morgan RV. Ultrasonography of retrobulbar diseases of the dog and cat. *J Am Anim Hosp Assoc* 1989; 25: 393–399.
15. Stuhr CM, Scagliotti RH. Retrobulbar ultrasound in the mesaticephalic and dolichocephalic dog using a temporal approach. *Vet Comp Ophthalmol* 1996; 6: 91–99.
16. Mason DR, Lamb CR, McLellan GJ. Ultrasonographic findings in 50 dogs with retrobulbar disease. *J Am Anim Hosp Assoc* 2001; 27: 3757–3762.
17. Schiffer SP, Rantanen NW, Leary GA, Bryan GM. Biometric study of the canine eye, using A-mode ultrasonography. *Am J Vet Res* 1982; 43: 826–830.
18. Cottrill NB, Banks WJ, Pechman RD. Ultrasonographic and biometric evaluation of the eye and orbit of dogs. *Am J Vet Res* 1989; 50: 898–903.
19. Ekesten B, Torrang I. Age-related changes in ocular distances in normal eyes of Samoyeds. *Am J Vet Res* 1995; 56: 127–133.
20. Neumann W. Biometrie am Hundeauge. *Kleintierpraxis* 1988; 33: 127–130.
21. Gaiddon J, Rosolen SG, Steru I, Cook CS, Peiffer R Jr. Use of biometry and keratometry for determining optimal power for intraocular lens implants in dogs. *Am J Vet Res* 1991; 52: 781–783.
22. Gilger BC, Davidson MG, Colitz CM. Experimental implantation of posterior chamber prototype intraocular lenses for the feline eye. *Am J Vet Res* 1998; 59: 787–790.
23. Gilger BC, Davidson MG, Howard PB. Keratometry, ultrasonic biometry, and prediction of intraocular lens power in the feline eye. *Am J Vet Res* 1998; 59: 131–134.
24. Byrne SF, Green RL. *Ultrasound of the Eye and Orbit,* 2nd ed. St. Louis: Mosby, 2002.
25. Rantanen NW, Ewing RL. Principles of ultrasound application in animals. *Vet Radiol* 1981; 22: 196–203.
26. Rochels R. *Ultraschalldiagnostik in der Augenheilkunde.* Munich: Ecomed-Verlag, 1986.
27. Ossoinig KC. Standardized echography: Basic principles, clinical applications, and results. *Intern Ophthalmol Clin* 1979; 19: 127–210.
28. Coleman DJ, Dallow RL, Smith ME. A combined system of contact A-scan and B-scan. *Intern Ophthalmol Clin* 1979; 19: 211–224.
29. Dietrich U. Ultrasonographic examination of the eyes of dogs with cataracts using the combined B-mode/Vector A-scan system. Inaugural dissertation, Ludwig-Maximilians-Universitdät Mlünchen, Germany, 1996.
30. Berges O, Puech M, Assouline M, Letenneur L, Gastellu-Etchegorry M. B-mode guided vector-A-mode versus A-mode biometry to determine axial length and intraocular lens power. *J Cat Refract Surg* 1998; 24: 529–535.
31. Bentley E, Miller PE, Diehl KA. Use of high-resolution ultrasound as a diagnostic tool in veterinary ophthalmology. *J Am Vet Med Assoc* 2003; 223: 1617–1622.
32. Pavlin CJ, Foster FS. *Ultrasound Biomicroscopy of the Eye.* New York: Springer Verlag, 1995.
33. Dennis R. Use of magnetic resonance imaging for the investigation of orbital disease in small animals. *J Sm Anim Pract* 2000; 41: 145–155.
34. Penninck D, Daniel GB, Brawer R, Tidwell AS. Cross-sectional imaging techniques in veterinary ophthalmology. *Clin Tech Sm Anim Pract* 2001; 16: 22–39.
35. Pavlin CJ, Harasiewicz K, Sherar MD, Foster FS. Clinical use of ultrasound biomicroscopy. *Ophthalmology* 1991; 98: 287–295.
36. Pavlin CJ, Harasiewicz K, Foster FS. Ultrasound biomicroscopy of anterior segment structures in normal and glaucomatous eyes. *Am J Ophthalmol* 1992; 113: 381–389.
37. Pavlin CJ, McWhae JA, McGowan HD, Foster FS. Ultrasound biomicroscopy of anterior segment tumors. *Ophthalmology* 1992; 99: 1220–1228.
38. Avitabile T, Russo V, Uva MG, Marino A, Castiglione F, Reibaldi A. Ultrasound-biomicroscopic evaluation of filtering blebs after laser suture lysis trabeculectomy. *Ophthalmologica* 1998; 212(suppl): 17–21.

39. Bartholomew LR, Pang DX, Sam DA, Cavender JC. Ultrasound biomicroscopy of globes from young adult pigs. *Am J Vet Res* 1997; 58: 942–948.
40. Gibson TE, Roberts SM, Severin GA, et al. Comparison of gonioscopy and ultrasound biomicroscopy for evaluating the iridocorneal angle in dogs. *J Am Vet Med Assoc* 1998; 213: 635–638.
41. Dietrich U, Moore PA. Clinical application of ultrasound biomicroscopy in veterinary ophthalmology (abstract). *Vet Ophthalmol* 2002; 5: 292.
42. Aubin ML, Powell CC, Gionfriddo JR, Fails AD. Ultrasound biomicroscopy of the feline anterior segment. *Vet Ophthalmol* 2003; 6: 15–17.
43. Williamson TH, Harris A. Color Doppler ultrasound imaging of the eye and orbit. *Surv Ophthalmol* 1996; 40: 255–267.
44. Greenfield DS, Heggerick PA, Hedges TR 3rd. Color Doppler imaging of normal orbital vasculature. *Ophthalmology* 1995; 102: 1598–1605.
45. Gelatt KJ, Gelatt KN, Mackay E, et al. Comparative Doppler imaging of the ophthalmic vasculature in normal beagles and beagles with inherited primary open angle glaucoma. *Vet Ophthalmol* 1999; 2: 97–105.
46. Gelatt-Nicholson KJ, Gelatt KN, MacKay EO, et al. Doppler imaging of the ophthalmic vasculature of the normal dog: Blood velocity measurements and reproducibility. *Vet Ophthalmol* 1999; 2: 87–96.
47. Källberg ME, Brooks DE, Komaromy AM, Miyabayashi T, Bradshaw PT. The effect of an L-type calcium channel blocker on the hemodynamics of orbital arteries in dogs. *Vet Ophthalmol* 2003; 6: 141–146.
48. Netland PA, Chaturvedi N, Dreyer EB. Calcium channel blockers in the management of low-tension and open-angle glaucoma. *Am J Ophthalmol* 1993; 115: 608–613.
49. Schmid V, Murisier N. Color Doppler Imaging of the orbit in the dog. *Vet Ophthalmol* 1996; 6: 35–44.
50. Lee H, Chang D, Eom K, et al. Use of color Doppler imaging for determining the resistive index of the medial long posterior ciliary artery in clinically normal conscious dogs. *Am J Vet Res* 2002; 63: 211–214.

Chapter 9

Ophthalmic Examination and Diagnostics

Part 4: Electrodiagnostic Evaluation of Vision

Björn Ekesten

Electrodiagnostic testing provides unique, noninvasive opportunities to probe the visual system from the retina to the visual cortex in virtually any animal species. Unlike psychophysics, which establishes relationships between the physical properties of stimuli and the subjective sensations they produce, electrodiagnostic tests measure the electrical potentials generated in various parts of the visual system. Therefore, electrodiagnostic testing should not be considered a measure of vision per se.

The electroretinogram (ERG) is still the most widely used electrodiagnostic test in veterinary ophthalmology. The ERG, which is often used to diagnose outer retinal disease, is a complex response of different cells within the retina. The visual evoked potential (VEP), which is a cortical response, is less commonly tested. VEPs are particularly helpful in diagnosing visual impairment of postretinal origin. Additionally, the VEP has been used to predict subjective psychophysical contrast sensitivity or limits of spatial resolution. There are also some electrodiagnostic tests that are not commonly used in veterinary ophthalmology because they require very expensive equipment, are technically demanding, rely on patient cooperation, or provide results that are not yet well understood. The pattern electroretinogram (PERG), which can be used to evaluate retinal ganglion cell function, has received little attention in clinical veterinary ophthalmology because it is a technically demanding test. The multifocal ERG (MFERG), a technique for recording local cone ERGs in multiple areas in the central part of the retina, is also technically demanding and not widely used. The electrooculogram (EOG) is used to assess the function of the retinal pigment epithelium (RPE) in human patients. The EOG has rarely been used in animals because the patient is normally required to perform regular, horizontal, saccadic eye movements.

Combining different electrodiagnostic tests is a powerful way to both assess function and localize where in the visual system the dysfunction occurs. Using different stimulus and recording parameters, more specific information about the function of a particular cell type can be obtained. A patient with normal flash electroretinogram (FERG) and abolished flash visual evoked potential (FVEP) is likely to suffer from a severe ganglion cell or postretinal dysfunction. A normal PERG from this patient shows that the retinal ganglion cells are normal and the dysfunction has to occur in the higher visual pathways. The more tests that can be employed, the more detailed information can be obtained.

THE FLASH ELECTRORETINOGRAM

The ERG provides an opportunity to assess the function of a part of the central nervous system, the retina, which can easily be visualized, for instance, using an ophthalmoscope. It is an electrical mass response of the retina to light stimulation, which reflects the function and integrity of the photoreceptors and the retinal cell layers they contact, the inner nuclear layer, and, if a special recording technique is used, the RPE. The electrical responses of the different cell types are superimposed in the ERG, which makes the interpretation of the results more challenging.

Abrupt changes in retinal illumination causes recordable, transient electrical changes, a phenomenon already described in the 19th century by the Swedish physiologist Fridthiof Holmgren.[1] In the beginning of the 20th century, the initial negative deflection was named the a-wave, the subsequent positive peak the b-wave (Fig. 9.4.1), and the late, prolonged positive component the c-wave.[2] A few years later, in 1911, the first report on the canine and feline ERGs, recorded using a string galvanometer, was published.[3] The three components or processes making up the dark-adapted ERG, the PI, PII, and PIII (corresponding

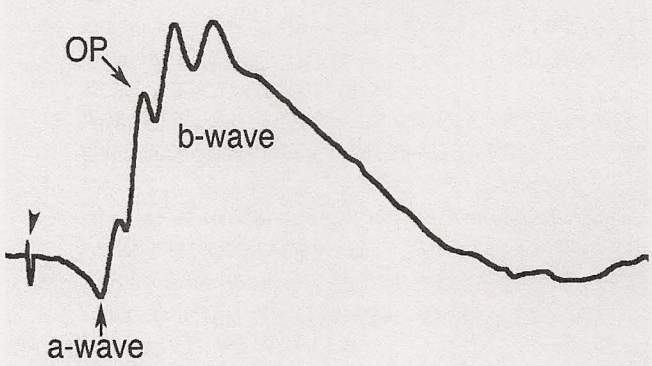

Figure 9.4.1. A dark-adapted canine electroretinogram in response to a brief, bright flash. Both rod and cone photoreceptors drive this response.

to the c-, b-, and a-waves), were analyzed more in detail in ether-anesthetized cats.[4] The order of disappearance in response to ether administration was from PI to PIII. Once PIII disappeared, the ERG was incapable of recovery, as was the patient.

PIII, forming the leading edge of the a-wave, reflects the negative change in the intracellular charge of photoreceptors (hyperpolarization) caused by light-evoked closure of the sodium channels in the cell membrane. The hyperpolarization diminishes the release of neurotransmitter, which in turn activates bipolar cells. The origin of the b-wave has been controversial for decades. Depolarization of Müller cells, caused by depolarization of bipolar cells, was long considered to result in a transretinal current along the Müller cell that was originally thought to be the major source of the b-wave. However, more recent results show that the b-wave directly relates to bipolar cell activity and not to K^+ currents flowing through the Müller cells.[5] The c-wave is a result of the transient hyperpolarization of the apical membrane of the RPE and a hyperpolarization of the Müller cells in response to light. However, the c-wave is usually not included in clinical animal protocols because direct current (DC) recordings are technically challenging and because it is recordable in only a fraction of normal adult dogs.[6]

The potential of the ERG as a diagnostic tool was demonstrated in 1945, when the ERGs of human patients with different ocular diseases were reported.[7] The appearance of the ERG in Irish Setters with and without ophthalmoscopic signs of retinal degeneration was published in 1953 by British researchers.[8] A century after Holmgren's discovery, the ERG became more widely used to diagnose and study retinal function in dogs.[9] The ERG has subsequently been used to evaluate retinal function in several species.

In veterinary ophthalmology, the ERG has been used to diagnose patients with acquired or inherited retinal diseases, assess retinal function in patients with opaque ocular media such as cataracts, and exclude an outer retinal component in patients with ganglion cell or postretinal dysfunction. The ERG provides more objective results than ophthalmoscopy and characterizes the function of specific cell types in the retina. Furthermore, the ERG usually allows much earlier diagnosis than does an ophthalmoscopic or behavioral examination.

Equipment for Recording and Light Stimulation

Electrodes

The electrical changes produced by light stimulation of the retina are usually recorded using an active electrode touching the cornea and a reference (passive) electrode either in contact with the eyelid margin (as in bipolar contact lens electrodes) or subcutaneously approximately 2-cm aboral to the lateral canthus. Furthermore, a ground electrode is normally placed in an indifferent location, such as the top portion of the skull.

Several types of electrodes can be used for animal ERGs. Corneal contact lens electrodes, such as the Burian-Allen (bipolar) or JET electrodes (monopolar) are safe, reliable, and easy to use in the cat and dog (Fig. 9.4.2A). Contact lens electrodes give significantly higher ERG amplitudes than active, subcutaneous electrodes.[10, 11] In addition, a contact lens electrode prevents the cornea from drying out during the recording. The space between the contact lens and the cornea is filled with an ionic solution of either saline or a more viscous solution depending on which type of electrode is used. Reusable contact lens electrodes have to be cleaned thoroughly between patients, both for good patient safety and for maintenance of reliable electrical coupling between the electrode and the eye. A metal clip attached to the conjunctiva close to the limbus is a more traumatic, low-cost alternative that has been shown to give reproducible recordings in dogs.[12] In sedated large animals, such as horses, active electrodes made from silver-impregnated microfibers[13] or thin,

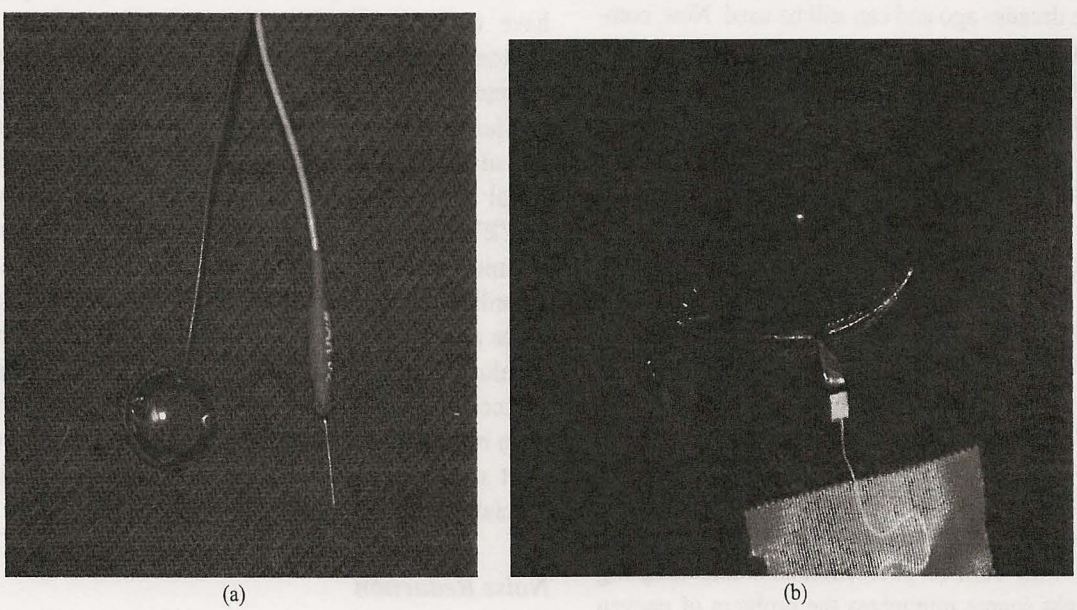

(a) (b)

Figure 9.4.2. **A.** The JET electrode is a monopolar corneal contact lens electrode that can be used in many species, such as the cat and dog. The platinum needle electrode is a reliable, easy-to-use, subcutaneous electrode. **B.** The gold-foil electrode can be used as an active electrode for recording the equine ERG. The plastic foil is bent over the canthus of the lower eyelid so the gold-coated side touches the corneal surface.

gold-coated foil strips[14] are easy to position and give reproducible results (Fig. 9.4.2B). Several types of active electrodes have been shown to give reliable FERG recordings in laboratory animals.[15] Metal needle electrodes, such as commercially available platinum needle electrodes, work well as subcutaneous reference and ground electrodes.

Impedance

It is important to measure the impedance to make sure that the electrodes, particularly the ground and reference electrodes, are in good contact with the tissue. This can easily be done using an impedance meter. Great caution should be used if the impedance over the active corneal or scleral electrodes is measured in order to make sure that the current passed through the electrodes (and the eye) does not damage the ocular tissues. Preferably, the impedance should be around 5 kOhms and not exceed 7 kOhms. Furthermore, it is important that the impedance is similar between the left and right sides if binocular recordings are made.

Data Acquisition

The electrical signals generated by the retina are small in amplitude (often less than 10^{-1} mV and certainly less than 10^{0} mV) and must be amplified approximately 10^{4} times to be properly visualized. Signal averaging reduces the impact of noise on the ERG signal,[16,17] and bandpass filters attenuate frequencies that do not contribute substantially to the ERG. It is recommended that the low filter (high pass) should be no higher than 1 Hz, and the high filter (low pass) should be no lower than 300 Hz.[18] These filter settings do not allow recording of the c-wave. However, recording of the c-wave is not normally included in standard ERG protocols.

Recording the FERG does not necessarily require very sophisticated equipment. Preamplifiers and amplifiers with vacuum tubes connected to a storage oscilloscope was high-end equipment some decades ago and can still be used. Now, computerized data acquisition systems are most commonly used. They are generally reliable, easy to use, reasonably priced, and provide excellent opportunities to store waveforms. It is recommended that the recording equipment meet the safety standards imposed on equipment used for human clinical ERGs.[18]

The Photostimulator

A light stimulus, such as a strobe flash or a light-emitting diode (LED), does not provide a uniform illumination of the entire retina. It produces a bright-light stimulus in the focal image of the light source on the retina and a weaker stimulus in nonfocal areas caused by scattered light.[19] The strongly and weakly stimulated areas of the retina generate responses with different amplitudes and time course. A full-field (*ganzfeld* in German) dome with built-in photostimulator and adapting (background) light source minimizes the problem of uneven retinal illumination and is strongly advocated (Fig. 9.4.3). Full-field stimulators have been used successfully in several animal species, including the dog.[18,20]

Figure 9.4.3. Both the stimulus and background light intensities must be measured to ensure that the same amount of light is delivered to the patient's eye. The detector of the photometer is positioned at the level of the eye of a patient. A xenon flash and a halogen bulb, used for steady adapting light, are built into the aluminum housing on top of this full-field (ganzfeld) stimulator.

A xenon strobe flash—a halogen, tungsten, or xenon arc lamp fitted with a mechanical shutter or LEDs—can provide an appropriate light stimulus in the full-field dome. The duration of the stimulus should not exceed 5 ms.[21,22] The adapting light source should provide a uniform, steady light. It should be possible to dim both the stimulus and adapting lights, for instance, by using different neutral density filters. According to international guidelines, the brightest light stimulus in the standard protocol should be 2 to 3 cd/m^2/s, whereas the stimulus for the dark-adapted rod tests should be 10^{2} dimmer, that is 0.02 to 0.03 cd/m^2/s.[18] The stimulus and adapting lights have to be measured and calibrated regularly using a photometer capable of measuring the stimulus and background light reflected off the surface in the full-field stimulator (luminance over time for the stimulus and luminance for the adapting light, respectively). According to the International Society for Clinical Electrophysiology of Vision (ISCEV) guidelines, which provide good information on the technical aspects of calibration of both the stimulus and recording equipment, the light should be calibrated at least twice a year.[23] Technical advances have made it possible to develop contact lens electrodes with built-in LEDs as light source,[24] but it has to be established that they provide uniform retinal illumination. Furthermore, calibration of such a light source requires both good knowledge of physics and specialized equipment.

Noise Reduction

Stable ERG responses without patient-related artifacts are keys to obtaining an adequate signal-to-noise ratio. Minimizing noise and artifacts can be a time-consuming task when the

electrodiagnostic system is first set up, but the time is well invested, and clean responses that do not require additional manipulation will increase the diagnostic potential. Thus, keeping the electrodiagnostic equipment in a dedicated area and not disassembling the equipment between examinations usually saves time. Electrodes and leads should be properly cleaned and maintained or replaced. Reducing and matching the electrode impedances usually reduces the noise considerably.[25]

Important generators of noise are stray electromagnetic and electrostatic fields, including unshielded power lines, switches, fluorescent tubes, transformers, computers, network equipment, and monitors. Notch filters, filters that reduce noise caused by the main's frequency (60 Hz in the U.S.A. and 50 Hz in the rest of the world), should be avoided because they partially block frequencies that contribute to the a- and b-wave of the ERG.[18] Proper shielding of the equipment and, if necessary, putting the patient inside a Faraday's cage will improve the ERG.

Patient Preparation

Allowing the Light to Reach the Retina

Miotic pupils reduce the amount of light reaching the retina, which reduces the response amplitudes and increases the implicit times in a way that may suggest retinal disease. Therefore, topical mydriatics should be instilled ahead of the ERG so the pupils are fully dilated throughout the examination. To make sure that aberration from normal is not caused by reduced retinal illumination due to incomplete dilation of the pupils, it is recommended that pupil size be checked immediately before and after the examination.

The visual field of the patient should not be blocked by a protruded third eyelid or equipment, which can interfere with the stimulus light. Stay sutures attached to the limbal conjunctiva help position the globe and keep the third eyelid out of the way. Retrobulbar injections of saline have been used for the same purpose[26] but may cause transient increases in IOP that can have deleterious effects on the ERG.

Anesthetic Protocol

The FERG can readily be recorded in conscious, cooperative human patients. However, most animals are less eager to perform well during a full recording session. Therefore, general anesthesia is recommended for more comprehensive ERG testing in order to maintain proper fixation and stable position of electrodes as well as to minimize movement artifacts and patient stress.

It is well known that FERG responses are affected by general anesthesia since the Nobel laureate Ragnar Granit's seminal analyses of the components of the feline ERG.[4] In clinical electrophysiology, the effects of anesthetics are generally of less importance for the interpretation of the ERG than are the large artifacts frequently seen during recording from awake animals. Several anesthetic protocols (including thiopentone and propofol; halothane, isoflurane, or sevoflurane with or without nitrous oxide; ketamine combined with xylazine or medetomedine hydrochloride) have been used for FERGs in dogs[12,18,27–31] and cats.[32,33]

Most common effects of general anesthesia are decreases in response amplitudes and increases in implicit times for both rod- and cone-driven responses of the FERG.[29,34,35] In experiments in which FERG recordings were performed in dogs both under halothane anesthesia and under succinylcholine akinesia, the b-wave amplitude was reduced by 36% to 77%, implicit times were prolonged, and waveforms were altered.[34] After prolonged dark-adaptation, the rod b-waves and, in particular, the scotopic threshold responses (STRs), were decreased in dogs anesthetized with halothane or sevoflurane.[29] Interestingly, both amplitudes and, at least initially, implicit times for oscillatory potentials (OPs) increased during anesthesia. The exact mechanism of suppression of the b-wave and STR, and at the same time increase in amplitude of OPs, is not well understood. An increase in GABA, glycine, or both, in the retina caused by the volatile anesthetics would explain the effects on the b-wave and STR, but not on the OPs, at least not to our current knowledge. Isoflurane has been shown to have some deleterious effects on the canine ERG as well.[36]

In horses, FERGs have been recorded under halothane anesthesia.[37,38] However, general anesthesia in horses (and other large animals) is associated with a higher incidence of potentially life-threatening complications, which justifies FERG recording in sedated patients. Flash electroretinograms have been successfully recorded in horses sedated with 5 to 15 μg/kg of detomidine hydrochloride.[13,14] However, it has also been shown that it is possible, but not necessarily easy, to record FERG in awake, unsedated horses and cattle.[14, 39, 40]

Proper oxygenation is important for obtaining a reliable and reproducible FERG. In cats, the c-wave is sensitive to hypoxemia beginning at PaO as high as 60 mm Hg.[41] The feline a-wave amplitude decreased approximately 9% at PaO between 50 and 60 mm Hg, whereas the b-wave amplitude was stable at this level.[42] During more severe hypoxemia, PaO of 20 to 30 mm Hg, the b-wave amplitude was decreased by 35% on average, whereas the decrease in mean a-wave amplitude was close to 9%. The STR, a response driven by the inner retina, has been reported to be stable until the PaO is close to 40 mm Hg in the cat.[41] It is believed that the inner retinal responses are relatively spared because of the efficient regulation of inner retinal PaO by the retinal circulation. A study of the effects of hypoxemia on the canine ERG reports that the b-wave is affected first, with decreased amplitude and increased latency at a PaO of 45 mm Hg.[43] Again, the a-wave was more resistant to severe hypoxemia and remained after the b-wave was extinguished. In contrast, hyperventilation enhanced the b-wave in anesthetized dogs, and this effect was attributed to reduction of carbon dioxide.[44]

The effects on response amplitudes and implicit times caused by anesthetics, drugs used for premedication, and sedatives can generally be neglected if both the normal data and the patient data are obtained using identical protocols for

patient preparation and anesthesia (including measures that ensure proper oxygenation throughout the recording).

Components of the FERG and Reporting the Results

Different stimulus and recording paradigms allow separation of responses contributed by different types of cells in the retina. Although the separation of different components is usually not complete, enhancing responses driven by one system and suppressing responses from other systems in the retina will increase the diagnostic value of the FERG considerably. Varying the stimulus and background light wavelengths and intensities, stimulus duration and frequency and bandpass filter settings will enhance different components of the FERG.

The ERG is usually reported by providing values for the implicit times and amplitudes for the a- and b-waves. The amplitude of the a-wave is measured from the (prestimulus) baseline to the trough of the a-wave. By convention, the b-wave is measured from the trough of the a-wave to the peak of the b-wave. The implicit time of the a-wave refers to the time between stimulus onset and the trough of the a-wave, whereas the b-wave implicit time is measured from the onset of the stimulus to the peak of the b-wave. In addition, it has been recommended that an illustration of the dark-adaptation curve, such as plotting the amplitude on the ordinate and dark adaptation time on the abscissa, including normal limits for a dog of similar breed, similarly anesthetized and of similar age, should be included.[18]

Separation of Rod and Cone Function

The rod system is designed for detecting minimum amounts of light in the dark of the night, whereas the cone system operates under bright-light conditions. Rods and cones contribute their signals to the FERG independently. Taking advantage of the inherent, physiological differences of the two systems allows separation of rod- and cone-driven responses in a number of ways (Fig. 9.4.4).

1. A dim stimulus will be relatively more effective in stimulating the rods than the cones. Dim stimuli under dark-adapted (scotopic) conditions will bring out the rod-driven responses, whereas the cone-driven response will be insignificant because the cones will be too poorly stimulated. Monitoring the responses for a number of minutes after the room light or the adapting light has been turned off will prove that the rod system has its normal ability to generate successively larger responses (dark-adapt) until a maximum is reached, usually in less than an hour in most domestic species. For practical reasons, usually only the first part of the dynamic process of dark adaptation, that is, the process when rods become more sensitive and consequently more responsive, is monitored in clinical FERG protocols.
2. A bright background light, mimicking daylight conditions, will bleach the rhodopsin and saturate the rods, making them unable to respond to light stimuli. Using bright stimuli under light-adapted (photopic) conditions will give responses almost exclusively driven by the cone system.[45]
3. Rods are incapable of following rapidly flickering lights. It has been demonstrated that the human cone ERG can be isolated from the rod-driven responses using stimulus frequencies above 30 Hz.[46] Flickering stimuli presented at 30 Hz or higher will produce pure cone responses in cats and dogs too. Given that canine (and feline) cones can follow frequencies up to 70 Hz or higher, it is possible to employ even higher stimulus frequencies to test the cone function. However, technical limitations usually force the examiner to use stimulus frequencies far below the cone flicker fusion frequencies in these species. Flicker photometry has proven to be useful in assessing the spectral sensitivity of the two classes of canine cones.[47]

Chromatic stimuli carefully chosen to stimulate one photoreceptor mechanism maximally presented on a chromatic background, suppressing responses from the other photoreceptor mechanisms (selective chromatic adaptation), may serve to assess the function of one cone mechanism compared with the other. Cone responses can also be examined in the dark. Altering the stimulus luminance over time so that the amplitude of dark-adapted responses to red and blue stimuli become identical can provide clues to whether a residual dark-adapted response is rod- or cone-driven. The dark-adapted response to red light is normally bipartite with the faster, medium wavelength–sensitive (green) cone response first, whereas the rod response has longer implicit time. The

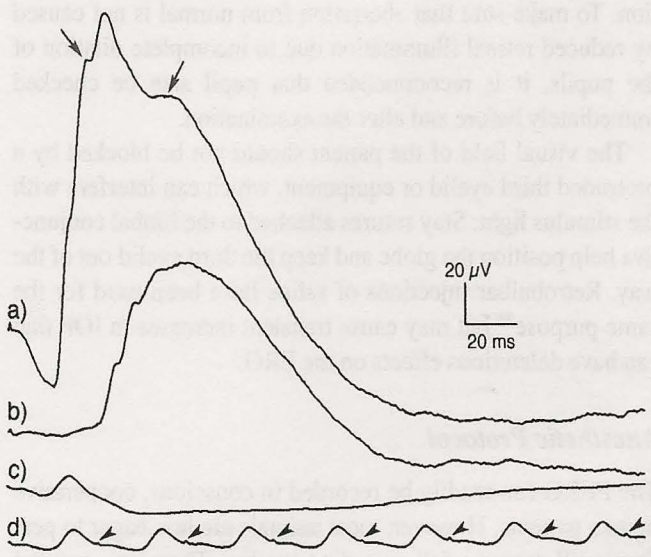

Figure 9.4.4. Four ERG responses from a normal dog. **A.** A mixed, dark-adapted rod-cone response. The small positive deflection just below the letter is a stimulus artifact, which shows when a brief, white flash (3.0 cd/m²/s) is delivered. The response has a conspicuous, negative a-wave followed by the large, positive b-wave. Superimposed on the ascending limb are a few OPs (*open arrow*). The peak of the b-wave is bipartite: the later peak reflects the slower rod b-wave (*black arrow*). **B.** A dark-adapted, mainly rod-driven ERG in response to a dim white flash (0.03 cd/m²/s). Notice that there is no obvious a-wave and that the implicit time of the b wave is similar to the rod-driven peak in A. **C.** A cone response to a bright, white flash (3.0 cd/m²/s) presented on a rod-saturating background (40 cd/m²). The amplitude is considerably smaller than that of the dark-adapted responses, but both an a- and a b-wave can be seen. **D.** A cone response (arrowheads) to a bright, white flickering stimulus (30 Hz) in presence of the steady, adapting light.

response to blue light is dominated by the rod-driven response, whereas the contribution from the short wavelength–sensitive cones is very small because of their low number in the retina and the dim stimulus. Subtracting the blue response from the red response will yield the dark-adapted cone response, mainly driven by the middle wavelength–sensitive (green) cones.[48]

Oscillatory Potentials

OPs are a series of wavelets superimposed mainly on the ascending limb of the b-wave reported in several animal species, such as the cat[49,50] and dog.[51,52] Their number and appearance may vary between individuals and species. In cats and dogs, usually 3 to 5 conspicuous OPs can be observed, whereas they are not easily detectable at all in the horse.

It has been suggested that the OPs represent radial current flows involving inhibitory circuits driven by amacrine cells. Intraretinal recordings have indicated that they arise in the inner plexiform layer, and pharmacological studies show that dopamine, GABA, and glycine blockers all diminish the OPs.[53–55] However, pharmacological blockade of the retinal ganglion cells in the rat has been shown to reduce the amplitudes of the light-adapted OPs, indicating that intact ganglion cell function is important for generation of the photopic OPs.[56] Retinal ischemia causes reduction of the OPs, which supports that these high-frequency, low-amplitude components of the FERG are generated by inner retinal cells supplied by the retinal circulation. The input to these inhibitory circuits is likely to come from both the rod and cone systems as well as from interactions between the rod and cone systems.[57–59] Each peak has been suggested to have a slightly different origin,[60,61] which means that the wavelets are not reverberations as the name suggests.

The OPs are readily visible on the dark-adapted ERG of cats and dogs elicited by bright stimuli (Fig. 9.4.5). OPs can be recorded similarly to the way a- and b-waves are recorded, but manipulation of the bandpass filter settings and stimulus conditions enhance the OPs. Changing the high-pass setting of the bandpass filter to 70 to 100 Hz will block the frequencies mainly contributing to the a- and b-waves, around 25 Hz, and allow the higher frequencies that dominate the OPs, about 100 to 160 Hz, to pass.[18,58] Dim stimuli presented to the dark-adapted eye will provide rod-driven OPs. Cone-driven OPs, which are most commonly included in the ERG protocols, can be obtained by first presenting a bright, white conditioning flash (2–3 cd/m^2/s) to the dark-adapted eye and then, 15 to 30 seconds later, present an average of 3 to 4 responses to additional flashes at 15-second intervals.[57]

OPs will be abnormal in conditions that cause widespread retinal ischemia. The amplitudes will decrease and the implicit times increase if the IOP is elevated. A threefold increase in IOP in dogs for 3 to 5 minutes has been shown to obliterate the OPs (and the ERG).

The changes in OPs and ERG were reversible and the responses returned to normal when IOP was reduced to baseline. However, it should always be borne in mind that the OPs will be abnormal in disorders primarily affecting the outer retina too, because the input from the outer retinal cells to the amacrine and interplexiform cells will be reduced. For instance, a rod-cone dystrophy will hence cause reduced OPs and a- and b- wave amplitudes.

Other Components of the ERG

Several other components of the ERG, except for the a- and b-waves and the OPs, have been recorded in different species. Some of these components, reflecting electrical activity in a certain group of retinal cells or in a certain pathway or circuit, cannot be isolated without injection of pharmacological blockers into the posterior segment, or they require more specialized recording techniques, such as DC recording.[6,62–68] Other components, such as the i-wave (discussed shortly), are of potential clinical value, but their retinal origin is not yet well understood.

The Scotopic Threshold Response

The STR is a negative response of the dark-adapted retina to very dim stimuli below the threshold for detecting a- and b-waves[69,70] (Fig. 9.4.6). Dim adapting light or brighter stimuli will immediately reduce or abolish the STR. In fully dark-adapted animals, the amplitude can exceed 100 μV, whereas the trough of the STR appears later than the positive-going b-wave peak. An average implicit time of 82 ± 7 ms (mean ± SD) has been reported in dogs.[71] Volatile anesthetics, such as halothane and isoflurane, reduce the amplitude of the STR in dogs significantly.[29]

The STR reflects inner retinal activity driven by the rod photoreceptors.[29,69,70] It has been shown that the STR in the rat depends on intact retinal ganglion cell responses, whereas the

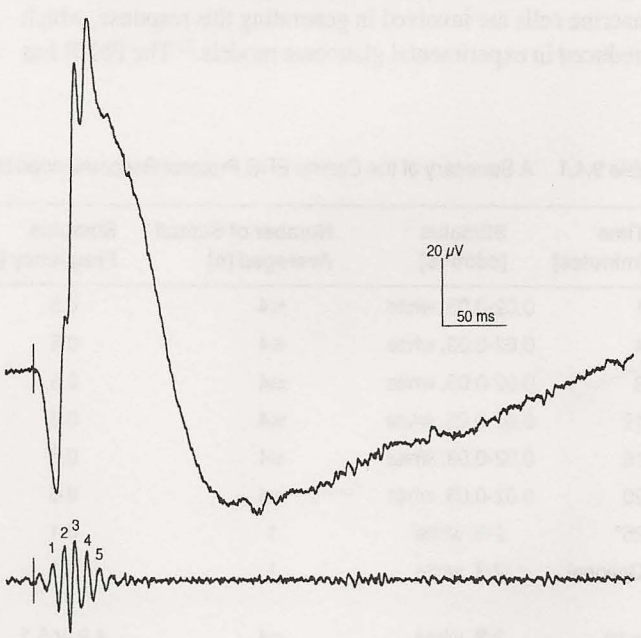

Figure 9.4.5. *Top:* A single, dark-adapted response to a bright flash (3.0 cd/m^2/s). A conditioning flash was presented 15 seconds earlier. The bandpass filter setting was 0.5 to 1000 Hz. *Bottom:* Oscillatory potentials extracted from the mixed rod-cone response using a bandpass filter from 100 to 1000 Hz. Numbers indicate OPs 1 thru 5. The stimulus is indicated by a vertical line.

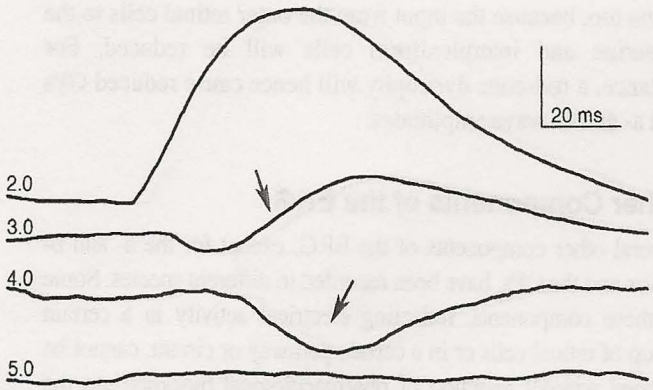

Figure 9.4.6. The STR is a dark-adapted inner retinal response that appears before the b-wave. A very dim flash, $3/10^{-5}$ cd/s/m^2 does not produce a response (*lowermost tracing*). Increasing the stimulus intensity by factor 10 results in a small STR (*blue arrow*) in this anesthetized dog. Using a brighter stimulus causes the b-wave (*red arrow*) to partially fill out the STR. Using an ECVO rod stimulus ($3/10^{-2}$ cd/s/m^2) produces only a b-wave. The stimulus is presented at the beginning of each tracing. Numbers indicate the neutral density filter in front of the stimulus light. Vertical calibration is 20μV for the three lowermost tracings and 40μV for the uppermost tracing.

contribution from the amacrine cells is relatively small.[56] Therefore, it is of potential interest in diseases primarily affecting the inner retina, in particular the ganglion cells. However, diseases impairing rod function will also reduce the STR, because the circuits in the inner retina will be poorly driven.

The Photopic Negative Response (PhNR)

The PhNR is a late negative response elicited by bright stimuli presented to the light-adapted retina, somewhat like a light-adapted counterpart to the STR. Ganglion cells and possibly amacrine cells are involved in generating this response, which is reduced in experimental glaucoma models.[72] The PhNR has been shown to be selectively reduced in human patients with optic nerve atrophy, which supports that the PhNR can be used to evaluate retinal ganglion cell function.[73]

The I-Wave

The i-wave is a positive wavelet of the light-adapted FERG that appears after the b-wave. Its precise origin in animals is still not clearly established, but it has been suggested that the i-wave is evoked at the level of the optic nerve[74] or ganglion cell layer.[75] An inner retinal origin of the i-wave was supported by its being the only FERG component that was altered in minipigs with experimental glaucoma with considerable loss of retinal ganglion cells.[76] The i-wave can be recorded in several pet species, including cats and dogs.[77]

ERG Protocols

The European College of Veterinary Ophthalmologists has proposed guidelines to ERG procedures in canine clinical practice in order to permit reproducible canine ERGs to be obtained under specifically defined conditions.[18] Basically, two types of procedures have been described:

- A very brief ERG protocol that determines whether a retinal response is present or absent, which was mainly intended as a preoperative ERG before cataract surgery.
- A more comprehensive protocol including selective rod and cone tests that could be used to diagnose generalized, often hereditary, outer retinal disease (Table 9.4.1).

These protocols should be considered a minimal functional study of the retina, which do not preclude the use of additional ERG responses that can provide important information if used and interpreted correctly. For instance, a luminance-response or Naka-Rushton-like function (Fig. 9.4.7) can give hints about the nature of a retinal dystrophy, such as

Table 9.4.1 A Summary of the Canine ERG Protocol Recommended by the ECVO for Detection of Generalized, Retinal Dystrophies

Time [minutes]	Stimulus [cd/m^2/s]	Number of Stimuli Averaged [n]	Stimulus Frequency [Hz]	Background Light [cd/m^2]	Bandpass Filter [Hz]	Responses Mainly Driven By
1	0.02-0.03, white	≤4	0.5	0 (darkness)	≤1 to ≥300	rods
4	0.02-0.03, white	≤4	0.5	0 (darkness)	≤1 to ≥300	rods
8	0.02-0.03, white	≤4	0.5	0 (darkness)	≤1 to ≥300	rods
12	0.02-0.03, white	≤4	0.5	0 (darkness)	≤1 to ≥300	rods
16	0.02-0.03, white	≤4	0.5	0 (darkness)	≤1 to ≥300	rods
20	0.02-0.03, white	≤4	0.5	0 (darkness)	≤1 to ≥300	rods
25*	2-3, white	1	0.1	0 (darkness)	≤1 to ≥300	rods and cones
Optional	2-3, white	1	0.1	0 (darkness)	70-100 to ≥300	rod- and cone-driven OPs
+10	2-3, white	≥4	4.9 or 5.1	30-40	≤1 to ≥300	cones
+15*	2-3, white	≥16*	31	30-40	≤1 to ≥300	cones

Numbers marked with a * represent the author's suggestions, because they are not provided in the published guidelines. The cone-driven responses should be performed after 10 minutes of light adaptation. Hence, the + sign indicates the number of minutes that should have passed since the white background light was turned on. The last column indicates the type of photoreceptors mainly driving the response, but the ERGs certainly reflect the function of more types of retinal cells as discussed in the text

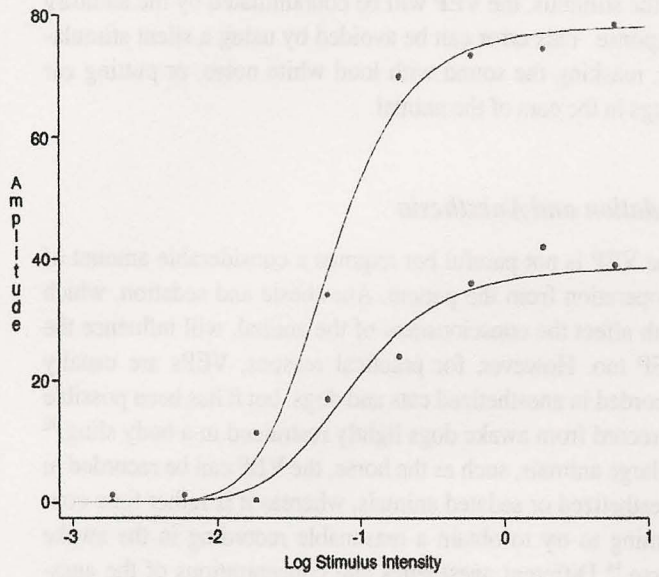

Figure 9.4.7. B-wave amplitudes in μV as a function of log stimulus intensity in log cd/s/m² from a normal dog (*green dots*) and a young Labrador Retriever affected by a rod-cone dystrophy, *prcd (red dots)*. Naka-Rushton-like equations have been used to fit curves to the data. The retinal sensitivity is decreased in the affected dog, which implies that its photoreceptors require more light in order to respond (notice the shift along the abscissa). Furthermore, there are fewer cells capable of generating a b-wave, which implies that the maximum amplitude is lower than in the normal dog. Finally, the slope of the rapidly rising part of the curve is flatter in the affected dog, which suggests that the retinal homogenetty is altered in the affected dog.

if the photoreceptors are completely lost or unable to respond to light in some areas or if the photoreceptors have a decreased sensitivity to light.[78–81]

Variations in visual stimuli, anesthetic protocols, electronic and other equipment used, and the examiner's experience will inevitably lead to differences in average normal values and variability. Furthermore, species, breed, age, diurnal fluctuations, and other factors will add to the variability. Therefore, normal values have to be established in each clinic performing electrodiagnostic testing. The number of animals needed will depend on the variability between individuals and the required precision of the test. Obtaining normal values is often time consuming but is nonetheless essential.

VISUAL EVOKED POTENTIALS

The VEP is a cortical response elicited by a visual stimulus, such as a flash (flash-VEP, FVEP) or a contrast-reversing pattern (pattern-VEP, PVEP). Multifocal VEP is a technique developed to obtain independent response from multiple areas of the visual field simultaneously, which requires considerable patient cooperation and sophisticated equipment.

The postretinal origin of the VEP has been substantiated by recording VEPs both before and after unilateral optic nerve transections in several species, such as the dog, with normal retinal function.[82] Postsurgically, the VEP was absent when the eye on the operated side was stimulated, whereas stimulation of the contralateral eye produced a slightly delayed VEP with the same waveform shape. Hence, a normal VEP indicates that the visual pathway from the retina to the visual cortex is intact.

More than 30 visual areas have been identified in the primate brain. The supragranular layers of the primary visual cortex have been reported to be the primary source of the PVEP,[83] although it is likely that other visual areas contribute as well. In primates, it is clear that responses driven by the central visual field dominate the VEP, because the cortical representation of the central visual field is located in the part of the striate cortex closest to the occipital pole (and the active electrodes) and the foveal projection is magnified at the cortical surface. In lower mammals, there is evidence for that the VEP primarily reflects cortical responses generated by stimulation of the most cone-rich retinal area, the area centralis. Feline FERGs, PERGs, and VEPs recorded after long-term monocular visual deprivation, accomplished by lid sutures, revealed that the VEPs were virtually eliminated when the deprived eye was tested, whereas the FERGs and PERGs were normal.[33] Furthermore, this shows again that combining different electrodiagnostic tests probing different parts of the visual system will enhance localization of the site of dysfunction.

Recording the VEP

Methods for recording the VEP have been reported in several species, including the cat,[33,84–88] dog,[82,89–93] horse,[14] cattle,[40] and small ruminants.[94–97] A large number of reports regarding VEPs in rodents and other laboratory animals are also available.

There are considerable differences both between and within species in these reports. The variations in amplitudes, latencies, and appearance of the VEP reflect both true differences between species and different recording strategies, stimulus parameters, and patient preparation protocols. Therefore, normative data has to be obtained by each lab performing VEPs.

Electrodes and Impedance

A canine VEP can be recorded from subcutaneous electrodes overlying the cortex in response to flash or pattern-reversal. Using active electrodes positioned over both hemispheres as well as the midline will aid in localization of chiasmal and postchiasmal abnormalities in the visual pathways as well as in hemifield stimulation. However, the normal variation in the distribution of the signals over the scalp between animals, including human beings, limits the clinical sensitivity of the VEP. The interhemispheric variability in VEPs has been shown to relate to the percentage of fibers that cross the midline in the optic chiasm.[88]

In the horse, cutaneous cup electrodes filled with conductive gel and positioned according to a modified 10 to 20 system have been used.[14] The reference electrode was placed caudal to a line joining the medial canthi, and the ground electrode was positioned halfway between the nuchal crest and a line joining the medial canthi along the midline (corresponding to the vertex position in human patients). The impedance was reported to not exceed 3 kOhms in this study, although values less than

5 kOhms between the active and reference electrodes are likely to be acceptable. If more than one active electrode is used, it is important that the impedance is similar for all channels.

Data Acquisition and Signal Averaging

The VEP amplitudes are in the 10^1 μV range and normally smaller than the amplitudes of the ongoing EEG and corneal ERG. Thus, signal averaging is required to isolate the VEP from the EEG. In addition, correct positioning of the scalp electrodes will reduce contamination from the ERG. The signals have to be amplified at least 10^4 times to be properly visualized. Online artifact rejection is advantageous to eliminate electrical artifacts caused by movements and muscle tension if the VEP is performed in awake or sedated patients. A bandpass filter setting from 1 to 100 Hz allows the dominant frequencies of the VEP to be sampled.

The VEP Stimulus

FVEPs as well as PVEPs have been performed in animals. The FVEP is more variable between individuals than the PVEP, limiting its clinical utility, but requires less complicated equipment and is easier to perform. Flash stimulation can easily be performed using a full-field stimulator. A strobe stimulating the central part of the retina will also provide reliable VEP responses, given that the peripheral retina is less important in generating the VEP responses than it is for the FERG.

Both dark- and light-adapted VEPs have been recorded in various animal species. The light-adapted FVEP will receive less contamination from the FERG because the cone responses have considerably smaller amplitudes than the dark-adapted, mixed rod-cone responses. The ISCEV standard recommends that the human FVEP is performed under light-adapted conditions, 15 to 30 cd/m^2, using a bright, white stimulus, 1.5 to 3.0 cd/m^2/s.[98]

The FVEP is quite similar regardless of which eye is stimulated. Monocular stimulation, after the opposite eye has been carefully patched, allows localization of prechiasmatic dysfunction of the visual pathways.

Pattern-reversal stimulation is produced by a video monitor connected to a pattern generator or computer. Human patients are asked to fix the eyes at the center of the pattern on the monitor and to maintain focus throughout the procedure, a situation that cannot be easily achieved when awake or sedated animals are tested. The reversing, isoluminant pattern stimulates different retinal cells than does a brief flash that produces a large, transient change in luminance. The organization of receptive fields is not uniform across the entire retina, so the pattern that best stimulates retinal components may vary between species. If patterned stimuli are used in awake or sedated patients, it should be possible to immediately stop recording whenever the animal looks away from the stimulus.

A noisy stimulator, such as one that clicks each time a flash is delivered, will produce an auditory evoked response as well as a visual one. Given that both responses will be time-locked to the stimulus, the VEP will be contaminated by the auditory response. This error can be avoided by using a silent stimulator, masking the sound with loud white noise, or putting ear plugs in the ears of the animal.

Sedation and Anesthesia

The VEP is not painful but requires a considerable amount of cooperation from the patient. Anesthesia and sedation, which both affect the consciousness of the animal, will influence the VEP too. However, for practical reasons, VEPs are usually recorded in anesthetized cats and dogs, but it has been possible to record from awake dogs lightly restrained in a body sling.[92] In large animals, such as the horse, the VEP can be recorded in anesthetized or sedated animals, whereas it is rather time consuming to try to obtain a reasonable recording in the awake horse.[14] Different anesthetics and concentrations of the anesthetic influence the VEP, although reported changes can be surprisingly small compared to the normal variation.[87,91,99] Maintaining the body temperature throughout anesthesia has been shown to be important in dogs.[100] Given that different anesthetic and sedation protocols might affect the VEP differently, it is important that the normal data is obtained from animals prepared in exactly the same way as the clinical patients.

VEP Response Parameters

The VEP waveforms in animals are polyphasic and consist of both positive and negative voltages (Fig. 9.4.8). The exact waveform of the response depends on the type and level of anesthesia, placement of electrodes, method of stimulation, and body temperature of the animal.[100] Two parameters, response amplitude and latency, can be measured. The amplitudes are generally more variable than

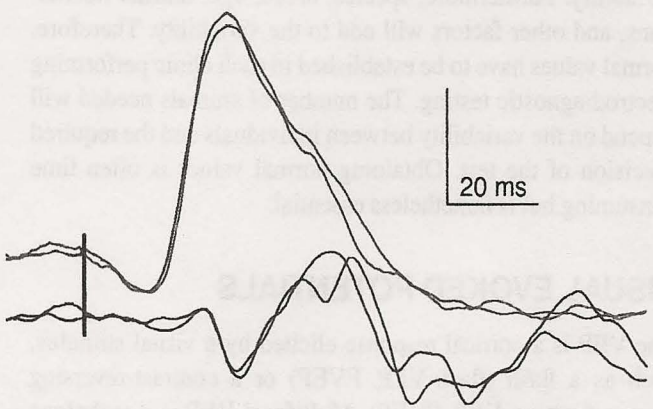

Figure 9.4.8. Simultaneous FERG (*red traces*) and FVEP (*blue traces*) from a sedated, normal horse. The active, cutaneous FVEP electrode was positioned in the midline between the left and right visual cortices. A bright, white stimulus, 3 cd/s/m^2 (the onset of the stimulus is indicated by the vertical black line), was used under light-adapted conditions (17 cd/m^2) to stimulate one eye (the other eye was covered with an opaque, light-tight patch). The FERG has a small, negative a-wave and a conspicuous, positive-going b-wave. Between 64 and 128 responses were averaged to obtain the VEP, which consists of multiple positive- and negative-going wavelets. Vertical calibration is 20μV for the FERG and 5μV for the FVEP.

latencies, both between and within patients. By convention, the amplitude is measured from the peak of a wavelet to the trough of the preceding component, and the latency is measured from the stimulus event to the peak or trough of the component.

Positive peaks of the FVEP are normally labeled *P* and negative troughs *N*, followed by its sequential number (N1, P1, N2, P2, etc.). For the PVEP, the positive and negative voltages recorded from the active electrode are named *P* and *N* respectively, followed by the approximate, normal latency in milliseconds. For example, the P100 is a stable, positive peak of the PVEP occurring about 100 ms after the stimulus in human subjects.

OTHER ELECTRODIAGNOSTIC TESTS

The Pattern Electroretinogram (PERG)

The PERG is used to evaluate macular function in primates and retinal ganglion cell function.[101–103] A reversing, structured stimulus, usually a black-and-white checkerboard or grating displayed on a video monitor, is used to stimulate the eye of cooperative human patients. The luminance of the stimulus remains constant (isoluminant), and the retina is essentially stimulated by a pattern. Hence, other retinal cells and circuits contribute to the PERG responses than to FERG. In primates, the PERG is cone-driven, whereas it has been reported to depend on both cone and rod inputs in the cat,[104] implying that outer retinal disease also will affect the inner retinal components of the PERG.

The PERG is typically just a few μV in amplitude and therefore more sensitive to noise than the FERG (Fig. 9.4.9). The stimulus has to be perfectly focused onto the retina, which means that the patient should be refracted and corrected and has to fixate on a target if a video monitor is used. To overcome the problems with fixation and patient cooperation in lower mammals, the stimulus is usually projected onto the retina of the anesthetized animal instead of using a reversing pattern on a monitor. Excellent optics has to be required to assure that the pattern is focused on the photoreceptors, especially in small eyes.

In cats, the transient PERG consists primarily of a negative afterpotential peaking at approximately 120 to 200 ms proceeded by a small positive deflection with a latency about 35 ms.[105–107] In dogs, PERGs have been reported using square-wave, vertical grating patterns presented at spatial frequencies ranging from 0.015 to 1.920 cycles/degree.[108] The waveform of the PERG elicited by a reversing, vertical grating with low spatial resolution (i.e., wide stripes) was similar to the feline PERG and characterized by a small negative peak (N1), a large positive peak (P1), and a very large negative peak (N2). Increased spatial frequencies caused decreased amplitudes of P1 and N2 and increased peak times of N1 and P1.

The PERG has been used in dogs[109,110] and cats[111] to assess the limits of visual resolution. The resolution of the central 15 degrees in dogs was estimated at 4.3 cycles per degree, whereas cats had lower resolution in the area centralis, 3.5 cycles per degree. This is in line with the lower number of ganglion cells and optic nerve fibers in cats.

The PERG has been used to study inner retinal function in a Beagle model for primary open-angle glaucoma.[110] In this study, the PERG failed to identify significant differences between normal and young glaucomatous dogs, both in the central 15 degrees and in a more peripheral, toroidal area surrounding the central field. However, altered recovery of the toroidal segment in glaucomatous Beagles was observed when the

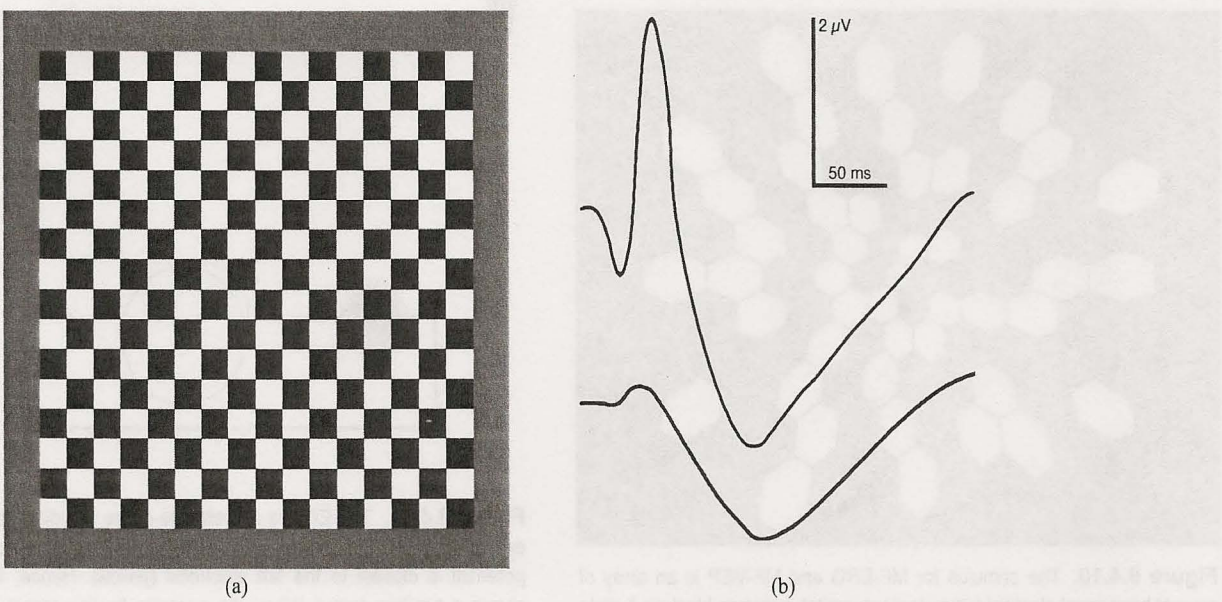

Figure 9.4.9. The PERG stimulus is a reversing checkerboard **(A)**, or grating, in which the black elements turn white at the same time as the white elements turn black. Hence, the overall luminance of the stimulus is equal (in contrast to the FERG, which is the retinal response to changes in luminance), and the retina is stimulated by the pattern. **B.** A schematic drawing of the PERG in a healthy, emmetropic human subject (*top*) and a normal dog (*bottom*).

PERG was repeated 2 hours after induction of anesthesia with an ultra-short-acting thiobarbiturate (thiamylal sodium).[112] PERGs were more sensitive than FERGs to experimental, short-term increases in IOP in mixed-breed dogs even before histological changes could be detected in the retina.[113]

The Multifocal ERG (MF-ERG)

The MF-ERG is a sophisticated technique to obtain local ERGs from multiple areas across the central part of the retina.[114] The stimulus for the MF-ERG is usually an array of hexagonal elements presented on a video monitor (Fig. 9.4.10). The elements are scaled with eccentricity, following the cone density profile of the retina, so the amplitudes of each focal response are equalized. Fifty percent of the elements are black at any given time; the other 50% are white. The luminance of each element, bright (white) or dark (black), is determined by a pseudorandom sequence, the m-sequence. The stimulus pattern is typically changed a number of times every second, and the duration of the test in a human patient is often close to 10 minutes. The responses are recorded from an active, corneal electrode. Powerful computer software then links the responses to each retinal area. It has been shown that the MF-ERG can be used to obtain information about both outer and inner retinal function.[115,116] The MF-ERG normally requires the subject to fixate on a central target, which makes the test difficult to perform in patients with poor central vision and in uncooperative patients. However, it is possible to project the stimulus array onto the retinal surface using a modified scanning laser ophthalmoscope. This has been used experimentally in anesthetized cats.[117]

The Electrooculogram (EOG)

The electrooculogram estimates the standing potential of the eye, a current in the millivolt range that is generated mainly across the RPE. It has been shown in human subjects that the clinically most useful information is obtained by comparing the dark- and light-adapted EOG amplitudes.[118,119] The recording technique employed for human subjects is based on that the subject is cooperative and voluntarily makes regular, horizontal eye movements (Fig. 9.4.11). The EOG is therefore technically challenging to perform in lower mammals. However, a study in which the feline EOG was recorded using a mechanical device that moved the eyes showed that the average light-adapted–dark-adapted ratio of the amplitudes (Arden ratio) was 1.83 (range 1.70–1.99), which is similar to the ratio considered to be normal in human patients.[120]

POSTNATAL DEVELOPMENT OF ELECTRODIAGNOSTIC RESPONSES

Electrodiagnostic procedures have become important in the early diagnosis of selected eye diseases among animals. Unaffected littermates may provide age-matched controls, but data collected during the maturation of normal animals are also needed if entire litters are affected or if normal littermates are unavailable for various reasons. Most animals have retinas in which both rods and cones develop with age, even though they develop at different rates.

The ERG

At birth, the photoreceptor layer in the canine retina is not formed (i.e., the two granular layers have not separated). The ERG is absent at birth. It begins to appear in puppies at approximately 10 to 15 days of age, and it is completely formed by 15 to 28 days of age.[121,122] The first response to occur is a small

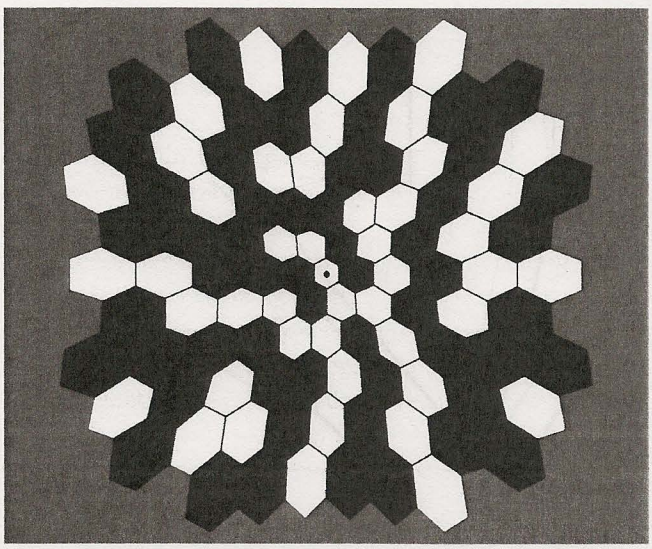

Figure 9.4.10. The stimulus for MF-ERG and MF-VEP is an array of several hexagonal elements; the elements switch between black and white according to a pseudorandom sequence. Hence, each retinal location is stimulated by both light and dark, but the sequence is lagged by different amounts for each location. Then, the computer software extracts the focal response to each element.

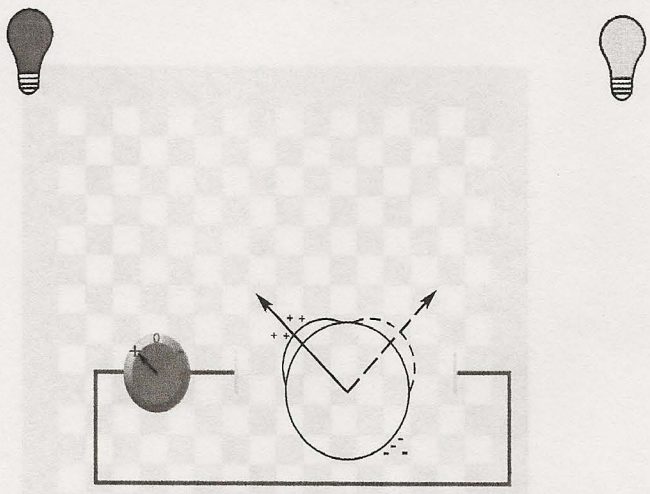

Figure 9.4.11. The EOG is an estimate of the standing potential of the eye. When the patient is looking toward the red light, the positive corneal potential is closest to the left electrode (*yellow*). Hence, the voltmeter shows a positive output. When the opposite fixation target is lit and the patient changes the direction of gaze, the negative posterior segment will be closer to the left electrode and the output will turn negative on the voltmeter. Thus, repeated saccadic eye movements will produce a square-wave response that reflects the standing potential of the eye.

negative wave that appears at the beginning of a nascent a-wave. This small negative response occurs at the time of differentiation of the rods and cones. In dogs, the cone system develops more rapidly than the rod system.[123] During development, amplitudes increase and latencies decrease until they approximate adult values between the fifth and eighth weeks of age.[121,122] In vitro recordings of transretinal mass potentials in 9- to 10-week-old dogs indicate that changes across the photoreceptors is the primary cause of the amplitude increase.[124] The waveform of the ERG changes from being dominated by the a-wave to being dominated by the b-wave, and these events are paralleled by development of the outer plexiform layer. The greatest changes in ERG amplitude are expected to occur between the third and fourth weeks of age, at a time corresponding with maturation of the inner and outer nuclear layers.[121,125] In red Irish Setters, the b-wave reaches its full size between 40 and 50 days.[8] By 60 days of age, both the rod and cone responses to flickering stimuli were essentially the same as those in adult dogs.[123] OPs appear on the b-wave of the ERG at approximately 3 weeks of age with high light intensities.[126] By 11 weeks, the potentials are well developed and become apparent with lower intensities.

Kittens are born with an immature visual system that requires approximately 4 months to mature. Photoreceptors are mature by the end of the first month, and the remainder of the maturational process occurs in more proximal elements, such as ganglion cells. Development of the ERG in kittens has also been reported to occur in phases.[127] The first stage is marked by appearance of the b-wave during the first 10 days after birth, and the second phase corresponds to the increase in amplitude of the b-wave between 10 and 49 days. The b-wave evoked by high-intensity stimulation matures by 5 to 7 weeks of age, whereas maturation of the b-wave evoked by low-level stimulation requires an additional 3 to 5 weeks. The third phase is required for attainment of adult implicit time values and OP development. Feline cone b-wave amplitudes have been reported to be normal or supernormal between 25 and 94 days of age.[128] These supernormal responses, seen in other species too, are likely to occur during a period when there actually are more functional cells in the immature retina than in the adult retina, and that the decline to adult values reflects normal degeneration. Adults values for the feline cone b-wave were attained after 100 days, implicit times reached adult levels by 80 days, and flicker fusion matured at approximately 74 days.[128] Before 7 weeks of age, the OPs differed from adults in numbers, amplitude, and time between peaks. By 18 weeks of age, values were similar to those of adults. The maturation of the retina and its ability to generate electrical responses has been studied in other species too, such as the sheep.[97]

The VEP

During the first 5 weeks after birth, maturation of the VEP closely parallels neuronal development in the visual cortex.[93] Generally, VEPs in maturing animals are quite variable between individuals and more fatigable than in adults.[129]

The development of VEPs in puppies was reported to begin as early as the second day after birth, with a negative wave characterized by a latency that exceeded 500 milliseconds.[130] By day 3 or 4, the peak had shortened, and this was followed by the addition of another negative peak. The number of peaks increased between 2 and 3 weeks of age, accompanied by a decrease in peak latencies. By the fifth week, the response simplified somewhat, with considerably shortened latencies. In a subsequent study conducted in puppies from 7 to 100 days of age, it was shown that the latency for P1 of the VEP was mature as early as 11 days, and 38 days were required for the latency of N1 and P2.[131] The latencies of later components were not mature by the end of the study.

Long latency VEPs appear in the feline visual cortex on approximately the second day of life, and short latency responses appear at 5 days to 2 weeks of age. The first potential reported to appear was a negative wave, which would become the N2 in the adult.[133, 134] The long latency response resembles that in adult cats between 30 and 40 days.

Sequential maturation of VEP components was reported in lambs during the first 30 days after birth.[97] The early component, N1, did not show a significant decrease in latency, whereas the later potential, P2, did. It was suggested that the primary nerve tracts (i.e., N1) were mature at birth, but that increasing myelination and integration in the cortex accounted for the shorter latencies for P2.

CLINICAL APPLICATION OF ELECTRODIAGNOSTIC TESTING

In clinical electrophysiology, correlating electrodiagnostic findings to clinical findings and history is essential. An unexpected finding not in line with the results of the clinical examination may turn out to be a very important discovery but is more often caused by technical problems or erroneous patient preparation. Therefore, an unexpected electrodiagnostic result should always alert the examiner, and the result should be validated against questions such as the following:

Is the result reproducible?
Will changing the electrodes and amplifiers affect the result?
Is it possible to probe the function of the same part of the visual system in a different way with a similar result?
Do electrodiagnostic tests at other levels of the visual system support the result?

Electrodiagnostic tests can provide information about the location of a lesion in the visual system and often more specific information regarding what type of cells are involved. Only two parameters are usually objectively assessed: the amplitude of the response and the timing of the response in relation to the stimulus (i.e., the implicit time or latency). The shape of the curve, the waveform, is usually subjectively judged by the examiner, although advances in computer technology open up for more sophisticated analyses of the waveforms.

The effects of lesions on the amplitude or implicit time or latency of the ERG and VEP are somewhat predictable. A large, degenerating area in the retina (or a generalized retinal

dystrophy) will result in decreased amplitudes and prolonged implicit times of the ERG, whereas focal, chronic lesions may result in decreased amplitudes but unchanged implicit times. A demyelinating optic neuropathy will slow down the conduction velocity and prolong the latency, whereas complete loss of axons will reduce the amplitude.

The diagnostic ability of electrodiagnostic tests depends on the variability between subjects, the difference between normal and affected subjects, the resolution of method employed, and the test protocol used. A lab where tests are performed by experienced personnel under highly standardized conditions with well-calibrated, upgraded equipment and a suitable protocol can detect to patients at an earlier stage or when the disease is less widely spread than can a lab where the conditions are less optimal. Therefore, the age when a patient can be diagnosed with reasonable accuracy will vary between labs.

REFERENCES

1. Holmgren F. En method att objektivera effecten af ljusintryck på retina. *Upsala Läkareförenings Förhandlingar* 1865; 1: 177–191.
2. Einthoven W, Jolly W. The form and magnitude of the electrical response of the eye to stimulation by light at various intensities. *Q J Exp Physiol* 1908; 1: 373–416.
3. Piper H. Über die Netzhautströme. *Arch Anat Physiol Lpz Physiol Abt* 1911: 85–132.
4. Granit R. The components of the retinal action potential in mammals and their relation to the discharge in the optic nerve. *J Physiol Lond* 1933; 23: 678–683.
5. Kofuji P, Ceelen P, Zahs KR, Surbeck LW, Lester HA, Newman EA. Genetic inactivation of an inwardly rectifying potassium channel (Kir4.1 subunit) in mice: Phenotypic impact in retina. *J Neurosci* 2000; 20(15): 5733–5740.
6. Dawson WW, Kommonen B. The late positive retinal potential in dogs. *Exp Eye Res* 1995; 60(2): 173–179.
7. Karpe G. The basis of clinical electroretinography. *Acta Ophthalmol Copenh* 1945; (suppl 24): 1–118.
8. Parry HB, Tansley K, Thomson LC. The electroretinogram of the dog. *J Physiol Lond* 1953; 120: 28–40.
9. Rubin LF. Clinical electroretinography in dogs. *J Am Vet Med Assoc* 1967; 151: 1456–1469.
10. Steiss JE, Storrs DP, Wright JC. Comparisons of electroretinograms recorded with a contact lens versus needle electrode in the clinically normal dogs. *Prog Vet Comp Ophthalmol* 1992; 2(4): 143–146.
11. Witzel DA, Johnson JH, Pitts DG, Smith EL III. Scleral contact lens electrodes for electroretinography in domesticated animals. *Am J Vet Res* 1976; 37(8): 983–985.
12. Rosolen SG, Rigaudiére F, Lachapelle P. A practical method to obtain reproducible binocular electroretinograms in dogs. *Doc Ophthalmol* 2002; 105: 93–103.
13. Komaromy AM, Andrew SE, Sapp HL Jr, Brooks DE, Dawson WW. Flash electroretinography in standing horses using the DTL microfiber electrode. *Vet Ophthalmol* 2003; 6(1): 27–33.
14. Ström L. Visual evoked potentials in the horse. [In Swedish.]. 2004, Department of Large Animal Medicine & Surgery, SLU: Uppsala. p. 21.
15. Bayer AU, Mittag T, Cook P, Brodie SE, Podos SM, Maag KP. Comparisons of amplitude size and the reproducibility of three different electrodes to record the corneal flash electroretinogram in rodents. *Doc Ophthalmol* 1999; 98(3): 233–246.
16. Coulter DB, Martin CL. Signal averaging of electroretinograms. *Georgia Vet* 1978; 30: 14–20.
17. Howard DR, Keller WF, Blanchard GL. Clinical electroretinography. A protocol for testing the retina. *J Am Anim Hosp Assoc* 1973; 9: 219–226.
18. Narfström K, Ekesten B, Rosolen SG, Spiess BM, Percicot CL, Ofri R. Guidelines for clinical electroretinography in the dog. *Doc Ophthalmol* 2002; 105(2): 83–92.
19. Gouras P. Electroretinography: Some basic principles. *Invest Ophthalmol* 1970; 9: 557–569.
20. Schaeppi U, Liverani F. Procedures for routine clinical electroretinography (ERG) in dogs. *Agents Actions* 1977; 7(3): 347–351.
21. Marmor MF, Holder GE, Seeliger MW, Yamamoto S. Standard for clinical electroretinography (2004 update). *Doc Ophthalmol* 2004; 108: 107–114.
22. Marmor MF, Zrenner E. Standard for clinical electroretinography (1999 update). *Doc Ophthalmol* 1999; 97: 143–156.
23. Brigell M, Bach M, Barber C, Moskowitz A, Robson JG. Guidelines for calibration of stimulus and recording parameters used in clinical electrophysiology of vision. *Doc Ophthalmol* 2003; 107: 185–193.
24. Maehara S, Itoh N, Wakaiki S, et al. Electroretinography using contact lens electrode with built-in light source in dogs. *J Vet Med Sci* 2005; 67(5): 509–514.
25. Komaromy AM, Brooks DE, Dawson WW, Källberg M, Ollivier FJ, Ofri R. Technical issues in electrodiagnostic recording. *Vet Ophthalmol* 2002; 5(2): 85–91.
26. Spiess BM. Elektrophysiologische Untersuchung des Auges be Hund und Katze. Stuttgart: *Ferdinand Enke Verlag* 1994: 351.
27. Acland GM. Diagnosis and differentiation of retinal diseases in small animals by electroretinography. *Semin Vet Med Surg Sm Anim* 1988; 3(1): 15–27.
28. Kommonen B. The DC-recorded dog electroretinogram in ketamine-medetomidine anesthesia. *Acta Vet Scand* 1988; 29(1): 35–41.
29. Yanase J, Ogawa H. Effects of halothane and sevoflurane on the electroretinogram of dogs. *Am J Vet Res* 1997; 58(8): 904–909.
30. Spiess BM, Leber-Zürcher AC. Clinical electroretinography in the dog. Part III. [In German.]. *Schweiz Arch Tierheilk* 1992; 134: 61–74.
31. Tanskanen P, Kylmä T, Kommonen B, Karhunen U. Propofol influences the electroretinogram to a lesser degree than thiopentone. *Acta Anaesthesiol Scand* 1996; 40(4): 480–485.
32. Narfström K, Nilsson SE, Andersson BE. Progressive retinal atrophy in the Abyssinian cat: Studies of the DC-recorded electroretinogram and the standing potential of the eye. *Br J Ophthalmol* 1985; 69: 618–623.
33. Baro JA, Lehmkühle S, Kratz KE. Electroretinograms and visual evoked potentials in long-term monocularly deprived cats. *Invest Ophthalmol Vis Sci* 1990; 31(7): 1405–1409.
34. Acland GM, Forte S, Aguirre GD. Halothane effect on the canine electroretinogram in Trans. *Am Coll Vet Ophthalmol* 1981.
35. Kommonen B, Karhunen U, Raitta C. Effects of thiopentone, halothane-nitrous oxide anesthesia compared to

ketamine-xylazine anesthesia on the D.C. recorded dog electroretinogram. *Acta Vet Scand* 1988; 29(1): 23–33.
36. Jones RD, Brenneke CJ, Hoss HE, Loney ML. An electroretinogram protocol for toxicological screening in the canine model. *Toxicol Lett* 1994; 70: 223–234.
37. François J, Wouters L, Victoria-Troncoso V, de Rouck A, van Gerven A. Morphometric and electrophysiologic study of the photoreceptors in the horse. *Ophthalmol Basel* 1980; 181: 340–349.
38. Wouters L, de Moor A, Moens Y. Rod and cone components in the electroretinogram of the horse. *Zbl Vet Med Assoc* 1980; 27: 330–338.
39. Kotani T, Kurosawa T, Numata Y, Izumisawa Y, Satoh H, Brooks DE. The normal electroretinogram in cattle and its clinical application in calves with visual defects. *Prog Vet Comp Ophthalmol* 1993; 3(1): 37–44.
40. Strain GM, Olcott BM, Hokett LD. Electroretinogram and visual-evoked potential measurements in Holstein cows. *Am J Vet Res* 1986; 47: 1079–1081.
41. Niemeyer G, Nagahara K, Demant E. Effects of changes in arterial PO2 and PCO2 on the electroretinogram in the cat. *Invest Ophthalmol Vis Sci* 1982; 24: 678–683.
42. Kang Derwent J, Linsenmeier RA. Effects of hypoxemia on the a- and b-waves of the electroretinogram in the cat retina. *Invest Ophthalmol Vis Sci* 2000; 41: 3634–3642.
43. Howard DR, Sawyer DC. Electroretinography of acute hypoxic and increased intraocular pressure status in the dog. *Am J Vet Res* 1975; 36(1): 81–84.
44. Murray MJ, Borda RP. Physiologic correlates of the ERG hyperventilatory response in dogs. *Acta Ophthalmol Copenh* 1984; 62(5): 808–818.
45. Gouras P. Saturation of the rods in Rhesus monkey. *J Opt Soc Am* 1965; 55: 86.
46. Dodt E. Cone electroretinography by flicker. *Nature* 1951; 168(4278): 738.
47. Jacobs GH, Deegan 2nd JF, Crognale MA, Fenwick JA. Photopigments of dogs and foxes and their implications for canine vision. *Vis Neurosci* 1993; 10(1): 173–180.
48. Estevez O, Spekreijse H. The "silent substitution" method in visual research. *Vis Res* 1982; 22(6): 681–691.
49. Doty RW, Kimura DS. Oscillatory potentials in the visual system of cats and monkeys. *J Physiol Lond* 1963; 168: 205–218.
50. Sims MH, Sackman JE, McLean RA, Slaymaker C. Effects of stimulus intensity and conditioning on the electroretinogram and oscillatory potentials in dark-adapted cats. *Prog Vet Comp Ophthalmol* 1991; 3: 177–185.
51. Brooks DE, Sims MH, Gum GG, Blackstock MJ. Changes in oscillatory potentials of the canine electroretinogram during acute sequential elevations in intraocular pressure. *Prog Vet Comp Ophthalmol* 1992; 2(2): 80–89.
52. Sims MH, Brooks DE. Changes in oscillatory potentials in the canine electroretinogram during dark adaptation. *Am J Vet Res* 1990; 51: 1580–1586.
53. Wachtmeister L, Dowling JE. The oscillatory potentials of the mudpuppy retina. *Invest Ophthalmol Vis Sci* 1978; 17(12): 1176–1188.
54. Wachtmeister L. Further studies of the chemical sensitivity of the oscillatory potentials of the electroretinogram (ERG). I. GABA and glycine antagonists. *Acta Ophthalmol Copenh* 1980; 58: 712–725.
55. Wachtmeister L. Oscillatory potentials in the retina: What do they reveal? *Prog Retin Eye Res* 1998; 17: 485–521.
56. Bui BV, Fortune B. Ganglion cell contributions to the rat full-field electroretinogram. *J Physiol Lond* 2003: 153–173.
57. Peachey NS, Alexander KR, Fishman GA. Rod and cone system contributions to oscillatory potentials: An explanation for the conditioning flash effect. *Vis Res* 1987; 27: 859–866.
58. Speros P, Price J. Oscillatory potentials: History techniques and potential evaluation of disturbances of retinal circulation. *Surv Ophthalmol* 1981; 25: 237–252.
59. King-Smith PE, Loffing DH, Jones R. Rod and cone ERGs and their oscillatory potentials. *Invest Ophthalmol Vis Sci* 1986; 27: 270–273.
60. Yanagida T, Koshimizu M, Kawasaki K, Yonemura D. Microelectrode depth study of the electroretinographic oscillatory potentials in the frog retina. *Doc Ophthalmol* 1988; 67: 355–361.
61. el Azizi M, Wang L, Eklund A, Wachtmeister L. Background light adaptation of the retinal neuronal adaptive system II. Dynamic effects. *Doc Ophthalmol* 2004; 109: 201–213.
62. Shirao Y, Wajima R, Kaneko T, Nishimura A. Neural retinal contribution to the slow negative potential of the canine electroretinogram. *Doc Ophthalmol* 1998; 94: 293–306.
63. Ekesten B, Narfström K. Cone positive off-responses in normal and dystrophic cats. *Doc Ophthalmol* 1999; 97(1): 9–21.
64. Kang Derwent J, Linsenmeier RA. Intraretinal analysis of the a-wave of the electroretinogram (ERG) in dark-adapted intact cat retina. *Vis Neurosci* 2001; 18: 353–363.
65. Nilsson SEG, Armstrong D, Koppang N, Persson P, Milde K. Study on the retina and the pigment epithelium in hereditary canine ceroid lipofuscinosis. IV: Changes in the electroretinogram and the standing potential of the eye. *Invest Ophthalmol Vis Sci* 1983; 24: 77–84.
66. Nilsson SEG, Wrigstad A, Narfström K. Changes in the DC electroretinogram in Briard dogs with hereditary congenital night blindness and partial day blindness. *Invest Ophthalmol Vis Sci* 1992; 54: 291–296.
67. Narfström K. Retinal degeneration in a strain of Abyssinian cats. A hereditary, clinical electrophysiological and morphological study. 1985, Linköping University and Swedish University of Agricultural Sciences, Uppsala.
68. Kommonen B, Dawson WW, Parmer R. Pigment epithelial function in the retina. *Am J Vet Res* 1991; 52: 1341–1344.
69. Sieving PA, Nino C. Scotopic threshold response (STR) of the human electroretinogram. *Invest Ophthalmol Vis Sci* 1988; 29: 1608–1614.
70. Sieving PA, Frishman LJ, Steinberg RH. Scotopic threshold response of the proximal retina in the cat. *J Neurophysiol* 1986; 56(4): 1049–1061.
71. Yanase J, Ogawa H, Ohtsuka H. Scotopic threshold response of the electroretinogram of dogs. *Am. J Vet. Res* 1996; 57(3): 361–366.
72. Viswanathan S, Frishman LJ, Robson JG. The photopic negative response of the macaque electroretinogram: Reduction by experimental glaucoma. *Invest Ophthalmol Vis Sci* 1999; 40: 1124–1136.
73. Gotoh Y, Machida S, Tazawa Y. Selective loss of the photopic negative response in patients with optic nerve atrophy. *Arch Ophthalmol* 2004; 122(3): 341–346.
74. Gouras P, Mackay CJ. Detecting early post-chiasmatic visually evoked responses. *Clin Vis Sci* 1988; 3: 119–124.

75. Rousseau S, McKerral M, Lachapelle P. The i-wave: Bridging flash and pattern electroretinography. *Electroencephalogr Clin Neurophysiol* 1996; 46(suppl): 165–171.
76. Rosolen SG, Rigaudiére F, LeGargasson JF. A new model of induced ocular hyperpressure using the minipig. [In French.]. *J Fr Ophthalmol* 2003; 26(3): 259–267.
77. Rosolen SG, Rigaudiére F, LeGargasson JF, et al. Comparing the photopic ERG i-wave in different species. *Vet Ophthalmol* 2004; 7(3): 189–192.
78. Peachey NS, Alexander KR, Fishman GA. The luminance-response function of the dark-adapted human electroretinogram. *Vis Res* 1989; 29(3): 263–270.
79. Naka K, Rushton WAH. The generation and spread of S-potentials in fish (Cyprinidae). *J Physiol Lond* 1970; 192: 437–461.
80. Narfström K, Arden GB, Nilsson SEG. Retinal sensitivity in hereditary retinal degeneration in Abyssinian cats: Electrophysiological similarities between man and cat. *Br J Ophthalmol* 1989; 73: 516–521.
81. Ekesten B, Narfström K. Abnormal dark-adapted ERG in cats heterozygous for a recessively inherited rod-cone degeneration. *Vet Ophthalmol* 2004; 7(1): 63–67.
82. Sims MH, Laratta LJ, Bubb WJ, Morgan RV. Waveform analysis and reproducibility of visual-evoked potentials in dogs. *Am J Vet Res* 1989; 50(11): 1823–1828.
83. Schroeder CE, Tenke CE, Givre SJ, Arezzo JC, Vaughan HG Jr. Striate cortical contribution to the surface-recorded pattern-reversal VEP in the alert monkey. *Vis Res* 1991; 31: 1143–1157.
84. Sims MH, Laratta LJ. Visual-evoked potentials in cats, using a light-emitting diode stimulator. *Am J Vet Res* 1988; 49(11): 1876–1881.
85. Strain GM, Tedford BL, Littlefield-Chabaud MA, Trevino LT. Air- and bone-conduction brainstem auditory evoked potentials and flash visual evoked potentials in cats. *Am J Vet Res* 1998; 59(2): 135–137.
86. Perez-Cobo JC, Lopez de Armentia M, Sanchez-Suero S, Perez-Arroyo M. Visual evoked potentials in response to pattern reversal in the cat cortex. *Rev Esp Fisiol* 1994; 50(4): 205–210.
87. Uzuka Y, Doi S, Tokuriki M, Matsumoto H. The establishment of a clinical diagnostic method of visual evoked potentials (VEPs) in the cat: The effects of recording electrode positions, stimulus intensity and level of anesthesia. *Nippon Juigaku Zasshi* 1989; 51(3): 547–553.
88. Creel DJ, Dustman RE, Beck EC. Visually evoked responses in the rat, guinea pig, cat, monkey and man. *Exp Neurol* 1973; 40: 351–366.
89. Howard DR, Breazile JE. Normal visual cortical-evoked response in the dog. *Am J Vet Res* 1972; 33(11): 2155–2157.
90. Malnati GA, Marshall AE, Coulter DB. Electroretinographic components of the canine visual evoked responses. *Am J Vet Res* 1981; 42(1): 159–163.
91. Bichsel P, Oliver Jr JE, Coulter DB, Brown J. Recording of visual-evoked potentials in dogs with scalp electrodes. *J Vet Int Med* 1988; 2(3): 145–149.
92. Strain GM, Jackson RM, Tedford BL. Visual evoked potentials in the clinically normal dog. *J Vet Int Med* 1990; 4(4): 222–225.
93. Fox MW. Neuronal development and ontogeny of evoked potentials in auditory and visual cortex of the dog. *Electroencephalogr Clin Neurophysiol* 1968; 24(3): 213–226.
94. Gregory NG, Wotton SB. Studies on the central nervous system: Visually evoked cortical responses in sheep. *Res Vet Sci* 1983; 4: 315–319.
95. Daly CC, Gregory NG, Wotton SB, Whittington PE. Concussive methods of preslaughter stunning in sheep: Assessment of brain function using cortical evoked responses. *Res Vet Sci* 1986; 1: 349–352.
96. Strain GM, Claxton MS, Olcott BM, Turnquist SE. Visual-evoked potentials and electroretinograms in ruminants with thiamine-responsive polioencephalomalacia or suspected listeriosis. *Am J Vet Res* 1990; 1(10): 1513–1517.
97. Woods JR, Parisi V, Coppes V, Brooks DE. Maturational sequence of the visual system: Serial measurements of visual evoked potential and electroretinogram in the healthy neonatal lamb. *J Obstet Gynaecol* 1983; 45(6): 738–743.
98. Odom JV, Bach M, Barber C, et al. Visual evoked potentials standard (2004). *Doc Ophthalmol* 2004; 108: 105–123.
99. Margalit E, Weiland JD, Clatterbuck RE, et al. Visual and electrical evoked response recorded from subdural electrodes implanted above the visual cortex in normal dogs under two methods of anesthesia. *J Neurosci Meth* 2003; 23: 129–137.
100. Aunon JI, Weirich WE, Nyholm R. Effects of hypothermia on the visual-evoked brain potential in dogs. *Am. J. Vet. Res* 1977; 38: 383–385.
101. Lawwill T. The bar-pattern electroretinogram for clinical evaluation of the central retina. *Am J Ophthalmol* 1974; 78: 121–126.
102. Maffei L, Fiorentini A. Electroretinographic responses to altering gratings before and after section of the optic nerve. *Science* 1981; 211: 953–955.
103. Riggs LA, Johnson EP, Schrick AML. Electrical responses of the human eye to moving stimulus patterns. *Science* 1964; 144: 567–570.
104. Maffei L, Fiorentini A. Pattern visual evoked potentials and electroretinograms in man and animals. In: Desmedt JE, ed. *Visual Evoked Potentials.* New York: Elsevier Science, 1990: 25–33.
105. Ohzawa I, Freeman RD. Pattern evoked potentials from the cat's retina. *J Neurophysiol* 1985; 54(3): 691–700.
106. Vaegan, Anderton PJ, Millar TJ. Transient and steady state focal and pattern electroretinogram losses with unilateral nerve section. *Doc Ophthalmol* 2002; 105: 105–127.
107. Vaegan, Arora A, Crewther SG, Millar TJ. The effect of various anaesthetics on spatial tuning of two major wave peaks in the transient pattern electroretinogram of the cat: Evidence for pattern and luminance components. *Vis Res* 1990; 30(10): 1401–1407.
108. Sims MH, Ward DA. Response of pattern-electroretinograms (PERG) in dogs to alterations in the spatial frequency of the stimulus. *Prog Vet Comp Ophthalmol* 1992; 2(3): 106–112.
109. Odom JV, Bromberg NM, Dawson WW. Canine visual acuity: Retinal and cortical field potentials evoked by pattern stimulation. *Am J Physiol* 1983; 245: R637.
110. Ofri R, Dawson WW, Gelatt KN. Visual resolution in normal and glaucomatous dogs determined by pattern electroretinogram. *Prog Vet Comp Ophthalmol* 1993; 3(3): 111–116.
111. Schuurmans RP, Berninger T. Pattern reversal responses in man and cat: A comparison. *Ophthalmic Res* 1984; 16(1–2): 67–72.
112. Ofri R, Dawson WW, Foli K, Gelatt KN. Primary open angle glaucoma alters retinal recovery from a thiobarbiturate. *Br J Ophthalmol* 1993; 77: 502–508.

113. Hamor RE, Gerding Jr PA, Ramsey DT, Whiteley HE, Benson GJ, Schaeffer DJ. Evaluation of short-term increased intraocular pressure on flash- and pattern-generated electroretinograms of dogs. *Am J Vet Res* 2000; 61(9): 1087–1091.
114. Sutter EE, Tran D. The field topography of ERG components in man – I. The photopic luminance. *Vis Res* 1992; 32(3): 433–446.
115. Sutter EE, Bearse MA Jr. The optic nerve head component of the human ERG. *Vis Res* 1999; 39: 419–436.
116. Hood DC, Frishman LJ, Viswanathan S, Robson JG, Ahmed J. Evidence for a ganglion cell contribution to the primate electroretinogram (ERG): Effects of TTX on the multifocal ERG in the macaque. *Vis Neurosci* 1999; 16: 411–416.
117. Seeliger MW, Narfström K. Functional assessment of the regional distribution of disease in a cat model of hereditary retinal degeneration. *Invest Ophthalmol Vis Sci* 2000; 41(7): 1998–2005.
118. Arden GB, Fojas MR. Electrophysiological abnormalities in pigmentary degenerations of the retina. *Arch Ophthalmol* 1962; 68: 369–389.
119. Arden GB, Kelsey JH. Changes produced by light in the standing potential of the human eye. *J Radiol Electrol Med Nucl* 1962; 161: 189–204.
120. Sakai H, Mitsui Y. Measurement of electrooculogram in the cat. [In Japanese]. *Nippon Ganka Gakkai Zasshi* 1995; 99(6): 659–662.
121. Gum GG, Gelatt KN, Samuelson DA. Maturation of the retina of the canine neonate as determined by electroretinography and histology. *Am J Vet Res* 1984; 45(6): 1166–1171.
122. Kirk GR, Boyer SF. Maturation of the electroretinogram in the dog. *Exp Neurol* 1973; 38(2): 252–264.
123. Acland GM, Aguirre GD. Retinal degenerations in the dog: IV. Early retinal degeneration (ERD) in Norwegian Elkhounds. *Exp Eye Res* 1987; 44: 491–521.
124. Millichamp NJ, Arden GB. Transretinal mass receptor potentials from the canine retina in vitro. *Am J Vet Res* 1989; 0(10): 1710–1714.
125. Gum GG. Electrophysiology in veterinary ophthalmology. *Vet Clin North Am Sm Anim Pract* 1980; 10(2): 437–453.
126. Leon A, Hussain AA, Curtis R. Autosomal dominant rod-cone dysplasia in the Rdy cat. 2. Electrophysiological findings. *Exp Eye Res* 1991; 53(4): 489–502.
127. Hamasaki DI, Maguire GW. Physiological development of the kitten's retina: An ERG study. *Vis Res* 1985; 25(11): 1537–1543.
128. Jacobson SG, Ikeda H, Ruddock K. Cone-mediated retinal function in cats during development. *Doc Ophthalmol* 1987; 65(1): 7–14.
129. Boyer S, Kirk GR. Maturation of the visual evoked response in the dog. *Exp Neurol* 1973; 38(3): 449–457.
130. Myslivecek J. The development of the response to light flashes in the visual cortex of the dog. *Brain Res* 1968; 10: 418–430.
131. Strain GM, Jackson RM, Tedford BL. Postnatal development of the visual-evoked potential in dogs. *Am J Vet Res* 1991; 52: 231–235.
132. Ellingson RJ, Wilcott RC. Development of evoked potentials in visual and auditory cortices of kittens. *J Neurophysiol* 1960; 23: 363–375.
133. Rose GH, Gruenau SP, Spencer JW. Maturation of visual electrocortical responses in unanesthetized kittens: Effects of barbiturate anesthesia. *Electroencephalogr Clin Neurophysiol* 1972; 33(2): 141–158.
134. Rose GH, Lindsley DB. Development of visually evoked potentials in kittens: Specific and non-specific responses. *J Neurophysiol* 1968; 31(4): 607–623.